
LN's

Endless

STEM Notes



Art:

Kira, by @Ekkoberry

M1. ALGEBRA	6
1.1. Mathematical Syntax and Techniques	6
1.2. Algebraic Identities	10
1.3. Trigonometric Identities	18
1.4. Sequences and Series	21
1.5. Complex Numbers	24
1.6. Discrete Mathematics and Abstract Algebra	26
1.7. Special Functions and Identities	30
M2. GEOMETRY	38
2.1. Properties of 2D and 3D Shapes	38
2.2. Angle, Triangle and Circle Theorems	45
2.3. 2D Coordinate Geometry	54
2.4. Vectors and 3D Geometry	61
M3. CALCULUS	67
3.1. Limits and Numerical Methods	67
3.2. Series Expansions	75
3.3. Differentiation and Integration	79
3.4. Ordinary Differential Equations, Laplace and Z-Transforms	87
3.5. Multivariable and Vector Calculus	98
3.6. Fourier Series and Fourier Transforms	110
3.7. Partial Differential Equations and Variational Calculus	117
M4. LINEAR ALGEBRA	122
4.1. Vector and Matrix Algebra	122
4.2. Transformation Matrices	130
4.3. Fundamental Subspaces and Matrix Decompositions	132
4.4. Matrix and Tensor Calculus	139
M5. STATISTICS	142
5.1. Axioms, Combinatorial Probability and Basic Statistics	142
5.2. Probability Distributions and Random Variables	147
5.3. Hypothesis Testing	162
5.4. Stochastic Processes, Signals and Information Theory	171
5.5. Machine Learning and Computational Statistics	186
5.6. Computer Vision and Computer Graphics	210
5.7. Accounting, Finance and Business	218

P6. MECHANICS, STRUCTURES AND MATERIALS	237
6.1. Kinematics, Forces and Dynamics	237
6.2. Linear Systems and Mechanical Vibrations	255
6.3. Solid Mechanics and Structural Mechanics	269
6.4. Geotechnical and Civil Engineering	293
6.5. Fracture Mechanics and Failure Analysis	308
6.6. Materials Processing, Design and Datasets	316
6.7. Sustainability and Energy Engineering	359
P7. THERMOFLUID MECHANICS	371
7.1. Fluid Mechanics	371
7.2. Thermofluid Dynamics	384
7.3. Heat Transfer	402
7.4. Thermodynamic Data of Fluids	410
P8. ELECTRICITY AND ELECTROMAGNETISM	427
8.1. Electrostatics and Magnetostatics	427
8.2. DC Circuits	434
8.3. AC Circuits	439
8.4. Electrical Power Engineering	444
8.5. Optics, Electromagnetic Waves and Plasma Physics	451
8.6. Functional Materials and Solid State Physics	463
8.7. Semiconductor Devices and Transistor Circuits	497
P9. DIGITAL ELECTRONICS, INSTRUMENTATION AND CONTROL	509
9.1. Digital Electronics	509
9.2. Computer Engineering and Communications	515
9.3. Data Structures, Algorithms and Programming	529
9.4. Control Theory	545
P10. ASTROPHYSICS AND COSMOLOGY	570
10.1. Aerospace Engineering and Orbital Mechanics	570
10.2. Astronomy	576
10.3. Cosmology and Relativity	581
P11. NUCLEAR, QUANTUM AND MEDICAL PHYSICS	586
11.1. Quantum Physics and The Standard Model	586
11.2. Radioactivity and Nuclear Power Engineering	595
11.3. Acoustics and Medical Imaging	605

C12. CHEMICAL DATA AND STANDARDS	616
12.1. Practical Chemistry in the Laboratory	616
12.2. Chemical Data	621
12.3. General Nomenclature of Organic Compounds	631
C13. PHYSICAL CHEMISTRY	633
13.1. Atomic Structure and Quantum Chemistry	633
13.2. Crystallography and Solid State Chemistry	651
13.3. Theory of Kinetics, Energetics and Thermodynamics	670
13.4. Solutions and Heterogeneous Equilibria	683
13.5. Electrochemistry	697
13.6. Acid-Base Chemistry	721
C14. SURFACE AND PARTICLE CHEMISTRY	728
14.1. Catalysis	728
14.2. Separation Processes and Chemical Engineering	732
14.3. Colloids and Nanoparticle Chemistry	744
C15. INORGANIC AND ENVIRONMENTAL CHEMISTRY	754
15.1. Metallurgy	754
15.2. Earth Science, Geochemistry and Physical Geography	762
15.3. Reactions of Inorganic Compounds	775
15.4. Periodicity Trends	786
15.5. Coordination and Organometallic Chemistry	788
C16. ORGANIC AND BIOCHEMISTRY	803
16.1. Bonding and Forces in Organic Molecules	803
16.2. Structure of Organic Molecules	813
16.3. Synthetic Organic Chemistry	818
16.4. Analytical Methods in Chemistry and Molecular Biology	842
16.5. Polymers and Biochemistry	858

B17. MOLECULAR BIOLOGY	870
17.1. Cellular Biology and Metabolism	870
17.2. Genetics and Evolutionary Developmental Biology	880
17.3. Biomechanics	897
17.4. Biotechnology and Bioengineering	910
17.5. Systems Chemistry, Origin of Life and Astrobiology	930
B18. MICROBIOLOGY	937
18.1. Bacteria and Archaea	937
18.2. Virology and Parasitic Agents	941
18.3. Mycology	945
B19. ANIMALS AND PLANTS	946
19.1. Ecology and Evolutionary Biology	946
19.2. Botany and Agriculture	953
19.3. Zoology and Paleontology	960
19.4. Primatology, Paleoanthropology and Archaeology	962
B20. MEDICAL BIOLOGY	971
20.1. Immunology	971
20.2. Human Anatomy and Physiology	985
20.3. Pharmacology	993
20.4. Diseases	1002
20.5. Biopsychology, Health, Fitness and Nutrition	1006
20.6. Medical Physics, Biointerfaces and Bioelectronics	1022
L21. CHINESE (中文)	1025
21.1. Basics of Chinese	1025
21.2. Basic Vocabulary	1027
21.3. Themed Vocabulary	1032
21.4. Basic Grammar Points	1044
21.5. Sentences for Reference by Theme	1050
L22. KOREAN (한국어)	1054
22.1. Basics of Korean	1054

M1. ALGEBRA

1.1. Mathematical Syntax and Techniques

1.1.1. Symbols for Relationships and Operators

$x : y$	ratio of x to y , representing quantities $\frac{x}{x+y}$ and $\frac{y}{x+y}$
$\lfloor x \rfloor$	floor of x , $\max\{a \in \mathbb{Z} : a \leq x\}$, round down to integer towards $-\infty$
$\lceil x \rceil$	ceiling of x , $\min\{a \in \mathbb{Z} : a \geq x\}$, round up to integer towards $+\infty$
$\{x\}$	fractional part, $x - \lfloor x \rfloor$
$1.238\overline{307}$	recurring decimal, $1.238307307307307\dots$, or in dot notation $1.238\dot{3}0\dot{7}$
\equiv	is identical to; is congruent to
$:=$	is defined as
\therefore	therefore
\because	because
$P \Rightarrow Q$	P implies Q ; if P then Q ; Q is necessary for P , P is sufficient for Q
$P \Leftarrow Q$	P is implied by Q ; if Q then P ; P is necessary for Q , Q is sufficient for P
$P \Leftrightarrow Q$	P and Q are equivalent; P if and only if (iff) Q ; P is necessary and sufficient for Q
$f: A \mapsto B$	function mapping domain A to codomain B
\bar{y}	sample mean of y ; Laplace transform of $y(t)$ into s domain
\hat{y}	estimate of y ; least-squares solution y ; unit vector y
$f_X(x)$	probability density function (pdf) for random variable X , taking value x
$F_X(x)$	cumulative density function (cdf) for random variable X , taking value x
\cong	is isomorphic to; is geometrically congruent to
$\prod_{r=a}^b f(r)$	product over integers; $\prod_{r=a}^b f(r) = f(a) \times f(a+1) \times \dots \times f(b)$
$(f \circ g)(x)$	composition; $fg(x)$; $f(g(x))$
$(f * g)(t)$	convolution of $f(t)$ and $g(t)$
$(f \star g)(t)$	correlation of $f(t)$ and $g(t)$
$[\mathbf{a} \ \mathbf{b} \ \mathbf{c}]$	scalar triple product; $\mathbf{a} \cdot (\mathbf{b} \times \mathbf{c})$
$[a, b, c]$	row vector; $[a, b, c]^T$; alternative way of denoting vectors
$[a; b; c]$	column vector; $[a, b, c]^T$; most common conventional way of denoting vectors
\dot{x}, \ddot{x}	time derivatives of x ; $\frac{dx}{dt}, \frac{d^2x}{dt^2}$
$y^{(n)}(x)$	n th derivative of y with respect to x ; $\frac{d^n y}{dx^n}$
$f_{xy}(x, y)$	partial derivative; $\frac{\partial f}{\partial y \partial x} = \frac{\partial}{\partial y} \left(\frac{\partial f}{\partial x} \right)$
Δf	change in f ; Laplacian of multivariable function f ; $\nabla^2 f$
δf	small change in f

1.1.2. Symbols in Set Theory and Logic

\in	is an element of	$n(A)$	number of elements in A
\notin	is not an element of	\emptyset	the empty set
\subseteq	is a subset of	ξ	the universal set
\subset	is a proper subset of	\forall	for all
$\{x: \dots\}$	the set of all x such that ...	\exists	there exists
A'	complement of A	$A \setminus B$	the set A minus B
$A \cup B$	union of A and B	$A \cap B$	intersection of A and B
\mathbb{P}	prime numbers; $\{2, 3, 5, \dots\}$	\mathbb{Q}	rationals; $\{1, 2, 1/2, \dots\}$
\mathbb{N}	natural numbers; $n; \{1, 2, 3, \dots\}$	\mathbb{R}	reals; x
\mathbb{Z}	integers; $\{\dots, -2, -1, 0, 1, 2, \dots\}$	\mathbb{C}	complex numbers; $z = x + yi$
\mathbb{Z}^*	nonnegative integers; $\{0, 1, 2, \dots\}$	\mathbb{H}	quaternions; $q = w + xi + yj + zk$
\mathbb{R}^n	n -dimensional vectors; \mathbf{x}	$\mathbb{R}^{m \times n}$	$m \times n$ matrices; \mathbf{A}

Algebraic numbers are roots of real-valued polynomials with rational (or integer) coefficients. Transcendental numbers (e, π) are irrational numbers which are **not** algebraic.

Note that $\mathbb{P} \subset \mathbb{N} \subset \mathbb{Z} \subset \mathbb{R} \subset \mathbb{C} \subset \mathbb{H}$. Irrational numbers can be designated as $\mathbb{R} \setminus \mathbb{Q}$.

1.1.3. Greek Alphabet

A α	alpha <i>άλφα</i>	H η	eta <i>ήτα</i>	N ν	nu <i>νι</i>	T τ	tau <i>ταυ</i>
B β	beta <i>βήτα</i>	Θ θ, ϑ	theta <i>θήτα</i>	Ξ ξ	xi <i>ξι</i>	Υ υ	upsilon <i>ύψιλον</i>
Γ γ	gamma <i>γάμμα</i>	I ι	iota <i>ιώτα</i>	O o	omicron <i>όμικρον</i>	Φ φ, ϕ	phi <i>φεϊ</i>
Δ δ	delta <i>δέλτα</i>	K κ	kappa <i>κάπα</i>	Π π	pi <i>πι</i>	X χ	chi <i>χϊ</i>
E ϵ	epsilon <i>έψιλο</i>	Λ λ	lambda <i>λάμδα</i>	P ρ	rho <i>ρο</i>	Ψ ψ	psi <i>ψι</i>
Z ζ	zeta <i>ζήτα</i>	M μ	mu <i>μι</i>	Σ σ, ς	sigma <i>σίγμα</i>	Ω ω	omega <i>ωμέγα</i>

- The lowercase letters $\{\vartheta, \iota, o, \varsigma, \upsilon\}$ are typically not used as symbols in mathematics.
- The uppercase letters are typed upright. The lowercase letters are typed in *italic*.
- When using Latin letters ($A a$) as symbols, both uppercase and lowercase are typed *italic*.
- In LaTeX, the Greek letters can be written using e.g. `\gamma` (lower) or `\Gamma` (upper).

1.1.4. Functions

Domain:	the set of all x for which $f(x)$ is defined	
Codomain:	any set containing all the values of $f(x)$.	
Range:	the set containing only the values of $f(x)$, so $\text{range} \subseteq \text{codomain}$.	
Injective:	one-to-one; there is exactly one $f(x)$ for every x ;	$f(x) = f(y) \Leftrightarrow x = y$.
Surjective:	many-to-one; there is at least one x for every $f(x)$;	$f(x) = f(y) \Leftarrow x = y$.
Bijjective:	two-way one-to-one; both injective and surjective;	$y = f(x) \Leftrightarrow x = f^{-1}(y)$.
Involution:	a function whose inverse is identical to itself;	$f(f(x)) = x$
Idempotent:	a function whose nesting is an involution;	$f(f(x)) = f(x)$
Endofunction:	a function whose codomain is identical to its domain	

1.1.5. Rounding of Numbers

A number can be rounded to a given number of decimal places (d.p.) or significant figures (s.f.).

Examples:

- 309.51547 rounded to 2 d.p. is 309.52 (5 rounds up)
- 0.00194105 rounded to 2 s.f. is 0.0019 (leading zeroes are not significant)

When working with physical quantities with finite precision, the least number of available significant figures should be used to most fairly represent the quoted precision.

1.1.6. Standard Form of Numbers

Very large or very small numbers can be written in the form $x = a \times 10^n$

($1 \leq a < 10$: mantissa, integer n : exponent). This number is said to have order of magnitude 10^n .

Numbers in standard form can be added by converting both to the same exponent.

1.1.7. Factorisation of Numbers

A divisor q is a factor of a dividend p if the quotient $\frac{p}{q}$ is an integer (i.e. p is a multiple of q).

Prime factorisation: expressing a number uniquely as a product of powers of prime numbers. The different prime factorisation of two numbers can be represented as a Venn diagram.

Greatest Common Factor (GCF) of a and b : product of intersection of prime factors of a and a .

Lowest Common Multiple (LCM) of a and b : product of union of prime factors of a and b .

The GCF and LCM are related by $\text{lcm}(a, b) \times \text{gcd}(a, b) = |ab|$.

1.1.8. Power-Law and Exponential Relationships

Variables x and y may be related by nonlinear relationships such as:

Relationship	Equation	Inverse	Linearised form ($Y = MX + C$)	Linear plot
Power Law	$y = k x^n$	$x = \left(\frac{y}{k}\right)^{1/n}$	$\underbrace{\ln y}_Y = \underbrace{n}_M \underbrace{\ln x}_X + \underbrace{\ln k}_C$	$\ln y$ vs $\ln x$
Exponential	$y = k a^x$	$x = \log_a \left(\frac{y}{k}\right)$	$\underbrace{\ln y}_Y = \underbrace{(\ln a)}_M \underbrace{x}_X + \underbrace{\ln k}_C$	$\ln y$ vs x

1.1.9. Dimensional Analysis and Scaling

Dimensions of base SI physical quantities:: mass (**M**), length (**L**), time (**T**), temperature (**Θ**), moles (**N**), electric current (**I**) and luminous intensity (**J**).

The number of parameters in a problem is reduced by expressing the relationship in non-dimensional form. Quantities are $\{q\}_i$. Dimensionless groups are $\{\pi\}_i$.

Buckingham's π Theorem: For N variables containing M dimensions, the number of dimensionless groups is at least $N - M$.

For a physical equation $f(q_1, q_2, \dots, q_N) = 0$ or $q_1 = f(q_2, \dots, q_N)$, where f may be unknown, there exists an equivalent dimensionless formulation $F(\pi_1, \pi_2, \dots, \pi_M) = 0$ or $\pi_1 = F(\pi_2, \dots, \pi_M)$, where each dimensionless group can be expressed as a power law function of a subset of the physical quantities:

$$\pi_i = (q_1)^{a_{i1}} (q_2)^{a_{i2}} \dots (q_N)^{a_{iN}}$$

For problems with 1 dimensionless group, the simple indicial method can be used, in which $F(\pi) = 0 \rightarrow \pi = C$, some dimensionless constant. Find the powers $\{a\}_i$ such that the expression for π has no dimensions.

Geometric similarity: where all length-ratio dimensionless groups are identical.

Dynamic similarity: where all independent dimensionless groups are identical.

Example with two dimensionless groups: power required to stir a fluid

($[P] = \mathbf{ML}^2\mathbf{T}^{-3}$: power, $[\rho] = \mathbf{ML}^{-3}$: density, $[\mu] = \mathbf{ML}^{-1}\mathbf{T}^{-1}$: viscosity, $[d] = \mathbf{L}$: diameter, $[\omega] = \mathbf{T}^{-1}$: angular speed)

$P = f(\rho, \mu, d, \omega)$: 5 quantities in 3 dimensions \rightarrow at least 2 dimensionless groups (1 dependent, at least 1 independent).

Typical dimensionless groups: $\frac{P}{\rho \omega^3 d^5} = F\left(\frac{\rho \omega d^2}{\mu}\right) \rightarrow$ graphing $\frac{P}{\rho \omega^3 d^5}$ vs $\frac{\rho \omega d^2}{\mu}$ specifies the relationship fully.

1.2. Algebraic Identities

1.2.1. Factorisation and Common Algebraic Manipulations

Factorisation

Difference of two squares:	$a^2 - b^2 = (a + b)(a - b)$
Sum of two squares (complex):	$a^2 + b^2 = (a + ib)(a - ib)$
Differences of two cubes:	$a^3 - b^3 = (a - b)(a^2 + ab + b^2)$
Sum of two cubes:	$a^3 + b^3 = (a + b)(a^2 - ab + b^2)$
Sum of two fourth-powers:	$a^4 + b^4 = (a^2 + \sqrt{2}ab + b^2)(a^2 - \sqrt{2}ab + b^2)$
Difference of two fourth-powers:	$a^4 - b^4 = (a^2 + b^2)(a + b)(a - b)$
Sophie-Germain identity:	$a^4 + 4b^4 = (a^2 + 2b^2 + 2ab)(a^2 + 2b^2 - 2ab)$

Expansion: derived by 'FOIL (first-outer-inner-last)'

$$(a + b)^2 = a^2 + 2ab + b^2 = (a - b)^2 + 4ab$$

$$(a + b)^3 = a^3 + 3a^2b + 3ab^2 + b^3$$

$$(a + b + c)^2 = a^2 + b^2 + c^2 + 2(ab + bc + ca)$$

$$(a + b + c)^3 = a^3 + b^3 + c^3 + 3(a^2b + a^2c + b^2a + b^2c + c^2a + c^2b) + 6abc$$

Completing the Square:
$$x^2 + bx + c = \left(x + \frac{b}{2}\right)^2 + \left(c - \frac{b^2}{4}\right)$$

Girard-Newton Identities: if $S = \{\alpha, \beta, \gamma, \dots\}$ are a set of K variables then

- $\sum \alpha^2 = (\sum \alpha)^2 - \sum \alpha\beta$
- $\sum \alpha^3 = (\sum \alpha)^3 - 3(\sum \alpha)(\sum \alpha\beta) + \sum \alpha\beta\gamma$
- $\sum \alpha^n = (\sum \alpha)\sum \alpha^{n-1} - (\sum \alpha\beta)\sum \alpha^{n-2} + (\sum \alpha\beta\gamma)\sum \alpha^{n-3} - \dots$

where sums over non-repeated combinations are $\sum \alpha = \alpha + \beta + \gamma + \dots$, $\sum \alpha\beta = \alpha\beta + \beta\gamma + \gamma\alpha + \dots$

These are commonly applied to roots of polynomials (see Vieta's formulas, Section 1.2.5).

If $K > n$ then the $\sum \alpha^{n-i}$ term will include terms such as $\sum \frac{1}{\alpha}$, $\sum \frac{1}{\alpha^2}$, etc. These can be

solved for by substituting previously found expressions recursively. The sum terminates with the $(-1)^{K-1} (\prod \alpha) (\sum \alpha^{n-K})$ term.

Componendo-Dividendo identities (corollaries of cross-multiplication):

If $\frac{a}{b} = \frac{c}{d}$, then $ad = bc$, $\frac{a+b}{b} = \frac{c+d}{d}$, $\frac{a-b}{b} = \frac{c-d}{d}$ and $\frac{a+b}{a-b} = \frac{c+d}{c-d}$.

1.2.2. Binomial Theorem and Trinomial Theorem

For any positive integer n , the binomial and trinomial theorems are, respectively,

$$(a + b)^n = \sum_{r=0}^n {}^n C_r a^r b^{n-r}$$

$$\text{where } {}^n C_r = \frac{n!}{r!(n-r)!}$$

$$(a + b + c)^n = \sum_{m=0}^n \sum_{k=0}^m {}^n C_m {}^m C_k a^{n-m} b^{m-k} c^k$$

$$\text{where } {}^n C_m {}^m C_k = \frac{n!}{(n-m)!(m-k)!k!}$$

1.2.3. Properties of Quadratic Polynomials

If $f(x) = ax^2 + bx + c$ then:

(the quadratic formula)

The turning point of $f(x)$ is at $x = -\frac{b}{2a}$. The roots of $f(x)$ are at $x = \frac{-b \pm \sqrt{b^2 - 4ac}}{2a}$.

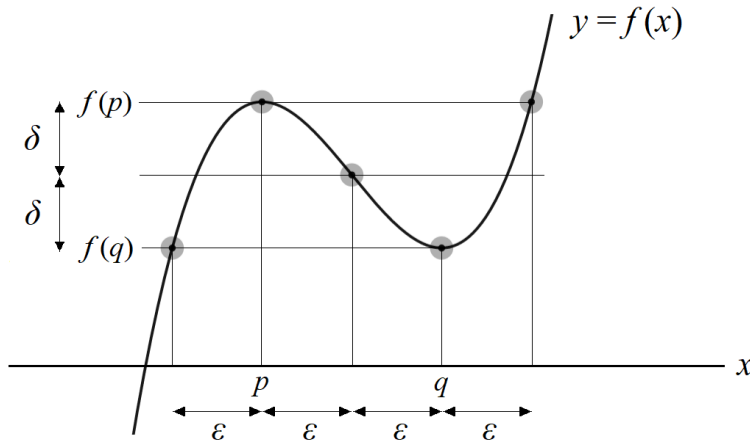
For real coefficients, the discriminant, $\Delta = b^2 - 4ac$, determines the nature of the roots:

- If $\Delta > 0 \rightarrow$ two distinct real roots.
- If $\Delta < 0 \rightarrow$ two complex roots (complex conjugates).
- If $\Delta = 0 \rightarrow$ a single repeated real root.

1.2.4. Properties of Cubic Polynomials

For a cubic $f(x) = ax^3 + bx^2 + cx + d$, it can be transformed to a ‘depressed cubic’ using the substitution $x = t - \frac{b}{3a}$ into $f(t) = t^3 + pt + q$ where $p = \frac{3ac - b^2}{3a^2}$ and $q = \frac{2b^3 - 9abc + 27a^2d}{27a^3}$.

The inflection point of $f(x)$ is at $x = -\frac{b}{3a}$ i.e. $t = 0$.



The graph of $f(x)$ will have real turning points if $b^2 - 3ac > 0$.

In this case, there is rotational symmetry order 2 about the inflection point, with the lengths shown being

$$\epsilon = \frac{\sqrt{b^2 - 3ac}}{3a} \quad \delta = 2a \epsilon^3$$

For real coefficients, the discriminant is, $\Delta = \frac{4(b^2 - 3ac)^3 - (2b^3 - 9abc + 27a^2d)^2}{27a^2} = \frac{p^3}{27} + \frac{q^2}{4}$.

- If $\Delta > 0 \rightarrow$ three distinct real roots;
- If $\Delta < 0 \rightarrow$ one real root and two complex conjugate roots;
- If $\Delta = 0 \rightarrow$ a repeated root of multiplicity 2 or 3.

The transformed roots of $f(t) = 0$ are $t_1 = \sqrt[3]{-\frac{q}{2} + \Delta} + \sqrt[3]{-\frac{q}{2} - \Delta}$,

$$t_2 = \omega \sqrt[3]{-\frac{q}{2} + \Delta} + \omega^2 \sqrt[3]{-\frac{q}{2} - \Delta} \text{ and } t_3 = \omega^2 \sqrt[3]{-\frac{q}{2} + \Delta} + \omega \sqrt[3]{-\frac{q}{2} - \Delta}$$

where $x_i = t_i - \frac{b}{3a}$ and ω is a primitive cube root of unity:

$$\omega = \frac{-1 + i\sqrt{3}}{2}, \quad \omega^2 = \frac{-1 - i\sqrt{3}}{2}, \quad \omega^3 = 1$$

1.2.5. Relations Between Roots of Polynomials

For a polynomial $P(x)$ of degree n given by

$$P(x) = \sum_{r=0}^n a_r x^r = a_n x^n + a_{n-1} x^{n-1} + a_{n-2} x^{n-2} + \dots + a_1 x + a_0$$

the n roots of the equation $P(x) = 0$, denoted $\alpha_1, \alpha_2, \dots, \alpha_n$, are related by:

- Fundamental theorem of algebra: all α are complex, and number of roots = degree.
- Factor theorem: $P(x) = a_n(x - \alpha_1)(x - \alpha_2)\dots(x - \alpha_n)$
- Rational root theorem: $\alpha = \frac{p}{q} \in \mathbb{Q} \Rightarrow |p|$ is a factor of a_0 and $|q|$ is a factor of a_n
- Vieta formulas:

$$\begin{array}{cccc} \Sigma \alpha = -\frac{a_{n-1}}{a_n} & \Sigma \alpha\beta = \frac{a_{n-2}}{a_n} & \Sigma \alpha\beta\gamma = -\frac{a_{n-3}}{a_n} & \Pi \alpha = (-1)^n \frac{a_0}{a_n} \\ \text{(sum of roots)} & \text{(sum of product pairs)} & \text{(sum of product triplets)} & \text{(product of roots)} \end{array}$$

- Conjugacy:
 - (1) if all a_r are real and $\alpha_1 = u + iv$ is a root then $\alpha_2 = \alpha_1^* = u - iv$ is also a root.
 - (2) if all a_r are rational and $\alpha_1 = u \pm \sqrt{v}$ is an irrational root then $\alpha_2 = u \mp \sqrt{v}$ is also a root.

For a monic polynomial (monocubic, monoquartic, etc), $a_n = 1$, so these formulas simplify.

1.2.6. Division of Polynomials

Polynomials can be divided into the form $\frac{A(x)}{B(x)} = Q(x) + \frac{R(x)}{B(x)}$.

(A : dividend, B : divisor (same or higher degree than A), Q : quotient, R : remainder, deg: degree of)

- $\deg A \geq \deg B$
- $\deg Q = \deg A - \deg B$
- $\deg R < \deg B$

Factorisation: $R = 0$ iff B divides A i.e. B is a factor of A .

Techniques: examples to evaluate $\frac{x^3 - 2x^2 - 4}{x - 3} = x^2 + x + 3 + \frac{5}{x - 3}$:

<p>Polynomial Long Division</p> $ \begin{array}{r} \overline{) x^3 - 2x^2 + 0x - 4} \\ \underline{- x^3 + 3x^2} \\ x^2 + 0x - 4 \\ \underline{- x^2 + 3x} \\ 3x - 4 \\ \underline{- 3x + 9} \\ 5 \end{array} $	<p>Synthetic Division (requires $B = x - a$)</p> $ \begin{array}{r} \overline{) 1 \quad -2 \quad 0 \quad -4} \\ \underline{3 \quad 3 \quad 9} \\ 1 \quad 1 \quad 3 \quad 5 \end{array} $
--	---

If it is known that $R = 0$ beforehand, then an alternative method is to equate coefficients with a general polynomial e.g. $Q(x) = ax^2 + bx + c$, solving for each a , b and c .

1.2.7. Divisibility Rules for Integers

A positive integer n is divisible by...

- | | |
|---|--|
| <ul style="list-style-type: none"> • 2, if the last digit is even • 3, if the sum of the digits is divisible by 3 • 4, if the last two digits form a number divisible by 4 • 5, if the last digit is 5 or 0 | <ul style="list-style-type: none"> • 6, if the number is divisible by both 2 and 3 • 7, if subtracting twice the last digit from the rest of the number gives a multiple of 7 • 8, if the last three digits form a number divisible by 8 • 9, if the sum of the digits is divisible by 9 |
|---|--|

These results can be derived from modular arithmetic.

1.2.8. The Triangle Inequality

For any real or complex numbers a, b : $|a + b| \leq |a| + |b|$

This is also valid for any vectors \mathbf{a} and \mathbf{b} : $|\mathbf{a} + \mathbf{b}| \leq |\mathbf{a}| + |\mathbf{b}|$

The Inverse Triangle Inequality: $|a - b| \geq ||a| - |b||$

$$|\mathbf{a} - \mathbf{b}| \geq ||\mathbf{a}| - |\mathbf{b}||$$

1.2.9. The Cauchy-Schwarz Inequality

For any n -dimensional vectors \mathbf{u} and \mathbf{v} : $\left(\sum_{i=1}^n u_i v_i \right)^2 \leq \left(\sum_{i=1}^n u_i^2 \right) \left(\sum_{i=1}^n v_i^2 \right)$

For $n = 2$, this can be stated as $(ac + bd)^2 \leq (a^2 + b^2)(c^2 + d^2)$

1.2.10. The Harmonic-Geometric-Arithmetic-Quadratic Mean Inequalities

For any real-valued set of n positive variables x with i th variable x_i :

$$0 < \frac{n}{\sum_{i=1}^n \frac{1}{x_i}} \leq \sqrt[n]{\prod_{i=1}^n x_i} \leq \frac{1}{n} \sum_{i=1}^n x_i \leq \sqrt{\frac{1}{n} \sum_{i=1}^n x_i^2}$$

$$\text{HM} \leq \text{GM} \leq \text{AM} \leq \text{QM}$$

For $n = 2$, this can be stated as: given $a, b > 0$, we have

$$\frac{2ab}{a+b} \leq \sqrt{ab} \leq \frac{a+b}{2} \leq \sqrt{\frac{a^2+b^2}{2}} \quad \text{or} \quad \frac{8a^2b^2}{(a+b)^2} \leq 2ab \leq \frac{1}{2}(a+b)^2 \leq a^2 + b^2$$

Weighted AM-GM inequality: $\frac{x_1 y_1 + x_2 y_2 + \dots + x_n y_n}{x_1 + x_2 + \dots + x_n} \geq \left(y_1^{x_1} y_2^{x_2} \dots y_n^{x_n} \right)^{\frac{1}{x_1 + x_2 + \dots + x_n}}$

1.2.11. Muirhead's Inequality

For two N -length sequences $\{a_i\}$ and $\{b_i\}$, the notation $\{a_i\} \succ \{b_i\}$ means that $\{a_i\}$ 'majorises' $\{b_i\}$, which is defined by

$$\sum_{i=1}^n a_i \geq \sum_{i=1}^n b_i \quad \forall n \in [1, \dots, N] \quad \text{and} \quad \sum_{i=1}^N a_i = \sum_{i=1}^N b_i \quad \Leftrightarrow \quad \{a_i\} \succ \{b_i\}.$$

Muirhead's inequality: if $\{a_i\} \succ \{b_i\}$ then $\sum_{\text{sym } x} x_1^{a_1} x_2^{a_2} \dots x_N^{a_N} \geq \sum_{\text{sym } x} x_1^{b_1} x_2^{b_2} \dots x_N^{b_N}$

where the sum is over all permutations of any chosen set of variables.

Example: the sequence (5, 1) majorises (4, 2). Therefore $x^5 y + xy^5 \geq x^4 y^2 + x^2 y^4$.

1.2.12. Schur's Inequality

For all real a, b, c and all $r > 0$,

$$a^r(a-b)(a-c) + b^r(b-a)(b-c) + c^r(c-a)(c-b) \geq 0.$$

Case $r=1$: $a^3 + b^3 + c^3 + 3abc \geq a^2b + a^2c + b^2a + b^2c + c^2a + c^2b$

Case $r=2$: $a^4 + b^4 + c^4 + abc(a+b+c) \geq a^3b + a^3c + b^3a + b^3c + c^3a + c^3b$

Generalisation: for all real a, b, c, x, y, z , where $a \geq b \geq c$ and $(x \geq y \geq z \text{ or } z \geq y \geq x)$, and some convex or monotonic function $f: \mathbb{R} \rightarrow \mathbb{R}^+$, and some constant $k \in \mathbb{Z}^+$,

$$f(x)(a-b)^k(a-c)^k + f(y)(b-a)^k(b-c)^k + f(z)(c-a)^k(c-b)^k \geq 0.$$

1.2.13. Jordan's Inequality

For all $0 \leq x \leq \frac{\pi}{2}$, we have $\frac{2}{\pi}x \leq \sin x \leq x$ i.e. $\frac{2}{\pi} \leq \text{sinc } x \leq 1$

1.2.14. Fermat's Last Theorem

If $n \geq 3$, then there are no positive integer solutions (a, b, c) to the equation $a^n + b^n = c^n$.

(The case of $n=2$ has infinitely many solutions - the Pythagorean triples.)

1.2.15. Diophantine Equations

The linear Diophantine equation $ax + by = c$ has integer solutions (x, y) iff (a, b, c) are all integers and $c \mid \gcd(a, b)$. If (x, y) is a solution then the other solutions are given by $(x + kv, y - ku)$ where k is an arbitrary integer, and $u = a / \gcd(a, b)$ and $v = b / \gcd(a, b)$.

Proofs on the solutions to Diophantine equations typically include:

- Chinese Remainder Theorem (CRT): see Section 1.6.5.
- Infinite descent: assume a supposedly minimal solution exists, show this implies the existence of a smaller solution, which is a contradiction (similar: Vieta jumping)

1.3. Trigonometric Identities

1.3.1. Trigonometric Functions and Identities

$$\sin(x + y) = \sin x \cos y + \cos x \sin y$$

$$\sin(x - y) = \sin x \cos y - \cos x \sin y$$

$$\cos(x + y) = \cos x \cos y - \sin x \sin y$$

$$\cos(x - y) = \cos x \cos y + \sin x \sin y$$

$$\tan(x + y) = \frac{\tan x + \tan y}{1 - \tan x \tan y}$$

$$\tan(x - y) = \frac{\tan x - \tan y}{1 + \tan x \tan y}$$

$$\sin 2x = 2 \sin x \cos x$$

$$\sin 3x = 3 \sin x - 4 \sin^3 x$$

$$\sin \frac{x}{2} = \pm \sqrt{\frac{1 - \cos x}{2}}$$

$$\cos 2x = 2 \cos^2 x - 1$$

$$\cos 3x = 4 \cos^3 x - 3 \cos x$$

$$\cos \frac{x}{2} = \pm \sqrt{\frac{1 + \cos x}{2}}$$

$$= 1 - 2 \sin^2 x$$

$$= \cos^2 x - \sin^2 x$$

$$\tan 2x = \frac{2 \tan x}{1 - \tan^2 x}$$

$$\tan 3x = \frac{3 \tan x - \tan^3 x}{1 - 3 \tan^2 x}$$

$$\tan \frac{x}{2} = \pm \sqrt{\frac{1 - \cos x}{1 + \cos x}}$$

$$= \frac{\sin x}{1 + \cos x} = \frac{1 - \cos x}{\sin x}$$

$$\sec x = \frac{1}{\cos x}$$

$$\csc x = \frac{1}{\sin x}$$

$$\cot x = \frac{1}{\tan x}$$

$$\sin^2 x + \cos^2 x = 1$$

$$\sec^2 x = 1 + \tan^2 x$$

$$\csc^2 x = 1 + \cot^2 x$$

$$\sin(-x) = -\sin x$$

$$\cos(-x) = \cos x$$

$$\tan(-x) = -\tan x$$

$$\sin\left(\frac{\pi}{2} - x\right) = \cos x$$

$$\cos\left(\frac{\pi}{2} - x\right) = \sin x$$

$$\tan\left(\frac{\pi}{2} - x\right) = \cot x$$

$$\sin(\pi - x) = \sin x$$

$$\cos(\pi - x) = -\cos x$$

$$\tan(\pi - x) = -\tan x$$

$$\sin\left(x + \frac{\pi}{2}\right) = \cos x$$

$$\cos\left(x + \frac{\pi}{2}\right) = -\sin x$$

$$\tan\left(x + \frac{\pi}{2}\right) = \tan x$$

$$\sin(x + \pi) = -\sin x$$

$$\cos(x + \pi) = -\cos x$$

$$\tan(x + \pi) = \tan x$$

$$\sin x + \sin y = 2 \sin \frac{x+y}{2} \cos \frac{x-y}{2}$$

$$\sin x - \sin y = 2 \cos \frac{x+y}{2} \sin \frac{x-y}{2}$$

$$\cos x + \cos y = 2 \cos \frac{x+y}{2} \cos \frac{x-y}{2}$$

$$\cos x - \cos y = -2 \sin \frac{x+y}{2} \sin \frac{x-y}{2}$$

$$2 \sin x \sin y = \cos(x - y) - \cos(x + y)$$

$$2 \cos x \cos y = \cos(x + y) + \cos(x - y)$$

$$2 \sin x \cos y = \sin(x + y) + \sin(x - y)$$

1.3.2. Hyperbolic Functions and Identities

$$\sinh x = \frac{1}{2}(e^x - e^{-x})$$

$$\cosh x = \frac{1}{2}(e^x + e^{-x})$$

$$\tanh x = \frac{e^x - e^{-x}}{e^x + e^{-x}}$$

$$\operatorname{csch} x = \frac{1}{\sinh x}$$

$$\operatorname{sech} x = \frac{1}{\cosh x}$$

$$\operatorname{coth} x = \frac{1}{\tanh x}$$

$$\sinh(x + y) = \sinh x \cosh y + \cosh x \sinh y$$

$$\sinh(x - y) = \sinh x \cosh y - \cosh x \sinh y$$

$$\cosh(x + y) = \cosh x \cosh y + \sinh x \sinh y$$

$$\cosh(x - y) = \cosh x \cosh y - \sinh x \sinh y$$

$$\tanh(x + y) = \frac{\tanh x + \tanh y}{1 + \tanh x \tanh y}$$

$$\tanh(x - y) = \frac{\tanh x - \tanh y}{1 - \tanh x \tanh y}$$

$$\sinh 2x = 2 \sinh x \cosh x$$

$$\sinh 3x = 3 \sinh x + 4 \sinh^3 x$$

$$\sinh \frac{x}{2} = \pm \sqrt{\frac{\cosh x - 1}{2}}$$

$$\cosh 2x = 2 \cosh^2 x - 1$$

$$\cosh 3x = 4 \cosh^3 x - 3 \cosh x$$

$$\cosh \frac{x}{2} = \sqrt{\frac{\cosh x + 1}{2}}$$

$$= 1 + 2 \sinh^2 x$$

$$= \cosh^2 x + \sinh^2 x$$

$$\tanh 2x = \frac{2 \tanh x}{1 + \tanh^2 x}$$

$$\tanh 3x = \frac{3 \tanh x - \tanh^3 x}{1 - 3 \tanh^2 x}$$

$$\tanh \frac{x}{2} = \pm \sqrt{\frac{\cosh x - 1}{\cosh x + 1}}$$

$$= \frac{\sinh x}{1 + \cosh x}$$

$$= \frac{\cosh x - 1}{\sinh x}$$

$$\operatorname{sech} x = \frac{1}{\cosh x}$$

$$\operatorname{csch} x = \frac{1}{\sinh x}$$

$$\operatorname{coth} x = \frac{1}{\tanh x}$$

$$\cosh^2 x - \sinh^2 x = 1$$

$$\operatorname{sech}^2 x = 1 - \tanh^2 x$$

$$\operatorname{coth}^2 x - \operatorname{csch}^2 x = 1$$

$$\sinh(-x) = -\sinh x$$

$$\cosh(-x) = \cosh x$$

$$\tanh(-x) = -\tanh x$$

$$\sinh x + \sinh y = 2 \sinh \frac{x+y}{2} \cosh \frac{x-y}{2}$$

$$\sinh x - \sinh y = 2 \cosh \frac{x+y}{2} \sinh \frac{x-y}{2}$$

$$\cosh x + \cosh y = 2 \cosh \frac{x+y}{2} \cosh \frac{x-y}{2}$$

$$\cosh x - \cosh y = -2 \sinh \frac{x+y}{2} \sinh \frac{x-y}{2}$$

$$2 \sinh x \sinh y = \cosh(x+y) - \cosh(x-y)$$

$$2 \cosh x \cosh y = \cosh(x+y) + \cosh(x-y)$$

$$2 \sinh x \cosh y = \sinh(x+y) + \sinh(x-y)$$

Osborn's Rule: for a trig identity, for a product of sines, change the sign, to get the hyperbolic identity.

1.3.3. Inverse Trigonometric Functions

$$\sec^{-1} x = \cos^{-1} \frac{1}{x}$$

$$\csc^{-1} x = \sin^{-1} \frac{1}{x}$$

$$\cot^{-1} x = \tan^{-1} \frac{1}{x}$$

$$\sin^{-1} x + \cos^{-1} x = \frac{\pi}{2}$$

$$\tan^{-1} x + \cot^{-1} x = \frac{\pi}{2}$$

$$\sec^{-1} x + \csc^{-1} x = \frac{\pi}{2}$$

$$\sin^{-1} x \pm \sin^{-1} y = \sin^{-1} \left(x\sqrt{1-y^2} \pm y\sqrt{1-x^2} \right)$$

$$\cos^{-1} x \pm \cos^{-1} y = \cos^{-1} \left(xy \mp \sqrt{1-x^2}\sqrt{1-y^2} \right)$$

$$\sin^{-1} x \pm \cos^{-1} y = \sin^{-1} \left(xy \pm \sqrt{1-x^2}\sqrt{1-y^2} \right) = \cos^{-1} \left(y\sqrt{1-x^2} \mp x\sqrt{1-y^2} \right)$$

$$\tan^{-1} x \pm \tan^{-1} y = \tan^{-1} \left(\frac{x \pm y}{1 \mp xy} \right)$$

1.3.4. Inverse Hyperbolic Functions

$$\sinh^{-1} x = \ln(x + \sqrt{x^2 + 1})$$

$$\cosh^{-1} x = \ln(x + \sqrt{x^2 - 1})$$

$$\tanh^{-1} x = \frac{1}{2} \ln \frac{1+x}{1-x}$$

$$\operatorname{csch}^{-1} x = \sinh^{-1} \frac{1}{x}$$

$$\operatorname{sech}^{-1} x = \cosh^{-1} \frac{1}{x}$$

$$\operatorname{coth}^{-1} x = \tanh^{-1} \frac{1}{x}$$

$$\sinh^{-1} x \pm \sinh^{-1} y = \sinh^{-1} \left(x\sqrt{1+y^2} \pm y\sqrt{1+x^2} \right)$$

$$\cosh^{-1} x \pm \cosh^{-1} y = \cosh^{-1} \left(xy \pm \sqrt{x^2-1}\sqrt{y^2-1} \right)$$

$$\sinh^{-1} x + \cosh^{-1} y = \sinh^{-1} \left(xy + \sqrt{1-x^2}\sqrt{y^2-1} \right) = \cosh^{-1} \left(y\sqrt{1+x^2} + x\sqrt{y^2-1} \right)$$

$$\tanh^{-1} x \pm \tanh^{-1} y = \tanh^{-1} \left(\frac{x \pm y}{1 \pm xy} \right)$$

1.4. Sequences and Series

1.4.1. Arithmetic Sequence

For an arithmetic sequence with first term a and common difference d , terms are

$$a, a + d, a + 2d, a + 3d, \dots$$

n th term: $u_n = a + (n - 1)d$

n th partial sum: $S_n = \sum_{r=1}^n u_n = \frac{n}{2}(2a + (n - 1)d)$

1.4.2. Geometric Sequence

For a geometric sequence with first term a and common ratio r , terms are

$$a, ar, ar^2, ar^3, \dots$$

n th term: $u_n = ar^{n-1}$

n th partial sum: $S_n = \sum_{r=1}^n u_n = \frac{a(1 - r^n)}{1 - r}$

Infinite sum: $S_\infty = \sum_{r=1}^{\infty} u_n = \frac{a}{1 - r}$ convergent if $0 < |r| < 1$

1.4.3. Harmonic Sequence

In a harmonic sequence, terms are the reciprocal of an arithmetic sequence.

$$\frac{1}{a}, \frac{1}{a + d}, \frac{1}{a + 2d}, \frac{1}{a + 3d}, \dots$$

n th term: $u_n = \frac{1}{a + (n - 1)d}$

n th partial sum: $S_n = \sum_{r=1}^n u_n \leq \ln(a + (n - 1)d) + \gamma + \frac{1}{2(a + (n - 1)d)}$

Infinite sum: diverges, always

1.4.4. Arithmetico-Geometric Sequence

In an arithmetico-geometric sequence, terms are a product of an arithmetic and geometric sequence.

$$ab, (a + d)br, (a + 2d)br^2, (a + 3d)br^3, \dots$$

*n*th term: $u_n = (a + (n - 1)d)br^{n-1}$

*n*th partial sum: $S_n = \sum_{r=1}^n u_r = \frac{ab - (a + nd)br^n}{1 - r} + \frac{dbr(1 - r^n)}{(1 - r)^2}$

Infinite sum: $S_\infty = \sum_{r=1}^\infty u_r = \frac{ab}{1 - r} + \frac{dbr}{(1 - r)^2}$ convergent if $|r| < 1$

1.4.5. Partial Sums of Series

$$\sum_{r=1}^n r = \frac{1}{2}n(n + 1) \qquad \sum_{r=1}^n r^2 = \frac{1}{6}n(n + 1)(2n + 1) \qquad \sum_{r=1}^n r^3 = \frac{1}{4}n^2(n + 1)^2$$

$$\sum_{r=1}^n \frac{1}{r} \geq \ln n + \gamma + O(n^{-1}) \quad \text{where } \gamma = 0.5772156649\dots \text{ is the Euler-Mascheroni constant.}$$

$$\sum_{r=0}^n {}^nC_r = 2^n \qquad \sum_{r=0}^n {}^pC_r \times {}^qC_{n-r} = {}^{p+q}C_n \qquad \text{(Chu-Vandermonde identity)}$$

$$\sum_{r=1}^n \cos r\theta = \frac{\sin \frac{n\theta}{2} \cos \frac{(n+1)\theta}{2}}{\sin \frac{\theta}{2}} \qquad \sum_{r=1}^n \sin r\theta = \frac{\sin \frac{n\theta}{2} \sin \frac{(n+1)\theta}{2}}{\sin \frac{\theta}{2}} \qquad \text{Often useful: } u_n = S_n - S_{n-1}.$$

1.4.6. Infinite Sums of Series

The numerical results below require advanced techniques to prove (e.g. special functions).

$$\sum_{r=1}^\infty \frac{1}{r} \text{ diverges} \qquad \sum_{r=1}^\infty \frac{1}{r^2} = \frac{\pi^2}{6} \qquad \sum_{r=1}^\infty \frac{1}{r^3} = \zeta(3) \approx 1.2021 \qquad \sum_{r=1}^\infty \frac{1}{r^4} = \frac{\pi^4}{90}$$

$$\sum_{r=1}^\infty \frac{(-1)^{r+1}}{r} = \ln 2 \qquad \sum_{r=1}^\infty \frac{(-1)^{r+1}}{r^2} = \frac{\pi^2}{12} \qquad \sum_{r=1}^\infty \frac{(-1)^{r+1}}{r^3} = \frac{3}{4}\zeta(3) \approx 0.90154 \qquad \sum_{r=1}^\infty \frac{(-1)^{r+1}}{r^4} = \frac{7\pi^4}{720}$$

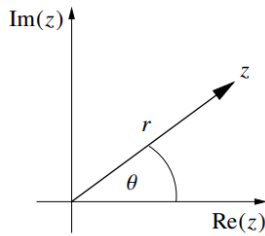
$$\sum_{r=-\infty}^\infty \frac{1}{a + br} = \frac{\pi}{b} \cot \frac{\pi a}{b} \qquad \sum_{r=-\infty}^\infty \frac{1}{a + br^2} = \frac{\pi}{\sqrt{ab}} \coth \pi \sqrt{\frac{a}{b}} \qquad \sum_{r=0}^\infty \frac{1}{1 + r^2} = \frac{1 + \pi \coth \pi}{2}$$

1.4.7. Common Techniques (Tests) for Proving Convergence or Divergence of Series

- **Divergence Test:** for $\sum_{n=1}^{\infty} a_n$, evaluate $\lim_{n \rightarrow \infty} a_n$.
 If $\lim_{n \rightarrow \infty} a_n \neq 0$ then the series **diverges**. Otherwise, inconclusive.
- **Geometric Series:** for $\sum_{n=1}^{\infty} a r^{n-1}$, evaluate r .
 If $|r| < 1$ then the series **converges** to $\frac{a}{1-r}$. Otherwise the series **diverges**.
- **Power Series:** for $\sum_{n=1}^{\infty} \frac{1}{n^p}$, evaluate p .
 If $p > 1$ then the series **converges** to $\zeta(p)$. Otherwise the series **diverges** (in the usual sense).
- **Comparison Test:** for $\sum_{n=1}^{\infty} a_n$ with all $a_n \geq 0$, compare to a known series $\sum_{n=1}^{\infty} b_n$.
 If there exists some N such that $a_n \leq b_n$ i.e. $\frac{a_n}{b_n} \leq 1$ for all $n > N$, and $\sum_{n=1}^{\infty} b_n$ converges then the series **converges**. Otherwise the series **diverges**.
- **Limit Comparison Test:** for $\sum_{n=1}^{\infty} a_n$ (all $a_n > 0$), compare to known $\sum_{n=1}^{\infty} b_n$ and evaluate $L = \lim_{n \rightarrow \infty} \frac{a_n}{b_n}$.
 If L is finite and nonzero then $\sum_{n=1}^{\infty} a_n$ and $\sum_{n=1}^{\infty} b_n$ either both converge or both diverge.
 If $L = 0$ and $\sum_{n=1}^{\infty} b_n$ converges then the series **converges**.
 If $L \rightarrow \infty$ and $\sum_{n=1}^{\infty} b_n$ diverges then the series **diverges**.
- **Integral Test:** for $\sum_{n=1}^{\infty} a_n$, if $f(n) = a_n$ is positive and decreasing for all $n > N$, evaluate $I = \int_N^{\infty} f(x) dx$.
 If I is finite then the series **converges**. If I diverges then the series **diverges**.
- **Alternating Series Test:** for $\sum_{n=1}^{\infty} (-1)^n a_n$, if $a_{n+1} \leq a_n$ for all $n \geq 1$ and $\lim_{n \rightarrow \infty} a_n = 0$ then the series **converges**.
- **Ratio Test and Root Test:** for any $\sum_{n=1}^{\infty} a_n$, evaluate either $\rho = \lim_{n \rightarrow \infty} \left| \frac{a_{n+1}}{a_n} \right|$ or $\rho = \lim_{n \rightarrow \infty} |a_n|^{1/n}$.
 If $0 \leq \rho < 1$ then the series **converges**. If $\rho > 1$ then the series **diverges**. If $\rho = 1$ then inconclusive.

1.5. Complex Numbers

1.5.1. Complex Number Definition



Any complex number $z \in \mathbb{C}$ can be represented as
 $z = x + yi = r(\cos \theta + i \sin \theta) = r e^{i\theta} = r \text{cis } \theta$ (Euler's formula)

The components are related and defined by
 $x = \text{Re}(z); y = \text{Im}(z); r = |z|; \theta = \arg z; -\pi < \theta \leq \pi$
 (r : magnitude, θ : argument/phase, x : real part, y : imaginary part)

1.5.2. Complex Conjugate

$$z^* = x - iy = r e^{-i\theta} = r \text{cis}(-\theta)$$

$$zz^* = |z|^2 \text{ is purely real}$$

$$(z_1 + z_2)^* = z_1^* + z_2^*$$

$$(z_1 z_2)^* = z_1^* z_2^*$$

$$\left(\frac{z_1}{z_2}\right)^* = \frac{z_1^*}{z_2^*}$$

1.5.3. Cyclic Nature of Exponentials and Logarithms

- Periodicity: $e^{2\pi ni} = 1, z = r e^{i(\theta + 2\pi n)}$, for any integer n
- De Moivre's theorem: $z = e^{i\theta} \rightarrow z^a = (\cos \theta + i \sin \theta)^a = \exp(ia(\theta + 2\pi n)) = \cos a\theta + i \sin a\theta$
- Natural logarithm: $z = r e^{i\theta} \rightarrow \ln z = \ln r + i(\theta + 2\pi n)$
- n th roots of unity: $\omega_k = e^{i \frac{2\pi k}{n}}, \omega_k^n = 1, \omega_{k+n} = \omega_k, \omega_1^k = \omega_k, \sum_{r=0}^{n-1} \omega^r = 0$

The roots of unity form a regular n -polygon around the origin.

1.5.4. Trigonometric and Hyperbolic Functions

$$\sin x = \frac{e^{ix} - e^{-ix}}{2i}$$

$$\cos x = \frac{e^{ix} + e^{-ix}}{2}$$

$$\tan x = \frac{e^{ix} - e^{-ix}}{e^{ix} + e^{-ix}}$$

$$z = e^{i\theta} \rightarrow z + \frac{1}{z} = 2 \cos \theta$$

$$z - \frac{1}{z} = 2i \sin \theta$$

$$\frac{z^2 - 1}{z^2 + 1} = i \tan \theta$$

$$\sin ix = i \sinh x$$

$$\cos ix = \cosh x$$

$$\sinh ix = i \sin x$$

$$\cosh ix = \cos x$$

$$\sin(x \pm iy) = \sin x \cosh y \pm i \cos x \sinh y$$

$$\cos(x \pm iy) = \cos x \cosh y \mp i \sin x \sinh y$$

$$\sinh(x \pm iy) = \sinh x \cos y \pm i \cosh x \sin y$$

$$\cosh(x \pm iy) = \cosh x \cos y \pm i \sinh x \sin y$$

$$\sin^{-1} z = \ln \left(iz + \sqrt{1 - z^2} \right) = i \sinh^{-1}(-iz)$$

$$\tan^{-1} z = \frac{i}{2} \ln \frac{1 - iz}{1 + iz} = i \tanh^{-1}(-iz)$$

1.5.5. Exponentiation of Complex Numbers

Let $z = a + bi = r e^{i\theta}$. Then, for integers n , the value of $f(z)$ is given by $R e^{i\phi}$, where:

$f(z)$	$R = f(z) $	$\phi = \arg f(z)$
z^i	$e^{-(\theta + 2\pi n)}$	$\ln r$
i^z	$e^{-\frac{4n+1}{2}\pi r \sin \theta}$	$\frac{4n+1}{2}\pi r \cos \theta$
z^{c+di}	$r^c e^{-d(\theta + 2\pi n)}$	$d \ln r + c(\theta + 2\pi n)$

The principal value is for when $n = 0$.

$i^{\pm i} = e^{\mp\pi/2}$ is purely real.

1.5.6. Root of Unity Filter

For a series $f(x) = \sum_{k=0}^{\infty} a_k x^k$, the value of $\sum_{k=0}^{N-1} f(\omega^k) = N \sum_{k=0}^{\infty} a_{kN}$ where $\omega = e^{\frac{2\pi}{N}i}$ for $N \geq 1$.

This is often useful when working with generating functions (series multisection) whose coefficients are periodic modulo N .

1.6. Discrete Mathematics and Abstract Algebra

1.6.1. Binary Operators

Let $*$ be a binary operator. We say that $*$ is

- Commutative: $a * b = b * a$
- Associative: $(a * b) * c = a * (b * c)$
- Distributive (over $+$): $a * (b + c) = a * b + a * c$

1.6.2. Axioms of Group Theory

A set S and an operation $*$ form a group $(S, *)$ if and only if all of the following are true:

- Closure: $*$ is a binary operation on S i.e. $a * b$ is in S for every $a, b \in S$.
- Identity: there exists exactly one element a in S such that $z * a = z$ for all z in S .
- Associative: $(a * b) * c = a * (b * c)$ for all $a, b, c \in S$.
- Inverse: every element a in S has exactly one corresponding element b in S such that $a * b$ equals the identity element for the group.

An Abelian group is a group in which $*$ is commutative in S .

Equivalently, the group is Abelian if its Cayley table is symmetric about the leading diagonal.

Examples of groups and their identity elements:

- If S is the integers and $*$ is multiplication, then the identity element is 1.
- If S is the real numbers and $*$ is addition, then the identity element is 0.
- If S is a set of geometric transformations and $*$ is composition, then the identity element is the transformation which does nothing (i.e. the identity matrix, if represented by affine transformation matrices).

For finite field groups, see Section 8.8.10.

For point and space (symmetry) groups and their character tables, see Section 13.2.8.

1.6.3. Axioms of Ring Theory

A set S and two operations $+$ and $*$ form a ring $(S, +, *)$ if and only if all of the following are true:

- $(S, +)$ is an Abelian group.
- S is a closed under $*$.
- $*$ is associative.
- $*$ is distributive over $+$.

A commutative ring is a ring in which $*$ is commutative on S .

A field is a ring in which every nonzero element in S has an inverse element under $*$. Equivalently, a field is a group under both $+$ and $*$.

1.6.5. Modular Arithmetic

Definition of modulo operator: $a \equiv b \pmod{n} \Leftrightarrow \frac{a}{n}$ and $\frac{b}{n}$ have the same remainder, where a, b and n are all integers.

If $a \equiv b \pmod{n}$ then $\frac{a-b}{n}$ is an integer.

Euler's totient function: $\phi(n)$ is the number of integers between 1 and n which are coprime with n (no common divisors except 1):

$$\phi(n) = \prod_{a \in N: a < n, \gcd(a, n) = 1} a = n \prod_{p \in P: p | n} \left(1 - \frac{1}{p}\right)$$

Fermat's little theorem: $a^p \equiv a \pmod{p}$ for prime p which does not divide a

Euler's theorem: $a^{\phi(n)} \equiv 1 \pmod{n}$ for coprime a and n

Wilson's theorem: $(p-1)! \equiv -1 \pmod{p} \Leftrightarrow p$ is prime

Chinese remainder theorem:

A system of N congruences $\bigcap_{i=1}^N \{x \equiv a_i \pmod{n_i}\}$ where all n_i are pairwise coprime has solutions x , any two of which x_i and x_j satisfy $x_i \equiv x_j \pmod{N}$.

The residue class of a modulo n is the set $\overline{a}_n = \{\dots, a-2n, a-n, a, a+n, a+2n, \dots\}$.

The ring of integers modulo n is the set of all residue classes modulo n , represented by

$$\mathbb{Z}/n\mathbb{Z} = \{\overline{a}_n \mid a \in \mathbb{Z}\} = \{\overline{0}_n, \overline{1}_n, \overline{2}_n, \dots, \overline{n-1}_n\}$$

and when $n = 0$, this ring is isomorphic to \mathbb{Z} since $\overline{a}_0 = \{a\}$.

This ring is commutative as $\overline{a}_n \pm \overline{b}_n = \overline{(a \pm b)}_n$ and $\overline{a}_n \overline{b}_n = \overline{(ab)}_n$.

$\mathbb{Z}/n\mathbb{Z}$ is a finite field if and only if n is prime.

1.6.6. Kuratowski's Theorem for Planarity of Graphs

1.6.7. Minimax Cut-Flow Theorem for Networks

1.6.8. Simplex Algorithm for Linear Programming

1.6.9. Lagrange Multipliers for Nonlinear Programming

A typical problem is stated as “Minimise / Maximise $f(\mathbf{x})$ subject to $g(\mathbf{x}) = 0$ ”, where \mathbf{x} is a vector of n scalar independent unknown variables. The Lagrangian is defined as $L(\mathbf{x}, \lambda) = f(\mathbf{x}) - \lambda g(\mathbf{x})$. The solution is given by $\nabla L(\mathbf{x}, \lambda) = 0$ (a system of $n + 1$ equations). Note that these are critical points, not necessarily extrema (may be saddle points).

For multiple constraints, formulated as “Minimise / Maximise $f(\mathbf{x})$ subject to $\mathbf{g}(\mathbf{x}) = \mathbf{0}$ ”, where \mathbf{g} is a vector-valued function for each of the m constraints, the Lagrangian is

$$L(\mathbf{x}, \boldsymbol{\lambda}) = f(\mathbf{x}) - \boldsymbol{\lambda} \cdot \mathbf{g}(\mathbf{x}) = f(\mathbf{x}) - \sum_{i=1}^m \lambda_i g_i(\mathbf{x})$$

where $\boldsymbol{\lambda}$ is a vector of m unknown multipliers.

The solution is again given by $\nabla L(\mathbf{x}, \boldsymbol{\lambda}) = 0$ (a system of $n + m$ equations).

In the Hamiltonian formulation, $H(\mathbf{x}) = f(\mathbf{x}) + \boldsymbol{\lambda} \cdot \mathbf{g}(\mathbf{x})$, which ensures **minima**.

1.6.10. Game Theory for Zero-Order and Higher-Order Games

1.7. Special Functions and Identities

1.7.1. Factorials and Related Functions

- Factorial: $n! = \prod_{k=1}^n k = n(n-1)(n-2)\dots 2 \times 1$ for positive integers n , and $0! = 1$.
- Double factorial:

$$n!! = n(n-2)(n-4)\dots 2 \text{ if } n \text{ even; } \quad n!! = n(n-2)(n-4)\dots 3 \text{ if } n \text{ odd.}$$

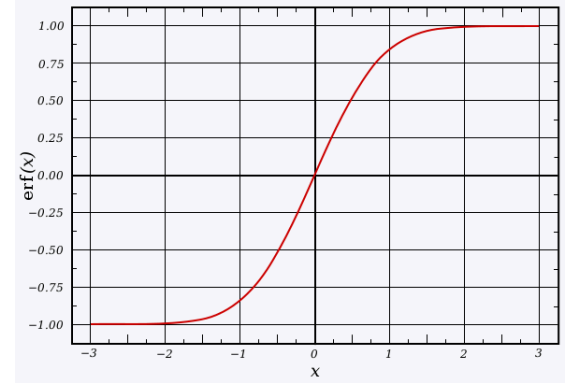
$$n!! = 2^{n/2} \left(\frac{n}{2}\right)! \text{ if } n \text{ even; } \quad n!! = 2^{\left(\frac{1-n}{2}\right)} \times \frac{n!}{\left(\frac{n-1}{2}\right)!} \text{ if } n \text{ odd.}$$
- Asymptotic growth: $n^k \ll n!! \ll n! \ll n^n$ as $n \rightarrow \infty$:
- Stirling's approximation: $\ln n! \sim n \ln n - n$ and $n! \sim \sqrt{2\pi n} \left(\frac{n}{e}\right)^n$ as $n \rightarrow \infty$
- Double factorial ratio: $\frac{(2n)!!}{(2n-1)!!} \sim \sqrt{\pi n}$ as $n \rightarrow \infty$
- Rising factorial: $x^{(n)} = x^{\overline{n}} = \prod_{k=0}^{n-1} (x+k) = x(x+1)(x+2)\dots(x+n-1) = \frac{(x+n-1)!}{(x-1)!}$
- Falling factorial: $(x)_n = \prod_{k=0}^{n-1} (x-k) = x(x-1)(x-2)\dots(x-n+1) = \frac{x!}{(x-n)!}$

1.7.2. Gamma Function, $\Gamma(x)$ and Digamma Function, $\psi(x)$

- Gamma function as a generalised factorial: $\Gamma(x) = (x-1)!$ i.e. $x! = x \Gamma(x)$
- Gamma function as an integral: $\Gamma(z) = \int_0^{\infty} t^{z-1} e^{-t} dt$ for $\text{Re}(z) > 0$
- Reflection identity: $\Gamma(z) \Gamma(1-z) = \frac{\pi}{\sin \pi z}$ for non-integer z
- Half-integer identity: $\Gamma(z) \Gamma\left(z + \frac{1}{2}\right) = 2^{1-2z} \sqrt{\pi} \Gamma(2z)$ for non-integer z
- Useful exact values: $\Gamma\left(\frac{1}{2}\right) = \sqrt{\pi}$ $\Gamma\left(-\frac{1}{2}\right) = -2\sqrt{\pi}$
- Digamma function: $\psi(x) = \frac{d}{dx} \ln \Gamma(x) = \frac{\Gamma'(x)}{\Gamma(x)}$
- Reflection identity: $\psi(1-x) - \psi(x) = \frac{\pi}{\tan \pi x}$ for non-integer x
- Integer identity: $\psi(x+1) = \psi(x) + \frac{1}{x}$

1.7.3. Error Function, erf x

- Error function: $\text{erf } x = \frac{2}{\sqrt{\pi}} \int_0^x e^{-t^2} dt$
- Relation to Normal distribution:
 $\text{erf } x = 2 \Phi(\sqrt{2}x) - 1$ (Φ : standard normal c.d.f.)
- Complementary error function: $\text{erfc } z = 1 - \text{erf } z$
- Imaginary error function: $\text{erfi } z = -i \text{erf } iz$



Graph of $y = \text{erf } x$

1.7.4. Beta Function, $B(x, y)$

- Beta function: $B(x, y) = \int_0^1 t^{x-1} (1 - t)^{y-1} dt$
- Relation to gamma function: $B(x, y) = \frac{\Gamma(x) \Gamma(y)}{\Gamma(x + y)}$
- Pascal's identity: $B(x, y) = B(x, y + 1) + B(x + 1, y)$
- For integers m, n : $B(m, n) = \frac{m + n}{mn} \times \frac{1}{\binom{m+n}{m}}$

1.7.5. Hypergeometric Functions, including ${}_2F_1(a, b; c; z)$

- Gaussian hypergeometric function: ${}_2F_1(a, b; c; z) = \sum_{n=0}^{\infty} \frac{(a)_n (b)_n}{(c)_n} \frac{z^n}{n!}$, for $|z| < 1$
 This series terminates if b or c is an integer, forming a binomial series.
- Euler's integral formula: $B(b, c - b) {}_2F_1(a, b; c; z) = \int_0^1 x^{b-1} (1 - x)^{c-b-1} (1 - zx)^{-a} dx$
- Gauss summation theorem: ${}_2F_1(a, b; c; 1) = \frac{\Gamma(c) \Gamma(c - a - b)}{\Gamma(c - a) \Gamma(c - b)}$, for $\text{Re}(c) > \text{Re}(a + b)$
- Barnes' contour integral: ${}_2F_1(a, b; c; z) = \frac{\Gamma(c)}{\Gamma(a) \Gamma(b)} \times \frac{1}{2\pi i} \int_{-i\infty}^{i\infty} \frac{\Gamma(a + s) \Gamma(b + s) \Gamma(-s)}{\Gamma(c + s)} (-z)^s ds$
- Generalised HGF: ${}_pF_q(a_1, \dots, a_p; b_1, \dots, b_q; z) = \sum_{n=0}^{\infty} \frac{(a_1)_n \dots (a_p)_n}{(b_1)_n \dots (b_q)_n} \frac{z^n}{n!}$, for $|z| < 1$
- Regularised HGF: $\widehat{F}_p(a_1, \dots, a_p; b_1, \dots, b_q; z) = \frac{{}_pF_q(a_1, \dots, a_p; b_1, \dots, b_q; z)}{\Gamma(b_1) \dots \Gamma(b_q)}$
- Kummer's confluent HGF, first kind: $M(a, b; z) = {}_1F_1(a, b; z) = \lim_{c \rightarrow \infty} {}_2F_1(a, c; b; \frac{z}{c})$
- Kummer's confluent HGF, second kind: $U(a, b; z) = z^{-a} {}_2F_0(a, 1 + a - b; ; -\frac{1}{z})$

1.7.7. Elliptic Integrals, $K(k)$, $E(k)$ and $\Pi(n, k)$

- Complete elliptic integral, first kind: $K(k) = \int_0^{\pi/2} \frac{d\theta}{\sqrt{1-k^2 \sin^2 \theta}} = \int_0^1 \frac{dt}{\sqrt{(1-t^2)(1-k^2 t^2)}}$
- Complete elliptic integral, second kind: $E(k) = \int_0^{\pi/2} \sqrt{1-k^2 \sin^2 \theta} d\theta = \int_0^1 \frac{\sqrt{1-k^2 t^2}}{\sqrt{1-t^2}} dt$
- Complete elliptic integral, third kind: $\Pi(n, k) = \int_0^{\pi/2} \frac{d\theta}{(1-n \sin^2 \theta) \sqrt{1-k^2 \sin^2 \theta}}$
- Incomplete elliptic integral, first kind: $F(\varphi, k) = \int_0^{\varphi} \frac{d\theta}{\sqrt{1-k^2 \sin^2 \theta}}, F(x; k) = \int_0^x \frac{dt}{\sqrt{(1-t^2)(1-k^2 t^2)}}$
- Incomplete elliptic integral, second kind: $E(\varphi, k) = \int_0^{\varphi} \sqrt{1-k^2 \sin^2 \theta} d\theta, E(x; k) = \int_0^x \frac{\sqrt{1-k^2 t^2}}{\sqrt{1-t^2}} dt$
- Incomplete elliptic integral, third kind: $\Pi(n; \varphi \setminus \alpha) = \int_0^{\varphi} \frac{d\theta}{(1-n \sin^2 \theta) \sqrt{1-(\sin \alpha \sin \theta)^2}}$

Substitutions used above are $t = \sin \theta$ and $x = \sin \varphi$.

Legendre's relation: $K(k) E(\sqrt{1-k^2}) + E(k) K(\sqrt{1-k^2}) - K(k) K(\sqrt{1-k^2}) = \frac{\pi}{2}$

Arithmetic-Geometric mean identity: $K(k) = \frac{\pi}{2 \operatorname{agm}(1, \sqrt{1-k^2})}$

Inverse elliptic integrals (Jacobi functions): with $u = F(\varphi, k) = \int_0^{\varphi} \frac{d\theta}{\sqrt{1-k^2 \sin^2 \theta}}$ then

- Jacobi amplitude function: $\operatorname{am}(u, k) = \varphi$
- Elliptic sine: $\operatorname{sn}(u, k) = \sin(\operatorname{am}(u, k)) = \sin \varphi$
- Elliptic cosine: $\operatorname{cn}(u, k) = \cos(\operatorname{am}(u, k)) = \cos \varphi$
- Delta amplitude: $\operatorname{dn}(u, k) = \frac{d\varphi}{du} \operatorname{am}(u, k) = \frac{d\varphi}{du} = \sqrt{1-k^2 \sin^2 \varphi}$

1.7.8. Zeta Function, $\zeta(z)$

- Zeta function as a series: $\zeta(z) = \sum_{r=1}^{\infty} r^{-z} = \frac{1}{\Gamma(z)} \int_0^{\infty} \frac{x^{z-1}}{e^x - 1} dx, \quad \text{for } \operatorname{Re}(z) > 1$
- Euler's product formula: $\zeta(z) = \prod_{p \in P} \frac{1}{1-p^{-z}}, \quad \text{a product over all primes } p$
- Riemann's functional equation: $\zeta(z) = 2^z \pi^{z-1} \sin \frac{\pi z}{2} \Gamma(1-z) \zeta(1-z)$
- Riemann hypothesis: does $\zeta(z) = 0 \Leftrightarrow \operatorname{Re}(z) = \frac{1}{2}$ or $z \in \{-2, -4, -6, \dots\}$?

(critical line)
(trivial zeroes)

1.7.9. Bessel Functions, $J_n(x)$ and $Y_n(x)$, and Hankel Functions, $H_\alpha^{(1)}(x)$ and $H_\alpha^{(2)}(x)$

Bessel functions, $J_n(x)$ and $Y_n(x)$:

1st kind: $J_n(x) = \frac{1}{\pi} \int_0^\pi \cos(n\tau - x \sin \tau) d\tau$

2nd kind: $Y_n(x) = \frac{1}{\pi} \int_0^\pi \sin(x \sin \tau - n\tau) d\tau$

Hankel function, $H_\alpha^{(1)}(x)$ and $H_\alpha^{(2)}(x)$:

1st kind: $H_\alpha^{(1)}(x) = J_\alpha(x) + iY_\alpha(x) = \frac{J_{-\alpha}(x) - e^{-\alpha\pi i} J_\alpha(x)}{i \sin \alpha\pi}$

2nd kind: $H_\alpha^{(2)}(x) = J_\alpha(x) - iY_\alpha(x) = \frac{J_{-\alpha}(x) - e^{\alpha\pi i} J_\alpha(x)}{-i \sin \alpha\pi}$

Modified Bessel Functions, $I_\alpha(x)$ and $K_\alpha(x)$:

1st kind: $I_\alpha(x) = i^{-\alpha} J_\alpha(ix) = \sum_{m=0}^{\infty} \frac{(x/2)^{2m+\alpha}}{m! \Gamma(m+\alpha+1)}$

2nd kind: $K_\alpha(x) = \frac{\pi}{2} \frac{I_{-\alpha}(x) - I_\alpha(x)}{\sin \alpha\pi}$

Spherical Bessel functions, $j_n(x)$ and $y_n(x)$:

1st kind: $j_n(x) = \sqrt{\frac{\pi}{2x}} J_{n+\frac{1}{2}}(x)$

2nd kind: $y_n(x) = \sqrt{\frac{\pi}{2x}} Y_{n+\frac{1}{2}}(x) = (-1)^{n+1} j_{-n-1}(x)$

1.7.10. Associated Legendre Polynomials, $P_l^m(x)$

Associated Legendre Polynomials: $P_l^m(x) = \frac{(-1)^m}{2^l l!} (1-x^2)^{m/2} \frac{d^{l+m}}{dx^{l+m}} (x^2-1)^l, \quad -l \leq m \leq l$

$P_l^m(x)$	$m = 0$	$m = 1$	$m = 2$	$m = 3$
$l = 0$	1			
$l = 1$	x	$-(1-x^2)^{1/2}$		
$l = 2$	$\frac{1}{2}(3x^2-1)$	$-3x(1-x^2)^{1/2}$	$3(1-x^2)$	
$l = 3$	$\frac{1}{2}(5x^3-3x)$	$\frac{3}{2}(1-5x^2)(1-x^2)^{1/2}$	$15x(1-x^2)$	$-15(1-x^2)^{3/2}$

For negative index m : $P_l^{-m}(x) = (-1)^m \frac{(l-m)!}{(l+m)!} P_l^m(x)$

1.7.11. Hermite Polynomials, $H_n(x)$

Hermite polynomials as a derivative: $H_n(x) = (-1)^n e^{x^2} \frac{d^n}{dx^n} e^{-x^2}$

Recurrence relation: $H_{n+1}(x) = 2x H_n(x) - H_n'(x)$

The first few Hermite polynomials are

$$H_0(x) = 1; H_1(x) = 2x; H_2(x) = 4x^2 - 2; H_3(x) = 8x^3 - 12x;$$

$$H_4(x) = 16x^4 - 48x^2 + 12; H_5(x) = 32x^5 - 160x^3 + 120x$$

1.7.12. Generalised Laguerre Polynomials, $L_n^{(\alpha)}(x)$

Recurrence relation: $(k + 1) L_{k+1}^{(\alpha)}(x) = (2k + 1 + \alpha - x) L_k^{(\alpha)}(x) - (k + \alpha) L_{k-1}^{(\alpha)}(x)$

The first few generalised Laguerre polynomials are:

$$L_0^{(\alpha)}(x) = 1; L_1^{(\alpha)}(x) = -x + (\alpha + 1); L_2^{(\alpha)}(x) = \frac{1}{2}x^2 + (\alpha + 2)x + \frac{1}{2}(\alpha + 1)(\alpha + 2)$$

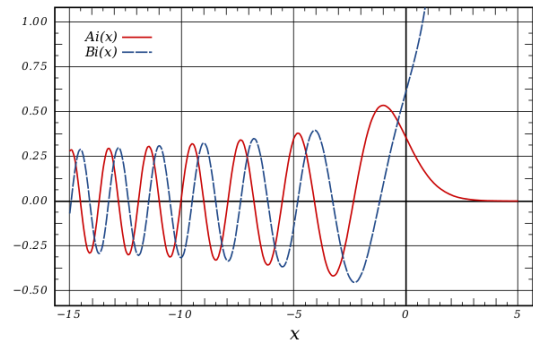
1.7.13. Airy Functions, $Ai(x)$ and $Bi(x)$

Airy equation: $\frac{d^2 y}{dx^2} - xy = 0$

Linearly independent solutions are:

$$Ai(x) = \frac{1}{\pi} \int_0^{\infty} \cos\left(xt + \frac{t^3}{3}\right) dt$$

$$Bi(x) = \frac{1}{\pi} \int_0^{\infty} \exp\left(xt - \frac{t^3}{3}\right) + \sin\left(xt + \frac{t^3}{3}\right) dt$$

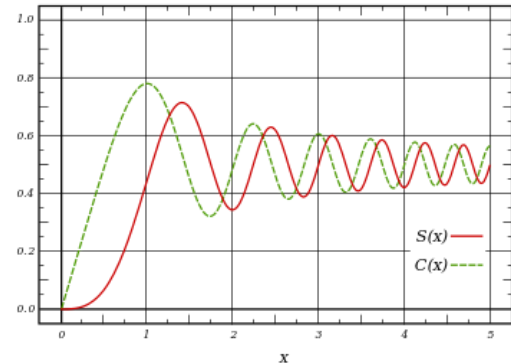


1.7.14. Fresnel Integrals, $S(x)$ and $C(x)$

Fresnel sine and cosine:

$$S(x) = \int_0^x \sin(t^2) dt = \sum_{n=0}^{\infty} (-1)^n \frac{x^{4n+3}}{(2n+1)!(4n+3)},$$

$$C(x) = \int_0^x \cos(t^2) dt = \sum_{n=0}^{\infty} (-1)^n \frac{x^{4n+1}}{(2n)!(4n+1)}.$$



Clothoid curve: $\{x(t) = C(t), y(t) = S(t)\}$.

which has a constant rate of change of curvature: $\frac{d\kappa}{ds} = 2$ and $\frac{ds}{dt} = 1$.

Limiting value: $\lim_{x \rightarrow \infty} S(x) = \lim_{x \rightarrow \infty} C(x) = \sqrt{\frac{\pi}{8}}$.

1.7.15. Lambert W Function, $W_k(z)$

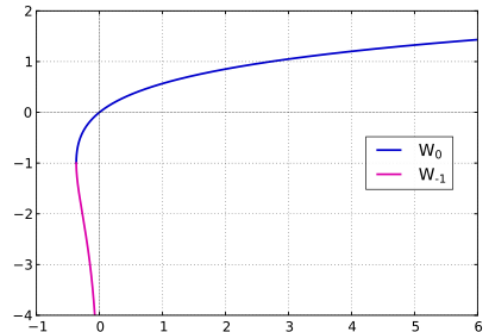
The Lambert W function is the inverse function of $f(z) = ze^z$ i.e. $W_k(z) e^{W_k(z)} = z$ ($k \in \mathbb{Z}$).

For real x , the two branches $y = W_0(x)$ and $y = W_{-1}(x)$ are the solutions to $y e^y = x$ for $x \geq 0$ and $-1/e \leq x < 0$ respectively.

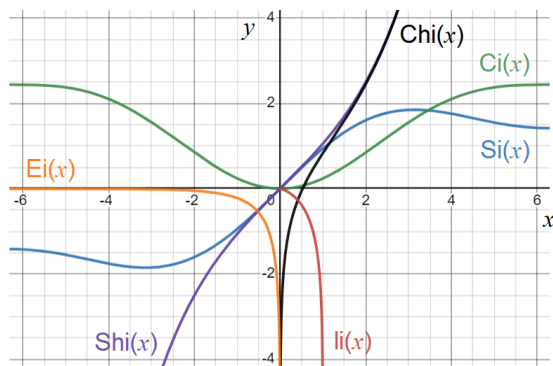
Taylor series: $W_0(x) = \sum_{n=1}^{\infty} \frac{(-n)^{n-1}}{n!} x^n, \quad |x| < 1/e$

Lambert differential equation: $x(1 + y) \frac{dy}{dx} = y$

All branches are solutions to this DE ($y = W_n(x)$).



1.7.16. Trigonometric Integral Functions, Si(x), Ci(x), Shi(x), Chi(x), li(x), Ei(x)



$$\lim_{x \rightarrow \pm\infty} Si(x) = \int_0^{\pm\infty} \frac{\sin t}{t} dt = \pm \frac{\pi}{2}$$

$$\lim_{x \rightarrow \pm\infty} Ci(x) = \int_0^{\pm\infty} \frac{1 - \cos t}{t} dt \text{ diverges to } \infty$$

$$\lim_{x \rightarrow 1} li(x) = \int_0^1 \frac{dt}{\ln t} \text{ diverges to } -\infty$$

- Sine integral: $Si(x) = \int_0^x \text{sinc } t \, dt = \int_0^x \frac{\sin t}{t} dt$
- Cosine integral: $Ci(x) = \int_0^x \frac{1 - \cos t}{t} dt = \gamma + \ln x + \int_x^{\infty} \frac{\cos t}{t} dt$
- Hyperbolic sine integral: $Shi(x) = \int_0^x \frac{\sinh t}{t} dt$ ($\gamma = 0.577216\dots$: Euler-Mascheroni constant)
- Hyperbolic cosine integral: $Chi(x) = \gamma + \ln x - \int_0^x \frac{1 - \cosh t}{t} dt, \quad x > 0$
- Logarithmic integral: $li(x) = \int_0^x \frac{dt}{\ln t}, \quad 0 \leq x < 1$
- Exponential integral: $Ei(x) = - \int_{-x}^{\infty} \frac{e^{-t}}{t} dt = \int_{-\infty}^x \frac{e^t}{t} dt, \quad x < 0$

1.7.17. Spherical Harmonics, $Y_l^m(\theta, \phi)$

Spherical harmonic: $Y_l^m(\theta, \phi) = \sqrt{\frac{(2l+1)(l-m)!}{4\pi(l+m)!}} P_l^m(\cos \theta) e^{im\phi} = \sqrt{\frac{2l+1}{4\pi}} C_{lm}(\theta, \phi)$ for $|m| \leq l$

The 'Condon-Shortley phase' is due to the term $(-1)^m$, which is included in the definition of P_l^m .

Expressions for C_{lm} in angular spherical coordinates (θ, ϕ) and Cartesian coordinates (x, y, z) are

$$C_{00} = 1; \quad C_{10} = \cos \theta = \frac{z}{r}; \quad C_{1,\pm 1} = \mp \sqrt{\frac{1}{2}} \sin \theta e^{\pm i\phi} = \mp \sqrt{\frac{1}{2}} \frac{x \pm iy}{r}$$

$$C_{20} = \frac{1}{2} (3 \cos^2 \theta - 1) = \frac{3z^2 - r^2}{2r^2} \quad (r = \sqrt{x^2 + y^2 + z^2})$$

$$C_{2,\pm 1} = \mp \sqrt{\frac{3}{2}} \cos \theta \sin \theta e^{\pm i\phi} = \mp \sqrt{\frac{3}{2}} \frac{zx \pm izy}{r^2}; \quad C_{2,\pm 2} = \sqrt{\frac{3}{8}} \sin^2 \theta e^{\pm 2i\phi} = \sqrt{\frac{3}{8}} \frac{x^2 - y^2 \pm 2ixy}{r^2}$$

Real Spherical Harmonics: real-valued alternative definition

$$Y_{lm} = \begin{cases} \frac{i}{\sqrt{2}} (Y_\ell^m - (-1)^m Y_\ell^{-m}) & \text{if } m < 0 \\ Y_\ell^0 & \text{if } m = 0 \\ \frac{1}{\sqrt{2}} (Y_\ell^{-m} + (-1)^m Y_\ell^m) & \text{if } m > 0. \end{cases} = \begin{cases} \sqrt{2} (-1)^m \Im[Y_\ell^{|m|}] & \text{if } m < 0 \\ Y_\ell^0 & \text{if } m = 0 \\ \sqrt{2} (-1)^m \Re[Y_\ell^{|m|}] & \text{if } m > 0. \end{cases}$$

Vector Spherical Harmonics: a complex vector-valued function.

$$\mathbf{Y}_{lm}(\theta, \phi) = Y_l^m(\theta, \phi) \hat{\mathbf{r}}, \quad \mathbf{\Psi}_{lm}(r, \theta, \phi) = r \nabla Y_l^m, \quad \mathbf{\Phi}_{lm}(r, \theta, \phi) = r \hat{\mathbf{r}} \times \nabla Y_l^m$$

Spherical Harmonic Transform: for a function in angular spherical coordinates $f(\theta, \phi)$,

$$f(\theta, \phi) = \sum_{l=0}^{\infty} \sum_{m=-l}^l \hat{a}_{lm} Y_l^m(\theta, \phi) \quad \text{where} \quad \hat{a}_{lm} = \int_0^{2\pi} \int_0^\pi f(\theta, \phi) Y_l^m(\theta, \phi) \sin \theta d\theta d\phi$$

This is analogous to a Fourier series (Section 3.6), with \hat{a}_{lm} as complex coefficients of the basis functions Y_l^m . The Jacobian term is sometimes written as the solid angle $d\Omega = \sin \theta d\theta d\phi$.

$$\text{Normalisation: } \int_0^{2\pi} \int_0^\pi |Y_l^m|^2 d\Omega = 1. \quad \text{Orthogonality: } \int_0^{2\pi} \int_0^\pi (Y_l^m)(Y_{l'}^{m'})^* d\Omega = \delta_{ll'} \delta_{mm'}.$$

1.7.18. Miscellaneous Special Functions

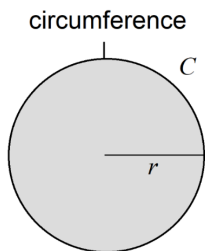
Generalised Marcum Q -function:
$$Q_\nu(a, b) = \frac{1}{a^{\nu-1}} \int_b^\infty x^\nu e^{-\frac{1}{2}(x^2 + a^2)} I_{\nu-1}(ax) dx$$

M2. GEOMETRY

2.1. Properties of 2D and 3D Shapes

2.1.1. Properties of Simple 2D Shapes

Circles and Parts of Circles

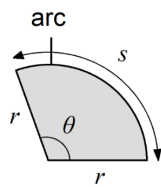


Circle

Area: $A = \pi r^2$

Diameter: $d = 2r$

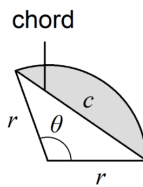
Circumference: $C = 2\pi r = \pi d$



Sector

Area: $A = \frac{1}{2}r^2\theta$

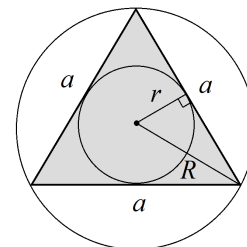
Arc length: $s = r\theta$



Segment

Area: $A = \frac{1}{2}r^2(\theta - \sin \theta)$

Chord length: $c = 2r \sin \frac{\theta}{2}$

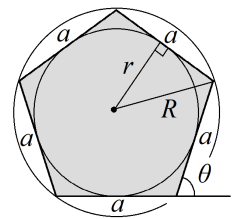


Equilateral Triangle

Area: $A = \frac{\sqrt{3}}{4}a^2$

$r = \frac{\sqrt{3}}{6}a$

$R = \frac{\sqrt{3}}{3}a$



Regular n-gon

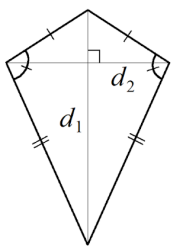
Area: $A = \frac{na^2}{4 \tan \frac{\pi}{n}}$

$r = \frac{a}{2 \tan \frac{\pi}{n}}, R = \frac{a}{2 \sin \frac{\pi}{n}}$

External angle: $\theta = \frac{2\pi}{n}$

Special Quadrilaterals

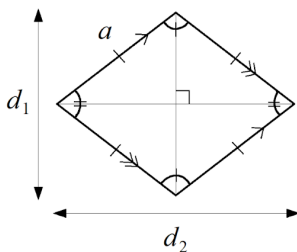
(For properties of scalene/right triangles, see Section 2.2.7.)



Kite (Deltoid)

Area: $A = \frac{1}{2}d_1d_2$

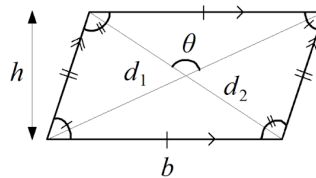
diagonals perpendicular



Rhombus

Area: $A = \frac{1}{2}d_1d_2$

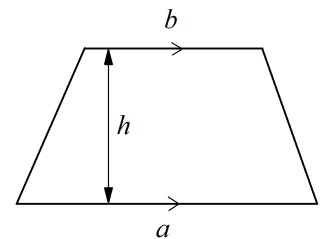
diagonals perp. bisectors



Parallelogram

Area: $A = bh = \frac{1}{2}d_1d_2 \sin \theta$

diagonals bisect



Trapezium (Trapezoid)

$A = \frac{1}{2}h(a + b)$

2.1.2. Symmetry

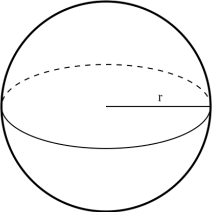
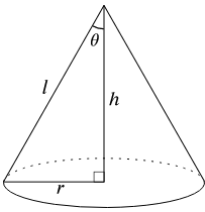
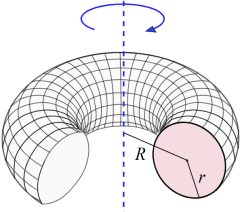
Rotational symmetry of order n : identical after turning through $360^\circ / n$

Reflective/mirror symmetry of order n : identical after reflecting in n different axes

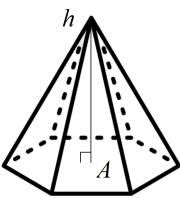
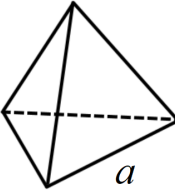
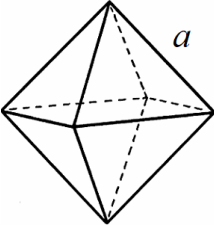
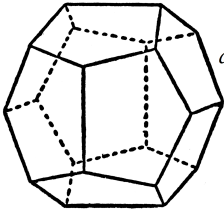
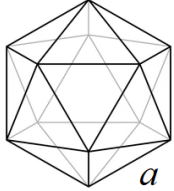
A regular polygon is both rotational and mirror symmetry order n

2.1.3. Volumes and Surface Areas of 3D Solid Figures

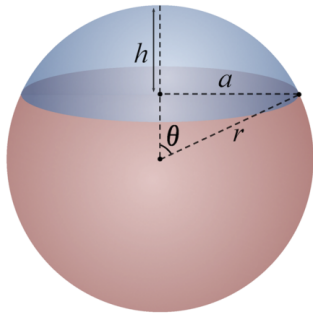
Curved bodies:

			
	Sphere	Cone	Torus
Volume	$\frac{4}{3}\pi r^3$	$\frac{1}{3}\pi r^2 h$	$2\pi^2 Rr^2$
Surface Area	$4\pi r^2$	$\pi r l + \pi r^2$	$4\pi^2 Rr$

Pyramidal and Platonic solids (f: faces, v: vertices, e: edges):

					
	Pyramid	Tetrahedron (4 f, 4 v, 6 e)	Octahedron (8 f, 6 v, 12 e)	Dodecahedron (12 f, 20 v, 30 e)	Icosahedron (20 f, 12 v, 30 e)
Volume	$\frac{1}{3}Ah$	$\frac{\sqrt{2}}{12} a^3$	$\frac{\sqrt{2}}{3} a^3$	$\frac{15 + 7\sqrt{5}}{4} a^3$	$\frac{5(3 + \sqrt{5})}{12} a^3$
Surface Area	$\frac{1}{2}pL + A$ (p: base perimeter L: slant length)	$\sqrt{3} a^2$	$2\sqrt{3} a^2$	$3\sqrt{25 + 10\sqrt{5}} a^2$	$5\sqrt{3} a^2$

2.1.4. Sections of Spheres (Sections of Revolution)



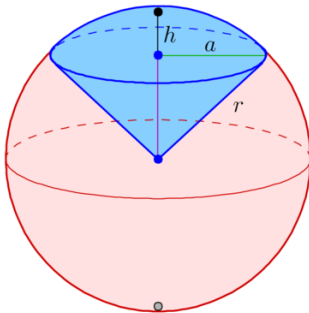
Spherical Cap (blue): radius r , flat radius a , height h , half-angle θ :

Volume:

$$V = \frac{\pi h^2}{3} (3r - h) = \frac{\pi h}{6} (3a^2 + h^2) = \frac{\pi r^3}{h} (2 + \cos \theta)(1 - \cos \theta)^2$$

Curved surface area: (circular plane face area: πa^2)

$$A = 2\pi r h = \pi(a^2 + h^2) = 2\pi r^2 (1 - \cos \theta)$$



Spherical Sector (blue): radius r , flat radius a , height h , half-angle θ :

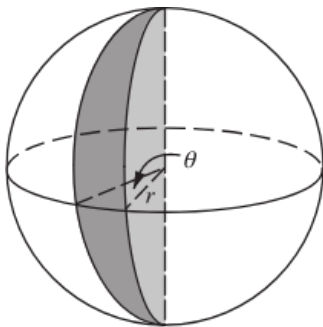
Volume:

$$V = \frac{2\pi r^2 h}{3} = \frac{\pi}{6h} (a^2 + h^2)^2 = \frac{2\pi r^3}{3} (1 - \cos \theta)$$

Curved surface area: (cone area: $\pi a r$)

$$A = 2\pi r h = \Omega r^2 = 2\pi r^2 (1 - \cos \theta)$$

(Ω : solid angle, in steradians (by definition))



Spherical Wedge: radius r , dihedral angle θ :

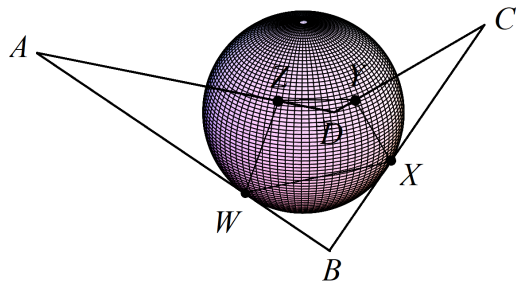
Volume:

$$V = \frac{2\pi r^3 \theta}{3}$$

Curved surface area (lune):

$$A = 2r^2 \theta$$

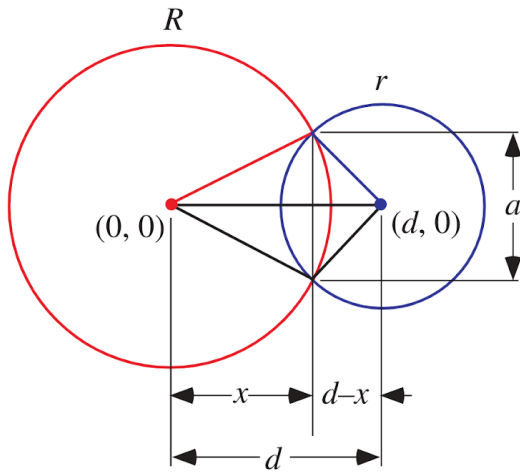
A plane intersects a sphere in a circle. The maximum area of this circle occurs when the plane cuts the sphere in two equal parts (hemisphere caps separated by a 'great circle').

2.1.5. Some Geometric Results in 3D**3D Quadrilateral Coffin Problem**

AB, BC, CD, AD tangent to a sphere at W, X, Y, Z

W, X, Y, Z are coplanar

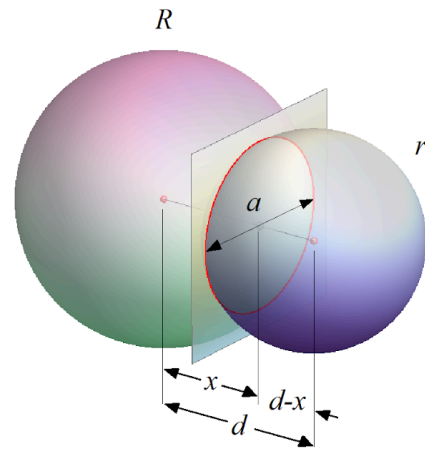
2.1.6. Circle-Circle and Sphere-Sphere Intersections



Circle-Circle Intersection

Area of overlapping lens region:

$$A = r^2 \cos^{-1} \frac{d^2 + r^2 - R^2}{2dr} + R^2 \cos^{-1} \frac{d^2 + R^2 - r^2}{2dR} - \frac{1}{2} \sqrt{4d^2 R^2 - (d^2 - r^2 + R^2)^2}$$



Sphere-Sphere Intersection

Volume of overlapping lens region:

$$V = \frac{\pi}{12d} (R + r - d)^2 \times (d^2 + 2dr - 3r^2 + 2dR + 6rR - 3R^2)$$

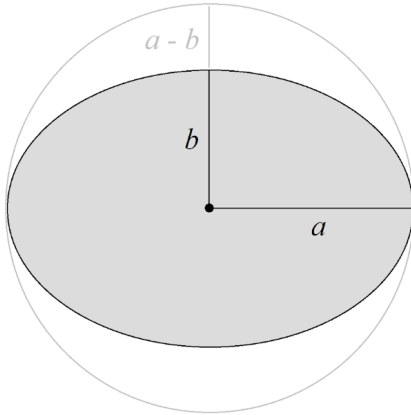
In both cases,

Distance to intersection chord or intersection plane: $x = \frac{d^2 - r^2 + R^2}{2d}$

Length of intersection chord or diameter of intersection circle: $a = \frac{1}{d} \sqrt{4d^2 R^2 - (d^2 - r^2 + R^2)^2}$

2.1.7. Ellipses and Ellipsoids

Ellipse (2D): an elongated circle.

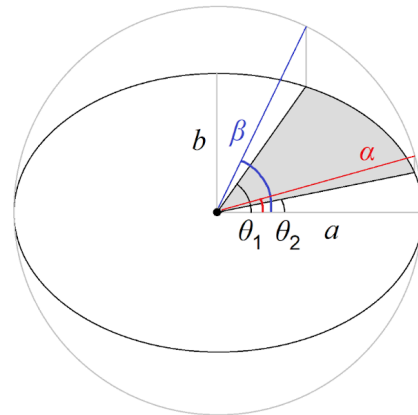


Ellipse

Area: $A = \pi ab$

Eccentricity: $e^2 = 1 - \frac{b^2}{a^2}$

Perimeter: $P = 4a E(e)$



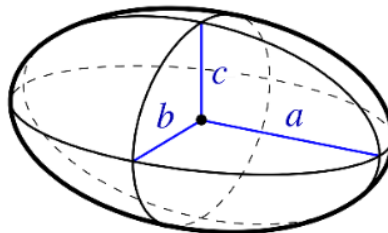
Elliptical Sector

$\cos^2 \theta_1 + \sin^2 \alpha = 1$ and $\cos^2 \theta_2 + \sin^2 \beta = 1$

Area: $\frac{ab}{2}(\beta - \alpha - \sin(\beta - \alpha))$

Elliptical arc length: $a(E(\beta, e) - E(\alpha, e))$

Ellipsoid (3D): an elongated sphere along two axes (radii a, b, c)



Volume: $\frac{4}{3} \pi abc$ ($a \geq b \geq c$)

Surface area: $2\pi \left[c^2 + \frac{ab}{\sin \varphi} (K(\varphi, k) \cos^2 \varphi + E(\varphi, k) \sin^2 \varphi) \right]$, $\cos \varphi = \frac{c}{a}$ and $k^2 = \frac{a^2(b^2 - c^2)}{b^2(a^2 - c^2)}$

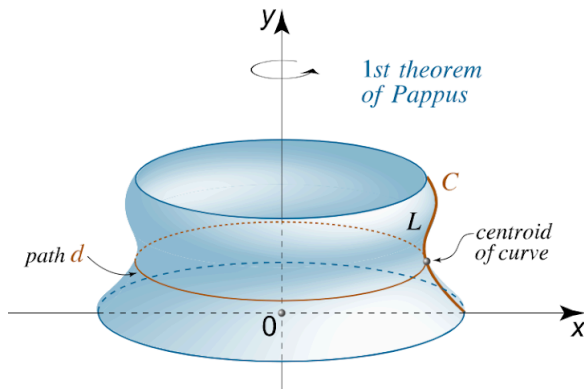
Spheroid: a sphere compressed (oblate) or elongated (prolate) along **one** axis (radii a, a, c)

Surface area, oblate ($c < a$): $2\pi a^2 \left(1 + \frac{1 - e^2}{e} \tanh^{-1} e \right)$, $e^2 = 1 - \frac{c^2}{a^2}$

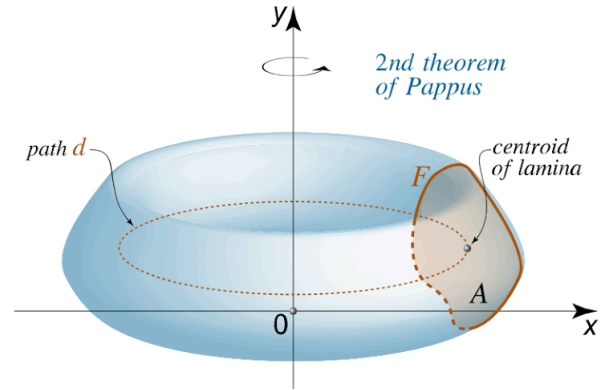
Surface area, prolate ($c > a$): $2\pi a^2 \left(1 + \frac{c}{ae} \sin^{-1} e \right)$, $e^2 = 1 - \frac{a^2}{c^2}$

A plane whose normal is parallel to the axis of stretching intersects the spheroid in a circle.

2.1.8. Pappus' Theorems



Surface Area = $L \times d$



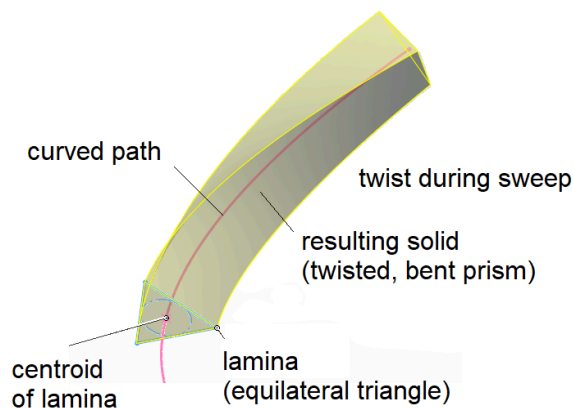
Volume = $A \times d$

For partial revolutions, use the arc length instead of the circumference as d .

Generalisation to Pappus' theorems:

The path traced out by the centroid does not need to be circular: it can be any simple curved path (e.g. linear, parabolic, helical). This will result in a 'swept' solid or surface. The appropriate length d is then the arc length along this path.

Additionally, the curve/lamina being swept may rotate in its plane (torsion: remaining perpendicular to the path) along the path, as long as the angle of twist is continuous. E.g:



Volume = area of lamina \times path length

Surface area = perimeter of lamina \times path length

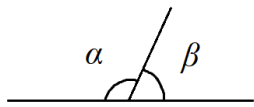
The resulting solid or surface must not be self-intersecting to produce valid results.

2.2. Angle, Triangle and Circle Theorems

2.2.1. Angle Theorems

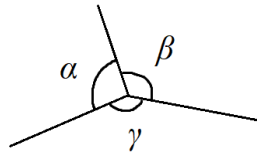
Types of angles: acute ($0^\circ < \theta < 90^\circ$), right angle ($\theta = 90^\circ$), obtuse ($90^\circ < \theta < 180^\circ$), straight line ($\theta = 180^\circ$), reflex ($180^\circ < \theta < 360^\circ$)

For angles at a given point,



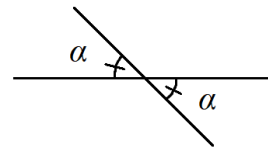
Angles on a line

$$\alpha + \beta = 180^\circ$$



Angles around a point

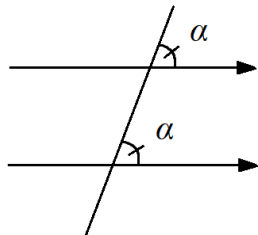
$$\alpha + \beta + \gamma = 360^\circ$$



Opposite angles

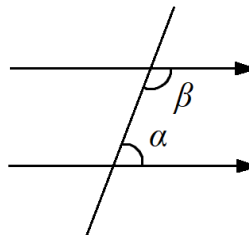
are equal

For parallel lines intersected by a single transversal line,



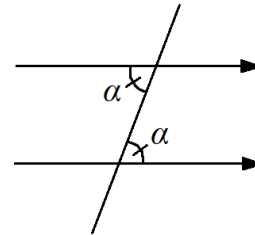
Corresponding Angles ('F')

are equal



Co-Interior Angles ('C')

$$\alpha + \beta = 180^\circ$$



Alternate Angles ('Z')

are equal

2.2.2. Measures of Angles

Common measures of angles are: ($1 \text{ rad} = \frac{180}{\pi} \approx 57.29^\circ$)

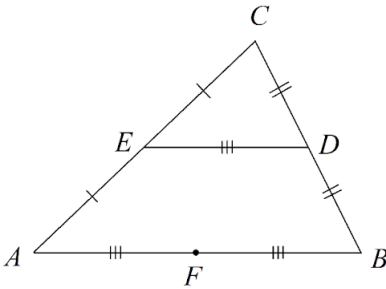
- Degrees: a full turn is 360° .
- Radians: a full turn is 2π rad. Assumed in all calculations (natural units).
- Gradians: a full turn is 400^g (archaic).

Units for small angles include the DMS (degrees-minutes-seconds, $D^\circ M' S''$) system:

- 1 degree = 60 arcminutes ($1^\circ = 60'$)
- 1 arcminute = 60 arcseconds ($1' = 60''$)

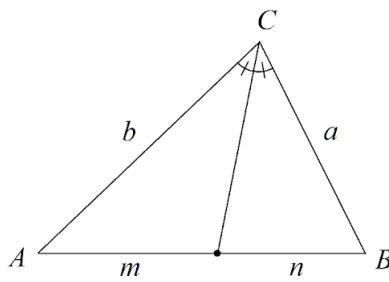
Three-figure bearings, used in navigation, are given in degrees clockwise from North, using three digits by convention (e.g. "050" for 50° clockwise from North).

2.2.3. Triangle and Quadrilateral Theorems



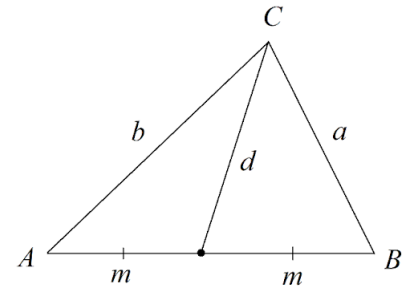
Midpoint Theorem

$$|DE| = \frac{1}{2} |AB|$$



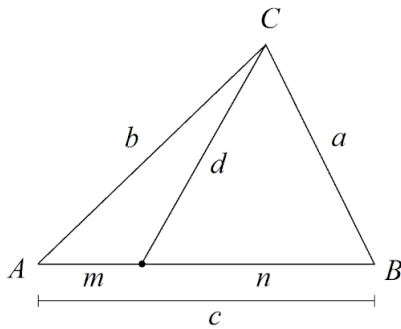
Angle Bisector Theorem

$$\frac{b}{a} = \frac{m}{n}$$



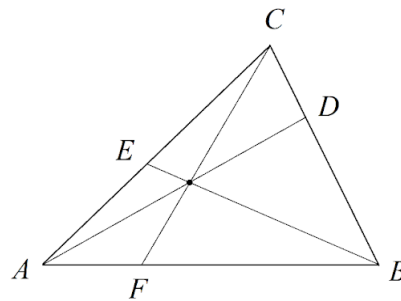
Apollonius' Theorem

$$a^2 + b^2 = 2(d^2 + m^2)$$



Stewart's Theorem

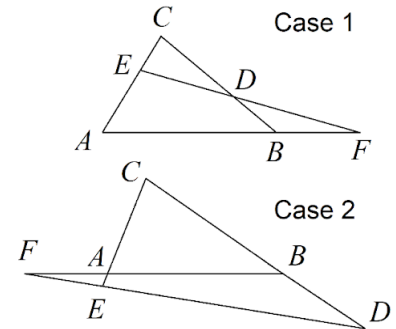
$$b^2 n + a^2 m = c(d^2 + mn)$$



Ceva's Theorem

$$\frac{|AF|}{|FB|} \times \frac{|BD|}{|DC|} \times \frac{|CE|}{|EA|} = 1$$

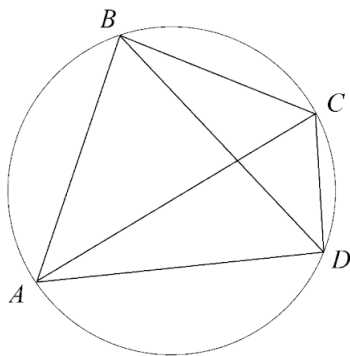
$$\frac{\sin \angle ABE}{\sin \angle CBE} \times \frac{\sin \angle BCF}{\sin \angle ACF} \times \frac{\sin \angle CAD}{\sin \angle BAD} = 1$$



Menelaus' Theorem

$$\frac{|AF|}{|FB|} \times \frac{|BD|}{|DC|} \times \frac{|CE|}{|EA|} = 1$$

in both cases

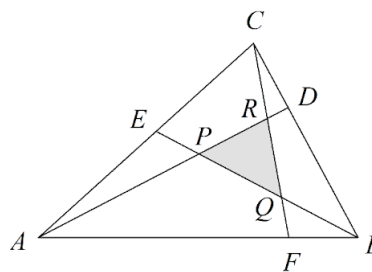


Ptolemy's Theorem

$$|AB||CD| + |BC||DA| = |AC||BD|$$

If ABCD is **not** cyclic, then:

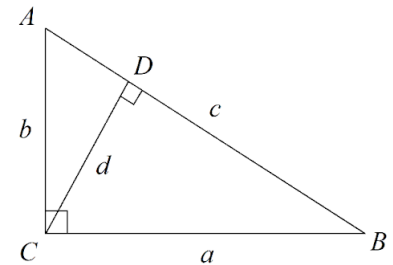
$$|AB||CD| + |BC||DA| \geq |AC||BD|$$



Routh's Theorem

$$\frac{\Delta PQR}{\Delta ABC} = \frac{(xyz-1)^2}{(xy+y+1)(yz+z+1)(xz+x+1)}$$

where $x = \frac{|BD|}{|DC|}$, $y = \frac{|CE|}{|EA|}$, $z = \frac{|AF|}{|BF|}$

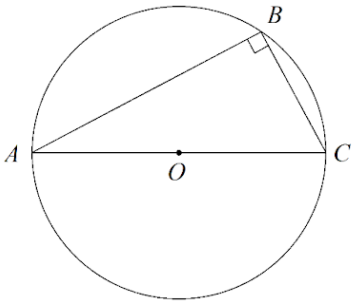


Pythagoras' Theorem

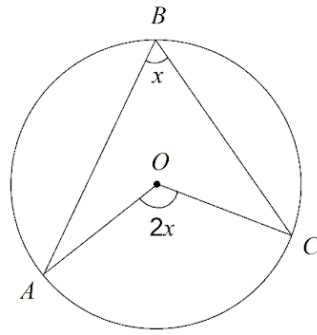
$$a^2 + b^2 = c^2$$

$$\frac{1}{a^2} + \frac{1}{b^2} = \frac{1}{d^2}$$

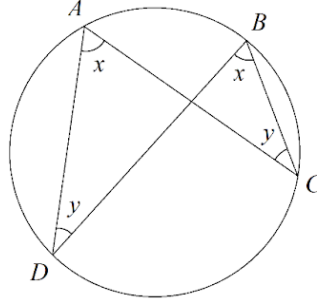
2.2.4. Circle Theorems



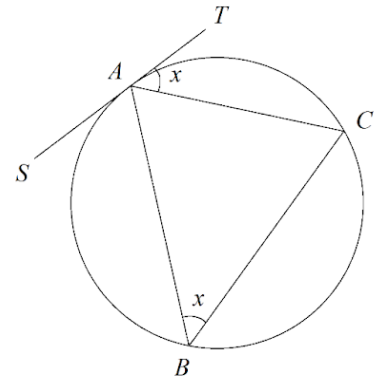
Thales' Theorem
 (Angle in a semicircle)
 AC is a diameter
 $\angle ABC = 90^\circ$



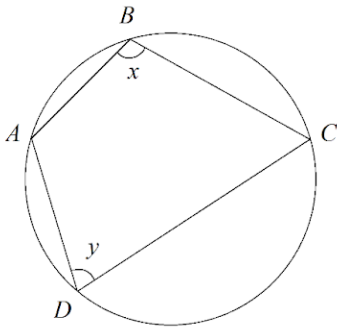
Inscribed Angle Theorems
 Angle at the centre
 $\angle AOC = 2 \angle ABC$



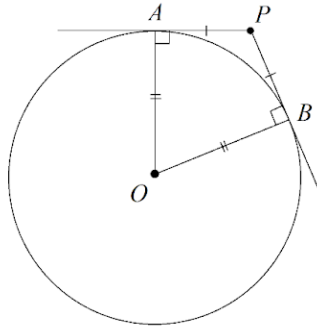
Angles subtended by an arc
 $\angle DAC = \angle DBC$



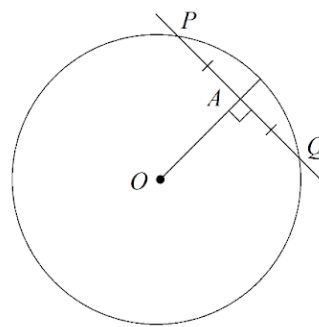
Alternate Segment Theorem
 ST tangent at A
 $\angle TAC = \angle ABC$



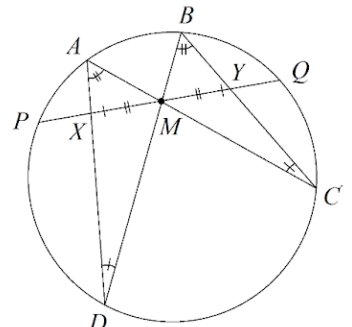
Cyclic Quadrilaterals
 $\angle ABC + \angle ADC = 180^\circ$
 opposite angles add to 180°



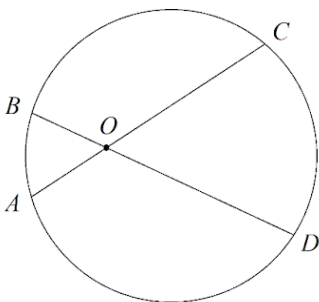
Tangent Theorem
 $|AP| = |BP|$, $OA \perp AP$
 OAPB is a cyclic kite



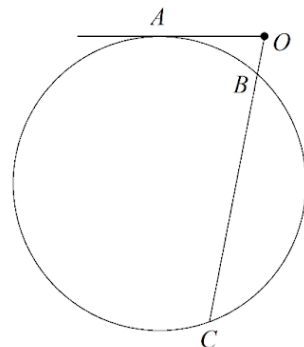
Chord Bisector Theorem
 PQ is a chord
 $OA \perp PQ$, $|AP| = |AQ|$



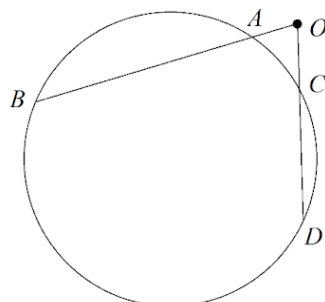
Butterfly Theorem
 M midpoint of chord PQ
 $|MX| = |MY|$



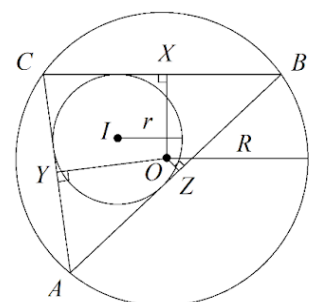
Intersecting Chords
 $|OA||OC| = |OB||OD|$



Tangent-Secant
 $|OA|^2 = |OB||OC|$



Intersecting Secants
 $|OA||OB| = |OC||OD|$

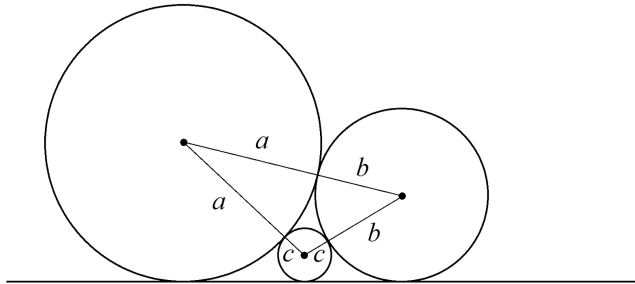


Carnot-Euler Theorems
 $|OX| + |OY| + |OZ| = R + r$
 $|OI|^2 + r^2 = (R - r)^2$
 distances **negative**
 if entirely outside triangle

Three Cases of the Power of a Point Theorem

2.2.5. Some Special Geometric Constructions

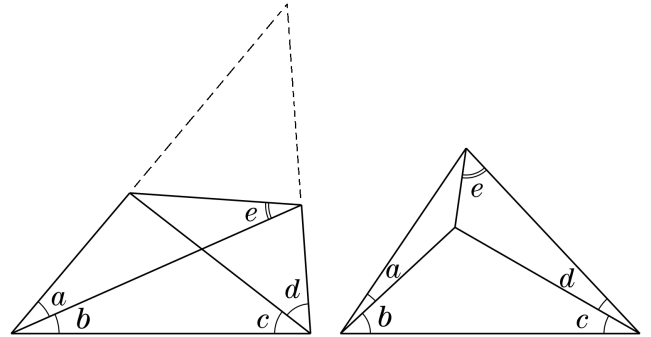
These setups may require unique methods of solving, and are extremely difficult without knowing the technique.



Ford Circles

Three circles tangent to each other, as well as one common tangent line

$$c^{-1/2} = a^{-1/2} + b^{-1/2}$$

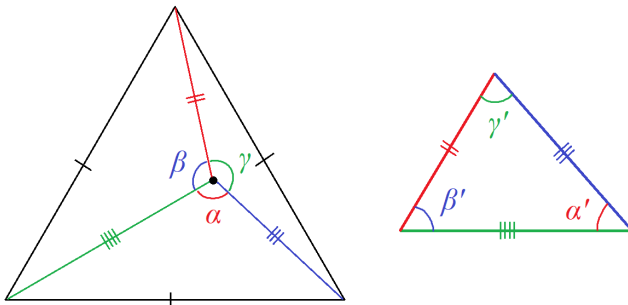


Langley's Adventitious Angles

Given a, b, c, d , find e .

In general, it is extremely difficult without trigonometry.

Techniques include: trigonometric Ceva's theorem, identifying congruent/equilateral triangles, three circumcentres method



Triangle Construction Coffin Problem

The line segments between a point in an equilateral triangle and its vertices are used to form a new triangle.

Angles: $\alpha' = \alpha - 60^\circ, \beta' = \beta - 60^\circ, \gamma' = \gamma - 60^\circ$

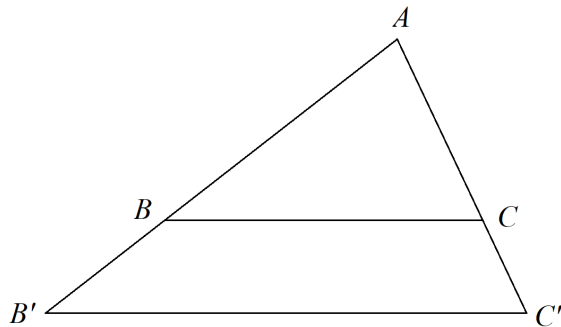
Can be solved by rotating the diagram 60° about a vertex.

2.2.6. Similarity and Congruence of Triangles

Two triangles are similar ($\triangle ABC \sim \triangle PQR$) if one is an enlargement of the other (AAA).

Two triangles are congruent ($\triangle ABC \cong \triangle PQR$) if they are identical (SSS / SAS / ASA / AAS / RHS).

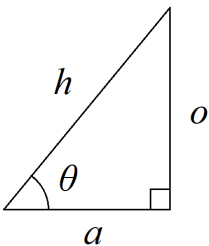
(S / A / R / H: a side / angle / right-angle / hypotenuse known to be equal in both triangles.)



Fundamental theorem of similarity: $\triangle ABC \sim \triangle AB'C'$

$$\frac{|AB|}{|BB'|} = \frac{|AC|}{|CC'|} \Leftrightarrow \frac{|AB|}{|AB'|} = \frac{|AC|}{|AC'|} \Leftrightarrow BC \parallel B'C'$$

2.2.7. Trigonometry of Right-Angled Triangles



The sides are said to be a (adjacent), o (opposite), h (hypotenuse) relative to acute angle θ .

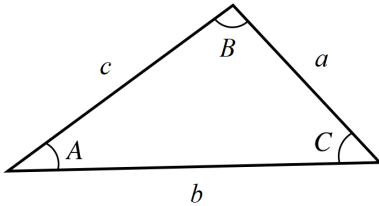
Definitions: $\sin \theta = \frac{o}{h}$ $\cos \theta = \frac{a}{h}$ $\tan \theta = \frac{o}{a}$ (SohCahToa)

Pythagoras' Theorem: $a^2 + o^2 = h^2$ (more often written $a^2 + b^2 = c^2$)

2.2.8. Trigonometry of Triangles

The results here are valid for any cyclic permutation of $\{a, b, c\}$ and $\{A, B, C\}$.

Area of a triangle, $\triangle ABC = \frac{1}{2}bh = \frac{1}{2}ab \sin C = \frac{c^2 \sin A \sin B}{2 \sin(A+B)}$ (h : height perpendicular to b)



Law of Sines (Sine Rule):

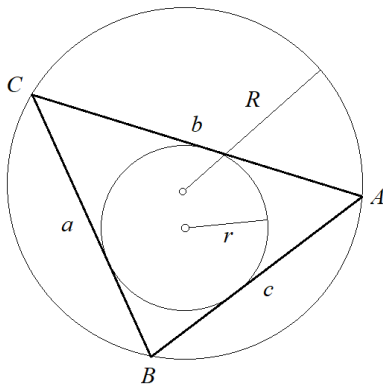
$$\frac{a}{\sin A} = \frac{b}{\sin B} = \frac{c}{\sin C}$$

Law of Cosines (Cosine Rule):

$$c^2 = a^2 + b^2 - 2ab \cos C$$

Law of Tangents (Tangent Rule):

$$\frac{a-b}{a+b} = \frac{\tan \frac{1}{2}(A-B)}{\tan \frac{1}{2}(A+B)}$$



Law of Cotangents (Cotangent Rule): $\frac{\cot \frac{1}{2}A}{s-a} = \frac{\cot \frac{1}{2}B}{s-b} = \frac{\cot \frac{1}{2}C}{s-c} = \frac{1}{r}$

Inscribed Circle Radius:

$$r = \frac{\triangle ABC}{s} = \frac{ab \sin C}{a+b+c}$$

Circumscribed Circle Radius:

$$R = \frac{abc}{4 \triangle ABC} = \frac{a}{2 \sin A}$$

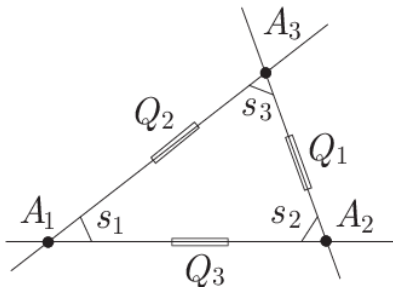
Heron's Theorem: $\triangle ABC = \sqrt{s(s-a)(s-b)(s-c)}$

Mollweide's formulas: $\frac{a+b}{c} = \frac{\cos \frac{1}{2}(A-B)}{\sin \frac{1}{2}C}$ and $\frac{a-b}{c} = \frac{\sin \frac{1}{2}(A-B)}{\cos \frac{1}{2}C}$

(s : semiperimeter, $s = \frac{a+b+c}{2}$, $\triangle ABC$: area of triangle ABC , r : inradius, R : circumradius)

2.2.9. Rational Trigonometry

Rational trigonometry is an alternative formulation of trigonometry in Euclidean geometry that uses 'spreads' and 'quadrances' instead of angles and lengths, which avoids the use of transcendental functions and irrational numbers.



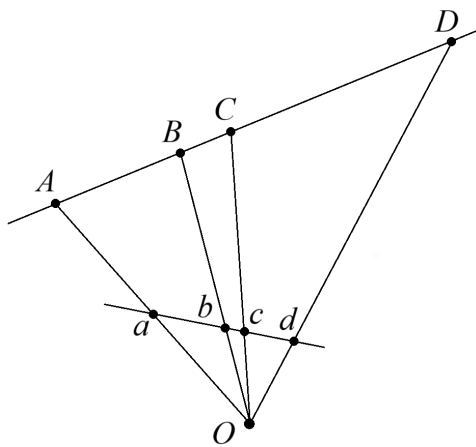
A line with equation $ax + by + c = 0$ is represented as $\langle a : b : c \rangle$.

$$\text{Spread: } s(l_1, l_2) = \frac{(a_1 a_2 - b_1 b_2)^2}{(a_1^2 + b_1^2)(a_2^2 + b_2^2)} \quad (\text{equal to } \sin^2 \theta)$$

Quadrance: Q is equal to distance squared. (equal to a^2)

A triangle is considered a set of three lines. Identities are:

- Pythagorean Theorem: $Q_1 + Q_2 = Q_3 \Leftrightarrow Q_1 \perp Q_2$.
- Triple Spread Formula: $(s_1 + s_2 + s_3)^2 = 2(s_1^2 + s_2^2 + s_3^2) + 4s_1 s_2 s_3$ (angle sum)
- Spread Law: $\frac{s_1}{Q_1} = \frac{s_2}{Q_2} = \frac{s_3}{Q_3}$ (sine rule)
- Cross Law: $(Q_1 + Q_2 - Q_3)^2 = 4Q_1 Q_2 (1 - s_3)$ (cosine rule)

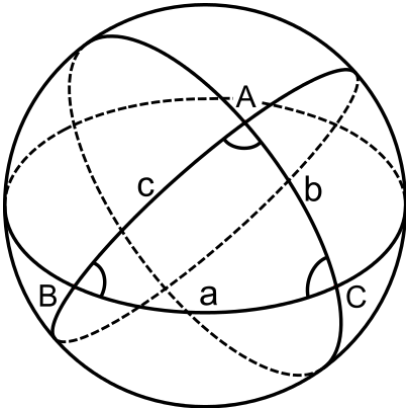
2.2.10. Projective Geometry

The cross ratio (anharmonic ratio) of any four collinear points is invariant under perspective projection:

$$\text{Cross ratio} = \frac{|AC||BD|}{|BC||AD|} = \frac{|ac||bd|}{|bc||ad|}$$

2.2.11. Mass Point Geometry (Barycentric Coordinates)

2.2.12. Spherical Geometry and Trigonometry (Non-Euclidean Geometry)



For a triangle made from three **great circle arcs of unit radius**:

a, b, c represent both (arc) lengths **and** angles subtended from the centre of the sphere O (in radians) i.e. $\angle AOB = c, \angle BOC = a, \angle COA = b$.

Spherical Cosine Rule: $\cos a = \cos b \cos c + \sin b \sin c \cos A$

Spherical Sine Rule: $\frac{\sin A}{\sin a} = \frac{\sin B}{\sin b} = \frac{\sin C}{\sin c}$

Inverse Cosine Rule: $\cos A = \sin B \sin C \cos a - \cos B \cos C$

Area of triangle $\triangle ABC$ (on sphere) = $A + B + C - \pi$ (Girard's Theorem)

Solid Angles: trihedral angles measured from O (units: steradians [sr]; full sphere = 4π sr.)

- Spherical triangle, ABC from O : $\Omega_o = A + B + C - \pi$
- Cone, vertex O , apex angle 2θ : $\Omega_o = 4\pi \sin^2 \frac{\theta}{2}$
- Irregular tetrahedron $OABC$: $\tan \frac{\Omega_o}{2} = \frac{\overline{OA} \cdot \overline{OB} \times \overline{OC}}{|\overline{OA}| |\overline{OB}| |\overline{OC}| + (\overline{OA} \cdot \overline{OB}) |\overline{OC}| + (\overline{OB} \cdot \overline{OC}) |\overline{OA}| + (\overline{OC} \cdot \overline{OA}) |\overline{OB}|}$
 $\cos \Omega_o = \frac{1}{3} (\cos \angle AOB + \cos \angle BOC + \cos \angle COA)$

The solid angle of a polyhedron is the sum of solid angles of the non-overlapping tetrahedra sharing the vertex (e.g. compute from Delauney tetrahedral mesh of 3D point cloud).

2.2.13. Hyperbolic Geometry (Non-Euclidean, Lobachevsky Geometry)

Klein disk model (projective model): points represented as being inside a unit disk.

2.3. 2D Coordinate Geometry

2.3.1. Coordinates

A point P can lie in the xy Cartesian coordinate plane with origin O (frame xOy).

The coordinates of P can be written as $P(x, y)$. (x : abscissa of P , y : ordinate of P)

2.3.2. Equations of Lines

Gradient-Intercept:

$$y = mx + c$$

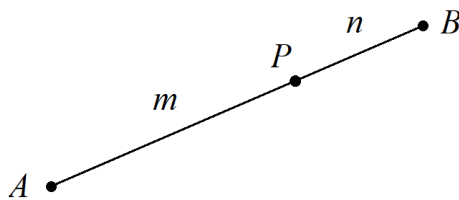
Point-Slope:

$$y - y_1 = m(x - x_1)$$

Two-point Interpolation:

$$\frac{y - y_1}{x - x_1} = \frac{y_2 - y_1}{x_2 - x_1}$$

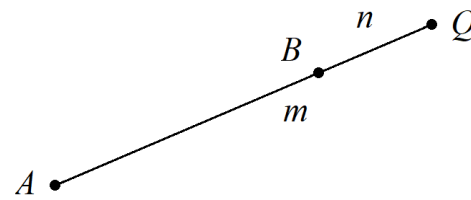
2.3.3. Ratio Division of a Line Segment



Internal Division:

If $|AP| : |PB| = m : n$, then

$$P = \left(\frac{nx_A + mx_B}{m + n}, \frac{ny_A + my_B}{m + n} \right)$$



External Division:

If $|AQ| : |BQ| = m : n$, then

$$Q = \left(\frac{mx_B - nx_A}{m + n}, \frac{my_B - ny_A}{m + n} \right)$$

2.3.4. Tangential Angle and Angle Between Lines

For a tangent line of gradient m , the angle with the x -axis is ψ , where

$$m = \frac{dy}{dx} = \tan \psi$$

$$\Delta\psi = \tan^{-1} \left| \frac{m_1 - m_2}{1 + m_1 m_2} \right|$$

2.3.5. Parallel and Perpendicular Lines

If lines L_1 and L_2 have gradients m_1 and m_2 then

$$m_1 = m_2 \Leftrightarrow L_1 \parallel L_2 \quad \text{and} \quad m_1 m_2 = -1 \Leftrightarrow L_1 \perp L_2.$$

2.3.6. Area of an Irregular Plane Polygon From Coordinates

Shoelace formula: if an n -sided irregular polygon has vertices (ordered cyclically anticlockwise) at coordinates $(x_1, y_1), (x_2, y_2), \dots, (x_n, y_n)$ then the area enclosed is

$$A = \frac{1}{2} \sum_{i=1}^n \begin{vmatrix} x_i & x_{i+1} \\ y_i & y_{i+1} \end{vmatrix} = \frac{1}{2} \left(\begin{vmatrix} x_1 & x_2 \\ y_1 & y_2 \end{vmatrix} + \begin{vmatrix} x_2 & x_3 \\ y_2 & y_3 \end{vmatrix} + \dots + \begin{vmatrix} x_n & x_1 \\ y_n & y_1 \end{vmatrix} \right)$$

In the case of a triangle, $n = 3$, this is equivalent to

$$A = \frac{1}{2} \begin{vmatrix} x_1 & y_1 & 1 \\ x_2 & y_2 & 1 \\ x_3 & y_3 & 1 \end{vmatrix} = \frac{1}{2} (x_1y_2 - x_2y_1 + x_2y_3 - x_3y_2 + x_3y_1 - x_1y_3)$$

2.3.7. Collinearity of Points and Concurrency of Lines

Collinearity: three points $(x_1, y_1), (x_2, y_2), (x_3, y_3)$ lie on the same line if

$$\begin{vmatrix} x_1 & y_1 & 1 \\ x_2 & y_2 & 1 \\ x_3 & y_3 & 1 \end{vmatrix} = 0 \quad \Leftrightarrow \quad x_1y_2 - x_2y_1 + x_2y_3 - x_3y_2 + x_3y_1 - x_1y_3 = 0.$$

Concurrency: three lines $a_1x + b_1y + c_1 = 0$, $a_2x + b_2y + c_2 = 0$ and $a_3x + b_3y + c_3 = 0$ intersect at a single point if

$$\begin{vmatrix} a_1 & b_1 & c_1 \\ a_2 & b_2 & c_2 \\ a_3 & b_3 & c_3 \end{vmatrix} = 0 \quad \Leftrightarrow \quad a_1(b_2c_3 - b_3c_2) - b_1(a_2c_3 - a_3c_2) + c_1(a_2b_3 - a_3b_2) = 0$$

In homogeneous coordinates (Section 4.2.3), there is a duality between collinearity of points (X, Y, Z) and lines (A, B, C) .

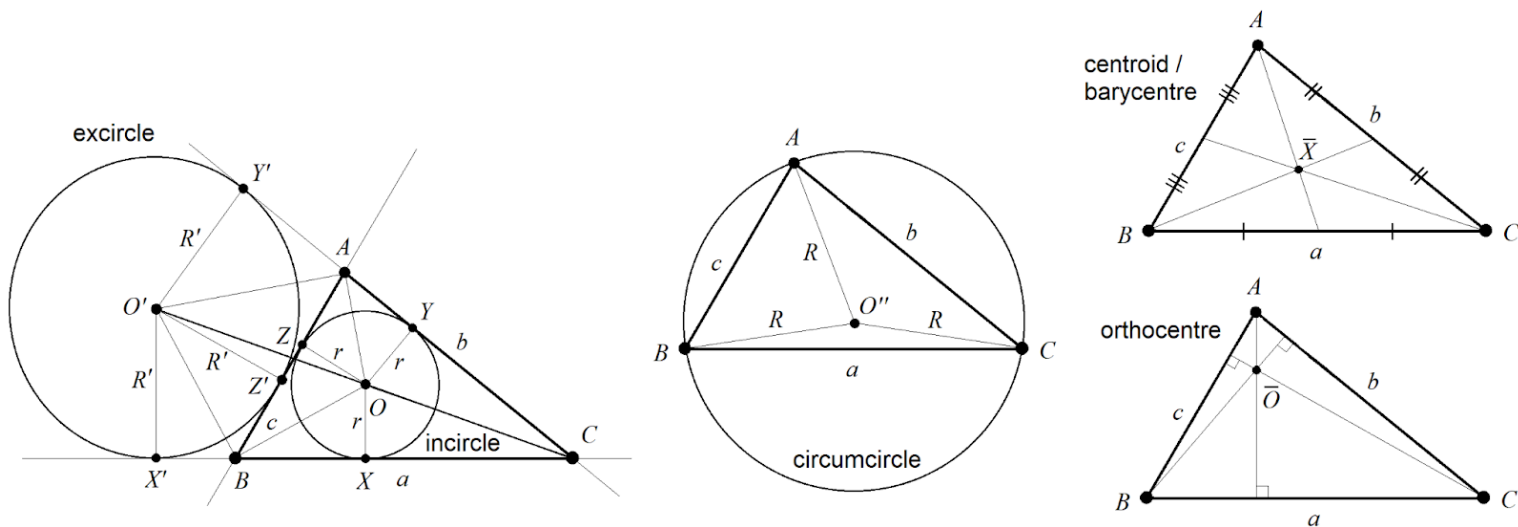
2.3.8. Equation of a Circle

For a circle with centre (x_0, y_0) and radius r , the equation is $(x - x_0)^2 + (y - y_0)^2 = r^2$

Standard form: $\frac{(x - x_0)^2}{r^2} + \frac{(y - y_0)^2}{r^2} = 1$

2.3.9. Centres of a Triangle: Incentre, Excentres, Circumcentre, Barycentre, Orthocentre

For a triangle with vertices $A = (x_A, y_A)$, $B = (x_B, y_B)$, $C = (x_C, y_C)$ opposite sides of length a, b, c :



Incentre: $O = \left(\frac{ax_A + bx_B + cx_C}{a + b + c}, \frac{ay_A + by_B + cy_C}{a + b + c} \right)$ Inradius: $r = \frac{2 \Delta_{ABC}}{a + b + c}$

Excentre (of C): $O' = \left(\frac{ax_A + bx_B - cx_C}{a + b - c}, \frac{ay_A + by_B - cy_C}{a + b - c} \right)$ Exradius: $R' = \frac{2 \Delta_{ABC}}{a + b - c}$ (on AB)

Circumcentre: $O'' = \left(\frac{(x_A^2 + y_A^2)(y_B - y_C) + (x_B^2 + y_B^2)(y_C - y_A) + (x_C^2 + y_C^2)(y_A - y_B)}{2(x_A(y_B - y_C) + x_B(y_C - y_A) + x_C(y_A - y_B))}, \frac{(x_A^2 + y_A^2)(x_C - x_B) + (x_B^2 + y_B^2)(x_A - x_C) + (x_C^2 + y_C^2)(x_B - x_A)}{2(x_A(y_B - y_C) + x_B(y_C - y_A) + x_C(y_A - y_B))} \right)$

Circumradius: $R = \frac{abc}{4 \Delta_{ABC}}$

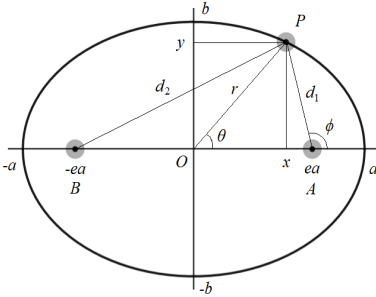
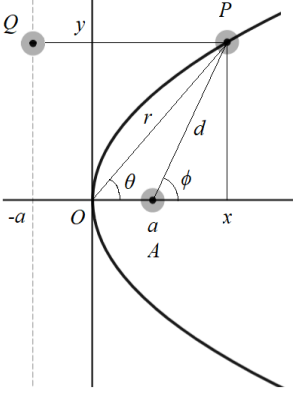
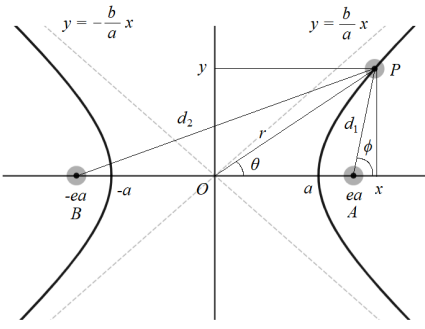
Barycentre: $\bar{X} = \left(\frac{x_A + x_B + x_C}{3}, \frac{y_A + y_B + y_C}{3} \right)$ $\frac{2}{3}$ along any median line from vertex

Orthocentre: $\bar{O} = \left(\frac{x_A \tan A + x_B \tan B + x_C \tan C}{\tan A + \tan B + \tan C}, \frac{y_A \tan A + y_B \tan B + y_C \tan C}{\tan A + \tan B + \tan C} \right)$ (A, B, C : angles)

- Every triangle has a unique incentre, circumcentre, barycentre (centroid) and orthocentre.
- Every triangle has **three** distinct excentres.
- The size order of the excircles follows the size order of the lengths of the tangent edges, or equivalently, the size order of the opposite internal angles.
- The incentre, excentre and external point (O, O', C) are collinear.
- Area relations for incircle and excircle:
 $\Delta_{ABC} = \Delta_{AOB} + \Delta_{BOC} + \Delta_{COA} = \frac{1}{2}ar + \frac{1}{2}br + \frac{1}{2}cr = sr$
 $\Delta_{ABC} = \Delta_{O'BC} + \Delta_{O'AC} - \Delta_{O'AB} = \frac{1}{2}aR' + \frac{1}{2}bR' - \frac{1}{2}cR' = (s - c)R'$

- The Apollonius circle to the three excircles is internally tangent to all three and has radius $\frac{r^2 + s^2}{4r}$.

2.3.10. Properties of Conic Sections

	Ellipse	Parabola	Hyperbola
Diagram			
Cartesian equation	$\frac{x^2}{a^2} + \frac{y^2}{b^2} = 1$	$y^2 = 4ax$	$\frac{x^2}{a^2} - \frac{y^2}{b^2} = 1$
Polar equations	$r = \frac{b}{\sqrt{1 - e^2 \cos^2 \theta}}$ (pole at O) $d_1 = \frac{b^2}{a(1 + e \cos \phi)}$ (pole at A)	$r = \frac{4a \cos \theta}{\sin^2 \theta}$ (pole at O) $d = \frac{2a}{1 - \cos \phi}$ (pole at A)	$r = \frac{b}{\sqrt{e^2 \cos^2 \theta - 1}}$ (pole at O) $d_1 = \frac{b^2}{a(1 - e \cos \phi)}$ (pole at A)
Parametric equations	$x = a \cos t, y = b \sin t$ $x = \pm a \operatorname{sech} t, y = b \tanh t$	$x = \frac{1}{4a} t^2, y = t$	$x = a \sec t, y = b \tan t$ $x = \pm a \cosh t, y = b \sinh t$
Definitions	O : centre A, B : focal points (foci) a : semi-major axis b : semi-minor axis e : eccentricity	O : vertex A : focal point (focus) a : focal length e : eccentricity $x = -a$: directrix	O : centre A, B : focal points (foci) a : semi-major axis e : eccentricity $y = \pm \frac{b}{a}x$: asymptotes
Eccentricity	$e^2 = 1 - \left(\frac{b}{a}\right)^2; \quad 0 \leq e < 1$	$e = 1$	$e^2 = 1 + \left(\frac{b}{a}\right)^2; \quad e > 1$
Plane-cone intersection	Plane gradient shallower than the cone.	Plane gradient equals that of the cone.	Plane gradient steeper than the cone.
Reflective property	Internal rays on AP are reflected into B .	Incident rays on PQ are reflected into A .	External rays parallel to AP are reflected towards B .
Distance property	$ AP + BP = d_1 + d_2 = 2a$	$ AP = PQ = d = x + a$	$ AP - BP = d_1 - d_2 = 2a$

2.3.11. Conic-Line Intersections

For a line $L: y = mx + c$, and conics translated to the origin given by

$$\text{ellipse } E: \frac{x^2}{a^2} + \frac{y^2}{b^2} = 1, \quad \text{hyperbola } H: \frac{x^2}{a^2} - \frac{y^2}{b^2} = 1, \quad \text{parabola } P: y^2 = 4ax$$

Then L makes either zero, one or two intersections with any conic, with x -coordinates of all intersections at the roots of

- Ellipse-line: $(a^2 m^2 + b^2)x^2 + 2a^2 mc x + a^2(c^2 - b^2) = 0$
- Hyperbola-line: $(a^2 m^2 - b^2)x^2 + 2a^2 mc x + a^2(c^2 + b^2) = 0$
- Parabola-line: $m^2 x^2 + (2mc - 4a)x + c^2 = 0$

Condition for tangency: discriminant of the quadratic is zero.

2.3.12. Canonical Matrix Equation of Conic Sections (Homogeneous Coordinates)

Any conic section plane curve can be represented by the equation

$$A x^2 + B y^2 + 2C xy + 2D x + 2E y + F = 0$$

which can be represented in homogeneous coordinates (see Section 4.2.3) as

$$\mathbf{x}^T \mathbf{Q} \mathbf{x} = 0$$

where $\mathbf{x} = \begin{bmatrix} x \\ y \\ 1 \end{bmatrix}$ and $\mathbf{Q} = \begin{bmatrix} A & B & D \\ B & C & E \\ D & E & F \end{bmatrix}$ is a symmetric 3×3 matrix.

For the analogous forms of conics in 3D (quadrics), see Section 2.4.10-11.

Equations from Section 2.4.12-14 (matrix transformations, line intersections, SVD of matrix) remain valid in 2D.

2.3.13. Radius of Curvature

A curve in 2D space has a curvature κ , with associated circular radius of curvature R , where

$$\text{Cartesian, } y(x): \quad R = \frac{(1 + (y')^2)^{3/2}}{y''} \quad (x: \text{ independent var, } y: \text{ dependent var})$$

$$\text{Parametric, } \{x(t), y(t)\}: \quad R = \frac{((x')^2 + (y')^2)^{3/2}}{x'y'' - x''y'} \quad (t: \text{ parameter})$$

$$\text{Polar, } r(\theta): \quad R = \frac{(r^2 + (r')^2)^{3/2}}{r^2 + 2(r')^2 - rr''} \quad (r: \text{ radial distance, } \theta: \text{ polar angle})$$

$$\text{Intrinsic, } s(\psi): \quad R = s' \quad (s: \text{ arc length, } \psi: \text{ tangential angle})$$

where f' is the derivative with respect to its argument.

2.3.14. Areas, Arc Lengths and Centres of Mass for Plane Curves by Integration

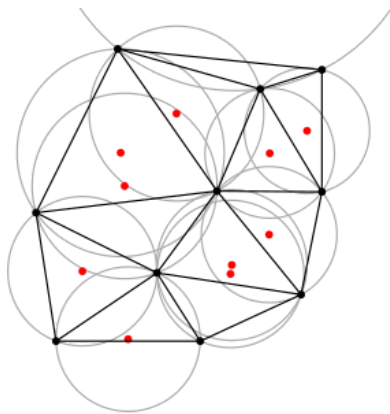
	Area A	Arc Length s	Centre of Mass (of plane region under curve)
Cartesian	$\int_a^b y \, dx$	$\int_a^b \sqrt{1 + \left(\frac{dy}{dx}\right)^2} \, dx$	$\bar{x} = \frac{1}{A} \int_a^b xy \, dx, \quad \bar{y} = \frac{1}{2A} \int_a^b y^2 \, dx$
Parametric	$\int_{t_1}^{t_2} y \frac{dx}{dt} \, dt$	$\int_{t_1}^{t_2} \sqrt{\left(\frac{dx}{dt}\right)^2 + \left(\frac{dy}{dt}\right)^2} \, dt$	$\bar{x} = \frac{1}{A} \int_{t_1}^{t_2} xy \frac{dx}{dt} \, dt, \quad \bar{y} = \frac{1}{2A} \int_{t_1}^{t_2} y^2 \frac{dx}{dt} \, dt$
Polar	$\frac{1}{2} \int_{\theta_1}^{\theta_2} r^2 \, d\theta$	$\int_{\theta_1}^{\theta_2} \sqrt{r^2 + \left(\frac{dr}{d\theta}\right)^2} \, d\theta$	(use Cartesian substitutions)

2.3.15. Tessellation (Tiling) and Partitioning of the Plane

Tessellation uses a fixed set of tile shapes to tile the plane completely, using only rotation and translation of the tiles to form unit cells which span the plane.

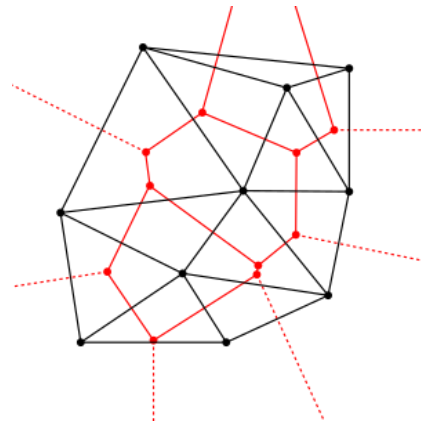
Delaunay triangulation (DT) is a mapping from a set of vertex points $\{P\}_i$ to a set of triangles $\{T\}_j$ connecting the points $\{P\}_i$ such that no point in $\{P\}_i$ is inside any triangle in the set. DT results in the maximisation of the smallest angle in every triangle. The convex hull of the vertices is the smallest convex polygon containing all vertices. If there are n vertices, of which h are on the convex hull, then there are $2n - 2 - h$ triangles and $3n - 3 - h$ edges on the Delaunay triangulation.

The **Voronoi diagram** of a set of vertex points $\{P\}_i$ is a partitioning of the plane into convex irregular polygonal cells. The vertices of these polygons are the circumcentres of the corresponding Delaunay triangles (duality). Gradually expanding circles at equal rates from each vertex produces the Voronoi diagram when any two circles 'collide'. The closest vertex to any given point is the vertex contained within the cell.



Delaunay Triangulation

vertices in black, circumcentres in red



Voronoi Diagram

vertices in black, cells (partitions) in red

The Delaunay and Voronoi partitions are useful in modelling a wide variety of phenomena. They can also be extended to higher dimensions.

The Bowyer-Watson algorithm computes the Delaunay triangulation of a vertex set.

2.4. Vectors and 3D Geometry

2.4.1. Direction Cosines

If a vector $\mathbf{a} = (a_x, a_y, a_z)$ makes angles α, β, γ with an orthogonal set of x -, y - and z -axes, then:

- the quantities $\cos \alpha, \cos \beta$ and $\cos \gamma$ are the direction cosines of \mathbf{a} .
- $\cos \alpha = a_x / |\mathbf{a}|$, etc.
- $\mathbf{a} = |\mathbf{a}| (\cos \alpha \mathbf{i} + \cos \beta \mathbf{j} + \cos \gamma \mathbf{k})$.

The direction cosines represent the component of a unit vector along \mathbf{a} parallel to each axis.

2.4.2. Scalar Product (Dot Product) and Vector Product (Cross Product) Algebra

The scalar and vector products are defined by components as

$$\mathbf{a} \cdot \mathbf{b} = \mathbf{a}^\top \mathbf{b} = \sum_i a_i b_i = a_x b_x + a_y b_y + a_z b_z$$

$$\mathbf{a} \times \mathbf{b} = \begin{vmatrix} \mathbf{i} & \mathbf{j} & \mathbf{k} \\ a_x & a_y & a_z \\ b_x & b_y & b_z \end{vmatrix} = (a_y b_z - a_z b_y) \mathbf{i} + (a_z b_x - a_x b_z) \mathbf{j} + (a_x b_y - a_y b_x) \mathbf{k}$$

In terms of magnitudes and angles,

$$\mathbf{a} \cdot \mathbf{b} = |\mathbf{a}| |\mathbf{b}| \cos \theta \qquad \mathbf{a} \times \mathbf{b} = |\mathbf{a}| |\mathbf{b}| \sin \theta \hat{\mathbf{n}}$$

Commutative / anticommutative properties:

$$\mathbf{a} \cdot \mathbf{b} = \mathbf{b} \cdot \mathbf{a} \qquad \mathbf{a} \times \mathbf{b} = -\mathbf{b} \times \mathbf{a}$$

Useful identities: (for the triple product identities see Section 2.4.4)

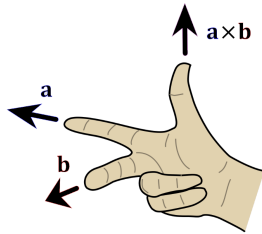
$$|\mathbf{a} \times \mathbf{b}|^2 + |\mathbf{a} \cdot \mathbf{b}|^2 = (|\mathbf{a}| |\mathbf{b}|)^2 \qquad \text{(Lagrange's identity)}$$

$$|\mathbf{a} \pm \mathbf{b}|^2 = \mathbf{a} \cdot \mathbf{a} + \mathbf{b} \cdot \mathbf{b} \pm 2(\mathbf{a} \cdot \mathbf{b}) \qquad \text{(from cosine rule)}$$

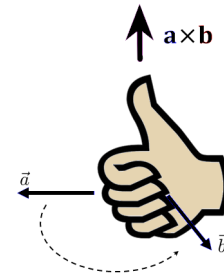
$$\mathbf{a} \times (\mathbf{b} \times \mathbf{c}) + \mathbf{c} \times (\mathbf{a} \times \mathbf{b}) + \mathbf{b} \times (\mathbf{c} \times \mathbf{a}) = \mathbf{0} \qquad \text{(Jacobi identity)}$$

$$(\mathbf{a} \times \mathbf{b}) \cdot (\mathbf{c} \times \mathbf{d}) = (\mathbf{a} \cdot \mathbf{c})(\mathbf{b} \cdot \mathbf{d}) - (\mathbf{b} \cdot \mathbf{c})(\mathbf{a} \cdot \mathbf{d}) \qquad \text{(Binet-Cauchy identity)}$$

2.4.3. Right-Hand Rules for Vector Product Orientation



Right hand rule:

Right hand grip rule:
for rotations

2.4.4. Triple Products

Scalar triple product:

$$\begin{aligned} \mathbf{a} \cdot (\mathbf{b} \times \mathbf{c}) &= \begin{vmatrix} a_x & a_y & a_z \\ b_x & b_y & b_z \\ c_x & c_y & c_z \end{vmatrix} = \begin{vmatrix} a_x & b_x & c_x \\ a_y & b_y & c_y \\ a_z & b_z & c_z \end{vmatrix} \\ &= \mathbf{b} \cdot (\mathbf{c} \times \mathbf{a}) = \mathbf{c} \cdot (\mathbf{a} \times \mathbf{b}) \\ &= -\mathbf{a} \cdot (\mathbf{c} \times \mathbf{b}) = -\mathbf{c} \cdot (\mathbf{b} \times \mathbf{a}) = -\mathbf{b} \cdot (\mathbf{a} \times \mathbf{c}) \end{aligned}$$

Vector triple product:

$$\begin{aligned} \mathbf{a} \times (\mathbf{b} \times \mathbf{c}) &= (\mathbf{a} \cdot \mathbf{c})\mathbf{b} - (\mathbf{a} \cdot \mathbf{b})\mathbf{c} \\ (\mathbf{a} \times \mathbf{b}) \times \mathbf{c} &= (\mathbf{a} \cdot \mathbf{c})\mathbf{b} - (\mathbf{b} \cdot \mathbf{c})\mathbf{a} \end{aligned}$$

2.4.5. Vector Products for Areas and Volumes

Area of triangle spanned by \mathbf{a} and \mathbf{b} : $A = \frac{1}{2} |\mathbf{a} \times \mathbf{b}|$

Volume of parallelepiped spanned by \mathbf{a} , \mathbf{b} and \mathbf{c} : $V = |\mathbf{a} \cdot (\mathbf{b} \times \mathbf{c})|$

Volume of tetrahedron spanned by \mathbf{a} , \mathbf{b} and \mathbf{c} : $V = \frac{1}{6} |\mathbf{a} \cdot (\mathbf{b} \times \mathbf{c})|$

Volume of a polyhedron of N faces, triangulated as $\bigcap_{i=1}^N \{\mathbf{a}_i, \mathbf{b}_i, \mathbf{c}_i\}$: $V = \frac{1}{6} \left| \sum_{i=1}^N \mathbf{a}_i \cdot (\mathbf{b}_i \times \mathbf{c}_i) \right|$

2.4.6. Equations of Lines and Planes

Line ($\mathbf{p} = [p_x \ p_y \ p_z]^T$: point on line, $\mathbf{d} = [d_x \ d_y \ d_z]^T$: direction vector):

$$\frac{x-p_x}{d_x} = \frac{y-p_y}{d_y} = \frac{z-p_z}{d_z} (= t) \quad \mathbf{r} = \mathbf{p} + t \mathbf{d} \quad (\mathbf{r} - \mathbf{p}) \times \mathbf{d} = \mathbf{0}$$

scalar (if not parallel to any axis) parametric non-parametric

Plane (\mathbf{p} : point on plane, $\{\mathbf{a}, \mathbf{b}\}$: vectors in plane, $\mathbf{n} = [n_x \ n_y \ n_z]^T$: normal vector to plane):

$$n_x x + n_y y + n_z z = d \quad \mathbf{r} = \mathbf{p} + s \mathbf{a} + t \mathbf{b} \quad (\mathbf{r} - \mathbf{p}) \cdot \mathbf{n} = 0$$

scalar parametric non-parametric

Plane-Plane Intersection: $\Pi_1: (\mathbf{r} - \mathbf{p}_1) \cdot \mathbf{n}_1 = 0$ and $\Pi_2: (\mathbf{r} - \mathbf{p}_2) \cdot \mathbf{n}_2 = 0$ intersect in a line with direction vector given by $(\mathbf{n}_1 \times \mathbf{n}_2)$. In a view parallel to this vector, the two planes are projected as straight lines parallel to all viewing planes, which can simplify problems.

2.4.7. Shortest Distances Between Points, Planes and Lines

Point \mathbf{c} to line $\mathbf{r} = \mathbf{p} + t \mathbf{d}$:

$$d_{\min} = |(\mathbf{c} - \mathbf{p}) \times \mathbf{d}|$$

Point \mathbf{c} to plane $(\mathbf{r} - \mathbf{p}) \cdot \mathbf{n} = 0$:

$$d_{\min} = \frac{|(\mathbf{c} - \mathbf{p}) \cdot \mathbf{n}|}{|\mathbf{n}|}$$

Skew lines $\mathbf{r}_1 = \mathbf{p}_1 + t \mathbf{d}_1$ and $\mathbf{r}_2 = \mathbf{p}_2 + t \mathbf{d}_2$:

$$d_{\min} = \frac{|(\mathbf{p}_1 - \mathbf{p}_2) \cdot (\mathbf{d}_1 \times \mathbf{d}_2)|}{|\mathbf{d}_1 \times \mathbf{d}_2|}$$

To find the point(s) of closest approach, define generalised point(s) (\mathbf{r}_1 and \mathbf{r}_2) on the object(s) in parametric form and assert perpendicularity: solve $(\mathbf{r}_1 - \mathbf{r}_2) \cdot \mathbf{d}_1 = 0$ and $(\mathbf{r}_1 - \mathbf{r}_2) \cdot \mathbf{d}_2 = 0$ for parameters t_1 and t_2 .

Shortest distance to an (external) sphere is shortest distance to its centre, minus the radius of the sphere.

Shortest distance to an (external) cylinder is the shortest distance to its axis, minus the radius of the cylinder.

2.4.8. Vector Equations of Curved Surfaces

Sphere, centre \mathbf{c} , radius R :

$$(\mathbf{r} - \mathbf{c}) \cdot (\mathbf{r} - \mathbf{c}) = R^2 \quad \text{or} \quad |\mathbf{r} - \mathbf{c}| = R$$

Double cone, axis \mathbf{n} , opening half-angle θ :

$$(\mathbf{r} \cdot \mathbf{n})^2 = \mathbf{r} \cdot \mathbf{r} \cos^2 \theta \quad \text{or} \quad \mathbf{r} \cdot \mathbf{n} = |\mathbf{r}| \cos \theta$$

Cylinder, axis \mathbf{n} , radius R :

$$(\mathbf{r} \times \mathbf{n}) \cdot (\mathbf{r} \times \mathbf{n}) = R^2 \quad \text{or} \quad |\mathbf{r} \times \mathbf{n}| = R$$

Ellipsoid of revolution,
foci \mathbf{f}_1 and \mathbf{f}_2 , semi-major axis a :

$$|\mathbf{r} - \mathbf{f}_1| + |\mathbf{r} - \mathbf{f}_2| = 2a$$

Hyperboloid of revolution (two sheets),
foci \mathbf{f}_1 and \mathbf{f}_2 , semi-major axis a :

$$||\mathbf{r} - \mathbf{f}_1| - |\mathbf{r} - \mathbf{f}_2|| = 2a$$

2.4.9. Surfaces and Volumes of Revolution and their Centres of Mass

For a plane curve rotated 360° about a horizontal axis to produce an axisymmetric solid or surface (shell), properties are:

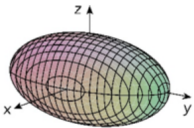
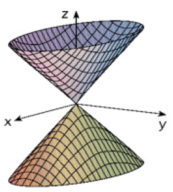
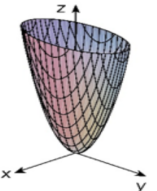
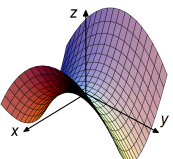
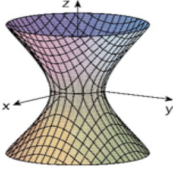
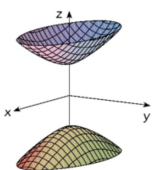
	Volume	COM (solid)	Surface area	COM (shell)
Cartesian, $y(x)$ revolving around the x -axis	$\pi \int_a^b y^2 dx$	$\frac{\int_a^b xy^2 dx}{\int_a^b y^2 dx}$	$2\pi \int_a^b y \sqrt{1 + (y')^2} dx$	$\frac{\int_a^b y^2 \sqrt{1 + (y')^2} dx}{\int_a^b y \sqrt{1 + (y')^2} dx}$
Parametric, $\{x(t), y(t)\}$ revolving around the x -axis	$\pi \int_a^b y^2 x' dt$	$\frac{\int_a^b xy^2 x' dt}{\int_a^b y^2 x' dt}$	$2\pi \int_a^b y \sqrt{(x')^2 + (y')^2} dt$	$\frac{\int_a^b x'y^2 \sqrt{(x')^2 + (y')^2} dt}{\int_a^b x'y \sqrt{(x')^2 + (y')^2} dt}$

The COM (centre of mass) is given as its x -coordinate, \bar{x} , and assumes uniform density. The other ordinates are $\bar{y} = \bar{z} = 0$.

For COMs of common geometric figures, see Section 6.3.

For Pappus' theorems for solids of revolution and solids swept along a curve, see Section 2.1.5.

2.4.10. Quadric Surfaces (3D Extensions of Conic Sections)

Surface	Cartesian	Parametric	Canonical Matrix Q
 <p>Ellipsoid</p>	$\frac{x^2}{a^2} + \frac{y^2}{b^2} + \frac{z^2}{c^2} = 1$ <p>a, b, c: semi-axes</p>	$\begin{aligned} x &= a \cos u \sin v \\ y &= b \sin u \sin v \\ z &= c \cos v \end{aligned}$ <p>$0 \leq u < 2\pi, 0 \leq v < \pi$</p>	$\begin{bmatrix} \frac{1}{a^2} & 0 & 0 & 0 \\ 0 & \frac{1}{b^2} & 0 & 0 \\ 0 & 0 & \frac{1}{c^2} & 0 \\ 0 & 0 & 0 & -1 \end{bmatrix}$
 <p>Cone</p>	$\frac{z^2}{c^2} = \frac{x^2}{a^2} + \frac{y^2}{b^2}$ <p>$\frac{c}{a}, \frac{c}{b}$: slopes in xz and yz planes</p>	$\begin{aligned} x &= av \cos u \\ y &= bv \sin u \\ z &= cv \end{aligned}$ <p>$0 \leq u < 2\pi$</p>	$\begin{bmatrix} \frac{1}{a^2} & 0 & 0 & 0 \\ 0 & \frac{1}{b^2} & 0 & 0 \\ 0 & 0 & -\frac{1}{c^2} & 0 \\ 0 & 0 & 0 & 0 \end{bmatrix}$
 <p>Elliptic Paraboloid</p>	$\frac{z}{c} = \frac{x^2}{a^2} + \frac{y^2}{b^2}$ <p>$\sqrt{\frac{z}{c}} a, \sqrt{\frac{z}{c}} b$: semi-axes of ellipse cross-section at z</p>	$\begin{aligned} x &= av \cos u \\ y &= bv \sin u \\ z &= cv^2 \end{aligned}$ <p>$0 \leq u < 2\pi, v \geq 0$</p>	$\begin{bmatrix} \frac{1}{a^2} & 0 & 0 & 0 \\ 0 & \frac{1}{b^2} & 0 & 0 \\ 0 & 0 & 0 & -\frac{1}{2c} \\ 0 & 0 & -\frac{1}{2c} & 0 \end{bmatrix}$
 <p>Hyperbolic Paraboloid</p>	$\frac{z}{c} = \frac{x^2}{a^2} - \frac{y^2}{b^2}$ <p>$\sqrt{\frac{z}{c}} a$: focal length of hyperbola cross-section at z</p>	$\begin{aligned} x &= av \cosh u \\ y &= bv \sinh u \\ z &= cv^2, \end{aligned}$ <p>(only for $\frac{y}{x} \leq \frac{b}{a}$)</p>	$\begin{bmatrix} \frac{1}{a^2} & 0 & 0 & 0 \\ 0 & -\frac{1}{b^2} & 0 & 0 \\ 0 & 0 & 0 & -\frac{1}{2c} \\ 0 & 0 & -\frac{1}{2c} & 0 \end{bmatrix}$
 <p>Hyperboloid, one sheet</p>	$\frac{x^2}{a^2} + \frac{y^2}{b^2} - \frac{z^2}{c^2} = 1$ <p>$\sqrt{1 + \frac{z^2}{c^2}} a, \sqrt{1 + \frac{z^2}{c^2}} b$: semi-axes of ellipse cross-section at z</p>	$\begin{aligned} x &= a \cos u \cosh v \\ y &= b \sin u \cosh v \\ z &= c \sinh v \end{aligned}$ <p>$0 \leq u < 2\pi$</p>	$\begin{bmatrix} \frac{1}{a^2} & 0 & 0 & 0 \\ 0 & \frac{1}{b^2} & 0 & 0 \\ 0 & 0 & -\frac{1}{c^2} & 0 \\ 0 & 0 & 0 & -1 \end{bmatrix}$
 <p>Hyperboloid, two sheets</p>	$-\frac{x^2}{a^2} - \frac{y^2}{b^2} + \frac{z^2}{c^2} = 1$ <p>$\sqrt{\frac{z^2}{c^2} - 1} a, \sqrt{\frac{z^2}{c^2} - 1} b$: semi-axes of ellipse cross-section at z</p>	$\begin{aligned} x &= a \cos u \sinh v \\ y &= b \sin u \sinh v \\ z &= \pm c \cosh v \end{aligned}$ <p>$0 \leq u < \pi$</p>	$\begin{bmatrix} -\frac{1}{a^2} & 0 & 0 & 0 \\ 0 & -\frac{1}{b^2} & 0 & 0 \\ 0 & 0 & \frac{1}{c^2} & 0 \\ 0 & 0 & 0 & -1 \end{bmatrix}$

2.4.11. Quadrics in Homogeneous Coordinates

Any quadric surface can be represented by the equation

$$a_{xx}x^2 + a_{yy}y^2 + a_{zz}z^2 + a_1 + 2a_{xy}xy + 2a_{yz}yz + 2a_{xz}xz + 2a_x x + 2a_y y + 2a_z z = 0$$

which can be represented in matrix form as $\mathbf{x}^T \mathbf{Q} \mathbf{x} = 0$ (canonical form) where

$$\mathbf{x} = \begin{bmatrix} x \\ y \\ z \\ 1 \end{bmatrix} \quad \text{and} \quad \mathbf{Q} = \begin{bmatrix} a_{xx} & a_{xy} & a_{xz} & a_x \\ a_{xy} & a_{yy} & a_{yz} & a_y \\ a_{xz} & a_{yz} & a_{zz} & a_z \\ a_x & a_y & a_z & a_1 \end{bmatrix} \quad \text{is a symmetric } 4 \times 4 \text{ matrix.}$$

Quadric-Line Intersection (Raytracing of Quadric Surfaces)

A line $\mathbf{x} = \mathbf{p} + \lambda \mathbf{n}$ intersects a quadric $\mathbf{x}^T \mathbf{Q} \mathbf{x} = 0$ at values of λ satisfying the quadratic

$$(\mathbf{n}^T \mathbf{Q} \mathbf{n}) \lambda^2 + (2 \mathbf{n}^T \mathbf{Q} \mathbf{p}) \lambda + (\mathbf{p}^T \mathbf{Q} \mathbf{p}) = 0.$$

A quadric generally intersects a **plane** in a conic section curve in the plane.

Affine Transformations on Quadric Surfaces

Transformations can be applied to a quadric using

$$\mathbf{Q}' = (\mathbf{R}^{-1})^T \mathbf{Q} \mathbf{R}^{-1} \quad \text{where } \mathbf{R} \text{ is a } 4 \times 4 \text{ affine transformation matrix mapping a quadric represented by } \mathbf{Q} \text{ into a quadric represented by } \mathbf{Q}'$$

For the general form of the affine transformation matrix \mathbf{R} , see Section 4.2.3.

Singular Value Decomposition of a Quadric Canonical Matrix

For any quadric $\mathbf{x}^T \mathbf{Q}' \mathbf{x} = 0$, define the matrix \mathbf{M} as the 3×3 matrix formed from the first three rows and columns of \mathbf{Q}' (i.e. $\mathbf{M} : \mathbf{Q} \rightarrow \mathbf{Q}'$ is a linear transformation matrix from a quadric \mathbf{Q} aligned with the $\{\mathbf{i}, \mathbf{j}, \mathbf{k}\}$ axes into the quadric represented by \mathbf{Q}' translated to the origin).

If the singular value decomposition (SVD, see Section 4.3.7) is written as $\mathbf{M} = \mathbf{U}\mathbf{\Sigma}\mathbf{V}^T$, then:

- The columns of \mathbf{U} represent the normalised principal axes of \mathbf{Q}' .
- The columns of \mathbf{V} (rows of \mathbf{V}^T) represent the vectors on the **original** quadric \mathbf{Q} which are mapped to the principal axes of \mathbf{Q}' .
- The singular values are the linear scale factors in the corresponding axes.

M3. CALCULUS

3.1. Limits and Numerical Methods

3.1.1. Formal Definition of Limits

Let $f(x)$ be defined for all real $x \neq a$ over an open interval containing a . We say that

$$\lim_{x \rightarrow a} f(x) = L \quad (\text{the (two-sided) limit of } f(x) \text{ as } x \text{ approaches } a \text{ is } L)$$

if, for every $\varepsilon > 0$, there exists some $\delta > 0$, such that if $0 < |x - a| < \delta$, then $|f(x) - L| < \varepsilon$:

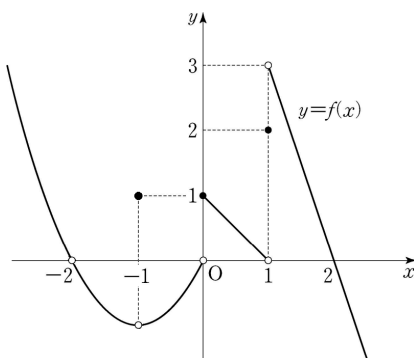
$$\lim_{x \rightarrow a} f(x) = L \Leftrightarrow (\forall \varepsilon > 0)(\exists \delta > 0)(\forall x \in D): (0 < |x - a| < \delta \Rightarrow |f(x) - L| < \varepsilon)$$

The one-sided limits are $\lim_{x \rightarrow a^+} f(x)$ (right-sided) and $\lim_{x \rightarrow a^-} f(x)$ (left-sided).

- For limits to infinity, the condition is $x > \delta$ (if a is $+\infty$) or $x < -\delta$ (if a is $-\infty$).
- For one-sided limits, use $0 < x - a < \delta$ (right-sided) or $0 < a - x < \delta$ (left-sided).

3.1.2. Limits at Discontinuities and Circle Notation

A graph of a function $y = f(x)$ should include open circles \circ for limiting values and closed circles \bullet for defined values. For example:



$$\lim_{x \rightarrow -2} f(x) = 0 \quad (\text{removable discontinuity})$$

$$\lim_{x \rightarrow -1} f(x) = -1 \quad \text{but} \quad f(-1) = 1 \quad (\text{jump discontinuity})$$

$$\lim_{x \rightarrow 0^-} f(x) = 0 \quad \text{and} \quad \lim_{x \rightarrow 0^+} f(x) = f(0) = 1$$

$$\lim_{x \rightarrow 1^-} f(x) = 0 \quad \text{and} \quad \lim_{x \rightarrow 1^+} f(x) = 3 \quad \text{and} \quad f(1) = 2$$

$$\lim_{x \rightarrow 0} f(x) \quad \text{and} \quad \lim_{x \rightarrow 1} f(x) \quad \text{do not exist.}$$

A discontinuity at $x = a$ is said to be removable if $\lim_{x \rightarrow a} f(x)$ exists. Continuity can be

established by including $x = a$ in the domain of $f(x)$, at which $f(a) := \lim_{x \rightarrow a} f(x) = \lim_{x \rightarrow a^\pm} f(x)$.

3.1.2. Standard Limits

Asymptotic ($x \rightarrow \infty$) growth order: $x^x \gg x! \gg a^x \gg x^a, x^2 \gg x \log x \gg x \gg \log x \gg 1$.

Limits to values:

- | | |
|---|---|
| <ul style="list-style-type: none"> • $\lim_{x \rightarrow \infty} (x^a p^x) = 0 \quad p < 1, \forall a \in \mathbb{R}.$ • $\lim_{x \rightarrow 0} (x^a \ln x) = 0, \quad \forall a > 0.$ • $\lim_{x \rightarrow 0} \frac{\sin ax}{x} = \lim_{x \rightarrow 0} \frac{\tan ax}{x} = a$ • $\lim_{x \rightarrow \infty} \left(\frac{a^x}{x!} \right) = 0.$ | <ul style="list-style-type: none"> • $\lim_{x \rightarrow a} \frac{x^n - a^n}{x - a} = na^{n-1}, \quad n \in \mathbb{Q}.$ • $\lim_{x \rightarrow 0} \frac{e^x - 1}{x} = 1.$ • $\lim_{x \rightarrow 0} \frac{a^x - 1}{x} = \ln a, \quad a > 0.$ |
|---|---|

Limits to functions:

- $\lim_{n \rightarrow \infty} \left(1 + \frac{x}{n} \right)^n = \lim_{n \rightarrow 0} (1 + nx)^{1/n} = e^x$
- $\lim_{n \rightarrow \infty} \cos^n \left(\frac{x}{\sqrt{n}} \right) = e^{-\frac{1}{2}x^2}$
- $\lim_{n \rightarrow \infty} \cosh^n \left(\frac{x}{\sqrt{n}} \right) = e^{\frac{1}{2}x^2}$

Derivative and integral as limit definitions:

- $\lim_{n \rightarrow \infty} n \left(f \left(x + \frac{a}{n} \right) - f(x) \right) = af'(x), \quad \forall a \in \mathbb{R} \quad \text{(forward difference)}$
- $\lim_{n \rightarrow \infty} \frac{1}{n} \sum_{k=0}^n f \left(\frac{k}{n} \right) = \int_0^1 f(x) \, dx \quad \text{(Riemann summation: rectangular rule)}$

For Stirling's formula involving asymptotic expressions for $n!$ and $\ln n!$, see Section 1.7.1.

3.1.3. Numerical Differentiation

Difference Quotients (finite difference approximations to derivatives):

- First derivative, forward difference: $f'(x) \approx \frac{f(x+h) - f(x)}{h} + O(h)$
- First derivative, backward difference: $f'(x) \approx \frac{f(x) - f(x-h)}{h} + O(h)$
- First derivative, central difference: $f'(x) \approx \frac{f(x+h) - f(x-h)}{2h} + O(h^2)$
- Second derivative, central difference: $f''(x) \approx \frac{f(x+h) - 2f(x) + f(x-h)}{h^2} + O(h^2)$

For partial derivatives (central differences):

- First partials: $\frac{\partial f(x, y)}{\partial x} \approx \frac{f(x+h, y) - f(x-h, y)}{2h}$ and $\frac{\partial f(x, y)}{\partial y} \approx \frac{f(x, y+h) - f(x, y-h)}{2h}$
- Second partials: $\frac{\partial^2 f(x, y)}{\partial x^2} \approx \frac{f(x+h, y) - 2f(x, y) + f(x-h, y)}{h^2}$
- Mixed partials: $\frac{\partial^2 f(x, y)}{\partial x \partial y} \approx \frac{f(x+h, y+h) - f(x-h, y+h) - f(x+h, y-h) + f(x-h, y-h)}{4h^2}$

For discrete sequences:

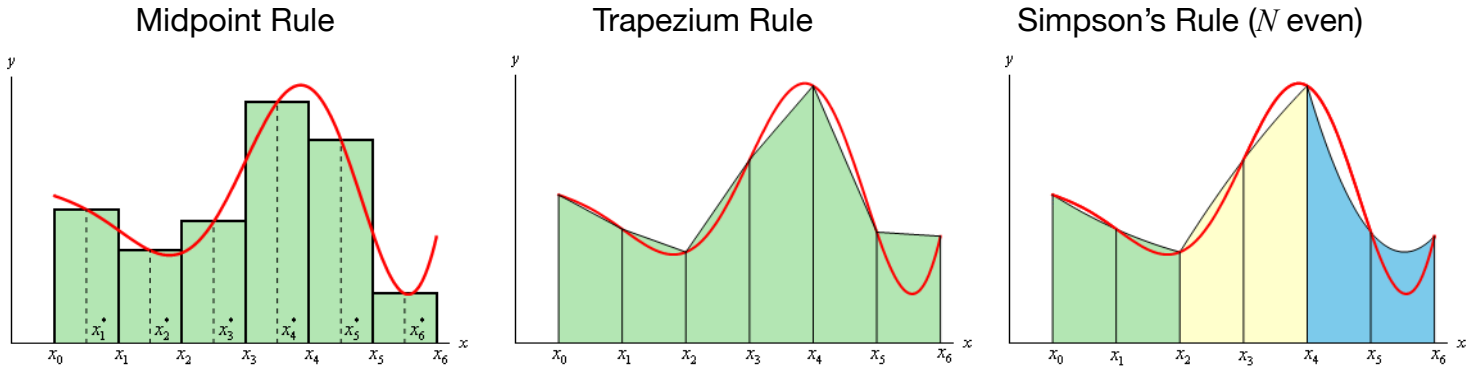
- One-sided: $\frac{u_{n+1} - u_n}{\Delta t} = \frac{du}{dt} + \frac{d^2u}{dt^2} \frac{\Delta t}{2!} + \dots$
- Two-sided: $\frac{u_{n+1} - u_{n-1}}{2\Delta t} = \frac{du}{dt} + \frac{d^3u}{dt^3} \frac{\Delta t^2}{3!} + \dots$

Python (SciPy): `f` is a callable function

```
from scipy.misc import derivative
gradient = derivative(f, x, dx=h)
```


3.1.4. Numerical Integration by Riemann Summation

A definite integral $I = \int_a^b f(x) dx$ can be approximated by splitting the interval $[a, b]$ into N equally-spaced intervals containing $N + 1$ ordinates from $x_0 = a$ to $x_N = b$ inclusive.



- Midpoint Rule:
$$I \approx \sum_{i=1}^N f(x_i^*) \cdot \Delta x$$
- Trapezium Rule:
$$I \approx \frac{\Delta x}{2} \left(f(x_0) + f(x_N) + 2 \sum_{i=1}^{N-1} f(x_i) \right)$$
- Simpson's Rule:
$$I \approx \frac{\Delta x}{2} \left(f(x_0) + f(x_N) + 4 \sum_{i=1}^{\frac{N}{2}} f(x_{2i-1}) + 2 \sum_{i=1}^{\frac{N}{2}-1} f(x_{2i}) \right)$$

(Simpsons' pattern of factors: 1, 4, 2, 4, 2, ..., 4, 1)

Maximum error bounds: if E is the absolute error in the approximation to I , then

Midpoint Error	Trapezium Error	Simpson's Error
$ E_M \leq \frac{K(b-a)^3}{24N^2}$,	$ E_T \leq \frac{K(b-a)^3}{12N^2}$,	$ E_S \leq \frac{M(b-a)^5}{180N^4}$.

where $|f''(x)| \leq K$ and $|f^{(4)}(x)| \leq M$ for all $a \leq x \leq b$.

Python (SciPy): f is a callable function representing the integrand

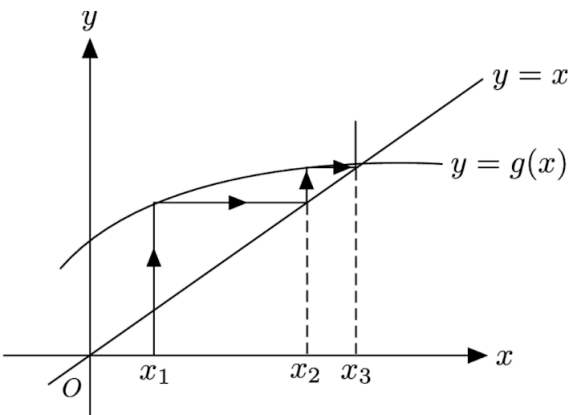
```
from scipy import integrate
val, abserr = integrate.quad(f, a, b)
```

3.1.5. Fixed Point Iteration for Solving Algebraic Equations

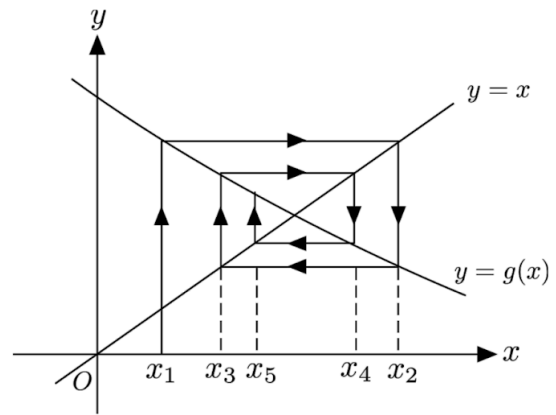
A root $x = \alpha$ to a single-variable equation $f(x) = 0$ can sometimes be found by writing the equation in the form $g(x) = x$ (so that $g(x) = f(x) + x$) and iterating (for suitable x_1):

$$x_{n+1} = g(x_n) \quad \Leftrightarrow \quad \lim_{n \rightarrow \infty} x_n = \alpha = g(\alpha) \text{ if } |g'(\alpha)| \leq 1$$

The iteration process, if it converges, can be represented as:



Convergent Staircase



Convergent Cobweb

Convergence Behaviour: the type of iteration depends on the gradient of $g(x)$ in the region between the initial point and the true root. Convergence requires $|g'(x)| < 1$. If the true root is $x = \alpha$ then the behaviour around the root is:

- Convergent Staircase: when $0 \leq g'(\alpha) \leq 1$.
- Convergent Cobweb: when $-1 \leq g'(\alpha) < 0$.
- Divergent Staircase: when $g'(\alpha) > 1$.
- Divergent Cobweb: when $g'(\alpha) < -1$.

If $0 < |g'(x)| < 1$ then convergence is linear:

$$\lim_{n \rightarrow \infty} \frac{x_{n+1} - \alpha}{x_n - \alpha} = g'(\alpha).$$

If $g'(\alpha) = 0$ then convergence is quadratic:

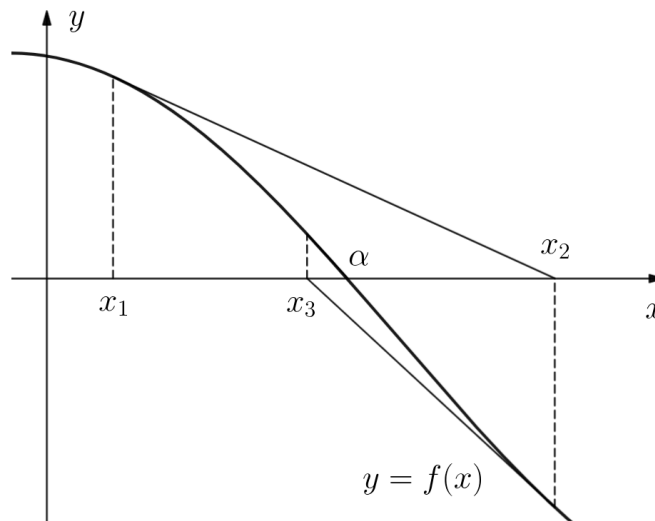
$$\lim_{n \rightarrow \infty} \frac{|x_{n+1} - \alpha|}{|x_n - \alpha|^2} = \lambda \text{ (some constant).}$$

3.1.6. Newton-Raphson Method (Gradient Descent) For Solving Algebraic Equations

A root $x = \alpha$ to a single-variable equation $f(x) = 0$ can be found by iterating (for suitable x_1):

$$x_{n+1} = x_n - \frac{f(x_n)}{f'(x_n)} \quad \Leftrightarrow \quad \lim_{n \rightarrow \infty} x_n = \alpha \quad (\text{if convergent})$$

The iteration process forms a pattern as follows:



Convergence Behaviour: convergence of Newton's method is generally difficult to predict.

If the root is a single root then convergence is quadratic.

If the root is repeated (algebraic multiplicity m) then convergence is linear, but can be accelerated to quadratic by using the iteration $x_{n+1} = x_n - m \times \frac{f(x_n)}{f'(x_n)}$ instead.

Generalisation to Multivariable Equations: for systems of algebraic equations of the form $\mathbf{f}(\mathbf{x}) = \mathbf{0}$, where \mathbf{f} is a vector-valued function containing each equation and \mathbf{x} is a vector of variables, Newton's method is $\mathbf{x}_{n+1} = \mathbf{x}_n - \mathbf{J}^{-1}(\mathbf{x}_n) \mathbf{f}(\mathbf{x}_n)$ where \mathbf{J} is the Jacobian matrix (Section 3.5.2) of \mathbf{f} . For increased efficiency and numerical stability, instead of computing \mathbf{J}^{-1} , the system of linear equations $\mathbf{J}(\mathbf{x}_n) (\mathbf{x}_{n+1} - \mathbf{x}_n) = -\mathbf{f}(\mathbf{x}_n)$ can be solved for $\mathbf{x}_{n+1} - \mathbf{x}_n$ at each iteration.

Python: f is a callable function representing the system (input: array \mathbf{x} ; output: array $\mathbf{f}(\mathbf{x})$)

```
from scipy.optimize import fsolve
root = fsolve(f, x0)
```

3.1.7. Numerical Methods for ODEs

An ODE integrator operates on either an individual ODE ($y' = f(t, y)$) or a system of coupled ODEs ($\mathbf{y}' = \mathbf{f}(t, \mathbf{y})$). The iteration is of fixed step size h , i.e. $t_{n+1} = t_n + h$.

Euler's Method:

$$y_{n+1} = y_n + hf(t_n, y_n)$$

Euler's Improved Method:

$$y_{n+1} = y_{n-1} + 2hf(t_n, y_n)$$

Predictor-Corrector (Heun's method):

$$\hat{y}_{n+1} = y_n + hf(t_n, y_n)$$

$$y_{n+1} = y_n + \frac{h}{2}[f(t_n, y_n) + f(t_{n+1}, \hat{y}_{n+1})]$$

Störmer-Verlet Integrator (symplectic: ideal for position-velocity-acceleration equations)

For a **2nd-order** ODE given by $\mathbf{x}'' = \mathbf{A}(t, \mathbf{x}, \mathbf{v})$, (with $\mathbf{v} = \mathbf{x}'$ and $t_{n+1} = t_n + \Delta t$)

1. set $\mathbf{x}_1 = \mathbf{x}_0 + \mathbf{v}_0 \Delta t + \frac{1}{2} \mathbf{A}(\mathbf{x}_0) \Delta t^2$,
2. for $n = 1, 2, \dots$ iterate

$$\mathbf{x}_{n+1} = 2\mathbf{x}_n - \mathbf{x}_{n-1} + \mathbf{A}(\mathbf{x}_n) \Delta t^2.$$

For the more sophisticated Gauss-Jackson integration algorithm, see Section 9.1.6.

Runge-Kutta Method (RK4; implicit 4th order):

$$y_{n+1} = y_n + \frac{h}{6} (k_{n1} + 2k_{n2} + 2k_{n3} + k_{n4})$$

$$k_{n1} = f(t_n, y_n)$$

$$k_{n2} = f(t_n + 0.5h, y_n + 0.5hk_{n1})$$

$$k_{n3} = f(t_n + 0.5h, y_n + 0.5hk_{n2})$$

$$k_{n4} = f(t_n + h, y_n + hk_{n3})$$

Butcher Tableau for RK4

(see Section 3.1.7.)

0				
1/2	1/2			
1/2	0	1/2		
1	0	0	1	
	1/6	1/3	1/3	1/6

Programming:

MATLAB: implements RK4. f is a callable function for the RHS.

```
[t, y] = ode45(f, [t_start, t_end], y0)
```

Python (SciPy): f is a callable function representing the RHS (inputs: t and \mathbf{y} ; output: \mathbf{y}')

```
from scipy.integrate import odeint
y = odeint(f, y0, t_array)
```

3.1.8. Butcher Tableau for Generalised Runge-Kutta ODE Integrators

A general RK method has an iteration step of the form $y_{n+1} = y_n + h \sum_{i=1}^s b_i k_{ni}$.

(s : order of the method, b_i : coefficients, k_{ni} evaluations of f near t_n and y_n (below)).

Explicit Scheme

$$k_{ni} = f\left(t_n + c_i h, y_n + h \sum_{j=1}^{i-1} a_{ij} k_{nj}\right)$$

0					
c_2	a_{21}				
c_3	a_{31}	a_{32}			
\vdots	\vdots		\ddots		
c_s	a_{s1}	a_{s2}	\cdots	$a_{s,s-1}$	
	b_1	b_2	\cdots	b_{s-1}	b_s

Implicit Scheme

$$k_{ni} = f\left(t_n + c_i h, y_n + h \sum_{j=1}^s a_{ij} k_{nj}\right)$$

c_1	a_{11}	a_{12}	\cdots	a_{1s}
c_2	a_{21}	a_{22}	\cdots	a_{2s}
\vdots	\vdots		\ddots	\vdots
c_s	a_{s1}	a_{s2}	\cdots	$a_{s,s}$
	b_1	b_2	\cdots	b_s

This allows any RK method to be represented as a matrix \mathbf{a} , a vector \mathbf{b} and a vector \mathbf{c} , allowing for efficient computation.

3.2. Series Expansions

3.2.1. Single Variable Definitions of Maclaurin Series and Taylor Series

The **Maclaurin series** about $x = 0$:

$$f(x) = \sum_{r=0}^{\infty} \frac{f^{(r)}(0)}{r!} \cdot x^r = f(0) + f'(0)x + \frac{1}{2}f''(0)x^2 + \frac{1}{6}f'''(0)x^3 + \dots$$

The sequence of coefficients of x^n is given by $\mathcal{Z}^{-1}[f(x^{-1})](n)$ where \mathcal{Z}^{-1} is the inverse z -transform (see Section 3.4.12).

The **Taylor series** about some value a :

$$f(x) = \sum_{r=0}^{\infty} \frac{f^{(r)}(a)}{r!} \cdot (x - a)^r = f(a) + f'(a)(x - a) + \frac{1}{2}f''(a)(x - a)^2 + \dots$$

This can also be written in the form (expanding about a fixed x)

$$f(x + \delta x) = \sum_{r=0}^{\infty} \frac{f^{(r)}(x)}{r!} \cdot h^r = f(x) + f'(x)\delta x + \frac{1}{2}f''(x)(\delta x)^2 + \dots$$

3.2.3. Maclaurin Series Expansions of Common Functions

Exponentials and Logarithms:

$$e^x = 1 + x + \frac{x^2}{2!} + \frac{x^3}{3!} + \cdots = \sum_{n=0}^{\infty} \frac{x^n}{n!} \quad \text{for all complex } x$$

$$e^{-x} = 1 - x + \frac{x^2}{2!} - \frac{x^3}{3!} + \cdots = \sum_{n=0}^{\infty} (-1)^n \frac{x^n}{n!} \quad \text{for all complex } x$$

$$\ln(1+x) = x - \frac{x^2}{2} + \frac{x^3}{3} - \cdots = \sum_{n=0}^{\infty} (-1)^n \frac{x^{n+1}}{n+1} \quad \text{for all } |x| \leq 1, x \neq -1, \text{ principal value}$$

$$\ln\left(\frac{1}{1-x}\right) = x + \frac{x^2}{2} + \frac{x^3}{3} + \cdots = \sum_{n=0}^{\infty} \frac{x^{n+1}}{n+1} \quad \text{for all } |x| \leq 1, x \neq -1, \text{ principal value}$$

Generalised binomial series expansion:

$$(1+x)^n = 1 + nx + \frac{n(n-1)}{2!}x^2 + \frac{n(n-1)(n-2)}{3!}x^3 + \cdots = \sum_{r=0}^{\infty} {}^n C_r x^r \quad \text{for all } |x| < 1$$

Trigonometric and hyperbolic functions:

$$\sin x = x - \frac{x^3}{3!} + \frac{x^5}{5!} - \cdots = \sum_{n=0}^{\infty} (-1)^n \frac{x^{2n+1}}{(2n+1)!} \quad \text{for all complex } x$$

$$\cos x = 1 - \frac{x^2}{2!} + \frac{x^4}{4!} - \cdots = \sum_{n=0}^{\infty} (-1)^n \frac{x^{2n}}{(2n)!} \quad \text{for all complex } x$$

$$\tan x = x + \frac{1}{3}x^3 + \frac{2}{15}x^5 + \frac{17}{315}x^7 + \cdots \quad \text{for all } |x| < \frac{\pi}{2}$$

$$\sec x = 1 + \frac{1}{2}x^2 + \frac{5}{24}x^4 + \frac{61}{720}x^6 + \cdots \quad \text{for all } |x| < \frac{\pi}{2}$$

$$\sinh x = x + \frac{x^3}{3!} + \frac{x^5}{5!} + \cdots = \sum_{n=0}^{\infty} \frac{x^{2n+1}}{(2n+1)!} \quad \text{for all complex } x$$

$$\cosh x = 1 + \frac{x^2}{2!} + \frac{x^4}{4!} + \cdots = \sum_{n=0}^{\infty} \frac{x^{2n}}{(2n)!} \quad \text{for all complex } x$$

$$\tanh x = x - \frac{1}{3}x^3 + \frac{2}{15}x^5 - \frac{17}{315}x^7 + \cdots \quad \text{for all } |x| < \frac{\pi}{2}$$

$$\operatorname{sech} x = 1 - \frac{1}{2}x^2 + \frac{5}{24}x^4 - \frac{61}{720}x^6 + \cdots \quad \text{for all } |x| < \frac{\pi}{2}$$

Inverse trigonometric and inverse hyperbolic functions:

$$\sin^{-1} x = x + \frac{1}{6}x^3 + \frac{3}{40}x^5 + \frac{5}{112}x^7 + \dots \quad \text{for all } |x| \leq 1$$

$$\cos^{-1} x = \frac{\pi}{2} - x - \frac{1}{6}x^3 - \frac{3}{40}x^5 - \frac{5}{112}x^7 - \dots \quad \text{for all } |x| \leq 1$$

$$\tan^{-1} x = x - \frac{x^3}{3} + \frac{x^5}{5} - \frac{x^7}{7} + \dots = \sum_{n=0}^{\infty} (-1)^n \frac{x^{2n+1}}{2n+1} \quad \text{for all } |x| \leq 1, x \neq \pm i$$

$$\cot^{-1} x = \frac{\pi}{2} - x + \frac{x^3}{3} - \frac{x^5}{5} + \frac{x^7}{7} = \frac{\pi}{2} - \sum_{n=0}^{\infty} (-1)^n \frac{x^{2n+1}}{2n+1} \quad \text{for all } |x| \leq 1, x \neq \pm i$$

$$\sinh^{-1} x = x - \frac{1}{6}x^3 + \frac{3}{40}x^5 - \frac{5}{112}x^7 + \dots = \sum_{n=0}^{\infty} \frac{(-1)^n (2n)! x^{2n+1}}{2^{2n} (n!)^2 (2n+1)} \quad \text{for all } |x| < 1$$

$$\tanh^{-1} x = x + \frac{x^3}{3} + \frac{x^5}{5} + \frac{x^7}{7} + \dots = \sum_{n=0}^{\infty} \frac{x^{2n+1}}{2n+1} \quad \text{for all } |x| < 1$$

Special Functions:

$$\operatorname{erf} x = \frac{2}{\sqrt{\pi}}x - \frac{2}{3\sqrt{\pi}}x^3 + \frac{1}{5\sqrt{\pi}}x^5 - \frac{1}{21\sqrt{\pi}}x^7 + \dots = \frac{2}{\sqrt{\pi}} \sum_{n=0}^{\infty} (-1)^n \frac{x^{2n+1}}{(2n+1)n!} \quad \text{for all } x$$

3.2.4. Lagrange's Inversion Theorem

If $y = f(x)$ and therefore $x = f^{-1}(y)$ then a Taylor series for x about a is given by

$$f^{-1}(y) = x = a + \sum_{n=1}^{\infty} \frac{g_n}{n!} (y - f(a))^n$$

The coefficients are $\frac{g_n}{n!}$ where $g_n = \lim_{x \rightarrow a} \frac{d^{n-1}}{dx^{n-1}} \left(\frac{x - a}{f(x) - f(a)} \right)^n$.

For shifting of Maclaurin series, the inverse function of $f(x + a)$ is $f^{-1}(x) - a$.

The radius of convergence is not easily determined from the function alone.

3.2.5. Laurent Series

Laurent series allow for inclusion of poles by summing over all integer powers of x , often used for complex functions $f(z)$. The Laurent series for $f(z)$ about c is given by

$$f(z) = \sum_{n=-\infty}^{\infty} g_n (z - c)^n$$

The coefficients are $g_n = \frac{1}{2\pi i} \oint_{\gamma} \frac{f(z)}{(z - c)^{n+1}} dz$.

(Cauchy contour integral around γ : counterclockwise Jordan curve where $f(z)$ holomorphic)

3.3. Differentiation and Integration

3.3.1. Continuity, Differentiability and Smoothness

A function $f(x)$ is said to be

- Continuous at $x = a$: if $\lim_{x \rightarrow a} f(x) = f(a)$
- Differentiable at $x = a$: if $\lim_{h \rightarrow 0} \frac{f(a+h) - f(a)}{h}$ exists
- Smooth (infinitely differentiable) at $x = a$: if $f^{(n)}(x)$ is continuous at $x = a$ for all nonnegative integer n .

If these terms are used without specifying a point $x = a$, then the condition must hold for all values of a in the domain of f .

3.3.2. Limit Definition of a Derivative

The first and second derivatives as limits are (as forward differences, assuming they exist):

$$f'(x) = \lim_{h \rightarrow 0} \frac{f(x+h) - f(x)}{h} \qquad f''(x) = \frac{f(x+h) - 2f(x) + f(x-h)}{h^2}$$

3.3.3. Limit Definition of a Definite Integral (Riemann Sum)

In general,
$$\int_a^b f(x) \, dx = \lim_{n \rightarrow \infty} \sum_{r=1}^n f(x_r) \Delta x$$

where $\Delta x = \frac{b-a}{n}$ and $x_r = a + (r-1)\Delta x$.

3.3.4. Mean Value Theorem and Intermediate Value Theorem

Mean Value Theorem: for a monotonically increasing function $f(x)$, we have $f(a) \leq M \leq f(b)$

where $M = \frac{1}{b-a} \int_a^b f(x) \, dx$ is the mean value of $f(x)$ on $a < x < b$.

Intermediate Value Theorem: for a continuous function $f(x)$ on the domain $[a, b]$, for all y such that $f(a) \leq y \leq f(b)$, there exists some $a \leq x \leq b$ such that $y = f(x)$.

Bolzano's Theorem: if a continuous function has values of opposite sign inside an interval, then it has a root in that interval.

3.3.5. Derivatives and Integrals of Functions

Algebraic, Exponential, Logarithmic, Trigonometric and Hyperbolic functions:

Function, $f(x)$	Derivative, $f'(x)$	Integral, $F(x) (+ C)$
1	0	x
x^n	nx^{n-1}	$\frac{1}{n+1}x^{n+1}$
\sqrt{x}	$\frac{1}{2\sqrt{x}}$	$\frac{2}{3}x^{3/2}$
e^x	e^x	e^x
a^x	$(\ln a)a^x$	$\frac{x^a}{\ln a}$
$\ln x $	$\frac{1}{x}$	$x(\ln x - 1)$
$\sin x$	$\cos x$	$-\cos x$
$\cos x$	$-\sin x$	$\sin x$
$\tan x$	$\sec^2 x$	$\ln \sec x $
$\sec x$	$\sec x \tan x$	$\ln \sec x + \tan x = \ln \left \tan \frac{x}{2} + \frac{\pi}{4} \right $
$\csc x$	$-\csc x \cot x$	$-\ln \csc x + \cot x = \ln \left \tan \frac{x}{2} \right $
$\cot x$	$-\csc^2 x$	$\ln \sin x $
$\sinh x$	$\cosh x$	$\cosh x$
$\cosh x$	$\sinh x$	$\sinh x$
$\tanh x$	$\operatorname{sech}^2 x$	$\ln \cosh x$
$\operatorname{sech} x$	$-\operatorname{sech} x \tanh x$	$2 \tan^{-1} \tanh \frac{x}{2} = \tan^{-1} \sinh x$
$\operatorname{csch} x$	$-\operatorname{csch} x \coth x$	$-\ln \operatorname{csch} x + \coth x = \ln \left \tanh \frac{x}{2} \right $
$\coth x$	$-\operatorname{csch}^2 x$	$\ln \sinh x $

Rationals with Radicals and Inverse Trigonometric / Inverse Hyperbolic Functions:

Function, $f(x)$	Derivative, $f'(x)$	Function, $f(x)$	Integral, $F(x) (+ C)$
$\sin^{-1} x$	$\frac{1}{\sqrt{1-x^2}}$	$\frac{1}{\sqrt{a^2-x^2}}$	$\sin^{-1} \frac{x}{a}$
$\cos^{-1} x$	$\frac{-1}{\sqrt{1-x^2}}$	$\frac{a}{\sqrt{x^4-a^2x^2}}$	$\sec^{-1} \frac{x}{a}$
$\tan^{-1} x$	$\frac{1}{1+x^2}$	$\frac{1}{\sqrt{a^2+x^2}}$	$\sinh^{-1} \frac{x}{a}$
$\sec^{-1} x$	$\frac{1}{ x \sqrt{x^2-1}}$	$\frac{1}{\sqrt{x^2-a^2}}$	$\cosh^{-1} \frac{x}{a}$
$\sinh^{-1} x$	$\frac{1}{\sqrt{1+x^2}}$	$\frac{1}{a^2+x^2}$	$\frac{1}{a} \tan^{-1} \frac{x}{a}$
$\cosh^{-1} x$	$\frac{1}{\sqrt{x^2-1}}$	$\frac{1}{a^2-x^2} (x < a)$	$\frac{1}{a} \tanh^{-1} \frac{x}{a}$
$\tanh^{-1} x,$ $\coth^{-1} x$	$\frac{1}{1-x^2}$	$\frac{1}{a^2-x^2} (x > a)$	$\frac{1}{a} \coth^{-1} \frac{x}{a}$

Integrals of radical functions:

$$\int \sqrt{a^2+x^2} dx = \frac{1}{2} \left(x\sqrt{a^2+x^2} + a^2 \sinh^{-1} \frac{x}{a} \right) + C$$

$$\int \sqrt{a^2-x^2} dx = \frac{1}{2} \left(x\sqrt{a^2-x^2} + a^2 \sin^{-1} \frac{x}{a} \right) + C$$

$$\int \sqrt{x^2-a^2} dx = \frac{1}{2} \left(x\sqrt{x^2-a^2} - a^2 \cosh^{-1} \frac{x}{a} \right) + C$$

Other common useful integrands:

$$\int \sec^3 x dx = \frac{1}{2} (\sec x \tan x + \ln |\sec x + \tan x|) + C$$

$$\int e^{ax} \sin bx dx = \frac{e^{ax} (a \sin bx - b \cos bx)}{a^2 + b^2} + C = \frac{e^{ax} \sin(bx - \tan^{-1} \frac{b}{a})}{\sqrt{a^2 + b^2}} + C$$

$$\int e^{ax} \cos bx dx = \frac{e^{ax} (a \cos bx + b \sin bx)}{a^2 + b^2} + C = \frac{e^{ax} \cos(bx - \tan^{-1} \frac{b}{a})}{\sqrt{a^2 + b^2}} + C$$

3.3.6. Indefinite Integral Reduction Formulas

Integral, I_n	Recurrence Relation
$I_n = \int \frac{x^n}{\sqrt{ax+b}} dx$	$I_n = \frac{2x^n \sqrt{ax+b}}{a(2n+1)} - \frac{2nb}{a(2n+1)} I_{n-1}$
$I_n = \int \frac{dx}{x^n \sqrt{ax+b}}$	$I_n = -\frac{\sqrt{ax+b}}{(n-1)bx^{n-1}} - \frac{a(2n-3)}{2b(n-1)} I_{n-1}$
$I_n = \int x^n \sqrt{ax+b} dx$	$I_n = \frac{2x^n \sqrt{(ax+b)^3}}{a(2n+3)} - \frac{2nb}{a(2n+3)} I_{n-1}$
$I_n = \int \frac{dx}{(px+q)^n \sqrt{ax+b}}$	$I_n = -\frac{\sqrt{ax+b}}{(n-1)(aq-bp)(px+q)^{n-1}} + \frac{a(2n-3)}{2(n-1)(aq-bp)} I_{n-1}$
$I_{m,n} = \int \frac{x^m dx}{(ax^2+bx+c)^n}$	$I_{m,n} = -\frac{x^{m-1}}{a(2n-m-1)(ax^2+bx+c)^{n-1}} - \frac{b(n-m)}{a(2n-m-1)} I_{m-1,n} + \frac{c(m-1)}{a(2n-m-1)} I_{m-2,n}$
$I_{m,n} = \int \frac{dx}{x^m (ax^2+bx+c)^n}$	$-c(m-1)I_{m,n} = \frac{1}{x^{m-1}(ax^2+bx+c)^{n-1}} + a(m+2n-3)I_{m-2,n} + b(m+n-2)I_{m-1,n}$
$I_n = \int \sin^n ax dx$	$I_n = -\frac{1}{an} \sin^{n-1} ax \cos ax + \frac{n-1}{n} I_{n-2}$
$I_n = \int \cos^n ax dx$	$I_n = \frac{1}{an} \sin ax \cos^{n-1} ax + \frac{n-1}{n} I_{n-2}$
$I_n = \int e^{ax} \sin^n bx dx$	$I_n = \frac{e^{ax} \sin^{n-1} bx}{a^2 + (bn)^2} (a \sin bx - bn \cos bx) + \frac{n(n-1)b^2}{a^2 + (bn)^2} I_{n-2}$
$I_n = \int e^{ax} \cos^n bx dx$	$I_n = \frac{e^{ax} \cos^{n-1} bx}{a^2 + (bn)^2} (a \cos bx + bn \sin bx) + \frac{n(n-1)b^2}{a^2 + (bn)^2} I_{n-2}$
$I_{m,n} = \int \sin^m ax \cos^n bx dx$	$I_{m,n} = \begin{cases} \frac{1}{a(n-1) \sin^{m-1} ax \cos^{n-1} ax} + \frac{m+n-2}{n-1} I_{m,n-2} \\ -\frac{1}{a(m-1) \sin^{m-1} ax \cos^{n-1} ax} + \frac{m+n-2}{m-1} I_{m-2,n} \end{cases}$

3.3.7. Special Definite and Improper Integrals

$$\int_{-\infty}^{\infty} \exp(-ax^2) \, dx = \sqrt{\frac{\pi}{a}}$$

$$\int_{-\infty}^{\infty} x^{2n} \exp(-ax^2) \, dx = \frac{(2n-1)!!}{(2a)^n} \sqrt{\frac{\pi}{a}}$$

$$\int_0^{\infty} x^n \exp(-ax) \, dx = \frac{n!}{a^{n+1}}$$

$$\int_{-\infty}^{\infty} \frac{\sin ax}{x} \, dx = \pi$$

$$\int_0^{\pi/2} \sin^m x \cos^n x \, dx = \frac{(m-1)!!(n-1)!!}{(m+n)!!} \times C, \quad C = \begin{cases} \pi/2 & \text{if } m, n \text{ both even} \\ 1 & \text{otherwise} \end{cases}$$

$$\int_{-\infty}^{\infty} \frac{dx}{a^n + x^n} = \frac{2\pi}{na^{n-1}} \csc \frac{\pi}{n} \quad (\text{for even } n)$$

$k!!$ is the double factorial, see Section 1.7.7.

3.3.8. Differentiation Rules: Product Rule, Quotient Rule, Chain Rule

If u, v, w, \dots are functions then:

- Product rule: $(uv)' = uv' + u'v$ $(uvw)' = uvw' + uv'w + u'vw$

- Leibniz rule for repeated differentiation of a product:

$$(uv)^{(n)} = u^{(n)}v + nu^{(n-1)}v' + \dots + {}^nC_p u^{(n-p)}v^{(p)} + \dots + uv^{(n)} = \sum_{p=0}^n {}^nC_p u^{(n-p)}v^{(p)}$$

- Quotient rule: $\left(\frac{u}{v}\right)' = \frac{u'v - v'u}{v^2}$

- Chain rule and Implicit differentiation: if $z = u(v(x))$ then

$$z' = (u \circ v)' = u(v)' = u'(v) v' \quad \frac{dz}{dx} = \frac{dz}{dv} \times \frac{dv}{dx}$$

3.3.9. Integration Rules: Integration by Parts, Integration by Substitution

Integration by parts: $\int_a^b u \frac{dv}{dx} dx = [uv]_a^b - \int_a^b v \frac{du}{dx} dx$

Integration by substitution: $\int_a^b u(v) \frac{dv}{dx} dx = \int_{v(a)}^{v(b)} u dv$

Leibniz Integral Rule for differentiation under the integral sign (Feynman's Technique):

$$\frac{d}{dx} \int_{a(x)}^{b(x)} f(x, y) dy = f(x, b) \frac{db}{dx} - f(x, a) \frac{da}{dx} + \int_{a(x)}^{b(x)} \frac{\partial f(x, y)}{\partial x} dy$$

3.3.10. Dirac Delta Functions (Impulse Function) and the Sifting Theorem

The delta function $\delta(x)$ is zero for all $x \neq 0$ and 'spikes' to $+\infty$ at $x = 0$, such that $\int_{-\infty}^{\infty} \delta(x) dx = 1$.

Integral of delta function: $\int_{-\infty}^x \delta(x - a) dx = H(x - a)$ (H : Heaviside unit step function)

Sifting property: $\int_{-\infty}^{\infty} f(x) \delta(x - a) dx = f(a)$ (Convolution: $f(x) * \delta(x - a) = f(x - a)$.)

For unilateral convolutions (integrating from 0 to x), the RHS is multiplied by $H(x)$.

3.3.11. Standard Substitutions for Integration

Integrals of radicals should use trigonometric (trig sub) or hyperbolic substitutions:

- $(a^2 - x^2)$ or $\sqrt{a^2 - x^2}$ → let $x = a \sin \theta$ or $x = a \cos \theta$
- $(a^2 + x^2)$ or $\sqrt{a^2 + x^2}$ → let $x = a \tan \theta$ or $x = a \sinh \theta$
- $(x^2 - a^2)$ or $\sqrt{x^2 - a^2}$ → let $x = a \sec \theta$ or $x = a \cosh \theta$

Integrals of rational functions of x and radicals should use:

- $\frac{1}{(ax + b)\sqrt{px + q}}$ → let $u^2 = px + q$
- $\frac{1}{(ax + b)\sqrt{px^2 + qx + r}}$ → let $\frac{1}{u} = ax + b$

More complicated rational functions of x and $\sqrt{px^2 + qx + r}$ should use Euler substitutions:

- if $p > 0$: → let $\sqrt{px^2 + qx + r} = u \pm x\sqrt{p}$ → $x = \frac{r - u^2}{\pm 2u\sqrt{p} - q}$
- if $r > 0$: → let $\sqrt{px^2 + qx + r} = xu \pm \sqrt{r}$ → $x = \frac{\pm 2u\sqrt{r} - q}{p - u^2}$
- if $q^2 - 4pr > 0$: → let $\sqrt{px^2 + qx + r} = \sqrt{p(x - \alpha)(x - \beta)} = (x - \alpha)u$ → $x = \frac{p\beta - \alpha u^2}{p - u^2}$

Integrals of rational functions of $(\sin x$ and/or $\cos x)$ or $(\sinh x$ and/or $\cosh x)$ should use the Weierstrass substitution (tangent half-angle substitution):

- $\frac{P(\sin x, \cos x)}{Q(\sin x, \cos x)}$ → let $t = \tan \frac{x}{2}$ → $\sin x = \frac{2t}{1 + t^2}$, $\cos x = \frac{1 - t^2}{1 + t^2}$, $dx = \frac{2 dt}{1 + t^2}$
- $\frac{P(\sinh x, \cosh x)}{Q(\sinh x, \cosh x)}$ → let $t = \tanh \frac{x}{2}$ → $\sinh x = \frac{2t}{1 - t^2}$, $\cosh x = \frac{1 + t^2}{1 - t^2}$, $dx = \frac{2 dt}{1 - t^2}$

3.3.12. Identities for Definite Integrals

Simple identities:
$$\int_a^b f(x) dx = - \int_b^a f(x) dx, \quad \int_a^b f(x) dx = \int_a^b f(y) dy$$

Reflections (King's rules):
$$\int_a^b f(x) dx = \int_a^b f(a+b-x) dx, \quad \int_a^b \frac{f(x)}{f(x)+f(a+b-x)} dx = \frac{b-a}{2}$$

Periodic function, T :
$$\int_a^{a+nT} f(x) dx = n \int_b^{b+T} f(x) dx \text{ for any } a, b \text{ and integers } n$$

Parity:
$$\text{odd: } \int_{-a}^a f(x) dx = 0, \quad \text{even: } \int_{-a}^a f(x) dx = 2 \int_0^a f(x) dx$$

Absolute values:
$$\int_a^b f(x) dx \leq \left| \int_a^b f(x) dx \right| \leq \int_a^b |f(x)| dx$$

Cauchy-Schwarz inequality:
$$\left| \int_a^b f(x) g(x) dx \right|^2 \leq \left(\int_a^b f(x)^2 dx \right) \left(\int_a^b g(x)^2 dx \right)$$

Monotonically increasing:
$$\int_a^b f(x) dx + \int_{f(a)}^{f(b)} f^{-1}(x) dx = b f(b) - a f(a)$$

3.4. Ordinary Differential Equations, Laplace and Z-Transforms

3.4.1. Classification of Ordinary Differential Equations (ODEs)

Ordinary differential equation (ODE): an equation relating a dependent variable y and its derivatives (y' , y'' , etc) with respect to a single independent variable x .

(The dependent function is sometimes also written as $y(x)$ or $x(t)$, or any other variables.)

Linear ODE: $\sum_{r=0}^n a_r(x) y^{(r)}(x) = f(x)$ (n : order, a_r : coefficient functions)

Homogeneous ODE: linear ODE with $f(x) = 0$. (**nonhomogeneous:** $f(x) \neq 0$)

Autonomous ODEs have no explicit dependence on x e.g. $y \, dy/dx = 1 - y$.

Nonlinear ODEs may have functions of the derivatives or products of variables e.g. xy , y^2 , $\exp y'$. The **degree** of a nonlinear ODE is the exponent on the highest-order derivative e.g. $x(y'')^3 - (y')^4 = 1$ is a nonlinear second-order ordinary differential equation with degree 3.

3.4.2. Separable DEs (First Order, Nonlinear)

For a separated ODE of the form $f(y) \, dy = g(x) \, dx$, the solution can be found by

integrating both sides. Initial conditions $y(x_0) = y_0$ can be applied with $\int_{y_0}^y f(y) \, dy = \int_{x_0}^x g(x) \, dx$.

3.4.3. Linear DEs (First Order, Linear)

To solve an ODE of the form $\frac{dy}{dx} + P(x) y = Q(x)$, multiply both sides by the integrating factor $I(x) = \exp(\int P(x) \, dx)$ and use the product rule so that the solution is given by $I(x) y(x) = \int I(x) Q(x) \, dx$. The computation of $I(x)$ does not require an arbitrary constant $+C$, even if initial conditions are not given.

3.4.4. Homogeneous DEs (First Order, Nonlinear) and Common Substitutions

To solve an ODE of the form $\frac{dy}{dx} = f\left(\frac{y}{x}\right)$, substitute $u = \frac{y}{x}$ so that $\frac{dy}{dx} = u + x \frac{du}{dx}$, which yields $\frac{du}{f(u) - u} = \frac{dx}{x}$, which is a separable DE in $u(x)$.

To solve an ODE of the form $\frac{dy}{dx} = f(ax + by + c)$, substitute $u = ax + by + c$ so that $\frac{dy}{dx} = \frac{1}{b} \frac{du}{dx} - \frac{a}{b}$, which yields $\frac{du}{dx} = bf(u) + a$, which is a separable DE in $u(x)$.

To solve an ODE of the form $\frac{dy}{dx} = \frac{a_1x + b_1y + c_1}{a_2x + b_2y + c_2}$, substitute $x = u + h$ and $y = v + k$, where h and k are the constant solutions to the system $\{a_1h + b_1k + c_1 = 0, a_2h + b_2k + c_2 = 0\}$.

Then, $\frac{dy}{dx} = \frac{dv}{du}$ and the DE becomes $\frac{dv}{du} = -\frac{a_1 + b_1 \frac{v}{u}}{a_2 + b_2 \frac{v}{u}}$, which is a homogeneous DE in $\frac{v}{u}$.

3.4.5. Linear DEs with Constant Coefficients (Second Order, Linear)

To solve an ODE of the form $a \frac{d^2 y}{dx^2} + b \frac{dy}{dx} + c y = f(x)$: (or with higher order)

- Solve the characteristic equation, $a\lambda^2 + b\lambda + c = 0$. (or with higher order)
- Depending on the nature of the roots λ , find the complementary function, y_{CF} :

- If λ_1 and λ_2 are **real and distinct**,

$$y_{CF}(x) = A e^{\lambda_1 x} + B e^{\lambda_2 x} \quad \text{or} \quad y_{CF}(x) = C \cosh \lambda_1 x + D \sinh \lambda_2 x$$

- If $\lambda_1 = \lambda_2 = \lambda$ is the **real repeated root**,

$$y_{CF}(x) = (A + Bt)e^{\lambda t}$$

- If $\lambda_1 = \alpha + i\beta$ and $\lambda_2 = \alpha - i\beta$ are the **distinct complex conjugate roots**,

$$y_{CF}(x) = e^{\alpha x} (A \cos \beta x + B \sin \beta x) \quad \text{or} \quad y_{CF} = C e^{\alpha x} \sin(\beta x - D)$$

- Find the particular integral y_{PI} using one of the following methods:

(note that if $f(x) = 0$ (homogeneous) then $y_{PI}(x) = 0$.)

- **Method of Undetermined Coefficients:** choose a suitable trial function based on the form of $f(x)$ from the table in Section 3.4.5, substituting it into the differential equation and equating linearly independent terms to solve for the coefficients.

- **Variation of Parameters:** evaluate the Wronskian, where y_1 and y_2 are the basis functions of y_{CF} .

$$W(x) = \begin{vmatrix} y_1(x) & y_2(x) \\ y_1'(x) & y_2'(x) \end{vmatrix}$$

The particular integral is then

$$y_{PI}(x) = -y_1(x) \int \frac{y_2(x) f(x)}{W(x)} dx + y_2(x) \int \frac{y_1(x) f(x)}{W(x)} dx$$

- By superposition, the solution is $y(x) = y_{CF}(x) + y_{PI}(x)$,
- The remaining constants in the $y_{CF}(x)$ term can be found using initial/boundary conditions.

Alternative methods without solving the characteristic equation are:

- **Laplace transform** (Section 3.4.15.): take LT of both sides, rearrange for $Y(s)$, take ILT

- **Convolution:** if the impulse response $g(t)$ is known, then $y(t) = (f * g)(t)$.

Note that for an LTI system with $y(0) = 0$ the impulse response is the derivative of the step response i.e. let $f(x) = 1$ and differentiate the solution. This is the 1D Green's function approach.

3.4.6. Trial Functions for Nonhomogeneous Differential Equations

For linear differential equations with constant coefficients, where $f(x)$ is linearly independent of the complementary function:

$f(x)$	Trial function
1	C
x^n , for integer n	$Cx^n + Dx^{n-1} + \dots + C_0$
k^x	Ck^x
e^{kx}	Ce^{kx}
$x e^{kx}$	$(Cx + D)e^{kx}$
$x^n e^{kx}$	$(Cx^n + Dx^{n-1} + \dots + C_0)e^{kx}$
$\sin px$ or $\cos px$	$C \sin px + D \cos px$
$e^{kx} \sin px$ or $e^{kx} \cos px$	$(C \sin px + D \cos px)e^{kx}$
$x^n e^{kx} \sin px$ or $x^n e^{kx} \cos px$	$(Cx^n + Dx^{n-1} + \dots + C_0)(C_S \sin px + C_C \cos px)e^{kx}$

where C, D, \dots, C_C, C_S are undetermined coefficients.

If $f(x)$ has a component which is not linearly independent of $y_{CF}(x)$, then the corresponding component in the trial function must be multiplied by x , or by x^2 in the case where this is still not linearly independent (i.e. repeated real roots solution with the same form as $f(x)$.)

3.4.7. Cauchy-Euler DEs (Second Order, Linear)

To solve an ODE of the form $ax^2 \frac{d^2y}{dx^2} + bx \frac{dy}{dx} + cy = f(x)$, substitute $u = \ln x$ so that

$$\frac{dy}{dx} = \frac{1}{x} \frac{dy}{du} \quad \text{and} \quad \frac{d^2y}{dx^2} = \frac{1}{x^2} \left(\frac{d^2y}{du^2} - \frac{dy}{du} \right),$$

which yields a second-order differential equation with constant coefficients. The resulting RHS will be $f(e^u)$, for which a particular integral may often be found.

3.4.8. Bernoulli DEs (First Order, Nonlinear)

To solve an ODE of the form $\frac{dy}{dx} + P(x)y(x) = Q(x)[y(x)]^n$, substitute $u(x) = y^{1-n}(x)$ so that

$$\frac{dy}{dx} = \frac{1}{1-n} u^{\frac{n}{1-n}} \frac{du}{dx}, \quad \text{which yields a linear ODE in } u(x): \frac{du}{dx} + (1-n)P(x)u = (1-n)Q(x).$$

3.4.9. Exact DEs (First Order, Nonlinear)

An ODE $M(x, y) dx + N(x, y) dy = 0 \leftrightarrow N(x, y) \frac{dy}{dx} + M(x, y) = 0$ is exact if there exists a 'potential function' $F(x, y)$ such that $\frac{\partial F}{\partial x} = M(x, y)$ and $\frac{\partial F}{\partial y} = N(x, y)$.

The condition for exactness is met if $\frac{\partial M}{\partial y} = \frac{\partial N}{\partial x}$ (by Clairhaut's theorem).

To solve, find $F(x, y)$ by integrating M and N , separating the components for each variable. Use unknown functions $f(x)$ and $g(y)$ for the arbitrary constants of integration, and solve to make the antiderivatives equal to each other. The solutions are the contour lines of $F(x, y)$, implicitly satisfying $F(x, y) = C$ for some arbitrary constant C .

Almost Exact DEs:

An ODE $M(x, y) dx + N(x, y) dy = 0$ that is **not** exact can sometimes be multiplied by an integrating factor $\mu(x, y)$ on both sides to make an ODE $\widehat{M}(x, y) dx + \widehat{N}(x, y) dy = 0$ that is exact i.e. $\frac{\partial \widehat{M}}{\partial y} = \frac{\partial \widehat{N}}{\partial x}$ (where $\widehat{M}(x, y) = \mu(x, y) M(x, y)$ and $\widehat{N}(x, y) = \mu(x, y) N(x, y)$).

Techniques for finding such an integrating factor, if it exists:

- If $\frac{1}{N(x, y)} \left(\frac{\partial M}{\partial y} - \frac{\partial N}{\partial x} \right)$ is a function of x only, then $\mu(x) = \exp \int \frac{1}{N(x, y)} \left(\frac{\partial M}{\partial y} - \frac{\partial N}{\partial x} \right) dx$.
- If $\frac{1}{M(x, y)} \left(\frac{\partial N}{\partial x} - \frac{\partial M}{\partial y} \right)$ is a function of y only, then $\mu(y) = \exp \int \frac{1}{M(x, y)} \left(\frac{\partial N}{\partial x} - \frac{\partial M}{\partial y} \right) dy$.

3.4.10. Power Series Solution of DEs (Taylor Series Expansions) (Any Order, Linear)

To find the power series expansion $y(x) = \sum_{n=0}^{\infty} a_n x^n$ of the solution to a DE of the form

$$\sum_{k=0}^N p_k(x) y^{(k)}(x) = f(x), \text{ valid in some neighbourhood around } x = 0:$$

Power Series Method:

- Let $y(x) = \sum_{n=0}^{\infty} a_n x^n \Rightarrow y'(x) = \sum_{n=0}^{\infty} n a_n x^{n-1} \Rightarrow y''(x) = \sum_{n=0}^{\infty} n(n-1) a_n x^{n-2} \dots$ in the DE.
- Write the power series for each $p_k(x)$ and $f(x)$ and absorb these powers into the $y^{(n)}$ series.
- Re-index the summations to make them all have the same exponents of x .
- Pull out the first few terms of summations to make them all start at the same index n .
- Combine the summations and factor out the x^n term.
- Set everything inside the summation to zero to yield a recurrence relation in a_n , and set the pulled out terms to zero.
- Use initial conditions e.g. $a_n = \frac{y^{(n)}(0)}{n!}$, or let $(a_0, a_1, \dots) \in \{(1, 0), (0, 1), \dots\}$ for a linearly independent set of basis solutions.

Leibniz Method:

- Differentiate both sides of the differential equation with respect to x , n times, using the general Leibniz rule for differentiating products.
- Let $x = 0$, convert the derivatives to series coefficients i.e. $a_n = \frac{y^{(n)}(0)}{n!}$ to yield a recurrence relation in a_n .
- If there are undetermined coefficients, evaluate the original DE at $x = 0$ to find them.

Frobenius Method: used when any $p_k(x)$ and $f(x)$ is not infinitely differentiable at $x = 0$.

For the DE $y'' + p(x)y' + q(x)y = 0$:

- Solve the indicial equation, $r(r-1) + u_0r + v_0 = 0$, where u_0 and v_0 are the constant terms in the Taylor series expansion of $u(x) = xp(x)$ and $v(x) = x^2q(x)$ respectively, for r .
- Case 1: Distinct real roots where r_1 and r_2 do not differ by an integer:
 - Use power series method with $y = \sum_{n=0}^{\infty} a_n x^{n+r}$, find recurrence relation in terms of r
 - Sub in each root: $y = A \sum_{n=0}^{\infty} a_n x^{n+r_1} + B \sum_{n=0}^{\infty} b_n x^{n+r_2}$
- Case 2: repeated roots. $y = (A + B \ln x) \sum_{n=0}^{\infty} a_n x^{n+r} + B \sum_{n=1}^{\infty} b_n x^{n+r}$, $b_n = \frac{da_n}{dr}(0)$
- Case 3: roots that differ by an integer. $y = (A + B \ln x) \sum_{n=0}^{\infty} a_n x^{n+r_1} + B \sum_{n=0}^{\infty} b_n x^{n+r_1}$, $b_n = \frac{da_n}{dr}(0)$

Fuch's theorem: radius of convergence of Frobenius series, $R \geq \min\{R_{p(x)}, R_{q(x)}, R_{r(x)}\}$.

If $x = 0$ is the only 'regular singular point' ($u(x)$ and $v(x)$ infinitely differentiable at $x = 0$) then the Frobenius series converges everywhere. Otherwise, R is the distance to the nearest singular point.

3.4.11. Higher Order DEs as Systems of First Order DEs

An N th order ODE $\sum_{n=0}^N a_n(x) y^{(n)}(x) = f(x)$ can be written as a set of N first-order ODEs.

Label the N new dependent variables $\left\{ y \rightarrow y_0, \frac{dy}{dx} \rightarrow y_1, \dots, \frac{d^{N-1}y}{dx^{N-1}} \rightarrow y_{N-1} \right\}$.

The system is then $\left\{ \frac{dy_0}{dx} = y_1, \frac{dy_1}{dx} = y_2, \dots, \frac{dy_{N-2}}{dx} = y_{N-1}, \frac{dy_{N-1}}{dx} = f(x) - \sum_{n=0}^{N-1} a_n(x) y_n \right\}$.

Initial conditions correspond directly to the initial condition for each equation in the system.

The method still works for nonlinear higher order ODEs but the resulting system will be nonlinear.

ODEs in this form are readily solved by computer/numerical methods.

3.4.12. Systems of Differential Equations

A system of n first-order ODEs can be written in the form $\dot{\mathbf{x}} = \mathbf{f}(\mathbf{x}, t)$ where \mathbf{x} is a vector of unknown functions: $\mathbf{x} = [x_1(t), x_2(t), \dots, x_n(t)]^T$.

An autonomous system is one in which $\mathbf{f}(\mathbf{x}, t) = \mathbf{f}(\mathbf{x})$ i.e. explicitly independent of t .

Linear homogeneous systems with constant coefficients:

- Standard form: $\dot{\mathbf{x}} = \mathbf{A}\mathbf{x}$ (\mathbf{A} : square $n \times n$ matrix of constant coefficients)
- Ansatz: $\mathbf{x} = \exp(\mathbf{A}t) \mathbf{x}_0$ (\mathbf{x}_0 : initial conditions at $t = 0$)
- General solution (for a 2×2 system): (\mathbf{u} : eigenvectors of \mathbf{A} , λ : eigenvalues of \mathbf{A})

$$\mathbf{x}(t) = \begin{cases} c_1 e^{\lambda_1 t} \mathbf{u}_1 + c_2 e^{\lambda_2 t} \mathbf{u}_2 & \text{if } \lambda_{1,2} \text{ are real} \\ c_1 e^{\alpha t} (\mathbf{u}_1 \cos \beta t + \mathbf{u}_2 \sin \beta t) + c_2 e^{\alpha t} (\mathbf{u}_1 \sin \beta t - \mathbf{u}_2 \cos \beta t) & \text{if } \lambda_{1,2} = \alpha \pm \beta i \text{ are complex} \\ c_1 e^{\lambda t} \mathbf{u} + c_2 e^{\lambda t} (\mathbf{u}t + \mathbf{v}), \text{ for any } \mathbf{v} : (\mathbf{A} - \lambda \mathbf{I})\mathbf{v} = \mathbf{u} & \text{if } \lambda \text{ is a repeated defective eigenvalue} \end{cases}$$

(\mathbf{u} : eigenvectors of \mathbf{A} , λ : eigenvalues of \mathbf{A})

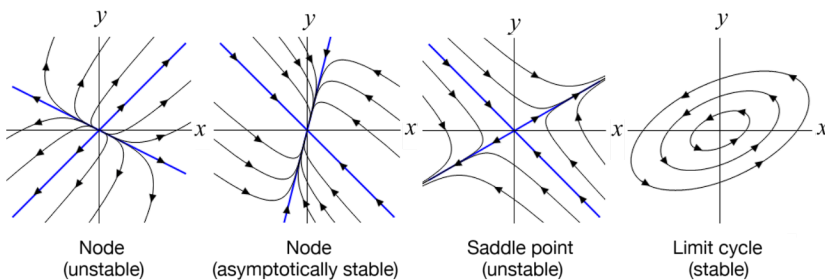
Linear nonhomogeneous systems with constant coefficients:

- Standard form: $\dot{\mathbf{x}} = \mathbf{A}\mathbf{x} + \mathbf{f}(t)$

Solution methods include the method of undetermined coefficients (using the complementary solution from the homogeneous case) or variation of parameters. The formula for variation of parameters is

$$\mathbf{x}_{PI}(t) = \mathbf{X} \int \mathbf{X}^{-1} \mathbf{f}(t) dt \quad (\mathbf{X}: \text{matrix where each column is a linearly independent part of the complementary solution})$$

Phase plane and equilibrium point stability: equilibrium point(s) occur when $d\mathbf{x}/dt = \mathbf{0}$.



Type	Eigenvalues	Stability
Node	Real λ , same signs	$\lambda < 0$, stable $\lambda > 0$, unstable
Saddle	Real λ opposite signs	Mostly Unstable
Center	λ pure imaginary	—
Focus/Spiral	Complex λ , $\text{Re}(\lambda) \neq 0$	$\text{Re}(\lambda) < 0$, stable $\text{Re}(\lambda) > 0$, unstable
Degenerate Node	Repeated roots,	$\lambda > 0$, stable
Lines of Equilibria	One zero eigenvalue	$\lambda < 0$, stable

- For linear homogeneous systems, the origin is the only equilibrium point.
- The eigenvectors of \mathbf{A} are directed along the asymptotic trajectories of the system (**nullclines**).
- An equilibrium point is the intersection of the x and y nullclines, for which $\frac{dx}{dt} = 0$ and $\frac{dy}{dt} = 0$.
- For nonlinear systems, the nullclines may be curved.

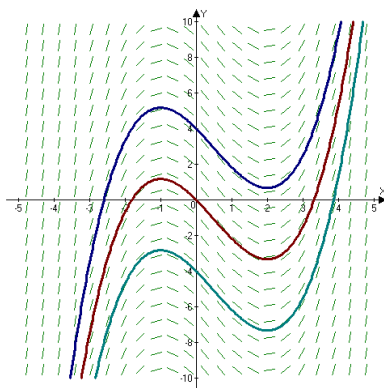
3.4.13. Graphical Representations of Differential Equations

Slope Field (Direction Field) of a Differential Equation

For a differential equation $\frac{dy}{dx} = f(x, y)$, the slope field is a unit vector field in the x - y plane given by $\mathbf{u}(x, y) = \frac{1}{\sqrt{1 + f(x, y)^2}} \mathbf{i} + \frac{f(x, y)}{\sqrt{1 + f(x, y)^2}} \mathbf{j}$.

Every solution to the differential equation is a **field line** of the vector field.

Curves with $\frac{dy}{dx} = f(x, y) = k$ for constant k are 'isoclines'.



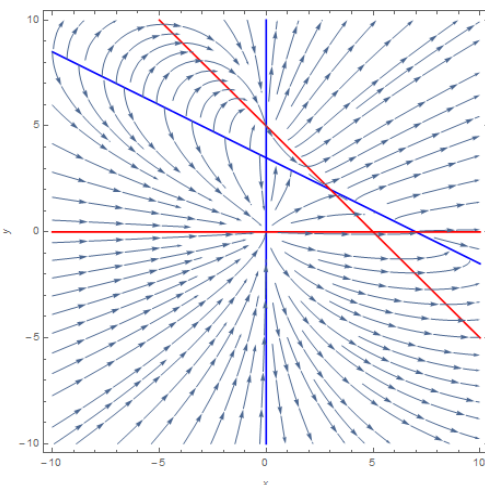
Example: slope field for $\frac{dy}{dx} = x^2 - x - 2$.

The curves represent solutions for initial conditions $y(0) = 4$, $y(0) = 0$ and $y(0) = -4$.

Phase Plane of a System of Differential Equations

For a system of two ODEs $\left\{ \frac{dx}{dt} = f(x, y, t), \frac{dy}{dt} = g(x, y, t) \right\}$, the phase space plot is a vector field in the x - y plane given by $\mathbf{u}(x, y, t) = \frac{f(x, y, t)}{\sqrt{f(x, y, t)^2 + g(x, y, t)^2}} \mathbf{i} + \frac{g(x, y, t)}{\sqrt{f(x, y, t)^2 + g(x, y, t)^2}} \mathbf{j}$.

If the system is autonomous (no t dependence), this is a static vector field.



Example: phase portrait for $\left\{ \frac{dx}{dt} = x(7 - x - 2y), \frac{dy}{dt} = y(5 - y - x) \right\}$

Lines for $\frac{dy}{dx} = 0$ are shown in red (x -nullcline)

Lines for $\frac{dx}{dy} = 0$ are shown in blue (y -nullcline)

A fixed point occurs at the intersection of nullclines.

3.4.14. Special Forms of DEs (Second Order, Nonlinear)**Bessel's differential equation** (generalised):

$$x^2 \frac{d^2 y}{dx^2} + (2p+1)x \frac{dy}{dx} + (\lambda^2 x^{2q} + \alpha^2) y = 0 \Rightarrow y = x^{-p} \left(A \cdot J_{\frac{\sqrt{p^2 - \alpha^2}}{q}} \left(\frac{\lambda}{q} x^q \right) + B \cdot Y_{\frac{\sqrt{p^2 - \alpha^2}}{q}} \left(\frac{\lambda}{q} x^q \right) \right)$$

Spherical Bessel's differential equation (a particular case of the above):

$$x^2 \frac{d^2 y}{dx^2} + 2x \frac{dy}{dx} + (\lambda^2 x^2 - n(n+1)) y = 0$$

$$\Rightarrow y = A \cdot \frac{J_{n+\frac{1}{2}}(\lambda x)}{\sqrt{\lambda x}} + B \cdot \frac{Y_{n+\frac{1}{2}}(\lambda x)}{\sqrt{\lambda x}} = A' \cdot j_n(\lambda x) + B' \cdot y_n(\lambda x)$$

In the case $n = 0$, the solution is $y = A' \frac{\sin \lambda x}{\lambda x} - B' \frac{\cos \lambda x}{\lambda x}$, for which $B' = 0$ if $y(0)$ is finite.**Generalised Laguerre differential equation:**

$$x \frac{d^2 y}{dx^2} + (\alpha + 1 - x) \frac{dy}{dx} + ny = 0 \Rightarrow y = A \cdot L_n^{(\alpha)}(x) + B \cdot U(-n, \alpha + 1, x)$$

Hypergeometric differential equation:

$$x(1-x) \frac{d^2 y}{dx^2} + (c - (a+b+1)x) \frac{dy}{dx} - aby = 0$$

$$\Rightarrow y = A \cdot {}_2F_1(a, b; c; x) + B \cdot (-x)^{1-c} {}_2F_1(a-c+1, b-c+1; 2-c; x)$$

Confluent Hypergeometric differential equation:

$$x \frac{d^2 y}{dx^2} + (c-x) \frac{dy}{dx} - ay = 0 \Rightarrow y = A \cdot {}_1F_1(a; c; x) + B \cdot U(a, c, x)$$

Hermite's differential equation:

$$\frac{d}{dx} \left(e^{-\frac{1}{2}x^2} \frac{dy}{dx} \right) + \lambda e^{-\frac{1}{2}x^2} y = 0 \Rightarrow y = A \cdot H_\lambda \left(\frac{x}{\sqrt{2}} \right) + B \cdot {}_1F_1 \left(-\frac{\lambda}{2}; \frac{1}{2}; \frac{x^2}{2} \right)$$

(For the special function definitions, see Section 1.7.)

3.4.15. Laplace Transforms

$$F(s) = \mathcal{L}\{f(t)\} = \int_0^{\infty} f(t) e^{-st} dt$$

Derivatives, Integrals, Deltas and Algebraic Functions:

$f(t)$	$F(s)$
$e^{-at}x(t)$	$\bar{x}(s+a)$
$x(t-\tau)H(t-\tau)$	$e^{-s\tau}\bar{x}(s)$
$\frac{dx(t)}{dt} = x'(t)$	$s\bar{x}(s) - x(0)$
$\frac{d^2x(t)}{dt^2} = x''(t)$	$s^2\bar{x}(s) - sx(0) - x'(0)$
$\frac{d^nx(t)}{dt^n} = x^{(n)}(t)$	$s^n\bar{x}(s) - s^{n-1}x(0) - s^{n-2}x'(0) - \dots - sx^{(n-2)}(0) - x^{(n-1)}(0)$
$\int_0^t x(\tau) d\tau$	$s^{-1}\bar{x}(s)$
$\int_0^t x_1(\tau)x_2(t-\tau) d\tau$	$\bar{x}_1(s)\bar{x}_2(s)$
$tx(t)$	$-\frac{d}{ds}\bar{x}(s)$
$1 = H(t)$	s^{-1}
$\delta(t)$	1
$H(t-\tau)$	$s^{-1}e^{-s\tau}$
$\delta(t-\tau)$	$e^{-s\tau}$

Powers, Exponential, Trigonometric and Hyperbolic:

$f(t)$	$F(s)$	$f(t)$	$F(s)$
t	s^{-2}	t^n	$n!s^{-n-1}$
e^{-at}	$(s+a)^{-1}$	$t^n e^{-at}$	$\frac{n!}{(s+a)^{n+1}}$
$\sin \omega t$	$\frac{\omega}{s^2 + \omega^2}$	$\cos \omega t$	$\frac{s}{s^2 + \omega^2}$
$e^{-at} \sin \omega t$	$\frac{\omega}{(s+a)^2 + \omega^2}$	$e^{-at} \cos \omega t$	$\frac{(s+a)}{(s+a)^2 + \omega^2}$
$t \sin \omega t$	$\frac{2s\omega}{(s^2 + \omega^2)^2}$	$t \cos \omega t$	$\frac{s^2 - \omega^2}{(s^2 + \omega^2)^2}$
$\sinh \omega t$	$\frac{\omega}{s^2 - \omega^2}$	$\cosh \omega t$	$\frac{s}{s^2 - \omega^2}$

Initial Value / Final Value Theorem: $f(0^+) = \lim_{s \rightarrow \infty} s F(s)$ and $\lim_{t \rightarrow \infty} f(t) = \lim_{s \rightarrow 0} s F(s)$.

3.4.16. Convolution Theorem

$$(f * g)(t) = \int_0^t f(t - \tau)g(\tau) d\tau$$

The Laplace transform of a convolution is the product of their transforms:

$$\mathcal{L}\{(f * g)(t)\} = F(s) \cdot G(s) \quad \text{equivalently} \quad \mathcal{L}^{-1}\{F(s)G(s)\} = (f * g)(t)$$

The convolution theorem also applies to Fourier transforms (Section 3.6.5).

3.4.17. Inverse Laplace Transform by the Cauchy Residue Theorem

The inverse Laplace transform is defined as

(Mellin's formula)

$$f(t) = \mathcal{L}^{-1}\{F(s)\} = \frac{1}{2\pi i} \int_{\gamma-i\infty}^{\gamma+i\infty} F(s) e^{st} ds$$

where γ is a constant larger than the real part of any pole of $F(s)$.

If $\gamma = 0$ (i.e. no unstable poles: $\text{Re}(s_k) < 0$) then this is similar to the inverse Fourier transform.

Using the Residue Theorem and Jordan's Lemma (using a semicircular contour), this is equivalent to (by complex analysis):

$$f(t) = 2\pi i \sum_k \text{Res}[F(s), s_k]$$

with the sum over all residues at the poles of $F(s)$. The residue is defined as

$$\text{Res}[F(s), s_k] = \frac{1}{(n-1)!} \lim_{s \rightarrow s_k} \frac{d^{n-1}}{dx^{n-1}} (s - s_k)^n F(s)$$

where n is the multiplicity of pole s_k .

If $n = 1$ then the residue simplifies to $\text{Res}(F, s_k) = \lim_{s \rightarrow s_k} (s - s_k)F(s)$.

which is the formalised 'cover-up method' of partial fractions if F is rational.

3.4.18. Linear Difference Equations

Difference Equations are discretised differential equations, expressed as a recurrence relation between terms of a sequence $\{y\}_n$ for $n = 0, 1, 2, \dots$

To solve a second-order difference equation of the form (or higher order)

$$a y_n + b y_{n-1} + c y_{n-2} = f(n),$$

- Solve the characteristic equation, $a\lambda^2 + b\lambda + c = 0$. (or higher order)
- Depending on the nature of the roots λ , find the complementary function, $y_n^{(CF)}$:

- If λ_1 and λ_2 are **real and distinct**,

$$y_n^{(CF)} = A \lambda_1^n + B \lambda_2^n$$

- If $\lambda_1 = \lambda_2 = \lambda$ is the **real repeated root**,

$$y_n^{(CF)} = A \lambda_1^n + B n \lambda_2^n$$

- If $\lambda_1 = R \exp i\theta$ and $\lambda_2 = R \exp -i\theta$ are the **distinct complex conjugate roots**,

$$y_n^{(CF)} = R^n (A \cos n\theta + B \sin n\theta)$$

- Use the Method of Undetermined Coefficients to determine the particular ‘integral’, $y_n^{(PI)}$ (note that if $f(n) = 0$ then $y_n^{(PI)} = 0$). The trial functions are identical to the case of a nonhomogeneous differential equation (Section 3.4.5.), with x replaced by n .
- By superposition, the solution is $y_n = y_n^{(CF)} + y_n^{(PI)}$ where the remaining constants can be found using given conditions.

Alternative methods without solving the characteristic equation are:

- **Z-transform / generating function** (Section 3.4.19): $y_n = Z^{-1}(Y(z))$, where $Y(z)$ is the generating function with $x = z^{-1}$ given by $Y(z) = \sum_n y_n z^{-n}$ (the Z transform). (The generating function is $Y(x) = \sum_n y_n x^n$.)
- **Convolution**: if the impulse response g_n is known, then $y_n = (f * g)[n]$. For the definition of the discrete convolution, see Section 5.4.7.

3.4.19. Z-Transforms, Inverse Z Transforms and Generating Functions

Sequence:

$$y_n = \mathcal{Z}^{-1}[Y(z)][n], \quad n = 0, 1, 2, \dots$$

Z-transform:

$$Y(z) = \mathcal{Z}[y_n](z) = \sum_{n=0}^{\infty} y_n z^{-n}$$

Generating function:

$$Y(x) = \mathcal{Z}[y_n](x^{-1}) = \sum_{n=0}^{\infty} y_n x^n$$

1 (unit step)	$\frac{1}{1 - z^{-1}}$	$\frac{1}{1 - x}$
nT	$\frac{Tz^{-1}}{(1 - z^{-1})^2}$	$\frac{Tx}{(1 - x)^2}$
$\frac{(n + m - 1)!}{n!(m - 1)!} = {}^{n+m-1}C_n$	$\frac{1}{(1 - z^{-1})^m}$	$\frac{1}{(1 - x)^m}$
e^{-anT}	$\frac{1}{1 - e^{-aT}z^{-1}}$	$\frac{1}{1 - e^{-aT}x}$
$\sin(\omega_0 nT)$	$\frac{\sin(\omega_0 T)z^{-1}}{1 - 2 \cos(\omega_0 T)z^{-1} + z^{-2}}$	$\frac{\sin(\omega_0 T)x}{1 - 2 \cos(\omega_0 T)x + x^2}$
$\cos(\omega_0 nT)$	$\frac{1 - \cos(\omega_0 T)z^{-1}}{1 - 2 \cos(\omega_0 T)z^{-1} + z^{-2}}$	$\frac{1 - \cos(\omega_0 T)x}{1 - 2 \cos(\omega_0 T)x + x^2}$
$\frac{r^{n-1}}{\sin(\omega_0 T)} [r \sin(\omega_0(n + 1)T) - a \sin(\omega_0 nT)]$	$\frac{1 - az^{-1}}{1 - 2r \cos(\omega_0 T)z^{-1} + r^2 z^{-2}}$	$\frac{1 - ax}{1 - 2r \cos(\omega_0 T)x + r^2 x^2}$
$r^n [A \cos(\omega_0 nT) + B \sin(\omega_0 nT)]$	$\frac{A + rz^{-1}(B \sin(\omega_0 T) - A \cos(\omega_0 T))}{1 - 2r \cos(\omega_0 T)z^{-1} + r^2 z^{-2}}$	$\frac{A + rx(B \sin(\omega_0 T) - A \cos(\omega_0 T))}{1 - 2r \cos(\omega_0 T)x + r^2 x^2}$
$r^n y_n$	$Y(r^{-1}z)$	$Y(r^{-1}x^{-1})$
y_{n+1}	$zY(z) - zy_0$	$x^{-1}Y(x^{-1}) - x^{-1}y_0$
y_{n-1}	$z^{-1}Y(z) + y_{-1}$	$xY(x^{-1}) + y_{-1}$
y_{n+m}	$z^m G(z) - (z^m y_0 + \dots + zy_{m-1})$	$x^{-m}G(x^{-1}) - (x^{-m}y_0 + \dots + x^{-1}y_{m-1})$
y_{n-m}	$z^{-m}G(z) + (z^{-(m-1)}y_{-1} + \dots + y_{-m})$	$x^m G(x^{-1}) + (x^{m-1}y_{-1} + \dots + y_{-m})$

Initial Value / Final Value Theorem: $y_0 = \lim_{z \rightarrow \infty} Y(z)$ and $\lim_{n \rightarrow \infty} y_n = \lim_{z \rightarrow 1} (z - 1) Y(z)$

Note: the final value theorem requires the poles of $(z - 1) Y(z)$ to have $|z| < 1$.

The Laplace-analogous residue formula for the Inverse Z-Transform is

$$g_n = \mathcal{Z}^{-1}\{G(z)\} = \frac{1}{2\pi i} \oint_C G(z) z^{n-1} dz = \sum_k \text{Res} [G(z)z^{n-1}, z_k]$$

where the residue Res is defined in Section 3.4.10. Note the extra factor of z^{n-1} .

3.5. Multivariable and Vector Calculus

3.5.1. Differentiation of Vector Products

For vector-valued functions $\mathbf{a}(t)$, $\mathbf{b}(t)$, and scalar-valued functions $u(t)$ of a single variable,

$$(\mathbf{a} \cdot \mathbf{b})' = \mathbf{a}' \cdot \mathbf{b} + \mathbf{a} \cdot \mathbf{b}' \quad (\mathbf{a} \times \mathbf{b})' = \mathbf{a}' \times \mathbf{b} + \mathbf{a} \times \mathbf{b}' \quad (u\mathbf{a})' = u'\mathbf{a} + u\mathbf{a}'$$

3.5.2. Jacobian Matrix

For a **vector valued** function \mathbf{f} of n variables $x_1 \dots x_n$, the Jacobian \mathbf{J} is $J_{ij} = \frac{\partial f_i}{\partial x_j}$:

$$\mathbf{J} = \begin{bmatrix} \frac{\partial \mathbf{f}}{\partial x_1} & \cdots & \frac{\partial \mathbf{f}}{\partial x_n} \end{bmatrix} = \begin{bmatrix} \nabla^T f_1 \\ \vdots \\ \nabla^T f_m \end{bmatrix} = \begin{bmatrix} \frac{\partial f_1}{\partial x_1} & \cdots & \frac{\partial f_1}{\partial x_n} \\ \vdots & \ddots & \vdots \\ \frac{\partial f_m}{\partial x_1} & \cdots & \frac{\partial f_m}{\partial x_n} \end{bmatrix}$$

3.5.3. Hessian Matrix

For a **scalar valued** function f of n variables $x_1 \dots x_n$, the Hessian \mathbf{H} is $H_{ij} = \frac{\partial^2 f}{\partial x_i \partial x_j}$:

$$\mathbf{H}_f = \begin{bmatrix} \frac{\partial^2 f}{\partial x_1^2} & \frac{\partial^2 f}{\partial x_1 \partial x_2} & \cdots & \frac{\partial^2 f}{\partial x_1 \partial x_n} \\ \frac{\partial^2 f}{\partial x_2 \partial x_1} & \frac{\partial^2 f}{\partial x_2^2} & \cdots & \frac{\partial^2 f}{\partial x_2 \partial x_n} \\ \vdots & \vdots & \ddots & \vdots \\ \frac{\partial^2 f}{\partial x_n \partial x_1} & \frac{\partial^2 f}{\partial x_n \partial x_2} & \cdots & \frac{\partial^2 f}{\partial x_n^2} \end{bmatrix},$$

The Hessian for a vector-valued function $\mathbf{f} = [f_1, f_2, \dots, f_n]$ is the third-rank Hessian tensor whose elements are $[\mathbf{H}_{f_1}, \mathbf{H}_{f_2}, \dots, \mathbf{H}_{f_n}]$, where \mathbf{H}_{f_i} is the Hessian matrix of f_i .

3.2.3. Multivariable Taylor Series

For a **scalar-valued** function $f(\mathbf{x})$ about \mathbf{x}_0 ,

$$f(\mathbf{x}_0 + \mathbf{h}) = f(\mathbf{x}_0) + (\mathbf{h} \cdot \nabla) f(\mathbf{x}_0) + \frac{1}{2!} (\mathbf{h} \cdot \nabla)(\mathbf{h} \cdot \nabla) f(\mathbf{x}_0) + \frac{1}{3!} (\mathbf{h} \cdot \nabla)(\mathbf{h} \cdot \nabla)(\mathbf{h} \cdot \nabla) f(\mathbf{x}_0) + \dots$$

In the case of a two-variable scalar function f about (x_0, y_0) ,

$$f(x_0 + h, y_0 + k) = \sum_{n=0}^{\infty} \left[\frac{1}{n!} \sum_{i=0}^n \binom{n}{i} h^i k^{n-i} \frac{\partial^n f}{\partial x^i \partial y^{n-i}} \right]$$

$$f(x_0 + h, y_0 + k) = f(x_0, y_0) + \left[h \frac{\partial f}{\partial x} + k \frac{\partial f}{\partial y} \right] + \frac{1}{2!} \left[h^2 \frac{\partial^2 f}{\partial x^2} + 2hk \frac{\partial^2 f}{\partial x \partial y} + k^2 \frac{\partial^2 f}{\partial y^2} \right] + \dots$$

The quadratic approximation is

$$f(\mathbf{x}_0 + \mathbf{h}) \approx f(\mathbf{x}_0) + \mathbf{h}^T \nabla f + \frac{1}{2!} \mathbf{h}^T \mathbf{H}(\mathbf{x}_0) \mathbf{h} + \dots$$

where $\mathbf{H}(\mathbf{x}_0)$ is the Hessian matrix of f (Section 3.5.3) at \mathbf{x}_0 . The linear term $\mathbf{h}^T \nabla f$ is the directional derivative of f in the direction of \mathbf{h} , also written as $D_{\mathbf{h}} f(\mathbf{x}_0) = \nabla f \cdot \mathbf{h}$.

For a **vector-valued** function $\mathbf{f}(\mathbf{x})$ about \mathbf{x}_0 ,

The quadratic approximation is

$$\mathbf{f}(\mathbf{x}_0 + \mathbf{h}) \approx \mathbf{f}(\mathbf{x}_0) + \mathbf{J}(\mathbf{x}_0) \mathbf{h} + \frac{1}{2!} \mathbf{h}^T \mathbf{H}(\mathbf{x}_0) \mathbf{h} + \dots$$

where $\mathbf{H}(\mathbf{x}_0)$ is the Hessian tensor of \mathbf{f} (Section 3.5.3) at \mathbf{x}_0 , and $\mathbf{J}(\mathbf{x}_0)$ is the Jacobian matrix of \mathbf{f} at \mathbf{x}_0 . In Einstein summation notation (Section 4.4.1), this quadratic approximation is

$$f_i(\mathbf{x}_0 + \mathbf{h}) \approx f_i(\mathbf{x}_0) + J_{ij}(\mathbf{x}_0) h_j + \frac{1}{2!} H_{ijk}(\mathbf{x}_0) h_j h_k + \dots$$

3.5.4. Stationary Points of a Scalar-Valued Multivariable Function

A function $\phi(x_1, \dots, x_n)$ has a **stationary point** when $\nabla\phi = \mathbf{0}$ i.e. $\frac{\partial\phi}{\partial x_1} = \frac{\partial\phi}{\partial x_2} = \dots = \frac{\partial\phi}{\partial x_n} = 0$.

If the determinant of the Hessian matrix $\Delta = |\mathbf{H}| \neq 0$ at a stationary point, then

- **Minimum point:** $\Delta > 0$ and all $\frac{\partial^2\phi}{\partial x_i^2} > 0$. (ϕ is locally **convex**)
- **Maximum point:** $\Delta < 0$ and all $\frac{\partial^2\phi}{\partial x_i^2} < 0$. (ϕ is locally **concave**)
- **Saddle point:** all other cases for which $\Delta \neq 0$.

The case $\Delta = 0$ can be a maximum, a minimum, a saddle point, or none of these.

For two variables, $\phi(x, y)$, $\Delta = \frac{\partial^2\phi}{\partial x^2} \frac{\partial^2\phi}{\partial y^2} - \left(\frac{\partial^2\phi}{\partial x \partial y}\right)^2$.

Second partial derivatives are symmetric (Clairhaut's theorem): $\frac{\partial^2\phi}{\partial x \partial y} = \frac{\partial^2\phi}{\partial y \partial x}$.

3.5.5. Total Differentials

For a function $\phi(x, y, z, \dots)$, $d\phi = \frac{d\phi}{dx} dx + \frac{d\phi}{dy} dy + \frac{d\phi}{dz} dz + \dots$

If $f(x, y) dx + g(x, y) dy = d\phi$, then $\frac{\partial f}{\partial y} = \frac{\partial g}{\partial x}$ (an exact differential).

3.5.6. Multivariable Chain Rule

If x, y, z are functions of u, v, w, \dots

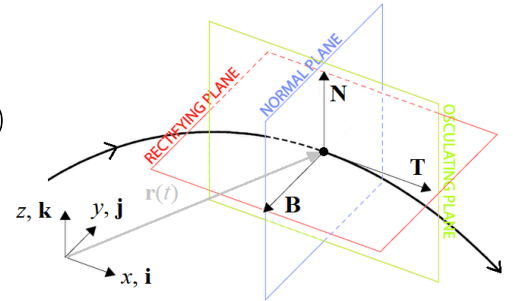
$$\left(\frac{\partial\phi}{\partial u}\right)_{v,w,\dots} = \frac{\partial\phi}{\partial x} \left(\frac{\partial x}{\partial u}\right)_{v,w,\dots} + \frac{\partial\phi}{\partial y} \left(\frac{\partial y}{\partial u}\right)_{v,w,\dots} + \frac{\partial\phi}{\partial z} \left(\frac{\partial z}{\partial u}\right)_{v,w,\dots} + \dots$$

3.5.7. Derivatives on Curved Lines and Curved Surfaces

For a **curve** defined parametrically as $\mathbf{r}(t) = [x(t) \ y(t) \ z(t)]^T$, the unit tangent vector \mathbf{T} , unit normal vector \mathbf{N} and unit binormal vector \mathbf{B} are given by

$$\hat{\mathbf{T}}(t) = \frac{\dot{\mathbf{r}}}{|\dot{\mathbf{r}}|} = \frac{\frac{d\mathbf{r}}{dt}}{\left|\frac{d\mathbf{r}}{dt}\right|} \quad \hat{\mathbf{N}}(t) = \frac{\frac{d\hat{\mathbf{T}}}{dt}}{\left|\frac{d\hat{\mathbf{T}}}{dt}\right|} \quad \hat{\mathbf{B}}(t) = \hat{\mathbf{T}}(t) \times \hat{\mathbf{N}}(t)$$

so that $\{\mathbf{T}, \mathbf{N}, \mathbf{B}\}$ forms a right-handed orthonormal set.



The equation of the tangent line at $\mathbf{r} = \mathbf{r}_0$ is then $(\mathbf{r} - \mathbf{r}_0) \times \mathbf{r}' = \mathbf{0}$.

The vectors \mathbf{T} , \mathbf{N} and \mathbf{B} vary with arc length s along the curve by (Frenet-Serret formulas):

$$\frac{d}{ds} \begin{bmatrix} \hat{\mathbf{T}} \\ \hat{\mathbf{N}} \\ \hat{\mathbf{B}} \end{bmatrix} = \begin{bmatrix} 0 & \kappa & 0 \\ -\kappa & 0 & \tau \\ 0 & -\tau & 0 \end{bmatrix} \begin{bmatrix} \hat{\mathbf{T}} \\ \hat{\mathbf{N}} \\ \hat{\mathbf{B}} \end{bmatrix} \quad (\kappa: \text{curvature}, \quad \tau: \text{torsion})$$

$$\kappa = \frac{|\dot{\mathbf{r}} \times \ddot{\mathbf{r}}|}{|\dot{\mathbf{r}}|^3} \quad \text{and} \quad \tau = \frac{(\dot{\mathbf{r}} \times \ddot{\mathbf{r}}) \cdot \dddot{\mathbf{r}}}{|\dot{\mathbf{r}} \times \ddot{\mathbf{r}}|^2}$$

The associated radius of curvature is $R = \kappa^{-1}$ and the ‘osculating circle’ lies in the plane spanned by \mathbf{T} and \mathbf{N} , with \mathbf{B} as its normal.

For a **surface** defined implicitly as $\phi(x, y, z) = 0$, the unit tangent vector \mathbf{T} (defined as being the projection of some vector \mathbf{u} in (x, y) -space onto the surface) and unit normal vector \mathbf{N} are

$$\hat{\mathbf{T}}(x, y, z) = \frac{(D_{\hat{\mathbf{k}}}\phi)\hat{\mathbf{u}} - (D_{\hat{\mathbf{u}}}\phi)\hat{\mathbf{k}}}{|\nabla\phi|} \quad \hat{\mathbf{N}}(x, y, z) = \frac{\nabla\phi}{|\nabla\phi|}$$

where \mathbf{k} is the unit vector in the z -direction and $D_{\mathbf{a}}f$ is the **directional derivative**, defined as $D_{\mathbf{a}}f = \nabla f \cdot \mathbf{a}$, representing the component of the gradient parallel to \mathbf{a} .

The equation of the tangent plane at $\mathbf{r} = \mathbf{r}_0$ is then $(\mathbf{r} - \mathbf{r}_0) \cdot \nabla\phi(\mathbf{r}_0) = 0$.

If \mathbf{N} is evaluated at a vector \mathbf{r}_0 which does not lie on the surface, then \mathbf{N} can instead be interpreted as the direction of steepest ascent for ϕ at $\mathbf{r} = \mathbf{r}_0$ (since $\phi \neq 0$ off the surface).

For a scalar-valued function $\phi(\mathbf{r})$, the regions of constant ϕ are called **isosurfaces** (contour surfaces; level surfaces) in 3D or **isolines** (contour lines) in 2D.

These results are easily generalisable to other dimensional functions, except the binormal vector which is only uniquely defined in \mathbb{R}^3 .

3.5.8. Reduction of a Multiple Integral with Common Bounds to a Single Integral

Double integral to single integral:
$$\int_a^x \int_a^u f(t) dt du = \int_a^x (x - t) f(t) dt$$

Triple integral to single integral:
$$\int_a^x \int_a^u \int_a^v f(t) dt dv du = \frac{1}{2} \int_a^x (x - t)^2 f(t) dt$$

These can be useful for simplifying numerical integration of multiple integrals.

3.5.9. Change of Variables for Multiple Integration

Surface Integrals:

For a change of variables in a surface integral from $(x, y) \rightarrow (u(x, y), v(x, y))$,

$$\iint_S f(x, y) dx dy = \iint_{S'} F(u, v) |J| du dv \quad J = \frac{\partial(x, y)}{\partial(u, v)} = \begin{vmatrix} \frac{\partial x}{\partial u} & \frac{\partial x}{\partial v} \\ \frac{\partial y}{\partial u} & \frac{\partial y}{\partial v} \end{vmatrix}$$

For surface integrals involving vector normals, where the sign is chosen to preserve the sense.

$$\mathbf{n} dA = \mathbf{n} dx dy = \pm \frac{\partial \mathbf{r}}{\partial u} \times \frac{\partial \mathbf{r}}{\partial v} du dv$$

Volume integrals:

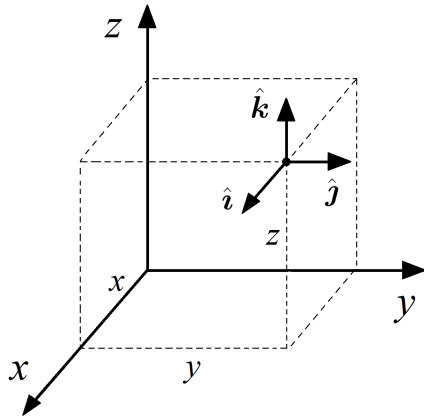
For a change of variables in a volume integral from $(x, y, z) \rightarrow (u(x, y, z), v(x, y, z), w(x, y, z))$,

$$\iiint_V f(x, y, z) dx dy dz = \iiint_{V'} F(u, v, w) |J| du dv dw \quad J = \frac{\partial(x, y, z)}{\partial(u, v, w)} = \begin{vmatrix} \frac{\partial x}{\partial u} & \frac{\partial x}{\partial v} & \frac{\partial x}{\partial w} \\ \frac{\partial y}{\partial u} & \frac{\partial y}{\partial v} & \frac{\partial y}{\partial w} \\ \frac{\partial z}{\partial u} & \frac{\partial z}{\partial v} & \frac{\partial z}{\partial w} \end{vmatrix}$$

The inverse Jacobian determinant is the same as that of the inverse substitution:

$$\frac{1}{J} = \frac{\partial(u, v, \dots)}{\partial(x, y, \dots)}$$

3.5.10. Vector Calculus in Cartesian Coordinates



Parameters: (x, y, z) , all real ordinates

Scalar field: $r = x\hat{i} + y\hat{j} + z\hat{k}$

Vector field: $u = u_x\hat{i} + u_y\hat{j} + u_z\hat{k}$

Kinematics:

Position: $r = x\hat{i} + y\hat{j} + z\hat{k}$

Velocity: $\dot{r} = \dot{x}\hat{i} + \dot{y}\hat{j} + \dot{z}\hat{k}$

Acceleration: $\ddot{r} = \ddot{x}\hat{i} + \ddot{y}\hat{j} + \ddot{z}\hat{k}$

Angular velocity: $\omega = 0$ (fixed)

Unit vectors: $\dot{\hat{i}} = 0, \dot{\hat{j}} = 0, \dot{\hat{k}} = 0$ (fixed)

Differential Elements

Line element: $dr = dx\hat{i} + dy\hat{j} + dz\hat{k}$

Volume element: $dV = dxdydz$

Surface elements: $dS_x = dydz, dS_y = dxdz, dS_z = dxdy$

Distance:

$$d = \sqrt{x^2 + y^2 + z^2}$$

Vector Operators:

Gradient: $\nabla f = \frac{\partial f}{\partial x}\hat{i} + \frac{\partial f}{\partial y}\hat{j} + \frac{\partial f}{\partial z}\hat{k}$

Divergence: $\nabla \cdot u = \frac{\partial u_x}{\partial x} + \frac{\partial u_y}{\partial y} + \frac{\partial u_z}{\partial z}$

Curl: $\nabla \times u = \begin{vmatrix} \hat{i} & \hat{j} & \hat{k} \\ \partial/\partial x & \partial/\partial y & \partial/\partial z \\ u_x & u_y & u_z \end{vmatrix}$

Laplacian: $\nabla^2 f = \Delta f = \frac{\partial^2 f}{\partial x^2} + \frac{\partial^2 f}{\partial y^2} + \frac{\partial^2 f}{\partial z^2}$

Biharmonic: $\nabla^4 f = \Delta^2 f = \frac{\partial^4 f}{\partial x^4} + \frac{\partial^4 f}{\partial y^4} + \frac{\partial^4 f}{\partial z^4} + 2\frac{\partial^4 f}{\partial x^2 \partial y^2} + 2\frac{\partial^4 f}{\partial y^2 \partial z^2} + 2\frac{\partial^4 f}{\partial x^2 \partial z^2}$

3.5.11. Vector Calculus in Spherically Symmetric (Radial) Coordinates

Parameters: $r \geq 0$ (radial coordinate): uniform in every direction

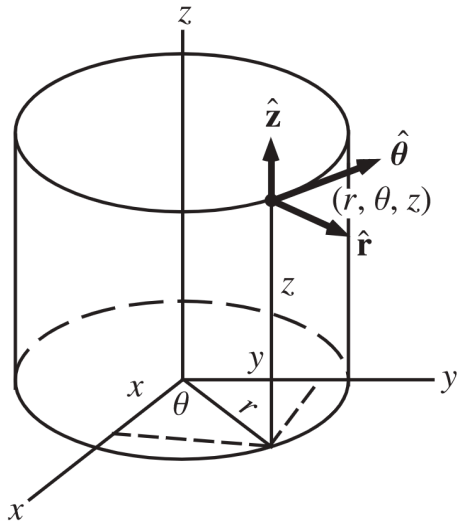
Gradient: $\nabla f = \frac{df}{dr}\hat{r}$ Divergence: $\nabla \cdot u = \frac{1}{r^2} \frac{d}{dr} (r^2 u_r)$ Curl: $\nabla \times u = 0$

Laplacian: $\nabla^2 f = \Delta f = \frac{d^2 f}{dr^2} + \frac{2}{r} \frac{df}{dr} = \frac{1}{r^2} \frac{d}{dr} \left(r^2 \frac{df}{dr} \right)$ (auxiliary function: $u(r) = r f(r)$)

Biharmonic: $\nabla^4 f = \Delta^2 f = \frac{d^4 f}{dr^4} + \frac{2}{r} \frac{d^3 f}{dr^3} - \frac{1}{r^2} \frac{d^2 f}{dr^2} + \frac{1}{r^3} \frac{df}{dr}$ $\rightarrow \nabla^2 f = \frac{1}{r} \frac{d^2 u}{dr^2}$

Volume element: $dV = 4\pi r^2 dr$ (shell element)

3.5.12. Vector Calculus in Cylindrical Coordinates



Parameters: r : radius, $0 \leq \theta \leq 2\pi$: polar angle, z : elevation

Scalar field: $\mathbf{r} = r \hat{\mathbf{r}} + z \hat{\mathbf{z}}$

Vector field: $\mathbf{u} = u_r \hat{\mathbf{r}} + u_\theta \hat{\boldsymbol{\theta}} + u_z \hat{\mathbf{z}}$

Coordinate Conversions to and from Cartesian (x, y, z) :

$$x = r \cos \theta, \quad y = r \sin \theta, \quad z = z$$

$$r = \sqrt{x^2 + y^2}, \quad \theta = \text{atan2}(y, x), \quad z = z$$

Unit Vector Conversions to and from Cartesian $(\hat{i}, \hat{j}, \hat{k})$:

$$\hat{\mathbf{r}} = \cos \theta \hat{\mathbf{i}} + \sin \theta \hat{\mathbf{j}}, \quad \hat{\boldsymbol{\theta}} = -\sin \theta \hat{\mathbf{i}} + \cos \theta \hat{\mathbf{j}}, \quad \hat{\mathbf{z}} = \hat{\mathbf{k}}$$

$$\hat{\mathbf{i}} = \cos \theta \hat{\mathbf{r}} - \sin \theta \hat{\boldsymbol{\theta}}, \quad \hat{\mathbf{j}} = \sin \theta \hat{\mathbf{r}} + \cos \theta \hat{\boldsymbol{\theta}}, \quad \hat{\mathbf{k}} = \hat{\mathbf{z}}$$

Kinematics: time derivatives of displacement \mathbf{r}

Position: $\mathbf{r} = r \hat{\mathbf{r}} + z \hat{\mathbf{z}}$

Velocity: $\dot{\mathbf{r}} = \dot{r} \hat{\mathbf{r}} + r \dot{\theta} \hat{\boldsymbol{\theta}} + \dot{z} \hat{\mathbf{z}}$

Acceleration: $\ddot{\mathbf{r}} = (\ddot{r} - r \dot{\theta}^2) \hat{\mathbf{r}} + (2\dot{r} \dot{\theta} + r \ddot{\theta}) \hat{\boldsymbol{\theta}} + \ddot{z} \hat{\mathbf{z}}$

Angular Velocity: $\boldsymbol{\omega} = \dot{\theta} \hat{\mathbf{z}}$

Unit vectors: $\dot{\hat{\mathbf{r}}} = \dot{\theta} \hat{\boldsymbol{\theta}}, \quad \dot{\hat{\boldsymbol{\theta}}} = -\dot{\theta} \hat{\mathbf{r}}, \quad \dot{\hat{\mathbf{z}}} = \mathbf{0}$

Differential Elements

Line element: $d\mathbf{r} = dr \hat{\mathbf{r}} + r d\theta \hat{\boldsymbol{\theta}} + dz \hat{\mathbf{z}}$

Volume element: $dV = r dr d\theta dz$

(Jacobian: $\frac{\partial(x, y, z)}{\partial(r, \theta, z)} = r$)

Surface elements: $dS_r = r d\theta dz, \quad dS_\theta = r dr dz, \quad dS_z = r dr d\theta$

Distance: $d = \sqrt{r_1^2 + r_2^2 - 2r_1 r_2 \cos(\theta_1 - \theta_2) + (z_1 - z_2)^2}$

Vector Operators

Gradient: $\nabla f = \frac{\partial f}{\partial r} \hat{\mathbf{r}} + \frac{1}{r} \frac{\partial f}{\partial \theta} \hat{\boldsymbol{\theta}} + \frac{\partial f}{\partial z} \hat{\mathbf{z}}$

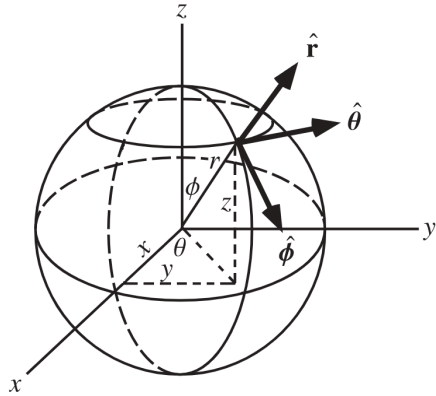
Divergence: $\nabla \cdot \mathbf{u} = \frac{1}{r} \frac{\partial(r u_r)}{\partial r} + \frac{1}{r} \frac{\partial u_\theta}{\partial \theta} + \frac{\partial u_z}{\partial z}$

Curl: $\nabla \times \mathbf{u} = \frac{1}{r} \begin{vmatrix} \hat{\mathbf{r}} & r \hat{\boldsymbol{\theta}} & \hat{\mathbf{z}} \\ \frac{\partial}{\partial r} & \frac{\partial}{\partial \theta} & \frac{\partial}{\partial z} \\ u_r & r u_\theta & u_z \end{vmatrix}$

Laplacian: $\nabla^2 f = \frac{1}{r} \frac{\partial}{\partial r} \left(r \frac{\partial f}{\partial r} \right) + \frac{1}{r^2} \frac{\partial^2 f}{\partial \theta^2} + \frac{\partial^2 f}{\partial z^2}$

Biharmonic: $\Delta^2 f = \nabla^4 f = \frac{\partial^4 f}{\partial r^4} + \frac{2}{r^2} \frac{\partial^4 f}{\partial r^2 \partial \theta^2} + \frac{1}{r^4} \frac{\partial^4 f}{\partial \theta^4} + \frac{2}{r} \frac{\partial^3 f}{\partial r^3} - \frac{2}{r^3} \frac{\partial^3 f}{\partial r \partial \theta^2} - \frac{1}{r^2} \frac{\partial^2 f}{\partial r^2} + \frac{4}{r^4} \frac{\partial^2 f}{\partial \theta^2} + \frac{1}{r^3} \frac{\partial f}{\partial r} + \frac{\partial^4 f}{\partial z^4}$

3.5.13. Vector Calculus in Spherical Coordinates



Parameters: r : radius, $0 \leq \theta \leq 2\pi$: azimuth/longitude angle, $0 \leq \phi \leq \pi$: zenith/colatitude angle

Vector field: $\mathbf{u} = u_r \hat{\mathbf{r}} + u_\theta \hat{\boldsymbol{\theta}} + u_\phi \hat{\boldsymbol{\phi}}$

Coordinate Conversions to and from Cartesian (x, y, z) :

$$x = r \sin \phi \cos \theta, \quad y = r \sin \phi \sin \theta, \quad z = r \cos \phi$$

$$r = \sqrt{x^2 + y^2 + z^2}, \quad \theta = \text{atan2}(y, x), \quad \phi = \cos^{-1} \frac{z}{r}$$

Unit Vector Conversions to and from Cartesian $(\hat{\mathbf{i}}, \hat{\mathbf{j}}, \hat{\mathbf{k}})$:

$$\hat{\mathbf{r}} = \sin \phi \cos \theta \hat{\mathbf{i}} + \sin \phi \sin \theta \hat{\mathbf{j}} + \cos \phi \hat{\mathbf{k}}, \quad \hat{\mathbf{i}} = \cos \theta \sin \phi \hat{\mathbf{r}} - \sin \theta \hat{\boldsymbol{\theta}} + \cos \theta \cos \phi \hat{\boldsymbol{\phi}}$$

$$\hat{\boldsymbol{\theta}} = -\sin \theta \hat{\mathbf{i}} + \cos \theta \hat{\mathbf{j}}, \quad \hat{\mathbf{j}} = \sin \theta \sin \phi \hat{\mathbf{r}} + \cos \theta \hat{\boldsymbol{\theta}} + \sin \theta \cos \phi \hat{\boldsymbol{\phi}}$$

$$\hat{\boldsymbol{\phi}} = \cos \theta \cos \phi \hat{\mathbf{i}} + \sin \theta \cos \phi \hat{\mathbf{j}} - \sin \phi \hat{\mathbf{k}}, \quad \hat{\mathbf{k}} = \cos \phi \hat{\mathbf{r}} - \sin \phi \hat{\boldsymbol{\phi}}$$

Kinematics: time derivatives of displacement \mathbf{r}

Position: $\mathbf{r} = r \hat{\mathbf{r}}$

Velocity: $\dot{\mathbf{r}} = \dot{r} \hat{\mathbf{r}} + r \dot{\theta} \sin \phi \hat{\boldsymbol{\theta}} + r \dot{\phi} \hat{\boldsymbol{\phi}}$

Acceleration: $\ddot{\mathbf{r}} = (\ddot{r} - r\dot{\theta}^2 \sin^2 \phi - r\dot{\phi}^2) \hat{\mathbf{r}} + ((r\ddot{\theta} + 2\dot{r}\dot{\theta}) \sin \phi + 2r\dot{\theta}\dot{\phi} \cos \phi) \hat{\boldsymbol{\theta}} + (r\ddot{\phi} + 2\dot{r}\dot{\phi} - r\dot{\theta}^2 \sin \phi \cos \phi) \hat{\boldsymbol{\phi}}$

Angular Velocity: $\boldsymbol{\omega} = \dot{\theta} \cos \phi \hat{\mathbf{r}} + \dot{\phi} \hat{\boldsymbol{\theta}} - \dot{\theta} \sin \phi \hat{\boldsymbol{\phi}} = \dot{\phi} \hat{\boldsymbol{\theta}} + \dot{\theta} \hat{\mathbf{k}}$

Unit vectors: $\dot{\hat{\mathbf{r}}} = -\dot{\theta} \sin \phi \hat{\boldsymbol{\theta}} + \dot{\phi} \hat{\boldsymbol{\phi}}, \quad \dot{\hat{\boldsymbol{\theta}}} = -\dot{\theta} \sin \phi \hat{\mathbf{r}} + \dot{\theta} \cos \phi \hat{\boldsymbol{\phi}}, \quad \dot{\hat{\boldsymbol{\phi}}} = \dot{\phi} \hat{\mathbf{r}} - \dot{\theta} \cos \phi \hat{\boldsymbol{\theta}}$

Differential Elements

Line element: $d\mathbf{r} = dr \hat{\mathbf{r}} + r \sin \phi d\theta \hat{\boldsymbol{\theta}} + r d\phi \hat{\boldsymbol{\phi}}$

Volume element: $dV = r^2 \sin \phi dr d\theta d\phi$ (Jacobian: $\frac{\partial(x, y, z)}{\partial(r, \phi, \theta)} = r^2 \sin \phi$)

Surface elements: $dS_r = r^2 \sin \phi d\theta d\phi, \quad dS_\theta = r dr d\phi, \quad dS_\phi = r \sin \phi dr d\theta$

Distance: $d = \sqrt{r_1^2 + r_2^2 - 2r_1 r_2 (\sin \phi_1 \sin \phi_2 \cos(\theta_1 - \theta_2) + \cos \phi_1 \cos \phi_2)}$

Vector Operators

Gradient: $\nabla f = \frac{\partial f}{\partial r} \hat{\mathbf{r}} + \frac{1}{r} \frac{\partial f}{\partial \phi} \hat{\boldsymbol{\phi}} + \frac{1}{r \sin \phi} \frac{\partial f}{\partial \theta} \hat{\boldsymbol{\theta}}$ Divergence: $\nabla \cdot \mathbf{u} = \frac{1}{r^2} \frac{\partial(r^2 u_r)}{\partial r} + \frac{1}{r \sin \phi} \frac{\partial(\sin \phi u_\phi)}{\partial \phi} + \frac{1}{r \sin \phi} \frac{\partial u_\theta}{\partial \theta}$

Curl: $\nabla \times \mathbf{u} = \frac{1}{r^2 \sin \phi} \begin{vmatrix} \hat{\mathbf{r}} & r \hat{\boldsymbol{\phi}} & r \sin \phi \hat{\boldsymbol{\theta}} \\ \partial/\partial r & \partial/\partial \phi & \partial/\partial \theta \\ u_r & r u_\phi & r \sin \phi u_\theta \end{vmatrix}$

Laplacian: $\nabla^2 f = \frac{1}{r^2} \frac{\partial}{\partial r} \left(r^2 \frac{\partial f}{\partial r} \right) + \frac{1}{r^2 \sin \phi} \frac{\partial}{\partial \phi} \left(\sin \phi \frac{\partial f}{\partial \phi} \right) + \frac{1}{r^2 \sin^2 \phi} \frac{\partial^2 f}{\partial \theta^2}$

3.5.14. Vector Fields

Field Lines of a Vector Field

The plot of a vector-valued function $\mathbf{u} = \mathbf{f}(x, y, z) = \mathbf{f}(\mathbf{r}) = u_x \mathbf{i} + u_y \mathbf{j} + u_z \mathbf{k}$ is a vector field.

The equations of the field lines (curves with tangent vectors \mathbf{u}) are given by $\frac{dx}{u_x} = \frac{dy}{u_y} = \frac{dz}{u_z}$,

so that e.g. the field lines in the plane $z = 0$ satisfy $\frac{dy}{dx} = \frac{u_y(x, y, 0)}{u_x(x, y, 0)}$.

Potentials of Vector Fields

- **Irrotational (conservative) field:** if $\nabla \times \mathbf{u} = 0$ (curl free). In this case, then there exists a scalar potential f such that $\mathbf{u} = \nabla f$. For some applications it is more natural to use $\mathbf{u} = -\nabla f$. The isosurfaces of f are the equipotentials of \mathbf{u} , and \mathbf{u} is perpendicular to these isosurfaces (the normal vectors of \mathbf{u}) everywhere.
- **Solenoidal (incompressible) field:** if $\nabla \cdot \mathbf{u} = 0$ (divergence free). In this case, then there exists a vector potential \mathbf{A} such that $\mathbf{u} = \nabla \times \mathbf{A}$.
 \mathbf{A} is usually chosen so that $\nabla \cdot \mathbf{A} = 0$. Then, \mathbf{u} is the vorticity field of \mathbf{A} .

Decompositions of Vector Fields

- **Helmholtz Decomposition:** a field \mathbf{u} can be written as $\mathbf{u} = -\nabla f + \nabla \times \mathbf{A}$ (irrotational part plus solenoidal part). The expressions for f and \mathbf{A} are

$$4\pi f(\mathbf{r}) = \iiint_V \frac{\nabla_{\mathbf{r}'} \cdot \mathbf{u}(\mathbf{r}')}{|\mathbf{r} - \mathbf{r}'|} dV' - \iint_S \hat{\mathbf{n}}' \cdot \frac{\mathbf{u}(\mathbf{r}')}{|\mathbf{r} - \mathbf{r}'|} dS', \quad 4\pi \mathbf{A}(\mathbf{r}) = \iiint_V \frac{\nabla_{\mathbf{r}'} \times \mathbf{u}(\mathbf{r}')}{|\mathbf{r} - \mathbf{r}'|} dV' - \iint_S \hat{\mathbf{n}}' \times \frac{\mathbf{u}(\mathbf{r}')}{|\mathbf{r} - \mathbf{r}'|} dS'$$

- **Poloidal-Toroidal (Chandrasekhar-Kendall) Decomposition:** if $\nabla \cdot \mathbf{u} = 0$ (solenoidal) and \mathbf{u} is defined in spherical coordinates $\{\mathbf{e}_r, \mathbf{e}_\theta, \mathbf{e}_\phi\}$, then the vector potential $\mathbf{u} = \nabla \times \mathbf{A}$ can be written as $\mathbf{A} = \mathbf{T} + \mathbf{P}$, where $\mathbf{T} = T \mathbf{e}_r$ (toroidal part) and $\mathbf{P} = \nabla \times (P \mathbf{e}_r) = \nabla P \times \mathbf{e}_r$ (poloidal part). The toroidal part satisfies $\mathbf{e}_r \cdot \mathbf{T} = 0$. The poloidal part satisfies $\mathbf{e}_r \cdot (\nabla \times \mathbf{P}) = 0$.

$T(\mathbf{r})$ and $P(\mathbf{r})$ are scalar fields that satisfy the Poisson equations $\mathbf{e}_r \cdot (\nabla \times \mathbf{u}) = -\Delta_H T$ and $\mathbf{e}_r \cdot \mathbf{u} = -\Delta_H P$, where Δ_H is the scalar Laplacian containing only the $\{\theta, \phi\}$ ('horizon') terms.

3.5.15. Vector Calculus Identities

Properties of Vector Calculus Operators with Vector Operators: for scalar-valued functions f and vector-valued functions \mathbf{u} ,

$$\nabla(f_1 + f_2) = \nabla f_1 + \nabla f_2$$

$$\nabla \cdot (\mathbf{u}_1 + \mathbf{u}_2) = \nabla \cdot \mathbf{u}_1 + \nabla \cdot \mathbf{u}_2$$

$$\nabla \times (\mathbf{u}_1 + \mathbf{u}_2) = \nabla \times \mathbf{u}_1 + \nabla \times \mathbf{u}_2$$

$$\nabla \cdot (f\mathbf{u}) = f\nabla \cdot \mathbf{u} + (\nabla f) \cdot \mathbf{u}$$

$$\nabla \times (f\mathbf{u}) = f\nabla \times \mathbf{u} + (\nabla f) \times \mathbf{u}$$

$$\nabla \cdot (\mathbf{u}_1 \times \mathbf{u}_2) = \mathbf{u}_2 \cdot \nabla \times \mathbf{u}_1 - \mathbf{u}_1 \cdot \nabla \times \mathbf{u}_2$$

$$\nabla \cdot \nabla \times \mathbf{u} = 0$$

$$\nabla \times \nabla f = \mathbf{0}$$

$$\nabla \times (\nabla \times \mathbf{u}) = \nabla(\nabla \cdot \mathbf{u}) - \nabla^2 \mathbf{u}$$

$$\nabla \times (\mathbf{u}_1 \times \mathbf{u}_2) = \mathbf{u}_1 \nabla \cdot \mathbf{u}_2 - \mathbf{u}_2 \nabla \cdot \mathbf{u}_1 + (\mathbf{u}_2 \cdot \nabla) \mathbf{u}_1 - (\mathbf{u}_1 \cdot \nabla) \mathbf{u}_2$$

$$\mathbf{u} \times (\nabla \times \mathbf{u}) + (\mathbf{u} \cdot \nabla) \mathbf{u} = \frac{1}{2} \nabla(\mathbf{u}^2)$$

$$(\nabla^2 \mathbf{u} = [\nabla^2 u_x, \nabla^2 u_y, \nabla^2 u_z]^T: \text{vector Laplacian.})$$

Gauss Theorem (divergence theorem): for a closed surface S enclosing a volume V , with the outward normal taken for $d\mathbf{A}$, the total emitted flux Φ is equal to the net internal divergence

$$\Phi = \iiint_V \nabla \cdot \mathbf{u} \, dV = \oiint_S \mathbf{u} \cdot d\mathbf{A}$$

Stokes Theorem (curl theorem): for an open surface S bounded by a closed curve C circulating S anti-clockwise, the circulation Γ is equal to the net enclosed rotation (flux of vorticity):

$$\Gamma = \oint_C \mathbf{u} \cdot d\mathbf{l} = \iint_S \nabla \times \mathbf{u} \cdot d\mathbf{A}$$

Green's Theorem: in planar 2D space, Stokes' theorem reduces to:

$$\Gamma = \oint_C \mathbf{u} \cdot d\mathbf{l} = \oint_C u_x \, dx + u_y \, dy = \iint_S \frac{\partial u_y}{\partial x} - \frac{\partial u_x}{\partial y} \, dx dy$$

Green's First Identity: divergence theorem with $\mathbf{u} = f\nabla g$ and $\nabla \cdot (f\nabla g) = \nabla f \cdot \nabla g + f\nabla \cdot \nabla g$.

$$\oiint_S f\nabla g \cdot d\mathbf{A} = \iiint_V (\nabla f \cdot \nabla g) dV + \iiint_V f\nabla^2 g \, dV$$

Green's Second Identity: difference of symmetric forms of first identity.

$$\oiint_S (f\nabla g - g\nabla f) \cdot d\mathbf{A} = \iiint_V (f\nabla^2 g - g\nabla^2 f) \, dV$$

Green's Third Identity: in the second identity, let $f = G$ (a Green's function, Section 3.7.4), chosen suitably for the PDE to be solved such that $G = 0$ on the boundary. Substitute solutions for ∇G and $\nabla^2 G$.

3.5.16. Differential Operators

Expressions of derivatives of functions can be written as operators acting on functions.

$$n\text{th partial differential operator: } D_x^n = \frac{\partial^n}{\partial x^n} \Rightarrow D_x^n y = \frac{\partial^n y}{\partial x^n}$$

$$\text{Example: } DxD = \frac{d}{dx} \left(x \frac{d}{dx} \right) = \frac{d}{dx} + x \frac{d^2}{dx^2} = D + xD^2$$

$$\text{General operators can be constructed e.g. } L = 2D_x^2 - xD_x D_y \Rightarrow L\phi = 2 \frac{\partial^2 \phi}{\partial x^2} - x \frac{\partial \phi}{\partial x} \frac{\partial \phi}{\partial y}$$

Differential operators are generally not commutative.

Linear differential operators with constant coefficients are commutative.

Separation of a coupled system of linear partial differential equations: using operators

If L_i are **commutative** linear differential operators with $L_1L_3 = L_3L_1$ and $L_2L_4 = L_4L_2$ then the coupled system of PDEs $\{L_1u + L_2v = f; L_3u + L_4v = g\}$ can be uncoupled to yield the two PDEs

$$\{(L_4L_1 - L_2L_3)u = L_4f - L_2g; (L_3L_2 - L_1L_4)v = L_3f - L_1g\}$$

($u = u(x, y, \dots)$, $v = v(x, y, \dots)$): dependent variables, L_i : linear differential operators of $\{x, y, \dots\}$ with constant coefficients, $\{f = f(x, y, \dots), g = g(x, y, \dots)\}$: differentiable functions)

3.5.17. Multivariable (Spatial) Continuous Fourier Transform

For the ordinary Fourier transform, see Section 3.6.4. When the input domain is multi-dimensional (e.g. position space $\mathbf{x} = [x, y, z]$ rather than time t), the output frequency domain is also multi-dimensional (e.g. spatial frequency $\mathbf{k} = [k_x, k_y, k_z]$ rather than temporal frequency ω).

$$F(\mathbf{k}) = \int_{C^n} f(\mathbf{x}) \exp(-j \mathbf{k} \cdot \mathbf{x}) d\mathbf{x} \qquad f(\mathbf{x}) = \frac{1}{(2\pi)^n} \int_{C^n} F(\mathbf{k}) \exp(j \mathbf{k} \cdot \mathbf{x}) d\mathbf{k}$$

Forward Fourier Transform **Inverse Fourier Transform**

The integration is generally performed over all $\mathbf{x} \in C^n$ and $\mathbf{k} \in C^n$. In many practical applications, the function $f(\mathbf{x})$ is real and even so $F(\mathbf{k})$ is real and even so $\mathbf{x} \in R^n$ and $\mathbf{k} \in R^n$. In quantum mechanics $f = \psi \in C$ and \mathbf{k} -space is momentum space (since $\mathbf{p} = \hbar \mathbf{k}$).

Multivariable Parseval's Theorem:
$$\int_{-\infty}^{\infty} \dots \int_{-\infty}^{\infty} |f(\mathbf{x})|^2 d\mathbf{x} = \frac{1}{(2\pi)^n} \int_{-\infty}^{\infty} \dots \int_{-\infty}^{\infty} |F(\mathbf{k})|^2 d\mathbf{k}$$

3.5.18. Multivariable (Spatial) Discrete Fourier Transform

For the ordinary discrete Fourier transform (DFT), see Section 3.6.5.

When the input domain is discrete multi-dimensional (e.g. pixel space $\mathbf{w} = [u, v]$), the output frequency domain is also discrete multi-dimensional (e.g. discrete spatial frequency $\mathbf{k} = [k_u, k_v]$).

$$F(\mathbf{k}) = \sum_{n_1=0}^{N_1-1} \dots \sum_{n_m=0}^{N_m-1} f(\mathbf{w}) \exp\left(-\sum_{a=1}^m \frac{2\pi i k_a n_a}{N_a}\right) \qquad f(\mathbf{w}) = \frac{1}{N_1 \dots N_m} \sum_{k_1=0}^{N_1-1} \dots \sum_{k_m=0}^{N_m-1} F(\mathbf{k}) \exp\left(\sum_{a=1}^m \frac{2\pi i k_a n_a}{N_a}\right)$$

Forward Discrete Fourier Transform **Inverse Discrete Fourier Transform**

Multivariable Convolution Theorem: $F(\mathbf{k}) G(\mathbf{k}) = \text{DFT}\{(f * g)(\mathbf{w})\}$ (DFT: discrete FT) where the convolution is circular (periodic). Common application: image filtering (Section 5.6.1).

3.5.18. Multivariable Z-Transform

For the ordinary Z-transform, see Section 3.4.19.

Forward Z-transform:
$$F(z_1, \dots, z_m) = \sum_{n_1=-\infty}^{\infty} \dots \sum_{n_m=-\infty}^{\infty} f(n_1, \dots, n_m) \times (z_1^{n_1} \dots z_m^{n_m})$$

3.6. Fourier Series and Fourier Transforms

3.6.1. General Fourier Series Definition

Real-Valued Fourier Series

The real-valued Fourier series is defined for a function $f(t)$ on $0 \leq t < T$ as

$$f(t) = d + \sum_{n=1}^{\infty} \left(a_n \cos \frac{2\pi nt}{T} + b_n \sin \frac{2\pi nt}{T} \right)$$

$$\text{where } d = \frac{1}{T} \int_0^T f(t) dt, \quad a_n = \frac{2}{T} \int_0^T f(t) \cos \frac{2\pi nt}{T} dt, \quad b_n = \frac{2}{T} \int_0^T f(t) \sin \frac{2\pi nt}{T} dt$$

If the function $f(t)$ is periodic, of period T , then these relationships are valid for all t . The integrals may then be taken over any range of T .

- If $f(t)$ is even then $b_n = 0$.
- If $f(t)$ is odd then $a_n = 0$.
- If $f(t)$ has zero mean value then $d = 0$.

The rate of convergence, $O(n^{-(k+1)})$, is such that the k -th derivative of $f(t)$ is discontinuous.

Complex-Valued Fourier Series

Equivalently, the complex-valued Fourier series is

$$f(t) = \sum_{n=-\infty}^{\infty} c_n e^{i2\pi nt/T} \quad \text{where} \quad c_n = \frac{1}{T} \int_0^T f(t) e^{-i2\pi nt/T} dt$$

$$\text{i.e. } f(t) = \sum_{n=-\infty}^{\infty} c_n e^{in\omega_0 t} \quad \text{where} \quad c_n = \frac{1}{T} \int_0^T f(t) e^{-in\omega_0 t} dt$$

The relationship between the complex and real forms of the coefficients is

$$c_n = \begin{cases} \frac{1}{2}(a_n - ib_n) & \text{for } n > 0 \\ d & \text{for } n = 0 \end{cases}$$

and, for real functions $f(t)$, we have $c_{-n} = c_n^*$.

The (scientific) fundamental frequency is $\omega_0 = \frac{2\pi}{T}$ and the (scientific) n th harmonic is $n\omega_0$.

3.6.2. Half-Range Fourier Series Definition

If a Fourier series representation of $f(x)$ is required to be valid only in $0 \leq x \leq L$, then it only needs to contain either the sine terms alone or the cosine terms alone. For example

$$f(x) = \sum_{n=1}^{\infty} b_n \sin \frac{n\pi x}{L}$$

$$\text{where } b_n = \frac{2}{L} \int_0^L f(x) \sin \frac{n\pi x}{L} dx$$

Note that the wavelength of the first term in the series ($n = 1$) is $2L$ rather than L (as would be the case for the full-range series).

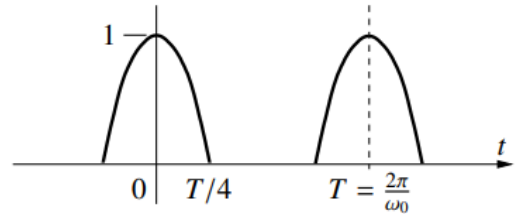
3.6.3. Fourier Series of Common Waveforms

Half-wave Rectified Cosine

$$f(t) = \frac{1}{\pi} + \frac{1}{2} \cos \omega_0 t + \frac{2}{\pi} \sum_{m=1}^{\infty} (-1)^{m+1} \frac{\cos 2m\omega_0 t}{4m^2 - 1}$$

$$f(t) = \frac{1}{\pi} + \frac{1}{4} e^{i\omega_0 t} + \frac{1}{4} e^{-i\omega_0 t} + \frac{1}{\pi} \sum_{\substack{n=-\infty \\ n \text{ even} \\ n \neq 0}}^{\infty} (\pm 1) \frac{e^{in\omega_0 t}}{n^2 - 1}$$

signs alternate, + for $n = 2$

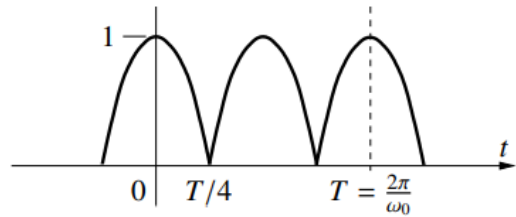


Full-wave Rectified Cosine

$$f(t) = \frac{2}{\pi} \left[1 + 2 \sum_{m=1}^{\infty} (-1)^{m+1} \frac{\cos 2m\omega_0 t}{4m^2 - 1} \right]$$

$$f(t) = \frac{2}{\pi} \left[1 + \sum_{\substack{n=-\infty \\ n \text{ even} \\ n \neq 0}}^{\infty} (\pm 1) \frac{e^{in\omega_0 t}}{n^2 - 1} \right]$$

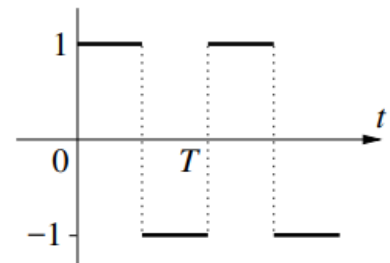
signs alternate, + for $n = 2$



Square Wave

$$f(t) = \frac{4}{\pi} \sum_{m=1}^{\infty} \frac{\sin(2m-1)\omega_0 t}{2m-1}$$

$$f(t) = \sum_{\substack{n=-\infty \\ n \text{ odd}}}^{\infty} \frac{2}{i\pi n} e^{in\omega_0 t}$$

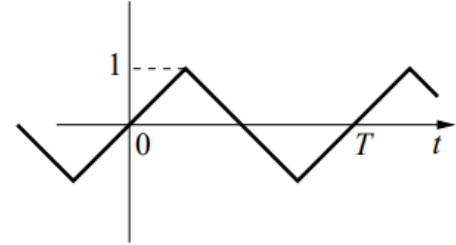


Triangular Wave

$$f(t) = \frac{8}{\pi^2} \sum_{m=1}^{\infty} (-1)^{m+1} \frac{\sin(2m-1)\omega_0 t}{(2m-1)^2}$$

$$f(t) = \frac{4}{i\pi^2} \sum_{\substack{n=-\infty \\ n \text{ odd}}}^{\infty} (\pm 1) \frac{e^{in\omega_0 t}}{n^2}$$

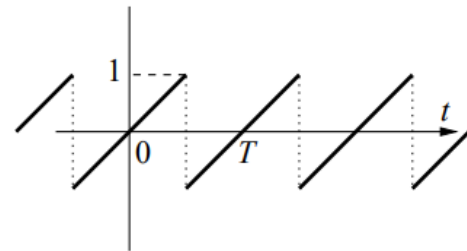
signs alternate, + for $n = 1$

**Sawtooth Wave**

$$f(t) = \frac{2}{\pi} \sum_{n=1}^{\infty} (-1)^{n+1} \frac{\sin n\omega_0 t}{n}$$

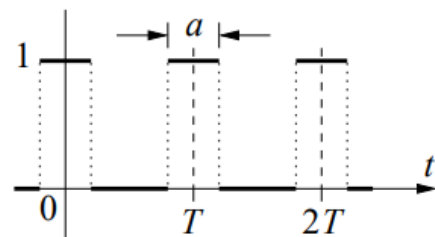
$$f(t) = \frac{1}{i\pi} \sum_{\substack{n=-\infty \\ n \neq 0}}^{\infty} (\pm 1) \frac{e^{in\omega_0 t}}{n}$$

signs alternate, + for $n = 1$

**Pulse Wave**

$$f(t) = \frac{a}{T} \left[1 + 2 \sum_{n=1}^{\infty} \frac{\sin \frac{n\pi a}{T}}{\frac{n\pi a}{T}} \cos n\omega_0 t \right]$$

$$f(t) = \frac{a}{T} \left[1 + \sum_{\substack{n=-\infty \\ n \neq 0}}^{\infty} \frac{\sin \frac{n\pi a}{T}}{\frac{n\pi a}{T}} e^{in\omega_0 t} \right]$$



3.6.4. Fourier Transforms

The Fourier transform maps a continuous time domain t to a continuous frequency domain ω :

$$\hat{y}(\omega) = \int_{-\infty}^{\infty} y(t) e^{-i\omega t} dt$$

Forward Fourier Transform

$$y(t) = \frac{1}{2\pi} \int_{-\infty}^{\infty} \hat{y}(\omega) e^{i\omega t} d\omega$$

Inverse Fourier Transform

- Some sources handle the 2π factor differently and define transforms with differences in signs of the exponent. All transform theorems are valid as long as it is done consistently.
- Fourier transforms are sometimes written in terms of frequency $f = \omega / 2\pi$ (as done below in the analogous discrete Fourier transform).
- The Fourier transform is a slice along the imaginary axis of the Laplace transform: $s = i\omega$; $\omega = \text{Im}\{s\}$.

3.6.5. Discrete Fourier Transforms

The discrete Fourier transform (DFT) maps a finite sequence ($x_n, n = 0, 1, \dots, N-1$) to a finite sequence of discrete frequencies ($X_k, k = 0, 1, \dots, N-1$)

$$X_k = \sum_{n=0}^{N-1} x_n e^{-2\pi i k n / N}$$

Forward Discrete Fourier Transform

$$x_n = \frac{1}{N} \sum_{k=0}^{N-1} X_k e^{2\pi i k n / N}$$

Inverse Discrete Fourier Transform

Notes:

- The DFT gives a discrete approximation to the frequency spectrum of a continuous function passing through all points x_n containing frequency components no higher than $\frac{1}{2T}$, where T is the sampling period. The Nyquist frequency is equal to twice the highest frequency contained in the original signal before sampling. Sampling at a rate below the Nyquist frequency leads to high-frequency information loss and aliasing effects (distorsion).
- Time and frequency parameter relation: $f_k = \frac{k}{NT}$ [] and $t_n = nT$ [s] for integers $0 \leq n, k < N$.
- Total sampling time: NT . Fundamental frequency: $f_1 = \frac{1}{NT}$. Sampling rate: $f_N = \frac{1}{T}$.
- For real sequences, $X_k^* = X_{N-k}$, since the cosine waves at these frequencies pass the same points.

Common DFTs (for $N = 4$):

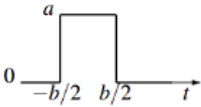
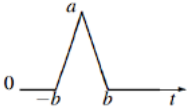
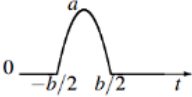
- Cosine: $x_n = \cos \frac{n\pi}{2}$ i.e. $x_n = [1, 0, -1, 0] \rightarrow X_k = [0, 2, 0, 2]$ ($f_1 = \frac{1}{4T}, f_3 = \frac{3}{4T}$)
- Sine: $x_n = \sin \frac{n\pi}{2}$ i.e. $x_n = [0, 1, 0, -1] \rightarrow X_k = [0, -2i, 0, 2i]$

For infinite discrete sequences ($N \rightarrow \infty$ and summing in both directions), the DFT is called the

'Discrete-Time Fourier Transform' (DTFT), $X(\omega) = \sum_{n=-\infty}^{\infty} x_n e^{-i\omega n}$, which is equivalent to the the

bilateral Z -transform $\hat{X}(z)$ of x_n with $z = e^{i\omega}$.

3.6.6. Fourier Transforms of Common Signals

Time-domain waveform $g(t)$	Frequency spectrum $G(\omega)$
1 (DC level)	$2\pi \delta(\omega) = \delta(f)$
$H(t)$ (Heaviside step)	$\pi \delta(\omega) + \frac{1}{j\omega}$
$e^{j\omega_0 t}$ (complex sinusoid)	$2\pi \delta(\omega - \omega_0)$
$\cos \omega_0 t$	$\pi [\delta(\omega - \omega_0) + \delta(\omega + \omega_0)]$
$\sin \omega_0 t$	$\frac{\pi}{j} [\delta(\omega - \omega_0) - \delta(\omega + \omega_0)]$
e^{-at^2} (Gaussian)	$\sqrt{\frac{\pi}{a}} e^{-\frac{1}{4a}\omega^2}$
$\sum_{n=-\infty}^{\infty} \delta(t - nT)$ (impulse train)	$\frac{2\pi}{T} \sum_{m=-\infty}^{\infty} \delta(\omega - \frac{2\pi m}{T})$
 $a \text{ rect } \frac{t}{b}$ (rectangle function)	$ab \text{ sinc } \frac{\omega b}{2}$ where $\text{sinc } x := (\sin x) / x$
 $a \text{ tri } \frac{t}{b}$ (triangle function)	$ab \text{ sinc}^2 \frac{\omega b}{2}$ main lobe bandwidth: $1 / b$
 $a \cos \frac{\pi t}{b} \cdot H(\frac{t}{b} - x)$	$\frac{ab}{2} [\text{sinc } \frac{\omega b - \pi}{2} + \text{sinc } \frac{\omega b + \pi}{2}]$
$a f(t) + b g(t)$	$a F(\omega) + b G(\omega)$ (linearity)
$g(t - t_0)$ (time shift)	$e^{-j\omega t_0} G(\omega)$
$e^{j\omega_0 t} g(t)$	$G(\omega - \omega_0)$ (frequency shift)
$\frac{d^n g(t)}{dt^n}$ (differentiation)	$(j\omega)^n G(\omega)$
$(f * g)(t) = \int_{-\infty}^{\infty} f(\tau) g(t - \tau) d\tau$ (convolution)	$F(\omega) G(\omega)$ (multiplication)
$f(t) g(t)$ (multiplication)	$\frac{1}{2\pi} (F * G)(\omega)$ (convolution)
$G(t)$ (duality)	$2\pi g(-\omega)$
if $g(t) \rightarrow G(\omega)$ then $G(t) \rightarrow 2\pi g(-\omega)$	
$g(t)^*$ (complex conjugate)	$G(-\omega)^*$
real-valued even function $g(t)$	real-valued even function $G(\omega)$
real-valued odd function $g(t)$	imaginary-valued odd function $G(\omega)$

3.6.7. Signal Energy, Power and Parseval's Theorem of Energy Conservation

The energy of a signal $g(t)$ is defined as $E_g = \int_{-\infty}^{\infty} |g(t)|^2 dt$.

The power of a signal $g(t)$ is defined as $P_g = \lim_{T \rightarrow \infty} \frac{1}{T} \int_{-T/2}^{T/2} |g(t)|^2 dt$.

The power spectral density (power spectrum) is $S_{gg}(\omega) = \frac{1}{2\pi} |G(\omega)|^2 = |G(f)|^2$.

Parseval's Theorem: The energy in the time and frequency domain must be the same:

$$E_g = \int_{-\infty}^{\infty} |g(t)|^2 dt = \frac{1}{2\pi} \int_{-\infty}^{\infty} |G(\omega)|^2 d\omega$$

For more on signal analysis, see Section 5.4.

3.7. Partial Differential Equations and Variational Calculus

3.7.1. Classification of Linear Second-Order Partial Differential Equations (PDEs)

A PDE of the form

$$A \frac{\partial^2 u}{\partial x^2} + 2B \frac{\partial^2 u}{\partial x \partial y} + C \frac{\partial^2 u}{\partial y^2} + D \frac{\partial u}{\partial x} + E \frac{\partial u}{\partial y} + Fu + G = 0$$

is said to be

- **Elliptic:** if $B^2 < AC$ (e.g. Laplace equation, Poisson equation)
- **Parabolic:** if $B^2 = AC$ (e.g. Heat equation, Diffusion equation)
- **Hyperbolic:** if $B^2 > AC$ (e.g. Wave equation)

3.7.2. Classification of Boundary Conditions

A PDE requires initial conditions (ICs: $u = f(x, 0)$) and boundary conditions (BCs) to be fully specified. The BCs constrain the value of the dependent variable on the boundary of the region satisfying the PDE. The types of BCs are:

- **Dirichlet:** dependent variable specified on boundary
e.g. $u = 0$ when $x = 0$; $u = 1 - e^{-3t}$ when $x = 1$
- **Neumann:** gradient of dependent variable specified on boundary
e.g. $\frac{du}{dx} = 0$ when $x = 0$ and $x = 1$
- **Robin:** an ODE for the dependent variable is specified on the boundary
e.g. $\frac{du}{dx} + 2u = x$ when $|x| = 1$, defined for $|x| \leq 1$.
- **Mixed:** the boundary is split into several parts, each with different conditions
e.g. $u = 4t$ when $x = 0$; $\frac{du}{dx} = 1 - u$ when $x = 1$, defined on $0 \leq x \leq 1$.

3.7.3. Common PDEs and their 2D General Solutions

Partial Differential Equations

$$\frac{\partial T}{\partial t} = \alpha \nabla^2 T + \frac{\alpha}{k} \dot{q}_{\text{gen}}$$

Heat Equation

(T : temperature,
 α : thermal diffusivity,
 k : thermal conductivity,
 q : heat source per volume)

$$\frac{\partial c}{\partial t} = D \nabla^2 c + \dot{c}_{\text{gen}}$$

Diffusion Equation

(c : concentration,
 D : diffusion coefficient)

$$\nabla^2 \phi = \rho_{\text{gen}}$$

Poisson's Equation

(Laplace's Equation if $\rho_{\text{gen}} = 0$)
 (ϕ : scalar potential,
 ρ : source density)

$$\frac{\partial^2 \psi}{\partial t^2} = c^2 \nabla^2 \psi$$

Wave Equation

(ψ : scalar displacement,
 c : phase velocity)

Heat Equation / Diffusion Equation: 2D Solutions

Separation of variables using $T(x, t) = X(x) \bar{T}(t)$ with a negative separation constant $-\lambda^2$ gives $X'' + \lambda^2 X = 0$ and $\bar{T}' + \alpha \lambda^2 \bar{T} = 0$ with solutions $X(x) = A \sin \lambda x + B \cos \lambda x$ and $\bar{T}(t) = C \exp(-\alpha \lambda^2 t)$.

Self-similar solution: let $\eta = \frac{x}{\sqrt{\alpha t}}$, separate as $T(x, t) = H(\eta) \bar{T}(t)$. Find an ODE in $H(\eta)$.

Heat flux: $\mathbf{q} = -k \nabla T$; Diffusion flux: $\mathbf{J} = -D \nabla c$; Convection boundary condition: $k \frac{\partial T}{\partial n_{\text{out}}} = h(T_{\infty} - T)$

Normalisation condition: all solutions satisfy $\frac{d}{dt} \int_{-\infty}^{\infty} T(x, t) dx = 0$ (conservation law).

Laplace's Equation: 2D Solutions

General solutions may be

$$\begin{aligned} \phi(x, y) = X(x) Y(y) &= (A \sinh \lambda x + B \cosh \lambda x)(C \sin \lambda y + D \cos \lambda y) \\ &= (A \sin \lambda x + B \cos \lambda x)(C \sinh \lambda y + D \cosh \lambda y) \\ &= (Ax + B)(Cy + D) \end{aligned}$$

Separation constant

using $+\lambda^2$
 using $-\lambda^2$
 using 0

Wave Equation: 1D Solutions

Separation of variables using $Y(x, t) = X(x) T(t)$ with a negative separation constant $-\lambda^2$ gives $X'' + \lambda^2 X = 0$ and $\bar{T}' + \alpha \lambda^2 \bar{T} = 0$ with solutions $X(x) = A \sin \lambda x + B \cos \lambda x$ and $T(t) = C \cos \lambda ct + D \sin \lambda ct$.

D'Alembert's solution: consider the PDEs $\frac{\partial y}{\partial t} \pm c \frac{\partial y}{\partial x} = 0$ and let $\eta = ct \mp x$. It is clear that any $y = f(\eta)$ is a solution, so the general solution is $y(x, t) = f(ct - x) + g(ct + x)$. The lines $ct - x = \text{constant}$ and $ct + x = \text{constant}$, along which the right and left running waves move in the (x, t) plane, are the characteristics of the PDE. By differentiation, these PDEs are jointly equivalent to the wave equation.

3.7.4. Techniques for Solving Partial Differential Equations

For a typical PDE for a multivariable function u in terms of space x and time t ,

Separation of Variables: assume $u(x, t) = X(x) T(t)$.

1. Substitute $u = XT$ where X is a function of x only and T is a function of t only. Compute the derivatives as e.g. $u_{xx} = X''(x) T(x)$, $u_t = X(x) T'(t)$ etc.
2. Rearrange so that all X terms and all T terms are on opposite sides. Set both sides equal to a separation constant, initially $\pm\lambda^2$.
3. Solve each ODE for $X(x)$ and $T(t)$ in terms of λ , selecting the appropriate sign (or zero) depending on whether the behaviour can meet the boundary conditions: it may be oscillatory, exponential, or linear.
4. Use initial conditions and boundary conditions to constrain or discretise λ and the undetermined coefficients.
5. Use superposition to sum over remaining undetermined indices, if required.

Laplace Transforms: defined such that $L\{u(x, t)\} = U(x, s) = \int_0^{\infty} u(x, t) e^{-st} dt$

1. Transform the PDE using e.g. $L\{u_x\} = U_x(x, s)$, $L\{u_t\} = s U(x, s) - u(x, 0)$, etc. Also transform the boundary conditions e.g. $\{u(0, t) = f(t)\} \rightarrow \{U(0, s) = F(s)\}$, and substitute the initial condition for $u(x, 0)$.
2. Solve the resulting ODE for $U(x, s)$ and apply boundary conditions.
3. The inverse Laplace transform of $U(x, s)$ (considering x as a constant) is $u(x, t)$.

Fourier and other integral transforms may also be used.

Green's Functions: multivariable convolution of input function with the impulse response to solve the equation $L[u] = f$.

1. Identify independent linear differential operators L and the forcing functions (nonhomogeneous components) f .
2. Find or look up (Section 3.7.5) the Green's function $G(\mathbf{x})$ for the operator L .
3. Apply initial conditions and boundary conditions to constrain G .
4. Apply the convolution theorem as $u(\mathbf{x}) = \int f(\boldsymbol{\eta}) G(\mathbf{x} - \boldsymbol{\eta}) d\boldsymbol{\eta}$.

3.7.5. Green's Functions

A Green's function G is the impulse response of a linear differential operator: $L [G] = \delta(\mathbf{x}, t)$

In the table, $r^2 = x^2 + y^2 (+ z^2)$ in 2D (or 3D). (H : step function, I : Bessel functions)

Differential operator L	Green's function $G(x, y, [z, t])$
∇_{2D}^2 2D Poisson equation	$\frac{1}{2\pi} \ln r$
∇_{3D}^2 3D Poisson equation	$-\frac{1}{4\pi r}$
$\nabla_{3D}^2 + k^2$ Schrodinger equation	$-\frac{e^{-ikr}}{4\pi r}$
$\frac{\partial^2}{\partial t^2} - c^2 \frac{\partial^2}{\partial x^2}$ 1D wave equation	$\frac{1}{2c} H\left(t - \left \frac{x}{c}\right \right)$
$\frac{\partial^2}{\partial t^2} - c^2 \nabla_{2D}^2$ 2D wave equation	$\frac{1}{2\pi c \sqrt{c^2 t^2 - r^2}} H\left(t - \frac{r}{c}\right)$
$\frac{1}{c^2} \frac{\partial^2}{\partial t^2} - \nabla_{3D}^2$ 3D wave equation	$\frac{1}{4\pi r} \delta\left(t - \frac{r}{c}\right)$
$\frac{\partial}{\partial t} - k \frac{\partial^2}{\partial x^2}$ 1D diffusion equation	$\left(\frac{1}{4\pi kt}\right)^{1/2} \exp\left(-\frac{x^2}{4kt}\right) H(t)$
$\frac{\partial}{\partial t} - k \nabla_{2D}^2$ 2D diffusion equation	$\frac{1}{4\pi kt} \exp\left(-\frac{r^2}{4kt}\right) H(t)$
$\frac{\partial}{\partial t} - k \nabla_{3D}^2$ 3D diffusion equation	$\left(\frac{1}{4\pi kt}\right)^{3/2} \exp\left(-\frac{r^2}{4kt}\right) H(t)$
$\frac{\partial^2}{\partial t^2} + 2\gamma \frac{\partial}{\partial t} - c^2 \frac{\partial^2}{\partial x^2}$ Telegrapher's equation	$\frac{1}{2} e^{-\gamma t} \left[\delta(ct - x) + \delta(ct + x) + H(ct - x) \left(\frac{\gamma}{c} I_0\left(\frac{\gamma u}{c}\right) + \frac{\gamma t}{u} I_1\left(\frac{\gamma u}{c}\right) \right) \right]$ where $u = \sqrt{c^2 t^2 - r^2}$

3.7.6. Fundamental Lemma of Calculus of Variations

If a continuous function f on an open interval (a, b) satisfies $\int_a^b f(x)h(x) dx = 0$ for all compactly supported smooth functions h on (a, b) , then $f(x) \equiv 0$.

Corollary: if $\int_a^b f(x)h(x) + g(x)h'(x) dx = 0$ then $g'(x) = f(x)$ (same conditions as above).

3.7.7. Euler-Lagrange Equation

A 'variation' (or perturbation) $f + \delta f$ of a function $f(x)$ constrained to satisfy $f(a) = A$ and $f(b) = B$ can be written as $g_\varepsilon(x) = f(x) + \varepsilon \eta(x)$ where ε is small and $\eta(x)$ is a differentiable function satisfying $\eta(a) = \eta(b) = 0$.

Let S be a functional defined as $S[f] = \int_a^b f(t, x, \dot{x}) dt$

The function f for which S is stationary i.e. local gradient to small variations is zero, satisfies the differential equation

$$\frac{\partial f}{\partial x} = \frac{d}{dt} \left(\frac{\partial f}{\partial \dot{x}} \right).$$

If f is explicitly a function of higher derivatives of x , then the equation is

$$\frac{\partial f}{\partial x} - \frac{d}{dt} \left(\frac{\partial f}{\partial \dot{x}} \right) + \frac{d^2}{dt^2} \left(\frac{\partial f}{\partial \ddot{x}} \right) - \dots + (-1)^k \frac{d^k}{dt^k} \left(\frac{\partial f}{\partial x^{(k)}} \right) = 0.$$

Note that x, x' etc. are considered **independent** variables.

Common applications:

- Minimum action (Lagrangian / Hamiltonian for mechanical systems, see Section 6.2.12).
- Minimum distance on a curved surface (geodesics)
- Minimum energy configuration of a system

M4. LINEAR ALGEBRA

4.1. Vector and Matrix Algebra

4.1.1. Properties of Real Matrices

Zero, Ones and Identity Matrices:

- Zero matrix: $\mathbf{0}$; Ones matrix $\mathbf{1}$; Identity matrix \mathbf{I}_n ($n \times n$ matrix with 1's on leading diagonal)

Singular Matrices:

- If $|\mathbf{A}| = 0$ then \mathbf{A} is singular (non-invertible) and \mathbf{A}^{-1} does not exist.

Symmetric and Antisymmetric Matrices

- If $\mathbf{A} = \mathbf{A}^T$ then \mathbf{A} is symmetric ($A_{ij} = A_{ji}$) and \mathbf{A}^{-1} exists.
- If $\mathbf{A} = -\mathbf{A}^T$ then \mathbf{A} is antisymmetric (skew-symmetric) ($A_{ij} = -A_{ji}$), \mathbf{A}^{-1} does **not** exist and \mathbf{A} has zeros on the leading diagonal.

Diagonal, Triangular and Sparse Matrices: special cases of square matrices

- If $A_{ij} = 0$ for all $i \neq j$ then \mathbf{A} is diagonal.
- If $A_{ij} = 0$ for all $i > j$ then \mathbf{A} is upper-triangular.
- If $A_{ij} = 0$ for all $i < j$ then \mathbf{A} is lower-triangular.
- If $A_{ij} = 0$ for 'most' $i \neq j$ then \mathbf{A} is sparse (informal definition but computationally useful)

Orthogonal Matrices:

- If $\mathbf{A}\mathbf{A}^T = \mathbf{A}^T\mathbf{A} = \mathbf{I}$ then \mathbf{A} is orthogonal (orthonormal), $\mathbf{A} = \mathbf{A}^T = \mathbf{A}^{-1}$, the rows and columns of \mathbf{A} are orthonormal vectors.

Full-Rank Matrices:

- If $\text{rank}(\mathbf{A}) = \min(\text{dim}(\mathbf{A}))$ then \mathbf{A} is full-rank.

Defective Matrices:

- If \mathbf{A} does not have a full set of eigenvectors then \mathbf{A} is defective (non-diagonalisable). A defective $n \times n$ matrix \mathbf{A} has at least one eigenvalue with algebraic multiplicity $m > 1$, with less than m associated eigenvectors.

Idempotent Matrices: for square matrices \mathbf{A} ,

- If $\mathbf{A}^2 = \mathbf{A}$ then \mathbf{A} is idempotent.
- All $\mathbf{A} = \mathbf{I}_n$ are idempotent. If $\mathbf{A} \neq \mathbf{I}_n$ is idempotent, then \mathbf{A} is singular.

Positive Definite and Positive Semi-Definite Matrices: for symmetric matrices $\mathbf{A} = \mathbf{A}^\top$,

- If $\mathbf{x}^\top \mathbf{A} \mathbf{x} > 0$ for all $\mathbf{x} \neq \mathbf{0}$ then \mathbf{A} is positive definite ($\mathbf{A} > 0$), and \mathbf{A} has all positive eigenvalues.
- If $\mathbf{x}^\top \mathbf{A} \mathbf{x} \geq 0$ for all \mathbf{x} then \mathbf{A} is positive semi-definite ($\mathbf{A} \geq 0$), and \mathbf{A} has all nonnegative eigenvalues.

Row Echelon Form and Reduced Row Echelon Form:

- \mathbf{A} is in row echelon form if 1) all rows having only zero entries are at the bottom and 2) the leading entry (the left-most nonzero entry) of every nonzero row (the pivot) is on the right of the leading entry of every row above.
- \mathbf{A} is in reduced row echelon form (RREF) if 1) \mathbf{A} is in row echelon form, 2) the leading entry in each nonzero row is 1 (a 'leading one') and 3) each column containing a leading 1 has zeros in all its other entries.

4.1.2. Properties of Complex Matrices

Normal and Unitary Matrices:

- If $\mathbf{A}\mathbf{A}^* = \mathbf{A}^*\mathbf{A}$ then \mathbf{A} is normal.
- If $\mathbf{A}\mathbf{A}^* = \mathbf{A}^*\mathbf{A} = \mathbf{I}$ then \mathbf{A} is unitary and $\mathbf{A} = \mathbf{A}^* = \mathbf{A}^{-1}$. The matrix can be written as $\mathbf{A} = \exp(i\mathbf{H})$ where \mathbf{H} is a Hermitian matrix, or diagonalised to $\mathbf{A} = \mathbf{U}\mathbf{D}\mathbf{U}^*$ where \mathbf{U} is unitary and \mathbf{D} is diagonal and unitary.

Hermitian and Anti-Hermitian Matrices:

- If $\mathbf{A} = \mathbf{A}^*$ ($\mathbf{A} = \mathbf{A}^H$) ($A_{ij} = \overline{A_{ji}}$) then \mathbf{A} is Hermitian (self-adjoint). $\mathbf{x}^* \mathbf{A} \mathbf{x}$ is real for all complex vectors \mathbf{x} . \mathbf{A} has spectral decomposition $\mathbf{A} = \mathbf{U}\mathbf{D}\mathbf{U}^*$ where \mathbf{U} is unitary and \mathbf{D} is diagonal. $|\mathbf{A}|$ is real.
- If $\mathbf{A} = -\mathbf{A}^*$ ($\mathbf{A} = -\mathbf{A}^H$) then \mathbf{A} is anti-Hermitian (skew-Hermitian) ($A_{ij} = -\overline{A_{ji}}$). The entries of \mathbf{A} on the leading diagonal have no real part.

For matrix decompositions, see Section 4.3.

4.1.2. Simple Properties of Matrix Operations

Matrix Multiplication:

- $\mathbf{ABC} = (\mathbf{AB})\mathbf{C} = \mathbf{A}(\mathbf{BC})$ (grouping / associative)
- $\mathbf{A}(\mathbf{B} + \mathbf{C}) = \mathbf{AB} + \mathbf{AC}$ (factorisation / distributive over addition)
- $\mathbf{AB} \neq \mathbf{BA}$ (**not** commutative in general)

Matrix Algebra: identical to scalar algebra, **except:**

- multiplication is not commutative e.g. $(\mathbf{A} + \mathbf{B})^2 = \mathbf{A}^2 + \mathbf{AB} + \mathbf{BA} + \mathbf{B}^2 \neq \mathbf{A}^2 + 2\mathbf{AB} + \mathbf{B}^2$
- vectors squared become $\mathbf{x}^T \mathbf{x}$
- divisions become matrix inverses \mathbf{A}^{-1}

Determinants, Transpose, Conjugate Transpose, Inverse (if it exists) and Trace:

- $\text{tr}(\mathbf{A})$ is the sum of all leading diagonal elements of \mathbf{A} .
- \mathbf{A}^* is the conjugate transpose: element-wise complex conjugate **and** transpose

$$|\mathbf{A}^T| = |\mathbf{A}| \quad |\mathbf{A}^*| = |\mathbf{A}|^* \quad |\mathbf{A}^{-1}| = |\mathbf{A}|^{-1}$$

$$|\mathbf{AB}| = |\mathbf{A}||\mathbf{B}| \quad (\mathbf{AB})^T = \mathbf{B}^T \mathbf{A}^T \quad (\mathbf{AB})^* = \mathbf{B}^* \mathbf{A}^* \quad (\mathbf{AB})^{-1} = \mathbf{B}^{-1} \mathbf{A}^{-1}$$

$$(\mathbf{A}^T)^T = (\mathbf{A}^*)^* = (\mathbf{A}^{-1})^{-1} = \mathbf{A}$$

$$\text{tr}(a\mathbf{A} + b\mathbf{B}) = a \text{tr}(\mathbf{A}) + b \text{tr}(\mathbf{B}) \quad \text{tr}(\mathbf{AB}) = \text{tr}(\mathbf{BA}) \quad \text{tr}(\mathbf{ab}^T) = \mathbf{b}^T \mathbf{a}$$

(\mathbf{a} and \mathbf{b} are column vectors of equal length)

4.1.3. Determinant of a Matrix

The determinant of a matrix \mathbf{A} is written $|\mathbf{A}|$ or $\det \mathbf{A}$.

For a 2×2 matrix:
$$\begin{vmatrix} a & b \\ c & d \end{vmatrix} = ad - bc$$

For a 3×3 matrix:
$$\begin{vmatrix} a & b & c \\ d & e & f \\ g & h & i \end{vmatrix} = a(ei - fh) - b(di - fg) + c(dh - eg)$$

In general, the determinant of a larger square matrix is the alternating sum of products of entries along any row or column with the determinant of the matrix formed by the remaining entries (not in that row or column). **Any** row or column can be chosen: in the above expression, the top row was used.

4.1.4. Inverse Matrix, Transpose and Conjugate Transpose

Inverse of a 2×2 matrix:
$$\mathbf{A} = \begin{bmatrix} a & b \\ c & d \end{bmatrix} \Rightarrow \mathbf{A}^{-1} = \frac{1}{ad - bc} \begin{bmatrix} d & -b \\ -c & a \end{bmatrix}$$

Inverse of a 3×3 matrix:
$$\mathbf{A}^{-1} = \frac{1}{|\mathbf{A}|} \mathbf{C}^T$$

where \mathbf{C} is the matrix of cofactors, which is the determinant of the 2×2 matrix formed by the elements not in the corresponding row or column, multiplied by an alternating sign of +1 or -1 (starting with +1 in the top left).

Transpose:
$$\begin{bmatrix} a & b & c \\ d & e & f \\ g & h & i \end{bmatrix}^T = \begin{bmatrix} a & d & g \\ b & e & h \\ c & f & i \end{bmatrix} \Leftrightarrow (\mathbf{A}^T)_{ij} = \mathbf{A}_{ji}$$

Conjugate Transpose (Hermitian transpose):

$$\begin{bmatrix} \alpha + \beta i & \gamma + \delta i \\ \varepsilon + \zeta i & \eta + \kappa i \end{bmatrix}^* = \begin{bmatrix} \alpha - \beta i & \varepsilon - \zeta i \\ \gamma - \delta i & \eta - \kappa i \end{bmatrix} \Leftrightarrow (\mathbf{A}^*)_{ij} = \mathbf{A}_{ji}^*$$

Results for complex matrices typically use \mathbf{A}^* instead of \mathbf{A}^T . For real matrices, $\mathbf{A}^* = \mathbf{A}^T$.

4.1.5. Outer Product

Outer product: $\mathbf{a} \otimes \mathbf{b} = \mathbf{ab}^T$ so that the elements are $(\mathbf{a} \otimes \mathbf{b})_{ij} = a_i b_j$.

Self outer product: If \mathbf{n} is a column vector, then $\mathbf{n} \otimes \mathbf{n} = \mathbf{nn}^T$ is a square, symmetric matrix.

$$\mathbf{nn}^T = \begin{bmatrix} n_1 \\ n_2 \\ n_3 \end{bmatrix} \begin{bmatrix} n_1 & n_2 & n_3 \end{bmatrix} = \begin{bmatrix} n_1^2 & n_1 n_2 & n_1 n_3 \\ n_1 n_2 & n_2^2 & n_2 n_3 \\ n_1 n_3 & n_2 n_3 & n_3^2 \end{bmatrix}$$

4.1.6. Cross Product Matrix

The cross product matrix of a vector \mathbf{n} is denoted $[\mathbf{n}]_{\times}$ and has the property $[\mathbf{n}]_{\times} \mathbf{a} = \mathbf{n} \times \mathbf{a}$ for any vector $\mathbf{a} \in \mathbb{R}^3$. i.e. it represents a cross product as a linear transformation. It is defined as

$$[\mathbf{n}]_{\times} = \begin{bmatrix} 0 & -n_3 & n_2 \\ n_3 & 0 & -n_1 \\ -n_2 & n_1 & 0 \end{bmatrix}$$

The cross product matrix $[\mathbf{n}]_{\times}$ is always skew-symmetric. The columns of $[\mathbf{n}]_{\times}$ are the cross products of \mathbf{n} with each unit basis vector $\{\mathbf{i}, \mathbf{j}, \mathbf{k}\}$.

4.1.7. Eigenvalues and Eigenvectors

Definitions: for a square $n \times n$ matrix \mathbf{A} , the eigenvalues are denoted λ and eigenvectors are denoted \mathbf{u} .

- Definition: $\mathbf{A}\mathbf{u} = \lambda\mathbf{u} \leftrightarrow (\mathbf{A} - \lambda\mathbf{I})\mathbf{u} = \mathbf{0} \leftrightarrow |\mathbf{A} - \lambda\mathbf{I}| = 0$ (characteristic equation, degree n)
- Non-defective matrix: every λ (including repeated) has a unique corresponding \mathbf{u} .
- Algebraic multiplicity a : the exponent of the factor $(\lambda - e)^a$ in the characteristic polynomial.
- Geometric multiplicity g : the number of linearly independent eigenvectors associated i.e. the dimension of the null space of $\mathbf{A} - e\mathbf{I}$.
- Eigenbasis / eigenspace: the space spanned by the eigenvectors. If \mathbf{A} is symmetric and the eigenvectors are normalised, then the eigenbasis is an orthonormal basis.

Geometric interpretation: $\mathbf{A} : \mathbb{R}^n \rightarrow \mathbb{R}^n$ is viewed as a linear transformation (Sections 4.2.2. and 4.3).

- The eigenvectors point along the invariant lines under \mathbf{A} . These vectors are not rotated (only scaled).
- If $\lambda = 1$ then the corresponding line is a line of invariant points under \mathbf{A} .
- A repeated eigenvalue represents an invariant plane under \mathbf{A} (spanned by the eigenvectors).

Relationships Between Eigenvalues and Eigenvectors:

- **Sums and products of eigenvalues:** $\lambda_1 + \lambda_2 + \dots + \lambda_n = \text{tr}(\mathbf{A})$ and $\lambda_1\lambda_2\dots\lambda_n = \det(\mathbf{A})$.
Sum of $(n-1)$ -permutations: $\lambda_2\lambda_3\dots\lambda_n + \lambda_1\lambda_3\dots\lambda_n + \lambda_1\lambda_2\dots\lambda_{n-1} = \lambda_1\lambda_2\lambda_3\dots\lambda_n (\lambda_1^{-1} + \lambda_2^{-1} + \dots + \lambda_n^{-1}) = \text{tr}(\mathbf{C})$
where \mathbf{C} is the matrix of cofactors of \mathbf{A} . The Faddeev-LeVerrier algorithm computes the coefficients of the characteristic polynomial via Vieta's formulas by applying Newton's identities to these expressions.
- **Linearity:** eigenvalues of $a\mathbf{A}$ are $a\lambda$; eigenvalues of $\mathbf{A} + a\mathbf{I}$ are $\lambda + a$; eigenvalues of \mathbf{A}^n are λ^n (including $n = -1$ as the inverse).
- **Commutative matrices:** if \mathbf{A} and \mathbf{B} have the same eigenvectors, then $\mathbf{AB} = \mathbf{BA}$.
- **Polynomial of a matrix:** for any polynomial $f(x)$, the eigenvalues of $f(\mathbf{A})$ are $f(\lambda)$ (with the constant term taken to be a multiple of \mathbf{I}).
- **Cayley-Hamilton theorem:** a matrix \mathbf{A} satisfies its own characteristic equation.
- **Rayleigh's quotient:** if \mathbf{A} is Hermitian, then the quantity $C = \frac{\mathbf{x}^\top \mathbf{A} \mathbf{x}}{\mathbf{x}^\top \mathbf{x}} = \hat{\mathbf{x}} \cdot \mathbf{A} \hat{\mathbf{x}} = \hat{\mathbf{x}}^\top \mathbf{A} \hat{\mathbf{x}}$ is bounded by $\lambda_1 \leq C \leq \lambda_n$, where λ_1 and λ_n are the smallest and largest eigenvalues of \mathbf{A} respectively, and \mathbf{x} is **any** vector. Also, if $\mathbf{x} \approx \mathbf{u}$ then $C \approx \lambda$, the (approximate) corresponding eigenvalue to eigenvector \mathbf{u} of \mathbf{A} .
- **Spectral radius:** the smallest circle in the complex plane containing all eigenvalues, $\rho(\mathbf{A}) = \max |\lambda_i|$.
For any integer $k \geq 1$ and norm (Section 4.1.9), $\rho(\mathbf{A}) \leq \|\mathbf{A}^k\|^{1/k}$, with equality in the limit of $k \rightarrow \infty$.
- **Gershgorin circle theorem:** every complex eigenvalue of \mathbf{A} lies within the union of circles in the complex plane, centred at the diagonal entries of \mathbf{A} , with radii given by the sum of the magnitudes of all off-diagonal entries in that row i.e. $\lambda \in \{z : \bigcup_{i=1}^n |z - A_{ii}| \leq \sum_{j \neq i} |A_{ij}|\}$.
- **Singular values:** the singular values σ of \mathbf{A} are the square roots of the eigenvalues of $\mathbf{A}\mathbf{A}^\top$ or $\mathbf{A}^\top\mathbf{A}$.

4.1.8. Approximations for Eigenvalues and Eigenvectors

Shifted Inverse Power Method

To approximate an eigenvalue of \mathbf{A} :

- Choose an initial approximation α to the target eigenvalue of \mathbf{A} .
- Calculate the matrix $\mathbf{B} = \mathbf{A} - \alpha\mathbf{I}$.
- Choose any initial normalised vector \mathbf{r}_0 .
- Iterate: starting with $n = 0$ and incrementing,
 - Solve the system $\mathbf{B} \mathbf{r}_{n+1} = \mathbf{r}_n$, typically using efficient LU decomposition.
 - Calculate $\mu_{n+1} = \mathbf{r}_{n+1} \cdot \mathbf{r}_n$ as an estimate for the shifted eigenvalue.
 - Normalise \mathbf{r}_{n+1} (in-place) and continue.
- Once sufficient convergence is achieved, calculate $\lambda = \frac{1}{\mu_\infty} + \alpha$ as the target eigenvalue of \mathbf{A} , where μ_∞ is the limiting (converged) value of sequence μ_n . The unit vector \mathbf{r}_n has simultaneously converged to the corresponding eigenvector.

Note that if \mathbf{r}_0 happens to be chosen as a different eigenvector of \mathbf{A} , the method will not converge.

An initial estimate for α can often be found using the Gershgorin Circle Theorem (see Section 4.1.7.), which works best when the matrix is sparse or near-diagonal (most off-diagonal entries are zero or much smaller than the diagonal entries).

Rayleigh's quotient (Section 4.1.7) can also be used to approximate the eigenvalue from an eigenvector approximation, and bounds the eigenvalues.

4.1.9. Normed Vector Spaces and Matrix Norms

Norms are scalar-valued measures of the ‘typical size’ of an object (vector/function/matrix).

Vector Norms: if \mathbf{x} is a vector with elements x_i , four common norms are

- 1-norm: $\|\mathbf{x}\|_1 = \sum_i |x_i|$ (L_1 norm / l_1 norm / Manhattan norm / Taxicab norm)
- 2-norm: $\|\mathbf{x}\|_2 = \sqrt{\sum_i x_i^2}$ (L_2 norm / l_2 norm / quadratic norm / Euclidean norm)
Inner product form: $\|\mathbf{x}\|_2^2 = \mathbf{x} \cdot \mathbf{x}$ (in a Hilbert space)
- p -norm: $\|\mathbf{x}\|_p = \left(\sum_i |x_i|^p\right)^{1/p}$ (for $p \geq 1$; l^p norm / Lebesgue norm)
- ∞ -norm: $\|\mathbf{x}\|_\infty = \max \{x_i\}$ (infinity norm / supremum norm)

Generalisation to Infinite Dimensions (Banach Spaces)

Discrete or continuous functions $f: \mathbb{R} \rightarrow \mathbb{R}$ can be considered infinite-dimensional vectors.

- l_p norm: $\|x\|_p = \left(\sum_i |x_i|^p\right)^{1/p}$
- L_p norm: $\|f\|_p = \left(\int_\Omega |f(x)|^p dx\right)^{1/p}$ (f defined in a Lebesgue space $L_p(\Omega)$)

Matrix Norms: if \mathbf{A} is a matrix with elements a_{ij} , four common norms are

- 1-norm: the maximum absolute column sum, $\|\mathbf{A}\|_1 = \max_j \sum_i |a_{ij}|$
- Infinity-norm: the maximum absolute row sum, $\|\mathbf{A}\|_\infty = \max_i \sum_j |a_{ij}|$
- Euclidean norm: $\|\mathbf{A}\|_E = \sqrt{\sum_i \sum_j |a_{ij}|^2}$ (Frobenius norm)
- 2-norm: the largest singular value of \mathbf{A} . (spectral norm)

The condition number of an invertible square matrix \mathbf{A} is defined by $\kappa = \|\mathbf{A}\| \|\mathbf{A}^{-1}\|$ evaluated using one of these norms (the same one in both places. If the 2-norm is used, the condition number is the ratio of the largest to the smallest singular value of \mathbf{A}).

4.2. Transformation Matrices

4.2.1. Rotations, Reflections, Shears and Projections as Transformation Matrices

Rotation Matrices: for a counterclockwise rotation about the origin, angle θ ,

$$\begin{matrix} \begin{bmatrix} \cos \theta & -\sin \theta \\ \sin \theta & \cos \theta \end{bmatrix} & \begin{bmatrix} 1 & 0 & 0 \\ 0 & \cos \theta & -\sin \theta \\ 0 & \sin \theta & \cos \theta \end{bmatrix} & \begin{bmatrix} \cos \theta & 0 & \sin \theta \\ 0 & 1 & 0 \\ -\sin \theta & 0 & \cos \theta \end{bmatrix} & \begin{bmatrix} \cos \theta & -\sin \theta & 0 \\ \sin \theta & \cos \theta & 0 \\ 0 & 0 & 1 \end{bmatrix} \\ \text{2D} & \text{3D, about } x\text{-axis} & \text{3D, about } y\text{-axis} & \text{3D, about } z\text{-axis} \end{matrix}$$

The general rotation about line $\mathbf{r} \times \mathbf{n} = \mathbf{0}$ is given by $(\cos \theta) \mathbf{I} + (\sin \theta) [\mathbf{n}]_{\times} + (1 - \cos \theta) (\mathbf{n} \otimes \mathbf{n})$.

In 3D, the rotation is considered counterclockwise when viewed inwards from the positive axis, towards the origin. The eigenvalues are $\{1, e^{i\theta}, e^{-i\theta}\}$. The real eigenvector corresponding to $\lambda = 1$ is the axis of rotation. The trace is $1 + 2 \cos \theta$. The determinant is 1.

Reflection Matrices:

In 2D, the reflection in the line $y = (\tan \theta)x$ is given by $\begin{bmatrix} \cos 2\theta & \sin 2\theta \\ \sin 2\theta & -\cos 2\theta \end{bmatrix}$. Determinant is -1.

In 3D, the reflection in the plane $\mathbf{r} \cdot \mathbf{n} = 0$ is given by $\mathbf{I} - 2\mathbf{nn}^T = \begin{bmatrix} 1 - 2n_1^2 & -2n_1n_2 & -2n_1n_3 \\ -2n_1n_2 & 1 - 2n_2^2 & -2n_2n_3 \\ -2n_1n_3 & -2n_2n_3 & 1 - 2n_3^2 \end{bmatrix}$ where \mathbf{n} is the **unit** normal vector of the plane.

Shear Matrices: shear factor λ is given by $\mathbf{I} + \lambda \mathbf{n} \begin{bmatrix} 1 & 1 & 1 \end{bmatrix}$: angle of shear: $\tan \gamma = \lambda$

$$\begin{matrix} \begin{bmatrix} 1 & \lambda \\ 0 & 1 \end{bmatrix} & \begin{bmatrix} 1 & 0 \\ \lambda & 1 \end{bmatrix} & \begin{bmatrix} 1 + \lambda n_1 & \lambda n_1 & \lambda n_1 \\ \lambda n_2 & 1 + \lambda n_2 & \lambda n_2 \\ \lambda n_3 & \lambda n_3 & 1 + \lambda n_3 \end{bmatrix} \\ \text{in } x\text{-axis} & \text{in } y\text{-axis} & \text{general 3D shear in line } \mathbf{r} \times \mathbf{n} = \mathbf{0} \end{matrix}$$

Orthogonal Projection: the projection matrix of \mathbb{R}^3 onto the plane $\mathbf{r} \cdot \mathbf{n} = 0$, where \mathbf{n} is the **unit** normal vector of the plane, is

$$\mathbf{I} - \mathbf{nn}^T = \begin{bmatrix} 1 - n_1^2 & -n_1n_2 & -n_1n_3 \\ -n_1n_2 & 1 - n_2^2 & -n_2n_3 \\ -n_1n_3 & -n_2n_3 & 1 - n_3^2 \end{bmatrix}.$$

This is a singular matrix since it involves a reduction in dimensionality ($3 \rightarrow 2$).

4.2.2. Geometric Interpretation of Invariance, Eigenvalues and Eigenvectors

For all linear transformations, the origin is invariant, which is not considered to ‘count’ here.

In 2D (or higher):

Invariant point: if $\mathbf{A}\mathbf{p} = \mathbf{p}$ then \mathbf{p} is invariant under \mathbf{A} (\mathbf{p} does not move).

\mathbf{p} is an eigenvector of \mathbf{A} , with eigenvalue 1.

Line of invariant points: a line $\mathbf{r} = \lambda\mathbf{n}$ for which all points on the line are invariant.

\mathbf{n} is an eigenvector of \mathbf{A} with eigenvalue 1.

Invariant line: a line $\mathbf{r} = \lambda\mathbf{n}$ for which points on the line are mapped to another point on the line, so that the line as a whole does not move.

\mathbf{n} is an eigenvector of \mathbf{A} , with points being scaled by the eigenvalue.

In 3D (or higher):

Plane of invariant points: a plane $\mathbf{r} = \lambda\mathbf{u} + \mu\mathbf{v}$ for which all points on the plane are invariant.

\mathbf{u} and \mathbf{v} are eigenvectors with repeated eigenvalue 1.

Invariant plane: a line $\mathbf{r} = \lambda\mathbf{u} + \mu\mathbf{v}$ for which points on the plane are mapped to another point on the plane, so that the plane as a whole does not move.

\mathbf{u} and \mathbf{v} are eigenvectors with the same repeated eigenvalue.

4.2.3. Affine Transformations

An affine transformation represents the combination of a linear transformation followed by a translation in space. In 3D, they can be represented as 4×4 matrices, with space vectors taking the form $[x \ y \ z \ 1]^T$, known as homogeneous coordinates (with $w = 1$, WLOG).

A 3D affine transformation matrix \mathbf{R} has the form

$$\mathbf{R} = \begin{bmatrix} M_{ii} & M_{ji} & M_{ki} & \Delta x \\ M_{ij} & M_{jj} & M_{kj} & \Delta y \\ M_{ik} & M_{jk} & M_{kk} & \Delta z \\ 0 & 0 & 0 & 1 \end{bmatrix} = \underbrace{\begin{bmatrix} 1 & 0 & 0 & \Delta x \\ 0 & 1 & 0 & \Delta y \\ 0 & 0 & 1 & \Delta z \\ 0 & 0 & 0 & 1 \end{bmatrix}}_{\text{translations}} \underbrace{\begin{bmatrix} M_{ii} & M_{ji} & M_{ki} & 0 \\ M_{ij} & M_{jj} & M_{kj} & 0 \\ M_{ik} & M_{jk} & M_{kk} & 0 \\ 0 & 0 & 0 & 1 \end{bmatrix}}_{\text{rotations, shears, projections...}}$$

where M_{xx} are the entries of a 3×3 linear transformation matrix \mathbf{M} and $(\Delta x, \Delta y, \Delta z)$ are translations parallel to the coordinate axes.

4.3. Fundamental Subspaces and Matrix Decompositions

4.3.1. Fundamental Subspaces

For any $m \times n$ matrix A of rank r , with $y = Ax$, (dims = number of dimensions in the space)

	Subspace	Form	Dims	Basis	Projection matrix onto subspace
Input space (dim = n)	Row space (domain)	$C(A^T)$	r_{col}	nonzero rows of $rref(A)$	$A^T(AA^T)^{-1}A$
	Null space (kernel)	$N(A)$	$n - r_{col}$	$Ax = 0$ i.e. $x^T A = 0^T$	$I - A^T(AA^T)^{-1}A$
Output space (dim = m)	Column space (image; range)	$C(A)$	r_{row}	columns of A corresponding to columns of $rref(A)$ with leading 1's	$A(A^T A)^{-1}A^T$
	Left null space (cokernel)	$N(A^T)$	$m - r_{col}$	$y^T A = 0^T$ i.e. $A^T y = 0$	$I - A(A^T A)^{-1}A^T$

For any matrix A acting as a transformation of space R^n into space R^m ,

- Vectors in the row space are mapped to the column space.
- Vectors in the null space are mapped to the origin.
- No vector is mapped to the left null space.
- The eigenvectors span the column space.

Orthogonal complements:

- The row space and the null space are orthogonal.
- The column space and the left null space are orthogonal.

Ranks:

- The column rank is the dimension of the row space. Full column rank: $r = n$.
- The row rank is the dimension of the column space. Full row rank: $r = m$.
- If A has full row rank then a solution x to the system $Ax = b$ exists.
- If A has full rank (i.e. square, invertible) then the solution x to $Ax = b$ is unique.

4.3.2. The Gram-Schmidt Orthonormalisation Process

Given a set of vectors a_i , the Gram-Schmidt process gives a set of orthonormal vectors q_i which span the same space as a_i , by subtracting off components parallel to each q_i .

Taking normalised a_1 as q_1 , the vector q_i is the normalised vector of $q_i' = a_i - \sum_{k=1}^{i-1} (a_i \cdot q_k) q_k$.

The complete set q_i is obtained when the resulting vector is 0 .

4.3.3. LU Decomposition

For any $m \times n$ matrix \mathbf{A} ,

$$\mathbf{PA} = \mathbf{LU}$$

where \mathbf{P} is a permutation matrix (sometimes omitted), \mathbf{L} a square $m \times m$ lower triangular matrix and \mathbf{U} an $m \times n$ echelon matrix.

Manual computation:

- To compute \mathbf{U} , use Gaussian elimination to convert \mathbf{A} into row echelon form, using row operations of the form $\mathbf{r}_j' = \mathbf{r}_j - a \mathbf{r}_i$ where $j > i$. If using partial pivoting, swap rows **before** each elimination such that the pivot (diagonal entry of \mathbf{U}) is maximised (by magnitude), equivalently ensuring that the multiplier (entry in \mathbf{L}) has $|a| \leq 1$.
- To compute \mathbf{L} , let each lower-triangular entry be equal to the coefficient a used in the Gaussian elimination step to form a zero in the corresponding position in \mathbf{U} . The diagonal entries of \mathbf{L} are all 1 and the upper-triangular entries are all 0. If using partial pivoting, swap entries in \mathbf{L} **only** when they are below the diagonal of the column, and only in the column in which the swap was performed.
- To compute \mathbf{P} , start with \mathbf{I} and swap the same rows as done during the process of computing \mathbf{U} . If partial pivoting was **not** used, then $\mathbf{P} = \mathbf{I}$ and can be omitted.

Programming functions:

- MATLAB: `[L, U, P] = lu(A)`
- Python: `P, L, U = scipy.linalg.lu(A)` where \mathbf{A} is a NumPy array

Basis of subspaces:

- Column space: the columns of \mathbf{L} corresponding to nonzero rows of \mathbf{U}
- Left nullspace: the nullspace of \mathbf{A}^T
- Row space: the nonzero rows of \mathbf{U}
- Nullspace: the nullspace of \mathbf{U}

To solve a system of equations of the form $\mathbf{Ax} = \mathbf{b}$:

- Transform $\mathbf{Ax} = \mathbf{b}$ into $\mathbf{Ux} = \mathbf{c}$ where $\mathbf{Lc} = \mathbf{b}$ can be solved by forward-substitution.
- Set all free variables to zero and find a particular solution \mathbf{x}_0 .
- Set the RHS to zero, give each free variable in turn the value 1 while the others are zero, and solve to find a set of vectors which span the null space of \mathbf{A} : $\mathbf{n}_1, \mathbf{n}_2$, etc.
- The general solution is $\mathbf{x} = \mathbf{x}_0 + \lambda \mathbf{n}_1 + \mu \mathbf{n}_2 + \dots$, where λ, μ , etc. are arbitrary.

4.3.4. Cholesky Decomposition

For a Hermitian (if real, then symmetric), positive-definite matrix \mathbf{A} ,

$$\mathbf{A} = \mathbf{L}\mathbf{L}^* \quad \text{in general, or} \quad \mathbf{A} = \mathbf{L}\mathbf{L}^T \quad \text{for real matrices}$$

where \mathbf{L} is a lower triangular matrix. \mathbf{L}^* is the conjugate transpose.

Manual computation:

- For each row of \mathbf{L} , compute the diagonal entry using this first formula below, starting with the top left.
- Then compute the remaining entries on that row using the second formula below, starting from the left and moving right until the diagonal. All other entries are 0.
- Move down to the next row, repeating until all rows of \mathbf{L} are filled.

$$L_{j,j} = (\pm) \sqrt{A_{j,j} - \sum_{k=1}^{j-1} L_{j,k}^2}, \quad L_{j,j} = \sqrt{A_{j,j} - \sum_{k=1}^{j-1} L_{j,k} L_{j,k}^*},$$

$$L_{i,j} = \frac{1}{L_{j,j}} \left(A_{i,j} - \sum_{k=1}^{j-1} L_{i,k} L_{j,k} \right) \quad \text{for } i > j. \quad L_{i,j} = \frac{1}{L_{j,j}} \left(A_{i,j} - \sum_{k=1}^{j-1} L_{i,k} L_{j,k}^* \right) \quad \text{for } i > j.$$

for real matrices for complex matrices

Programming functions:

- MATLAB: $\mathbf{L} = \text{chol}(\mathbf{A})$
- Python: $\mathbf{L} = \text{scipy.linalg.cholesky}(\mathbf{A})$ where \mathbf{A} is a NumPy array

To solve a system of equations of the form $\mathbf{A}\mathbf{x} = \mathbf{b}$:

- Transform $\mathbf{A}\mathbf{x} = \mathbf{b}$ into $\mathbf{L}^*\mathbf{x} = \mathbf{c}$ where $\mathbf{L}\mathbf{c} = \mathbf{b}$ can be solved by forward-substitution.
- Solve $\mathbf{L}^*\mathbf{x} = \mathbf{c}$ by back-substitution.

This method is approximately twice as fast as a solution using LU decomposition.

4.3.5. QR Decomposition and Least Squares Fitting

For any $m \times n$ matrix \mathbf{A} ,

$$\mathbf{A} = \mathbf{QR}$$

where \mathbf{Q} is an orthonormal $m \times r$ matrix and \mathbf{R} is an invertible upper-triangular $r \times n$ matrix, where r is the rank of \mathbf{A} .

Manual computation:

- To compute \mathbf{Q} , use the Gram-Schmidt process (Section 4.3.2.) to find an orthonormal set from the columns of \mathbf{A} . These vectors form the columns of \mathbf{Q} .
- To compute \mathbf{R} , use

$$\mathbf{R}_{ij} = \mathbf{q}_i \cdot \mathbf{a}_j \quad \text{if } i \leq j; \quad \text{otherwise } \mathbf{R}_{ij} = 0$$

where \mathbf{q}_i is the i th column vector of \mathbf{Q} and \mathbf{a}_j is the j th column vector of \mathbf{A} .

Programming functions:

- MATLAB: `[Q, R] = qr(A)`
- Python: `Q, R = scipy.linalg.qr(A)` where \mathbf{A} is a NumPy array

To solve a least-squares system $\mathbf{Ax}^* = \mathbf{b}$: in general, $\mathbf{x}^* = (\mathbf{A}^T \mathbf{A})^{-1} \mathbf{A}^T \mathbf{b}$, or more efficiently,

- Find $\mathbf{A} = \mathbf{QR}$.
- Solve $\mathbf{Rx}^* = \mathbf{Q}^T \mathbf{b}$ by back-substitution.
- The solution $\mathbf{x} = \mathbf{x}^*$ satisfies $\min \{\mathbf{x} \in \mathbb{R}^n : \|\mathbf{Ax} - \mathbf{b}\|_2^2\} = \min \{\mathbf{x} \in \mathbb{R}^n : \sum_i |\mathbf{A}_i \cdot \mathbf{x} - b_i|^2\}$.

Least-squares system in tabulated form: mapping x_i to y_i ($1 \leq i \leq n$), the coefficients of a best-fit line $y = a + bx$ or parabola $y = a + bx + cx^2$ can be found by solving the systems

$$\begin{array}{l} \text{Straight line: } y = a + bx \\ \text{Quadratic: } y = a + bx + cx^2 \end{array} \quad \left\{ \begin{array}{l} an + b \sum_i x_i = \sum_i y_i \\ a \sum_i x_i + b \sum_i x_i^2 = \sum_i x_i y_i \\ \\ an + b \sum_i x_i + c \sum_i x_i^2 = \sum_i y_i \\ a \sum_i x_i + b \sum_i x_i^2 + c \sum_i x_i^3 = \sum_i x_i y_i \\ a \sum_i x_i^2 + b \sum_i x_i^3 + c \sum_i x_i^4 = \sum_i x_i^2 y_i \end{array} \right.$$

4.3.6. Eigendecomposition (Diagonalisation)

If \mathbf{A} is a square $n \times n$ matrix with n linearly independent eigenvectors (diagonalisable, nondefective), then

$$\mathbf{A} = \mathbf{S}\mathbf{\Lambda}\mathbf{S}^{-1} \quad \text{and} \quad \mathbf{A}^n = \mathbf{S}\mathbf{\Lambda}^n\mathbf{S}^{-1}$$

where \mathbf{S} has the eigenvectors of \mathbf{A} as its columns, and $\mathbf{\Lambda}$ is a diagonal matrix with the corresponding eigenvalues along the diagonal. Matrices \mathbf{A} and $\mathbf{\Lambda}$ are said to be similar, so that they represent the same geometric transformation with a change of basis given by \mathbf{S} .

Spectral theorem: If \mathbf{A} is Hermitian then $\mathbf{A} = \mathbf{S}\mathbf{\Lambda}\mathbf{S}^*$

Spectral decomposition: If \mathbf{A} is real and symmetric then $\mathbf{A} = \mathbf{S}\mathbf{\Lambda}\mathbf{S}^T$.

where \mathbf{S} the orthonormal matrix of **normalised** eigenvectors as its columns.

Programming functions (where $\mathbf{D} \leftrightarrow \mathbf{\Lambda}$)

- MATLAB: `[S, D] = eig(A)`.
- Python: `D, S = np.linalg.eig(A)` # can use `eigh(A)` if Hermitian

4.3.7. Singular Value Decomposition (SVD)

For any $m \times n$ matrix \mathbf{A} ,

$$\mathbf{A} = \mathbf{Q}_1\mathbf{\Sigma}\mathbf{Q}_2^T$$

- \mathbf{Q}_1 is an $m \times m$ orthonormal matrix with the normalised eigenvectors of $\mathbf{A}\mathbf{A}^T$ as its columns.
- \mathbf{Q}_2 is an $n \times n$ orthonormal matrix with the normalised eigenvectors of $\mathbf{A}^T\mathbf{A}$ as its columns.
- $\mathbf{\Sigma}$ is an $m \times n$ diagonal matrix containing the r singular values, arranged in descending order on the leading diagonal, which are the square roots of the non-zero eigenvalues of both $\mathbf{A}\mathbf{A}^T$ and $\mathbf{A}^T\mathbf{A}$, where r is the rank of \mathbf{A} .

Programming functions:

- MATLAB: `[Q1, S, Q2] = svd(A)`
- Python: `Q1, S, Q2_T = np.linalg.svd(A)` where \mathbf{A} is a NumPy array

Basis of subspaces of \mathbf{A} :

- Column space: the first r columns of \mathbf{Q}_1
- Left nullspace: the last $m - r$ columns of \mathbf{Q}_1
- Row space: the first r columns of \mathbf{Q}_2
- Nullspace: the last $n - r$ columns of \mathbf{Q}_2

4.3.8. Other Matrix Decompositions

Schur Decomposition: for any square matrix \mathbf{A} ,

$$\mathbf{A} = \mathbf{U}\mathbf{T}\mathbf{U}^*$$

where \mathbf{U} is unitary, and \mathbf{T} is upper-triangular with the eigenvalues of \mathbf{A} along its diagonal. If \mathbf{A} is normal then \mathbf{T} is diagonal and the Schur form matches the spectral decomposition.

Polar Decomposition: for any square matrix \mathbf{A} ,

$$\mathbf{A} = \mathbf{U}\mathbf{P}$$

where \mathbf{U} is unitary and \mathbf{P} is positive semi-definite and Hermitian. \mathbf{P} is unique with $\mathbf{P}^2 = \mathbf{A}\mathbf{A}^*$. If \mathbf{P} has spectral decomposition $\mathbf{P} = \mathbf{V}\mathbf{D}\mathbf{V}^*$ and $\mathbf{W} = \mathbf{U}\mathbf{V}$ then the SVD is $\mathbf{A} = \mathbf{W}\mathbf{D}\mathbf{V}^*$.

Toeplitz decomposition: for any square matrix \mathbf{A} ,

$$\mathbf{A} = \mathbf{H} + \mathbf{G}$$

where \mathbf{H} is Hermitian and \mathbf{G} is skew-Hermitian, with $\mathbf{H} = (\mathbf{A} + \mathbf{A}^*)/2$ and $\mathbf{G} = (\mathbf{A} - \mathbf{A}^*)/2$.

4.3.9. Matrix Exponentials

For a square $m \times m$ matrix \mathbf{A} , the matrix exponential $\exp(\mathbf{A})$ is defined as

$$\exp(\mathbf{A}) = e^{\mathbf{A}} = \sum_{n=0}^{\infty} \frac{\mathbf{A}^n}{n!} = \mathbf{I} + \mathbf{A} + \frac{1}{2}\mathbf{A}^2 + \dots$$

To compute $\exp(\mathbf{A})$ from its eigenvalues and eigenvectors, let $\mathbf{A} = \mathbf{S}\mathbf{\Lambda}\mathbf{S}^{-1}$ (eigendecomposition: Section 4.3.6). Then $\exp(\mathbf{A}) = \mathbf{S} \exp(\mathbf{\Lambda}) \mathbf{S}^{-1}$.

Properties:

- $\exp(\mathbf{A}^T) = \exp(\mathbf{A})^T$ and $\exp(\mathbf{A}^*) = \exp(\mathbf{A})^*$
- If $\mathbf{A}\mathbf{B} = \mathbf{B}\mathbf{A}$ then $e^{\mathbf{A}}e^{\mathbf{B}} = e^{\mathbf{B}}e^{\mathbf{A}} = e^{\mathbf{A}+\mathbf{B}}$

4.3.10. Statement of a Convex Optimisation Problem

Objective: to find \mathbf{x} that minimises $f_0(\mathbf{x})$ such that $f_i(\mathbf{x}) \leq b_i$ and $h_i(\mathbf{x}) = 0$, where

- $\mathbf{x} = [x_1, x_2, \dots, x_n]^T$ is an input state vector
- $f_0(\mathbf{x})$ is the objective function (scalar)
- $f_i(\mathbf{x}) \leq b_i$ are bounds for valid regions (feasible region) of the input \mathbf{x}
- $h_i(\mathbf{x}) = 0$ are constraints for valid contour lines (level sets) of the input \mathbf{x}

Convex function: $f_i(\alpha\mathbf{x} + \beta\mathbf{y}) \leq \alpha f_i(\mathbf{x}) + \beta f_i(\mathbf{y})$ for all $\alpha + \beta = 1$, $\alpha \geq 0$, $\beta \geq 0$

In a **convex** optimisation problem, the objective and inequality constraint functions f_0 and f_i are convex functions. Convex optimisation problems are guaranteed to have no more than one local minima: if a minimum exists, then it is the global minimum.

The global minimum solution is denoted $\mathbf{x} = \mathbf{x}^*$, so that $f_0(\mathbf{x}^*) = \min \{\mathbf{x} \in \mathbb{R}^n : f_0(\mathbf{x})\}$ within the specified constraints.

Least-Squares Optimisation

Objective: minimise $f_0(\mathbf{x}) = \|\mathbf{A}\mathbf{x} - \mathbf{b}\|_2^2$ (l_2 -norm of residual vector)

Constraints: (arbitrary)

The solution is given by $\mathbf{x}^* = \mathbf{A}^+\mathbf{b}$ ($\mathbf{A}^+ = (\mathbf{A}^T\mathbf{A})^{-1}\mathbf{A}^T$: Moore-Penrose pseudoinverse).

Linear Programming (LP Problems)

Objective: minimise $f_0(\mathbf{x}) = \mathbf{c}^T\mathbf{x}$ (linear combination of variables)

Constraints: $\mathbf{a}_i^T\mathbf{x} \leq b_i$ and $\mathbf{x} \geq 0$

The solution \mathbf{x}^* is guaranteed to lie on the vertex of the boundary of the constraint region.

Danzig's simplex algorithm: visualise feasible region as a polytope (n -D polyhedron with hyperplane faces) in a uniform gradient field $\nabla f_0 = \mathbf{c}$. Traverse edges of the polytope until optimum vertex found.

Quadratic Programming

Objective: minimise $f_0(\mathbf{x}) = \frac{1}{2}\mathbf{x}^T\mathbf{P}\mathbf{x} + \mathbf{q}^T\mathbf{x} + \mathbf{r}$ (\mathbf{P} : positive semi-definite matrix)

Constraints: $\mathbf{G}\mathbf{x} \leq \mathbf{h}$ and $\mathbf{A}\mathbf{x} = \mathbf{b}$

4.4. Matrix and Tensor Calculus

4.4.1. Indicial Tensor Notation

Einstein summation notation: repeated indices imply summation over indices.

- Component form: $\mathbf{a} = a_i \mathbf{e}_i = \sum_i a_i \mathbf{e}_i$
- Inner product: $\mathbf{a} \cdot \mathbf{b} = a_i b_i$
- Outer product: if $\mathbf{A} = \mathbf{a} \otimes \mathbf{b}$ then $A_{ij} = a_i b_j$
- Kronecker delta: $\delta_{ij} = 1$ if $i = j$ else $\delta_{ij} = 0$; for orthonormal \mathbf{e} , then $\delta_{ij} = \mathbf{e}_i \cdot \mathbf{e}_j$.
- Permutation symbol:
 - $e_{ijk} = 1$, when i, j, k are in cyclic order
 - $e_{ijk} = -1$, when i, j, k are in anti-cyclic order
 - $e_{ijk} = 0$, when any indices repeat
- Triple product contraction: $e_{ijk} e_{ipq} = \delta_{jp} \delta_{kq} - \delta_{jq} \delta_{kp}$ (epsilon-delta identity)
- Gradient field: $\nabla \phi = (\partial \phi / \partial x_i) \mathbf{e}_i = \phi_{,i} \mathbf{e}_i$
- Divergence field: $\nabla \cdot \mathbf{v} = v_{i,i}$
- Curl field: $\nabla \times \mathbf{v} = e_{ijk} v_{k,j} \mathbf{e}_i$
- Gauss' divergence theorem: $\int_V \frac{\partial A_{ij}}{\partial x_j} dV = \oint_S A_{ij} n_j dS$
- Stokes' curl theorem: $\int_S e_{ijk} \frac{\partial A_{pk}}{\partial x_j} n_i dS = \oint_C A_{pk} dx_k$

4.4.2. Differentiation with Respect to Vectors and Matrices

$$\left[\frac{\partial \mathbf{x}}{\partial y} \right]_i = \frac{\partial x_i}{\partial y}$$

Vector-valued function $\mathbf{x}(y)$

$$\left[\frac{\partial x}{\partial \mathbf{y}} \right]_i = \frac{\partial x}{\partial y_i}$$

Multivariable function $x(\mathbf{y})$

$$\left[\frac{\partial \mathbf{x}}{\partial \mathbf{y}} \right]_{ij} = \frac{\partial x_i}{\partial y_j}$$

Vector field $\mathbf{x}(\mathbf{y})$

Differential of matrix expressions (\mathbf{X}, \mathbf{Y} : matrix-valued functions)

$$\begin{aligned} \partial \mathbf{A} &= 0 && (\mathbf{A} \text{ is a constant}) \\ \partial(\alpha \mathbf{X}) &= \alpha \partial \mathbf{X} \\ \partial(\mathbf{X} + \mathbf{Y}) &= \partial \mathbf{X} + \partial \mathbf{Y} \\ \partial(\text{Tr}(\mathbf{X})) &= \text{Tr}(\partial \mathbf{X}) \\ \partial(\mathbf{X}\mathbf{Y}) &= (\partial \mathbf{X})\mathbf{Y} + \mathbf{X}(\partial \mathbf{Y}) \\ \partial(\mathbf{X} \circ \mathbf{Y}) &= (\partial \mathbf{X}) \circ \mathbf{Y} + \mathbf{X} \circ (\partial \mathbf{Y}) \\ \partial(\mathbf{X} \otimes \mathbf{Y}) &= (\partial \mathbf{X}) \otimes \mathbf{Y} + \mathbf{X} \otimes (\partial \mathbf{Y}) \\ \partial(\mathbf{X}^{-1}) &= -\mathbf{X}^{-1}(\partial \mathbf{X})\mathbf{X}^{-1} \\ \partial(\det(\mathbf{X})) &= \text{Tr}(\text{adj}(\mathbf{X})\partial \mathbf{X}) \\ \partial(\det(\mathbf{X})) &= \det(\mathbf{X})\text{Tr}(\mathbf{X}^{-1}\partial \mathbf{X}) \\ \partial(\ln(\det(\mathbf{X}))) &= \text{Tr}(\mathbf{X}^{-1}\partial \mathbf{X}) \\ \partial \mathbf{X}^T &= (\partial \mathbf{X})^T \\ \partial \mathbf{X}^H &= (\partial \mathbf{X})^H \end{aligned}$$

Derivative of determinant: $\frac{\partial \det(\mathbf{Y})}{\partial x} = \det(\mathbf{Y})\text{Tr} \left[\mathbf{Y}^{-1} \frac{\partial \mathbf{Y}}{\partial x} \right]$

Derivative of inverse: $\frac{\partial \mathbf{Y}^{-1}}{\partial x} = -\mathbf{Y}^{-1} \frac{\partial \mathbf{Y}}{\partial x} \mathbf{Y}^{-1}$

Derivative of eigenvalues: $\frac{\partial}{\partial \mathbf{X}} \sum \text{eig}(\mathbf{X}) = \frac{\partial}{\partial \mathbf{X}} \text{Tr}(\mathbf{X}) = \mathbf{I}$
 $\frac{\partial}{\partial \mathbf{X}} \prod \text{eig}(\mathbf{X}) = \frac{\partial}{\partial \mathbf{X}} \det(\mathbf{X}) = \det(\mathbf{X})\mathbf{X}^{-T}$

Derivatives of linear forms: $\frac{\partial \mathbf{x}^T \mathbf{a}}{\partial \mathbf{x}} = \frac{\partial \mathbf{a}^T \mathbf{x}}{\partial \mathbf{x}} = \mathbf{a}$ $\frac{\partial \mathbf{a}^T \mathbf{X} \mathbf{b}}{\partial \mathbf{X}} = \mathbf{a} \mathbf{b}^T$ $\frac{\partial \mathbf{a}^T \mathbf{X}^T \mathbf{b}}{\partial \mathbf{X}} = \mathbf{b} \mathbf{a}^T$

Derivatives of quadratic forms: $\frac{\partial \mathbf{x}^T \mathbf{B} \mathbf{x}}{\partial \mathbf{x}} = (\mathbf{B} + \mathbf{B}^T)\mathbf{x}$

Gradient and Hessian: if $f = \mathbf{x}^T \mathbf{A} \mathbf{x} + \mathbf{b}^T \mathbf{x}$ then $\nabla_{\mathbf{x}} f = \frac{\partial f}{\partial \mathbf{x}} = (\mathbf{A} + \mathbf{A}^T)\mathbf{x} + \mathbf{b}$; $\frac{\partial^2 f}{\partial \mathbf{x} \partial \mathbf{x}^T} = \mathbf{A} + \mathbf{A}^T$

Derivative of trace: if $f(x) = \frac{dF(\mathbf{X})}{dx}$ then $\frac{\partial \text{Tr}(F(\mathbf{X}))}{\partial \mathbf{X}} = f(\mathbf{X})^T$

4.4.3. Quadratic Forms

A quadratic form is a scalar-valued function of the form

$$f(\mathbf{x}) = \mathbf{x}^T \mathbf{A} \mathbf{x} + \mathbf{b}^T \mathbf{x}, \quad f: \mathbb{R}^n \rightarrow \mathbb{R}, \quad \mathbf{A} = \mathbf{A}^T \in \mathbb{R}^{n \times n}, \quad \mathbf{b} \in \mathbb{R}^n.$$

If $\mathbf{x} = [x_1 \dots x_n]$ then the $\mathbf{x}^T \mathbf{A} \mathbf{x}$ term expands to a weighted sum over all combinations of $x_i x_j$ and the $\mathbf{b}^T \mathbf{x}$ term expands to a weighted sum over all x_i .

Iff $\mathbf{A} > 0$ then f is a strictly convex function.

4.4.4. Block Matrices

A block matrix is a matrix in which the entries can be matrices, vectors or scalars.

$$\mathbf{P} = \begin{bmatrix} 1 & 2 & 2 & 7 \\ 1 & 5 & 6 & 2 \\ 3 & 3 & 4 & 5 \\ 3 & 3 & 6 & 7 \end{bmatrix} \quad \mathbf{P}_{11} = \begin{bmatrix} 1 & 2 \\ 1 & 5 \end{bmatrix}, \quad \mathbf{P}_{12} = \begin{bmatrix} 2 & 7 \\ 6 & 2 \end{bmatrix}, \quad \mathbf{P}_{21} = \begin{bmatrix} 3 & 3 \\ 3 & 3 \end{bmatrix}, \quad \mathbf{P}_{22} = \begin{bmatrix} 4 & 5 \\ 6 & 7 \end{bmatrix}.$$

$$\mathbf{P} = \begin{bmatrix} \mathbf{P}_{11} & \mathbf{P}_{12} \\ \mathbf{P}_{21} & \mathbf{P}_{22} \end{bmatrix}.$$

Block matrix \mathbf{P} is said to be $(m \times n)$ if it has m row partitions and n column partitions. Its full dimensions are at least as large as $m \times n$.

- **Multiplication:** if \mathbf{A} is $(m \times n)$ and \mathbf{B} is $(p \times n)$ then $\mathbf{C} = \mathbf{AB}$ is $(m \times n)$: $\mathbf{C}_{qr} = \mathbf{A}_{qi} \mathbf{B}_{ir}$. All partitions must be conformable such that # columns in $\mathbf{A}_{qi} = \#$ rows in \mathbf{B}_{ir} for all i .

M5. STATISTICS

5.1. Axioms, Combinatorial Probability and Basic Statistics

5.1.1. Axioms of Probability

Axioms: The probability P is a measure that verifies the following:

- Probability of an event: $P(A) \in R, P(A) \geq 0, \forall A \subseteq \Omega$
- Sample space is a certain event: $P(\Omega) = 1$
- Additivity for disjoint sets: $P(A \cup B) = P(A) + P(B), \text{ if } A \cap B = \emptyset$

Immediate Consequences: these can be demonstrated easily from a Venn diagram.

- Monotonicity: if $A \subseteq B$ then $P(A) \leq P(B)$.
- Empty set: $P(\emptyset) = 0$.
- Complement: $P(\bar{A}) = 1 - P(A)$
- Bound: $0 \leq P(A) \leq 1, \forall A \subseteq \Omega$.

5.1.2. Rules of Probability

- Addition: $P(A \cup B) = P(A) + P(B) - P(A \cap B)$.
- Sum rule: $P(A \cap B) + P(A \cap \bar{B}) = P(A)$.
- Conditional probability: $P(A | B) = \frac{P(A \cap B)}{P(B)}$ if $P(B) \neq 0$.
- Law of total probability: $P(A) = P(A | B) P(B) + P(A | \bar{B}) P(\bar{B})$.
- Bayes' rule: $P(B | A) = \frac{P(B)}{P(A)} P(A | B) = \frac{P(A | B) P(B)}{P(A | B) P(B) + P(A | \bar{B}) P(\bar{B})}$.

5.1.3. Combinatorial (Frequentist) Definition of Probability

Assuming that the event occurs with equal likelihood in all outcomes:

$$\text{Probability of an event } A = \frac{\text{number of outcomes in which } A \text{ occurs}}{\text{total number of outcomes}}.$$

5.1.4. Definitions of Mean and Variance

For a single variable dataset $\{x_1, x_2, \dots, x_n\}$, the sample mean and variance are

$$\bar{x} = \frac{1}{n} \sum_{i=1}^n x_i \quad s^2 = \frac{1}{n-1} \sum_{i=1}^n (x_i - \bar{x})^2 = \frac{1}{n-1} \sum_{i=1}^n x_i^2 - \frac{1}{n(n-1)} \left(\sum_{i=1}^n x_i \right)^2$$

If $n \rightarrow N$ is large and representative of the population, then the population mean and variance are

$$\mu = \frac{1}{N} \sum_{i=1}^N x_i \quad \sigma^2 = \frac{1}{N} \sum_{i=1}^N (x_i - \mu)^2 = \frac{1}{N} \sum_{i=1}^N x_i^2 - \frac{1}{N^2} \left(\sum_{i=1}^N x_i \right)^2$$

The quantities $\sum_{i=1}^n x_i$ and $\sum_{i=1}^n x_i^2$ are known as summary statistics.

Standard deviation: σ

Coefficient of Variation: $\text{CoV} = \frac{\sigma}{\mu}$

5.1.5. Data Presentation

For categorical or discrete data:

- Pie chart: angle of the pie represents fraction of total frequency.
- Bar chart: bar height represents frequency. May have error bars, be grouped and/or stacked.
- Frequency table: lists the frequencies explicitly.
- Pictogram / tally chart: shows icons representing a given unit frequency.
- Choropleth map: colour-coded values or buckets. Often used for geographical data.

For numerical and continuous data:

- Histogram: shows frequency density = frequency (area) / bin size, of the intervals
- Line chart: shows values as \times on the graph, connected. Can also be used for discrete.
- Stem and leaf plot: lists of numerical data grouped by the most significant digit.
- Box and whisker plot: shows the min, max, quartiles and mean.
Conventionally, outliers are identified as $x > \text{UQ} + 1.5 \times \text{IQR}$ or $x < \text{LQ} - 1.5 \times \text{IQR}$.
(UQ: upper quartile, LQ: lower quartile, IQR = UQ - LQ: interquartile range)

For bivariate data:

- Scatter graph: shows values as \times on the graph, not connected.

5.1.6. Common Numbers and Operators in Combinatorics

- Factorial:
$$n! = n(n - 1)(n - 2)\dots 2 \times 1$$
 - First few factorials: $0! = 1, 1! = 1, 2! = 2, 3! = 6, 4! = 24, 5! = 120, 6! = 720\dots$
 - For identities involving factorials and other types of factorials, see Section 1.7.1.
- Derangement (subfactorial):
$$!n = n! \times \sum_{k=0}^n \frac{(-1)^k}{k!} = \text{round}\left(\frac{n!}{e}\right), \text{ with } !0 = 1$$
- Combinations (binomial coefficient):
$${}^n C_r = \frac{n!}{r!(n-r)!}$$
- Permutations:
$${}^n P_r = \frac{n!}{(n-r)!} = r! \times {}^n C_r$$
- Bell numbers:
$$B_{n+1} = \sum_{k=0}^n {}^n C_k \times B_k$$
 - Explicit formula (Dobiński's formula):
$$B_n = \frac{1}{e} \sum_{k=0}^{\infty} \frac{k^n}{k!}$$
 - First few Bell numbers: $B_0 = 1, B_1 = 1, B_2 = 2, B_3 = 5, B_4 = 15, B_5 = 52, B_6 = 203\dots$
 - Exponential generating function:
$$EG(B_n; z) = \sum_{n=0}^{\infty} \frac{B_n}{n!} z^n = e^{e^z - 1}$$
- Harmonic numbers:
$$H_n = \sum_{r=1}^n \frac{1}{r}$$
- Stirling numbers of the 1st kind: coefficients s such that $(x)_n = \sum_{k=0}^n s(n, k) x^k$
- Stirling numbers of the 2nd kind:
$$S(n, k) = \sum_{i=0}^k \frac{(-1)^{k-i} i^n}{(k-i)! i!}$$
- Lah numbers:
$$L(n, k) = {}^{n-1} C_{k-1} \times \frac{n!}{k!}$$

5.1.7. Counting Problems of Unordered Sets (Combinations and Partitions)

Consider a set S of n objects, all of which are **unique**, e.g. $S = \{\text{red circle}, \text{yellow heart}, \text{green heart}, \text{blue circle}, \text{purple heart}\}$

A **combination** is an **unordered** non-empty subset of S of any length r , e.g. $\{\text{red circle}, \text{green heart}, \text{blue circle}\}$.

A **partition** is a superset of S containing any number k of non-overlapping (mutually disjoint) combinations of S , e.g. $\{\{\text{red circle}, \text{purple heart}\}, \{\text{yellow heart}, \text{green heart}\}, \{\text{blue circle}\}\}$.

A combination may (if specified) include the same element(s) of S multiple times. If this is the case, we say it has “repeats” or “with replacement”.

- Number of r -length **combinations without replacement** $= {}^n C_r = \frac{n!}{r!(n-r)!}$
- Number of r -length **combinations with replacement** $= {}^{n+r-1} C_r = \frac{(n+r-1)!}{r!(n-1)!}$
- Number of **partitions** $= B_n$ (Bell numbers)
- Number of **partitions into k combinations** $= S(n, k)$ (Stirling numbers of the second kind)

5.1.8. Counting Problems of Ordered Sets (Permutations and Derangements)

Consider a set S of n objects, all of which are **unique**, e.g. $S = \{\text{red circle}, \text{yellow heart}, \text{green heart}, \text{blue circle}, \text{purple heart}\}$

A **permutation** is a linearly **ordered** non-empty subset of S of any length r , e.g. $(\text{red circle}, \text{blue circle}, \text{yellow heart})$.

A **cyclic permutation** is a permutation where left/right shifting is considered an identical permutation.

A **derangement** is an n -length permutation without replacement of an **ordered** set S such that no object remains in its original position, e.g. $(\text{red circle}, \text{yellow heart}, \text{green heart}, \text{blue circle}, \text{purple heart}) \rightarrow (\text{yellow heart}, \text{blue circle}, \text{red circle}, \text{purple heart}, \text{green heart})$.

A permutation may (if specified) include the same element(s) of S multiple times. If this is the case, we say it has “repeats” or “with replacement”.

- Number of r -length **permutations without replacement** $= {}^n P_r = \frac{n!}{(n-r)!}$
- Number of r -length **permutations with replacement** $= n^r$
- Number of **derangements** $= !n$ (derangement)
- Number of **partitions into k cyclic permutations** $= s(n, k)$ (Stirling numbers of the 1st kind)
- Number of **partitions into k permutations** $= L(n, k)$ (Lah numbers / Stirling numbers of the 3rd kind)

If the set contains items considered to be **identical** e.g. $S = \{\text{red circle}, \text{red circle}, \text{yellow heart}, \text{green heart}, \text{green heart}, \text{green heart}, \text{blue circle}, \text{blue circle}, \text{purple heart}\}$, where each item red circle , yellow heart , green heart ... appears n_1, n_2, n_3, \dots times respectively ($n_1 + n_2 + n_3 + \dots = n$):

- Number of n -length **multiset permutations without replacement** $= \frac{n!}{n_1! n_2! n_3! \dots}$

5.1.9. Common Counting Problems

Coupon Collector Problem: Each box contains one coupon. Each coupon can come in n different kinds, uniformly distributed. Let T be the number of boxes opened once at least one of each coupon kind has been found, where $T \geq n$.

- Probability distribution: $P(T = t) = \frac{n!}{n^t} S(t-1, n-1) = n^{1-t} \sum_{r=0}^{n-1} {}^{n-1}C_r (-1)^{n-1-r} r^{t-1}$
- Cumulative distribution: $P(T \leq t) = \frac{n!}{n^t} S(t, n) = \sum_{i=0}^n {}^n C_i (-1)^{n-i} \left(\frac{i}{n}\right)^t$
(S : Stirling numbers of the 2nd kind)
- Expected number of boxes required: $E[T] = n H_n$ (H_n : harmonic numbers)
- Variance in number of boxes required: $Var[T] = n^2 \left(\sum_{r=1}^n \frac{1}{r^2} \right) - n H_n$
- Expected remaining number of boxes required when $m < n$ already found: $E[T_m] = n H_{n-m}$
- Asymptotic limit for large n : $E[T] \sim n \ln n + \gamma n + \frac{1}{2} + O(n^{-1})$ ($\gamma \approx 0.5772$: Euler-Mascheroni constant)

Hat Check Problem: A group of n men put their n unique hats into a box. Afterwards, the men then randomly take back one hat each from the box without replacement. Let M be the number of men who correctly retrieved their own hat, where $0 \leq M \leq n$.

- Probability distribution: $P(M = m) = \frac{{}^n C_m \times !(n-m)}{n!}$ ($!$: derangement)
- Probability that no men find their hat: $P(0) = 1/e \approx 0.3679\dots$
- Expected number of correct hats: $E[M] = 1$
- Variance in number of correct hats: $Var[M] = 1$

Birthday Problem: In a room of n people, find the probability that any two share a birthday.

- $P(\text{at least two shared birthdays}) = 1 - \frac{{}^{365}P_n}{365^n}$
- For two groups (a men and b women, with $a + b = n$):
 - $P(\text{a man shares a birthday with a woman}) = \frac{1}{365^n} \sum_{i=1}^a \sum_{j=1}^b S(a, i) S(b, j) \prod_{k=0}^{i+j-1} (365 - k)$

5.2. Probability Distributions and Random Variables

5.2.1. Discrete Probability Distributions

Distribution	$P(X=r)$ PMF	$E(X)$ expectation	$Var(X)$ variance	$G_X(z)$ PGF	$H(X)$ differential entropy
Bernoulli $r \in \{0, 1\}$ $X \sim \text{Ber}(p)$	$p^r q^{1-r}$ $q = 1 - p$	p	pq	$q + pz$	$-q \log q + p \log p$
Discrete Uniform $r \in \{a, \dots, b\}$ $X \sim U(a, b)$	$\frac{1}{n}$ $n = b - a + 1$	$\frac{a+b}{2}$	$\frac{n^2 - 1}{12}$	$\frac{z^a - z^{b+1}}{n(1-z)}$	$\log n$
Binomial $r \in \{0, 1, 2, \dots, n\}$ $X \sim B(n, p)$	${}^n C_r p^r q^{n-r}$	np	npq	$(q + pz)^n$	$\log \sqrt{2\pi n p q} + O(n^{-1})$
Negative Binomial $r \in \{0, 1, 2, \dots\}$ $X \sim \text{NB}(n, p)$	${}^{r+n-1} C_r p^n q^r$	$\frac{nq}{p}$	$\frac{nq}{p^2}$	$\left(\frac{p}{1-qz}\right)^n$	-
Beta-Binomial $r \in \{0, 1, 2, \dots, n\}$ $X \sim \text{BetaBin}(n, \alpha, \beta)$	$\frac{{}^n C_r B(r+\alpha, n-r+\beta)}{B(\alpha, \beta)}$	$\frac{n\alpha}{\alpha + \beta}$	$\frac{n\alpha\beta(\alpha+\beta+n)}{(\alpha+\beta)^2(\alpha+\beta+1)}$	-	-
Geometric $r \in \{1, 2, 3, \dots\}$ $X \sim \text{Geo}(p)$	$q^{r-1} p$	p^{-1}	qp^{-2}	$\frac{pz}{1-qz}$	$\frac{-q}{p} \log q - \log p$
Hypergeometric $r \in \{\max(0, n+K-N), \dots, \min(n, K)\}$ $X \sim \text{HG}(N, K, n)$	$\frac{{}^K C_r {}^{N-K} C_{n-r}}{{}^N C_n}$	$\frac{nK}{N}$	$\frac{nK(N-K)(N-n)}{N^2(N-1)}$	$\frac{{}^{N-K} C_n}{{}^N C_n} \times {}_2F_1(-n, -K; N-K-n+1; z)$	-
Negative Hypergeometric $r \in \{0, \dots, K\}$ $X \sim \text{NHG}(N, K, n)$	$\frac{{}^{r+n-1} C_r {}^{N-n-r} C_{K-r}}{{}^N C_K}$	$\frac{nK}{N-K+1}$	$\frac{nK(N+1)(N-K+1-n)}{N-K+2}$	-	-
Poisson $r \in \{0, 1, 2, \dots\}$ $X \sim \text{Po}(\lambda)$	$\frac{e^{-\lambda} \lambda^r}{r!}$	λ	λ	$e^{\lambda(z-1)}$	$\log \sqrt{2\pi e \lambda} + O(\lambda^{-1})$

5.2.2. Continuous Probability Distributions

Distribution	$f_X(x)$ PDF	$E(X)$ expectation	$Var(X)$ variance	$M_X(s)$ MGF	$H(X)$ differential entropy
Rectangular $x \in [a, b]$ $X \sim \text{Rect}(a, b)$	$\frac{1}{b-a}$	$\frac{a+b}{2}$	$\frac{(b-a)^2}{12}$	$\frac{e^{bs} - e^{as}}{s(b-a)}$	$\log(b-a)$
Normal $x \in \mathbb{R}$ $X \sim N(\mu, \sigma^2)$	$\frac{1}{\sigma\sqrt{2\pi}} e^{-\frac{1}{2}\left(\frac{x-\mu}{\sigma}\right)^2}$	μ	σ^2	$e^{\mu s + \frac{1}{2}\sigma^2 s^2}$	$\frac{1}{2} (1 + \log(2\pi\sigma^2))$
Student's t $x \in \mathbb{R}$ $X \sim t_\nu$	$\frac{\Gamma\left(\frac{\nu+1}{2}\right)}{\sqrt{\nu\pi} \Gamma\left(\frac{\nu}{2}\right)} \left(1 + \frac{x^2}{\nu}\right)^{-\frac{1}{2}(\nu+1)}$	0	$\frac{\nu}{\nu-2}$	(undefined for tail ranges of t)	$\frac{\nu+1}{2} \left(\psi\left(\frac{\nu+1}{2}\right) - \psi\left(\frac{\nu}{2}\right)\right) + \log(\nu^{1/2} B\left(\frac{\nu}{2}, \frac{1}{2}\right))$
Exponential $x \geq 0$ $X \sim \text{Exp}(\lambda)$	$\lambda e^{-\lambda x}$	$\frac{1}{\lambda}$	$\frac{1}{\lambda^2}$	$\frac{\lambda}{\lambda-s}$	$1 - \log \lambda$
Rayleigh $x \geq 0$ $X \sim \text{Rayleigh}(\sigma)$	$\frac{x}{\sigma^2} e^{-\frac{x^2}{2\sigma^2}}$	$\sqrt{\frac{\pi\sigma^2}{2}}$	$\frac{4-\pi}{2} \sigma^2$	-	$1 + \frac{\gamma}{2} + \log \frac{\sigma}{\sqrt{2}}$
Beta $x \in [0, 1]$ $X \sim \text{Beta}(\alpha, \beta)$	$\frac{\Gamma(\alpha+\beta)}{\Gamma(\alpha)\Gamma(\beta)} x^{\alpha-1} (1-x)^{\beta-1}$	$\frac{\alpha}{\alpha+\beta}$	$\frac{\alpha\beta}{(\alpha+\beta)^2(\alpha+\beta+1)}$	$1 + \sum_{k=1}^{\infty} \left(\prod_{r=0}^{k-1} \frac{\alpha+r}{\alpha+\beta+r} \right) \frac{s^k}{k!}$	$\log B(\alpha, \beta) - (\alpha-1)\psi(\alpha) - (\beta-1)\psi(\beta) + (\alpha+\beta-2)\psi(\alpha+\beta)$

For the multivariate Normal distribution, see Section 5.4.1.

5.2.3. Typical Modelling Cases for Probability Distributions

Urn Model (With Replacements / Repeats): Consider an urn (container) of balls, of which a proportion p are **green** (success) and the rest $(1 - p)$ are **red** (failure). Suppose that balls are sampled **with replacement** (each ball is returned before taking the next ball).

Binomial	A total of n balls are sampled. The number of green balls sampled is distributed as $X \sim B(n, p)$.
Geometric	Samples are drawn until the first green ball is sampled. The total number of balls sampled (including the green) is distributed as $X \sim \text{Geo}(p)$. The number of red balls sampled is then $X - 1$.
Negative Binomial	Samples are drawn until the first n green balls are sampled. The number of red balls sampled is distributed as $X \sim \text{NB}(n, p)$.
Beta	A fixed number of balls are drawn. It is observed that $\alpha - 1$ are green and that $\beta - 1$ are red . The prior for the number of green balls is uniform. The (posterior) probability of drawing green is distributed as $p \sim \text{Beta}(\alpha, \beta)$.
Beta Binomial	A total of n balls are sampled. The probability p of drawing green is unknown and is distributed as $p \sim \text{Beta}(\alpha, \beta)$. The number of green balls sampled is distributed as $X \sim \text{BetaBin}(n, \alpha, \beta)$.

Urn Model (Without Replacement / Repeats): Consider an urn of N balls, of which K are **green** and the rest $(N - K)$ are **red**. Suppose that balls are sampled **without replacement** (the combination of balls is taken at once, so the sample must contain unique balls).

Hypergeometric	A total of n balls are sampled. The number of green balls sampled is distributed as $X \sim \text{HG}(N, K, n)$. If $n \ll N \rightarrow \infty$ then $X \sim B(n, K/N)$ ($K = pN$).
Negative Hypergeometric	Samples are drawn until the first n red balls are sampled. The number of green balls sampled is distributed as $X \sim \text{NHG}(N, K, n)$. If $n \ll N \rightarrow \infty$ then $X \sim \text{BetaBin}(K, n, N - K - n + 1)$ ($K = \frac{\alpha}{p}$ and $N - K = \frac{\beta}{1 - p}$).

Event Model: Consider a period over which point events can occur at an average rate λ events per unit interval (often time, sometimes distance or number of transitions).

Poisson	The number of events per unit interval is distributed as $X \sim \text{Po}(\lambda)$.
Exponential	The interval between two consecutive events is distributed as $X \sim \text{Exp}(\lambda)$.

5.2.4. Sampling From Normal Distributions

If X is Normally distributed as $X \sim N(\mu, \sigma^2)$, then:

- The standard score $Z = \frac{X - \mu}{\sigma}$ is distributed as $Z \sim N(0, 1)$.

For a random sample of n observations X_n from X with sample standard deviation s :

- The sample mean \bar{X} is distributed as $\bar{X} \sim N(\mu, \frac{\sigma^2}{n})$. ($Var(\bar{X}) = \frac{\sigma_x^2}{n}$ for any iid sample)
- The sample mean standard score $\bar{Z} = \frac{\bar{X} - \mu}{s^2/n}$ is distributed as $\bar{Z} \sim t_{n-1}$.
- If n is sufficiently large ($n > 30$) then $s \approx \sigma$ and $\bar{Z} \sim N(0, 1)$.

5.2.5. Central Limit Theorem

For a set of n independent random variables X_1, X_2, \dots, X_n , each having means and variances $(\mu_1, \sigma_1^2), (\mu_2, \sigma_2^2), \dots, (\mu_n, \sigma_n^2)$, the CLT states that

- The random variable $S_n = \sum_{i=1}^n X_i$ is approximately Normally distributed (weak CLT),
- $\lim_{n \rightarrow \infty} S_n \sim N\left(\sum_{i=1}^n \mu_i, \sum_{i=1}^n \sigma_i^2\right)$ i.e. the approximation is exact as $n \rightarrow \infty$.

If all X_i are i.i.d. with mean μ and variance σ^2 then $\frac{S_n - n\mu}{\sigma\sqrt{n}} \sim N(0, 1)$ as $n \rightarrow \infty$.

These results hold **regardless** of the distribution of X .

The Berry-Esseen Theorem (improved by Shevtsova, 2010) bounds the error in the weak CLT Normal approximation by the value of its CDF (z is the value of standardised S_n):

$$\left| \underbrace{P\left(\frac{\sum_{i=1}^n (X_i - \mu_i)}{\sqrt{\sum_{i=1}^n \sigma_i^2}} \leq z\right)}_{\text{exact CDF at } z} - \underbrace{\frac{1}{\sqrt{2\pi}} \int_{-\infty}^z e^{-x^2/2} dx}_{\text{approximate CDF at } z} \right| \leq \underbrace{0.56 \times \frac{\max_i \{E(|X_i|^3)\}}{\sqrt{n} \cdot \max_i \{\sigma_i^3\}}}_{\text{upper bound for error}}$$

Therefore error $\sim n^{-1/2}$. Practically, the CLT is ‘good’ when the sample size is $n \geq 30$.

5.2.6. Expectation from Probability Density Function

Expectation (mean) of a random variable given PMF or PDF:

$$\text{Discrete: } E[X] = \sum_{x=-\infty}^{\infty} x P(X = x) = \mu \quad \text{Continuous: } E[X] = \int_{-\infty}^{\infty} x f_X(x) dx = \mu$$

Tail formula for nonnegative random variables ($X \geq 0$):

$$\text{Discrete: } E[X] = \sum_{x=0}^{\infty} P(X \geq x) \quad \text{Continuous: } E[X] = \int_0^{\infty} (1 - F_X(x)) dx$$

Law of the Unconscious Statistician (LOTUS theorem): if $Y = g(X)$ then

$$\text{Discrete: } E[Y] = \sum_{x=-\infty}^{\infty} g(x) P(X = x) \quad \text{Continuous: } E[Y] = \int_{-\infty}^{\infty} g(x) f_X(x) dx$$

Variance of a random variable given PMF or PDF and mean (2nd central moment):

$$\text{Discrete: } \text{Var}[X] = \sum_{x=-\infty}^{\infty} (x - \mu)^2 P(X = x) \quad \text{Continuous: } \text{Var}[X] = \int_{-\infty}^{\infty} (x - \mu)^2 f_X(x) dx$$

5.2.7. Moments of Distributions

Moments of a random variable X are defined as:

- **n th raw moment:** $\mu_n' = E[X^n]$
- **n th central moment:** $\mu_n = E[(X - \mu)^n] = \sum_{r=0}^n (-1)^r \binom{n}{r} \mu^r \mu_{n-r}'$
- **n th central moment, standardised:** $\frac{\mu_n}{\sigma^n} = \frac{E[(X - \mu)^n]}{E[(X - \mu)^{2n/2}]}$

Some important moment-related measures are:

- **Mean:** $\mu = E[X] = \mu_1'$ (central tendency)
- **Variance:** $\sigma^2 = \text{Var}[X] = E[X^2] - E[X]^2 = \mu_2$ (spread about the mean)
- **Skewness:** $\gamma = \text{Skew}[X] = \mu_3 / \sigma^3$ (asymmetry)
 $\gamma > 0$: smaller values more likely
 $\gamma < 0$: larger values more likely
- **Kurtosis:** $\kappa = \text{Kurt}[X] = \mu_4 / \sigma^4$ (tailedness / outlier frequency)
- **Excess Kurtosis:** $\bar{\kappa} = \kappa - 3$ (Fisher kurtosis)
 mesokurtic: $\bar{\kappa} = 0$ (Gaussian)
 leptokurtic: $\bar{\kappa} > 0$ (tail-heavy)
 platykurtic: $\bar{\kappa} < 0$ (tail-light)

5.2.8. Generating Functions

For a **discrete** random variable X :

- **Probability generating function (PGF):** $G_X(z) = E[z^X] = \sum_{k=-\infty}^{\infty} P(X = k) z^k$

For any variable X , the PGF is a polynomial in z where the coefficients give the PMF. The PGF is the Z -transform (discretised Mellin transform) of the PMF $P(X = k)$.

For a **continuous** random variable X :

- **Moment generating function (MGF):** $M_X(s) = E[e^{sX}] = \int_{-\infty}^{\infty} f_X(x) e^{sx} dx$

The MGF is the bilateral Laplace transform of $f_X(x)$ (or ordinary LT if X has support $X \geq 0$). The PGF and MGF definitions are related by $z = e^s$.

- **Characteristic function (CF):** $\varphi_X(t) = E[e^{itX}] = \int_{-\infty}^{\infty} f_X(x) e^{ixt} dx$

The CF is the Fourier transform of $f_X(x)$ (signs reversed; using t as the Fourier 'frequency'). The MGF and CF definitions are related by $s = it$ so that $M_X(t) = \varphi_X(-it)$.

Identities with Generating Functions: manipulating random variables

- Shift and scale: $Y = aX + b \Rightarrow M_Y(s) = e^{sb} M_X(as)$
- Sum of RVs: $Y = X_1 + X_2 \Rightarrow G_Y(z) = G_{X_1}(z) G_{X_2}(z); M_Y(s) = M_{X_1}(s) M_{X_2}(s)$
- Difference of RVs: $Y = X_1 - X_2 \Rightarrow G_Y(z) = G_{X_1}(z) G_{X_2}(\frac{1}{z}); M_Y(s) = M_{X_1}(s) M_{X_2}(-s)$
- Joint GF of X, Y : $G_{X,Y}(z, w) = E[z^X w^Y]; M_{X,Y}(s, t) = E[e^{sX+tY}]$
- Marginal GF: $G_X(z) = G_{X,Y}(z, 0); M_X(s) = M_{X,Y}(s, 0)$

Important Quantities (Moments) from the PGF and MGF: see Section 5.2.7 for definitions

The coefficient of z^k in the expansion of the PGF $G_X(z)$ is the PMF of X i.e. $P(X = k)$.

The coefficient of s^n in the expansion of the MGF $M_X(s)$ is proportional to the n th raw moment of X :

$$M_X(s) = \sum_{n=0}^{\infty} \frac{s^n \mu_n'}{n!} \text{ since } \mu_n' = M_X^{(n)}(s)$$

Expectation: $E[X] = M_X'(0) = G_X'(1)$ since $E[X^n] = M_X^{(n)}(0) = G_X^{(n)}(1)$

Variance: $\text{Var}[X] = E[X^2] - E[X]^2$
 $= M_X''(0) - M_X'(0)^2$
 $= G_X''(1) + G_X'(1) - (G_X'(1))^2$

5.2.10. Inverse Transform Sampling

Let U be a uniformly distributed random variable on $0 \leq U \leq 1$. If X is a random variable with cdf or cmf $F_X(x)$, then $X = F_X^{-1}(U)$. This can be used to generate samples with a given pdf or cdf, given a system to generate uniformly distributed random numbers.

To generate RVs with a truncated distribution $a \leq X \leq b$, let $F(a) \leq U \leq F(b)$ and $X = F_X^{-1}(U)$.

5.2.11. Inequalities for the Expectation of Random Variables

- **Markov's Inequality:** $P(X \geq a) \leq \frac{E[X]}{a}$ for nonnegative X i.e. $X \geq 0$
- **Jensen's Inequality:** $E[g(X)] \geq g(E[X])$ for convex functions g i.e. $g''(x) \geq 0$
- **Chebyshev's Inequality:** $P(|X - E[X]| > a) \leq \frac{\text{Var}[X]}{a^2}$ for $a > 0$
- **Minkowski's Inequality:** $(E[|X + Y|^p])^{1/p} \leq (E[|X|^p])^{1/p} + (E[|Y|^p])^{1/p}$ for $p \geq 1$
- **Hölder's Inequality:** $E[|XY|] \leq (E[|X|^p])^{1/p} (E[|Y|^q])^{1/q}$ for $p, q > 1$ with $\frac{1}{p} + \frac{1}{q} = 1$

5.2.12. Distributions of Functions of Random Variables

To find the PDF of Y , $f_Y(y)$, write down $F_Y(y) = P(Y \leq y)$ and let $Y = g(X)$. Solve the resulting inequality for X to write $F_Y(y)$ in terms of $F_X(y)$. Finally, use $f_Y(y) = \frac{dF_Y}{dy}$ and $F_X(x) = \int_{-\infty}^x f_X(x) dx$.

Common functions:

- If $Y = aX + b$ then $f_Y(y) = \frac{1}{a} f_X\left(\frac{y-b}{a}\right)$ where $a > 0$
- If $Y = X^2$ then $f_Y(y) = \frac{f_X(\sqrt{y}) + f_X(-\sqrt{y})}{2\sqrt{y}}$
- If $Y = X^3$ then $f_Y(y) = \frac{1}{3} y^{-2/3} f_X(y^{1/3})$
- If $Y = \sqrt{X}$ then $f_Y(y) = 2y f_X(y^2)$
- If $Y = \min(X, a)$ then $F_Y(y) = F_X(y)$ if $y \leq a$ else 1 ($f_Y(y)$ contains a delta function)
- If $Y = \max(X, a)$ then $F_Y(y) = F_X(y)$ if $y \geq a$ else 0 ($f_Y(y)$ contains a delta function)

For a multivariable function e.g. two RVs, $Y = g(X_1, X_2)$, use (for the CDF):

$$F_Y(y) = \iint_S f_{X_1 X_2}(x_1, x_2) dx_1 dx_2, \quad \text{where } S = \{(x_1, x_2) \in \mathbb{R}^2 : g(x_1, x_2) \leq y\}$$

Common functions:

- If $Y = \max\{X_1, X_2, \dots, X_n\}$ then $F_Y(y) = F_{X_1}(y) F_{X_2}(y) \dots F_{X_n}(y)$ (**parallel system**)
- If $Y = \min\{X_1, X_2, \dots, X_n\}$ then $F_Y(y) = \left(1 - F_{X_1}(y)\right) \left(1 - F_{X_2}(y)\right) \dots \left(1 - F_{X_n}(y)\right)$
(**series system**: models 'weakest link' failure)

5.2.13. Manipulating Independent Random Variables and their Distributions

Let X_1 and X_2 be **independent** random variables. Then:

Linear Transformations (green: also valid when X_1 and X_2 are not independent.)

Transform	$E[Y]$	$Var[Y]$	$f_Y(y)$	$M_Y(s)$
Scale $Y = aX$	$a E[X]$	$a^2 Var[X]$	$\frac{1}{a} f_X\left(\frac{y}{a}\right)$	$M_X(as)$
Scale and Shift $Y = aX + b$	$a E[X] + b$	$a^2 Var[X]$	$\frac{1}{a} f_X\left(\frac{y-b}{a}\right)$	$e^{sb} M_X(as)$
Sum $Y = X_1 + X_2$	$E[X_1] + E[X_2]$	$Var[X_1] + Var[X_2]$	$(f_{X_1} * f_{X_2})(y)$	$M_{X_1}(s) M_{X_2}(s)$

Nonlinear Transformations (all the below require **independence**)

- **Product:** if $Y = X_1 X_2$ then

$$E[Y] = E[X_1] E[X_2]$$

$$Var[Y] = Var[X_1] Var[X_2] + Var[X_1] E[X_2]^2 + Var[X_2] E[X_1]^2$$

The new distribution is $f_Y(y) = \int_{-\infty}^{\infty} f_{X_1}(x) f_{X_2}\left(\frac{y}{x}\right) \frac{1}{|x|} dx$ (product distribution)

- **Ratio:** if $Y = X_1 / X_2$ then

$E[Y]$ can be found by LOTUS, and $Var[Y] = E[X_1^2] E\left[\frac{1}{X_2^2}\right] - E[X_1]^2 E\left[\frac{1}{X_2}\right]^2$.

The new distribution is $f_Y(y) = \int_{-\infty}^{\infty} |x| f_{X_1}(xy) f_{X_2}(x) dx$ (ratio distribution)

Combinations of Common Distributions: for independent random variables,

- If $X_1 \sim N(\mu_1, \sigma_1^2)$ and $X_2 \sim N(\mu_2, \sigma_2^2)$ then $X_1 + X_2 \sim N(\mu_1 + \mu_2, \sigma_1^2 + \sigma_2^2)$.
- If $X_1 \sim Po(\lambda_1)$ and $X_2 \sim Po(\lambda_2)$ then $X_1 + X_2 \sim Po(\lambda_1 + \lambda_2)$.
- If $X_1 \sim B(n_1, p)$ and $X_2 \sim B(n_2, p)$ then $X_1 + X_2 \sim B(n_1 + n_2, p)$.
- If $X \sim B(N, p)$ and $N \sim Po(\lambda)$ then $X \sim Po(p\lambda)$.
- If $X_1 \sim N(0, \sigma^2)$ and $X_2 \sim N(0, \sigma^2)$ then $X_1^2 + X_2^2 \sim Exp\left(\frac{1}{2\sigma^2}\right)$.
- If $X_i \sim N(0, 1)$ then $\sum_{i=1}^N X_i^2 \sim \chi^2_N$ (Chi-Square distribution with N degrees of freedom).
- If $X_1 \sim N(0, \sigma^2)$ and $X_2 \sim N(0, \sigma^2)$ then $\sqrt{X_1^2 + X_2^2} \sim Rayleigh(\sigma)$.

Reciprocal Normal Distribution: if $X \sim N(\mu, \sigma^2)$ and $Y = 1/X$ then $f_Y(y) = \frac{1}{\sqrt{2\pi\sigma^2}} \exp\left(-\frac{(1-\mu y)^2}{2\sigma^2 y^2}\right)$.

5.2.14. Multivariable Probability: Joint and Marginal Distributions

For jointly distributed random variables (X, Y) , let $p(x, y) = f_{XY}(x, y)$ denote the joint pmf if (X, Y) are discrete, or the joint pdf if (X, Y) are jointly continuous. $p(x) = f_X(x)$ is the marginal pmf/pdf of X . $p(x | y) = f_{X|Y}(x | y)$ is the pmf/pdf of X , conditioned on some value of $Y = y$.

- Definition of joint density: $P(a \leq X \leq b \cap c \leq Y \leq d) = \int_c^d \int_a^b p(x, y) dx dy$
- Definition from joint CDF: $p(x, y) = \frac{\partial^2}{\partial x \partial y} F_{XY}(x, y)$ (also written $f_{XY}(x, y)$)
- Conditional PMF / PDF: $p(x | y) = \frac{p(x, y)}{p(y)}$, $p(y) \neq 0$ (also written $f_{X|Y}(x | y)$)
- Bayes' rule: $p(x | y) = \frac{p(y | x) p(x)}{p(y)} = \frac{p(y | x) p(x)}{\sum_x p(x) p(x | y)}$ ($p(x)$: prior distribution)

Independence between random variables $\mathbf{X} = \{X_1, X_2, \dots\}$: (\mathbf{X} is a random vector)

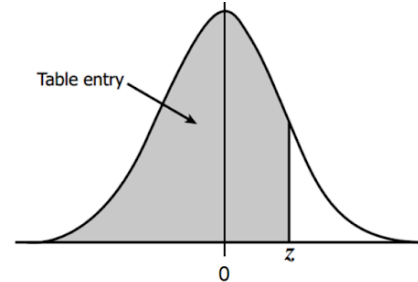
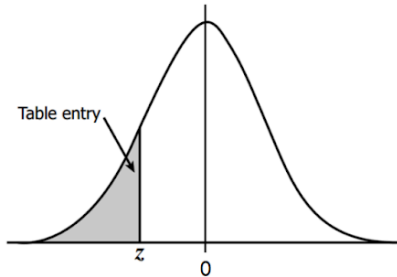
- Conditional independence: $p(x_1, x_2 | y) = p(x_1 | y) p(x_2 | y)$, $p(y) \neq 0$
- Pairwise independence: $p(x_i, x_j) = p(x_i) p(x_j)$ for every pair i, j
- (Mutual) independence: $p(\text{union of all } x_i) = \text{product of all } p(x_i)$ (stronger than pairwise)
- Conditional expectation: $E[X | Y] = \sum_x x p(x | y)$ (= $E[X]$ if independent)
- Linearity of conditionals: $E[(aX + bY) | Z] = a E[X | Z] + b E[Y | Z]$

Quantification of dependence and association:

- Covariance: $\text{Cov}[X, Y] = E[(X - E[X])(Y - E[Y])] = E[XY] - E[X] E[Y]$
- Law of total probability: $p(x) = \sum_y p(x, y)$
- Law of total expectation: $E[X] = E[E[X | Y]]$
- Law of total variance: $\text{Var}[X] = E[\text{Var}[Y | X]] + \text{Var}[E[Y | X]]$
- Law of total covariance: $\text{Cov}[X, Y] = E[\text{Cov}[X, Y | Z]] + \text{Cov}[E[X | Z], E[Y | Z]]$
- Linearity of covariance: $\text{Cov}[aX, Y] = \text{Cov}[X, aY] = a \text{Cov}[X, Y]$, and $\text{Cov}[X + Y, Z] = \text{Cov}[X, Z] + \text{Cov}[Y, Z]$
- Pearson Correlation Coefficient: $\rho_{XY} = \text{Corr}[X, Y] = \frac{\text{Cov}(X, Y)}{\sqrt{\text{Var}(X) \text{Var}(Y)}} = \frac{\text{Cov}(X, Y)}{\sigma_X \sigma_Y}$ (PMCC)
- General variance of sums: $\text{Var}[aX \pm bY + c] = a^2 \text{Var}[X] + b^2 \text{Var}[Y] \pm 2ab \text{Cov}[X, Y]$

5.2.15. Standard Normal Distribution: Critical Values (z table and its Inverse)

The table gives the values of $P(Z \leq z)$ for a given z , with $Z \sim N(0, 1)$. These are left tail probabilities.



z	.00	.01	.02	.03	.04	.05	.06	.07	.08	.09
-3.4	.0003	.0003	.0003	.0003	.0003	.0003	.0003	.0003	.0003	.0002
-3.3	.0005	.0005	.0005	.0004	.0004	.0004	.0004	.0004	.0004	.0003
-3.2	.0007	.0007	.0006	.0006	.0006	.0006	.0006	.0005	.0005	.0005
-3.1	.0010	.0009	.0009	.0009	.0008	.0008	.0008	.0008	.0007	.0007
-3.0	.0013	.0013	.0013	.0012	.0012	.0011	.0011	.0011	.0010	.0010
-2.9	.0019	.0018	.0018	.0017	.0016	.0016	.0015	.0015	.0014	.0014
-2.8	.0026	.0025	.0024	.0023	.0023	.0022	.0021	.0021	.0020	.0019
-2.7	.0035	.0034	.0033	.0032	.0031	.0030	.0029	.0028	.0027	.0026
-2.6	.0047	.0045	.0044	.0043	.0041	.0040	.0039	.0038	.0037	.0036
-2.5	.0062	.0060	.0059	.0057	.0055	.0054	.0052	.0051	.0049	.0048
-2.4	.0082	.0080	.0078	.0075	.0073	.0071	.0069	.0068	.0066	.0064
-2.3	.0107	.0104	.0102	.0099	.0096	.0094	.0091	.0089	.0087	.0084
-2.2	.0139	.0136	.0132	.0129	.0125	.0122	.0119	.0116	.0113	.0110
-2.1	.0179	.0174	.0170	.0166	.0162	.0158	.0154	.0150	.0146	.0143
-2.0	.0228	.0222	.0217	.0212	.0207	.0202	.0197	.0192	.0188	.0183
-1.9	.0287	.0281	.0274	.0268	.0262	.0256	.0250	.0244	.0239	.0233
-1.8	.0359	.0351	.0344	.0336	.0329	.0322	.0314	.0307	.0301	.0294
-1.7	.0446	.0436	.0427	.0418	.0409	.0401	.0392	.0384	.0375	.0367
-1.6	.0548	.0537	.0526	.0516	.0505	.0495	.0485	.0475	.0465	.0455
-1.5	.0668	.0655	.0643	.0630	.0618	.0606	.0594	.0582	.0571	.0559
-1.4	.0808	.0793	.0778	.0764	.0749	.0735	.0721	.0708	.0694	.0681
-1.3	.0968	.0951	.0934	.0918	.0901	.0885	.0869	.0853	.0838	.0823
-1.2	.1151	.1131	.1112	.1093	.1075	.1056	.1038	.1020	.1003	.0985
-1.1	.1357	.1335	.1314	.1292	.1271	.1251	.1230	.1210	.1190	.1170
-1.0	.1587	.1562	.1539	.1515	.1492	.1469	.1446	.1423	.1401	.1379
-0.9	.1841	.1814	.1788	.1762	.1736	.1711	.1685	.1660	.1635	.1611
-0.8	.2119	.2090	.2061	.2033	.2005	.1977	.1949	.1922	.1894	.1867
-0.7	.2420	.2389	.2358	.2327	.2296	.2266	.2236	.2206	.2177	.2148
-0.6	.2743	.2709	.2676	.2643	.2611	.2578	.2546	.2514	.2483	.2451
-0.5	.3085	.3050	.3015	.2981	.2946	.2912	.2877	.2843	.2810	.2776
-0.4	.3446	.3409	.3372	.3336	.3300	.3264	.3228	.3192	.3156	.3121
-0.3	.3821	.3783	.3745	.3707	.3669	.3632	.3594	.3557	.3520	.3483
-0.2	.4207	.4168	.4129	.4090	.4052	.4013	.3974	.3936	.3897	.3859
-0.1	.4602	.4562	.4522	.4483	.4443	.4404	.4364	.4325	.4286	.4247
-0.0	.5000	.4960	.4920	.4880	.4840	.4801	.4761	.4721	.4681	.4641

z	.00	.01	.02	.03	.04	.05	.06	.07	.08	.09
0.0	.5000	.5040	.5080	.5120	.5160	.5199	.5239	.5279	.5319	.5359
0.1	.5398	.5438	.5478	.5517	.5557	.5596	.5636	.5675	.5714	.5753
0.2	.5793	.5832	.5871	.5910	.5948	.5987	.6026	.6064	.6103	.6141
0.3	.6179	.6217	.6255	.6293	.6331	.6368	.6406	.6443	.6480	.6517
0.4	.6554	.6591	.6628	.6664	.6700	.6736	.6772	.6808	.6844	.6879
0.5	.6915	.6950	.6985	.7019	.7054	.7088	.7123	.7157	.7190	.7224
0.6	.7257	.7291	.7324	.7357	.7389	.7422	.7454	.7486	.7517	.7549
0.7	.7580	.7611	.7642	.7673	.7704	.7734	.7764	.7794	.7823	.7852
0.8	.7881	.7910	.7939	.7967	.7995	.8023	.8051	.8078	.8106	.8133
0.9	.8159	.8186	.8212	.8238	.8264	.8289	.8315	.8340	.8365	.8389
1.0	.8413	.8438	.8461	.8485	.8508	.8531	.8554	.8577	.8599	.8621
1.1	.8643	.8665	.8686	.8708	.8729	.8749	.8770	.8790	.8810	.8830
1.2	.8849	.8869	.8888	.8907	.8925	.8944	.8962	.8980	.8997	.9015
1.3	.9032	.9049	.9066	.9082	.9099	.9115	.9131	.9147	.9162	.9177
1.4	.9192	.9207	.9222	.9236	.9251	.9265	.9279	.9292	.9306	.9319
1.5	.9332	.9345	.9357	.9370	.9382	.9394	.9406	.9418	.9429	.9441
1.6	.9452	.9463	.9474	.9484	.9495	.9505	.9515	.9525	.9535	.9545
1.7	.9554	.9564	.9573	.9582	.9591	.9599	.9608	.9616	.9625	.9633
1.8	.9641	.9649	.9656	.9664	.9671	.9678	.9686	.9693	.9699	.9706
1.9	.9713	.9719	.9726	.9732	.9738	.9744	.9750	.9756	.9761	.9767
2.0	.9772	.9778	.9783	.9788	.9793	.9798	.9803	.9808	.9812	.9817
2.1	.9821	.9826	.9830	.9834	.9838	.9842	.9846	.9850	.9854	.9857
2.2	.9861	.9864	.9868	.9871	.9875	.9878	.9881	.9884	.9887	.9890
2.3	.9893	.9896	.9898	.9901	.9904	.9906	.9909	.9911	.9913	.9916
2.4	.9918	.9920	.9922	.9925	.9927	.9929	.9931	.9932	.9934	.9936
2.5	.9938	.9940	.9941	.9943	.9945	.9946	.9948	.9949	.9951	.9952
2.6	.9953	.9955	.9956	.9957	.9959	.9960	.9961	.9962	.9963	.9964
2.7	.9965	.9966	.9967	.9968	.9969	.9970	.9971	.9972	.9973	.9974
2.8	.9974	.9975	.9976	.9977	.9977	.9978	.9979	.9979	.9980	.9981
2.9	.9981	.9982	.9982	.9983	.9984	.9984	.9985	.9985	.9986	.9986
3.0	.9987	.9987	.9987	.9988	.9988	.9989	.9989	.9989	.9990	.9990
3.1	.9990	.9991	.9991	.9991	.9992	.9992	.9992	.9992	.9993	.9993
3.2	.9993	.9993	.9994	.9994	.9994	.9994	.9994	.9995	.9995	.9995
3.3	.9995	.9995	.9995	.9996	.9996	.9996	.9996	.9996	.9996	.9997
3.4	.9997	.9997	.9997	.9997	.9997	.9997	.9997	.9997	.9997	.9998

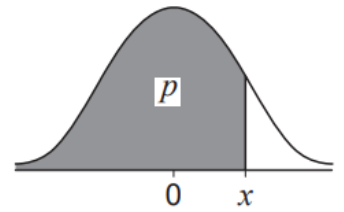
Inverse z Table: $z = \Phi^{-1}(P(Z \leq z))$

$P(Z \leq z)$	0.001	0.005	0.01	0.05	0.1	0.5
z	-3.090232	-2.575829	-2.326347	-1.644854	-1.281552	0

$P(Z \leq z)$	0.9	0.9995	0.95	0.99	0.995	0.999
z	1.281552	3.290527	1.644854	2.326347	2.575829	3.090232

5.2.16. Student's t -Distribution: Critical Values (Inverse t table)

The table gives the values of x satisfying $P(X \leq x) = p$, where X is a random variable having the t distribution with ν degrees of freedom.



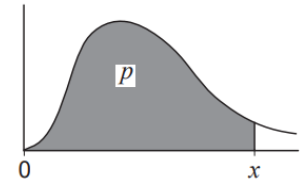
p	0.9	0.95	0.975	0.99	0.995
ν					
1	3.078	6.314	12.706	31.821	63.657
2	1.886	2.920	4.303	6.965	9.925
3	1.638	2.353	3.182	4.541	5.841
4	1.533	2.132	2.776	3.747	4.604
5	1.476	2.015	2.571	3.365	4.032
6	1.440	1.943	2.447	3.143	3.707
7	1.415	1.895	2.365	2.998	3.499
8	1.397	1.860	2.306	2.896	3.355
9	1.383	1.833	2.262	2.821	3.250
10	1.372	1.812	2.228	2.764	3.169
11	1.363	1.796	2.201	2.718	3.106
12	1.356	1.782	2.179	2.681	3.055
13	1.350	1.771	2.160	2.650	3.012
14	1.345	1.761	2.145	2.624	2.977
15	1.341	1.753	2.131	2.602	2.947
16	1.337	1.746	2.121	2.583	2.921
17	1.333	1.740	2.110	2.567	2.898
18	1.330	1.734	2.101	2.552	2.878
19	1.328	1.729	2.093	2.539	2.861
20	1.325	1.725	2.086	2.528	2.845
21	1.323	1.721	2.080	2.518	2.831
22	1.321	1.717	2.074	2.508	2.819
23	1.319	1.714	2.069	2.500	2.807
24	1.318	1.711	2.064	2.492	2.797
25	1.316	1.708	2.060	2.485	2.787
26	1.315	1.706	2.056	2.479	2.779
27	1.314	1.703	2.052	2.473	2.771
28	1.313	1.701	2.048	2.467	2.763

p	0.9	0.95	0.975	0.99	0.995
ν					
29	1.311	1.699	2.045	2.462	2.756
30	1.310	1.697	2.042	2.457	2.750
31	1.309	1.696	2.040	2.453	2.744
32	1.309	1.694	2.037	2.449	2.738
33	1.308	1.692	2.035	2.445	2.733
34	1.307	1.691	2.032	2.441	2.728
35	1.306	1.690	2.030	2.438	2.724
36	1.306	1.688	2.028	2.434	2.719
37	1.305	1.687	2.026	2.431	2.715
38	1.304	1.686	2.024	2.429	2.712
39	1.304	1.685	2.023	2.426	2.708
40	1.303	1.684	2.021	2.423	2.704
45	1.301	1.679	2.014	2.412	2.690
50	1.299	1.676	2.009	2.403	2.678
55	1.297	1.673	2.004	2.396	2.668
60	1.296	1.671	2.000	2.390	2.660
65	1.295	1.669	1.997	2.385	2.654
70	1.294	1.667	1.994	2.381	2.648
75	1.293	1.665	1.992	2.377	2.643
80	1.292	1.664	1.990	2.374	2.639
85	1.292	1.663	1.988	2.371	2.635
90	1.291	1.662	1.987	2.368	2.632
95	1.291	1.661	1.985	2.366	2.629
100	1.290	1.660	1.984	2.364	2.626
125	1.288	1.657	1.979	2.357	2.616
150	1.287	1.655	1.976	2.351	2.609
200	1.286	1.653	1.972	2.345	2.601
∞	1.282	1.645	1.960	2.326	2.576

PDF of the t -distribution:
$$f_t(x; \nu) = \frac{\Gamma\left(\frac{\nu+1}{2}\right)}{\sqrt{\nu\pi}\Gamma\left(\frac{\nu}{2}\right)} \left(1 + \frac{x^2}{\nu}\right)^{-\frac{\nu+1}{2}}$$

5.2.17. Chi-Squared (χ^2) Distribution: Critical Values (Inverse Chi square table)

The table gives the values of x satisfying $P(X \leq x) = p$, where X is a random variable having the χ^2 distribution with ν degrees of freedom.



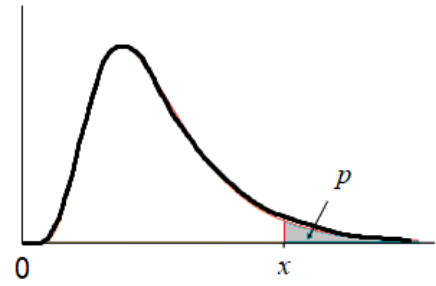
p	0.005	0.01	0.025	0.05	0.1	0.9	0.95	0.975	0.99	0.995	p
ν											ν
1	0.00004	0.0002	0.001	0.004	0.016	2.706	3.841	5.024	6.635	7.879	1
2	0.010	0.020	0.051	0.103	0.211	4.605	5.991	7.378	9.210	10.597	2
3	0.072	0.115	0.216	0.352	0.584	6.251	7.815	9.348	11.345	12.838	3
4	0.207	0.297	0.484	0.711	1.064	7.779	9.488	11.143	13.277	14.860	4
5	0.412	0.554	0.831	1.145	1.610	9.236	11.070	12.833	15.086	16.750	5
6	0.676	0.872	1.237	1.635	2.204	10.645	12.592	14.449	16.812	18.548	6
7	0.989	1.239	1.690	2.167	2.833	12.017	14.067	16.013	18.475	20.278	7
8	1.344	1.646	2.180	2.733	3.490	13.362	15.507	17.535	20.090	21.955	8
9	1.735	2.088	2.700	3.325	4.168	14.684	16.919	19.023	21.666	23.589	9
10	2.156	2.558	3.247	3.940	4.865	15.987	18.307	20.483	23.209	25.188	10
11	2.603	3.053	3.816	4.575	5.578	17.275	19.675	21.920	24.725	26.757	11
12	3.074	3.571	4.404	5.226	6.304	18.549	21.026	23.337	26.217	28.300	12
13	3.565	4.107	5.009	5.892	7.042	19.812	22.362	24.736	27.688	29.819	13
14	4.075	4.660	5.629	6.571	7.790	21.064	23.685	26.119	29.141	31.319	14
15	4.601	5.229	6.262	7.261	8.547	22.307	24.996	27.488	30.578	32.801	15
16	5.142	5.812	6.908	7.962	9.312	23.542	26.296	28.845	32.000	34.267	16
17	5.697	6.408	7.564	8.672	10.085	24.769	27.587	30.191	33.409	35.718	17
18	6.265	7.015	8.231	9.390	10.865	25.989	28.869	31.526	34.805	37.156	18
19	6.844	7.633	8.907	10.117	11.651	27.204	30.144	32.852	36.191	38.582	19
20	7.434	8.260	9.591	10.851	12.443	28.412	31.410	34.170	37.566	39.997	20
21	8.034	8.897	10.283	11.591	13.240	29.615	32.671	35.479	38.932	41.401	21
22	8.643	9.542	10.982	12.338	14.041	30.813	33.924	36.781	40.289	42.796	22
23	9.260	10.196	11.689	13.091	14.848	32.007	35.172	38.076	41.638	44.181	23
24	9.886	10.856	12.401	13.848	15.659	33.196	36.415	39.364	42.980	45.559	24
25	10.520	11.524	13.120	14.611	16.473	34.382	37.652	40.646	44.314	46.928	25
26	11.160	12.198	13.844	15.379	17.292	35.563	38.885	41.923	45.642	48.290	26
27	11.808	12.879	14.573	16.151	18.114	36.741	40.113	43.195	46.963	49.645	27
28	12.461	13.565	15.308	16.928	18.939	37.916	41.337	44.461	48.278	50.993	28
29	13.121	14.256	16.047	17.708	19.768	39.087	42.557	45.722	49.588	52.336	29
30	13.787	14.953	16.791	18.493	20.599	40.256	43.773	46.979	50.892	53.672	30
31	14.458	15.655	17.539	19.281	21.434	41.422	44.985	48.232	52.191	55.003	31
32	15.134	16.362	18.291	20.072	22.271	42.585	46.194	49.480	53.486	56.328	32
33	15.815	17.074	19.047	20.867	23.110	43.745	47.400	50.725	54.776	57.648	33
34	16.501	17.789	19.806	21.664	23.952	44.903	48.602	51.996	56.061	58.964	34
35	17.192	18.509	20.569	22.465	24.797	46.059	49.802	53.203	57.342	60.275	35
36	17.887	19.223	21.336	23.269	25.643	47.212	50.998	54.437	58.619	61.581	36
37	18.586	19.960	22.106	24.075	26.492	48.363	52.192	55.668	59.892	62.883	37
38	19.289	20.691	22.878	24.884	27.343	49.513	53.384	56.896	61.162	64.181	38
39	19.996	21.426	23.654	25.695	28.196	50.660	54.572	58.120	62.428	65.476	39
40	20.707	22.164	24.433	26.509	29.051	51.805	55.758	59.342	63.691	66.766	40
45	24.311	25.901	28.366	30.612	33.350	57.505	61.656	65.410	69.957	73.166	45
50	27.991	29.707	32.357	34.764	37.689	63.167	67.505	71.420	76.154	79.490	50
55	31.735	33.570	36.398	38.958	42.060	68.796	73.311	77.380	82.292	85.749	55
60	35.534	37.485	40.482	43.188	46.459	74.397	79.082	83.298	88.379	91.952	60
65	39.383	41.444	44.603	47.450	50.883	79.973	84.821	89.177	94.422	98.105	65
70	43.275	45.442	48.758	51.739	55.329	85.527	90.531	95.023	100.425	104.215	70
75	47.206	49.475	52.942	56.054	59.795	91.061	96.217	100.839	106.393	110.286	75
80	51.172	53.540	57.153	60.391	64.278	96.578	101.879	106.629	112.329	116.321	80
85	55.170	57.634	61.389	64.749	68.777	102.079	107.522	112.393	118.236	122.325	85
90	59.196	61.754	65.647	69.126	73.291	107.565	113.145	118.136	124.116	128.299	90
95	63.250	65.898	69.925	73.520	77.818	113.038	118.752	123.858	129.973	134.247	95
100	67.328	70.065	74.222	77.929	82.358	118.498	124.342	129.561	135.807	140.169	100

PDF of the Chi-Square distribution:

$$f_{\chi^2}(x; \nu) = \frac{x^{\nu/2-1} e^{-x/2}}{2^{\nu/2} \Gamma(\frac{\nu}{2})}$$

5.3.18. F-Distribution: Critical Values (Inverse F table)

The table gives the values of x satisfying $P(X \geq x) = p$, where X is a random variable having the F distribution formed by $X = \frac{\chi_1^2/\nu_1}{\chi_2^2/\nu_2}$, where χ_1 and χ_2 are χ^2 -distributed with ν_1 and ν_2 degrees of freedom respectively.



degrees of freedom in the numerator, ν_1

		degrees of freedom in the denominator, ν_2									
		p	1	2	3	4	5	6	7	8	9
1	.100	39.86	49.50	53.59	55.83	57.24	58.20	58.91	59.44	59.86	60.19
	.050	161.45	199.50	215.71	224.58	230.16	233.99	236.77	238.88	240.54	241.88
	.025	647.79	799.50	864.16	899.58	921.85	937.11	948.22	956.66	963.28	968.63
	.010	4052.2	4999.5	5403.4	5624.6	5763.6	5859.0	5928.4	5981.1	6022.5	6055.8
	.001	405284	500000	540379	562500	576405	585937	592873	598144	602284	605621
2	.100	8.53	9.00	9.16	9.24	9.29	9.33	9.35	9.37	9.38	9.39
	.050	18.51	19.00	19.16	19.25	19.30	19.33	19.35	19.37	19.38	19.40
	.025	38.51	39.00	39.17	39.25	39.30	39.33	39.36	39.37	39.39	39.40
	.010	98.50	99.00	99.17	99.25	99.30	99.33	99.36	99.37	99.39	99.40
	.001	998.50	999.00	999.17	999.25	999.30	999.33	999.36	999.37	999.39	999.40
3	.100	5.54	5.46	5.39	5.34	5.31	5.28	5.27	5.25	5.24	5.23
	.050	10.13	9.55	9.28	9.12	9.01	8.94	8.89	8.85	8.81	8.79
	.025	17.44	16.04	15.44	15.10	14.88	14.73	14.62	14.54	14.47	14.42
	.010	34.12	30.82	29.46	28.71	28.24	27.91	27.67	27.49	27.35	27.23
	.001	167.03	148.50	141.11	137.10	134.58	132.85	131.58	130.62	129.86	129.25
4	.100	4.54	4.32	4.19	4.11	4.05	4.01	3.98	3.95	3.94	3.92
	.050	7.71	6.94	6.59	6.39	6.26	6.16	6.09	6.04	6.00	5.96
	.025	12.22	10.65	9.98	9.60	9.36	9.20	9.07	8.98	8.90	8.84
	.010	21.20	18.00	16.69	15.98	15.52	15.21	14.98	14.80	14.66	14.55
	.001	74.14	61.25	56.18	53.44	51.71	50.53	49.66	49.00	48.47	48.05
5	.100	4.06	3.78	3.62	3.52	3.45	3.40	3.37	3.34	3.32	3.30
	.050	6.61	5.79	5.41	5.19	5.05	4.95	4.88	4.82	4.77	4.74
	.025	10.01	8.43	7.76	7.39	7.15	6.98	6.85	6.76	6.68	6.62
	.010	16.26	13.27	12.06	11.39	10.97	10.67	10.46	10.29	10.16	10.05
	.001	47.18	37.12	33.20	31.09	29.75	28.83	28.16	27.65	27.24	26.92
6	.100	3.78	3.46	3.29	3.18	3.11	3.05	3.01	2.98	2.96	2.94
	.050	5.99	5.14	4.76	4.53	4.39	4.28	4.21	4.15	4.10	4.06
	.025	8.81	7.26	6.60	6.23	5.99	5.82	5.70	5.60	5.52	5.46
	.010	13.75	10.92	9.78	9.15	8.75	8.47	8.26	8.10	7.98	7.87
	.001	35.51	27.00	23.70	21.92	20.80	20.03	19.46	19.03	18.69	18.41
7	.100	3.59	3.26	3.07	2.96	2.88	2.83	2.78	2.75	2.72	2.70
	.050	5.59	4.74	4.35	4.12	3.97	3.87	3.79	3.73	3.68	3.64
	.025	8.07	6.54	5.89	5.52	5.29	5.12	4.99	4.90	4.82	4.76
	.010	12.25	9.55	8.45	7.85	7.46	7.19	6.99	6.84	6.72	6.62
	.001	29.25	21.69	18.77	17.20	16.21	15.52	15.02	14.63	14.33	14.08
8	.100	3.46	3.11	2.92	2.81	2.73	2.67	2.62	2.59	2.56	2.54
	.050	5.32	4.46	4.07	3.84	3.69	3.58	3.50	3.44	3.39	3.35
	.025	7.57	6.06	5.42	5.05	4.82	4.65	4.53	4.43	4.36	4.30
	.010	11.26	8.65	7.59	7.01	6.63	6.37	6.18	6.03	5.91	5.81
	.001	25.41	18.49	15.83	14.39	13.48	12.86	12.40	12.05	11.77	11.54
9	.100	3.36	3.01	2.81	2.69	2.61	2.55	2.51	2.47	2.44	2.42
	.050	5.12	4.26	3.86	3.63	3.48	3.37	3.29	3.23	3.18	3.14
	.025	7.21	5.71	5.08	4.72	4.48	4.32	4.20	4.10	4.03	3.96
	.010	10.56	8.02	6.99	6.42	6.06	5.80	5.61	5.47	5.35	5.26
	.001	22.86	16.39	13.90	12.56	11.71	11.13	10.70	10.37	10.11	9.89
10	.100	3.29	2.92	2.73	2.61	2.52	2.46	2.41	2.38	2.35	2.32
	.050	4.96	4.10	3.71	3.48	3.33	3.22	3.14	3.07	3.02	2.98
	.025	6.94	5.46	4.83	4.47	4.24	4.07	3.95	3.85	3.78	3.72
	.010	10.04	7.56	6.55	5.99	5.64	5.39	5.20	5.06	4.94	4.85
	.001	21.04	14.91	12.55	11.28	10.48	9.93	9.52	9.20	8.96	8.75

PDF of the F -distribution:

$$f_F(x; \nu_1, \nu_2) = \frac{1}{B\left(\frac{\nu_1}{2}, \frac{\nu_2}{2}\right)} \left(\frac{\nu_1}{\nu_2}\right)^{\nu_1/2} x^{\nu_1/2-1} \left(1 + \frac{\nu_1}{\nu_2}x\right)^{-\frac{\nu_1+\nu_2}{2}} \quad 163$$

5.2.19. Product Moment Correlation Coefficient (PMCC): Critical Values (Inverse rho table)

The table gives the critical values, for different significance levels, of the Pearson's product moment correlation coefficient (PMCC), ρ , for varying sample sizes, n .

One tail Two tail	10% 20%	5% 10%	2.5% 5%	1% 2%	0.5% 1%	One tail Two tail
<i>n</i>						<i>n</i>
4	0.8000	0.9000	0.9500	0.9800	0.9900	4
5	0.6870	0.8054	0.8783	0.9343	0.9587	5
6	0.6084	0.7293	0.8114	0.8822	0.9172	6
7	0.5509	0.6694	0.7545	0.8329	0.8745	7
8	0.5067	0.6215	0.7067	0.7887	0.8343	8
9	0.4716	0.5822	0.6664	0.7498	0.7977	9
10	0.4428	0.5494	0.6319	0.7155	0.7646	10
11	0.4187	0.5214	0.6021	0.6851	0.7348	11
12	0.3981	0.4973	0.5760	0.6581	0.7079	12
13	0.3802	0.4762	0.5529	0.6339	0.6835	13
14	0.3646	0.4575	0.5324	0.6120	0.6614	14
15	0.3507	0.4409	0.5140	0.5923	0.6411	15
16	0.3383	0.4259	0.4973	0.5742	0.6226	16
17	0.3271	0.4124	0.4821	0.5577	0.6055	17
18	0.3170	0.4000	0.4683	0.5425	0.5897	18
19	0.3077	0.3887	0.4555	0.5285	0.5751	19
20	0.2992	0.3783	0.4438	0.5155	0.5614	20
21	0.2914	0.3687	0.4329	0.5034	0.5487	21
22	0.2841	0.3598	0.4227	0.4921	0.5368	22
23	0.2774	0.3515	0.4132	0.4815	0.5256	23
24	0.2711	0.3438	0.4044	0.4716	0.5151	24
25	0.2653	0.3365	0.3961	0.4622	0.5052	25
26	0.2598	0.3297	0.3882	0.4534	0.4958	26
27	0.2546	0.3233	0.3809	0.4451	0.4869	27
28	0.2497	0.3172	0.3739	0.4372	0.4785	28
29	0.2451	0.3115	0.3673	0.4297	0.4705	29
30	0.2407	0.3061	0.3610	0.4226	0.4629	30
31	0.2366	0.3009	0.3550	0.4158	0.4556	31
32	0.2327	0.2960	0.3494	0.4093	0.4487	32
33	0.2289	0.2913	0.3440	0.4032	0.4421	33
34	0.2254	0.2869	0.3388	0.3972	0.4357	34
35	0.2220	0.2826	0.3338	0.3916	0.4296	35
36	0.2187	0.2785	0.3291	0.3862	0.4238	36
37	0.2156	0.2746	0.3246	0.3810	0.4182	37
38	0.2126	0.2709	0.3202	0.3760	0.4128	38
39	0.2097	0.2673	0.3160	0.3712	0.4076	39
40	0.2070	0.2638	0.3120	0.3665	0.4026	40
41	0.2043	0.2605	0.3081	0.3621	0.3978	41
42	0.2018	0.2573	0.3044	0.3578	0.3932	42
43	0.1993	0.2542	0.3008	0.3536	0.3887	43
44	0.1970	0.2512	0.2973	0.3496	0.3843	44
45	0.1947	0.2483	0.2940	0.3457	0.3801	45
46	0.1925	0.2455	0.2907	0.3420	0.3761	46
47	0.1903	0.2429	0.2876	0.3384	0.3721	47
48	0.1883	0.2403	0.2845	0.3348	0.3683	48
49	0.1863	0.2377	0.2816	0.3314	0.3646	49
50	0.1843	0.2353	0.2787	0.3281	0.3610	50
60	0.1678	0.2144	0.2542	0.2997	0.3301	60
70	0.1550	0.1982	0.2352	0.2776	0.3060	70
80	0.1448	0.1852	0.2199	0.2597	0.2864	80
90	0.1364	0.1745	0.2072	0.2449	0.2702	90
100	0.1292	0.1654	0.1966	0.2324	0.2565	100

5.3. Hypothesis Testing

5.3.1. Decision and Estimation Theory

Definitions:

- For a set of i iid observations $\mathbf{x} = [x_1, x_2, \dots, x_i]$ of a random variable $\mathbf{X} = [X_1, X_2, \dots, X_i]$, the distribution of each X_i depends on x and some unknown parameter(s) θ .
- The estimate (decision) for θ is a function of the observations: $\hat{\theta}(\mathbf{x})$.
- The estimator (decision rule) for a parameter θ is given by $\hat{\Theta} = \hat{\theta}(\mathbf{X})$.

5.3.2. Bayesian Statistics

In Bayesian statistics, the unknown parameter θ is viewed as the value of a random variable Θ . The distribution of the sample is then interpreted as the conditional distribution $f_{\mathbf{X}|\Theta}(\mathbf{x} | \theta)$.

- Prior function: $f_{\Theta}(\theta)$ (prior to any measurements)
- Likelihood function: $f_{\mathbf{X}|\Theta}(\mathbf{x} | \theta)$.
- Posterior function: $f_{\Theta|\mathbf{X}}(\theta | \mathbf{x})$ (after the measurements)

5.3.3. Estimator Metrics

Maximum likelihood estimator (ML): $\hat{\theta}_{\text{ML}}(\mathbf{x}) = \underset{\theta}{\operatorname{argmax}} f_{\mathbf{X}|\Theta}(\mathbf{x}|\theta)$

Maximum a posteriori estimator (MAP): $\hat{\theta}_{\text{MAP}}(\mathbf{x}) = \underset{\theta}{\operatorname{argmax}} f_{\Theta|\mathbf{X}}(\theta|\mathbf{x})$

Minimum mean squared error (MMSE): $\hat{\theta}_{\text{MMSE}}(\mathbf{x}) = \mathbb{E}[\Theta|\mathbf{X} = \mathbf{x}] = \int \theta f_{\Theta|\mathbf{X}}(\theta|\mathbf{x}) d\theta$
which minimises the value of $\mathbb{E}[(\theta - \Theta)^2|\mathbf{X} = \mathbf{x}]$.

The posterior function is obtained from Bayes' rule (see Section 5.2.9) as

$$f_{\Theta|\mathbf{X}}(\theta|\mathbf{x}) = \frac{f_{\mathbf{X}|\Theta}(\mathbf{x}|\theta) \cdot f_{\Theta}(\theta)}{f_{\mathbf{X}}(\mathbf{x})}.$$

Note that if $f_{\Theta}(\theta) = \text{constant}$ (i.e. Θ is uniformly distributed) then $\hat{\theta}_{\text{ML}} = \hat{\theta}_{\text{MAP}}$.

5.3.4. Principles of Hypothesis Testing

Hypothesis testing involves assessing the probability of observing a given dataset, given the assumption of a particular null hypothesis (H_0).

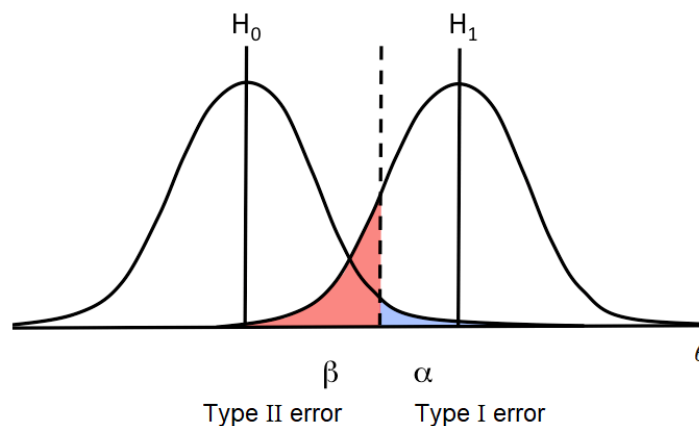
Alternative hypothesis (H_1): a potential alternative statement to explain a dataset, attributed to an external effect influencing the data.

- p-value (p): the probability of obtaining a result at least as extreme as the given data, under the assumption that H_0 is true.
- $p = P(\text{data or further from } H_0 \mid H_0)$. The p-value is **not** the probability of H_0 .
- Significance level (α): if $p \leq \alpha$, the result is unlikely to happen under H_0 so we reject H_0 and the result is said to be statistically significant.

Analysis of a Hypothesis Test

If H_1 is of the form $\theta \neq a$, the p-value must be found on the basis of a two-tailed test in which the critical region is central to the distribution of θ under H_0 i.e. use an effective significance level of $\alpha/2$ in each tail.

The diagram illustrates the conditional distributions $f_{\theta}(\theta \mid H_0)$ and $f_{\theta}(\theta \mid H_1)$.



- **Type I error:** falsely **rejecting** H_0 when in reality, H_0 is true ($\alpha = P(\text{reject } H_0 \mid H_0)$)
- **Type II error:** falsely **accepting** H_0 when in reality, H_1 is true ($\beta = P(\text{accept } H_0 \mid H_1)$)
- **Critical (rejection) region** under H_0 : $\theta \geq \theta^*$ such that $P(\theta \geq \theta^* \mid H_0) \leq \alpha$
- **Power** of a test = $1 - \beta$

5.3.5. Specified Distribution Hypothesis Tests

After sampling a random variable X , a test can be performed to investigate whether the sample is expected under a particular null hypothesis distribution. Commonly used for Binomial, Normal...

Assumptions: all assumptions made by the underlying distribution being proposed.

The p -value is the probability of observing the sample **or more extreme** given the null hypothesis.

Example (Binomial): a coin is flipped 16 times and lands tails 11 times. Investigate at 5% significance whether the coin is fair or biased. Find the power of the test if the true probability of tails is 0.6.

- Assume that the number of tails X is binomially distributed as $X \sim B(16, p)$ (independent trials, binary outcomes, constant probability of success p).
- $H_0: p = 0.5$ (the coin is unbiased / fair).
- $H_1: p \neq 0.5$ (the coin is biased / unfair) (two-tailed test).
- Under H_0 , $X \sim B(16, 0.5)$. The test statistic is $X = 11$.
- $P(X \geq 11 | H_0) = 0.1051$ (p -value).
- Since $0.1051 > 0.025$ (half the significance level), we accept H_0 .
- There is insufficient evidence to suggest that the coin is biased.
- Critical region: $X \geq 13$ and $X \leq 3$, Acceptance region: $4 \leq X \leq 12$. Critical values: 3 and 13.
- $P(\text{Type I error}) = 0.05$ (significance level).
- $P(\text{Type II error} | \text{true } p = 0.6) = P(\text{accept } H_0 | p = 0.6) = P(4 \leq X \leq 12 | p = 0.6) = 0.9339$.
- Power of the test = $1 - 0.9339 = 0.0661$.

Example (Normal): a particular make and model of car is known to have an average fuel mileage of 25.0 miles per gallon (mpg) with variance 6.1 mpg². When a new additive is added to the fuel of 35 cars, their mean mileage rises to 25.9 mpg. Test at 5% significance whether the additive increased the mean mileage, and construct a 99% confidence interval for the population mean mileage with the additive.

- Assume that the mileage X is Normally distributed as $X \sim N(\mu, 6.1)$.
- $H_0: \mu = 25$ (the mileage has not increased).
- $H_1: \mu > 25$ (the mileage has increased).
- Under H_0 , $X \sim N(25, 6.1)$ and therefore the sample mean $\bar{X} \sim N(25, \frac{6.1}{35}) = N(25, 0.1743)$.
- $p = P(\bar{X} > 25.9 | H_0) = 0.0156$ (or using z -statistic: $z = \frac{25.9 - 25}{\sqrt{0.1743}} = 2.1557 \rightarrow p = 1 - \Phi(z) = 0.0156$)
- Since $0.0156 < 0.05$ (significance level), we reject H_0 .
- There is sufficient evidence to suggest the population mean mileage has increased.
- Critical region: $z > \Phi^{-1}(0.95) \rightarrow z > 1.6449 \rightarrow \bar{X} > 25 + 1.6449 \times \sqrt{0.1743} \rightarrow \bar{X} > 25.6867$.
Acceptance region: $\bar{X} < 25.6867$. Critical value: 25.6867.
- $P(\text{Type I error}) = 0.05$ (significance level).
- 99% confidence interval for new mean: $z = \Phi^{-1}(0.995) = 2.5758$
 $\rightarrow \mu \in (25.9 - 2.5758\sqrt{0.1743}, 25.9 + 2.5758\sqrt{0.1743}) \rightarrow \mu \in (24.8246, 26.9754)$.
This interval captures the true mean mileage with fuel additives with 99% confidence.

5.3.6. Chi-Square Tests

Chi-Square Test for Goodness of Fit or Association

A Chi-Square (χ^2) test can be performed to investigate whether a discrete categorical random variable X obeys a particular distribution, or for association between two categorical variables X and Y (a non-parametric test).

H_0 : there is no association between X and Y

H_1 : there is an association between X and Y

Degrees of freedom for an $a \times b$ observed contingency table O : $v = (a - 1)(b - 1)$

Expected value under H_0 (no association): $E_{ij} = \frac{(\text{row total})_i \times (\text{column total})_j}{\text{grand total}}$

Test statistic: $\chi^2 = \sum_{i,j} \frac{(O_{ij} - E_{ij})^2}{E_{ij}}$

Critical value, χ^2_c , found from the table in Section 5.2.12.

If $\chi^2 < \chi^2_c$ then we accept H_0 (evidence to suggest independence)

If $\chi^2 > \chi^2_c$ then we reject H_0 (evidence to suggest association)

Modifications to the test methodology include:

- Pooling: if observed frequencies are less than 5, rows / columns should be combined.
- Yates' continuity correction: if the contingency table is 2×2 (1 degree of freedom) and at least one frequency is less than 5 (and so cannot be pooled), the test statistic is

$$\chi^2_{Yates} = \sum_{i,j} \frac{(|O_{ij} - E_{ij}| - 0.5)^2}{E_{ij}}$$

Yates' correction is not universally accepted. Applying it decreases the test statistic, increases the p-value and increases the probability of a type II error.

Software implementations:

Python: `scipy.stats.chisquare(f_obs, f_exp=None)`

R: `chisq.test(data) # `correct=False` to disable Yates`

Excel: `=CHITEST(obs_range, exp_range)`

Chi-Square Test for Variance

After sampling a random variable X , a Chi-Square (χ^2) test can be performed to investigate whether X has a given population variance.

$H_0: \sigma^2_X = a^2$

$H_1: \sigma^2_X \neq a^2$ (two tailed test) or $\sigma^2_X < a^2$ or $\sigma^2_X > a^2$ (one tailed test).

Test statistic: $\chi^2 = \frac{(N - 1) s^2}{a^2}$ (s^2 : sample variance)

Critical value, χ^2_c , found from the table in Section 5.2.12.

If $\chi^2 < \chi^2_c$ then we accept H_0 ; If $\chi^2 > \chi^2_c$ then we reject H_0

5.3.7. Inferential Parametric Tests: t -Tests and Analysis of Variance (ANOVA)

One-Sample t -Test for the Mean of a Normal Distribution

One sample, Normal distribution, unknown variance. $H_0: \mu = a$; $H_1: \mu \neq a$ (if two-tail).

Test statistic: $t = \frac{\bar{x} - a}{S/\sqrt{n}}$ (\bar{x} : sample mean, S : sample std.dev, n : sample size)

The test statistic has a t -distribution with $\nu = n - 1$ degrees of freedom.

Critical values in table in Section 5.2.16.

Student's Two-Sample t -Test for Independent Means of Homoscedastic Normal Distributions

Two samples A and B , Normal distributions, equal variance. $H_0: \mu_A = \mu_B$; $H_1: \mu_A \neq \mu_B$ (if two-tail)

Test statistic: $t = \frac{\bar{x}_A - \bar{x}_B}{\sqrt{\frac{S^2}{n_A} + \frac{S^2}{n_B}}}$ ($\bar{x}_A = \frac{\sum x_i}{n_A}$: sample mean of A , $S^2 = \frac{\sum(x_i - \bar{x}_A)^2 + \sum(x_j - \bar{x}_B)^2}{n_A + n_B - 2}$: pooled sample variance)

The test statistic has a t -distribution with $\nu = n_A + n_B - 2$ degrees of freedom.

Critical values in table in Section 5.2.16.

Welch's Two-Sample t -Test for Independent Means of Heteroscedastic Normal Distributions

Two samples A and B , Normal distributions, unequal variance. $H_0: \mu_A = \mu_B$; $H_1: \mu_A \neq \mu_B$ (if two-tail)

Test statistic: $t = \frac{\bar{x}_A - \bar{x}_B}{\sqrt{\frac{S_A^2}{n_A} + \frac{S_B^2}{n_B}}}$. The test statistic has a t -distribution with $\nu = \frac{\left(\frac{S_A^2}{n_A} + \frac{S_B^2}{n_B}\right)^2}{\frac{S_A^4}{n_A^2(n_A-1)} + \frac{S_B^4}{n_B^2(n_B-1)}}$ dof.

Critical values in table in Section 5.2.16.

Fisher's ANOVA Test for Independent Means of Homoscedastic Normal Distributions

N variables $\{X_j\}_i$ (i th observation of X_j , $1 \leq j \leq N$), Normal distributions, equal variance. H_0 : all μ_i equal; H_1 : not all μ_i equal.

Test statistic: $F = \frac{S_{between}^2}{S_{within}^2}$ ($S_{between}^2 = \frac{\sum_j (\bar{X}_j - \bar{X})^2}{\left(\sum_j n_j\right) - N}$, $S_{within}^2 = \frac{\sum_{j,i} (X_{ji} - \bar{X}_j)^2}{N - 1}$)

The test statistic has an F -distribution with $\nu_1 = \left(\sum_j n_j\right) - N$ and $\nu_2 = N - 1$ degrees of freedom.

Critical values in table in Section 5.2.18. **Post-hoc analysis:** Tukey's range test.

Welch's ANOVA Test for Independent Means of Heteroscedastic Normal Distributions

N variables $\{X_j\}_i$ (i th observation of X_j , $1 \leq j \leq N$), Normal distributions, unequal variance. H_0 : all μ_i equal; H_1 : not all μ_i equal.

Test statistic: $F = \frac{S_{between}^2}{S_{within}^2}$ ($S_{between}^2 = \frac{\sum_j \frac{n_j}{s_j^2} \left(\bar{X}_j - \frac{\sum_j \frac{n_j \bar{X}_j}{s_j^2}}{\sum_j \frac{n_j}{s_j^2}} \right)^2}{N - 1}$, $S_{within}^2 = 1 + \frac{2(N-2)}{N^2-1} T$, $T = \sum_j \frac{1}{n_j - 1} \left(1 - \frac{\frac{n_j}{s_j^2}}{\sum_j \frac{n_j}{s_j^2}} \right)^2$)

The test statistic has an F -distribution with $\nu_1 = N - 1$ and $\nu_2 = \frac{N^2 - 1}{3T}$ degrees of freedom.

Critical values in table in Section 5.2.18. **Post-hoc analysis:** Games-Howell test.

5.3.8. Other Inferential Hypothesis Tests

Mann-Whitney U -Test (Wilcoxon Rank Sum Test)

Two samples A and B , unknown distributions. H_0 : A and B from same distributions; H_1 : A and B from different distributions.

Kruskal-Wallis H -Test (Non-Parametric One-Way ANOVA)

N variables $\{X_j\}_i$ (i th observation of X_j , $1 \leq j \leq N$), unknown distributions. H_0 : all distributions equal; H_1 : not all distributions equal. Post-hoc analysis: Dunn's test or Conover-Iman test.

Shapiro-Wilk Test for Normality

One sample X , unknown distribution. H_0 : X has a Normal distribution, H_1 : X does not have a Normal distribution.

Pearson's Test for Linear Correlation

Paired (bivariate) dataset $\mathbf{X} = \{X, Y\}$, Normal joint distribution. H_0 : X and Y are uncorrelated, H_1 : X and Y are correlated.

Test statistic: Pearson's PMCC:

Critical values in table in Section 5.2.19.

$$r_{xy} = \frac{\sum_{i=1}^n (x_i - \bar{x})(y_i - \bar{y})}{\sqrt{\sum_{i=1}^n (x_i - \bar{x})^2} \sqrt{\sum_{i=1}^n (y_i - \bar{y})^2}}, \quad |r_{xy}| \leq 1.$$

Spearman's Rank-Order Test for Monotonic Correlation

Paired (bivariate) dataset $\mathbf{X} = \{X, Y\}$, unknown distributions. H_0 : X and Y are uncorrelated, H_1 : X and Y are correlated.

Test statistic: Spearman's rho,

Similar alternative: Kendall's Tau Test.

$$\rho = 1 - \frac{6 \sum d_i^2}{n(n^2 - 1)} \quad (d_i: \text{rank difference of observation } i) \\ \text{rank is the index in the ordered list.}$$

Levene's Test for Homoscedasticity (Equal Variances)

N variables $\{X_j\}_i$ (i th observation of X_j , $1 \leq j \leq N$), unknown distributions. H_0 : all distributions equal; H_1 : not all distributions equal. Post-hoc analysis: Dunn's test or Conover-Iman test.

Similar alternative: Brown-Forsythe test.

Cohen's d Statistic for Mean Effect Size

The d metric is related to the t -statistic in testing for independent means by $d = \sqrt{\frac{1}{N_1} + \frac{1}{N_2}} \times t$.

It is typically used in the context of quantifying the effect size of a test group against a control group.

Egger's Regression Test for Intervention Effects

For a collection of univariate datasets, a funnel plot is made of standard error σ_x / \sqrt{N} against a measure of effect size: depending on context, this may be a raw mean value, a correlation coefficient, odds ratio, or Cohen's d metric. One point is made per dataset. H_0 : funnel plot regression line is vertical (implies no bias), H_1 : funnel plot regression line is sloped (implies bias). Egger's test is commonly used in meta-analyses to test for publication bias.

5.3.9. Common Fallacies in Statistical Inference, Interpretation and Discourse

Interpretation of Statistical Tests: issues arising when concluding and communicating.

- **Texas Sharpshooter:** the cherry-picking of a cluster of data to fit a conclusion, or asserting that a pattern has an underlying cause other than randomness. A related concept in data misuse is 'p-hacking', in which the same (or slightly modified) tests are conducted on the same dataset until statistical significance is found (the multiple comparisons problem).
- **False Cause:** asserting that correlation implies causation, rather than randomness or a common cause.
- **Gambler's Fallacy:** assuming that the outcome of an event occurring after a series of the event has already been observed is lower than observing the event in general, when in fact they are independent.
- **Prosecutor's Fallacy:** assuming that the probability of observing an outcome given some evidence is the same as the probability of observing the evidence given the outcome.
- **Composition Fallacy:** assuming that the properties of the parts of a system completely determine those of the whole system, when they may be different (e.g. interaction effects, 'emergent properties').
- **Slippery Slope:** asserting that if one event happens, then a subsequent chain of events will also happen, without clearly establishing the validity of these links.
- **Begging the Question:** presenting a circular argument; presupposing the conclusion within the premise.
- **Ambiguity:** using language with multiple meanings, from which readers from different target audiences may interpret in different ways. Can occur when using terms of art.
- **Confirmation Bias:** favouring arguments and evidence which align with a person's existing beliefs while downplaying opposing evidence, regardless of its merit.
- **Post-hoc Rationalisation:** constructing (often improvised) arguments to justify behaviour or beliefs that are otherwise incompatible with one's beliefs. Often used when one is experiencing 'cognitive dissonance', in which a person simultaneously supports two logically irreconcilable beliefs, sometimes without being consciously aware of it. Also used to justify hypocrisy.

Methodology of Experiments and Studies: issues arising when conducting a study.

- **Loaded Question:** posing a question with a strong built-in bias towards a known outcome, which can hamper the validity of the testing methodology.
- **Survivorship Bias:** the sample under study may be self-selecting, making the results unrepresentative.
- **Observer Effect:** subjects under study may alter their behaviour if they know they are under study, in captivity, or respond differently depending on who is studying them.
- **Placebo Effect:** common in medicine. If subjects are told they can expect to see an effect from taking a treatment, they may genuinely experience the effect, even if the treatment itself does nothing.
- **Replication Crisis:** the observation that many studies, particularly in the social sciences which study complex population-level interactions, can often not be reproduced precisely. However, this does not imply the results are always invalid, rather, if different studies can investigate hypotheses from different perspectives and come to similar conclusions (triangulation), it implies that there is a deeper effect at play. Neglecting this nuance and extrapolating it to where it does not apply can lead to undue public distrust in the scientific method and the body of science as a whole.
- **Confounding variables:** factors which may influence a study but were not controlled for, either because they were not considered when the study was conducted or the control measures taken were inadequate to suppress their influence.

Argumentation and Discourse: logical fallacies and rhetorical techniques.

- **Strawman:** misrepresenting a statement in order to make it easier to argue against.
- **Anecdotes:** personal experiences or isolated incidents are statistically meaningless (typically $n \sim 1$ sample size) but are often far more compelling due to their tangibility or use of emotive language.
- **Appeal to Authority:** claims made by a perceived authority should not be considered valid based solely on their status of authority, but rather the rigorousness of their investigative methodology and access to empirical evidence e.g. peer-reviewed scientific literature.
- **Bandwagon:** the validity of a claim is not inherently dependent on how popular the claim is.
- **False Dichotomy:** asserting that there are only two possible outcomes (binary decision), when there may be more than two. The reverse of this is assuming a middle ground in a *true* dichotomy.
- **Non Sequitur:** any statement that can be demonstrated to be formally illogical or self-contradictory.
- **Slander / Libel:** public defamation by making false statements aimed at damaging one's reputation.
- **Burden of Proof:** the burden of proof lies with the individual making the claim against the current consensus i.e. what is presented without evidence can be dismissed without evidence. This is sometimes referred to as '(dis)proof beyond reasonable doubt'. If there is no current consensus, then all sides have a burden of proof.
- **Argumentum Ad Hominem:** attempting to discredit an opposing view by attacking irrelevant qualities of the person (whether true or false) who holds that view, without attacking the view itself.
- **Gish Gallop:** presenting a large number of claims in a short amount of time, making it seem as if one has an endless list of strong arguments, without allowing time to respond, and without explaining anything that could reveal that the arguments are not independent and/or strong.
- **Tu Quoque (Whataboutism):** claiming that one's opponent is a hypocrite because they committed the same act that one is being accused of, without actually defending oneself against the accusation. Whataboutism is the general propagandistic tactic of diverting attention to another scenario, without elaborating on whether such a comparison is valid to make.
- **Motte and Bailey Fallacy:** presenting a more outlandish (less well-supported) claim before falling back to a more well-established claim once it is criticised, and implying they use the same reasoning.
- **Socratic Method:** the use of open-ended questions and well-defined terminology to promote a non-confrontational discussion where opinionated people can reflect on their own perspectives. It can challenge presuppositions and expose unrealised self-contradictions.
- **Hegel's Dialectics:** presenting an initial idea (thesis), a contradictory idea (antithesis) and a higher-level resolution that integrates ideas discussed in each (synthesis).

5.3.10. The Scientific Method

The scientific method is the empirical process of reliably acquiring new knowledge about the natural world.

1. **Question:** identify something in the natural world, and ask a question about it.
2. **Fact-Finding:** consult existing scientific literature to research the topic at hand. Gather preliminary information that will be useful in studying the topic.
3. **Hypothesis:** formulate a potential explanation or answer to the question based on initial knowledge gained.
4. **Predictions:** before investigations begin, make testable, falsifiable predictions as to what the expected outcome would be if the hypothesis put forward is correct.
5. **Test:** design an experiment to investigate the question. Conduct the experiment in a safe, ethical and reproducible manner to investigate the question and record all observations.
6. **Analysis:** process the results to obtain useful data. If appropriate, perform statistical tests to quantify the likelihood of these results under a null and alternative hypothesis.
7. **Interpretations:** draw conclusions from the data analysis. These conclusions may serve as the starting point for new investigations.

Writing Scientific Literature:

For experimental work, the paper should outline the ‘story’ of how the topic is introduced:

1) abstract (succinct statement of the problem, approach and results), **2) introduction**, **3) materials and methods**, **4) results and discussion**, **5) conclusions**, **6) references** (from existing primary scientific literature, cited in a standard style). Sections are field-dependent.

Submit the work conducted in the form of a paper to a peer-reviewed journal. Designate a ‘corresponding author’ who can be contacted to answer questions about the work. When in proceedings, respond to suggestions and criticism from peer-reviewers and be open to assisting others in replicating your work.

Reading Scientific Literature:

An often useful approach when researching a topic comprehensively is to find a ‘review’ paper of the topic via Google Scholar. For papers, read: 1) abstract, 2) look at the figures, 3) conclusions, 4) the rest of the paper, 5) search for author’s discussions of their work in other sources. If seeking to examine methodology, check for any supplementary materials.

5.4. Stochastic Processes, Signals and Information Theory

5.4.1. Identities for Random Vectors

$$\mathbf{X} = \{X_1 \ X_2 \ \dots\}$$

These identities hold when X_i are scalar RVs. If X_i are n -vectors, then variances should be divided by $\frac{1}{n}$ for population quantities and by $\frac{1}{n-1}$ for sample quantities (as in Section 5.4.1).

- Covariance matrix (autocovariance): $\Sigma_{\mathbf{X}\mathbf{X}} = \text{Var}[\mathbf{X}] = \text{Cov}[\mathbf{X}, \mathbf{X}] = E[\mathbf{X}\mathbf{X}^T] - E[\mathbf{X}] E[\mathbf{X}]^T$; $\Sigma_{ij} = \text{Cov}[X_i, X_j]$
- Cross-Covariance (joint variance): $\Sigma_{\mathbf{X}\mathbf{Y}} = \text{Cov}[\mathbf{X}, \mathbf{Y}] = E[\mathbf{X}\mathbf{Y}^T] - E[\mathbf{X}] E[\mathbf{Y}]^T$; $\Sigma_{ij} = \text{Cov}[X_i, Y_j]$
- Autocorrelation and cross-correlation: $\mathbf{R}_{\mathbf{X}\mathbf{X}} = E[\mathbf{X}\mathbf{X}^T]$; $\mathbf{R}_{\mathbf{X}\mathbf{Y}} = E[\mathbf{X}\mathbf{Y}^T]$; $(\mathbf{R}_{\mathbf{X}\mathbf{Y}})_{ij} = \text{Corr}[X_i, Y_j]$
- Covariance of a sum: if $\mathbf{Z} = \mathbf{X} + \mathbf{Y}$ then $\Sigma_{\mathbf{Z}\mathbf{Z}} = \Sigma_{\mathbf{X}\mathbf{X}} + \Sigma_{\mathbf{X}\mathbf{Y}} + \Sigma_{\mathbf{Y}\mathbf{X}} + \Sigma_{\mathbf{Y}\mathbf{Y}}$ (note that $\Sigma_{\mathbf{X}\mathbf{Y}} = \Sigma_{\mathbf{Y}\mathbf{X}}^T$)
- Covariance of a transformation: if $\mathbf{Y} = \mathbf{A}\mathbf{X} + \mathbf{b}$ (\mathbf{A}, \mathbf{b} : constants) then $\Sigma_{\mathbf{Y}\mathbf{Y}} = \mathbf{A}\Sigma_{\mathbf{X}\mathbf{X}}\mathbf{A}^T$

5.4.2. Convolution, Cross-Correlation and Autocorrelation on LTI Systems

For discrete signals $x[nT]$ and $y[nT]$, and continuous signals $f(t)$ and $g(t)$ (where $t = nT$),

	Convolution $f * g$	Cross-Correlation $f * g$	Autocorrelation $f * f$
Discrete	$\sum_{m=-\infty}^{\infty} x[mT] y[(n - m)T]$	$\sum_{m=-\infty}^{\infty} x[mT] y[(n + m)T]$	$\sum_{m=-\infty}^{\infty} x[mT] x[(n + m)T]$
Continuous	$\int_{-\infty}^{\infty} f(\tau) g(t - \tau) d\tau$	$\int_{-\infty}^{\infty} f(\tau) g(t + \tau) d\tau$	$\int_{-\infty}^{\infty} f(\tau) f(t + \tau) d\tau$
Stochastic	$E[X_t Y_{t-\tau}^*]$	$E[X_t Y_{t+\tau}^*]$	$E[X_t X_{t+\tau}^*]$

For the convolution theorem as it applies to discrete signals via the Z -transform and to continuous signals via the Fourier transform and Laplace transform, see Section 3.4.

5.4.3. Discrete Multidimensional Convolution

Let \mathbf{X} be an $M \times N$ matrix ($x(i, j) = X_{ij}$) and \mathbf{H} be a $K \times L$ matrix ($h(u, v) = H_{uv}$).

The convolution $\mathbf{Y} = \mathbf{H} * \mathbf{X}$ ($y = x * h$) is a $(M - K + 1) \times (N - L + 1)$ matrix, where

$$y(i, j) = \sum_{k=0}^{K-1} \sum_{l=0}^{L-1} h(k, l) x(i - k, j - l), \quad \text{for } 1 \leq i \leq M - K + 1, 1 \leq j \leq N - L + 1.$$

Typical application: \mathbf{X} is a general input, \mathbf{H} is the impulse response of a filter, \mathbf{Y} is the output.

5.4.3. Wiener-Khinchin Theorem

The power spectrum $S(\omega) = |X(\omega)|^2$ of a signal $x(t)$ and the autocorrelation of $x(t)$ form a Fourier-inverse pair:

$$\int_{-\infty}^{\infty} (x \star x)(t) e^{-j\omega t} dt = S(\omega) \qquad \int_{-\infty}^{\infty} S(\omega) e^{j\omega t} d\omega = (x \star x)(t)$$

forward transform inverse transform

5.4.4. FIR and IIR Filters

The pulse function is defined as $\delta_k = \{1 \text{ if } k = 0 \text{ else } 0\} = \{1, 0, 0, 0, \dots\}$ (Kronecker Delta; discrete version of Dirac Delta function).

A discrete-time system has a transfer function given by the Z-transform of its pulse response. (Analogous to continuous-time transfer functions as the Laplace transform of the impulse response).

For a discrete-time system (digital filter) with transfer function $G(z)$, input u_k and output y_k :

- $G(z)$ is the Z-transform of g_k (the pulse response when $u_k = \delta_k$).
- For a general input, the output is given by $y_k = (g_k \star u_k)$ (discrete convolution theorem).
- Causal system: if $g_k = 0$ for all $k < 0$. All physically realisable systems are causal, in which k represents a discretisation of real time.
- Finite impulse response (FIR): if $g_k = 0$ for all $k > n$ for some smallest finite n . Otherwise, it is an Infinite impulse response (IIR) filter.
- Stability: a system is BIBO stable if, for any bounded $\{u_k\}$, the output $\{y_k\}$ is bounded. (A signal $\{u_k\}$ is bounded such that $|u_k| < M$ for some positive M for all k .)
- Step response: if $u_k = 1$ for all k then $y_k \rightarrow G(1)$ as $k \rightarrow \infty$ (final value theorem).
- Frequency response: if $u_k = \cos k\theta$ then at steady state, $y_{ss}(k) = |G(e^{j\theta})| \cos(k\theta + \angle G(e^{j\theta}))$.
- Causal system transfer function: $G(z) = \sum_{k=0}^{\infty} g_k z^{-k}$ (For IIR, all poles are at $z = 0$.)

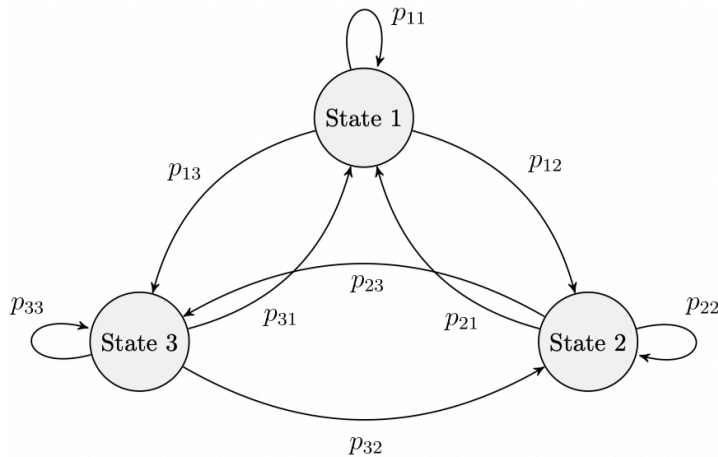
Stability criterion: a rational TF $G(z) = \frac{n(z)}{d(z)} = \frac{\sum_{k=0}^m b_k z^{m-k}}{\sum_{k=0}^n a_k z^{n-k}} = \frac{b_0 z^m + b_1 z^{m-1} + \dots + b_m}{z^n + a_1 z^{n-1} + \dots + a_n}$ must have $m \leq n$.

For such a system, $G(z)$ is stable, all of the roots p_i of $d(z)$ satisfy $|p_i| < 1$ and $\sum_{k=0}^{\infty} |g_k|$ is finite.

A stable filter has a decaying transient response, so that its steady state is independent of the initial conditions. Any linear filter can be written as $A(z) Y(z) = B(z) U(z) + C(z, y_i)$, where C accounts for the initial conditions.

5.4.6. Discrete-Time Markov Chains (DTMCs)

A Markov process is a stochastic process in which the distribution of the next state is a function of only the current state, and not the previous states: $p(X_{n+1} | X_1, X_2, \dots, X_n) = p(X_{n+1} | X_n)$, where $p(X)$ is a **row** vector of probabilities of the random variable X being in each state.



		to		
		State 1	State 2	State 3
from	State 1	p_{11}	p_{12}	p_{13}
	State 2	p_{21}	p_{22}	p_{23}
	State 3	p_{31}	p_{32}	p_{33}

Definitions

- State space: the enumeration of the different states i.e. the domain of $X_n \in S$
- Absorbing state: if $p_{ii} = 1$ (on the leading diagonal of \mathbf{M}) then state i is an absorbing state.
- Recurrent set / Equivalence class: a set of states within which any state can reach any other state
- Irreducible chain: if all states are recurrent (i.e. no absorbing states; one equivalence class)
- Periodicity: for a chain of period δ , the nonzero eigenvalues of \mathbf{M} are the δ th roots of unity.
- Regular ergodic: an irreducible and aperiodic chain, which has limiting (stationary) distribution.

Probability Relationships

- Transition matrix: $(\mathbf{M})_{ij} = p_{ij} = P(X_{n+1} = j | X_n = i)$
- Columns of \mathbf{M} sum to 1: $\sum_j p_{ij} = 1$. (right stochastic matrix)
- Joint distribution: $p(X_0 = i_0, X_1 = i_1, \dots, X_n = i_n) = P(X_0 = i_0) \times p_{i_0 i_1} p_{i_1 i_2} \dots p_{i_{n-1} i_n}$
- State transition probabilities: $p(X_{n+1}) = p(X_n) \mathbf{M}$ and $p(X_{n+k}) = p(X_n) \mathbf{M}^k$
- Higher order transition probability: $p_{ij}^{(m+n)} = (\mathbf{M}^{m+n})_{ij} = \sum_k p_{ik}^{(m)} p_{kj}^{(n)}$ (Chapman-Kolmogorov equation)
- Stationary (ergodic) state: if $p(X_n) = \boldsymbol{\pi}$ then $\boldsymbol{\pi} \mathbf{M} = \boldsymbol{\pi}$ ($\boldsymbol{\pi}$ is an eigenvector of \mathbf{M} with eigenvalue 1)
- Unconditional probability: $P(X_n = j) = \sum_i p_{ij}^{(n)} P(X_0 = i) = \text{mean value of column } j \text{ in } \mathbf{M}^n$

First Step Transition Analysis / Waiting Time Problems

- Transitions between neighbouring states $i \rightarrow i + 1$ occur with time $T = \text{Geo}(p_{i(i+1)})$, so $E[T] = 1 / p_{i(i+1)}$.
- Expected steps μ_{ij} required for a transition from i to j : $\mu_{ij} = E[\min(n \geq 1: X_n = j) | X_0 = i] = 1 + \sum_{k \neq j} p_{ik} \mu_{kj}$.

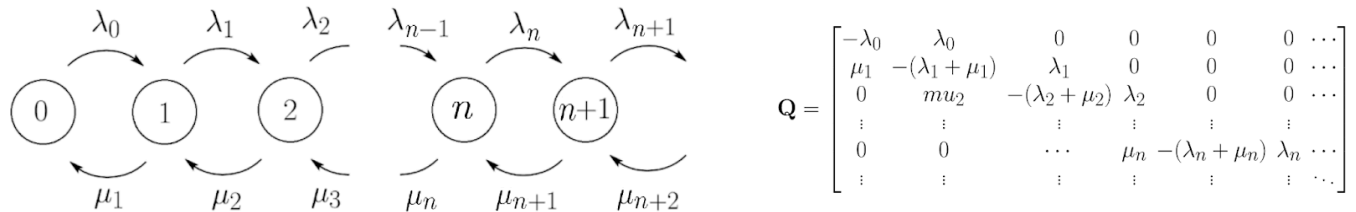
5.4.7. Continuous-Time Markov Chains (CTMCs, Discrete State Space)

The Markov matrix \mathbf{Q} for a continuous-time process is infinite dimensional: $\mathbf{x}' = \mathbf{x} \mathbf{Q}$

- $x_n(t) = P_n(t) = P(X(t) = n)$, $\mathbf{x} = [x_1(t), x_2(t), \dots]$ (**row vector**) and $(\mathbf{Q})_{ij} = \frac{\partial(x_j')}{\partial x_i}$. Entries of \mathbf{x} sum to 1.
- Rows of \mathbf{Q} sum to zero: $\sum_j (\mathbf{Q})_{ij} = 0$ (probability mass conserved).
- Discrete state space: $X(t)$ takes discrete values; $X \in \{0, 1, 2, \dots, n, \dots\}$ (to infinity, in general)
- Continuous state space: $X(t)$ takes continuous values (a range); $X \in S$.

Note that in solving $\mathbf{x}\mathbf{Q} = 0$ for the stationary state, one equation obtained from the columns of \mathbf{Q} is degenerate, and should be replaced with $\sum_j x_j = 1$ to give a determinate system.

The Birth-Death Process: the state $X(t)$ represents the number n of some entity at time t

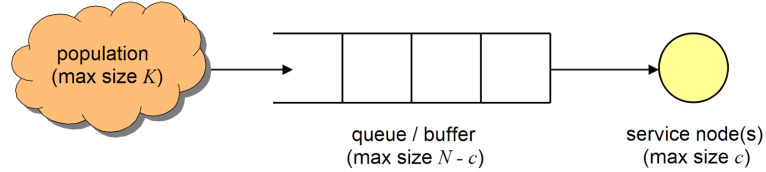


- Birth: transition from state n to state $n + 1$, occurring at a rate λ_n per unit time ($T_{n \rightarrow n+1} \sim \text{Exp}(\lambda_n)$).
- Death: transition from state n to state $n - 1$, occurring at a rate μ_n per unit time ($T_{n \rightarrow n-1} \sim \text{Exp}(\mu_n)$).
- Transitioning to the same state is also possible in general, with rate $1 - \lambda_n - \mu_n$ (allowable if $\lambda_n + \mu_n \neq 1$).
- Equation: $x_n(t + \Delta t) = x_n(t) (1 - \lambda_n \Delta t - \mu_n \Delta t) + x_{n-1}(t) (\lambda_{n-1} \Delta t) + x_{n+1}(t) (\mu_{n+1} \Delta t)$ for $n > 1$.
- Differential Equation: $\frac{dx_n}{dt} = \lambda_{n-1} x_{n-1} + \mu_{n+1} x_{n+1} - (\lambda_n + \mu_n) x_n$ for $n > 1$, and $\frac{dx_0}{dt} = \mu_1 x_1 - \lambda_0 x_0$.
- **Pure birth process (Yule-Furry process):** $\mu_n = 0$ (no deaths) and $\lambda_n = n\lambda$ (proportional growth rate).
Solution: $x_n(t) = {}^{n-1}C_{n-n_0} e^{-\lambda n_0 t} (1 - e^{-\lambda t})^{n-n_0}$ if $x_{n_0}(0) = 1$ i.e. given initial state is $X(0) = n_0$.
- **Poisson process:** $\mu_n = 0, \lambda_n = \lambda$ (constant birth rate) and $X(0) = 0$. Solution: $x_n(t) = \frac{(\lambda t)^n}{n!} e^{-\lambda t}$.

For results of other CTMCs which can be interpreted as FIFO queues, see Section 5.4.8.

5.4.8. Queueing Theory

Kendall notation: a queue model is named $A/B/c/N/K$ where:



A: inter-arrival time distribution (M: Markovian (exponential), D: deterministic (constant), G: general)

B: service time distribution (M: Markovian (exponential), D: deterministic (constant), G: general)

c : number of parallel servers (each serves 1 at a time)

N : system size (maximum queue length + c) (assumed ∞ if omitted)

K : population size (absolute maximum system size) (assumed ∞ if omitted)

(L : number of customers in the system, T : time of a customer in the system,

L_Q : number of customers in the queue, T_Q : time of a customer in the queue,

$\rho = \frac{\lambda_{eff}}{c\mu}$: server utilisation (load factor) - the queue is ergodic (a stationary state exists) if $\rho < 1$.)

Little's lemma: $mean\ throughput = \frac{mean\ number\ in\ system}{mean\ service\ time} \Leftrightarrow \lambda_{eff} = \frac{E[L]}{E[T]} = \frac{E[L_Q]}{E[T_Q]}$, always.

Coefficient of variation: $(cv)^2 = Var[X] / (E[X])^2$ for a specified random variable X . If $X \sim Exp$, $cv = 1$.

M/M/c/N/N Queue: those who leave the service node immediately rejoin the population (closed queue)

$$\pi_0 = \left[\sum_{n=0}^{c-1} {}^N C_n (c\rho)^n + \sum_{n=c}^N \frac{N! (c\rho)^n}{(N-n)! c! c^{n-c}} \right]^{-1}, \quad \pi_n = \left\{ \pi_0 {}^N C_n (c\rho)^n \text{ if } 0 \leq n < c, \text{ else } \frac{N! (c\rho)^n}{(N-n)! c! c^{n-c}} \right\},$$

$$E[L] = \sum_{n=0}^N n \pi_n, \quad \lambda_{eff} = \sum_{n=0}^N (N-n)\lambda \pi_n.$$

M/M/c/N Queue: capped system size. Functionally identical to an M/M/c/ ∞ /N queue.

$$\pi_0 = \left[1 + \sum_{n=1}^c \frac{(c\rho)^n}{n!} + \frac{(c\rho)^c}{c!} \sum_{n=c+1}^N \rho^{n-c} \right]^{-1}, \quad \pi_n = \left\{ \pi_0 \frac{(c\rho)^n}{n!} \text{ if } 0 \leq n < c, \text{ else } \pi_0 \frac{(c\rho)^n c^{c-n}}{c!} \right\}, \quad \pi_N = \frac{(c\rho)^N}{c! c^{N-c}} \pi_0,$$

$$E[L_Q] = \frac{\pi_0 (c\rho)^c \rho}{c! (1-\rho)^2} (1 - \rho^{N-c} - (N-c)(1-\rho)\rho^{N-c}), \quad \lambda_{eff} = \lambda(1 - \pi_N) = \frac{E[L_Q]}{E[T_Q]} = \frac{E[L]}{E[T]}, \quad E[T] = E[T_Q] + \mu^{-1}$$

M/M/c Queue (Erlang-C Model): birth-death process with $\lambda_n = \lambda$ and $\mu_n = \min\{c, n\} \mu$.

$$\pi_0 = \left[\left(\sum_{n=0}^{c-1} \frac{(c\rho)^n}{n!} \right) + \frac{(c\rho)^c}{c! (1-\rho)} \right]^{-1}, \quad P(L \geq c) = \sum_{n=c}^{\infty} \pi_n = \frac{(c\rho)^c}{c! (1-\rho)} \pi_0, \quad E[L] = c\rho + \frac{\rho}{1-\rho} P(L \geq c),$$

$$E[L_Q] = \frac{\rho}{1-\rho} P(L \geq c), \quad E[L - L_Q] = c\rho, \quad \pi_n = \left\{ \pi_0 \frac{(c\rho)^n}{n!} \text{ if } 0 \leq n < c, \text{ else } \pi_0 \frac{(c\rho)^n c^{c-n}}{c!} \right\}, \quad \lambda_{eff} = \lambda.$$

M/M/1 Queue: birth-death process with $\lambda_n = \lambda$ and $\mu_n = \mu$.

$$\pi_0 = 1 - \rho, \quad \pi_n = \pi_0 \rho^n, \quad E[L] = \frac{\rho}{1-\rho}, \quad E[T] = \frac{1}{\mu - \lambda}, \quad E[L_Q] = \frac{\rho^2}{1-\rho}, \quad E[T_Q] = \frac{\rho}{\mu(1-\rho)}, \quad \lambda_{eff} = \lambda.$$

M/G/1 Queue: service times are randomly distributed with mean time μ^{-1} and variance σ^2 .

$$\rho = \frac{\lambda}{\mu}, \quad \pi_0 = 1 - \rho, \quad E[L_Q] = \frac{\rho^2(1 + \sigma^2 \mu^2)}{2(1-\rho)}, \quad E[T_Q] = \frac{\lambda(\mu^{-2} + \sigma^2)}{2(1-\rho)}, \quad E[L] = \rho + E[L_Q], \quad E[T] = \mu^{-1} + E[T_Q].$$

5.4.9. Priority Queues and Networks

Service Disciplines

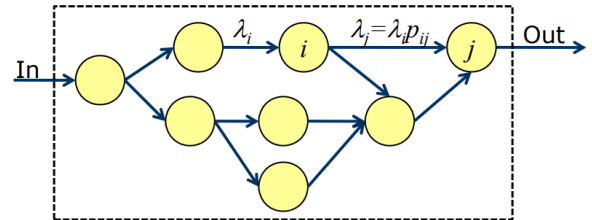
- First-in, first-out (FIFO) / first-come, first-served (FCFS): longest waiting served first.
- Last-in, first out (LIFO) / stack: shortest waiting served first.
- Processor sharing: service capacity is shared equally among customers.
- Priority queue: customers are assigned a priority and can jump to the front of the queue on arrival or even displace a customer being served (preemptive).

Customer Waiting Behaviour

- Balking: customers decide not to join the queue if it is too long, as if an M/M/c/N queue.
- Jockeying: when there are multiple queues, customers move to the shortest at any time.
- Reneging: customers will leave the queue if they have waited too long.

Queuing Networks

- A network of queues is represented as m nodes (queue + service) each with population x_i and black-box parameters i.e. $M/M/c_i, \lambda_i^{(eff)}, \mu_i$.



- Transition probability for leaving node i to enter node j : p_{ij} (can also leave system with p_i)
- Overall arrival rate into queue j : $\lambda_j = a_j + \sum_i \lambda_i p_{ij}$ (a_j : arrival rate from outside the system)
- Matrix / vector form: $\lambda = (\mathbf{I} - \mathbf{P}^T)^{-1} \mathbf{a}$
- Utilisation of queue j : $\rho_j = \lambda_j / (c_j \mu_j)$
- The flow of customers through a network at steady-state can often (not always) be thought of as a fluid flowing through ‘pipes’ (the fluid limit).

- Jackson network: an open network of m M/M/ c_i queues.

Joint steady-state distribution product form:
$$\pi(\mathbf{x}) = \prod_{i=1}^m \pi(x_i) \quad (\text{independence})$$

Discrete event simulation (DES) can be used to investigate complex queuing systems, such as the simple module in Python, the SimEvents MATLAB add-on or enterprise software.

Simulations of queueing are subject to initialisation bias, in which the initial state can influence the averaged statistics even after a long time has elapsed. To mitigate this, data collection can be delayed until a given ‘warm-up period’ has passed. Determining the ideal length of this period may be challenging, with several methods proposed (e.g. Welch plot). Alternatively, a known/theoretical average steady state can be set at the start (although this may affect measures of variability).

5.4.9. Continuous-Time, Continuous State Space Markov Chains

The Wiener Process: continuous random walk (Brownian motion).

Discrete Brownian motion: Let $X_n = \sum_{k=1}^n \zeta_k$ where $\zeta_k \in \{-\delta, \delta\}$ with $P(\zeta_k = -\delta) = P(\zeta_k = \delta) = 1/2$.

The limiting distribution of X_n as $n \rightarrow \infty$ where time $t = n\delta$ as $\delta \rightarrow 0$ (so t is finite) is $p(x, t) \sim N_x(0, t)$.

In general, the Fokker-Planck equation is $\frac{\partial p}{\partial t} = \frac{\partial^2}{\partial x^2} (\alpha p)$ (diffusion equation).

If $p(x, 0) = \delta(x - a)$ then $p(x, t) \sim N_x(a, 2\alpha t)$. The standard deviation is unbounded: $\sigma = \sqrt{2\alpha t}$.

The Ornstein-Uhlenbeck Process: continuous analogue of the AR(1) process.

The stochastic differential equation is $dx = -\beta x dt + \sqrt{2\alpha} dW$ (W : Wiener process)

(α : diffusion term, β : drift term)

The Fokker-Planck equation is $\frac{\partial p}{\partial t} = \frac{\partial}{\partial x} (\beta x p) + \frac{\partial^2}{\partial x^2} (\alpha p)$.

If $p(x, 0) = \delta(x - a)$ then $p(x, t) \sim N_x(a e^{-\beta t}, \frac{\alpha}{\beta}(1 - e^{-2\beta t}))$. At steady state, $\lim_{t \rightarrow \infty} p(x, t) \sim N(0, \frac{\alpha}{\beta})$.

The Renewal Process: how many observations of an RV in series before a given time t

Let $X_t = \max \left\{ n: \left(\sum_{i=1}^n S_i \right) \leq t \right\}$, where S is a random variable with known distribution

(with support $S > 0$), and S_i is the i th i.i.d. observation of S .

- X_t is a generalised Poisson process, known as the renewal process.
- Renewal function equation: if $m(t) = E[X_t]$, then $m(t) = F_S(t) + \int_0^t m(t - \tau) f_S(\tau)$
where $F_S(t)$ is the CDF of S and $f_S(t)$ is the PDF of S .
- Strong law of large numbers: $\lim_{t \rightarrow \infty} \frac{X_t}{t} = \frac{1}{E[S]}$
- Central limit theorem: for large t , X_t is asymptotically Gaussian: $X_t \sim N\left(\frac{t}{E[S]}, \frac{t \times \text{Var}[S]}{E[S]^3}\right)$

5.4.10. Sampling from Unnormalised Distributions

Consider a distribution $p(x) = \frac{f(x)}{C}$ where $f(x)$ is a known function but C is an unknown normalising constant. To approximate the drawing of samples from $p(x)$, we can use:

Rejection Sampling: Define a proposal distribution $q(x)$ and a constant k such that $f(x) \leq kq(x)$ for all x . Draw a candidate sample $Q \sim q(x)$, then draw another sample $U \sim \text{Uniform}(0, kq(Q))$. If $U \leq f(Q)$ then we accept the sample Q ; otherwise we reject. The accepted samples approach the distribution of $p(x)$.

Markov Chain Monte Carlo (MCMC): Construct a discrete-time Markov chain in which the states are the support (non-zero domain) of $f(x)$ and the 'time' is the sample number (index). The goal is to find the transition probabilities \mathbf{M} such that the stationary distribution is $p(x)$.

Detailed balance of equilibrium: $p(x)p(y|x) = p(y)p(x|y)$ equivalently $pM = p$.

Metropolis-Hastings Algorithm: Define a proposal distribution $q(x_{n+1}|x_n)$.

Generate samples of $x_{n+1} \sim q(x_{n+1}|x_n)$ and accept them with probability $A(x_{n+1}|x_n)$. (Note that $f = Aq$)

Detailed balance: $\frac{A(x_{n+1}|x_n)}{A(x_n|x_{n+1})} = \frac{f(x_{n+1})}{f(x_n)} \times \frac{q(x_n|x_{n+1})}{q(x_{n+1}|x_n)}$. Then $A(x_{n+1}|x_n) = \min \left\{ 1, \frac{f(x_{n+1})}{f(x_n)} \times \frac{q(x_n|x_{n+1})}{q(x_{n+1}|x_n)} \right\}$.

Gibbs Sampling: when $f = f(\mathbf{x})$ is a multivariable distribution and sampling from the joint pdf is difficult but from the conditional pdfs is easier. Choose an initial \mathbf{x}_0 . For each variable $x^{(i)}$, sample $x^{(i)}_{n+1} \sim p(x^{(i)}_{n+1} | \mathbf{x}^*_n)$ where \mathbf{x}^*_n is either \mathbf{x}_n or its partly/fully updated entries depending on implementation.

5.4.13. Wiener Deconvolution Filter

Given $y(t) = (h * x)(t) + n(t)$ (h : impulse response, n : noise), the goal is to find the MMSE estimate $\hat{x}(t) = (g * y)(t)$.

Signal-to-Noise ratio: $SNR(\omega) = \frac{S_{xx}(\omega)}{N(\omega)}$ ($S_{xx}(\omega)$: power spectrum of x)

Frequency spectrum of g : $G(\omega) = \frac{H^*(\omega) S_{xx}(\omega)}{|H(\omega)|^2 S_{xx}(\omega) + N(\omega)} = \frac{H^*(\omega) SNR(\omega)}{1 + |H(\omega)|^2 SNR(\omega)}$

Therefore $\hat{X}(\omega) = G(\omega) Y(\omega) \Rightarrow \hat{x}(t) = \frac{1}{2\pi} \int_{-\infty}^{\infty} G(\omega) Y(\omega) e^{i\omega t} d\omega$.

5.4.14. Stationary Time Series Analysis: AR, RA and ARMA Models

Gaussian noise: Let W_n be a sequence of random variables such that $E(W_n) = 0$ for all n and $E(W_i W_j) = \sigma^2$ if $i = j$ else 0.

Wide sense stationary (WSS): fixed mean, fixed correlation (independent of n).

The augmented Dickey-Fuller test (ADF test) can be used to test against the null hypothesis of a unit root (non-stationarity). Python: `statsmodels.tsa.stattools.adfuller(x)`

AR Model (Autoregressive Model)

AR(p) (order p) process: $X_n = \sum_{i=1}^p a_i X_{n-i} + W_n$

Correlation of AR(1): $R_{XX}(k) = E[X_n X_{n+k}] = a^k \sigma_X^2$

MA Model (Moving Average Model)

MA(p) (order p) process: $X_n = \mu + \sum_{i=1}^p a_i W_i$ where $\mu = E[X]$.

ARMA Model (Autoregressive Moving Average Model)

ARMA(p, q) process: $X_n = \mu + W_n + \sum_{i=1}^p a_i X_{n-i} + \sum_{j=1}^q b_j W_j$

Autocorrelation: $R_{XX}(k) = E[X_n X_{n+k}]$; Partial autocorrelation: $\phi(k) = E[(X_n - \bar{X}_n)(X_{n+k} - \bar{X}_{n+k})]$

The ARMA process the white noise response of an IIR filter.

Model Fitting: estimating the hyperparameters of an ARMA process to fit observed data.

- The value of p is optimal at the elbow or peak of $|\phi(k)|$ (PACF).
- The value of q is optimal at the elbow or peak of $|R_{XX}(k)|$ (ACF, correlogram).

5.4.15. ARIMA Model (Autoregressive Integrated Moving Average Model)

ARIMA(p, d, q) process: $Y_n = (1 - L)^d X_n = \sum_{k=0}^d C_k (-1)^k X_{n-k}$ ($L^k X_n = X_{n-k}$: lag operator)

where X_n is an ARMA(p, q) process.

The ARIMA process Y_n is non-stationary, while the ARMA process X_n is stationary.

For time series analysis, the W_n (noise) terms are evaluated as the model error, which is assumed to be Gaussian. A time series can be made stationary by repeatedly differentiating (differencing) until sufficiently stationary. This is equivalent to removing polynomial terms from the Taylor series of a smoothed version of the series.

Akaike Information Criterion: $AIC = 2k - 2 \ln(\max\{\hat{L}\})$ (can be applied to any model)

(k : number of estimated parameters, L : likelihood function)

Further enhancements include the SARIMAX model (seasonal components and exogenous (externally supplied) variables). These are available in Python via the `statsmodels` module, with a similar interface to `tensorflow.keras` models.

5.4.16. Noise Response of an LTI System

Let $H y = x$ where H : linear time invariant (LTI) system, y : system state, x : system input.

If H has impulse response h , the system response is given by $y = h * x$.

If $x = X(t)$ where X is a WSS stochastic process, then the response y is also WSS.

- Power spectral density (PSD) of y : $S_{YY}(\omega) = |H(\omega)|^2 S_{XX}(\omega)$ (H : FT of $h(t)$).
- Cross-spectral density (CSD): $S_{XY}(\omega) = S_{XX}(\omega) H(\omega)$

5.4.17. Multivariate Gaussian Distribution

A D -dimensional Gaussian random vector \mathbf{x} with mean vector $\boldsymbol{\mu}$ and covariance matrix $\boldsymbol{\Sigma}$ has a joint pdf given by

$$N(\mathbf{x}; \boldsymbol{\mu}, \boldsymbol{\Sigma}) = \frac{1}{\sqrt{(2\pi)^D |\boldsymbol{\Sigma}|}} \exp\left(-\frac{1}{2}(\mathbf{x} - \boldsymbol{\mu})^\top \boldsymbol{\Sigma}^{-1}(\mathbf{x} - \boldsymbol{\mu})\right).$$

where $\boldsymbol{\mu}$ is a D -dimensional vector, $\boldsymbol{\Sigma}$ is a $D \times D$ positive definite symmetric matrix, and $|\boldsymbol{\Sigma}|$ its determinant.

- Distribution notation: writing $p(\mathbf{x}) = N(\mathbf{x}; \boldsymbol{\mu}, \boldsymbol{\Sigma})$ is equivalent to $\mathbf{x} \sim N(\boldsymbol{\mu}, \boldsymbol{\Sigma})$.
- If \mathbf{x} and \mathbf{y} are jointly Gaussian random vectors with marginal pdfs $p(\mathbf{x}) = N(\mathbf{x}; \mathbf{a}, \mathbf{A})$ and $p(\mathbf{y}) = N(\mathbf{y}; \mathbf{b}, \mathbf{B})$, with cross-covariance matrix $\mathbf{C} = \text{Cov}[\mathbf{x}, \mathbf{y}]$, then the joint pdf is

$$p\left(\begin{bmatrix} \mathbf{x} \\ \mathbf{y} \end{bmatrix}\right) = N\left(\begin{bmatrix} \mathbf{x} \\ \mathbf{y} \end{bmatrix}; \begin{bmatrix} \mathbf{a} \\ \mathbf{b} \end{bmatrix}, \begin{bmatrix} \mathbf{A} & \mathbf{C} \\ \mathbf{C}^\top & \mathbf{B} \end{bmatrix}\right),$$

and the conditional pdf is $p(\mathbf{x} | \mathbf{y}) = N(\mathbf{x}; \mathbf{a} + \mathbf{C}\mathbf{B}^{-1}(\mathbf{y} - \mathbf{b}), \mathbf{A} - \mathbf{C}\mathbf{B}^{-1}\mathbf{C}^\top)$.

- Linear projection: if $p(\mathbf{x}) = N(\mathbf{x}; \boldsymbol{\mu}, \boldsymbol{\Sigma})$ and $\mathbf{y} = \mathbf{A}\mathbf{x} + \mathbf{b}$ then $p(\mathbf{y}) = N(\mathbf{y}; \mathbf{A}\boldsymbol{\mu} + \mathbf{b}, \mathbf{A}\boldsymbol{\Sigma}\mathbf{A}^\top)$.
- The product of Gaussian densities is an unnormalised Gaussian:

$$N(\mathbf{x}; \mathbf{a}, \mathbf{A}) N(\mathbf{x}; \mathbf{b}, \mathbf{B}) = Z^{-1} N(\mathbf{x}; \mathbf{c}, \mathbf{C})$$

where $\mathbf{C} = (\mathbf{A}^{-1} + \mathbf{B}^{-1})^{-1}$, $\mathbf{c} = \mathbf{C}(\mathbf{A}^{-1}\mathbf{a} + \mathbf{B}^{-1}\mathbf{b})$ and the normalising constant is Gaussian in both \mathbf{a} and \mathbf{b} : $Z^{-1} = (2\pi)^{-D/2} |\mathbf{A} + \mathbf{B}|^{-1/2} \exp(-(\mathbf{a} - \mathbf{b})^\top (\mathbf{A} + \mathbf{B})^{-1} (\mathbf{a} - \mathbf{b}) / 2)$.

- The (differential) entropy of a D -dimensional Gaussian random vector \mathbf{X} with pdf $p(\mathbf{x}) = N(\mathbf{x}; \boldsymbol{\mu}, \boldsymbol{\Sigma})$ is

$$h(\mathbf{X}) = \int p(\mathbf{x}) \log \frac{1}{p(\mathbf{x})} d\mathbf{x} = \frac{1}{2} \log((2\pi e)^D |\boldsymbol{\Sigma}|).$$

- KL (Kullback-Leibler) divergence between Gaussians:

If $p(\mathbf{x}) = N(\mathbf{x}; \boldsymbol{\mu}_1, \boldsymbol{\Sigma}_1)$ and $q(\mathbf{x}) = N(\mathbf{x}; \boldsymbol{\mu}_2, \boldsymbol{\Sigma}_2)$ then

$$KL(p, q) = \int p(\mathbf{x}) \log \frac{p(\mathbf{x})}{q(\mathbf{x})} d\mathbf{x} = \frac{1}{2} \left(\log \frac{|\boldsymbol{\Sigma}_2|}{|\boldsymbol{\Sigma}_1|} - D + \text{tr}(\boldsymbol{\Sigma}_2^{-1}\boldsymbol{\Sigma}_1) + (\boldsymbol{\mu}_1 - \boldsymbol{\mu}_2)^\top \boldsymbol{\Sigma}_2^{-1}(\boldsymbol{\mu}_1 - \boldsymbol{\mu}_2) \right).$$

5.4.18. Gaussian Process

Formally, if $X: T \times \Omega \rightarrow \mathbb{R}$ is a Gaussian process with mean function m and covariance function K , then for every $t_1, \dots, t_k \in T$, the random vector $[X(t_1), \dots, X(t_k)]$ has a multivariate normal distribution with mean vector $\boldsymbol{\mu}_k = m(t_k)$ and covariance matrix $\boldsymbol{\Sigma}_{ij} = K(t_i, t_j)$.

(T : set of indices for Gaussian process, Ω : sample space of X)

Informally, X can be considered a ‘function’ that returns a distribution $N(x; m(t), K(t, t))$ for any given t , i.e. $X(t)$ has a univariate Normal distribution (with a specified covariance between any two different t). Function $X(t)$ has domain T and sample space Ω , returning a real-valued probability.

$X(t) \sim \text{GP}(m(t), K(t, t'))$ where $m(x)$ is the mean function, $K(t, t')$ is the covariance function with another given input x' .

It is useful to note that a Gaussian process can also be considered as an infinite-variable Gaussian distribution, with an infinite-length mean vector and infinity-by-infinity covariance matrix, since:

- An infinite-dimensional vector can be considered a scalar function of a single variable.
- An infinity-by-infinity matrix can be considered a scalar function of two variables:

Regression: let $y = X(t) + \varepsilon\sigma_y$, where $X(t)$ is a Gaussian process (the model \hat{y}), $\varepsilon \sim N(0, 1)$ and σ_y is the constant standard deviation of the model errors.

Assume a zero-mean Gaussian process prior distribution $f(x) | \theta \sim \text{GP}(0, K(x, x'))$ (θ : model hyperparameters used to define function K). Then $y | \theta \sim \text{GP}(0, K(x, x') + \mathbf{I}\sigma_y)$.

A common choice of K is $K(t, t') = \exp\left(-\frac{|t - t'|^2}{2\sigma}\right)$, where length-scale σ is a hyperparameter.

Prediction: let some given data be $\mathbf{y}_2 \sim N(\mathbf{b}, \mathbf{B})$ (finite dimensional) and data to predict $\mathbf{y}_1 \sim N(\mathbf{a}, \mathbf{A})$ (infinite dimensional). The joint distribution of \mathbf{y}_1 and \mathbf{y}_2 (Section 5.4.17) is a Gaussian process: $p(\mathbf{y}_1, \mathbf{y}_2) = N([\mathbf{y}_1; \mathbf{y}_2]; [\mathbf{a}; \mathbf{b}], [[\mathbf{A}, \mathbf{C}]; [\mathbf{C}^\top, \mathbf{B}]])$.

Consider $p(\mathbf{y}_1 | \mathbf{y}_2) = \frac{p(\mathbf{y}_1, \mathbf{y}_2)}{p(\mathbf{y}_2)} = N(\mathbf{y}_1; \mathbf{a} + \mathbf{CB}^{-1}(\mathbf{y}_2 - \mathbf{b}), \mathbf{A} - \mathbf{CB}^{-1}\mathbf{C}^\top)$.

The predictive mean is $E[\mathbf{y}_1 | \mathbf{y}_2] = \mathbf{a} + \mathbf{CB}^{-1}(\mathbf{y}_2 - \mathbf{b}) = \mathbf{CB}^{-1}\mathbf{y}_2$ ($\mathbf{a} = \mathbf{b} = \mathbf{0}$ for zero mean prior), which is linear in the given data \mathbf{y}_2 . The predictive covariance is $\text{Cov}[\mathbf{y}_1 | \mathbf{y}_2] = \mathbf{A} - \mathbf{CB}^{-1}\mathbf{C}^\top$ i.e. the uncertainty has been reduced from \mathbf{A} (prior uncertainty) by $\mathbf{CB}^{-1}\mathbf{C}^\top$.

5.4.19. Information Entropy

For a discrete random variable X with a probability mass function $P_X(x)$:

- **Shannon information content** ('surprise') of an outcome: $I_X(x) = -\log P_X(x)$
- The **entropy** of an r.v. X with pmf P is the expected information, $E[I_X(x)]$:

$$H(X) = \sum_x P(x) \log \frac{1}{P(x)} = -\mathbb{E}[\log(P(x))].$$

The entropy is measured in 'bits' if using log base 2, and 'nats' if using log base e.

- The **joint entropy** of random variables X_1, \dots, X_n with joint pmf $P_{X_1 \dots X_n}$ is

$$H(X_1, X_2, \dots, X_n) = \sum_{x_1, \dots, x_n} P_{X_1 \dots X_n}(x_1, \dots, x_n) \log \frac{1}{P_{X_1 \dots X_n}(x_1, \dots, x_n)}.$$

- The **conditional entropy** of Y given X is

$$H(Y|X) = \sum_x P_X(x) \underbrace{\sum_y P_{Y|X}(y|x) \log \frac{1}{P_{Y|X}(y|x)}}_{H(Y|X=x)} = \sum_x P_X(x) H(Y|X=x).$$

Note that a similar formula holds if we condition on a collection of random variables (X_1, \dots, X_n) instead of a single random variable X .

- **Chain rule for entropy:** The joint entropy of X_1, \dots, X_n can be written as

$$\begin{aligned} H(X_1, X_2, \dots, X_n) &= H(X_1) + H(X_2|X_1) + H(X_3|X_2, X_1) + \dots + H(X_n|X_{n-1}, \dots, X_1) \\ &= \sum_{i=1}^n H(X_i|X_{i-1}, \dots, X_1), \quad \text{where} \end{aligned}$$

$$H(X_i|X_{i-1}, \dots, X_1) = -\sum_{x_1, \dots, x_i} P_{X_1, \dots, X_i}(x_1, \dots, x_i) \log P_{X_i|X_1, \dots, X_{i-1}}(x_i|x_1, \dots, x_{i-1}).$$

- The **relative entropy or KL divergence** between two PMFs P and Q (defined on the same alphabet) is the information loss by using Q to represent P , given by

$$D(P||Q) = \sum_{x \in \mathcal{X}} P(x) \log \frac{P(x)}{Q(x)}.$$

- The **differential entropy** of a continuous random variable X with pdf p is

$$h(X) = \int_{-\infty}^{\infty} p(x) \log \frac{1}{p(x)} dx.$$

Joint differential entropy, conditional differential entropy, relative entropy/KL divergence, mutual information, chain rules for continuous random variables are all defined similarly to the discrete case with integrals replacing sums.

5.4.20. Mutual Information

The mutual information between random variables X and Y represents the average reduction in uncertainty about X by knowing Y . For a joint pmf P_{XY} , mutual information is

$$\begin{aligned} I(X;Y) &= H(X) - H(X|Y) \\ &= H(Y) - H(Y|X) \\ &= H(X) + H(Y) - H(X,Y) \\ &= D(P_{XY} || P_X P_Y). \end{aligned}$$

Chain rule for mutual information:

$$\begin{aligned} I(X_1, X_2, \dots, X_n; Y) &= I(X_1; Y) + I(X_2; Y|X_1) + \dots + I(X_n; Y|X_{n-1}, \dots, X_1) \\ &= \sum_{i=1}^n I(X_i; Y|X_{i-1}, X_{i-2}, \dots, X_1). \end{aligned}$$

For maximum coding efficiency (optimal encoding), the mutual information / KL divergence $I(X; Y) = D_{\text{KL}}(P_{XY} || P_X P_Y)$ between an 'output' X and an 'input' Y must be maximised.

5.4.21. Decoding with Information Loss due to Noise

Data Processing Inequality: If X, Y, Z form a Markov chain, then

$$I(X; Y) \geq I(X; Z).$$

Discrete random variables X, Y, Z are said to form a Markov chain if their joint pmf can be written as $P_{XYZ} = P_X P_{Y|X} P_{Z|Y}$.

This is analogous to the second law of thermodynamics for statistical entropy (mutual information never increases with deterministic processing (conditioning)).

Fano's Inequality: Let X be a random variable taking values in a set χ with cardinality denoted by $|\chi|$. Let Y be a random variable jointly distributed with X , and $\hat{X} = f(Y)$ be any estimator of X from Y . Then the probability of error $P_e = P(\hat{X} \neq X)$ satisfies

$$1 + P_e \log |\chi| \geq H(X | Y).$$

5.4.22. Maximum Entropy Distributions

The entropy, representing the ‘surprise’ we get when making an observation. A random variable with a maximum entropy distribution (subject to given constraints) represents the most efficient coding of the information in the variable.

Constraint type	Constraint definition(s)	Maximum entropy distribution, $f_X(x)$	Distribution name
Limited range	$a \leq X \leq b$	$\frac{1}{b-a}$	Uniform
Nonnegative integers, limited range, fixed mean	$X \in \{0, 1, \dots, n\},$ $E[X] = \mu_x$	${}^n C_x \left(\frac{\mu_x}{n}\right)^x \left(1 - \frac{\mu_x}{n}\right)^{n-x}$	Binomial
Positive integers, fixed mean	$X \in \{1, 2, 3, \dots\},$ $E[X] = \mu_x$	$\frac{1}{\mu_x} \left(1 - \frac{1}{\mu_x}\right)^{x-1}$	Geometric
Nonnegative integers, fixed mean	$X \in \{0, 1, 2, \dots\},$ $E[X] = \mu_x$	$\frac{\mu_x^x e^{-\mu_x}}{x!}$	Poisson
Nonnegative, fixed mean	$X \geq 0, E[X] = \mu_x$	$\frac{1}{\mu_x} \exp \frac{-x}{\mu_x}$	Exponential
Fixed mean, fixed variance	$E[X] = \mu_x, Var[X] = \sigma_x^2$	$\frac{1}{\sqrt{2\pi\sigma_x^2}} \exp \frac{-(x-\mu_x)^2}{2\sigma_x^2}$	Normal

5.5. Machine Learning and Computational Statistics

5.5.1. Data Matrix and Notation for Datasets

The p ‘independent variables’ (features) are $\{x_1, x_2, \dots, x_p\}$. The single dependent variable is y . In a complete dataset, there are n recorded observations of each variable. A data matrix $\mathbf{X} \in \mathbb{R}^{n \times p}$ and label column vector $\mathbf{y} \in \mathbb{R}^n$ is constructed:

Observation	Feature 1 (x_1)	Feature 2 (x_2)	...	Feature p (x_p)	Label ($y \in \mathbb{R}^n$)
1	X_{11}	X_{12}	...	X_{1p}	y_1
2	X_{21}	X_{22}	...	X_{2p}	y_2
...
n	X_{n1}	X_{n2}	...	X_{np}	y_n

X_{ij} is the i th observation of variable x_j .

The goal of an ML model is to find a mapping $f: \mathbf{X} \rightarrow \mathbf{y}$.

- Each row of \mathbf{X} can be considered a random vector.
- Each column of \mathbf{X} can be considered a set of observations from a random variable X_j .
- A ‘centred dataset’ contains features whose observations have zero mean: $\mathbf{x}_j' = \mathbf{x}_j - \overline{X_j}$.
- A ‘standardised dataset’ contains features whose observations have zero mean and unit standard deviation: $\mathbf{x}_j' = (\mathbf{x}_j - \overline{X_j}) / s_{X_j}$. The standardised X_j is comparable to (but not necessarily has) a standard normal (Gaussian) distribution.

5.5.2. Principal Component Analysis (PCA)

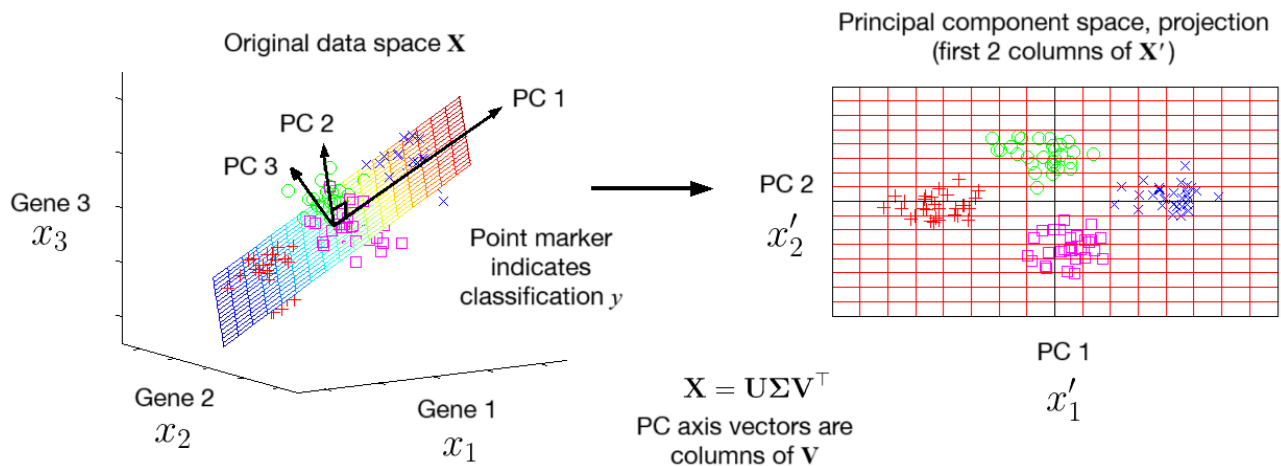
PCA is a method of constructing new features $\{x_1', x_2', \dots, x_p'\}$ that retain the information required to reconstruct y . Mathematically, it is a rotation of the coordinate axes used to specify the data into axes along which variance is maximised and covariance is minimised.

For a **standardised** ($\mu_i = 0, \sigma_i = 1$) dataset represented with data matrix $\mathbf{X} \in \mathbb{R}^{n \times p}$ ($n \geq 2$):

- Singular value decomposition (SVD, Section 4.3.7): $\mathbf{X} = \mathbf{U}\mathbf{\Sigma}\mathbf{V}^T$
($\mathbf{U} \in \mathbb{R}^{n \times n}$, orthonormal; $\mathbf{\Sigma} \in \mathbb{R}^{n \times p}$, non-square diagonal; $\mathbf{V} \in \mathbb{R}^{p \times p}$, orthonormal, $\mathbf{V}^{-1} = \mathbf{V}^T$)
- Covariance matrix: $\mathbf{C} = \text{Cov}[\mathbf{X}, \mathbf{X}] = \frac{1}{n-1} \mathbf{X}^T \mathbf{X}$ such that $C_{ij} = \text{Cov}[X_i, X_j]$ ($\mathbf{C} \in \mathbb{R}^{p \times p}$, symmetric)
- Eigendecomposition (Section 4.3.6): $\mathbf{C} = \frac{1}{n-1} \mathbf{V}\mathbf{\Sigma}^2\mathbf{V}^T$ or $\mathbf{X}^T \mathbf{X} = \mathbf{V}\mathbf{\Sigma}^2\mathbf{V}^T$,
with eigenvalues in $\mathbf{\Sigma}^2 / (n - 1)$ or singular values in $\mathbf{\Sigma}$ are ordered descending.
- Data matrix in PC space: $\mathbf{X}' = \mathbf{X}\mathbf{V} = \mathbf{U}\mathbf{\Sigma}$. Each column of \mathbf{X}' is a principal component.
- The V_{ij} are the 'loadings' of X_i (coefficient in the expression for computing PC X'_j).
- The columns of \mathbf{V} are orthonormal vectors. This means that the PCs are independent i.e. uncorrelated: the new covariance matrix $\mathbf{C}' = \text{Cov}[\mathbf{X}', \mathbf{X}'] = \mathbf{V}^T \mathbf{C} \mathbf{V}$ is diagonal.
- Eigenvalues of \mathbf{C} are $\lambda_i = \sigma_i^2 / (n - 1)$, representing the variances of data in each PC.

PCA can be used for model dimensionality reduction by truncating $\mathbf{\Sigma}$ to retain only the $k \leq p$ largest singular values (projection: $\mathbb{R}^p \rightarrow \mathbb{R}^k$). The corresponding eigenvectors (rows of \mathbf{V}^T) are the dominant components. Then, $\mathbf{\Sigma}$ becomes a $n \times k$ matrix and \mathbf{V} becomes a $p \times k$ matrix. k can be chosen by plotting the eigenvalues in descending order and selecting the ones significantly larger than the rest (the 'elbow' of a 'scree plot'). For visualisation, $k = 2$ is often chosen (obtain PC1 and PC2).

For a multivariate distribution of zero-mean Normal variables, the principal components are along the axes of the p -dimensional hyper-ellipsoid formed by contours of the joint PDF. If the data has categorical labels, they can be colour-coded, around which 95% confidence ellipses can be drawn. This can sometimes help separate clusters before a clustering algorithm is applied (Section 5.5.6). A 'loading plot' shows the weights of the features (loadings) to a PC. A 'biplot' shows each loading as a vector to the point (PC1, PC2) in PC space, with a circle of radius 1 surrounding them, and the dataset in PC space optionally superimposed. Example (gene expression):



5.5.3. Scaling and Encoding (Pre-Processing)

Data can be normalised to remove potential variation due to physical units or magnitudes.

- Standard scaling: $x' = \frac{x - \mu}{\sigma}$ (sklearn.preprocessing.StandardScaler)
- Min-max scaling: $x' = \frac{x - \min(x)}{\max(x) - \min(x)}$ (sklearn.preprocessing.MinMaxScaler)

Non-numerical (categorical) data can be encoded into numerical data.

- Ordinal encoding: $x' \in \{0, 1, 2, \dots\}$ (sklearn.preprocessing.OrdinalEncoder)
- One-hot encoding: $x'_i \in \{0, 1\}$ (sklearn.preprocessing.OneHotEncoder)

where i is the number of distinct categories. Each one-hot feature is essentially a boolean for “is X equal to i ?”, where feature X takes values i .

5.5.4. Metrics for Evaluating Model Performance

Metrics for Evaluating Regression Models:

$$MSE = \frac{1}{n} \sum_i (y_i - \hat{y}_i)^2$$

Mean Squared Error (MSE)

$$MAE = \frac{1}{n} \sum_i |y_i - \hat{y}_i|$$

Mean Absolute Error (MAE)

$$MAPE = \frac{1}{n} \sum_i \left| \frac{y_i - \hat{y}_i}{y_i} \right|$$

Mean Absolute Percentage Error (MAPE)

$$R^2 = 1 - \frac{RSS}{TSS} = 1 - \frac{SSE}{SSE \text{ with } \hat{y}_i = \bar{y}} = 1 - \frac{\sum_i (y_i - \hat{y}_i)^2}{\sum_i (y_i - \bar{y})^2}$$

Coefficient of Determination (R^2)

(SSE (sum of squared errors) = RSS (residual sum of squares); SSE with $\hat{y} = \bar{y}$ = TSS (total sum of squares))

If the errors can be assumed to have zero mean (symmetric), then the MSE is equivalent to the variance of \hat{y} , and the RMSE = \sqrt{MSE} = std. dev.

Metrics for Evaluating Classification Models:

Confusion matrix: a contingency table showing frequency of classifications.

	Predicted Positive	Predicted Negative	Total
True Positive	TP True Positive	FN False Negative (Type II Error)	P
True Negative	FP False Positive (Type I Error)	TN True Negative	N
Total	PP	PN	$P + N = PP + PN$

$$\text{Accuracy} = \frac{TP + TN}{P + N}; \quad \text{Precision} = \frac{TP}{PP}; \quad \text{Sensitivity} = \frac{TP}{P}; \quad \text{Specificity} = \frac{TN}{N}; \quad F_1 \text{ Score} = \frac{2 TP}{PP + P}$$

Precision is also known as Positive Predictive Value (PPV).

Sensitivity is also known as True Positive Rate (TPR), Recall, Hit Rate, or Power.

Specificity is also known as True Negative Rate (TNR) or Selectivity.

Metrics for Evaluating Clustering Models:

- Silhouette Score: $s_i = \frac{b_i - a_i}{\max\{a_i, b_i\}}$, compute for each point; measures separation.
(a_i : average distance between i and other points in same cluster; b_i : distance between i and centroid of nearest other cluster)
- Adjusted Rand Index: fraction of pairs of points in the correct same cluster, adjusted for randomness.
- Adjusted Mutual Information: measured between two given clusters; adjusted for the entropies of each cluster, see Section 5.5.3.
- Calinski-Harabasz Index (variance criterion): ratio of within-cluster dispersion to inter-cluster dispersion.

Many of these metrics are available in `scikit-learn`.

5.5.5. Traditional (Non Neural Network Based) Supervised Classification Algorithms

Naive Bayes Classifier

A Bayes classifier assumes conditional independence between each x given y . Classification labels \hat{y}_j are chosen to maximise the MAP, given by $p(y) \prod_i p(x_i | y)$ where $p(y) = 1 / (\# \text{ labels})$ is the prior relative frequency of y and $p(y | x_i)$ is calculated from a given distribution e.g. Gaussian.

Python (scikit-learn): `from sklearn.naive_bayes import GaussianNB`

Random Forest Classifier

A supervised classification method in which binary decision trees are created and optimised on their decision rule to minimise a loss function (often Gini impurity).

Python (scikit-learn): `from sklearn.ensemble import RandomForestClassifier`

XGBoost (extreme gradient boosting) is a powerful tree-based model implemented in C++.

Support Vector Classifier

For maximum margin classification, use a hinge loss:
$$L(\hat{y}, y) = \begin{cases} \max\{0, \varepsilon - \hat{y}\}, & \text{if } y > 0 \\ \max\{0, \varepsilon + \hat{y}\}, & \text{if } y < 0 \end{cases}$$

Python (scikit-learn): `from sklearn.svm import SVC`

K Nearest Neighbours

A simple classification algorithm in which data points are classified according to the most common label among that of the K nearest training data points (majority voting).

KD tree algorithm: constructs a binary tree in which each node represents a decision on the point coordinates (typically “above/below the median feature value?”), and the leaves of the tree are all the points within a class under these decision rules.

Python (scikit-learn): `from sklearn.neighbors import KNeighborsClassifier`

5.5.6. Clustering Algorithms (Unsupervised)

***K* Means Clustering**

For a dataset of n observations $\mathbf{x} = \{x_1, x_2, \dots, x_n\}$, centroidal points \hat{y}_j ($0 \leq j < K$) are chosen such that $\sum_i \text{dist}(x_i, \hat{y}_{\text{closest}(i)})^2$ is minimised, where $\text{closest}(i)$ returns the centroidal point index which is closest to x_i . This is a nonlinear and non-smooth optimisation problem. The clusters are then given by $S_j = \{x_i: \text{closest}(i) = \hat{y}_j\}$.

Main limitation: cannot produce cluster boundaries whose centroids are necessarily far from any of their points (e.g. concentric rings).

Python (scikit-learn): `from sklearn.cluster import KMeans`

DBSCAN

DBSCAN (Density-Based Spatial Clustering of Applications with Noise) groups points of similar densities, without reference to any centroids. Can produce more complex cluster boundary topologies, including shapes with holes (annuli).

A modification is HDBSCAN (hierarchical DBSCAN) which has easier hyperparameter tuning.

Python (scikit-learn): `from sklearn.cluster import DBSCAN`

5.5.7. Generalised Linear Regression (Regression, Supervised)

Linear regression model: $\hat{y}(\mathbf{x}) = \mathbf{w}^T \mathbf{x} + w_0 = w_1 x_1 + w_2 x_2 + \dots + w_p x_p + w_0$. (linear combination of features)

The values of \mathbf{w} and b are chosen to minimise a particular cost function: $\mathbf{w}^*, w_0^* = \operatorname{argmin} C(\mathbf{w}, w_0)$.

- Ordinary least squares (OLS): $C(\mathbf{w}) = \sum_{i=1}^n (y_i - \hat{y}_i)^2$ (SSE: sum of squared errors)
- LASSO regression: $C(\mathbf{w}) = \sum_{i=1}^n (y_i - \hat{y}_i)^2 + \lambda \sum_{j=1}^p |w_j|$ (l^1 norm regularisation)
- Ridge regression: $C(\mathbf{w}) = \sum_{i=1}^n (y_i - \hat{y}_i)^2 + \lambda \sum_{j=1}^p w_j^2$ (l^2 norm regularisation)
- Support vector regression (SVR): $C(\mathbf{w}, b) = \lambda \sum_{i=1}^n \max\{0, |y_i - \hat{y}_i| - \varepsilon\} + \frac{1}{2} \sum_{j=1}^p w_j^2$ (hinge loss)

(n : number of observations, p : number of features; $\mathbf{X} \in \mathbb{R}^{n \times p}$; and λ, ε are hyperparameters.)

Regularisation terms penalise large components in \mathbf{w} , ensuring weight decay to prevent overfitting.

For polynomial regression up to order k , extend \mathbf{X} with new features given by

$x_1^{\alpha_1} x_2^{\alpha_2} x_3^{\alpha_3} \dots x_n^{\alpha_n}$ for all $0 \leq \alpha_i \leq k$ such that $2 \leq \sum_{i=1}^n \alpha_i \leq k$, then apply linear regression as

usual. E.g. for $k = 2$ and $n = 3$ (original features: $\mathbf{X} = \{x, y, z\}$), extend with $\{xy, yz, xz, x^2, y^2, z^2\}$.

Python (scikit-learn):

```
from sklearn.linear_model import LinearRegression # also: Ridge / Lasso / sklearn.svm.SVM
from sklearn.preprocessing import PolynomialFeatures
from sklearn.model_selection import train_test_split
from sklearn.metrics import mean_absolute_percentage_error

poly_features = PolynomialFeatures(degree=3, include_bias=False).fit_transform(X_data)
X_train, X_test, y_train, y_test = train_test_split(poly_features, y_data,
    test_size=0.2)

poly_model = LinearRegression(fit_intercept=True).fit(X_train, y_train)
y_pred = poly_model.predict(X_test) # use the model to estimate y(X_test)
mpe = mean_absolute_percentage_error(y_test, y_pred) # quantify accuracy
```

5.5.8. Gaussian Process Regression (Uncertainty Regression, Supervised)

Gaussian process regression allows quantification of the uncertainty associated with a regression model about a mean predicted value. GPR is a useful form of nonlinear regression in which the computational complexity is independent of the form of the data: input x may be a scalar, a vector, a string, a graph, etc. It is suited when only a small training dataset is available.

- For a given training dataset $\{(\mathbf{x}_i, y_i)\}_{i=1}^n$ such that all y_i are centralised (zero mean), the aim of the model is to produce predictive distributions on test points $\{(\mathbf{x}_i^*, y_i^*)\}_{i=1}^m$.
- Assume noisy observations of a Gaussian process (Section 5.4.18) f , i.e. $y_i = f(\mathbf{x}_i) + \varepsilon_i$, where $\varepsilon_i \sim \mathcal{N}(0, \sigma_\varepsilon^2)$.
- Notation: \mathbf{X} = training data matrix, \mathbf{X}^* = testing data matrix, \mathbf{y} = training labels, $\mathbf{f} = \mathbf{f}(\mathbf{X})$, $\mathbf{f}^* = \mathbf{f}(\mathbf{X}^*)$.
- Kernel function (autocovariance): $\mathbf{K}_{\mathbf{X}\mathbf{X}}$ where element (i, j) is a function $K: \{\mathbb{R}^p \times \mathbb{R}^p\} \rightarrow \mathbb{R}$ evaluated as $K(\mathbf{x}_i, \mathbf{x}_j)$. A common choice of kernel for numeric \mathbf{x} is the radial basis function (RBF), $K(\mathbf{x}, \mathbf{x}') = \lambda \exp[-|\mathbf{x} - \mathbf{x}'| / 2\sigma]$ where $\boldsymbol{\tau} = \{\lambda: \text{output correlation scale}, \sigma: \text{input correlation scale}\}$ are hyperparameters. Kernel functions can be combined additively (and **approximately**, not formally, multiplicatively) to produce better fits to observed data. $\mathbf{K}_{\mathbf{X}\mathbf{X}^*}$, $\mathbf{K}_{\mathbf{X}^*\mathbf{X}}$ and $\mathbf{K}_{\mathbf{X}^*\mathbf{X}^*}$ are defined similarly. Note that $\mathbf{K}_{\mathbf{X}^*\mathbf{X}} = \mathbf{K}_{\mathbf{X}\mathbf{X}^*}^\top$ by the property in Section 5.4.17.
- Assume that \mathbf{y} and \mathbf{f}^* together form a joint $(n + m)$ -dimensional normal distribution:

$$\begin{bmatrix} \mathbf{y} \\ \mathbf{f}^* \end{bmatrix} \sim \mathcal{N} \left(\begin{bmatrix} \mathbf{0} \\ \mathbf{0} \end{bmatrix}, \begin{bmatrix} \hat{\mathbf{K}}_{\mathbf{X}\mathbf{X}} & \mathbf{K}_{\mathbf{X}\mathbf{X}^*} \\ \mathbf{K}_{\mathbf{X}^*\mathbf{X}} & \mathbf{K}_{\mathbf{X}^*\mathbf{X}^*} \end{bmatrix} \right) \quad \text{where} \quad \hat{\mathbf{K}}_{\mathbf{X}\mathbf{X}} = \mathbf{K}_{\mathbf{X}\mathbf{X}} + \sigma_\varepsilon^2 \mathbf{I} \quad (\text{block matrices}).$$

The training dataset provides a marginalisation (conditioning) of one observation from this distribution, from which the distribution of the testing set can be inferred.

- The posterior distribution is then $\mathbf{f}^* | \mathbf{X}^*, \mathbf{X}, \mathbf{y} \sim \mathcal{N}(\boldsymbol{\mu}, \boldsymbol{\Sigma})$ where

$$\boldsymbol{\mu}_{\mathbf{f}^*} = \mathbf{K}_{\mathbf{X}^*\mathbf{X}} \hat{\mathbf{K}}_{\mathbf{X}\mathbf{X}}^{-1} \mathbf{y}, \quad \boldsymbol{\Sigma}_{\mathbf{f}^*} = \mathbf{K}_{\mathbf{X}^*\mathbf{X}^*} - \mathbf{K}_{\mathbf{X}^*\mathbf{X}} \hat{\mathbf{K}}_{\mathbf{X}\mathbf{X}}^{-1} \mathbf{K}_{\mathbf{X}\mathbf{X}^*}$$

- Individual posterior output distributions for y have 1D normal distributions with mean given by an entry in $\boldsymbol{\mu}_{\mathbf{f}^*}$ and variance given by the corresponding diagonal entry in $\boldsymbol{\Sigma}_{\mathbf{f}^*}$.
- Hyperparameter selection: choose $\boldsymbol{\theta} = \{\sigma_\varepsilon^2, \boldsymbol{\tau}\}$ such that $\boldsymbol{\theta}^* = \arg \max_{\boldsymbol{\theta}} \log p(\mathbf{y} | \mathbf{X}, \boldsymbol{\theta})$ (maximum log-likelihood prior). By algebra, $\boldsymbol{\theta}^* = \arg \max_{\boldsymbol{\theta}} \log p(\mathbf{y} | \mathbf{X}, \boldsymbol{\theta}) = \arg \max_{\boldsymbol{\theta}} \log \mathcal{N}(\mathbf{y} | \mathbf{0}, \hat{\mathbf{K}}_{\mathbf{X}\mathbf{X}})$

This is a differentiable function, allowing gradient-based optimisation techniques.

Python: (scikit-learn)

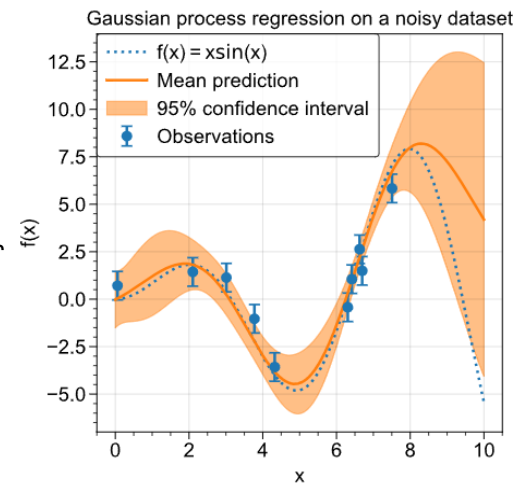
Gaussian process regression with one feature using the RBF kernel, showing the function $f(x)$ (mean) and $\pm 2\sigma$ range (95% confidence CI).

```
import numpy as np
import matplotlib.pyplot as plt
from sklearn.gaussian_process import GaussianProcessRegressor
from sklearn.gaussian_process.kernels import RBF

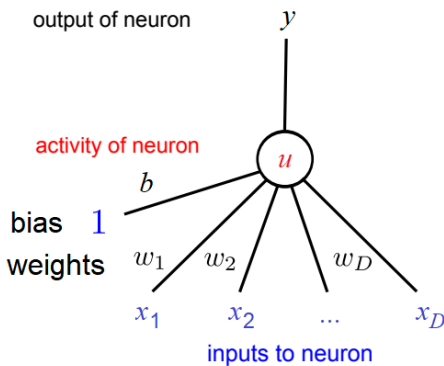
X = np.linspace(start=0, stop=10, num=1_000).reshape(-1, 1)
y = np.squeeze(X * np.sin(X))

training_indices = np.random.choice(np.arange(y.size),
                                     size=10, replace=False)
X_train, y_train = X[training_indices], y[training_indices]
NOISE_STD = 0.75 # measurement noise  $\epsilon$ 
y_train_noisy = y_train + np.random.normal(loc=0.0,
                                             scale=noise_std, size=y_train.shape)
kernel = 1 * RBF(length_scale=1.0, length_scale_bounds=(1e-2, 1e2)) # kernel function K
gaussian_process = GaussianProcessRegressor(kernel=kernel, alpha=NOISE_STD**2,
                                           n_restarts_optimizer=9)
gaussian_process.fit(X_train, y_train) # fit to observed data
print(gaussian_process.kernel_) # K multiplied by optimal  $\lambda$ 
mean_prediction, std_prediction = gaussian_process.predict(X, return_std=True)

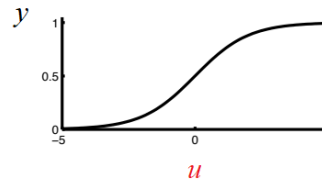
plt.plot(X, y, label=r"$f(x) = x \sin(x)$", linestyle="dotted")
plt.errorbar(X_train, y_train_noisy, NOISE_STD, linestyle="None", color="tab:blue",
             marker=".", markersize=10, label="Observations")
plt.plot(X, mean_prediction, label="Mean prediction")
plt.fill_between(X.ravel(), mean_prediction - 1.96 * std_prediction,
                 mean_prediction + 1.96 * std_prediction, color="tab:orange",
                 alpha=0.5, label=r"95% confidence interval")
plt.legend(); plt.xlabel("$x$"); plt.ylabel("$f(x)$")
plt.title("Gaussian process regression on a noisy dataset")
```



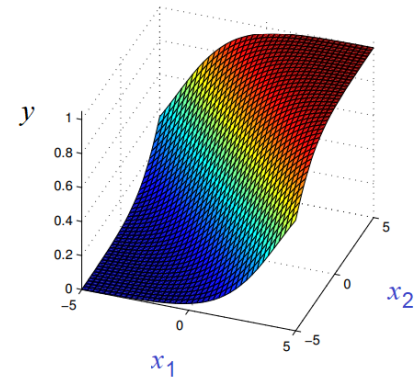
5.5.9. Logistic Regression (Classification, Supervised)



Schematic of a single neuron



Sigmoid: nonlinear activation function

Output for a binary classification task ($D=2$)

Activity (weighted sum): $u = w_1 x_1 + w_2 x_2 + \dots + w_D x_D + b$

Output: $z = \sigma(u) = \frac{1}{1 + \exp(-u)}$ (sigmoid: logistic curve)

The output of the network can be written as $y = f(\mathbf{x}; \mathbf{w})$. This can be interpreted as a (posterior) probability between 0 and 1 i.e. $y = p(z = 1 | \mathbf{x}, \mathbf{w})$ for a known label z .

The goodness-of-fit is measured by the log-likelihood objective function evaluated over N data points in a batch:

$$G(\mathbf{w}) = - \sum_{i=1}^N z^{(i)} \log y^{(i)} + (1 - z^{(i)}) \log (1 - y^{(i)}) \quad (\text{binary cross-entropy})$$

For multi-class classification i.e. $y = p(z = \mathbf{1} | \mathbf{x}, \mathbf{w})$, the softmax activation is applied before computing the loss (the categorical cross-entropy). (Note that if errors are Normally distributed i.e. in a regression / estimation problem, the ideal objective function is the mean-squared error (MSE):

$$G(\mathbf{w}) = \frac{1}{N} \sum (z^{(i)} - y^{(i)})^2$$

The aim of training is to find \mathbf{w} such that $G(\mathbf{w})$ is minimised i.e. $\mathbf{w}^* = \text{argmin} G(\mathbf{w})$. This is done by gradient descent i.e. $\mathbf{w} \leftarrow \mathbf{w} - \eta \nabla G$ i.e. $w_i \leftarrow w_i - \eta \frac{\partial G}{\partial w_i}$ (η : learning rate)

Common improvements to the gradient descent method are:

- Stochastic gradient descent (SGD): compute ∇G over a smaller sample (mini-batch).
- Adaptive step: allow η to vary e.g. AdaGrad, RMSProp, Adam)
- Regularisation: add $\alpha E(\mathbf{w}) = \frac{1}{2} \alpha \mathbf{w}^T \mathbf{w}$ to objective function, penalises extreme weights, preventing overfitting. α controls trade-off.

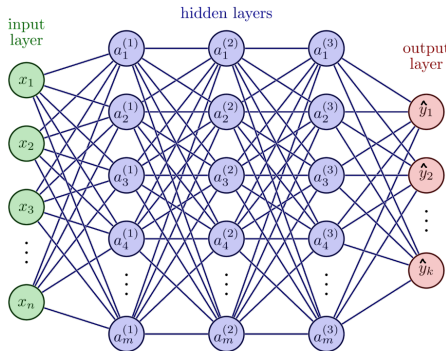
Single layer perceptrons generate linear decision regions, and can only be generalised by 1) manual 'feature engineering' or 2) adding more layers (MLPs, Section 5.5.10) to learn the feature transforms. The hidden layer activations represent the new features in latent space.

Python (scikit-learn):

```
from sklearn.linear_model import LogisticRegression
ans = LogisticRegression(penalty='l2', C=1.0).fit(X_train) # C = 1/alpha
y_pred = ans.predict(X_test)
```

5.5.10. Multilayer Perceptron (Feedforward / Fully Connected Neural Networks)

An MLP is a neural network which uses multiple neurons to allow multiple output dimensions. There are often 'hidden layers' of neurons which help in hierarchical pattern matching in the data.



- $a_j^{(L)}$: activation of neuron j in layer L of the network.
- $w_{j,i}^{(L)}$ ($i_{L-1} \rightarrow j_L$): weight from neuron i in layer $L - 1$ to neuron j in layer L .
- $b_j^{(L)}$ indicates the bias of neuron j in layer L .

These are typically compressed into vectors $\mathbf{a}^{(L)}$, $\mathbf{b}^{(L)}$ and matrices $\mathbf{W}^{(L)}$ for each layer.

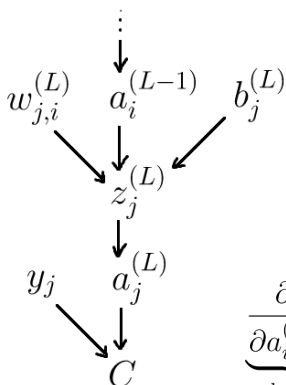
- Weighted sum: $\mathbf{z}^{(L)} = \mathbf{W}^{(L)} \mathbf{a}^{(L-1)} + \mathbf{b}^{(L)}$ (in batch normalisation, \mathbf{a} is standard scaled)
- Feedforward activation: $\mathbf{a}^{(L)} = \mathbf{f}(\mathbf{z}^{(L)})$ (\mathbf{f} : nonlinear function e.g. sigmoid, ReLU, tanh)
- Output cost: $C(\hat{\mathbf{y}}, \mathbf{y}) = \frac{1}{2} \sum_i (\hat{y}_i - y_i)^2$

Nonlinear Functions:

- Sigmoid: $\sigma(x) = (1 + e^{-x})^{-1}$, $\sigma'(x) = e^{-x} (1 + e^{-x})^{-2}$
- ReLU (rectified linear unit): $\text{ReLU}(x) = \max\{0, x\}$, $\text{ReLU}'(x) = \mathbf{I}_{\{x>0\}}$ ($x \neq 0$)
- Softmax: $(\mathbf{p}(\mathbf{x}))_i = e^{x_i} / \sum_j e^{x_j}$, $\left(\frac{\partial p}{\partial x_j}\right)_i = p_i(\mathbf{I}_{\{i=j\}} - p_j)$

Backpropagation: derivatives on computational graphs use the chain rule ($\dots \rightarrow h_{L-2} \rightarrow i_{L-1} \rightarrow j_L$)

To compute the gradient of C with respect to a weight in the **final** layer $w_{j,i}^{(L)}$:



$$\underbrace{\frac{\partial C}{\partial w_{j,i}^{(L)}}}_{\text{component of } \nabla C} = \underbrace{\frac{\partial C}{\partial a_j^{(L)}}}_{(a_j^{(L)} - y_j)} \times \underbrace{\frac{\partial a_j^{(L)}}{\partial z_j^{(L)}}}_{f'(z_j^{(L)})} \times \underbrace{\frac{\partial z_j^{(L)}}{\partial w_{j,i}^{(L)}}}_{a_i^{(L-1)}}$$

To compute the gradient of C with respect to a weight in a **further** layer $w_{i,h}^{(L-1)}$, sum over all final layer contributions when computing $\partial C / \partial a_i^{(L-1)}$:

$$\underbrace{\frac{\partial C}{\partial a_i^{(L-1)}}}_{\text{deeper layer}} = \sum_{j=1}^{n_L} \underbrace{\frac{\partial C}{\partial a_j^{(L)}}}_{(a_j^{(L)} - y_j)} \times \underbrace{\frac{\partial a_j^{(L)}}{\partial z_j^{(L)}}}_{f'(z_j^{(L)})} \times \underbrace{\frac{\partial z_j^{(L)}}{\partial a_i^{(L-1)}}}_{w_{j,i}^{(L)}} \quad \text{and} \quad \underbrace{\frac{\partial C}{\partial w_{i,h}^{(L-1)}}}_{\text{component of } \nabla C} = \underbrace{\frac{\partial C}{\partial a_i^{(L-1)}}}_{\text{deeper layer}} \times \underbrace{\frac{\partial a_i^{(L-1)}}{\partial z_i^{(L-1)}}}_{f'(z_i^{(L-1)})} \times \underbrace{\frac{\partial z_i^{(L-1)}}{\partial w_{i,h}^{(L-1)}}}_{a_h^{(L-2)}}$$

Gradient Descent: update weights by $\Delta \mathbf{W}_{n+1}^{(L)} = -\eta \nabla_{\mathbf{W}_n^{(L)}} C$. (C averaged over whole training set.)

Python Typical Implementation (TensorFlow with the Keras API):

```
from tensorflow.keras import Input, layers, models
model = models.Sequential(); model.add(Input(num_inputs, ...))
model.add(layers.Dense(num_neurons, ...)) # add as many hidden layers as desired
model.compile(optimizer=..., loss=..., metrics=...)
model.fit(X, y, epochs=..., batch_size=...) # training
model.evaluate(...); # check loss; model.predict(...) # testing
```

5.5.11. Techniques for Training Deep Neural Networks

Optimisations of the gradient descent algorithm:

- **Stochastic gradient descent (SGD):** compute ∇C per training example, rather than averaging over the whole training set (i.e. use batch size = 1). Decrease η over time to allow convergence.
- **Adam (adaptive moment estimation):** combines AdaGrad and RMSProp by keeping track of an exponentially decaying average (EMA) of past gradients and their squares.

Problems faced by deep neural networks and their solutions:

- **Unstable gradient problem** (vanishing gradient / exploding gradient): layers further from the output are harder to train in backpropagation. Resolved by using non-saturating activation functions (gradients do not fall to zero as $x \rightarrow \pm\infty$, e.g. leaky ReLU), using batch normalisation ($\mathbf{a}^{(L-1)}$ is standard scaled over a batch of values before evaluating the sum), and layer normalisation (or batch) can also be used in which $\mathbf{a}^{(L-1)}$ is standard scaled over the neurons in the layer.
- **Overfitting:** a model may perform well on training data but bad in unseen test data. Resolved by using a regularisation term in the loss function to prevent large weights from forming; using a recurrent dilution / dropout to randomly temporarily shrink / exclude neurons in training to force the network to generalise to wider patterns; and using pruning to drop unimportant weights, all of which reduce model complexity.
- **Internal covariate shift:** the erratic change in the distribution of neuron activations due to fluctuating data inputs and hence sharp changes to the weights. Mitigated by batch normalisation ($\mathbf{a}^{(L-1)}$ is standard scaled over a mini-batch of values before evaluating the sum).

Metric evaluation:

- **K-fold cross-validation:** Shuffle the data. Allocate a fixed proportion as the test data. Split the remaining data into K equal groups (folds). For each fold i in the folds, allocate fold i as the validation set and the remaining data as the training set, and train the data, and find performance on the validation set. Python: `from sklearn.model_selection import KFold`
- **Leave-one-out cross-validation (LOOCV):** K -fold CV but with $K =$ number of data points in training set i.e. use every data point once as the validation 'set'.

Hyperparameter optimisation: in Python, can use the keras-tuner library for TensorFlow models.

- **Grid search:** train models with all combinations of hyperparameters within a search space.
- **Random search:** train models with randomly chosen hyperparameters and locate good clusters.
- **Gradient-based optimisation** (hypernetworks): use gradient descent to find the optimal hyperparameters in the same way as a regular neural network finds its optimal weights.
- **Bayesian optimisation:** a probabilistic approach to estimate the optimal hyperparameters.
- **Evolutionary algorithm:** use a fitness function (e.g. CV) to rank performance, then select the best for crossover and mutation of (encoded) hyperparameters, run until desired performance is observed.

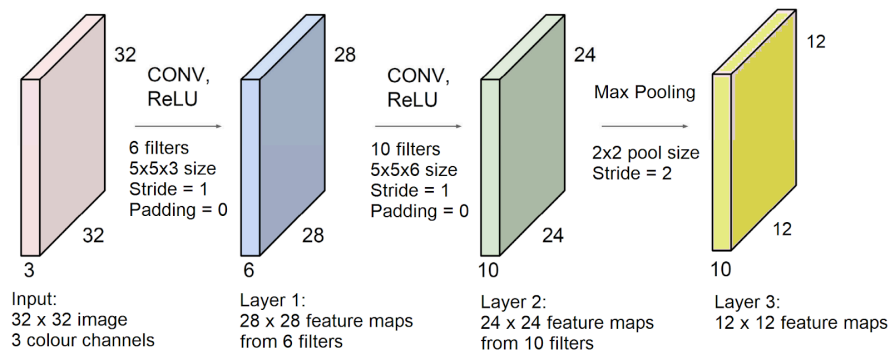
5.5.12. Convolutional Neural Networks (CNNs, ConvNets)

A CNN uses hidden layers consisting of convolution cells. CNNs are often used for computer vision, with each weight kernel representing a filter to identify a particular feature e.g. edges / blobs in early layers, more complex features in later layers. Each kernel is convolved against the input (Section 5.4.3) then adds an array-wide bias to produce a set of N activation maps, which are stacked into a 3 dimensional array and then subject to a pointwise nonlinear function.

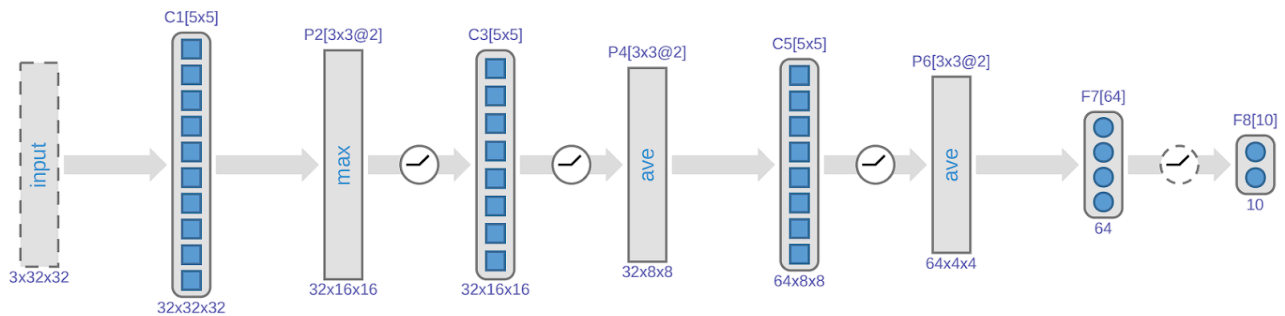
The hyperparameters for a convolutional layer are the number of filters N (number of neurons), the dimension of the filters $K \times K$ (kernel size), the stride S (step size) and the padding P (extend with zeros).

A convolutional layer takes an input array of dimension $W_1 \times H_1 \times D_1$ and produces an output of $W_2 \times H_2 \times D_2$, where $W_2 = \frac{W_1 - K + 2P}{S} + 1$, $H_2 = \frac{H_1 - K + 2P}{S} + 1$ and $D_2 = N$. An optional pooling layer (using an operation such as max pooling or average pooling) reduces the output size by subdividing the output into square arrays (per layer) and choosing the maximum or mean value. The stride for a pooling layer is usually equal to the pool size, so that there is no overlap between subarrays. With parameter sharing, it introduces a total of $(K^2 D_1 + 1)N$ parameters (weights + biases) per layer.

CNNs can be represented visually as transforming an array into different dimensions as blocks:



Another common notation is to label each layer symbolically:



($C_n[a \times b @ s]$: convolutional layer # n using $a \times b$ kernel and stride s , $P_n[a \times b @ s]$: pooling layer # n (max / average) using $a \times b$ subsampling and stride s , $F_n[N]$: fully connected layer # n with N neurons, $_/:$ ReLU activation, dashed border: applies dropout. The number of neurons is inferred from the last dimension $D = K$. Zero padding is assumed unless otherwise specified.)

The last layer of a convolutional neural network for classification is typically a fully connected (FC, dense) layer, with softmax activation, which takes in the flattened output array and produces a vector representing the classification probabilities.

1D convolutions can be used for short-term time series forecasting, for which they are faster to train than LSTMs, but are less capable of detecting longer term patterns. Hybrid CNN-LSTMs can be used to combine the strengths of both, and are useful for e.g. anomaly detection.

Data augmentation (image manipulation e.g. cropping, reflecting) can be used to artificially enlarge an image dataset to generate more images. This can also be used in the testing stage, where the testing set is augmented and predictions are based on the modification with the maximum output.

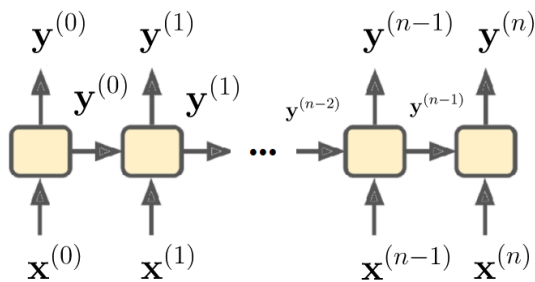
Python (Keras, TensorFlow): convolutional layers are added separately to pooling layers, e.g.

```
# for 32x32 pixel input RGB (3 dimensions) images
model.add(layers.Conv2D(32, (3, 3), activation='relu', input_shape=(32, 32, 3)))
model.add(layers.MaxPooling2D((2, 2)))
```

5.5.13. Recurrent Neural Networks

RNNs make predictions based on a sequence of inputs (typically in time) rather than a single input. Each input sequence can be represented by a data matrix \mathbf{X} (d variables \times n observations; transpose of convention used in Section 5.5.6). A batch of inputs can be represented as a rank 3 tensor (data matrices stacked along a third dimension: d variables \times n observations \times b sequences):

$$\mathbf{X} = \begin{bmatrix} x_0^{(0)} & x_0^{(1)} & \cdots & x_0^{(n)} \\ x_1^{(0)} & x_1^{(1)} & \cdots & x_1^{(n)} \\ \vdots & \vdots & \ddots & \vdots \\ x_d^{(0)} & x_d^{(1)} & & x_d^{(n)} \end{bmatrix} \quad \underline{\mathbf{B}} = [^{(0)}\mathbf{X} \quad ^{(1)}\mathbf{X} \quad \cdots \quad ^{(b)}\mathbf{X}]$$

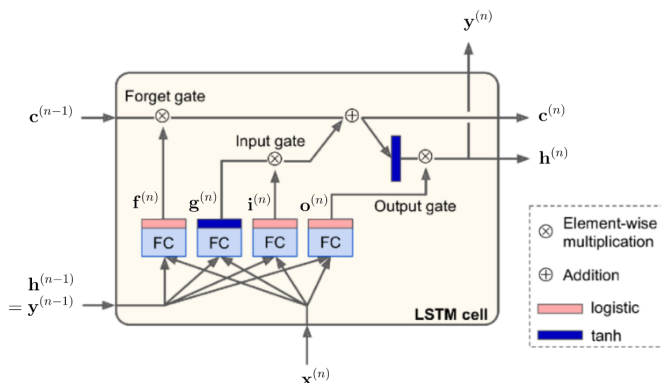


Each recurrent cell takes both an input observation $\mathbf{x}^{(j)}$ as well as the output of the previous cell (as its 'hidden state') $\mathbf{h}^{(j-1)} = \mathbf{y}^{(j-1)}$ to produce an output $\mathbf{y}^{(j)}$, giving the network an ability to recall previous values: $\mathbf{y}^{(j)} = \sigma(\mathbf{W}_x \mathbf{x}^{(j)} + \mathbf{W}_h \mathbf{y}^{(j-1)} + \mathbf{b}) = \sigma(\underline{\mathbf{W}} \mathbf{X}^{(j)})$ (\mathbf{W}_x : weight matrix for input, \mathbf{W}_h : weight matrix for hidden input, \mathbf{b} : bias vector, all identical over j)

Backpropagation Through Time (BPTT): unroll the network through time (as shown above), then use regular NN backpropagation. The cost function is based on the T most recent outputs (where T is a hyperparameter in truncated BPTT).

Layer Normalisation: standardise inputs to (or outputs from) $\sigma(\cdot)$ by learning an offset (mean) and scale (std.dev) for each observation.

Long Short Term Memory (LSTM): memory cells can recall further back.



Layer outputs are: $\mathbf{f}, \mathbf{g}, \mathbf{i}, \mathbf{o} = \sigma(\mathbf{W}_x \mathbf{x} + \mathbf{W}_h \mathbf{h} + \mathbf{b})$ for different weights in each FC.

Then $\mathbf{c}^{(n)} = \mathbf{c}^{(n-1)} \otimes \mathbf{f}^{(n)} + \mathbf{g}^{(n)} \otimes \mathbf{i}^{(n)}$ and $\mathbf{y}^{(n)} = \mathbf{o}^{(n)} \otimes \tanh \mathbf{c}^{(n)}$.

(FC: fully-connected (dense) layer, \mathbf{f} : forget gate controller, \mathbf{g}, \mathbf{i} : input gate controllers, \mathbf{o} : output gate controllers, \mathbf{c} : cell state, $\mathbf{h} = \mathbf{y}$: hidden state (output), \otimes : Hadamard (simple elementwise) matrix product)

Gated Recurrent Unit (GRU): a simplified LSTM which maintains similar performance.

5.5.14. Transformer Networks

Embeddings

Each token i is assigned an embedding vector e_i based on a lookup table. The token position is encoded by adding an orthogonal set of sinusoids.

Single Head Self Attention Mechanism: updates embeddings

- Compute the queries $\mathbf{Q} = \mathbf{W}_q \mathbf{E}$, keys $\mathbf{K} = \mathbf{W}_k \mathbf{E}$ and values $\mathbf{V} = \mathbf{W}_v \mathbf{E}$.
- Compute the attention pattern, $\mathbf{A} = \text{softmax}(\mathbf{Q}\mathbf{K}^T / d_k)$.
(input may be 'masked' setting all entries below the leading diagonal to $-\infty$, \mathbf{Q} : matrix of q_i , \mathbf{K} : matrix of k_i , d_k : dimension of query/key space, softmax is computed columnwise.)
- Compute the attention output $\Delta \mathbf{E} = \mathbf{A}\mathbf{V}$. The new embedding is then $\mathbf{E}' = \mathbf{E} + \Delta \mathbf{E}$.

The value weights \mathbf{W}_v is a low rank transformation matrix, implemented in non-square factorised form as $\mathbf{W}_v = \mathbf{W}_v^{(1)} \mathbf{W}_v^{(l)}$.

The attention pattern matrix size is $O(N^2)$ where N is the context size, making this a bottleneck in transformer architectures. Recent modifications have allowed for more scalable models (e.g. sparse attention mechanisms, blockwise attention, ring attention...).

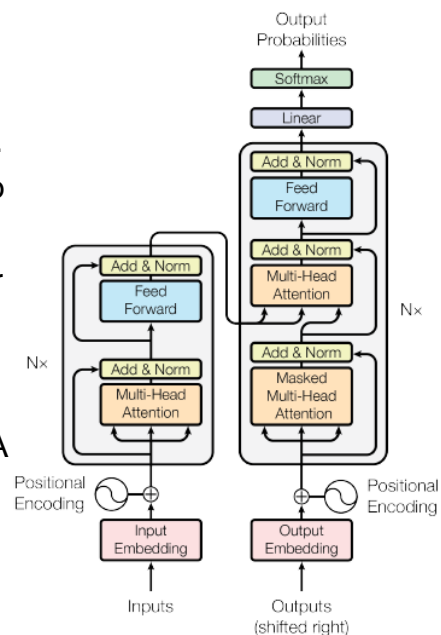
Cross Attention: the key and query matrices act on embeddings of two different token sets.

Multi Head Attention (MHA): run parallel single-head attentions, each with different parameters. Each head produces a change $\Delta \mathbf{E}^{(h)}$ which contributes to the overall change in \mathbf{E} . The computation $\Delta \mathbf{E} = \mathbf{A}\mathbf{V}$ is performed using only $\mathbf{W}_v^{(l)}$ in each head, then concatenating all $\mathbf{W}_v^{(1)}$ (output matrix) to compute the summed $\Delta \mathbf{E}$.

Transformer Architecture:

- The **encoder** block is an unmasked MHA followed by an MLP layer.
- The **decoder** block is a masked MHA, then an unmasked MHA also accepting inputs from the encoder block output, and an MLP layer.
- The transformer as a whole consists of a series of encoder-decoder blocks in series.

If the encoder is fed inputs, the decoder is fed outputs, and the decoder unmasked MHA takes the concatenation of the output MHA and encoder output (shown right), the transformer will be trained to predict the **next** token in the input (trained on shifted examples).



5.6.15. Modern Machine Learning Techniques

Large Datasets: used for Training in Machine Learning in Computer Vision

- **MNIST:** 70,000 28×28 grayscale images of 10 handwritten numerical digits (0-9).
- **CIFAR-10:** 60,000 32×32 RGB images of 10 object classes. (Also: CIFAR-100, 100 classes)
- **ImageNet:** 14 million images of 20,000 classes. (Also: ILSVRC 2012 subset for classification).
- **COCO:** 330,000 images of scenes segmented to 91 classes.
- **Labelled faces in the wild (LFW):** 13,000 images of labelled faces, for face recognition.

Successful Architectures in Computer Vision

- **VGG-16:** CNN, small kernels, frequent max pooling to reduce the number of parameters.
- **AlexNet:** 8-layer CNN, trained on ILSVRC 2012 on GPU.
- **ResNet:** deep CNN, residual blocks (identity layer/skip connections), trained on ILSVRC 2012.
- **Fully convolutional network (FCN):** replaces FC layers with 1×1 convolutional layers. Used for semantic segmentation (using interpolation, each pixel gets a prediction).
- **YOLO:** uses ResNet for instance segmentation (object detection). Can be run fast enough for real-time segmentation from live video on mid-range mobile GPUs.
- **Siamese network:** same weights applied to image pairs, trained with triplet/contrastive loss.
- **U-net:** downsampling (pooling) and upsampling (transposed convolution), extendable with e.g. spatial attention, skip connections in between. Used in biomedical image segmentation.
- **FaceNet:** face recognition, trained on LFW, generates embeddings per face, triplet loss.
- **Variational autoencoder:** input to encoder, output of decoder (with transposed convolution to scale up image). Uses 'evidence lower bound' (ELBO) loss function.
- **ViT (vision transformer).** Uses a transformer network with patches as tokens.

Some of these models are available pretrained in `tensorflow.keras`, others are open source elsewhere, trained on a particular dataset.

Successful Models in Natural Language Processing (NLP, LLMs) and Generative AI:

- **BERT:** first modern transformer used for various NLP purposes. Relatively hard to fine-tune.
- **GPT:** decoder-only transformer for text prediction. GPT-3 is single mode (text → text), while GPT-4 is multimodal (text/image → text). Has found commercial success (ChatGPT).
- **Gemini:** encoder-decoder transformer for (text → text), considered to outperform GPT-4.
- **DALL-E / Stable Diffusion / Midjourney:** generative AI using prompts (text → image).

These models are typically called from an API client side (MaaS: model as a service) rather than being embedded locally, as they contain billions to trillions of parameters (large file sizes).

Other notable leaps in AI technology have occurred in protein folding prediction (AlphaFold 3) and computational fluid dynamics. Generative models for (text → audio) and (text → video, e.g. Sora) have also emerged, with some debate as to their safety and practical usefulness, especially regarding the risks of distributing misleading or false content (e.g. deepfakes, misinformation, LLM hallucinations).

Adversarial Attacks: exploiting backpropagation (fast gradient sign method) to find the smallest possible change to an input image that would result in misclassification due to crossing decision boundaries in latent space. This is a serious concern for high dimensional networks ('the curse of dimensionality').

Transfer Learning: using a pretrained high-performing model as part of the architecture for another neural network with a different task, by freezing its weights and only training the additional layers. The base model acts as a feature extractor from which the additional layers complete the task. Fine tuning is achieved by unfreezing the base model weights.

Few-Shot Learning: learning with only a very small training dataset (few / one / zero per class).

Self-Supervised Learning (SSL): a method of training that can be applied to transformers (e.g. ViT). Models learn useful representations from unlabeled data by predicting parts of the data from other parts (e.g. predicting image patches or masked tokens in NLP).

Reinforcement Learning from Human Feedback (RLHF): the model learns a reward policy based on ranking feedback from human annotators, as a way to improve AI safety or content moderation.

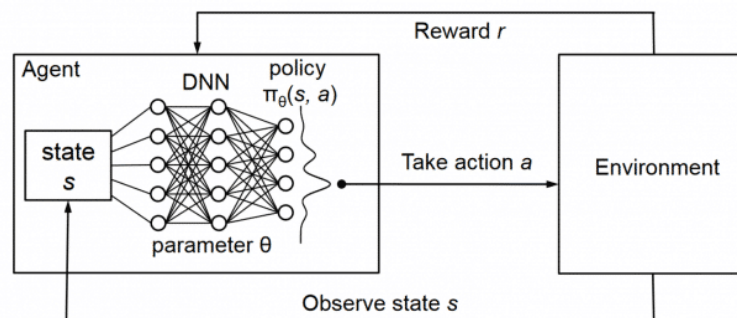
5.5.16. Reinforcement Learning (RL, Unsupervised Learning)

An agent makes decisions (actions) A based on the state of the environment S , using a decision rule (policy) $\pi : S \mapsto A$ (the function $p_\pi(a_n | s_n)$). Each action results in a transition to a new state with probability $p(s_{n+1} | s_n, a_n)$, and a reward signal $r_n(s_n, a_n)$.

- Discounted return: $G_n = \sum_{r=n}^{\infty} \gamma^{r-n} R_{r+1}$ where $0 < \gamma < 1$ is the discount rate.
- State-value function: $V_\pi(s_n) = E[G_n | S_n = s_n]$
- Action-value function: $Q_\pi(s_n, a_n) = E[G_n | S_n = s_n, A_n = a_n]$
- TD(0) update rule at time $n + 1$: $V(s_n) \leftarrow V(s_n) + \alpha(r_{n+1} + \gamma V(s_{n+1}) - V(s_n))$
- ϵ -greedy policy: choose optimal (greedy) $a_n = \operatorname{argmax} Q(s_n, a_n)$ with probability ϵ and choose a random (exploratory) $a_n \in A$ with probability $1 - \epsilon$.
- Q -learning (off-policy TD): find $\pi \in \Pi$ such that $Q_\pi(s_0, a_0)$ is maximised (optimal policy π^*)

$$Q(s_n, a_n) \leftarrow Q(s_n, a_n) + \alpha \left(r_{n+1} + \gamma \max_{a_{n+1}} \{Q(s_{n+1}, a_{n+1})\} - Q(s_n, a_n) \right)$$

Deep Reinforcement Learning / Deep Q Networks (DQN): parameterise $V(s_n; \theta)$ and/or $Q(s_n, a_n; \theta)$ where θ are the weights and biases of a neural network used to estimate the value functions given the state and action, instead of calculating explicitly, which is infeasible for large search spaces.



- Experience replay: store the agent's observations of $(s_n = s, a_n, r_n, s_{n+1} = s')$ in a replay buffer until a given batch size. Train a copy of the network by sampling from the buffer using the original action-values as the truth.
- Gradient of loss function with respect to parameter θ_i :

$$\nabla_{\theta_i} L(\theta_i) = \mathbb{E}_{s, a, r, s'} \left[\left(r + \gamma \max_{a'} Q(s', a'; \theta_i^-) - Q(s, a; \theta_i) \right) \nabla_{\theta_i} Q(s, a; \theta_i) \right]$$

5.5.17. Evolutionary (Genetic) Algorithms for Optimisation

Evolutionary algorithms (EAs) mimic the biological concept of ‘natural selection’ in order to optimise an objective function of the state \mathbf{x} . They are useful when this objective is a ‘black box’ function of a high-dimensional \mathbf{x} .

- Individual: a particular candidate solution \mathbf{x} to the optimisation problem
- Population: a set of individuals
- Genes: encodes the state \mathbf{x} of an individual

Topology Optimisation

Evolutionary algorithms have been applied to topology optimisation in engineering design of load-efficient structures, using e.g. the solid isotropic material with penalisation (SIMP).

5.5.18. Python Examples of Various Machine Learning Tasks

For exploratory data analysis (EDA), Jupyter Notebooks (.ipynb files) can be used to execute one cell block of code at a time, view results step by step, and annotate code.

Loading and Cleaning a Dataset: in this example, from an Excel workbook (.xlsx file)

```
import pandas as pd
X = pd.read_excel('path/to/dataset.xlsx', sheet_name='InputData')
y = pd.read_excel('path/to/dataset.xlsx', sheet_name='OutputData')
null_indices = y[y.isnull().any(axis=1)].index # get rows with null values
X.drop(null_indices, inplace=True) # X: pd.DataFrame
y.drop(null_indices, inplace=True) # y: pd.DataFrame
```

Exploratory Data Analysis: display a report showing various useful metrics.

```
from ydata_profiling import ProfileReport
ProfileReport(df)
```

Standard Scaling and Exploratory Principal Component Analysis: show a scree plot.

```
from matplotlib import pyplot as plt
import numpy as np
from sklearn.preprocessing import StandardScaler
from sklearn.decomposition import PCA

X_std = StandardScaler().fit_transform(X)
pca = PCA(n_components=None)
df_pca = pd.DataFrame(pca.fit_transform(X_std))
explained_variance = pca.explained_variance_ratio_
plt.plot(range(1, len(explained_variance) + 1), explained_variance,
         label='Explained Variance')
plt.plot(range(1, len(explained_variance) + 1),
         np.cumsum(explained_variance), label='Cumulative Explained Variance')
plt.xlabel('Number of Components \n ($n$th largest eigenvalue, descending)')
plt.ylabel('Explained Variance \n (proportion of total variance)')
plt.legend()
plt.title('Principal Component Analysis: Scree plot')
plt.show()
```

Pipelines for Regression Algorithms: train models for 1) linear regression and 2) support vector regression including PCA and polynomial regression with regularisation (lasso). K -fold cross-validation is used and grid search is used for hyperparameter optimisation. The models are evaluated on various error metrics and then saved/loaded to/from the disk.

```

from sklearn.model_selection import train_test_split, GridSearchCV
from sklearn.preprocessing import StandardScaler, PolynomialFeatures
from sklearn.decomposition import PCA
from sklearn.linear_model import Lasso
from sklearn.pipeline import Pipeline
from sklearn.metrics import mean_absolute_error, mean_squared_error
from sklearn.svm import SVR
from sklearn.multioutput import MultiOutputRegressor
import joblib

pipeline_lasso = Pipeline([('scaler', StandardScaler()),
                           ('pca', PCA(n_components=5)), ('poly', PolynomialFeatures(degree=2)),
                           ('lasso', Lasso())])
pipeline_svr = Pipeline([('scaler', StandardScaler()),
                          ('svr', MultiOutputRegressor(SVR()))])

param_grid_lasso = {'lasso__alpha': [0.001, 0.005, 0.01, 0.05, 0.1, 0.5, 1.0]}
param_grid_svr = {'svr__estimator__C': [0.001, 0.01, 0.1],
                  'svr__estimator__epsilon': [0.001, 0.01, 0.1]}

def train_model(X: np.ndarray, y: np.ndarray, pipeline: Pipeline,
                param_grid: dict[str: list], model_name: str = '',
                test_size: float = 0.2, cv: int = 10,
                scoring: str = 'neg_mean_squared_error') -> Pipeline:

    mae = lambda y_test, y_pred: mean_absolute_error(y_test, y_pred)
    rmse = lambda y_test, y_pred: mean_squared_error(y_test, y_pred, squared=False)

    X_train, X_test, y_train, y_test = train_test_split(X, y, test_size=test_size)
    search = GridSearchCV(estimator=pipeline, param_grid=param_grid, cv=cv,
                          scoring=scoring)
    search.fit(X_train, y_train)
    best_model = search.best_estimator_
    y_pred = best_model.predict(X_test)
    print(f'{model_name} - Best hyperparameters: {search.best_params_}')
    print(f'MAE: {mae(y_test, y_pred)}, RMSE: {rmse(y_test, y_pred)}')
    return best_model

lasso_model = train_model(X, y, pipeline_lasso, param_grid_lasso, model_name='Lasso')
svr_model = train_model(X, y, pipeline_svr, param_grid_svr, model_name='SVR')
joblib.dump(lasso_model, 'path/to/output/lasso_model.joblib')
lasso_model = joblib.load('path/to/output/lasso_model.joblib')

```

Pipelines for Neural Networks: train a CNN for multi-class image classification with one-hot encoding with pooling, dropout and batch normalisation layers, a validation set, and hyperparameter optimisation. Training neural networks can be computationally intensive, so it can help to use cloud computing (e.g. Google Colab/Cloud Platform, AWS) with access to hardware accelerators (GPUs and TPUs).

```

from matplotlib import pyplot as plt
import numpy as np; import pandas as pd; import cv2; import os
from sklearn.model_selection import train_test_split
from tensorflow.keras.models import Sequential, load_model
from tensorflow.keras.layers import Input, MaxPooling2D, \
    Reshape, Flatten, Dense, Dropout, Conv2D, BatchNormalization
from tensorflow.keras.callbacks import TensorBoard
from keras_tuner.tuners import BayesianOptimization
from keras_tuner.engine.hyperparameters import HyperParameters

tensorboard_callback = TensorBoard(log_dir='model_logs/fit', histogram_freq=1,
    write_graph=True, update_freq='epoch')
df_X = pd.DataFrame(columns=['img', 'gender'], index=None)
folder_names = ['imgs/men', 'imgs/women']
for folder_name in folder_names:
    for file in os.listdir(folder_name):
        img_arr = cv2.imread(os.path.join(folder_name, file), cv2.IMREAD_GRAYSCALE)
        img_arr = cv2.resize(img_arr, (96, 96))
        row = pd.DataFrame({'img': [img_arr], 'gender': [folder_name.split('/')[-1]]})
        df_X = pd.concat([df_X, row], ignore_index=True)
df_y = pd.get_dummies(df_X['gender'])
df_X.drop('gender', axis=1, inplace=True)
X, y = np.array(df_X['img'].tolist()), df_y.values.astype(np.float32)
X_train, X_test, y_train, y_test = train_test_split(X, y, test_size=1/10)
X_train, X_val, y_train, y_val = train_test_split(X_train, y_train, test_size=1/9)

def build_convnet_model(hp: HyperParameters) -> Sequential:
    model_cnn = Sequential()
    model_cnn.add(Input(shape=(96, 96)))
    model_cnn.add(Reshape((96, 96, 1)))
    model_cnn.add(Conv2D(hp.Int('filters_1', min_value=64, max_value=256, step=32),
        kernel_size=hp.Int('size_1', min_value=2, max_value=4, step=1), activation='relu'))
    model_cnn.add(BatchNormalization())
    model_cnn.add(MaxPooling2D(pool_size=(2, 2)))
    model_cnn.add(Dropout(0.25))
    model_cnn.add(Conv2D(hp.Int('filters_2', min_value=8, max_value=32, step=8),
        kernel_size=hp.Int('size_2', min_value=4, max_value=8, step=2), activation='relu'))
    model_cnn.add(BatchNormalization())
    model_cnn.add(MaxPooling2D(pool_size=(2, 2)))
    model_cnn.add(Dropout(0.25))
    model_cnn.add(Flatten())
    model_cnn.add(Dense(hp.Int('nodes_fc', min_value=32, max_value=96, step=32), activation='relu'))
    model_cnn.add(Dense(2, activation='softmax'))
    model_cnn.compile(optimizer='adam', loss='categorical_crossentropy', metrics=['accuracy'])
    return model_cnn

tuner = BayesianOptimization(build_convnet_model, objective='val_loss', max_trials=10,
    directory='tuner_dir', project_name='model_tuner')
tuner.search(X_train, y_train, epochs=100, validation_data=(X_val, y_val))
best_model = tuner.get_best_models(num_models=1)[0]
best_hyperparameters = tuner.get_best_hyperparameters(num_trials=1)[0]
best_hist = best_model.fit(X_train, y_train, epochs=200, batch_size=128,
    validation_data=(X_val, y_val), callbacks=[tensorboard_callback])
plt.plot(best_hist.history['loss'], label='Training Loss')
plt.plot(best_hist.history['val_loss'], label='Validation Loss')
plt.xlabel('Epoch'); plt.ylabel('Loss'); plt.yscale('log'); plt.legend(loc='upper right'); plt.show()
best_loss = best_model.evaluate(X_test, y_test)
print(f'{best_hyperparameters.values}, loss: {best_loss}')
best_model.save('path/to/output/image_classifier.keras')
best_model = load_model('path/to/output/image_classifier.keras')

```

Pipelines for Neural Networks: train a hybrid CNN-LSTM for one-step-ahead multivariate time series forecasting, with pooling/dropout layers, a validation set, and hyperparameter optimisation.

```
import numpy as np; from matplotlib import pyplot as plt
from sklearn.preprocessing import StandardScaler; from sklearn.model_selection import train_test_split
from tensorflow.keras.models import Sequential
from tensorflow.keras.layers import Input, MaxPooling1D, TimeDistributed,
    Reshape, Flatten, Dense, Dropout, LSTM, Conv1D
from tensorflow.keras.callbacks import TensorBoard
from keras_tuner.tuners import BayesianOptimization; from keras_tuner.engine.hyperparameters import HyperParameters

tensorboard_callback = TensorBoard(log_dir='model_logs/fit', histogram_freq=1,
    write_graph=True, update_freq='epoch')
df = pd.read_excel('time_series_data.xlsx', sheet_name='Daily')
LOOKBACK, FEATURES = 30, 2 # predict the 31st value of a given subsequence with 2 features
scaler = StandardScaler() # df: pd.DataFrame with features in columns
df_scaled = scaler.fit_transform(df[['adj_close_returns', 'volume_change']].values.reshape(-1, FEATURES))
# generate sliding window arrays (subsequences) from time series data
X = np.lib.stride_tricks.sliding_window_view(df_scaled, (LOOKBACK, FEATURES))
X = X.reshape((X.shape[0], X.shape[2], FEATURES)); y = X[1:, -1, :]; X = X[:-1, :, :]
X_train, X_test, y_train, y_test = train_test_split(X, y, test_size=1/10) # train:val:test = 80:10:10
X_train, X_val, y_train, y_val = train_test_split(X_train, y_train, test_size=1/9)

def build_model(hp: HyperParameters) -> Sequential:
    model = Sequential()
    model.add(Input(shape=(LOOKBACK, FEATURES)))
    model.add(Reshape((-1, LOOKBACK, FEATURES)))
    model.add(TimeDistributed(Conv1D(filters=hp.Int('filters_1', min_value=64, max_value=256, step=32),
        kernel_size=hp.Choice('kernel_1', values=[3, 5]), activation='relu')))
    model.add(TimeDistributed(Conv1D(filters=hp.Int('filters_2', min_value=32, max_value=128, step=32),
        kernel_size=hp.Choice('kernel_2', values=[3, 5]), activation='relu')))
    model.add(TimeDistributed(MaxPooling1D(pool_size=2)))
    model.add(TimeDistributed(Flatten()))
    model.add(LSTM(units=hp.Int('units_1', min_value=32, max_value=128, step=32), activation='relu',
        return_sequences=True))
    model.add(Dropout(rate=hp.Float('dropout_1', min_value=0.1, max_value=0.5, step=0.1)))
    model.add(LSTM(units=hp.Int('units_2', min_value=16, max_value=64, step=16), activation='relu'))
    model.add(Dropout(rate=hp.Float('dropout_2', min_value=0.1, max_value=0.5, step=0.1)))
    model.add(Dense(units=FEATURES, activation='linear'))
    model.compile(optimizer='adam', loss='mse')
    return model

tuner = BayesianOptimization(build_model, objective='val_loss', max_trials=10,
    directory='tuner_dir', project_name='model_tuner')
tuner.search(X_train, y_train, epochs=100, validation_data=(X_val, y_val))
best_model = tuner.get_best_models(num_models=1)[0]
best_hyperparameters = tuner.get_best_hyperparameters(num_trials=1)[0]
best_hist = best_model.fit(X_train, y_train, epochs=200, batch_size=128, validation_data=(X_val, y_val),
    callbacks=[tensorboard_callback])
plt.plot(best_history.history['loss'], label='Training Loss')
plt.plot(best_history.history['val_loss'], label='Validation Loss')
plt.xlabel('Epoch'); plt.ylabel('Loss'); plt.yscale('log'); plt.legend(loc='upper right'); plt.show()
best_loss = best_model.evaluate(X_test, y_test)
print(f'{best_hyperparameters.values}, MSE: {best_loss}')
best_model.save('path/to/output/time_series_forecasting.keras')
best_model = load_model('path/to/output/time_series_forecasting.keras')
```

5.6. Computer Vision and Computer Graphics

5.6.1. Representation and Processing of Digital Images

An image can be represented as a $w \times h \times c$ array (w : width in pixels, h : height in pixels, c : number of colour channels e.g. 3 for RGB, 1 for grayscale or monochrome). Each entry in the array is a binary number representing the intensity of the indicated pixel colour. The number of bits used per component channel is the 'bit depth'.

Common standard image dimensions are 640×480 (VGA), 1280×720 (HD), 4096×2160 (4K).

Common colour spaces are RGB(A) (red, green, blue, (alpha)), HSV (hue, saturation, value), CMYK (cyan, yellow, magenta, key/black), L*a*b* (lightness, green-red, blue-yellow), YUV / YCbCr.

Gamma correction: adjusts displayed intensities to account for the perceived nonlinearity of the different colour channels over the range of displayable colours (the gamut).

Image size [MB] = $\frac{\text{bit depth [b]}}{8} \times c \times h \times w \times 10^{-6}$ (+ storage of metadata, no coding/compression)

Conversion of the 3D World to a 2D Image: information is inevitably lost.

The intensity of a pixel $I(x, y)$ is dependent on the position/orientation of the camera, the geometry of the scene, the nature and distribution of light sources, the reflectance spectra of the surfaces (specular or diffuse/Lambertian), and the properties of the lens and CCD. Occlusion may obscure features of specific objects in a scene. In most practical situations, these factors do not affect the desired outcome, so data processing is required to prepare images with features independent of this 'noise'.

Image Processing in the Fourier Domain: useful for analysing filtering operations

Operations can be represented as convolution with a kernel, or multiplication in the Fourier domain.

1D Gaussian kernel: $g_{\sigma}(x) = \frac{1}{\sigma\sqrt{2\pi}} e^{-\frac{x^2}{2\sigma^2}} \Rightarrow G_{\sigma}(k) = e^{-\frac{k^2\sigma^2}{2}}$ (unnormalised Gaussian with std.dev $\frac{1}{\sigma}$)

2D Gaussian kernel: $g_{\sigma}(x, y) = \frac{1}{2\pi\sigma^2} e^{-\frac{x^2+y^2}{2\sigma^2}} \Rightarrow G_{\sigma}(k_x, k_y) = e^{-\frac{(k_x^2+k_y^2)\sigma^2}{2}}$, discretised: $(-n, -n) \leq (x, y) \leq (n, n)$

2D discrete convolution: $(w * I)(x, y) = \sum_{i=-n}^n \sum_{j=-n}^n w(i, j) I(x - i, y - j)$ (\mathbf{W} : $(2n + 1) \times (2n + 1)$ kernel array)

$O(n^2)$ 2D convolution as repeated $O(n)$ 1D convolution: $(w * I)(x, y) = w(x) * (w(y) * I(x, y))$

Differentiation as a convolution: $\frac{\partial S}{\partial x} = \frac{S(x+1, y) - S(x-y)}{2} = S(x, y) * [\frac{1}{2}, 0, \frac{-1}{2}]$

Directional derivative: $\nabla S \cdot \mathbf{n} = D_{\mathbf{n}} S(\mathbf{x}) = S_{\mathbf{n}}(\mathbf{x}) \approx S(\mathbf{x} + \mathbf{n}) - S(\mathbf{x})$.

Gradient of a convolution: $\nabla^n s_{\sigma}(x, y) = \nabla^n G_{\sigma}(x, y) * I(x, y)$

Laplacian is approximately a Difference of Gaussians (DoG): $g_{k\sigma}(x, y) - g_{\sigma}(x, y) \approx (k - 1)\sigma^2 \times \nabla^2 g_{\sigma}(x, y)$

Smoothing (low pass filter): $S(x, y) = (g_{\sigma} * I)(x, y) = \sum_{i=-n}^n \sum_{j=-n}^n g_{\sigma}(i, j) I(x - i, y - j)$

5.6.2. Feature Detection

Edge Detection: edges represent regions of sharp change in intensity (max gradient).

Canny edge detection algorithm: **1)** smooth: $s_\sigma = g_\sigma * I$, **2)** gradient: ∇_{s_σ} , **3)** non-maximal suppression: place 'edgels' where $|\nabla_{s_\sigma}|$ exceeds neighbours in directions $\pm \nabla_{s_\sigma}$, **4)** threshold by $|\nabla_{s_\sigma}|$.

Marr-Hildreth detection algorithm: **1)** Laplacian: $\nabla^2 g_\sigma * I$ by DoG approximation, **2)** find zeroes.

The motion of an edge cannot be inferred by looking at edges along (the aperture problem).

Corner Detection: corners have discontinuity in two separate directions (cross correlation)

$$C_n(x, y) = \frac{\mathbf{n}^T \mathbf{A} \mathbf{n}}{\mathbf{n}^T \mathbf{n}} \quad \mathbf{A} = \begin{bmatrix} \langle S_x^2 \rangle & \langle S_x S_y \rangle \\ \langle S_x S_y \rangle & \langle S_y^2 \rangle \end{bmatrix} \quad \lambda_1 \leq C_n(x, y) \leq \lambda_2$$

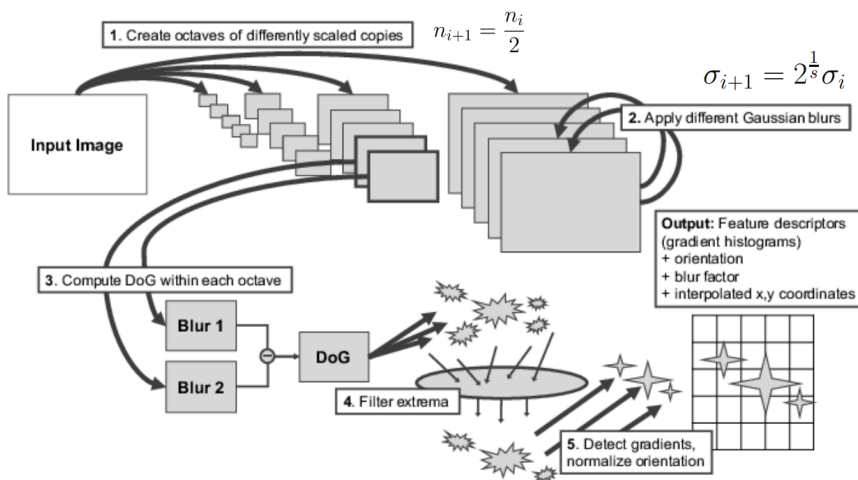
Smoothed directional derivative of $I(x, y)$ in the direction of \mathbf{n} where $\langle S \rangle = s_\sigma = g_\sigma * I$ and $S_x = \partial S / \partial x$, etc. (λ_1, λ_2) : eigenvalues of \mathbf{A}

Harris-Stephens corner detection algorithm: **1)** cross-correlation: $\mathbf{A}(x, y)$, **2)** find $\lambda_1 \lambda_2 = \det \mathbf{A}$ and $\lambda_1 + \lambda_2 = \text{tr } \mathbf{A}$, **3)** threshold by $\lambda_1 \lambda_2 - \kappa(\lambda_1 + \lambda_2)^2$ for some small parameter κ .

If the eigenvalues are both large and distinct, then a corner is likely present.

Blob Detection: round regions enclosed by edges, indicative of keypoints

$|\sigma^2 \nabla^2 s_\sigma(x, y)|$ acts as a normalised 'blob detector' for features at length scale σ (it is a band pass filter). The circular blob diameter with maximum response is $d = 2\sqrt{2}\sigma$.



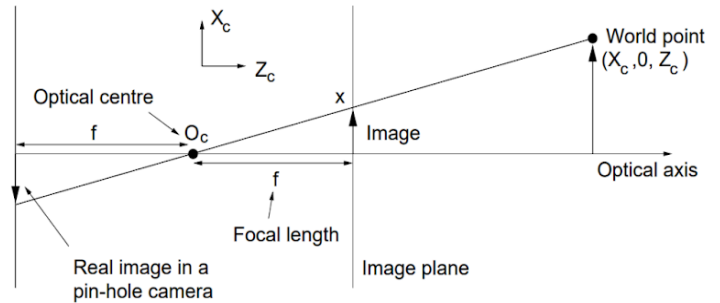
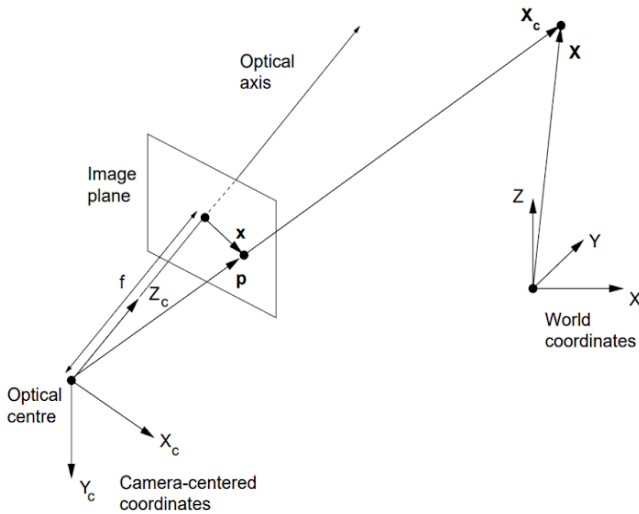
SIFT Feature Detection: **1)** create copies at sizes $n_{i+1} = n_i / 2$ by subsampling (i : octave number), **2)** apply sequential blurs in each octave, $\sigma_{j+1} = 2^{1/8} \sigma_j$ (j : index within octave), **3)** find $s_{j+1} - s_j$ in each octave (represents $\propto \nabla^2 s_j$ due to DoG approx), **4)** threshold to identify keypoints, **5)** sample Gaussian-weighted 16×16 patch at correct scale around keypoint, **6)** histogram of oriented gradients (HoG) in 4×4 subcells, **7)** concat to a vector, **8)** normalise, truncate outliers ($> 0.2 \rightarrow 0.2$), renormalise. The output is a 128-vector per patch.

The SIFT descriptors for a given keypoint feature can be compared (for recognition tasks) by k nearest neighbours on a k -D tree (Section 5.5.16) or passed to a neural network for classification.

Image texture can be characterised by a repeated feature patch (textons).

5.6.3. Planar Perspective Projection

A planar perspective projection of a 3D object in the world is the enlargement about an optical centre point onto an image plane. Assumptions: pinhole camera, no nonlinear distortion.



$$\mathbf{X}_c = (X_c, Y_c, Z_c), \quad \mathbf{x} = (x, y) \text{ at } z = f$$

$$\text{Images are projected through } O_c: \tilde{\mathbf{x}} = \frac{f}{Z_c} \mathbf{X}_c$$

Homogeneous Coordinates: point $\mathbf{X} = (X, Y, Z)$ represented as $\tilde{\mathbf{X}} = [sX, sY, sZ, s]^T$. (WLOG $s = 1$).

If $\tilde{\mathbf{X}} = [X_1, X_2, X_3, X_4]^T$ then $\mathbf{X} = (X_1/X_4, X_2/X_4, X_3/X_4)$.

If $X_4 = 0$ then \mathbf{X} is the point at infinity in direction $[X_1, X_2, X_3]^T$.

1. Rotation in Homogeneous Coordinates:

where $\tilde{\mathbf{X}} = [X, Y, Z, 1]^T$ and $\tilde{\mathbf{X}}_c = [X_c, Y_c, Z_c, 1]^T$.

(\mathbf{R} : 3×3 rotation matrix, \mathbf{T} : 3×1 translation vector; in Cartesian, $\mathbf{X}_c = \mathbf{R}\mathbf{X} + \mathbf{T}$.)

$$\tilde{\mathbf{X}}_c = \underbrace{\begin{bmatrix} r_{xx} & r_{xy} & r_{xz} & t_x \\ r_{yx} & r_{yy} & r_{yz} & t_y \\ r_{zx} & r_{zy} & r_{zz} & t_z \\ 0 & 0 & 0 & 1 \end{bmatrix}}_{\text{affine rotation: } \mathbf{P}_r = [\mathbf{R}|\mathbf{T}]} \tilde{\mathbf{X}}$$

2. Projection in Homogeneous Coordinates:

for perspective projection, $3D \rightarrow 2D$.

(f : focal length for perspective projection)

$$\tilde{\mathbf{x}} = \underbrace{\begin{bmatrix} f & 0 & 0 & 0 \\ 0 & f & 0 & 0 \\ 0 & 0 & 1 & 0 \end{bmatrix}}_{\tilde{\mathbf{P}}_p: \text{projection}} \tilde{\mathbf{X}}_c = \begin{bmatrix} fX_c \\ fY_c \\ Z_c \end{bmatrix} \rightarrow \mathbf{x} = \begin{bmatrix} fX_c/Z_c \\ fY_c/Z_c \end{bmatrix}$$

3. CCD Imaging in Homogeneous Coordinates:

where $\tilde{\mathbf{w}} = [u, v, 1]^T$ and $\tilde{\mathbf{x}} = [x, y, 1]^T$

((k_u, k_v): pixel length scales, (u_0, v_0): optical centre offset)

$$\tilde{\mathbf{w}} = \underbrace{\begin{bmatrix} k_u & 0 & u_0 \\ 0 & k_v & v_0 \\ 0 & 0 & 1 \end{bmatrix}}_{\mathbf{P}_c: \text{imaging}} \tilde{\mathbf{x}}$$

Overall, $\tilde{\mathbf{w}} = \mathbf{P}_c \mathbf{P}_p \tilde{\mathbf{X}}$. Intrinsic camera calibration matrix is $\mathbf{K} = \mathbf{P}_c \mathbf{P}_p$. Matrix $\mathbf{P}_r = [\mathbf{R}|\mathbf{T}]$ is extrinsic.

Then, $\tilde{\mathbf{w}} = \mathbf{K}[\mathbf{R}|\mathbf{T}] \tilde{\mathbf{X}} = \mathbf{P}_{ps} \tilde{\mathbf{X}}$ where \mathbf{P}_{ps} is the camera projection matrix (3×4 , 10 dof).

A general 'projective camera model' refers to any 3×4 matrix \mathbf{P}_{ps} , which can have 11 dof (constrain by either enforcing $\|\mathbf{P}\| = 1$ or setting $P_{34} = 1$.)

Geometry in Homogeneous Coordinates

- Point in image: $\mathbf{w} = [u, v]^T \rightarrow \tilde{\mathbf{w}} = [u, v, 1]^T$, with reconstructed ray in camera coordinates $\mathbf{X}_c = \mathbf{0} + \lambda \tilde{\mathbf{w}} \rightarrow \mathbf{r} = \lambda [u, v, 1]^T$ (from the optical centre through the point in image plane)
- Line in image: $\mathbf{l}^T \tilde{\mathbf{w}} = 0 \rightarrow l_1 u + l_2 v + l_3 = 0$.
- Intersection of two image lines $\mathbf{l}_1^T \tilde{\mathbf{w}} = 0$ and $\mathbf{l}_2^T \tilde{\mathbf{w}} = 0$ occurs at $\tilde{\mathbf{w}} = \mathbf{l}_1 \times \mathbf{l}_2$.
- Vanishing point (VP) of a line: $\lim_{\lambda \rightarrow \infty} \mathbf{X} = \mathbf{a} + \lambda [a, b, c]^T$ projects to $\tilde{\mathbf{w}} = \mathbf{P}_{ps}[a, b, c, 0]^T$.
- Horizon of a plane $\mathbf{X} = \mathbf{a} + \lambda [a, b, c]^T + \mu [d, e, f]^T$ projects to the line connecting the vanishing points $\tilde{\mathbf{w}}_1 = \mathbf{P}_{ps}[a, b, c, 0]^T$ and $\tilde{\mathbf{w}}_2 = \mathbf{P}_{ps}[d, e, f, 0]^T$, equivalently $\mathbf{l} = \tilde{\mathbf{w}}_1 \times \tilde{\mathbf{w}}_2$.
- Parallel world **lines** have the **same vanishing point**.
- Parallel world **planes** have the **same horizon**.

Camera Calibration: find 3×4 projective camera matrix $\mathbf{w} = \mathbf{P}_{ps}\mathbf{X}$ (11 dof) from a known set $\{\mathbf{w}, \mathbf{X}\}_i$

Points $\mathbf{w}_i = [su_i, sv_i, s]^T$ and $\mathbf{X}_i = [X_i, Y_i, Z_i, 1]^T$ are given. The equations to solve are

$$u_i = \frac{su_i}{s} = \frac{p_{11}X_i + p_{12}Y_i + p_{13}Z_i + p_{14}}{p_{31}X_i + p_{32}Y_i + p_{33}Z_i + p_{34}} \quad \text{and} \quad v_i = \frac{sv_i}{s} = \frac{p_{21}X_i + p_{22}Y_i + p_{23}Z_i + p_{24}}{p_{31}X_i + p_{32}Y_i + p_{33}Z_i + p_{34}}$$

$$\begin{bmatrix} X_1 & Y_1 & Z_1 & 1 & 0 & 0 & 0 & -u_1 X_1 & -u_1 Y_1 & -u_1 Z_1 & -u_1 \\ 0 & 0 & 0 & 0 & X_1 & Y_1 & Z_1 & -v_1 X_1 & -v_1 Y_1 & -v_1 Z_1 & -v_1 \\ \vdots & \vdots & \vdots & \vdots & \vdots & \vdots & \vdots & \vdots & \vdots & \vdots & \vdots \\ X_n & Y_n & Z_n & 1 & 0 & 0 & 0 & -u_n X_n & -u_n Y_n & -u_n Z_n & -u_n \\ 0 & 0 & 0 & 0 & X_n & Y_n & Z_n & -v_n X_n & -v_n Y_n & -v_n Z_n & -v_n \end{bmatrix} \begin{bmatrix} p_{11} \\ p_{12} \\ p_{13} \\ p_{14} \\ p_{21} \\ p_{22} \\ p_{23} \\ p_{24} \\ p_{31} \\ p_{32} \\ p_{33} \\ p_{34} \end{bmatrix} = \mathbf{0}$$

← n points yields the linear system of equations $\mathbf{A}\mathbf{p} = \mathbf{0}$. Solve by orthogonal least squares (\mathbf{p} = eigenvector of $\mathbf{A}^T\mathbf{A}$ corresponding to smallest eigenvalue, found via SVD: last column of \mathbf{V} in $\mathbf{A} = \mathbf{U}\mathbf{\Sigma}\mathbf{V}^T$)

If using the constraint $P_{34} = 1$, can write in the form $\mathbf{A}\mathbf{p} = \mathbf{b}$ and solve by (psuedo)inverse (i.e. ordinary least squares) $\mathbf{p} = (\mathbf{A}^T\mathbf{A})^{-1}\mathbf{A}^T\mathbf{b}$.

Refine \mathbf{p} to optimise the reprojection errors: $\mathbf{P}_{ps} = \text{argmin} \left\{ \sum_{i=1}^N (u_i - \hat{u}_i)^2 + (v_i - \hat{v}_i)^2 \right\}$ where $[s\hat{u}_i, s\hat{v}_i, s]^T = \mathbf{P}_{ps}\mathbf{X}_i$.

The ‘RQ’ decomposition of top-left 3×3 submatrix of \mathbf{P}_{ps} yields $\mathbf{K}\mathbf{R}$, and $\mathbf{T} = \mathbf{K}^{-1} [P_{14}, P_{24}, P_{34}]^T$.

Image Mosaicing: any two images of a general scene with the same camera centre are related by a planar projective transformation (homography) given by $\tilde{\mathbf{w}}' = \mathbf{K}\mathbf{R}\mathbf{K}^{-1}\tilde{\mathbf{w}}$ (\mathbf{K} : camera calibration matrix, \mathbf{R} : rotation between views).

Given key points in an image (e.g. by SIFT), the RANSAC (random sample consensus) algorithm robustly fits keypoints to compute the homography.

5.6.4. Affine Projection

Weak Perspective Projection: when the whole scene has a similar Z_c , orthographic projection is a good approximation of perspective projection.

The weak perspective projection is $\tilde{\mathbf{x}} = \underbrace{\begin{bmatrix} f & 0 & 0 & 0 \\ 0 & f & 0 & 0 \\ 0 & 0 & 0 & Z_{av} \end{bmatrix}}_{\mathbf{P}_{pl}: \text{ weak perspective}} \tilde{\mathbf{X}}_c$ where Z_{av} is the average scene Z_c .

The overall image is then $\tilde{\mathbf{w}} = \mathbf{P}_c \mathbf{P}_{ppi} \mathbf{P}_r \tilde{\mathbf{X}} = \mathbf{P}_{aff} \tilde{\mathbf{X}}$, where $\mathbf{P}_{aff} = \begin{bmatrix} p_{11} & p_{12} & p_{13} & p_{14} \\ p_{21} & p_{22} & p_{23} & p_{24} \\ 0 & 0 & 0 & p_{34} \end{bmatrix}$ is the **affine camera** projection matrix (8 dof).

Planar Weak Perspective Projection: if Z_c is **exactly** constant across the scene, then the projection matrix can be simplified further. The third column can be removed, giving 6 dof.

Cross-Ratio (Section 2.2.10): for four ordered **collinear** points $\{A, B, C, D\} \rightarrow \{a, b, c, d\}$,

The cross ratio of $\{A, B, C, D\}$ is conserved under any perspective projection: $\frac{|AD||BC|}{|BD||AC|} = \frac{|ad||bc|}{|bd||ac|}$.

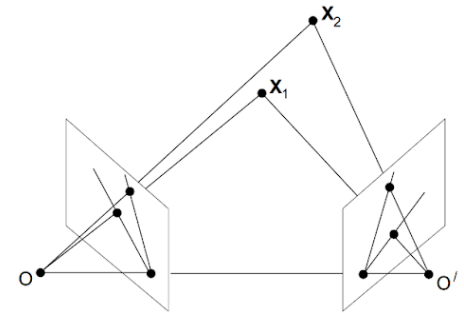
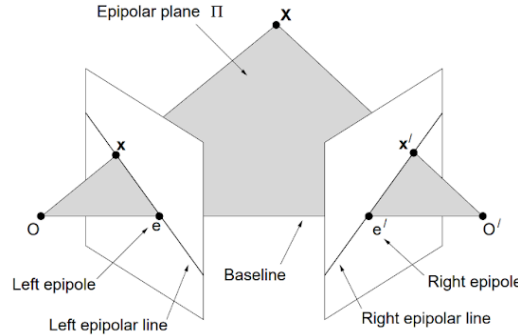
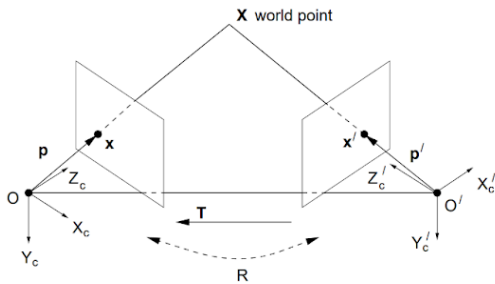
For five **coplanar** points $\{A, B, C, D, E\} \rightarrow \{a, b, c, d, e\}$, two conserved cross-ratios exist using specially constructed points: if $F = AB \cap CD$, $G = BC \cap AD$, $E_1 = EF \cap AG$, $E_2 = AF \cap EG$, then the cross-ratios of $\{A, E_2, B, F\}$ and $\{A, E_1, D, G\}$ are conserved under any perspective projection. (Notation: $AB \cap CD$ is the intersection of lines AB and CD .)

Another way to form projective invariant quantities is by ‘canonical views’, by constructing a canonical frame curve given two views of an object in perspective projection. A calibration operation aims to map four key points onto the corners of a unit square, giving an ‘invariant signature’.

5.6.5. Stereoscopic Vision (Stereo Vision)

Epipolar Geometry: relation between projections onto different image planes

Viewing a point X from two angles in perspective projection allows for triangulation of the point in 3D, by the intersection of the corresponding rays. **Epipolar lines** constrain the positions of a projected point in each image.



X from two views $\rightarrow x$ and x'
 Coords relate by $X_c' = R X_c + T$
 X_c' is p_1 , X_c is p_2

Epipolar plane Π contains X and the optical centres.

As X moves, the epipoles are invariant and Π rotates about OO' .

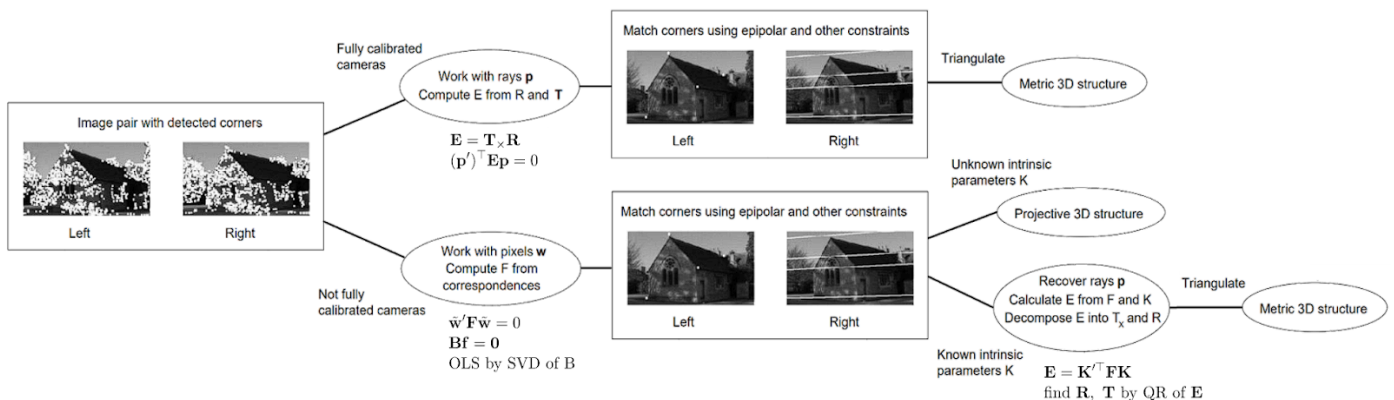
For two correspondences (1 and 2) of one world point X (as a projected ray in camera coordinates $p = \tilde{x} = [x, y, f]^T$) related by a **homography** (linear transformation R , translation T),

- **Epipolar constraint** (ray coordinates): $p_1^T E p_2 = 0$
 ($E = T_x R$: essential matrix, T_x : cross product matrix of T , Section 4.1.6)
 The **epipoles** lie in the **nullspace** of E ($Ee = 0$ and $E^T e' = 0$; and of F^T).

In the limit of parallel cameras, the epipoles approach infinity, allowing depth perception: if $T = [-d, 0, 0]^T$ and $R = I$ then $Z_c = df / (x - x')$.

- **Epipolar constraint** (pixel coordinates): $\tilde{w}_1^T F \tilde{w}_2 = 0$
 ($F = (K_1^{-1})^T E K_2^{-1}$: fundamental matrix, $\tilde{w} = Kp$: imaged ray, K : camera intrinsics).
 The equation of the epipolar line in the right image is $\tilde{l}'^T \tilde{w}' = 0$ where $\tilde{l}' = F \tilde{w}$.

Other constraints to identify correspondences are uniqueness and ordering (for opaque surfaces). The metric structure information (R, T) up to a scale can be computed from the SVD of E .



Summary

Camera Calibration: robust method using RANSAC and nonlinear optimisation

1. Randomly sample 6 out of N image points and world points to form a set of $\{\tilde{\mathbf{w}}_i, \tilde{\mathbf{X}}_i\}$ ($1 \leq i \leq 6$)
2. Using $\tilde{\mathbf{w}} = \mathbf{P}\tilde{\mathbf{X}}$, write a system of 12 equations: $\mathbf{A}\mathbf{p} = \mathbf{0}$ (\mathbf{A} : 12×12 , \mathbf{p} : 12×1)
3. Calculate the SVD decomposition and take $\mathbf{p} = [\text{last row of } \mathbf{V}^T]$ where $\mathbf{A} = \mathbf{U}\mathbf{\Sigma}\mathbf{V}^T$
4. Calculate $|\mathbf{A}\mathbf{p}|$ for the full set of N points and count the 'inliers' (sufficiently close to zero)
5. Iterate from step 1 until the count of inliers is maximised. Use this \mathbf{P} as a seed for Step 6.
6. Minimise the reprojection errors: $\mathbf{P} = \operatorname{argmin} \left\{ \sum_{i=1}^N (u_i - \hat{u}_i)^2 + (v_i - \hat{v}_i)^2 \right\}$ where $[s\hat{u}_i, s\hat{v}_i, s]^T = \mathbf{P}\mathbf{X}_i$.
7. The 'RQ' decomposition of top-left 3×3 submatrix of \mathbf{P} yields \mathbf{KR} .
8. Calculate $\mathbf{T} = \mathbf{K}^{-1} [p_{14} \ p_{24} \ p_{34}]^T \rightarrow \mathbf{P} = \mathbf{K}[\mathbf{R}|\mathbf{T}]$.

Stereoscopic Correspondences: recover 3D structure from two calibrated cameras

1. Given two images related by an unknown homography, identify keypoints.
2. Use SIFT to register invariant features $\mathbf{x}_i \in \mathbb{R}^{128}$ and $\mathbf{x}'_j \in \mathbb{R}^{128}$ in a k -D tree.
3. Find nearest neighbour correspondence estimates $\{\mathbf{x}_i, \mathbf{x}'_j\}$ from the images.
4. Refine the correspondence estimates using the RANSAC algorithm:
 - a. Randomly sample 8 pairs of correspondences $\{\tilde{\mathbf{w}}_i, \tilde{\mathbf{w}}'_i\}$.
 - b. Using $\tilde{\mathbf{w}}'^T \mathbf{F} \tilde{\mathbf{w}} = 0$, write a system of 8 equations: $\mathbf{A}\mathbf{f} = \mathbf{0}$ (\mathbf{A} : 8×9 , \mathbf{f} : 9×1), solve with SVD as before to find 3×3 fundamental matrix \mathbf{F} with $F_{33} = f_9 = 1$.
 - c. Find $\tilde{\mathbf{w}}'^T \mathbf{F} \tilde{\mathbf{w}}$ using this estimate for \mathbf{F} on the whole dataset. Count the number of correspondences for which this value is sufficiently close to zero.
 - d. Iterate, finding new \mathbf{F} 's until the count of inliers is maximised. Take this as \mathbf{F} .
5. Enforce rank 2 constraint in \mathbf{F} by setting its smallest singular value to zero.
6. Compute $\mathbf{E} = \mathbf{K}'^T \mathbf{F} \mathbf{K}$.
7. Calculate the SVD decomposition $\mathbf{E} = \mathbf{U}\mathbf{\Sigma}\mathbf{V}^T$. Then $\mathbf{R} = \mathbf{U}\mathbf{Y}\mathbf{V}^T$ and $\mathbf{T} = [\text{last column of } \mathbf{U}]$, where $\mathbf{Y} = [[0, -1, 0]; [1, 0, 0]; [0, 0, 1]] = \{\text{rotation about } V_z \text{ by } 90^\circ \text{ anticlockwise}\}$
8. There are 4 possible solutions for using $\pm\mathbf{T}$ and $\{\mathbf{R}, \mathbf{R}^T\}$: resolve ambiguity by ensuring all visible points lie in front of both cameras. Then $\mathbf{P}' = \mathbf{K}'[\mathbf{R}|\mathbf{T}]$ and $\mathbf{P} = \mathbf{K}[\mathbf{I}|\mathbf{0}]$.
9. To compute $\tilde{\mathbf{X}}$, solve $\tilde{\mathbf{w}}' = \mathbf{P}'\tilde{\mathbf{X}}$ and $\tilde{\mathbf{w}} = \mathbf{P}\tilde{\mathbf{X}}$ (4 equations in 3 unknowns: least squares).

5.6.6. Hough Transform and Radon Transform

Hough Transform: detects lines in 2D images.

Straight lines in images can be parameterised by (r, θ) , the polar coordinates of the closest point on the line to the origin of the image coordinate system. The equation of the line is then

$$r = x \cos \theta + y \sin \theta \quad (\text{Hough transform in } (r, \theta) \text{ space: Hesse normal form}).$$

A given (x, y) point corresponds to a sinusoid in (r, θ) space. Sinusoids are superposed for each pixel to build the transformed image in Hough (r, θ) space. The intersections of these sinusoids (represented as maxima in total amplitude) occur at values of (r, θ) where a line with these parameters exists in the original image.

The intersections are thresholded and returned as detected lines in the image.

Radon Transform:

An image $f(x, y)$ can be mapped to (r, θ) directly using the Radon transform:

$$Rf(r, \theta) = \int_{-\infty}^{\infty} \int_{-\infty}^{\infty} f(x, y) \delta(r - x \cos \theta - y \sin \theta) dx dy$$

This is mathematically equivalent to the Hough transform in the continuous infinite size limit.

The **inverse Radon transform** is useful in tomography (reconstructing solid 3D objects from a stack of 2D image slices through), widely used in biomedical imaging (e.g. CT scans) to reconstruct from X-ray transmission intensity data. It is computed using the filtered backprojection formula.

5.7. Accounting, Finance and Business

5.7.1. Basics of Accounting for Businesses

Types of Entities

- **Non-Business Organisation:** exists to meet a societal need where making profit is not the goal.
- **Business Organisation:** exists to sell goods and/or services where making profit is a goal.
 - **Sole Trader / Proprietorship:** owned by one person, the same legal entity.
 - **Limited Company (LTD):** owned by one person, a different legal entity.
 - **Partnership:** owned by two or more associated people.
 - **Corporation:** owned by one or more shareholders.
 - **Publicly Accountable Enterprise:** sells shares on the stock exchange (after IPO).
 - **Private Enterprise:** shares owned by a group of associated people.
 - **Limited Liability (LLC):** shareholders are not personally responsible for debts.

Types of Accounting:

- **Financial Accounting:** reports the breakdown of financial decisions of a company, aimed at informing external stakeholders. Standardised according to GAAP / IFRS, enforced depending on locality (US: FASB, elsewhere: IASB).
- **Managerial Accounting:** reports the internal performance of the company, aimed at informing managers about decisions on projects and employees.
- **Tax Accounting:** reports the overall profits made by a company to facilitate collection of tax revenue by the government (US: IRS, UK: HMRC)

Incentives: actors may be incentivised to bias a report e.g. managers aim to minimise reported profits for a tax return (to pay less tax), but maximise profits when presenting to investors. This also applies for external bodies e.g. consultants, auditors and credit rating agencies which are paid by the company for evaluation, though these entities are typically more reputable as third parties.

Key Actors in Accounting

- **Financial Accountants:** hired by the firm to prepare their financial reports. Supervised by the Chief Financial Officer (CFO).
- **Auditors:** external agents hired by the firm to assess and verify the financial reporting quality of the firm. Typically works for an accounting firm (the 'Big 4': Deloitte, KPMG, EY, PwC). Auditors use statistical methods to determine the risk of a significant deviation from accounting standards.
- **Forensic Accountants:** investigates fraud and financial irregularities, and advises on financial disputes.
- **Investors:** sources of finance for developing companies, especially at the entrepreneurial stage. Seed funding may be received from angel investors, venture capitalists and banks (investment bankers) can provide sources of funding as well as advice on decision making, though VCs typically require a position on the company board (equity stake) for their services.
- **Standards Setters:** the entities making and enforcing the rules on accounting.

5.7.2. Financial Statements (Books)

Stakeholders may make major investment decisions based on financial reports:

- **Income Statement:** shows the breakdown of **revenue and expenses**, as summed flows over time.
- **Balance Sheet:** shows the total **assets, liabilities and equity**, at a point in time.
- **Cash Flow Statement:** shows the total sum of transactions of the company.
- **Environmental, Social and Governance (ESG Data):** currently being formalised, but is not yet universally mandatory as audit quality varies. Used to inform policymakers.

The ‘aggregation exercise’ is performed in each accounting cycle: ongoing accruals are recorded in a **journal**, noting the date, account debited and credited. To prepare the accounts, **T-accounts** are drawn up, grouping transactions by account. The balance for each account is found by summing and the necessary financial books are written.

Double Entry Bookkeeping: any one transaction affects two variables in the **accounting equation**, **Assets = Liabilities + Equity**. Financial statements are structured using ‘T-accounts’ to reflect this:

Ledger	General Ledger						Temporary Ledger			
Account Type	Assets Debits Credits		Liabilities Debits Credits		Equity (Shares) Debits Credits		Revenue Debits Credits		Expense Debits Credits	
Increase or Decrease										

Debits (Dr) increase the **assets**. For the temp ledger, **credits (Cr)** increase the **equity** (which decreases the assets). The temporary ledger balance (revenue - expense) is realised as ‘retained earnings’ in Equity.

Company Name Income Statement For the month or year ended xx/xx/xxxx	
Sales Revenue or Service Revenue	_____
Cost of Goods Sold (COGS)	_____
Gross Margin	_____
Operating Expenses	_____
e.g. Depreciation Expense	
e.g. Selling, General and Administrative Expense (SG&A)	
e.g. Research and Development Expense (R&D)	
Operating Income or Loss	_____
Other Revenues or Expenses	_____
e.g. Gain or Loss from disposal of long-term assets	
e.g. Impairment Loss	
Earnings Before Interest and Tax (EBIT)	_____
Interest Expense	_____
Tax Expense	_____
Net Income or Loss	_____

Company Name Statement of Cash Flow For the month or year ended xx/xx/xxxx	
Cash flow from operating activities:	_____
Net Income	_____
Adjust for non-cash items from the Income Statement:	
e.g. +depreciation/amortisation expense	
e.g. -gain/+loss from disposal of long-term assets	
e.g. + bad debt expense	
Adjust for changes in non-cash current assets and current liabilities:	
e.g. - increase in non-cash current assets	
e.g. + increase in current liabilities	
Total Cash flow from operating activities	_____
Cash flow from investing activities:	_____
Cash used to purchase long-term assets	_____
Cash received from disposal of long-term assets	_____
Total cash flow from investing activities	_____
Cash flow from financial activities:	_____
Cash payment of long-term liabilities	_____
Acquisition of long-term liabilities for cash	_____
Cash repurchase of share capital	_____
Issuance of new shares for cash	_____
Cash payment of dividends	_____
Total cash flow from financing activities	_____
Net Increase (Decrease) in cash	_____
Cash Balance at the beginning of the year	_____
Cash Balance at the end of the year	_____

Company Name Balance Sheet As at xx/xx/xxxx	
Assets	Liabilities and Shareholders' Equity
Current Assets	Liabilities
e.g. Cash	Current liabilities
e.g. Inventory	e.g. Accounts Payable (A/P)
e.g. Accounts Receivable (A/R)	e.g. Salaries Payable
Non-Current Assets	e.g. Interests Payable
e.g. Property, plant and equipment (PPE)	Non-Current liabilities
e.g. Research and Development	e.g. Bank Loans
e.g. Goodwill	Total Liabilities
Total Assets	_____
	Shareholders' Equities
	e.g. Share Capital
	e.g. Retained Earnings
	Total Equity

	Total Liability and Shareholders' Equity

5.7.3. Simple Metrics in Financial Accounting

Metrics of profitability:

- Gross Profit Ratio = Gross Profit / Sales Revenue
- Profit Margin Ratio = Net Income / Sales Revenue
- Return on Assets = Net Income / Total Assets

Metrics of liquidity:

- Working Capital = Current Assets - Current Liabilities
- Current Ratio = Current Assets / Current Liabilities.

Negative numbers on books are recorded in parentheses e.g. (100) is \$ -100.

Quantitative easing: a monetary policy in which a central bank buys government bonds, increasing the assets of commercial banks, stimulating economic activity. First used to mitigate the 2008 financial crisis.

5.7.4. Revenue Recognition and Bad Debt

- Revenue is earned when a product or service has been delivered and accepted by the customer.
- When money is received before a service is delivered, record the revenue as **'deferred revenue' (a liability)** until the service is delivered, since the company owes a refund until this time.
- When a service is delivered before money is received, record the value as **'accounts receivable' (A/R, an asset)** until the bill/invoice is fully paid. In B2B, many companies offer credit to customers when they make sales.
- If the customer seems unable to pay off their debt, the reported A/R value is now inaccurate, and an estimate of the loss is recorded in **'allowances for bad debt' (AFDA)**, a contra-asset valuation account). If the firm gives up on recovering this bad debt, it is **written off**, balancing the AFDA and crediting from the A/R account.
- To compute the bad debt expense, statistical methods based on an **ageing schedule (arrears)** are used. The longer the account remains overdue, the higher the probability it will default. Established firms have long histories of data to estimate probability of defaulting by lateness of the payment. Increment to ending AFDA = A/R amount due × Probability of default (summed over arrears buckets).

5.7.5. Statement of Cash Flows and Fraud in Accounting

The balance sheet and income statement are not sufficient to assess a company's financial health. Without cash, a company cannot operate and goes bankrupt (even if it owns assets). To predict this, financial analysts look at the cash inflows and outflows over a period, described in the cash flow statement.

The cash flow statement's net change in cash in year t gives the increase in balance sheet cash between years $t - 1$ and t .

Cash Flow Statement: divided into three sections

- Cash flow from **operations**: from income statement/balance sheet changes, also paying off interest on debts (as of US-GAAP ASC 230).
- Cash flow from **investing**: from investments and long-term assets.
- Cash flow from **financing**: obtaining long-term debt (borrowing), paying off principal of debt, issuing equity, paying dividends.

Operating cash flow is usually computed indirectly, subtracting **non-cash operations from 'net income'** on the income statement.

Gains and **Losses** are increases and decreases in equity (net assets), except those that result from revenues or investments by owners.

Fraud in Accounting: exploiting grey areas of accounting to misrepresent cash flow data.

- Channel stuffing: selling more products to distributors than they are capable of selling to the end customers in order to inflate sales.
- Underestimating default probabilities for a bad debt expense account to inflate net A/R income.

5.7.6. Financial Interest and the Time Value of Money

Interest: accrual of money per unit time

- Simple interest: $A = P(1 + rt)$ (interest = $A - P = Prt$)
- Compound interest: $A = P\left(1 + \frac{r}{n}\right)^{nt}$
- Continuous compound interest: $A = P e^{rt}$
- Annual percentage rate (APR): $APR = \frac{\text{interest } [\text{\$}] + \text{fees } [\text{\$}]}{\text{principal } [\text{\$}]} \times \frac{365 [\text{days}]}{\text{loan term } [\text{days}]}$ (effective interest rate)
- Return on investment (ROI) = % increase in $P = \frac{A - P}{P} = \frac{\text{profits}}{P}$ ($\times 100\%$)

(A : accrued amount; future value FV, P : premium (present value PV), r : interest rate (as $\frac{r [\%]}{100}$) per year, t : time (years), n : number of compounding periods per year e.g. weekly $\rightarrow n = 52$, monthly $\rightarrow n = 12$. When working with r as an inflation rate, A in the future has the same purchasing power as P now.)

Time Value of Money: a unit of money is generally 'more valuable' now than in the future.

Cash amounts are only comparable when referring to the same point in time.

- Future Value (FV) = Present Value (PV) $\times (1 + r)^n$ (where $r > 0 \rightarrow FV > PV$)
- Present Value (PV) = $\frac{\text{Future Value (FV)}}{(1 + r)^n}$

If the net present value (NPV) of an investment is negative, it is likely not worthwhile, as the discounting exceeds the interest.

Perpetuities and Annuities: cash flows vary between times due to interest and inflation

- **Perpetuity:** stream of constant cash flows. $PV = \sum_{n=1}^{\infty} \frac{C}{(1+r)^n} = \frac{C_1}{r}$
- **Growing perpetuity:** stream of rising cash flows. $PV = \sum_{n=1}^{\infty} \frac{C_1(1+r_g)^{n-1}}{(1+r)^n} = \frac{C_1}{r-r_g}$ ($C_1 = C_0(1+r_g)$)
- **Annuity:** stream of N cash flows. $PV = \sum_{n=1}^N \frac{C}{(1+r)^n} = \frac{C}{r} \left(1 - \frac{1}{(1+r)^N}\right)$
- **Growing annuity:** stream of N rising cash flows. $PV = \sum_{n=1}^N \frac{C_1(1+r_g)^{n-1}}{(1+r)^n} = \frac{C_1}{r-r_g} \left(1 - \left(\frac{1+r_g}{1+r}\right)^N\right)$

(r : discount rate / hurdle rate / (opportunity) cost of capital, r_g : long-term growth rate)

5.7.7. Valuation of Stocks and Shares

Types of shares:

- Growth shares: investors expect to benefit from capital gains (future growth of earnings)
- Income shares: investors seek cash dividends

Metrics of share valuation:

- Book equity per share (BVPS) = $\frac{\text{value of common equity on balance sheet}}{\text{number of shares outstanding}}$
- Earnings per share (EPS) = $\frac{\text{net income} - \text{dividends to preferred shares}}{\text{number of shares outstanding}}$
- Return on equity (RoE) = $\frac{\text{net income}}{\text{shareholders' equity}} = \frac{\text{EPS}}{\text{BVPS}} = \frac{\text{net income} - \text{dividends to preferred shares}}{\text{value of common equity on balance sheet}}$
- Payout ratio = $\frac{\text{dividends}}{\text{EPS}}$
- Plowback / Retention ratio, $b = 1 - \text{Payout ratio}$
- Price per earning (P/E ratio) = $\frac{\text{market value per share (share price)}}{\text{EPS}}$

Valuation of Shares: common shares can be paid out as either dividends or capital gains.

(D : dividends, P : share price, discount rate: $r = \frac{D_1}{P_0} + r_g$, growth rate: $r_g = b$ (plowback) \times RoE.)

DCF share price is the sum of discounted future dividends (PV): $P_0 = \frac{P_1 + D_1}{1+r} = \sum_{n=1}^{\infty} \frac{D_n}{(1+r)^n}$.

Gordon-Shapiro growth model: $D_n = D_0(1+r_g)^n$ then $P_0 = \sum_{n=1}^{\infty} \frac{D_1(1+r_g)^{n-1}}{(1+r)^n} = \frac{D_1}{r-r_g}$ and so $P_n = \frac{D_{n+1}}{r-r_g}$.

For nonlinear growth then linear, use $P_0 = \frac{P_N}{(1+r)^N} + \sum_{n=1}^N \frac{D_n}{1+r}$ (where $P_N = D_N(1+r_g) / (r-r_g)$).

Valuation of Straight Bonds: investor (lender) buys the bond to receive fixed returns (like a loan)

- Maturity date: bond expiry date, issuer returns the face value amount to the lender
- Face value F / Par value: the amount promised to pay the investor on the maturity date
- Coupon C : periodic interest paid while the bond is held (before maturity):

$$\text{Coupon, } C [\text{\$}] = \text{Face Value, } F [\text{\$}] \times \text{Coupon rate, } r_C [\%]$$

- Yield to maturity r_{YTM} (YTM): annual expected return for the investor.
- Current yield: annual coupon divided by price

Fair value of bond is the sum of discounted debt cash flows: $P_0 = \frac{F}{(1+r_{\text{YTM}})^N} + \sum_{n=1}^N \frac{C}{(1+r_{\text{YTM}})^n}$.

Investors are at risks e.g. default risk, liquidity risk, regulatory risk, interest rate risk.

5.7.8. Cash Flow Analysis

The net present value (NPV) concept can be used to check feasibility of an investment (e.g. for a project):

$$\text{Net Present Value (NPV)} = \left(\sum_{n=1}^N \frac{C_n}{(1+r)^n} \right) - P_0 \text{ (PV of returns - } P_0 \text{: initial investment / cash outlay)}$$

Considerations in conducting a cash flow analysis:

- Use **incremental** cash flows: differences between revenue with and without the project.
- Account for **side effects** on other cash flows e.g. erosion (decrease) or synergy (increase).
- **Ignore sunk costs**: costs in the past cannot influence future decisions.
- Consider potential revenues excluded by the project as **opportunity costs**.
- Allocated cost should be included entirely when budgeting (as opposed to in accounting).

Free cash flow to the firm (FCFF) method: typical tabular layout

- EBIT (earnings before interest and tax) = (sales revenue – costs) – depreciation [on income statement]
- NOPDAT (net operating profit after tax) = EBIT × (1 – r_{tax})
- CFO = NOPDAT + depreciation + amortisation
- Depreciation = Initial Outlay / Project Length (using ‘straight line’ depreciation method)

	Year 0	Year 1	Year 2 ...	Year N
Cash flow from operations (CFO)	0	CFO	CFO	CFO
Capital investment (CapEx)	(initial outlay) (-ve)	0	0	0
Investment in working capital (ΔNWC)	(WC) (-ve)	0	0	WC (+ve)
Free cash flow [sum down columns]	C_0	C_1	C_2	C_N
Discounted cash flow (DCF)	C_0	$C_1 / (1+r)$	$C_2 / (1+r)^2$	$C_N / (1+r)^N$
Net Present Value (NPV) = sum of DCFs				

If $\text{NPV} > 0$ then the project is expected to be profitable. If $\text{NPV} < 0$ then the project is unprofitable.

5.7.9. Break-even Analysis

Internal rate of return (IRR): the discount rate r such that a cash flow analysis returns $\text{NPV} = 0$.

If $\text{IRR} > r_{\text{required}}$ then the project is profitable. If $\text{IRR} < r_{\text{required}}$ then the project is unprofitable.

- If the function $\text{NPV}(r)$ has multiple zeros, this method may be invalid (need to graph curve).
- When comparing two projects, higher IRR does not always imply higher NPV.

$$\text{Profitability Index} = \frac{\text{NPV [at fixed } r]}{\text{initial investment}}$$

Sensitivity analysis: study how NPV varies with inputs e.g. $\frac{\Delta\text{NPV}}{\Delta x}$ or $\frac{d(\text{NPV})}{dr}$.

5.7.10. International Business

An international business conducts some aspect of their business across borders e.g. products and services, capital (trading), people (employees) and information (digital companies).

Incentives for internationalisation of business:

- Market seeking: economic growth, infrastructure, less competition
- Efficiency seeking: regulatory arbitrage, lower labour costs, lower taxes / tax avoidance
- Innovation seeking: access to talent and specialist workforce
- Resource seeking: critical materials

Barriers to internationalisation of businesses:

- Trade tensions: politicians may legislate against trade with some countries
- Armed conflict: international business is deprioritised in times of war
- Disruptions: (e.g. Houthi attacks on ships in the Red Sea/Suez canal in 2024).
- Climate Change: shortages or failures of land-based raw materials

Strategy of internationalisation: experience or experimentation?

- Deliberate: top-down, global strategy with careful planning.
- Emergent: bottom-up, local strategy embracing learning the new cultural norms.

Modes of entry: resource commitment usually starts low and increases over time (Uppsala model).

- Non-equity modes: import/export, outsourcing, licensing, franchising.
- Joint venture / partial acquisition. Can help with gaining local knowledge.
- Equity modes: green field / full acquisition.

Increasing global supply chain resilience (reconfiguration):

- Shorter supply chains: onshoring / near-shoring
- Political alignment: friend-shoring
- Diversification: dual/multi-sourcing e.g. 'China Plus One' strategy for the West
- Bifurcations: separate supply chains for different markets

Examples of Internationalisation in Tech and Energy Industries

- Tesla expands into China in 2014: to take advantage of the EV market, manufacturing in China is necessary to avoid high tariffs.
- Many tech companies (Arm, Nvidia, etc) set up in high-talent areas e.g. Silicon Valley (California) or Cambridge.
- LG Chem builds a factory in the US in 2024 to take advantage of the IRA tax credits for making EV battery cathodes.

Factors affecting International Business for Energy and Tech Industry

- **US-China Trade War** (President Trump, 2019): nationalist protectionism increasing barriers to trade between the USA and China.
- **US Inflation Reduction Act** (President Biden, 2022): promotes US decarbonisation by subsidising domestic clean energy production with tax credits.
- **Critical minerals**: top producers (mining and refining) include China (Sb, Co, Ga, graphite, In, Mg, REE oxides, Si, Te, Sn, W, V), Vietnam (Bi), Australia (Li), DR Congo (Ta), South Africa (Pt), Brazil (Nb).
- **Artificial intelligence**: potential rise of LLMs and AGI in the near-to-medium future may force a restructuring of the software workforce.
- **Fragility in Semiconductor Industry**: impacts all technology and associated supply chains.
 - US firms design chips using software relying on IP licences from Europe.
 - Manufacturing equipment developed in the US, Japan and Europe. ASML (Europe) is the only producer of extreme UV lithography systems as of 2024: they sell to chip makers.
 - Silicon is mined and refined in the US, processed into wafers in Japan and South Korea.
 - Chips are manufactured and packaged in Taiwan and Malaysia. TSMC makes 92% of global advanced semiconductor chips.
 - Processors are assembled into electronic products in China.

5.7.11. Institutional Theory in International Business

Institution: a taken-for-granted set of organising principles ('rules of the game; social scripts').

Institutional theory was developed to criticise the 19th century 'economic man' theory, explaining how and why business and people behave irrationally. Modern (neo-institutionalism) theory explores why some organisations of the same type always have a very **similar structure** everywhere in the world, due to **regulative, normative and cognitive forces** driving uniformity.

Examples of institutions: democracy, marriage, banks, places of religious worship, schools...

Properties of institutions: persist for a long time, are collective, are mostly taken for granted, **guide and constrain social behaviour**, simplify decision-making, provide order, build trust and legitimacy, are hard to change (inertia).

5.7.12. Analysis of Institutional Distance for Internationalisation

Institutions in International Business:

- Institutional arrangements are highly context dependent. They may be literal (geographic), formal (legal, political, economic) or informal (cultural, religious, linguistic).
- Institutions are incredibly powerful structures: underestimating or misunderstanding 'the rules of the game' while entering a given country may lead to failure. However, it is hard to fully understand the institutional environment from the outside due to its taken-for-granted nature (liability of outsidership).
- If we need to change the institutional environment in order to enter a country, we need to understand it entirely, and will still be a very challenging task.

Analysing Potential for Internationalisation:

- Why is the company successful currently in the home country?
- What is their positioning (reputation, service type) in the market?
- Identify regulations responsible for forming institutions.
- Identify the cultural forces that drive these regulations.
- What are the implications of these differences on the current business model? Is adaptation feasible?

Types of Institutional Distance: may be literal (**geographic**), formal (**legal, political, economic**) or informal (**cultural, religious, linguistic**).

Approaches to Reduce Institutional Distance: adapt to the target, or influence the target?

- Cultural legitimisation ('glocalisation'): localisation, polycentric pricing, omnichannel marketing, workforce training, social responsibility. May require ethnographic studies for market research.
- Market to the diaspora of the target country, then attract locals (e.g. bubble tea in the West).
- Use cultural interests to promote associated products (e.g. K-pop/Korean wave → Asian food supermarket)
- Joint ventures with a local company to gain trust or avoid negative perception of host country.
- Institutional entrepreneurship: lobbying to relax regulations, marketing, PR, strategic collaboration with industry groups.

Example: commerce in the US (e.g. Walmart). Relevant institutional norms in the US include:

1. Economies of scale: a more capitalist free market allows monopolisation by rapid growth.
2. Driving culture: can have large stores, spaced apart.
3. Very high standards of customer service: requires more rigorous management of employees).
4. Low price guarantees: requires lower wages for employees.

These factors are unlikely to work in Europe (hence Walmart's failure in Germany) due to institutional distance: e.g. more government oversight, regulations on employee rights, salaries and environmentalism, limited store opening hours, stronger unions for employees, mandatory holidays, less emphasis on customer service and the appearance of friendliness.

5.7.13. Cross-Cultural Communication

Models for Understanding Culture:

- **Human mental programming hierarchy:** 1) human nature (universal; inherited), 2) culture (specific to group; learned), 3) personality (specific to person; inherited and learned).
- **Cultural iceberg:** only behaviours and practices are observable. The hidden factors informing them are the perceptions, attitudes, beliefs, values, which in turn are influenced by climate, geography, demographics, economics, media, education, ideology, religion.
- A nation is often not the best unit to study a culture: the cultural unit may be larger or smaller, and may not be geographically united.

Dimensions determined by culture (Hofstede and more recent critical work):

1. **Individualism vs Collectivism.** Integration of people into primary groups. Most significant.
2. **High vs Low power distance.** Solutions to basic inequality.
3. **Low vs High uncertainty avoidance.** Response to stress in the presence of unknowns.
4. **Motivation towards Achievement / “Masculinity vs Femininity”.** Division of emotional and gender roles in society, into competitive/tough/assertive vs cooperation/relationship building.
5. **Long vs Short term orientation.** Focus of people’s efforts in the present or the future.

Other important dimensions are **Indulgence vs Restraint** (Personal happiness, freedom of expression, and the importance of leisure) and **Perception of Time** (Sequential vs Overlapping).

Differences along any of these dimensions can lead to unexpected clashes in many social interactions while doing business.

5.7.14. Institutional Voids and Developmental Distances

Developing economies may have a lack of formal institutions (voids): within each dimension of institutional distance, there is also a developmental distance (informality). Often occurs in:

- Functioning political, economic and legal systems
- Hard infrastructure e.g. roads, rail, airports, seaports, telecomms, energy
- Soft infrastructure (business ecosystems) e.g. talent, logistics, information availability

Conglomerates (highly diversified, often family-founded corporations) tend to perform well in countries with voids as they provide all necessary services at once, becoming MNCs.

Network Effects: some services become intrinsically better when more people use them. Commonly exploited by digital companies to cement a monopoly in a void.

Examples: taxi apps (more drivers, more users), e-commerce (more buyers, more sellers), social media (more users, more engagement), shopping malls (more shops, more buyers).

'Super-apps' are all-in-one digital service apps, proving highly successful in 'recently' developed countries, combining the benefits of conglomerate-style void-filling and the network effects. Localisation helps to tailor services to the local market e.g. Grab in South-East Asia. Super apps are not popular in the West due to anti-competition laws, already matured institutions, data privacy concerns etc.

Technological leapfrogging: using voids as opportunities by building the service around what is already there on the ground, not worrying about the necessary infrastructure in the home country e.g. mobile internet in Africa, mobile fintech, renewable energy in Asia, electric mobility.

5.7.15. Business in the Anthropocene Epoch (Climate Change and Pollution)

The 'anthropocene epoch' refers to the observation that collective human activity is impacting the planet itself.

Climate risk: the negative financial effects of climate change on business e.g. supply chain disruption, higher costs, lower sales, transportation disruption, food shortages, regulatory risk.

Double materiality: the recognition that companies have a significant impact on the climate and should be held responsible for the waste they produce (rather than the consumer). Implementations include ESG data reporting (Section 5.7.2), extended producer responsibility (EPR) schemes, right to repair laws and results-based government funding.

Scopes of climate reporting (e.g. greenhouse gas emissions):

- Operational emissions: company-owned vehicles and facilities.
- Operational resources: purchased heating, cooling, energy, steam...
- Upstream activity (suppliers): assets, employee commuting, purchased goods/services, business travel, waste, fuel/energy, transport/distribution, capital goods
- Downstream activity (consumers): processing of sold product, use of product, leased facilities, investments, franchisees activity, end of life treatment (LCA)

Wastage per person is increasing over time due to increased consumerism and illegal business practices e.g. planned obsolescence, proprietary interfaces, fast fashion, as well as growth in emerging economies. In developed economies, 'degrowth' has become a viable strategy for decreasing waste without short-term economic loss. Companies producing in underdeveloped countries are being scrutinised for the ethics of their supply chains e.g. slavery, poor working conditions, sometimes resulting in supply-chain restructuring.

Recently, advanced technologies have been used to make deep supply chains more transparent (e.g. blockchain, molecular tagging in cotton supply chains), but this approach may not be locally suitable. Other methods include supplier code of conduct, monitoring the workplaces (auditing) of direct suppliers, publishing of supplier details for information transparency and industry alliances. However, the reputation of segments of the public remains almost the only incentive to comply, limiting full-scale adoption.

Companies are being pressured to take stances on these issues, as well as some social issues ('cancel culture': more controversial, less universally accepted). Companies must decide whether they want to risk alienating certain demographics with their choices.

5.7.16. Important Companies in the Semiconductor Industry

- **Arm** (UK): designs chips and licences the design as IP to manufacturers e.g. Nvidia, Intel, TSMC, Apple, Samsung.
- **Applied Materials** (USA): supplies equipment, services and software for manufacturing chips.
- **Nvidia** (USA): fabless tech company producing GPUs widely used to train large-scale machine learning models.
- **ASML** (Netherlands): the only producer of ‘extreme UV lithography’ machines, used to print ICs on silicon for high-performance chips. ASML was formed from the unification of several industry experts, and they sells their machines to chip makers, used to surpass the ‘7 nm’ process node from 2019. Its subsidiary, Cymer, is based in the US.
- **TSMC** (Taiwan): the world’s largest contract semiconductor manufacturer (foundry), selling to ‘fabless’ companies who rely on TSMC to produce their chips. TSMC does not try to compete with its customers. TSMC’s largest customer is Apple.
- **FoxConn** (China and Taiwan): a competitor to TSMC, which has much friendlier relations with the Chinese government, used to a smaller extent by Western companies.
- **Samsung** (South Korea): ‘chaebol’ (Korean conglomerate) with in-house manufacturing for their own electronics products, especially for memory chips.
- **Intel** (USA): manufactures its own high-end microprocessors and GPUs.

5.7.2. Income Tax (UK, FY2022):

Tax brackets vary over time and between different countries, as well as various special circumstances. The table is only useful as an example and should not be relied on.

The annual tax brackets for the fiscal year 2022 (6th April 2022 – 5th April 2023) in the UK using tax code 1257L (single source of fully taxable income) are:

Bracket	Taxable range	Progressive tax rate
Personal allowance	£ 0 – £ P	0%
Basic rate	£ $P+1$ – £ 50,270	20%
Higher rate	£ 50,271 – £ 150,000	40%
Additional rate	£ 150,001 and above	45%

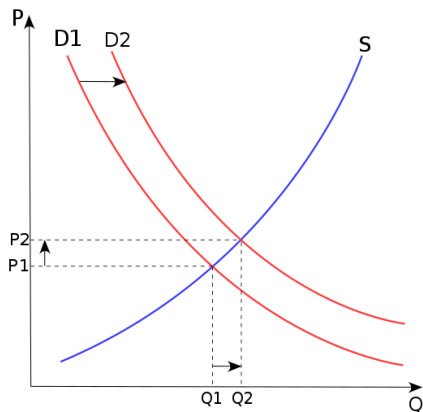
The standard personal allowance $P = 12,570$, which holds when income is less than £ 100,000. If the income I is more than £ 100,000, then $P = \max\{12,570 - 0.5(I - 100,000), 0\}$.

Example calculation: if income before tax is £ 61,000, then the tax payable is

$$(12,570 - 0) * 0.00 + (50,270 - 12,571) * 0.20 + (61,000 - 50,271) * 0.40 = \text{£ } 11,831.40.$$

Effective tax rate = (tax paid) / (income before tax) ($\times 100\%$).

5.7.3. Supply and Demand



In a perfectly competitive market, per-unit price of a good varies until quantity demanded equals quantity supplied (economic equilibrium).

(P : price of product, Q : quantity of product sold, S : supply curve, D : demand curve)

Isoelastic supply curve: $Q = k P^n$ (power law expression)

The graph on the left shows that an increase in demand ($D_1 \rightarrow D_2$) results in an increase in both price P and quantity Q .

Elasticity: sensitivity of demand to variations in environmental factors.

Liquidity: ease of buying/selling quickly and without affecting the price.

5.7.4. Inflation

Inflation is the reduction in value of money and the resulting decrease in consumer purchasing power.

Hyperinflation is caused primarily by excessive unsustainable growth in the money supply. Keynesian economics does not suggest moderate inflation directly results from growth, but rather that it is caused by excessive demand.

Real (inflation adjusted) rate of return = $1 + \frac{1 + \text{nominal rate}}{1 + \text{inflation rate}}$ (all expressed as decimals)

5.7.5. Pareto Principle

The Pareto principle (aka the 80-20 rule) is an empirical observation applicable to some scenarios. It states that 80% of consequences (data) come from 20% of the causes.

It is often used qualitatively, where the goal is to identify the dominant few actions (or problems to solve) that would generate the most results (profits).

5.7.6. Inventory Models

In operations research, an inventory model advises on the time and quantity of a supply to purchase in anticipation of a distribution of orders.

Let p : unit sale price, c : unit order cost, h : unit leftover holding cost, b : unit shortage penalty, D : random demand, x : initial inventory level, y : base stock level, $F_D(d) = P(D \leq d)$.

Assuming that $p + b > c$, the optimal order quantity q^* aims to maximise the expected profits:

$$q^* = \operatorname{argmax}_q \mathbb{E} \left[\underbrace{-cq}_{\text{order cost}} + \underbrace{p \min\{x + q, D\}}_{\text{products sold}} - \underbrace{h \max\{x + q - D, 0\}}_{\text{holding costs}} - \underbrace{b \max\{D - x - q, 0\}}_{\text{shortage penalties}} \right]$$

The solution (optimal order up to level) is $y^* = F_D^{-1}\left(\frac{p+b-c}{p+b-h}\right)$, where $y^* = \max\{q^*, 0\} + x$
 $\leftrightarrow q^* = \max\{y^* - x, 0\}$ and F_D^{-1} is the inverse cumulative distribution function (ICDF) of D .

Probability of running out of stock = $P(D > y^*) = 1 - \frac{p+b-c}{p+b-h}$.

If $D \sim N(\mu, \sigma^2)$ then $y^* = \mu + \sigma \times \Phi^{-1}\left(\frac{p+b-c}{p+b-h}\right)$ and the optimal (maximum) profit is $cx + (p-c)\mu - \sigma((h+c)z^* + (p+h+b)L(z^*))$ where $z^* = (y^* - \mu) / \sigma = \Phi^{-1}\left(\frac{p+b-c}{p+b-h}\right)$ and

$L(w)$ is the loss function defined as $L(w) = \frac{1}{\sqrt{2\pi}} \int_w^\infty (t-w) e^{-\frac{1}{2}t^2} dt = \phi(w) - w(1 - \Phi(w))$.

For an additional fixed (base) order cost K , the optimal reorder point s is defined as the value such that when $x < s$ we should order up to level ($q = q^*$) and when $x > s$ we do not order. The value of s is the smallest s such that $\text{Profit}(y^*) - \text{Profit}(s) = K$, which can be solved using the profit expression above.

5.7.7. Financial Instruments

Stocks (equities, shares): represent a fixed fraction of a single company's market capitalisation (value).

Bonds (fixed income securities): debt instruments with fixed interest rate returns and time to maturity (repay time to avoid defaulting), issued by governments (gilts / treasury notes) or corporations.

Commodities: raw materials such as fuels (e.g. crude oil, natural gas), agricultural produce (e.g. corn, sugar, live cattle), base metals (e.g. lead, copper), precious metals (e.g. gold, platinum), precious stones (e.g. diamond), lumber, rubber and water rights.

Currencies: the exchange rates of one currency relative to another, including cryptocurrencies, fluctuating due to national economics.

Derivatives: high-leverage instruments based on an underlying asset, used to hedge risk. May be contracts to purchase assets for a fixed price in the future (futures, options, forwards), or by exchanging loans with different interest rates (swaps).

Exchange-Traded Funds (ETFs): a collection of assets, whose price varies throughout the day as trading occurs.

5.7.7. Time Series Forecasting

A stock ticker represents time series data of the value of a stock over time. Various statistical and machine learning methods (e.g. SARIMAX, ES, LSTM, transformer etc) can be used to estimate (forecast) \hat{X}_{n+1} given $X_1 \dots X_n$.

The return of a stock $(\frac{X_n}{X_{n-1}} - 1)$ is typically more stationary (WSS) than the values X_n , and these returns are closer to a Normal or t -distribution, making use of standard scaling (Section 5.5.7) optimal in preprocessing.

Backtesting is used to test a trained model. For a large span of historic data \mathbf{b} , split \mathbf{b} into a set of adjacent sliding windows $\mathbf{X} = [\mathbf{x}^{(1)}, \mathbf{x}^{(2)}, \dots]$ and process each $\mathbf{x}^{(i)}$,

Processing involves checking data suitability (e.g. checking for stationarity in ARMA), computing the forecast, and evaluating the performance using a metric.

Stock tickers which perform well in backtesting can be ranked, with the top selection being used in real-time trading (diversification helps smooth out random variation).

White noise hypothesis: there is no actual pattern to stock data, and any model is as good as drawing from a Normal distribution with the same mean and variance as the training data. This is a good reference to see whether a model outperforms the 'naive'

P6. MECHANICS, STRUCTURES AND MATERIALS

6.1. Kinematics, Forces and Dynamics

6.1.1. Constant Acceleration Kinematics

Linear Motion: for constant a (the SUVAT equations):

$$\begin{aligned} v &= u + at & s &= ut + \frac{1}{2}at^2 & s &= vt - \frac{1}{2}at^2 \\ v^2 &= u^2 + 2as & s &= \frac{1}{2}t(u + v) \end{aligned}$$

(s : displacement, u : initial velocity, v : final velocity, a : acceleration, t : time.)

These equations also apply in 2D and 3D, using coplanar vectors (\mathbf{s} , \mathbf{u} , \mathbf{v} , \mathbf{a}), except $v^2 = u^2 + 2as$ which must be evaluated component-wise. The equations $|\mathbf{v}|^2 = |\mathbf{u}|^2 + 2\mathbf{a} \cdot \mathbf{s}$ and $\mathbf{s} \times \mathbf{a} = \mathbf{v} \times \mathbf{u}$ also apply but provide incomplete additional information.

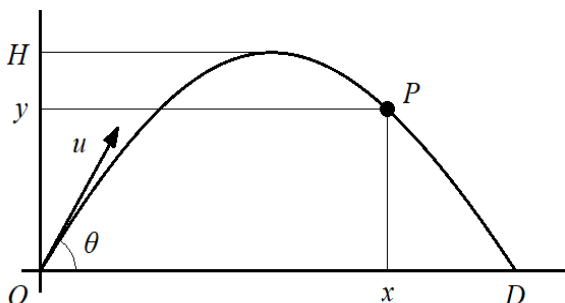
Rotational Motion: for constant α :

$$\begin{aligned} \omega &= \omega_0 + \alpha t & \theta &= \omega_0 t + \frac{1}{2}\alpha t^2 & \theta &= \omega t - \frac{1}{2}\alpha t^2 \\ \omega^2 &= \omega_0^2 + 2\alpha\theta & \theta &= \frac{1}{2}t(\omega_0 + \omega) \end{aligned}$$

(θ : angular displacement, ω_0 : initial angular velocity, ω : final angular velocity, α : angular acceleration, t : time.)

6.1.2. Simple Projectile Motion

For a point particle subject to only uniform gravitational field $g \text{ ms}^{-2}$, the trajectory is parabolic.



Position: $x = (u \cos \theta)t$ and $y = (u \sin \theta)t - \frac{1}{2}gt^2$

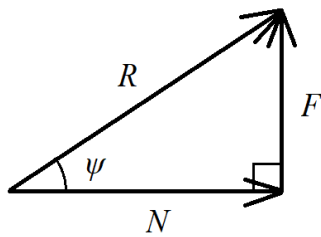
Range: $D = \frac{u^2 \sin 2\theta}{g}$; Maximum height: $H = \frac{u^2 \sin^2 \theta}{2g}$;

Flight time: $T = \frac{2u \sin \theta}{g}$

6.1.3. Mechanical Forces

Resultant force:	$\mathbf{F} = \dot{\mathbf{p}} = m\mathbf{a} + \dot{m}\mathbf{v}$	Newton's Second Law: $\mathbf{F} = m\mathbf{a}$ if mass is constant
Weight:	$W = mg$	uniform gravitational field g
Upthrust:	$U = \rho_f V g$	buoyancy in fluids ($W - U$); Archimedes principle.
Pressure:	$F = pA$	distributed loading normal to a surface
Friction force:	$F \leq \mu_s N, F = \mu_k N$	angle of friction: $\tan \psi = \mu_s$
Spring force:	$\mathbf{F} = -k\mathbf{x}$	for linear elastic media (Hooke's law)
Dashpot force:	$\mathbf{F} = -\lambda\mathbf{v}$	for linear viscous media (Stokes' law)
Centripetal force:	$\mathbf{F} = -\frac{mv^2}{r} \mathbf{e}_r = -mr\omega^2 \mathbf{e}_r$	radial force in uniform circular motion
Rolling resistance:	$F = C_{rr}N$	due to deformation of rolling bodies
Air resistance / lift:	$F = \frac{1}{2} C \rho_f A v^2$	distributed force due to fluid flow
Power and torque:	$P = Fv + \tau\omega, \boldsymbol{\tau} = \mathbf{r} \times \mathbf{F}$	torque is an unbalanced net moment
Work and impulse:	$E = \int \mathbf{F} \cdot d\mathbf{s}, \mathbf{J} = \int \mathbf{F} dt$	E is change in energy, \mathbf{J} is change in momentum

6.1.4 Friction



At a rough contact, there is a normal force N and a friction force F , forming a net reaction force R .

Stationary: $F \leq \mu_s N$ Moving: $F = \mu_k N$ where $\mu_s > \mu_k$

Angle of friction: $\tan \psi = \frac{F}{N} \leq \mu$.

Typical values of the coefficient of static friction, assuming all surfaces are clean and dry:

Surface 1	Surface 2	μ_s	Surface 1	Surface 2	μ_s
steel	steel	0.65	copper	copper	1.6
rubber	rubber	1.16	ice	steel	0.03
car tyre	asphalt	0.72	ice	wood	0.05
car tyre	grass	0.35	human skin	metals	0.9

Rolling resistance (e.g. in wheels) is **not** due to surface friction, but rather due to hysteresis losses in the wheel material. The harder the wheel and surface, the lower the coefficient of rolling resistance C_{rr} . Typical values of C_{rr} are:

car tyres (pneumatic, rubber)		train wheels (cast iron)	
concrete, asphalt	0.014	steel rail	0.0003
field, sand	0.2		

6.1.5. Vector Momentum and Impulse

Angular velocity $\boldsymbol{\omega}$:	$\mathbf{v} = \boldsymbol{\omega} \times \mathbf{r}$	\mathbf{r} : displacement from axis
Linear momentum \mathbf{p} :	$\mathbf{p} = m\mathbf{v}_G$	\mathbf{v}_G : velocity of COM
Angular momentum \mathbf{h} :	$\mathbf{h} = \mathbf{I}\boldsymbol{\omega} = \mathbf{r} \times \mathbf{p}$	\mathbf{I} : inertia matrix (Section 6.3.3, scalar if 2D)
Force-momentum:	$\mathbf{F} = \dot{\mathbf{p}}$	Linear impulse: $\mathbf{J} = \Delta\mathbf{p} = \mathbf{F}\Delta t$
Torque-angular momentum:	$\mathbf{Q} = \dot{\mathbf{h}}$	Angular impulse: $\mathbf{r} \times \mathbf{J} = \Delta\mathbf{h} = \mathbf{Q}\Delta t$

Note: (\mathbf{Q} , \mathbf{h} , \mathbf{I} , $\boldsymbol{\omega}$) must be taken about the same axis, and must include inertial forces and torques if this axis does not pass through the COM. If \mathbf{h} is taken about a moving point P , add a correction term $\mathbf{Q}_P = \dot{\mathbf{h}}_P + \mathbf{v}_P \times \mathbf{p}$.

6.1.6. Relative Velocity and Angular Momentum in a Rigid Body

Relative position, velocity and acceleration:

$$\mathbf{r}_{G/P} = -\mathbf{r}_{P/G} = \mathbf{r}_G - \mathbf{r}_P \quad \dot{\mathbf{r}}_{G/P} = -\dot{\mathbf{r}}_{P/G} = \dot{\mathbf{r}}_G - \dot{\mathbf{r}}_P \quad \ddot{\mathbf{r}}_{G/P} = -\ddot{\mathbf{r}}_{P/G} = \ddot{\mathbf{r}}_G - \ddot{\mathbf{r}}_P$$

For planar (fixed-axis) rotation, angular momentum about a point P :

$$\mathbf{h}_P = \mathbf{h}_G + \mathbf{r}_{G/P} \times \mathbf{p} \quad (\text{from parallel axis theorem})$$

If P is a moving point then G must be the centre of mass (COM).

6.1.7. Variable Mass Problems

When a body B gains or loses mass in the form of particles P :

$$\mathbf{F} = m\mathbf{a} - \dot{m}\mathbf{v}_{P/B}$$

(\mathbf{F} : force exerted on B , \mathbf{a} : acceleration of B , $\mathbf{v}_{P/B}$: velocity of P relative to B ,
 m : mass of B , \dot{m} : rate of change of mass of B)

In general, mechanical energy is **not** conserved in a variable mass process. For example, lifting a coiled chain results in net energy loss due to inelastic collisions.

6.1.8. Collisions and the Coefficient of Restitution

For two objects moving at initial velocities \mathbf{u}_A and \mathbf{u}_B , colliding to new velocities \mathbf{v}_A and \mathbf{v}_B ,

- Coefficient of restitution: $e = \frac{\text{relative speed of separation}}{\text{relative speed of approach}}$.

$$1\text{D: } e = \frac{v_B - v_A}{u_A - u_B} \quad 2\text{D: } e = \frac{(\mathbf{v}_B - \mathbf{v}_A) \cdot \hat{\mathbf{n}}}{(\mathbf{u}_B - \mathbf{u}_A) \cdot \hat{\mathbf{n}}} \quad (\hat{\mathbf{n}}: \text{unit normal vector to plane of contact})$$

- Fraction of total kinetic energy retained = e^2 .

Perfectly elastic collision: $e = 1$, kinetic energy is conserved,

Perfectly inelastic collision: $e = 0$, kinetic energy is lost entirely (converted to heat)

Oblique Collision Between Smooth Inelastic Spheres

(m_1 and m_2 : masses of spheres, \mathbf{u}_1 and \mathbf{u}_2 : initial velocities of spheres, \mathbf{v}_1 and \mathbf{v}_2 : final velocities of spheres after collision, e : coefficient of restitution between spheres, \mathbf{r}_1 and \mathbf{r}_2 : position vectors of sphere COMs at moment of collision. Indices i, j are from $\{1, 2\}$ as properties are symmetric.)

- Velocity of zero momentum frame of reference: $\mathbf{v}_{\text{ZM}} = \frac{1}{m_1 + m_2}(m_1\mathbf{u}_1 + m_2\mathbf{u}_2)$
- Final velocities: $\mathbf{v}_i = \mathbf{u}_i + \frac{m_j(1+e)(\mathbf{u}_j - \mathbf{u}_i) \cdot \hat{\mathbf{n}}}{m_i + m_j} \hat{\mathbf{n}}$ where $\hat{\mathbf{n}} = \frac{\mathbf{r}_i - \mathbf{r}_j}{|\mathbf{r}_i - \mathbf{r}_j|}$
- Impulse: $\mathbf{J}_i = m_i(\mathbf{v}_i - \mathbf{u}_i) = \frac{m_i m_j}{m_i + m_j} (1+e)((\mathbf{u}_j - \mathbf{u}_i) \cdot \hat{\mathbf{n}}) \hat{\mathbf{n}}$

6.1.9. Principles of Mechanical Systems (Simple Mechanical Machines)

- Mechanical advantage (force amplification factor) = $\frac{F_{load}}{F_{effort}} = \frac{F_{output}}{F_{input}}$
- Energy balance on static machines: $\sum \mathbf{F} \cdot \mathbf{x} + \sum \boldsymbol{\tau} \cdot \boldsymbol{\theta} = 0$
- Power balance on dynamic mechanisms: $\sum \mathbf{F} \cdot \mathbf{v} + \sum \boldsymbol{\tau} \cdot \boldsymbol{\omega} = 0$

Levers

Principle of moments: sum of moments $M = Fx$ of all forces on the beam about the fulcrum must be zero for rotational equilibrium. Force balance is also required, via a contact force at the fulcrum (which it must be able to support without failing). Using an 'effort' force (input), a load's moment is balanced.

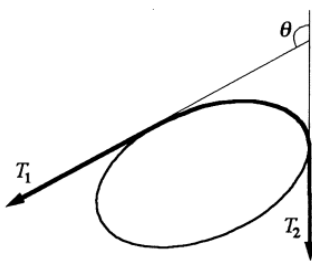
- Class 1 lever: load and effort are on opposite sides of a fulcrum.
- Class 2 lever: load and effort are on one side of a fulcrum, with the effort further away.
- Class 3 lever: load and effort are on one side of a fulcrum, with the load further away.

Pulleys

The tension in a light flexible inextensible rope in contact with small, light, frictionless pulleys is constant. The sum of the forces acting on any static pulley must be zero. For a suspended pulley, the ratio of displacements, velocities and accelerations is equal to the ratio of the numbers of attached ropes.

If any of these assumptions about the system are broken, the tension forces either side of the pulley will be unequal, even at static equilibrium, due to inertial/frictional forces and torques.

Belts (Capstans/Winches, Conveyors)



For a belt or cable passing over a rounded rough contact (subtending angle θ) of distributed coefficient of friction μ , sliding begins when

$$\frac{T_1}{T_2} \geq e^{\mu\theta} \quad \text{or} \quad \frac{T_1}{T_2} \leq e^{-\mu\theta} \quad \text{(the capstan equation)}$$

For a motor powered conveyor belt, the input torque equals the moment of the friction force, μWr .

Pistons and Hydraulic Jacks

Pistons are often actuated by plane mechanisms (Section 6.1.10) to convert rotary motion into linear motion.

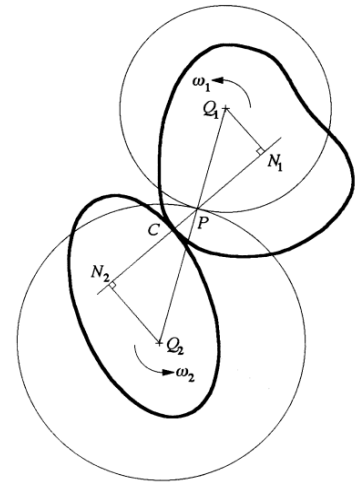
Hydraulic jacks are used to transmit forces over distance through a fluid: $p_{fluid} = \frac{F_{input}}{A_{input}} = \frac{F_{output}}{A_{output}}$

Cams and Wheels (Rolling Body Kinematics)

For pure rolling, the speed of the contact point of a wheel is zero. For pure sliding, the speed of the contact point of a wheel is equal to the translational speed of the wheel.

Equivalent rolling circles at instantaneous centres Q_1 and Q_2 are shown, with angular velocities related by $\frac{\omega_2}{\omega_1} = -\frac{|Q_1N_1|}{|Q_2N_2|} = -\frac{|Q_1P|}{|Q_2P|}$.

Sliding speed at C : $(\omega_1 - \omega_2) PC$.

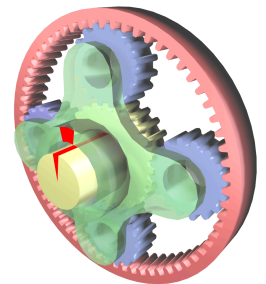


Gears

Gears roll on each other at constant angular velocity with slipping at the teeth. For two coplanar circular gears in contact, they rotate in opposite directions.

- Gear tooth module, $m = \frac{\text{pitch circle diameter, } d}{\text{number of teeth, } n}$ (meshing gears must have same m)
- Rotation rate, $\omega = \frac{\text{contact speed, } v}{\text{gear radius, } r}$ (meshing gears must have same v)
- Gear ratio: $\frac{\omega_1}{\omega_2} = \frac{n_1}{n_2} = \frac{r_2}{r_1} = \frac{\tau_2}{\tau_1}$ (torque amplification factor)
- Compound gears: two concentric gears with the same ω in the same direction.
- Rack and pinion: straight track with one gear (either moving or fixed) so that $v = \omega r$.

Planetary gears (epicyclic gears): a central sun gear (s) meshing with N planetary gears (p) translating uniformly with a carrier frame (c), also meshing with an outer ring gear (r). For meshing, $n_s + n_r = kN$ (k : an integer). The four angular velocities satisfy $n_s\omega_s + n_p\omega_p = (n_s + n_p)\omega_c$ and $n_p\omega_p + (n_r - n_p)\omega_c = n_r\omega_r$ (two degrees of freedom).



Arbitrary gear shape design: using kinematics to find target geometry

Let $f: \mathbb{R} \rightarrow \mathbb{C}$ be a parameterisation $f(s)$ of the first gear shape in the complex plane with its axle at the origin $\{x = \text{Re}(f), y = \text{Im}(f)\}$. During rotation with a second gear, the shape is

$$\gamma(s, t) = (f(s) e^{i\omega t} + R) e^{i\Omega t}$$

(ω : first gear angular velocity, Ω : second gear angular velocity, R : axle separation, t : time). The second gear shape is the envelope of this curve, given by $\gamma(s, t)$, where

$$t = \frac{-\phi(s) \pm \alpha(s)}{\omega}, \quad \phi(s) = \angle f'(s) \quad \text{and} \quad \alpha(s) = \cos^{-1}\left(-\frac{\omega + \Omega}{R\Omega} \text{Re}\left(\frac{f'(s)^*}{|f'(s)|} f(s)\right)\right).$$

This method does not work if the resulting gear has retrograde motion or is self-intersecting.

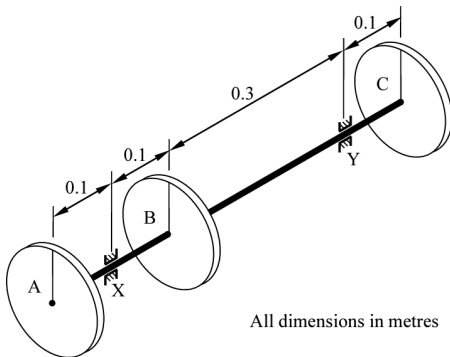
Crank Shafts and Rotors

A slender shaft is loaded with heavy rotors along its length which rotate about the shaft.

Imbalance of a rotor, U [kg mm] = Rotor mass, M [kg] \times Rotor COM to shaft distance, e [mm]

- **Static balance:** COM of the system lies on shaft axis \rightarrow resultant bearing force is zero.
- **Dynamic balance:** resultant moment of the bearing forces about any point on the shaft is zero.

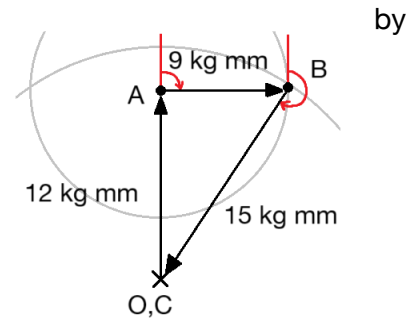
An imbalanced rotor can be modelled as a uniform rotor plus an imbalance mass m at its outer radius r , for a net imbalance $U = mr$.



Example (left): bearings X and Y, rotors A, B, C (diameter: 0.2 m). Imbalances: A = 12 kg mm, B = 9 kg mm, C = 15 kg mm, along the lines on the rotors. Shaft rotation speed: 5000 rpm.

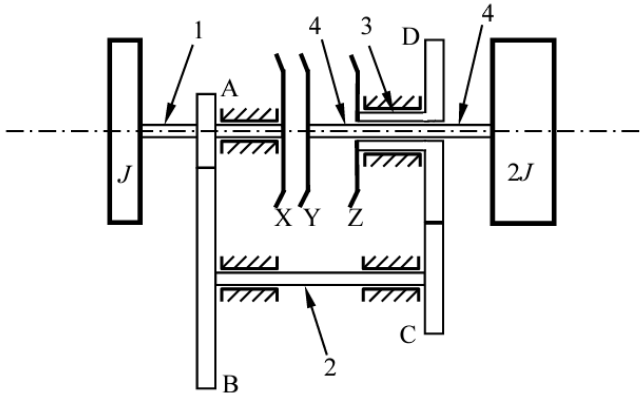
Diagram of imbalances: need to rotate B 90° and C by 216.9° to achieve static balance (zero resultant).

Dynamic moment about X due to centrifugal loading: $M_A = \frac{U_A \omega_A^2 d_{AX}}{1000} \dots$



Bearing force at Y supplies out-of-balance (net) moment. Material of mass m can be cut from the outsides of A and C at angular positions in the direction of the bearing force to achieve dynamic balance ($mr\omega^2 d_{AC} = M_{net}$).

Clutches and Gearboxes



Example (left): two-speed gearbox. Shafts 1, 2 and 3 are mounted in rigid bearings and are axially constrained. Shaft 4 is mounted inside shaft 3 (can slide relative to shaft 3 and rotate at different speed). When shaft 4 slides to the left, clutch plates X and Y engage, so that shafts 1 and 4 rotate together; when it slides to the right, clutch plates Y and Z engage, so that shafts 3 and 4 rotate together. If shafts 1 and 4 carry rotors with polar moment of inertia of J and $2J$ respectively, while gear wheels A, B, C, and D have $N_A = 12$, $N_B = 36$, $N_C = 18$ and $N_D = 30$ teeth respectively, then:

Gear speeds: $\omega_1 N_A = \omega_2 N_B$ and $\omega_2 N_C = \omega_3 N_D$
 Impulse between gears: $I_{AB} N_B = I_{CD} N_C$ (equilibrium of BC)

The total angular momentum of the system about the axis of the rotors is **not** conserved even when not slipping at the clutch since gear contact forces exert moments about the shafts.

After starting with Y at X, consider 'rotational impact' of clutch moving to engage Z:

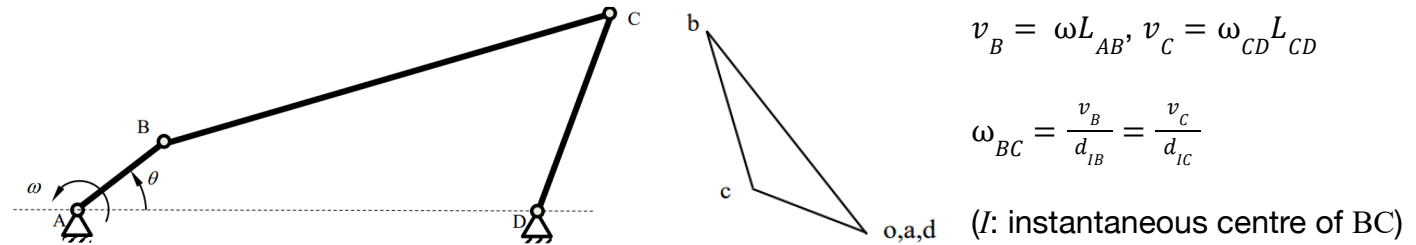
Angular momenta before/after: on rotor J : $J\omega_1 + I_{AB} r_A = J\omega_1'$; on rotor $2J$: $2J\omega_1 - I_{CD} r_D = 2J \frac{N_A N_C}{N_B N_D} \omega_1'$

Kinetic energy before: $\frac{1}{2} (3J)\omega_1^2$; Kinetic energy after: $\frac{1}{2} J\omega_1'^2 + \frac{1}{2} (2J) \left(\frac{N_A N_C}{N_B N_D} \omega_1' \right)^2$; Efficiency = $\frac{KE_{after}}{KE_{before}}$

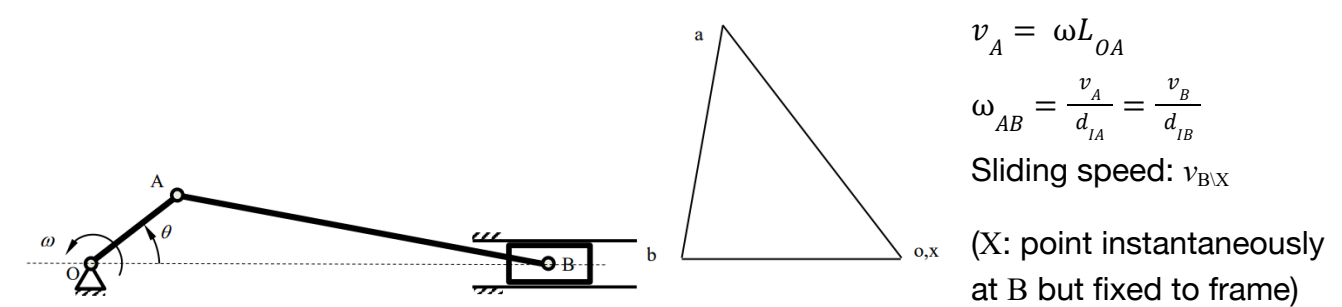
6.1.10. Kinematics of Plane Mechanisms

A mechanistic assembly of rigid rods connected by pin joints can be actuated by applying a torque to one of the joints. Common types of ‘four-bar mechanisms’ with their **velocity diagrams** are shown:

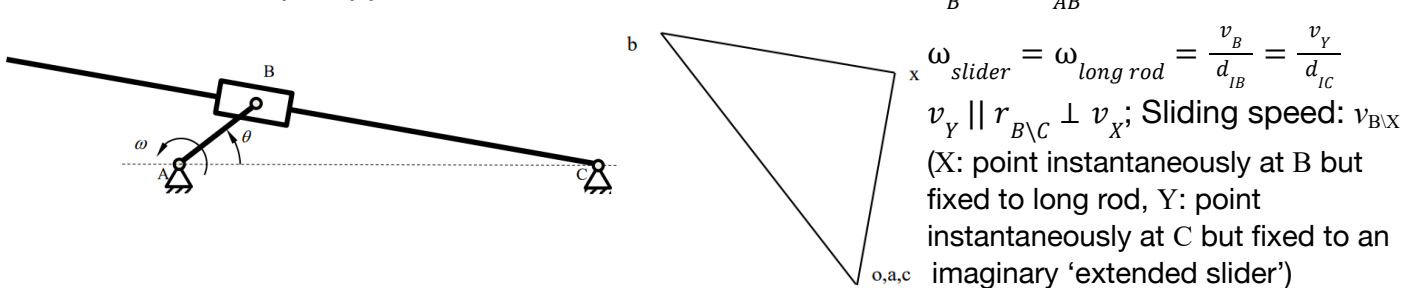
Crank Rocker: torque applied at A, rocker CD oscillates about D



Slider Crank: torque applied at O, slider B oscillates in a line



Quick Return: torque applied at A, rod BC oscillates



Velocity Image Theorem: for any rigid lamina ABC rotating at ω , the corresponding velocity diagram is obtained by rotating the lamina 90° in the direction of ω and scaling by factor ω .

Acceleration Diagrams: for rigid link AB (length L , angular speed ω , angular acceleration α):
 $\mathbf{a}_{B \setminus A} = -L\omega^2 \mathbf{e}_r + L\alpha \mathbf{e}_\theta$ (\mathbf{e}_r : unit vector of $\mathbf{r}_{B \setminus A}$, \mathbf{e}_θ : unit vector perpendicular to \mathbf{e}_r in direction of ω).
 The acceleration image is a rotation of the lamina by some angle (not necessarily 90°).

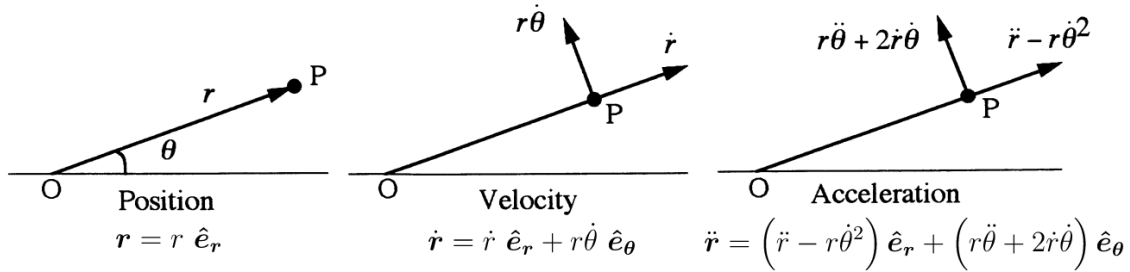
Virtual Work and Virtual Power: $\sum_i \mathbf{F}_i \cdot \mathbf{v}_i + \sum_i T_i \omega_i = 0$

Include both real and D’Alembert (inertial) forces/torques to balance member accelerations ($\mathbf{F}_{COM} = -m\mathbf{a}_{COM}$ and $T_{COM} = -I\alpha_{COM}$) if links are not light. Frictional torques T_{fr} acting at joints should use the relative angular velocity between the links. Power loss by frictional torque: $|P| = T_{fr}(\omega_1 - \omega_2)$.

6.1.11. Vector Kinematics in 2D Polar and Intrinsic Coordinates

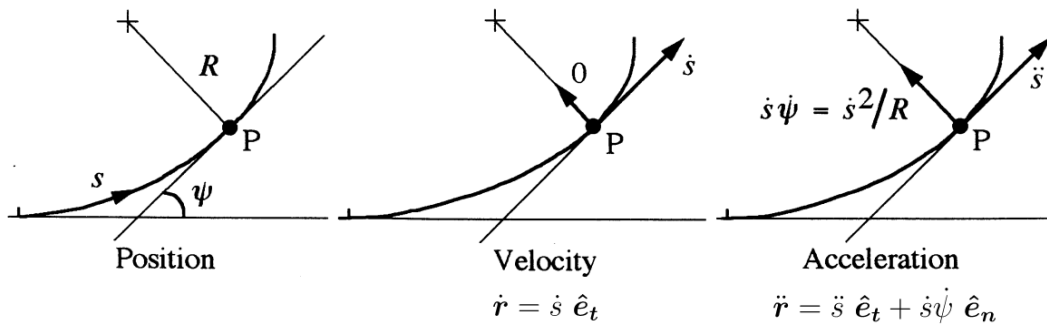
(r : displacement, R : radius of curvature, ω : angular velocity, (e, e^*) orthonormal vectors.)

Polar Coordinates (r, θ): $\dot{e}_r = \dot{\theta} e_\theta$ $\dot{e}_\theta = -\dot{\theta} e_r$



Acceleration components: $\{r\ddot{\theta}$: tangential; $2\dot{r}\dot{\theta}$: Coriolis; \ddot{r} : radial; $-r\dot{\theta}^2$: centripetal}

Intrinsic Coordinates (s, ψ): $\dot{e}_t = \dot{\psi} e_n$ $\dot{e}_n = -\dot{\psi} e_t$



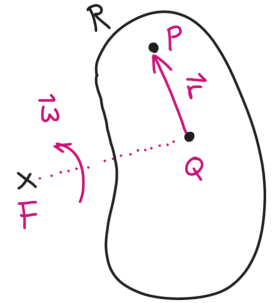
Differentiation of a rotating vector:

For any unit vector rotating at rate ω , $\dot{e} = \omega \times \hat{e}^*$

For vector kinematics in 3D spherical coordinates, see Section 3.5.13.

6.1.12. Vector Kinematics in Non-Inertial Reference Frames

A body R moves and rotates with angular velocity ω with respect to a reference frame F. If point Q is fixed on the body, and another point P moves relative to the body with \mathbf{r} as the position vector of P relative to Q, then the displacement \mathbf{r}_P , velocity \mathbf{v}_P and acceleration \mathbf{a}_P of P relative to frame F are given by:



$$\mathbf{r}_P = \mathbf{r}_Q + \mathbf{r},$$

$$\mathbf{v}_P = \underbrace{\mathbf{v}_Q}_{\text{velocity of Q in frame F}} + \left[\frac{d\mathbf{r}}{dt} \right]_F = \mathbf{v}_Q + \underbrace{\left[\frac{d\mathbf{r}}{dt} \right]_R}_{\text{apparent motion of P relative to body R}} + \underbrace{\omega \times \mathbf{r}}_{\text{contribution due to rotation of body R}}$$

$$\mathbf{a}_P = \underbrace{\mathbf{a}_Q}_{\text{acceleration of Q in frame F}} + \underbrace{\left[\frac{d^2\mathbf{r}}{dt^2} \right]_R}_{\text{apparent acceleration relative to body R}} + \underbrace{\frac{d\omega}{dt} \times \mathbf{r}}_{\text{Euler acceleration}} + \underbrace{2\omega \times \left[\frac{d\mathbf{r}}{dt} \right]_R}_{\text{Coriolis acceleration}} + \underbrace{\omega \times (\omega \times \mathbf{r})}_{\text{centripetal acceleration}}$$

Reference frame conversion: if the non-inertial ‘body frame’ R translating at velocity \mathbf{U} and rotating at rate ω relative to a reference frame F, then the rate of change of any vector \mathbf{x} in the two frames are related by: $((\mathbf{U} \cdot \nabla)\mathbf{x}$: advection operator)

$$\underbrace{\left[\frac{d\mathbf{x}}{dt} \right]_F}_{\text{rate of change in frame F}} = \underbrace{\left[\frac{d\mathbf{x}}{dt} \right]_R}_{\text{rate of change in frame R}} + \underbrace{\omega \times \mathbf{x}}_{\text{contribution due to rotation of F relative to R}} + \underbrace{(\mathbf{U} \cdot \nabla)\mathbf{x}}_{\text{contribution due to translation of F relative to R}}$$

If frame F is inertial then it is in frame F that forces and torques can be computed via Newton’s second law.

Example (left): kinematics of a horizontal-axis wind turbine with yaw control. Constant speeds: blade rotation rate is Ω , housing rotation rate is ω .

- P: the tip of a turbine blade, at distance l from the housing ($\Omega = -\Omega\mathbf{j}$ in frame R)
- Q: the housing, at distance d from the tower
- R: the frame rotating with the housing at angular velocity $\omega = \omega\mathbf{k}$ relative to F
- F: the frame fixed to the tower $\{\mathbf{i}, \mathbf{j}, \mathbf{k}\}$

$$\mathbf{r}_P = (-l \sin \theta)\mathbf{i} + (-d)\mathbf{j} + (l \cos \theta)\mathbf{k} \qquad (\mathbf{r}_Q = -d\mathbf{j}, \mathbf{r} = -l \sin \theta \mathbf{i} + l \cos \theta \mathbf{k})$$

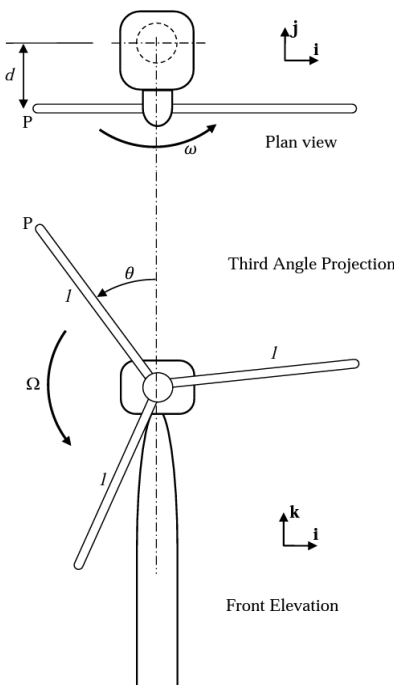
$$\mathbf{v}_P = (\omega d - \Omega l \cos \theta)\mathbf{i} + (-\omega l \sin \theta)\mathbf{j} + (-\Omega l \sin \theta)\mathbf{k}$$

$$(\mathbf{v}_Q = \omega d\mathbf{i}, [\mathbf{v}]_R = -\Omega l \cos \theta \mathbf{i} - \Omega l \sin \theta \mathbf{k}, \omega \times \mathbf{r} = -\omega l \sin \theta \mathbf{j})$$

$$\mathbf{a}_P = ((\Omega^2 + \omega^2) l \sin \theta)\mathbf{i} + (\omega^2 d - 2\omega\Omega l \cos \theta)\mathbf{j} + (-\Omega^2 l \cos \theta)\mathbf{k}$$

$$(\mathbf{a}_Q = \omega^2 d\mathbf{j}, [\mathbf{a}]_R = \Omega^2 l \sin \theta \mathbf{i} - \Omega^2 l \cos \theta \mathbf{k}, \mathbf{a}_{\text{Euler}} = \mathbf{0}, \mathbf{a}_{\text{Coriolis}} = -2\omega\Omega l \cos \theta \mathbf{j}, \mathbf{a}_{\text{centripetal}} = \omega^2 l \sin \theta \mathbf{i})$$

The inertial force loading (per unit length along the blade) is $\mathbf{w}(x) = -\rho A \mathbf{a}(x)$. This loading gives rise to an internal shear force $\mathbf{S}(x)$ and bending moment $\mathbf{M}(x)$, which can be found by taking a free-body cut at x .



6.1.13. Moments of Inertia

Moments of inertia:

$$I_{xx} = \int (y^2 + z^2) dm = mk_x^2, \quad k_x: \text{radius of gyration about } x\text{-axis}$$

$$I_{yy} = \int (x^2 + z^2) dm = mk_y^2, \quad k_y: \text{radius of gyration about } y\text{-axis}$$

$$I_{zz} = \int (x^2 + y^2) dm = mk_z^2, \quad k_z: \text{radius of gyration about } z\text{-axis}$$

Products of inertia: $I_{xy} = \int xy dm, I_{yz} = \int yz dm, I_{xz} = \int xz dm$

Parallel Axis Theorem: $I_{x'x'} = I_{xx} + m((\Delta y)^2 + (\Delta z)^2)$ etc, and $I_{x'y'} = I_{xy} + m(\Delta x)(\Delta y)$ etc.

Perpendicular Axis Theorem: for a lamina in the xy plane only, $I_{z'z'} = I_{x'x'} + I_{y'y'}$.

Inertia matrix:
$$\mathbf{I} = \begin{bmatrix} I_{xx} & -I_{xy} & -I_{xz} \\ -I_{xy} & I_{yy} & -I_{yz} \\ -I_{xz} & -I_{yz} & I_{zz} \end{bmatrix}$$

The eigenvalues of \mathbf{I} are the principal moments of inertia, and the eigenvectors are the principal axes, about which $\mathbf{h} = I\boldsymbol{\omega}$ i.e. $\mathbf{h} \parallel \boldsymbol{\omega}$.

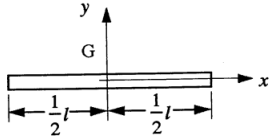
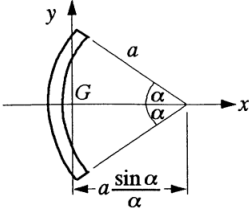
For a body with a plane of symmetry, two principal axes lie in the plane while the third is normal to the plane. An 'AAC' body is axisymmetric (e.g. prisms, all laminas). An 'AAA' body is symmetric in all three axes and has dynamic similarity.

Inertia matrix in the body frame of reference, with \mathbf{R} as a rotation matrix from the inertial frame to the body frame: $\mathbf{I}_{\text{body}} = \mathbf{R}\mathbf{I}_{\text{principal}}\mathbf{R}^T$, where all products of inertia are zero and the diagonal entries of $\mathbf{I}_{\text{principal}}$ are the principal moments of inertia (Sylvester's law of inertia).

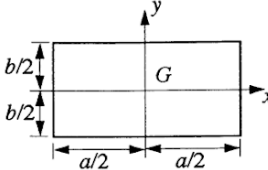
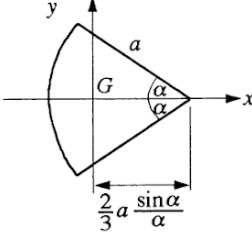
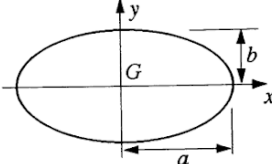
For formulas for moments of inertia of specific geometries, see Section 6.3.

6.1.14. Moments of Inertia and Centroids of 1D Bodies

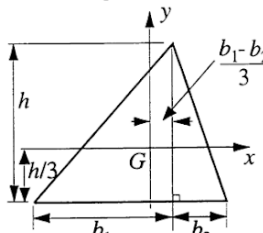
Rods:

	k_x^2	k_y^2
<p>Straight rod</p> 	0	$\frac{1}{12}l^2$
<p>Curved rod</p> 	$\frac{1}{2}a^2\left(1 - \frac{\sin 2\alpha}{2\alpha}\right)$	$\frac{1}{2}a^2\left\{1 - 2\left(\frac{\sin \alpha}{\alpha}\right)^2 + \frac{\sin 2\alpha}{2\alpha}\right\}$

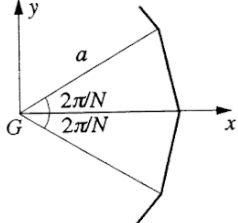
Laminas:

<p>Rectangular lamina</p> 	A ab	k_x^2 $\frac{1}{12}b^2$	k_y^2 $\frac{1}{12}a^2$
<p>Sectorial lamina</p> 	αa^2	$\frac{a^2}{4}\left(1 - \frac{\sin 2\alpha}{2\alpha}\right)$	$\frac{a^2}{4}\left\{1 - \left(\frac{4 \sin \alpha}{3\alpha}\right)^2 + \frac{\sin 2\alpha}{2\alpha}\right\}$
<p>Elliptic lamina</p> 	πab	$\frac{b^2}{4}$	$\frac{a^2}{4}$

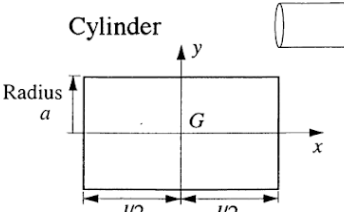
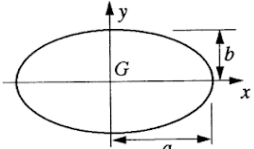
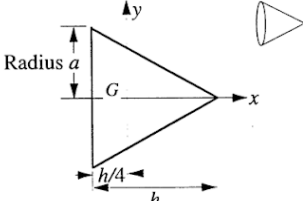
Laminas (continued):

	A	k_x^2	k_y^2
Triangular lamina			
	$\frac{h}{2}(b_1 + b_2)$	$\frac{h^2}{18}$	$\frac{(b_1^2 + b_1b_2 + b_2^2)}{18}$
		$I_{xy} = m \cdot \frac{h}{36}(b_1 - b_2)$	

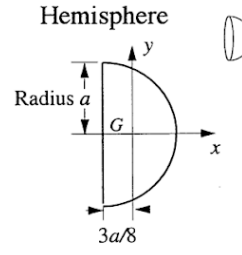
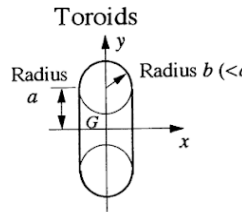
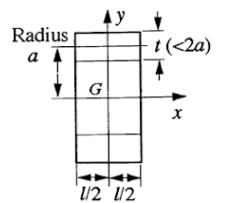
Regular polygonal lamina with N sides ($N > 2$)

	$\pi a^2 \left(\frac{\sin \frac{2\pi}{N}}{\frac{2\pi}{N}} \right)$	$\frac{a^2}{12} \left(2 + \cos \frac{2\pi}{N} \right)$	$\frac{a^2}{12} \left(2 + \cos \frac{2\pi}{N} \right)$
---	---	---	---

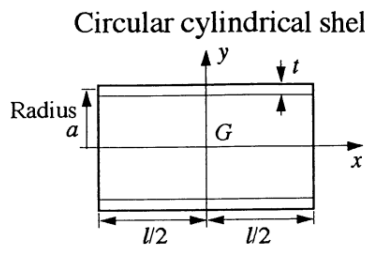
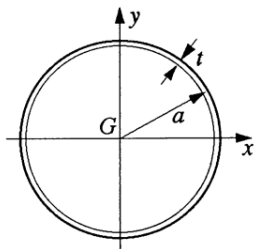
3D Solids of Revolution (Axisymmetric Bodies):

	V	k_x^2	$k_y^2 = k_z^2$
Cylinder			
	$\pi a^2 l$	$\frac{a^2}{2}$	$\frac{a^2}{4} + \frac{l^2}{12}$
Spheroid			
	$\frac{4\pi ab^2}{3}$	$\frac{2b^2}{5}$	$\frac{(a^2 + b^2)}{5}$
Cone			
	$\frac{\pi a^2 h}{3}$	$\frac{3a^2}{10}$	$\frac{3(4a^2 + h^2)}{80}$

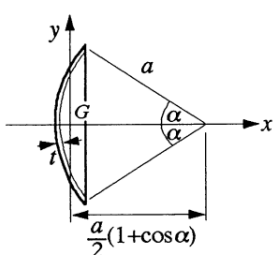
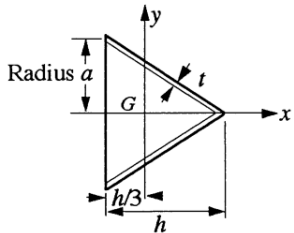
3D Solids of Revolution (Axisymmetric Bodies) (continued):

	V	k_x^2	$k_y^2 = k_z^2$
<p>Hemisphere</p> 	$\frac{2\pi a^3}{3}$	$\frac{2a^2}{5}$	$\frac{83a^2}{320}$
<p>Toroids</p> 	$2\pi^2 ab^2$	$a^2 + \frac{3b^2}{4}$	$\frac{a^2}{2} + \frac{5b^2}{8}$
	$2\pi a t l$	$a^2 + \frac{t^2}{4}$	$\frac{a^2}{2} + \frac{t^2}{8} + \frac{l^2}{12}$

3D Shells of Revolution

	V	k_x^2	$k_y^2 = k_z^2$
<p>Circular cylindrical shell</p> 	$2\pi a t l$	a^2	$\frac{a^2}{2} + \frac{l^2}{12}$
<p>Spherical shell</p> 	$4\pi a^2 t$	$\frac{2a^2}{3}$	$\frac{2a^2}{3}$

3D Shells of Revolution (continued):

	V	k_x^2	$k_y^2 = k_z^2$
Spherical cap shell			
	$2\pi a^2 t (1 - \cos \alpha)$		$\frac{a^2}{12} (1 - \cos \alpha)(5 + \cos \alpha)$
		$\frac{a^2}{3} (1 - \cos \alpha)(2 + \cos \alpha)$	
Conical shell			
	$\pi a t (a^2 + h^2)^{1/2}$	$\frac{a^2}{2}$	$\frac{a^2}{4} + \frac{h^2}{18}$

6.1.15. Second Moments of Area

The second moment of area of a plane cross-section about the x axis is denoted I_{xx} :

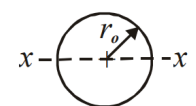
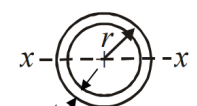
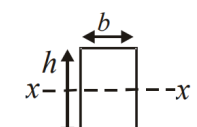
$$I_{xx} = \int y^2 dA$$

Warning: both moment of inertia and second moment of area use the symbol I . Moment of inertia has dimensions of \mathbf{ML}^2 . Second moment of area has dimensions \mathbf{L}^4 .

If the mass-per-unit-area σ is uniform across the cross-section, then

$$\text{moment of inertia} = \sigma \times \text{second moment of area}$$

Second moments of area for common beam cross-sections:

Solid circular section	Thin-walled circular section	Solid rectangle
		
$I_{xx} = \frac{\pi r_o^4}{4}$	$I_{xx} \approx \pi r^3 t$	$I_{xx} = \frac{bh^3}{12}$

6.1.16. Polar Second Moments of Area

The polar second moment of area of a plane cross-section in the xy plane is denoted J :

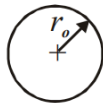
$$I_{zz} = J = \int (x^2 + y^2) dA$$

If the mass-per-unit-area σ is uniform across the cross-section, then

$$\text{polar moment of inertia} = \sigma \times \text{polar second moment of area}$$

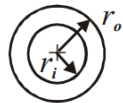
For common cross-sections:

Solid circular section



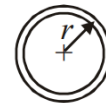
$$J = \frac{\pi r_o^4}{2}$$

Thick-walled circular section



$$J = \frac{\pi (r_o^4 - r_i^4)}{2}$$

Thin-walled circular section



$$J \approx 2\pi r^3 t$$

Main applications of I and J :

- Moment of inertia I is important for kinematics of rotating bodies.
- Second moment of area I is important for bending stresses in beams.
- Polar second moment of area J is important for torsional stresses in shafts.

6.1.17. Gyroscope Dynamics

For motion relative to axes aligned with the rotation of a rigid body (the body frame B , rotating at ω relative to the rest frame):

Rate of change of a vector: $\frac{d}{dt}\mathbf{x} = \dot{\mathbf{x}}_B + \boldsymbol{\omega} \times \mathbf{x}_B$

Euler's Equations: Torque-angular momentum in the body frame.

If A, B and C are the principal moments of inertia about P which is either at a fixed point or at the centre of mass, the angular velocity of the body is $\boldsymbol{\omega} = [\omega_1, \omega_2, \omega_3]^T$ and the moment about P of external forces is $\mathbf{Q} = [Q_1, Q_2, Q_3]$, then

Body-fixed reference frame:

$$A\dot{\omega}_1 - (B - C)\omega_2\omega_3 = Q_1$$

$$B\dot{\omega}_2 - (C - A)\omega_3\omega_1 = Q_2$$

$$C\dot{\omega}_3 - (A - B)\omega_1\omega_2 = Q_3$$

using axes aligned with the principal axes of inertia of the body at P

Non-body-fixed reference frame:
(the AAC gyroscope equations)

$$A\dot{\Omega}_1 - (A\Omega_3 - C\omega_3)\Omega_2 = Q_1$$

$$A\dot{\Omega}_2 + (A\Omega_3 - C\omega_3)\Omega_1 = Q_2$$

$$C\dot{\omega}_3 = Q_3$$

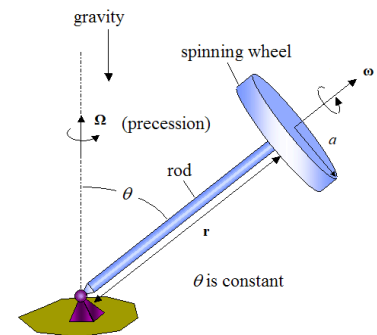
using axes such that ω_3 and Q_3 are aligned with the symmetry axis of the body

The reference frame when not fixed in the body rotates with angular velocity $\boldsymbol{\Omega} = [\Omega_1, \Omega_2, \Omega_3]^T$ with $\Omega_1 = \omega_1$ and $\Omega_2 = \omega_2$.

For a simple gyroscope (J : polar moment of inertia parallel to $\boldsymbol{\omega}$):

$$\mathbf{Q} = \mathbf{r} \times m\mathbf{g} = J\boldsymbol{\Omega} \times \boldsymbol{\omega}$$

In general, resultant torque is $\mathbf{Q} = \mathbf{I}\boldsymbol{\alpha} + \boldsymbol{\omega} \times \mathbf{h}$, where the additional $\boldsymbol{\omega} \times \mathbf{h}$ term is the Coriolis torque.



6.1.18. Representations of 3D Rigid Body Orientation

Three consecutive rotations applied starting from the rest frame to transform it into the body frame. The rotations may be ‘intrinsic’ (referring to the successively transformed body axes) or ‘extrinsic’ (always referring to the fixed rest frame axes). Two common schemes are:

Proper Euler Angles $\{\alpha, \beta, \gamma\}$: uses only two reference axes (first and last are the same)

Most common convention: $z-x'-z''$ (intrinsic). Rotate α about body z -axis, rotate β about new body x -axis (x'), rotate γ about new body z -axis (z''). If the body-frame unit vectors are measured in the rest frame as ($\hat{X} = X_1\mathbf{i} + X_2\mathbf{j} + X_3\mathbf{k}$, etc), then:

$$\alpha = \cos^{-1} \frac{-Z_2}{\sqrt{1-Z_3^2}} = \text{atan2}(Z_1, -Z_2), \quad \beta = \cos^{-1} Z_3, \quad \gamma = \cos^{-1} \frac{Y_3}{\sqrt{1-Z_3^2}} = \text{atan2}(X_3, Y_3)$$

Tait-Bryan / Nautical Angles $\{\varphi, \theta, \psi\}$: uses all three reference axes

Most common convention: $z-y'-x''$ (intrinsic). Rotate ψ about body z -axis, rotate θ about new body y axis (y'), rotate φ about new body x -axis (x''). If the body-frame unit vectors are measured in the rest frame as ($\hat{X} = X_1\mathbf{i} + X_2\mathbf{j} + X_3\mathbf{k}$, etc), then:

$$\varphi = \sin^{-1} \frac{X_2}{\sqrt{1-X_3^2}}, \quad \theta = \sin^{-1}(-X_3), \quad \psi = \sin^{-1} \frac{Y_3}{\sqrt{1-X_3^2}}$$

The Tait-Bryan angles are often used for vehicle navigation (e.g. aeroplanes, ships), in which the $\{X, Y, Z\}$ axes are specific to the vehicle. In the $z-y'-x''$ convention:

The 3×3 linear transformation matrix from fixed to body frames: $\mathbf{M} = \mathbf{R}_z(\psi) \mathbf{R}_y(\theta) \mathbf{R}_x(\varphi)$, where \mathbf{R} are the rotation matrices (Section 4.2.1).

- ψ : yaw angle, giving the bearing about the Z -axis, aligned in the ‘down’ direction.
- θ : pitch angle, giving the elevation about the Y -axis, aligned in the ‘right’ direction.
- φ : roll angle, giving the bank about the X -axis, aligned in the ‘forward’ direction.

Axis-Angle and Quaternion Representation of Rotations

Any sequence of 3D rotations can be represented as a single rotation φ about an axis $\mathbf{X} = [X_1, X_2, X_3]$, due to the Rodriguez formula (Section 4.2.1).

Quaternions can be considered an extension of how complex numbers can represent 2D rotations. A quaternion $q = w + xi + yj + zk$, such that $\{w, x, y, z\}$ are real and $i^2 = j^2 = k^2 = ijk = -1$.

Unit quaternion $q = \cos \frac{\varphi}{2} + X_1 \sin \frac{\varphi}{2} \mathbf{i} + X_2 \sin \frac{\varphi}{2} \mathbf{j} + X_3 \sin \frac{\varphi}{2} \mathbf{k}$ represents $\mathbf{R}_x(\varphi)$ via $x' = qxq^{-1}$.

Working in terms of quaternions instead of matrices results in significant computational speedups, and also avoids the issue of ‘gimbal lock’ for degenerate rotations.

6.2. Linear Systems and Mechanical Vibrations

6.2.1. Equations for Natural Oscillations

Angular velocity, period and frequency: $\omega = 2\pi f = \frac{2\pi}{T}$ (T : time period)

Simple 1D SHM kinematics: $x = A \cos \omega t$, $v = -A\omega \sin \omega t$, $a = -A\omega^2 \cos \omega t$
 $v = \pm \omega \sqrt{A^2 - x^2}$, $a = -\omega^2 x$

Max speed = $A\omega$ Max acceleration = $A\omega^2$

Energy balance (no external forces): $T + V = \text{constant} \Leftrightarrow \frac{d}{dt}(T + V) = 0$

6.2.2. Common Undamped Oscillating Systems

For a linear spring-mass system: $\omega^2 = \frac{k}{m}$, $T = 2\pi \sqrt{\frac{m}{k}}$, $\frac{1}{2}mv^2 + \frac{1}{2}kx^2 = C$

For a plane pendulum: $\Omega^2 = \frac{g}{L}$, $T = 2\pi \sqrt{\frac{L}{g}}$, $\frac{1}{2}m\omega^2 L^2 - mgL \cos \theta = C$

For a rotational spring-flywheel: $\Omega^2 = \frac{\kappa}{J}$, $T = 2\pi \sqrt{\frac{J}{\kappa}}$, $\frac{1}{2}J\omega^2 + \frac{1}{2}\kappa\theta^2 = C$

For a standing wave on a string: $\omega^2 = \frac{\pi^2 P}{L^2 \rho}$, $T = 2L \sqrt{\frac{\rho}{P}}$

(k : spring constant, m : mass, g : gravity, L : length, κ : rotational stiffness, J : polar moment of inertia, P : string tension, ρ : string mass per unit length)

6.2.3. Step Response of a Linear Second Order System

For a model of the form $\frac{1}{\omega_n^2}y'' + \frac{2\zeta}{\omega_n}y' + y = x$ with $y(0) = y'(0) = 0$ and $x = KH(t)$,

$$\frac{y}{K} = 1 - \frac{1}{2\omega_n\sqrt{\zeta^2 - 1}} \left(\lambda^{(+)} e^{\lambda^{(+)}t} - \lambda^{(-)} e^{\lambda^{(-)}t} \right), \quad \text{if overdamped } (\zeta > 1)$$

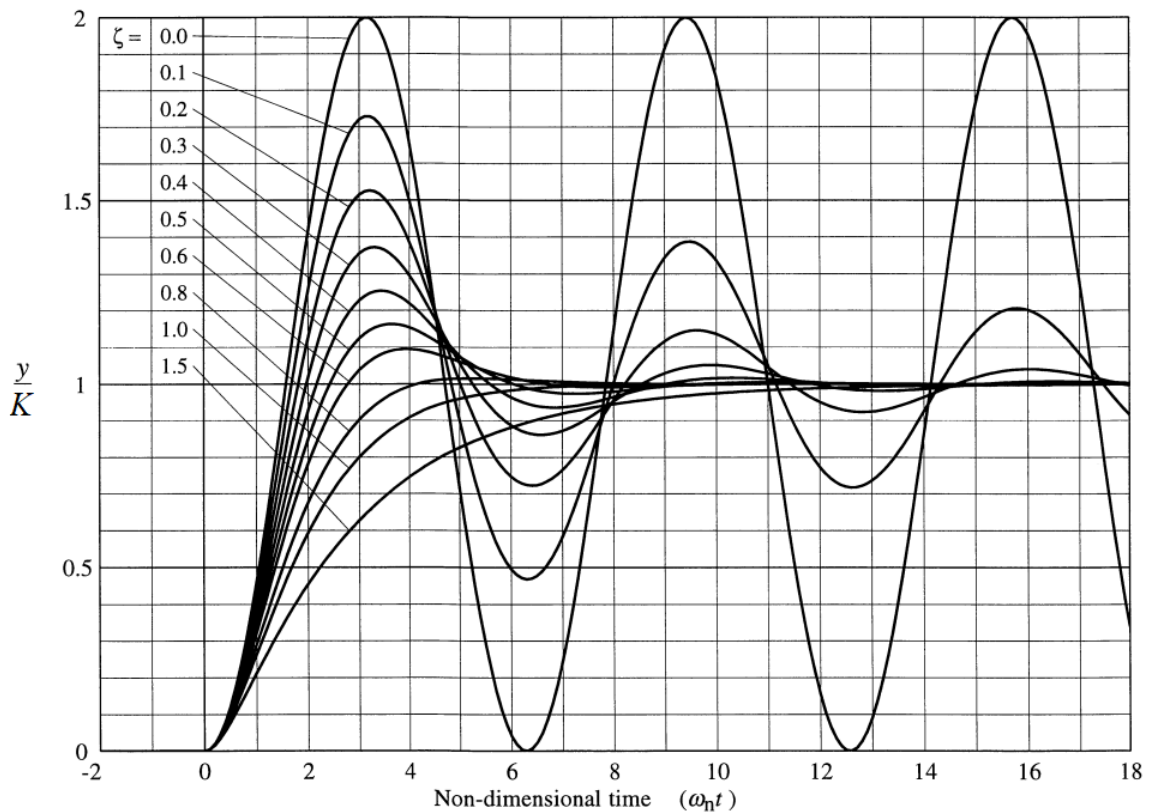
$$\frac{y}{K} = 1 - (1 + \omega_n t) e^{-\omega_n t}, \quad \text{if critically damped } (\zeta = 1)$$

$$\frac{y}{K} = 1 - \frac{1}{\sqrt{1 - \zeta^2}} e^{-\zeta\omega_n t} \cos(\omega_d t - \psi), \quad \text{if underdamped } (\zeta < 1)$$

$$\frac{y}{K} \approx 1 - e^{-\zeta\omega_n t} \cos \omega_n t, \quad \text{if lightly damped } (\zeta \ll 1)$$

where $\lambda^{(\pm)} = \left(-\zeta \pm \sqrt{\zeta^2 - 1} \right) \omega_n$, $\omega_d = \omega_n \sqrt{1 - \zeta^2}$, $\sin \psi = \zeta$.

Dimensionless plots of step response:



6.2.4. Impulse Response of a Linear Second Order System

For a model of the form $\frac{1}{\omega_n^2}\ddot{y} + \frac{2\zeta}{\omega_n}\dot{y} + y = x$ with $y(0) = \dot{y}(0) = 0$, $x(t) = N\delta(t)$,

$$\frac{y(t)}{\omega_n N} = \frac{1}{2\sqrt{\zeta^2 - 1}} (e^{\lambda_+ t} - e^{\lambda_- t}) \quad \text{if overdamped } (\zeta > 1)$$

$$\frac{y(t)}{\omega_n N} = \omega_n t e^{-\omega_n t} \quad \text{if critically damped } (\zeta = 1)$$

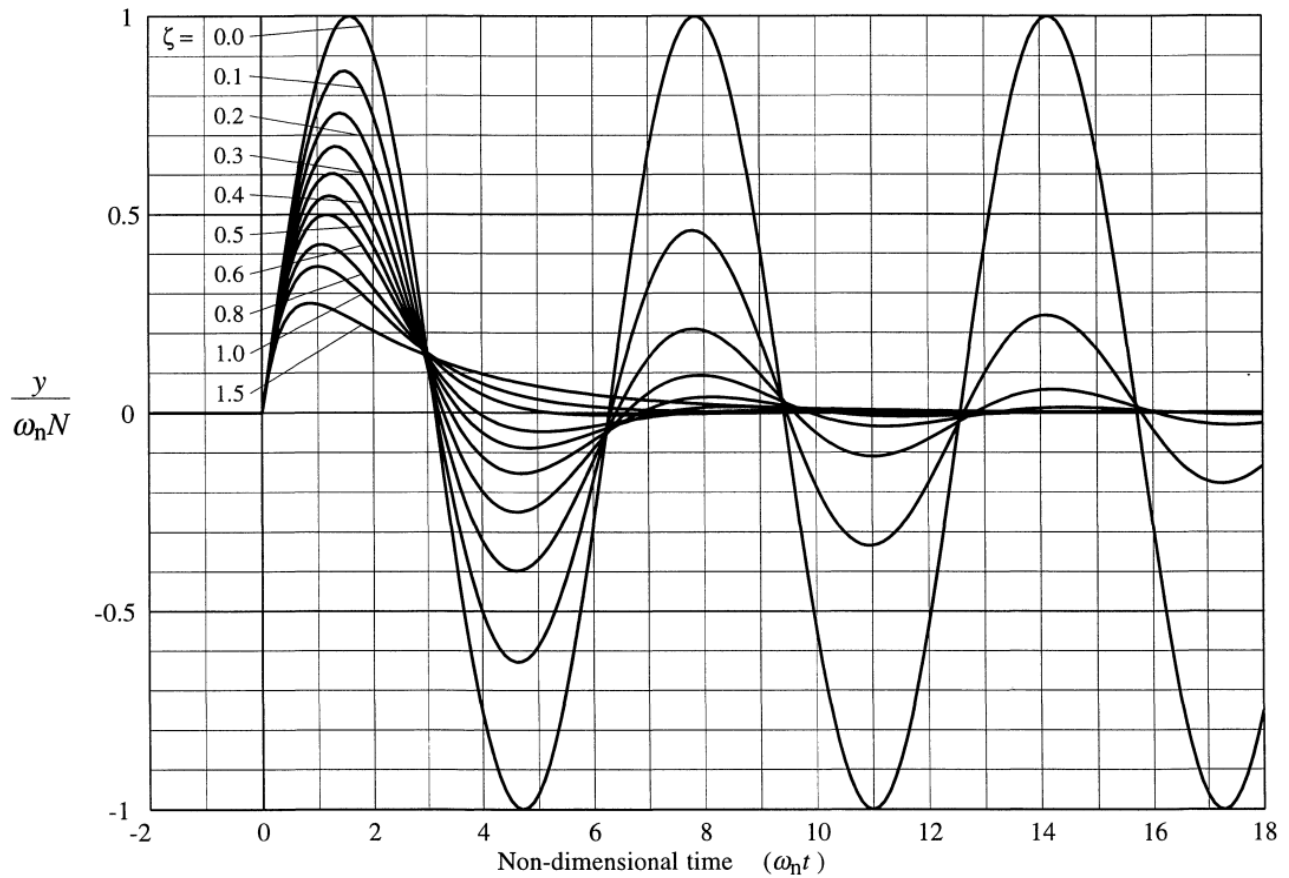
$$\frac{y(t)}{\omega_n N} = \frac{1}{\sqrt{1 - \zeta^2}} e^{-\zeta\omega_n t} \sin \omega_d t \quad \text{if underdamped } (\zeta < 1)$$

$$\frac{y(t)}{\omega_n N} \approx e^{-\zeta\omega_n t} \sin \omega_n t \quad \text{if very lightly damped } (\zeta \ll 1)$$

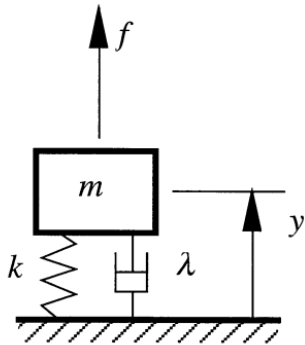
where $\lambda_{\pm} = (-\zeta \pm \sqrt{\zeta^2 - 1}) \omega_n$ (system s -domain poles), $\omega_d = \omega_n \sqrt{1 - \zeta^2}$, and $\sin \psi = \zeta$.

Transfer function in s -domain: $\frac{\hat{y}(s)}{\hat{x}(s)} = \frac{N\omega_n^2}{s^2 + 2\omega_n\zeta s + \omega_n^2}$

Dimensionless plots of impulse response for a variety of damping rates ζ :



6.2.5. Harmonic Response of a Linear Second Order System (Forced Displacements)



For a model of the form $\frac{1}{\omega_n^2} \ddot{y} + \frac{2\zeta}{\omega_n} \dot{y} + y = x$, the harmonic gain is

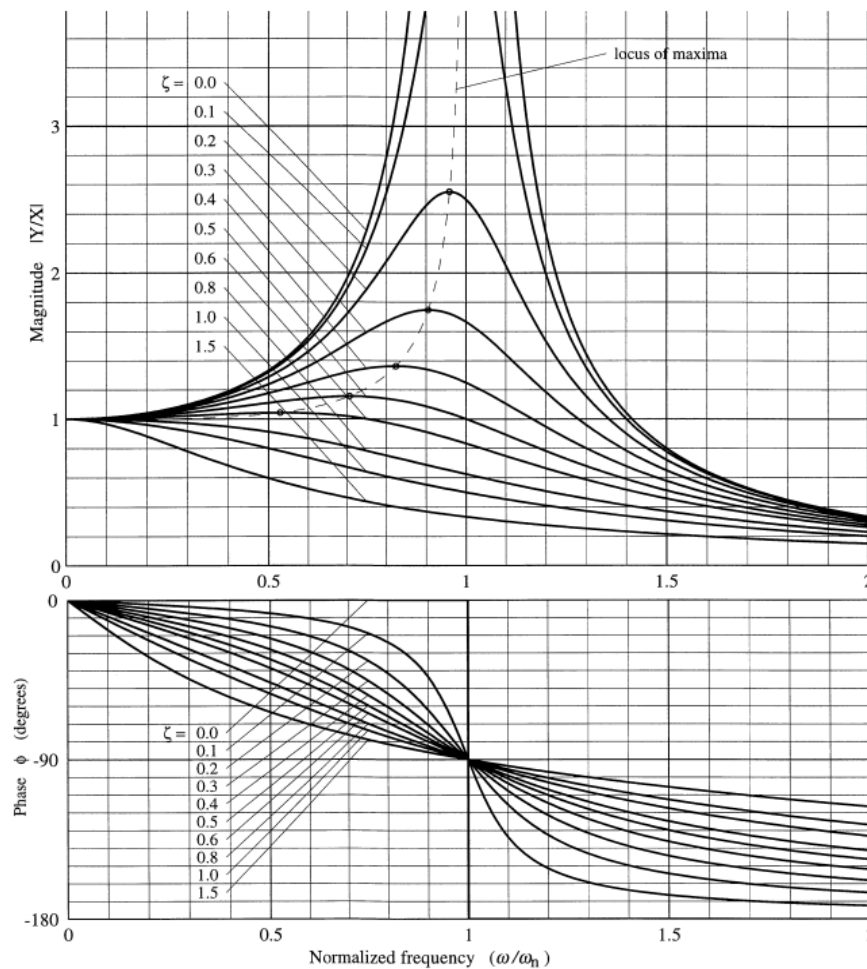
$$\frac{Y}{X} = \frac{1}{-\tilde{\omega}^2 + 2i\zeta\tilde{\omega} + 1}, \quad \left| \frac{Y}{X} \right| = \frac{1}{\sqrt{(1 - \tilde{\omega}^2)^2 + (2\zeta\tilde{\omega})^2}}$$

$(x = \text{Re}(X e^{i\omega t}) = X \cos \omega t, y = \text{Re}(Y e^{i\omega t}) = |Y| \cos(\omega t + \phi), \tan \phi = \frac{-2\tilde{\omega}}{1 - \tilde{\omega}^2}, \tilde{\omega} = \frac{\omega}{\omega_n})$

For a mass-spring-damper system (Section 6.2.8), let $x = \frac{f}{k}, \omega_n = \sqrt{\frac{k}{m}}, \zeta = \frac{\lambda}{2\sqrt{km}}$.

Maximum response: $|Y_{\max}| = \frac{X}{2\zeta\sqrt{1 - \zeta^2}}$ when $\frac{\omega}{\omega_n} = \sqrt{1 - 2\zeta^2}$, existing if $\zeta < \frac{1}{\sqrt{2}}$.

Dimensionless frequency response (Bode plot) at steady-state:

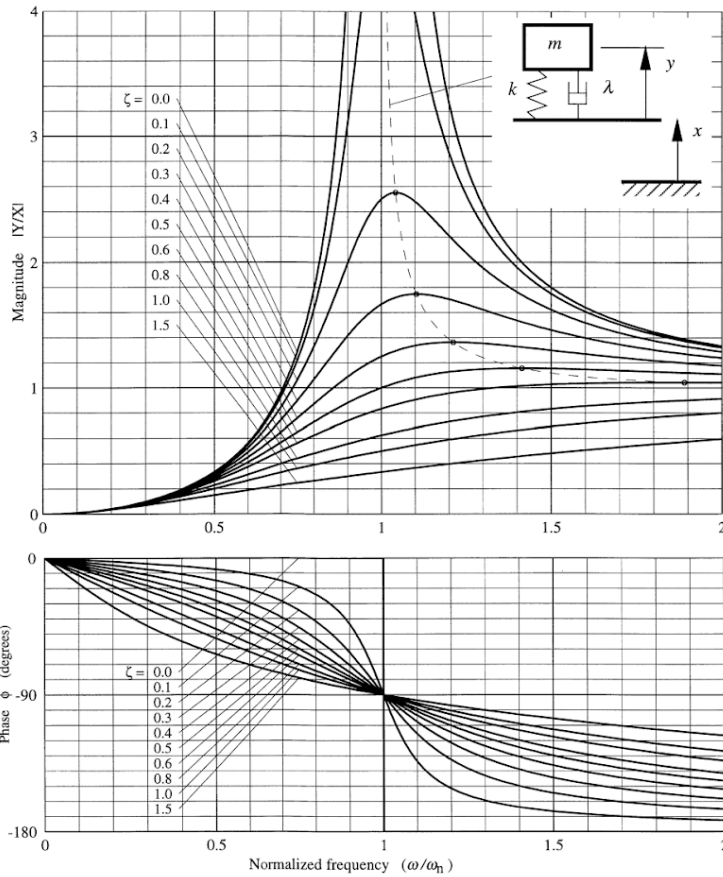


6.2.6. Harmonic Response of a Linear Second Order System (Base Displacements)

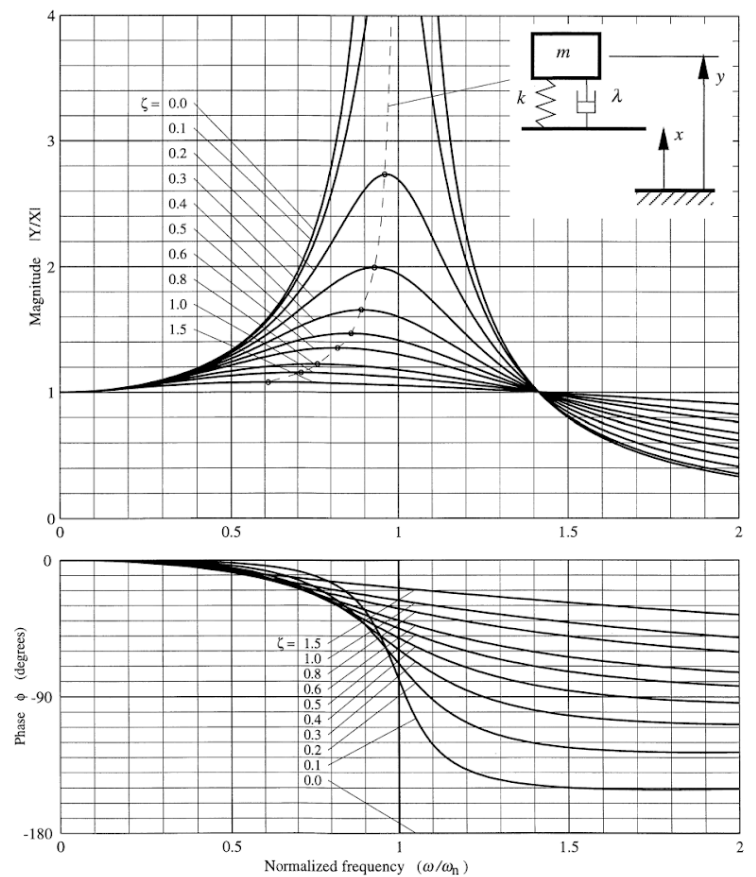
In cases where the input is a base displacement rather than a force, the RHS takes the form of a D'Alembert force. The two common cases (aside from that in Section 6.2.5) are shown.

If $x = \text{Re}(X e^{i\omega t}) = X \cos \omega t$, $y = \text{Re}(Y e^{i\omega t}) = |Y| \cos(\omega t + \phi)$ then: $\left(\omega_n = \sqrt{\frac{k}{m}}, \zeta = \frac{\lambda}{2\sqrt{km}}\right)$

Relative Response to Base Displacement:



Absolute Response to Base Displacement



$$\frac{1}{\omega_n^2} y'' + \frac{2\zeta}{\omega_n} y' + y = -\frac{1}{\omega_n^2} x'' \quad \left(\tilde{\omega} = \frac{\omega}{\omega_n}\right)$$

$$\frac{1}{\omega_n^2} y'' + \frac{2\zeta}{\omega_n} y' + y = \frac{2\zeta}{\omega_n} x' + x$$

$$\frac{Y}{X} = \frac{\tilde{\omega}}{-\tilde{\omega}^2 + 2i\zeta\tilde{\omega} + 1}$$

$$\frac{Y}{X} = \frac{2i\zeta\tilde{\omega} + 1}{-\tilde{\omega}^2 + 2i\zeta\tilde{\omega} + 1}$$

$$\left|\frac{Y}{X}\right| = \tilde{\omega}^2 \left[(1 - \tilde{\omega}^2)^2 + 2\zeta\tilde{\omega} \right]^{-1/2}, \quad \tan \phi = \frac{-2\zeta\tilde{\omega}}{1 - \tilde{\omega}^2}$$

$$\left|\frac{Y}{X}\right| = \left(\frac{1 + (2\zeta\tilde{\omega})^2}{(1 - \tilde{\omega}^2)^2 + (2\zeta\tilde{\omega})^2} \right)^{1/2}, \quad \tan \phi = \frac{-2\zeta\tilde{\omega}^3}{1 - (1 - 4\zeta^2)\tilde{\omega}^2}$$

$$|Y_{\max}| = \frac{X}{2\zeta\sqrt{1 - \zeta^2}} \quad \text{when} \quad \tilde{\omega} = \frac{1}{\sqrt{1 - 2\zeta^2}}$$

$$|Y_{\max}| \approx \frac{X}{2\zeta} \left(1 + \frac{5}{2}\zeta^2 \right) \quad \text{when} \quad \tilde{\omega} = 1 - \zeta^2$$

existing if $\zeta < 1/\sqrt{2}$

existing always, but valid only if $\zeta \ll 1$

6.2.7. Measures of Damping and Stiffness for an Underdamped System

If y_0 and y_N are peaks of a step or impulse response separated by N periods, then the logarithmic decrement is

$$N\Delta = \ln \frac{y_0}{y_N} = \frac{2\pi N \zeta}{\sqrt{1 - \zeta^2}}$$

Time constant τ and attenuation rate α of exponential envelope $e^{-t/\tau}$: $\tau = \frac{2Q}{\omega_n} = \frac{1}{\zeta\omega_n} = \frac{1}{\alpha}$.

Q-factor: $Q = 2\pi \times \frac{\text{energy stored}}{\text{energy dissipated per cycle}} = \frac{1}{2\zeta}$

Loss factor: η , often used to suppress frequency dependence of ζ for practical systems.
At resonance, $\eta = 2\zeta$.

Proportion of energy lost per cycle = $2\pi\eta$.

Complex stiffness: $k^* = k(1 + j\eta)$

Loss tangent: $\tan \delta$, equal to the tangent of the phase shift, $\tan \phi$ (δ : loss angle)
 $\delta = \arg k^*$ (dissipative modulus / elastic modulus)

Sinusoidal Forced Loading: if $\varepsilon(t) = e^{j\omega t}$ and $\sigma(t) = G^*(\omega) e^{j\omega t}$, then:

Dynamic modulus: $G^*(\omega) = G'(\omega) + j G''(\omega)$ (G' : storage, G'' : loss)

In the Laplace domain: $\overline{G'}(s) \overline{G''}(s) = s^{-2}$

For more on viscoelasticity and the electrical circuit analogy see Section 6.2.9.

(Note that this is the **opposite** of the analogous electrical system, in which real and imaginary parts of impedance are effectively swapped in terms of dissipation (resistance) vs exchange (reactance).)

For lightly damped systems ($\zeta \ll 1$):

Logarithmic decrement: $N\Delta \approx 2\pi N\zeta$

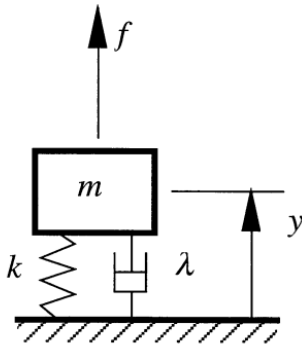
Loss factor and loss tangent: $\eta \approx \frac{2\zeta\omega}{\omega_n}$ and $\tan \delta \approx \eta$ (δ : loss angle)

Q factor: $Q = \frac{1}{2\zeta}$

Half-power bandwidth: $\Delta\omega = \frac{\omega_n}{Q} = 2\omega_n\zeta = \frac{2}{\tau}$ for which $|Y| \geq \frac{1}{\sqrt{2}} |Y_{\max}|$

(valid for both forced displacements and base displacements)

6.2.8. Mass-Spring-Damper Systems



The spring and damper exert resistive forces of magnitude ky and $\lambda y'$ respectively. This system has dynamic model

$$my'' + \lambda y' + ky = f \Leftrightarrow \frac{1}{\omega_n^2} y'' + \frac{2\zeta}{\omega_n} y' + y = x, \text{ where}$$

$$x = \frac{f}{k} \quad \omega_n = \sqrt{\frac{k}{m}} \quad \zeta = \frac{\lambda}{2\sqrt{km}}$$

$$T = \frac{2\pi}{\omega_d} = \frac{2\pi}{\omega_n \sqrt{1 - \zeta^2}} \quad Q = \frac{\sqrt{mk}}{\lambda} \quad \Delta\omega = \frac{\lambda}{m}$$

Mechanical power balance: $\frac{d}{dt} \left(\underbrace{\frac{1}{2} m \dot{y}^2}_{\text{kinetic energy}} + \underbrace{mgy}_{\text{gravitational potential energy}} + \underbrace{\frac{1}{2} k y^2}_{\text{elastic strain energy}} \right) = \underbrace{f\dot{y}}_{\text{driving power}} - \underbrace{\lambda \dot{y}^2}_{\text{damper dissipation}}$

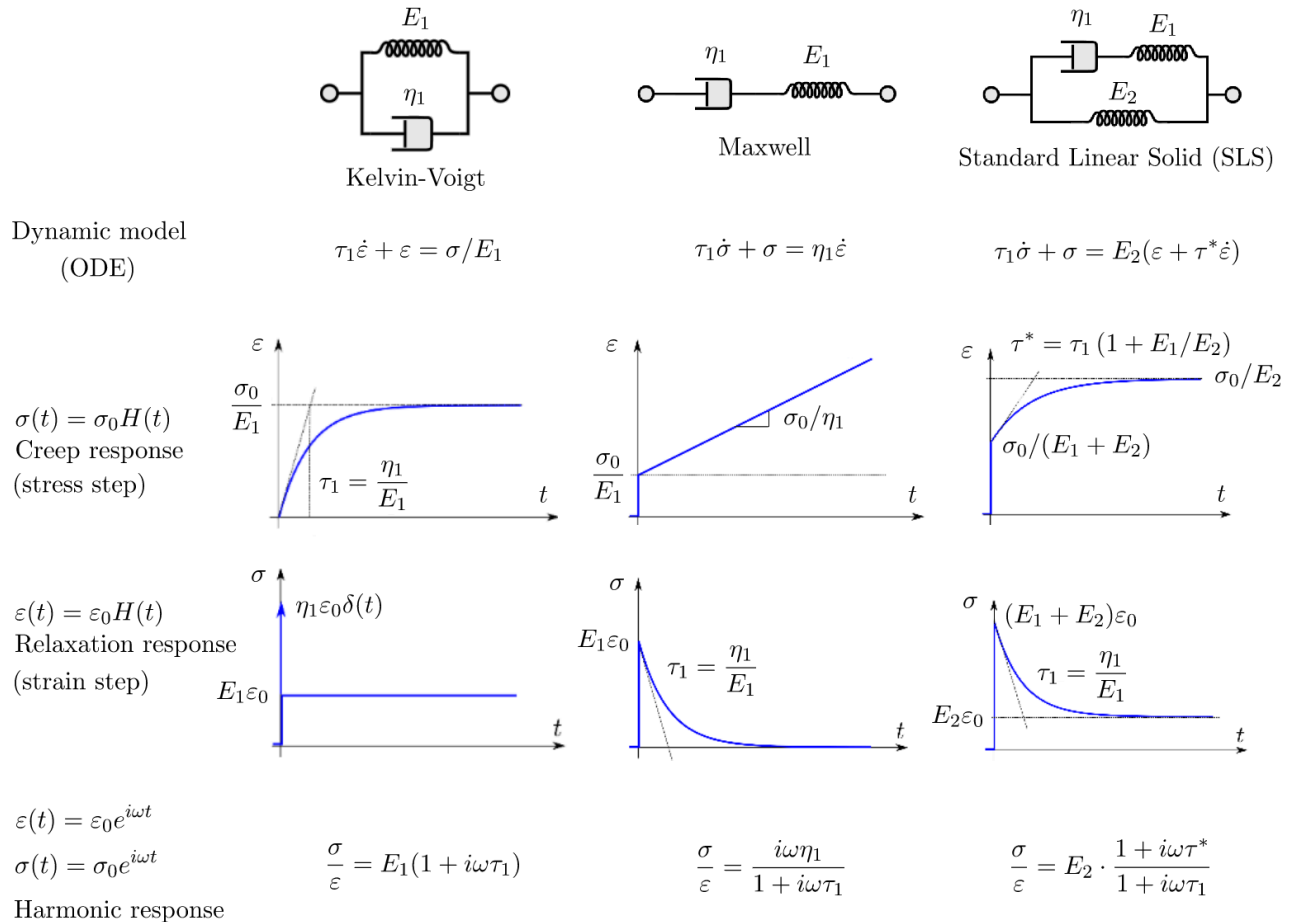
Transfer function: $\frac{\bar{y}}{\bar{f}} = \frac{1}{ms^2 + \lambda s + k}$

Combining in:	Series	Parallel
Springs k_1 and k_2	$\frac{1}{k'} = \frac{1}{k_1} + \frac{1}{k_2}$	$k' = k_1 + k_2$
Dampers λ_1 and λ_2	$\frac{1}{\lambda'} = \frac{1}{\lambda_1} + \frac{1}{\lambda_2}$	$\lambda' = \lambda_1 + \lambda_2$

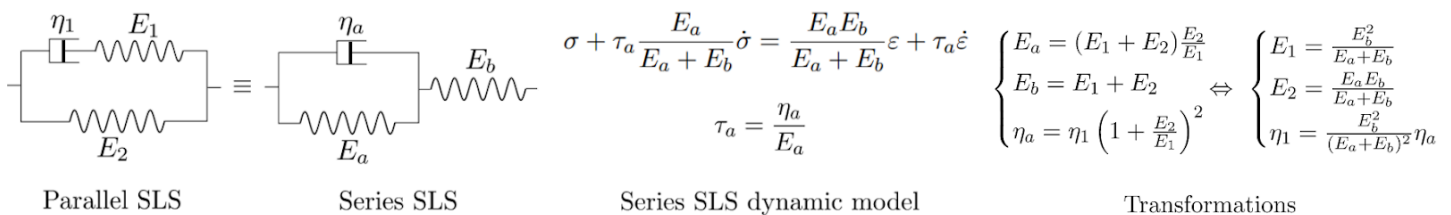
6.2.9. Fundamental Models of Viscoelasticity and their Dynamic Responses

Viscoelastic materials can be modelled by ‘springs’ with Young’s modulus E and ‘dampers’ with dynamic viscosity η , for which the stress σ , strain ε and strain rate $\dot{\varepsilon}$ are related by $\sigma = E\varepsilon$ and $\sigma = \eta\dot{\varepsilon}$. (For shear phenomena, τ , γ and G may be used instead.)

The Kelvin-Voigt, Maxwell, and Standard Linear Solid (SLS) models are shown below.



The SLS model may alternatively be formulated in series, which are dynamically equivalent:



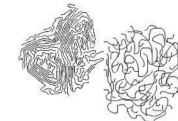
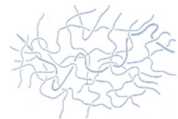
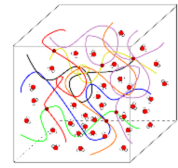
Combining models: Creep responses add in series. Relaxation responses add in parallel.

Electrical circuit analogy: $v \leftrightarrow \sigma$, $i \leftrightarrow \varepsilon$, $\sigma = \varepsilon Z$; $Z_{\text{spring}} = E$ (‘resistor’), $Z_{\text{damper}} = j\omega\eta$ (‘inductor’)
(If formulated instead with $v \leftrightarrow \varepsilon$ and $i \leftrightarrow \sigma$ then use admittances instead.)

6.2.10. Applications of Viscoelasticity and Nonlinear Elasticity

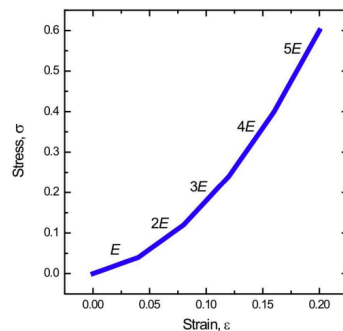
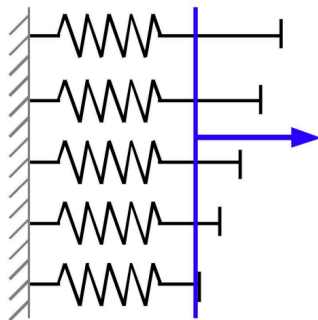
Linear models work well for certain classes of substances as first-order approximations:

- The **Kelvin-Voigt model** best represents viscous gelatinous substances such as hydrogels. The stresses in the polymer chains approximately represent the spring while the stresses in the water approximately represent the dashpot.
- The **Maxwell model** best represents long chain mobile molecules which slide over each other, binding and unbinding.
- The **Standard Linear Solid model** best represents thermoplastic polymers below their glass transition temperature.



The Sequential Recruitment Model works for some materials where stiffness increases with strain e.g. biomaterials such as collagen (see Section 16.5.7).

This may occur when material fibres are reorienting themselves under strain to help carry the imposed stress, effectively ‘recruiting’ linear elastic elements in parallel.



For a stress-strain response of the form

$$\sigma = a\varepsilon^2 + b\varepsilon,$$

this is modelled by an incremental stiffness of $\frac{dE}{d\varepsilon} = a$

and an initial stiffness of $E(0) = b$.

Mechanical properties of matter can be investigated experimentally using a universal mechanical tester (UMT), dynamic mechanical analyser (DMA), or rheometer.

6.2.11. Routh-Hurwitz Stability Criteria of Higher Order Systems

For a higher order system with **positive** coefficients of y and its derivatives i.e. all $a_i > 0$,

2nd-order: $a_2 y'' + a_1 y' + a_0 y = x$ is stable, always (provided $a_i > 0$)

3rd-order: $a_3 y''' + a_2 y'' + a_1 y' + a_0 y = x$ is stable if also $a_1 a_2 > a_0 a_3$

4th-order: $a_4 y'''' + a_3 y''' + a_2 y'' + a_1 y' + a_0 y = x$ is stable if also $a_1 a_2 a_3 > a_0 a_3^2 + a_4 a_1^2$

6.2.12. Vibration of a Conservative System with One Degree of Freedom

Potential energy: $V(q)$ Kinetic energy: $T = \frac{1}{2}M(q)\dot{q}^2$

At an equilibrium position $q = q_0$: $V'(q_0) = 0$ which is stable if $V''(q_0) > 0$.

Small oscillations about this equilibrium have natural frequency $\omega_n^2 = \frac{V''(q_0)}{M(q_0)}$

6.2.13. Lagrangian Mechanics

For mechanical systems, the Lagrangian is defined as $\mathcal{L} = T - V$. The action is $S = \int L dt$. The path of a system in phase space (q, q') will minimise the action S , so the equations of motion are given by applying the Euler-Lagrange equation to S . Then, for a holonomic system with generalised coordinates q_i ,

$$\frac{d}{dt} \left(\frac{\partial \mathcal{L}}{\partial \dot{q}_i} \right) = \frac{\partial \mathcal{L}}{\partial q_i} + Q_i \quad \text{or expanding,} \quad \frac{d}{dt} \left[\frac{\partial T}{\partial \dot{q}_i} \right] - \frac{\partial T}{\partial q_i} + \frac{\partial V}{\partial q_i} = Q_i$$

where T is the total kinetic energy, V is the total potential energy, and Q_i are the nonconservative generalised forces.

Noether's theorem: every differentiable symmetry of the action of a physical system with conservative forces has a corresponding conservation law.

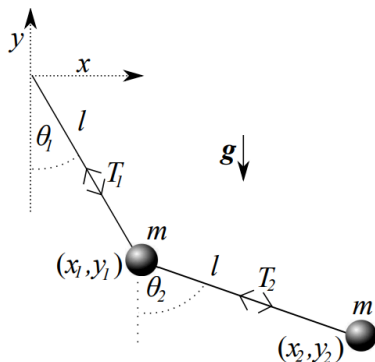
Linearisation about an equilibrium \mathbf{q}_0 : let $\mathbf{q} = \mathbf{q}_0 + \delta\mathbf{q}$, $\dot{\mathbf{q}} = \delta\dot{\mathbf{q}}$, $\ddot{\mathbf{q}} = \delta\ddot{\mathbf{q}}$.
Expand the Lagrangian to **second** order in $\delta\mathbf{q}$ and its derivatives.

In general, with \mathbf{M} as the mass matrix and \mathbf{K} as the stiffness matrix,

$$M_{ij} = \left. \frac{\partial^2 T}{\partial \dot{q}_i \partial \dot{q}_j} \right|_{\mathbf{q}=\mathbf{q}_0} \quad K_{ij} = \left. \frac{\partial^2 V}{\partial q_i \partial q_j} \right|_{\mathbf{q}=\mathbf{q}_0}$$

Then the Lagrangian linearised about \mathbf{q}_0 is

$$\mathcal{L}(\delta\mathbf{q}, \delta\dot{\mathbf{q}}) \approx V(\mathbf{q}_0) + \frac{1}{2}\delta\dot{\mathbf{q}}^T M \delta\dot{\mathbf{q}} - \frac{1}{2}\delta\mathbf{q}^T K \delta\mathbf{q}$$



Typical Lagrangian of a double pendulum (polar coords):

$$\mathcal{L}(\theta_1, \theta_2, \dot{\theta}_1, \dot{\theta}_2) = \frac{1}{2}ml^2 \left(2\dot{\theta}_1^2 + \dot{\theta}_2^2 + 2\dot{\theta}_1\dot{\theta}_2 \cos(\theta_2 - \theta_1) \right) + mgl(2 \cos \theta_1 + \cos \theta_2).$$

6.2.14. Parametric Resonance

When the mass, stiffness or damping factors are functions of time t , the governing equation has the form $\ddot{q} + \omega_0^2 q = h\omega_0^2 \cos(\omega t)q$ for $h \ll 1$. (Matthieu's equation)

For simple systems without coupling of modes, the resonant frequency of a parametrically resonating system is **twice** the resonance frequency of the same nonparametric system.

Higher order terms in ω_0 lead to nonlinear vibrations.

6.2.15. Hamiltonian Mechanics

The generalised momentum p_i and the Hamiltonian $H(\mathbf{p}, \mathbf{q})$ are defined as

$$p_i = \frac{\partial T}{\partial \dot{q}_i}, \quad H(\mathbf{p}, \mathbf{q}) = \sum_i p_i \dot{q}_i - T + V$$

Note that the velocities must be expressed as a function of the generalised momenta p and the generalised displacements q .

Hamilton's equations are then $\dot{q}_i = \frac{\partial H}{\partial p_i}, \quad \dot{p}_i = -\frac{\partial H}{\partial q_i} + Q_i$.

For the Hamiltonian as it applies to quantum mechanics, see Section 10.1.9.

6.2.16. Canonical Transformation of Hamilton's Equation

The total time derivative of some function $f(\mathbf{p}, \mathbf{q}, t)$ can be expressed in terms of the Poisson bracket $\{f, H\}$ in the form

$$\frac{df}{dt} = \frac{\partial f}{\partial t} + \{f, H\}, \quad \{f, H\} \equiv \sum_i \left[\frac{\partial f}{\partial q_i} \frac{\partial H}{\partial p_i} - \frac{\partial f}{\partial p_i} \frac{\partial H}{\partial q_i} \right].$$

Common forms of Canonical Transform for Hamilton's equations (to the "Kamiltonian" K) are:

Type	Generating function	1st eqn	2nd eqn	Kamiltonian
1	$G_1(\mathbf{q}, \mathbf{Q}, t)$	$\mathbf{p} = \frac{\partial G_1}{\partial \mathbf{q}}$	$\mathbf{P} = -\frac{\partial G_1}{\partial \mathbf{Q}}$	$K = H + \frac{\partial G_1}{\partial t}$
2	$G_2(\mathbf{q}, \mathbf{P}, t)$	$\mathbf{p} = \frac{\partial G_2}{\partial \mathbf{q}}$	$\mathbf{Q} = \frac{\partial G_2}{\partial \mathbf{P}}$	$K = H + \frac{\partial G_2}{\partial t}$
3	$G_3(\mathbf{p}, \mathbf{Q}, t)$	$\mathbf{q} = -\frac{\partial G_3}{\partial \mathbf{p}}$	$\mathbf{P} = -\frac{\partial G_3}{\partial \mathbf{Q}}$	$K = H + \frac{\partial G_3}{\partial t}$
4	$G_4(\mathbf{p}, \mathbf{P}, t)$	$\mathbf{q} = -\frac{\partial G_4}{\partial \mathbf{p}}$	$\mathbf{Q} = \frac{\partial G_4}{\partial \mathbf{P}}$	$K = H + \frac{\partial G_4}{\partial t}$

6.2.17. Undamped Vibration Modes and Response

The forced vibration of an N -degree-of-freedom system with mass matrix \mathbf{M} and stiffness matrix \mathbf{K} (both symmetric and positive definite) is governed by

$$\mathbf{M}\ddot{\mathbf{y}} + \mathbf{K}\mathbf{y} = \mathbf{f}$$

where \mathbf{y} is the vector of displacements and \mathbf{f} is the vector of forces.

Kinetic energy and potential energy: $T = \frac{1}{2}\dot{\mathbf{y}}^T\mathbf{M}\dot{\mathbf{y}}$ $V = \frac{1}{2}\mathbf{y}^T\mathbf{K}\mathbf{y}$

Natural frequencies ω_n and mode shapes $\mathbf{u}^{(n)}$: $\mathbf{K}\mathbf{u}^{(n)} = \omega_n^2\mathbf{M}\mathbf{u}^{(n)}$

Orthogonality and normalisation of modes:

$$\int u_j(x)u_k(x)dm = \begin{cases} 0 & j \neq k \\ 1 & j = k \end{cases}$$

$$\mathbf{u}^{(j)T}\mathbf{M}\mathbf{u}^{(k)} = \begin{cases} 0 & j \neq k \\ 1 & j = k \end{cases}$$

$$\mathbf{u}^{(j)T}\mathbf{K}\mathbf{u}^{(k)} = \begin{cases} 0 & j \neq k \\ \omega_j^2 & j = k \end{cases}$$

6.2.18. General Response in Modal Coordinates

The general response of the system can be written as a sum of modal responses:

$$\mathbf{y}(t) = \sum_{j=1}^N q_j(t) \mathbf{u}^{(j)} = \mathbf{U} \mathbf{q}(t)$$

where \mathbf{U} is a matrix whose N columns are the normalised eigenvectors $\mathbf{u}^{(j)}$ and q_j can be thought of as the ‘quantity’ of the j th mode.

Modal coordinates satisfy $\ddot{\mathbf{q}} + [\text{diag}(\omega_j^2)] \mathbf{q} = \mathbf{Q}$ $\mathbf{y} = \mathbf{U} \mathbf{q}$, modal force $\mathbf{Q} = \mathbf{U}^T \mathbf{f}$

Transfer functions for the general responses are

Step Response:

$$h(j, k, t) = y_k(t) = \sum_{n=1}^N \frac{u_j^{(n)} u_k^{(n)}}{\omega_n^2} [1 - \cos \omega_n t]$$

for $t \geq 0$ (with no damping), or

$$h(j, k, t) \approx \sum_{n=1}^N \frac{u_j^{(n)} u_k^{(n)}}{\omega_n^2} [1 - e^{-\omega_n \zeta_n t} \cos \omega_n t]$$

for $t \geq 0$ (with small damping).

Impulse Response:

$$g(j, k, t) = y_k(t) = \sum_{n=1}^N \frac{u_j^{(n)} u_k^{(n)}}{\omega_n} \sin \omega_n t$$

for $t \geq 0$ (with no damping), or

$$g(j, k, t) \approx \sum_{n=1}^N \frac{u_j^{(n)} u_k^{(n)}}{\omega_n} e^{-\omega_n \zeta_n t} \sin \omega_n t$$

for $t \geq 0$ (with small damping).

Harmonic Response:

$$H(j, k, \omega) = \frac{y_k}{f_j} = \sum_{n=1}^N \frac{u_j^{(n)} u_k^{(n)}}{\omega_n^2 - \omega^2}$$

(with no damping), or

$$H(j, k, \omega) = \frac{y_k}{f_j} \approx \sum_{n=1}^N \frac{u_j^{(n)} u_k^{(n)}}{\omega_n^2 + 2i\omega\omega_n\zeta_n - \omega^2}$$

(with small damping)

Pattern of antiresonances: For a system with well-separated resonances (low modal overlap), if the factor $u_j^{(n)} u_k^{(n)}$ has the same sign for two adjacent resonances then the transfer function will have an anti resonance between the two peaks. If it has opposite signs, there will be no antiresonance.

6.2.19. Governing Equations for Continuous Systems**Transverse Vibration of a Stretched String:**

Equation of motion

$$m \frac{\partial^2 y}{\partial t^2} - P \frac{\partial^2 y}{\partial x^2} = f(x, t)$$

Potential energy

$$V = \frac{1}{2} P \int \left(\frac{\partial y}{\partial x} \right)^2 dx$$

Kinetic energy

$$T = \frac{1}{2} m \int \left(\frac{\partial y}{\partial t} \right)^2 dx$$

(P : tension, m : mass per unit length, $y(x, t)$: transverse displacement, $f(x, t)$: applied lateral force per unit length.)

Torsional Vibration of a Circular Shaft:

Equation of motion

$$\rho J \frac{\partial^2 \theta}{\partial t^2} - GJ \frac{\partial^2 \theta}{\partial x^2} = \tau(x, t)$$

Potential energy

$$V = \frac{1}{2} GJ \int \left(\frac{\partial \theta}{\partial x} \right)^2 dx$$

Kinetic energy

$$T = \frac{1}{2} \rho J \int \left(\frac{\partial \theta}{\partial t} \right)^2 dx$$

(G : shear modulus, $J = \frac{\pi}{2}(a^4 - b^4)$: second polar moment of area, ρ : density, $\theta(x, t)$: angular displacement, $\tau(x, t)$: applied torque per unit length. a : external radius, b : internal radius ($b = 0$ if solid).)

Axial Vibration of Rod or Column:

Equation of motion

$$\rho A \frac{\partial^2 y}{\partial t^2} - EA \frac{\partial^2 y}{\partial x^2} = f(x, t)$$

Potential energy

$$V = \frac{1}{2} EA \int \left(\frac{\partial y}{\partial x} \right)^2 dx$$

Kinetic energy

$$T = \frac{1}{2} \rho A \int \left(\frac{\partial y}{\partial t} \right)^2 dx$$

(E : Young's modulus, ρ : density, A : cross-sectional area, $y(x, t)$: transverse displacement, $f(x, t)$: applied lateral force per unit length.)

Bending Vibration of an Euler Beam:

Equation of motion

$$\rho A \frac{\partial^2 y}{\partial t^2} + EI \frac{\partial^4 y}{\partial x^4} = f(x, t)$$

Potential energy

$$V = \frac{1}{2} EI \int \left(\frac{\partial^2 y}{\partial x^2} \right)^2 dx$$

Kinetic energy

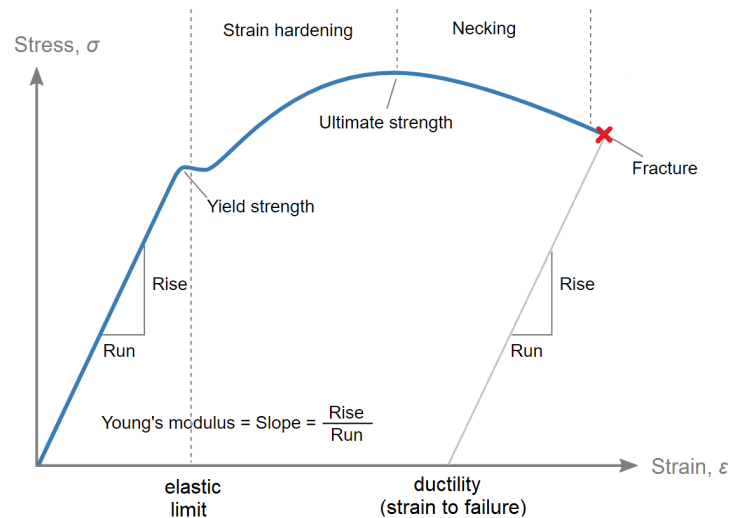
$$T = \frac{1}{2} \rho A \int \left(\frac{\partial y}{\partial t} \right)^2 dx$$

(E : Young's modulus, ρ : density, A : cross-sectional area, I : second moment of area, $y(x, t)$: transverse displacement, $f(x, t)$: applied lateral force per unit length.)

6.3. Solid Mechanics and Structural Mechanics

6.3.1. Uniaxial Stress and Strain

For a homogeneous isotropic specimen in a simple uniaxial tensile test (e.g. a metal rod):



- Nominal stress: $\sigma_n = \frac{F}{A_0}$ (F : tensile force, A_0 : initial cross-sectional area)
- Nominal strain: $\epsilon_n = \frac{x}{l_0} = \frac{l - l_0}{l_0}$ (x : extension, l : length, l_0 : initial length)
(‘nominal stress/strain’ is also known as ‘engineering stress/strain’.)
- True stress: $\sigma_t = \frac{F}{A} = \sigma_n(1 + \epsilon_n)$ (A : cross-sectional area)
- True strain: $\epsilon_t = \int_{l_0}^l \frac{dl}{l} = \ln\left(\frac{l}{l_0}\right) = \ln(1 + \epsilon_n)$ (true strains are additive)

In the elastic region (from unloaded to yield stress σ_y ; slope = E : Young’s modulus)

- Hooke’s law for linear elasticity: $F = kx = k(l - l_0)$ or $E = \frac{\sigma}{\epsilon} = \frac{Fl_0}{Ax}$
- Elastic potential energy (strain energy): $U = \frac{1}{2} kx^2 = \frac{1}{2} Fx$ (area under F - x graph)

In the plastic region:

- Strain energy per unit volume: $U/V = \int_0^{\epsilon} \sigma_n d\epsilon_n$ (area under σ - ϵ graph)
- Plastic strains occur at constant volume. Strain hardening occurs up to the ultimate tensile strength (UTS). Necking decreases the cross-sectional area until the point of rupture if perfectly ductile. On failure, the specimen suddenly contracts by relaxing the elastic strain.

6.3.2. Stress-Strain Relationships for Homogeneous Isotropic Elastic Solids

Elastic moduli: material properties

- Young's modulus: $E = \frac{\sigma}{\varepsilon}$ (uniaxial only - effective E_{xx} is $\frac{\sigma_{xx}}{\varepsilon_{xx}}$ etc.)
- Poisson's ratio: $\nu = -\frac{\text{lateral strain}}{\text{tensile strain}}$ (lateral strain is **not** for volume conservation)
- Dilatation (volumetric strain): $\Delta = \frac{\text{change in volume}}{\text{initial volume}} = \ln\left(\frac{\rho_{\text{initial}}}{\rho_{\text{final}}}\right) = \varepsilon_{xx} + \varepsilon_{yy} + \varepsilon_{zz} (+ O(\varepsilon^2))$
- Shear modulus: $G = \frac{\tau}{\gamma} = \frac{E}{2(1+\nu)}$
- Bulk modulus: $K = \frac{\text{hydrostatic stress}}{\text{volumetric strain}} = \frac{p}{\Delta} = \frac{E}{3(1-2\nu)}$
- Compressibility: $1/K$; Speed of sound in solid/liquid: $a = \sqrt{K/\rho}$

Stresses and strains induced by temperature changes:

- Thermal strain: $\varepsilon = \alpha \Delta T$ (α : linear coefficient of thermal expansion, equal in all directions)
- Axial material law: $\varepsilon_{xx} = \frac{1}{E} (\sigma_{xx} - \nu\sigma_{yy} - \nu\sigma_{zz}) + \alpha \Delta T$, similar for other directions
- Shear material law: $\gamma_{xy} = \frac{1}{G} \tau_{xy}$, similar for other directions (pure elastic strains)
- Complementary shear: $\tau_{xy} = \tau_{yx}$ and $\gamma_{xy} = \gamma_{yx}$.

The axial and shear elastic laws can be combined into a constitutive law with tensors.

In matrix form, the axial stress $\sigma = [\sigma_{xx} \ \sigma_{yy} \ \sigma_{zz}]^T$ and strain $\varepsilon = [\varepsilon_{xx} \ \varepsilon_{yy} \ \varepsilon_{zz}]^T$ vectors are related by:

$$\varepsilon = \frac{1}{E} \begin{bmatrix} 1 & -\nu & -\nu \\ -\nu & 1 & -\nu \\ -\nu & -\nu & 1 \end{bmatrix} \sigma + \begin{bmatrix} 1 \\ 1 \\ 1 \end{bmatrix} \alpha \Delta T \quad \Leftrightarrow \quad \sigma = \frac{E}{(1+\nu)(1-2\nu)} \begin{bmatrix} 1-\nu & \nu & \nu \\ \nu & 1-\nu & \nu \\ \nu & \nu & 1-\nu \end{bmatrix} \left(\varepsilon - \begin{bmatrix} 1 \\ 1 \\ 1 \end{bmatrix} \alpha \Delta T \right)$$

Constrained thermal displacements are resisted by tensile/compressive stresses.

Biaxial constraint: for plane stress with the z face unstressed and $\Delta T = 0$, the stresses are

$$\sigma_{xx} = \frac{E}{1-\nu^2} (\varepsilon_{xx} + \nu \varepsilon_{yy}) \quad \text{and} \quad \sigma_{yy} = \frac{E}{1-\nu^2} (\nu \varepsilon_{xx} + \varepsilon_{yy})$$

Common cases:

- Contraction of a constrained thin surface layer: biaxial surface stress $\sigma = \frac{E}{1-\nu} (\alpha_{\text{surface}} - \alpha_{\text{bulk}}) \Delta T$.
- Freezing of water: $p = K_{\text{ice}} \ln\left(\frac{\rho_{\text{water}}}{\rho_{\text{ice}}}\right)$, $\varepsilon_{\text{cont}} = \alpha \Delta T$, then pressure vessel formulas (Section 6.4.6).

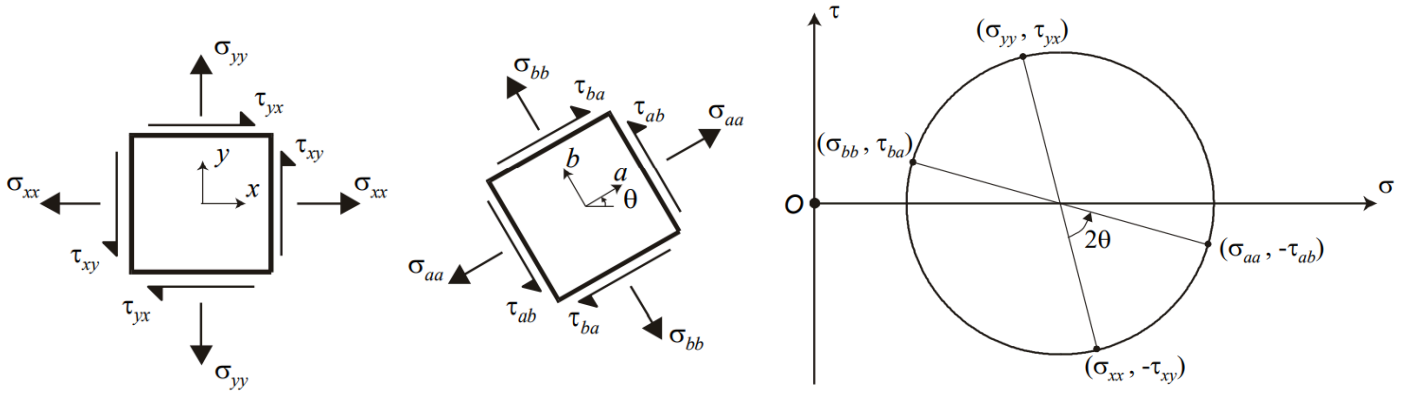
Special cases:

Large strain bending in materials with high ν (e.g. rubber, $\nu = 0.5$) produces anticlastic curvature, and these materials are incompressible under hydrostatic loading.

Auxetic metamaterials expand in both directions (i.e. negative ν) and can occur in specially designed mesh geometries e.g. minimal surfaces.

6.3.3. Planar Transformations of Stress and Strain

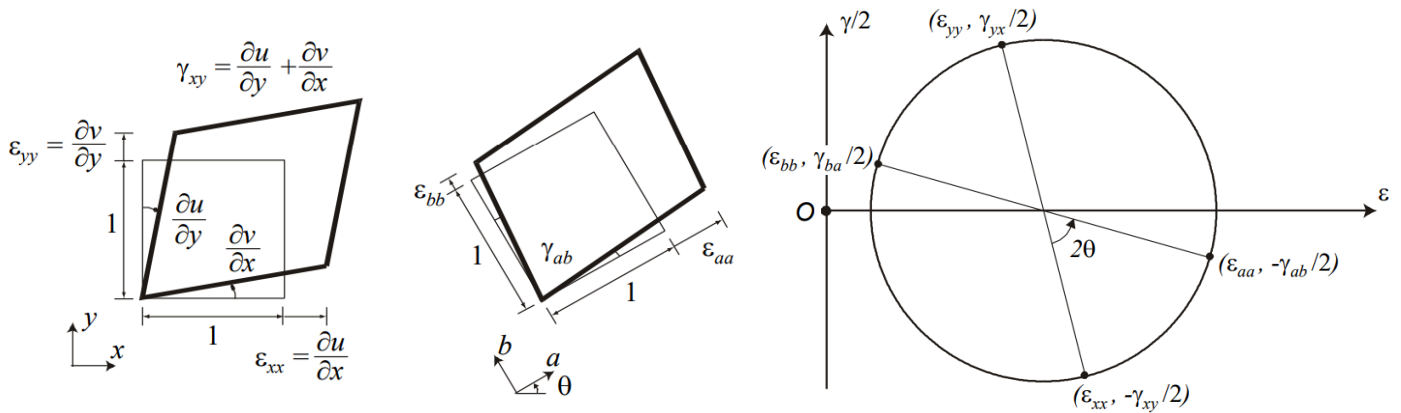
Mohr's circle of stress. Shear stress is plotted as positive when acting clockwise.



$$\sigma_{aa} = \sigma_{xx} \cos^2 \theta + \sigma_{yy} \sin^2 \theta + 2\tau_{xy} \sin \theta \cos \theta$$

$$\tau_{ab} = -\sigma_{xx} \sin \theta \cos \theta + \sigma_{yy} \sin \theta \cos \theta + \tau_{xy} (\cos^2 \theta - \sin^2 \theta)$$

Mohr's circle of strain. Shear strain is plotted as positive when acting clockwise.



$$\epsilon_{aa} = \epsilon_{xx} \cos^2 \theta + \epsilon_{yy} \sin^2 \theta + \gamma_{xy} \sin \theta \cos \theta$$

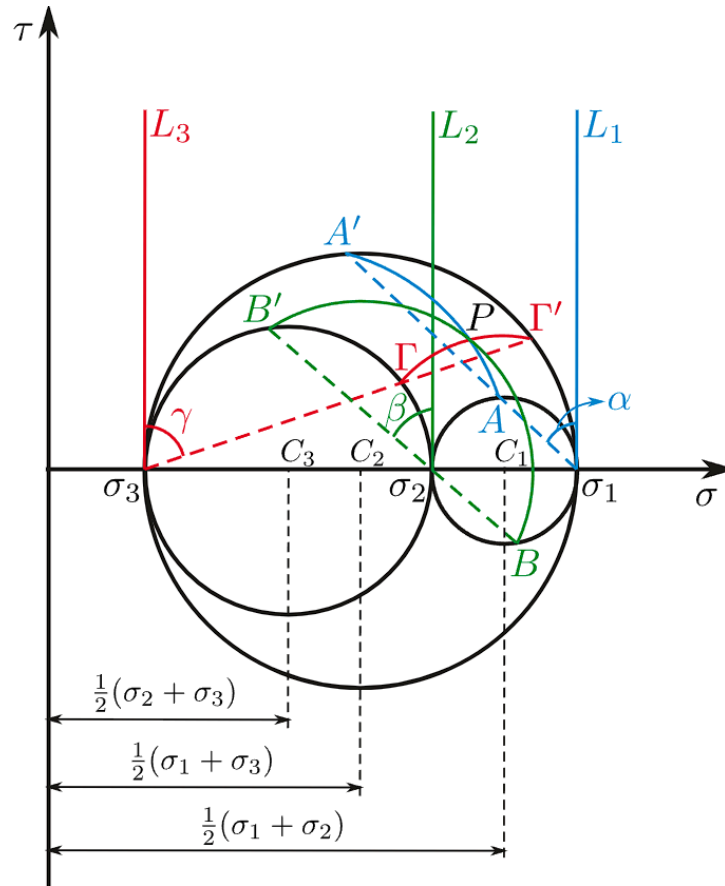
$$\gamma_{ab} = -2\epsilon_{xx} \sin \theta \cos \theta + 2\epsilon_{yy} \sin \theta \cos \theta + \gamma_{xy} (\cos^2 \theta - \sin^2 \theta)$$

6.3.4. Principal Stresses in 3D

The principal stresses can be calculated as the eigenvalues of the stress tensor σ , and the orthogonal principal directions are the corresponding eigenvectors: $\sigma = \mathbf{D}\Sigma\mathbf{D}^T$ (since $\sigma = \sigma^T$).

$$\underline{\sigma} = \begin{bmatrix} \sigma_{xx} & \tau_{xy} & \tau_{xz} \\ \tau_{yx} & \sigma_{yy} & \tau_{yz} \\ \tau_{zx} & \tau_{zy} & \sigma_{zz} \end{bmatrix}$$

3D Mohr's Circle:

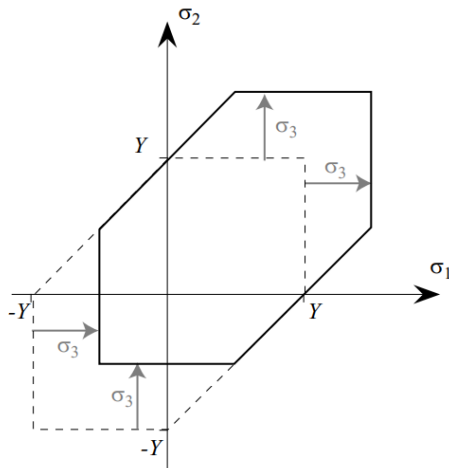


6.3.5. Yield Criteria for Isotropic Solids

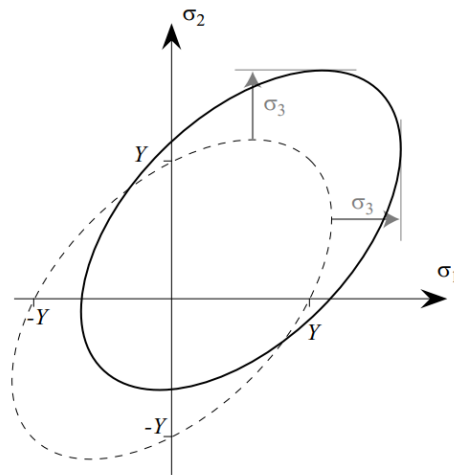
If Y is the yield stress in simple uniaxial tension and $(\sigma_1, \sigma_2, \sigma_3)$ are the principal stresses of a given stress state, then yielding is predicted to occur according to

- Hydrostatic component: $\sigma_h = (\sigma_1 + \sigma_2 + \sigma_3) / 3$, which does **not** contribute to yielding
- Tresca's Criterion: $\max\{|\sigma_1 - \sigma_2|, |\sigma_2 - \sigma_3|, |\sigma_3 - \sigma_1|\} = Y$
- Von Mises' Criterion: $(\sigma_1 - \sigma_2)^2 + (\sigma_2 - \sigma_3)^2 + (\sigma_3 - \sigma_1)^2 = 2Y^2$

Failure surfaces according to each criterion:



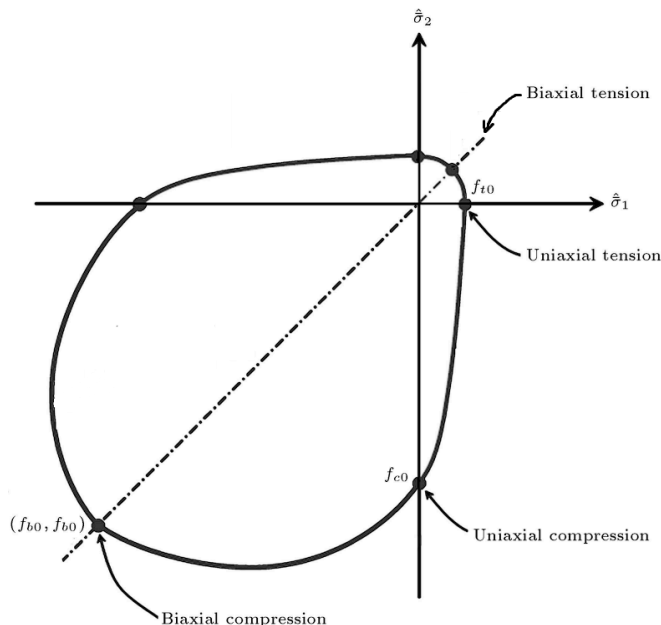
Tresca criterion failure surface



Von Mises criterion failure surface

The Von Mises ellipse exactly circumscribes the Tresca hexagon. The maximum discrepancy is for pure shear ($\sigma_1 = -\sigma_2$) where the difference is about 15%.

When the failure surfaces are projected parallel to the hydrostatic axis ($\sigma_1 = \sigma_2 = \sigma_3$), both Tresca and Von Mises become a regular hexagon and a circle respectively. The components along the axes in this projection are the deviatoric stresses $\sigma_{dev} = \sigma - \sigma_h \mathbf{I}$.



← Failure Surface for Concrete:

Concrete is weak in tension and strong in compression. The largest flaw governs tensile fracture, whereas compression leads initially to stable crack growth and material crushing.

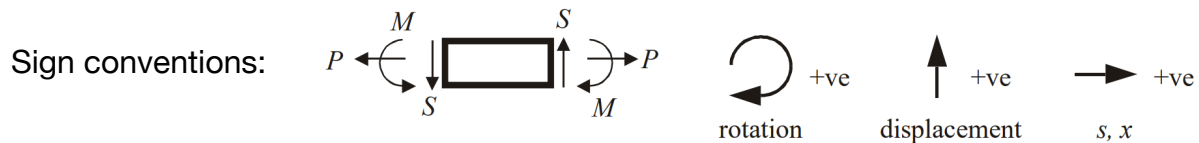
The Coulomb-Mohr and modified Mohr failure theories approximate brittle failure.

6.3.6. Thin-Walled Cylinders Under Uniform Pressure (Hydrostatic Loading)

(σ_h : hoop stress (circumferential / azimuthal), σ_l : longitudinal (axial) stress, t : thickness, r : radius, p : gauge pressure = $p_{in} - p_{out}$. If $p > 0$ then stresses are tensile; else compressive.)

- Stresses: $\sigma_h = \frac{pr}{t}, \sigma_l = \frac{pr}{2t}, \sigma_t \approx 0$ (away from ends; $t \ll r$)
- Strains: $\epsilon_h = \frac{pr}{2Et}(2 - \nu), \epsilon_l = \frac{pr}{2Et}(1 - 2\nu), \epsilon_t = \frac{-pr}{2Et}(3\nu)$
- Dimensional changes: $\frac{\Delta l}{l} = \epsilon_l, \frac{\Delta r}{r} = \frac{\Delta C}{C} = \epsilon_h, \frac{\Delta t}{t} = \epsilon_t$

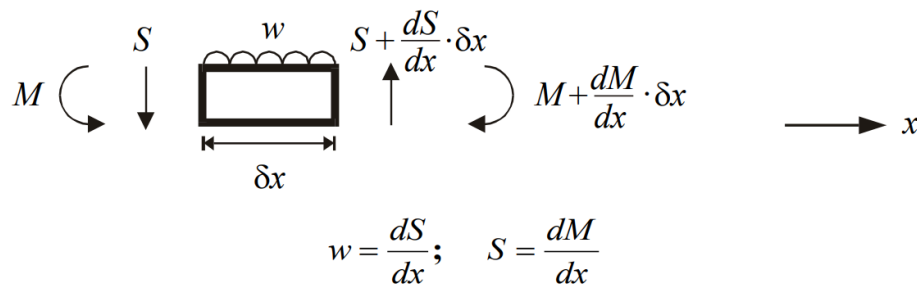
6.3.7. Forces, Moments and Displacements of Beams



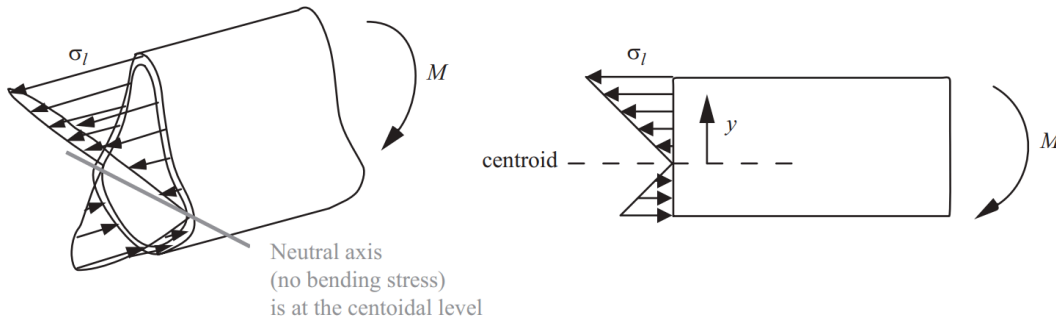
(x : distance parallel to beam, y : position on section from neutral axis, v : transverse deflection, ψ : beam rotation, κ : beam curvature, R : radius of curvature, ϵ : axial strain, s : arc length along beam, P : axial force, M : bending moment, S : shear force, w : shear force per unit length parallel to beam)

- Compatibility of rotations ψ and curvatures κ : $\kappa = \frac{1}{R} = \frac{d\psi}{ds}$
- Plane sections remain plane: $\epsilon = \kappa y$
- Transverse deflections due to a load: $\psi = -\frac{dv}{dx}$ and $\kappa = -\frac{d^2v}{dx^2}$

Equilibrium of transverse force per unit length w , shear force S and bending moment M :

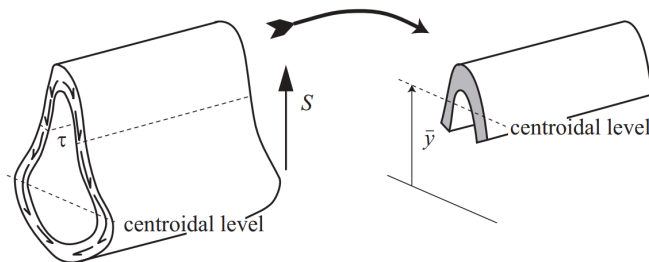


6.3.8. Elastic Bending of Beams



- Longitudinal stress due to a bending moment: $\frac{\sigma_l}{y} = \frac{M}{I} = E \Delta\kappa$
- Transverse displacement due to a bending moment: $M(x) = -EI \frac{d^2v}{dx^2}$.

(σ_l : longitudinal stress, y : distance from neutral axis, v : transverse displacement, M : bending moment, $\Delta\kappa$: change in curvature, I : second moment of area of section about the neutral axis, E : Young’s modulus. The ‘flexural rigidity’ is denoted $B = EI$.)



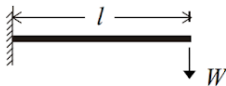
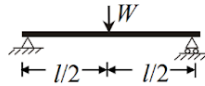
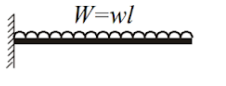
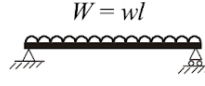

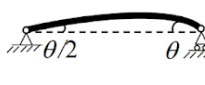
- Shear flow due to a shear force: $q = \frac{S}{I} \int_{A_c} y dA = \frac{S A_c \bar{y}}{I}$
- Shear stress (average over cut length): $\tau_{avg} = \frac{q}{a} = \frac{S A_c \bar{y}}{Ia}$ (Zhuravskii’s formula)

(q : shear flow (total longitudinal shear force per unit longitudinal length of the beam), S : shear force, $A_c \bar{y}$: first moment of area of the cut-off portion (area \times distance from centroid to neutral axis), I : second moment of area of the section about the neutral axis, a : total length of the cut through the beam in the plane of the cross-section)

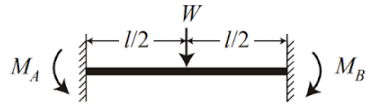
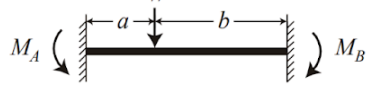
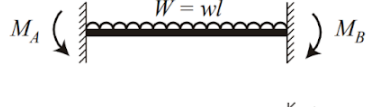
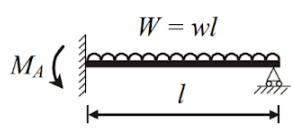

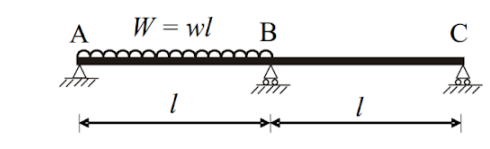

Analysis of sections with longitudinal stiffeners (e.g. semi-monocoque structures) can be simplified by ‘smearing’ the stiffener area into the beam, increasing its thickness slightly.

6.3.9. Standard Cases of Elastic Beam Bending

Bending of statically determinate beams:

	end rotation $\frac{Wl^2}{2EI}$	end deflection $\frac{Wl^3}{3EI}$		end rotation $\frac{Wl^2}{16EI}$	central deflection $\frac{Wl^3}{48EI}$	M_{MID} $\frac{Wl}{4}$
	$\frac{Wl^2}{6EI} = \frac{wl^3}{6EI}$	$\frac{Wl^3}{8EI} = \frac{wl^4}{8EI}$		$\frac{Wl^2}{24EI} = \frac{wl^3}{24EI}$	$\frac{5Wl^3}{384EI} = \frac{5wl^4}{384EI}$	$\frac{Wl}{8} = \frac{wl^2}{8}$
	$\frac{Ml}{EI}$	$\frac{Ml^2}{2EI}$		$\theta = \frac{Ml}{3EI}$		

Clamping moments of statically indeterminate beams:

	M_A	M_B		M_A	M_B
	$\frac{Wl}{8}$	$\frac{Wl}{8}$		$\frac{Wb^2a}{l^2}$	$\frac{Wa^2b}{l^2}$
	M_A	M_B		M_A	M_B
	$\frac{Wl}{12} = \frac{wl^2}{12}$	$\frac{Wl}{12} = \frac{wl^2}{12}$		$\frac{Wl}{8} = \frac{wl^2}{8}$	
	M_A	M_B		M_A	M_B
	$\frac{6EI\delta}{l^2}$	$\frac{6EI\delta}{l^2}$		$\frac{Wl}{16} = \frac{wl^2}{16}$	
	M_A	M_B			
	$\frac{2EI\theta}{l}$	$\frac{4EI\theta}{l}$			

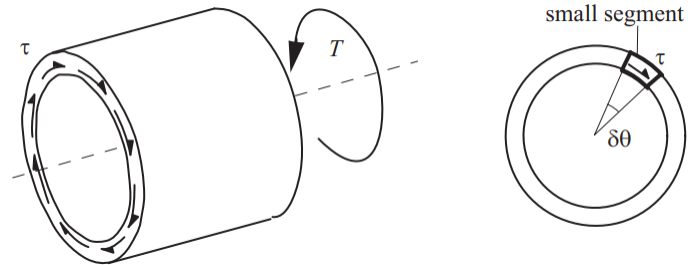
Saint-Venant's principle: the difference in the effects* induced by two different but statically equivalent loads is negligible in regions located very far from the loads.

* e.g. displacements, induced shear forces, bending moments, stress states etc.

6.3.10. Elastic Torsion of Beams

Hollow Circular Beams: (r : radius, J : polar second moment of inertia (aka torsion constant), T : torque, τ : shear stress, G : shear modulus)

- Torque-stress relationship: $\frac{\tau}{r} = \frac{T}{J}$
- Angular displacement **per unit beam length:** $\phi' = \frac{T}{GJ}$
(GJ : torsional rigidity)



General Cross-Sections: (q : shear flow, $t = t(s)$: section thickness (may be non-uniform), γ : shear strain, s : arc length around section, A_e : area enclosed by section at mid-thickness)

- Circulating shear flow and shear stress: $q = \frac{T}{2 A_e}, \quad \tau = \frac{q}{t}$
- Angular displacement **per unit beam length:** $\phi' = \frac{\oint \gamma ds}{2 A_e}$ (Bredt-Batho equation)
- Torque: $T = GJ\phi'$ where $J = \frac{4 A_e^2}{\oint \frac{ds}{t}}$

Warping: non-circular cross-sections warp out of plane under torsion.

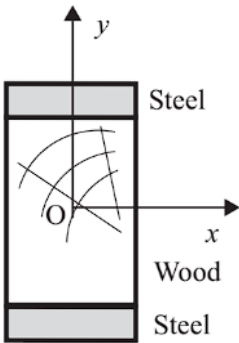
(I, J : second moments for **minor** axis, Γ : cross-sectional constant for warping, $E\Gamma$: warping rigidity, h : distance between flange centroids in a symmetric I-beam)

- End-moment for elastic lateral torsional buckling: $M_{LT} = \frac{\pi}{L} \sqrt{EIGJ \left(1 + \frac{\pi^2}{L^2} \frac{E\Gamma}{GJ} \right)}$
- For I-beams, $\Gamma \approx \frac{1}{4} I h^2$ and the bimoment (warping moment) is $B = Th = - E\Gamma \frac{d^2\phi}{dx^2}$

6.3.11. Elastic Bending of Composite Beams

Composite beams are made of two or more materials.

Sandwich Beams: e.g. timber/honeycomb/foam interior with Al-alloy face sheets

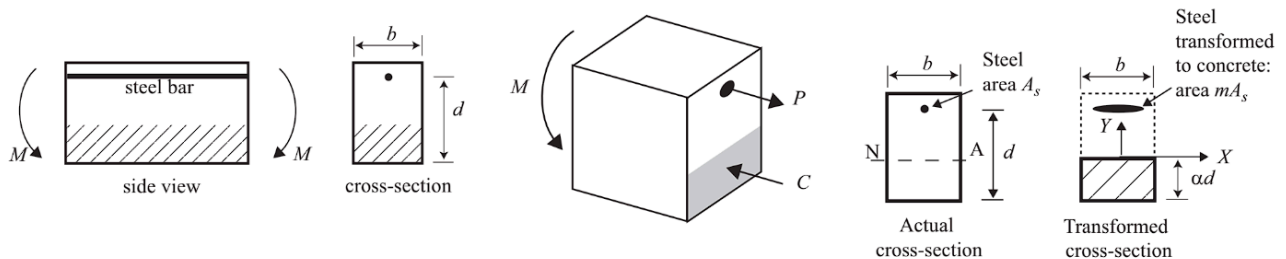


The wood section (width w) can be 'transformed' into an equivalent steel section of width $w \times (E_{\text{wood}} / E_{\text{steel}})$ (like the web of an I-beam).

Stress in steel: $\sigma_l = \frac{My}{I_{\text{steel}}}$, Stress in wood: $\sigma_l = \frac{My}{I_{\text{wood}}}$ where

Shear stress in adhesive: $\tau = \frac{S(\bar{A}y)_{\text{steel}}}{I_{\text{transformed}} w}$

Reinforced Concrete Beams: concrete with carbon steel rebar through the tensile side



The 'transformed' beam is all concrete ($m = E_{\text{steel}} / E_{\text{concrete (compression)}}$), with all tensile concrete becoming imaginary. The neutral axis position α satisfies $\frac{bd}{2mA_s} \alpha^2 + \alpha - 1 = 0$.

The maximum stresses in the steel and concrete are $\left| \frac{\sigma_{\text{steel}}}{\sigma_{\text{concrete}}} \right|_{\text{max}} = \frac{m(1-\alpha)}{\alpha}$.

If $\left| \frac{\sigma_{\text{steel}}}{\sigma_{\text{concrete}}} \right|_{\text{max}} = \frac{\sigma_y^{(\text{steel, tension})}}{\sigma_f^{(\text{concrete, compression})}}$ then this is a 'balanced design' (neither part is limiting).

6.3.11. Cables, Ropes, Chains and Segmented Arches

Friction due to Cable or Belt Contact (The Capstan Equation)

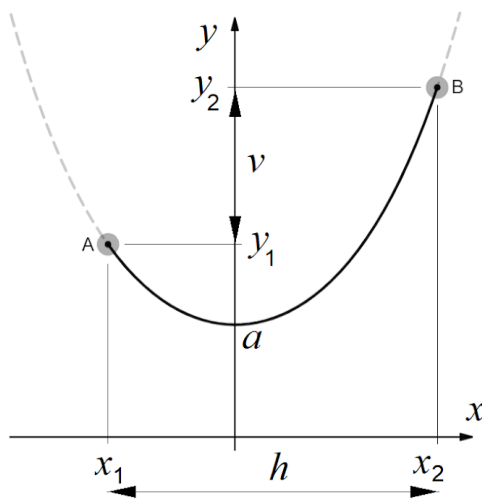
A flexible inextensible cable in contact with a curved surface develops different tensions either side of the contact due to friction, such that

$$\frac{T_2}{T_1} \leq e^{\mu\theta} \quad (\mu: \text{coefficient of friction, } \theta: \text{angle subtended by contact, } T: \text{tension})$$

with equality when on the limit of sliding in either direction.

Tension in a Hanging Cable, Rope or Chain (The Catenary Equation)

A freely hanging inextensible cable, rope or chain suspended between any two points forms a catenary curve under its own self-weight. In Cartesian coordinates, this curve has the general shape $y = a \cosh x/a$. If the mass per unit cable length is λ then:

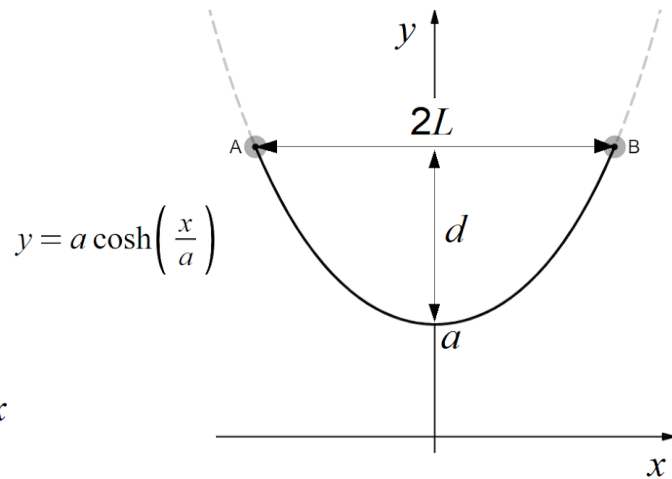


Different Elevations

Arc length: $s = a \left(\sinh \frac{x_2}{a} - \sinh \frac{x_1}{a} \right)$

Parameters: $\sqrt{s^2 - v^2} = 2a \sinh \frac{h}{2a}$

Tension: $|T_x| = \lambda ga, \quad T_y = \lambda ga \sinh \frac{|x|}{a} \Rightarrow |T| = \sqrt{T_x^2 + T_y^2} = \lambda ga \cosh \frac{x}{a} \quad (m = \lambda s)$



Same Elevation

$s = 2a \sinh \frac{L}{a} \approx 2L + \frac{4d^2}{3L}$ for small $\frac{d}{L}$

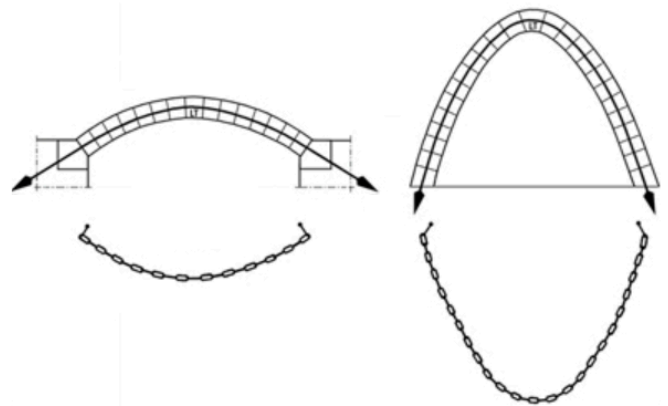
$a = \frac{s^2}{8d} - \frac{d}{2}$ and $L = a \cosh^{-1} \left(1 + \frac{d}{a} \right)$

Compressive Forces in Arches

Arches carry loads, including their self-weight, via compression. They are typically made of brick or stone, which are cheap and strong in compression (masonry).

For a segmented arch, each segment (voussoir) exerts compressive contact forces on each neighbouring segment, with the end segments in contact with the base (buttress). For any arch, the locus of contact forces (**thrust line**) must be contained within the geometry of the arch itself in order to be stable. Friction between the segments is not required for stability, although friction can help improve resilience to varying loads.

A **hanging chain** illustrates the geometry of the thrust line in an unloaded arch (self-weight only, producing a catenary curve): the thrust line in the arch is simply the **reflection** of this. This also applies to rigid arches. By hanging weights from the chain of a desired design mass, the shape of the thrust line in the corresponding arch can be deduced, allowing architects to easily design arbitrarily shaped segmented arches (**funicular analysis for form finding**).



Both 'chain' and 'arch' models can be useful in construction: for example, an arch bridge and a suspension bridge are the inversions of each other. In these cases, the weight distribution is uniform in the horizontal direction, transforming the catenary into the parabola.

The bending moment at any point within an arch (or frame) is proportional to the distance between the point and the closest point on the thrust line. The tensile side of the arch is usually the outer edge (when loads are vertically downwards). The point of maximum bending moment is therefore the point furthest from this line. In a pinned arch, the thrust line must pass through the pins, since there can be no bending moment at a frictionless pin.

A 'tied arch' can be formed by connecting the two supports together with a rod, which will be placed into tension in order to carry the horizontal components of the reaction force. This allows for vertical, frictionless supports to be used for the arch instead.

6.3.12. Stress Distribution in a Rotating Axisymmetric Bodies

Rotating Thin Disk or Plate: The force balance on an infinitesimal sector element with zero axial stress rotating at angular speed ω about the axis gives

$$\sigma_r = A + \frac{B}{r^2} - \frac{3 + \nu}{8} \rho \omega^2 r^2 \qquad \sigma_\theta = A - \frac{B}{r^2} - \frac{1 + 3\nu}{8} \rho \omega^2 r^2$$

(σ_r : radial stress, σ_θ : hoop stress, r : radial distance, ν : Poisson's ratio, ρ : density)

- Solid disk, radius R : $A = \frac{1}{8} \rho R^2 \omega^2$ and $B = 0$
- Disk of radius R_2 with hole of radius R_1 : $A = \frac{(3 + \nu)(R_1^2 + R_2^2) \rho \omega^2}{8}$ and $B = -A$

Rotating Long Cylinder or Shaft: The force balance on an infinitesimal sector element rotating at angular speed ω about the axis gives

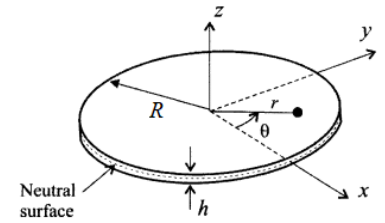
$$\sigma_r = A - \frac{B}{r^2} - \frac{3 - 2\nu}{8(1 - \nu)} \rho \omega^2 r^2 \qquad \sigma_\theta = A + \frac{B}{r^2} - \frac{1 + 2\nu}{8(1 - \nu)} \rho \omega^2 r^2$$

(σ_r : radial stress, σ_θ : hoop stress, r : radial distance, ν : Poisson's ratio, ρ : density)

- Solid cylinder, radius R : $A = \frac{(3 - 2\nu) \rho R^2 \omega^2}{8(1 - \nu)}$ and $B = 0$
- Cylinder R_2 with hollow radius R_1 : $A = \frac{(3 - 2\nu)(R_1^2 + R_2^2) \rho \omega^2}{8(1 - \nu)}$ and $B = \frac{(3 - 2\nu) \rho R_1^2 R_2^2 \omega^2}{8(1 - \nu)}$

6.3.13. Transverse Loading of a Circular Plate (2D Deflection)

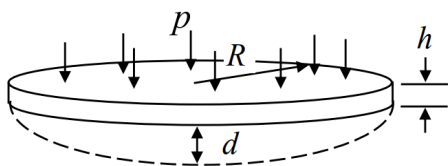
For axisymmetric loading, the peak deflection and stress is at the centre (σ_r : radial stress, σ_t : hoop stress). For **small** (linear) deflections:



Conditions	Central deflection	Central stress	
		$\sigma_{r, max}$	$\sigma_{z, max}$
Uniform loading, clamped edges	$\frac{3pR^4}{16Eh^3} (1 - \nu)$	$\frac{3pR^2}{4h^2}$	$\frac{3pR^2}{8h^2} (1 + \nu)$
Uniform loading, simply supported circumference	$\frac{3pR^4}{16Eh^3} (5 + \nu)(1 - \nu)$	$\frac{3pR^2}{8h^2} (3 + \nu)$	$\frac{3pR^2}{8h^2} (3 + \nu)$
Central load, clamped edges	$\frac{3FR^2}{4\pi Eh^3} (1 - \nu^2)$	$\frac{3F}{2\pi h^2}$	$\frac{3\nu F}{2\pi h^2}$
Central load, simply supported circumference	$\frac{3FR^2}{4\pi Eh^3} (3 + \nu)(1 - \nu)$	$\frac{3F}{2\pi h^2} (1 + \nu) \ln \frac{R}{r}$	$\frac{3F}{2\pi h^2} [(1 + \nu) \ln \frac{R}{r} + (1 - \nu)]$

Large Deflections of Thin Elastic Membranes: numerical data given for $\nu = 0.3$

Boundary conditions		A	B	Centre		Edge			
				$\alpha_r = \alpha_t$	$\beta_r = \beta_t$	α_r	α_t	β_r	β_t
Clamped	Fixed	0.471	0.171	0.976	2.86	0.476	0.143	-4.40	-1.32
	Free to move	0.146	0.171	0.500	2.86	0	-0.333	-4.40	-1.32
Simply supported	Fixed	1.852	0.696	0.905	1.778	0.610	0.183	0	0.755
	Free to move	0.262	0.696	0.295	1.778	0	-0.427	0	0.755

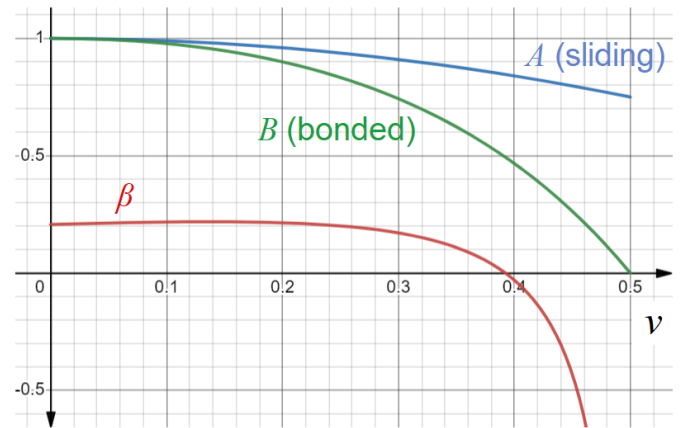
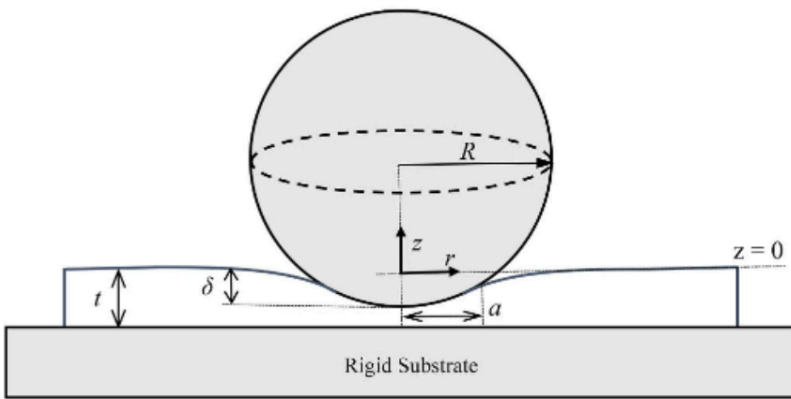


Central deflection: $\frac{d}{h} + A\left(\frac{d}{h}\right)^3 = B \frac{p}{E} \left(\frac{R}{h}\right)^4$

Middle plane stress: $\sigma_r = \alpha_r E \left(\frac{d}{R}\right)^2, \quad \sigma_t = \alpha_t E \left(\frac{d}{R}\right)^2$

Extreme fibre stress: $\sigma'_r = \beta_r E \frac{dh}{R^2}, \quad \sigma'_t = \beta_t E \frac{dh}{R^2}$

6.3.14. Spherical Indentation into an Infinite Compressible Elastic Plate

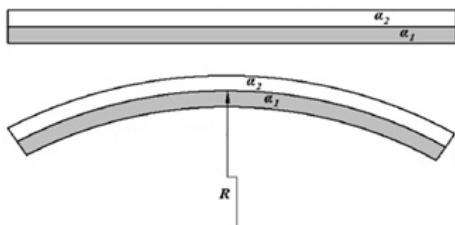


The deflection of the compressible elastic layer depends on whether it is bonded to the rigid substrate or allowed to slide. The values of constants β, A, B depend on ν of the layer.

	a and δ	F and a	F and δ
Sliding	$\frac{\delta R}{a^2} = \frac{1}{2}$	$\frac{1}{8} \frac{a}{R} \left(\frac{a}{t}\right)^3 = \frac{FA}{2\pi Et^2}$	$\frac{R\delta^2}{t} = \frac{FA}{\pi E}$
Bonded	$\frac{\delta R}{a^2} = \frac{1}{2} + \beta \left(\frac{t}{a}\right)$	$\frac{a}{R} \left(\frac{1}{8} + \frac{\beta t}{2a}\right) \left(\frac{a}{t}\right)^3 = \frac{FB}{2\pi Et^2}$	$\frac{R\delta^2}{t} = \frac{FB}{\pi E}$

6.3.15. Curvature of a Bimetallic Strip due to Differential Strains with Constraint

When two thin films (thickness t_1, t_2) are bound at a plane interface and subject to e.g. thermal strain by heating, there is an induced curvature κ and radius ρ given by



$$\kappa = \frac{1}{R} = \frac{6(1+m)^2}{h \left(3(1+m)^2 + (1+mn) \left(m^2 + \frac{1}{mn} \right) \right)} \cdot (\varepsilon_2 - \varepsilon_1)$$

$$= \frac{3(\varepsilon_2 - \varepsilon_1)}{2h} \quad \text{if } m = n = 1.$$

where $\varepsilon = \alpha \Delta T$, $m = \frac{t_1}{t_2}$, $h = t_1 + t_2$, $n = \frac{E_1}{E_2}$.

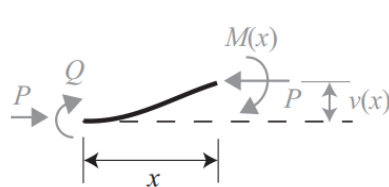
(α [K^{-1}]: linear expansion coefficient, ΔT [K]: increase in temperature)

Other responsive stimuli to strain follow a similar pattern.

6.3.16. Euler Buckling of Elastic Columns

The axial compressive buckling load P of a **perfectly straight** elastic beam is given by

$$P = \frac{\pi^2 EI}{L_e^2} \quad (I: \text{second moment of inertia, } L_e: \text{effective buckling length})$$



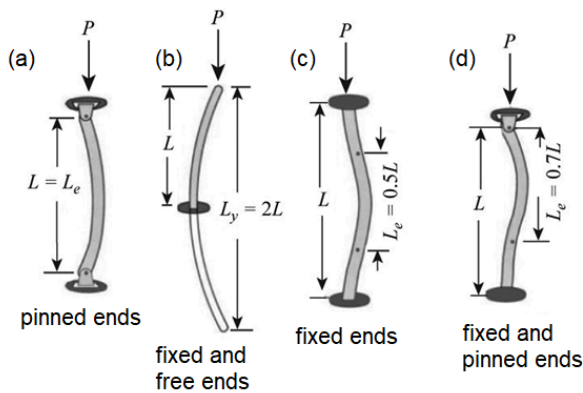
If $P = \alpha^2 EI$, the critical value of α can be found by solving

Equilibrium:

$$P v(x) = M(x) + Q$$

Compatibility:

$$M(x) = -EI \frac{d^2 v(x)}{dx^2}$$



← **Typical support cases:**

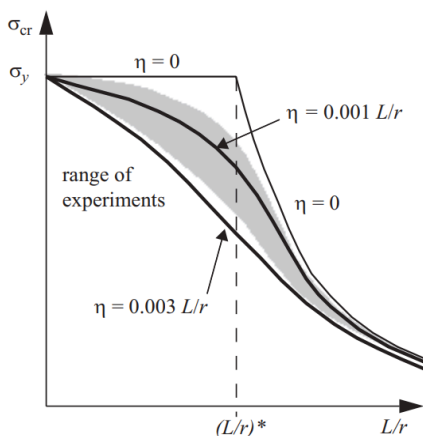
For a beam of length L , the value of L_e can sometimes be inferred from symmetry as the distance between inflection points on the deformed beam. For simple supports, $L_e = L$.

An exact value for case (d) is $L_e = \frac{\pi L}{\beta}$, where $\beta \approx 4.49341\dots$ is the smallest positive solution to the equation $\beta = \tan \beta$.

Buckling stress: for a beam with cross-sectional area A ,

- Euler buckling stress: $\sigma_E = \frac{P}{A} = \frac{\pi^2 E}{(L_e/r)^2}$ ($\frac{L_e}{r}$: slenderness, $r = \sqrt{\frac{I}{A}}$: radius of gyration)
- If $\sigma_E > \sigma_y$ then the column will yield in compression (crushing) before buckling, which occurs for slenderness values of $\frac{L_e}{r} < \pi \sqrt{\frac{E}{\sigma_y}}$.

Imperfect Buckling of an Elastic Column: small initial deformations lower the buckling load



For an initial deformation with first mode shape $v(x) = \delta_0 \sin \frac{\pi x}{L}$, the buckling stress falls from $P/A = \sigma_E$ to σ_{cr} , where (Perry's formula)

$$(\sigma_y - \sigma_{cr})(\sigma_E - \sigma_{cr}) = \eta \sigma_{cr} \sigma_E \quad \text{where } \eta = \frac{\delta_0 y_{max}}{r^2}.$$

(y_{max} : maximum section distance from neutral axis)

An experimental correlation is $\eta \approx 0.001 \times \frac{L}{r}$, with

$\eta = 0.003 \times \frac{L}{r}$ as a safe lower bound.

(Robertson's correlation, incorporated into Eurocode 3 (EN 1993)).

6.3.18. Statically Determinate Trusses

A plane pin-jointed truss is a 2D assembly of light elastic bars, frictionless point joints and supports (pinned, roller or built-in/encastre), with loads applied at joints only, so that the bars carry only axial forces at equilibrium.

In 2D, the components of the truss satisfy $b - 2j + r = s - m$ (Maxwell-Calladine rule).

(b : number of bars, j : number of joints, r : number of reaction force components (restraints), s : number of states of self-stress, m : number of mechanistic degrees of freedom)

- If $s - m < 0$ then the assembly is a mechanism.
- If $s - m > 0$ then the assembly is redundant and rigid.
- The condition $s - m = 0$ is necessary (but not sufficient) for a non-redundant rigid assembly. It is possible for an assembly to have $s = m \neq 0$.
- If $s = 0$ then the assembly is **statically determinate** (bar forces independent of materials)
- If $m = 0$ then the assembly is kinematically determinate (displacements are fixed)

Force Methods in a Statically Determinate Truss: first-order linear elastic analysis

Denote the b bar forces T_i and the r reaction forces R_j . These can be found by either:

- **Method of joints:** take a free body cut through the bars around every joint and resolve the forces: solve the system ($2j$ equations in $(b + r)$ unknowns) algebraically.
- **Method of sections:** choose free body cuts to expose a small number (typically 3-5) of forces; balance forces and take moments about where many lines of action of forces intersect to find their values. Continue until all unknowns are found.

Exploit symmetry and anti-symmetry and identify zero-force members to simplify analysis.

Displacement Methods in a Kinematically Determinate Truss: first-order small displacements

Once all internal forces T_i under a given load have been found, bar extensions can be found using $e_i = T_i L_i / AE$ (L : bar length, A : bar area, E : bar Young's modulus). Joint displacements δ_i can be found by either:

- **Displacement diagram:** mark all known fixed joints at a common reference point $o \dots$. For each bar connected to a fixed joint, draw a solid line segment to a distance e_i in the direction of the endpoint, and if the bar is free to rotate, then draw a perpendicular dashed line from it. The endpoint displacement lies on this line. Repeat until intersections of the lines are found to identify the displacement vectors δ_i of the joints, measured using scale drawings relative to o .
- **Virtual work (Castigliano's Theorem):** for **any** system of external forces F_i at the joints in equilibrium with bar tensions T_j (equilibrium set), and any system of joint displacements δ_i compatible with member extensions e_j (compatibility set): the equation $\sum_i F_i \cdot \delta_i = \sum_j T_j e_j$, (external work = internal work) can be used by applying virtual load(s) $F_i^* = 1$ at a joint where the displacement is desired, and finding the new virtual tensions T_j^* under this load. Solve for the desired real displacement(s) δ_i using the real extensions e_j . If there is only one virtual load and it is parallel to the only real applied load F , then $\delta = \sum_j T_j^2 L_j / AEF$ (since $T_j = FT_j^*$).

6.3.19. Statically Indeterminate Trusses and Frames

A linear-elastic, pin-jointed (no bending moments), joint-loaded truss can be represented by:

- An equilibrium matrix, \mathbf{A} , such that $\mathbf{A}\mathbf{t} = \mathbf{f}$, formed by resolving in two orthogonal directions at each joint. Solutions to $\mathbf{A}\mathbf{t} = \mathbf{0}$ are states of self-stress.
- A compliance matrix, \mathbf{C} , such that $\mathbf{e} = \mathbf{C}\mathbf{t} + \mathbf{e}_0$, given by $C_{ii} = \frac{L_i}{A_i E_i}$ and zero off-diagonal.

The compatibility constraint is represented as $\mathbf{e} = \mathbf{A}^T \delta$ (\mathbf{A}^T : compatibility matrix).

Solutions to $\mathbf{A}^T \delta = \mathbf{0}$ are internal/rigid body mechanisms.

(\mathbf{t} : unknown bar tensions, \mathbf{f} : external loads, \mathbf{e} : bar extensions, δ : bar displacements

\mathbf{e}_0 : initial (misfit) bar extensions e.g. thermal expansion gives $(\mathbf{e}_0)_i = \alpha_i L_i \Delta T_i$)

If the truss is statically indeterminate, then $\mathbf{A}\mathbf{t} = \mathbf{f}$ is an underconstrained system of equations, providing the 'particular solution' \mathbf{t}_0 and a set of 'states of self-stress' \mathbf{s}_i .

- To find \mathbf{t}_0 , identify and remove (set force to zero) redundant bars to make the truss statically determinate, and solve for equilibrium with the applied load.
- To find each \mathbf{s}_i , remove all loads and remove (set force to zero) all but one redundant bars, which can be set to any arbitrary value e.g. 1, and solve again. Note that \mathbf{s}_i are vectors spanning the null space of \mathbf{A} since $\mathbf{A}\mathbf{s}_i = \mathbf{0}$ (Section 4.3.1).
- To find each x_i , invoke virtual work using $\mathbf{e} \cdot \mathbf{s}_i = 0$, for all i , solving for x_i .
- The equilibrium solutions are then $\mathbf{t} = \mathbf{t}_0 + \sum x_i \mathbf{s}_i$ and $\mathbf{e} = \mathbf{C}\mathbf{t} + \mathbf{e}_0$.

For frame structures which are statically indeterminate:

- Remove redundant supports and replace them with pins and reinstated unknown point bending moments.
- Find displacements and rotations of sections using compatibility or virtual work. The virtual work equations are $P^* \delta = \int_{frame} M \kappa^* ds$ and $Q^* \psi = \int_{frame} M \kappa^* ds$, or if bulk solid bodies are involved then $p^* V = \int_{solid} \sigma \varepsilon^* dV = \int_{solid} \tau \gamma^* dV$
(P^* , Q^* : virtual loads and torques, $\kappa^* = M^* / EI$: virtual curvature, M : bending moment, ds : incremental distance along the frame, p^* : virtual pressure, V : volume change, σ : axial stress, ε^* : virtual axial strain, τ : shear stress, γ^* : virtual shear strain.)
- For each added pin, invoke continuity to set rotations either side equal.
- Solve for the required value(s) of the pin bending moments.
- Solve for reaction forces and plot shear forces/bending moments as required.

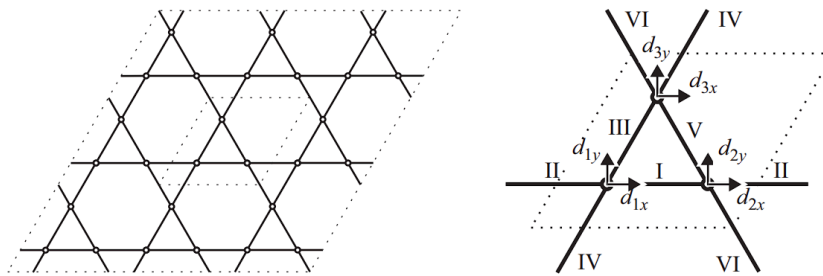
6.4.20. Periodic and Amorphous Rigid-Jointed Frameworks (Lattices and Foams)

In a rigid-jointed mechanistic assembly, bars parallel to applied forces do not develop a force, but other bars develop elastic bending moments (curvature) and the joints translate. For rigid-perfectly plastic modes, joints act as plastic hinges (Section 6.6.13).

Plane (2D) lattices will be stiff for $Z \geq 4$ and mechanistic for $Z < 4$.

Space (3D) lattices will be stiff for $Z \geq 6$ and mechanistic for $Z < 6$.

Example: Kagome plane lattice



$$\begin{bmatrix}
 -1 & 0 & 1 & 0 & 0 & 0 \\
 1 & 0 & -1 & 0 & 0 & 0 \\
 -1/2 & -\sqrt{3}/2 & 0 & 0 & 1/2 & \sqrt{3}/2 \\
 1/2 & \sqrt{3}/2 & 0 & 0 & -1/2 & -\sqrt{3}/2 \\
 0 & 0 & 1/2 & -\sqrt{3}/2 & -1/2 & \sqrt{3}/2 \\
 0 & 0 & -1/2 & \sqrt{3}/2 & 1/2 & -\sqrt{3}/2
 \end{bmatrix}
 \begin{bmatrix}
 d_{1x} \\
 d_{1y} \\
 d_{2x} \\
 d_{2y} \\
 d_{3x} \\
 d_{3y}
 \end{bmatrix}
 =
 \begin{bmatrix}
 e_I \\
 e_{II} \\
 e_{III} \\
 e_{IV} \\
 e_V \\
 e_{VI}
 \end{bmatrix}$$

6.3.21. Plastic Theory

(For the prediction of failure in elastic deformation modes with Tresca and Von Mises theory), see Section 6.4.4.)

Plasticity theory is a failure-oriented design theory, assuming a flat stress-strain curve after yield (rigid-perfectly plastic: with ductility and neglects work hardening) and identical properties in tension and compression.

Elastic section modulus (Z_e) and Plastic section modulus (Z_p)

$$Z_e = \sum_{\text{region } i} A_i |\bar{y}_i| \qquad Z_p = \sum_{\text{region } i} A_i |\bar{y}_{i(EA)}|$$

(\bar{y}_i : centroid of region i to **neutral axis**, $\bar{y}_{i(EA)}$: centroid of region i to **equal-area axis**)

The sum is over areas which are bending or yielding in either tension or compression. The equal-area axis is also known as the ‘plastic neutral axis’ (PNA).

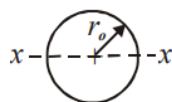
The bending moment at which the extreme fibre of a beam yields plastically is the moment at first yield (elastic moment capacity), M_y .

The bending moment at which the entirety of a beam section yields plastically is the plastic moment capacity, M_p .

These are related to the material yield stress σ_y by $M_y = Z_e \sigma_y$ and $M_p = Z_p \sigma_y$.

Values of Z_e and Z_p for some cross-section are given.

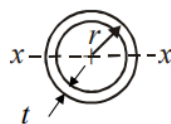
Solid circular section



$$Z_e = \frac{\pi r_o^3}{4}$$

$$Z_p = \frac{4 r_o^3}{3}$$

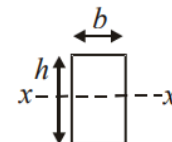
Thin circular section



$$Z_e \approx \pi r^2 t$$

$$Z_p \approx 4 r^2 t$$

Rectangular section



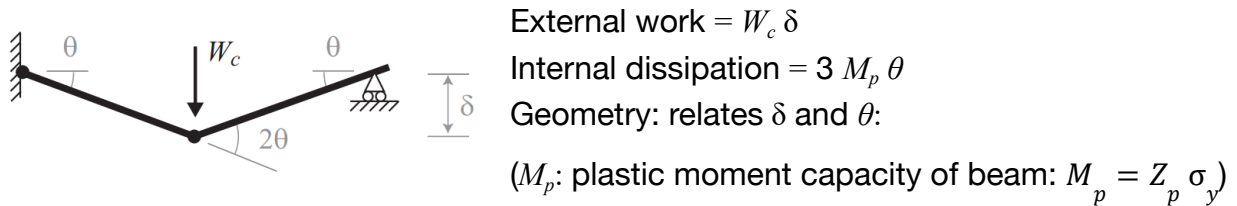
$$Z_e = \frac{bh^2}{6}$$

$$Z_p = \frac{bh^2}{4}$$

6.3.22. Upper Bound Theorem for Plastic Failure of Structures

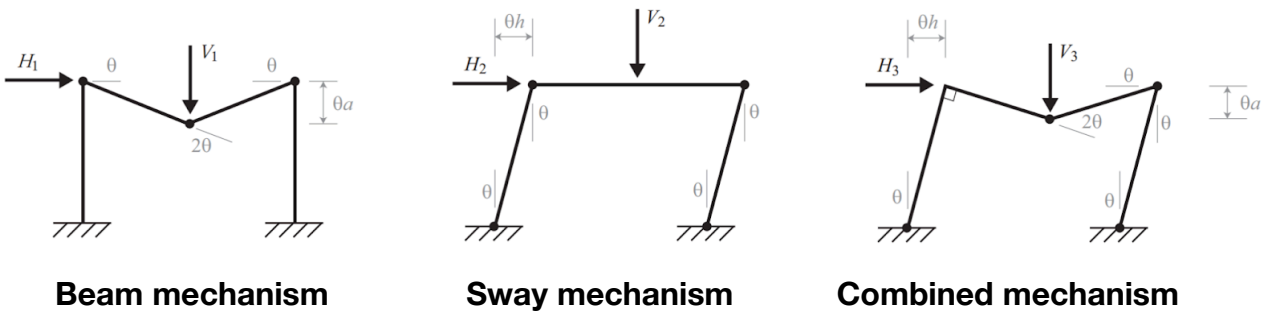
If an estimate of the plastic collapse load W_{mech} is calculated for any arbitrary compatible mechanism by equating the work done by the applied load, and the plastic energy dissipated, and the actual collapse load is W_c , then $W_{mech} \geq W_c$.

Typical application: plastic failure load of frame or beam due to **plastic hinge** formation.



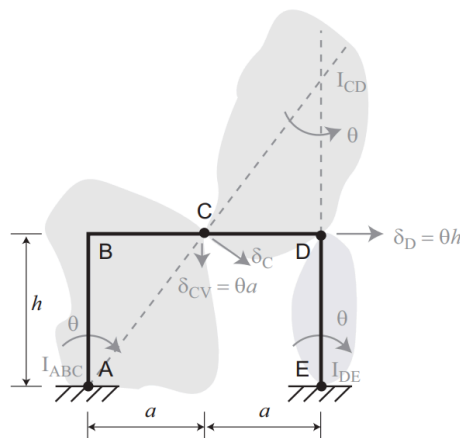
Statically determinate structures collapse with **one** plastic hinge. Statically indeterminate structures (e.g. multi-span beams, frames) collapse with **multiple** plastic hinges.

6.3.23. Plastic Failure Modes of Portal Frames (Plastic Hinge Mechanisms)

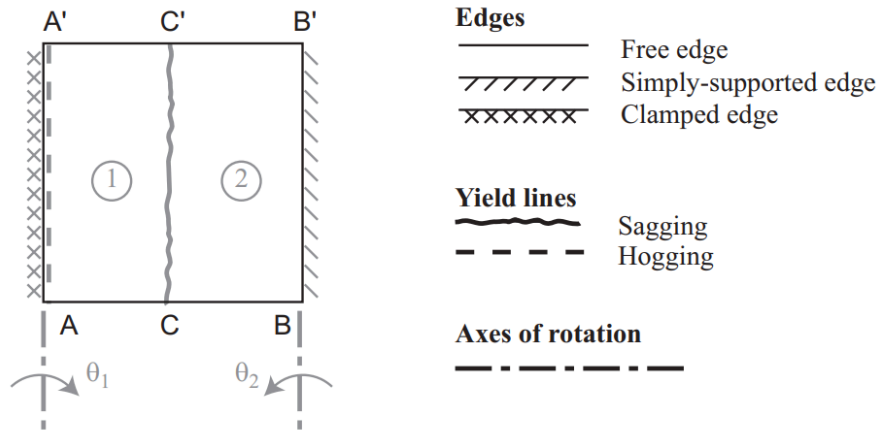


An ‘interaction diagram’ shows the regions of each mode as a function of H and V .

The geometry of combined mechanisms can be deduced using the method of instantaneous centres for each of the rigid regions between plastic hinges:



6.3.24. Yield Line and Slip Plane Analysis of Slabs, Plates and Continua



Plastic moment capacity per unit length of a yield line: $m = \frac{M_p}{b} = \frac{Z_p \sigma_y}{b} = \frac{1}{4} d^2 \sigma_y$
 (d : thickness of rectangular plate cross section)

By the upper bound theorem, $\sum_{forces} F \delta + \sum_{pressures} p \Delta V = \sum_{yield\ lines} mL \Delta \theta$.

If the volume generated ΔV due to a pressure loading is difficult to calculate, an alternative way of writing this term is $pA \Delta z_g$, where A is the plane area of the region and Δz_g is the distance descended by the centroid of the region, which can be related to δ by similarity.

The $L \Delta \theta$ terms can be found using either a displacement diagram (yield line length \times relative angle of rotation) or the projection method (resolve into component of yield line parallel to axis \times rotation about axis).

Slabs made of reinforced concrete do fail by yield lines, but the energy absorbed is all in the steel reinforcement, and the above calculation for moment capacity is not valid. For calculations on reinforced concrete, see Section 6.5.7. Similar analyses can be done for soil slippage in shear (Section 6.5.4).

For continua (rigid plastic solids), the upper bound theorem is

$$\sum_{forces} F \delta + \sum_{pressures} p \Delta V = \sum_{shear\ zones} kA \Delta x$$

where k is the shear yield stress, A is the area of the slip plane and Δx is the relative displacement of each rigid block. For continuum mechanics analysis, see Section 6.2.27.

6.3.25. Lower Bound Theorem for Plastic Failure of Structures

If a set of internal stresses can be found in the structure that are in equilibrium with an applied load W_{equil} , and nowhere violate the yield condition, and the actual collapse load is W_c , then $W_c \geq W_{equil}$.

To perform a lower bound analysis:

- Make the structure statically determinate by adding unknown bending moments M_x at newly-positioned pins.
- Determine the generalised bending moment distribution in terms of M_x .
- Optimise the distribution so that the peaks and troughs are as close to M_p as possible with no larger value. Calculate the value of M_x at which this occurs.

For beam section optimisation, plastic moduli Z_p are given for common steel UBs in Section 6.5.9.

6.3.26. Continuum Mechanics Formulation of Deformation

For tensor notation, see Section 4.4.1.

Isotropic Linear Elasticity

(σ_{ij} : stress tensor, ε_{ij} : infinitesimal strain tensor, b_i : body force vector, t_i^e : external traction vector, u_i : displacement vector, U : strain energy density scalar)

- Equilibrium: $\sigma_{ij,j} + b_i = 0$ and $\sigma_{ij} = \sigma_{ji}$
- Compatibility: $\varepsilon_{ij,kp} + \varepsilon_{kp,ij} - \varepsilon_{pj,ki} - \varepsilon_{ki,pj} = 0$
- Constitutive law: $\sigma_{ij} = \frac{E}{1+\nu} \varepsilon_{ij} + \frac{\nu E}{(1+\nu)(1-2\nu)} \varepsilon_{kk} \delta_{ij}$
- Lamé's constants: $\mu = G = \frac{E}{2(1+\nu)}$, $\lambda = \frac{\nu E}{(1+\nu)(1-2\nu)}$
- Strain energy density: $\sigma_{ij} = \frac{\partial U}{\partial \varepsilon_{ij}}$

At equilibrium, the potential energy Π is minimised. Hence, for any small kinematically admissible perturbation δu_i ,

$$\delta \Pi = \int_V \delta U dV - \int_S t_i^e \delta u_i dS - \int_V b_i \delta u_i dV = 0$$

Isotropic Linear Viscoelasticity

(E_r : relaxation modulus, J_c : creep compliance, $H(t)$: Heaviside step function)

- Relaxation response: if $\varepsilon(t) = \varepsilon_0 H(t)$ then $\sigma(t) = \varepsilon_0 E_r(t)$
- Creep response: if $\sigma(t) = \sigma_0 H(t)$ then $\varepsilon(t) = \sigma_0 J_c(t)$
- Laplace domain: $\overline{E_r}(s) \overline{J_c}(s) = s^{-2}$

Boltzmann superposition principle in 1D (convolution theorem for impulse responses):

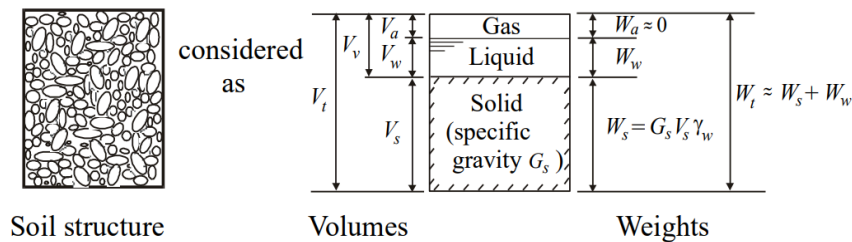
$$\sigma(t) = \int_0^t \frac{\partial \varepsilon(\tau)}{\partial \tau} E_r(t - \tau) d\tau \quad \varepsilon(t) = \int_0^t \frac{\partial \sigma(\tau)}{\partial \tau} J_c(t - \tau) d\tau$$

Correspondence principle: in the Laplace domain, the viscoelastic solution corresponds to the elastic solution, with the substitutions $E \rightarrow s \overline{E_r}(s)$ and $\nu \rightarrow s \overline{\nu_r}(s)$ (for any time-dependent moduli).

6.4. Geotechnical and Civil Engineering

6.4.1. Definitions in Soil Mechanics

The structure of soil can be divided into a solid phase, liquid phase and gas phase:



Quantities defining the composition are given by: (Unit weight of water: $\gamma_w = 9.81 \text{ kN m}^{-3}$)

- Specific gravity of soil solids: $G_s = \frac{\rho_s}{\rho_{\text{water}}}$
- Voids ratio: $e = \frac{V_v}{V_s}$
- Water content: $w = \frac{W_w}{W_s}$
- Degree of saturation: $S_r = \frac{V_w}{V_v} = w \frac{G_s}{e}$
- Bulk unit weight of soil: $\gamma = \frac{W_t}{V_t} = \frac{\gamma_w (G_s + S_r e)}{1 + e}$
- Dry unit weight of soil: $\gamma = \frac{W_s}{V_t} = \frac{\gamma_w G_s}{1 + e}$
- Buoyant unit weight of soil: $\gamma' = \gamma - \gamma_w = \frac{\gamma_w (G_s - 1)}{1 + e}$
- Relative density: $I_D = \frac{e_{\text{max}} - e}{e_{\text{max}} - e_{\text{min}}}$

where e_{max} is the maximum voids ratio achievable in a quick tilt test, and e_{min} is the minimum voids ratio achievable by vibratory compaction.

6.4.2. Classification of Particle Sizes

Clay: smaller than 0.002 mm (two microns)

Silt: between 0.002 and 0.06 mm

Sand: between 0.06 and 2 mm

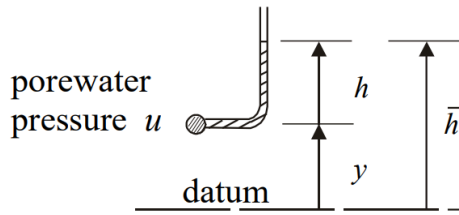
Gravel: between 2 and 60 mm

Cobbles: between 60 and 200 mm

Boulders: larger than 200 mm

D_x : particle size such that $x\%$ by weight of a soil sample is composed of finer grains.

6.4.3. Groundwater Seepage



Head	$h = u / \gamma_w$
Potential	$\bar{h} = h + y$
Hydraulic gradient	$i = -\nabla \bar{h}$

Darcy's law for laminar flow:

$$v = ki \quad (v: \text{superficial seepage velocity, } k: \text{coefficient of permeability})$$

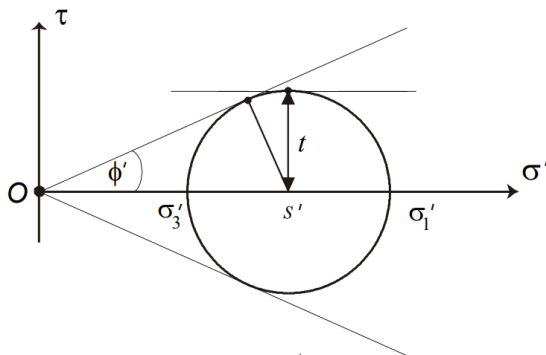
Typical values:

- Clays: k between 10^{-11} ms^{-1} and 10^{-9} ms^{-1}
- 1 micron $< D_{10} < 10 \text{ mm}$: $k \approx 0.01 \times (D_{10} \text{ in mm})^2 \text{ ms}^{-1}$
- $D_{10} > 10 \text{ mm}$: non-laminar flow.

6.4.4. Plane-Strain Soil Stresses

In this section only, compressive stresses are taken as positive.

The effective stress in saturated soil the difference between the total stress and the pore water pressure: $\sigma = \sigma' + u$ and $\tau = \tau' (+ 0)$.



Mohr's circle:

Mobilised angle of shearing: ϕ'

Mean effective stress: $s' = \frac{\sigma'_1 + \sigma'_3}{2}$

Mobilised shear strength: $t = \frac{\sigma'_1 - \sigma'_3}{2} = \frac{\sigma_1 - \sigma_3}{2}$

$$\sin \phi' = \frac{t}{s'} = \frac{\sigma_1 - \sigma_3}{\sigma_1 + \sigma_3}$$

6.4.5. Undrained Strength of Soil: Tresca Cohesion Hypothesis

Undrained behaviour is exhibited by clays in the short term.

In constant-volume tests on clay, failure occurs when t reaches $t_{max} = c_u$ where c_u is the undrained shear strength, which depends primarily on the voids ratio e .

The active and passive total horizontal stresses (σ_a and σ_p) are related to the vertical total stress σ_v by

$$\sigma_a = \sigma_v - 2c_u \quad \text{and} \quad \sigma_p = \sigma_v + 2c_u$$

6.4.6. Drained Strength of Soil: Coulomb Friction hypothesis

Drained behaviour is exhibited by sands in the short term and all soils in the long term.

Earth pressure coefficient: K , such that $\sigma_h' = K \sigma_v'$

Active pressure ($\sigma_v' > \sigma_h'$): $K_A = \frac{1 - \sin \phi'}{1 + \sin \phi'}$

Passive pressure ($\sigma_v' < \sigma_h'$): $K_P = \frac{1 + \sin \phi'}{1 - \sin \phi'}$

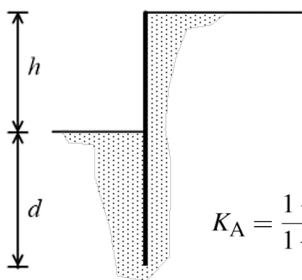
(Assuming principal stresses are vertical and horizontal.)

Angle of shearing resistance: ϕ'_{max} at peak strength, ϕ'_{crit} at large strain (critical state).

$$\phi'_{max} = \phi'_{crit} + \phi'_{dilatancy}$$

where ϕ'_{crit} is the ultimate angle of shearing resistance of a random aggregate deforming at constant volume, and $\phi'_{dilatancy} \rightarrow 0$ as $I_D \rightarrow 0$, or s' becomes large.

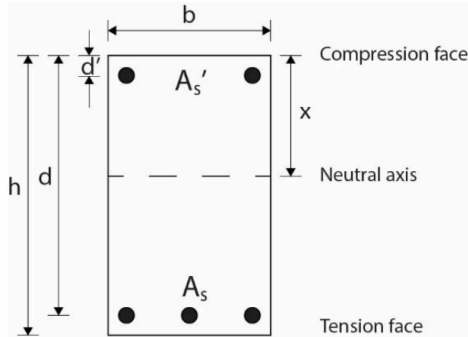
Typical properties for a quartz sand: $\phi'_{crit} = 33^\circ$, $\phi'_{max} = 53^\circ$ ($I_D = 1$, $s' < 150 \text{ kN m}^{-2}$)



Geotechnical engineering of deep excavations with a cantilevered pile wall support: if passive side mobilised friction is δ , then the static solutions are (Lancellotta, 2002)

$$K_A = \frac{1 - \sin \phi'}{1 + \sin \phi'} \quad K_P = \frac{\cos \delta}{1 - \sin \phi'} \left[\cos \delta + \sqrt{\sin^2 \phi' - \sin^2 \delta} \right] e^{2\Theta \tan \phi'} \quad 2\Theta = \sin^{-1} \left[\frac{\sin \delta}{\sin \phi'} \right] + \delta$$

6.4.7. Design Standards of Reinforced Concrete



Design compressive strength of concrete is based on the characteristic cylinder or cube strength f_{ck} [MPa]:

$$f_{cd} = \frac{2}{3} \alpha_{cc} f_{ck}$$

$\alpha_{cc} = 0.85$ for compression in flexure and axial loading and $\alpha_{cc} = 1.0$ for other phenomena.

Design tensile strength of steel is based on the characteristic tensile yield stress of steel f_{yk} :

$$f_{yd} = \frac{f_{yk}}{1.15}$$

At failure in bending, the stress in the concrete is $0.6 f_{cd}$ over the whole area of concrete in compression and the stress in the steel is f_{yd} .

Moment capacity of singly reinforced beam:

$$M = f_{yd} A_s \left(d - \frac{x}{2} \right) \quad x = \frac{5}{3} \frac{f_{yd}}{f_{cd}} \frac{A_s}{b} \quad (\leq 0.5d \text{ to avoid over-reinforcement})$$

Moment capacity of doubly reinforced beam (if compression reinforcement is yielding):

$$M = 0.6 f_{cd} b x \left(d - \frac{x}{2} \right) + A_s' f_{yd} (d - d')$$

Shear capacity of unreinforced webs:

$$V_{Rd,c} = \frac{0.18}{\gamma_c} \left(k (100 \rho_l f_{ck})^{1/3} \right) b_w d \geq 0.035 k^{3/2} f_{ck}^{1/2} b_w d$$

where $k = 1 + \sqrt{\frac{200}{d}} \leq 2$ (with d in mm), b_w : width of the web,

ρ_l : reinforcement ratio of the anchored steel with $\rho_l = \frac{A_s}{b_w d} \leq 0.02$.

If this resistance is insufficient to carry the applied load, internal stirrups are required, designed (assuming a 45 degrees truss angle) according to:

$$V_s = \frac{A_{sw} f_{yd} (0.9 d)}{1.15 s} \quad (A_{sw}: \text{area of stirrup legs, } s: \text{stirrup spacing})$$

$$V_{max} = \frac{1}{2} f_{c,max} (0.9 b d) \quad \text{where } f_{c,max} = 0.4 f_{ck} \left(1 - \frac{f_{ck}}{250} \right)$$

The shear resistance is controlled by the smaller of V_s or V_{max} .

6.4.8. Standard Bar Sizes and Reinforcement Areas

Available steel types:

Deformed high yield steel: $f_{yk} = 500 \text{ N mm}^{-2}$

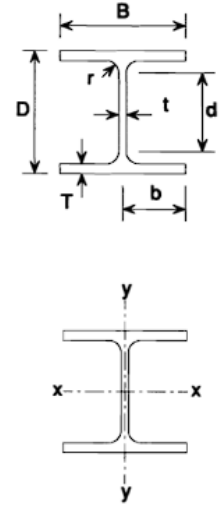
Plain mild steel: $f_{yk} = 250 \text{ N mm}^{-2}$

Reinforcement area (in mm^2) per metre width from bar diameter and bar spacing:

	Spacing of bars (mm)									
	75	100	125	150	175	200	225	250	275	300
Bar Dia. (mm)										
6	377	283	226	189	162	142	126	113	103	94.3
8	671	503	402	335	287	252	224	201	183	168
10	1050	785	628	523	449	393	349	314	285	262
12	1510	1130	905	754	646	566	503	452	411	377
16	2680	2010	1610	1340	1150	1010	894	804	731	670
20	4190	3140	2510	2090	1800	1570	1400	1260	1140	1050
25	6550	4910	3930	3270	2810	2450	2180	1960	1790	1640
32	10700	8040	6430	5360	4600	4020	3570	3220	2920	2680
40	16800	12600	10100	8380	7180	6280	5580	5030	4570	4190

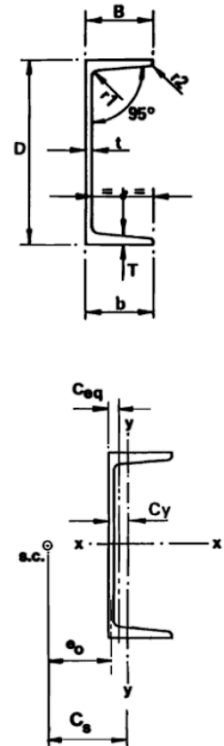
Universal Columns: designation $a \times b \times c$ where $a \approx$ depth [mm], $b \approx$ width [mm], $c \approx$ mass/length [kg/m]

Section Designation	Mass Per Metre kg/m	Depth Of Section D mm	Width Of Section B mm	Thickness		Second Moment Of Area		Radius Of Gyration		Elastic Modulus		Plastic Modulus		Torsional Constant J cm ⁴	Area Of Section A cm ²
				Web t mm	Flange T mm	Axis x-x cm ⁴	Axis y-y cm ⁴	Axis x-x cm	Axis y-y cm	Axis x-x cm ³	Axis y-y cm ³	Axis x-x cm ³	Axis y-y cm ³		
356x406x634	633.9	474.6	424.0	47.6	77.0	274800	98130	18.4	11.0	11580	4629	14240	7108	13720	808
356x406x551	551.0	455.6	418.5	42.1	67.5	226900	82670	18.0	10.9	9962	3951	12080	6058	9240	702
356x406x467	467.0	436.6	412.2	35.8	58.0	183000	67830	17.5	10.7	8383	3291	10000	5034	5809	595
356x406x393	393.0	419.0	407.0	30.6	49.2	146600	55370	17.1	10.5	6998	2721	8222	4154	3545	501
356x406x340	339.9	406.4	403.0	26.6	42.9	122500	46850	16.8	10.4	6031	2325	6999	3544	2343	433
356x406x287	287.1	393.6	399.0	22.6	36.5	99880	38680	16.5	10.3	5075	1939	5812	2949	1441	366
356x406x235	235.1	381.0	394.8	18.4	30.2	79080	30990	16.3	10.2	4151	1570	4687	2383	812	299
356x368x202	201.9	374.6	374.7	16.5	27.0	66260	23690	16.1	9.60	3538	1264	3972	1920	558	257
356x368x177	177.0	368.2	372.6	14.4	23.8	57120	20530	15.9	9.54	3103	1102	3455	1671	381	226
356x368x153	152.9	362.0	370.5	12.3	20.7	48590	17550	15.8	9.49	2684	948	2965	1435	251	195
356x368x129	129.0	355.6	368.6	10.4	17.5	40250	14610	15.6	9.43	2264	793	2479	1199	153	164
305x305x283	282.9	365.3	322.2	26.8	44.1	78870	24630	14.8	8.27	4318	1529	5105	2342	2034	360
305x305x240	240.0	352.5	318.4	23.0	37.7	64200	20310	14.5	8.15	3643	1276	4247	1951	1271	306
305x305x198	198.1	339.9	314.5	19.1	31.4	50900	16300	14.2	8.04	2995	1037	3440	1581	734	252
305x305x158	158.1	327.1	311.2	15.8	25.0	38750	12570	13.9	7.90	2369	808	2680	1230	378	201
305x305x137	136.9	320.5	309.2	13.8	21.7	32810	10700	13.7	7.83	2048	692	2297	1053	249	174
305x305x118	117.9	314.5	307.4	12.0	18.7	27670	9059	13.6	7.77	1760	589	1958	895	161	150
305x305x97	96.9	307.9	305.3	9.9	15.4	22250	7308	13.4	7.69	1445	479	1592	726	91.2	123
254x254x167	167.1	289.1	285.2	19.2	31.7	30000	9870	11.9	6.81	2075	744	2424	1137	626	213
254x254x132	132.0	276.3	281.3	15.3	25.3	22530	7531	11.6	6.69	1631	576	1869	878	319	168
254x254x107	107.1	266.7	258.8	12.8	20.5	17510	5928	11.3	6.59	1313	458	1484	697	172	136
254x254x89	88.9	260.3	256.3	10.3	17.3	14270	4857	11.2	6.55	1096	379	1224	575	102	113
254x254x73	73.1	254.1	254.6	8.6	14.2	11410	3908	11.1	6.48	898	307	992	465	57.6	93.1
203x203x86	86.1	222.2	209.1	12.7	20.5	9449	3127	9.28	5.34	850	299	977	456	137	110
203x203x71	71.0	215.8	206.4	10.0	17.3	7618	2537	9.18	5.30	706	246	799	374	80.2	90.4
203x203x60	60.0	209.6	205.8	9.4	14.2	6125	2065	8.96	5.20	584	201	656	305	47.2	76.4
203x203x52	52.0	206.2	204.3	7.9	12.5	5259	1778	8.91	5.18	510	174	567	264	31.8	66.3
203x203x46	46.1	203.2	203.6	7.2	11.0	4568	1548	8.82	5.13	450	152	497	231	22.2	58.7
152x152x37	37.0	161.8	154.4	8.0	11.5	2210	706	6.85	3.87	273	91.5	309	140	19.2	47.1
152x152x30	30.0	157.6	152.9	6.5	9.4	1748	560	6.76	3.83	222	73.3	248	112	10.5	38.3
152x152x23	23.0	152.4	152.2	5.8	6.8	1250	400	6.54	3.70	164	52.6	182	80.2	4.63	29.2



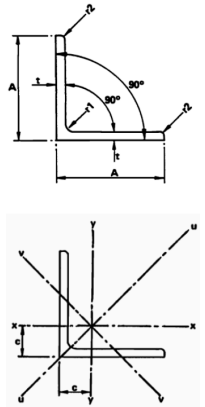
Channels:

Designation		Depth Of Section D mm	Width Of Section B mm	Thickness		Second Moment Of Area		Radius Of Gyration		Elastic Modulus		Plastic Modulus		Torsional Constant J cm ⁴	Area Of Section A cm ²
Nominal Size mm	Mass Per Metre kg			Web t mm	Flange T mm	Axis x-x cm ⁴	Axis y-y cm ⁴	Axis x-x cm	Axis y-y cm	Axis x-x cm ³	Axis y-y cm ³	Axis x-x cm ³	Axis y-y cm ³		
432x102	65.54	431.8	101.6	12.2	16.8	21370	627	16.0	2.74	990	79.9	1205	153	61.5	83.4
381x102	55.10	381.0	101.6	10.4	16.3	14870	579	14.6	2.87	781	75.7	931	144	46.4	70.1
305x102	46.18	304.8	101.6	10.2	14.8	8208	499	11.8	2.91	539	66.5	638	128	35.9	58.9
305x89	41.69	304.8	88.9	10.2	13.7	7078	326	11.5	2.47	464	48.6	559	92.9	28.1	53.3
254x89	35.74	254.0	88.9	9.1	13.6	4445	302	9.89	2.58	350	46.7	414	89.6	23.2	45.4
254x76	28.29	254.0	76.2	8.1	10.9	3355	162	9.67	2.12	264	28.1	316	53.9	12.3	35.9
229x89	32.76	228.6	88.9	8.6	13.3	3383	285	9.01	2.61	296	44.8	348	86.3	20.6	41.6
229x76	26.06	228.6	76.2	7.6	11.2	2615	159	8.87	2.19	229	28.3	271	54.5	11.6	33.2
203x89	29.78	203.2	88.9	8.1	12.9	2492	265	8.11	2.64	245	42.4	287	81.7	18.1	37.9
203x76	23.82	203.2	76.2	7.1	11.2	1955	152	8.02	2.24	192	27.7	226	53.5	10.6	30.4
178x89	26.81	177.8	88.9	7.6	12.3	1753	241	7.17	2.66	197	39.3	230	75.4	15.3	34.1
178x76	20.84	177.8	76.2	6.6	10.3	1338	134	7.10	2.25	151	24.8	176	48.1	8.26	26.6
152x89	23.84	152.4	88.9	7.1	11.6	1168	216	6.20	2.66	153	35.8	178	68.3	12.7	30.4
152x76	17.88	152.4	76.2	6.4	9.0	852	114	6.11	2.23	112	21.0	130	41.2	6.05	22.8
127x64	14.90	127.0	63.5	6.4	9.2	482	67.2	5.04	1.88	76.0	15.2	89.4	29.3	5.00	19.0
102x51	10.42	101.6	50.8	6.1	7.6	207	29.0	3.95	1.48	40.8	8.14	48.7	15.7	2.58	13.3
76x38	6.70	76.2	38.1	5.1	6.8	74.3	10.7	2.95	1.12	19.5	4.09	23.5	7.78	1.26	8.56



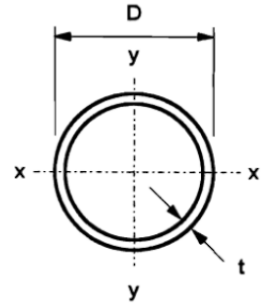
Equal Angles:

Designation		Mass Per Metre kg	Radius		Area Of Section cm ²	Distance Of Centre Of Gravity cx and cy cm	Second Moment Of Area			Radius Of Gyration			Elastic Modulus Axis x-x, y-y cm ³
Size A mm	Thickness t mm		Root r1 mm	Toe r2 mm			Axis x-x, y-y cm ⁴	Axis u-u cm ⁴	Axis v-v cm ⁴	Axis x-x, y-y cm	Axis u-u cm	Axis v-v cm	
250x250	35	128	20.0	4.8	164	7.51	9305	14720	3886	7.54	9.49	4.88	532
	32	118	20.0	4.8	151	7.40	8650	13710	3592	7.58	9.54	4.89	491
	28	104	20.0	4.8	133	7.25	7741	12290	3194	7.63	9.61	4.90	436
	25	93.6	20.0	4.8	120	7.14	7030	11170	2890	7.67	9.67	4.92	394
200x200	24	71.1	18.0	4.8	90.8	5.85	3356	5322	1391	6.08	7.65	3.91	237
	20	59.9	18.0	4.8	76.6	5.70	2877	4569	1185	6.13	7.72	3.93	201
	18	54.2	18.0	4.8	69.4	5.62	2627	4174	1080	6.15	7.76	3.95	183
	16	48.5	18.0	4.8	62.0	5.54	2369	3765	973	6.18	7.79	3.96	164
150x150	18	40.1	16.0	4.8	51.2	4.38	1060	1680	440	4.55	5.73	2.93	99.8
	15	33.8	16.0	4.8	43.2	4.26	909	1442	375	4.59	5.78	2.95	84.6
	12	27.3	16.0	4.8	35.0	4.14	748	1187	308	4.62	5.82	2.97	68.9
	10	23.0	16.0	4.8	29.5	4.06	635	1008	262	4.64	5.85	2.99	58.0
120x120	15	26.6	13.0	4.8	34.0	3.52	448	710	186	3.63	4.57	2.34	52.8
	12	21.6	13.0	4.8	27.6	3.41	371	589	153	3.66	4.62	2.35	43.1
	10	18.2	13.0	4.8	23.3	3.32	316	502	130	3.69	4.65	2.37	36.4
	8	14.7	13.0	4.8	18.8	3.24	259	411	107	3.71	4.67	2.38	29.5
100x100	15	21.9	12.0	4.8	28.0	3.02	250	395	105	2.99	3.76	1.94	35.8
	12	17.8	12.0	4.8	22.8	2.91	208	330	86.5	3.02	3.81	1.95	29.4
	10+	15.0	12.0	4.8	19.2	2.83	178	283	73.7	3.05	3.84	1.96	24.8
	8	12.2	12.0	4.8	15.6	2.75	146	232	60.5	3.07	3.86	1.97	20.2
90x90	12	15.9	11.0	4.8	20.3	2.66	149	235	62.0	2.70	3.40	1.75	23.5
	10	13.4	11.0	4.8	17.2	2.58	128	202	52.9	2.73	3.43	1.76	19.9
	8	10.9	11.0	4.8	13.9	2.50	105	167	43.4	2.75	3.46	1.77	16.2
	7♦	9.61	11.0	4.8	12.3	2.46	93.2	148	38.6	2.76	3.47	1.77	14.3
	6	8.30	11.0	4.8	10.6	2.41	81.0	128	33.6	2.76	3.48	1.78	12.3
80x80	10	11.9	10.0	4.8	15.1	2.34	87.6	139	36.4	2.41	3.03	1.55	15.5
	8	9.63	10.0	4.8	12.3	2.26	72.4	115	29.9	2.43	3.06	1.56	12.6
	6	7.34	10.0	4.8	9.36	2.17	56.0	88.7	23.2	2.45	3.08	1.57	9.60
70x70	10	10.3	9.0	2.4	13.1	2.10	58.0	91.6	24.4	2.10	2.64	1.36	11.8
	8	8.36	9.0	2.4	10.7	2.02	48.3	76.5	20.1	2.12	2.67	1.37	9.70
	6	6.38	9.0	2.4	8.19	1.94	37.7	59.8	15.6	2.15	2.70	1.38	7.45
60x60	10	8.69	8.0	2.4	11.1	1.85	35.3	55.6	15.0	1.78	2.24	1.16	8.51
	8	7.09	8.0	2.4	9.07	1.78	29.6	46.7	12.4	1.80	2.27	1.17	7.00
	6	5.42	8.0	2.4	6.95	1.70	23.2	36.8	9.64	1.83	2.30	1.18	5.39
	5	4.57	8.0	2.4	5.86	1.65	19.8	31.4	8.23	1.84	2.31	1.18	4.56
50x50	8	5.82	7.0	2.4	7.44	1.53	16.5	25.9	6.96	1.49	1.87	0.968	4.74
	6	4.47	7.0	2.4	5.72	1.45	13.0	20.6	5.43	1.51	1.90	0.974	3.67
	5	3.77	7.0	2.4	4.83	1.41	11.1	17.7	4.63	1.52	1.91	0.979	3.11
	4	3.06	7.0	2.4	3.92	1.37	9.16	14.5	3.82	1.53	1.92	0.987	2.52
	3	2.33	7.0	2.4	2.99	1.32	7.06	11.1	2.97	1.54	1.93	0.996	1.92
45x45	6	4.00	7.0	2.4	5.12	1.33	9.30	14.7	3.90	1.35	1.69	0.872	2.93
	5	3.38	7.0	2.4	4.33	1.29	7.99	12.6	3.33	1.36	1.71	0.877	2.49
	4	2.74	7.0	2.4	3.52	1.24	6.58	10.4	2.75	1.37	1.72	0.883	2.02
	3	2.09	7.0	2.4	2.69	1.20	5.08	8.03	2.14	1.37	1.73	0.892	1.54
40x40	6	3.52	6.0	2.4	4.49	1.20	6.37	10.1	2.68	1.19	1.50	0.773	2.28
	5	2.97	6.0	2.4	3.80	1.17	5.48	8.68	2.29	1.20	1.51	0.776	1.93
	4	2.42	6.0	2.4	3.09	1.12	4.53	7.18	1.89	1.21	1.52	0.781	1.58
	3	1.84	6.0	2.4	2.36	1.08	3.51	5.55	1.47	1.22	1.53	0.788	1.20
30x30	5	2.18	5.0	2.4	2.78	0.919	2.17	3.42	0.919	0.883	1.11	0.575	1.04
	4	1.78	5.0	2.4	2.27	0.879	1.81	2.86	0.756	0.893	1.12	0.577	0.852
	3	1.36	5.0	2.4	1.74	0.836	1.41	2.23	0.588	0.900	1.13	0.581	0.652
25x25	5	1.77	3.5	2.4	2.25	0.796	1.19	1.87	0.515	0.728	0.912	0.478	0.701
	4	1.45	3.5	2.4	1.84	0.758	1.00	1.58	0.421	0.737	0.926	0.478	0.574
	3	1.11	3.5	2.4	1.41	0.718	0.784	1.24	0.325	0.745	0.939	0.480	0.440



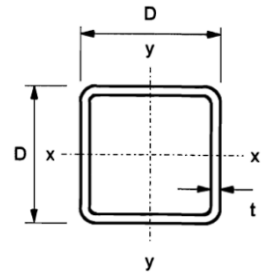
Circular Hollow Sections:

Designation		Mass per Metre kg	Area of Section A cm ²	Ratio for Local Buckling D / t	Second Moment of Area I cm ⁴	Radius of Gyration r cm	Elastic Modulus Z cm ³	Plastic Modulus S cm ³	Torsional Constants		Surface Area per Metre m ²
Outside Diameter D mm	Thickness t mm								J cm ⁴	C cm ³	
21.3	3.2Δ	1.43	1.82	6.66	0.768	0.650	0.722	1.06	1.54	1.44	0.0669
26.9	3.2Δ	1.87	2.38	8.41	1.70	0.846	1.27	1.81	3.41	2.53	0.0845
33.7	2.6Δ	1.99	2.54	13.0	3.09	1.10	1.84	2.52	6.19	3.67	0.106
	3.2Δ	2.41	3.07	10.5	3.60	1.08	2.14	2.99	7.21	4.28	0.106
	4.0Δ	2.93	3.73	8.43	4.19	1.06	2.49	3.55	8.38	4.97	0.106
42.4	2.6Δ	2.55	3.25	16.3	6.46	1.41	3.05	4.12	12.9	6.10	0.133
	3.2Δ	3.09	3.94	13.3	7.62	1.39	3.59	4.93	15.2	7.19	0.133
	4.0Δ	3.79	4.83	10.6	8.99	1.36	4.24	5.92	18.0	8.48	0.133
48.3	3.2	3.56	4.53	15.1	11.6	1.60	4.80	6.52	23.2	9.59	0.152
	4.0	4.37	5.57	12.1	13.8	1.57	5.70	7.87	27.5	11.4	0.152
	5.0	5.34	6.80	9.66	16.2	1.54	6.69	9.42	32.3	13.4	0.152
60.3	3.2	4.51	5.74	18.8	23.5	2.02	7.78	10.4	46.9	15.6	0.189
	4.0	5.55	7.07	15.1	28.2	2.00	9.34	12.7	56.3	18.7	0.189
	5.0	6.82	8.69	12.1	33.5	1.96	11.1	15.3	67.0	22.2	0.189
76.1	3.2	5.75	7.33	23.8	48.8	2.58	12.8	17.0	97.6	25.6	0.239
	4.0	7.11	9.06	19.0	59.1	2.55	15.5	20.8	118	31.0	0.239
	5.0	8.77	11.2	15.2	70.9	2.52	18.6	25.3	142	37.3	0.239
88.9	3.2	6.76	8.62	27.8	79.2	3.03	17.8	23.5	158	35.6	0.279
	4.0	8.38	10.7	22.2	96.3	3.00	21.7	28.9	193	43.3	0.279
	5.0	10.3	13.2	17.8	116	2.97	26.2	35.2	233	52.4	0.279
114.3	3.6	9.83	12.5	31.8	192	3.92	33.6	44.1	384	67.2	0.359
	5.0	13.5	17.2	22.9	257	3.87	45.0	59.8	514	89.9	0.359
	6.3	16.8	21.4	18.1	313	3.82	54.7	73.6	625	109	0.359
139.7	5.0	16.6	21.2	27.9	481	4.77	68.8	90.8	961	138	0.439
	6.3	20.7	26.4	22.2	589	4.72	84.3	112	1177	169	0.439
	8.0	26.0	33.1	17.5	720	4.66	103	139	1441	206	0.439
	10.0	32.0	40.7	14.0	862	4.60	123	169	1724	247	0.439
168.3	5.0	20.1	25.7	33.7	856	5.78	102	133	1712	203	0.529
	6.3	25.2	32.1	26.7	1053	5.73	125	165	2107	250	0.529
	8.0	31.6	40.3	21.0	1297	5.67	154	206	2595	308	0.529
	10.0	39.0	49.7	16.8	1564	5.61	186	251	3128	372	0.529
	12.5	48.0	61.2	13.5	1868	5.53	222	304	3737	444	0.529
193.7	5.0	23.3	29.6	38.7	1320	6.67	136	178	2640	273	0.609
	6.3	29.1	37.1	30.7	1630	6.63	168	221	3260	337	0.609
	8.0	36.6	46.7	24.2	2016	6.57	208	276	4031	416	0.609
	10.0	45.3	57.7	19.4	2442	6.50	252	338	4883	504	0.609
	12.5	55.9	71.2	15.5	2934	6.42	303	411	5869	606	0.609
	16.0♦	70.1	89.3	12.1	3554	6.31	367	507	7109	734	0.609



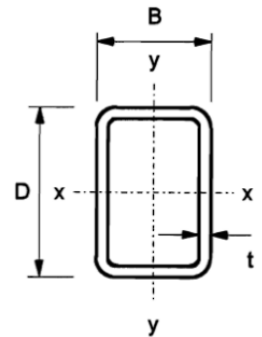
Square Hollow Sections:

Designation		Mass per Metre kg	Area of Section A cm ²	Ratio for Local Buckling d / t ⁽¹⁾	Second Moment of Area I cm ⁴	Radius of Gyration r cm	Elastic Modulus Z cm ³	Plastic Modulus S cm ³	Torsional Constants		Surface Area per Metre m ²
Size D D mm	Thickness t mm								J cm ⁴	C cm ³	
40x40	2.5	2.89	3.68	13.0	8.54	1.52	4.27	5.14	13.6	6.22	0.154
	3.0	3.41	4.34	10.3	9.78	1.50	4.89	5.97	15.7	7.10	0.152
	3.2	3.61	4.60	9.50	10.2	1.49	5.11	6.28	16.5	7.42	0.152
	4.0	4.39	5.59	7.00	11.8	1.45	5.91	7.44	19.5	8.54	0.150
	5.0	5.28	6.73	5.00	13.4	1.41	6.68	8.66	22.5	9.60	0.147
50x50	2.5	3.68	4.68	17.0	17.5	1.93	6.99	8.29	27.5	10.2	0.194
	3.0	4.35	5.54	13.7	20.2	1.91	8.08	9.70	32.1	11.8	0.192
	3.2	4.62	5.88	12.6	21.2	1.90	8.49	10.2	33.8	12.4	0.192
	4.0	5.64	7.19	9.50	25.0	1.86	9.99	12.3	40.4	14.5	0.190
	5.0	6.85	8.73	7.00	28.9	1.82	11.6	14.5	47.6	16.7	0.187
6.3	8.31	10.6	4.94	32.8	1.76	13.1	17.0	55.2	18.8	0.184	
60x60	3.0	5.29	6.74	17.0	36.2	2.32	12.1	14.3	56.9	17.7	0.232
	3.2	5.62	7.16	15.8	38.2	2.31	12.7	15.2	60.2	18.6	0.232
	4.0	6.90	8.79	12.0	45.4	2.27	15.1	18.3	72.5	22.0	0.230
	5.0	8.42	10.7	9.00	53.3	2.23	17.8	21.9	86.4	25.7	0.227
	6.3	10.3	13.1	6.52	61.6	2.17	20.5	26.0	102	29.6	0.224
8.0	12.5	16.0	4.50	69.7	2.09	23.2	30.4	118	33.4	0.219	
70x70	3.0	6.24	7.94	20.3	59.0	2.73	16.9	19.9	92.2	24.8	0.272
	3.6	7.40	9.42	16.4	68.6	2.70	19.6	23.3	108	28.7	0.271
	5.0	9.99	12.7	11.0	88.5	2.64	25.3	30.8	142	36.8	0.267
	6.3	12.3	15.6	8.11	104	2.58	29.7	36.9	169	42.9	0.264
	8.0	15.0	19.2	5.75	120	2.50	34.2	43.8	200	49.2	0.259
80x80	3.0	7.18	9.14	23.7	89.8	3.13	22.5	26.3	140	33.0	0.312
	3.6	8.53	10.9	19.2	105	3.11	26.2	31.0	164	38.5	0.311
	5.0	11.6	14.7	13.0	137	3.05	34.2	41.1	217	49.8	0.307
	6.3	14.2	18.1	9.70	162	2.99	40.5	49.7	262	58.7	0.304
	8.0	17.5	22.4	7.00	189	2.91	47.3	59.5	312	68.3	0.299
90x90	3.6	9.66	12.3	22.0	152	3.52	33.8	39.7	237	49.7	0.351
	5.0	13.1	16.7	15.0	200	3.45	44.4	53.0	316	64.8	0.347
	6.3	16.2	20.7	11.3	238	3.40	53.0	64.3	382	77.0	0.344
	8.0	20.1	25.6	8.25	281	3.32	62.6	77.6	459	90.5	0.339
100x100	4.0	11.9	15.2	22.0	232	3.91	46.4	54.4	361	68.2	0.390
	5.0	14.7	18.7	17.0	279	3.86	55.9	66.4	439	81.8	0.387
	6.3	18.2	23.2	12.9	336	3.80	67.1	80.9	534	97.8	0.384
	8.0	22.6	28.8	9.50	400	3.73	79.9	98.2	646	116	0.379
	10.0	27.4	34.9	7.00	462	3.64	92.4	116	761	133	0.374
120x120	4.0	14.4	18.4	27.0	410	4.72	68.4	79.7	635	101	0.470
	5.0	17.8	22.7	21.0	498	4.68	83.0	97.6	777	122	0.467
	6.3	22.2	28.2	16.0	603	4.62	100	120	950	147	0.464
	8.0	27.6	35.2	12.0	726	4.55	121	146	1160	176	0.459
	10.0	33.7	42.9	9.00	852	4.46	142	175	1382	206	0.454
	12.5	40.9	52.1	6.60	982	4.34	164	207	1623	236	0.448



Rectangular Hollow Sections:

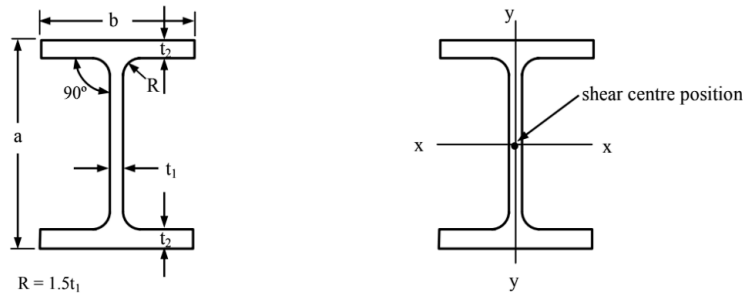
Designation		Mass per Metre	Area of Section	Ratios for Local Buckling		Second Moment of Area		Radius of Gyration		Elastic Modulus		Plastic Modulus		Torsional Constants		Surface Area per Metre	
Size	Thickness			(1)	(1)	Axis x-x	Axis y-y	Axis x-x	Axis y-y	Axis x-x	Axis y-y	Axis x-x	Axis y-y	J	C		
D mm	B mm	t mm	A cm ²	d/t	b/t	cm ⁴	cm ⁴	cm	cm	cm ³	cm ³	cm ³	cm ³	cm ⁴	cm ³	m ²	
50x30		2.5	3.68	17.0	9.00	11.8	5.22	1.79	1.19	4.73	3.48	5.92	4.11	11.7	5.73	0.154	
		3.0	3.41	4.34	13.7	7.00	13.6	5.94	1.77	1.17	5.43	3.96	6.88	4.76	13.5	6.51	0.152
		3.2	3.61	4.60	12.6	6.38	14.2	6.20	1.76	1.16	5.68	4.13	7.25	5.00	14.2	6.80	0.152
		4.0	4.39	5.59	9.50	4.50	16.5	7.08	1.72	1.13	6.60	4.72	8.59	5.88	16.6	7.77	0.150
		5.0	5.28	6.73	7.00	3.00	18.7	7.89	1.67	1.08	7.49	5.26	10.0	6.80	19.0	8.67	0.147
60x40		2.5	3.68	4.68	21.0	13.0	22.8	12.1	2.21	1.60	7.61	6.03	9.32	7.02	25.1	9.73	0.194
		3.0	4.35	5.54	17.0	10.3	26.5	13.9	2.18	1.58	8.82	6.95	10.9	8.19	29.2	11.2	0.192
		3.2	4.62	5.88	15.8	9.50	27.8	14.6	2.18	1.57	9.27	7.29	11.5	8.64	30.8	11.7	0.192
		4.0	5.64	7.19	12.0	7.00	32.8	17.0	2.14	1.54	10.9	8.52	13.8	10.3	36.7	13.7	0.190
		5.0	6.85	8.73	9.00	5.00	38.1	19.5	2.09	1.50	12.7	9.77	16.4	12.2	43.0	15.7	0.187
6.3	8.31	10.6	6.52	3.35	43.4	21.9	2.02	1.44	14.5	11.0	19.2	14.2	49.5	17.6	0.184		
80x40		3.0	5.29	6.74	23.7	10.3	54.2	18.0	2.84	1.63	13.6	9.00	17.1	10.4	43.8	15.3	0.232
		3.2	5.62	7.16	22.0	9.50	57.2	18.9	2.83	1.63	14.3	9.46	18.0	11.0	46.2	16.1	0.232
		4.0	6.90	8.79	17.0	7.00	68.2	22.2	2.79	1.59	17.1	11.1	21.8	13.2	55.2	18.9	0.230
		5.0	8.42	10.7	13.0	5.00	80.3	25.7	2.74	1.55	20.1	12.9	26.1	15.7	65.1	21.9	0.227
		6.3	10.3	13.1	9.70	3.35	93.3	29.2	2.67	1.49	23.3	14.6	31.1	18.4	75.6	24.8	0.224
8.0	12.5	16.0	7.00	2.00	106	32.1	2.58	1.42	26.5	16.1	36.5	21.2	85.8	27.4	0.219		
90x50		3.0	6.24	7.94	27.0	13.7	84.4	33.5	3.26	2.05	18.8	13.4	23.2	15.3	76.5	22.4	0.272
		3.6	7.40	9.42	22.0	10.9	98.3	38.7	3.23	2.03	21.8	15.5	27.2	18.0	89.4	25.9	0.271
		5.0	9.99	12.7	15.0	7.00	127	49.2	3.16	1.97	28.3	19.7	36.0	23.5	116	32.9	0.267
		6.3	12.3	15.6	11.3	4.94	150	57.0	3.10	1.91	33.3	22.8	43.2	28.0	138	38.1	0.264
		8.0	15.0	19.2	8.25	3.25	174	64.6	3.01	1.84	38.6	25.8	51.4	32.9	160	43.2	0.259
100x50		3.0	6.71	8.54	30.3	13.7	110	36.8	3.58	2.08	21.9	14.7	27.3	16.8	88.4	25.0	0.292
		3.2	7.13	9.08	28.3	12.6	116	38.8	3.57	2.07	23.2	15.5	28.9	17.7	93.4	26.4	0.292
		4.0	8.78	11.2	22.0	9.50	140	46.2	3.53	2.03	27.9	18.5	35.2	21.5	113	31.4	0.290
		5.0	10.8	13.7	17.0	7.00	167	54.3	3.48	1.99	33.3	21.7	42.6	25.8	135	36.9	0.287
		6.3	13.3	16.9	12.9	4.94	197	63.0	3.42	1.93	39.4	25.2	51.3	30.8	160	42.9	0.284
8.0	16.3	20.8	9.50	3.25	230	71.7	3.33	1.86	46.0	28.7	61.4	36.3	186	48.9	0.279		
100x60		3.0	7.18	9.14	30.3	17.0	124	55.7	3.68	2.47	24.7	18.6	30.2	21.2	121	30.7	0.312
		3.6	8.53	10.9	24.8	13.7	145	64.8	3.65	2.44	28.9	21.6	35.6	24.9	142	35.6	0.311
		5.0	11.6	14.7	17.0	9.00	189	83.6	3.58	2.38	37.8	27.9	47.4	32.9	188	45.9	0.307
		6.3	14.2	18.1	12.9	6.52	225	98.1	3.52	2.33	45.0	32.7	57.3	39.5	224	53.8	0.304
		8.0	17.5	22.4	9.50	4.50	264	113	3.44	2.25	52.8	37.8	68.7	47.1	265	62.2	0.299
120x60		3.6	9.66	12.3	30.3	13.7	227	76.3	4.30	2.49	37.9	25.4	47.2	28.9	183	43.3	0.351
		5.0	13.1	16.7	21.0	9.00	299	98.8	4.23	2.43	49.9	32.9	63.1	38.4	242	56.0	0.347
		6.3	16.2	20.7	16.0	6.52	358	116	4.16	2.37	59.7	38.8	76.7	46.3	290	65.9	0.344
		8.0	20.1	25.6	12.0	4.50	425	135	4.08	2.30	70.8	45.0	92.7	55.4	344	76.6	0.339
120x80		5.0	14.7	18.7	21.0	13.0	365	193	4.42	3.21	60.9	48.2	74.6	56.1	401	77.9	0.387
		6.3	18.2	23.2	16.0	9.70	440	230	4.36	3.15	73.3	57.6	91.0	68.2	487	92.9	0.384
		8.0	22.6	28.8	12.0	7.00	525	273	4.27	3.08	87.5	68.1	111	82.6	587	110	0.379
		10.0	27.4	34.9	9.00	5.00	609	313	4.18	2.99	102	78.1	131	97.3	688	126	0.374
150x100		4.0	15.1	19.2	34.5	22.0	607	324	5.63	4.11	81.0	64.8	97.4	73.6	660	105	0.490
		5.0	18.6	23.7	27.0	17.0	739	392	5.58	4.07	98.5	78.5	119	90.1	807	127	0.487
		6.3	23.1	29.5	20.8	12.9	898	474	5.52	4.01	120	94.8	147	110	986	153	0.484
		8.0	28.9	36.8	15.8	9.50	1087	569	5.44	3.94	145	114	180	135	1203	183	0.479
		10.0	35.3	44.9	12.0	7.00	1282	665	5.34	3.85	171	133	216	161	1432	214	0.474
12.5	42.8	54.6	9.00	5.00	1488	763	5.22	3.74	198	153	256	190	1679	246	0.468		



6.4.10. Properties of Aluminium Sections (Extrusions)

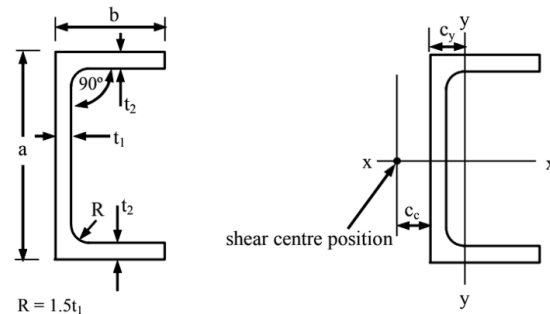
When designing with aluminium there is limited use of standard sections since the extrusion process is very versatile and it is possible to achieve a wide variety of section shapes. Standard profiles are covered by British Standard BS1161.

I-Beams:



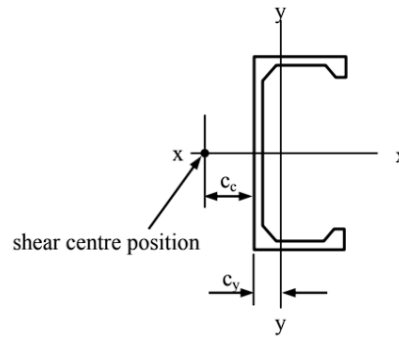
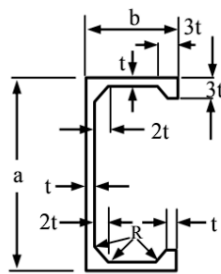
Size (mm)	Thickness (mm)		Mass/unit length (kg/m)	Area of section (mm ² × 10 ²)	Centroid (mm)		Second moments of area (mm ⁴ × 10 ⁴)		Radii of gyration (mm)		Moduli of section (mm ³ × 10 ³)		Torsion constant (mm ⁴ × 10 ⁴)
	web t ₁	flange t ₂			W	A	c _x and c _y	I _x	I _y	r _x	r _y	Z _x	
60 × 30	4	6	1.59	5.83	0	31.6	2.76	23.3	6.89	10.5	1.84	0.753	
80 × 40	5	7	2.54	9.38	0	91.6	7.63	31.2	9.02	22.9	3.82	1.69	
100 × 50	6	8	3.72	13.7	0	210	17.0	39.2	11.1	42.1	6.80	3.30	
120 × 60	6	9	4.77	17.6	0	403	32.8	47.8	13.6	67.2	10.9	4.76	
140 × 70	7	10	6.33	23.4	0	725	57.9	55.7	15.7	104	16.5	8.00	
160 × 80	7	11	7.64	28.2	0	1170	94.6	64.5	18.3	147	23.7	10.8	

Channel Sections:



Size (mm)	Thickness (mm)		Mass/unit length (kg/m)	Area of section (mm ² × 10 ²)	Centroid (mm)		Second moments of area (mm ⁴ × 10 ⁴)		Radii of gyration (mm)		Moduli of section (mm ³ × 10 ³)		Torsion constant (mm ⁴ × 10 ⁴)	Shear centre from back of section (mm)
	web t ₁	flange t ₂			W	A	c _x	c _y	I _x	I _y	r _x	r _y		
60 × 30	5	6	1.69	6.24	0	9.87	32.2	5.03	22.7	8.98	10.7	2.50	0.690	11.7
80 × 35	5	7	2.29	8.44	0	11.3	79.8	9.57	30.8	10.6	20.0	4.04	1.12	13.8
100 × 40	6	8	3.20	11.8	0	12.4	171	16.9	38.1	11.9	34.2	6.12	2.07	15.2
120 × 50	6	9	4.19	15.5	0	15.9	339	36.8	46.8	15.4	56.5	10.8	3.22	19.7
140 × 60	7	10	5.66	20.9	0	18.9	625	71.5	54.7	18.5	89.2	17.4	5.51	23.6
160 × 70	7	10	6.58	24.3	0	21.8	970	116	63.2	21.8	121	24.0	6.41	27.6
180 × 75	8	11	8.06	29.8	0	22.7	1480	159	70.5	23.1	164	30.5	9.63	29.0
200 × 80	8	12	9.19	33.9	0	24.5	2110	210	78.8	24.9	211	37.8	12.4	31.3
240 × 100	9	13	12.5	46.0	0	30.3	4170	450	95.2	31.2	345	64.6	20.2	39.2

Lipped Channel Sections:

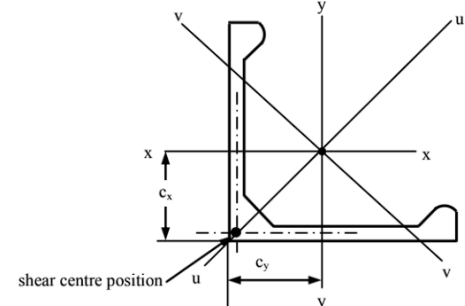
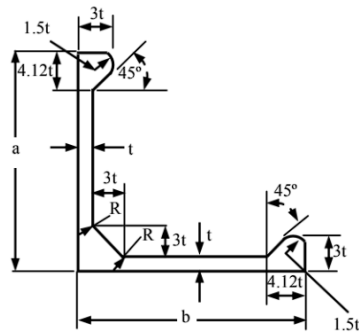


$*A = 74.00t^2$
 $R = 2t$
 $a = 32t$
 $b = 16t$
 $c_x = 0$
 $c_y = 5.36t$
 $c_c = 6.91t$
 $I_x = 12371t^4$
 $I_y = 2407t^4$
 $r_x = 12.93t$
 $r_y = 5.70t$
 $Z_{x-x} = 773t^3$
 $Z_{y-y} = 226t^3$
 $J = 41.29t^4$

*Excludes small areas present at internal radii ($4 \times \dots^2$)

Size (mm)	Thickness (mm)	Mass/unit length (kg/m)	Area of section ($\text{mm}^2 \times 10^2$)	Centroid (mm)		Second moments of area ($\text{mm}^4 \times 10^4$)		Radii of gyration (mm)		Moduli of section ($\text{mm}^3 \times 10^3$)		Torsion constant ($\text{mm}^4 \times 10^3$)	Shear centre from back of section (mm)
				c_x	c_y	I_x	I_y	r_x	r_y	Z_x	Z_y		
$a \times b$	t	W	A	c_x	c_y	I_x	I_y	r_x	r_y	Z_x	Z_y	J	c_c
80 × 40	2.5	1.25	4.62	0	13.4	48.3	9.40	32.3	14.2	12.1	3.53	1.61	17.3
100 × 50	3.13	1.96	7.23	0	16.8	118	23.0	40.4	17.8	23.6	6.90	3.94	21.6
120 × 60	3.75	2.82	10.4	0	20.1	245	47.6	48.5	21.4	40.8	11.9	8.16	25.9
140 × 70	4.38	3.84	14.2	0	23.5	453	88.2	56.6	24.9	64.8	18.9	15.1	30.2

Equal Bulb Angle Sections:



u-u and v-v are principal axes

$*A = 54.92t^2$
 $R = 2t$
 $a = b = 20t$
 *Excludes small areas present at internal radii ($4 \times 0.086t^2$)

$c_x = 6.07t$
 $c_y = 6.07t$
 $I_x = 2605t^4$
 $I_y = 2605t^4$
 $I_u = 4030t^4$
 $I_v = 1180t^4$

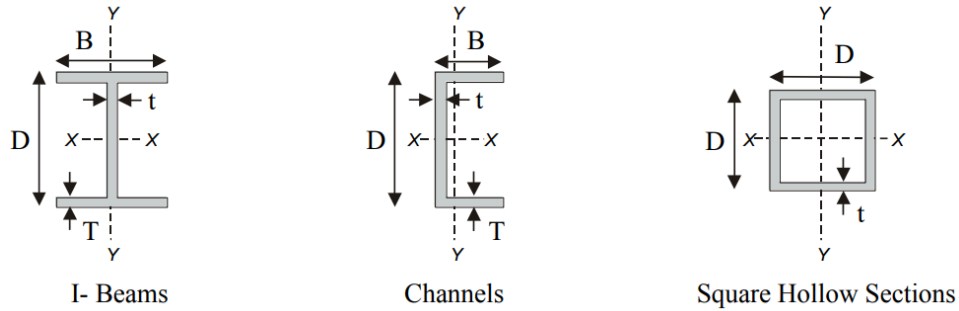
$r_x = 6.89t$
 $r_y = 6.89t$
 $r_u = 8.57t$
 $r_v = 4.64t$
 $Z_x = 187t^3$
 $Z_y = 187t^3$

$Z_u = 285t^3$
 $Z_v = 138t^3$
 $\alpha = 45^\circ$
 $\tan \alpha = 1$
 $J = 51.32t^4$

Size (mm)	Thickness (mm)	Mass/unit length (kg/m)	Area of section ($\text{mm}^2 \times 10^2$)	Centroid (mm)	Second moments of area ($\text{mm}^4 \times 10^4$)			Radii of gyration (mm)			Moduli of section ($\text{mm}^3 \times 10^3$)			Torsion constant ($\text{mm}^4 \times 10^4$)
					c_x and c_y	I_x and I_y	I_u	I_v	r_x and r_y	r_u	r_v	Z_x and Z_y	Z_u	
$a \times b$	t	W	A	c_x and c_y	I_x and I_y	I_u	I_v	r_x and r_y	r_u	r_v	Z_x and Z_y	Z_u	Z_v	J
50 × 50	2.5	0.930	3.43	15.2	10.2	15.7	4.61	17.2	21.4	11.6	2.92	4.45	2.16	0.200
60 × 60	3	1.34	4.94	18.2	21.1	32.6	9.56	20.7	25.7	13.9	5.05	7.70	3.73	0.416
80 × 80	4	2.38	8.79	24.3	66.7	103	30.2	27.6	34.3	18.6	12.0	18.2	8.82	1.31
100 × 100	5	3.72	13.7	30.3	163	252	73.8	34.4	42.8	23.2	23.4	35.6	17.2	3.21
120 × 120	6	5.36	19.8	36.4	338	522	153	41.3	51.4	27.8	40.4	61.6	29.8	6.65

6.4.11. Properties of Glass Fibre Reinforced Plastic (GFRP) Sections (Pultrusions)

A wide variety of shapes is also possible with the pultrusion process and each GFRP manufacturer will produce a different standard product range. Typical examples:



I-beams:

Section Designation	Depth D (mm)	Width B (mm)	Web t (mm)	Flange T (mm)	I_{xx} (cm ⁴)	I_{yy} (cm ⁴)	Area A (cm ²)
53 × 50	53	50	7	7	40.8	14.7	9.73
102 × 51	102	51	6.35	6.35	186	14.2	12.1
150 × 150	150	150	10	10	1660	564	43.0
200 × 200	200	200	10	10	4100	1330	58.0

Channels:

Section Designation	Depth D (mm)	Width B (mm)	Web t (mm)	Flange T (mm)	I_{xx} (cm ⁴)	I_{yy} (cm ⁴)	Area A (cm ²)
50.8 × 25.4	50.8	25.4	3.2	3.2	11.6	1.82	3.05
73 × 25	73	25	5.0	5.0	39.4	2.76	5.65
100 × 40	100	40	5.0	5.0	121	11.9	8.50
200 × 50	200	50	10	10	1390	48.0	28.0
200 × 60	200	60	8.0	8.0	1300	68.9	24.3
500 × 60	500	60	7.0	7.0	11800	73.9	42.4

Square Hollow Sections:

Designation		Area A (cm ²)	$I_{xx} = I_{yy}$ (cm ⁴)
Size D D (mm)	Thickness t (mm)		
31.8 × 31.8	3.0	3.46	4.83
44.0 × 44.0	6.0	9.12	22.5
51.0 × 51.0	3.2	6.12	23.4
100 × 100	4.0	15.3	236

6.4.12. Building Codes for Structural Design

Building codes are sets of practical experimentally-determined guidelines for safe and reliable structural design. Their adoption and legislature varies by region and sector.

Eurocodes: collection of ten standards (EN 1990 - EN 1999). Used in the EU and UK.

- | | |
|---|--------------------------------|
| 0. Basis of structural design | 5. Timber structures |
| 1. Actions on structures (loading conditions) | 6. Masonry structures |
| 2. Concrete structures | 7. Geotechnical design |
| 3. Steel structures | 8. Earthquake resistant design |
| 4. Composite steel-concrete structures | 9. Aluminium structures |

Other sources of design information, often extending beyond structural design, include:

- ISO: wide range of standards e.g. production, performance, management; used worldwide
- ASME: standards for mechanical devices requiring structural integrity; used in USA

6.5. Fracture Mechanics and Failure Analysis

6.5.1. Dislocations, Plastic Flow and Hardness

Dislocations are line defects in crystalline solids which can glide along the lattice and are important for many plasticity and failure mechanisms in materials.

- Burger's vector, \mathbf{b} : additional lattice spacing created around a dislocation core
- Force on dislocation due to applied shear stress: $F = \tau b$
(F : force per unit length of dislocation, τ : remote shear stress, $b = |\mathbf{b}|$)
- Line tension in dislocation: $T \approx \frac{1}{2}Gb^2$ (G : shear modulus)
- Shear stress for dislocation movement on a single slip plane: $\tau_y = \frac{cT}{bL}$
(L : inter-obstacle distance, c : constant. For strong obstacles, $c \approx 2$, and for weaker obstacles, $c < 2$.)
- Shear yield stress of a polycrystalline solid: $k \approx \frac{3}{2}\tau_y$
- Uniaxial yield stress of a polycrystalline solid: $\sigma_y \approx 2k$.
- Hardness: $H \approx 3\sigma_y$, expressed in MPa.
- Vickers Hardness: $HV = H/g$, expressed in kgf mm^{-2} (g : acceleration due to gravity).

For a microscopic analysis of dislocations and their stress fields, see Section 13.2.4.

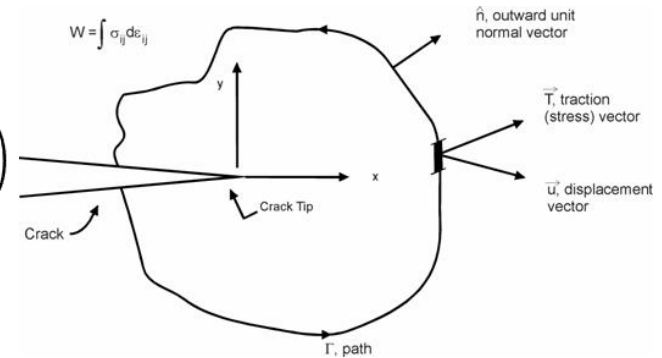
6.5.2. Fast Fracture

Material defects cause stress concentrations, forming plastic zones and contributing to crack growth, which can lead to fast fracture if a critical size is reached under stress.

- Stress intensity factor: $K = Y\sigma\sqrt{\pi a}$. Fast fracture occurs for $K \geq K_{IC}$, a material property. (Y : dimensionless constant dependent on geometry - typically $Y \approx 1$, σ : remote tensile stress, $2a$: total closed crack length)

- J -integral for strain energy release rate:

$$J = G = -\frac{\partial U}{\partial A} = \oint_{\Gamma} \left(W dy - \mathbf{T} \cdot \frac{\partial \mathbf{u}}{\partial x} ds \right)$$



- Strain energy release rate and compliance:

$$G = \frac{P^2}{2} \frac{dC}{da}$$

	Plane stress	Plane strain
Stress-energy relations	$K_I = \sqrt{EG_I}$, $K_{II} = \sqrt{EG_{II}}$ $K_{III} = \sqrt{2\mu G_{III}}$	$K_I = \sqrt{\frac{EG_I}{1-\nu^2}}$, $K_{II} = \sqrt{\frac{EG_{II}}{1-\nu^2}}$ $K_{III} = \sqrt{\frac{2\mu G_{III}}{1-\nu^2}}$
Crack tip plastic zone size (mode I)	$d_p = \frac{1}{\pi} \left(\frac{K_I}{\sigma_y} \right)^2$	$d_p = \frac{1}{3\pi} \left(\frac{K_I}{\sigma_y} \right)^2$
Crack opening displacement	$\delta = \frac{K_I^2}{\sigma_y E}$	$\delta = \frac{K_I^2}{2\sigma_y E}$

(σ_y : remote yield stress, K_{IC} : plane strain fracture toughness, G_{IC} : critical strain energy release rate, E : Young's modulus, ν : Poisson's ratio, $C = E^{-1}$: compliance, P : applied force)

K_{IC} and G_{IC} are only valid when conditions for linear elastic fracture mechanics apply. Typically the crack length and specimen dimensions must be at least 50 times the process zone size.

Micromechanisms of fracture

- Metals: plastic zone formation at crack tips → void nucleation → void linkage
- Ceramics: fast fracture of 'worst' flaw (tension); mode II shear failure (compression)
- Polymers: crazing (opening of cracks bridged by fibres), shear yielding, cold drawing
- Composites: fibres pulled out from sockets in matrix, impeding crack advance

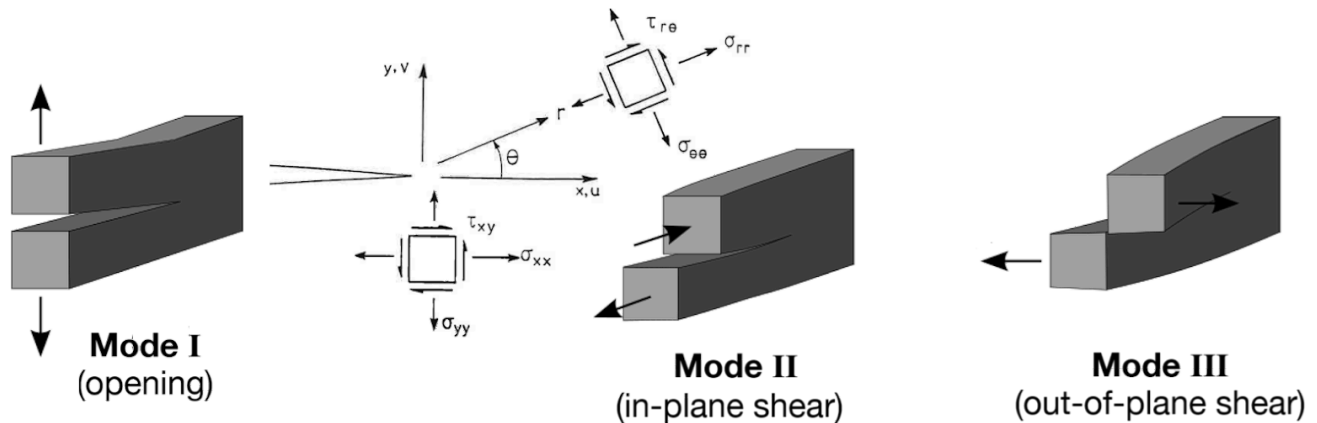
Statistics of Fracture

1D 'weakest link' theory implies a **Weibull distribution**:

$$P_s(V) = \exp \left[- \int_V \left(\frac{\sigma}{\sigma_0} \right)^m \frac{dV}{V_0} \right]$$

(P_s : survival probability of component, V : volume of component σ : tensile stress on component, V_0 : volume of test sample σ_0 : reference failure stress for volume V_0 which gives $P_s = 1/e \approx 0.37$, m : Weibull modulus (measure of variability: high $m \rightarrow$ small spread).)

6.5.4. Asymptotic Crack Tip Stress Fields in a Linear Elastic Solid



$$\begin{aligned} \sigma_{yy} &= \frac{K_I}{\sqrt{2\pi r}} \cos \frac{\theta}{2} \left(1 + \sin \frac{\theta}{2} \sin \frac{3\theta}{2} \right) \\ \sigma_{xx} &= \frac{K_I}{\sqrt{2\pi r}} \cos \frac{\theta}{2} \left(1 - \sin \frac{\theta}{2} \sin \frac{3\theta}{2} \right) \\ \tau_{xy} &= \frac{K_I}{\sqrt{2\pi r}} \cos \frac{\theta}{2} \sin \frac{\theta}{2} \cos \frac{3\theta}{2} \\ \sigma_{rr} &= \frac{K_I}{\sqrt{2\pi r}} \left(\frac{5}{4} \cos \frac{\theta}{2} - \frac{1}{4} \cos \frac{3\theta}{2} \right) \\ \sigma_{\theta\theta} &= \frac{K_I}{\sqrt{2\pi r}} \left(\frac{3}{4} \cos \frac{\theta}{2} + \frac{1}{4} \cos \frac{3\theta}{2} \right) \\ \tau_{r\theta} &= \frac{K_I}{\sqrt{2\pi r}} \left(\frac{1}{4} \sin \frac{\theta}{2} + \frac{1}{4} \sin \frac{3\theta}{2} \right) \end{aligned}$$

$$\begin{aligned} u &= \begin{cases} \frac{K_I}{G} \sqrt{\frac{r}{2\pi}} \left(\frac{1-\nu}{1+\nu} + \sin^2 \frac{\theta}{2} \right) \cos \frac{\theta}{2} & \text{Plane stress} \\ \frac{K_I}{G} \sqrt{\frac{r}{2\pi}} \left(1 - 2\nu + \sin^2 \frac{\theta}{2} \right) \cos \frac{\theta}{2} & \text{Plane strain} \end{cases} \\ v &= \begin{cases} \frac{K_I}{G} \sqrt{\frac{r}{2\pi}} \left(\frac{2}{1+\nu} - \cos^2 \frac{\theta}{2} \right) \sin \frac{\theta}{2} & \text{Plane stress} \\ \frac{K_I}{G} \sqrt{\frac{r}{2\pi}} \left(2 - 2\nu - \cos^2 \frac{\theta}{2} \right) \sin \frac{\theta}{2} & \text{Plane strain} \end{cases} \end{aligned}$$

$w = 0$

$$\begin{aligned} \sigma_{yy} &= \frac{K_{II}}{\sqrt{2\pi r}} \cos \frac{\theta}{2} \sin \frac{\theta}{2} \cos \frac{3\theta}{2} \\ \sigma_{xx} &= -\frac{K_{II}}{\sqrt{2\pi r}} \sin \frac{\theta}{2} \left(2 + \cos \frac{\theta}{2} \cos \frac{3\theta}{2} \right) \\ \tau_{xy} &= \frac{K_{II}}{\sqrt{2\pi r}} \cos \frac{\theta}{2} \left(1 - \sin \frac{\theta}{2} \sin \frac{3\theta}{2} \right) \\ \sigma_{rr} &= \frac{K_{II}}{\sqrt{2\pi r}} \left(-\frac{5}{4} \sin \frac{\theta}{2} + \frac{3}{4} \sin \frac{3\theta}{2} \right) \\ \sigma_{\theta\theta} &= -\frac{K_{II}}{\sqrt{2\pi r}} \left(\frac{3}{4} \sin \frac{\theta}{2} + \frac{3}{4} \sin \frac{3\theta}{2} \right) \\ \tau_{r\theta} &= \frac{K_{II}}{\sqrt{2\pi r}} \left(\frac{1}{4} \cos \frac{\theta}{2} + \frac{3}{4} \cos \frac{3\theta}{2} \right) \end{aligned}$$

$$\begin{aligned} u &= \begin{cases} \frac{K_{II}}{G} \sqrt{\frac{r}{2\pi}} \left(\frac{2}{1+\nu} + \cos^2 \frac{\theta}{2} \right) \sin \frac{\theta}{2} & \text{Plane stress} \\ \frac{K_{II}}{G} \sqrt{\frac{r}{2\pi}} \left(2 - 2\nu + \cos^2 \frac{\theta}{2} \right) \sin \frac{\theta}{2} & \text{Plane strain} \end{cases} \\ v &= \begin{cases} \frac{K_{II}}{G} \sqrt{\frac{r}{2\pi}} \left(\frac{\nu-1}{1+\nu} + \sin^2 \frac{\theta}{2} \right) \cos \frac{\theta}{2} & \text{Plane stress} \\ \frac{K_{II}}{G} \sqrt{\frac{r}{2\pi}} \left(-1 + 2\nu + \sin^2 \frac{\theta}{2} \right) \cos \frac{\theta}{2} & \text{Plane strain} \end{cases} \end{aligned}$$

$w = 0$

$$\begin{aligned} \tau_{zx} &= -\frac{K_{III}}{\sqrt{2\pi r}} \sin \frac{\theta}{2} \\ \tau_{yz} &= \frac{K_{III}}{\sqrt{2\pi r}} \cos \frac{\theta}{2} \\ \sigma_{xx} &= \sigma_{yy} = \sigma_{zz} = \tau_{xy} = 0 \\ w &= \frac{K_{III}}{G} \sqrt{\frac{2r}{\pi}} \sin \frac{\theta}{2} \\ u &= v = 0 \end{aligned}$$

6.5.5. Stress Intensity Factors Correlations (*J*-Integral Solutions) by Geometry and Mode

$K_I = \sigma_\infty \sqrt{\pi a}$

$K_{II} = \tau_\infty \sqrt{\pi a}$

$K_{III} = \tau_\infty \sqrt{\pi a}$

$K_I = 1.12 \sigma_\infty \sqrt{\pi a}$

$K_I = \sigma_\infty \sqrt{\pi a} \left(\frac{1-a/2W + 0.326a^2/W^2}{\sqrt{1-a/W}} \right)$

$K_I = \sigma_\infty \sqrt{\pi a} \left(1.12 - 0.23 \frac{a}{W} + 10.6 \frac{a^2}{W^2} - 21.7 \frac{a^3}{W^3} + 30.4 \frac{a^4}{W^4} \right)$

$K_I = \sigma_\infty \sqrt{\pi a} \left(\frac{1.12 - 0.61a/W + 0.13a^3/W^3}{\sqrt{1-a/W}} \right)$

$K_I = \sigma_\infty \sqrt{\pi a} \left(1.12 - 1.39 \frac{a}{W} + 7.3 \frac{a^2}{W^2} - 13 \frac{a^3}{W^3} + 14 \frac{a^4}{W^4} \right)$

$K_I = 0.683 \sigma_{\max} \sqrt{\pi a}$

$K_I = \frac{2P}{\sqrt{2\pi x_0}}$
 $K_{II} = \frac{2Q}{\sqrt{2\pi x_0}}$
 $K_{III} = \frac{2T}{\sqrt{2\pi x_0}}$

$K_I = \frac{P_1}{\sqrt{\pi a}} \sqrt{\frac{a+x_0}{a-x_0}}$
 $K_{II} = \frac{P_2}{\sqrt{\pi a}} \sqrt{\frac{a+x_0}{a-x_0}}$
 $K_{III} = \frac{P_3}{\sqrt{\pi a}} \sqrt{\frac{a+x_0}{a-x_0}}$

$K_I = \frac{2pb}{\sqrt{\pi a}} \arcsin \frac{b}{a}$

$K_I = \frac{2\sqrt{3} Pa}{h\sqrt{h} B}$
 $h \ll a \text{ and } h \ll b$

$K_I = \sqrt{\frac{1}{2\alpha H}} Eu \quad H \ll a \text{ and } H \ll b$
 $\alpha = \begin{cases} 1 - \nu^2 & \text{Plane stress} \\ 1 - 3\nu^2 - 2\nu^3 & \text{Plane strain} \end{cases}$

$K_I = \frac{1.12}{\Phi} \sigma_\infty \sqrt{\pi a}$

$\Phi = \int_0^{\pi/2} \left(1 - \frac{c^2 - a^2}{c^2} \sin^2 \theta \right)^{1/2} d\theta$

$K_I = \sigma_\infty \sqrt{\pi a} F \left(\frac{a}{r} \right)$

a/r	value of $F(a/r)^\dagger$			
	One crack		Two cracks	
	U	B	U	B
0.00	3.36	2.24	3.36	2.24
0.10	2.73	1.98	2.73	1.98
0.20	2.30	1.82	2.41	1.83
0.30	2.04	1.67	2.15	1.70
0.40	1.86	1.58	1.96	1.61
0.50	1.73	1.49	1.83	1.57
0.60	1.64	1.42	1.71	1.52
0.80	1.47	1.32	1.58	1.43
1.0	1.37	1.22	1.45	1.38
1.5	1.18	1.06	1.29	1.26
2.0	1.06	1.01	1.21	1.20
3.0	0.94	0.93	1.14	1.13
5.0	0.81	0.81	1.07	1.06
10.0	0.75	0.75	1.03	1.03
∞	0.707	0.707	1.00	1.00

$^\dagger U = \text{uniaxial } \sigma_\infty \quad B = \text{biaxial } \sigma_\infty.$

$K_I = \sigma_\infty \sqrt{\pi a} \left(\frac{D}{d} + \frac{1}{2} + \frac{3d}{8D} - 0.36 \frac{d^2}{D^2} + 0.73 \frac{d^3}{D^3} \right) \frac{1}{2} \sqrt{\frac{D}{d}}$

$K_{III} = \frac{16T}{\pi D^3} \sqrt{\pi a} \left(\frac{D^2}{d^2} + \frac{1D}{2d} + \frac{3}{8} + \frac{5d}{16D} + \frac{35d^2}{128D^2} + 0.21 \frac{d^3}{D^3} \right) \frac{3}{8} \sqrt{\frac{D}{d}}$

$K_I = \frac{4P}{B} \sqrt{\frac{\pi}{W}} \left\{ 1.6 \left(\frac{a}{W} \right)^{1/2} - 2.6 \left(\frac{a}{W} \right)^{3/2} + 12.3 \left(\frac{a}{W} \right)^{5/2} - 21.2 \left(\frac{a}{W} \right)^{7/2} + 21.8 \left(\frac{a}{W} \right)^{9/2} \right\}$

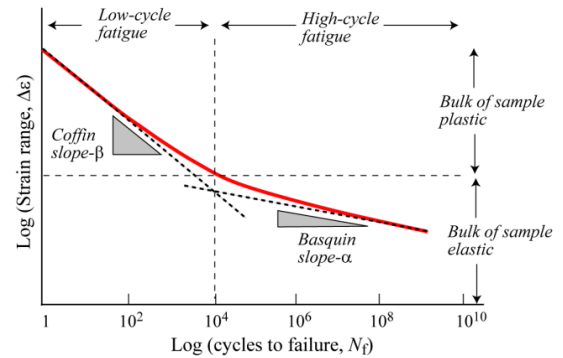
$K_I = \frac{P}{B} \sqrt{\frac{\pi}{W}} \left\{ 16.7 \left(\frac{a}{W} \right)^{1/2} - 104.7 \left(\frac{a}{W} \right)^{3/2} + 369.9 \left(\frac{a}{W} \right)^{5/2} - 573.8 \left(\frac{a}{W} \right)^{7/2} + 360.5 \left(\frac{a}{W} \right)^{9/2} \right\}$

6.5.6. Fatigue

Cyclic loading of a material can eventually lead to fatigue failure even if the applied stresses are below the yield stress due to crack propagation and fast fracture.

S-N curve for a given material specimen:

- **Basquin's law of high cycle fatigue:** $\Delta\sigma N_f^\alpha = C_1$
- **Coffin-Manson law of low cycle fatigue:** $\Delta\varepsilon^{pl} N_f^\beta = C_2$



Fatigue limit: the (practically) horizontal asymptote to the S-N curve, occurring in some materials. It is typically around $\sim 0.4-0.5\sigma_y$, if it exists. Some research suggests the fatigue limit may never truly exist in metals (i.e. N_f remains finite but very large for all nonzero $\Delta\sigma$).

($\Delta\sigma$: stress range, $\Delta\varepsilon^{pl}$: plastic strain range, N : number of cycles, N_f : cycles to failure, $\{\alpha, \beta, C_1, C_2\}$: constants, σ_{ts} : tensile strength.)

- **Goodman's rule:** for the same fatigue life, a stress range $\Delta\sigma$ operating with a mean stress σ_m is equivalent to a larger stress range $\Delta\sigma_0$ and zero mean stress, according to the relationship:

$$\Delta\sigma_0 = \frac{\Delta\sigma}{1 - (\sigma_m / \sigma_{ts})}$$

(other correlations exist: see Gerber parabola, Goodman-Haigh diagrams)

- **Miner's Rule** for cumulative damage (for i loading blocks, each of constant stress amplitude and duration N_i cycles):

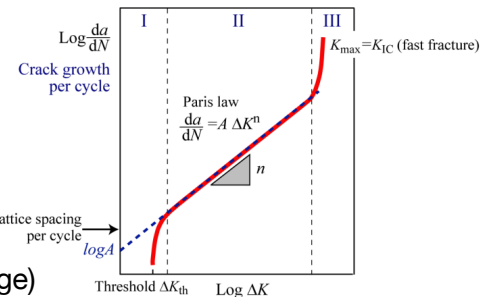
$$\sum_i \frac{N_i}{N_{fi}} = 1$$

(accuracy is variable)

- **Paris' law** for crack growth / propagation:

In the linear regime (phase II): $\frac{da}{dN} = A (\Delta K)^n$

(a : crack length, $\{A, n\}$: constants, ΔK : tensile stress intensity factor range)



Pressure Vessel Design: flaws in the shell are hazards for fast fracture (risk of explosion).

- For cylindrical vessels (Section 6.4.6), the dominant (hoop) stress is $\sigma_h = pr/t$.
- Proof test: pressurise a vessel to a level above its working pressure. If it survives, then we have an upper bound on the crack length present in the shell by $K_{IC} = Y\sigma_h\sqrt{\pi a}$.
- Critical crack length: $a_c = \frac{1}{\pi} \left(\frac{K_{IC}}{Y\sigma_h} \right)^2$ (need $a_c > t$ for leak before break criterion).

If $a_c \ll t \rightarrow$ break first. If $a_c \gg t \rightarrow$ leak first. Once a vessel has been proof tested, integrated Paris' law can find the remaining lifetime by solving for N . As the crack approaches the outside of the wall, the effective geometric factor Y may change (Section 6.5.5).

6.5.7. Tribology: Friction, Wear and Lubrication

Amontons-Coulomb's laws of friction:

1. Friction is directly proportional to the applied load: $F = \mu N$
2. Friction is independent of the apparent area of contact.
3. Kinetic friction is independent of sliding velocity.

The **static friction** μ_s is typically higher than the **kinetic friction** μ_k due increased adhesion, as well as due to the breakdown of asperities in the kinetic regime.

For **ductile** materials, the true contact area A_t due to a load W is related to the **hardness** H of the bulk material by $W = HA_t$.

This assumes linear elasticity. The friction F between two objects in contact is made up of shear stresses τ acting at microscopic asperities over a true contact area A_t , so that $F = \tau A_t$ with $\tau \leq \tau_y$. Sliding occurs when $\tau = \tau_y$, the shear yield stress of the surface material. In the case of non-noble metals, this is the oxide of the bulk metal and is much smaller.

The **wear rate** Q is defined by the volume worn away per unit sliding distance: $Q = -\Delta V / s$.

The wear coefficient K is defined by $Q = KA_t = K(W / H)$ (for ductile materials), which varies by wear mechanism (abrasion or adhesion).

Lubrication of an interface by inserting a fluid significantly reduces the wear rate.

Triboelectric charging (static electric charge accumulation) can occur at sliding interfaces, causing discharge when brought in contact with grounded conductors. For the triboelectric series, see Section 6.6.24.

6.5.8. Creep Deformation

Creep is a slow plastic deformation due to a sustained tensile or shear stress. In metals and polymers, this occurs typically for $T/T_m > 0.4$. The strain follows a similar curve to Paris' law (Section 6.6.6) with a (1) fast startup stage, (2) steady linear stage, (3) runaway to failure stage.

In metals, stage 2 creep occurs due to atom diffusion along **grain boundaries** or **dislocation cores** (Coble creep) or through the **lattice** (Nabarro-Herring creep), and **gliding dislocations** climbing obstacles (power-law creep). Stage 3 creep can occur due to increasing true stress (necking), near-yield plastic deformation or microstructural cavitation (void nucleation on grain boundaries), in which failure by yielding will follow quickly if the external stress continues.

Creep is an important failure mechanism in metals working at high temperatures. Creep lifetimes can be mitigated by using high melting point metals (e.g. Ni, Cr, Ti, W), lower operating temperatures (e.g. air cooling or a thermal barrier coating), casting with an elongated grain microstructure (or pure oriented single crystal), and forming crystals with coherent interfaces between ordered crystal structures to impede dislocation glide by creating a lattice strain (e.g. γ/γ' precipitate phase boundary).

Diffusion coefficient at temperature: $D = D_0 \exp\left(-\frac{Q}{RT}\right)$ (Section 6.6.6)

Stage 2 (diffusional creep): $\dot{\epsilon}_{ss} = A \sigma^n \exp\left(-\frac{Q}{RT}\right)$ or equivalently $\frac{\dot{\epsilon}_{ss}}{\dot{\epsilon}_0} = \exp\left(-\frac{Q}{RT}\right) \left(\frac{\sigma}{\sigma_0}\right)^n$

Stages 1 and 2 (Miller-Norton law): $\epsilon = \frac{C \sigma^n t^{m+1}}{m+1} \exp\left(-\frac{Q}{RT}\right)$ or equivalently $\dot{\epsilon} = C \sigma^n t^m \exp\left(-\frac{Q}{RT}\right)$

Estimated creep lifetime (Monkman-Grant relation): $t_f \times \dot{\epsilon}_{ss} = \text{constant}$

($\dot{\epsilon}_{ss}$: true plastic strain rate, (A, n, C, m, ϵ_0): power-law constants, σ : deviatoric Von Mises tensile stress, Q : creep activation energy, approximately equal to the diffusional energy (Section 6.6.10), ϵ_{cr} : true creep strain. For Coble creep, $n = 1$. For dislocation (power-law) creep, $3 < n < 8$.)

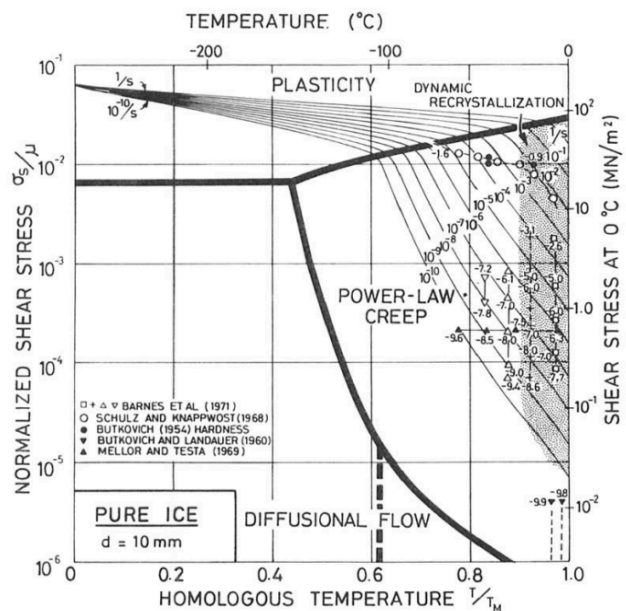
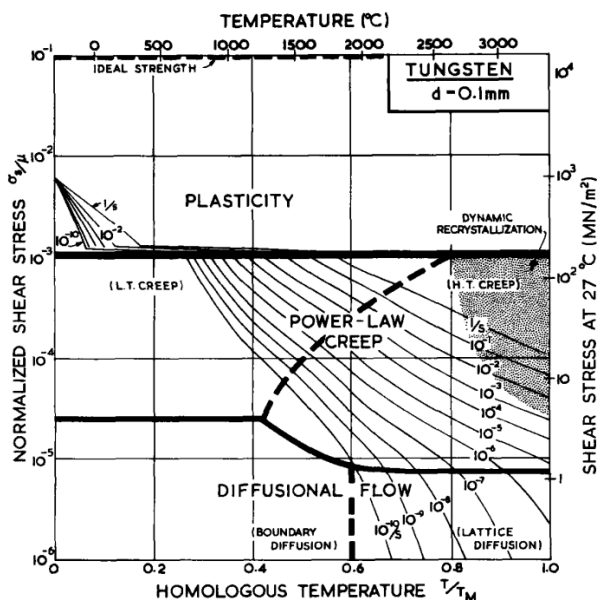
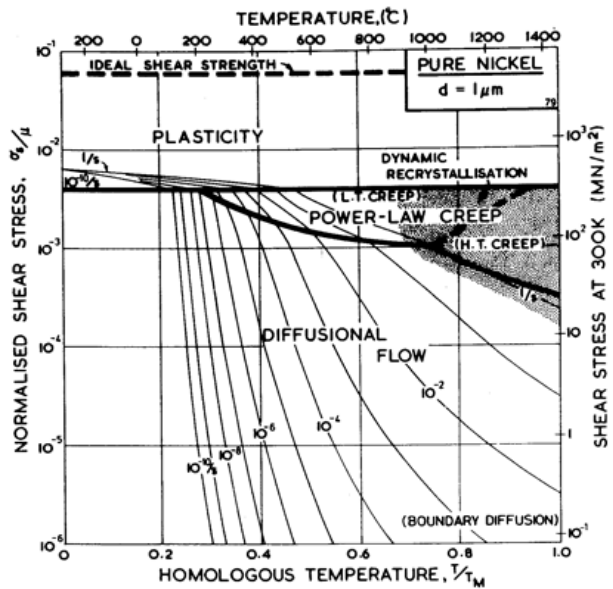
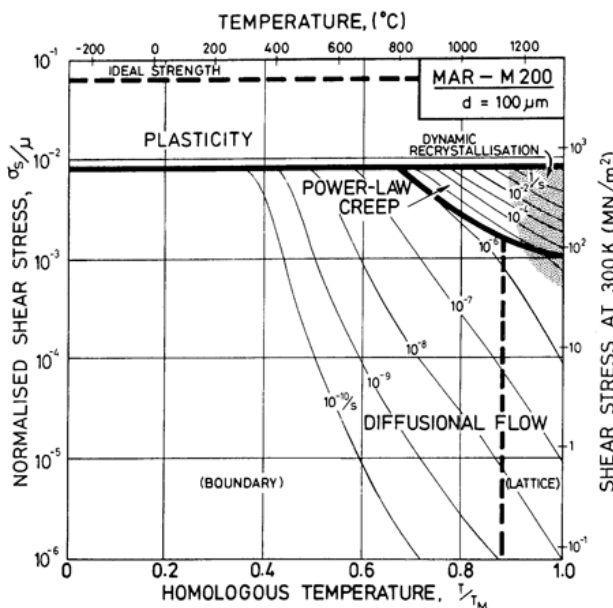
In high-temperature, high-stress applications (e.g. centrifugal loading on turbine blades), preventing creep is the primary design constraint. Single-crystal (SX) nickel superalloys (e.g. MAR-M200) have been developed which eliminate grain boundaries entirely which act as diffusional short-circuits.

6.5.9. Creep Mechanism Maps

Deformation mechanism maps with contours of strain rate in s^{-1} are shown below for

- nickel superalloy MAR-M200 (12.5% W, 10% Co, 9% Cr, 5% Al), grain size $100 \mu m$
 - pure nickel, grain size $1 \mu m$
 - pure tungsten, grain size $100 \mu m$
 - pure ice, grain size 10 mm
- (data from Ashby, 1983)

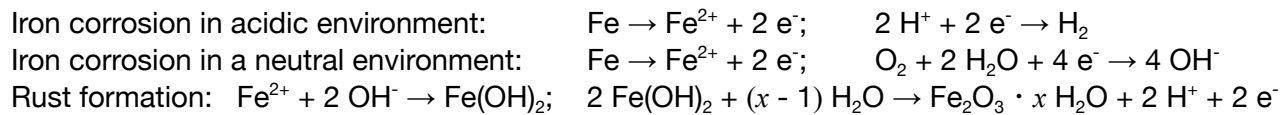
On the vertical axis, the shear stress is normalised by the shear modulus $\mu = G$.



6.5.10. Oxidation and Corrosion of Metals

For electrochemistry, see Section 13.5.

Metals of differing electrode potentials in contact with each other and an electrolyte (e.g. seawater) will progressively corrode due to electrochemical reactions, leading to the metals dissolving or oxidising.



Corrosion Kinetics

Metal components can gain or lose mass due to corrosion. The rate of change of mass can be:

- Linear decrease: for an oxide layer that falls off or is volatile
- Linear increase: for an oxide layer forming a porous or cracked structure allowing oxygen access
- Parabolic increase ($\sim t^{1/2}$): for an adhering oxide layer that provides a diffusion barrier to oxygen

Thickness of oxide layer: $\hat{h}(t) = \sqrt{1 + \hat{t}} - 1$ where $\hat{h} = \frac{k_{ox}}{D_{ox}} h$, $\hat{t} = \frac{2 M_{ox} c_g k_{ox}^2}{\rho D_{ox}} t$ (Deal-Grove model)

(k_{ox} : oxidation rate constant, D_{ox} : diffusion coefficient of O_2 in metal oxide layer,

M_{ox} : molar mass of oxide, c_g : O_2 concentration at oxide-gas interface, ρ : oxide density, h : thickness, t : time)

At higher temperatures, D_{ox} is increased, increasing the rate of oxide formation (corrosion rate).

For some metals (e.g. Al, Cr, Ti), the oxide layer is impermeable to oxygen, protecting the bulk metal.

Localised corrosion occurs when the materials promote the anodic reaction, due to:

- defects in a protective coating (paint, natural oxide layer, etc). This leads to pitting.
- electrolyte present in crevices (e.g. under nuts and bolts). Low oxygen favours the anodic reaction.
- cracks. Corrosion can directly promote crack growth under cyclic stresses (corrosion fatigue).

Stress corrosion cracking occurs under tensile stress, where cracks grow faster due to corrosion.

Hydrogen embrittlement (hydrogen-induced cracking): the cathodic reaction produces H_2 which can diffuse interstitially through most metals, initiating and propagating crack growth, worse at lower temperatures. Stainless steels and Al-alloys are less susceptible to this. At very high temperatures, hot hydrogen can dissociate into H^* atoms which de-carburise carbon steels to form trapped pressurised methane at grain boundaries and microcavities, which weakens the steel, presents a fire hazard, and accelerates crack growth ('high-temperature hydrogen attack').

Corrosion engineering: techniques to mitigate large-scale corrosion include:

- Galvanic (cathodic) protection: use of sacrificial anodes (e.g. zinc on iron) for preferential discharge.
- Impressed current: external voltage applied to decrease the potential of the structure.
- Coating: painting the surface with epoxy to create a physical barrier with the environment.
- Passivation in alkaline environments: e.g. hot bluing, concrete. Promotes insoluble oxide formation.
- Alloying steel: e.g. chromium. Cr forms a self-healing chromium oxide layer spontaneously. On heating, the Cr can deplete from the grains to form carbides on grain boundaries, risking intergranular corrosion. This is mitigated by adding stabilising elements in the alloy (e.g. Ti, Nb).

Corrosion Thermodynamics

Oxidation reactions of metals are exothermic ($\Delta H < 0$) and entropy-reducing ($\Delta S < 0$), and are spontaneous (thermodynamically favoured, exergonic, $\Delta G < 0$) for most metals at room temperature.

The **Ellingham diagram** (Section 15.1.3) shows the variation of ΔG for oxidation with temperature T , which becomes less exergonic with increasing T . However, the increased corrosion rate takes precedent for moderately high temperatures as oxidation remains spontaneous.

Some noble metals (e.g. Au) cannot be corroded at room temperature due to their high stability. Pure silver resists corrosion due to the activation energy barrier, but can tarnish in the presence of sulfur.

Standard Gibbs free energy of oxidation

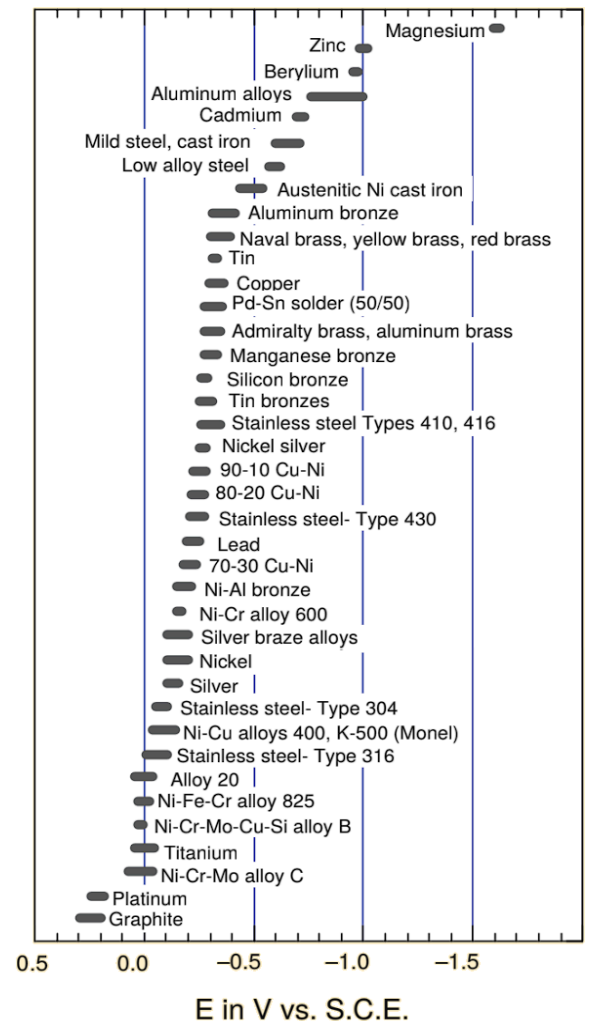
ΔG^\ominus in kJ per mole of oxygen: $x M + O_2 \rightarrow M_xO_2$ at $T = 298$ K.

Corrosion is feasible for exergonic reactions ($\Delta G < 0$).

Material	Oxide	Free energy (kJ/mol O ₂)
Beryllium	BeO	- 1182
Magnesium	MgO	- 1162
Aluminium	Al ₂ O ₃	- 1045
Zirconium	ZrO ₂	-1028
Titanium	TiO	- 848
Silicon	SiO ₂	- 836
Niobium	Nb ₂ O ₅	- 757
Chromium	Cr ₂ O ₃	- 701
Zinc	ZnO	- 636
Silicon nitride	3SiO ₂ + 2N ₂	- 629
Silicon carbide	SiO ₂ + CO ₂	- 580
Molybdenum	MoO ₂	- 534
Tungsten	WO ₃	- 510
Iron	Fe ₃ O ₄	- 508
Nickel	NiO	- 439
Most polymers	-	- 400
Diamond, graphite	CO ₂	- 389
Lead	Pb ₃ O ₄	- 309
Copper	CuO	- 254
Silver	Ag ₂ O	- 5
Gold	Au ₂ O ₃	+ 80

Galvanic series in seawater

Metals of different E in direct contact are at risk of corrosion. Seawater contains chloride ions which penetrate oxide layers and accelerate electrochemical reactions.



6.6. Materials Processing, Design and Datasets

6.6.1. Materials Selection

Process of material selection, single objective:

1. Identify **objective** (what is to be maximised or minimised? e.g. mass, cost, embodied CO₂)
2. Identify **functional constraints** (what is prescribed? e.g. stiffness-limited, strength-limited?)
3. Identify **geometrical constraints** (which dimensions are fixed, and which can vary?)
4. Eliminate free variables, and identify performance index of properties by proportionality.
5. Use material property charts (Section 6.6.14) or material selector software (e.g. Ansys Granta) to short-list the best materials.
6. Refine the selection using relevant secondary criteria: property limits (e.g. toughness), qualitative suitability (e.g. corrosion), manufacturing limits.

Performance indices for common optimisation problems

Function	Objective	Constraint	Index
Tie (tensile forces)	min mass	stiffness prescribed	E/ρ
Beam (bending moments)	min mass	stiffness prescribed	$E^{1/2}/\rho$
	min mass	strength prescribed	$\sigma_y^{2/3}/\rho$
Column (compressive forces)	min mass	buckling load prescribed	$E^{1/2}/\rho$
Shaft (torsion)	min mass	stiffness prescribed	$G^{1/2}/\rho$
Spring	min mass	strain energy prescribed	$\sigma_y^2/(\rho E)$
Thermal insulation	min mass	heat flux prescribed	$1/(\lambda c_p \rho)$
Electromagnet	max magnetic field	temperature rise prescribed	$c_p \rho / \rho_e$

(E : Young's modulus, σ_y : yield strength, ρ : density, C_m : material cost per unit mass, λ : thermal conductivity, c_p : specific heat capacity, ρ_e : electrical resistivity)

To design for minimum cost (or minimum embodied energy/CO₂...), replace ρ with ρC_m .

For material datasets including environmental resistance, see Section 6.6.2-3.

For the material property charts, see Section 6.6.4.

For process compatibility charts, see Section 6.6.5.

Shape Effects: designing axisymmetric components

If shape and/or area (of a cross-section) are free variables, shape factors can be used to measure geometric efficiency, and act as secondary constraints.

- Shape factor, stiffness-limited, in bending: $\Phi_E = \frac{I}{I_{\text{square}}} = \frac{12I}{A^2}$ (I : second moment of area)
- Shape factor, strength-limited, in bending: $\Phi_\sigma = \frac{Z_e}{Z_{e,\text{square}}} = \frac{6Z_e}{A^{3/2}}$ (Z_e : elastic section modulus)

Larger values of Φ correspond to more intricate shapes e.g. thin-flanged I-beam compared to a square or circle. Materials can be processed to a maximum Φ :

Material	Max Φ_E	Max Φ_σ	Material	Max Φ_E	Max Φ_σ
Steels	64	13	Fibre composites	36	9
Aluminium alloys	49	10	Wood	9	3

To incorporate shape factor into performance indices, replace E with $E\Phi_E$ (stiffness-limited) or replace σ_y with $\sigma_y\Phi_\sigma$ (strength-limited).

Multiple Constraints

If the design is simultaneously stiffness and strength limited (specified deflection and must not fail), compute the objective function for each functional constraint and evaluate both for each material. Rank the materials based on the worse of the two metrics.

Alternatively, plot a property chart with the two performance indices against each other and choose materials to maximise their product (above straight line $x + y$ on log-log axes).

Example: For a cantilever of fixed length L , it must carry a load F with maximum displacement δ , without failing. Identify materials to minimise materials cost C .

- Functional constraints: $\frac{F}{\delta} = \frac{3EI}{L^3} = \frac{E\Phi_E A^2}{4L^3}$ and $FL = Z_e \sigma_y = \frac{\Phi_\sigma A^{3/2} \sigma_y}{6}$.
- Eliminate free variable: $A = \left(\frac{4FL^3}{\delta E \Phi_E}\right)^{1/2}$ and $A = \left(\frac{6FL}{\Phi_\sigma \sigma_y}\right)^{2/3}$. $\{L, F, \delta\}$ are constants.
- Objective: $\min C = \max \frac{1}{C_m \rho A} = \max \frac{E^{1/2} \Phi_E^{1/2}}{C_m \rho}$ and $\max \frac{\sigma_y^{2/3} \Phi_\sigma^{2/3}}{C_m \rho}$ (performance indices).

$\min m \rightarrow$ CFRP; $\min C$, ignoring shape \rightarrow wood; $\min C$, considering shape \rightarrow aluminium alloy.

Use e.g. Section 6.4.10 to find the aluminium extruded I-beam with the highest $\Phi_E^{1/2} \Phi_\sigma^{2/3} = \frac{I^{1/2} Z_e^{2/3}}{A^2}$.

6.6.3. Process Selection

Once a raw material has been selected (Section 6.6.1), a process needs to be selected, to achieve both the 1) desired shape and 2) desired properties (by manipulating microstructure).



Primary shaping: raw material → component

- **Casting:** pour liquid metal into mould, solidify and cool, remove mould.
- **Moulding:** viscous flow of molten polymer or glass to fill a mould.
- **Forming:** plastically deform solid metal to shape (hot or cold).
- **Powder:** fill die with powder (metal/ceramic), hot press to shape

Consider suitability for the geometry e.g. prismatic → rolling/extrusion, sheet → metal forming.

Machining involves using e.g. lathe, mill to cut and remove material with high precision. **Heat treatment** exploits microstructural changes to achieve a particular range of physical properties.

To select a process, eliminate processes that cannot achieve the required product tolerances (Section 6.6.10). The feasible processes are then typically ranked on total cost, using a cost model:

$$C = C_m + \frac{C_c}{n} + \frac{\dot{C}_L}{\dot{n}}$$

(C_m : material cost per unit (including consumables), C_c : tooling cost per unit (dedicated machinery), \dot{C}_L : overhead cost per unit rate (labour, energy, share of capital), n : batch size, \dot{n} : production rate.)

The '**economic batch size**' of a process represents the range of n for which $\frac{C_c/n}{C_m}$ is small.

Technical evaluation is needed to determine process operating conditions (pressure, temperature, time etc) to form a target defect-free microstructure and associated properties.

6.6.4. Theory of Phase Diagrams

For any horizontal line (isotherm), each two-phase field is adjacent to a one-phase field.

Vertical line or thin field at w_B wt% B: chemical compound A_xB_y where $\frac{x}{y} = \frac{(100 - w_B) / M_{r,A}}{w_B / M_{r,B}}$

Single phase regions are labelled as their crystal polymorphs $\alpha, \beta, \gamma \dots$

Proportions of a two-phase mixture between α and β : $\frac{wt\% \alpha}{wt\% \beta} = \frac{(w_\beta - w) / (w_\beta - w_\alpha)}{(w - w_\alpha) / (w_\beta - w_\alpha)} = \frac{w_\beta - w}{w - w_\alpha}$ (lever rule)

Nucleation of solids (solidification/freezing) begins on cooling below the **liquidus** line. Melting of solids begins at the grain boundaries above the solidus line.

Special phase transformations during cooling of a melt at a particular mixture composition:

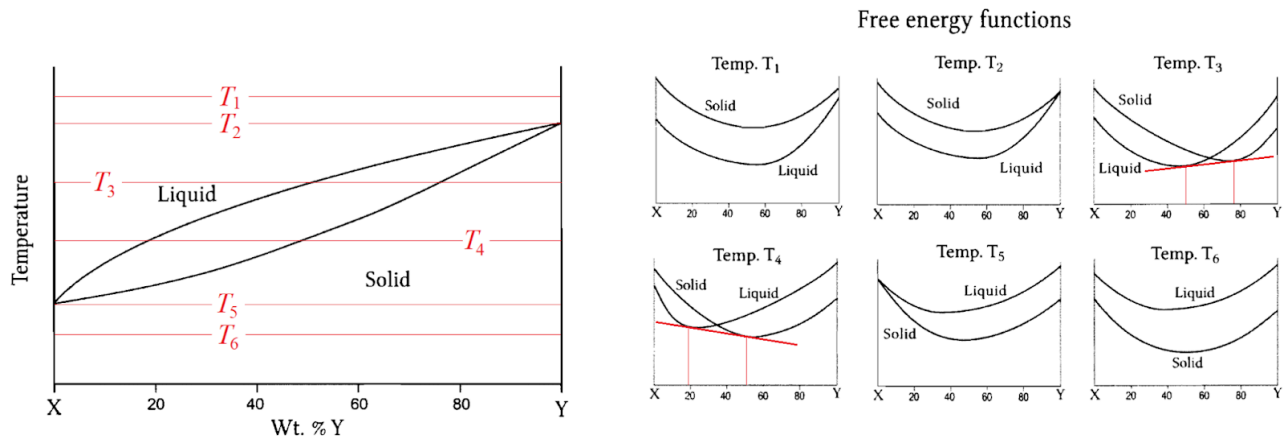
Eutectic reaction: $L(l) \rightarrow \alpha(s) + \beta(s)$

Peritectic reaction: $\alpha(s) + L(l) \rightarrow \beta(s)$

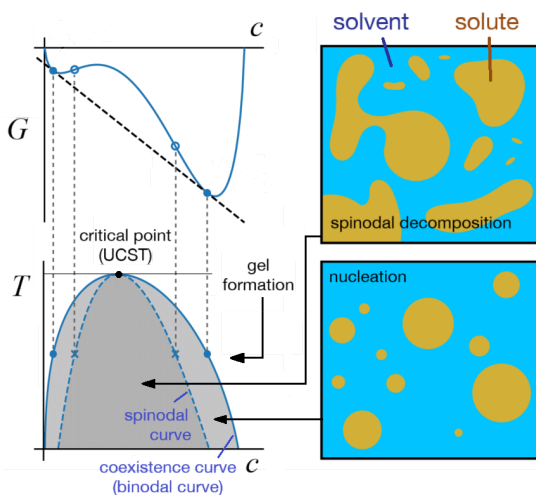
Eutectoid reaction: $\alpha(s) \rightarrow \beta(s) + \gamma(s)$

Peritectoid reaction: $\alpha(s) + \beta(s) \rightarrow \gamma(s)$

Total Gibbs Free Energy of Non-Eutectic (Non-Azeotropic) Binary Mixtures: at any given temperature, an equilibrium phase minimises its total Gibbs free energy. In a two-phase region (T_3 and T_4 below), the composition is at the common tangent intersection to the solid phase and liquid phase curves.



Phase Separation Thermodynamics



- **Spinodal curve:** limit of single phase stability, at free energy inflection points $d^2G/dx^2 = 0$. Phase separation occurs within the spinodal (unstable).
- **Binodal curve (coexistence curve):** limit of two-phase stability, at the common tangent to the free energy curve. The coexistence curve bounds the miscibility gap.
- Between the binodal and spinodal points, nucleation occurs with a metastable precipitate phase.

6.6.5. Microstructure from Phase Diagrams

While the phase diagram gives the thermodynamically favoured equilibrium phase proportions, it does not directly show their microscopic arrangement, dominated by diffusion kinetics. Common phase transformations and their resulting microstructures are:

- **Liquid to Concentrated Solid Solution:** under the liquidus line (upper melting point), grains of solid phase nucleate in the liquid and grow as cooling continues.
- **Single to Two-Phase Solid Solutions:** in solid grains, phase separation occurs by formation of nanoscopic precipitate clusters within the matrix. Atoms diffuse between matrix and precipitate.
- **Eutectic Solidification:** liquid phase spontaneously forms intricate microstructure of two solid phases. Grains are not observed.
- **Off-Eutectic Solidification:** solid phase nucleates first, liquid phase moves closer to eutectic composition. At the eutectic point, the remaining liquid undergoes eutectic solidification, and the other phase can develop precipitates within its grains.
- **Eutectoid Reaction:** in solid phase grains, new grains nucleate on the boundaries, consisting of lamellar (nanoscopic alternating plates, stacked normal to grain growth) microstructure of the two resulting solid phases. Atoms diffuse between the layers of the lamellar structure.
- **Off-Eutectoid Reaction:** one of the two solid phase grains undergoes the eutectoid reaction, developing the lamellar structure, and the other phase can develop precipitates within its grains. Commonly used in hypo-eutectoid steels, where lamellar structure (pearlite) is effective in obstructing dislocation motion, providing strength in addition to ferrite's intrinsic toughness.

6.6.6. Kinetics of Microstructural Evolution

Nucleation and Grain Growth

Free energy of a nucleated solid in a fluid for $T < T_m$: $G(r) = \frac{4}{3}\pi r^3 \Delta G_V + 4\pi r^2 \gamma$

Critical radius r for nucleation: $\frac{dG}{dr} = 0$ at $r = r^*$, where $r^* = \frac{2\gamma}{|\Delta G_V|} = \frac{2\gamma T_m}{|\Delta H_V| (T_m - T)}$

Some undercooling $T_m - T$ is required to begin solidification, which then occurs at T_m .

(ΔG_V : Gibbs free energy of fusion (per unit volume), ΔH_V : specific latent heat of fusion (per unit volume), T_m : liquid melting point (liquidus line), γ : solid-liquid surface energy)

Once solidification begins, the released heat from ΔH_V heats the mixture back up towards T_m .

Since r can be much larger for the same V in a spherical cap than a sphere, heterogeneous nucleation will always dominate over homogeneous nucleation.

Solid growth rate v : $v = \frac{\Delta H_V}{k_B T} \frac{T_m - T}{T_m} e^{-Q/(k_B T)}$; $\max v$ and w occur at some undercooling $T_m - T > 0$.

Rate of nucleation w : $w \propto e^{-\Delta G^*/(k_B T)} e^{-Q/(k_B T)}$, where $\Delta G^* = \Delta G_V(r^*) = \frac{16\pi\gamma^3 T_m^2}{3(\Delta H_V)^2 (T_m - T)^2}$.

Mass and Heat Transfer in Solids (Diffusion and Heat Conduction)

In 1D, mass and heat transfer are governed by analogous differential equations:

- 1D diffusional flow (Fick's law, steady state): $J = -D \frac{\partial C}{\partial x} \Rightarrow \frac{\partial C}{\partial t} = D \frac{\partial^2 C}{\partial x^2}$
- 1D heat flow (Fourier's law, steady state): $q' = -\lambda \frac{dT}{dx} \Rightarrow \frac{\partial T}{\partial t} = \alpha \frac{\partial^2 T}{\partial x^2}$

For the 2D or 3D forms of these PDEs, see Section 3.7.3.

- Diffusion coefficient D [$\text{m}^2 \text{s}^{-1}$]: $D = D_0 \exp\left(-\frac{Q_a}{RT}\right)$
- Thermal diffusivity α [$\text{m}^2 \text{s}^{-1}$]: $\alpha = \frac{\lambda}{\rho c_p}$

(J : diffusive flux per unit area [$\text{mol s}^{-1} \text{m}^{-2}$], C : concentration [mol m^{-3}], q' : heat flux per unit area [W m^{-2}], T : temperature [K], x : 1D position [m], t : time [s], Q_a : diffusional activation energy [J], λ : thermal conductivity [$\text{W m}^{-1} \text{K}^{-1}$], ρ : density [kg m^{-3}], c_p : specific heat capacity [$\text{J K}^{-1} \text{kg}^{-1}$].)

For many 1D problems of diffusion and heat flow, the solution for concentration or temperature depends on the error function distribution, erf (Section 1.7.3.):

$$C(x, t) = f\left[\text{erf}\left(\frac{x}{2\sqrt{Dt}}\right)\right] \quad \text{and} \quad T(x, t) = f\left[\text{erf}\left(\frac{x}{2\sqrt{\alpha t}}\right)\right]$$

A characteristic diffusion distance in all problems is given by $x \sim \sqrt{Dt}$, with the corresponding characteristic heat flow distance in thermal problems being $x \sim \sqrt{\alpha t}$.

Impulse Response: if $C(x, 0) = n_0 \delta(x)$, (n_0 is the initial amount (mol m^{-2}))

$$\Rightarrow C(x, t) = \frac{n_0}{2\sqrt{\pi Dt}} \exp\left(-\frac{x^2}{4Dt}\right) \quad (\text{bell curve, increasing width with } t)$$

Step Response: if $C(x, 0) = C_0 + (C_1 - C_0) H(x)$, (C_0 : external conc, C_1 : internal conc)

$$\Rightarrow C(x, t) = C_0 + (C_1 - C_0) \text{erf}\left(\frac{x}{2\sqrt{Dt}}\right) \\ (\text{slope from } C(0) = C_0, C(\infty) = C_1, \text{ increasing width with } t)$$

Harmonic Response: if $C(x, 0) = C_0 + (C_1 - C_0) \sin\left(\frac{2\pi x}{w}\right)$, (w : length period of variation)

$$\Rightarrow C(x, t) = C_0 + (C_1 - C_0) \sin\left(\frac{2\pi x}{w}\right) \exp\left(-\frac{4\pi^2 Dt}{w^2}\right)$$

The harmonic response can be used to find responses to arbitrary initial conditions using Fourier series.

6.6.7. Heat Treatment of Steel

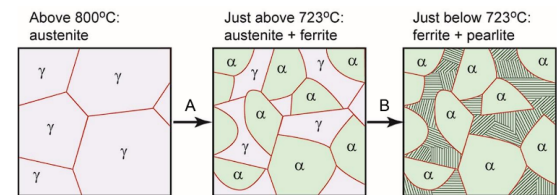
Heat treatment is used to form strong, tough microstructures, mainly by precipitation hardening (pinning of dislocations by hard second phase microparticles). This helps to alleviate the usual trade-off between strength and toughness. Heat treatment is primarily applied as a secondary process, but can also occur due to similar thermal histories in e.g. welding, hot rolling.

Heat treatable alloys require heating to a single solid phase and cooling to form a two-phase mixture of solids. All steels satisfy this requirement: austenitisation involves the initial heating stage to convert the steel to single solid phase austenite (γ). On cooling, microstructural hardness is dependent on the temperature-time curve (thermal history). The steel phase diagram is shown in Section 6.6.33.

Slow Cooling of Hypoeutectoid Steels: left of the eutectoid (0.8 wt% C) point on phase diagram

A: Between ~ 800 °C and 723 °C (eutectoid line), ferrite (α) grains nucleate on austenite (γ) grain boundaries

B: remaining austenite undergoes the eutectoid reaction to form lamellar pearlite (hard phase of $\alpha + \text{Fe}_3\text{C}$).



Slow-cooled steels are known as '**normalised**' steels, often occurring after hot rolling. The carbon content determines their properties: low carbon steel has $\sigma_y \sim 200$ MPa and high ductility, while normalised eutectoid steel (100% pearlite) has $\sigma_y \sim 450$ MPa with lower ductility.

Fast Cooling of Hypoeutectoid Steels: non-equilibrium states

The TTT diagram for hypoeutectoid steels (Section 6.6.34) implies four possible routes:

- Above the C-curves and above the eutectoid line (AC_1): forms ferrite + austenite.
- Above the C-curves and below the eutectoid line: forms ferrite + pearlite (lamellar $\alpha + \text{Fe}_3\text{C}$)
- Below the C-curves and above the martensite line (M_1): forms bainite (fine Fe_3C needles in α)
- Below the C-curves and below the martensite line: forms martensite (metastable α')

Martensite is the metastable SSSS state, formed by diffusionless transformation of γ . Martensite is initially in the FCC unit cell, but since the equilibrium state is BCC, it can undergo a sudden 'shock wave' lattice shear to a distorted BCC unit cell (Bain strain), forming long thin needles of martensite through the remaining unstable γ grains. The lower the final temperature, the more martensite formed. With higher carbon content, pearlite predominates at higher T , the times to transformations increase and the martensite lines move to lower temperatures. Bainite has $\sigma_y \sim 600$ MPa while martensite has $\sigma_y \sim 2$ GPa, but is impractically brittle as-quenched ($K_{IC} < 5$ MPa $\text{m}^{1/2}$), and must undergo tempering.

Quenching and Tempering of High Carbon Steels

Heating martensite to 450-600 °C reduces its yield stress to $\sigma_y = 450$ -800 MPa while providing it with essential toughness similar to normalised steels. A fine-scale dispersion of Fe_3C forms and the Fe lattice relaxes back to undistorted BCC. The tempering temperature also influences the softening rate and the volume fraction of precipitates formed.

Hardenability: ease of forming martensite on cooling, allowing larger bar diameters for through-hardening.

High hardenability is desired for cutting tools, requiring quenching and tempering.

Low hardenability is desired in welds, where weld fracture could occur in the heat-affected zone.

Surface Hardening of Steels

Many steel components used in machinery (e.g. gears, bearings, tool edges) are subjected to high surface stresses, due to friction and sliding contact. Surface engineering is used to harden the surface of the component ('case hardening') to increase its hardness and wear resistance without damaging the strength and toughness of the underlying steel.

Carburising: the steel is immersed in a carbon-rich atmosphere at high temperature e.g. gaseous CO or molten NaCN (older). Carbon diffuses into the surface of the component. The higher local C content increases both the hardness and hardenability, facilitating surface martensite formation which can then be tempered.

Thermal modelling (Section 6.6.1) can be used to estimate the carburisation time required for a

given case depth:
$$\operatorname{erf}\left(\frac{x_{\text{case}}}{2\sqrt{Dt_{\text{case}}}}\right) = 1 - \frac{C_{\text{min}} - C_0}{C_s - C_0}.$$

(C_{min} : minimum C concentration at depth x_{case} , t_{case} : time required, C_0 : initial bulk C concentration, C_s : maximum solubility of austenite at the carburising temperature, D : diffusion coefficient of C in steel at the carburising temperature)

Transformation Hardening: a heat source is applied to the surface, austenitising a thin layer, then cooling it quickly to form a layer of martensite. Surface heating may use a traversing flame, laser, electron gun or high frequency induction coils (induces surface eddy currents). Air cooling may be sufficient to form martensite, or a water-quench can be used.

Joining of Steels

Two metallic components can be joined at an interface using welding. Lower carbon-steels are suitable for welding, while high-carbon and high-alloy steels are less suitable, requiring preheating.

Metal-Inert Gas (MIG) Welding: a consumable (continuously fed) metal electrode at high voltage generates an electrical arc which melts the metal. When the components are melted together along an interface, they will re-solidify together, joining them. An inert gas stream is blown over the molten weld pool to prevent atmospheric contaminants entering the weld.

Tungsten-Inert Gas (TIG) Welding: an inert (fixed) tungsten electrode at high voltage arcs to a manually held metal welding rod, triple-melting the workpieces-rod interface. The TIG torch may be water-cooled to prevent overheating.

The '**heat affected zone**' (**HAZ**) is the region around the weld which did not melt but whose microstructure may still be affected by the process. The HAZ may undergo grain recrystallisation and growth (lower strength), over-ageing of precipitates, stress concentrations (thermal expansion, warping of thin sections), brittle martensite formation in steels on cooling (requiring post-weld tempering), or sensitisation of non-stabilised Cr-alloy steels (Cr is removed from grains to the boundaries, increasing susceptibility to intergranular corrosion).

6.6.8. Heat Treatment of Aluminium Alloys

Aluminium alloys are ‘light alloys’ (like titanium and magnesium). The strength of pure Al is very low ($\sigma_y = 40$ MPa) but can be increased $\sim 10x$ using Al alloys and heat treatment. Al-Si is a casting alloy. Al-Cu is a heat treatable alloy. Al-Mg is light and non-heat treatable.

Slow Cooling of Aluminium Alloys: equilibrium processes only

In slow cooling, temperature changes are slow enough to maintain equilibrium compositions throughout. After heating to the Al-rich solid field of the phase diagram (~ 550 °C), on cooling below the solvus line (~ 450 °C), the secondary phase is rejected from the solid solution. This forms a precipitate (usually of an intermetallic compound e.g. CuAl_2), first by heterogeneous nucleation on grain boundaries and slowly by homogeneous nucleation in grains. The hard phase precipitates are coarse (well spaced), giving low yield strength and high ductility due to weak dislocation pinning.

Fast Cooling of Aluminium Alloys: controllable non-equilibrium process

The rates of phase transformations due to nucleation thermodynamics (Section 6.6.6) result in a ‘C-curve’ distribution, with rapid phase transformation occurring at some optimal undercooling below T_E . This is displayed for a given alloy in a ‘TTT diagram’ (time-temperature transformation). Quenching (rapid cooling) to some $T < T_E$ followed by isothermal holding for a given time results in a certain fraction of transformation, before removing to room temperature. This provides solid solution hardening, but the solute atoms provide weak pinning, so the yield strength is low.

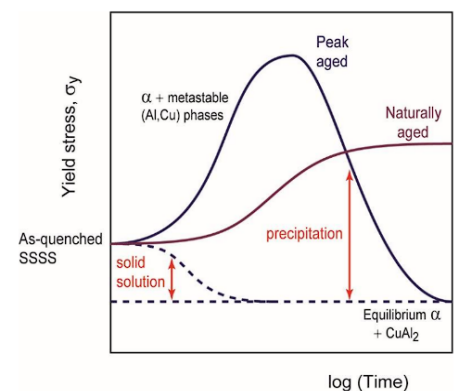
If the cooling rate is fast enough to miss the C-curves (critical cooling rate), no precipitate will form at all, and the resulting room-temperature composition will be a metastable ‘supersaturated solid solution’ (SSSS). Continuous cooling transformations are illustrated on a ‘CCT diagram’.

Age Hardening of Aluminium Alloys: increase the strength after fast cooling

A more complete thermal history to achieve hardness and strength in Al alloys is 1) solid solution heat treatment (dissolve alloy elements, forming single phase), 2) quenching (forms SSSS), 3) age hardening (reheating for precipitation). There are two methods of age hardening:

- Artificial ageing: reheat for a few hours at ~ 200 °C (two phase).
- Natural ageing: leave for several days at room temperature.

The precipitate lattice structure is coherent with the Al, reducing the interface energy penalty to nucleation, but loses coherence when they coarsen too much (grow and spread out). Age hardening therefore has a ‘peak aged’ state, where shear resistance to dislocation glide is maximised. Over-aged Al-alloys are soft. Natural ageing avoids this issue, though at slightly reduced strengths.



Non-Heat Treatable Aluminium Alloys

Al-Mg (‘5000 series’) and Al-Mg-Mn (‘3000 series’) cannot be age hardened, due to the difficult nucleation of Mg_5Al_8 intermetallic solute, so the precipitates do not form. These alloys remain metastable in operation and are hardened by solid solution and work hardening.

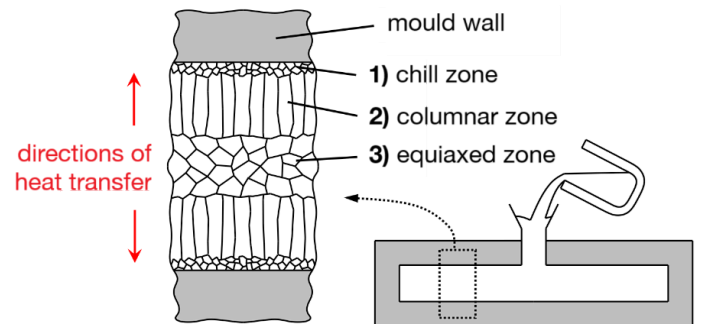
6.6.10. Casting of Metals (Cast Alloys)

A mould is filled with a molten metal or metal alloy, and it is allowed to cool and solidify. The resulting crystal grain structure (grain size and anisotropy) depends on the rates of internal heat conduction and so is highly shape-dependent.

Casting is often the first shaping step, forming large bulk metals (continuous casting, forming ingots, slabs, billets) and can be followed by deformation processing. Alloys can also be cast into 'near net shape', requiring only minimal secondary shaping processes to form the final product (e.g. die casting, sand casting, investment casting).

Grain Structure due to Cooling

1. **Chill zone:** rapid undercooling and large heterogeneous nucleation sites lead to numerous nuclei forming very small grains.
2. **Columnar zone:** grains oriented towards the centre can only grow in that direction.
3. **Equiaxed zone:** once the core liquid has undercooled, nucleation can begin slowly, forming larger grains in the centre.



Controlling Grain Structure

When casting with metal alloys, smaller grain size provides a more uniform distribution of alloying elements and impurities due to segregation. This can be achieved by adding 'inoculants' (e.g. TiB_2 microparticles for Al casting alloys) to the molten cast, promoting rapid heterogeneous nucleation.

Eutectic compositions are optimal for casting alloys (low melting point, uniform melting temperature → can fill mould completely before solidifying). Al-11.3 wt% Si is a eutectic casting alloy with high strength, but the brittle Si needles require further alloying. In cast iron (Fe-4.3 wt% C), a small addition of Mg improves toughness by causing the graphite phase to form as spheres instead of flakes ('poisoning').

Chvorinov's rule: solidification time is proportional to volume-to-surface area ratio squared.

The microstructural length scale (e.g. lamella plate spacing) is inversely proportional to solidification rate.

Segregation: alloy/impurity concentrations are typically anisotropic in casting

The first solid to form (centre of grains) is always purer than the average alloy composition due to the diverging solidus and liquidus lines away from the eutectic point. The same is true for the material in the chill zone, producing both macroscopic and microscopic variation. Diffusion occurs too slowly to homogenise these fluctuations. Impurities concentrate on grain boundaries, possibly forming brittle precipitates or gas-filled cavities, leading to variable strength and reduced toughness.

Segregation can be reduced using inoculants for a finer grain size, or by adding small alloying additions that react with impurities. This forms a fine dispersion of solid particles during solidification, trapping the impurity in a harmless state (e.g. Mn and Al in carbon steels, trapping impurity S and O as MnS and Al_2O_3). The casting can also be homogenised by reheating, redistributing the solute by faster diffusion.

6.6.11. Deformation of Metals (Wrought Alloys)

Ductile alloys can be shaped by inducing compressive plastic strains without failure (deformation processing), in processes such as forging, rolling, extrusion and sheet metal forming.

Cold Working: deformation processes at room temperature. Microstructural changes include:

1. The grains change shape, following the overall imposed strain ('pancaked grains').
2. Work hardening occurs due to increase in dislocation density, increasing yield strength.

Deformation to large plastic strains risks failure by fracture due to reduced ductility.

Annealing: heating to $\sim 0.5 T_m$ reverses the effects of work hardening

The thermal energy provided in annealing causes microstructural changes:

1. Recovery: at lower $\sim 0.1 T_m$, dislocations of opposite orientation can annihilate each other on collision, or many dislocations of similar orientation can migrate and align into 'sub-grains', reducing the overall strain energy in the lattice. There is a small reduction in yield stress.
2. Recrystallisation: at higher $\sim 0.3 T_m$, new defect-free grains are nucleated within the deformed work-hardened grains, significantly reducing dislocation density and dropping the yield strength.

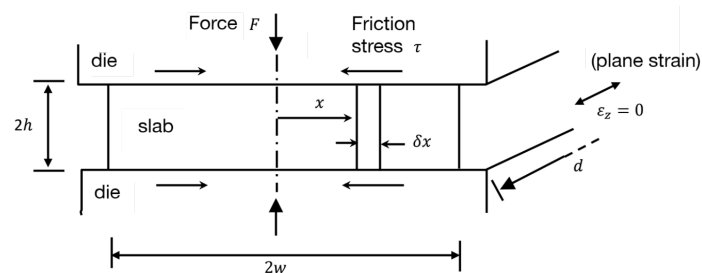
In cold-rolling, the yield stress increases and thickness decreases slightly with each pass. An annealing schedule is used to 'reset' the yield stress when it rises too high, before continuing passes.

Hot Working: combined deformation and annealing, around $\sim 0.7 T_m$

In hot working, strain hardening does not occur, reducing tooling forces and allowing larger strains.

Open-Die Hot Forging Analysis: workpiece struck with compressive plastic deformation by a die

Slab material flows away from the centre, resisted by friction stress at the lubricated die interface.



Equilibrium: $\frac{d\sigma_x}{dx} = \frac{-\tau}{h}$; Tresca yield criterion:

$$p - \sigma_x = Y \Rightarrow \frac{dp}{dx} = \frac{-\tau}{h}$$

Friction law: either Coulomb or Tresca

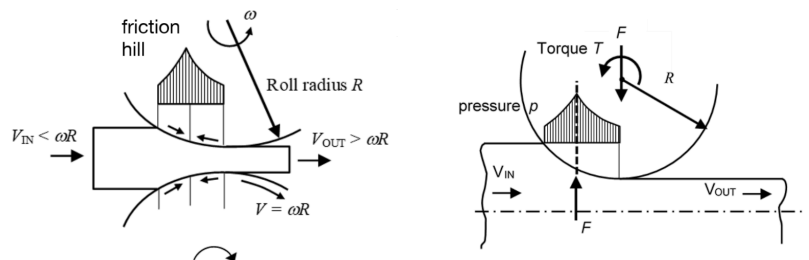
Coulomb friction: $\tau = \mu p$; Tresca friction: $\tau = mk = m \frac{Y}{2}$ ($m = 1$ represents 'sticking friction')

Applying Tresca friction, $\int_{p(x)} dp = \frac{-mY}{2h} \int_x^w dx \Rightarrow p(x) = Y \left(1 + \frac{m}{2h} (w - x \operatorname{sgn} x) \right)$ ('friction hill')

Total forging load per unit depth, $F = \int_{-w}^w p(x) dx = 2wY \left(1 + \frac{mw}{4h} \right)$.

Hot Rolling Analysis: pressure maximum at the 'neutral plane' ($V = \omega R$)

Rolling torque, $T = F\alpha R$ ($\alpha \sim 0.3$)



6.6.12. Processing of Thermoplastic Polymers

Solidification of Thermoplastic Polymers

Thermoplastics can solidify into a semi-crystalline structure, with regions of aligned (spherulites) and amorphous polymer chains. Higher crystallinity gives higher stiffness, higher density, higher glass transition temperature, lower ductility, lower toughness (more brittle) and lower optical transparency (scattering, birefringence and opacity).

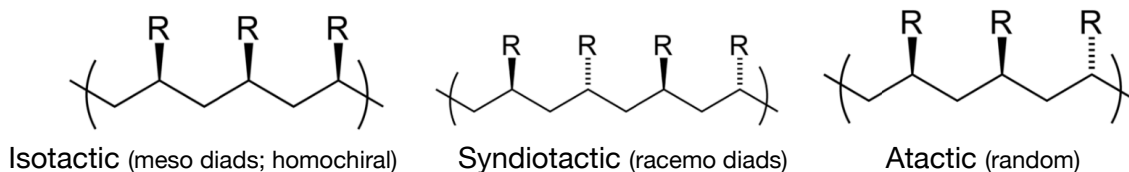
Polymers are strong (high elastic modulus E) and brittle below a glass transition temperature T_g , and rapidly degrade into viscous liquids above this point.

- Thermoset: high degree of cross-linking \rightarrow high T_g and E
- Elastomer: low degree of cross-linking \rightarrow medium T_g and E
- Thermoplastic: no cross-linking \rightarrow low T_g and E

Cross-linking can be induced by heat, pressure, acid catalysis, irradiation, or chemical agents (cross-linkers). In the vulcanisation process of rubber, elastomers are cured with sulfur or metal oxides to form stronger rubbers.

A complex monomer (large side groups, branching) will be slow to rearrange by diffusion and will therefore typically be difficult to crystallise. Low crystallinity (amorphous structure) is obtained when a polymer is formed by rapid cooling from a melt (e.g. film blowing). Crystallisation rate is maximum at some $T_g < T < T_m$, similar to C-curves on a TTT diagram (Section 6.6.7). Fast cooling rates, such as in producing thin sections of polymeric material, can avoid crystallinity.

Tacticity Control: relative stereochemistry of adjacent chiral centres between monomers



Tacticity cannot be changed after polymer formation as it is set by polymerisation conditions e.g. catalyst.

- Isotactic polymers are semi-crystalline. Most biopolymers are homochiral in this way.
- Syndiotactic polymers are highly crystalline.
- Atactic polymers are amorphous and are sometimes viscous liquids at room temperature.

Deformation Processing of Thermoplastics: variety of methods

- Fibre drawing: pressure screw extrudes thin polymer filament onto coiling drum.
- Stretch blow moulding: polymer preform ('parison') inflated to fill a mould. Anisotropic alignment.
- Film blowing: extruded polymer inflated, cooled and wound onto drum.

6.6.13. Powder Processing (Technical Ceramics)

Powder methods are suitable for near-net shape forming processes for ceramics and cemented carbides. It can provide good tolerances and surface finish with little final machining needed. It is easy to make complex shapes cost-effectively, and material wastage is very low.

Powder Manufacture

Metal powders are produced by atomisation (high pressure jets of water or gas directed at molten metal). Ceramic powders are typically made by crushing or grinding followed by sieving, producing very irregular particles.

Processing of Powders

- **Powder blending:** metal or ceramic powder is blended with various additives. Can be used for alloy steels. For ceramics, the additives are sintering aids (low melting phase to bind particles together), grain growth inhibitors (second-phase particles that pin grain boundaries) and a lubricant binder (e.g. zinc stearate, improves powder flow/mould filling, reduces die friction).
- **Compaction (cold isostatic pressing):** powder is pressed into a shaped mould/die at very high pressure to form a weak 'green compact', which can be 'green machined' to add holes/slots. On sintering, the ceramics shrink in dimensions due to loss in porosity, while metals do not shrink. Inhomogeneous porosity (due to non-uniform die friction) leads to undesirable internal stresses on contraction. Cold isostatic pressing is suitable for complex-shaped ceramics.
- **Pressureless sintering:** continuous conveying of powder through a furnace. The furnace atmosphere is controlled to prevent oxidation or decarburisation (e.g. of steels). Particles bond together, forming the grains in the bulk material. Sintering rate: $\frac{\partial \rho}{\partial t} = \frac{\gamma D}{a^3}$ (ρ : density, γ : surface energy, D : self-diffusion coefficient, a : particle diameter). Porosity goes from being interconnected to being discrete and then shrinking. Mechanical properties improve with decreased porosity.
- **Liquid phase sintering:** sintering is faster if a liquid phase is present, drawn by capillary action into the spaces between the particles e.g. sintering of alumina + 1% MgO which reacts to form a low melting-point glass which bonds the alumina grains together (e.g. for spark-plug insulator).
- **Hot isostatic pressing (hiping):** like cold isostatic pressing, but powder is canned in a metal container to provide shape and subjected simultaneously to high temperature. Hiping allows very low final porosity with short process time.
- **Metal Injection Moulding (MIM) and ceramic Powder Injection Moulding (PIM):** used for producing small, high-precision, low porosity components. Uses conventional polymer injection moulding technology with a blended polymer-metal or polymer-ceramic feedstock to make initial compacts which are then carefully treated to remove the polymer binder. Restricted to thin sections (limited by de-binding process).
- **Slip casting:** the 'traditional' manually handled process, often used for pottery and tiles. Clay slip (clay-water slurry) poured into mould, then the solid discs are pressed into a rotating tool, then transferred to racks for drying, followed by glazing and firing in a kiln.

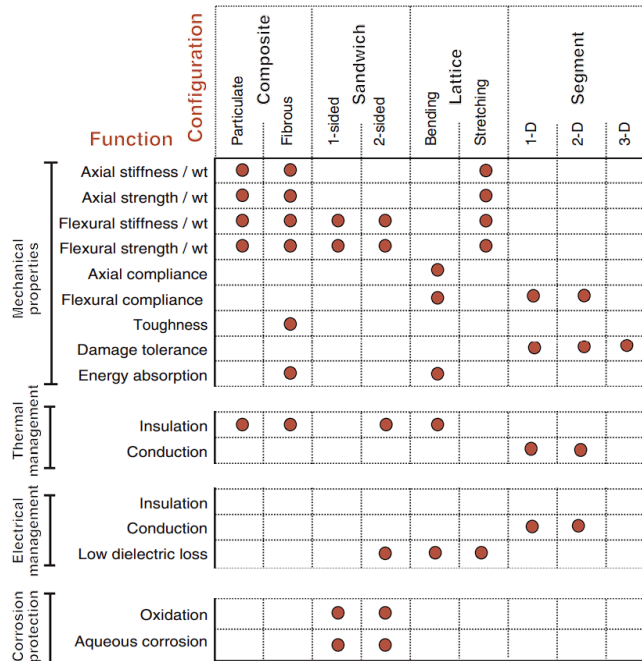
6.6.14. Composite Processing (Composites)

6.6.15. Design Against In-Service Failures

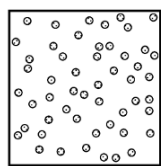
6.6.16. Designing with Hybrid Materials

Hybrid materials (composites, sandwich structures, lattices and segmented structures) can be used when no single material is suitable: hybrid materials fill in the empty spaces of the material property charts. The two materials, configuration and volume fractions are chosen to optimise the goal at hand.

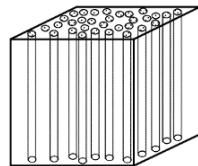
Properties of Hybrid Materials by Topology



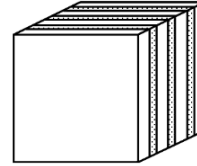
Types of Composites



Particulate



Fibre



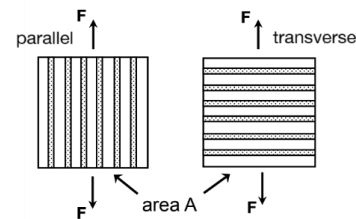
Laminate

Theoretical Ranges on Physical Properties (Voigt-Reuss equations)

Composite property	Lower bound	Upper bound
Young's modulus, E	$\left(\frac{V_f}{E_f} + \frac{1-V_f}{E_m}\right)^{-1}$	$V_f E_f + (1 - V_f)E_m$
Tensile strength, σ_{ts}	$\sigma_y^{(m)}\left(1 + \frac{\sqrt{f}}{16(1-\sqrt{f})}\right)$	$V_f \sigma_f^{(f)} + (1 - V_f)\sigma_y^{(m)}$
Thermal expansion coefficient, α	$\frac{E_f \alpha_f V_f + E_m \alpha_m (1 - V_f)}{E_f V_f + E_m (1 - V_f)}$	$\alpha_f V_f (1 + \nu_f) + \alpha_m (1 - V_f) (1 + \nu_m) - \alpha_{min} (V_f \nu_f + (1 - V_f) \nu_m)$
Thermal conductivity, λ	$\lambda_m \left(\frac{\lambda_f + 2\lambda_m - 2V_f(\lambda_m - \lambda_f)}{\lambda_f + 2\lambda_m + 2V_f(\lambda_m - \lambda_f)}\right)$	$V_f \lambda_f + (1 - V_f)\lambda_m$

Quantities independent of configuration:

- Density, ρ : $\rho = V_f \rho_f + (1 - V_f)\rho_m$
- Specific heat capacity, c_p : $c_p \approx c_v = \frac{1}{\rho} (V_f \rho_f c_p^{(f)} + (1 - V_f)\rho_m c_p^{(m)})$
- Dielectric constant, ϵ : $\epsilon = V_f \epsilon_f + (1 - V_f)\epsilon_m$



($\{m$: matrix, f : fibre}, V_f : volume fraction of fibres.) Anisotropy ratio = $\frac{\text{upper bound}}{\text{lower bound}}$.

For Young's modulus, tensile strength and conductivity, maximum is achieved for parallel fibres, minimum for transverse fibres.

For tensile strength, maximum assumes a continuous ductile matrix with strong reinforcing particles. Other correlations are known for specific configurations.

For conductivity, good interface properties are assumed. Debonding, interfacial layers and large differences in moduli can result in conductivity below the lower bound (reflects phonons, creating an interface impedance, on a structural scale which is shorter than the phonon wavelengths).

For electrical conductivity, correlations are the same as thermal conductivity if **percolation** is absent. For random packing of spheres, the percolation threshold is $p_c = 0.20$. For $V_f \gg p_c$, electrical conductivity is much closer to the maximum. For a random network of fibres of aspect ratio $\beta = L / d$, the percolation threshold falls to $\beta^{-1/2} p_c$.

6.6.17. Designing with Steel

UK Steel designations

There is no internationally agreed system for classifying steels - the current UK system is detailed in British Standard BS970, using 6 digit codes (e.g. 080M40, 304S12).

The first 3 numbers relate to the class of steel:

- 000-199: C steels, C-Mn steels (the figures give the mean Mn content, from 0-1.99%)
- 200-240: Free machining steels (2nd & 3rd figures indicate sulphur content, from 0-0.4%)
- 250: Spring steels (Si-Mn steels)
- 300-499: Stainless, Heat-resisting and Valve steels
- 500-999 Alloy steels (subdivided by main alloy types, e.g. Ni-Cr, Ni-Cr-Mo etc)

The character refers to the supply conditions, or indicates stainless steel: A = chemical composition only, H = hardenability requirements given, M = mechanical requirements given, S = stainless steel. The last 2 numbers give the mean carbon content, for A, H and M steels (from 0-0.99%).

Example: 080M40 = 0.8% Mn, 0.4% carbon steel with specified composition and properties

Many product forms are also covered by British Standards, e.g. steel sheet, forgings, reinforcing bar etc. The national steel trade association, UK Steel, maintains a data handbook for all steels available in the UK (over 1000 specifications).

6.6.17. Designing with Concrete (Reinforced Concrete and Prestressed Concrete)

For standard codes of concrete construction in civil engineering, see Section 6.4.6.

Concrete is a cheap, durable and versatile material used for static structures, composed of water, sand (fine aggregate), gravel (coarse aggregate) and cement. A typical mix (by mass) is cement : sand : gravel = 1 : 2 : 3. For concrete beams, 1 : 1.5 : 3 is often used. It is very strong in compression but weak in tension (fails by fracture).

Portland cement is made by crushing and roasting a mixture of limestone (CaCO_3), clay or shale (provides SiO_2 and Al_2O_3) and iron ore (Fe_2O_3). The limestone decomposes to lime (CaO , releasing CO_2), which then reacts to form a variety of silicates and aluminosilicates in the clinker.

For large outdoor concrete structures e.g. patios, supports, the ground must be suitably prepared, by removing grass and organic matter (topsoil), flattening and compacting the soil (subgrade). A base layer of stone/gravel provides support, and a wooden formwork around the perimeter helps maintain the shape. After pouring the concrete mix, spread and level with a screed, and leave to cure with plenty of moisture (e.g. wet burlap) for 28 days for maximum strength. When choosing location, consider rainwater runoff and drainage, as concrete is impermeable.

Concrete is non-flammable and fire-resistant but degrades at very high temperatures (not fireproof), as heat can reverse the curing reactions in the binder (cement), losing mass from water evaporation, dropping the compressive strength. In RC, the steel may also debond, fail or melt, losing tensile strength entirely, as well as concrete cracking from differential thermal expansion. At lower temperatures ($\sim 300^\circ\text{C}$), spalling can occur as water-filled pores evaporate. Refractory cement, using crushed firebrick (grog) and corundum aggregates, can be used for better fire resistance.

Reinforced Concrete (RC)

Steel rebar is used to provide tensile strength, especially at one edge of a beam in bending. The rebars are long and thin hot-rolled carbon steel cylinders. Glass fibre reinforced plastic (GFRP, fibreglass) can alternatively be used as the rebar material to make GFRC which is more lightweight than steel RC.

Prestressed Concrete (PC)

To reduce crack formation in the tensile side of RC, the concrete can be put into compression on its formation. There are two methods:

- Pre-tensioning: rebars (tendons) placed in tension in hydraulic jacks, and the concrete is poured around the rebars. Once cured, the tension is released, compressing the concrete.
- Post-tensioning: rebars pulled in tension and cured concrete compressed simultaneously.

6.6.18. Designing with Wood (Lumber, Timber, Glulam, Plywood, Veneer)**Classifications of Wood**

Hardwood comes from the logging of angiosperm trees (fruit-bearing plants). Softwood comes from the logging of gymnosperm trees (cone-bearing plants).

Lumber is unprocessed wood fibre, typically in beam, plank or board form. Engineered woods are physical or material composites of wood.

Processing of Wood Logs

Logs from trees can be converted into lumber by sawing (cutting with a rip saw), hewing (cutting with an axe) or splitting (cutting with a wedge, knife or froe).

Lumber is often cut to standard dimensions (e.g. 2×4 is a beam with section 50×100 mm).

6.6.19. Prototypical Manufacturing Methods

3D Printing: produces complex shapes by extrusion, typically ~1-20 cm dimensions

Compatible materials: many polymers (e.g. PLA, ABS, nylon, PC, PMMA), polymer composites (e.g. with wood, magnetic powder), carbon fibre, sandstone.

- Design a model of the part using computer aided design software (CAD).
- Save the part as an STL file (.stl), which saves the part as a triangulated mesh.
- Use 3D printing software to import the model. Check the filament material and automatically add supports if necessary. Slice the model to obtain the G-code instruction file (.gcode) for printing.
- Insert a USB thumb drive containing the .gcode file into the 3D printer.
- Check that the nozzle and stage temperatures are set correctly for the material.
- Start the print job; collect from the stage once finished.

Laser Cutting: produces flat shapes from thin soft materials (e.g. up to 5 mm plywood)

Compatible materials: wood, some polymers, cardboard, foam, fabric, thin metal sheets. Glass can be engraved but not be cut. Always check whether a specific polymer can be laser cut: some release toxic fumes (e.g. chlorine, hydrogen cyanide) due to photochemical breakdown of the polymer.

- Design a drawing of the part and save as a DXF file (.dxf).

Plasma Cutting: produces flat shapes from thicker metal pieces (e.g. up to 15 mm steel)

Welding

Mills and Lathes (Manual and CNC-Operated):

Printed Circuit Board (PCB) Fabrication

6.7.20. Mechanics of Materials Data

Metals, Alloys and Ceramics:

		Melting or softening temperature, T_m (°C)		Density, ρ (Mg m ⁻³)		Young's modulus, E (GPa)		Yield stress, σ_y (MPa)		Tensile strength, σ_{ts} (MPa)		Fracture toughness (plane strain), K_{IC} (MPa m ^{1/2})		
		Lower	Upper	Lower	Upper	Lower	Upper	Lower	Upper	Lower	Upper	Lower	Upper	
Metals	Cast irons	1130	1250	7.05	7.25	165	180	215	790	350	1000	22	54	
	Ferrous	High carbon steels	1289	1478	7.8	7.9	200	215	400	1155	550	1640	27	92
	Med carbon steels	1380	1514	7.8	7.9	200	216	305	900	410	1200	12	92	
	Low carbon steels	1480	1526	7.8	7.9	200	215	250	395	345	580	41	82	
	Low alloy steels	1382	1529	7.8	7.9	201	217	400	1100	460	1200	14	200	
	Stainless steels	1375	1450	7.6	8.1	189	210	170	1000	480	2240	62	280	
	Non-ferrous	Aluminium alloys	475	677	2.5	2.9	68	82	30	500	58	550	22	35
Copper alloys	982	1082	8.93	8.94	112	148	30	500	100	550	30	90		
Lead alloys	322	328	10	11.4	12.5	15	8	14	12	20	5	15		
Magnesium alloys	447	649	1.74	1.95	42	47	70	400	185	475	12	18		
Nickel alloys	1435	1466	8.83	8.95	190	220	70	1100	345	1200	80	110		
Titanium alloys	1477	1682	4.4	4.8	90	120	250	1245	300	1625	14	120		
Zinc alloys	375	492	4.95	7	68	95	80	450	135	520	10	100		
Ceramics														
Glasses	Borosilicate glass	450	602	2.2	2.3	61	64	264	384	22	32	0.5	0.7	
	Glass ceramic	563	1647	2.2	2.8	64	110	750	2129	62	177	1.4	1.7	
	Silica glass	957	1557	2.17	2.22	68	74	110	1600	45	155	0.6	0.8	
	Soda-lime glass	442	592	2.44	2.49	68	72	360	420	31	35	0.55	0.7	
Porous	Brick	927	1227	1.9	2.1	15	30	50	140	7	14	1	2	
	Concrete, typical	927	1227	2.2	2.6	15	25	32	60	2	6	0.35	0.45	
	Stone	1227	1427	2.5	3	20	60	34	248	5	17	0.7	1.5	
Technical	Alumina	2004	2096	3.5	3.98	215	413	690	5500	350	665	3.3	4.8	
	Aluminium nitride	2397	2507	3.26	3.33	302	348	1970	2700	197	270	2.5	3.4	
	Boron carbide	2372	2507	2.35	2.55	400	472	2583	5687	350	560	2.5	3.5	
	Silicon	1407	1412	2.3	2.35	140	155	3200	3460	160	180	0.83	0.94	
	Silicon carbide	2152	2500	3	3.21	300	460	1000	5250	370	680	2.5	5	
	Silicon nitride	2388	2496	3	3.29	280	310	524	5500	690	800	4	6	
Tungsten carbide	2827	2920	15.3	15.9	600	720	3347	6833	370	550	2	3.8		

Notes:

- For glasses, T_m is given as the glass transition temperature, above which the material properties degrade rapidly.
- For ceramics, σ_y is given as the compression strength (about ~10 times yield in tension).

Composites, Natural Materials and Polymers:

		Melting or softening temperature, T_m (°C)		Density, ρ (Mg m ⁻³)		Young's modulus, E (GPa)		Yield stress, σ_y (MPa)		Tensile strength, σ_{ts} (MPa)		Fracture toughness (plane strain), K_{IC} (MPa m ^{1/2})		
		Lower	Upper	Lower	Upper	Lower	Upper	Lower	Upper	Lower	Upper	Lower	Upper	
Composites	Metal	Al/SiC	525	627	2.66	2.9	81	100	280	324	290	365	15	24
	Polymer	CFRP	(decomposes)		1.5	1.6	69	150	550	1050	550	1050	6.1	88
		GFRP	(decomposes)		1.75	1.97	15	28	110	192	138	241	7	23
Natural														
	Bamboo	77	102	0.6	0.8	15	20	35	44	36	45	5	7	
	Cork	77	102	0.12	0.24	0.013	0.05	0.3	1.5	0.5	2.5	0.05	0.1	
	Leather	107	127	0.81	1.05	0.1	0.5	5	10	20	26	3	5	
	Wood, longitudinal	77	102	0.6	0.8	6	20	30	70	60	100	5	9	
	Wood, transverse	77	102	0.6	0.8	0.5	3	2	6	4	9	0.5	0.8	
Polymers														
Elastomer	Butyl rubber	-73	-63	0.9	0.92	0.001	0.002	2	3	5	10	0.07	0.1	
	EVA	-73	-23	0.945	0.955	0.01	0.04	12	18	16	20	0.5	0.7	
	Isoprene	-83	-78	0.93	0.94	0.0014	0.004	20	25	20	25	0.07	0.1	
	Natural rubber	-78	-63	0.92	0.93	0.0015	0.0025	20	30	22	32	0.15	0.25	
	Neoprene	-48	-43	1.23	1.25	0.0007	0.002	3.4	24	3.4	24	0.1	0.3	
	Polyurethane (elPU)	-73	-23	1.02	1.25	0.002	0.003	25	51	25	51	0.2	0.4	
	Silicones	-123	-73	1.3	1.8	0.005	0.02	2.4	5.5	2.4	5.5	0.03	0.5	
Thermo-plastic	ABS	88	128	1.02	1.21	1.1	2.9	18.5	51	27.6	55.2	1.19	4.3	
	Cellulose polymers	-9	107	0.98	1.3	1.6	2	25	45	25	50	1	2.5	
	Ionomer (I)	27	77	0.93	0.96	0.2	0.424	8.3	15.9	17.2	37.2	1.14	3.43	
	Nylons (PA)	44	56	1.12	1.14	2.62	3.2	50	94.8	90	165	2.22	5.62	
	Polycarbonate (PC)	142	205	1.14	1.21	2	2.44	59	70	60	72.4	2.1	4.6	
	PEEK	143	199	1.3	1.32	3.5	4.2	65	95	70	103	2.73	4.3	
	Polyethylene (PE)	-25	-15	0.939	0.96	0.621	0.896	17.9	29	20.7	44.8	1.44	1.72	
	PET	68	80	1.29	1.4	2.76	4.14	56.5	62.3	48.3	72.4	4.5	5.5	
	Acrylic (PMMA)	85	165	1.16	1.22	2.24	3.8	53.8	72.4	48.3	79.6	0.7	1.6	
	Acetal (POM)	-18	-8	1.39	1.43	2.5	5	48.6	72.4	60	89.6	1.71	4.2	
	Polypropylene (PP)	-25	-15	0.89	0.91	0.896	1.55	20.7	37.2	27.6	41.4	3	4.5	
	Polystyrene (PS)	74	110	1.04	1.05	2.28	3.34	28.7	56.2	35.9	56.5	0.7	1.1	
	Polyurethane (tpPU)	120	160	1.12	1.24	1.31	2.07	40	53.8	31	62	1.84	4.97	
	PVC	75	105	1.3	1.58	2.14	4.14	35.4	52.1	40.7	65.1	1.46	5.12	
	Teflon (PTFE)	107	123	2.14	2.2	0.4	0.552	15	25	20	30	1.32	1.8	
Thermosets	Epoxies	(decomposes)		1.11	1.4	2.35	3.075	36	71.7	45	89.6	0.4	2.22	
	Phenolics	(decomposes)		1.24	1.32	2.76	4.83	27.6	49.7	34.5	62.1	0.79	1.21	
	Polyester	(decomposes)		1.04	1.4	2.07	4.41	33	40	41.4	89.6	1.09	1.70	

Notes:

- For polymers, T_m is given as the glass transition temperature. Material properties degrade rapidly above this.
- Thermosets, CFRP (carbon fibre reinforced composite) and GFRP (glass fibre reinforced composite) decompose when heated rather than melt.
- For applications and full names/abbreviations of polymers, see Section 16.5.1.

Polymer Foams: properties are dependent mainly on the mesh/scaffold geometry.

Foams		Melting or softening temperature, T_m (°C)		Density, ρ (Mg m ⁻³)		Young's modulus, E (GPa)		Yield stress, σ_y (MPa)		Tensile strength, σ_{ts} (MPa)		Fracture toughness (plane strain), K_{IC} (MPa m ^{1/2})	
		Lower	Upper	Lower	Upper	Lower	Upper	Lower	Upper	Lower	Upper	Lower	Upper
Flexible	Very low density (VLD)	112	177	0.016	0.035	0.0003	0.001	0.01	0.12	0.24	0.85	0.005	0.02
	Low density (LD)	112	177	0.038	0.07	0.001	0.003	0.02	0.3	0.24	2.35	0.015	0.05
	Medium density (MD)	112	177	0.07	0.115	0.004	0.012	0.05	0.7	0.43	2.95	0.03	0.09
Rigid	Low density (LD)	67	171	0.036	0.07	0.023	0.08	0.3	1.7	0.45	2.25	0.002	0.02
	Medium density (MD)	67	157	0.078	0.165	0.08	0.2	0.4	3.5	0.65	5.1	0.007	0.049
	High density (HD)	67	171	0.17	0.47	0.2	0.48	0.8	12	1.2	12.4	0.024	0.091

6.6.21. Environmental Resistance and Durability

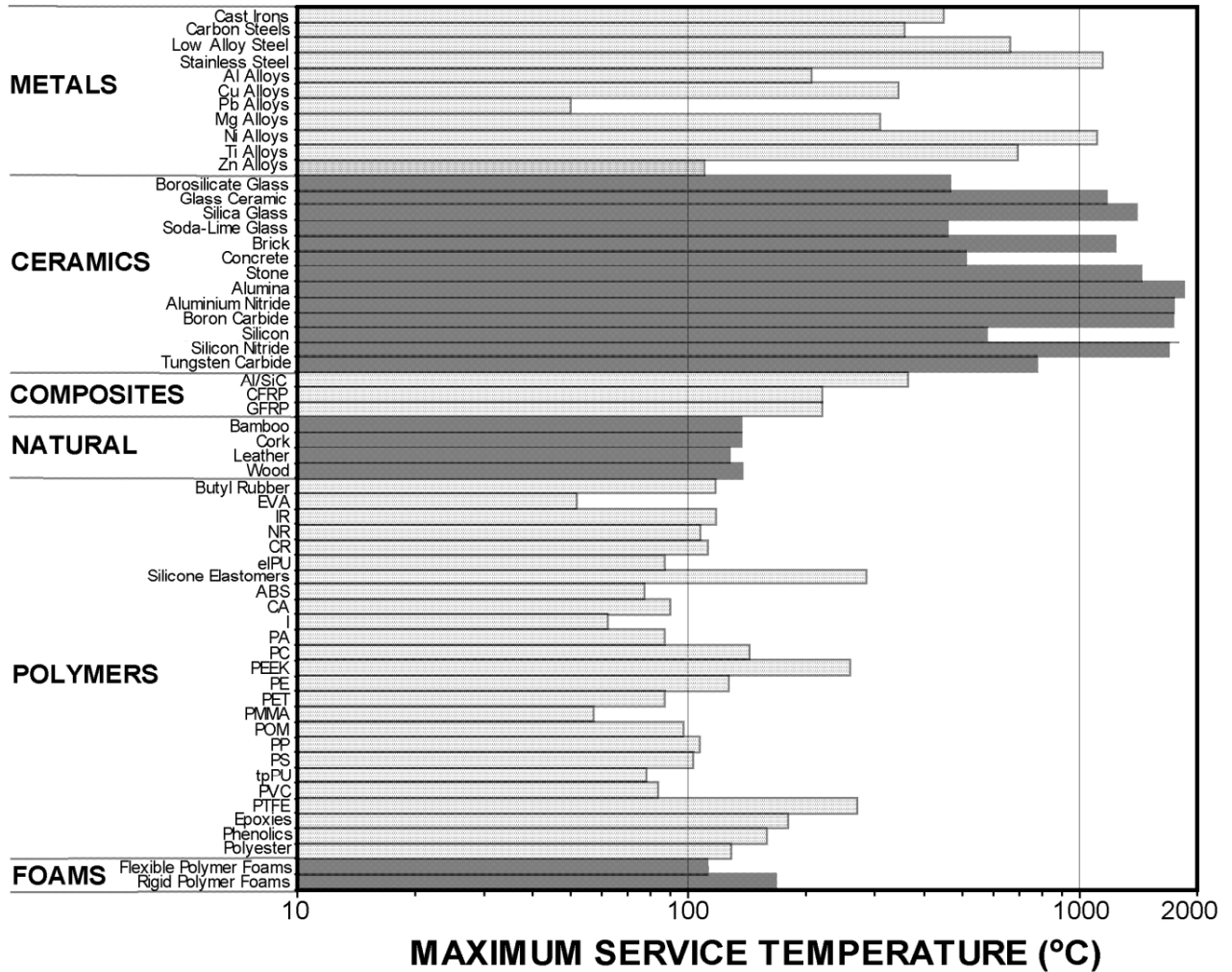
Qualitative assessment of material resilience in **fire, fresh water, salt water, sunlight (UV)** and **wearing** environments. **A** = very good; **B** = good; **C** = average; **D** = poor; **E** = very poor.

		Flammability	Fresh water	Salt water	Sunlight (UV)	Wear resistance			
Metals	Ferrous	Cast Irons	A	B	C	A	A		
		High Carbon Steels	A	B	C	A	A		
		Medium Carbon Steels	A	B	C	A	A		
		Low Carbon Steels	A	B	C	A	A		
		Low Alloy Steels	A	B	C	A	A		
	Non-ferrous	Stainless Steels	A	A	A	A	B		
		Aluminium Alloys	B	A	B	A	C		
		Copper Alloys	A	A	A	A	A		
		Lead Alloys	A	A	A	A	C		
		Magnesium Alloys	A	A	D	A	C		
		Nickel Alloys	A	A	A	A	B		
		Titanium Alloys	A	A	A	A	C		
		Zinc Alloys	A	A	C	A	E		
		Ceramics	Glasses	Borosilicate Glass	A	B	B	A	A
				Glass Ceramic	A	A	A	A	A
Silica Glass	A			A	A	A	B		
Soda-Lime Glass	A			A	A	A	A		
Porous Technical	Brick, Concrete, Stone		A	A	A	A	C		
	Alumina		A	A	A	A	A		
	Aluminium Nitride		A	A	A	A	A		
	Boron Carbide		A	A	A	A	A		
	Silicon		A	A	B	A	B		
	Silicon Carbide		A	A	A	A	A		
	Silicon Nitride		A	A	A	A	A		
	Tungsten Carbide		A	A	A	A	A		
	Composites		Metal Polymer	Aluminium/Silicon Carbide	A	A	B	A	B
				CFRP	B	A	A	B	C
				GFRP	B	A	A	B	C
Natural	Bamboo	D	C	C	B	D			
	Cork	D	B	B	A	B			
	Leather	D	B	B	B	B			
	Wood	D	C	C	B	D			

		Flammability	Fresh water	Salt water	Sunlight (UV)	Wear resistance		
Polymers¹	Elastomer	Butyl Rubber	E	A	A	B	B	
		EVA	E	A	A	B	B	
		Isoprene (IR)	E	A	A	B	B	
		Natural Rubber (NR)	E	A	A	B	B	
		Neoprene (CR)	E	A	A	B	B	
		Polyurethane Elastomers (elPU)	E	A	A	B	B	
		Silicone Elastomers	B	A	A	B	B	
		Thermoplastic	ABS	D	A	A	C	D
			Cellulose Polymers (CA)	D	A	A	B	C
			Ionomer (I)	D	A	A	B	C
	Nylons (PA)		C	A	A	C	C	
	Polycarbonate (PC)		B	A	A	B	C	
	PEEK		B	A	A	A	C	
	Polyethylene (PE)		D	A	A	D	C	
	PET		D	A	A	B	C	
	Acrylic (PMMA)		D	A	A	A	C	
	Acetal (POM)		D	A	A	C	B	
	Thermoset	Polypropylene (PP)	D	A	A	D	C	
		Polystyrene (PS)	D	A	A	C	D	
		Polyurethane Thermoplastics (tpPU)	C	A	A	B	C	
		PVC	A	A	A	A	C	
		Teflon (PTFE)	A	A	A	B	B	
		Epoxies	B	A	A	B	C	
		Phenolics	B	A	A	A	C	
		Polyester	D	A	A	A	C	
		Polymer Foams	Flexible Polymer Foams	E	A	A	C	D
			Rigid Polymer Foams	C	A	A	B	E

6.6.22. Maximum Service Temperature

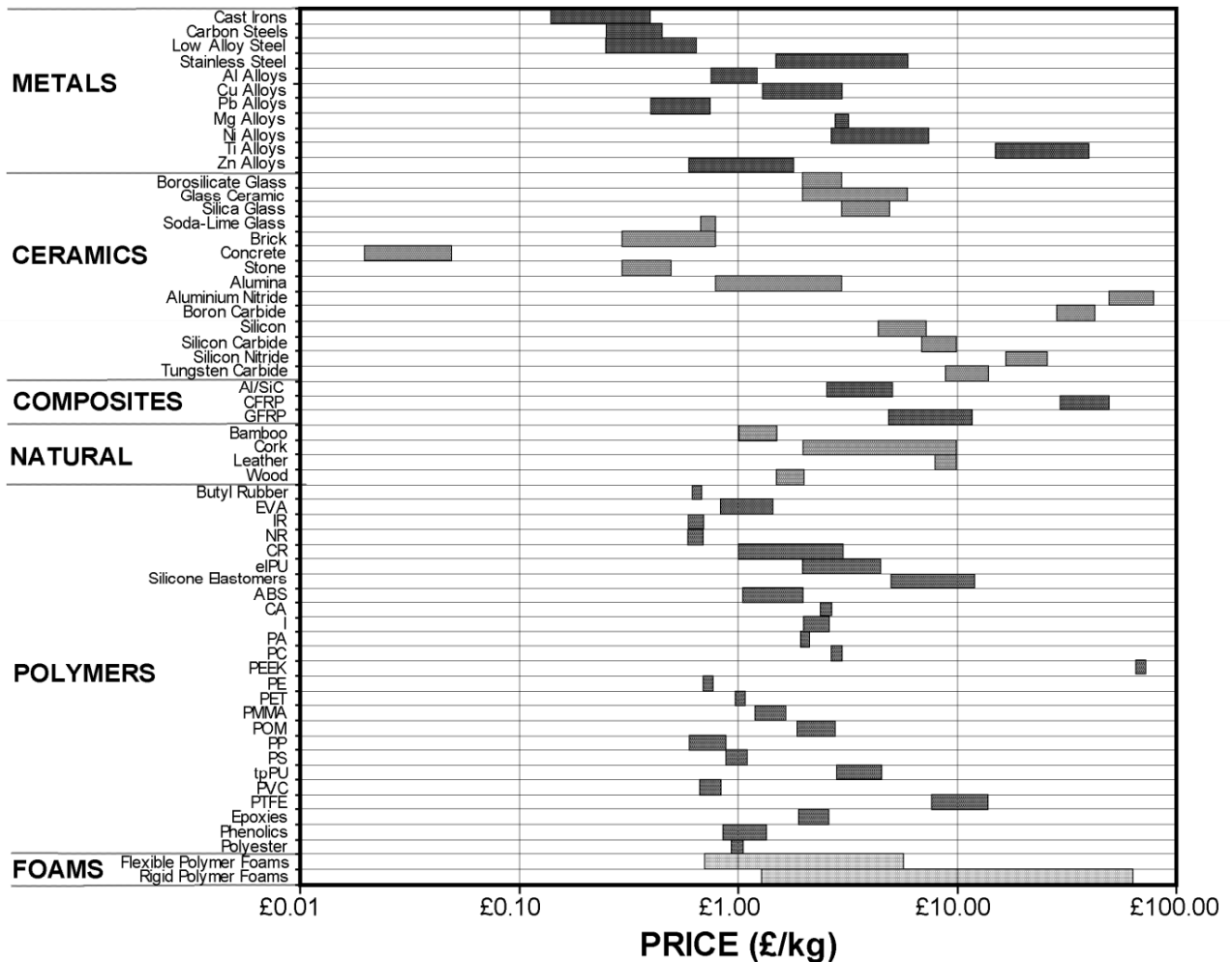
The shaded bars extend to the maximum service temperature – materials may be used safely for all temperatures up to this value, without significant property degradation. Note the logarithmic axis.



There is a modest range of maximum service temperature in a given material class – not all variants within a class may be used up to the temperature shown, so caution should be exercised if a material appears close to its limit.

6.6.23. Material Price

Material price per kg, C_m in £ (GBP). C_m represents raw material price/kg, and does not include manufacturing or end-of-life costs.

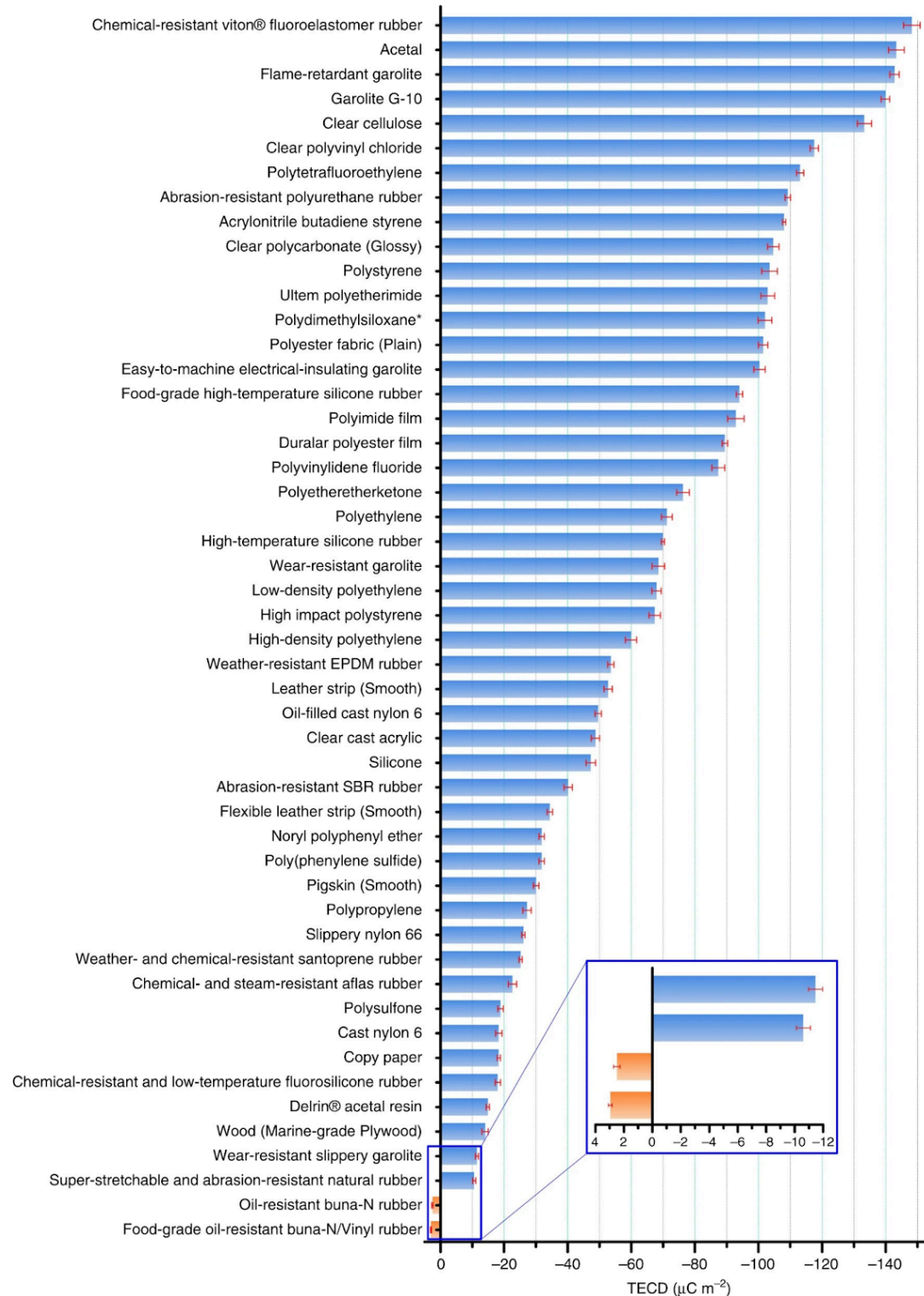


Note that this data is from 2003 and can vary over time due to inflation, currency exchange rates and supply/demand. For these reasons it should be used only for rough comparison between materials and not the raw numerical data.

Note the logarithmic axis.

6.6.24. Triboelectric Effect (Anti-Static Design)

Electrical insulators (ceramics, polymers, natural materials, foams) develop static electric charges on mechanical rubbing. The triboelectric series, quantified by surface charge density (in $\mu\text{C m}^{-2}$), is given.



6.6.25. Main Applications of Materials

Metals:

Metal class	Metal	Applications
Ferrous	Cast irons	Automotive parts, engine blocks, machine tool structural parts, lathe beds
	High carbon steels	Cutting tools, springs, bearings, cranks, shafts, railway track
	Medium carbon steels	General mechanical engineering (tools, bearings, gears, shafts)
	Low carbon steels	Steel structures (“mild steel”) – bridges, oil rigs, ships; rebar for reinforced concrete; automotive parts, car body panels; galvanised sheet; packaging (cans, drums)
	Low alloy steels	Springs, tools, ball bearings, automotive parts (gears connecting rods, etc.)
	Stainless steels	Transport, chemical and food processing plant, nuclear plant, domestic ware (cutlery, washing machines, stoves), surgical implements, pipes, pressure vessels, liquid gas containers
Non-ferrous	Casting aluminium alloys	Automotive parts (cylinder blocks), domestic appliances (irons)
	Non-heat-treatable aluminium alloys	Electrical conductors, heat exchangers, foil, tubes, saucepans, beverage cans, lightweight ships, architectural panels
	Heat-treatable aluminium alloys	Aerospace engineering, automotive bodies and panels, lightweight structures and ships
	Copper alloys	Electrical conductors and wire (oxygen-free copper, OFHC), electronic circuit boards, heat exchangers, boilers, cookware, coinage, sculptures
	Lead alloys	Roof and wall cladding, solder, X-ray shielding, battery electrodes
	Magnesium alloys	Automotive castings, wheels, general lightweight castings for transport, nuclear fuel containers; principal alloying addition to aluminium alloys
	Nickel alloys	Gas turbines and jet engines, thermocouples, coinage; alloying addition to austenitic stainless steels
	Titanium alloys	Aircraft turbine blades; general structural aerospace applications; biomedical implants.
	Zinc alloys	Die castings (automotive, domestic appliances, toys, handles); coating on galvanised steel

Ceramics, Natural Materials and Composites:

Ceramic class	Ceramic	Applications
Glasses	Borosilicate glass	Ovenware, laboratory ware, headlights
	Glass ceramic	Cookware, lasers, telescope mirrors
	Silica glass	High performance windows, crucibles, high temperature applications
	Soda-lime glass	Windows, bottles, tubing, light bulbs, pottery glazes
Porous	Brick	Buildings
	Concrete	General civil engineering construction
	Stone	Buildings, architecture, sculpture
Technical	Alumina	Cutting tools, spark plugs, microcircuit substrates, valves
	Aluminium nitride	Microcircuit substrates and heat sinks
	Boron carbide	Lightweight armour, nozzles, dies, precision tool parts
	Silicon	Microcircuits, semiconductors, precision instruments, IR windows, MEMS
	Silicon carbide	High temperature equipment, abrasive polishing grits, bearings, armour
	Silicon nitride	Bearings, cutting tools, dies, engine parts
	Tungsten carbide	Cutting tools, drills, abrasives

Natural Material	Applications
Bamboo	Building, scaffolding, paper, ropes, baskets, furniture
Cork	Corks and bungs, seals, floats, packaging, flooring
Leather	Shoes, clothing, bags, drive-belts
Wood	Construction, flooring, doors, furniture, packaging, sports goods

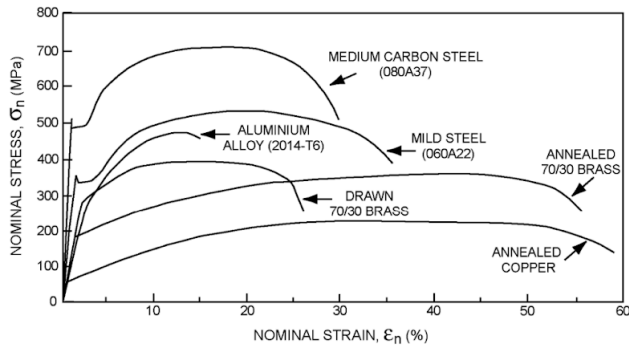
Composite class	Composite	Applications
Metal	AlSiC	Automotive parts, sports goods
Polymer	CFRP	Lightweight structural parts (aerospace, bike frames, sports goods, boat hulls and oars, springs)
	GFRP	Boat hulls, automotive parts, chemical plants, glass fibre reinforced concrete

Polymers and Foams

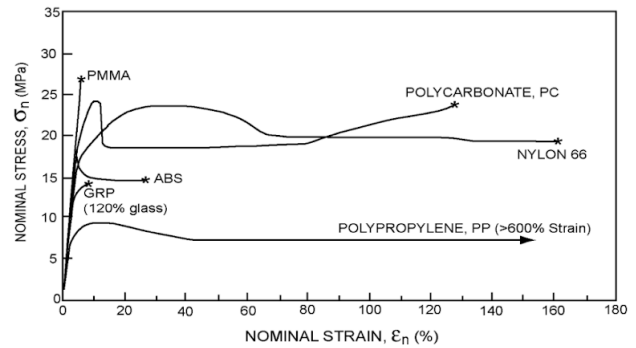
Polymer Class	Polymer	Abbr.	Applications
Elastomers	Butyl rubber		Tyres, seals, anti-vibration mountings, electrical insulation, tubing
	Ethylene-vinyl-acetate	EVA	Bags, films, packaging, gloves, insulation, running shoes
	Isoprene	IR	Tyres, inner tubes, insulation, tubing, shoes
	Natural rubber	NR	Gloves, tyres, electrical insulation, tubing
	Neoprene	CR	Wetsuits, O-rings and seals, footwear
	Polyurethane	el-PU	Packaging, hoses, adhesives, fabric coating
	Silicone		Electrical insulation, electronic encapsulation, medical implants
Thermo-plastics	Acrylonitrile butadiene styrene	ABS	Communication appliances, automotive interiors, luggage, toys, boats
	Cellulose polymers	CA	Tool and cutlery handles, decorative trim, pens
	Ionomers	I	Packaging, golf balls, blister packs, bottles
	Polyamides (nylons)	PA	Gears, bearings, plumbing, packaging, bottles, fabrics, textiles, ropes
	Polycarbonates	PC	Safety goggles, shields, helmets, light fittings, medical components
	Polyetheretherketone	PEEK	Electrical connectors, racing car parts, fibre composites
	Polyethylene	PE	Packaging, bags, squeeze tubes, toys, artificial joints
	Polyethylene terephthalate	PET	Blow moulded bags, film, audio/video tape, sails
	Polymethyl methacrylate (acrylic)	PMMA	Aircraft windows, 3D printer ink, lenses, reflectors, lights, CDs
	Polyoxymethylene (acetal)	POM	Zips, domestic and appliance parts, handles
	Polypropylene	PP	Ropes, garden furniture, pipes, kettles, electrical insulation, astroturf
	Polystyrene	PS	Toys, packaging, cutlery, audio cassette/CD cases
	Polyurethane	tp-PU	Cushioning, seating, shoe soles, hoses, car bumpers, insulation
	Polyvinylchloride	PVC	Pipes, gutters, window frames, packaging
Polytetrafluoroethylene (Teflon)	PTFE	Non-stick coatings, bearings, skis, electrical insulation, tape	
Thermo-sets	Epoxies	EP	Adhesives, fibre composites, electronic encapsulation
	Phenolics	PHEN	Electrical plugs, sockets, cookware, handles, adhesives
	Polyester	PEST	Furniture, boats, sports goods

Polymer Foam	Applications
Flexible polymer foam	Packaging, buoyancy, cushioning, sponges, sleeping mats
Rigid polymer foam	Thermal insulation, sandwich panels, packaging, buoyancy

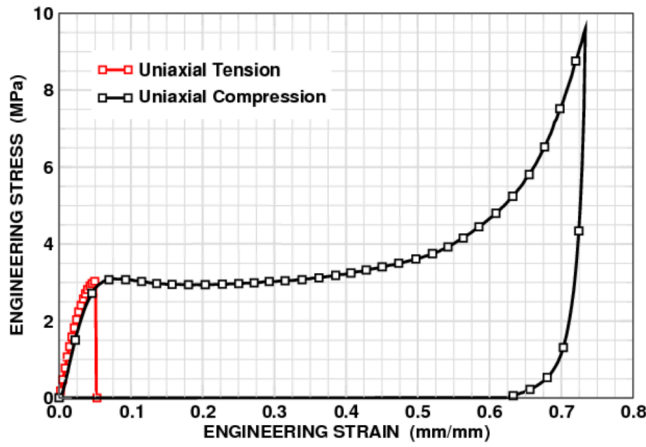
6.6.25. Uniaxial Tensile Response (Stress-Strain) Curves



Metals and Alloys



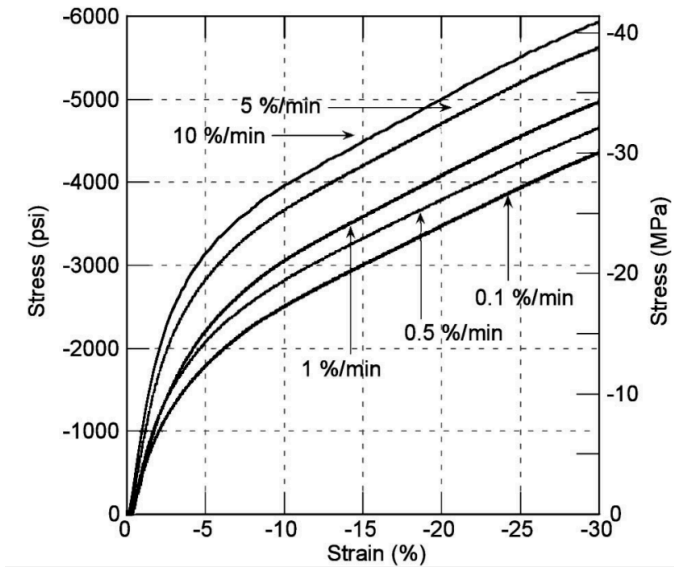
Polymers



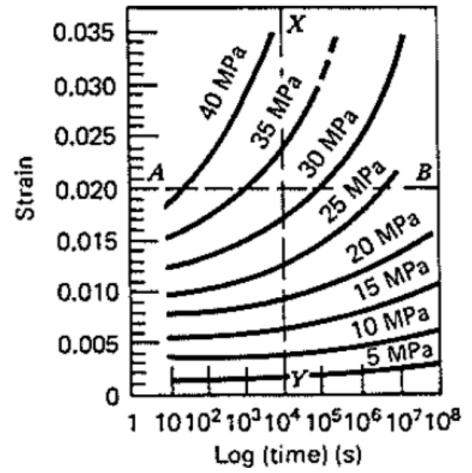
Polyurethane Foam, $\rho = 176 \text{ kg m}^{-3}$

6.6.26. Viscoelastic Stress-Strain Responses of Polymeric Materials

Data recorded at 25 °C.



HDPE (high-density polyethylene)

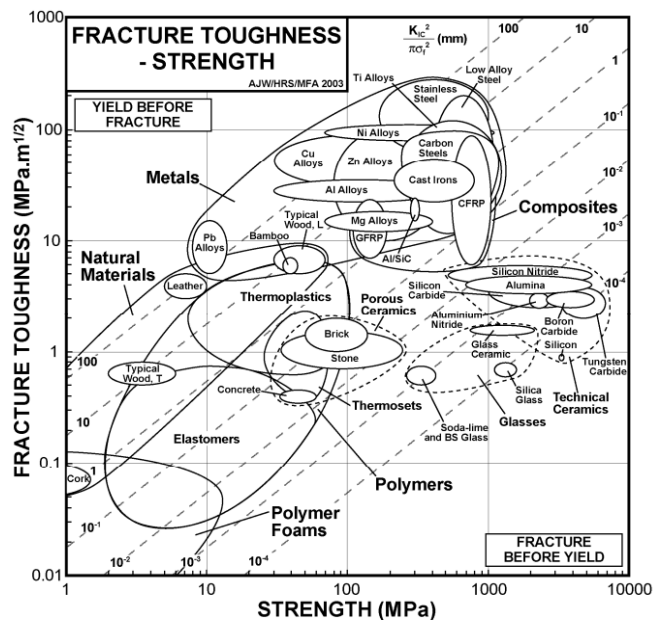
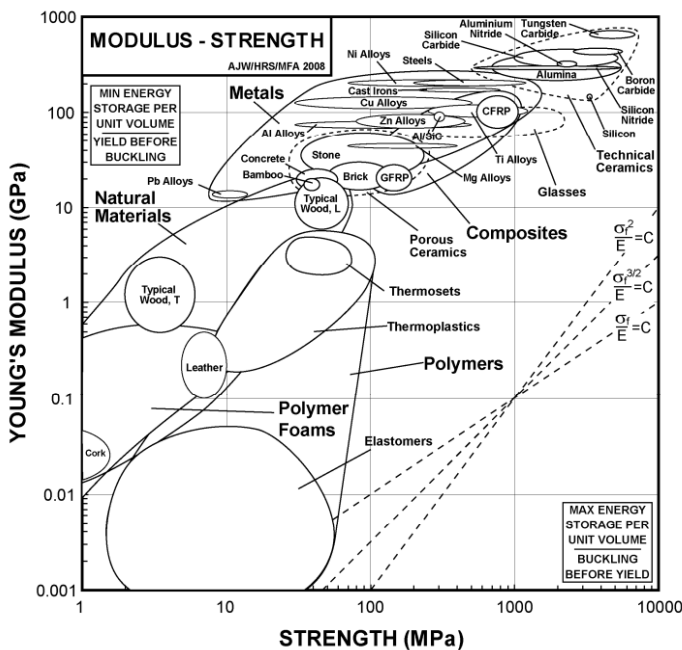
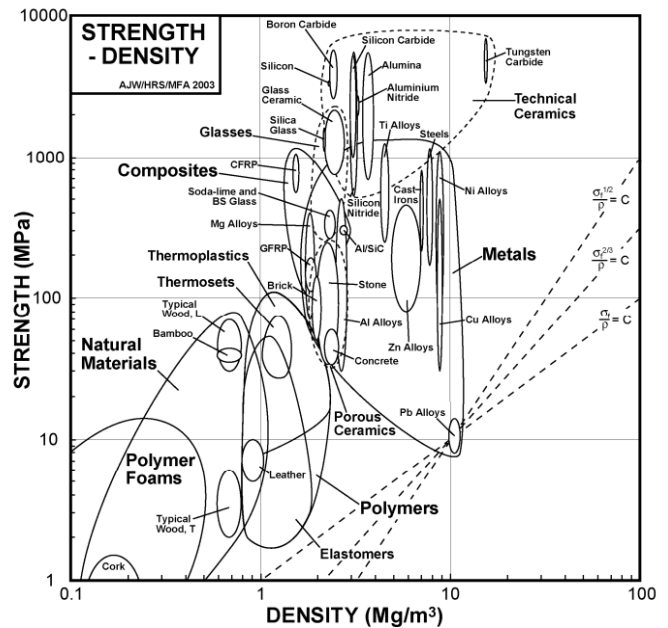
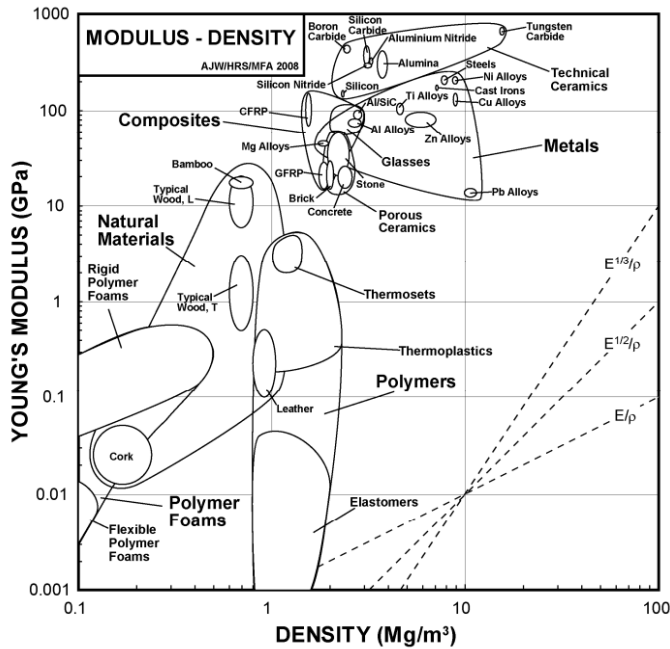


PVC (polyvinyl chloride)

For the high-temperature creep response of materials, see Section 6.6.6.

6.6.27. Material Property Charts for Performance-Limited Design

Materials can be ranked using various performance indices based on the charts below.

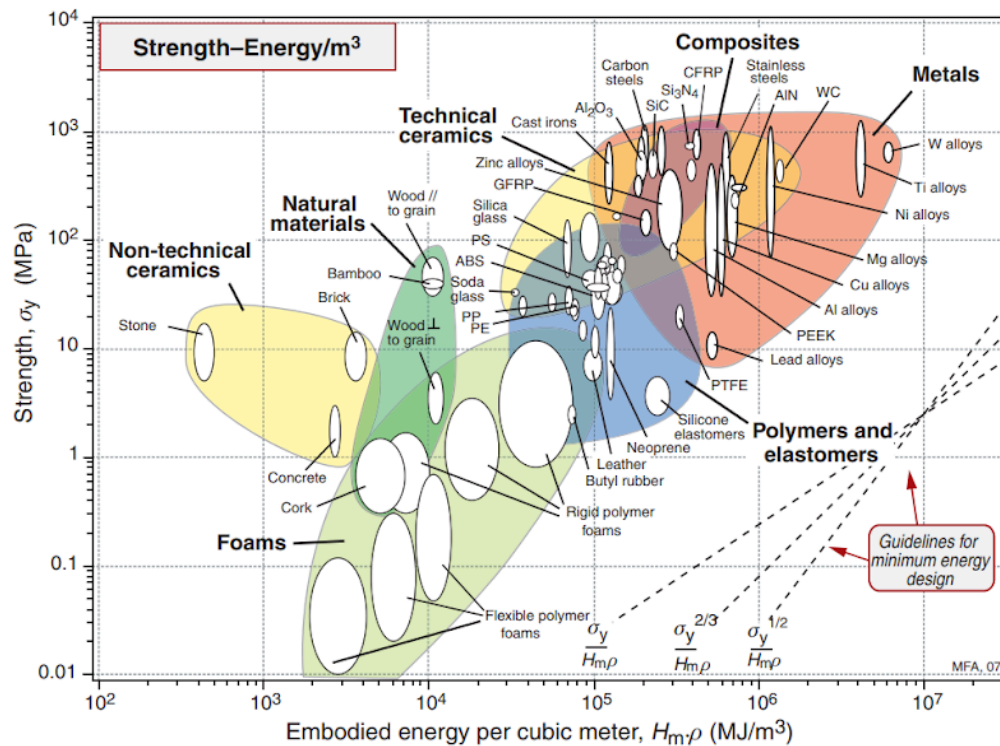
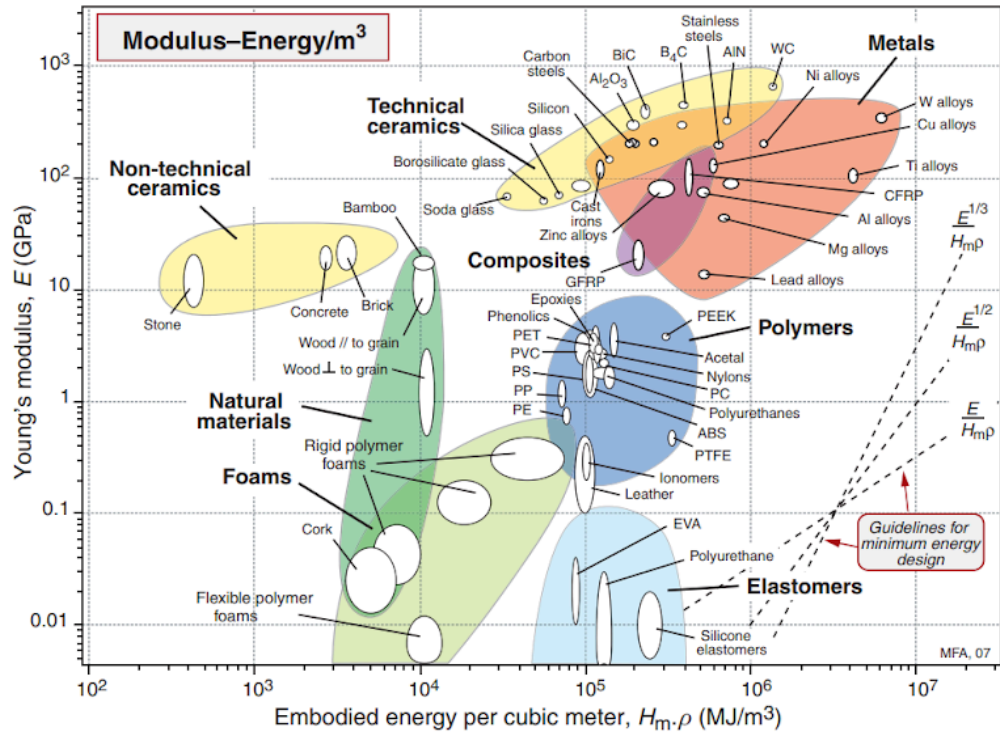


Failure strength is defined as the tensile elastic limit (usually yield stress) for all materials other than ceramics, for which it is the compressive strength.

The contours on the fracture toughness-strength graph represent process zone size, as per the definition in Section 6.6.2 (plane stress).

6.6.28. Material Property Charts for Energy-Limited Design

H_m : embodied energy per unit mass; ρH_m : embodied energy per unit volume.



6.6.29. Material Process Compatibility

Material processing techniques compatible with various materials are shown with • .

For metals:

Metals		Sand Casting	Die Casting	Investment Casting	Rolling/ Forging	Extrusion	Sheet Forming	Powder Methods	Machining
Ferrous	Cast Irons	•	•	•					
	Medium/High Carbon Steels	•		•	•			•	•
	Low Carbon Steels	•		•	•		•	•	•
	Low Alloy/Stainless Steels	•	•	•	•		•	•	•
Non-ferrous	Aluminium, Copper, Lead, Magnesium, Zinc Alloys	•	•	•	•	•	•	•	•
	Nickel Alloys	•	•	•	•		•	•	•
	Titanium Alloys		•		•	•	•	•	•

For polymers:

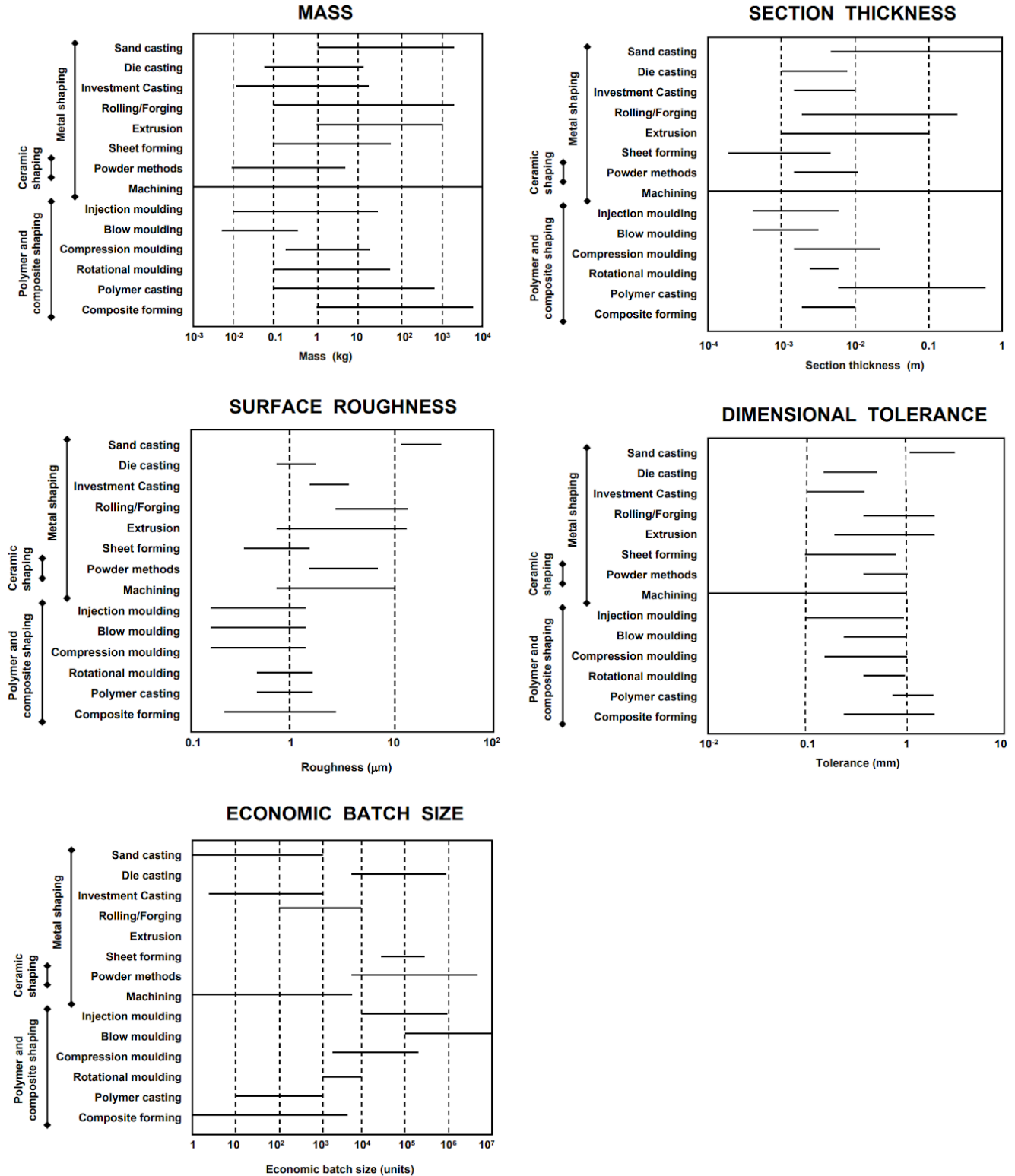
Polymers	Machining	Injection Moulding	Blow Moulding	Compression Moulding	Rotational Moulding	Polymer Casting	Composite Forming
Elastomers	•			•	•		
Thermoplastics	•	•	•	•	•		
Thermosets				•	•	•	•
Polymer Foams	•	•			•		

For other materials:

- Ceramics are all processed by powder compaction methods, and Glasses are also moulded. Both are difficult to machine.
- Polymer Composites are shaped by dedicated forming techniques, and are difficult to machine.
- Natural Materials can only be machined, though some woods are also hot formed.

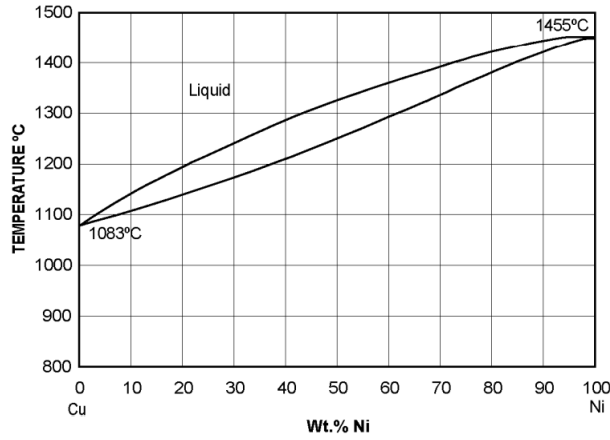
6.6.30. Attribute Charts for Shaping Processes

Typical attainable ranges are specified.

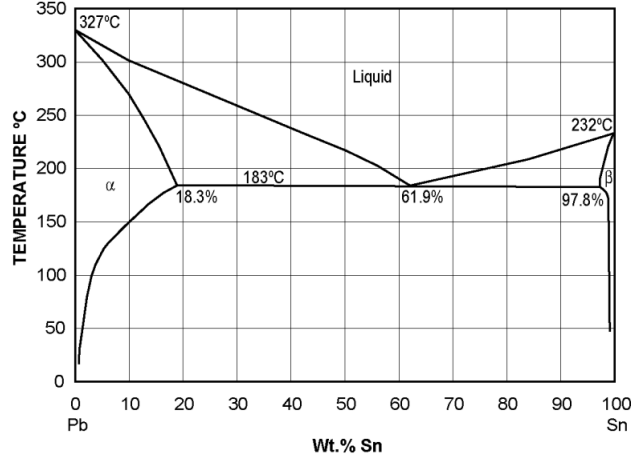


6.6.31. Binary Phase Diagrams Involving Metals

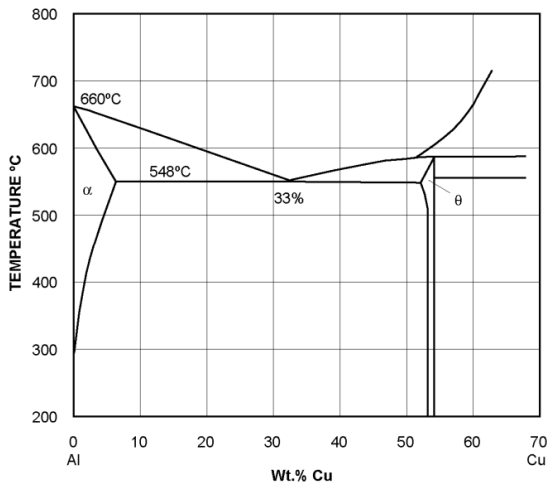
Copper-Nickel (Cu-Ni)



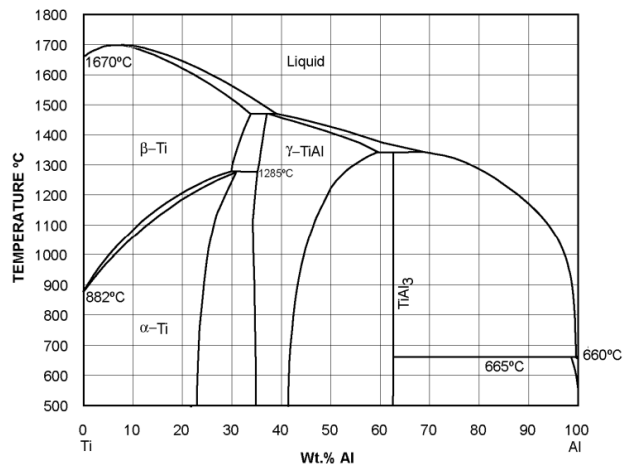
Lead-Tin (Pb-Sn)



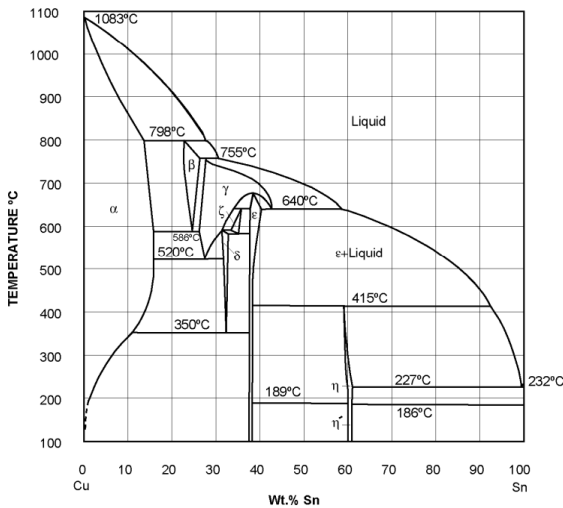
Aluminium-Copper (Al-Cu)



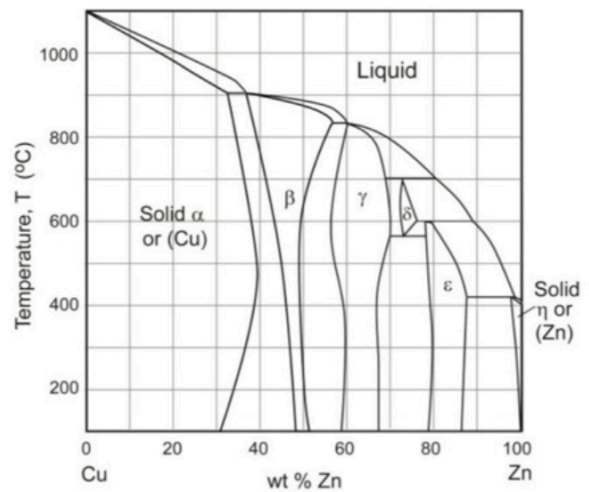
Titanium-Aluminium (Ti-Al)



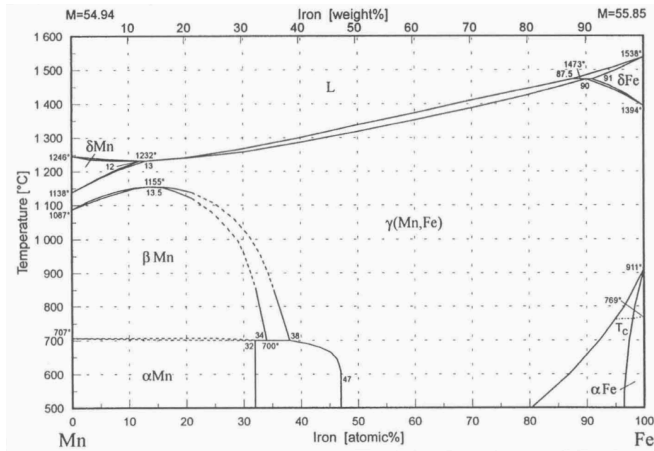
Copper-Tin (Cu-Sn)



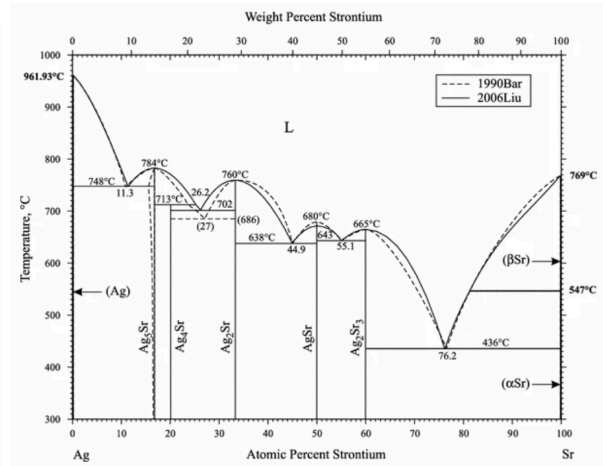
Copper-Zinc (Cu-Zn)



Manganese-Iron (Mn-Fe)



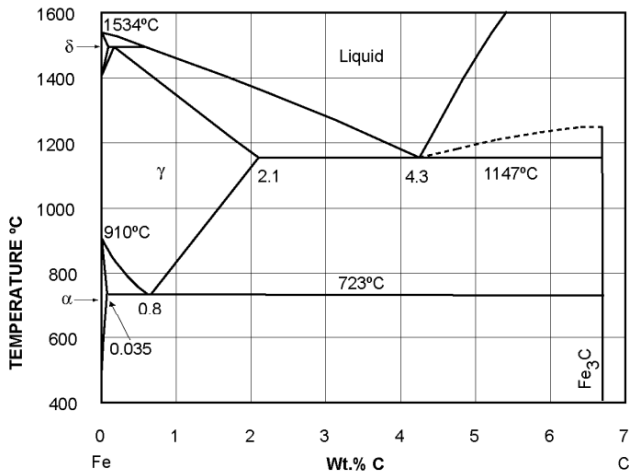
Silver-Strontium (Ag-Sr)



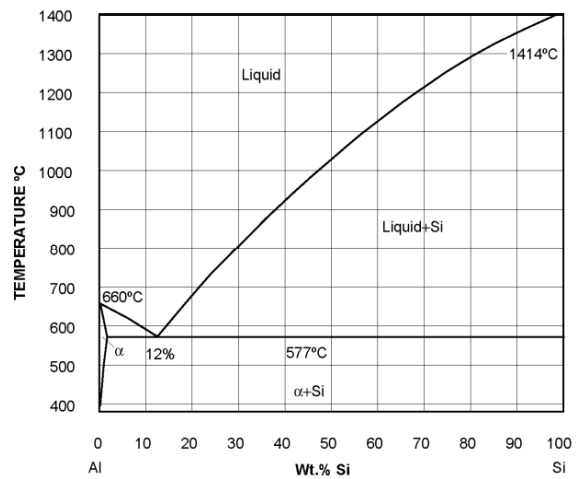
6.6.32. Binary Phase Diagrams Involving Non-Metals

* For a more detailed phase diagram for the iron-carbon system, see Section 6.6.15.

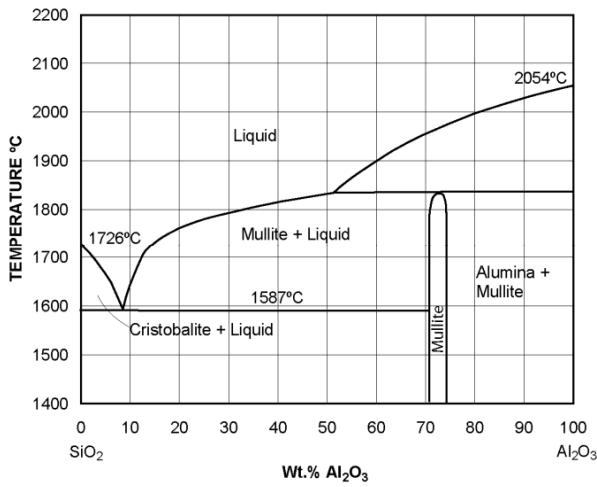
Iron-Carbon (Fe-C)*



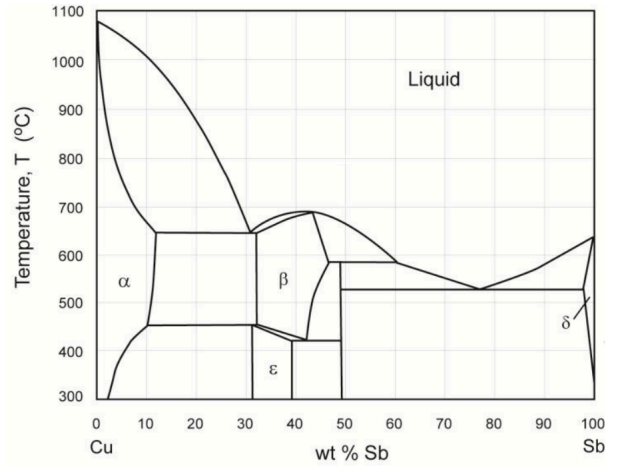
Aluminium-Silicon (Al-Si)



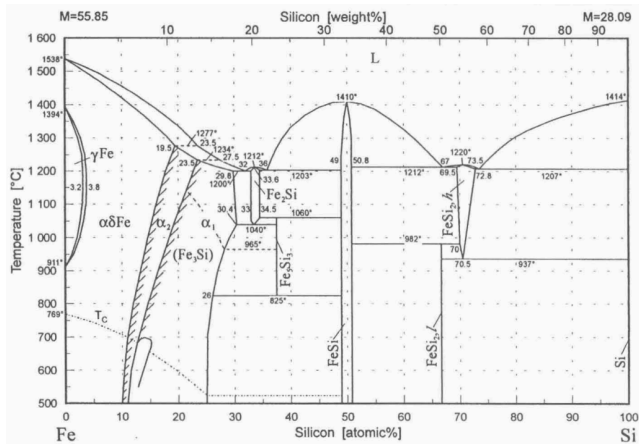
Silica-Alumina ($\text{SiO}_2\text{-Al}_2\text{O}_3$)



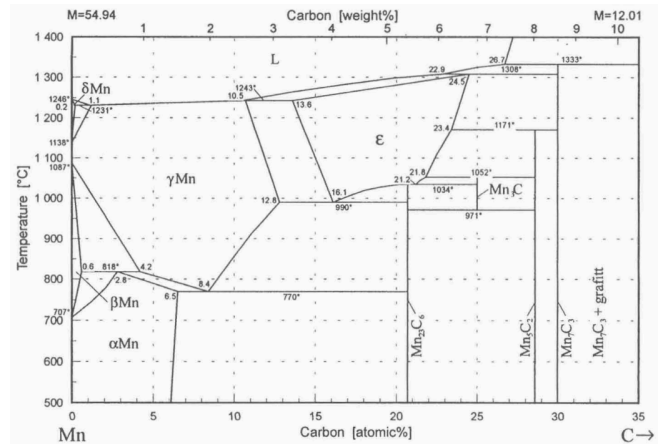
Copper-Antimony (Cu-Sb)



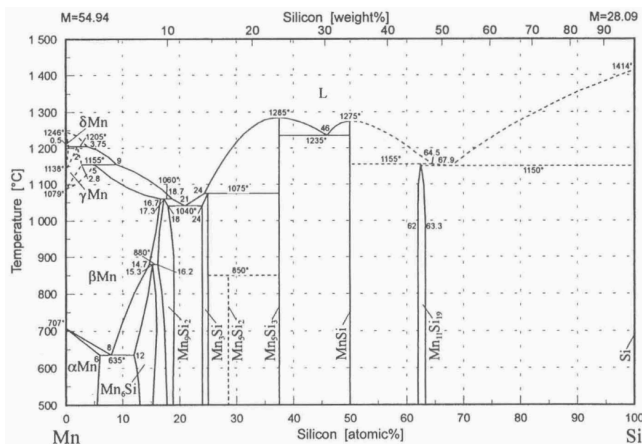
Iron-Silicon (Fe-Si)



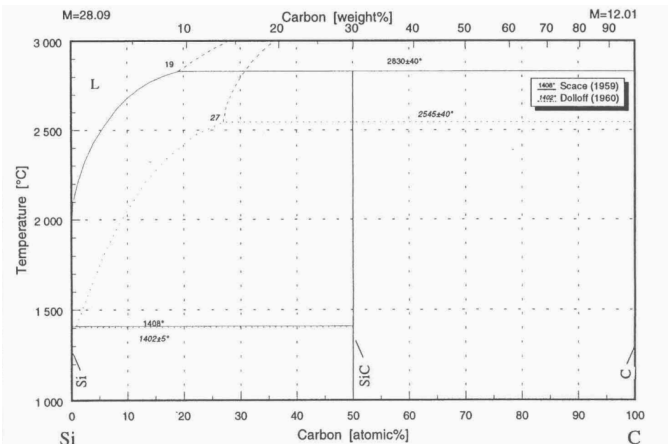
Manganese-Carbon (Mn-C)



Manganese-Silicon (Mn-Si)

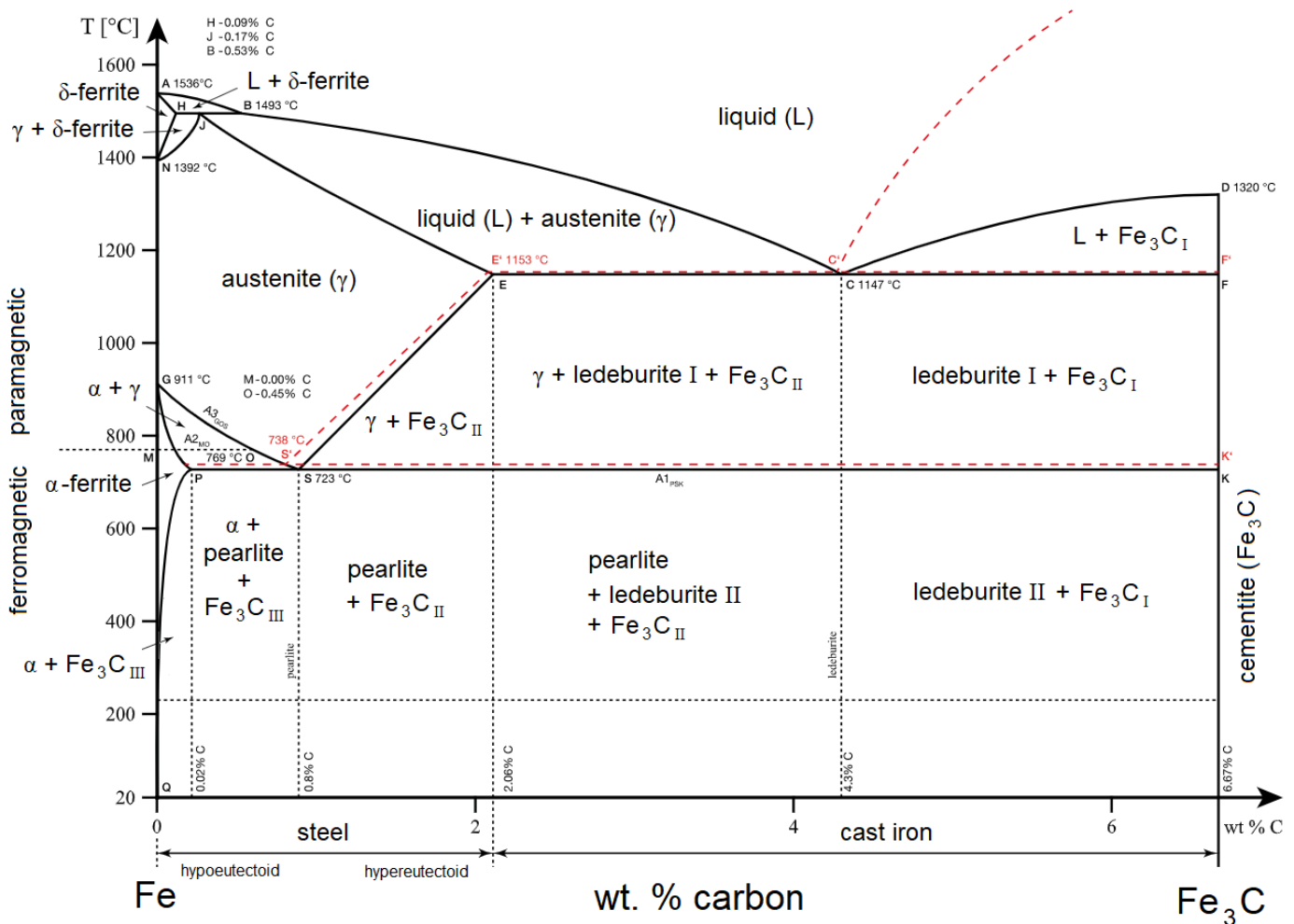


Silicon-Carbon (Si-C)



6.6.33. Equilibrium Microstructural Classification of Steels by Phase Composition

Phase diagram showing equilibrium microstructure, including the phases of pure Fe (ferrite (α , BCC), austenite (γ , FCC) and δ -iron (δ , BCC)), as well as ledeburite (fibrous $\alpha + \text{Fe}_3\text{C}$), pearlite (lamellar $\alpha + \text{Fe}_3\text{C}$) and cementite (Fe_3C). Compositions beyond cementite will form graphite (pure C), which are not shown.



The key labelled points and lines on the above phase diagram are:

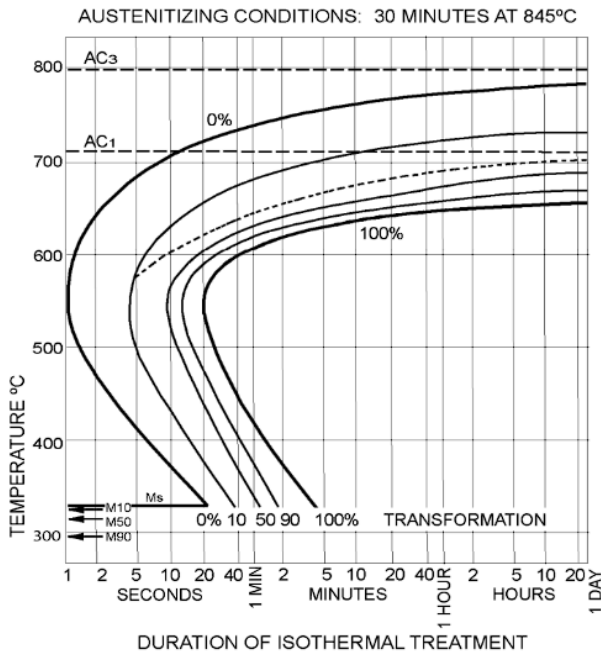
- | | | |
|-----------------------------------|------------------------------|---------------------------|
| A: melting point of pure Fe | ABCD: liquidus line | AHJECF: solidus line |
| C: eutectic point (4.3%, 1147 °C) | J: peritectic point | M: Curie point of pure Fe |
| S: eutectoid point (0.8%, 723 °C) | A _n : arrest line | X': metastable equivalent |

An equilibrium microstructure will be attained when the cooling rate from the melt is less than the critical cooling rate (CCR), which can be determined from a TTT diagram (Section 6.7.13.). Otherwise, a certain fraction of metastable bainite or martensite (quench to low temperature) will form, for which the transformations are shown by the red dashed lines.

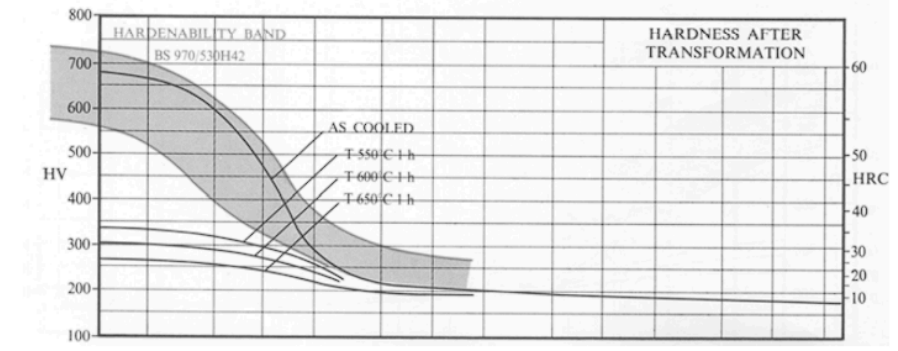
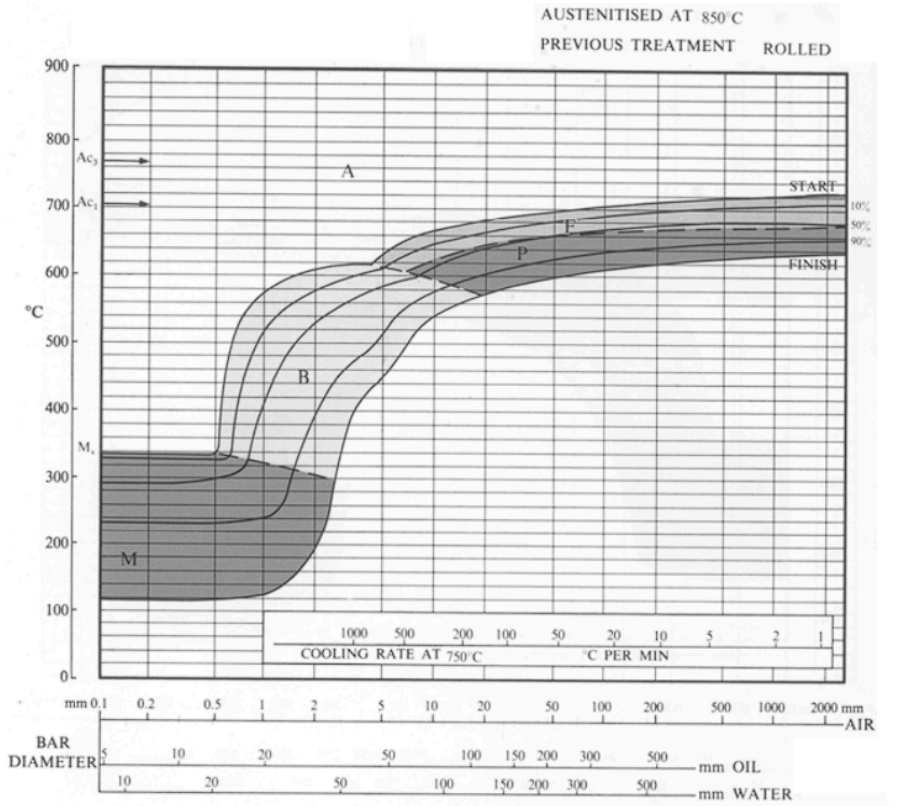
6.6.34. Heat Treatment Data for Steels

1% nickel steel, BS 503M40 (En12):

TTT Diagram



CCT Diagram



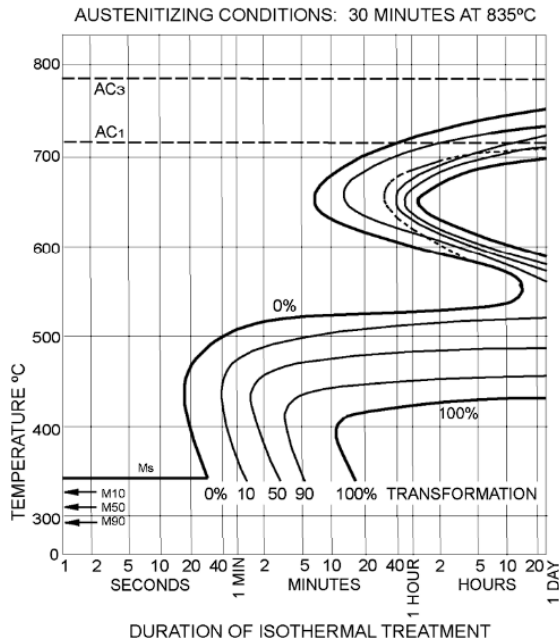
Jominy End-Quench Distance to Effective Diameter

Jominy End-Quench Hardenability Curves

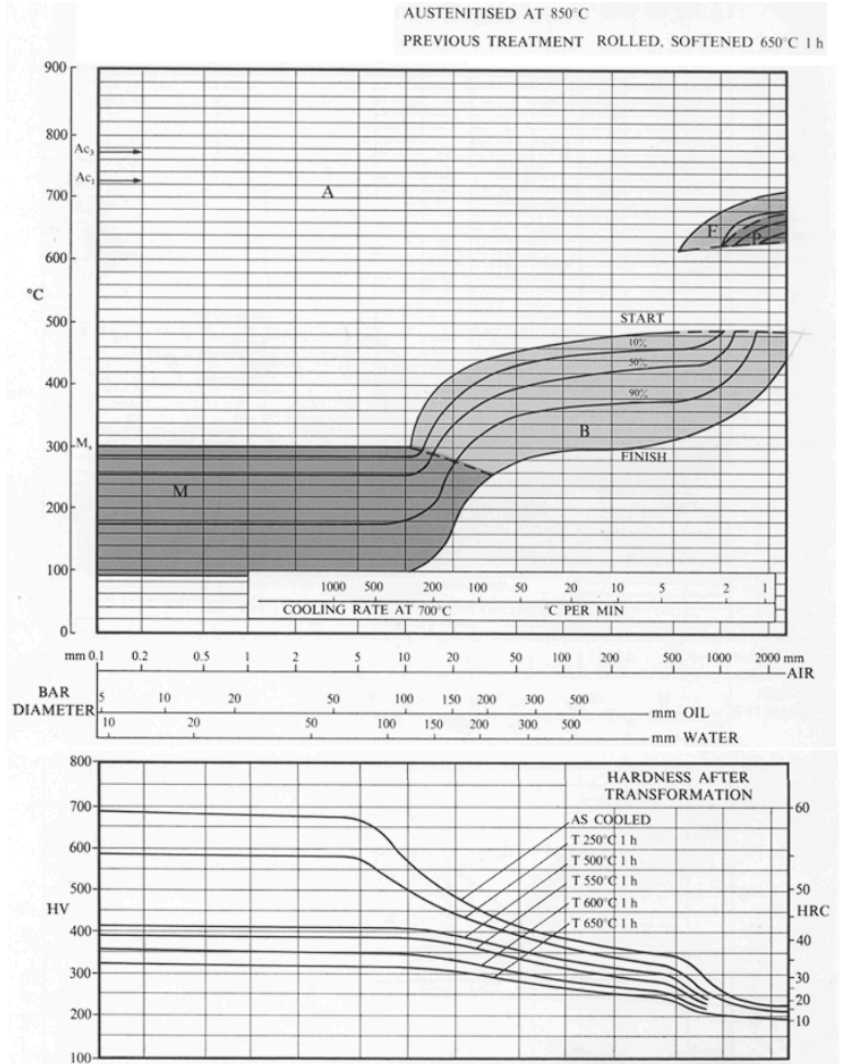
- TTT diagram: AC₁ = eutectoid line, dotted curve = carbide line (where ferrite growth stops and pearlite growth begins).
- CCT diagram, zones A = austenite, F = ferrite, P = pearlite, B = bainite, M = martensite.
- Conversion: correlation between bar diameter (oil-quenched) and distance along Jominy bar which have equivalent cooling rates. Independent of steel type (i.e. also applies for En24 below).

1.5% Ni-Cr-Mo steel, BS 817M40 (En24):

TTT Diagram



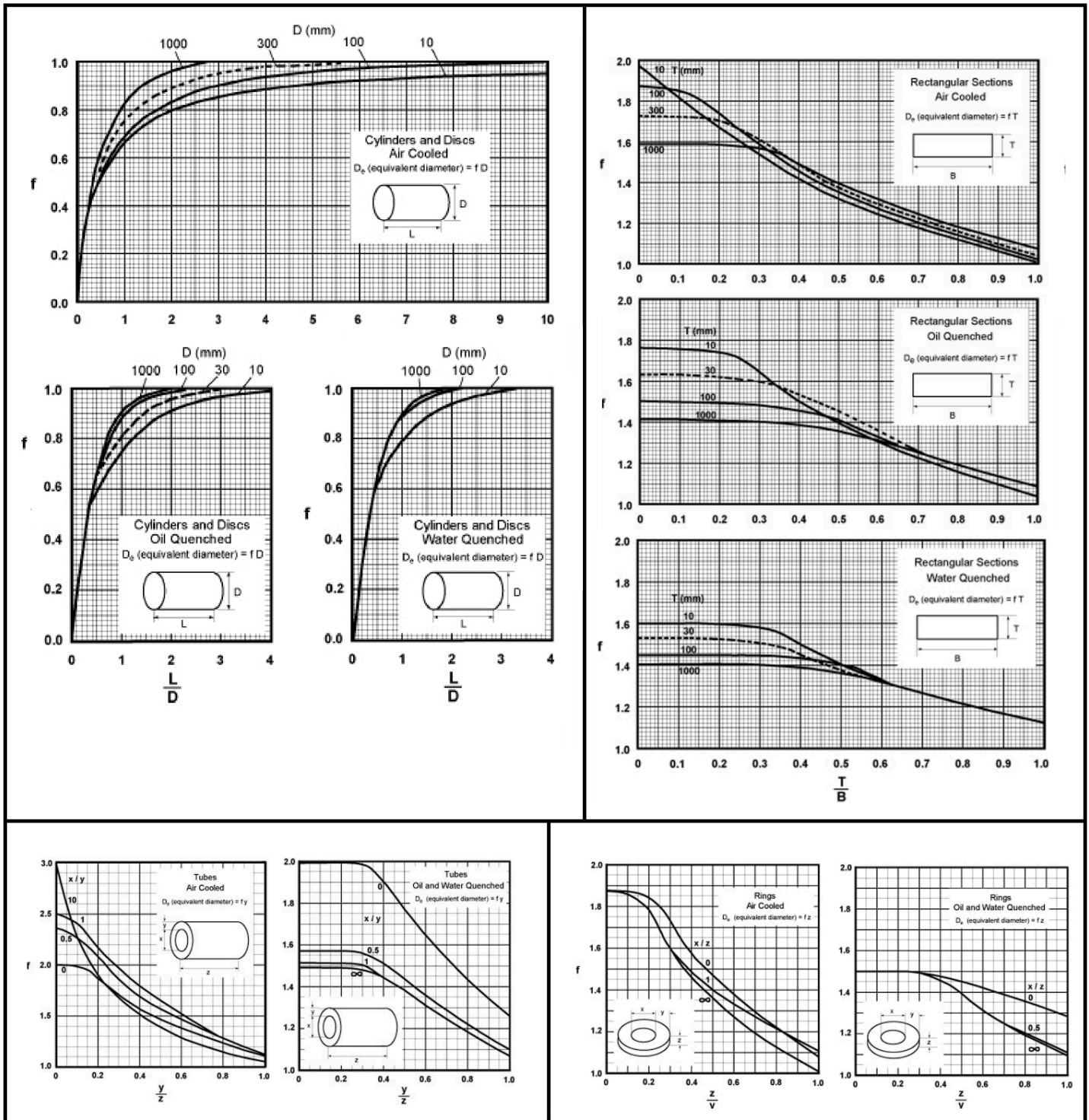
CCT Diagram



Jominy End-Quench Hardenability Curves

- TTT diagram: the lower set of C-curves correspond to precipitation of compounds with the alloyed metals rather than with carbon. AC_1 = eutectoid line, dotted curve = carbide line (where ferrite growth stops and pearlite growth begins).
- CCT diagram, zones A = austenite, F = ferrite, P = pearlite, B = bainite, M = martensite.

Equivalent Diameters for Standard Component Shapes



6.7. Sustainability and Energy Engineering

6.7.1. Quantification of Emissions and Economics of Power Systems

Metrics for Emissions: most energy systems release greenhouse gases to some extent

$$\text{Global Warming Potential of a gas, GWP} = \frac{\int_0^{T_h} a_x [x] dt}{\int_0^{T_h} a_{CO_2} [CO_2] dt}, \text{ for a specified time horizon } T_h$$

(Normalised relative to CO₂. a_x : radiative efficiency of the gas, $[x]$: time-dependent abundance of the gas in the atmosphere.)

The CO₂ mass equivalent of a gas is its GWP at $T_h = 100$ years e.g. 1 kg CH₄ = 28 kg CO₂e. Mass equivalent can also be written in tonnes e.g. 1 ton R-134a = 1.43 ktCO₂e.

Gas	Atmospheric lifetime (years)	GWP ($T_h = 20$ yrs)	GWP ($T_h = 100$ yrs) defines the CO ₂ mass equivalent (CO ₂ e)
CO ₂	>100	1	1
CH ₄	12.4	84	28
N ₂ O	121	264	265
R-134a (CF ₃ CH ₂ F)	14	3830	1430

Economic Metrics for Energy Systems: important for making investment decisions

Capital expenditure costs (CapEx): pre-development costs (adjusted for research over time), construction costs, infrastructure costs

Operating expenditure costs (OpEx): fixed + variable operating costs, connections, carbon transport/storage, decommissioning, insurance, heat revenues, fuel prices, carbon costs

Expected generation: plant capacity, expected availability and efficiency, load factor

$$\text{Net Present Value (NPV) of total costs [\$]} = \sum_{n=1}^{N_{\text{periods}}} \frac{\text{CapEx}_n + \text{OpEx}_n}{(1+r)^n} \quad (n: \text{period e.g. year})$$

$$\text{Net Present Value (NPV) of electricity generation [MWh]} = \sum_{n=1}^{N_{\text{periods}}} \frac{\text{net electricity generated in period } n}{(1+r)^n}$$

(r : rate of discount e.g. real rate of inflation)

Levelised Cost of Electricity (life-cycle cost, LCOE) [$\$ \text{ MWh}^{-1}$] = $\frac{\text{NPV of total costs}}{\text{NPV of electricity generation}}$,
the discounted lifetime cost of building, operating and decommissioning an energy generation system.

6.7.2. Climate Modelling

Simple 'one-tank' model:
$$\frac{dC}{dt} = k \left(E(t) - \frac{1}{\tau} (C(t) - C_{pre}(t)) \right)$$

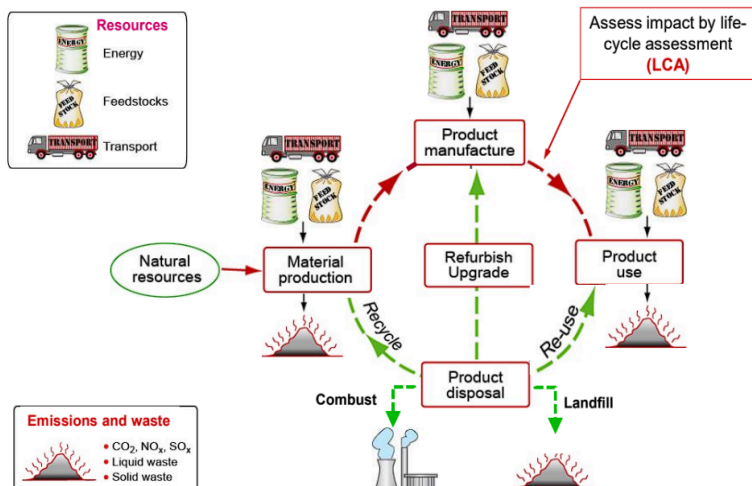
($C(t)$: carbon (**not** CO₂) content of the atmosphere, $E(t)$: carbon emissions from burning fossil fuels and cement production, $k \sim 0.5$: airborne fraction due to absorption into biosphere and ocean surface, $\tau \sim 200$ yrs: relaxation timescale due to mixing into deep ocean, $C_{pre} = 600$ GtC: pre-industrial level.)

6.7.3. Ashby Methodology for Sustainable Product Assessment

- 1. Define and articulate** the objective, scale, and timing.
(SMART goals: specific, measurable, achievable, relevant, time-bound.)
- 2. Stakeholder analysis:** consider influence vs interest, and interactions between groups (Government, the public, local communities, owners, manufacturers, suppliers, trade unions, customers, lobbyists, investors, National press, managers, colleagues, team.)
- 3. Fact-finding:** consider materials, environment, society, economics, legislation, energy.
- 4. Synthesis:** the corporate 'triple bottom line' (natural, human & financial capital).
- 5. Reflection:** is this a sustainable development?

6.7.4. Life-Cycle Assessment (LCA, Eco-Audit)

An LCA assesses the environmental impact of a product, considering e.g. CO₂ emissions, water consumption, energy consumption, at every stage, from mining the raw materials to disposing of the product after its useful lifetime.

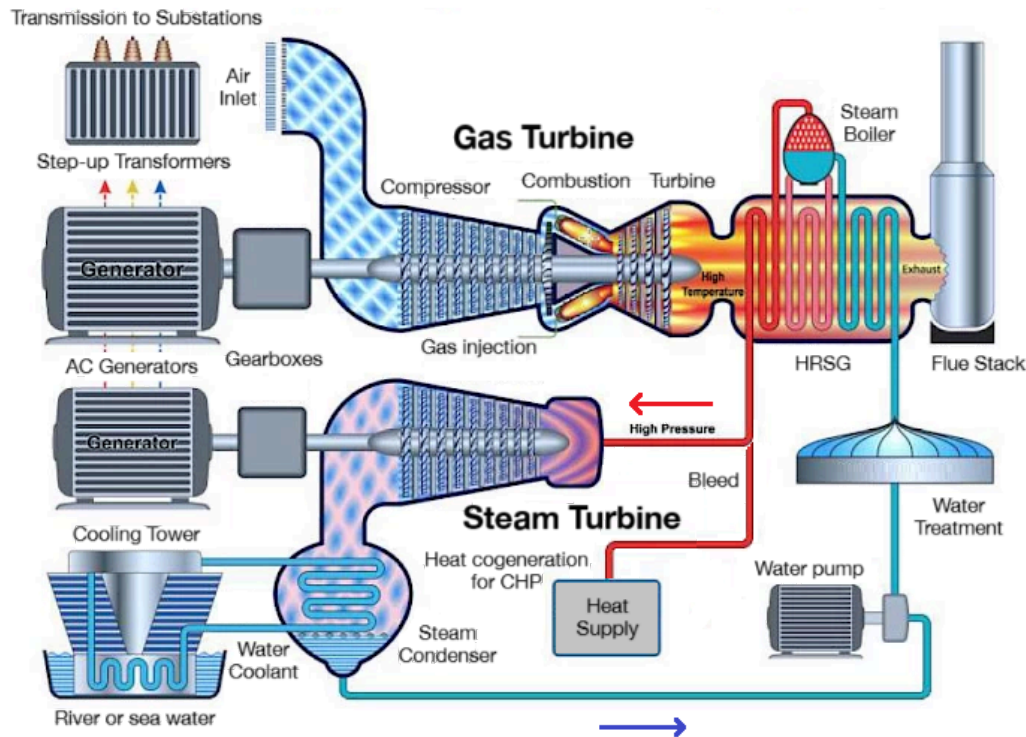


The metrics for environmental impact can be broken down into the stages of its lifecycle:

- **Materials:** minimise by materials selection, optimising for mass / embodied CO₂ / energy.
- **Manufacture:** minimise by choosing less energy-intensive materials processing
- **Transport:** minimise distance moved / lower energy modes of transport
- **Use:** minimise mass / thermal losses / electrical losses (max energy efficiency)
- **Disposal:** select non-toxic, recyclable materials

6.7.5. Improving the Sustainability of Existing Fossil-Fuel Power

Combined-cycle gas turbines (CCGTs) are the modern standard power station for burning natural gas, the least-polluting form of fossil fuel (other than hydrogen), achieving an efficiency of around ~60%. For the thermodynamics of CCGTs, see Section 7.2.8.

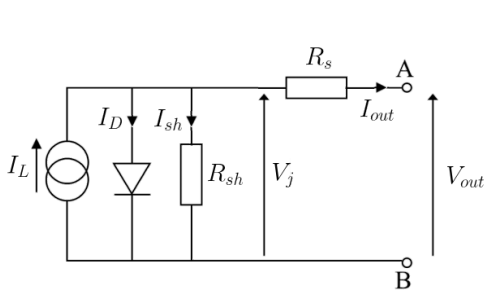


- **Superheating and reheating stages:** the steam cycle turbine can reach higher temperatures to increase turbine output power.
- **Combined heat and power (CHP):** heat can be extracted from any of the high-temperature points (e.g. HRSG outlet for hot steam, or pump outlet/coolant outlet for hot water) that can be sent directly to customers or used in thermal storage.
- **Carbon capture and storage (CCS)** from the flue output, removing some CO₂ at the expense of requiring some energy input.
- **Solid oxide fuel cells (SOFCs):** operate efficiently at high temperatures. They can generate extra electricity from supplied H₂ (waste heat utilisation) or from the gas supply (pre-combustion). Methane-fired plants can use steam-methane reforming (SMR) to convert CH₄ into H₂ for a SOFC.
- **Bioenergy with CCS (BECCS):** near-carbon-neutral biogas (~75% methane) as a natural gas source, with CCS for net-negative generation, with the possibility of SMR and SOFC cogeneration.
- **Further advances in turbomachinery (blade cooling, anti-creep ceramics):** can push turbine inlet temperatures higher, although there is only marginal room left for gains.

6.7.5. Solar Power Technologies (Solar PV, CSP)

Photovoltaic Cells (PV): conversion of sunlight to DC electricity using semiconductors

Electrical Circuit Analysis: solar cell modelled as a current source and diode with resistances



(I_L : luminous current, I_D : diode current, I_{sh} : leakage current, R_{sh} : shunt resistance, V_j : junction voltage, R_s : series resistance)

- Nodal analysis: $I_{out} = I_L - I_D - I_{sh}$; $V_j = V_{out} + I_{out} R_s$; $V_j = I_{sh} R_{sh}$
- Shockley diode equation: $I_D = I_0 \left[\exp\left(\frac{eV_j}{nkT}\right) - 1 \right]$
- Open-circuit: $I_{out} = 0 \Rightarrow V_{out} = V_{OC} \approx \frac{nkT}{e} \ln\left(\frac{I_L}{I_0} + 1\right)$ if $\frac{V_{out}}{R_{sh}} \ll I_L$
- Short-circuit: $V_{out} = 0 \Rightarrow I_{out} = I_{SC} \approx I_L$

Overall efficiency = $\frac{\text{electrical power output}}{\text{light power input}} = \frac{I [A] \times V [V]}{J [W m^{-2}] \times A [m^2]}$ (J : surface irradiance, A : normal absorbing area)

Fill factor = $\frac{P_{max}}{I_{sc} \times V_{oc}} = \frac{I_{max} \times V_{max}}{I_{sc} \times V_{oc}}$ (ideal operating point: load impedance $R = \frac{V_{max}}{I_{max}}$, for max power)

Factors affecting the light energy input include latitude, month of year, time of day, panel orientation relative to the Sun, cloud cover, reflections from environment, shading losses, dust accumulation. Maximum power point tracking (MPPT) is an online algorithm used to adjust the operating point by varying the duty ratio in a DC-to-DC converter, achieving maximum power in varying conditions.

Power production during the day follows a ‘duck curve’, with solar power meeting the bulk of daytime demand but not in the evening, where consumption is highest.

Solar water heating is a household alternative to gas-fired boilers using solar panels installed on a roof.

Traditional solar panels use the semiconductor silicon, in either polycrystalline or monocrystalline. Advances in functional materials (Section 8.6.10) has allowed for the use of thin-film materials (e.g. CdTe, CIGS), including use of multiple layers.

Shockley-Queisser limit: maximum single p-n junction solar-cell efficiency is ~33.16%.

Perovskite solar panels have shown to be highly efficient ($CsSnI_3$, ~31%) while being easy to manufacture. Organic hybrid perovskites (e.g. $CH_3NH_3PbX_3$) for PV cells are under research, especially lead-free organic perovskites. Control over the photonic properties (e.g. anti-reflection, scattering) can further improve efficiency.

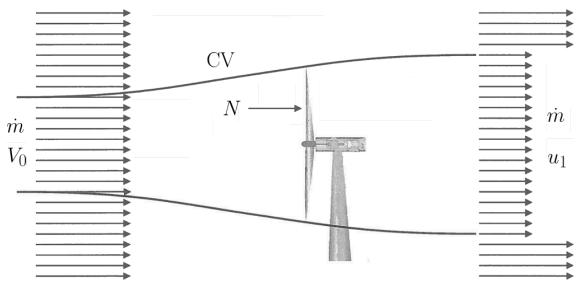
Concentrated Solar Power (CSP): mirrors reflect sunlight to produce heat.

The sunlight over a large area is focussed by parabolic mirrors and/or Fresnel lenses to generate heat, which can be used as the heat input to a steam turbine (Section 7.2.12) or to a reverse heat engine (refrigerator e.g. space cooling). It can also complement high-temperature energy processes such as molten salt battery storage with e.g. calcium potassium nitrate for night-time power generation (Section 13.5.13) or cogeneration schemes (CHP).

6.7.5. Wind Power Technologies (HAWT, VAWT, Offshore)

Good sites for large land-based wind turbines are at the top of gentle hills, where turbulent downstream eddy formation is minimised. The tops or bottoms of sharp cliffs are unsuitable, and the turbine should be a distance at least $10h$ away from any obstacles of height h , and taller than h .

Simple Model of Wind Turbine Aerodynamics



(CV: axisymmetric control volume following stream lines, \dot{m} : air mass flow rate, V_0 : upstream velocity, u_1 : downstream wake velocity, N : force on rotors, u : velocity at rotors, A : rotor area)

- Pressure drop across turbine: $\Delta p = \frac{1}{2}\rho(V_0^2 - u_1^2)$ (Bernoulli)
- Rotor force: $N = \Delta p A = \rho A u (V_0 - u_1)$ (SFME)
- Axial induction factor: a , where $u_1 = (1 - 2a)V_0$ ($0 < a < 1/2$)
- Power developed: $P = Nu = 2\rho V_0^3 a(1 - a)^2 A$
- Available power in flow: $P_{max} = \frac{1}{2}\dot{m}V_0^2 = \frac{1}{2}\rho A V_0^3$.
- Power coefficient: $C_p = \frac{P}{P_{max}} = 4a(1 - a^2)$, maximised at $a = \frac{1}{3}$, $C_p = 59\%$ (Betz efficiency limit)
- Capacity factor: $\frac{\text{total energy generated in reality}}{\text{maximum possible energy generated}} = \frac{\sum_i \min\{2\rho a(1 - a)^2 A (V_{0i})^3, P_{gen}\} \times t_i}{P_{gen}}$

(P_{gen} : generator power rating, t_i : fraction of total time where wind speed is V_{0i} (sum over buckets))

Wind Turbine Blade Design

For an aerodynamic analysis of wind turbines, see Section 7.2.17.

Wind turbines exploit electromagnetic induction, using AC generators (Section 8.4.11). The prime mover achieves high rpm by coupling with a gearbox in the housing.

The magnets used in wind turbines use rare-earth elements (Dy, Nd, Pr) which are critical materials, threatening the supply chains for their large-scale manufacture.

Horizontal axis wind turbines (HAWTs) can be fitted with anemometers and yaw controllers to face the oncoming wind at all times, improving the capacity. This requires some additional power to overcome the dynamic inertial forces (Coriolis force/gyroscopic torque) acting on the blades.

Offshore Wind Farms

Offshore wind farms experience higher wind speeds and therefore greater efficiencies than those on land. They also have less impact on the landscape view and land usage, helping to reduce opposition due to NIMBYism.

Vertical axis wind turbines (VAWTs) are a more convenient construction, but with lower efficiency.

6.7.6. Nuclear Fission Technologies

6.7.7. Nuclear Fusion Technologies

6.7.8. Geothermal Energy Technologies

6.7.9. Bioenergy Technologies

Plants and other biomass remove CO₂ from the atmosphere during their life due to photosynthesis, making plants a carbon sink by storing the carbon as carbohydrates.

When the biomass is burned, they release the CO₂ again, producing bioheat which can be used to produce electricity. This process is approximately carbon neutral, with some net operational emissions. Biomass can also be used to form biogas (by methanisation, Section 14.3.2), biofuel (by fermentation into bioethanol, Section 17.3.2) and biochar (by phytomining/pyrolysis, Section 15.1.5). When combined with carbon capture and storage (BECCS), the system becomes carbon negative.

Biofuel cells use enzymes or immobilised bacteria to carry out redox reactions that generate electricity. Glucose biofuel cells (Section 13.5.12) can act on the carbohydrates in plants. Nitrogenase bioelectrocatalysis cells are under research to cogenerate ammonia and hydrogen from atmospheric nitrogen gas: $\text{N}_2 + 8 \text{H}^+ + 8 \text{e}^- + 16 \text{ATP} \rightarrow 2 \text{NH}_3 + \text{H}_2 + 16 \text{ADP} + 16 \text{P}_i$. Genetic engineering can be used to optimise the enzymes and microorganisms operating in these processes e.g. directed evolution (Section 17.4.5) of the RuBisCo enzyme for photosynthesis.

6.7.9. Hydropower Technologies (Hydroelectric, Tidal Barrage, Wave Power)

6.7.10. Energy Storage

Pumped-Storage Hydroelectricity

Compressed Air Energy Storage

An improvement under research is adiabatic CAES.

Batteries and Supercapacitors

Molten salt batteries (Section 13.5.13) and redox flow batteries (Section 13.5.14).

These are dispatchable and fast-responding to varying grid demands.

These technologies are typically installed at grid-scale in battery energy storage systems (BESS). Currently, BESS primarily uses lithium-ion batteries.

Superconducting Magnetic Energy Storage (SMES)

Carbon Capture and Storage

Removal of CO₂ from gas supplies or exhausts is typically done by chemisorption. CO₂ dissolves in an alkaline solution to form carbonate precipitates which can be removed as solids. CCS requires energy input for compression and liquefaction which reduces the energy output of an attached power plant.

6.7.11. Renewable Heat Technologies

Heat Pumps:

Air-source heat pumps

Passive Daytime Radiative Cooling (PDRC): zero-input alternative to refrigeration/air-con.

PDRCs use thermally emissive materials to form a radiator with high performance. It is considered a type of geoengineering as it increases the thermal radiation emitted from the Earth, by emitting in the longwave IR range (through the infrared window). It can help to combat the urban heat island effect in dense cities.

PDRC systems can be coupled with thermoelectric generators that exploit the resulting temperature gradient to produce electricity.

Passive Solar Building Design:

Buildings can use Trombe walls which act as thermal capacitors, storing heat in the day and radiating it inside at night. The insulation material for the Trombe wall must have low thermal conductivity, such as nanoporous silica aerogel.

P7. THERMOFLUID MECHANICS

7.1. Fluid Mechanics

7.1.1. Hydrostatic Pressure

Pressure difference due to a column of liquid: $\Delta p = \rho g \Delta h$.

The equivalent resultant force per unit width on the wall of the container due to this triangular pressure distribution is

$$F = \int_0^h \rho g x \, dx = \frac{1}{2} \rho g h^2 \quad \text{acting at a depth } h^* = \frac{2}{3} h \text{ below the free surface.}$$

7.1.2. Buoyancy

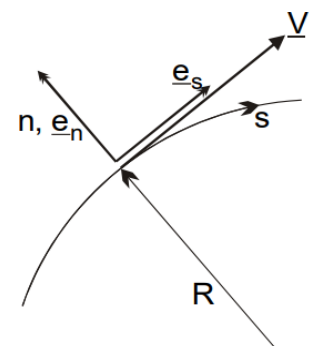
For a body of volume V completely submerged in a fluid of density ρ_f , the buoyant (upthrust) force is given by $F = \rho_f V g$. This is equal to the weight of the displaced fluid. For a body partially submerged to a depth $h(x, y)$ which varies over an area of fluid, the distributed buoyancy pressure $p(x, y)$ is given by $p = \rho_f h g$, normal to the body surface.

7.1.3. Radial Pressure Gradient on Curved Streamlines

An infinitesimal fluid parcel at a point on a curved streamline experiences radial pressure gradients due to centrifugal force.

The pressure gradient **normal** to a streamline with a radius of curvature R is given by $\frac{dp}{dn} = \frac{\rho V^2}{R} = \kappa \rho V^2$ (κ : curvature)

There is low pressure at the centre of the bend, increasing outwards.



7.1.4. Surface Tension, Excess Pressure and Capillary Action

Surface Tension: force per unit length in the plane of the liquid surface.

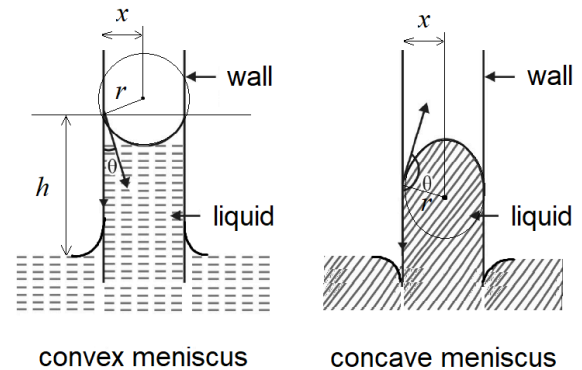
- Surface energy (excess potential energy per liquid surface area): $\Delta E = \gamma \Delta A$
(γ [N/m or J/m²]: surface tension).
- For a liquid-solid interface, a meniscus forms with contact angle θ and interfacial pressure p_i :
 - Adhesion > cohesion (wetable): $0^\circ < \theta < 90^\circ$, convex meniscus, pressure $p_l = p_\infty - \frac{2\gamma}{x}$.
 - Adhesion < cohesion (hydrophobic): $90^\circ < \theta < 180^\circ$, concave meniscus, pressure $p_l = p_\infty + \frac{2\gamma}{x}$.
 - Adhesion = cohesion: $\theta = 90^\circ$, flat meniscus, pressure $p_l = p_\infty$.
- Surface tension for liquids drops to zero at the critical temperature, decreasing linearly at other T .

Internal Excess Pressure: pressure change across interface

- Excess pressure in a liquid drop or bubble of radius r : $p_{in} - p_\infty = \frac{2\gamma}{r}$ (Young-Laplace equation)
- Excess pressure a film bubble (e.g. soap bubble): $p_{in} - p_\infty = \frac{4\gamma}{r}$ (two free surfaces)

Capillary action: excess pressure can do work against gravity

- Height ascended in capillary tube: $\Delta h = \frac{2\gamma \cos \theta}{x\rho g} = \frac{2\gamma}{r\rho g}$
(ρ : density, x : tube radius, r : radius of curvature of meniscus)
- Net vertical reaction force on tube: $F = 2\pi x\gamma$
- Tube of insufficient length to accommodate ascent: meniscus reshapes to curvature $r' = \frac{\Delta h r}{L}$. The tube will not overflow.

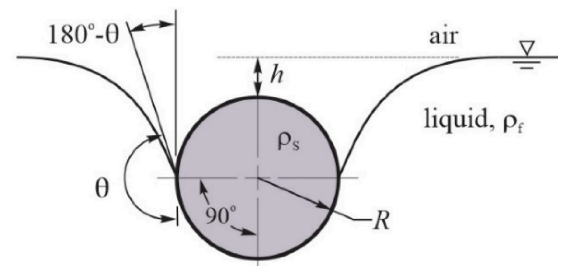


Floating Bodies with Surface Tension

Partially submerged bodies experience surface tension at their wetted perimeter. If $\theta > 90^\circ$ (hydrophobic) then the effective buoyancy increases (more weight can be supported without sinking). If $\theta < 90^\circ$ (wetable) then buoyancy is weakened.

For a **spherical** body in a fluid, force balance gives:

$$\underbrace{\frac{4}{3}\rho_s\pi R^3g}_{\text{sphere weight}} = \left(\underbrace{\frac{2}{3}\pi R^3}_{\text{submerged volume}} + \underbrace{\pi R^2(R+h)}_{\text{displaced volume}} \right) \rho_f g - \underbrace{2\pi R\gamma \cos \theta}_{\text{surface tension}}$$



For a **long horizontal cylindrical** body in a fluid, force balance (per unit length) gives:

$$\underbrace{\rho_s\pi R^2g}_{\text{cylinder weight}} = \left(\underbrace{\frac{1}{2}\pi R^2}_{\text{submerged volume}} + \underbrace{2R(R+h)}_{\text{displaced volume}} \right) \rho_f g - \underbrace{2\gamma \cos \theta}_{\text{surface tension}}$$

7.1.5. Conservation of Energy along Streamlines

Bernoulli's Equation for incompressible inviscid steady flow along a streamline (irrotational flows):

$$p + \frac{1}{2}\rho V^2 + \rho g z = C = \text{constant} \quad (\text{fluid mechanical energy per unit volume})$$

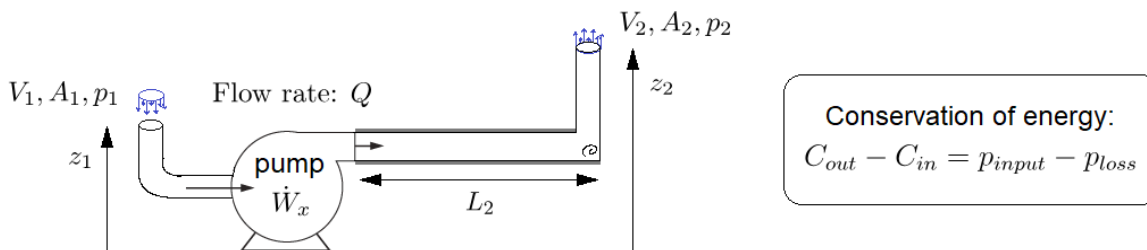
static pressure + dynamic pressure + hydrostatic pressure = total pressure (total)

The 'head' is related to the pressure by $H = \frac{p}{\rho g}$ and has units of length ('effective height').

Head gain/loss due to external work (e.g. pump: $W_x > 0$, turbine: $W_x < 0$) = $\frac{\dot{W}_x}{Q}$.
 (\dot{W}_x : external power input to flow, Q : volumetric flow rate).

Bernoulli's equation is not Gallileian invariant, since flow steadiness may depend on the reference frame.

Application of Bernoulli's equation: pipe flow with sources and resistances.



$$\underbrace{p_1 + \frac{1}{2}\rho \left(\frac{Q}{A_1}\right)^2 + \rho g z_1}_{\text{total pressure in, } C_{in}} + \underbrace{\frac{\dot{W}_x}{Q}}_{\text{pump}} = \underbrace{p_2 + \frac{1}{2}\rho \left(\frac{Q}{A_2}\right)^2 + \rho g z_2}_{\text{total pressure out, } C_{out}} + \underbrace{4c_f \frac{L_2}{d_2} \frac{1}{2}\rho \left(\frac{Q}{A_2}\right)^2}_{\text{pipe friction loss}} + \underbrace{\frac{\mu L_2 Q}{2\pi d_2^4}}_{\text{viscous loss}} + \underbrace{\frac{1}{2\rho} \left(\frac{Q}{C_d A_2}\right)^2}_{\text{corner loss}}$$

7.1.6. Viscosity and Reynolds Number

- Interfacial shear stress: $\tau = \mu \frac{dV}{dy}$ (μ : dynamic viscosity, $\frac{dV}{dy}$: transverse velocity gradient)
- Newtonian fluid: μ is independent of shear rate.
- Kinematic viscosity: $\nu = \frac{\mu}{\rho}$ (ρ : fluid density)
- Reynolds number: $Re_d = \frac{\rho V d}{\mu}$ (d : characteristic length dimension)
- Laminar flow for $Re < 2000$; turbulent flow for $Re > 4000$; transitional flow for $2000 < Re < 4000$
- Stokes' law (drag on sphere; x : diameter, V : relative speed; in creeping flow ($Re_x < 0.3$): $F_{drag} = 3\pi\mu x V$)
- Non-dimensional form (C_D : drag coefficient, Re_x : Reynolds number): $C_D = \frac{24}{Re_x}$ ($F_{drag} = \frac{1}{2} C_D \rho_f A V^2$)
 (ρ_f : fluid density, ρ_p : particle density, A : projected cross-sectional area normal to flow)
- Terminal velocity accounting for viscosity and buoyancy: $U_T = \frac{x^2(\rho_p - \rho_f)g}{18\mu}$

7.1.7. Fluid Dynamics of Control Volumes

A control volume is that region of space that is enclosed by a rigid control surface. For steady-flow, conditions within the control volume are not changing (on average) so that the mass, momentum, energy and entropy within the control volume remain constant.

- Volumetric flow rate: $Q = \iint_{cs} \mathbf{v} \cdot d\mathbf{A}$ (volume of fluid crossing CS per unit time)
- Mass flow rate: $\dot{m} = \rho Q$ (mass of fluid crossing CS per unit time)

For an incompressible flow, both m' and Q are conserved across a CV.

Conservation of Mass (the Continuity Equation):

$$\underbrace{\frac{d}{dt} \iiint_{cv} \rho dV}_{\text{internal change}} + \underbrace{\iint_{cs} \rho \mathbf{v} \cdot d\mathbf{A}}_{\text{mass flow}} = 0 \quad \Leftrightarrow \quad \frac{dm_{cv}}{dt} + \sum_{\text{out}} \dot{m} - \sum_{\text{in}} \dot{m} = 0$$

For steady flow, $dm_{cv}/dt = 0$, so that the sum of mass flows in and out are equal.

Conservation of Momentum (the Steady Flow Momentum Equation, SFME):

$$\underbrace{\frac{d}{dt} \iiint_{cv} \rho \mathbf{v} dV}_{\text{internal change}} + \underbrace{\iint_{cs} \rho \mathbf{v} \mathbf{v} \cdot d\mathbf{A}}_{\text{momentum flow}} = \underbrace{\mathbf{F}}_{\text{external forces}} - \underbrace{\iint_{cs} p d\mathbf{A}}_{\text{pressures}}$$

($d\mathbf{A}$: area normal element, oriented positive out of the CV, \mathbf{F} : non-pressure forces on flow)

For steady flow, the 'internal change' term is zero. $\sum \dot{m}_{out} V_{x,out} - \sum \dot{m}_{in} V_{x,in} = \sum F_x + (\sum pA)_x$

In scalar component form in Cartesian coordinates: $\sum \dot{m}_{out} V_{y,out} - \sum \dot{m}_{in} V_{y,in} = \sum F_y + (\sum pA)_y$

7.1.8. Navier-Stokes Equations and Euler Equations

For viscous unsteady flow of an incompressible fluid, the velocity profile \mathbf{V} satisfies

$$\nabla \cdot \underline{V} = 0 \quad \rho \left(\frac{\partial \underline{V}}{\partial t} + \underline{V} \cdot \nabla \underline{V} \right) = -\nabla p + \rho \underline{g} + \mu \nabla^2 \underline{V}$$

(p : static pressure scalar field, \underline{g} : gravity vector field, $\underline{V} \cdot \nabla$: advection operator, ∇^2 : vector (component-wise) Laplacian operator.)

If gravity and viscosity are neglected (inviscid flow) from the Navier-Stokes equation, this simplifies to the Euler equations: $\nabla \cdot \mathbf{V} = 0$ and $\rho \frac{\partial \mathbf{V}}{\partial t} + \rho \mathbf{V} \cdot \nabla \mathbf{V} = -\nabla p$

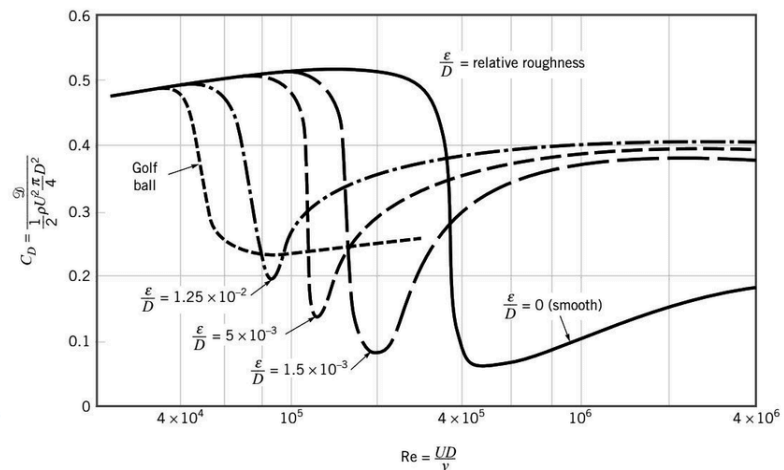
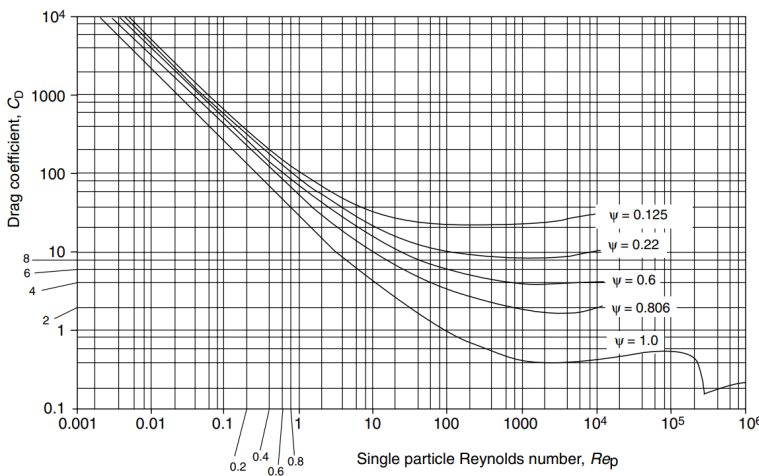
7.1.9. Drag Coefficient for Rough Spheres and Non-Spherical Bodies

Sphericity of an irregular particle: $\psi = \frac{A_s}{A_p} = \frac{6V_p}{x_p A_p} = (36\pi)^{1/3} \frac{V_p^{2/3}}{A_p}$.

(A_s : surface area of a sphere with the same volume as the particle, A_p : surface area of the particle, $x_p = x_{SV}$: equivalent diameter of the particle.)

Sphere: $\psi = 1$; Ellipsoid (2:1:1): $\psi = 0.929$; Cube: $\psi = 0.806$; Torus (2:1): $\psi = 0.710$, Tetrahedron: $\psi = 0.671$.

Sphere relative surface roughness: $\frac{\epsilon}{D}$ (ϵ : rms surface roughness amplitude, D : diameter)



Non-Spherical Bodies: $C_D = f(Re, \psi)$

Rough Spherical Bodies: $C_D = f(Re, \frac{\epsilon}{D})$

To determine terminal velocity U_T for a given particle size x ,

$$C_D Re_p^2 = \frac{4x^3 \rho_f (\rho_p - \rho_f) g}{3\mu^2} \quad (\text{straight line of gradient } -2 \text{ on log-log plot})$$

To determine particle size x for a given terminal velocity U_T ,

$$\frac{C_D}{Re_p} = \frac{4\mu (\rho_p - \rho_f) g}{3 U_T^3 \rho_f^2} \quad (\text{straight line of gradient } +1 \text{ on log-log plot})$$

where $Re_p = \frac{\rho_f U_T x}{\mu}$ and ρ_p is the density of the particle.

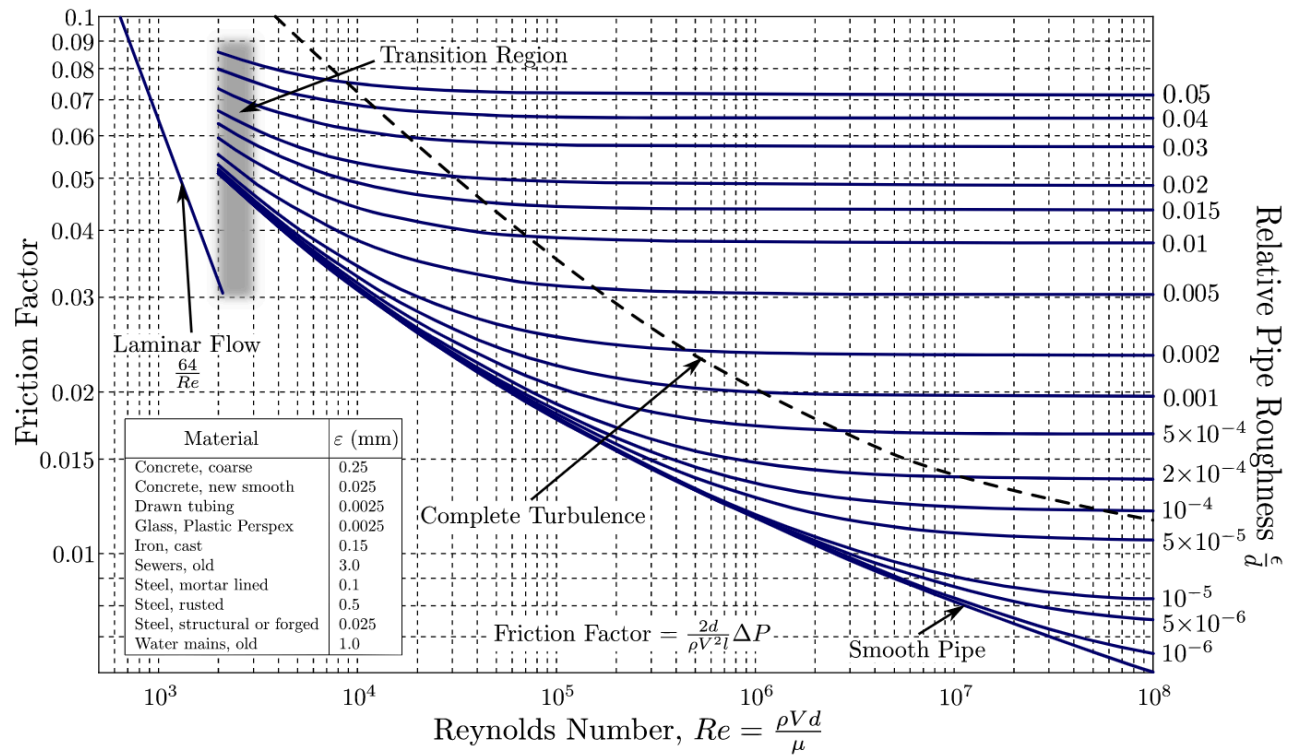
7.1.10. Frictional Losses in Pipes

The pressure drop along a pipe of constant diameter d and length L , with viscous flow is

$$\Delta p = 4c_f \frac{L}{d} \frac{1}{2} \rho V^2 = f \frac{L}{d} \frac{1}{2} \rho V^2$$

where c_f is the (Fanning) ‘friction coefficient’ and f is the (Darcy) ‘friction factor’.

If the rms surface roughness of the pipe is ϵ then f is found from the Moody diagram:



Laminar regime: $f = \frac{64}{Re}$ (Poiseuille’s law, dimensionless form)

Turbulent regime: $f^{-1/2} = -2 \log_{10} \left(\frac{\epsilon/d}{3.7} + \frac{2.51}{Re \times f^{1/2}} \right)$ (Colebrook equation, implicit)

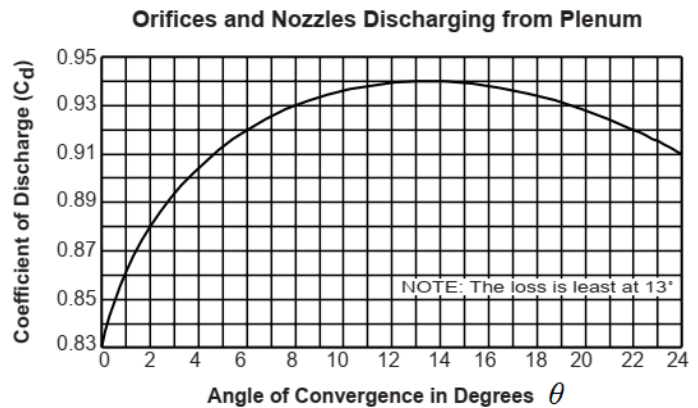
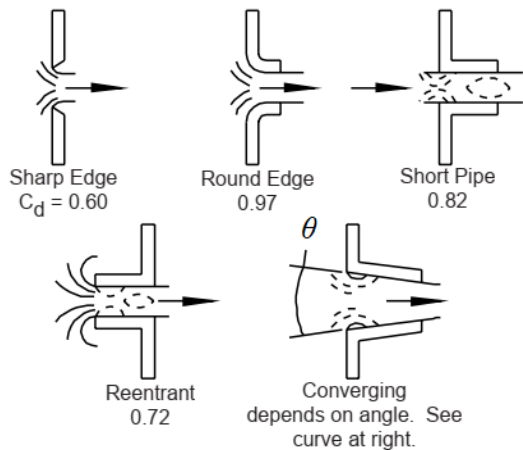
7.1.11. Flow Through Orifices, Weirs and Open Channels

Orifice Flow: a plate with a small hole placed into the flow to reduce the pressure.

For flow through an orifice plate,
$$Q = \frac{C_d}{\sqrt{1 - \beta^4}} \cdot \epsilon A \cdot \sqrt{2\rho \Delta p}$$

(Q : volumetric flow rate, C_d : discharge coefficient, $\beta = \frac{d_{orifice}}{d_{pipe}}$: diameter ratio, A : orifice area, ϵ : expansibility factor, ρ : fluid density, Δp : pressure drop across plate)

Values of the discharge coefficient C_d for various plate geometries are given.



Experimental expansibility factor correlation:
$$\epsilon = 1 - (0.351 + 0.256\beta^4 + 0.93\beta^8) \left[1 - \left(\frac{p_2}{p_1} \right)^{1/\gamma} \right]$$

For incompressible fluids e.g. water, $\gamma \rightarrow \infty$ so $\epsilon \rightarrow 1$.

(γ : adiabatic index of fluid, p_1 : static pressure upstream, p_2 : static pressure in plate)

Different correlations are appropriate for nozzles and Venturi tubes.

Weir Flow: flow from one upstream source to a downstream outlet, like a waterfall.

For a common man-made weir, the V-notch weir:
$$Q = \frac{8}{15} \sqrt{2g} C_e \tan \frac{\theta}{2} (h + k)^{5/2}$$

(g : acceleration due to gravity, C_e : flow correction factor, θ : opening angle of V-notch, h : height of inlet fluid above bottom of V-notch, k : head correction.)

Open Channel / Conduit Flow: flow is driven by gravity rather than pressure gradient

- Hydraulic radius: $R_h = \frac{A}{P}$ (A : flow cross-sectional area, P : wetted perimeter)

For an open channel, correlations for the cross-sectional average velocity u are:

- Chezy's formula: $u = C \times R_h^{1/2} S^{1/2}$ (C : Chezy coefficient, S : slope)
- Manning's formula: $u = \frac{1}{n} \times R_h^{2/3} S^{1/2}$ (n : Manning roughness coefficient, S : slope)

For a clean smooth channel, $n \sim 0.01 \text{ s m}^{-1/3}$. For a channel with stones/debris, $n \sim 0.06 \text{ s m}^{-1/3}$.

- Hazen-Williams formula: $u = 0.849 \times C_{HW} \times R_h^{0.63} S^{0.54}$ (C_{HW} : material dependent)

The volumetric flow rate (discharge, capacity) is then $Q = Au$.

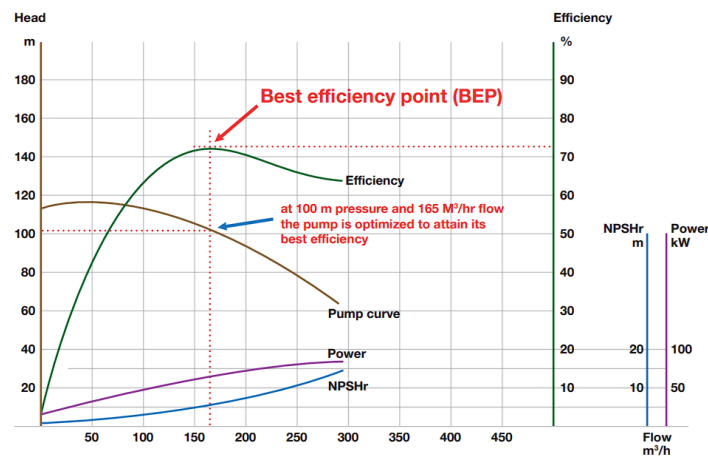
7.1.12. Pump Selection

Pumps (as well as fans and compressors) are turbomachinery components for providing flow and mechanical energy (as pressure) to a hydraulic fluid.

- Volumetric flow rate Q is typically given in m^3/hr , L/min or gpm (gallons per minute).
- Pressure head H is typically given in m or ft . The pump head rise is the value of $\frac{\Delta p_{\text{pump}}}{\rho g}$. (Δp_{pump} : change in total pressure across the pump.)

Centrifugal Pumps: motor-powered rotating impeller (rotor) pushes fluid around a volute channel

- **Characteristic curve:** plot of pump head rise H for a given flow rate Q . Often shows curves for different impeller diameters d and rotational speeds ω , as well as the efficiency η at Q . The 1st stage minimum input pressure required to avoid cavitation (NPSH_R , net positive suction head required) can also be shown as a function of Q . The absolute pressure minus the vapour pressure of the fluid at the inlet must be at least $\rho g \times \text{NPSH}_R$.



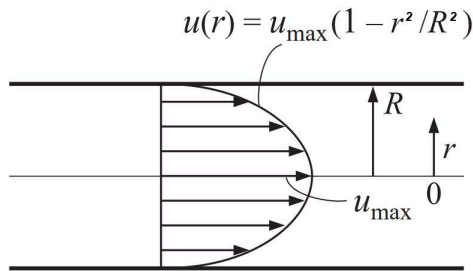
- Pump affinity laws (scaling laws for dynamically similar pumps): $Q \propto \omega d$, $H \propto \omega^2 d^2$, $P_s \propto \omega^3 d^3$.
- Shut-off head: pump head rise H when $Q = 0$.
- Free delivery flow rate: pump flow rate Q when $H = 0$ (often beyond optimal operation region).
- BEP (best efficiency point): point where η is maximum.
- Resistance coefficient, K_m : for a component or system with a head loss, $H = K_m Q^2$ (in SI units).
- Isentropic mechanical power input to flow from pump, $P_s = Q \Delta p_{\text{pump}} = \rho g Q H$ ('water horsepower', whp).
- Electrical power input to pump: $P_e = P_s / \eta = \rho g Q H / \eta$ (η : machine efficiency) ('brake horsepower', bhp. The rated power of the motor should be equal to the end-of-curve (maximum, not operating point) power for safety, to protect against overloading the motor).
- Variable speed/frequency drives (VSDs/VFDs): allows adjusting of the frequency of the AC motor input supply to set ω which allows the pump characteristic curve to move.

Positive Displacement Pumps: traps fluid within chamber and does work to move it out

- PD pumps have constant flow rate Q (dependent on speed only) i.e. their characteristic H vs Q curve is a straight vertical line at Q .

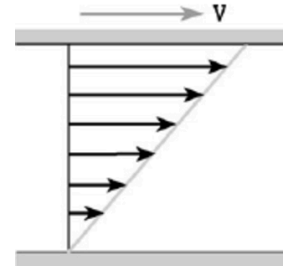
7.1.12. Laminar Viscous Flow in Pipes and Between Plates

Typical solutions for a viscous fluid moving in one direction between two plates:



Poiseuille Flow

Uniform pressure gradient
Parabolic velocity profile ($u_{\max} = 2Q/\pi R^2$)



Couette Flow

Moving boundary condition
Linear velocity profile

The profiles of these two cases can be superimposed to find solutions with both streamwise pressure gradients and moving boundary conditions.

An adverse streamwise pressure gradient on a Couette flow can induce flow reversal at the stationary plate edge.

Laminar Viscous Cylindrical Pipe Flow (Hagen-Poiseuille formula):

(Δp : pressure drop across pipe, Q : volumetric flow rate, r : pipe radius, $x = 2r$: pipe diameter, L : pipe length, Q' [W]: heat transfer rate)

- Hydraulic-electrical circuit analogy: $Q \sim$ current, $p \sim$ voltage, $R_{hyd} \sim$ resistance
- Flow rate: $Q = \frac{\Delta p}{R_{hyd}}$ where hydraulic resistance $R_{hyd} = \frac{8\mu L}{\pi r^4} = \frac{\mu L}{2\pi x^4}$
- Heat dissipation due to viscosity (thermal power): $Q' = Q \Delta p = \frac{(\Delta p)^2}{R_{hyd}} = Q^2 R_{hyd}$

In **turbulent** Poiseuille flow, the u_{\max} region is broadened as momentum is transferred by eddies, giving steeper velocity profiles at the walls and increasing heat transfer.

Viscous heat dissipation: $\dot{Q} = \int \tau \frac{\partial v_x}{\partial y} dV$

($\tau = \mu \frac{dv}{dy}$: interfacial shear stress, x : streamwise coordinate, y or r : transverse coordinate)

7.1.13. Boundary Layers and Aerodynamics of External Flows

Laminar Boundary Layers: thin boundary layer, gradual velocity gradient to free stream

Near a wall, viscosity cannot be neglected as the no-slip condition is always satisfied. A flowing fluid imposes a necessary velocity gradient, and the region where this gradient occurs is the boundary layer. Momentum diffuses away from the wall in the boundary layer.

$$\text{Boundary layer Reynolds: } Re_{\delta} = \frac{\rho_{\infty} V_{\infty} \delta}{\mu_{\infty}} \qquad \text{Streamwise Reynolds: } Re_x = \frac{\rho_{\infty} V_{\infty} x}{\mu_{\infty}}$$

$$\text{Boundary layer thickness along an infinite flat body (plate): } \delta \sim \sqrt{\frac{\mu_{\infty} x}{\rho_{\infty} V_{\infty}}} \Rightarrow \frac{\delta}{x} = 4.64 Re_x^{-1/2}$$

(x : distance along wall from stagnation)

Bernoulli's equation is **not** valid in a boundary layer due to viscous forces, which give rise to viscous drag on the body. Dimensionless viscous drag $C_D = 24 / Re_D$ (Stokes flow).

When an adverse pressure gradient acts on the flow, flow reversal can occur in the boundary layer, in a similar manner to Couette flow (Section 7.1.10). Regions of high curvature on a body (e.g. high angle of attack on an airfoil) result in large streamwise pressure drops as the fluid is unable to follow the surface, which can lead to boundary layer separation and transition to turbulence.

Turbulent Boundary Layers: wide boundary layer, steep velocity gradient, filled-out velocity profile

Turbulent boundary layers grow faster than laminar boundary layers, retaining the steep velocity gradient at the wall. The surrounding pressure field exerts forces on the body (form drag and lift), which dominate as turbulence increases. For $Re > 1000$, viscous drag (skin friction) is negligible.

If a turbulent boundary layer is about to experience flow reversal, the high-viscosity eddies can facilitate the diffusion of momentum flux from the full velocity profile region into the reversing region, providing it with momentum needed to prevent reversal, delaying boundary layer separation from bodies. For bluff bodies, this decreases the low pressure wake region, reducing form drag significantly.

Laminar boundary layers can be 'tripped' into turbulence by surface irregularities, where the sudden high curvature of the body forces subsequent boundary layer separation. If a laminar boundary layer becomes separated and transitions to turbulence, it may be able to re-attach to the body downstream, forming a 'separation bubble'. Aerofoil shapes are often designed to ensure that, once separated, the flow transitions to turbulence quickly, so that the separation bubble is short. If the transition occurs too far downstream, the bubble will cover a large area of the wing, or the flow may not even be able to re-attach at all (stall: sudden loss of lift and increase in drag).

The sudden reduction of drag for slightly larger velocities due to laminar/turbulent transition in the boundary layer, and the corresponding separation delay, can give rise to a resonance phenomenon. This can sometimes be observed in poles, chimneys and other slender objects, and needs to be addressed to avoid structural failure. When boundary layers separate, they create a shear layer. Shear layers are inherently unstable as their velocity profile has an inflection point. They develop waves that roll up into Kelvin-Helmholtz vortices (vortex shedding). Positive feedback produces a downstream Von Kármán vortex street at a constant frequency, which can resonate structures (aeroelastic flutter).

7.1.14. Properties of Velocity Fields (Flow Fields)

If \mathbf{u} is a velocity vector field for a flow, then a particle's position \mathbf{r} in the field obeys $\frac{d}{dt}\mathbf{r} = \mathbf{u}$. The streamlines of \mathbf{u} illustrate trajectories of the particle over time, $\mathbf{r}(t)$.

- Vorticity: $\boldsymbol{\omega} = \nabla \times \mathbf{u}$ (local angular velocity is equal to $\frac{1}{2}\boldsymbol{\omega}$)
- Material derivative: $\frac{Df}{Dt} = \frac{df}{dt} + \mathbf{u} \cdot \nabla f$ (derivative of quantity f moving with the fluid)
- Potential flow: if there exists ϕ such that $\mathbf{u} = \nabla\phi$, then $\boldsymbol{\omega} = \mathbf{0}$ (irrotational flow)
- Incompressible fluid: $\nabla \cdot \mathbf{u} = 0$ (isochoric flow)
- Mass continuity equation: $\nabla \cdot (\rho\mathbf{u}) + \frac{\partial\rho}{\partial t} = 0$ (if $\frac{\partial\rho}{\partial t} = 0$, ρ constant along streamlines of \mathbf{u})
- Kutta-Joukowski theorem: lift force per unit depth on a body in a 2D flow is $L' = \rho_{\infty} V_{\infty} \Gamma$ ($\mathbf{L} \perp \mathbf{V}_{\infty}$; ρ_{∞} : free stream density, V_{∞} : free stream velocity)

The circulation of \mathbf{u} around the body is given by $\Gamma = \oint_C \mathbf{u} \cdot d\mathbf{l}$ (Section 3.5.15).

(C : anticlockwise path around the body, away from the boundary layer, in potential flow region)

- For a rotating object in a flow, the lift force is responsible for the **Magnus effect**, with $\mathbf{L} \parallel (\boldsymbol{\omega} \times \mathbf{V}_{\infty})$. For a circular cross-section of the body, $\Gamma = 2\pi\omega r^2 \rightarrow L' = 2\pi\rho_{\infty} V_{\infty} \omega r^2$
- Kelvin's circulation theorem: $\frac{D\Gamma}{Dt} = 0$ for barotropic fluids in conservative forces.
- Coandă effect: fluid jet streamlines tend to follow convex surfaces, if the curvature is not too sharp. The curved streamlines generate a normal pressure gradient that can result in a net body force on the surface.

7.1.15. Taylor-Couette Flow

A viscous fluid between two concentric solid cylinders (radii r_1, r_2) driven to rotate at different relative rates (angular velocities ω_1, ω_2) exhibits Taylor-Couette flow.

Let $\eta = \frac{r_i}{r_o}$ and $\mu = \frac{\omega_o}{\omega_i}$. The Taylor number is $Ta = \frac{4\omega_i^2 r_i^4}{\nu^2} \frac{(1-\mu)(1-\frac{\mu}{\eta^2})}{(1-\eta^2)^2}$.

Azimuthal velocity profile for circular pure Couette flow (no axial throughput):

$$v_\theta(r) = Ar + Br^{-1} \quad \text{where } A = \omega_i \frac{\mu - \eta^2}{1 - \eta^2} \text{ and } B = \omega_i r_i^2 \frac{1 - \mu}{1 - \eta^2}$$

For thin-gap applications ($\eta \approx 1$), $Ta = -\frac{2A\omega_i r_o^4}{\nu^2} (1 - \eta)^4 (1 + \mu)$.

Taylor-Couette flow is exploited in some industrial chemical reactors (the Taylor-Couette reactor, TCR) using an axial input flow velocity u_{ax} . A TCR ($u_{ax} \approx \omega r$) can be considered intermediate between a PFR ($u_{ax} \gg \omega r$) (Section 14.2.7) and a CSTR ($\omega r \gg u_{ax}$) (Section 14.2.6).

Axial Reynolds number: $Re_{ax} = \frac{u_{ax} d}{\nu}$.

For low Re (laminar), the flow is analogous to Couette flow (Section 7.1.12).

- For $Ta < Ta_{c1}$, flow is steady, where the lower critical Taylor number is

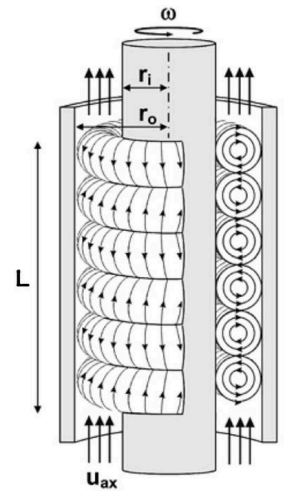
$$Ta_{c1} \approx 41.3 \times \frac{(1+\eta)^2}{2\eta\sqrt{(1-\eta)(3+\eta)}}$$

- For $Ta_{c1} < Ta < Ta_{c2}$, flow forms laminar toroidal vortices (shown right), where Ta_{c2} is an upper critical Taylor number.

Vortex aspect ratio, $\Gamma = \frac{L_{vortex}}{r_o - r_i}$. Typical range: $0.8 < \Gamma < 2.0$.

Using rotors with protruding ribs at regular axial intervals helps to stabilise the vortices within them.

- For $Ta > Ta_{c2}$, oscillating wavy vortices form, which become more turbulent for larger Ta.



Specialist applications of TCRs include continuous filtration/desalination (inner cylinder is a semi-permeable membrane), reactors for homogeneous catalysis (high mixing, high throughput, narrow residence time distribution), low-shear heterogeneous transport (cells, enzyme colloids), and selective crystallisation of pharmaceutical compound polymorphs.

7.2. Thermofluid Dynamics

7.2.1. Dimensionless Numbers in Thermofluid Dynamics

- Reynolds number: $Re = \frac{\rho_f V d}{\mu} = \frac{V d}{\nu}$ (fluid flow: flow is laminar for $Re < 2000$)
- Mach number: $M = \frac{V}{a}$ (flow is incompressible for $M < 0.3$)
- Froude number: $Fr = \frac{V}{\sqrt{gz}}$ (flow is supercritical for $Fr > 1$)
- Prandtl number: $Pr = \frac{\mu c_p}{\lambda} = \frac{\nu}{\alpha}$ (momentum diffusivity for $Pr > 1$, thermal diffusivity for $Pr < 1$)
- Biot number: $Bi = \frac{hs}{\lambda}$ (lumped heat transfer model valid for $Bi < 0.1$)
- Fourier number: $Fo = \frac{\alpha \tau}{s^2}$ (temperature reaches steady state for $Fo > 1$)
- Grashof number: $Gr = \frac{g d^3 \beta \Delta T}{\nu^2} = \frac{-g d^3 \rho \Delta \rho}{\mu^2}$ (natural convection: boundary layer is laminar for $Gr < 10^6$)
- Eötvös number: $Eo = \frac{\Delta \rho g d^2}{\gamma}$ (porous flow: capillary action dominant for $Eo < 1$)
- Nusselt number: $Nu = \frac{hd}{\lambda}$ (heat transfer: slug/laminar flow for $Nu < 10$)
- Rayleigh number: $Ra = Gr Pr = \frac{g d^3 \beta \Delta T}{\nu \alpha} = \frac{-g d^3 \Delta \rho}{\mu \alpha}$
- Stanton number: $St = \frac{Nu}{Re Pr} = \frac{h}{\rho_f V c_p}$
- Rossby number: $Ro = \frac{V}{2 \Omega L \sin \phi}$ (Coriolis forces dominate for $Ro < 1$)
- Taylor number: $Ta = \frac{4 \Omega^2 R^4}{\nu^2}$
- Strouhal number: $Sr = \frac{f L}{V}$
- Drag coefficient: $C_D = \frac{F_{drag}}{\frac{1}{2} \rho_f A V^2}$
- Lift coefficient: $C_L = \frac{F_{lift}}{\frac{1}{2} \rho_f A V^2}$
- Friction coefficient: $c_f = \frac{\tau_{wall}}{\frac{1}{2} \rho_f V^2}$ (Fanning skin friction coefficient)
- Friction factor: $f = 4 c_f$ (Darcy friction factor)
- Discharge coefficient: $C_d = \frac{m'_{actual}}{m'_{ideal}}$

(ρ_f : fluid density, V : fluid velocity relative to reference, d or L : body length (e.g. pipe diameter, plate length), μ : dynamic viscosity, ν : kinematic viscosity, a : speed of sound in fluid, g : acceleration due to gravity, z : fluid vertical elevation, c_p : isobaric specific heat capacity of fluid, λ : thermal conductivity of fluid, α : thermal diffusivity of fluid, h : heat transfer coefficient from body to fluid, s : volume-to-surface area ratio (length scale), τ : elapsed time, β : coefficient of volume expansion, ΔT : bulk-surface temperature difference, $\Delta \rho$: density difference between fluids, γ : surface tension, Ω : body angular velocity, ϕ : fluid latitude on spherical body, f : frequency of oscillation, A : body cross-sectional area, F : forces, τ_{wall} : shear stress at wall, m' : mass flow rate.)

7.2.2. Laws of Thermodynamics and Systems

Thermodynamic Systems:

A system is a quantity of matter occupying a control volume, enclosed by a control surface. The surroundings to a system is everything not contained within the control surface.

	Energy transfer allowed	Energy transfer not allowed
Mass transfer allowed	Open system	Insulated system
Mass transfer not allowed	Closed system	Isolated system

A system containing a constant mass is necessary but **not** sufficient to define a closed system: if mass enters and leaves the system at the same rate, this remains an open system.

A 'simple compressible system' is a system in which changes in bulk kinetic energy and gravitational potential energy are negligible (also the effects of surface tension, stress in deformed solids, and externally applied electromagnetic fields). The only contribution to the energy of a simple compressible system is the internal energy U .

Laws of Thermodynamics: in terms of energy and entropy,

- **First Law:** the energy in an isolated system is constant.
- **Second Law:** the entropy in an isolated system never decreases.
- **Third Law:** the entropy in a closed system at equilibrium is minimum at zero temperature.
- **'Zeroth Law':** if two thermodynamic systems are both in thermal equilibrium with a third system, then the two systems are in thermal equilibrium with each other.
- **'Fourth Law':** a system not at equilibrium evolves in such a way as to maximise its entropy production, constrained by the forces and fluxes that the system is subject to.

Thermodynamic Properties:

- **Extensive:** proportional to the system mass e.g. V, U, H, S
- **Intensive:** independent of the system mass e.g. p, T
- **Specific:** extensive property per unit mass e.g. v, u, h, s
- **Molar:** extensive property per mole e.g. $\bar{v}, \bar{u}, \bar{h}, \bar{s}$ (note: **kilomoles** used in this section)

Specific and molar properties are intensive, related by $\bar{x} [X/kmol] = x [X/kg] \times M_r [kg/kmol]$

Phases and Components: A phase is a quantity of homogeneous matter. A system may consist of a single phase or a number of co-existing phases.

- The three-phase state of H_2O (ice, water, steam) only exists in equilibrium along the triple-point line. The components of a phase are the minimum set of chemical substances which make up the phase. A single-component system is a pure substance.
- Air could be treated as a two-component mixture of N_2 and O_2 . However, if liquefaction does not occur the composition remains constant and it is usually more convenient to treat it as a pure substance. The single component is a mixture of 79% N_2 and 21% O_2 by volume.

7.2.2. Thermodynamic State Variables

For a closed system (m : mass, H : enthalpy, U : internal energy, G : Gibbs free energy, A : Helmholtz free energy, p : pressure, T : temperature, V : volume, S : entropy). Thermodynamics potentials are $\{H, U, G, A\}$. Conjugate variables are $\{p, T, V, S\}$. Without external work/heat, the system obeys:

$$dU = T dS - p dV, \quad H = U + pV, \quad G = H - TS, \quad A = U - TS$$

$$dH = T dS + V dp, \quad dG = V dp - S dT, \quad dA = -p dV - S dT$$

To account for chemical reactions, add μdN to each differential (e.g. $dU = T dS - p dV + \mu dN$).

(μ : chemical potential, N : particle or mole count, summed over each chemical species.)

All the above equations are also valid when replaced with their specific or molar intensive properties.

G : the maximum reversible work a system can do in an isothermal, **isobaric** process.

A : the maximum reversible work a system can do in an isothermal, **isochoric** process.

Most commonly useful: $T dS = dU + p dV = dH - V dp$

Specific heat capacities: isochoric: $c_v = \left(\frac{\partial u}{\partial T}\right)_v$, isobaric: $c_p = \left(\frac{\partial h}{\partial T}\right)_p$, adiabatic index: $\gamma = \frac{c_p}{c_v}$

Coefficients of expansion: volume expansion: $\beta = \frac{1}{v} \left(\frac{\partial v}{\partial T}\right)_p$, compressibility: $\kappa = -\frac{1}{v} \left(\frac{\partial v}{\partial p}\right)_T$

First law: $dU = \delta Q - \delta W$; Second law: $\delta Q = T dS$

Contributions to work W and heat Q can be expressed as products of an intensive variable and its conjugate infinitesimal extrinsic variable, e.g. mechanical work $\delta W = p dV$, elastic strain energy $\delta W = \sigma d\varepsilon$, heat transfer $\delta Q = T dS$.

7.2.3. Ideal Gas Relationships

An ideal gas is a collection of particles with negligible size moving randomly, making elastic collisions with the container and making no inter-particle interactions. For microscopic properties of ideal gases, see Section 14.1.1-7.

(p : pressure, V : volume, n : moles, m : mass, T : temperature, ρ : density, M_r : molar mass,

v : specific volume, $\bar{R} = 8.314 \text{ J K}^{-1} \text{ mol}^{-1}$: gas constant, γ : adiabatic index, f : molecular degrees of freedom)

- Ideal gas law: $pV = n\bar{R}T = mRT$ where $R = \frac{\bar{R}}{M_r [\text{kg mol}^{-1}]}$ so $mR = n\bar{R}$
- Specific ideal gas law: $pv = RT$ where $v = \frac{V}{m} = \frac{1}{\rho}$
- Density gas law: $p = \rho RT$
- Density change: isobaric: $\left(\frac{\partial \rho}{\partial T}\right)_p = -\rho\beta$, isothermal: $\left(\frac{\partial \rho}{\partial p}\right)_T = \rho\kappa$
- Specific heat capacities: $c_v = \frac{R}{\gamma-1}$, $c_p = \frac{\gamma R}{\gamma-1}$, $c_p - c_v = R$ where $\gamma = \frac{c_p}{c_v} = 1 + \frac{2}{f}$
Monatomic gas e.g. He, Ar: $f=3$; diatomic gas e.g. H₂, N₂, O₂: $f=5$. For dry air at 20 °C, $\gamma = 1.400$.
- Speed of sound: $a = \sqrt{\gamma RT}$

7.2.4. Perfect Gas Relationships for Non-Flow Processes

A perfect gas has specific heat capacities which are independent of T .

A semi-perfect gas has specific heat capacities which are dependent on T only.

An ideal gas has specific heat capacities which may vary with state.

- Change in specific internal energy: $\Delta u = u_2 - u_1 = c_v (T_2 - T_1)$
- Change in specific enthalpy: $\Delta h = h_2 - h_1 = c_p (T_2 - T_1)$
- Change in specific entropy: $\Delta s = s_2 - s_1 = c_v \ln \frac{T_2}{T_1} + R \ln \frac{v_2}{v_1} = c_p \ln \frac{T_2}{T_1} - R \ln \frac{p_2}{p_1}$
 $= c_v \ln \frac{p_2}{p_1} + c_p \ln \frac{v_2}{v_1}$

For a perfect gas, types of processes are:

Isobaric Processes: constant pressure p from state 1 \rightarrow state 2

- Charles' law: $v_1 / T_1 = v_2 / T_2$ (vT^{-1} is constant)
- Work done: $W = p \Delta V = - mR \Delta T$
- Heat transferred: $Q = \Delta H = m c_p \Delta T$

Isochoric Processes: constant volume v from state 1 \rightarrow state 2

- Gay-Lussac's law: $p_1 / T_1 = p_2 / T_2$ (pT^{-1} is constant)
- Work done: $W = 0$
- Heat transferred: $Q = \Delta U = m c_v \Delta T = \frac{m c_v}{R} v \Delta p$

Isothermal Processes: constant temperature T from state 1 \rightarrow state 2

- Boyle's law: $p_1 v_1 = p_2 v_2$ (pv is constant)
- Work done: $W = - mRT \ln \frac{v_2}{v_1} = - mRT \ln \frac{p_1}{p_2}$
- Heat transferred: $Q = mRT \ln \frac{v_2}{v_1} = mRT \ln \frac{p_1}{p_2}$

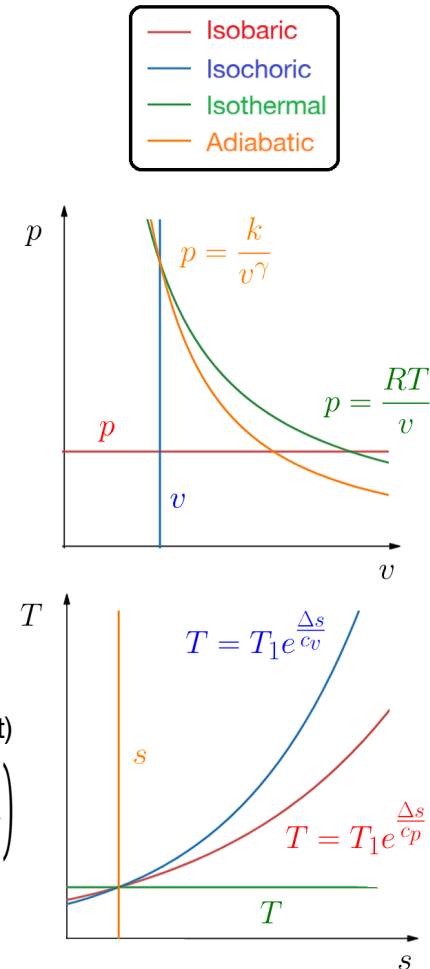
Adiabatic Processes: no heat transfer from state 1 \rightarrow state 2

- Adiabatic gas law: $p_1 v_1^\gamma = p_2 v_2^\gamma$ ($pv^\gamma, T v^{\gamma-1}, T p^{\frac{1-\gamma}{\gamma}}$ constant)
- Work done: $W = \frac{p_2 v_2 - p_1 v_1}{1-\gamma} = - \frac{1}{\gamma-1} mRT_1 \left(\left(\frac{p_2}{p_1} \right)^{\frac{\gamma-1}{\gamma}} - 1 \right)$
- Heat transferred: $Q = 0$

Any two of {adiabatic, reversible, isentropic} implies the third is also true.

Polytropic Processes: generalised power-law equation from state 1 \rightarrow state 2 (n : polytropic index)

- Polytropic gas law: $p_1 v_1^n = p_2 v_2^n$ ($pv^n, T v^{n-1}, T p^{\frac{1-n}{n}}$ are constant)
- Polytropic coefficient: $n = (1 - \gamma) \frac{\partial Q}{\partial W} + \gamma$ ($\frac{\partial Q}{\partial W}$: instantaneous heat to work transfer ratio)



7.2.5. Thermodynamics of Non-Flow Processes

For a closed system of mass m undergoing a process between state 1 and state 2 are defined as positive and in the absence of capillarity, electric and magnetic fields:

First Law of Thermodynamics: conservation of energy

$$Q - W = m \left(u_2 + \frac{1}{2}V_2^2 + gz_2 \right) - m \left(u_1 + \frac{1}{2}V_1^2 + gz_1 \right)$$

(Q : heat transferred to system, W : work done by system, m : system mass, u : specific internal energy, V : bulk translational velocity, g : gravitational field, z : elevation)

For a cyclic process: $\oint dQ = \oint dW$ Displacement work by pressure p : $W = \int_1^2 p dV$

Second Law of Thermodynamics: entropy and heat transfer

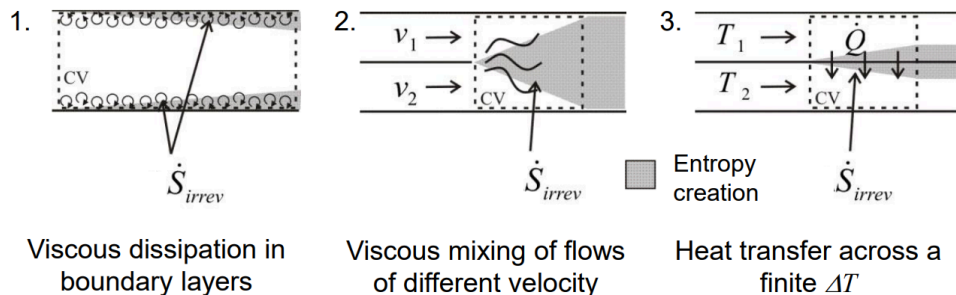
$$m(s_2 - s_1) = \int_1^2 \frac{dQ}{T} + \Delta S_{irrev}$$

(m : system mass, s : specific entropy, dQ : infinitesimal heat transfer to system, T : system temperature (on boundary), $\Delta S_{irrev} \geq 0$: entropy created by irreversibilities in the system)

For a fully reversible process: $m ds_{irrev} = \sigma = \Delta S_{irrev} = 0$.

For a cyclic process: $\oint \frac{dQ}{T} \leq 0$ (the Clausius inequality)

7.2.6. Sources of Irreversible Entropy Creation in Flow Processes



7.2.7. Thermodynamics of Control Volumes (Flow Processes and Open Systems)

A control volume is that region of space that is enclosed by a rigid control surface. For steady-flow, conditions within the control volume are not, on average, changing so that the mass, momentum, energy and entropy within the control volume remain constant.

Steady Flow Energy Equation (SFEE) (First Law of Thermodynamics): conservation of energy

$$\underbrace{\frac{dE_{cv}}{dt}}_{\text{internal change}} + \underbrace{\sum_{\text{out}} \dot{m} \left(h + \frac{1}{2}V^2 + gz \right)}_{\text{energy flow out of CV}} - \underbrace{\sum_{\text{in}} \dot{m} \left(h + \frac{1}{2}V^2 + gz \right)}_{\text{energy flow into CV}} = \underbrace{\dot{Q} - \dot{W}}_{\text{heat and work transferred to and from CV}}$$

(E_{cv} : total system energy, \dot{m} : mass flow rate, h : specific enthalpy at inlet/outlet, V : flow speed, g : gravitational field, z : elevation, \dot{Q} : heat transfer rate to CV, \dot{W} : shaft power output)

For steady flow, the 'internal change' term is zero.

Steady Flow Entropy Equation (SFSE) (Second Law of Thermodynamics): entropy accounting

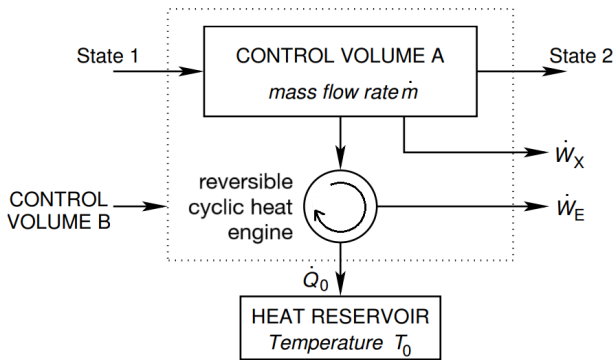
$$\underbrace{\frac{dS_{cv}}{dt}}_{\text{internal change}} + \underbrace{\sum_{\text{out}} \dot{m}s}_{\text{entropy flow out}} - \underbrace{\sum_{\text{in}} \dot{m}s}_{\text{entropy flow in}} = \underbrace{\oint_{cs} \frac{d\dot{Q}}{T}}_{\text{isothermal heat transfer}} + \underbrace{\dot{S}_{\text{irrev}}}_{\text{irreversible processes}}$$

(S_{cv} : total system entropy, \dot{m} : mass flow rate, s : specific entropy at inlet/outlet, $d\dot{Q}$: infinitesimal heat transfer rate to CV, T : system temperature (on boundary), $\dot{S}_{\text{irrev}} \geq 0$: rate of entropy creation within the CV due to irreversibilities)

For steady flow, the 'internal change' term is zero.

7.2.8. Exergy and Available Power in Control Volumes

Heat is not as ‘valuable’ as work, as a heat engine can only extract work from heat up to the Carnot efficiency factor.



Availability: the maximum useful work \dot{W}_X that can be obtained from CVA as it comes into equilibrium with its environment (i.e. using a hypothetical Carnot engine). Applying the SFEE (1st law) and SFSE (2nd law) to CVB:

$$[\dot{W}_X]_{MAX} = \dot{m}(b_1 - b_2) \quad \text{or} \quad [-\dot{W}_X]_{MIN} = \dot{m}(b_2 - b_1)$$

when work is the output when work is the input
 ($b = h - T_0 s$: specific steady flow availability function)

- Dead state: $p_D = 1 \text{ atm}, T_D = 298 \text{ K}$
- Specific exergy: $e = b - b_D$ so $\Delta e = \Delta b$ (dead state availability: $b_D = h_D - T_0 s_D$)

Steady Flow Exergy Equation (SFEXE): combination of first and second laws

$$\underbrace{\sum_{out} \dot{m} \left(e + \frac{1}{2}V^2 + gz \right) - \sum_{in} \dot{m} \left(e + \frac{1}{2}V^2 + gz \right)}_{\text{exergy flow rate}} = \underbrace{-\dot{W}_X}_{\text{shaft power output}} + \underbrace{\oint_{CS} \left(1 - \frac{T_0}{T_S} \right) d\dot{Q}_S}_{\dot{E}_Q: \text{ power potential of heat addition to system at } T_S} - \underbrace{\oint_{CS} \left(1 - \frac{T_0}{T_L} \right) d\dot{Q}_L}_{\dot{W}_{L,Q}: \text{ power potential of heat rejection to environment at } T_0} - \underbrace{T_0 \dot{S}_{irrev}}_{\dot{W}_{L,CR}: \text{ loss of available power due to irreversibilities}}$$

(T_0 : dead state, T_S : system temperature of heat addition, T_L : system temperature of heat rejection.)

p - V (boundary expansion) work is **not** counted as useful output work ($\dot{W}_X' = \dot{W}' - p \, dV/dt$).

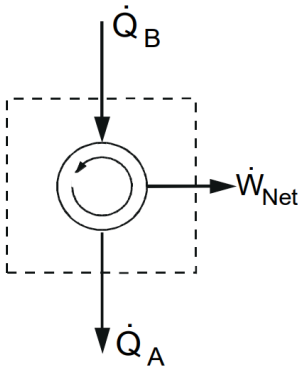
The fourth term on the RHS represents the irreversible exergy destruction rate (Gouy-Stodola theorem.)

An ‘exergy analysis’ of a component or system typically involves:

- 1) calculate the state properties of the working fluid around the system ($h_1, s_1, h_2, s_2, \dots$)
- 2) calculate the exergy of the fluid at each state ($e_1 = b_1 = h_1 - T_D s_1 \dots$) (take datum $b_D = 0$)
- 3) calculate $\dot{Q}, \dot{E}_Q, \dot{W}_X, \dot{W}_{L,Q}, \dot{W}_{L,CR}$ for each component or process
- 4) apply the a) SFEE and b) SFEXE to each component in turn
- 5) draw up overall a) energy and b) exergy balances showing how the heat supply rate is utilised
- 6) calculate the a) thermal efficiency (energy) and b) rational efficiency (exergy).

Components with the greatest contributions to exergy destruction can then be identified for targeting of potential improvements. For individual components, exergy efficiency is defined as:

7.2.8. Thermal Efficiency of Thermodynamic Cycles



First-Law (overall, thermal) Efficiency: how much of the *total* energy was used?

$$\eta_{1st} = \frac{\dot{W}_{net}}{\dot{Q}_B} = 1 - \frac{\dot{Q}_A}{\dot{Q}_B} \quad \text{where} \quad \dot{W}_{net} = \dot{Q}_B - \dot{Q}_A$$

Second-Law (rational, exergy) Efficiency: how much of the *available* energy was used?

$$\eta_{2nd} = \frac{\dot{W}_{net}}{\dot{m}\Delta b} = \frac{\eta_{1st}}{\eta_{Carnot}} \quad \text{where} \quad \eta_{Carnot} = 1 - \frac{T_A}{T_B}$$

T_A as the dead state and T_B as the system state.

The 2nd law efficiency is always higher than the 1st law efficiency, accounting for the fact that heat is not as 'valuable' as work ($\eta_{Carnot} < 1$ for finite T_B and nonzero T_A).

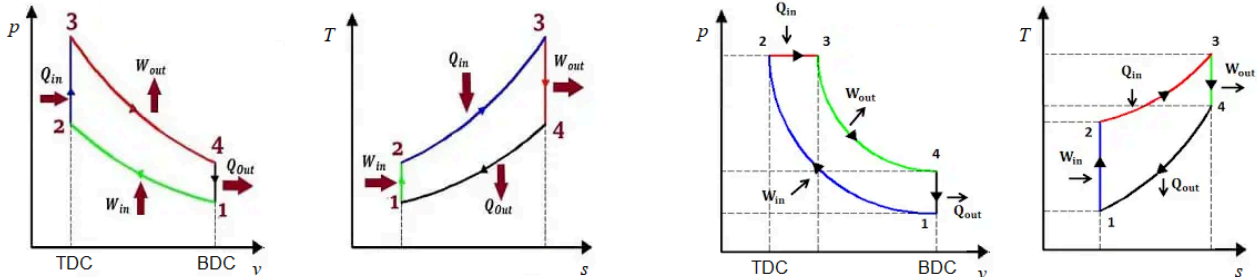
Carnot cycle: the only cycle with 100% second-law efficiency (fully reversible: maximum possible first-law efficiency). It consists of alternating isothermal and adiabatic processes, making a rectangle on a T - s indicator diagram. It cannot be achieved in reality.

Practical consequences of the second law of thermodynamics can be stated as:

- **Kelvin-Planck Statement** of the Second Law: no cyclic device can generate only work from only heat from a single thermal reservoir (work is more 'valuable' than heat).
- **Clausius Statement** of the Second Law: no cyclic device can transfer heat from a cold reservoir to a hot reservoir without work input (heat naturally flows from hot to cold spaces).

7.2.9. The Otto Cycle and Diesel Cycle (Fossil Fuel Powered Automobiles)

Indicator (P - v and T - s) diagrams for ideal air-standard Otto and Diesel cycles:



Otto Cycle (petrol/gasoline engines)

- 1 → 2: adiabatic compression
- 2 → 3: isochoric ignition from spark plug
- 3 → 4: adiabatic power stroke
- 4 → 1 → STP → 1: exhaust and intake

Diesel Cycle

- 1 → 2: adiabatic compression
- 2 → 3: isobaric ignition from glow plug
- 3 → 4: adiabatic power stroke
- 4 → 1 → STP → 1: exhaust and intake

TDC: top dead centre (piston before intake), BDC: bottom dead centre (piston after intake)

Real indicator diagrams have rounded corners since the crankshaft does not stop.

Engine Operation in Vehicles

- To initiate fuel combustion, a **spark plug** ignites the fuel-air mixture using electrical energy.
- In diesel engines, ignition occurs spontaneously (high T and p), but is assisted by a **glow plug**.
- The power stroke moves the piston down, turning the crankshaft, delivering torque to the drivetrain.
- A flywheel smooths the delivery of torque between cycles, providing maximum torque at a uniform engine speed, which is delivered to the drivetrain (wheels) by a gear system (by operating the clutch in a manual transmission vehicle).
- Four-stroke cycles require two revolutions of the crankshaft per cycle. Two-stroke cycles only require one, but are not used in automobiles due to fuel efficiency and emissions.
- Vehicles may have 3, 4, 6, 8 or more cylinders working together to supply torque to the crankshaft, in either e.g. V6 or I6 (inline) configurations.

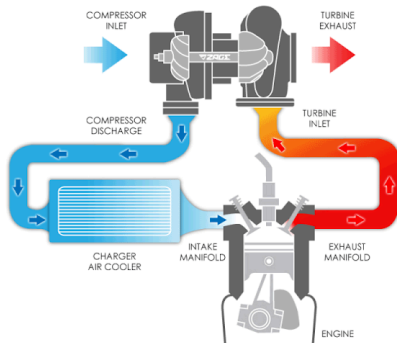
Power Development from Engines

- Input power from fuel combustion (as heat): $P_{\text{input}} = CV \times m'$
- Shaft power: $P_{\text{indicated}} = WfN_{\text{cyl}} = P_{\text{brake}} + P_{\text{lost}} = \eta_{\text{th}} P_{\text{input}}$
- Brake power (useful output power): $P_{\text{brake}} = T\omega = \eta_{\text{mech}} P_{\text{indicated}} = \eta_{\text{th}} \eta_{\text{mech}} P_{\text{input}} = \eta_{\text{overall}} P_{\text{input}}$

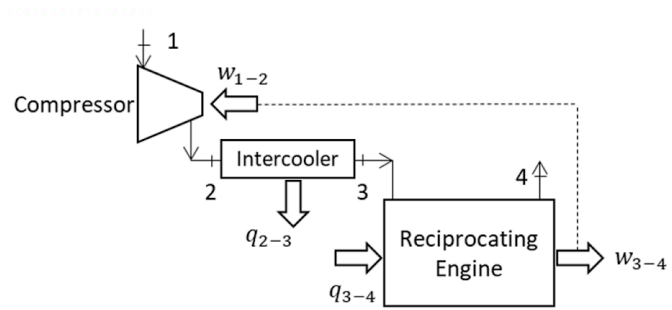
(CV : fuel calorific value, m' : mass flow rate, T : engine torque, ω : crankshaft angular velocity, W : work done per cycle, f : engine cycles per second, N_{cyl} : number of cylinders)

Additional devices used to enhance performance in automobiles include:

- Supercharger: compressor at inlet, powered by engine crankshaft via a belt drive
- Turbocharger: compressor at inlet, powered by hot exhaust flow
- Intercooler: a high-throughput heat exchanger used to prevent pre-ignition due to compression



Turbocharger (top) and intercooler (left) fitted to an engine (bottom)

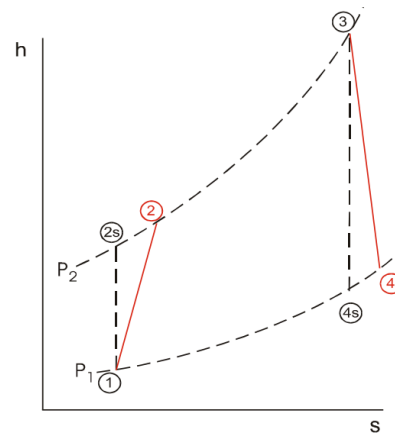
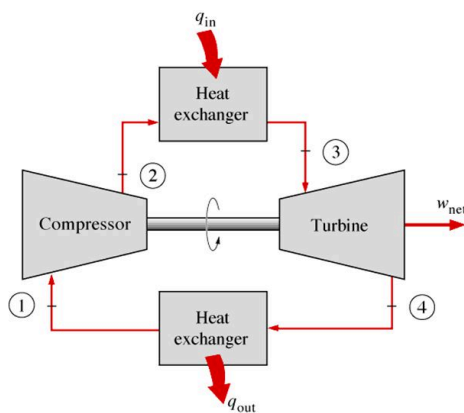


The supercharger supplies w_{1-2} from the engine shaft power w_{3-4}

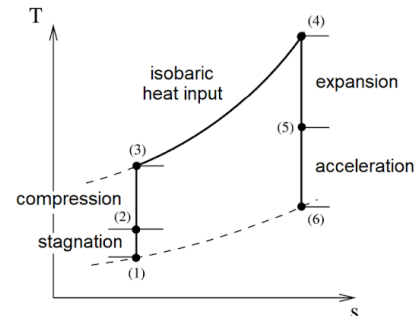
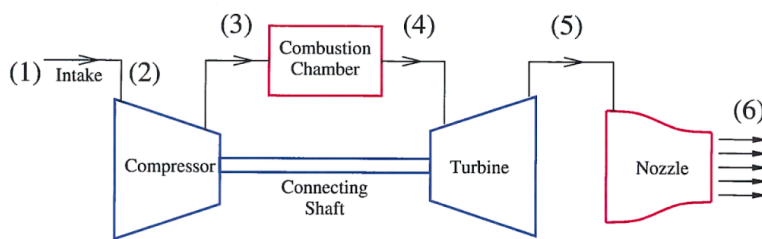
7.2.10. The Brayton Cycle / Joule Cycle (Gas Turbines and Jet Engines)

Used by aerospace vehicles (rockets), supersonic jets (airbreathing: turbojet and turbofan) and subsonic aircraft (turboprops). The gas can be hydrogen (rockets) or kerosene (jets).

Gas Turbine (imperfect cycle in red):



Jet engine:



Isentropic efficiency of a non-ideal compressor η_c and turbine η_t :

$$\eta_c \equiv \frac{\text{Ideal Work Input}}{\text{Actual Work Input}} = \frac{h_{2s} - h_1}{h_2 - h_1} \qquad \eta_t \equiv \frac{\text{Actual Work Output}}{\text{Ideal Work Output}} = \frac{h_3 - h_4}{h_3 - h_{4s}}$$

The non-ideal ending state lies on the same isobar as the ideal ending state (pressure losses are neglected), but at a higher entropy and temperature.

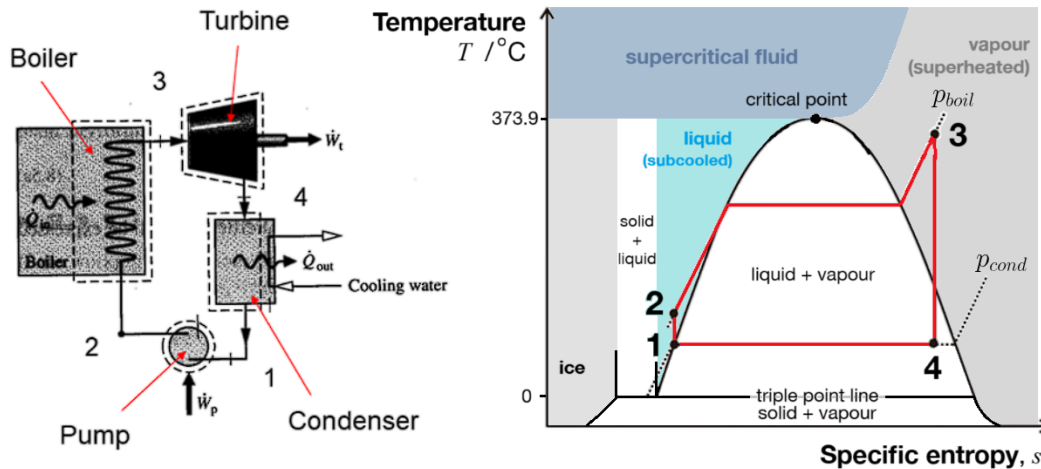
7.2.11. The Stirling Cycle

Uses two cylinders separated by a regenerator. Useful for some high-efficiency applications e.g. space vehicles (heat supplied by radioisotope thermoelectric generator (RTGs)).

Cycle: isothermal heat addition \rightarrow isochoric cooling \rightarrow isothermal heat rejection \rightarrow isochoric heating.

7.2.12. The Superheated Rankine Cycle (Steam Turbine)

An ideal Rankine cycle is shown, using mixtures of steam and condensate. It is often used in power plants to generate electricity, where the heat addition $q_{2 \rightarrow 3}$ comes from e.g. burning coal, oil, natural gas, biofuels, geothermal or solar thermal power. In a combined heat and power (CHP, cogeneration) scheme, both output heat $q_{4 \rightarrow 1}$ and work $w_{3 \rightarrow 4}$ are distributed to consumers.



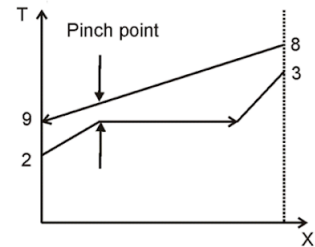
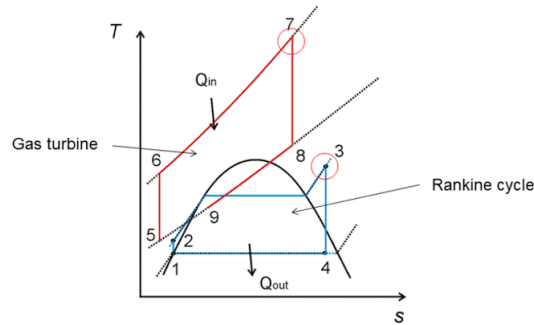
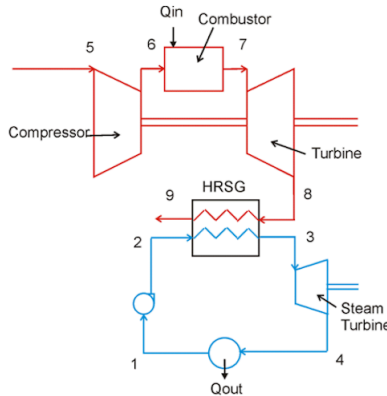
The turbine stage $w_{3 \rightarrow 4}$ may be split into **reheat stages** to increase the efficiency, up to a limit. Typically no more than two reheats are done due to practicalities and diminishing returns.

The steam quality (dryness fraction) at the turbine outlet (4) must be $>90\%$ to avoid water droplet condensation which leads to erosion of the turbine blades. The condenser pressure must be high enough to avoid ice crystal formation. The pump inlet total pressure must supply the required suction pressure at the pump inlet to avoid cavitation, achieved by physically positioning the pump at a lower elevation to gain hydrostatic pressure at the inlet.

A lower operating temperature alternative is to use an organic working fluid e.g. isopentane (organic Rankine cycle, ORC), useful for waste heat recovery. A recent development is the supercritical CO_2 Rankine cycle.

7.2.13. Combined-Cycle Gas Turbine (CCGT) and Heat Recovery Steam Generator (HRSG)

A CCGT uses the exhaust heat of a gas turbine to heat a steam turbine, improving efficiency.



Combined Cycle Gas Turbine

Indicator Diagrams

Thermal Gradient in HRSG

gas turbine feeds Rankine cycle

(X: fraction of heat transferred)

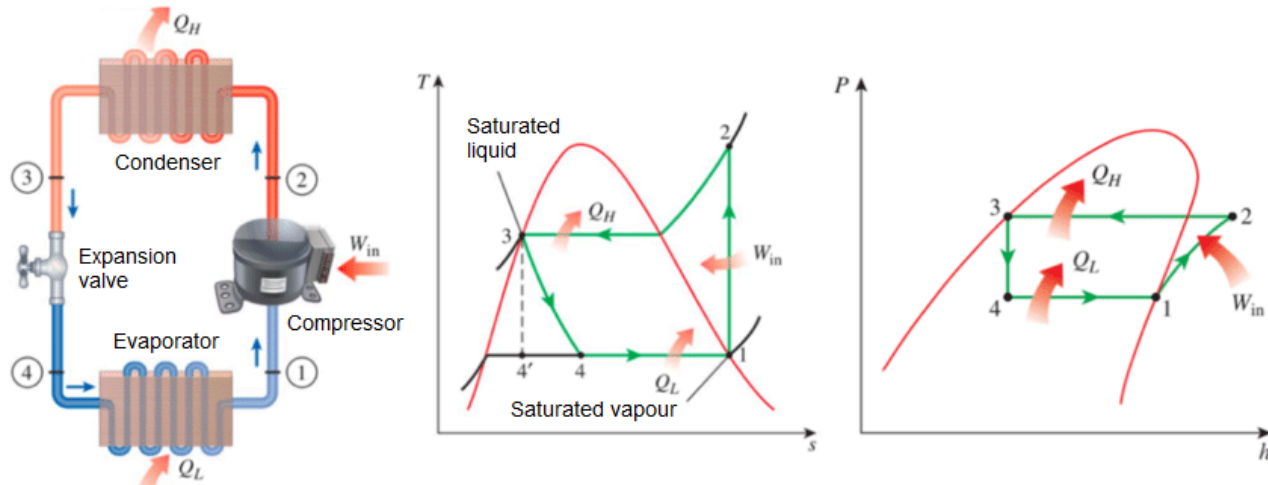
In the HRSG:
$$\frac{\dot{m}_{gas}}{\dot{m}_{H_2O}} = \frac{h_3 - h_2}{c_{p,gas} (T_8 - T_9)}$$
 (find h_2, h_3, s_2, s_3 for water from Section 7.4.4.)

Entropy in HRSG:
$$\Delta \dot{S}_{irrev} = \dot{m}_{H_2O} (s_3 - s_2) + \dot{m}_{gas} (s_9 - s_8) \quad (s_9 - s_8 = c_p \ln \frac{T_9}{T_8} - R \ln \frac{p_9}{p_8})$$

The HRSG steam side consists of the economiser (2 → wet sat), evaporator (wet sat → dry sat) and superheater (dry sat → 3). The pinch point is typically at the economiser outlet.

7.2.14. The Refrigeration Cycle (Refrigerators and Heat Pumps)

Representative indicator T - s and p - h diagrams are shown, with an ideal compressor. A typical working fluid is R-134a (a refrigerant / freon).



Coefficient of Performance: measures useful heat transfer per unit work input

$$\text{COP}_{\text{hp}} = \frac{\dot{Q}_H}{\dot{W}_{in}} \leq \frac{T_{\text{hot}}}{T_{\text{hot}} - T_{\text{cold}}} \quad \text{COP}_{\text{ref}} = \frac{\dot{Q}_L}{\dot{W}_{in}} \leq \frac{T_{\text{cold}}}{T_{\text{hot}} - T_{\text{cold}}} \quad \text{COP}_{\text{hp}} = 1 + \text{COP}_{\text{ref}}$$

COP can be considered the reciprocal of efficiency, since heat transfer is the desired output.

Heat removal ability: Q_L is often stated in any units of 1 TON = 3.516 kW = 12,000 BTU hr⁻¹. A rate of 1 TON is equivalent to freezing 1 ton of liquid water into ice at 0 °C in 24 hours.

Refrigeration cycles are used in household refrigerators, dehumidifiers, air conditioning units and heat pumps as an energy efficient alternative to air conditioning.

Specialised applications involve cryogenic cooling for superconductors using liquid helium or nitrogen, using dedicated cycles e.g. Stirling cryocooler, Brayton magnetocaloric cycle, Gifford-McMahon cycle.

7.2.15. Humidity and Psychrometry

If liquid water is added to dry air then the liquid layer will evaporate until the vapour pressure of steam in the gas mixture is attained (can be found in Section 7.4.4. as $p(T)$). At this point the air is said to be saturated. If a steam-air mixture is cooled below the dew point temperature, condensation to liquid water will occur similarly.

Specific humidity (humidity ratio):
$$\omega = \frac{m_{steam}}{m_{air}} = \frac{M_{r(H_2O)}}{M_{r(air)}} \times \frac{p_{steam}}{p_{air}} = 0.622 \frac{p_{steam}}{P_{tot} - p_{steam}}$$

Relative humidity:
$$\phi = \frac{p_{steam}}{p_{steam, sat}} \quad (\text{fraction of saturation pressure})$$

Psychrometric correlations or charts (e.g. flipped version of the Mollier diagram, Section 7.4.11, where $\phi = x$, dryness fraction) can be used to find the relative humidity and other state variables (e.g. specific enthalpy) from the dry bulb ($\phi = \phi_{mix}$) and wet bulb ($\phi = 1$) temperatures.

Dehumidifiers: condense water out of the air by dropping the temperature

A refrigeration cycle (Section 7.2.14) sets up a cold 'evaporator' coil and a hot 'condenser' coil. An external open air flow containing moisture is blown over the coils. The air meets the cold coil first, condensing out liquid water from the air, dropping the temperature and specific humidity. The cool, dry air is then warmed back up as it leaves over the hot coil.

An alternative refrigerant-free design is to use a desiccant to absorb water from the air without a temperature change.

Air conditioners operating in moist air will provide cooling as well as a dehumidification effect as their hot condenser coil rejects heat to the outside through a vent. Refrigerators can act as dehumidifiers for the food inside, reducing moisture content.

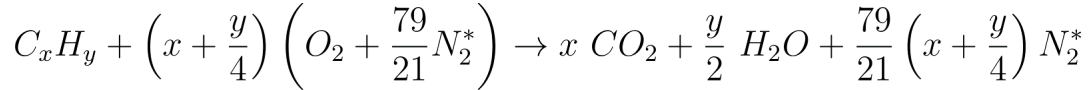
Humidifiers: add water vapour to the air directly

Water vapour is added to the air stream via simple evaporation. Liquid water is provided by the user in a reservoir, which can be dispersed as vapour by e.g. wick filter, mist formation by ultrasonic vibrator, or boiling of the water.

7.2.16. Thermochemistry of Combustion

Stoichiometry of Combustion Reactions

- **Stoichiometric combustion** of hydrocarbon fuels in atmospheric nitrogen-oxygen:



(Neglects small amounts of nitrogen oxidation to NO_x)

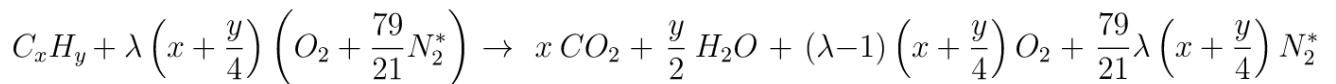
- **Air-to-fuel mass ratio (AFR):** $AFR = \frac{\dot{m}_{N_2^*, O_2}}{\dot{m}_{C_xH_y}}$ and $AFR_{stoichiometric} = \frac{28x + 7y}{12x + y}$

(M_r of atmospheric nitrogen, N₂* (diatomic nitrogen plus Ar, CO₂, etc.) = 28 g mol⁻¹.)

- **Lambda number:** $\lambda = \frac{AFR}{AFR_{stoichiometric}}$ and **equivalence ratio:** $\phi = \frac{1}{\lambda}$

(λ > 1 → lean, oxygen-rich, complete combustion; λ < 1 → (fuel)-rich, incomplete combustion. Optimal combustion typically requires some λ > 1: the value of λ - 1 is the 'excess air'.)

- **Reaction in lean conditions:**

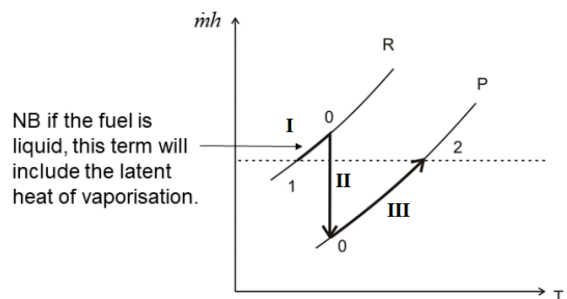
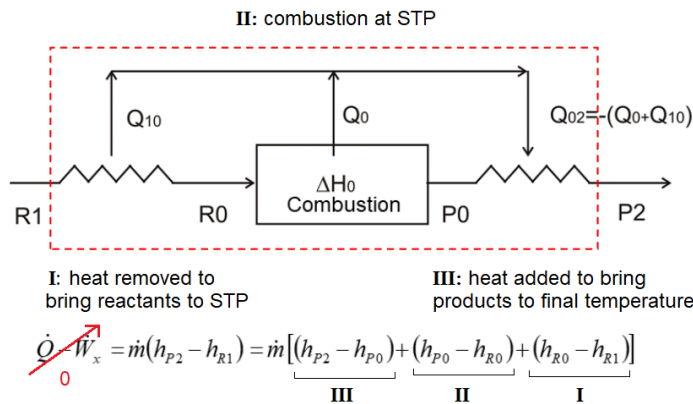


(Dry basis: water product is liquid (absent in gaseous mixture).)

Wet basis: water product is gas (present in gaseous mixture), assumed when T > 100 °C.)

If λ < 1 (oxygen-deficient) then combustion is incomplete and products are C / CO / CO₂ / H₂. Hydrogen is always fully oxidised first to H₂O. For reactions see Section 14.3.4.

Energetics of Combustion (1st law analysis). For useful data see Section 7.4.1-3.



7.2.17.

7.2.17. Aerodynamic Analysis of Turbines

(V_0 : upstream speed, A : turbine swept area, ρ : fluid density, θ : local twist angle of blade, ω : blade angular speed, $\sigma = \frac{cB}{2\pi r}$: rotor solidity, B : number of blades, c : chord length, $a = 1 - \frac{U}{V_0}$: axial induction factor, r : radial position)

Flow angle: $\tan \phi = \frac{(1-a)V_0}{(1+a')\omega R}$ Local angle of attack: $\alpha = \phi - \theta$

Lift and drag coefficient (below stall): $C_L \approx 2\pi\alpha$ $C_D \approx \text{const.}$ (for $\alpha < 15^\circ$; using radians)

Relative velocity: $V_{rel}^2 = V_0^2(1-a)^2 + r^2\omega^2(1+a')^2$

Force coefficients: $C_N = \frac{F_N}{\frac{1}{2}\rho V_{rel}^2 c} = C_L \cos \phi + C_D \sin \phi$ $C_T = \frac{F_T}{\frac{1}{2}\rho V_{rel}^2 c} = C_L \sin \phi - C_D \cos \phi$

Induction factors: axial: $a = \frac{1}{1 + \frac{4 \sin^2 \phi}{\sigma C_N}}$ angular: $a' = \frac{1}{1 + \frac{4 \sin \phi \cos \phi}{\sigma C_N}}$

Tip speed ratio: $\lambda = \frac{\omega R}{V_0}$

Aerodynamic loads: blade element forces/torques (BEM):

$$\delta N = 4\pi r \rho V_0^2 a(1-a) \delta r, \quad \delta T = 4\pi r^3 \rho V_0 (1-a) \omega a' \delta r$$

Total power: $P = \omega T = \omega \int_{r_0}^R \delta T = \omega B \int_{r_0}^R r F_T dr$

Available power: $P_{av} = \frac{1}{2} \rho A V_0^3$

Power coefficient: $C_P = \frac{P}{P_{av}} = \frac{P}{\frac{1}{2} \rho A U^3} = 4a(1-a^2)$ ($a = 1 - \frac{U}{V_0}$: axial induction factor)

Betz limit: $C_{P,max} = \frac{16}{27} \approx 59\%$ when $a = \frac{1}{3}$.

Capacity factor: $\frac{\text{energy generated over a long time}}{\text{rated power} \times \text{time}}$, a measure of installation effectiveness.

Additional loads are due to centrifugal force and self-weight. These are cyclic (periodic) with frequency $f = \frac{\omega B}{2\pi}$ (fatigue inducing: Section 6.6.6). Storm loading should also be considered. Wind loading is often modelled using the Wisper spectrum and generalisations to Miner's rule for fatigue modelling.

7.3. Heat Transfer

7.3.1. Heat Transfer by Conduction, Convection and Radiation

The rate of thermal energy transfer, \dot{Q} (units: W) is related to a temperature change ΔT by a thermal resistance R_{th} (units: $K W^{-1}$) such that $\Delta T = \dot{Q} R_{th}$. The mechanisms include:

- **Convection:** $\dot{Q} = hA (T_{body} - T_{surroundings})$, thermal resistance $R_{th} = \frac{1}{hA}$
(h : heat transfer coefficient, A : area of heat transfer)
- **Conduction:** axial $\dot{Q} = -\lambda A \frac{dT}{dx}$, thermal resistance $R_{th} = \frac{L}{\lambda A}$
(λ : rod thermal conductivity, A : rod cross-sectional area, dT/dx : temp gradient along rod)
- **Conduction:** radial $\dot{Q} = -2\pi r \lambda L \frac{dT}{dr}$, thermal resistance $R_{th} = \frac{\ln\left(\frac{r_2}{r_1}\right)}{2\pi \lambda L}$
(r : radial coordinate in cylindrical rod, L : rod length, dT/dr : radial temp gradient)
- **Radiation:** $\dot{Q} = \varepsilon \dot{Q}_{black} = \varepsilon \sigma A T^4$, circuit equivalent in Section 7.3.7.
(ε : grey body surface emissivity, A : surface area, $\sigma = 5.67 \times 10^{-8} W m^{-2} K^{-4}$: Stefan-Boltzmann constant. Note that the net rate of heat transfer will be less due to incident radiation.)

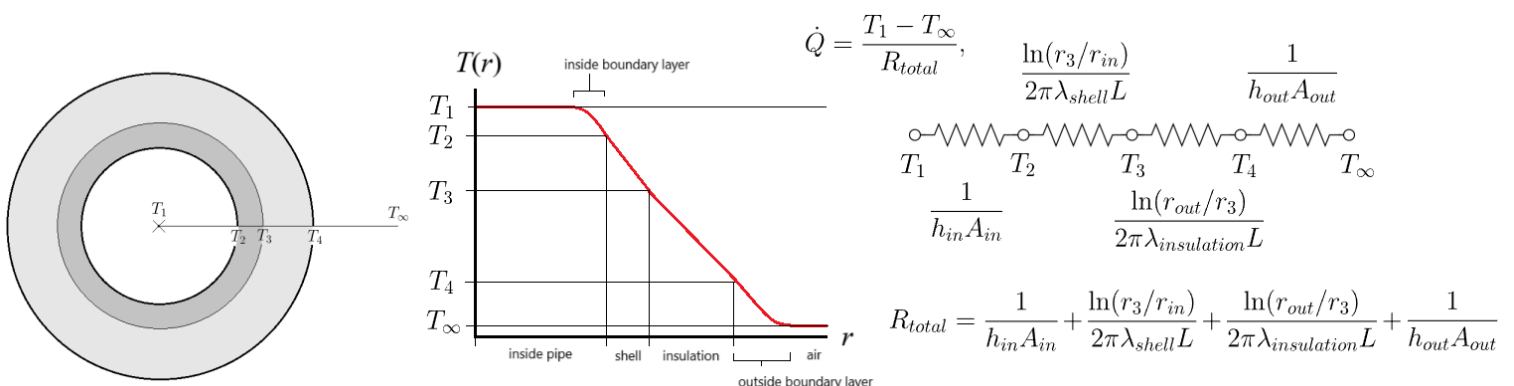
Lumped model: Newton's law of cooling

(assumes no internal heat generation, environment temp T_∞):

$$\frac{dT}{dt} = k (T_\infty - T) \quad \text{with solution} \quad \frac{T(t) - T_\infty}{T_0 - T_\infty} = \exp\left(-\frac{hA}{mc}t\right).$$

where $k = \frac{UA}{mc}$ and U is the overall heat transfer coefficient (primarily convection, so $U \approx h$).

Combined Conduction and Convection Models: insulated hot cylindrical pipe example



7.3.2. Coflow and Counterflow Heat Exchangers

In a co-flow or counter-flow heat exchanger, the log-mean temperature difference (LMTD, ΔT_{LM}) and arithmetic-mean temperature difference (AMTD, ΔT_{AM}) are given by

$$\Delta T_{LM} = \frac{\Delta T_1 - \Delta T_2}{\ln\left(\frac{\Delta T_1}{\Delta T_2}\right)} \quad \text{such that } Q' = UA \Delta T_{LM} \quad \text{and} \quad \Delta T_{AM} = \frac{1}{2}(\Delta T_1 + \Delta T_2).$$

where $\Delta T_1 = T_{h1} - T_{c1}$ and $\Delta T_2 = T_{h2} - T_{c2}$ are temperature differences between the **same ends** of the exchanger (**not** across each tube).

Effectiveness:
$$\varepsilon = \frac{\text{actual heat exchange}}{\text{maximum heat exchanged (counter flow)}} = \frac{Q'}{Q'_{max}}$$

Efficiency:
$$\eta = \frac{\text{actual heat exchange}}{\text{optimum heat exchanged}} = \frac{Q'}{Q'_{opt}}$$

Maximum heat exchanged:
$$\dot{Q}_{max} = (\dot{m}c_p)_{min} \times (\Delta T)_{max},$$

the product of the smallest heat capacity flow with the largest temperature difference between **any** two ends in the heat exchanger.

Optimum heat exchanged:
$$\dot{Q}_{opt} = UA \Delta T_{AM}$$

During a phase change:
$$\dot{Q} = \dot{m}h_{fg}$$

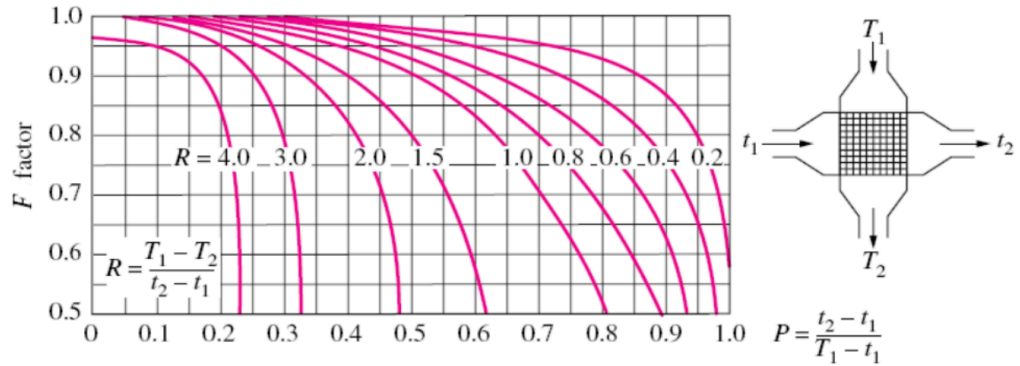
the product of the rate of evaporation or condensation with the enthalpy of the phase change.

7.3.3. Cross-Flow and Shell-Tube Heat Exchangers

For more complex geometry heat exchangers, an empirical correction factor (the F factor) is introduced, such that $\dot{Q} = F \times UA \Delta T_m$, (ΔT_m : LMTD of the equivalent counterflow HX).

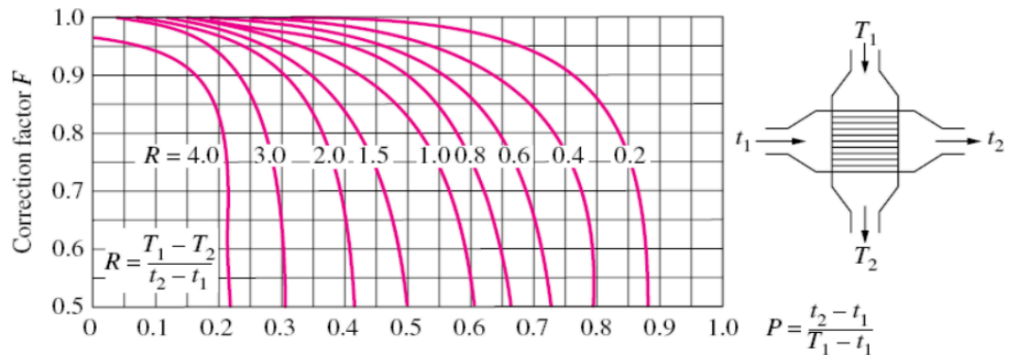
Cross-flow,
Single-pass,

Both flows
unmixed:

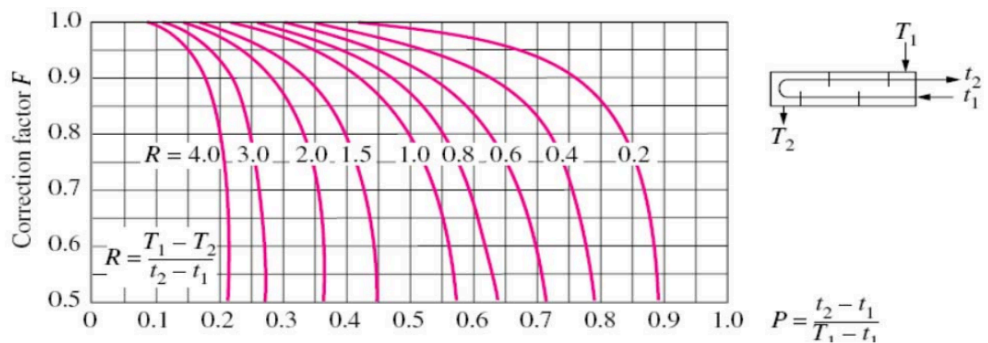


Cross-flow,
Single-pass,

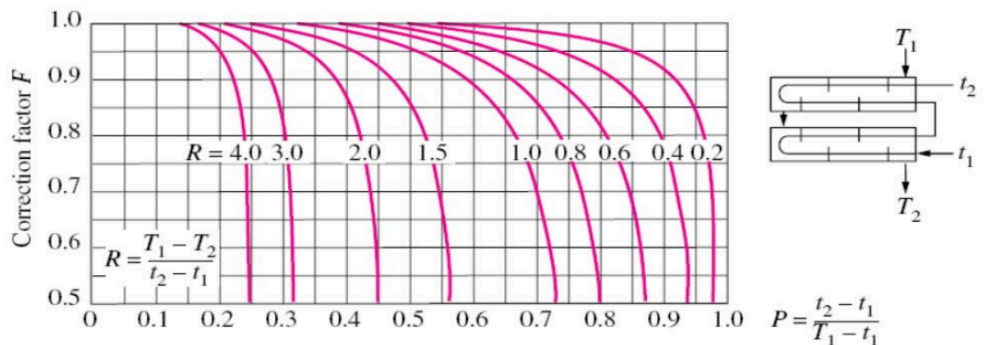
One flow (T) mixed
and the other (t)
unmixed:



Shell-and-tube,
One shell pass and
2, 4, 6, etc. tube
passes.



Shell-and-tube,
Two shell passes
and 4, 8, 12, etc.
tube passes.



7.3.4. Correlations for Heat Transfer by Natural Convection

For linear models, heat transfer coefficient $h = \frac{q'}{A(T_s - T_\infty)}$ and Nusselt number $Nu_L = \frac{hL}{\lambda}$.

General approximate ranges for h [W m⁻² K⁻¹] for different phase interfaces:

	Solid-Liquid	Solid-Gas	Liquid-Gas
Forced	500 - 20,000	20 - 300	20 - 3000
Natural	50 - 1,000	2 - 25	5 - 100

Natural (Free) Convection: heat is supplied or removed by buoyancy of surrounding fluid.

Correlations allow estimation of heat transfer coefficients h from the Nusselt number for a convection process.

Correlations for the Nusselt number, $Nu = f(Re, Pr)$ or $Nu = f(Ra, Pr)$ are:

<p>Vertical isothermal plate T_s: plate temperature T_∞: free stream temperature ($T_s > T_\infty$) x: position along plate from bottom of plate ($0 < x < L$). For a plate inclined at an angle of θ to the vertical, where $\theta < 60^\circ$, these correlations remain valid if $g \rightarrow g \cos \theta$ is used to calculate Ra_L.</p>	<p>All regimes: $\overline{Nu}_L = \left[0.825 + \frac{0.387 Ra_L^{1/6}}{\left[1 + \left(\frac{0.492}{Pr} \right)^{9/16} \right]^{8/27}} \right]^2$</p> <p>$Ra_L < 10^9$ (laminar): $\overline{Nu}_L = 0.68 + \frac{0.387 Ra_L^{1/4}}{\left[1 + \left(\frac{0.492}{Pr} \right)^{9/16} \right]^{4/9}}$</p>
<p>Horizontal isothermal plate T_s: plate temperature T_∞: free stream temperature x: position along plate from bottom of plate ($0 < x < L, T_s > T_\infty$) $L = \frac{\text{plate surface area}}{\text{plate face perimeter}}$</p>	<p>Upper surface of hot plate or lower surface of cold plate; $10^4 < Ra_L < 10^7$: $\overline{Nu}_L = 0.54 Ra_L^{1/4}$ $10^7 < Ra_L < 10^{11}$: $\overline{Nu}_L = 0.15 Ra_L^{1/3}$ Lower surface of hot plate or upper surface of cold plate; $10^5 < Ra_L < 10^{10}$: $\overline{Nu}_L = 0.27 Ra_L^{1/4}$</p>
<p>Horizontal isothermal cylinder T_s: cylinder temperature T_∞: free stream temperature D: cylinder diameter</p>	<p>$Ra_D < 10^{12}$: $\overline{Nu}_D = \left[0.60 + \frac{0.387 Ra_D^{1/6}}{\left[1 + \left(\frac{0.559}{Pr} \right)^{9/16} \right]^{8/27}} \right]^2$</p>
<p>Isothermal sphere T_s: sphere temperature T_∞: free stream temperature D: sphere diameter</p>	<p>$Ra_D < 10^{11}, Pr > 0.7$: $\overline{Nu}_D = 2 + \frac{0.589 Ra_D^{1/4}}{\left[1 + \left(\frac{0.469}{Pr} \right)^{9/16} \right]^{4/9}}$</p>

7.3.5. Correlations for Heat Transfer by Forced Convection

Forced Convection: heat is supplied or removed by constantly flowing surrounding fluid.

For forced convection into gases, the HTC is on the order of 10-100 W m⁻² K⁻¹.

The Reynolds analogy between heat and momentum transfer: $St = \frac{1}{2} c_f$

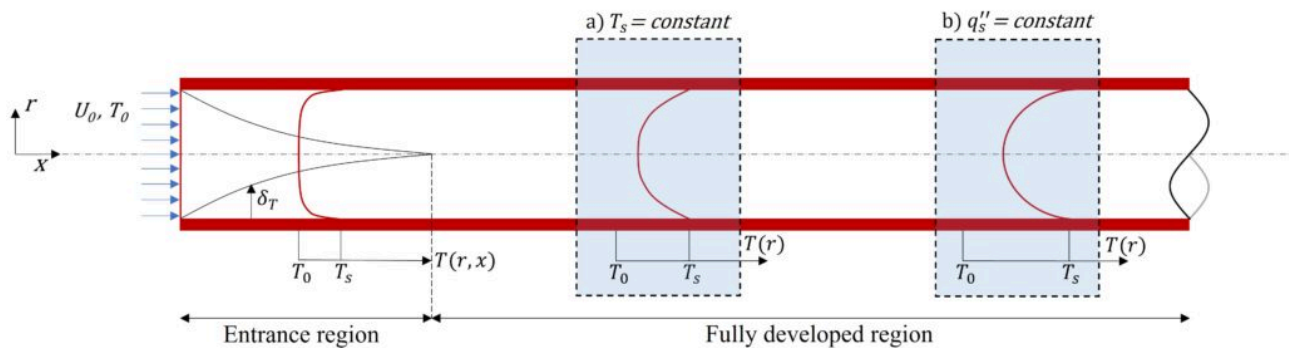
The film temperature between a temperature T and a flow at T_∞ : $T_{film} = \frac{1}{2} (T + T_\infty)$

<p>Flat isothermal plate oriented parallel to flow T_s: plate temperature U_∞: free stream velocity T_∞: free stream temperature x: position along plate from inlet edge of plate ($0 < x < L, T_s > T_\infty$)</p>	<p>Pr > 0.6 (laminar): $Nu_x = 0.332 Re_x^{1/2} Pr^{1/3}$ Pr > 0.6 (laminar): $\overline{Nu}_x = 2 Nu_x = 0.664 Re_x^{1/2} Pr^{1/3}$ 0.6 < Pr < 60 (turbulent): $Nu_x = 0.0296 Re_x^{4/5} Pr^{1/3}$ 0.6 < Pr < 60 (turbulent): $\overline{Nu}_x = 0.037 Re_x^{4/5} Pr^{1/3}$</p>
<p>Flat plate with uniform heat flux oriented parallel to flow U_∞: free stream velocity T_∞: free stream temperature x: position along plate from inlet edge of plate ($0 < x < L, T_s > T_\infty$)</p>	<p>Pr > 0.6 (laminar): $Nu_x = 0.453 Re_x^{1/2} Pr^{1/3}$ All regimes: $\overline{Nu}_x = 0.68 Re_x^{1/2} Pr^{1/3}$ 0.6 < Pr < 60 (turbulent): $Nu_x = 0.0308 Re_x^{4/5} Pr^{1/3}$</p>
<p>Isothermal cylinder in cross flow T_s: plate temperature U_∞: free stream velocity T_∞: free stream temperature D: diameter of cylinder</p>	<p>Re_D Pr > 0.2: $\overline{Nu}_D = 0.3 + \frac{0.62 Re_D^{1/2} Pr^{1/3} \left[1 + \left(\frac{Re_D}{282000} \right)^{5/8} \right]^{4/5}}{\left[1 + \left(\frac{0.4}{Pr} \right)^{2/3} \right]^{1/4}}$ 0.4 < Re_D < 4: $\overline{Nu}_D = 0.989 Re_D^{0.33} Pr^{1/3}$ 4 < Re_D < 40: $\overline{Nu}_D = 0.911 Re_D^{0.385} Pr^{1/3}$ 40 < Re_D < 4000: $\overline{Nu}_D = 0.683 Re_D^{0.466} Pr^{1/3}$ 4000 < Re_D < 4 × 10⁴: $\overline{Nu}_D = 0.193 Re_D^{0.618} Pr^{1/3}$ 4 × 10⁴ < Re_D < 4 × 10⁵: $\overline{Nu}_D = 0.027 Re_D^{0.805} Pr^{1/3}$</p>
<p>Sphere in cross flow D: diameter of sphere</p>	<p>Re < 5 × 10⁵: $Nu_D = 2 + \left(0.4 Re_D^{1/2} + 0.06 Re_D^{2/3} \right) Pr^{0.4}$</p>

Forced Convection in Pipe Flow: fluid-wall convection due to internal pipe flow

For pipe flow, fluid properties are taken at the local mean temperature $T_m = \frac{2}{u_m r_{max}^2} \int_0^{r_{max}} u T r dr$,

where u_m is the mean velocity, $u_m = \frac{2}{r_{max}} \int_0^{r_{max}} u(r, x) r dr$. (r_{max} : pipe internal radius)



<p>Laminar Pipe Flow T_s: pipe surface temperature U_∞: free stream velocity T_∞: free stream temperature D: diameter of cylinder</p>	<p>Case a): Isothermal, laminar: $Nu_D = 3.66$ Case b): Constant heat flux, laminar: $Nu_D = 4.36$ Full region including entrance effects: $\overline{Nu}_D = 1.86 \left(\frac{Re_D Pr}{L/D} \right)^{1/3} \left(\frac{\mu}{\mu_s} \right)^{0.14}$</p>
<p>Turbulent Pipe Flow T_s: pipe surface temperature U_∞: free stream velocity T_∞: free stream temperature D: diameter of cylinder</p>	<p>Small temperature differences: $Nu_D = 0.023 Re_D^{4/5} Pr^{0.3}$ Large temperature differences: $Nu_D = 0.027 Re_D^{4/5} Pr^{1/3} \left(\frac{\mu}{\mu_s} \right)^{0.14}$ For non-circular pipes, use the hydraulic diameter, $D_h = \frac{4 A_c}{P}$ (A_c: area, P: perimeter)</p>

Forced fluid boiling flow: evaporation in vertical tubes (Chen's correlation)

$$h = S \cdot \underbrace{\frac{\lambda^{0.79} c_p^{0.45} \rho_l^{0.49} g^{0.25} \Delta T^{0.24} \Delta p^{0.75}}{\sigma^{0.5} \mu^{0.29} h_{fg}^{0.24} \rho_v^{0.24}}}_{h_{pool}: \text{ nucleate pool boiling (Forster-Zuber corr.)}} + F \cdot \underbrace{\frac{Re^{0.8} Pr^{0.4} \lambda}{d_{eq}}}_{h_{conv}: \text{ forced convection (Dittus-Boelter corr.)}}$$

(λ : thermal conductivity, c_p : specific heat capacity, ρ : density, g : gravitational acceleration, $\Delta T = T_{wall} - T_{sat}$, Δp : bubble pressure drop, σ : surface tension, μ : dynamic viscosity, h_{fg} : specific latent heat of vaporisation, d_{eq} : hydraulic diameter, Re_{tp} : two-phase Reynolds, χ_{tt} : Lockhart-Martinelli parameter)

$$S = \frac{1}{1 + 2.53 \times 10^{-6} \times Re_{tp}^{1.17}}, \quad F = \left(\frac{Re_{tp}}{Re} \right)^{0.8} = 2.35 \times \left(\frac{1}{\chi_{tt}} + 0.213 \right)^{0.736}$$

7.3.6. Thermal Radiation

A ‘black body’ is an idealised object, which will completely absorb all radiation incident upon it, and emit the largest amount of power per unit area possible for a given temperature: ($\sigma = 5.67 \times 10^{-8} \text{ W m}^{-2} \text{ K}^{-4}$: Stefan-Boltzmann constant)

Total energy flux, $E_b \text{ [W m}^{-2}] = \sigma T^4$; **Total entropy flux**, $S_b \text{ [W K}^{-1} \text{ m}^{-2}] = \frac{4}{3} \sigma T^3$

Spectra, such that $E_b = \int_0^\infty E_{b\lambda} d\lambda$ and $S_b = \int_0^\infty S_{b\lambda} d\lambda$, are

Energy spectrum, $E_{b\lambda} = \frac{2hc^2}{\lambda^5 \left(\exp\left(\frac{hc}{\lambda T}\right) \right)}$ (λ : wavelength)

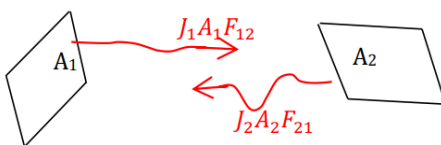
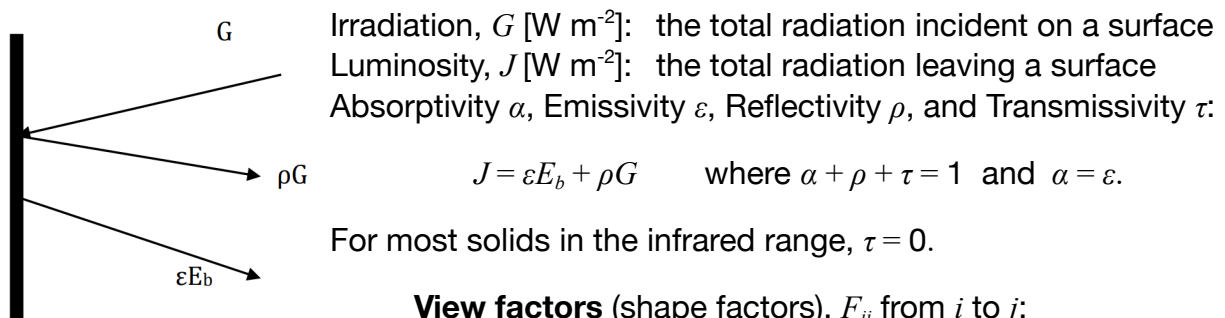
Entropy spectrum, $S_{b\lambda} = \frac{2n_0kc}{\lambda^4} \left[\left(1 + \frac{\lambda^5 E_{b\lambda}}{2n_0hc^2} \right) \ln \left(1 + \frac{\lambda^5 E_{b\lambda}}{2n_0hc^2} \right) - \frac{\lambda^5 E_{b\lambda}}{2n_0hc^2} \ln \frac{\lambda^5 E_{b\lambda}}{2n_0hc^2} \right]$ (λ : wavelength)

Exergy spectrum, $e_{b\lambda}(T) = [E_{b\lambda}(T) - E_{b\lambda}(T_0)] - T_0[S_{b\lambda}(T) - S_{b\lambda}(T_0)]$ (same expression for total).

(monochromatic emissive black body spectra i.e. between wavelengths λ and $\lambda + d\lambda$;
 $\sigma = 5.67 \times 10^{-8} \text{ W m}^{-2} \text{ K}^{-4}$: Stefan-Boltzmann constant, $c_1 = 2\pi hc^2 = 3.743 \times 10^{-16} \text{ W m}^{-2}$,
 $c_2 = hc / k_B = 1.4387 \times 10^4 \text{ } \mu\text{m K}$, with wavelength λ in numerical units of μm , ν []: frequency of radiation, $n_0 = \{1 \text{ if polarised rays; } 2 \text{ if unpolarised rays}\}$, T : emitter temperature, T_0 : dead state / receiver temperature)

Grey Body: has an emissive power proportional to a black body at the same temperature for all wavelengths, with an emissivity ϵ such that $E_\lambda = \epsilon E_{b\lambda}$ and $S_\lambda = \epsilon S_{b\lambda}$.

For **matte black** materials, $\epsilon \approx 1, \rho \approx 0$. For **shiny white** or mirror-like materials, $\epsilon \approx 0, \rho \approx 1$.



View factors (shape factors), F_{ij} from i to j :

$A_i F_{ij} = A_j F_{ji}$, $\sum_j F_{ij} = 1$, i is convex $\Leftrightarrow F_{ii} = 0$

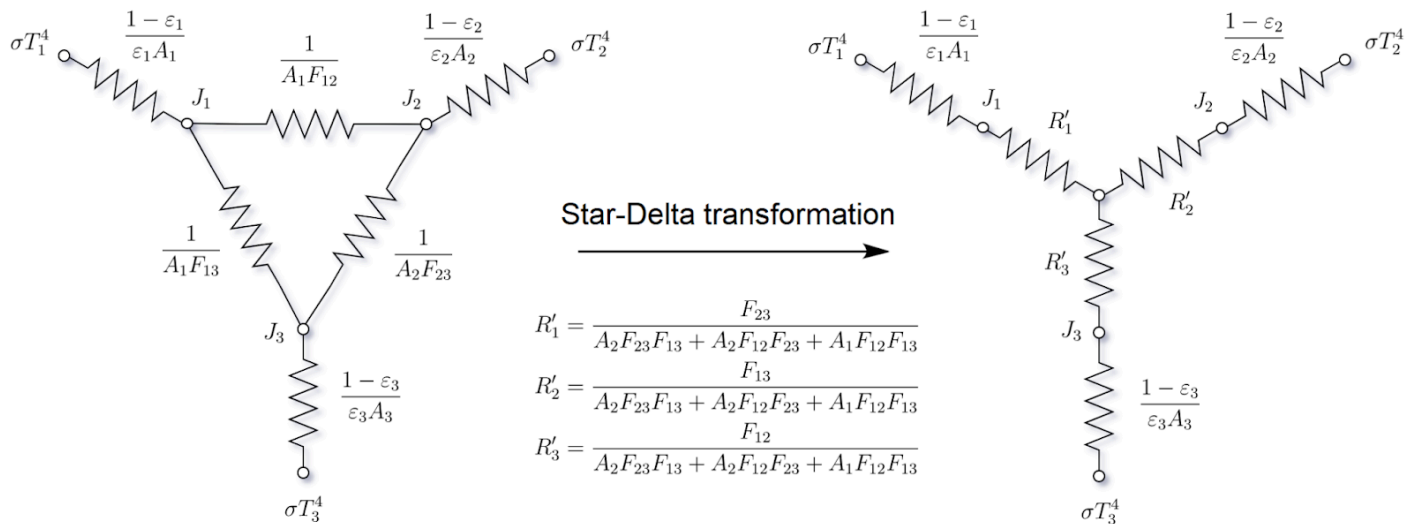
If the medium does not interact with infrared radiation

(i.e. $\tau_{medium} = 1$) then $Q = \frac{J_1 - J_2}{1/(A_1 F_{12})}$.

7.3.7. Electrical Analogy for Radiative Exchange Between Surfaces

- Electrical-radiative circuit analogy: $I = \frac{\Delta V}{R_{elec}} \Leftrightarrow \dot{Q} = \frac{\Delta E}{R_{th}}$ (Ohm's law)
 (ΔE : radiation intensity difference, \dot{Q} : radiative heat transfer rate, R_{th} : thermal resistance)
- Grey body emission: $R_{th} = \frac{1 - \varepsilon}{\varepsilon A}$ such that $E_b - J = \dot{Q} R_{th}$
 ($E_b = \sigma T^4$: black body intensity, J : luminosity, ε : emissivity, A : surface area)
- Radiative exchange: $R_{th} = \frac{1}{AF}$ such that $J_1 - J_2 = \dot{Q}' R_{th}$
 (A : area of this body, F : view factor from this body to another, \dot{Q}' : heat transfer rate between bodies when the system is loses no radiation to the environment)

A typical two-body setup (with the environment as a third 'body') can be represented as



For the details of the Star-Delta transformation, see Section 8.2.2. Other simplifications:

- If a surface is insulated, there is no net current flow into it, so it can be simplified to be considered a black body (i.e. short / remove its $\sigma T^4 - J$ resistor).
- For the environment, since $A \rightarrow \infty$, it can be simplified to a black body (i.e. short / remove its $\sigma T^4 - J$ resistor).

7.4. Thermodynamic Data of Fluids

7.4.1. Combustion and Calorific Values of Hydrocarbon-Based Fuels

When heat transfer to a control volume is defined as positive and in the absence of shaft work, changes in KE and PE, capillarity, electric and magnetic fields, the rate of heat transfer and the calorific value (CV) are related by

$$\dot{Q} = \dot{m}_{fuel}(-CV) = \dot{n}_{fuel}\Delta\bar{h} \quad \dot{m}_{fuel} = M\dot{n}_{fuel}$$

The calorific value is equal and opposite to the enthalpy of reaction when the reactants and products are at 25 °C and 1.01325 bar. In the evaluation of the lower calorific value and lower enthalpy of reaction, the steam is assumed to be dry saturated.

Stoichiometric Equation	Molar Mass M of Fuel kg kmol	Phase	Calorific Value MJ/kg	
			Higher: H_2O to water	Lower: H_2O to steam
$C + \frac{1}{2}O_2 \rightarrow CO$	12	solid	9.190	
$C + O_2 \rightarrow CO_2$	12	solid	32.760	
$CO + \frac{1}{2}O_2 \rightarrow CO_2$	28	gas	10.100	
$H_2 + \frac{1}{2}O_2 \rightarrow H_2O$	2.016	gas	142.000	120.000
$CH_4 + 2O_2 \rightarrow CO_2 + 2H_2O$	16	gas	55.500	50.010
$C_2H_6 + 3.5O_2 \rightarrow 2CO_2 + 3H_2O$	30	gas	51.870	47.470
$C_3H_8 + 5O_2 \rightarrow 3CO_2 + 4H_2O$	44	gas	50.360	46.360
$C_4H_{10} + 6.5O_2 \rightarrow 4CO_2 + 5H_2O$	58	gas	49.520	45.730
$C_8H_{18} + 12.5O_2 \rightarrow 8CO_2 + 9H_2O$	114	gas	48.270	44.800
$C_8H_{18} + 12.5O_2 \rightarrow 8CO_2 + 9H_2O$	114	liquid	47.900	44.430

A dry basis uses the higher CV, a wet basis uses the lower CV.

7.4.2. Properties of Perfect Gases

At normal atmospheric conditions, and over a limited range of temperature and pressure, the gases listed below may be assumed to behave as perfect gases. That is, they may be assumed to have the equation of state $p\bar{v} = \bar{R}T$, and to have constant specific heat capacities.

Gas	Molar mass M kg/kmol	Gas constant R kJ/kg K	c_p kJ/kg K	c_v kJ/kg K	$\gamma \equiv \frac{c_p}{c_v}$
Air [#]	29.0	0.287	1.005	0.718	1.40
Atmospheric nitrogen [†]	28.15	0.295	1.033	0.738	1.40
N ₂	28	0.297	1.04	0.74	1.40
O ₂	32	0.260	0.92	0.66	1.40
Ar	40	0.208	0.52	0.31	1.67
H ₂	2 [*]	4.120	14.20	10.08	1.41
He	4	2.080	5.19	3.11	1.67
CO	28	0.297	1.04	0.74	1.40
CO ₂	44	0.189	0.83	0.63	1.31
SO ₂	64	0.130	0.61	0.48	1.26
CH ₄	16	0.520	2.23	1.71	1.31
C ₂ H ₆	30	0.277	1.75	1.47	1.19
C ₃ H ₆	42	0.198	1.52	1.32	1.15

- Air contains 0.93 % of argon (Ar) and traces of other gases; these and the nitrogen together are called atmospheric nitrogen (atm N₂).
- Air contains 21.0% O₂ and 79.0% atm N₂ by **volume** (Volumetric / Molar Analysis).
- Air contains 23.2% O₂ and 76.8% atm N₂ by **weight** (Gravimetric Analysis).
- Molar volume: 1 kmol of any perfect gas occupies a volume of approximately 22.7 m³ at s.t.p. (0 °C and 1 bar) and contains 6.022×10^{26} particles.

7.4.3. Molar Enthalpies of Gases at High Temperature and Low Pressure

At low pressures, and over the temperature range quoted, the gases listed below behave as **semi-perfect** gases. That is, while having the molar equation of state $p\bar{v} = \bar{R}T$, their specific heat capacities c_p and c_v are not constant but are functions only of temperature.

Gas	Air	N ₂	O ₂	H ₂	CO	CO ₂	H ₂ O	Gas
Molar Mass kg/kmol	29	28	32	2†	28	44	18	Molar Mass kg/kmol
Temperature K	Molar enthalpy MJ/kmol							Temperature K
200	5.79	5.81	5.79	5.69	5.81	5.96	6.62	200
298.15=25°C	8.64	8.67	8.66	8.46	8.67	9.37	9.90	25°C=298.15
300	8.70	8.72	8.71	8.52	8.72	9.44	9.96	300
400	11.62	11.64	11.68	11.42	11.64	13.37	13.35	400
500	14.57	14.58	14.74	14.34	14.60	17.67	16.82	500
600	17.59	17.56	17.90	17.27	17.61	22.27	20.39	600
700	20.66	20.61	21.16	20.21	20.69	27.12	24.09	700
800	23.81	23.72	24.50	23.16	23.85	32.18	27.90	800
900	27.03	26.89	27.90	26.13	27.07	37.41	31.83	900
1000	30.30	30.14	31.37	29.14	30.36	42.78	35.90	1000
1100	33.64	33.44	34.88	32.18	33.71	48.27	40.09	1100
1200	37.02	36.79	38.43	35.26	37.11	53.87	44.41	1200
1300	40.44	40.19	42.01	38.38	40.54	59.55	48.84	1300
1400	43.90	43.62	45.63	41.54	44.02	65.31	53.39	1400
1500	47.39	47.09	49.27	44.75	47.53	71.13	58.05	1500
1600	50.92	50.59	52.94	48.00	51.07	77.01	62.81	1600
1700	54.47	54.12	56.63	51.29	54.63	82.94	67.65	1700
1800	58.04	57.67	60.35	54.62	58.21	88.92	72.58	1800
1900	61.63	61.25	64.09	58.00	61.81	94.93	77.59	1900
2000	65.24	64.84	67.86	61.40	65.42	100.97	82.67	2000
2100	68.87	68.44	71.65	64.84	69.06	107.05	87.81	2100
2200	72.52	72.06	75.46	68.31	72.70	113.15	93.01	2200
2300	76.18	75.70	79.29	71.82	76.36	119.28	98.27	2300
2400	79.86	79.35	83.14	75.35	80.03	125.43	103.58	2400
2500	83.55	83.01	87.02	78.90	83.71	131.61	108.94	2500
2600	87.25	86.68	90.92	82.48	87.40	137.80	114.34	2600
2700	90.96	90.36	94.83	86.09	91.10	144.02	119.78	2700
2800	94.69	94.05	98.77	89.72	94.80	150.25	125.26	2800
2900	98.42	97.74	102.72	93.37	98.51	156.50	130.77	2900
3000	102.16	101.44	106.70	97.04	102.23	162.76	136.31	3000

- The molar enthalpies listed are those in the ideal gas state at zero pressure, but the values given are also valid at and around atmospheric pressure.
- In this table, the arbitrary datum state for zero enthalpy is that of the substance in the ideal gas state at zero pressure and zero absolute temperature.
- The values for atmospheric nitrogen, N₂*, may be taken to be the same as those for N₂.

7.4.4. Saturated Water and Steam (Steam Tables)

Temperatures from the triple point to the critical point (showing $0.01\text{ }^{\circ}\text{C} \leq T \leq 100\text{ }^{\circ}\text{C}$):

Temp. $^{\circ}\text{C}$	Pressure bar	Specific volume m^3/kg		Spec. int. energy kJ/kg		Specific enthalpy kJ/kg			Specific entropy $\text{kJ}/\text{kg K}$		Temp. $^{\circ}\text{C}$
T	p	v_f	v_g	u_f	u_g	h_f	h_{fg}	h_g	s_f	s_g	T
0.01	0.00611	0.001000	206.005	0.0	2375.0	0.0	2500.9	2500.9	0.000	9.156	0.01
2	0.00706	0.001000	179.776	8.4	2377.6	8.4	2496.2	2504.6	0.031	9.103	2
4	0.00814	0.001000	157.135	16.8	2380.4	16.8	2491.4	2508.2	0.061	9.051	4
6	0.00935	0.001000	137.652	25.2	2383.1	25.2	2486.7	2511.9	0.091	8.999	6
8	0.01073	0.001000	120.846	33.6	2385.9	33.6	2481.9	2515.6	0.121	8.949	8
10	0.01228	0.001000	106.319	42.0	2388.6	42.0	2477.2	2519.2	0.151	8.900	10
12	0.01403	0.001001	93.732	50.4	2391.4	50.4	2472.5	2522.9	0.181	8.851	12
14	0.01599	0.001001	82.804	58.8	2394.1	58.8	2467.7	2526.5	0.210	8.804	14
16	0.01819	0.001001	73.295	67.2	2396.9	67.2	2463.0	2530.2	0.239	8.757	16
18	0.02065	0.001001	65.005	75.5	2399.6	75.5	2458.3	2533.8	0.268	8.711	18
20	0.02339	0.001002	57.762	83.9	2402.3	83.9	2453.5	2537.4	0.296	8.666	20
22	0.02645	0.001002	51.422	92.3	2405.0	92.3	2448.8	2541.1	0.325	8.622	22
24	0.02986	0.001003	45.861	100.6	2407.8	100.6	2444.1	2544.7	0.353	8.578	24
25	0.03170	0.001003	43.340	104.8	2409.1	104.8	2441.7	2546.5	0.367	8.557	25
26	0.03364	0.001003	40.975	109.0	2410.5	109.0	2439.3	2548.3	0.381	8.535	26
28	0.03783	0.001004	36.673	117.4	2413.2	117.4	2434.6	2551.9	0.409	8.493	28
30	0.04247	0.001004	32.879	125.7	2415.9	125.7	2429.8	2555.5	0.437	8.452	30
32	0.04760	0.001005	29.527	134.1	2418.6	134.1	2425.1	2559.2	0.464	8.411	32
34	0.05325	0.001006	26.560	142.4	2421.3	142.4	2420.3	2562.8	0.492	8.371	34
36	0.05948	0.001006	23.929	150.8	2424.0	150.8	2415.5	2566.3	0.519	8.332	36
38	0.06633	0.001007	21.593	159.2	2426.7	159.2	2410.8	2569.9	0.546	8.294	38
40	0.07385	0.001008	19.515	167.5	2429.4	167.5	2406.0	2573.5	0.572	8.256	40
42	0.08210	0.001009	17.663	175.9	2432.1	175.9	2401.2	2577.1	0.599	8.218	42
44	0.09113	0.001010	16.010	184.2	2434.7	184.2	2396.4	2580.6	0.625	8.181	44
46	0.10100	0.001010	14.534	192.6	2437.4	192.6	2391.6	2584.2	0.652	8.145	46
48	0.11178	0.001011	13.212	201.0	2440.1	201.0	2386.8	2587.8	0.678	8.110	48
50	0.12352	0.001012	12.026	209.3	2442.7	209.3	2382.0	2591.3	0.704	8.075	50
52	0.13632	0.001013	10.962	217.7	2445.4	217.7	2377.1	2594.8	0.730	8.040	52
54	0.15023	0.001014	10.006	226.0	2448.0	226.1	2372.3	2598.3	0.755	8.007	54
56	0.16534	0.001015	9.145	234.4	2450.7	234.4	2367.4	2601.8	0.781	7.973	56
58	0.18172	0.001016	8.368	242.8	2453.3	242.8	2362.5	2605.3	0.806	7.940	58
60	0.19947	0.001017	7.667	251.1	2455.9	251.2	2357.7	2608.8	0.831	7.908	60
62	0.21868	0.001018	7.033	259.5	2458.5	259.5	2352.8	2612.3	0.856	7.876	62
64	0.23944	0.001019	6.460	267.9	2461.1	267.9	2347.9	2615.8	0.881	7.845	64
66	0.26184	0.001020	5.940	276.3	2463.7	276.3	2342.9	2619.2	0.906	7.814	66
68	0.28600	0.001022	5.468	284.6	2466.3	284.7	2338.0	2622.7	0.931	7.784	68
70	0.31202	0.001023	5.040	293.0	2468.8	293.1	2333.0	2626.1	0.955	7.754	70
72	0.34002	0.001024	4.650	301.4	2471.4	301.4	2328.1	2629.5	0.979	7.725	72
74	0.37010	0.001025	4.295	309.8	2474.0	309.8	2323.1	2632.9	1.004	7.696	74
76	0.40240	0.001026	3.971	318.2	2476.5	318.2	2318.1	2636.3	1.028	7.667	76
78	0.43704	0.001028	3.675	326.6	2479.0	326.6	2313.1	2639.7	1.052	7.639	78
80	0.47416	0.001029	3.405	335.0	2481.5	335.0	2308.0	2643.0	1.076	7.611	80
82	0.51388	0.001030	3.158	343.3	2484.1	343.4	2303.0	2646.4	1.099	7.584	82
84	0.55636	0.001032	2.932	351.7	2486.5	351.8	2297.9	2649.7	1.123	7.557	84
86	0.60174	0.001033	2.725	360.1	2489.0	360.2	2292.8	2653.0	1.146	7.530	86
88	0.65018	0.001035	2.534	368.6	2491.5	368.6	2287.6	2656.3	1.170	7.504	88
90	0.70183	0.001036	2.359	377.0	2494.0	377.0	2282.5	2659.5	1.193	7.478	90
92	0.75685	0.001037	2.198	385.4	2496.4	385.4	2277.3	2662.8	1.216	7.453	92
94	0.81542	0.001039	2.050	393.8	2498.8	393.9	2272.1	2666.0	1.239	7.428	94
96	0.87771	0.001040	1.914	402.2	2501.2	402.3	2266.9	2669.2	1.262	7.403	96
98	0.94390	0.001042	1.788	410.6	2503.6	410.7	2261.7	2672.4	1.285	7.378	98
100	1.01418	0.001043	1.672	419.1	2506.0	419.2	2256.4	2675.6	1.307	7.354	100
T	p	v_f	v_g	u_f	u_g	h_f	h_{fg}	h_g	s_f	s_g	T

Temperatures from the triple point to the critical point (showing $100\text{ }^{\circ}\text{C} \leq T \leq 373.95\text{ }^{\circ}\text{C}$):

Temp. $^{\circ}\text{C}$	Pressure bar	Specific volume m^3/kg		Spec. int. energy kJ/kg		Specific enthalpy kJ/kg			Specific entropy kJ/kg K		Temp. $^{\circ}\text{C}$
T	p	v_f	v_g	u_f	u_g	h_f	h_{fg}	h_g	s_f	s_g	T
100	1.014	0.001043	1.67196	419.1	2506.0	419.2	2256.4	2675.6	1.307	7.354	100
105	1.209	0.001047	1.41856	440.1	2511.9	440.3	2243.1	2683.4	1.363	7.295	105
110	1.434	0.001052	1.20945	461.3	2517.7	461.4	2229.6	2691.1	1.419	7.238	110
115	1.692	0.001056	1.03598	482.4	2523.3	482.6	2216.0	2698.6	1.474	7.183	115
120	1.987	0.001060	0.89133	503.6	2528.8	503.8	2202.1	2705.9	1.528	7.129	120
125	2.322	0.001065	0.77012	524.8	2534.3	525.1	2188.0	2713.1	1.582	7.077	125
130	2.703	0.001070	0.66808	546.1	2539.5	546.4	2173.7	2720.1	1.635	7.026	130
135	3.132	0.001075	0.58179	567.4	2544.6	567.7	2159.1	2726.9	1.687	6.977	135
140	3.615	0.001080	0.50850	588.8	2549.6	589.2	2144.3	2733.4	1.739	6.929	140
145	4.157	0.001085	0.44600	610.2	2554.4	610.6	2129.2	2739.8	1.791	6.883	145
150	4.762	0.001091	0.39248	631.7	2559.0	632.2	2113.7	2745.9	1.842	6.837	150
155	5.435	0.001096	0.34648	653.2	2563.5	653.8	2098.0	2751.8	1.892	6.793	155
160	6.182	0.001102	0.30680	674.8	2567.8	675.5	2082.0	2757.4	1.943	6.749	160
165	7.009	0.001108	0.27244	696.5	2571.8	697.2	2065.6	2762.8	1.992	6.707	165
170	7.922	0.001114	0.24260	718.2	2575.7	719.1	2048.8	2767.9	2.042	6.665	170
175	8.926	0.001121	0.21659	740.0	2579.4	741.0	2031.7	2772.7	2.091	6.624	175
180	10.028	0.001127	0.19384	761.9	2582.8	763.1	2014.2	2777.2	2.139	6.584	180
185	11.235	0.001134	0.17390	783.9	2586.0	785.2	1996.2	2781.4	2.188	6.545	185
190	12.552	0.001141	0.15636	806.0	2589.0	807.4	1977.8	2785.3	2.235	6.506	190
195	13.988	0.001149	0.14089	828.2	2591.7	829.8	1959.0	2788.8	2.283	6.468	195
200	15.549	0.001157	0.12721	850.5	2594.2	852.3	1939.7	2792.0	2.331	6.430	200
205	17.243	0.001164	0.11508	872.9	2596.4	874.9	1919.9	2794.8	2.378	6.393	205
210	19.077	0.001173	0.10429	895.4	2598.3	897.6	1899.6	2797.3	2.424	6.356	210
215	21.059	0.001181	0.09468	918.0	2599.9	920.5	1878.8	2799.3	2.471	6.320	215
220	23.196	0.001190	0.08609	940.8	2601.2	943.6	1857.4	2800.9	2.518	6.284	220
225	25.497	0.001199	0.07841	963.7	2602.2	966.8	1835.3	2802.2	2.564	6.248	225
230	27.971	0.001209	0.07151	986.8	2602.9	990.2	1812.7	2802.9	2.610	6.213	230
235	30.626	0.001219	0.06530	1010.0	2603.2	1013.8	1789.4	2803.2	2.656	6.178	235
240	33.470	0.001229	0.05971	1033.4	2603.1	1037.6	1765.4	2803.0	2.702	6.142	240
245	36.512	0.001240	0.05466	1057.0	2602.7	1061.5	1740.7	2802.2	2.748	6.107	245
250	39.762	0.001252	0.05009	1080.8	2601.8	1085.8	1715.2	2800.9	2.793	6.072	250
255	43.229	0.001263	0.04594	1104.8	2600.5	1110.2	1688.9	2799.1	2.839	6.037	255
260	46.923	0.001276	0.04218	1129.0	2598.7	1134.9	1661.7	2796.6	2.885	6.002	260
265	50.853	0.001289	0.03875	1153.4	2596.5	1159.9	1633.6	2793.5	2.930	5.966	265
270	55.030	0.001303	0.03562	1178.1	2593.7	1185.2	1604.5	2789.7	2.976	5.930	270
275	59.464	0.001317	0.03277	1203.0	2590.3	1210.9	1574.3	2785.2	3.022	5.894	275
280	64.166	0.001333	0.03015	1228.3	2586.4	1236.8	1543.0	2779.9	3.068	5.858	280
285	69.146	0.001349	0.02776	1253.9	2581.8	1263.2	1510.5	2773.7	3.114	5.821	285
290	74.418	0.001366	0.02555	1279.8	2576.5	1290.0	1476.7	2766.7	3.161	5.783	290
295	79.991	0.001384	0.02353	1306.1	2570.5	1317.2	1441.5	2758.7	3.208	5.745	295
300	85.879	0.001404	0.02166	1332.8	2563.6	1344.9	1404.7	2749.6	3.255	5.706	300
305	92.094	0.001425	0.01993	1360.1	2555.8	1373.2	1366.2	2739.4	3.302	5.666	305
310	98.650	0.001447	0.01833	1387.8	2547.1	1402.1	1325.8	2727.9	3.351	5.624	310
315	105.561	0.001472	0.01685	1416.2	2537.2	1431.7	1283.3	2715.0	3.399	5.582	315
320	112.843	0.001499	0.01547	1445.2	2526.0	1462.1	1238.5	2700.6	3.449	5.537	320
325	120.510	0.001528	0.01418	1475.0	2513.4	1493.4	1190.9	2684.3	3.500	5.491	325
330	128.581	0.001560	0.01298	1505.7	2499.2	1525.8	1140.2	2666.0	3.552	5.442	330
335	137.073	0.001597	0.01185	1537.5	2483.0	1559.4	1086.0	2645.4	3.605	5.391	335
340	146.007	0.001638	0.01078	1570.7	2464.5	1594.6	1027.4	2621.9	3.660	5.336	340
345	155.406	0.001685	0.00977	1605.4	2443.2	1631.6	963.4	2595.1	3.718	5.276	345
350	165.293	0.001741	0.00881	1642.3	2418.3	1671.1	892.7	2563.8	3.779	5.211	350
355	175.700	0.001808	0.00787	1682.1	2388.6	1713.9	812.9	2526.9	3.844	5.138	355
360	186.660	0.001895	0.00695	1726.2	2351.8	1761.5	720.0	2481.6	3.916	5.054	360
365	198.218	0.002015	0.00601	1777.2	2303.6	1817.2	605.5	2422.7	4.000	4.949	365
370	210.438	0.002217	0.00495	1844.5	2230.1	1891.2	443.1	2334.3	4.112	4.801	370
373.95	220.640	0.003106	0.00311	2018.1	2018.1	2086.6	0.0	2086.6	4.410	4.410	373.95
T	p	v_f	v_g	u_f	u_g	h_f	h_{fg}	h_g	s_f	s_g	T

Pressures from the triple point to the critical point (showing $0.00611 \text{ bar} \leq p \leq 1.00 \text{ bar}$):

Pressure bar p	Temp. °C T	Specific volume m ³ /kg		Spec. int. energy kJ/kg		Specific enthalpy kJ/kg			Specific entropy kJ/kg K		Pressure bar p
		v_f	v_g	u_f	u_g	h_f	h_{fg}	h_g	s_f	s_g	
0.00611	0.01	0.001000	206.0005	0.0	2375.0	0.0	2500.9	2500.9	0.000	9.156	0.00611
0.02	17.50	0.001001	66.990	73.4	2398.9	73.4	2459.5	2532.9	0.261	8.723	0.02
0.04	28.96	0.001004	34.791	121.4	2414.5	121.4	2432.3	2553.7	0.422	8.473	0.04
0.06	36.16	0.001006	23.733	151.5	2424.2	151.5	2415.2	2566.6	0.521	8.329	0.06
0.08	41.51	0.001008	18.099	173.8	2431.4	173.8	2402.4	2576.2	0.592	8.227	0.08
0.10	45.81	0.001010	14.670	191.8	2437.2	191.8	2392.1	2583.9	0.649	8.149	0.10
0.12	49.42	0.001012	12.358	206.9	2442.0	206.9	2383.4	2590.3	0.696	8.085	0.12
0.14	52.55	0.001013	10.691	220.0	2446.1	220.0	2375.8	2595.8	0.737	8.031	0.14
0.16	55.31	0.001015	9.431	231.5	2449.8	231.6	2369.1	2600.6	0.772	7.985	0.16
0.18	57.80	0.001016	8.443	241.9	2453.0	241.9	2363.0	2605.0	0.804	7.944	0.18
0.20	60.06	0.001017	7.648	251.4	2456.0	251.4	2357.5	2608.9	0.832	7.907	0.20
0.22	62.13	0.001018	6.994	260.1	2458.7	260.1	2352.4	2612.5	0.858	7.874	0.22
0.24	64.05	0.001019	6.446	268.1	2461.2	268.1	2347.7	2615.9	0.882	7.844	0.24
0.26	65.84	0.001020	5.979	275.6	2463.5	275.6	2343.3	2619.0	0.904	7.817	0.26
0.28	67.52	0.001021	5.578	282.6	2465.7	282.6	2339.2	2621.8	0.925	7.791	0.28
0.30	69.09	0.001022	5.229	289.2	2467.7	289.3	2335.3	2624.5	0.944	7.767	0.30
0.32	70.58	0.001023	4.922	295.5	2469.6	295.5	2331.6	2627.1	0.962	7.745	0.32
0.34	72.00	0.001024	4.650	301.4	2471.4	301.4	2328.1	2629.5	0.979	7.725	0.34
0.36	73.34	0.001025	4.407	307.0	2473.1	307.1	2324.7	2631.8	0.996	7.705	0.36
0.38	74.63	0.001026	4.190	312.4	2474.8	312.5	2321.5	2634.0	1.011	7.687	0.38
0.40	75.86	0.001026	3.993	317.6	2476.3	317.6	2318.4	2636.1	1.026	7.669	0.40
0.42	77.03	0.001027	3.815	322.5	2477.8	322.6	2315.5	2638.0	1.040	7.652	0.42
0.44	78.16	0.001028	3.652	327.3	2479.2	327.3	2312.6	2639.9	1.054	7.637	0.44
0.46	79.25	0.001029	3.503	331.8	2480.6	331.9	2309.9	2641.8	1.067	7.621	0.46
0.48	80.30	0.001029	3.367	336.2	2481.9	336.3	2307.2	2643.5	1.079	7.607	0.48
0.50	81.32	0.001030	3.240	340.5	2483.2	340.5	2304.7	2645.2	1.091	7.593	0.50
0.52	82.30	0.001031	3.123	344.6	2484.4	344.6	2302.2	2646.8	1.103	7.580	0.52
0.54	83.25	0.001031	3.015	348.6	2485.6	348.6	2299.8	2648.4	1.114	7.567	0.54
0.56	84.17	0.001032	2.914	352.4	2486.8	352.5	2297.4	2649.9	1.125	7.555	0.56
0.58	85.06	0.001032	2.820	356.2	2487.9	356.3	2295.2	2651.4	1.135	7.543	0.58
0.60	85.93	0.001033	2.732	359.8	2488.9	359.9	2293.0	2652.9	1.145	7.531	0.60
0.62	86.77	0.001034	2.649	363.4	2490.0	363.4	2290.8	2654.2	1.155	7.520	0.62
0.64	87.59	0.001034	2.572	366.8	2491.0	366.9	2288.7	2655.6	1.165	7.509	0.64
0.66	88.39	0.001035	2.499	370.2	2492.0	370.3	2286.6	2656.9	1.174	7.499	0.66
0.68	89.17	0.001035	2.430	373.5	2492.9	373.5	2284.6	2658.2	1.183	7.489	0.68
0.70	89.93	0.001036	2.365	376.7	2493.9	376.7	2282.7	2659.4	1.192	7.479	0.70
0.72	90.67	0.001036	2.304	379.8	2494.8	379.9	2280.8	2660.6	1.201	7.470	0.72
0.74	91.40	0.001037	2.245	382.9	2495.7	382.9	2278.9	2661.8	1.209	7.460	0.74
0.76	92.11	0.001037	2.190	385.8	2496.5	385.9	2277.0	2663.0	1.217	7.451	0.76
0.78	92.81	0.001038	2.137	388.8	2497.4	388.8	2275.2	2664.1	1.225	7.443	0.78
0.80	93.49	0.001039	2.087	391.6	2498.2	391.7	2273.5	2665.2	1.233	7.434	0.80
0.82	94.15	0.001039	2.040	394.4	2499.0	394.5	2271.7	2666.3	1.241	7.426	0.82
0.84	94.80	0.001039	1.994	397.2	2499.8	397.3	2270.0	2667.3	1.248	7.418	0.84
0.86	95.44	0.001040	1.951	399.9	2500.6	400.0	2268.4	2668.3	1.255	7.410	0.86
0.88	96.07	0.001040	1.909	402.5	2501.3	402.6	2266.7	2669.3	1.263	7.402	0.88
0.90	96.69	0.001041	1.870	405.1	2502.1	405.2	2265.1	2670.3	1.270	7.394	0.90
0.92	97.29	0.001041	1.832	407.6	2502.8	407.7	2263.5	2671.3	1.277	7.387	0.92
0.94	97.89	0.001042	1.795	410.1	2503.5	410.2	2262.0	2672.2	1.283	7.380	0.94
0.96	98.47	0.001042	1.760	412.6	2504.2	412.7	2260.4	2673.1	1.290	7.373	0.96
0.98	99.04	0.001043	1.726	415.0	2504.9	415.1	2258.9	2674.1	1.296	7.366	0.98
1.00	99.61	0.001043	1.694	417.4	2505.5	417.5	2257.4	2674.9	1.303	7.359	1.00
p	T	v_f	v_g	u_f	u_g	h_f	h_{fg}	h_g	s_f	s_g	p

Pressures from the triple point to the critical point ($1.0 \text{ bar} \leq p \leq 25.5 \text{ bar}$):

Pressure bar p	Temp. °C T	Specific volume m^3/kg v_f v_g		Spec. int. energy kJ/kg u_f u_g		Specific enthalpy kJ/kg h_f h_{fg} h_g			Specific entropy kJ/kg K s_f s_g		Pressure bar p
1.0	99.61	0.001043	1.6941	417.4	2505.5	417.5	2257.4	2674.9	1.303	7.359	1.0
1.5	111.35	0.001053	1.1594	467.0	2519.2	467.1	2226.0	2693.1	1.434	7.223	1.5
2.0	120.21	0.001061	0.8858	504.5	2529.1	504.7	2201.5	2706.2	1.530	7.127	2.0
2.5	127.41	0.001067	0.7187	535.1	2536.8	535.3	2181.1	2716.5	1.607	7.053	2.5
3.0	133.52	0.001073	0.6058	561.1	2543.1	561.4	2163.5	2724.9	1.672	6.992	3.0
3.5	138.86	0.001079	0.5242	583.9	2548.5	584.3	2147.7	2732.0	1.727	6.940	3.5
4.0	143.61	0.001084	0.4624	604.2	2553.1	604.7	2133.4	2738.1	1.776	6.896	4.0
4.5	147.90	0.001088	0.4139	622.7	2557.1	623.1	2120.2	2743.4	1.820	6.856	4.5
5.0	151.83	0.001093	0.3748	639.5	2560.7	640.1	2108.0	2748.1	1.860	6.821	5.0
5.5	155.46	0.001097	0.3426	655.2	2563.9	655.8	2096.6	2752.3	1.897	6.789	5.5
6.0	158.83	0.001101	0.3156	669.7	2566.8	670.4	2085.8	2756.1	1.931	6.759	6.0
6.5	161.98	0.001104	0.2926	683.4	2569.4	684.1	2075.5	2759.6	1.962	6.732	6.5
7.0	164.95	0.001108	0.2728	696.2	2571.8	697.0	2065.8	2762.8	1.992	6.707	7.0
7.5	167.75	0.001111	0.2555	708.4	2574.0	709.2	2056.4	2765.6	2.019	6.684	7.5
8.0	170.41	0.001115	0.2403	720.0	2576.0	720.9	2047.4	2768.3	2.046	6.662	8.0
8.5	172.94	0.001118	0.2269	731.0	2577.9	732.0	2038.8	2770.8	2.070	6.641	8.5
9.0	175.35	0.001121	0.2149	741.6	2579.6	742.6	2030.5	2773.0	2.094	6.621	9.0
9.5	177.66	0.001124	0.2041	751.7	2581.2	752.7	2022.4	2775.1	2.117	6.603	9.5
10.0	179.88	0.001127	0.1944	761.4	2582.7	762.5	2014.6	2777.1	2.138	6.585	10.0
10.5	182.01	0.001130	0.1855	770.8	2584.1	771.9	2007.0	2778.9	2.159	6.568	10.5
11.0	184.06	0.001133	0.1775	779.8	2585.5	781.0	1999.6	2780.6	2.178	6.552	11.0
11.5	186.04	0.001136	0.1701	788.5	2586.7	789.8	1992.4	2782.2	2.198	6.537	11.5
12.0	187.96	0.001138	0.1633	797.0	2587.8	798.3	1985.4	2783.7	2.216	6.522	12.0
12.5	189.81	0.001141	0.1570	805.2	2588.9	806.6	1978.6	2785.1	2.234	6.507	12.5
13.0	191.60	0.001144	0.1512	813.1	2589.9	814.6	1971.9	2786.5	2.251	6.494	13.0
13.5	193.35	0.001146	0.1458	820.8	2590.9	822.4	1965.3	2787.7	2.267	6.480	13.5
14.0	195.04	0.001149	0.1408	828.4	2591.8	830.0	1958.9	2788.8	2.284	6.467	14.0
14.5	196.68	0.001151	0.1361	835.7	2592.6	837.4	1952.6	2789.9	2.299	6.455	14.5
15.0	198.29	0.001154	0.1317	842.8	2593.4	844.6	1946.4	2791.0	2.314	6.443	15.0
15.5	199.85	0.001156	0.1276	849.8	2594.1	851.6	1940.3	2791.9	2.329	6.431	15.5
16.0	201.37	0.001159	0.1237	856.6	2594.8	858.5	1934.4	2792.8	2.343	6.420	16.0
16.5	202.86	0.001161	0.1201	863.3	2595.5	865.2	1928.5	2793.7	2.357	6.409	16.5
17.0	204.31	0.001163	0.1167	869.8	2596.1	871.7	1922.7	2794.5	2.371	6.398	17.0
17.5	205.72	0.001166	0.1134	876.1	2596.7	878.2	1917.0	2795.2	2.384	6.388	17.5
18.0	207.11	0.001168	0.1104	882.4	2597.2	884.5	1911.4	2795.9	2.397	6.377	18.0
18.5	208.47	0.001170	0.1075	888.5	2597.8	890.7	1905.9	2796.6	2.410	6.368	18.5
19.0	209.80	0.001172	0.1047	894.5	2598.2	896.7	1900.5	2797.2	2.423	6.358	19.0
19.5	211.10	0.001175	0.1021	900.4	2598.7	902.7	1895.1	2797.8	2.435	6.348	19.5
20.0	212.38	0.001177	0.0996	906.2	2599.1	908.5	1889.8	2798.3	2.447	6.339	20.0
20.5	213.63	0.001179	0.0972	911.8	2599.5	914.2	1884.6	2798.8	2.458	6.330	20.5
21.0	214.86	0.001181	0.0949	917.4	2599.9	919.9	1879.4	2799.3	2.470	6.321	21.0
21.5	216.06	0.001183	0.0928	922.9	2600.2	925.4	1874.3	2799.7	2.481	6.312	21.5
22.0	217.25	0.001185	0.0907	928.3	2600.6	930.9	1869.2	2800.1	2.492	6.304	22.0
22.5	218.41	0.001187	0.0887	933.6	2600.9	936.3	1864.2	2800.5	2.503	6.295	22.5
23.0	219.56	0.001189	0.0868	938.8	2601.1	941.5	1859.3	2800.8	2.513	6.287	23.0
23.5	220.68	0.001191	0.0850	943.9	2601.4	946.7	1854.4	2801.1	2.524	6.279	23.5
24.0	221.79	0.001193	0.0832	949.0	2601.6	951.9	1849.6	2801.4	2.534	6.271	24.0
24.5	222.88	0.001195	0.0816	954.0	2601.9	956.9	1844.8	2801.7	2.544	6.263	24.5
25.0	223.95	0.001197	0.0800	958.9	2602.1	961.9	1840.0	2801.9	2.554	6.256	25.0
25.5	225.01	0.001199	0.0784	963.8	2602.2	966.8	1835.3	2802.2	2.564	6.248	25.5
p	T	v_f	v_g	u_f	u_g	h_f	h_{fg}	h_g	s_f	s_g	p

Pressures from the triple point to the critical point ($26.0 \text{ bar} \leq T \leq 145 \text{ bar}$):

Pressure bar	Temp. °C	Specific volume m ³ /kg		Spec. int. energy kJ/kg		Specific enthalpy kJ/kg			Specific entropy kJ/kg K		Pressure bar
p	T	v_f	v_g	u_f	u_g	h_f	h_{fg}	h_g	s_f	s_g	p
26.0	226.05	0.001201	0.0769	968.6	2602.4	971.7	1830.7	2802.3	2.574	6.241	26.0
26.5	227.07	0.001203	0.0755	973.3	2602.5	976.5	1826.1	2802.5	2.583	6.234	26.5
27.0	228.08	0.001205	0.0741	977.9	2602.7	981.2	1821.5	2802.7	2.592	6.226	27.0
27.5	229.07	0.001207	0.0727	982.5	2602.8	985.9	1816.9	2802.8	2.601	6.219	27.5
28.0	230.06	0.001209	0.0714	987.1	2602.9	990.5	1812.4	2802.9	2.611	6.212	28.0
28.5	231.02	0.001211	0.0702	991.6	2603.0	995.0	1808.0	2803.0	2.619	6.206	28.5
29.0	231.98	0.001213	0.0690	996.0	2603.1	999.5	1803.6	2803.1	2.628	6.199	29.0
29.5	232.92	0.001215	0.0678	1000.4	2603.1	1004.0	1799.2	2803.1	2.637	6.192	29.5
30	233.85	0.001217	0.06667	1004.7	2603.2	1008.4	1794.8	2803.2	2.645	6.186	30
32	237.46	0.001224	0.06248	1021.5	2603.2	1025.4	1777.7	2803.1	2.679	6.160	32
34	240.90	0.001231	0.05876	1037.7	2603.1	1041.8	1761.0	2802.9	2.710	6.136	34
36	244.18	0.001238	0.05545	1053.1	2602.8	1057.6	1744.8	2802.4	2.740	6.113	36
38	247.33	0.001245	0.05247	1068.1	2602.3	1072.8	1728.9	2801.7	2.769	6.091	38
40	250.35	0.001252	0.04978	1082.5	2601.7	1087.5	1713.3	2800.8	2.797	6.070	40
42	253.26	0.001259	0.04733	1096.4	2601.0	1101.7	1698.1	2799.8	2.823	6.049	42
44	256.07	0.001266	0.04510	1109.9	2600.1	1115.5	1683.1	2798.6	2.849	6.029	44
46	258.78	0.001273	0.04306	1123.0	2599.2	1128.9	1668.4	2797.3	2.874	6.010	46
48	261.40	0.001280	0.04118	1135.8	2598.1	1141.9	1653.9	2795.8	2.898	5.992	48
50	263.94	0.001286	0.03945	1148.2	2597.0	1154.6	1639.6	2794.2	2.921	5.974	50
52	266.40	0.001293	0.03784	1160.3	2595.7	1167.0	1625.5	2792.5	2.943	5.956	52
54	268.79	0.001299	0.03635	1172.1	2594.4	1179.1	1611.6	2790.7	2.965	5.939	54
56	271.12	0.001306	0.03496	1183.6	2593.0	1190.9	1597.8	2788.8	2.986	5.922	56
58	273.38	0.001312	0.03366	1194.9	2591.5	1202.5	1584.2	2786.7	3.007	5.906	58
60	275.58	0.001319	0.03245	1206.0	2589.9	1213.9	1570.7	2784.6	3.027	5.890	60
62	277.73	0.001326	0.03131	1216.8	2588.3	1225.0	1557.4	2782.4	3.047	5.875	62
64	279.83	0.001332	0.03024	1227.4	2586.5	1235.9	1544.1	2780.1	3.067	5.859	64
66	281.87	0.001339	0.02923	1237.8	2584.8	1246.7	1531.0	2777.7	3.085	5.844	66
68	283.87	0.001345	0.02828	1248.1	2582.9	1257.2	1518.0	2775.2	3.104	5.829	68
70	285.83	0.001352	0.02738	1258.1	2581.0	1267.6	1505.0	2772.6	3.122	5.815	70
72	287.74	0.001358	0.02653	1268.0	2579.0	1277.8	1492.2	2770.0	3.140	5.800	72
74	289.61	0.001365	0.02572	1277.8	2577.0	1287.9	1479.4	2767.3	3.157	5.786	74
76	291.45	0.001371	0.02495	1287.4	2574.9	1297.8	1466.7	2764.5	3.174	5.772	76
78	293.25	0.001378	0.02422	1296.8	2572.7	1307.6	1454.0	2761.6	3.191	5.759	78
80	295.01	0.001384	0.02352	1306.1	2570.5	1317.2	1441.4	2758.7	3.208	5.745	80
82	296.74	0.001391	0.02286	1315.3	2568.2	1326.7	1428.9	2755.7	3.224	5.732	82
84	298.43	0.001398	0.02223	1324.4	2565.9	1336.2	1416.4	2752.6	3.240	5.718	84
86	300.10	0.001404	0.02162	1333.4	2563.5	1345.5	1404.0	2749.4	3.256	5.705	86
88	301.74	0.001411	0.02104	1342.2	2561.0	1354.7	1391.5	2746.2	3.271	5.692	88
90	303.35	0.001418	0.02049	1351.0	2558.5	1363.8	1379.2	2742.9	3.287	5.679	90
92	304.93	0.001425	0.01996	1359.7	2556.0	1372.8	1366.8	2739.6	3.302	5.666	92
94	306.48	0.001431	0.01945	1368.2	2553.3	1381.7	1354.5	2736.1	3.317	5.654	94
96	308.01	0.001438	0.01895	1376.7	2550.7	1390.5	1342.1	2732.6	3.331	5.641	96
98	309.52	0.001445	0.01848	1385.1	2548.0	1399.3	1329.8	2729.1	3.346	5.628	98
100	311.00	0.001452	0.01803	1393.4	2545.2	1407.9	1317.5	2725.5	3.360	5.616	100
105	314.60	0.001470	0.01696	1413.9	2538.0	1429.3	1286.8	2716.1	3.396	5.585	105
110	318.08	0.001488	0.01599	1433.9	2530.4	1450.3	1256.0	2706.3	3.430	5.554	110
115	321.43	0.001507	0.01509	1453.6	2522.5	1471.0	1225.1	2696.1	3.464	5.524	115
120	324.68	0.001526	0.01426	1473.0	2514.3	1491.3	1194.1	2685.4	3.496	5.494	120
125	327.81	0.001546	0.01350	1492.2	2505.6	1511.5	1162.8	2674.3	3.529	5.464	125
130	330.85	0.001566	0.01278	1511.1	2496.5	1531.4	1131.3	2662.7	3.561	5.434	130
135	333.80	0.001588	0.01211	1529.8	2487.0	1551.2	1099.3	2650.6	3.592	5.403	135
140	336.67	0.001610	0.01149	1548.4	2477.1	1571.0	1067.0	2637.9	3.623	5.373	140
145	339.45	0.001633	0.01090	1566.9	2466.7	1590.6	1034.1	2624.7	3.654	5.342	145
p	T	v_f	v_g	u_f	u_g	h_f	h_{fg}	h_g	s_f	s_g	p

Pressures from the triple point to the critical point ($150 \text{ bar} \leq T \leq 220.64 \text{ bar}$):

Pressure bar p	Temp. °C T	Specific volume m ³ /kg v_f v_g		Spec. int. energy kJ/kg u_f u_g		Specific enthalpy kJ/kg h_f h_{fg} h_g			Specific entropy kJ/kg K s_f s_g		Pressure bar p
150	342.16	0.001657	0.01034	1585.4	2455.7	1610.3	1000.5	2610.8	3.685	5.311	150
155	344.79	0.001683	0.00981	1603.9	2444.2	1630.0	966.2	2596.3	3.715	5.279	155
160	347.35	0.001710	0.00931	1622.5	2432.0	1649.9	931.1	2581.0	3.746	5.247	160
165	349.86	0.001739	0.00883	1641.2	2419.1	1669.9	894.9	2564.8	3.777	5.213	165
170	352.29	0.001770	0.00837	1660.2	2405.4	1690.3	857.4	2547.7	3.808	5.179	170
175	354.67	0.001804	0.00793	1679.4	2390.7	1711.0	818.5	2529.5	3.840	5.143	175
180	356.99	0.001840	0.00750	1699.1	2374.9	1732.2	777.8	2510.0	3.872	5.106	180
185	359.26	0.001881	0.00709	1719.3	2357.9	1754.1	734.9	2489.0	3.905	5.067	185
190	361.47	0.001926	0.00668	1740.3	2339.1	1776.9	689.2	2466.0	3.940	5.026	190
195	363.63	0.001977	0.00627	1762.3	2318.4	1800.9	639.8	2440.7	3.976	4.981	195
200	365.75	0.002038	0.00586	1785.9	2294.8	1826.6	585.4	2412.1	4.015	4.931	200
205	367.81	0.002111	0.00544	1811.7	2267.3	1855.0	523.8	2378.9	4.057	4.875	205
210	369.83	0.002207	0.00499	1841.6	2233.5	1888.0	450.4	2338.4	4.107	4.808	210
215	371.79	0.002349	0.00448	1879.5	2187.4	1930.0	353.6	2283.6	4.171	4.719	215
220	373.71	0.002703	0.00364	1951.6	2092.4	2011.1	161.5	2172.6	4.294	4.544	220
220.64	373.95	0.003106	0.00311	2018.1	2018.1	2086.6	0.0	2086.6	4.410	4.410	220.64
p	T	v_f	v_g	u_f	u_g	h_f	h_{fg}	h_g	s_f	s_g	p

Above the critical temperature and pressure ($p \geq 220.64 \text{ bar}$, $T \geq 373.95 \text{ K}$), water enters the **supercritical** state, in which all properties of the liquid and vapour states become equal, so the two phases become fully miscible. The supercritical fluid properties can vary continuously between those of the liquid and vapour states depending on the values of p and T .

7.4.6. Transport Properties of Gases

The below values are correct for a pressure of 1 atm but may often be used with sufficient accuracy at other pressures. For air, $d\lambda_{air}/dp \sim 0.05 \text{ W K}^{-1} \text{ atm}^{-1}$.

Water and Steam Mixtures (H₂O (l) + H₂O (g))

Temp. °C	Specific volume m ³ /kg		Isobaric specific heat capacity kJ/kg K		Thermal conductivity W/m K		Dynamic viscosity kg/s m		Prandtl number = $\mu c_p / \lambda$		Temp. °C
	v_f	v_g	c_{p_f}	c_{p_g}	λ_f	λ_g	$\mu_f / 10^{-3}$	$\mu_g / 10^{-6}$	Pr_f	Pr_g	
0.01	0.00100	206.2	4.217	1.854	0.569	0.0173	1.755	8.8	13.02	0.942	0.01
10	0.00100	106.4	4.193	1.860	0.587	0.0185	1.301	9.1	9.29	0.915	10
20	0.00100	57.8	4.182	1.866	0.603	0.0191	1.002	9.4	6.95	0.918	20
30	0.00100	32.9	4.179	1.885	0.618	0.0198	0.797	9.7	5.39	0.923	30
40	0.00101	19.5	4.179	1.885	0.632	0.0204	0.651	10.1	4.31	0.930	40
50	0.00101	12.05	4.181	1.899	0.643	0.0210	0.544	10.4	3.53	0.939	50
60	0.00102	7.68	4.185	1.915	0.653	0.0217	0.462	10.7	2.96	0.947	60
70	0.00102	5.05	4.190	1.936	0.662	0.0224	0.400	11.1	2.53	0.956	70
80	0.00103	3.41	4.197	1.962	0.670	0.0231	0.350	11.4	2.19	0.966	80
90	0.00104	2.36	4.205	1.992	0.676	0.0240	0.311	11.7	1.93	0.976	90
100	0.00104	1.673	4.216	2.028	0.681	0.0249	0.278	12.1	1.723	0.986	100
125	0.00107	0.770	4.254	2.147	0.687	0.0272	0.219	13.3	1.358	1.047	125
150	0.00109	0.392	4.310	2.314	0.687	0.0300	0.180	14.4	1.133	1.110	150
175	0.00112	0.217	4.389	2.542	0.679	0.0334	0.153	15.6	0.990	1.185	175
200	0.00116	0.127	4.497	2.843	0.665	0.0375	0.133	16.7	0.902	1.270	200
225	0.00120	0.0783	4.648	3.238	0.644	0.0427	0.1182	17.9	0.853	1.36	225
250	0.00125	0.0500	4.867	3.772	0.616	0.0495	0.1065	19.1	0.841	1.45	250
275	0.00132	0.0327	5.202	4.561	0.582	0.0587	0.0972	20.2	0.869	1.56	275
300	0.00140	0.0216	5.762	5.863	0.541	0.0719	0.0897	21.4	0.955	1.74	300
325	0.00153	0.0142	6.861	8.440	0.493	0.0929	0.0790	23.0	1.100	2.09	325
350	0.00174	0.00880	10.10	17.15	0.437	0.1343	0.0648	25.8	1.50	3.29	350
360	0.00190	0.00694	14.6	25.1	0.400	0.168	0.0582	27.5	2.11	3.89	360
374.15	0.00317	0.00317	∞	∞	0.24	0.24	0.045	45.0	∞	∞	374.15

Superheated Steam (H₂O (g))

Temp. °C	Isobaric sp. heat capacity kJ/kg K	Thermal conductivity W/m K	Dynamic viscosity kg/s m	Prandtl number
	c_p	λ	$\mu / 10^{-6}$	$Pr = \mu c_p / \lambda$
100	2.028	0.0245	12.1	0.986
200	1.979	0.0331	16.2	0.968
300	2.010	0.0434	20.4	0.946
400	2.067	0.0548	24.6	0.928
500	2.132	0.0673	28.8	0.912
600	2.201	0.0805	32.9	0.898
700	2.268	0.0942	36.8	0.887
800	2.332	0.1080	40.6	0.876

Air (79% N₂* (g) + 21% O₂ (g))

Temp. °C	Isobaric sp. heat capacity kJ/kg K	Thermal conductivity W/m K	Dynamic viscosity kg/s m	Prandtl number
	c_p	λ	$\mu / 10^{-6}$	$Pr = \mu c_p / \lambda$
-100	1.01	0.016	12	0.75
0	1.01	0.024	17	0.72
100	1.02	0.032	22	0.70
200	1.03	0.039	26	0.69
300	1.05	0.045	30	0.69
400	1.07	0.051	33	0.70
500	1.10	0.056	36	0.70
600	1.12	0.061	39	0.71
700	1.14	0.066	42	0.72
800	1.16	0.071	44	0.73

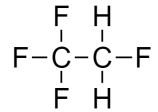
Carbon Dioxide (CO₂ (g))

Temp. °C	Isobaric sp. heat capacity kJ/kg K	Thermal conductivity W/m K	Dynamic viscosity kg/s m	Prandtl number
	c_p	λ	$\mu / 10^{-6}$	$Pr = \mu c_p / \lambda$
-50	0.79	0.011	11	0.79
0	0.83	0.015	14	0.78
100	0.92	0.022	18	0.75
200	1.00	0.030	22	0.73
300	1.06	0.038	26	0.72
400	1.11	0.046	29	0.71
500	1.16	0.053	32	0.70
600	1.20	0.061	35	0.69
700	1.23	0.069	38	0.68
800	1.25	0.078	41	0.67

Hydrogen (H₂ (g))

Temp. °C	Isobaric sp. heat capacity kJ/kg K	Thermal conductivity W/m K	Dynamic viscosity kg/s m	Prandtl number
	c_p	λ	$\mu / 10^{-6}$	$Pr = \mu c_p / \lambda$
-200	10.6	0.050	3.3	0.71
-100	13.1	0.112	6.2	0.72
0	14.2	0.172	8.4	0.69
100	14.5	0.220	10.3	0.68
200	14.5	0.307	12.1	0.67
300	14.5	0.307	13.8	0.66
400	14.6	0.348	15.4	0.65
500	14.7	0.387	16.9	0.64
600	14.8	0.427	18.3	0.63
700	14.9	0.476	19.9	0.62
800	15.1	0.528	21.1	0.61

7.4.9. Properties of Refrigerant (Freon) R-134a



R-134a is a hydrofluorocarbon (HFC) with chemical formula $\text{C}_2\text{H}_2\text{F}_4$.

It is non-toxic, non-flammable, non-corrosive and non-ozone depleting.

1,1,1,2-tetrafluoroethane
(R-134a)

Saturation Temp. °C	Saturation Pressure bar	Saturated						Superheated by				Saturation Temp. °C
		Specific volume m ³ /kg		Specific enthalpy kJ/kg		Specific entropy kJ/kg K		20K		40K		
		v_f	v_g	h_f	h_g	s_f	s_g	kJ/kg	kJ/kg K	kJ/kg	kJ/kg K	
T_{sat}	P_{sat}							h	s	h	s	T_{sat}
-45	0.39	0.00070	0.46458	141.9	370.8	0.7687	1.7722	385.8	1.8348	401.3	1.8949	-45
-40	0.51	0.00071	0.36094	148.1	374.0	0.7956	1.7643	389.2	1.8270	405.0	1.8869	-40
-35	0.66	0.00071	0.28390	154.4	377.2	0.8221	1.7574	392.7	1.8201	408.6	1.8797	-35
-30	0.84	0.00072	0.22585	160.8	380.3	0.8483	1.7512	396.1	1.8139	412.3	1.8734	-30
-25	1.06	0.00073	0.18155	167.2	383.4	0.8743	1.7458	399.5	1.8085	416.0	1.8678	-25
-20	1.33	0.00074	0.14735	173.6	386.5	0.8999	1.7410	402.9	1.8037	419.7	1.8629	-20
-15	1.64	0.00074	0.12065	180.1	389.6	0.9253	1.7368	406.3	1.7995	423.4	1.8587	-15
-10	2.01	0.00075	0.09959	186.7	392.7	0.9505	1.7331	409.7	1.7959	427.0	1.8550	-10
-5	2.43	0.00076	0.08281	193.3	395.6	0.9753	1.7299	413.1	1.7927	430.7	1.8518	-5
0	2.93	0.00077	0.06933	200.0	398.6	1.0000	1.7270	416.4	1.7900	434.3	1.8491	0
5	3.50	0.00078	0.05840	206.8	401.5	1.0244	1.7245	419.7	1.7877	437.9	1.8469	5
10	4.15	0.00079	0.04947	213.6	404.3	1.0486	1.7222	422.9	1.7857	441.5	1.8450	10
15	4.88	0.00080	0.04212	220.5	407.1	1.0726	1.7202	426.1	1.7840	445.0	1.8434	15
20	5.72	0.00082	0.03602	227.5	409.8	1.0965	1.7183	429.3	1.7825	448.5	1.8422	20
25	6.65	0.00083	0.03093	234.6	412.3	1.1202	1.7165	432.3	1.7813	452.0	1.8412	25
30	7.70	0.00084	0.02666	241.7	414.8	1.1438	1.7148	435.4	1.7803	455.4	1.8405	30
35	8.87	0.00086	0.02305	249.0	417.2	1.1672	1.7130	438.3	1.7794	458.8	1.8399	35
40	10.17	0.00087	0.01999	256.4	419.4	1.1906	1.7112	441.2	1.7786	462.1	1.8395	40
45	11.60	0.00089	0.01736	263.9	421.5	1.2140	1.7093	444.0	1.7779	465.4	1.8393	45
50	13.18	0.00091	0.01511	271.6	423.4	1.2374	1.7073	446.7	1.7772	468.6	1.8392	50
60	16.82	0.00095	0.01148	287.5	426.6	1.2846	1.7022	451.8	1.7759	474.8	1.8392	60
70	21.16	0.00101	0.00871	304.3	428.6	1.3329	1.6953	456.4	1.7743	480.7	1.8394	70
80	26.33	0.00108	0.00654	322.4	428.8	1.3834	1.6848	460.4	1.7722	486.2	1.8395	80
90	32.45	0.00119	0.00481	342.9	425.4	1.4393	1.6665	463.8	1.7692	491.3	1.8392	90
100	39.73	0.00148	0.00345	373.3	407.7	1.5183	1.6105	466.4	1.7650	495.9	1.8384	100

Boiling point: -26.1 °C (at $p = 1$ bar)

Solubility in water: 0.11 wt% (at 25 °C)

Ozone depletion level (ODL): 0

Autoignition temperature: 770 °C

Critical temperature: 122 °C

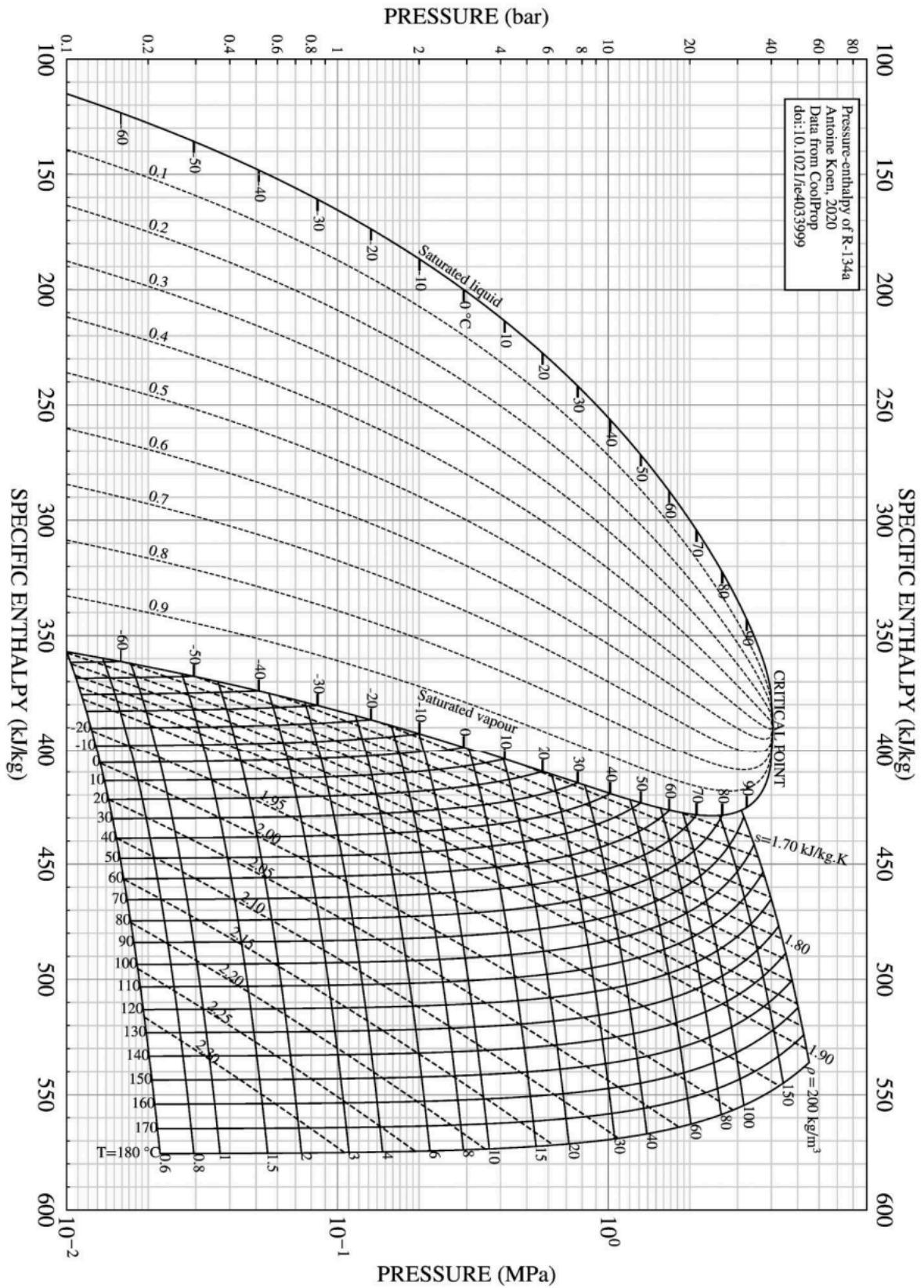
Global warming potential (GWP): 1430

Alternative Refrigerants: R-134a is being phased out as a refrigerant due to its high GWP

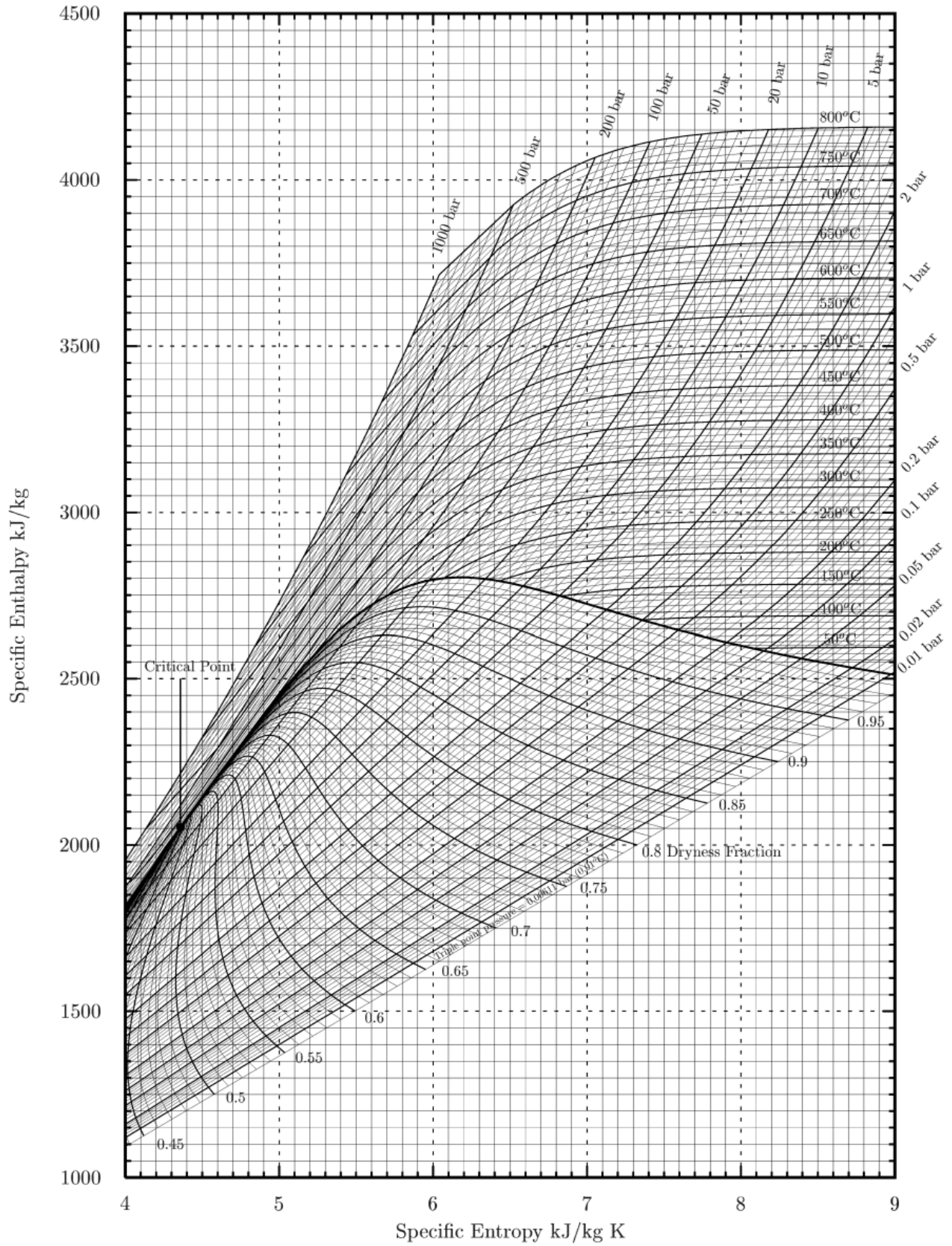
Refrigerant	Composition	GWP	ODL
R-515b	azeotrope of 91.1% R-1234ze: (E)-1,3,3,3-tetrafluoropropene + 8.9% R-227ea: 1,1,1,2,3,3,3-heptafluoropropane	299	0
HFO-1233zd	(Z)-1-chloro-3,3,3-trifluoropropene	6	0
R-12a	propane + isobutane	3	0
HFO-1234yf	2,3,3,3-tetrafluoroprop-1-ene	1	0

For reliable data on these and various other fluids used in refrigeration and power, the CoolProp library can be used, with interfaces in C++, Python, MATLAB, Excel, R, etc.

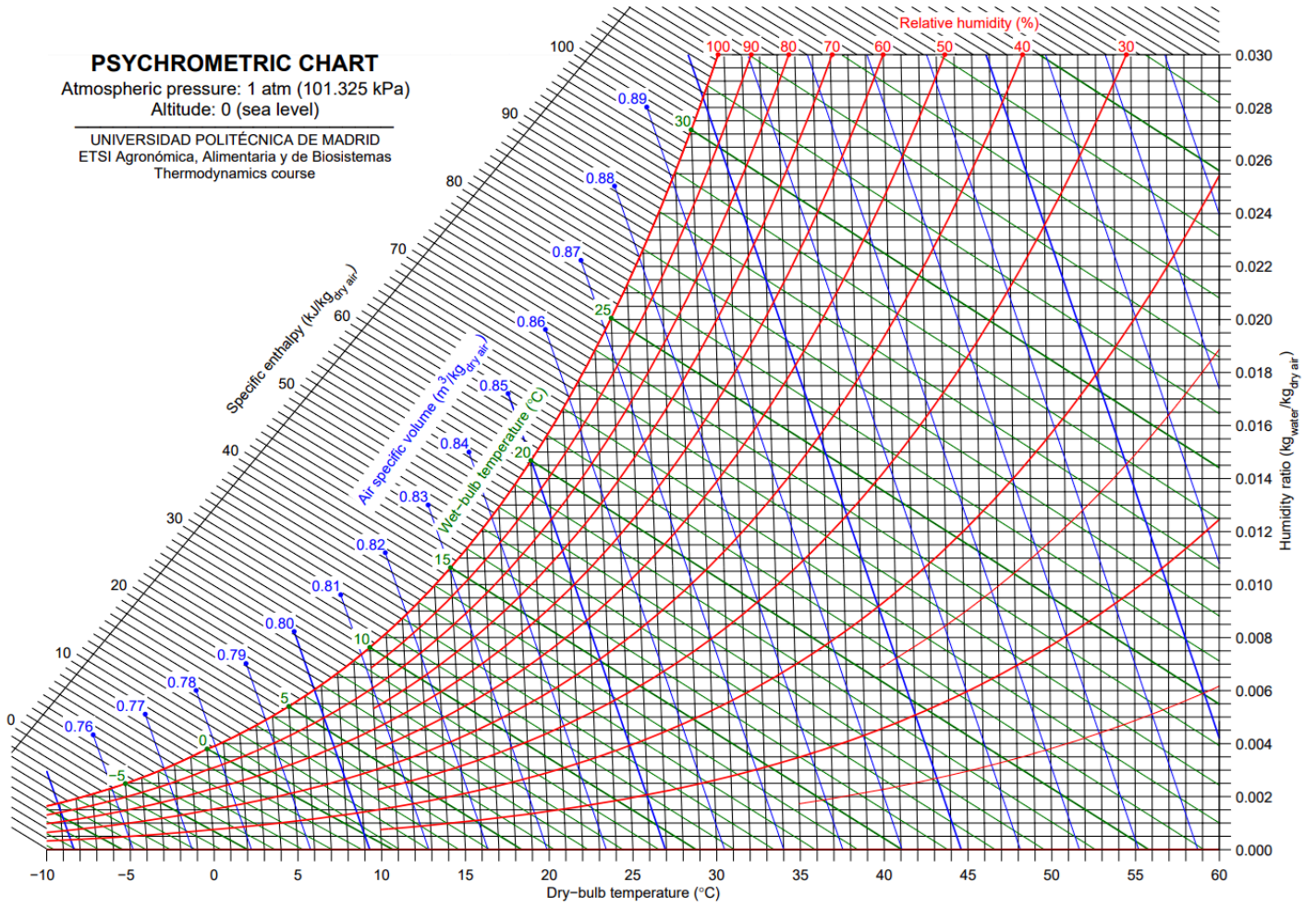
7.4.10. Pressure-Enthalpy ($p-h$) Phase Diagram of Refrigerant R-134a



7.4.11. Enthalpy-Entropy ($h-s$) Phase Diagram of Steam (Mollier Diagram)

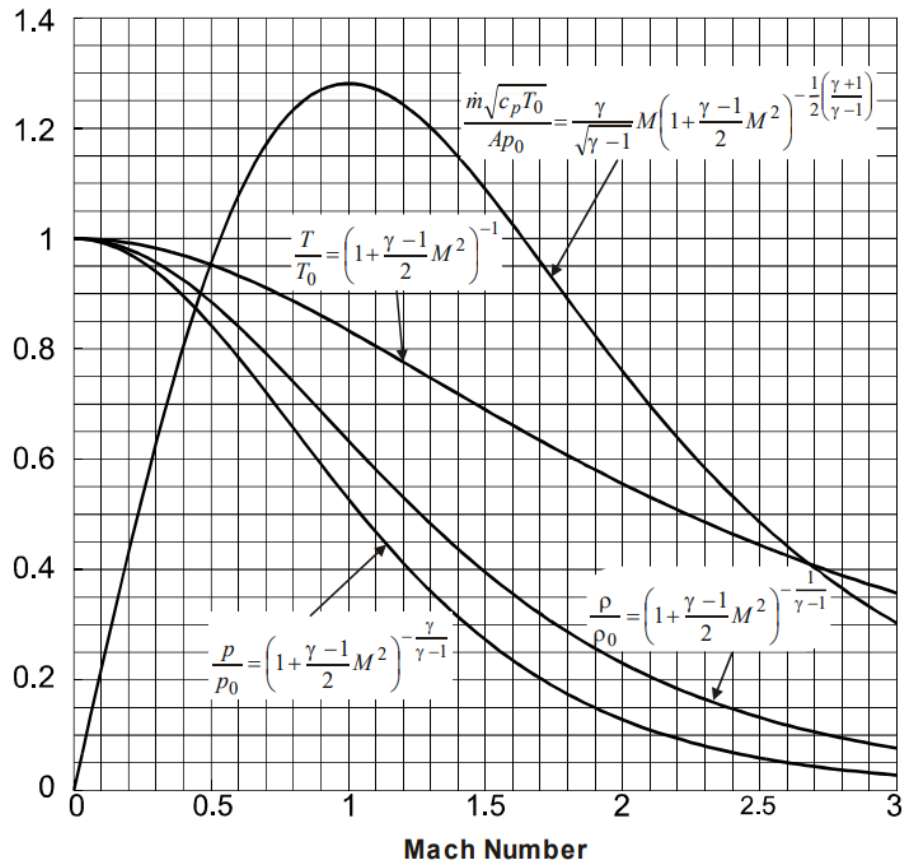


7.4.12. Enthalpy-Humidity (h - ω) Data for Water and Steam (Psychrometric Chart)



7.4.13. Perfect Gas Relations For Compressible Supersonic Flow

Nondimensional temperature, pressure, density and mass flow rate are plotted for $\gamma = 1.4$.



- $T_0 = \text{const}$ in adiabatic flow with no shaft work.
- If flow is isentropic, $p_0 = \text{const}$ and $\rho_0 = \text{const}$ when $T = \text{const}$.
- At Mach 1 and when $\gamma = 1.4$, $\frac{\dot{m} \sqrt{c_p T_0}}{A p_0} = 1.281$.

P8. ELECTRICITY AND ELECTROMAGNETISM

8.1. Electrostatics and Magnetostatics

8.1.1. Electric Fields

The electric field intensity \mathbf{E} [V m^{-1}], electric flux density \mathbf{D} [C m^{-2}] and electric polarisation \mathbf{P} [C m^{-2}] vector fields are related by the constitutive relation $\mathbf{D} = \epsilon_0 \mathbf{E} + \mathbf{P}$ ($\epsilon_0 = 8.854 \times 10^{-12} \text{ F m}^{-1}$; vacuum permittivity). Only the \mathbf{E} -field is physically meaningful.

- Electric field is irrotational: $\nabla \times \mathbf{E} = \mathbf{0}$ (with an unchanging magnetic field)
- Electrostatic potential V : $\mathbf{E} = -\nabla V$
- Electromotive force (EMF, electrostatic potential difference): $\varepsilon = V_2 - V_1 = \int_1^2 \mathbf{E} \cdot d\mathbf{l}$
- Electrostatic force on a point charge: $\mathbf{F} = q\mathbf{E}$
- Electrostatic potential energy: $E_e = qV$
- Capacitance: $C = \frac{q_{\text{free}}}{V}$ (V_2 on surface, $V_1 = 0$ taken at infinity)

Gauss's Law: flux of electric field is proportional to the enclosed charge

$$\begin{aligned} \Phi_E &= \oiint_S \mathbf{E} \cdot d\mathbf{S} = \frac{q}{\epsilon_0} & \Leftrightarrow & \nabla \cdot \mathbf{E} = \frac{\rho}{\epsilon_0} \\ \Phi_D &= \oiint_S \mathbf{D} \cdot d\mathbf{S} = q_{\text{free}} & \Leftrightarrow & \nabla \cdot \mathbf{D} = \rho_{\text{free}} \\ \Phi_P &= \oiint_S \mathbf{P} \cdot d\mathbf{S} = -q_{\text{bound}} & \Leftrightarrow & -\nabla \cdot \mathbf{P} = \rho_{\text{bound}} \end{aligned}$$

Charges: $\rho = \rho_{\text{free}} + \rho_{\text{bound}}$. Fluxes: $\epsilon_0 \Phi_E = \Phi_D - \Phi_P$.

The bound charges represent immobilised dipoles within a material.

Poisson's equation: $\nabla^2 V = \frac{\rho}{\epsilon_0}$ (if no charge, reduces to Laplace's equation: $\nabla^2 V = 0$)

In linear, homogeneous, isotropic media, the material dipoles respond to external electric fields such that $\mathbf{P} = \epsilon_0 \chi_e \mathbf{E}$, therefore $\mathbf{D} = \epsilon_0 \epsilon_r \mathbf{E} = \epsilon_0 (1 + \chi_e) \mathbf{E}$ ($\chi_e = \epsilon_r - 1$: electric susceptibility, $\epsilon_r > 1$: relative permittivity).

There are alternative systems of units for electrostatic quantities, based on the CGS (centimetre gram second) system, e.g. ESU/stat, EMU/ab, Gaussian. These systems are not widely used for computations, and instead are only occasionally used to simplify some equations. They are not used here (metric SI units only).

8.1.2. Magnetic Fields

The magnetic flux density \mathbf{B} [T], magnetic field intensity \mathbf{H} [A m⁻¹] and magnetisation \mathbf{M} [A m⁻¹] vector fields are related by the constitutive relation $\mathbf{B} = \mu_0(\mathbf{H} + \mathbf{M})$ ($\mu_0 = 4\pi \times 10^{-7}$ H m⁻¹: vacuum permeability).

- Magnetic field is irrotational: $\nabla \times \mathbf{H} = \mathbf{0}$ (with no current **and** an unchanging electric field)
- Magnetic flux is solenoidal: $\nabla \cdot \mathbf{B} = 0$ (Gauss's law for magnetism: no magnetic monopoles)
- Magnetostatic scalar potential Φ_M : $\mathbf{H} = -\nabla\Phi_M$
- Laplace's equation: $\nabla^2\Phi_M = 0$
- Magnetomotive force (MMF, magnetostatic potential difference): $\Phi_{M2} - \Phi_{M1} = \int_1^2 \mathbf{H} \cdot d\mathbf{l}$
- Magnetostatic vector potential \mathbf{A} : $\mathbf{B} = \nabla \times \mathbf{A}$
- Magnetic flux as circulation of \mathbf{A} : $\oint_{\Gamma} \mathbf{A} \cdot d\mathbf{\Gamma} = \iint_S \nabla \times \mathbf{A} \cdot d\mathbf{S} = \Phi_{\mathbf{B}}$.

In linear, homogeneous, isotropic media, the material dipoles respond to external magnetic fields such that $\mathbf{M} = \chi_m \mathbf{H}$, therefore $\mathbf{B} = \mu_0 \mu_r \mathbf{H}$ ($\chi_m = \mu_r - 1$: magnetic permeability, μ_r : relative permeability).

8.1.3. Fields due to Electric Currents

- Electric current density: $\nabla \cdot \mathbf{J} = -\dot{\rho}$ (total electric current: $I = \dot{Q} = \mathbf{J} \cdot \hat{\mathbf{n}}$)
- Other conceptual currents include:
 - Electric dipole current: $\mathbf{J}_P = \dot{\mathbf{P}}$
 - Magnetisation current: $\mathbf{J}_M = \nabla \times \mathbf{M}$ ($\mathbf{J}_M + \mathbf{J}_P =$ bound current)
 - Displacement current: $\mathbf{J}_D = \dot{\mathbf{D}}$
- Ohm's law (electric field due to current-carrying wire): $\mathbf{J} = \sigma \mathbf{E}$, $V = IR$ (σ : conductivity, R : resistance)
- Ampere's law (magnetic field due to a current loop): $\oint_C \mathbf{H} \cdot d\mathbf{l} = NI$ (MMF: circulation of \mathbf{H})
- Maxwell-Ampere circuital law: $\oint_C \mathbf{H} \cdot d\mathbf{l} = \int_S (\mathbf{J} + \dot{\mathbf{D}}) \cdot d\mathbf{S}$
- Biot-Savart law (magnetic field due to a current-carrying wire): $d\mathbf{H} = \frac{I}{4\pi r^2} d\mathbf{l} \times \hat{\mathbf{r}}$
($\mathbf{r} = r\hat{\mathbf{r}}$: displacement of a point on the wire relative to the fixed point of the field)

By the Biot-Savart law, an infinitesimal current produces a circular field around it.

- Power per unit area in electromagnetic field (Poynting vector): $\mathbf{S} = \frac{1}{\mu_0} \mathbf{E} \times \mathbf{B}$
- Momentum density in electromagnetic field: $\mathbf{g} = \mu_0 \epsilon_0 \mathbf{S} = \epsilon_0 \mathbf{E} \times \mathbf{B}$

8.1.4. Alternating Magnetic Fields

Electromagnetic Induction

- Induced EMF in a conductor due to changing flux: $\oint_C \mathbf{E} \cdot d\mathbf{l} = - \int_S \dot{\mathbf{B}} \cdot d\mathbf{S}$
- Induced EMF, scalar form (Faraday's law): $\varepsilon = -\dot{\Phi}_B$ ($\Phi_B = BAN \cos \theta$: magnetic flux linkage)

The electric field \mathbf{E} resulting from electromagnetic induction is non-conservative, so the resulting voltage between two points is path-dependent: $\nabla \times \mathbf{E} = -\partial \mathbf{B} / \partial t \neq \mathbf{0}$.

In conductors, this EMF generates a current flow with a magnetic field to oppose the change in flux that produced it (Lenz's law).

8.1.5. Forces due to Electric and Magnetic Fields

- Net force on a charge (electric + Lorentz): $\mathbf{F} = q\mathbf{E} + q\mathbf{v} \times \mathbf{B}$ (\mathbf{v} : velocity vector)
- Charge carrier drift velocity: $\mathbf{J} = \rho\mathbf{v}$ (scalar form: $I = nevA$)
- Force on a straight current-carrying wire: $\mathbf{F} = I \mathbf{l} \times \mathbf{B}$ (scalar form: $F = BIl$)

Current Loop Model of Magnetisation: magnetic dipole moment is $\boldsymbol{\mu} = NI\mathbf{A}$

- Atomic dipole moment: $\boldsymbol{\mu} = i \delta \mathbf{A}$ (for electron-counting calculation of $|\delta \mathbf{m}|$, see Section 15.5.10)
- Magnetisation due to aligned dipoles: $\mathbf{M} = \frac{N}{V} \boldsymbol{\mu}$ (N/V : number of dipoles per unit volume)
- Magnetostatic force on a dipole: $\mathbf{F} = \nabla(\boldsymbol{\mu} \cdot \mathbf{B})$ ($\boldsymbol{\mu}$: magnetic dipole moment)
- Magnetostatic torque on a dipole: $\boldsymbol{\tau} = \boldsymbol{\mu} \times \mathbf{B}$

8.1.6. Electric and Magnetic Fields for Common Geometries

Point: non-accelerating point charge or sphere, total charge Q , distance (centre to centre) r :

- Electric field E , electrostatic potential V and electrostatic potential energy U :

$$E = \frac{Q}{4\pi\epsilon r^2} \quad V = \frac{Q}{4\pi\epsilon r} \quad U = qV = \frac{Qq}{4\pi\epsilon r}$$

- Inside a conductive sphere, $E = 0$ as all charges distribute evenly on the surface.

Between two point charges: cylindrical coordinates, $+q$ at $+a$ and $-q$ at $-a$ on z -axis:
(By the method of images, this also applies to a conducting plane and an image charge.)

- Potential:
$$V(r, \theta, z) = \frac{1}{4\pi\epsilon} \left(\frac{Q}{\sqrt{r^2 + (z-a)^2}} - \frac{Q}{\sqrt{r^2 + (z+a)^2}} \right)$$
- Electric field: $\mathbf{E} = -\nabla V$ (for ∇ in cylindrical coordinates, see Section 3.5.9.)

Line: static linear charge density λ or straight wire carrying current I :

$$\text{Static line charge: } E = \frac{\lambda}{2\pi\epsilon r} \quad \text{Current-carrying wire: } B = \frac{\mu I}{2\pi r}$$

Circle: static loop of linear charge density λ or current loop I of radius R :

$$\text{Along central axis: } E = \frac{\lambda R z}{2\epsilon (z^2 + R^2)^{3/2}} \quad B = \frac{\mu R^2 I}{2 (z^2 + R^2)^{3/2}}$$

Plane: static planar charge density σ on two sides of a flat plane: $E = \frac{\sigma}{2\epsilon}$

Solenoid: current-carrying, N' turns per unit length, **inside:** $B = \mu N' I$

Toroid: current-carrying, N turns of centre-to-ring radius R , **inside:** $B = \mu N' I$ ($N' = \frac{N}{2\pi R}$)

Magnetic Dipole: dipole moment $\mathbf{m} = \mathbf{M}V = IA$:

$$\mathbf{B} = \frac{\mu}{4\pi r^3} [3(\mathbf{m} \cdot \mathbf{r})\mathbf{r} - \mathbf{m}] + \frac{2\mu}{3} \mathbf{m} \delta^3(\mathbf{r}) \quad (\mathbf{r} \text{ is the unit displacement vector: } \mathbf{x} = r \mathbf{r})$$

In polar coordinates (r, θ) relative to \mathbf{m} , $B_x = \frac{\mu}{4\pi} m \frac{3 \cos^2 \theta - 1}{r^3}$, $B_y = \frac{\mu}{4\pi} m \frac{3 \cos \theta \sin \theta}{r^3}$

Cuboidal Ferromagnet: side lengths $(2x_b, 2y_b, 2z_b)$, constant axial magnetisation $\mathbf{M} = M_0 \mathbf{j}$, magnet occupies region in Cartesian coordinates $\{(x, y, z): -x_b \leq x \leq x_b, -y_b \leq y \leq y_b, -z_b \leq z \leq z_b\}$.

$$H_x(x, y, z) = \frac{M_0}{4\pi} \sum_{k,l,m=1}^2 (-1)^{k+l+m} \ln\{z + (-1)^m z_b + \alpha_{klm}(x, y, z)\}$$

$$H_y(x, y, z) = -\frac{M_0}{4\pi} \sum_{k,l,m=1}^2 (-1)^{k+l+m} \operatorname{sgn}\{y + (-1)^l y_b\} \operatorname{sgn}\{x + (-1)^k x_b\} \tan^{-1} \left\{ \frac{|x + (-1)^k x_b| |z + (-1)^m z_b|}{|y + (-1)^l y_b| \alpha_{klm}(x, y, z)} \right\}$$

$$H_z(x, y, z) = \frac{M_0}{4\pi} \sum_{k,l,m=1}^2 (-1)^{k+l+m} \ln\{x + (-1)^k x_b + \alpha_{klm}(x, y, z)\}$$

(where $\alpha_{klm}(x, y, z) = \sqrt{\left(x + (-1)^k x_b\right)^2 + \left(y + (-1)^l y_b\right)^2 + \left(z + (-1)^m z_b\right)^2}$, $\operatorname{sgn}(x) = \frac{x}{|x|}$)

Cylindrical Ferromagnet: length $2L$, radius R , constant axial magnetisation $\mathbf{M} = M_0 \mathbf{z}$, magnet occupies region in cylindrical coordinates $\{(r, \theta, z): 0 \leq r \leq R, 0 \leq \theta < 2\pi, -L \leq z \leq L\}$

$$B_r(r, \theta, z) = \frac{\mu_0 M_0 R}{\pi} (\alpha_+ P_1(k_+) - \alpha_- P_1(k_-)); \quad B_\theta(r, \theta, z) = 0; \quad B_z(r, \theta, z) = \frac{\mu_0 M_0 R}{\pi(r+R)} (\beta_+ P_2(k_+) - \beta_- P_2(k_-))$$

(where $\alpha_\pm = \frac{1}{\sqrt{(z \pm L)^2 + (r+R)^2}}$, $\beta_\pm = (z \pm L)\alpha_\pm$, $\gamma = \frac{r-R}{r+R}$, $k_\pm^2 = \frac{(z \pm L)^2 + (r-R)^2}{(z \pm L)^2 + (r+R)^2}$,

$$P_1(k_\pm) = \frac{2E(\sqrt{1-k_\pm^2}) - (1+k_\pm^2)K(\sqrt{1-k_\pm^2})}{1-k_\pm^2}, \quad P_2(k_\pm) = \frac{(\gamma+1)K(\sqrt{1-k_\pm^2}) - \gamma(\gamma+1)\Pi(1-\gamma^2, \sqrt{1-k_\pm^2})}{1-\gamma^2},$$

K, E and Π are the first, second and third complete elliptic functions, Section 1.6.5)

Solenoid electromagnets have equivalent fields to cylindrical ferromagnets with $M_0 = N'I$ (N' : turns per unit length, I : solenoid current)

8.1.7. Forces and Torques for Common Geometries

- **Two separated point charges or spheres:** $F = \frac{Q_1 Q_2}{4\pi\epsilon r^2}$ (Coulomb force)
- **Current-carrying wire:** $F = BIL \sin \theta$ or $\mathbf{F} = I\mathbf{l} \times \mathbf{B}$ (Lorentz force)
Moving charges: $F = Bqv \sin \theta$ or $\mathbf{F} = q\mathbf{v} \times \mathbf{B}$

- **Two parallel current-carrying wires:** $F = \frac{\mu I_1 I_2}{2\pi R}$
(I_1 and I_2 parallel $\rightarrow F$ attractive; I_1 and I_2 anti-parallel $\rightarrow F$ repulsive)

- **Loop or solenoid** in uniform magnetic field, N turns:

$$\tau = NIAB \sin \theta \quad \text{or} \quad \boldsymbol{\tau} = \mathbf{m} \times \mathbf{B} \quad (\mathbf{m}: \text{dipole moment of } I, \mathbf{m} = INA)$$

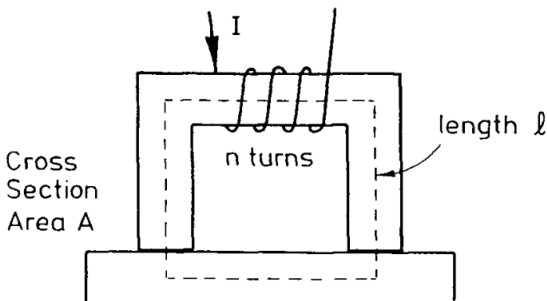
- **Two magnetic dipoles:** force exerted on dipole 2 due to dipole 1 ($\mathbf{r}_{2/1} = \mathbf{r}_2 - \mathbf{r}_1$):

$$\mathbf{F}_2 = \frac{3\mu}{4\pi r^5} [(\mathbf{m}_1 \cdot \mathbf{r}_{2/1})\mathbf{m}_2 + (\mathbf{m}_2 \cdot \mathbf{r}_{2/1})\mathbf{m}_1 + (\mathbf{m}_1 \cdot \mathbf{m}_1)\mathbf{r}_{2/1} - \frac{5}{r^2}(\mathbf{m}_1 \cdot \mathbf{r}_{2/1})(\mathbf{m}_2 \cdot \mathbf{r}_{2/1})\mathbf{r}_{2/1}]$$

If \mathbf{m}_1 and \mathbf{m}_2 are aligned parallel, then $F = -\frac{3\mu m_1 m_2}{2\pi r^4}$ and $F = U_1 m_2$.

Dipoles can approximate magnets ($\mathbf{m} \approx \mathbf{M}_0 V$) and solenoids ($\mathbf{m} \approx INA$), especially at longer distances.

8.1.8. Energy and Forces in an Electromagnet



Magnetostatic energy U per unit volume V :

$$\frac{U}{V} = \int_0^B H dB = \frac{B^2}{2\mu} \quad \text{if linear } (\mu_r \text{ constant})$$

Field strength due to electromagnet:

$$H_m = \frac{nI}{l}$$

Attractive force on the pickup bar: $F = 2A \int_0^B H dB$ (virtual work)

Volume of air gap created by a finite vertical bar displacement δx is $2A \delta x$ i.e. $U = F \delta x = \frac{U}{V} \delta V$.

For a permanent magnet, the relationship between B and H is non-linear: for $\int_0^B H dB$, the area under the B - H magnetisation curve will be required (see Section 8.6.2.)

8.1.9. Capacitances and Inductances for Common Geometries

Parallel plate capacitor:

- Single dielectric ϵ , shared area A , plate separation d :

$$C = \frac{\epsilon A}{d}$$

- Partially filled dielectric (thickness t_1 , vacuum/air thickness t_2):

$$C = \frac{\epsilon_0 A}{\frac{t_1}{\epsilon_r} + t_2}$$

Spheres:

- Single isolated sphere of radius R :

$$C = 4\pi\epsilon R$$

- Concentric spheres of radius r_1 and r_2 :

$$C = \frac{4\pi\epsilon}{\frac{1}{r_1} - \frac{1}{r_2}}$$

Cylinders or coaxial cables:

- Static concentric cylinders of length l and radii r_1, r_2 :

$$C = \frac{2\pi\epsilon l}{\ln \frac{r_2}{r_1}}$$

- Coaxial cables with current I , length l , radii r_1, r_2 :

$$L = \frac{\mu l}{2\pi} \ln \frac{r_2}{r_1}$$

Parallel wires (parasitics):

- Straight parallel wires of length l , separated by (centre-centre) distance s , with outer diameters d_1 and d_2 :

$$C = \frac{2\pi\epsilon l}{\cosh^{-1}\left(\frac{4s^2 - d_1^2 - d_2^2}{2d_1 d_2}\right)}; \text{ if } d_1 = d_2 = d \text{ then } C = \frac{\pi\epsilon l}{\cosh^{-1}\left(\frac{s}{d}\right)}$$

$$L = \frac{\mu l}{2\pi} \cosh^{-1}\left(\frac{4s^2 - d_1^2 - d_2^2}{2d_1 d_2}\right); \text{ if } d_1 = d_2 = d \text{ then } L = \frac{\mu}{\pi} \cosh^{-1} \frac{s}{d}$$

Solenoids and toroids:

- Solenoid with N turns, area $A = \pi r^2$, current I , length l :

$$L = \frac{\mu N^2 A}{l}$$

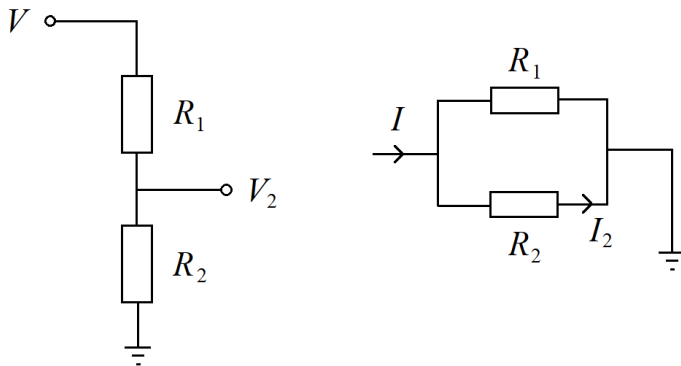
- Toroid with N turns, loop area $A = \pi r^2$, current I , centre-ring radius R :

$$L = \frac{\mu N^2 A}{2\pi R}$$

8.2. DC Circuits

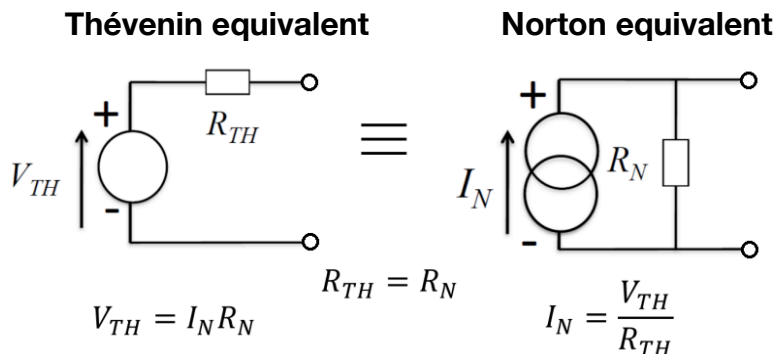
8.2.1. Circuit Resistance and the Norton/Thévenin Theorems

- Kirchoff's first law: sum of currents into a node is zero (conservation of charge)
- Kirchoff's second law: sum of voltages around a loop is zero (conservation of energy)
- For resistors in series: $R_{eq} = R_1 + R_2 + \dots + R_n$
- For resistors in parallel: $R_{eq} = R_1 \parallel R_2 \parallel \dots \parallel R_n = \left(\frac{1}{R_1} + \frac{1}{R_2} + \dots + \frac{1}{R_n} \right)^{-1}$
- For a cell with emf ε and internal resistance r , drawing current I into network resistance R : $\varepsilon - Ir = V = IR$ (Ohm's law)
(V : terminal p.d.)



- Potential Divider: $V_2 = \frac{R_2}{R_1 + R_2} V$
- Current Divider: $I_2 = \frac{R_1}{R_1 + R_2} I$

Norton's Theorem and Thévenin's Theorem: any linear two-terminal network can be replaced at its terminals by:



Norton: a current source I_N in parallel with a resistance R_N .

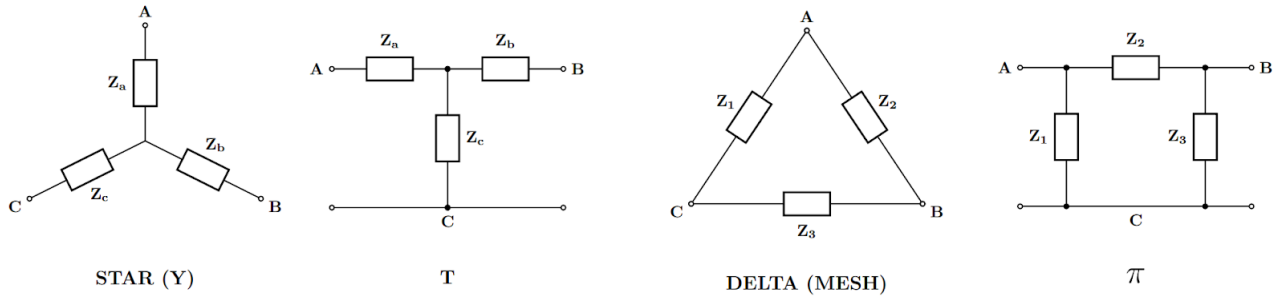
Thévenin: a voltage source V_{TH} in series with a resistance R_{TH} .

The Thévenin equivalent of a potential divider has $V_{TH} = \frac{R_2}{R_1 + R_2} V$ and $R_{TH} = R_1 \parallel R_2$.

(In general, the Thévenin / Norton 'resistances' may be complex impedances (Section 8.3).)

8.2.2. Three-Terminal Star-Delta Transformation of Impedances

The Star-Delta (also known as Y/wye-mesh or T- π) Transformation converts equivalent circuit topologies between three terminals A, B and C.



Star impedances:

$$Z_a = \frac{Z_1 Z_2}{Z_1 + Z_2 + Z_3}$$

$$Z_b = \frac{Z_2 Z_3}{Z_1 + Z_2 + Z_3}$$

$$Z_c = \frac{Z_3 Z_1}{Z_1 + Z_2 + Z_3}$$

Delta impedances:

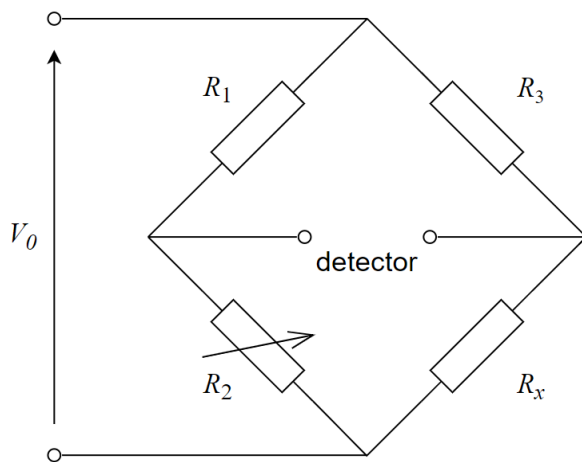
$$Z_1 = Z_c + Z_a + \frac{Z_c Z_a}{Z_b}$$

$$Z_2 = Z_a + Z_b + \frac{Z_a Z_b}{Z_c}$$

$$Z_3 = Z_b + Z_c + \frac{Z_b Z_c}{Z_a}$$

If all three impedance branches are equal, then $Z_{\text{Delta}} = 3 Z_{\text{Star}}$.

8.2.3. Wheatstone Bridge Circuit



The bridge is balanced (no current and voltage at the detector) when

$$R_1 R_x = R_2 R_3$$

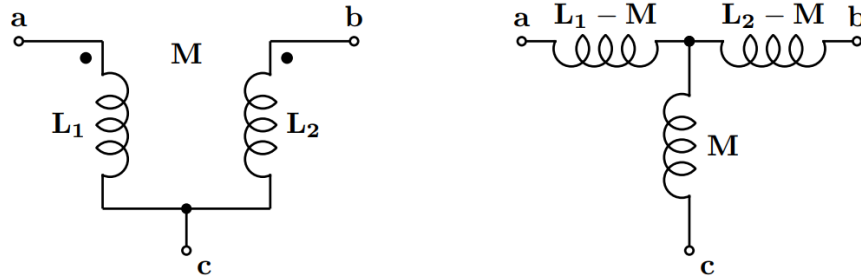
R_x is a fixed unknown resistance. R_2 is a known variable resistor (rheostat).

The detector may be a voltmeter, ammeter or galvanometer, which deflects when the bridge is unbalanced.

For other bridge circuits, see Section 8.3.5.

8.2.4. Three-Terminal Tee Transformation of Coupled Inductances

For inductances L_1 and L_2 connected with matching polarity as shown, with mutual inductance M , they can be replaced by the following network of three inductances:



(The dot on the inductor indicates the positive terminal. The convention is that when positive current flows into the positive terminal, the current flows anticlockwise when viewed inwards from the positive end.)

8.2.5. Combining Capacitances and Inductances in Series and Parallel

$$\begin{aligned} \text{In series: } C_{eq} &= \left(\frac{1}{C_1} + \frac{1}{C_2} + \dots + \frac{1}{C_n} \right)^{-1} & L_{eq} &= L_1 + L_2 + \dots + L_n \\ \text{In parallel: } C_{eq} &= C_1 + C_2 + \dots + C_n & L_{eq} &= \left(\frac{1}{L_1} + \frac{1}{L_2} + \dots + \frac{1}{L_n} \right)^{-1} \end{aligned}$$

8.2.6. Resistance, Capacitance and Inductance

For DC voltages and currents,

$$\text{Resistance: } R = \frac{V}{I} \quad \text{Capacitance: } C = \frac{Q}{V} \quad \text{Inductance: } L = \frac{\phi'}{I}$$

$$\text{Resistivity: } \rho = \frac{RA}{L} \quad \text{Conductance: } G = \frac{1}{R} \quad \text{Conductivity: } \sigma = \frac{GL}{A} = \frac{1}{\rho}$$

(V : voltage, I : current, Q : charge, ϕ' : magnetic flux linkage, A : cross-sectional area, L : length)

$$\text{Thermal power dissipated in a resistance: } P = I^2 R = \frac{V^2}{R} = IV$$

Maximum Power Transfer Theorem: if a fixed voltage V is divided across R_1 and R_2 , then maximum power is delivered to either resistor when $R_1 = R_2$.

8.2.7. Energy Transfer and Virtual Work for Capacitors and Inductors

Energy stored in a capacitor or inductor: $W = \frac{1}{2}CV^2$; $W = \frac{1}{2}LI^2$ (L : self-inductance)

Energy stored in coupled inductances: (+ if same polarity; - if opposite polarity)

$$W = \frac{1}{2}L_1I_1^2 + \frac{1}{2}L_2I_2^2 \pm MI_1I_2 \quad (M: \text{mutual inductance})$$

Coupling coefficient for inductors: $k = \frac{M}{\sqrt{L_1L_2}}$; full coupling when $k = 1$ i.e. $M \leq \sqrt{L_1L_2}$.

Force between capacitive or inductive conductors separated by distance x (virtual work):

$$F = \frac{1}{2}V^2 \frac{\partial C}{\partial x} \quad \text{and} \quad F = \frac{1}{2}I^2 \frac{\partial M}{\partial x}$$

8.2.8. Kinetics of Electrical Conductance

Charge-carrier density: $n = \frac{N_A \rho n_c}{A_r}$ (number density, per unit volume)

(N_A : Avogadro's number, A_r : relative atomic mass of metal, ρ : mass density, n_c : number of delocalised electrons per atom)

Drift velocity v , mobility μ and relaxation time τ : $\mu = \frac{v}{E} = \frac{e\tau}{m}$ and $I = nevA = \frac{Ane^2\tau E}{m}$

Resistivity: $\rho = \frac{m}{ne^2\tau}$

8.2.9. Resistor, Capacitor and Inductor Codes

Resistor colour codes: 4-colour code: $ab\ cd \rightarrow R = (ab) \times 10^c \pm d\% \Omega$
 5-colour code: $abc\ de \rightarrow R = (abc) \times 10^d \pm e\% \Omega$

Color	1 st Band	2 nd Band	3 rd Band	Multiplier	Tolerance
Black	0	0	0	10^0	
Brown	1	1	1	10^1	±1% (F)
Red	2	2	2	10^2	±2% (G)
Orange	3	3	3	10^3	
Yellow	4	4	4	10^4	
Green	5	5	5	10^5	±0.5% (D)
Blue	6	6	6	10^6	±0.25% (C)
Violet	7	7	7	10^7	±0.10% (B)
Grey	8	8	8		±0.05%
White	9	9	9		
Gold				10^{-1}	±5% (J)
Silver				10^{-2}	±10% (K)

Capacitor and inductor codes: code $xyz \rightarrow C = (xy) \times 10^z \text{ pF}$ or $L = (xy) \times 10^z \text{ μH}$

Number	1	100	101	102	103	104	105
<i>C</i>	1 pF	10 pF	100 pF	1 nF	10 nF	100 nF	1 μF
<i>L</i>	1 μH	10 μH	100 μH	1 mH	10 mH	100 mH	1 H

Letter	B	C	D	E	F	G	J	K	M	Z
Tolerance	± 0.1 pF	± 0.25 pF	± 0.5 pF	± 0.5 %	± 1 %	± 2 %	± 5 %	± 10 %	± 20 %	-20%, +80%

For electrolytic (polarised) capacitors, the longer leg is positive. For SMD (surface mounted) capacitors, the side with the coloured/black tab mark is negative.

8.3. AC Circuits

8.3.1. Differential Equation Formulation of AC Capacitor and Inductor Circuits

AC voltage input: $v(t) = V \cos \omega t = \text{Re}\{V e^{j\omega t}\} = \text{Re}\{\bar{v}(t)\}$

Device	Voltage and current	Impedance $\frac{\bar{v}(t)}{\bar{i}(t)}$	Reactance	Transfer function $\frac{\hat{v}(s)}{\hat{i}(s)}$
Resistor	$v(t) = R i(t)$ $i(t) = \frac{1}{R} v(t)$	$Z_R = R$	$X_R = 0$	R
Capacitor	$v(t) = \frac{1}{C} \int_0^t i(t) dt$ $i(t) = C \frac{dv(t)}{dt}$	$Z_C = \frac{1}{j\omega C}$	$X_C = \frac{-1}{\omega C}$	$\frac{1}{Cs}$
Inductor	$v(t) = L \frac{di(t)}{dt}$ $i(t) = \frac{1}{L} \int_0^t v(t) dt$	$Z_L = j\omega L$	$X_L = \omega L$	Ls

AC Ohm's law: $v = iZ$ ($Z = \frac{v}{i}$; 'complex resistance' accounting for phase difference)

In general, $Z = R + jX$ and $Y = G + jB$ where $Y = \frac{1}{Z} = \frac{i}{v}$ and $Z = \frac{1}{Y}$.

(Z : impedance, R : resistance, X : reactance, Y : admittance, G : conductance, B : susceptance)

Conversions: $Y = \frac{R - jX}{R^2 + X^2} = \frac{R - jX}{|Z|^2}$, $Z = \frac{G - jB}{G^2 + B^2} = \frac{G - jB}{|Y|^2}$

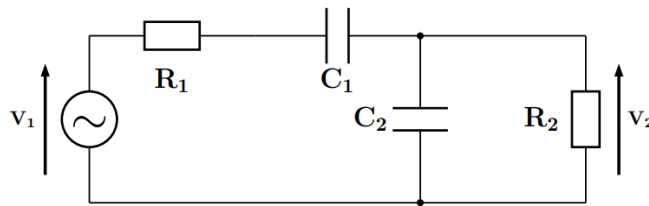
8.3.2. RMS Voltage and Single-Phase Mains Supply Standards

The root-mean-square value (rms value) of a signal is $V_{rms} = \frac{V_{peak}}{\sqrt{2}}$ and $I_{rms} = \frac{I_{peak}}{\sqrt{2}}$.

Unless otherwise specified, all a.c. voltages and currents are defined by their r.m.s. value.

Mains supplies: 220-240 V @ 50 in the UK, EU and Asia; 110-120 V @ 60 in the USA.

8.3.3. Capacitive Coupling Circuit



At midband, when the effects of C_1 and C_2 can be ignored, $v_2 = \frac{R_2}{R_1 + R_2} v_1$.

The -3 dB points (half-power, turnover) of the coupling circuit are:

- At high frequencies, v_2 drops to 70% of the midband value when $\frac{1}{\omega_2 C_2} = \frac{R_1 R_2}{R_1 + R_2}$.
- At low frequencies, v_2 drops to 70% of the midband value when $\frac{1}{\omega_1 C_1} = R_1 + R_2$.

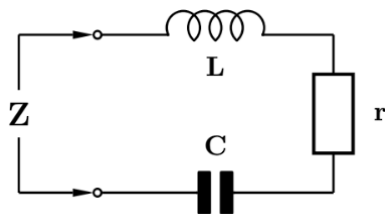
ω_1 and ω_2 are known as the lower and upper half power angular frequencies. At these frequencies, there is a 45° phase shift between v_2 and v_1 .

8.3.4. LC Resonant Circuit

Undamped resonant angular frequency, ω_0 , is given when $\omega_0^2 LC = 1 \Rightarrow \omega_0 = \frac{1}{\sqrt{LC}}$.

Quality factor: $Q = \frac{\omega U}{P}$ (U : total stored energy in the system, P : mean power dissipation)

Half power bandwidth = $\omega_2 - \omega_1 = \frac{1}{Q} \times$ resonant frequency ω_0 .

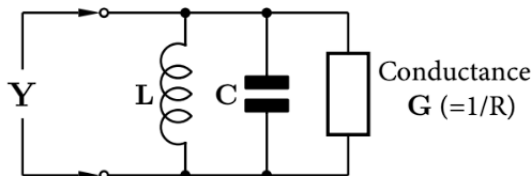


Series Resonant Circuit:

$$Q_0 = \frac{\omega_0 L}{r} = \frac{1}{r \omega_0 C},$$

$$Z \approx r \left(1 + 2jQ_0 \frac{\delta\omega}{\omega_0} \right), \text{ at frequencies close to resonance}$$

$$Z = r(1 \pm j) \text{ when } \frac{\delta\omega}{\omega_0} = \pm \frac{1}{2Q_0}.$$



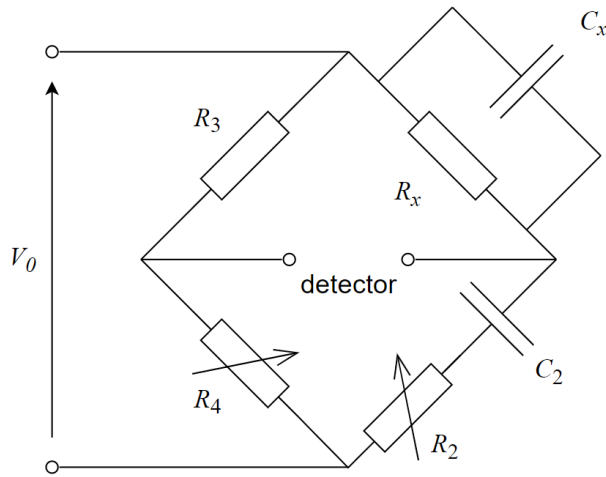
Parallel Resonant Circuit:

$$Q_0 = \frac{1}{\omega_0 L G} = \frac{\omega_0 C}{G} = \omega_0 RC,$$

$$Y \approx G \left(1 + 2jQ_0 \frac{\delta\omega}{\omega_0} \right), \text{ at frequencies close to resonance}$$

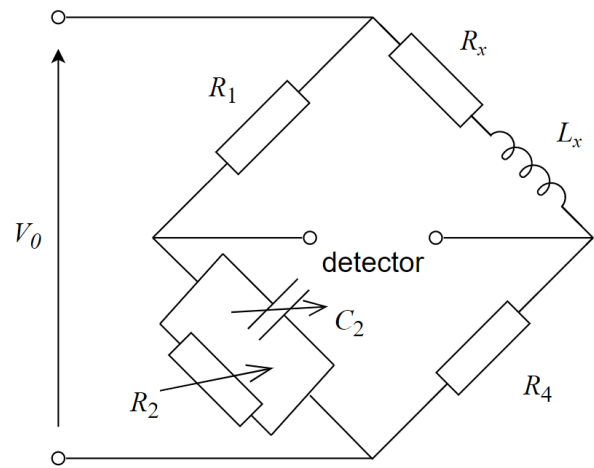
$$(Y = 1/Z: \text{ admittance})$$

8.3.5. Balance Conditions for AC Bridge Circuits



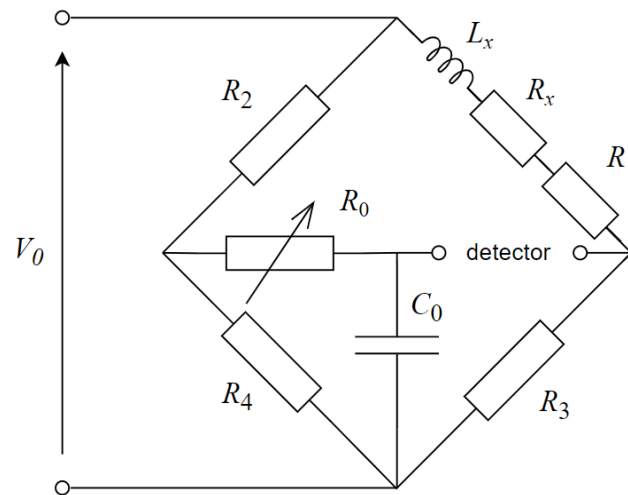
Wien Bridge: unknown $R_x \parallel C_x$

$$\omega^2 = \frac{1}{R_x R_2 C_x C_2} \text{ and } \frac{C_x}{C_2} = \frac{R_4}{R_3} - \frac{R_2}{R_x}$$



Maxwell Bridge: unknown $R_x + L_x$

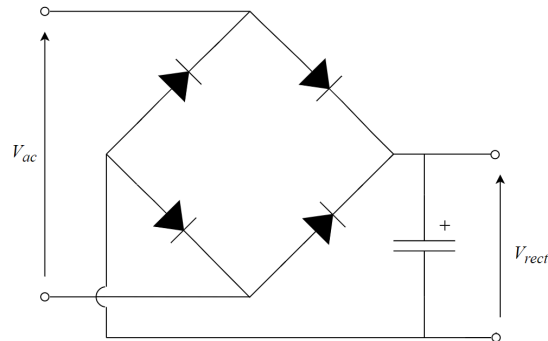
$$R_2 R_x = R_1 R_4 \text{ and } L_x = R_1 R_4 C_2$$



Anderson Bridge: unknown $R_x + L_x$

$$R_4(R_x + R_1) = R_2 R_3 \text{ and } L_x = \frac{R_3 C_0}{R_4} (R_2 R_4 + R_0(R_2 + R_4))$$

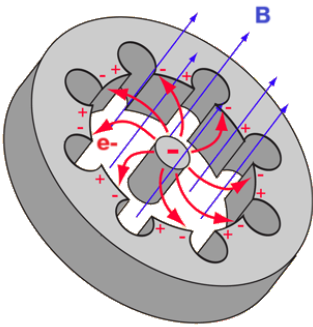
8.3.6. Full Wave Rectifier Bridge



The diode bridge effectively produces $|V_{ac}|$ (decreased by two small potential drops due to the diodes) at the output. The smoothing capacitor ensures that the voltage does not drop significantly between cycles. The resulting waveform V_{rect} is approximately d.c. with a small ripple voltage.

8.3.8. Microwave and Radio Frequency (RF) Circuits

Cavity Magnetron: produces microwaves, used in radar and microwave ovens



- A copper cathode is heated by a thoriated-tungsten filament, boiling off electrons (thermionic emission) into an evacuated space, attracted towards the copper anode.
- A permanent magnet produces a strong static axial magnetic field **B**.
- The electron trajectories in the space are curved into spiral-shaped paths by the Lorentz force of the **B**-field.
- The cavities in the anode act as *LC* resonators. As the electrons pass by the cavity ducts, AC current is induced around the cavities and radiation is generated inside.
- An antenna directs the microwaves into a waveguide for emission.

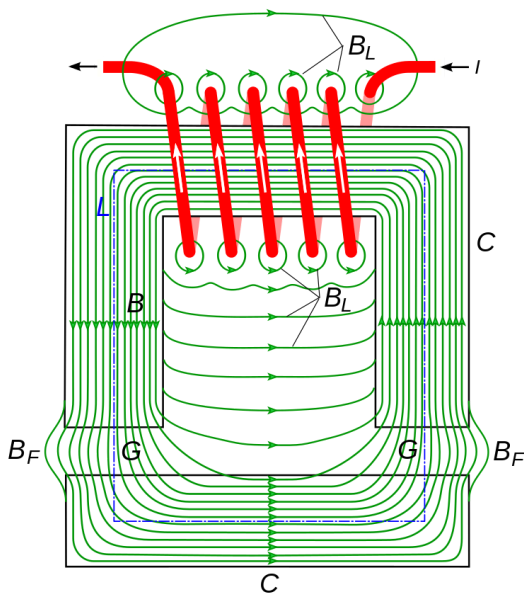
In a household microwave, the microwave radiation excites hydrogen bonds between water molecules in food creating phonons and thermal excitation (dielectric heating).

8.3.9. Switch-Mode Electronics

8.4. Electrical Power Engineering

8.4.1. Magnetic Circuits

A 'magnetic circuit' is a way to conceptualise the flow of magnetic flux.



- **Magnetomotive force (mmf):** the ampere-turns NI (for electromagnets), analogous to voltage/electromotive force
- **Magnetic flux, ϕ :** the magnetic flux through a material, analogous to electric current
- **Reluctance, $R = \frac{L}{\mu A}$:** analogous to resistance (magnetic Ohm's law: $NI = \phi R$)
- **Magnetic flux density, B :** analogous to current density J
- **Permeance, $P = \frac{1}{R}$:** analogous to conductance G
- **Permeability, μ :** analogous to conductivity κ , with $B = \mu H$.

(C : iron core, G : air gap, I : current, B : magnetic flux density, H : magnetic field intensity, B_F : fringing fields, B_L : leakage flux, L : magnetic circuit mean path length)

The mean path length L can be used in Ampere's circuital law: $\oint_L H \, dL = NI$ (Section 8.1.3).

Magnetic flux $\phi = BA$ is conserved across boundaries. In the above example:

- Ampere's law: $H_m(L - 2L_g) + H_g(2L_g) = NI$, neglecting leakage
- Flux conservation: $B_m = B_g = B$, neglecting air gap/corner fringing
- Constitutive law: $B = \mu_0 \mu_r H_m = \mu_0 H_g$, if core is a linear magnetic material

A good conductor of electric current (e.g. copper) has a low resistance (high conductivity).

A good conductor of magnetic flux (e.g. iron) has low reluctance (high permeability).

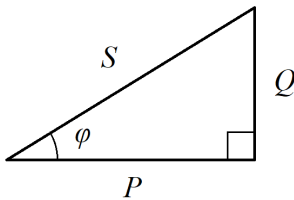
Good magnetic flux conductors will channel more of the flux, minimising flux leakage.

A permanent ferromagnet in a magnetic circuit has $NI = 0$ but drives a magnetic flux around the circuit. The operating point can be found by intersection of its B - H demagnetisation curve (Section 8.6.15) with the load line enforced by Ampere's law. Low-coercivity permanent magnets require a soft magnetic 'keeper' (armature) to prevent spontaneous loss of magnetisation over time due to e.g. stray magnetic interference.

8.4.2. AC Power

Electrical circuits may contain reactive components (complex impedance Z), causing AC voltages v and currents i to be out of phase. The phase difference is φ , defined as positive when i leads v i.e. if the phasors are $\hat{v} = V_{rms} e^{j\alpha}$ and $\hat{i} = I_{rms} e^{j\beta}$ then $\varphi = \beta - \alpha$.

Power triangle:



Apparent power:	$S = VI$ (units: volt-amperes, VA)
Power factor:	$\cos \varphi$ ($\varphi > 0$: i leads v . $\varphi < 0$: i lags v)
Real power:	$P = S \cos \varphi$ (units: watts, W)
Reactive power:	$Q = S \sin \varphi$ (units: volt-amperes reactive, VAR)

Reactive power indicates energy being exchanged between the source and reactive (inductive / capacitive) components and therefore not dissipated in any component.

Conventionally, reactive power is said to be 'consumed' if $Q > 0$ (inductive load e.g. heating element) and 'generated' if $Q < 0$ (capacitive load e.g. fluorescent light (CFLs)).

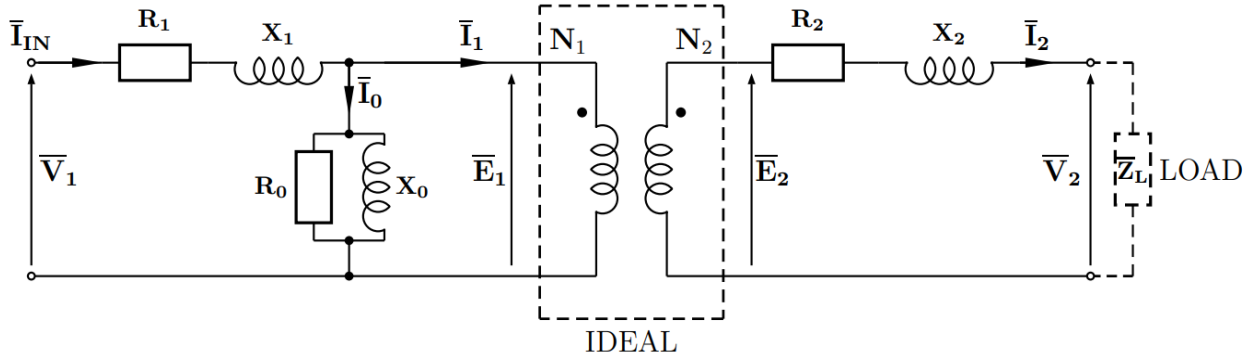
Ratings are based on apparent power S (volt-amperes), so larger reactive power Q is effectively a waste of power since real power delivered P must be lower.

Power factor correction: determine the reactive power which must be generated (per phase if three-phase) to make the desired power factor (typically 1: unity $\rightarrow Q_{\text{required}} = -Q_{\text{actual}}$ so $Q_{\text{total}} = 0$). Find the corresponding capacitor ($Q_C = -\omega CV^2$) or inductor ($Q_L = V^2 / \omega L$) value. Assume that the voltage across the load remains the same. The line current and its power losses will decrease.

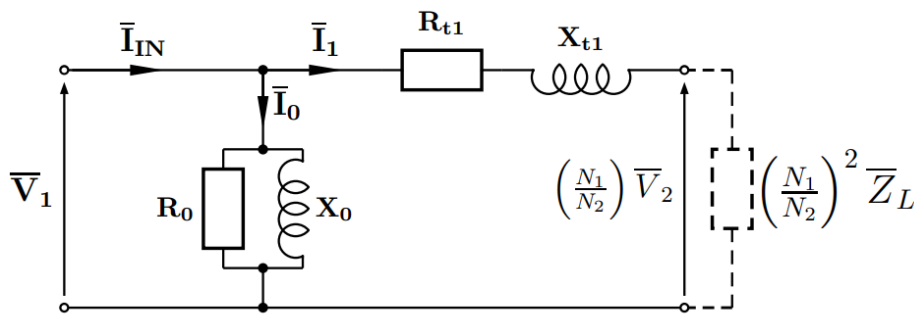
Most consumers of electricity are net inductive (due to the use of e.g. induction motors) requiring capacitor-based power factor correction. Industrial-scale consumers (e.g. factories, refineries) usually have low power factors and are charged for reactive power, requiring power factor correction. Household consumers are not charged and usually have near-unity power factors.

8.4.3. Single-Phase Transformer Equivalent Circuit

True circuit: $\bar{I}_1 N_1 = \bar{I}_2 N_2$ and $\bar{E}_1 / N_1 = \bar{E}_2 / N_2$.



Simplified circuit (all referred to the primary coil: $R_{t1} = R_1 + \left(\frac{N_1}{N_2}\right)^2 R_2$ and $X_{t1} = X_1 + \left(\frac{N_1}{N_2}\right)^2 X_2$):



Physical significances of each component:

- R_{t1} represents the winding resistance (variable copper losses) of the coils
- X_{t1} represents the winding reactance of the coils (acting as inductors).
- R_0 represents the fixed iron losses (conduction through the transformer metal core)
- X_0 represents the leakage reactance (loss of flux escaping the metal core)

R_0 can be maximised by laminating the core which minimises eddy currents. X_0 can be maximised by using a soft iron core to ensure high permeability and low hysteresis losses.

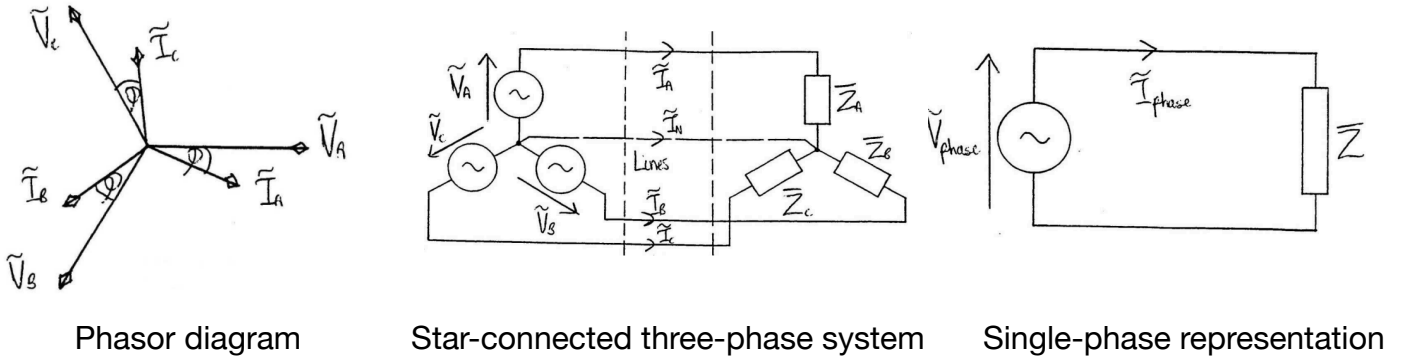
Transformer tests: experimental analysis of a transformer to determine circuit parameters

- Open-circuit test: excite primary coil, secondary is open. $I_1 = I_2 = 0 \rightarrow N_1/N_2 = E_1/E_2 = V_1/V_2$. The series branch can be eliminated, leaving only $R_0 \parallel X_0$. Power: $V_1^2 = PR_0$ and $V_1^2 = QX_0$.
- Short-circuit test: excite primary coil, secondary is shorted. $V_2 = E_2 = E_1 = 0$. The parallel branch can be eliminated, leaving only $R_{t1} + jX_{t1}$. Power: $P = I_1 R_{t1}^2$ and $Q = I_1 X_{t1}$.

Efficiency: $\eta = \frac{P_{out}}{P_{in}} = 1 - \frac{P_{losses}}{P_{in}} = 1 - \frac{V_1^2/R_0 + I_1^2 R_{t1}}{P_{in}}$, Regulation: $\frac{V_{2,OC} - V_2}{V_{2,OC}} = \frac{E_2 - V_2}{E_2} (\times 100\%)$

8.4.4. Three-Phase Power

In a three-phase power system, generators (sources) provide three separate voltages with (ideally) identical magnitude and frequency but separated by phases of 120°.



If the star-connected source is perfectly balanced then the neutral wire has $I_N = 0$.

The line voltage V_L is the voltage between any two transmission lines (at the source).

The phase voltage V_{ph} is the voltage between any line and the nodal point.

- For a **star-connected source:** $V_L = \sqrt{3} V_{ph}$ and $I_L = I_{ph}$.
- For a **delta-connected source:** $V_L = V_{ph}$ and $I_L = \sqrt{3} I_{ph}$.

Star and Delta connected loads can be interconverted using the star-delta transformations (see Section 8.2.2). When balanced, $Z_* = \frac{1}{3} Z_{\Delta}$.

With multiple loads in parallel, use conservation of real power P and reactive power Q on a per-phase basis:

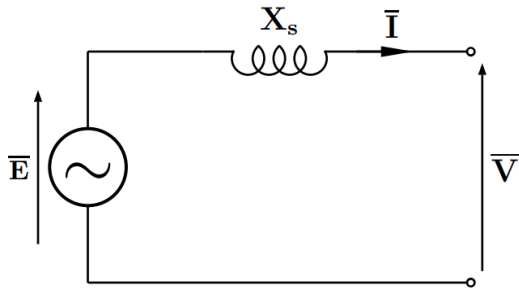
- For a **star-connected load:** $\frac{1}{3} P = Re\left(\frac{V_{ph}^2}{Z_*}\right)$ and $-\frac{1}{3} Q = Im\left(\frac{V_{ph}^2}{Z_*}\right)$
- For a **delta-connected load:** $\frac{1}{3} P = Re\left(\frac{V_L^2}{Z_*}\right)$ and $-\frac{1}{3} Q = Im\left(\frac{V_L^2}{Z_*}\right)$

Power factors can be corrected by adding a set of star or delta connected capacitors or inductors in parallel with the load (at each three-phase terminal).

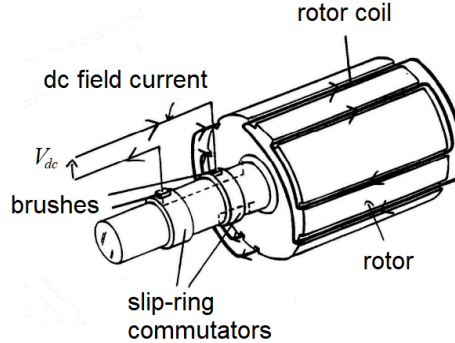
8.4.5. Three-Phase Synchronous Machine (Generator) Equivalent Circuit

A prime mover is driven and rotates the rotor coils in the presence of a static magnetic field (induced by dc field current on the stator coils). AC current is induced in the rotor.

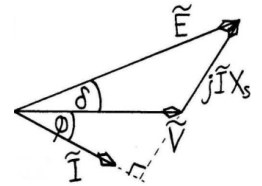
Equivalent circuit (generator convention):



Construction: (stator omitted)



Phasor diagram:



(E : phase excitation, X_s : synchronous reactance, I : input phase current, V : terminal phase pd, ϕ : phase difference, $\delta = \arg E - \arg V$: load angle, jIX_s : back-emf in stator)

$$\bar{E} = \bar{V} + jIX_s \quad \text{or as phasors,} \quad \bar{E} = \bar{V} + (IX_s) \angle \sin^{-1}(\cos \phi)$$

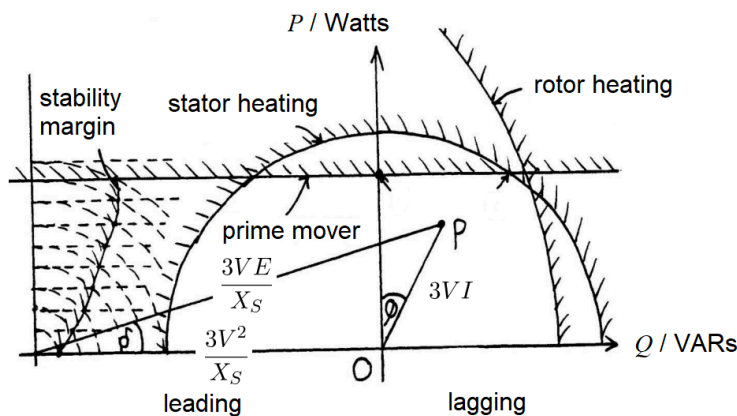
$\delta > 0$: **generator (alternator)**. $\delta < 0$: **motor**. If $|\delta| \geq \pi/2$ then the machine is prone to instability.

Conditions for synchronous power generation: $\omega_s = \frac{\omega}{p_s}$ and $p_s = p_R$.

(ω_s : synchronous rotation speed of prime mover, ω : generated electricity frequency, p_s : pole **pairs** on stator, p_R : pole **pairs** on rotor).

A **dynamo** is a DC generator, using split-ring commutators instead of slip rings.

Three-phase generators are optimal: increasing the number of phases has diminishing returns on efficiency while costing more for wiring. Most generators are connected to public supplies, so stator voltage output has fixed magnitude and frequency (infinite bus assumption: no single generator variation affects the grid).



Operating chart: scale lengths by $\frac{3V}{X_s}$

Maximum EM torque: $T_{max} = \frac{3VE}{\omega_s X_s}$

EM torque: $T = T_{max} \sin \delta$

Power: $P_{in} = P_{out} + T\omega_s$

Stator heating limit based on rated S_{max} :

$$S = 3 V_{ph} I_{ph}$$

8.4.6. Three-Phase Induction Motor (AC) Equivalent Circuit (Asynchronous Motor)

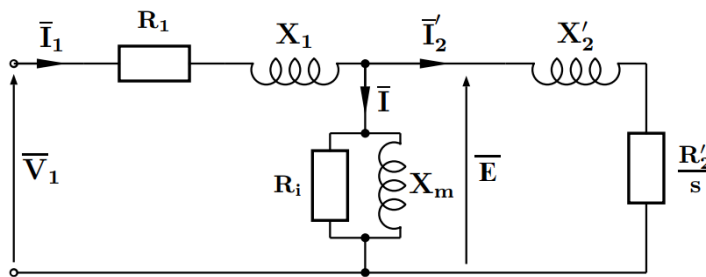
Conditions for steady torque production: $\omega_s = \omega_R = \frac{\omega}{p}$ and $p_s = p_R$.

Slip: $s = 1 - \frac{\omega_R}{\omega_s}$. If $s = 0$ then $\omega_R = \omega_s$. If $s = 1$ then $\omega_R = 0$.

At the synchronous speed, the relative magnetic field rotation rate is zero (stationary), so there is no induced emf or rotor current so no torque is produced.

Equivalent circuit: side 1 is the stator; side 2 is the rotor (referred).

Assume $R_0 \gg R_1$ and $X_m \gg X_1$. Physical significance is similar to the transformer (per phase).



$$\bar{E} = \bar{V}_1 - (R_1 + jX_1) \bar{I}_1$$

(motoring convention)

Motor tests:

- No-load test: let slip $s = 0$ (synchronous speed).

$$P_{ph} = \frac{V_{ph}^2}{R_0}, \quad Q_{ph} = \sqrt{(V_{ph} I)^2 - P_{ph}^2} = \frac{V_{ph}^2}{X_m}$$

- Locked-rotor test: let slip $s = 1$ (stationary transformer).

$$P_{ph} = I_{in}^2 \left(R_1 + \frac{R_2'}{s} \right), \quad Q_{ph} = \sqrt{(V_{ph} I)^2 - P_{ph}^2} = I_{in}^2 (X_1 + X_2')$$

Power, Torque and Efficiency: Electromagnetic torque: $T_{EM} = \frac{3(I_2')^2 R_2'}{s \omega_s}$.

To find I_2' , use a Thevenin circuit equivalent and take $I_2' = V_{TH} \left| Z_{TH} + \frac{R_2'}{s} \right|^{-1}$.

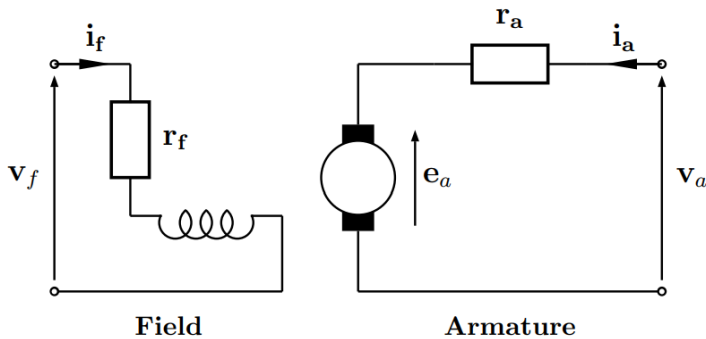
$$P = T\omega, \quad P_{loss} = T_{loss} \omega_R, \quad P_{out} = T_{out} \omega_R \text{ and } T_{out} = T_{EM} - T_{loss} \rightarrow \text{efficiency: } \eta = \frac{P_{out}}{3 V_{ph} I \cos \phi_{in}}$$

- Maximum torque: use Thevenin and max power transfer theorems: $\frac{R_2'}{s} = |Z_{TH}|$.

- Maximum output power: split as $\frac{R_2'}{s} = \underbrace{R_2}_{\text{wasted}} + \underbrace{\left(\frac{1}{s} - 1\right) R_2}_{\text{power out}}$, maximise similarly.
- Maximum starting torque:

$\omega_R = 0$ so let $s = 1$ and add the remaining (referred) rotor resistance to make $R_2'' = Z_{TH}$.

8.4.7. Separately Excited DC Motor Equivalent Circuit



Armature back emf, $e_a = K\phi\omega$; torque, $T = K\phi i_a$
 (K : emf constant, ϕ : flux per pole, ω : rotor speed, i_a : armature current)

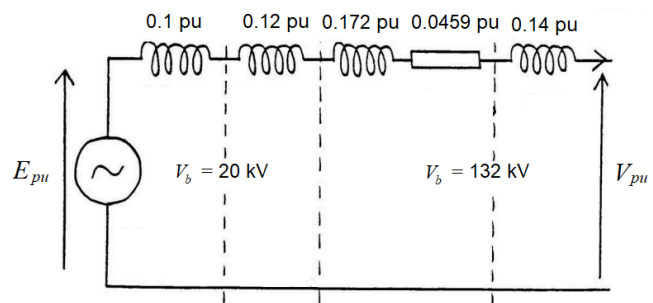
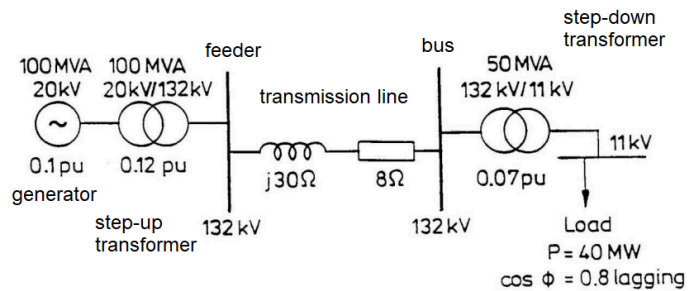
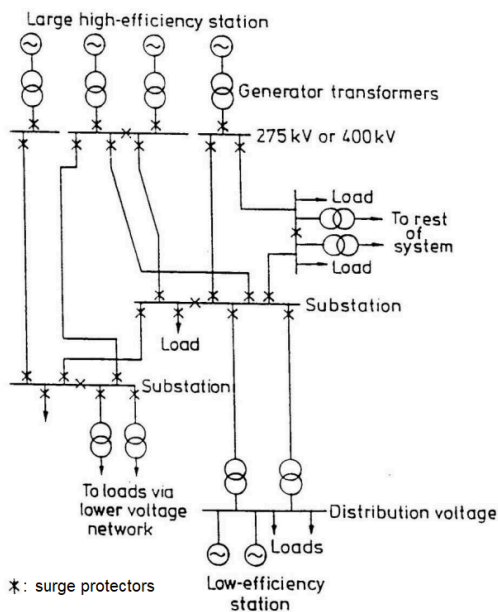
The field winding circuit represents the **stator** and the armature circuit is the **rotor**. Dynamics: (θ : rotor/shaft angular position, J : shaft polar moment of inertia, λ : rotor damping constant, $\{R_a, L_a\}$: armature resistance/inductance)

$$J\ddot{\theta} + \lambda\dot{\theta} = K\phi i_a, \quad L_a \frac{di_a}{dt} + R_a i_a = V_a - K\phi\dot{\theta}$$

8.4.8. Electrical Grid Transmission System and Per-Unit Calculations

Typical distribution system:

Example per-phase, per-unit representation to a single load:



Per-unit calculations: VA_b : base VA (three-phase), V_b : base line voltage, with

$$S_{pu} = V_{pu} I_{pu}, \quad Z_b = \frac{V_b^2}{VA_b} \text{ and } I_b = \frac{VA_b}{\sqrt{3} V_b}. \quad \text{Change of base: } Z_{pu}' = \frac{VA_b'}{VA_b} Z_{pu}$$

Per-unit reactances are often expressed as percentages e.g. 15% pu = 0.15 pu.

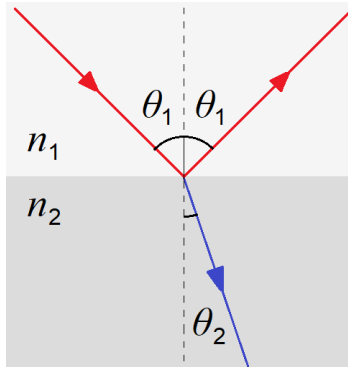
For a transformer, the rated voltage and reactance always refer to the primary coil.

Fault analysis: assume a three-phase symmetrical fault to earth (worst-case: max surge current)

Model all generators as $E_{pu} = 1 \angle 0^\circ$ pu emfs with their synchronous reactances so that all generators output to a common node. Neglect resistances and loads. Determine fault current and required VA rating of the circuit breaker.

8.5. Optics, Electromagnetic Waves and Plasma Physics

8.5.1. Reflection and Refraction



At a perfectly flat interface, an incoming ray can undergo **reflection** and/or **refraction** such that:

$$n_1 \sin \theta_1 = n_2 \sin \theta_2 \quad (\text{Snell's law of refraction})$$

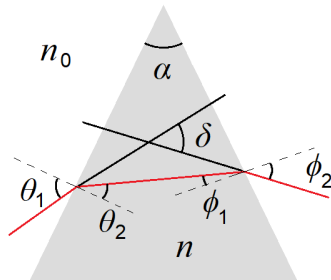
For any **reflected** component, angle of incidence = reflection.

Critical angle: $\sin \theta_c = \frac{n_2}{n_1} \quad (\theta_2 = 90^\circ)$

For total internal reflection: $n_1 > n_2$ and $\theta_1 > \theta_c$.

The refractive index depends on medium material, wavelength and temperature.

8.5.2. Angle of Dispersion in a Prism

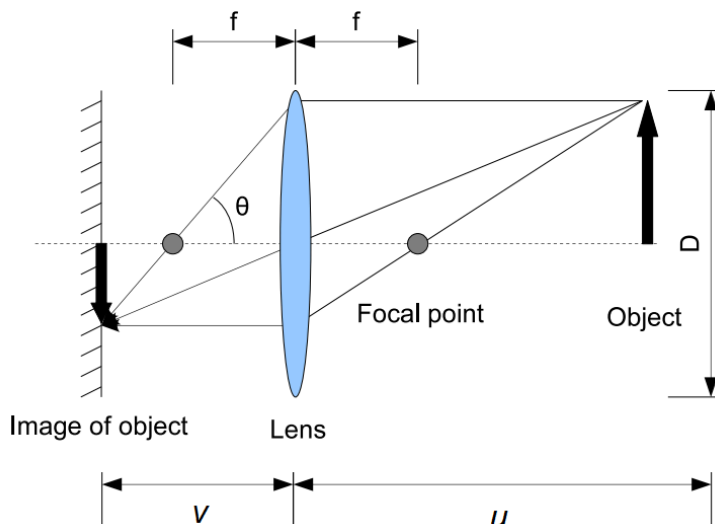


Geometry: $\theta_2 + \phi_1 = \alpha$ and $\delta = \theta_1 - \theta_2 + \phi_2 - \phi_1$

Refraction: $n_0 \sin \theta_1 = n \sin \theta_2$ and $n \sin \phi_1 = n_0 \sin \phi_2$

Angle of dispersion: $\frac{n}{n_0} = \frac{\sin \frac{1}{2}(\alpha + \delta)}{\sin \frac{1}{2}\alpha} \rightarrow \delta = 2 \sin^{-1} \left(\frac{n}{n_0} \sin \frac{\alpha}{2} \right) - \alpha$

8.5.3. Thin Convex (Converging) Lenses



Distances u and v relate to the focal length f by

$$\frac{1}{f} = \frac{1}{u} + \frac{1}{v}$$

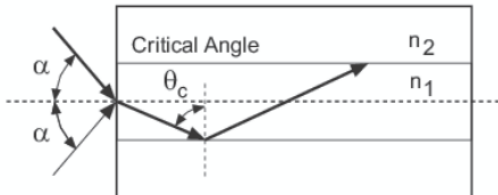
Magnification: $m = \frac{v}{u}$

Numerical aperture: $NA = n \sin \theta$

f -number ($f/\#$): $N = \frac{f}{D}$; $NA \approx \frac{n}{2N}$

8.5.4. Fibre Optics

For a single straight fibre of total length L , acceptance half-angle α , core index n_1 and cladding index n_2 (such that $n_1 > n_2$):



- Numerical aperture: $NA = \sin \alpha = \sqrt{n_1^2 - n_2^2}$
- Propagation time range: $\frac{Ln_1}{c} < T < \frac{Ln_1^2}{cn_2}$
- Chromatic dispersion: shorter wavelengths travel faster than longer wavelengths.

Fibre optic cables have a characteristic attenuation spectrum (due to Rayleigh scattering, impurity metal ions, absorption peaks, glass absorption), with varying losses (measured in signal power drop per length of cable, dB/km).

An impurity of 1 ppm of metal ions (e.g. Fe^{2+} , Cu^{2+}) causes ~ 1 dB/km loss.

The coating should be impermeable to hydrogen (produced from e.g. steel cable corrosion, bacterial presence) as H_2 and its OH^- byproducts also have absorption peaks.

Fibre optic cables that are bent sharply risk attenuation due to light incident below the critical angle at the bend. Sharp bends can also induce stresses and micro-scale flaws in the core interface, contributing to the dB/km losses. A common standard is to ensure no bends with radius of curvature $r < 15d$ exist (d : diameter of cable).

8.5.5. Polarisation and Malus' Law

EM waves can be plane-polarised i.e. all electric/magnetic field oscillations are in the same plane. The direction of polarisation refers to the plane of the electric field.

Radiation can be polarised by passing through a polariser. For polarisation by reflection, see Section 8.5.5.

Malus' law: for a perfect polariser, $\frac{I_t}{I_i} = \cos^2 \Delta\theta$

(I_t : transmitted intensity, I_i : incident intensity, $\Delta\theta$: difference between angle of initial and final polarisation.)

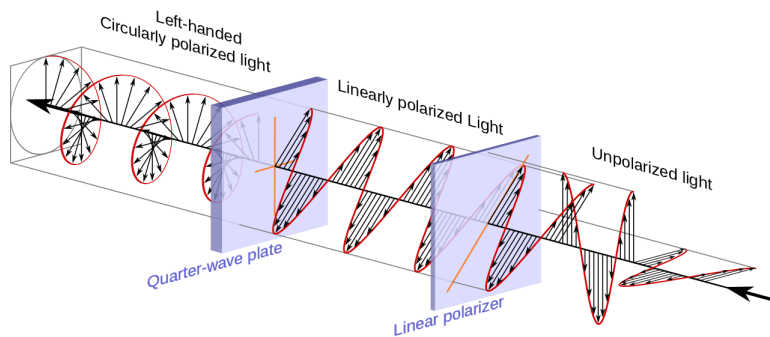
For initially unpolarised (uniformly distributed) radiation, transmission coefficient $\frac{I_t}{I_i} = \frac{1}{2}$.

Losses in a Polaroid filter result in actual $\frac{I_t}{I_i} \sim 0.38$.

Plane Polarised Light and Circularly Polarised Light as Superpositions of Coherent Waves

- Superposition of two perpendicularly plane-polarised waves with different amplitudes and/or phases produces **elliptically polarised light**. If the phase difference is 90° , then the axes of the ellipse align with the polarisation directions. If additionally the amplitudes are equal then the result is **circularly polarised light**.
- Superposition of coherent in-phase left- and right-circularly polarised light produces **plane polarised light**, with the polarisation direction being the coincident vectors of the waves.

Circularly polarised light can be created using a birefringent quarter-wave plate whose 'fast' (lower index) and 'slow' (higher index) axes are at 45° to the plane of polarisation. The thickness of the plate is chosen such that the component in the slow axis lags the component in the fast axis by 90° at their exit, creating circular polarisation.

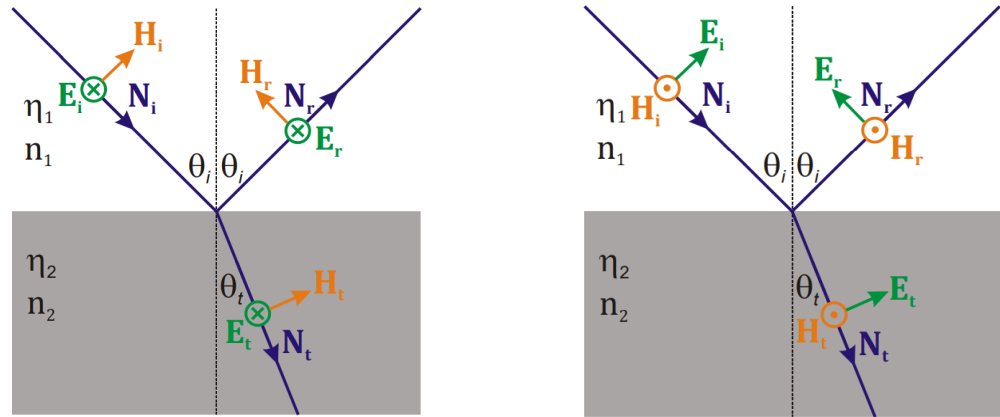


Required quarter-wave plate thickness: $d = \frac{\lambda_0}{4 |\Delta n|}$ (Δn : difference in refractive index in axes)

For values of Δn for different crystals see Section 8.5.12.

8.5.6. Waves at Interfaces: The Fresnel Equations and Polarisation by Reflection

Snell's law using impedances: $n_1 \sin \theta_i = n_2 \sin \theta_t$ so $\eta_2 \sin \theta_i = \eta_1 \sin \theta_t$ where $H = E / \eta$.



Electric field perpendicular to plane

Magnetic field perpendicular to plane

$$(E_i + E_r = E_t)$$

$$(H_i + H_r = H_t)$$

Transmission: $\left(\frac{E_t}{E_i}\right)_{\perp} = \frac{2\eta_2 \cos \theta_i}{\eta_2 \cos \theta_i + \eta_1 \cos \theta_t}$

Transmission: $\left(\frac{E_t}{E_i}\right)_{\parallel} = \frac{2\eta_2 \cos \theta_i}{\eta_1 \cos \theta_i + \eta_2 \cos \theta_t}$

Reflection: $\left(\frac{E_r}{E_i}\right)_{\perp} = \frac{\eta_2 \cos \theta_i - \eta_1 \cos \theta_t}{\eta_2 \cos \theta_i + \eta_1 \cos \theta_t}$

Reflection: $\left(\frac{E_r}{E_i}\right)_{\parallel} = \frac{\eta_1 \cos \theta_i - \eta_2 \cos \theta_t}{\eta_2 \cos \theta_i + \eta_1 \cos \theta_t}$

At normal incidence ($\theta_i = 0^\circ$), we have $\left(\frac{E_t}{E_i}\right)_{\perp} = \frac{2\eta_2}{\eta_1 + \eta_2}$, $\left(\frac{E_r}{E_i}\right)_{\perp} = \frac{\eta_2 - \eta_1}{\eta_1 + \eta_2}$, $\left(\frac{E_r}{E_i}\right)_{\parallel} = \frac{\eta_1 - \eta_2}{\eta_1 + \eta_2}$.

Polarisation by Reflection: if $\tan \theta_i = \frac{\eta_1}{\eta_2}$ (**Brewster angle**) then $\left(\frac{E_r}{E_i}\right)_{\parallel} = 0$ (**plane polarised**).

In this case the reflected wave is **plane-polarised** with the electric field perpendicular to the plane of incidence i.e. electric field oscillates in the plane of the **interface** surface.

Anti-Reflection Coatings: inserting a layer of material with $\eta = \sqrt{\eta_1 \eta_2}$ allows for quarter-wave matching (layer thickness is equal to $\frac{1}{4}$ of the wavelength within the layer).

However, this is only tuned to the one wavelength. An alternative is to use nanostructured materials with size much less than λ (metamaterials: see Section 8.5.15). In this case the electromagnetic wave does not interact with individual structures but sees a spatial average of the structure so the nanostructure can appear to modulate the characteristic impedance smoothly as a function of depth into the layer: reflections are minimised across a broad range of wavelengths.

8.5.7. Scattering of Light by Particles in a Medium

Rayleigh Scattering (particles with size $x \ll \lambda$): $I(r, \theta) = I_0 \frac{8\pi^4 \alpha^2}{\lambda^4 r^2} (1 + \cos^2 \theta)$

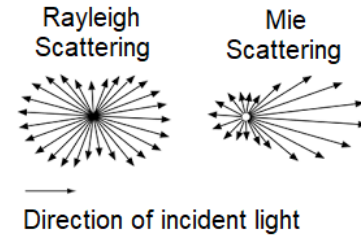
Mie Scattering (particles with size $x \sim \lambda$): more intense forward lobe, much less dependent on λ .

Molecular polarisability, $\alpha = \frac{3}{4\pi N} \left(\frac{\epsilon_r - 1}{\epsilon_r + 2} \right)$

(Clausius-Mossotti relation)

where $\epsilon_r = n^2$ for nonmagnetic media.

(N : number of scatterers per unit volume)



8.5.8. Maxwell's Equations and the Electromagnetic Wave Equations (Differential Form)

For the integral forms, see Section 8.1.4-6.

$\nabla \cdot \mathbf{D} = \rho$	Gauss' law for electricity: charge produces an electric field
$\nabla \cdot \mathbf{B} = 0$	Gauss' law for magnetism: magnetic monopoles do not exist
$\nabla \times \mathbf{E} = -\frac{\partial \mathbf{B}}{\partial t}$	Faraday's law: changing magnetic flux induces an electric field
$\nabla \times \mathbf{H} = \mathbf{J} + \frac{\partial \mathbf{D}}{\partial t}$	Ampere-Maxwell law: moving charge or changing electric flux both induces a magnetic field

To derive the electromagnetic wave equations in free space, set $\rho = 0$ and $\mathbf{J} = 0$ (no charge, no current). Take the curl of both sides of Faraday's law, use the vector product identity in Section 3.5.12 and substitute $\nabla \cdot \mathbf{E} = 0$ (from Gauss' law). The wave PDEs are then

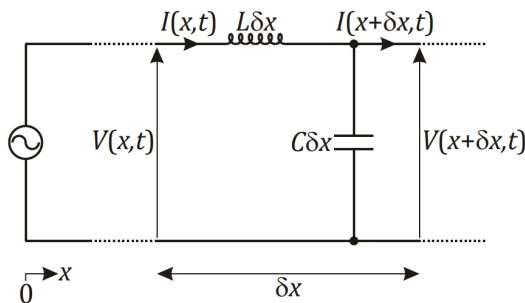
$$\nabla^2 \mathbf{E} = \frac{1}{c^2} \frac{\partial^2 \mathbf{E}}{\partial t^2} \quad \text{and} \quad \nabla^2 \mathbf{H} = \frac{1}{c^2} \frac{\partial^2 \mathbf{H}}{\partial t^2} \quad \text{where} \quad c = \frac{1}{\sqrt{\epsilon_0 \epsilon_r \mu_0 \mu_r}}.$$

8.5.9. Telegrapher's Wave Equations and the Loss Transmission Line Model

If the wavelength is of similar order to the physical length of the system we are looking at, then we can no longer consider the current to be behaving as an 'incompressible fluid' i.e. conventional circuit analysis. This is the case in e.g. transmission lines.

Let C and L be the capacitance and inductance **per unit length** of transmission line.

For a **lossless** transmission line (no series resistance, no shunt conductance):



Telegrapher's equations:

$$\frac{\partial V}{\partial x} = -L \frac{\partial I}{\partial t} \quad \text{and} \quad \frac{\partial I}{\partial x} = -C \frac{\partial V}{\partial t}$$

Wave equations:

$$\frac{\partial^2 V}{\partial x^2} = \frac{1}{c^2} \frac{\partial^2 V}{\partial t^2} \quad \text{and} \quad \frac{\partial^2 I}{\partial x^2} = \frac{1}{c^2} \frac{\partial^2 I}{\partial t^2} \quad \text{where} \quad c = \frac{1}{\sqrt{LC}}$$

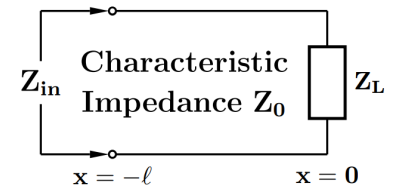
- General solution: $V = \bar{V}_F e^{j(\omega t - \beta x)} + \bar{V}_B e^{j(\omega t + \beta x)}$ and $I = \bar{I}_F e^{j(\omega t - \beta x)} + \bar{I}_B e^{j(\omega t + \beta x)}$
- Amplitudes: $V_F = I_F Z_0$ and $V_B = -I_B Z_0$

(Wavelength: $\lambda = \frac{2\pi c}{\omega}$. Characteristic impedance: $Z_0 = \sqrt{\frac{L}{C}}$. Propagation constant = $j\beta$.)

Phase constant (wavenumber): $\beta = k = \frac{2\pi}{\lambda} = \frac{\omega}{v}$. Speed of light in media: $v = c/n$.)

Connection to a Load: at $x = 0$, with load Z_L , voltage reflection ρ_L / transmission τ_L coefficients are ($\tau_L - \rho_L = 1$): $\rho_L = \frac{V_B}{V_F} = \frac{Z_L - Z_0}{Z_L + Z_0}$, $\tau_L = \frac{2Z_L}{Z_L + Z_0}$.

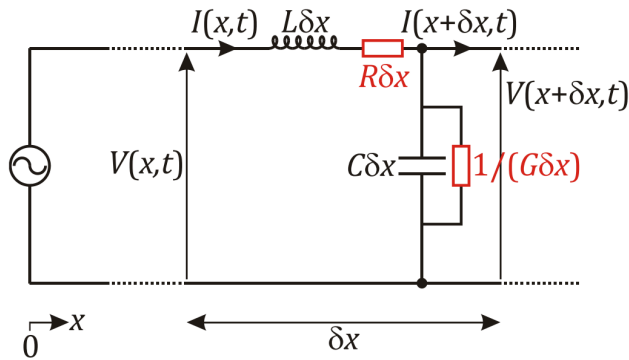
- For any value of x , $\rho(x) = \rho_L e^{j2\beta x}$.
- Input impedance: $Z_{in} = Z_0 \frac{Z_L + Z_0 j \tan \beta l}{Z_0 + Z_L j \tan \beta l}$.
- Voltage standing wave ratio (VSWR): $\frac{|V_F| + |V_B|}{|V_F| - |V_B|} = \frac{1 + |\rho_L|}{1 - |\rho_L|}$.
- Incident reflected power is proportional to $|\rho_L|^2$.



- Open circuit: $Z_L = \infty$ so $\rho_L = 1$ (0 shift). Perfect reflection with an antinode at the terminal.
- Closed circuit: $Z_L = 0$ so $\rho_L = -1$ (π shift). Perfect reflection with a node at the terminal.
- Load impedance matched: $Z_L = Z_0$ so $\rho_L = 0$. No reflection; perfect transmission.

8.5.10. Lossy Transmission Lines

There are incremental series resistances $R \delta x$ and shunt conductances $G \delta x$:



General wave solution is now

$$V(x,t) = (V_F e^{-\gamma x} + V_B e^{\gamma x}) e^{j\omega t}$$

$$I(x,t) = (I_F e^{-\gamma x} + I_B e^{\gamma x}) e^{j\omega t}$$

Propagation constant:

$$\gamma = \alpha + j\beta = \sqrt{(R + j\omega L)(G + j\omega C)}$$

Characteristic impedance: $Z_0 = \sqrt{\frac{R + j\omega L}{G + j\omega C}}$

For any value of x ,

$$\rho(x) = \rho_L e^{j2\gamma x}.$$

Input impedance: $Z_{in} = Z_0 \frac{Z_L + Z_0 j \tanh \gamma l}{Z_0 + Z_L j \tanh \gamma l}$

8.5.11. Propagation of Waves in Insulating Media

Electric and magnetic field wave solutions (1D):

$$E_x = \text{Re} \left\{ \mathbf{E}_{xF} e^{j(\omega t - \beta z)} + \mathbf{E}_{xB} e^{j(\omega t + \beta z)} \right\}$$

$$H_y = \text{Re} \left\{ \mathbf{H}_{yF} e^{j(\omega t - \beta z)} + \mathbf{H}_{yB} e^{j(\omega t + \beta z)} \right\}$$

Refractive index: $n = \sqrt{\epsilon_r \mu_r}$. Intrinsic impedance: $\eta = \sqrt{\mu / \epsilon}$. Wave speed: $v = \frac{1}{\sqrt{\epsilon \mu}}$.

For air or vacuum, $\eta = 377 \Omega$, $n = 1$, $\epsilon_r = 1$, $\mu_r = 1$, $v = c = 299,792,458 \text{ ms}^{-1} \approx 3 \times 10^8 \text{ ms}^{-1}$.

Intensity of an EM wave (complex Poynting vector): $I = \frac{1}{2} \text{Re} (\mathbf{E} \times \mathbf{H}^*)$

For the reflection and transmission coefficients, see Section 8.5.5.

8.5.12. Propagation of Waves in Conducting Media

Electric and magnetic field wave solutions (1D):

$$E_x = \text{Re} \left\{ \mathbf{E}_{xF} e^{-\gamma z} + \mathbf{E}_{xB} e^{\gamma z} \right\} e^{j\omega t}$$

$$H_y = \text{Re} \left\{ \mathbf{H}_{yF} e^{-\gamma z} + \mathbf{H}_{yB} e^{\gamma z} \right\} e^{j\omega t}$$

When conductivity $\sigma \neq 0$, the propagation constant is $\gamma = \alpha + j\beta = \sqrt{j\omega\mu(\sigma + j\omega\epsilon)}$.

Intrinsic impedance: $\eta = \sqrt{\frac{j\omega\mu}{\sigma + j\omega\epsilon}}$. Reflection coefficient: $\rho_L = \frac{\eta_2 - \eta_1}{\eta_1 + \eta_2}$. Skin depth: $\delta = \frac{1}{\alpha}$.

8.5.13. Skin Effect

AC signals (like all electromagnetic waves in conducting media) have maximum current density \mathbf{J} at the surfaces of any conductor, and minimum in the centre.

The skin depth is the reciprocal of the real part of the propagation constant γ (Section 8.5.10). The skin depth decreases with frequency, which increases the effective impedance.

For low frequencies $\omega \ll \sigma/\epsilon$, this simplifies to $\delta \approx \sqrt{\frac{2}{\sigma\omega\mu}}$.

For high frequencies $\omega \gg \sigma/\epsilon$, the asymptotic limit is $\delta \approx \frac{2}{\sigma} \sqrt{\frac{\epsilon}{\mu}}$.

Variation of current density \mathbf{J} with depth d from surface: $\mathbf{J}(d) = \mathbf{J}_s e^{-(1+j)\frac{d}{\delta}}$.

When $\delta \sim R$ (wire radius), the current density is (for circular sections):

$$\mathbf{J}(r) = \mathbf{I} \frac{k}{2\pi R} \frac{J_0(kr)}{J_1(kR)} = \mathbf{J}(R) \frac{J_0(kr)}{J_0(kR)}$$

(J_n : Bessel function (Section 1.7.10), $k = \sqrt{-j\omega\mu\sigma}$: wavenumber, \mathbf{I} : total current phasor)

In both cases, both the magnitude and phase (represented by the complex current density) vary with depth.

8.5.14. Antenna Design

Poynting vector: $\mathbf{N} = \mathbf{E} \times \mathbf{H}$ (\mathbf{N} is parallel to the direction of propagation / energy transfer)

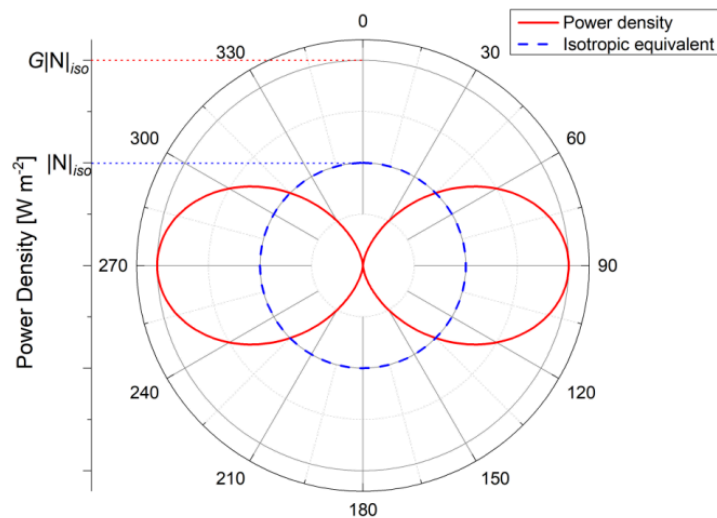
Instantaneous intensity (power density, W m^{-2}): $|\mathbf{N}(t)| = |\mathbf{E}(t)||\mathbf{H}(t)|$.

Mean intensity: $\frac{1}{2} |\mathbf{N}| = E_{\text{rms}} H_{\text{rms}}$

Half-wave dipole (grand plane) antenna: conductor of length $\frac{\lambda}{4}$ extending from a grounded plane (common for e.g. radio antenna). AC signal in the conductor produces circulating \mathbf{H} -field with \mathbf{E} -field parallel to the dipole so propagation is in all surrounding perpendicular directions.

Current variation is a standing wave: $i = i_0 \cos \omega t \cos kx$ ($k = \frac{2\pi}{\lambda}$, for $|x| \leq \frac{\lambda}{4}$)

Anisotropic far-field electric field: $E_\theta = \frac{I_0 Z_0}{2\pi r} \frac{\cos\left(\frac{\pi}{2} \cos \theta\right)}{\sin \theta} \sin(\omega t - kr)$

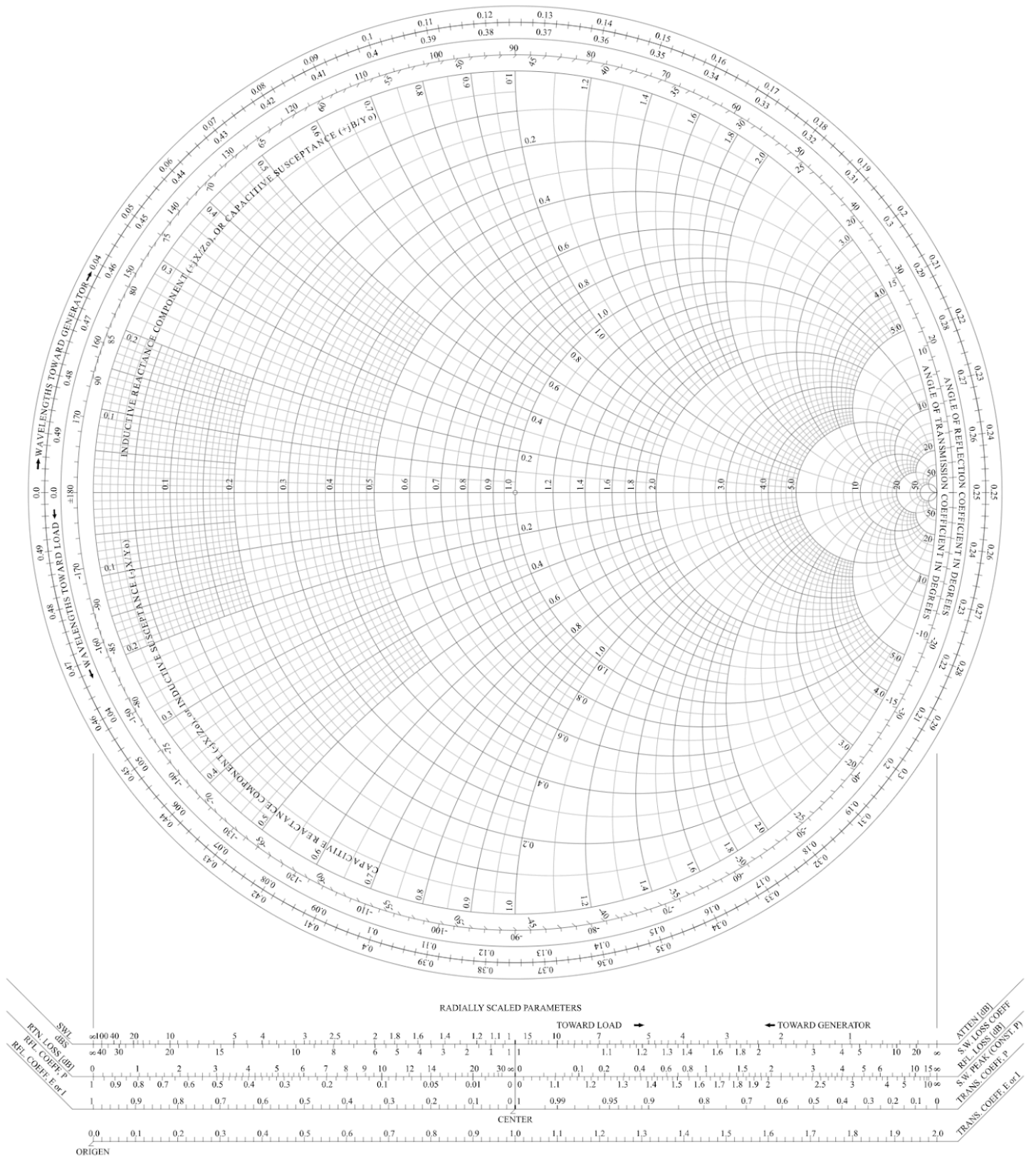


Antenna gain: $G = \frac{\text{maximum power density}}{\text{isotropic power density}}$ such that $I_{\text{max}} = \frac{GP}{4\pi r^2}$. For a $\frac{\lambda}{4}$ -dipole, $G = 1.64$.

The total power can be computed by integrating $\frac{|E_\theta|^2}{2Z_0}$ over all space.

Radiation resistance: $R_a = \frac{P}{I_{\text{rms}}^2}$. (P : total power emitted by antenna)

8.5.15. Smith Chart for Impedance Matching of Complex Reflection Coefficients



8.5.16. Magnetohydrodynamics (MHD)

Electrically conductive fluids (liquid metals, electrolytes, plasmas) respond to changing magnetic fields by developing an internal electric current (Faraday's law), which exert Lorentz forces on the fluid, which can produce fluid flow, unlike in solid conductors.

- Current density: $\mathbf{J} = \sum_i n_i q_i \mathbf{u}_i$ (n : number density, q : charge, \mathbf{u} : mean velocity, i : species)
- Fluid COM velocity: $\rho \mathbf{v} = \sum_i n_i m_i \mathbf{u}_i$ (ρ : fluid density, m : particle mass)
- Ampere's law: $\mu_0 \mathbf{J} = \nabla \times \mathbf{B}$ (\mathbf{B} : magnetic flux density)
- Faraday's law: $\partial \mathbf{B} / \partial t = -\nabla \times \mathbf{E}$ (\mathbf{E} : electric field strength)
- Ohm's law: $\mathbf{E} + \mathbf{v} \times \mathbf{B} = \rho_e \mathbf{J}$ ($\rho_e = 1 / \sigma$: electrical resistivity, σ : electrical conductivity)
- Cauchy momentum: $\rho D\mathbf{v} / Dt = \mathbf{J} \times \mathbf{B} - \nabla p$ ($D / Dt = d/dt + \mathbf{v} \cdot \nabla$: material derivative operator)
- Force per unit volume: $d\mathbf{F} = \mathbf{J} \times \mathbf{B} dV$ ($\mathbf{F} = \iiint_V \mathbf{J} \times \mathbf{B} dV$: body force on fluid control volume)
- **Induction equation:** $\partial \mathbf{B} / \partial t = \nabla \times (\mathbf{v} \times \mathbf{B}) + \eta \nabla^2 \mathbf{B}$ ($\eta = 1 / (\mu_0 \sigma)$: magnetic diffusivity)
In 'ideal MHD', it is assumed that $\eta \rightarrow 0$, while in 'resistive MHD', η is finite.

Dimensionless numbers in MHD:

- Magnetic Reynolds number: $Re_m = \frac{vL}{\eta}$ (v : velocity scale, L : length scale)

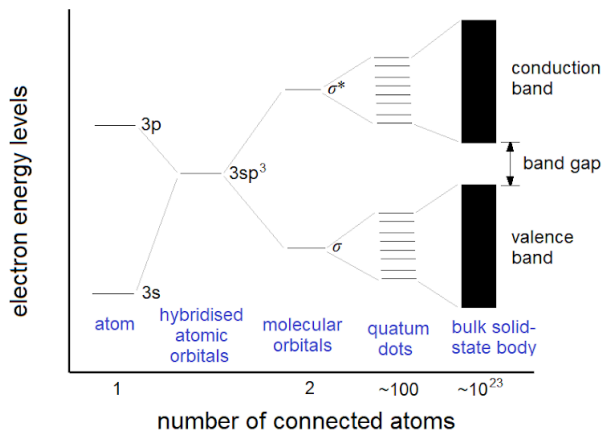
Alfvén's theorem: conducting fluid streamlines and magnetic flux lines are identical when $Re_m \rightarrow \infty$.

8.6. Functional Materials and Solid State Physics

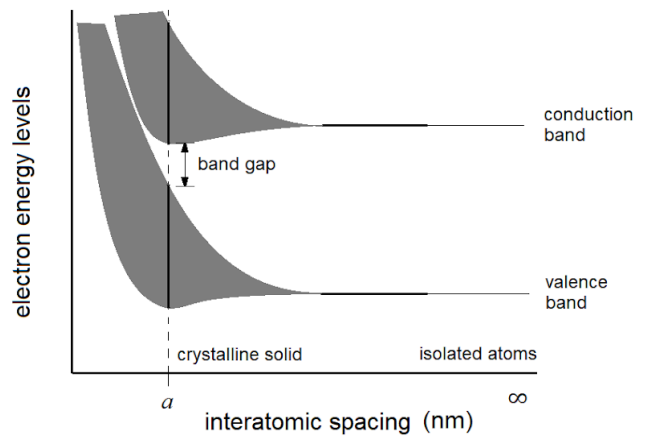
8.6.1. Band Theory of Network Solids

Overlap of atomic orbitals in close proximity causes energy level splitting. For a large network of atoms, the resulting orbitals (bonding is valence; $E \leq \text{HOMO}$ and antibonding is conduction; $E \geq \text{LUMO}$) approximate continuous bands of energies. The HOMO-LUMO gap (band gap) is zero in metals (due to overlap), small in semiconductors ($< 2\text{eV}$) and large in insulators ($> 2\text{eV}$). Thermal excitation can promote valence electrons to the conduction band.

Tight Binding Model: analogous the LCAO model from MO theory (Section 13.1.10)

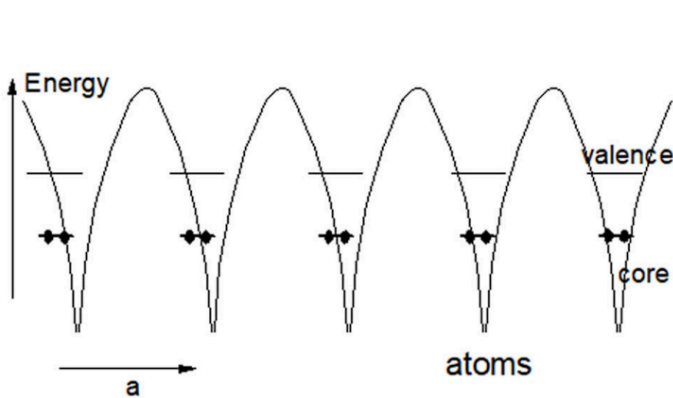


Number of splits increases with atom count
Hybridisation of AOs for covalent bond formation

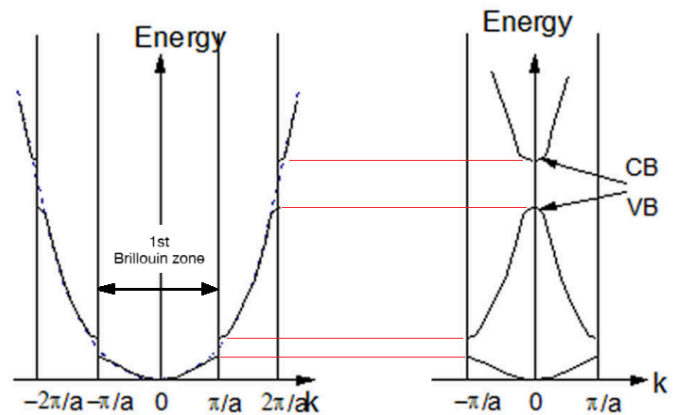


Magnitude of splitting energy increases with proximity to other atoms

Nearly-Free Electron Model: periodic lattice perturbations to free electron wavefunction



Lattice potential function, $V(x)$
Superposition of Coulomb potentials at lattice points



Repeated zone scheme
Band-stopped free electron

Folded zone scheme
Reflected: band gaps

8.6.2. Quantum Physics of Crystalline Semiconductors

- **Wavevector** \mathbf{k} is the quantum of momentum \mathbf{p} : $\mathbf{p} = \hbar\mathbf{k}$ ($\hbar = \frac{h}{2\pi} = 1.055 \times 10^{-34}$ J s)
A 3D Fourier transform maps position \mathbf{x} into spatial frequency \mathbf{k} (spatial frequency); if the domain of \mathbf{x} is a unit cell then the domain of \mathbf{k} is the union of all n th-order Brillouin zones (Section 13.2.7). The components of \mathbf{k} represent the frequency of the wavefunction for a state in each lattice direction, and the vector \mathbf{k} indicates the direction of its stationary oscillation in real space.
- **De Broglie wavelength** λ : $|\mathbf{k}| = k = \frac{2\pi}{\lambda}$
- **Kinetic energy**, by free electron model (Section 11.1.11): $E = \frac{p^2}{2m} = \frac{\hbar^2 k^2}{2m}$
- Lattice symmetry (size a) imposes **constraints on wavelength**:
 $\lambda_n = 2a/n \rightarrow k_n = \frac{2\pi}{\lambda_n} = \frac{2\pi}{a}n \rightarrow E_n = \frac{2\pi^2 \hbar^2 n^2}{ma^2}$ (particle in a box model)
- **Bloch's theorem of periodicity**, $u(\mathbf{r})$ is a unit cell wavefunction: $\psi(\mathbf{r}) = \exp(i \mathbf{k} \cdot \mathbf{r}) u(\mathbf{r})$
- **Effective mass** (electrons: $m^* > 0$, holes: $m^* < 0$): $m^* = \hbar^2 (d^2E / dk^2)^{-1}$
 m^* is typically quoted in multiples of the free electron mass, $m_e = 9.1 \times 10^{-31}$ kg.
- **Hydrogenic model of dopant levels**: $E_n = -\frac{R'_0}{n^2}$, $R'_0 = \frac{Z^2 m^*}{\epsilon_r^2} R_0$, $R_0 = 13.6$ eV.
(R'_0 : modified Rydberg constant (dopant binding energy).
 Z : dopant valency relative to host, m^* [m_e]: dopant effective mass, ϵ_r : host relative permittivity.)
- **Deep impurities / trap levels**: dopant binding energy R'_0 is large for **wide band gap** semiconductors, due to heavier carriers (high m^*) and poorer screening (low ϵ_r).
- **Linear dispersion**: $m^* = 0$ (zero second derivative). Charge carriers behave like bosons or zero rest mass fermions i.e. light, giving very **high mobility**.
- **Quadratic dispersion**: $m^* \neq 0$ (parabolic band edge).
- **Light carriers**: $|m^*|$ is small, band dispersion is **narrow** and mobility is higher.
- **Heavy carriers**: $|m^*|$ is large, band dispersion is **wide** and mobility is lower.
- **Doubly degenerate levels**: multiple bands coinciding at the same band edge.
- **Fermi level** E_f : HOMO energy at $T = 0$ K (minimum entropy, no lattice vibrations). At other temperatures, E_f is the energy at which the Fermi-Dirac distribution of electron energies,

$$f(E) = \frac{1}{1 + \exp\left(\frac{E - E_f}{kT}\right)} = \frac{1}{2}$$

8.6.3. Transport Properties of Crystalline Semiconductors

- **Ohm's law:** $\mathbf{J} = \sigma \mathbf{E}$ (\mathbf{J} [A m^{-2}]: current density, σ [S m^{-1}]: conductivity, \mathbf{E} [V m^{-1}]: electric field)
- **Fermi energy:** $E_F = \frac{3\hbar^2}{8m} \left(\frac{N}{V}\right)$, **Wavenumber:** $k_F = \left(\frac{2m^*E_F}{\hbar^2}\right)^{1/2}$ (m^* : effective carrier mass)
- **Density of states for nearly free electrons:** $g(E) = \frac{\sqrt{2(m^*)^3 E}}{\pi^2 \hbar^3}$ (E : relative to bottom band)
- **Conduction band density:** if $E_c - E_f > 3kT$ then $n = N_c \exp\left(-\frac{E_c - E_f}{kT}\right)$ where $N_c = \frac{2(2\pi m^* kT)^{3/2}}{h^3}$. (E_c : energy of conduction band min, N_c [m^{-3}]: effective density of states)
- **Mobility kinetics:** $\mu = \frac{v}{E} = \frac{e\tau}{m^*}$ (τ : mean time between collisions)
- Continuity equation for excess minority electrons: $\frac{\partial n}{\partial t} = -\frac{n}{\tau} + D \nabla^2 n + \mu \nabla \cdot (n\mathbf{E})$
- **Diffusion and mobility:** $D = \frac{kT}{e} \mu$ (Einstein's relation. μ : mobility, D : diffusion coefficient)
- **Thermal voltage:** $\frac{kT}{e} = \frac{D}{\mu}$. (thermal energy: kT)
- **Conductivity:** $\sigma = \sum_{\text{carriers}} n\mu|q| = e(n\mu_e + p\mu_h)$

Data for Some Crystalline Semiconductors:

Semiconductor	Crystal Struct.	Lattice Const. at 300 K (Å)	Bandgap (eV)		Band	Mobility at 300 K (cm ² /V-s)		Effective Mass		ϵ_s/ϵ_0
			300 K	0 K		μ_n	μ_p	m_n^*/m_0	m_p^*/m_0	
C Carbon (diamond)	D	3.56683	5.47	5.48	I	1,800	1,200	0.2	0.25	5.7
Ge Germanium	D	5.64613	0.66	0.74	I	3,900	1,900	1.64 ^l ,0.082 ^t	0.04 ^{lh} ,0.28 ^{hh}	16.0
Si Silicon	D	5.43102	1.12	1.17	I	1,450	500	0.98 ^l ,0.19 ^t	0.16 ^{lh} ,0.49 ^{hh}	11.9
IV-IV SiC Silicon carbide	W	$a=3.086,c=15.117$	2.996	3.03	I	400	50	0.60	1.00	9.66
III-V AlAs Aluminum arsenide	Z	5.6605	2.36	2.23	I	180		0.11	0.22	10.1
AlP Aluminum phosphide	Z	5.4635	2.42	2.51	I	60	450	0.212	0.145	9.8
AlSb Aluminum antimonide	Z	6.1355	1.58	1.68	I	200	420	0.12	0.98	14.4
BN Boron nitride	Z	3.6157	6.4		I	200	500	0.26	0.36	7.1
" "	W	$a=2.55,c=4.17$	5.8		D			0.24	0.88	6.85
BP Boron phosphide	Z	4.5383	2.0		I	40	500	0.67	0.042	11
GaAs Gallium arsenide	Z	5.6533	1.42	1.52	D	8,000	400	0.063	0.076 ^{lh} ,0.5 ^{hh}	12.9
GaN Gallium nitride	W	$a=3.189,c=5.182$	3.44	3.50	D	400	10	0.27	0.8	10.4
GaP Gallium phosphide	Z	5.4512	2.26	2.34	I	110	75	0.82	0.60	11.1
GaSb Gallium antimonide	Z	6.0959	0.72	0.81	D	5,000	850	0.042	0.40	15.7
InAs Indium arsenide	Z	6.0584	0.36	0.42	D	33,000	460	0.023	0.40	15.1
InP Indium phosphide	Z	5.8686	1.35	1.42	D	4,600	150	0.077	0.64	12.6
InSb Indium antimonide	Z	6.4794	0.17	0.23	D	80,000	1,250	0.0145	0.40	16.8
II-VI CdS Cadmium sulfide	Z	5.825	2.5		D			0.14	0.51	5.4
" "	W	$a=4.136,c=6.714$	2.49		D	350	40	0.20	0.7	9.1
CdSe Cadmium selenide	Z	6.050	1.70	1.85	D	800		0.13	0.45	10.0
CdTe Cadmium telluride	Z	6.482	1.56		D	1,050	100			10.2
ZnO Zinc oxide	R	4.580	3.35	3.42	D	200	180	0.27		9.0
ZnS Zinc sulfide	Z	5.410	3.66	3.84	D	600		0.39	0.23	8.4
" "	W	$a=3.822,c=6.26$	3.78		D	280	800	0.287	0.49	9.6
IV-VI PbS Lead sulfide	R	5.9362	0.41	0.286	I	600	700	0.25	0.25	17.0
PbTe Lead telluride	R	6.4620	0.31	0.19	I	6,000	4,000	0.17	0.20	30.0

D = diamond, W = wurtzite, Z = zinblende, R = rock salt (simple cubic). I/D = indirect/direct band gap.

l / t / lh / hh = longitudinal, transverse, light-hole, heavy-hole effective mass.

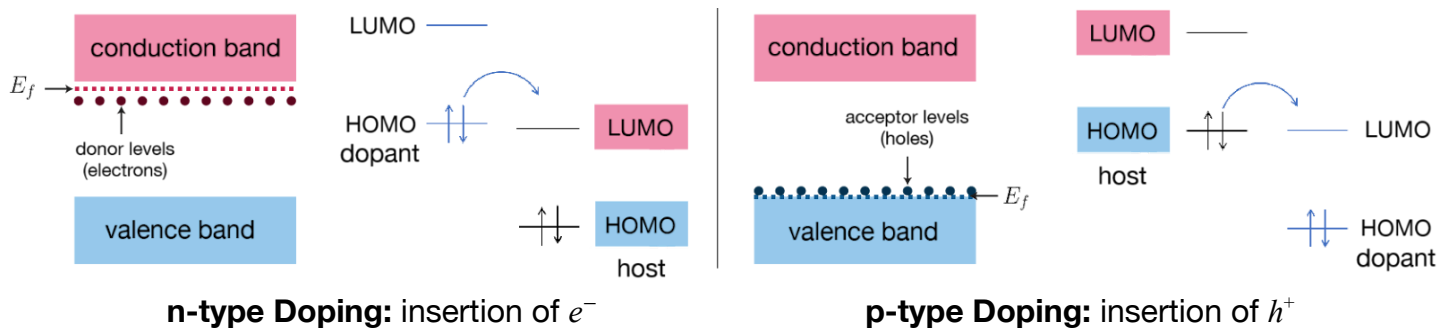
8.6.4. Optical and Transport Properties from Band Structure

For a **direct** band gap transition (carrier \mathbf{k} constant), energy E is conserved via photon exchange: (e^- : electron, h^+ : hole, γ : photon. Alternative notation - e^- : electron, h^+ : hole)

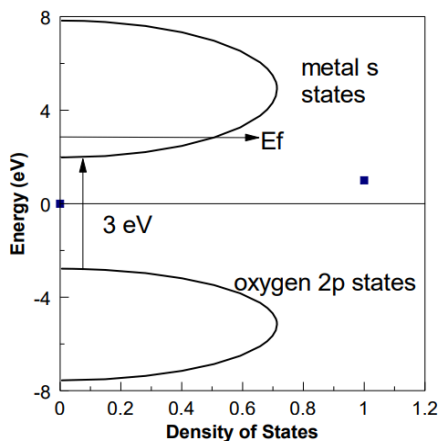
- **Photon Absorption:** e^- (low E) + $\gamma \rightarrow e^-$ (high E) or equivalently $\gamma \rightarrow e^- + h^+$
- **Radiative Recombination:** e^- (high E) $\rightarrow e^-$ (low E) + γ or equivalently $e^- + h^+ \rightarrow \gamma$

For an **indirect** band gap transition, momentum $\mathbf{p} = \hbar\mathbf{k}$ is conserved via phonon exchange from thermal lattice vibrations, which significantly lowers the rate (efficiency) of the photon exchange.

Extrinsic semiconductors can be formed by substitutional doping with impurities:



Transparent Extrinsic Semiconductors: needs band gap >3 eV and **shallow dopant levels**



More ionic lattices and smaller lattice constants have larger band gaps (s-block oxides, or III-V semiconductors) since molecular orbital splitting is decreased (less covalent).

Left: density of states (DoS) for n-doped metal oxide e.g. In_2O_3 with In^{3+} substituted by Sn^{4+} . E_f rises to the conduction band. The band gap remains >3 eV, so the resulting semiconductor (indium tin oxide, ITO) is transparent. Other transparent oxides include SnO_2 , ZnO .

Indirect band gap semiconductors e.g. GaP , can be n-doped to insert localised (small Δx) donor levels below the conduction min. Due to Heisenberg's uncertainty principle, Δk is large so the band gap becomes '**quasi-direct**', in which light emission does not require a phonon (**more efficient light emission**).

Intrinsic Defects: imperfections in crystalline lattices can degrade transparency

- **Lattice vacancies** forms a **dangling bond** (DB, unpaired / free radical), which falls in the middle of the band gap since there is no MO splitting. This also occurs at surfaces.
- DBs are recombination centres, trapping electrons and holes formed by light excitation (Schottky-Read-Hall model). **Passivation** with gas (e.g. O_2 or H_2) forms oxide or hydride bonds which remove the trap levels.

The radiative recombination of electrons and holes in current-carrying semiconductors is generally known as **electroluminescence**. Electroluminescent materials include $\text{ZnS}_2\text{:Cu/Ag/Mn}$, natural diamond with trace boron, InP, GaAs, GaN (used in LEDs), $[\text{Ru}(\text{bpy})_3]^{2+}(\text{PF}_6^-)_2$, $[\text{Ir}(\text{ppy})_3]$ and Tb_2O_3 .

Other mechanisms of light emission include:

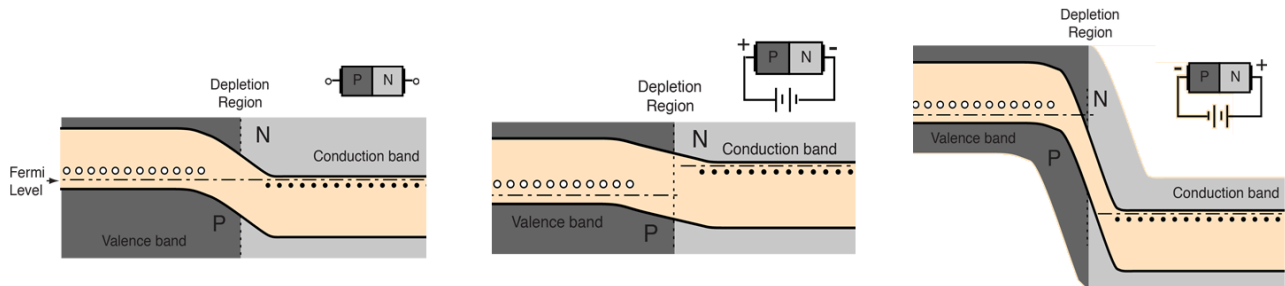
- **Incandescence:** all solids and liquids emit thermal radiation due to their temperature, with good emitters following the black-body spectrum. At around 798 K (the Draper point), hot objects begin to glow a dull red, moving towards brighter red, orange-yellow, white and blue at the hottest temperatures.
- **Photoluminescence:** excitation by UV photons and relaxation of electrons in atoms.
 - **Fluorescence:** fast relaxation from a singlet state.
 - **Phosphorescence:** slow relaxation from a triplet state after intersystem crossing.
- **Chemiluminescence:** a chemical reaction forms an excited species which then undergoes relaxation. In biological systems, this is known as **bioluminescence**, occurring in e.g. fireflies, anglerfish and the sea pansy (soft coral). In an electrochemical reaction, this is known as **electrochemiluminescence** (ECL), used in an ECL assay: e.g. an antibody linked with the complex $[\text{Ru}(\text{bpy})_3]^{2+}$, which undergoes a reaction with an oxidised radical species $(\text{CH}_3\text{CH}_2\text{CH}_2)_3\text{N}^{+\bullet}$ to form an excited complex which releases light.
- **Mechanoluminescence:** nanosecond-order radiation emission due to mechanical stress
 - **Sonoluminescence:** microbubbles in liquids rapidly collapse in high-intensity ultrasound, releasing light. The mechanism of light emission is not well understood.
 - **Triboluminescence:** triboelectric charging at sliding interfaces generates strong local electric fields that cause breakdowns at the microscopic level, releasing radiation. This can also occur during fast fracture (fractoluminescence).
 - **Crystalloluminescence:** emission of light on rapid crystallisation of some salts.
- **Radioluminescence:** light emission on absorption of ionising radiation (alpha/beta/gamma rays), usually using a phosphor material (scintillation). This also includes Cherenkov radiation (braking radiation of relativistic electrons in a dielectric).

8.6.5. Heterojunctions (p-n Junctions)

A p-n junction is formed between the interfaces of oppositely-doped semiconductors.

The Fermi level (electrochemical potential: indicates direction of electron flow) jumps at the interface of two oppositely doped semiconductors because the carrier levels are different. For a good heterojunction, dopants should insert localised energy levels inside or just below/above the host conduction/valence band.

Diode operation: applied electric field (p.d.) reroutes n-type electrons around an external circuit.



Equilibrium: depleting

Fermi level constant across junction

Forward Bias: conducting

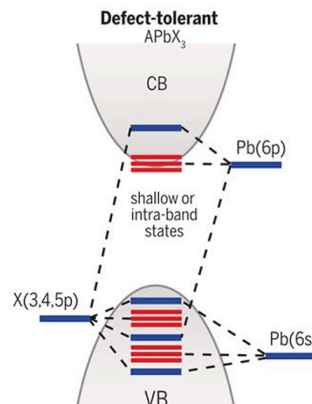
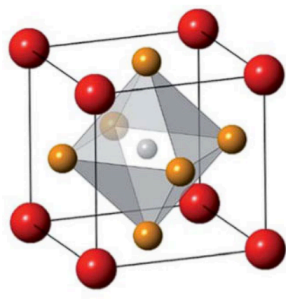
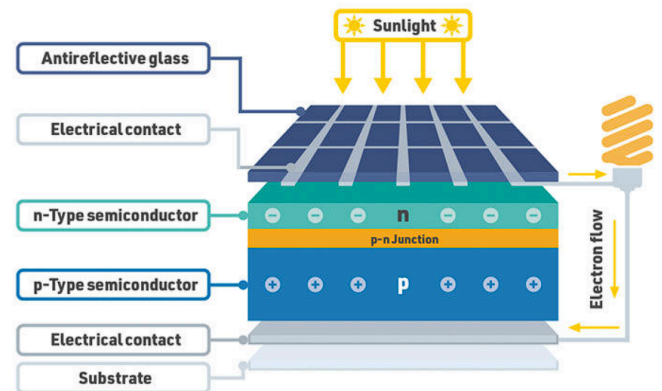
Reverse Bias: insulating

Electrons cannot flow

Carrier energy from p-n recombination is released as photons which heat the material unless the system is designed to allow emission (e.g. as a light-emitting diode (LED)).

Photovoltaic operation: excitation of n-type electrons and rerouting around an external circuit

- Silicon solar cell: uses a Si-based pn-junction
- **Perovskite solar cell:** uses an organic halide perovskite ABX_3 e.g. $CH_3NH_3PbI_3$ ($MAPbI_3$) crystal structure between an electron (ETL) and hole (HTL) transport layer (e.g. organic semiconductors, Section 8.6.8). Transparent electrodes are used (e.g. ITO).



The PbX_6 octahedra primarily sets the band gap (valence band: I (5p), conduction band: Pb (6p).)

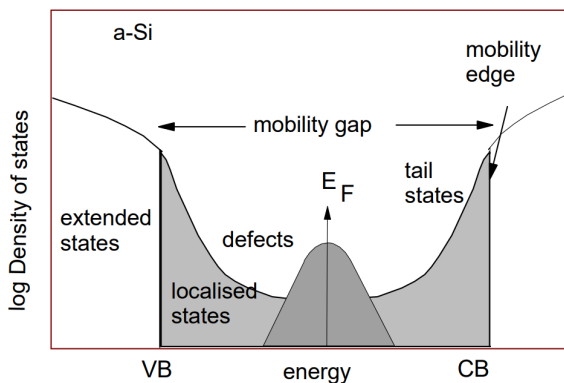
Differently sized A-sites (e.g. MA, FA) allow for tuning of lattice constant and band gap.

Perovskites are defect tolerant as the defect energy levels are shallow.

8.6.6. Amorphous Semiconductors

In non-crystalline semiconductors, the concept of k and direct/indirect band gaps are invalid as there is no symmetry element/unit cell. The band structure remains.

Amorphous silicon (a-Si): has no long-range order, but all atoms remain sp^3 hybridised (approximately tetrahedral) and bonded to 4 other atoms. There are a large number of dangling bonds, which produce a **continuous band structure**:

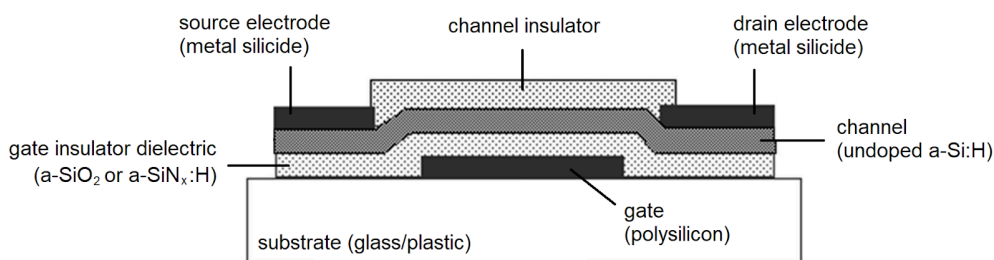


Defects produce a band in the middle. Bond distortion 'smears' the bands into **localised states**. Neither of these states conduct, so the material is still a semiconductor. The **mobility gap is larger** than the crystalline band gap. The efficiency of doping is decreased, as the dopants bond with defects rather than substitution, but is still practical for large area applications (e.g. thin film transistors (TFTs), solar cells).

a-Si:H is made by plasma deposition with SiH_4 . It is much cheaper, easier to make at large areas and lower temperatures, than c-Si.

Thin-Film Transistors: improved FETs which can use a-Si:H as the channel

The 'bottom gate, inverted staggered' architecture of an a-Si:H TFT is:



Polysilicon (polycrystalline silicon) has properties intermediate between a-Si and c-Si. The TFT is in enhancement mode, with the **E-field** pulling electrons into the channel to be conducted.

Other Amorphous Semiconductors: a-Si:H has low mobility and is unstable under constant E-field (gate threshold voltage drift). Oxides such as $InZnGaO_4$ (IGZO) have higher mobilities and are more stable.

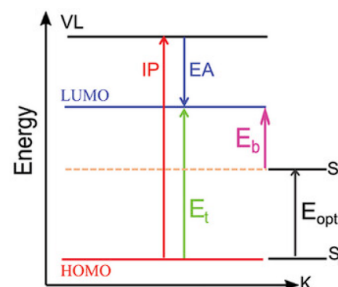
Glass: amorphous SiO_2 , very wide (**insulating**, ~ 9 eV) band gap. Doping with various substances (e.g. Na for soda glass) can insert trap levels throughout, giving specific colours of glass.

8.6.7. Organic Semiconductors

Organic materials such as polymers and small molecules open up new manufacturing pathways (spin-coating, inkjetting) which can be done at lower temperatures than a-Si:H. They typically have **low screening** (low ϵ_r).

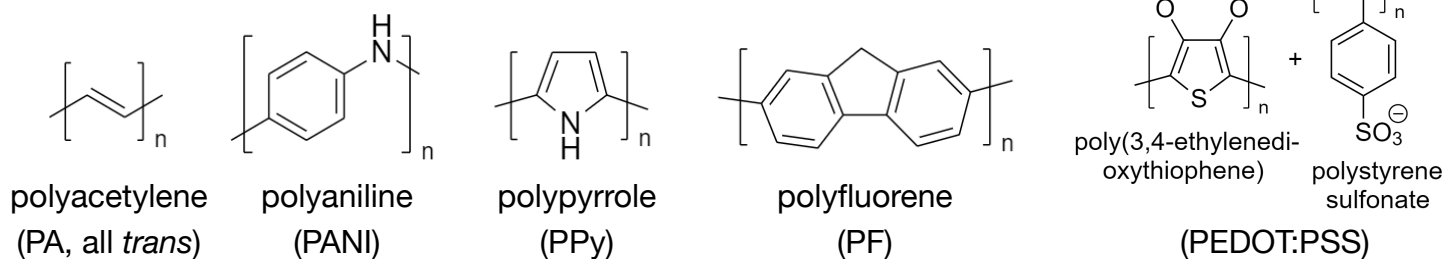
- **Band gap decreases as $1/N$** (N : chain length) due to splitting of π - π^* orbitals in conjugated polymer (electron in a box quantum model). Subject to Peierls instability. There is then a valence (π) band and a conduction (π^*) band.
- **Exciton:** short-range electron-hole pair quasiparticles, formed in light. Excitons dominate charge transfer phenomena in organic semiconductors, as their binding energy E_b (can be estimated with dopant hydrogenic model, Section 8.6.2) is large.

Exciton binding energy = HOMO-LUMO gap – Optical gap (singlet)



- **Exciton decay** is the mechanism of the photovoltaic effect (light \rightarrow exciton) and light emission (exciton \rightarrow light) in organic semiconductors (Section 8.6.8).
- **Doping:** oxidation (with I_2 , Br_2 , AsF_5) or reduction (with Na, Li) to give radical polycations (hole carriers) or polyanions (electron carriers), both known as **polarons** (another quasiparticle). Doping further increases the conductivity of these polymers.

Examples of conjugated semiconductive polymers:



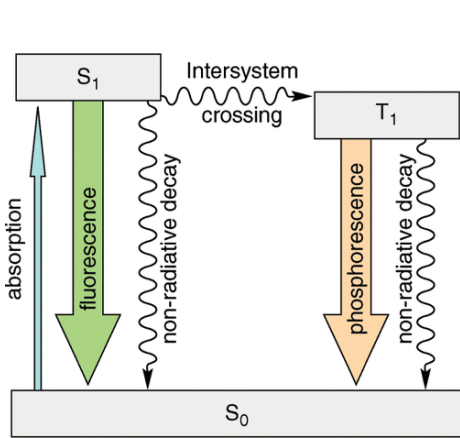
Small-Molecule Organic Semiconductors: fully conjugated monomer molecules with small HOMO-LUMO gaps e.g. anthracene, coronene, copper phthalocyanine (CuPc), tris(2-phenylpyridine)iridium(III) [$Ir(ppy)_3$] (a phosphorescent complex), buckminsterfullerene (C_{60} , ‘buckyballs’).

The optoelectronic properties of such small-molecule organic semiconductors are dependent on the crystallinity, crystal orientation, and size. Again, the exciton state dominates their optoelectronic behaviour. The complex charge transport mechanisms taking place in such weakly van-der-Waals bonded molecular crystals remains a subject of research and has implications for e.g. studying photosynthesis by chlorophyll molecules (conjugated porphyrin ring).

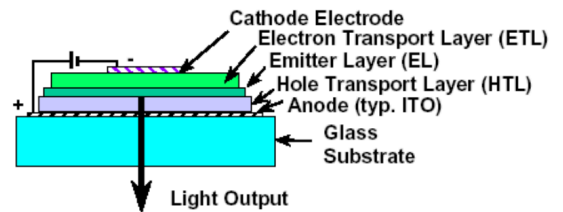
8.6.8. Organic Electronics

The excitons generated in organic semiconductors can dissociate at a heterojunction (photovoltaic effect: light → current). Excitons can also decay by recombination to produce light (current → light).

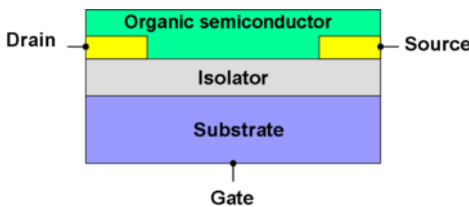
Organic Light-Emitting Diodes (OLEDs): exciton recombination at the heterojunction.



Conducting polymers comprise the emitter layer. Spin-orbit coupling in polymer compounds combines conduction band singlet (S_1) and triplet (T_1) states even more than in pure hydrocarbons, allowing phosphorescence ($T_1 \rightarrow S_0 + h\nu$) to become a permitted transfer by intersystem crossing in addition to fluorescence ($S_1 \rightarrow S_0 + h\nu$). Non-radiative decay emits a phonon without emitting a photon.

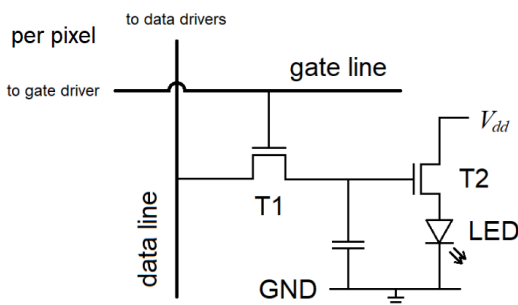


Organic Field-Effect Transistors (OTFTs / OFETs): organic semiconductor channel.



Polymers for p-type OFETs have HOMO energy between 5.0-5.5 eV and LUMO > 3.5 eV. Polymers for n-type OFETs may be fluorinated to reduce HOMO and LUMO. OFETs adopt the TFT (thin-film transistor, Section 8.6.6) architecture (as opposed to e.g. MOSFET, MeSFET).

OLED Displays: uses (O)TFTs to power OLEDs for each pixel (active matrix display architecture)



When TFTs are used in OLED displays (two (O)TFTs and one OLED per pixel), mobility translates to frame rate, so there are demands for higher performance.

T1 acts as a switch and is in linear bias.

T2 drives the current through the light modulator (LED) and is in saturation mode (current source depending only on gate voltage).

White light emission can be achieved by either 1) RGB tuned OLEDs, 2) down-conversion from blue LEDs using phosphorescent materials (excitons recombine from multiple triplet states) or 3) colour filters with white organic EML (protects against differential degradation).

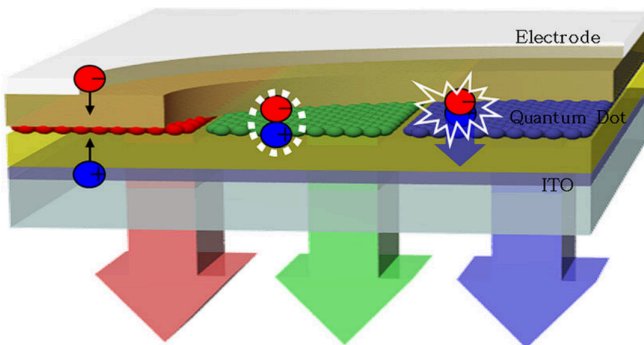
8.6.9. Quantum Dots (0D Nanomaterials)

Quantum dots (QDs) are semiconducting nanoparticles. Quantum dot optoelectronic properties are easily tunable by their size D .

Common photoluminescent QDs include CdSe, ZnS, CdTe.

- **Exciton ($e-h$) Bohr radius:** $a_{Bx} = \frac{4\pi\epsilon\hbar^2}{m_0 e^2} \left(\frac{1}{m_e^*} + \frac{1}{m_h^*} \right) \sim D$
- **Idealised energy levels (3D cubic well):** $E_n = \frac{3\hbar^2 \pi^2 n^2}{2m_e^* D^2}$ (D : quantum dot diameter)
- **Quantum dot band gap:** $\Delta E_{QD} = \Delta E_{bulk} + \Delta E_{well}(e^-) + \Delta E_{well}(h^+) + \Delta E_{Coulomb}$
 where $\Delta E_{Coulomb} \approx \frac{-3.6 \times e^2}{4\pi\epsilon_0 \epsilon_r D}$ and confinement energy $\Delta E_{well}(e^-) + \Delta E_{well}(h^+)$ scales with D^{-2} .
- **QD Emission Energy:** $\Delta E_{QD} \approx \Delta E_{bulk} + \frac{2\hbar^2 \pi^2}{D^2} \left(\frac{1}{m_e^*} + \frac{1}{m_h^*} \right)$ (Brus equation)

AMQLED Displays (Active Matrix QDs Light Emitting Diode)



An electroluminescent QD nanoparticle film is used as the emitter layer (EML). QDs are superior to organic luminescent materials due to their inherent luminescent properties, including narrow spectral emission bandwidths, high photoluminescence quantum efficiency, good photostability and controllable bandgap.

QDs naturally produce monochromatic light, so they are more efficient than white light sources when colour filtered and allow more saturated colours.

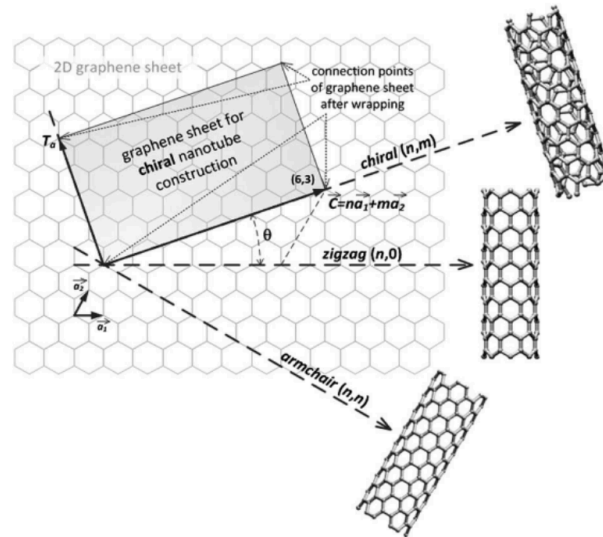
QDs often exhibit localised surface plasmon resonance, altering their reflectivity.

8.6.10. Nanotubes and Nanoribbons (1D Nanomaterials)

Nanotubes are 1D nanostructures, geometrically equivalent to a rolled-up cylindrical monolayer of conducting or semiconducting thin-film material.

Carbon Nanotubes (CNTs): cylindrical sp^2 carbons.

The orientation of a nanotube has two degrees of freedom (size and pitch). These are enumerated with a chiral vector (n, m) , for positive integers $m \leq n$ as defined in terms of a unit cell of graphene as shown.



Chiral vector: $\mathbf{c} = n\mathbf{a}_1 + m\mathbf{a}_2$ ($\mathbf{a}_1 = \frac{a}{2}(\sqrt{3}\mathbf{i} + \mathbf{j})$ and $\mathbf{a}_2 = \frac{a}{2}(\sqrt{3}\mathbf{i} - \mathbf{j})$, $a = 0.2461$ nm)

Tube diameter: $d = c/\pi = \frac{a\sqrt{n^2 + m^2 + mn}}{\pi}$ ($c = |\mathbf{c}|$: circumference of nanotube)

Chiral angle: $\tan \theta = \frac{\sqrt{3}m}{2n + m}$ ($0 \leq \theta \leq 30^\circ$)

Translational vector: $\mathbf{T}_a = \frac{2m+n}{d_R}\mathbf{a}_1 - \frac{2n+m}{d_R}\mathbf{a}_2$ ($d_R = \text{gcf}\{2m+n, 2n+m\}$, greatest common factor)

Length of unit cell: $|\mathbf{T}_a| = \frac{\sqrt{3}c}{d_R}$ (surface area of unit cell: $A = |\mathbf{c}||\mathbf{T}_a| = \frac{\sqrt{3}a^2(n^2 + m^2 + mn)}{d_R}$)

Number of atoms per unit cell: $N = \frac{4(n^2 + m^2 + mn)}{d_R}$ (number of hexagons per unit cell is $\frac{N}{2}$)

Types of nanotube based on geometry:

- **Metallic CNTs:** when $n = m$ (armchair). The 0 eV band gap is at the K point.
- **Semi-metallic CNTs:** when $n - m \equiv 0 \pmod{3}$. Band gap is on the order of $k_B T$ (< 0.1 eV).
- **Semiconductor CNTs:** when $n - m \not\equiv 0 \pmod{3}$. Larger band gap, inversely proportional to the nanotube diameter: E [eV] $\approx 0.85/d$ [nm]. (1, 0) and (2, 0) are insulators.

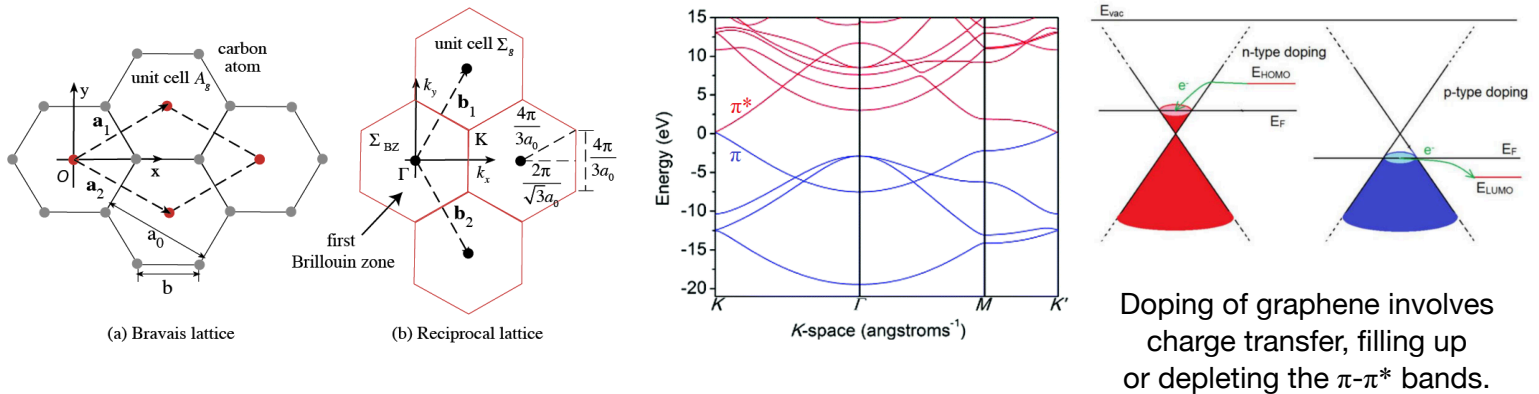
When grown, carbon nanotubes can naturally form multi-walled structures, consisting of concentric CNTs. These are typically metallic due to statistical probability of at least one layer being metallic. Other materials can also form nanotubes such as h-BN and MoS_2 . Heterostructures (analogous to multi-layer materials) can also be made from these materials.

Graphene Nanoribbons: narrow graphene; open nanotube. Semiconductive with **finite band gap**.

8.6.11. Thin-Film Materials (2D Nanomaterials)

Graphene: a 2D monolayer. Comprises the layers of graphite (stable carbon allotrope)

Graphene is a single layer hexagonal lattice of carbon, and is a fully conjugated system. It is a **zero band gap** semiconductor (0 eV, semi-metal) with **linear dispersion** around the K point giving **very high mobility**.



Graphene can be stacked into bilayers. The most stable conformation is the Bernal arrangement (AB: half of the sites are above/below hexagon centres). The layers can also be positioned at a small angle of deviation, forming a Moiré superlattice. These structures have **tunable bandgaps** (twistronics).

Hexagonal Boron Nitride (h-BN): isomorphous to graphene with alternating B and N

Due to the partial ionic character (III-V), h-BN has a **large band gap** (~6 eV, insulator). Due to its exceptional environmental, thermal, and chemical stability, atom thin h-BN is emerging as dielectric, support and barrier layer for nanoelectronics, and also as host material for quantum emitters. 3D amorphous oxides that work well in silicon technology have ill-defined interfaces with 2D materials and numerous defects. Currently, crystalline dielectrics like h-BN layers show most promise for 2D nanoelectronics despite having only moderate dielectric constants ($\epsilon \approx 3$). Specialised integrated processes are required for manufacture of these integrated heterogeneous monolayers.

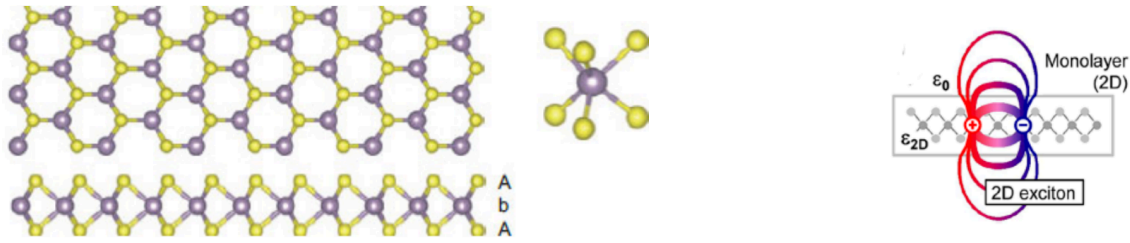
Amorphous Monolayers: can be used to test for tolerance of defects in monolayers

Monolayer sp^2 -bonded amorphous carbon films have been demonstrated, highlighting the possibility of stable amorphous material in the 2D monolayer limit. The amorphous structure consists of small crystallites embedded in a continuous random network, analogous to spherulites in semi-crystalline polymers (Section 16.5.3). Similar to 3D materials, **localised states** emerge. 2D silica glass has also been demonstrated. Amorphous BN does not form a planar layer, instead forming a 3D thin structure.

Phosphorene (Black Phosphorus): hexagonal structure like graphene, but not in-plane

Forms a puckered structure (fused chair conformations) and is a **direct bandgap** semiconductor (2.3 eV). Band gap decreases with more layers with **high mobility**.

Transition Metal Dichalcogenides (TMDs, MS₂):



MS₂ forms three-atom-thick layers with D_{3h} symmetry (trigonal prismatic).

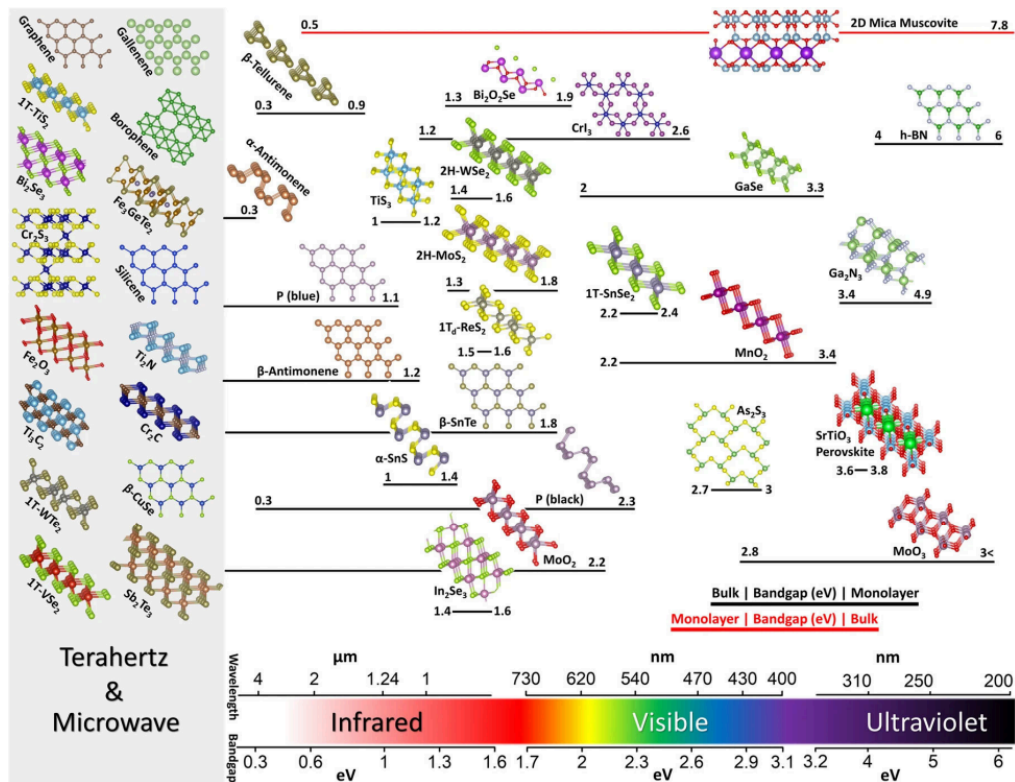
Weak dielectric screening enhances the $e-h$ Coulomb interaction, making excitons more strongly bound.

Monolayer MS₂ is a **direct bandgap** semiconductor (MoS₂: 1.9 eV) at the K point, while multiple layers gives an indirect and smaller bandgap from valence $\Gamma \rightarrow$ conduction near K . The strongly-bound Frenkel excitons dominate optical and charge-transport properties. Others include WS₂, WSe₂, MoTe₂.

MXenes: transition metal carbide, nitrides and borides of the form $M_{n+1}X_n$, with terminal groups.

MXenes are multi-layer (ML) or few-layer (FL) 2D materials. Monolayers are conductors while FL-MXenes are small band gap semiconductors. Intercalation is possible in between the layers, and have been used to replace graphite as electrodes in Li-ion batteries.

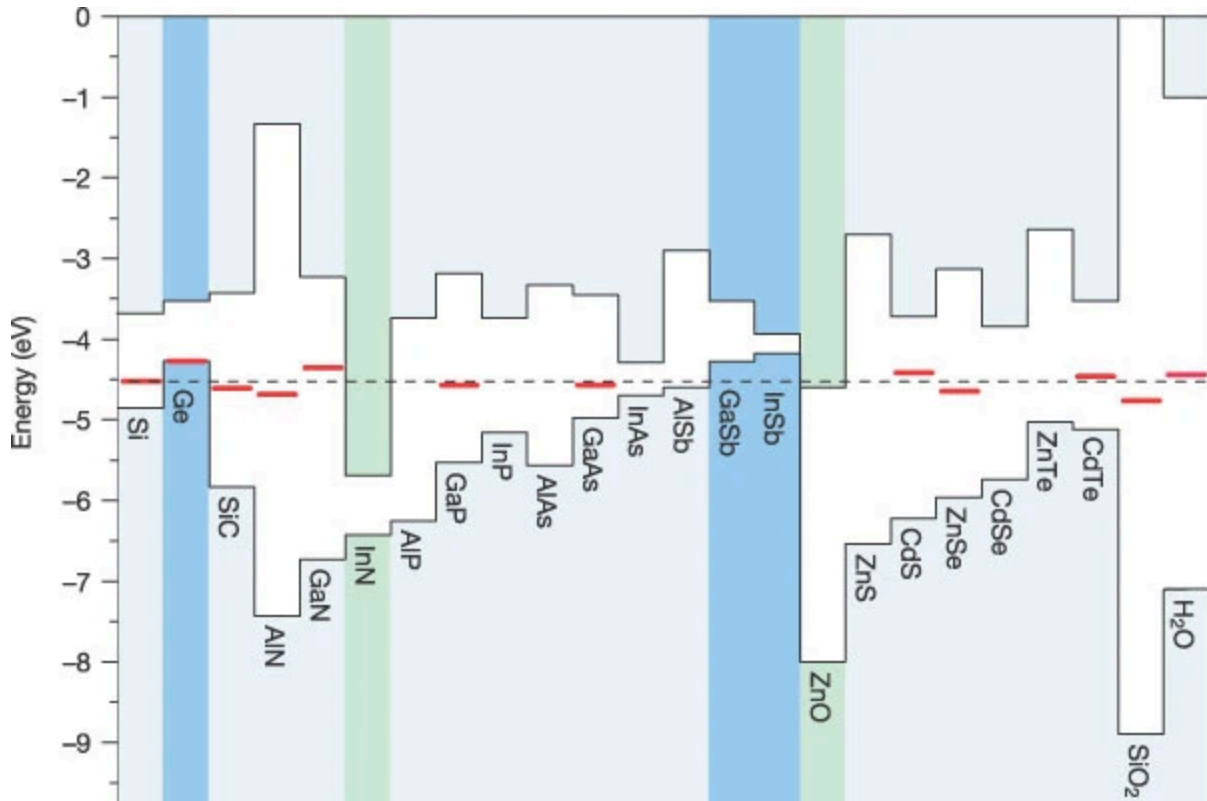
Band gaps of other layered materials:



8.6.12. Band Structure Engineering

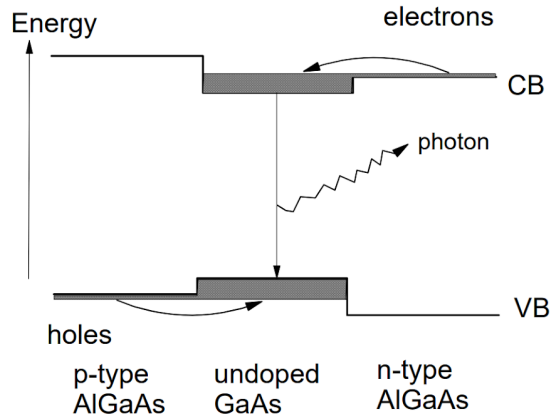
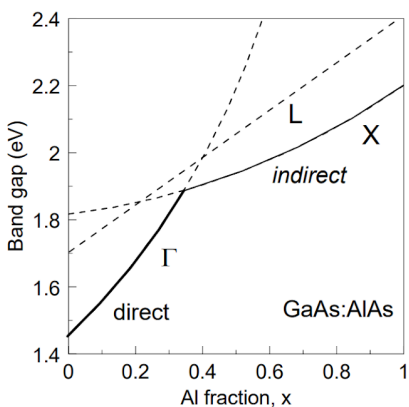
Interfaces between semiconductors allow for tuning of band gaps. This can be very useful to guide electrons or holes into the desired layers, either for recombination, or to separate them.

- **Electrons sink down** the conduction band surface (like water in a landscape).
- **Holes rise up** the valence band surface (like bubbles in water).



Band edge landscape for various semiconductors

red: hydrogen levels, green: H acts only as donor, blue: H acts only as acceptor



Transfer doping is used to exploit this flow of electrons and holes, e.g. in the GaAs diode laser.

8.6.12. Very Large Scale Integration (VLSI) Semiconductor Technologies

Oxides such as SiO_2 and Al_2O_3 are **defect tolerant**, remaining insulating (~ 9 eV band gap) even when doped or impure. Conduction occurs only at high electric fields. Impurities in metal oxides create trap levels where carriers can more easily enter the conduction band.

Non-breakdown (reversible) conduction mechanisms in defect-dense metal oxides:

- **Poole-Frenkel conduction:** thermal excitation over the potential barrier at a defect.
- **Quantum tunnelling:** probabilistic bypassing through the potential barrier.
- **Hot carrier injection:** acceleration of carrier by applied electric field over the barrier.

Non-volatile flash memory (programmable ROM, a type of EEPROM) consists of FETs with an additional floating gate and tunneling oxide in between the channel and gate oxide (to which the control gate is attached). In a high field, electrons are drawn into the floating gate, which shifts the gate threshold voltage to more positive values, so the charge can be stored for as long as needed (up to ~ 10 years).

- Use of **high K (high dielectric constant) oxides** (e.g. ZrO_2 , HfO_2 , ZrSiO_4) allows for scaling of FETs to **prevent tunneling through nanometre-scale gates** (thicker oxide, same capacitance per unit area). These oxides can be manufactured using atomic layer deposition (ALD), where localised surface chemical reactions with adsorbed reagents occur (e.g. $\text{HfCl}_4 + 2 \text{H}_2\text{O} \rightarrow \text{HfO}_2 + 4 \text{HCl}$).
- **High-speed FETs** require inter-layer dielectrics with **low K materials**, such as fluorinated SiO_2 or organo-silicon polymers. In high-power-density chips, high thermal conductivity is also required to dissipate heat quickly, with covalent organic frameworks and amorphous BN (Section 8.6.8) as suitable materials.
- **Strained Si or Ge**, in which the mechanical stress field **splits the degenerate (symmetric) conduction band valleys** (analogous to the Jahn-Teller effect, Section 15.5.15) to **reduce scattering**, can be used as a **high-mobility** channel material.
- III-V semiconductors (based on e.g. InSb , InGaAs_2) have also been used in complex stacked architectures: in III-V semiconductors, Si can act as either p or n type dopant depending on whether it substitutes the group III or V atom (amphoteric dopant).
- In **ultra-short channel FETs** (< 5 nm), drain-induced barrier lowering (DIBL) means that leakage becomes a significant problem, requiring semiconducting TMDs (Section 8.6.11) e.g. MoS_2 for the channel.

8.6.13. Linear Magnetic Materials (Diamagnetism and Paramagnetism)

Linear magnetic materials possess reversible spin alignment, magnetising in the presence of an externally applied magnetic field, and demagnetising when the field is removed.

- **Magnetic constitutive relation:** $\mathbf{B} = \mu_0(\mathbf{H} + \mathbf{M})$.
(\mathbf{B} [T]: magnetic flux density, \mathbf{H} : magnetic field intensity [A m^{-1}], \mathbf{M} [A m^{-1}]: magnetisation, $\mu_0 = 4\pi \times 10^{-7} \text{ N A}^{-2}$: vacuum permeability.)
- Outside of a magnetic material: $\mathbf{M} = 0$ and $\mathbf{B} = \mu_0 \mathbf{H}$ (non-magnetic: $\chi_m = 0$)
- **Inside a linear magnetic material:** $\mathbf{M} = \chi_v \mathbf{H}$ and $\mathbf{B} = \mu \mathbf{H}$.
($\chi_v = \mu_r - 1$: volume magnetic susceptibility, $\mu = \mu_0 \mu_r$: permeability)
- **Mass and molar magnetic susceptibility:** mass: $\chi_p = \chi_v / \rho$, molar: $\chi_m = M_r \chi_p$
- **Bulk saturation magnetisation,** \mathbf{M}_{sat} [A m^{-1}] = $\frac{\text{total dipole moment}}{V} = \frac{n_{\text{atoms/unit cell}}}{V_{\text{unit cell}}} \times \boldsymbol{\mu} = \frac{\rho N_A}{M_r} \boldsymbol{\mu}$
- **Magnetic moment $\boldsymbol{\mu}$** (per atom) is the sum of spin-only (intrinsic, unpaired electrons) and angular momentum (unbalanced $p / d / f$ orbitals) contributions (Section 15.5.10).

Magnetic Susceptibility of Weakly Magnetic Materials (diamagnetic or weakly paramagnetic):

- **Diamagnetic** materials produce weakly **repulsive** magnetisations ($-1 \leq \chi_v < 0$).
- **Paramagnetic** materials produce **attractive** magnetisations ($\chi_m > 0$) (Section 13.1.2).

Material	χ_v [-]	Material	χ_v [-]
mercury	-2.84×10^{-5}	air	$+2.6 \times 10^{-7}$
silver	-2.38×10^{-5}	oxygen	$+1.908 \times 10^{-6}$
lead	-1.7×10^{-5}	aluminium	$+2.11 \times 10^{-5}$
copper	-9.63×10^{-6}	neodymium	+0.00336
hydrogen	-2.23×10^{-9}	terbium	+0.112
fused silica glass	-1.13×10^{-5}	titanium	$+1.81 \times 10^{-4}$
graphite (parallel)	-6.14×10^{-4}	uranium	$+4.11 \times 10^{-4}$
graphite (perpendicular)	-1.4×10^{-5}	BMIM-FeCl ₄	+0.21
diamond	-2.2×10^{-5}		
water	-9.04×10^{-6}		
polyvinyl chloride	-1.07×10^{-5}		

Iron, cobalt and nickel are nonlinear ferromagnets with initial $\chi_v \sim 10^3 - 10^5$.

8.6.14. Nonlinear Magnetic Materials (Ferromagnetism)

Ferromagnetism occurs when a paramagnetic metal experiences quantum exchange interactions between neighbouring spins (which depends on crystal structure). Elevated temperatures can impede this alignment but below the Curie temperature T_c , the material remains ferromagnetic. The ferromagnetic elements at room temperature are BCC iron, FCC nickel, HCP cobalt and body-centred tetragonal ruthenium. Austenitic steels (contain FCC γ -Fe) are not ferromagnetic.

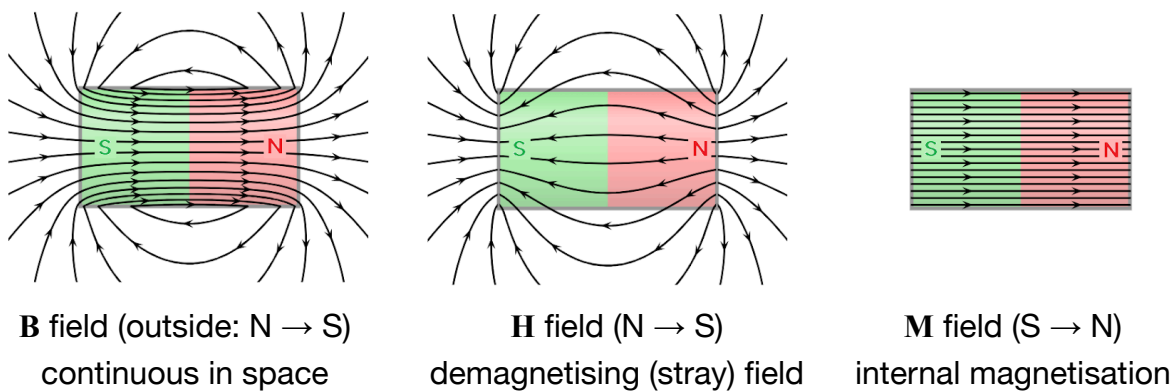
Neutron diffraction shows increased neutron scattering in ferromagnetic materials near the Curie point, as magnetic domains have larger fluctuations. Above T_c , the domains are fully randomised and the materials are paramagnetic with $\chi_m = \frac{C}{T - T_c}$ (Curie-Weiss law).

(C : Curie constant, theoretically given by $C = \frac{\mu_0 (N/V) \mu^2}{k_B}$ (N/V : dipole number density).)

Spin Exchange Interactions in Spontaneously Aligned Dipoles

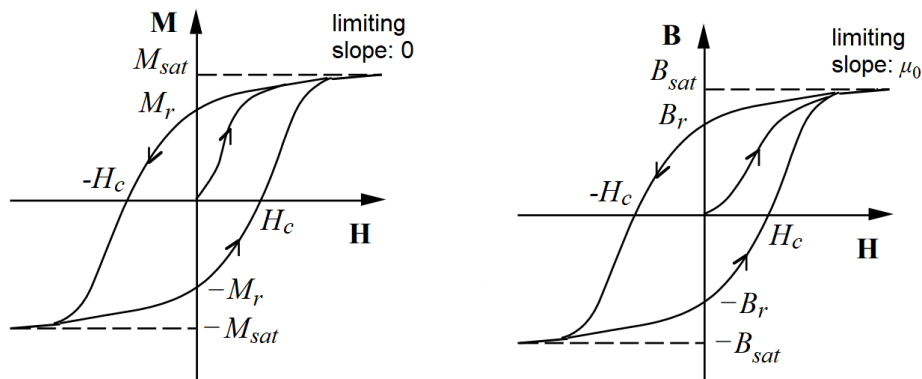
- **Soft Ferromagnetic:** spontaneous magnetic dipoles in domains (nonlinear B - H curve, no hysteresis).
- **Hard Ferromagnetic:** irreversible once magnetised into a single domain (hysteresis) (Section 8.6.15).
- **Antiferromagnetic:** all adjacent dipoles cancel, resulting in no net magnetisation
- **Ferrimagnetic:** antiferromagnetism with two opposing magnitudes (net ferromagnetism)

Field lines for a permanent bar ferromagnet (**N**: North-seeking pole, **S**: South-seeking pole)



Smelted (solidified from molten) iron forms magnetic 'domains' of locally saturated (fully aligned) magnetisations. The size of the domains are usually smaller than the grains in polycrystalline ferromagnets. When exposed to an external magnetic field for the first time, the domains align, reaching a net large saturation magnetisation M_s .

8.6.15. Hysteresis in Hard Ferromagnets



The fields are sometimes shown in CGS units: 1 Gauss = 100 μT and 1 Oersted = $\frac{1000}{4\pi}$ A m^{-1} . The energy loss per unit volume per cycle is the area of the B - H loop.

Initial Magnetisation

- Spins begin spontaneously aligned within domains. Each domain is randomised.
- As H increases, **domains aligned in the lattice 'easy' direction grow**; others shrink.
- For small H , this domain growth is reversible (no hysteresis).
- Growing domains can be **pinned on defects**, which snap off as H grows (Barkhausen effect).
- When the material is all one domain, further increases in H slowly **rotate the alignment towards the field**, up to its saturation magnetisation M_{sat} .

Demagnetisation

- As H is removed, the alignment relaxes back to the lattice 'easy' direction, retaining a 'remanence' M_r .
- The average **stray (demagnetising) self-field** (at $H = 0$) can be written as $\mathbf{H}_d = -N \mathbf{M}$. ($0 < N < 1$: shape factor, e.g. flat plate: $N = 1$, infinite parallel cylinder: $N = 0$.) Plotting this as a '**load line**' gives the **operating point** (intersection with B - H curve).
- The $(BH)_{\max}$ point contains the most magnetic energy (**optimal operating point**).
For a linear B - H line, $(BH)_{\max} = \mu_0 \left(\frac{M_{sat}}{2} \right)^2$, optimal for $N = \frac{1}{2}$, since $\frac{B}{H} = -\mu_0 \frac{1-N}{N}$.
- If a reversed H is applied, the magnetisation will remain aligned until exceeding the 'coercivity' $H < -H_c$. The process of reverse saturation and relaxation repeats, completing the magnetic cycle. If the operating H_d is close to H_c , the magnet is prone to spontaneous demagnetisation in operation.

Magnetostriction in Hard Ferromagnets: mechanical strain due to domain rotation in applied H

Material	Maximum magnetostrictive strain λ (microstrain ppm, $\times 10^{-6}$)	Saturation field $H_c / \text{kA m}^{-1}$
Terfenol-D ($\text{Tb}_x\text{Dy}_{1-x}\text{Fe}_2$)	-2000	160
Alperm ($\text{Fe}_x\text{Al}_{1-x}$)	-300	16
Metglas 2605SC ($\text{Fe}_{81}\text{Si}_{13.5}\text{B}_{13.5}\text{C}_2$)	-20	1
Cobalt ferrite (CoFe_2O_4)	-200	0.25

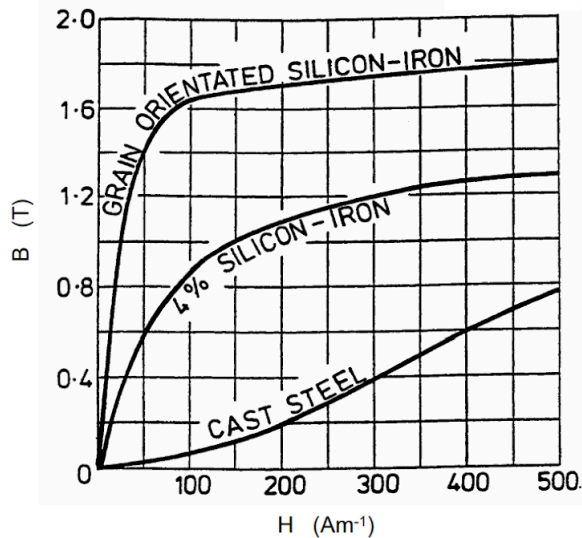
The **magnetoelastic effect** (Villari effect) is the inverse of magnetostriction (applied mechanical stress \rightarrow change in magnetic susceptibility \rightarrow change in M in applied H).

8.6.16. Properties of Soft Ferromagnetic Materials

Soft ferromagnetic materials are highly paramagnetic, with potentially large μ_r . They magnetise reversibly in the presence of an external field (very little hysteresis, small remanence/coercivity).

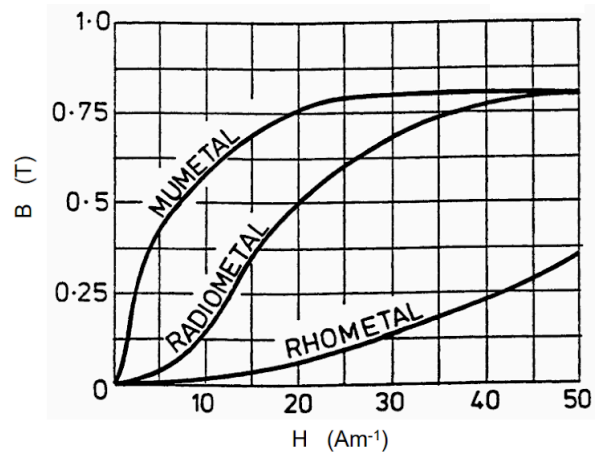
Soft ferromagnets are manufactured with **large grains** e.g. by annealing, to allow large domains.

B-H Magnetisation Curves of Group I and Group II Alloys (Soft Ferromagnetic Materials): grain-oriented silicon steel (GOSS), Fe-4% Si, cast steel, mumetal, radiometal, rhometal.



Group I

Materials used in the electrical power industry



Group II

The nickel-iron alloys

Properties of Silicon Steels (Electrical Steel): Group I, little hysteresis, high electrical resistivity

Fe-Si alloys are used as iron cores in AC power transformers as they have high resistivity (low eddy current loss), large grains (low magnetostriction, low stress sensitivity and transformer hum) and low magnetocrystalline anisotropy (high permeability). The Fe-Si phase diagram (Section 6.7.13) is such that the BCC phase is always stable for >2.5% Si. Thermo-mechanical treatment to form a Goss texture (fixed grain orientation) increases permeability further. Fe-Al is also used (e.g. Sendust, Fe-5.4% Al-9.6% Si), competitive with Mo-doped permalloy.

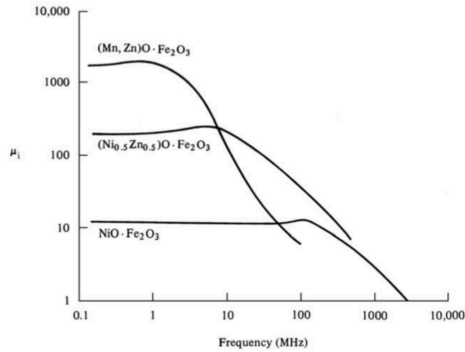
Properties of Nickel-Iron Alloys (Permalloys): Group II, very high μ_r

wt% Ni	Name	Initial μ_r	Maximum flux density [T]	Resistivity [Ω m]
70-90	Mumetal (Permalloy C)	10000-30000	0.8	6.0×10^{-7}
45-50	Radiometal (Permalloy B)	1800-2400	1.6	5.5×10^{-7}
35-45	Rhometal (Permalloy D)	1500-2000	1.3	9.0×10^{-7}

Mumetal is used in magnetic shielding as it channels the magnetic flux efficiently.

Properties of Ferrites: Group IV spinels with general formula $MO \cdot Fe_2O_3$.

Ferrite Alloy	Initial μ_r	AC frequency range []	Maximum flux density [T]	Resistivity [Ω m]
Mn-Zn	850 - 1500	1 k - 20 M	0.34 - 0.40	0.5 - 1.0
Ni-Zn	20 - 650	1 k - 200 M	0.19 - 0.32	1000



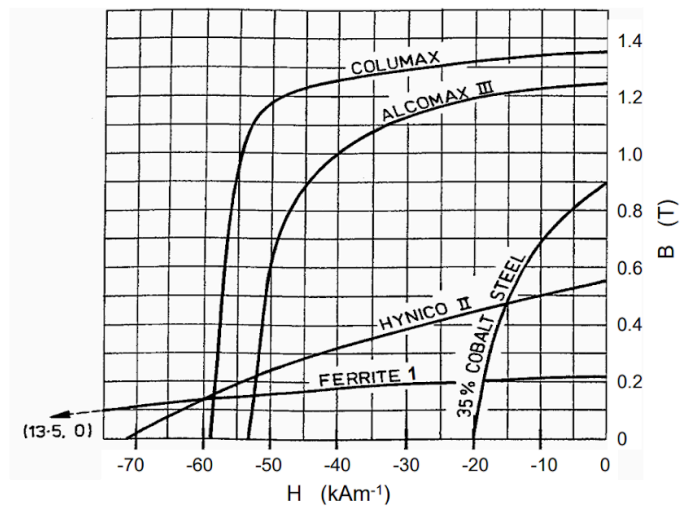
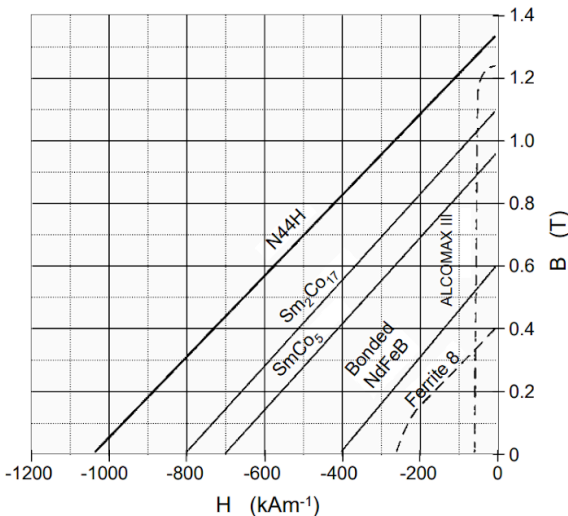
AC operation requires constant permeability over a frequency range: ferrites act as low pass filters. They are useful for switch-mode electronics (SMPS) and EM interference suppression as ferrite bead core inductors.

Gigahertz (>1000 M) applications (sub-millimetre, microwave radar, radio antennas) use specialised silicates and garnets (e.g. $Y_3Fe_5O_{12}$).

8.6.17. Properties of Hard Ferromagnetic Materials (Permanent Magnets)

Hard ferromagnets are manufactured with **small grains**, e.g. by sintering, to form many pinning sites.

Normal Demagnetisation Curves of Group III Alloys (Hard Ferromagnetic Materials, Permanent Magnets): neodymium, samarium-cobalt, ferrites, alcomax (alnico), columax, hynico, 35% Co-Fe.



N44H is a high grade of sintered NdFeB. Samarium-cobalt alloy is available in two forms and is machinable:

Sm-Co alloys	B_r , Remanent flux density / T	H_c , Coercive force / $A\ m^{-1}$
Sintered metal	0.87	1.280×10^6
Moulded powder in epoxy	0.435	6.40×10^5

Barium ferrites are permanent magnets with $B_r = 0.36\ T$ and $H_c = 1.1 \times 10^5\ A\ m^{-1}$.

8.6.18. Superconductivity

Superconductors exhibit zero electrical resistivity below a critical temperature T_c , critical current density J_c and applied magnetic field H_c .

- Superconducting order parameter (wavefunction), ψ : complex amplitude of electron density.
- **London penetration depth**, λ : length scale for the **magnetic field**, decaying from the surface inwards
- **Coherence length**, ξ : length scale for **electron density** ψ , rising from zero at the surface into the bulk.
- Ginzburg-Landau parameter, $\kappa = \lambda / \xi$: If $\kappa < 1 / \sqrt{2} \rightarrow$ type I. If $\kappa > 1 / \sqrt{2} \rightarrow$ type II.
- Bohr radius of Cooper pairs: $a_{CP} = \xi / \sqrt{2}$. If $a_{CP} >$ grain boundary gap, then good superconductor.

Type I Superconductivity: superdiamagnetism up to a critical field H_c . Most common in metals.

The quantum mechanical model of type I superconductivity is given by Bardeen-Cooper-Schrieffer theory (BCS theory). Conduction band electrons of opposite spin form **Cooper pairs**, which have lower energy than the Fermi level. The Cooper pairs act as bosons so **cannot be scattered by phonons** and propagate freely in a single degenerate quantum state. The electron spins can be realigned by an external magnetic field (Zeeman energy), giving a maximum field H_c and current capacity $I_c = 2\pi r H_c$ (Silsbee effect, r : radius of superconducting wire).

In the presence of an external magnetic field, a persistent **screening current** is set up at the surface which expels the field from the interior (for $x > \lambda$). Type I superconductors have low critical field and temperature ($T_c \sim 10$ K). Examples include Hg, Al, Pb, TaSi₂, SiC:B.

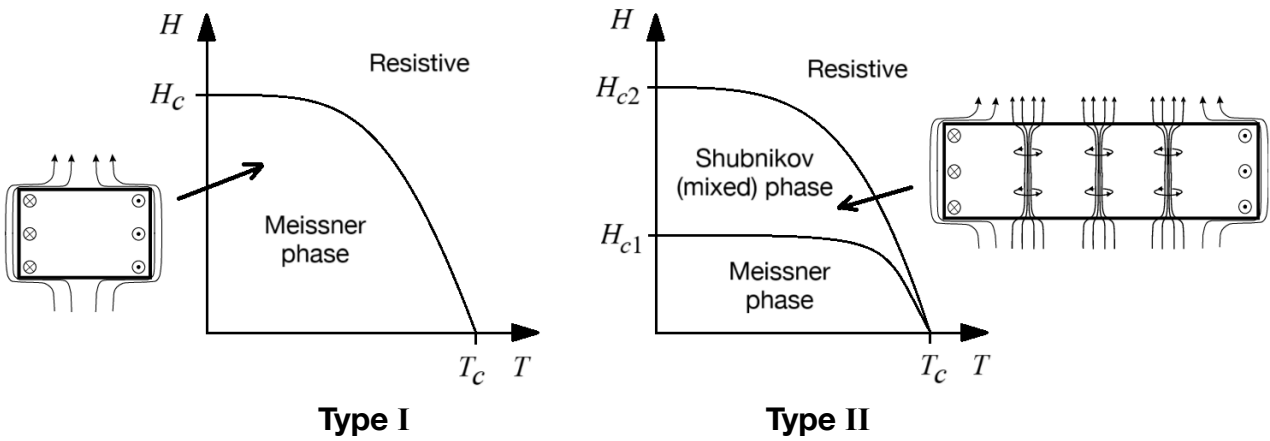
Type II Superconductivity: intermediate phase of flux penetration. Most common in ceramics.

Type II superconductivity currently lacks a complete theoretical model, but a starting point is the Ginzburg-Landau theory. If $\xi \ll \lambda$, then **magnetic fields and electron density can overlap significantly**. For intermediate fields ($H_{c1} < H < H_{c2}$), a **mixed (Shubnikov) state** forms instead, where local points of normal phase material form to channel incoming magnetic flux through flux tubes / **flux vortices** / fluxoids, with persistent screening **supercurrents** surrounding them (like a solenoid). In a current-carrying superconductor, the current will flow through the superconducting region as usual, but may move the flux vortices if they are not pinned strongly enough, which leads to dissipation (flux creep).

- **Magnetic flux per flux tube:** one quanta, $\Phi_0 = h / 2e = 2.07 \times 10^{-15}$ Wb
- Flux tube radius: approximately ξ (length scale over which surrounding current density can decay)
- Number of flux tubes per unit area: proportional to applied field, B / Φ_0
- Upper breakdown field H_{c2} : when the flux tubes become numerous enough to touch each other.

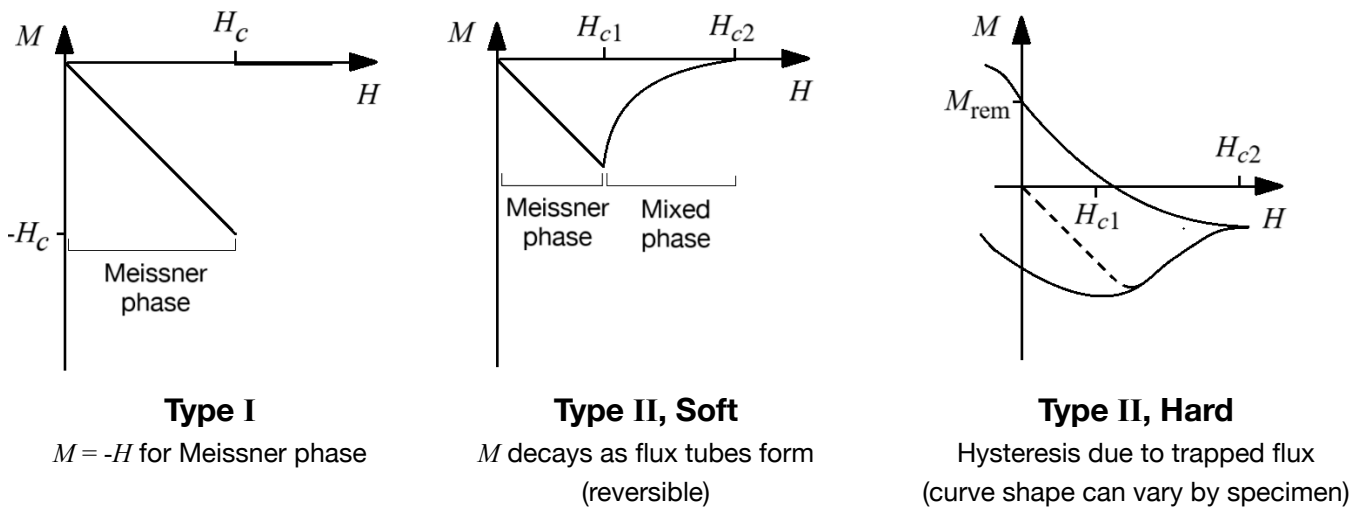
Type II superconductors may have a **hysteresis effect** when an external magnetic field is removed ('**hard**' superconductor). This occurs when the flux tubes are **pinned on hard obstacles** such as precipitate inclusions (other material phases). The flux vortices remain when the external field is removed (like a hard ferromagnet), while for soft superconductors the material returns to its Meissner phase (reversible magnetisation). The hysteresis effect in hard type II superconductors can be described by the **Bean critical state model**.

Temperature Dependence of Critical Field and Superconducting State

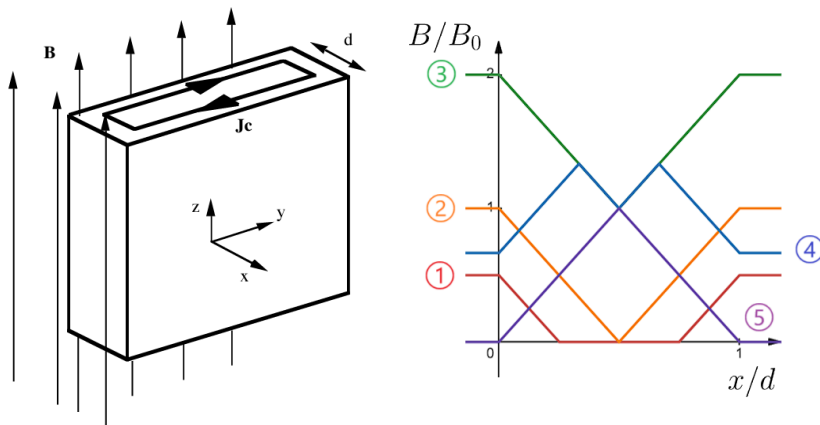


Empirical relation for critical field:
$$H_c(T) = H_c(0) \times \left[1 - \left(\frac{T}{T_c} \right)^2 \right]$$

M-H Curves for Superconductors: external **H**-field cycled from 0 to H_{c2} and back



Bean's Critical State Model: for a thin slab of hard type II superconducting material



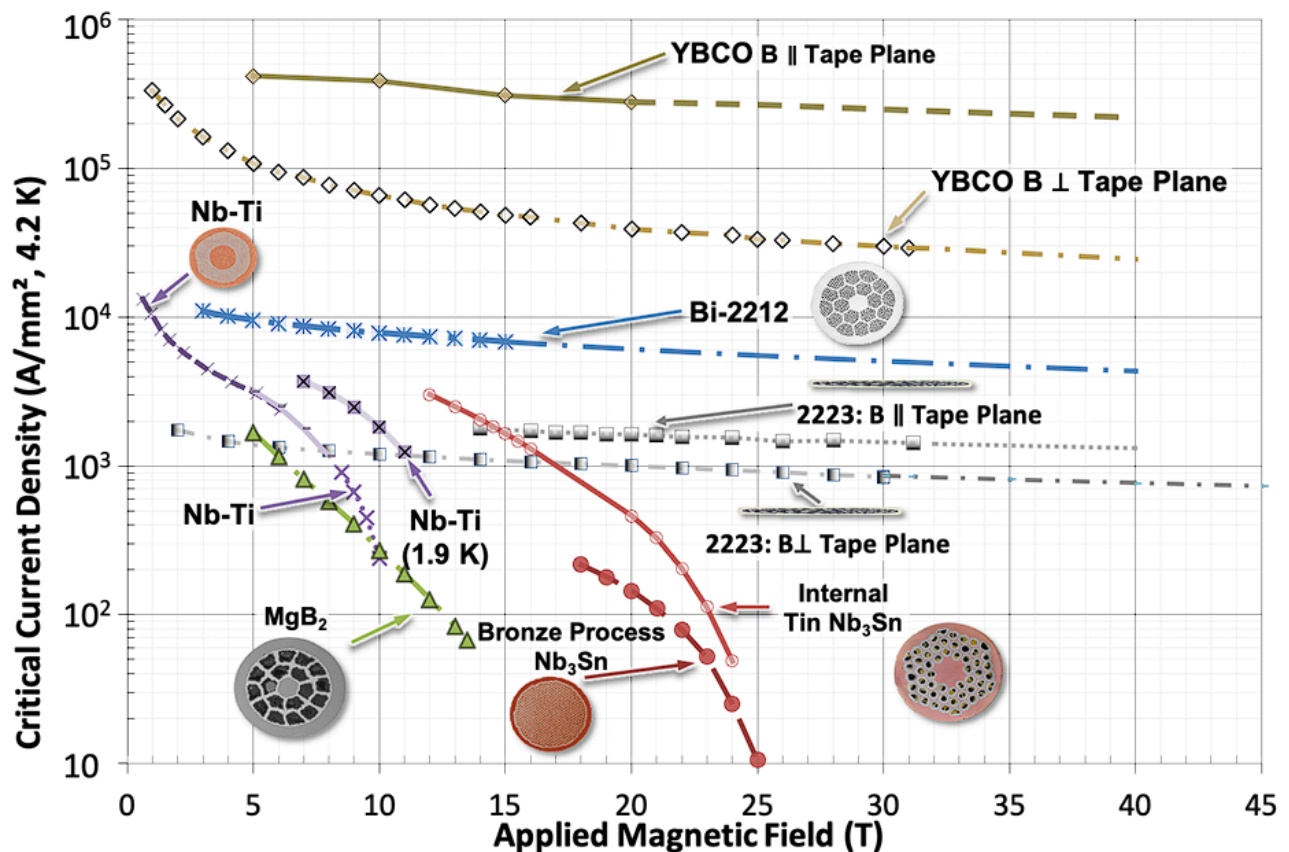
Field slope: $\frac{dB}{dx} = \mu_0 J$ (from 1D Ampere's law)

Assume that J is either $\pm J_c$ or 0.
In the 'critical state', $J = \pm J_c$ for all x .

By varying the external field up to $2B_0$ and back down (① → ⑤), a maximum field of B_0 can be trapped within the material.

8.6.19. Bulk Superconductors and Applications

Typically only **hard type II superconductors** are practically useful, and are used in their **mixed phase**. Transition metal and rare-earth (RE) cuprates are practical ceramic bulk superconductors with high critical temperatures (>90 K). Large-grain YBCO ($\text{YBa}_2\text{Cu}_3\text{O}_{7-x}$) is produced by peritectic cooling, with Y-211 (Y_2BaCuO_5) inclusions acting as the flux pinning centres. Practical lower T_c (~ 10 K) superconductors include NbTi, with α -Ti precipitates in Nb- β Ti acting as pinning centres. Nb_3Sn and Nb_3Al (A15 materials) are also used, as is MgB_2 (39 K). As a rule of thumb, mechanical/material fabrication properties and superconducting performance are a trade-off.



Superconducting wires must be manufactured carefully to maintain **thermal stability** (prevent thermal runaway due to local breakdown with fluctuation in operating conditions). They are made as multifilamentary **bundles of superconductors with copper conductor cores and shell** (shunt layer), for high thermal and electrical conductivity paths to divert excess heat and current generation. For AC applications, these fibres are also twisted to minimise coupling losses. Cryocoolers are used to achieve the low temperatures required. Low temperatures can be maintained by using superinsulating materials (e.g. multi-layer insulation (MLI): Kapton polyimide + aluminised mylar foil).

Applications: current and emerging, but somewhat limited by engineering constraints.

- **Magnetic bearings:** frictionless for high efficiency, used in high-performance flywheels and vibration isolators.
- **Magnetic resonance imaging (MRI):** generates high magnetic fields for imaging the body.
- **Maglev trains:** on-board superconductors and a track with ferromagnets to levitate the train for frictionless propulsion to high speeds.
- **Superconducting quantum interference devices (SQUIDs):** highly sensitive measuring device for tiny magnetic fields, through the use of Josephson junctions (superconductor-insulator-superconductor junctions). Used in magnetoencephalopathy (MEG, brain imaging based on magnetic activity, detecting fields ~ 100 fT).
- **Nuclear fusion:** strong magnetic fields are used to guide plasma in magnetic confinement fusion (MCF) tokamaks and stellarators.
- **Underwater DC transmission connectors:** AC currents experience impedance in superconductors, so is more suitable for DC submarine cables (no reactive dissipation).

Data for Superconductors

Critical current density is very variable:

- NbSn will carry 109 A/m^2 in a field of 5 T at 4.2 K in wire form.
- YBaCuO will carry 1010 A/m^2 in zero magnetic field at 77 K in thin film form.

Flux quantum $\frac{h}{2e} = 2.07 \times 10^{-15} \text{ V s}$. Energy gap $\approx 3500 T_c$.

	T_c K	B_c or B_{c2} at 0 K tesla (T)
Al	1.2	0.01
Pb	7.2	0.08
Nb	9.2	0.08
NbSn	18.4	24
YBaCuO	93	~ 100
TlBaCaCuO	125	~ 120

8.6.20. Properties of Electrical Conductors and Insulators

Electrically Conductive Materials:

	Resistivity at 20 °C $\Omega \text{ m}$	Temp. Coeff. of Resistance K^{-1} at 20°C	Temp. Coeff of Expansion K^{-1}	Specific Heat- Capacity J/kg K	Thermal Conducti- vity W/m K	Melting Point °C
Copper	1.72×10^{-8}	39×10^{-4}	25.5×10^{-6}	380	385	1083
Aluminium	2.8×10^{-8}	40×10^{-4}	16.7×10^{-6}	880	200	660
Tungsten	5.5×10^{-8}	45×10^{-4}	4.4×10^{-6}	140	160	3370
Manganin	44.5×10^{-8}	0.1×10^{-4}	18×10^{-6}		26	910
Nichrome	103×10^{-8}	1.5×10^{-4}	17×10^{-6}	450	13	1350
Carbon	4500×10^{-8}	-5×10^{-4}	5.4×10^{-6}	840	1.7	3500
Iron	100×10^{-8}	54×10^{-4}	11.6×10^{-6}	250	67	1537
Stainless steel	72×10^{-8}	-	9×10^{-6}	500	16	1427

Dielectric Materials:

	Relative Permit- tivity	Dielectric Strength MV/m	tan δ at			Resistivity $\Omega \text{ m}$
			50Hz	1MHz	1GHz	
Mica	6	200	25×10^{-4}	3×10^{-4}	3×10^{-4}	$10^{11} - 10^{15}$
Glass	5	20	6×10^{-4}	8×10^{-4}	12×10^{-4}	$10^9 - 10^{12}$
Porcelain	6	30	220×10^{-4}	75×10^{-4}	100×10^{-4}	-
Polystyrene	2.5	20	0.5×10^{-4}	0.7×10^{-4}	3.3×10^{-4}	-
P.T.F.E	2.1	20	5×10^{-4}	2×10^{-4}	2×10^{-4}	$10^{15} - 10^{19}$
Transfr. Oil	2.2	15	4×10^{-4}	5×10^{-4}	30×10^{-4}	-
Alumina	8.5	-	20×10^{-4}	-	-	-
Quartz	3.8	20	10×10^{-4}	-	-	10^{16}
Polythene	2.3	20	2×10^{-4}	-	-	$10^8 - 10^{14}$
Polycarbonates	3.1	-	50×10^{-4}	-	-	$10^{11} - 10^{14}$

8.6.21. Piezoelectric Materials

Electric properties of crystalline materials are intrinsically linked to their crystal structures. For the 32 point groups, see Section 13.2.9.

Piezoelectric point group: a lattice lacking an inversion symmetry i (exception: cubic group O). There are 20 such point groups.

Piezoelectric materials attain an induced polarisation (lattice dipole) in response to an electric field as the charges are displaced in different directions.

Crystal system	Point groups	Piezoelectric tensor	Surface representation
Cubic	23 (T) 43m (T_d)	$\begin{pmatrix} 0 & 0 & 0 & e_{14} & 0 & 0 \\ 0 & 0 & 0 & 0 & e_{14} & 0 \\ 0 & 0 & 0 & 0 & 0 & e_{14} \end{pmatrix}$	
Hexagonal, Tetragonal	6mm (C_{6v}) 4mm (C_{4v})	$\begin{pmatrix} 0 & 0 & 0 & 0 & e_{15} & 0 \\ 0 & 0 & 0 & 0 & 0 & 0 \\ e_{31} & e_{31} & e_{33} & 0 & 0 & 0 \end{pmatrix}$	
Hexagonal, Tetragonal	6 (C_6) 4 (C_4)	$\begin{pmatrix} 0 & 0 & 0 & e_{14} & e_{15} & 0 \\ 0 & 0 & 0 & e_{15} & -e_{14} & 0 \\ e_{31} & e_{31} & e_{33} & 0 & 0 & 0 \end{pmatrix}$	

Applications of piezoelectricity include microphones (direct) and buzzers / loudspeakers (converse). Piezoelectric materials in the form of structural frames can be used as energy harvesting devices, as vibrations on the frame generate internal stresses which produce current in a complete circuit.

Piezoelectric tensor \mathbf{d} is a rank 3 tensor typically written as a 3×6 matrix.

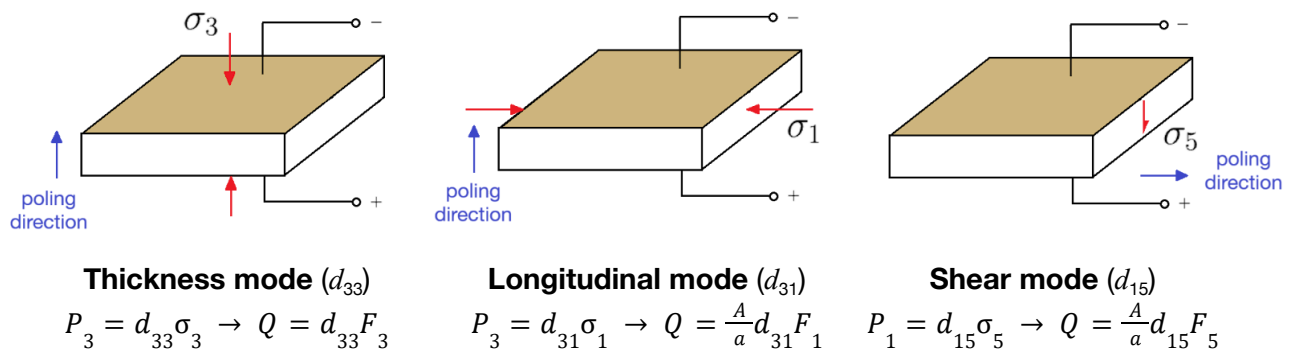
- Electric and mechanical tensors: $\mathbf{D} = \epsilon_0 \mathbf{E} + \mathbf{P}$ (ϵ : permittivity) and $\mathbf{S} = \mathbf{C}\boldsymbol{\sigma}$ (\mathbf{C} : elastic compliance)
- Piezoelectric effect: $\Delta \mathbf{P} = \mathbf{d}\boldsymbol{\sigma}$ (i.e. $\Delta P_i = d_{ij} \sigma_j$) (passive) and $\Delta \mathbf{S} = \mathbf{d}^T \mathbf{E}$ (active)
- **Piezoelectric equations:** $\mathbf{P} = \epsilon_0 \chi_e \mathbf{E} + \mathbf{d}\boldsymbol{\sigma}$ (direct effect) and $\mathbf{S} = \mathbf{C}\boldsymbol{\sigma} + \mathbf{d}^T \mathbf{E}$ (converse effect)

($\mathbf{P} = [P_1, P_2, P_3]^T$: polarisation field (bound charge density) [C m^{-2}], $\boldsymbol{\sigma} = [\sigma_1, \sigma_2, \sigma_3, \tau_{23}, \tau_{13}, \tau_{12}]^T$: stress, $\mathbf{d} = \{d_{ij}\}$: piezoelectric tensor, $\mathbf{S} = [\epsilon_1, \epsilon_2, \epsilon_3, \gamma_{23}, \gamma_{13}, \gamma_{23}]^T$: strain)

Piezoelectric tensor in another dimension: $d_{ijk}^* = M_{il} M_{jm} M_{kn} d_{lmn}$ (\mathbf{M} : transformation matrix from crystal frame)

Piezoelectric Modes of Operation: constraints reduce complexity of response.

Practical piezoelectric materials are usually made as thin slabs, where the only major electric field/strain is developed through the thickness direction. Using ferroelectrics (Section 8.6.22) allows poling control.



(A : electrode area, a : stressed area, Q : charge on electrodes, F : applied force, P : polarisation)
Applying a tensile stress instead of compressive stresses reverses the charge polarity.

8.6.22. Pyroelectric and Ferroelectric Materials

Pyroelectric point group: a piezoelectric point group with an **intrinsic dipole**. There are 10 such groups.

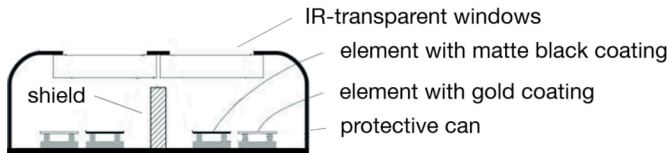
When temperature changes, the lattice becomes more or less disordered, changing the alignment of the dipoles and hence the polarisation changes.

Pyroelectric effect: $\Delta P = p \Delta T$ (p : pyroelectric coefficient. Typically, $p < 0$).

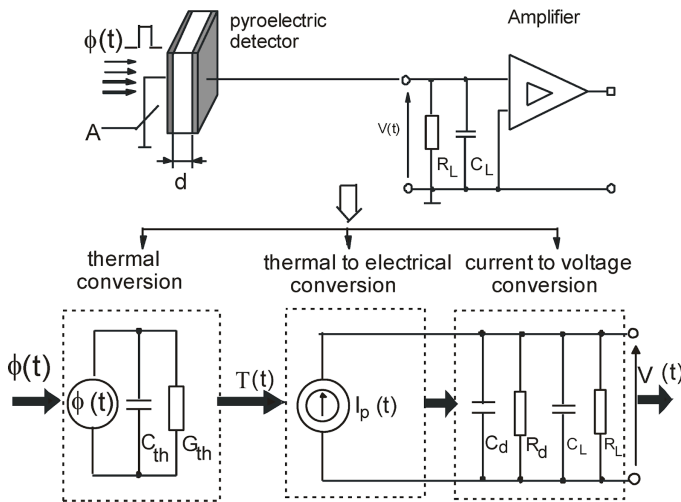
Measured coefficient: $D = p_g \Delta T = Q/A$ ($p_g = p + \frac{\partial \epsilon}{\partial T} E$. E : applied field, D : measured charge density)

Ferroelectric crystal (electret): a pyroelectric crystal where poling with an applied E gives **hysteresis** due to spontaneous formation of **domains** of polarisation.

Common application: Passive Infrared (PIR) motion sensor, detecting changes in IR radiation.



The detector unit is placed behind a multi-segment Fresnel lens which focuses IR radiation into the two detection zones. The **gold-coated** pyroelectric element ensures that the differential signal corrects for overall temperature changes (all IR radiation is reflected away). The two **zones** are positioned to receive IR radiation from different sides of the scene FOV, so that motion from IR-emitting objects (e.g. people, warm-blooded animals) across the scene produces a signal. High input impedance FET-based differential amplifiers are used to contrast the signals. The contact area of the pyroelectric element with the protective can is minimised to increase the thermal time constant of the sensor.



Thermal conversion ($C_{th} = cAd$: thermal capacitance, G_{th} : thermal conductance, c : vol. heat capacity, η : emissivity, $\Phi(t) = \Phi_0 e^{j\omega t}$: incident thermal power, $\tau_{th} = C_{th} / G_{th}$: thermal time constant)

$$C_{th} \frac{dT}{dt} + G_{th} T(t) = \eta \Phi(t) \Leftrightarrow T(t) = \frac{\eta \Phi_0}{G_{th}(1 + j\omega\tau_{th})} e^{j\omega t}$$

Thermal to electrical conversion ($i_p(t)$: pyroelectric current)

$$i_p(t) = pA \frac{dT}{dt} \Leftrightarrow i_p(t) = \frac{j\omega pA\eta \Phi_0}{G_{th}(1 + j\omega\tau_{th})} e^{j\omega t}$$

Current to voltage conversion ((R_d, C_d) : leakage, (R_L, C_L) : amplifier input), $R = R_d \parallel R_L$, $C = C_d + C_L$, $\tau_e = RC$: electrical time constant, $Y = R^{-1} + j\omega C = i_p / v$: input admittance)

$$C \frac{dv}{dt} + \frac{1}{R} v(t) = i_p(t) \Leftrightarrow v(t) = \frac{j\omega pA\eta \Phi_0}{G_{th}(1 + j\omega\tau_{th})(1 + j\omega\tau_e)} e^{j\omega t}$$

Current responsivity (current mode): $\left| \frac{i_p}{\Phi_0} \right| = \frac{pA\eta\omega}{G_{th}\sqrt{1 + \omega^2\tau_{th}^2}} \approx \frac{pA\eta}{G_{th}\tau_{th}} = \frac{p\eta}{cd}$ for $\omega \gg \tau_{th}^{-1}$.

Voltage responsivity (voltage mode): $\left| \frac{v}{\Phi_0} \right| = \frac{pA\eta\omega}{G_{th}\sqrt{(1 + \omega^2\tau_{th}^2)(1 + \omega^2\tau_e^2)}} \approx \frac{pA\eta}{G_{th}\tau_{th}\tau_e\omega} = \frac{p\eta}{cdC\omega}$ for $\omega \gg \tau_{th}^{-1}, \tau_e^{-1}$.

Data for Practical Pyroelectric Materials: data at 25 °C. All listed materials are **also** ferroelectric.

Material	p [$\mu\text{C m}^{-2} \text{K}^{-1}$]	Material	p [$\mu\text{C m}^{-2} \text{K}^{-1}$]
PMN-PT (lead magnesium niobate-lead titanate)	-1300	PZT (lead zirconium titanate)	-30
BST (barium strontium titanate)	-7570	triglycine sulfate	-550
LiTaO ₃ (lithium tantalate)	-230	PVDF (polyvinylidene fluoride)	-27
Ca ₁₀ (PO ₄) ₆ (OH) ₂ (hydroxyapatite)	-1 to -400	HfO ₂ (hafnium oxide)	-46
tourmaline	-6		

Pyroelectrics/ferroelectrics often have a perovskite structure. In ideal cubic perovskite ABO₃, the B-site ion is shifted away from its body centre position, forming lower energy covalent bonds with O atoms.

Electrostriction in Hard Ferroelectrics: mechanical strain due to dipole rotation

Electrostrictive strain: $S_{ij} = Q_{ijkl} P_k P_l$ (strain is proportional to P^2 , Q : 4th order electrostriction tensor)

Strains generated by electrostriction are typically smaller than by the piezoelectric effect.

Electrostriction is responsible for the 'equivalent series resistance' (ESR) in AC capacitor dielectrics.

Multiferroic Materials: both ferroelectric and ferromagnetic. The mechanism of ferroelectricity is typically different for multiferroics.

8.6.23. Thermoelectric Materials

The thermoelectric effect is the formation of a potential difference between two points on a material at different temperatures. The converse is applying a potential difference to two points on the material, which results in heat transfer in the material.

Seebeck effect electric field: $\mathbf{E} = -\nabla V - S \nabla T$ where $\mathbf{J} = \sigma \mathbf{E}$

Full steady-state heat transfer model (combined Joule heating, Seebeck, Peltier/Thompson effects):

$$-\dot{q}_{\text{ext}} = \underbrace{\nabla \cdot (\kappa \nabla T)}_{\text{heat conduction}} + \underbrace{\mathbf{J} \cdot (\sigma^{-1} \mathbf{J})}_{\text{Joule heating}} - \underbrace{T \mathbf{J} \cdot \nabla S}_{\text{Thompson effect}} \quad (q_{\text{ext}}: \text{external heat transfer rate per unit volume, } \kappa: \text{thermal conductivity, } \sigma: \text{electrical conductivity, } S: \text{Seebeck coefficient})$$

Seebeck coefficients are typically on the order of $S \sim 100 \mu\text{V K}^{-1}$. These materials can be doped to create spatial variations (∇S).

A thermoelectric generator uses a thermopile design to produce a current from heat.

- Power factor performance index: σS^2 (units: $\text{W m}^{-1} \text{K}^{-2}$)
- Thermoelectric material performance index: $z = \frac{\sigma S^2}{\kappa}$ (figure of merit: zT)
- Compatibility factor: $s = \frac{\sqrt{1 + z\bar{T}} - 1}{ST}$
- Maximum 1st law efficiency: $\eta_{th} = \frac{\text{electrical power generated}}{\text{heat absorbed at hot side}} \leq \frac{T_H - T_C}{T_H} \frac{\sqrt{1 + z\bar{T}} - 1}{\sqrt{1 + z\bar{T}} + \frac{T_C}{T_H}}$ (where $\bar{T} = \frac{T_C + T_H}{2}$)
- Maximum 2nd law efficiency (exergy): $\eta_{ex} = \frac{\text{maximum electrical power generated}}{\text{power generated by Carnot engine}} \leq \frac{\sqrt{1 + z\bar{T}} - 1}{\sqrt{1 + z\bar{T}} + \frac{T_C}{T_H}}$

In terms of exergy efficiency, thermoelectric generators are only competitive with heat engines for large $T_H - T_C \sim 1000 \text{ K}$, in materials having $zT \sim 3$, for which $\eta_{ex} \sim 0.4 - 0.5$. Around room temperatures, $zT \sim 1$. They are suitable only for low power applications at near-ambient conditions.

Thermoelectric Materials and their typical Figure of Merits

Material	zT	at T [K]	Material	zT	at T
Bi_2Te_3	0.8 - 1.0	298	PbTe:Ti	1.0	600
Bi_2Se_3	0.8 - 1.0	298	Sb_2Te_3	1.5	700
SnSe	2.6 (b axis)	923	PEDOT:PSS	0.42	298
$\text{Mg}_2\text{Si}_{0.55-x}\text{Sn}_{0.4}\text{Ge}_{0.05}\text{Bi}_x$	1.4	800			

8.6.24. Birefringence and the Permittivity / Refractive Index Tensors

Tensor constitutive relationship: $\mathbf{D} = \boldsymbol{\epsilon}\mathbf{E}$ ($\boldsymbol{\epsilon}$: 3×3 permittivity tensor: $\boldsymbol{\epsilon} = \epsilon_0 \begin{bmatrix} n_a^2 & 0 & 0 \\ 0 & n_b^2 & 0 \\ 0 & 0 & n_c^2 \end{bmatrix}$.)

The index ellipsoid (optical indicatrix) for a birefringent crystal represents the refractive indices for different orientations of wavefronts. The principal axes are the principal refractive indices n_a, n_b, n_c . (Uniaxial: two different, Biaxial: three different)

When this ellipsoid is cut through its centre by a plane parallel to the wavefront, the resulting intersection (central / diametral section) is an ellipse whose major and minor semi-axes have lengths equal to the two refractive indices for that orientation of the wavefront, and have the directions of the respective polarizations as expressed by the electric displacement vector \mathbf{D} .

Index ellipsoid equation: $\frac{\cos^2 \xi}{n_a^2} + \frac{\cos^2 \eta}{n_b^2} + \frac{\cos^2 \zeta}{n_c^2} = \frac{1}{n^2}$

Speed: $\nu^2 = a^2 \cos^2 \xi + b^2 \cos^2 \eta + c^2 \cos^2 \zeta$

($\cos \xi, \cos \eta$ and $\cos \zeta$ are the direction cosines (Section 2.4.1) with the principal axes. The principal refractive indices can also be replaced with the relative permittivities $\sqrt{\epsilon_{ra}}, \sqrt{\epsilon_{rb}}, \sqrt{\epsilon_{rc}}$.)

Sources of birefringence, other than natural anisotropy:

- Stress-induced birefringence: transparent isotropic (linear photoelastic) materials with stress fields have refractive indices as a function of the stress state.
- Circular birefringence: chiral substances (in the chemical sense) rotate plane-polarised light in opposite directions (circular dichroism).
- Magneto-optic Faraday effect: in the presence of an external static magnetic field directed parallel to the direction of propagation, and in a permeable material medium, plane-polarised light is rotated in one direction.

8.6.25. Principal Refractive Indices for Uniaxial and Biaxial Crystal Systems

Uniaxial crystals, at 590 nm

Material	Crystal system	n_o	n_e	Δn
barium borate BaB_2O_4	trigonal	1.6776	1.5534	-0.1242
beryl $\text{Be}_3\text{Al}_2(\text{SiO}_3)_6$	hexagonal	1.602	1.557	-0.045
calcite CaCO_3	trigonal	1.658	1.486	-0.172
ice H_2O (ice I_h)	hexagonal	1.3090	1.3104	+0.0014
lithium niobate LiNbO_3	trigonal	2.272	2.187	-0.085
magnesium fluoride MgF_2	tetragonal	1.380	1.385	+0.006
quartz SiO_2	trigonal	1.544	1.553	+0.009
ruby Al_2O_3	trigonal	1.770	1.762	-0.008
rutile TiO_2	tetragonal	2.616	2.903	+0.287
sapphire Al_2O_3	trigonal	1.768	1.760	-0.008
silicon carbide SiC	hexagonal	2.647	2.693	+0.046
tourmaline (complex silicate)	trigonal	1.669	1.638	-0.031
zircon, high ZrSiO_4	tetragonal	1.960	2.015	+0.055

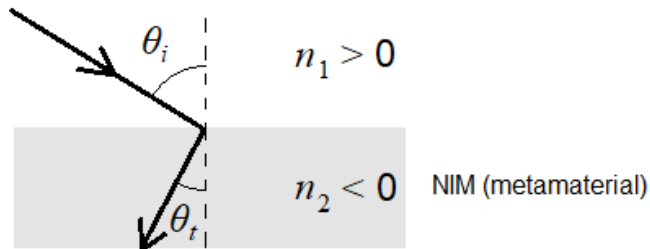
Biaxial crystals, at 590 nm

Material	Crystal system	n_α	n_β	n_γ
borax $\text{Na}_2(\text{B}_4\text{O}_5)(\text{OH})_4 \cdot 8\text{H}_2\text{O}$	mono- clinic	1.447	1.469	1.472
epsom salt $\text{MgSO}_4 \cdot 7\text{H}_2\text{O}$	mono- clinic	1.433	1.455	1.461
mica, biotite $\text{K}(\text{Mg},\text{Fe})_3(\text{AlSi}_3\text{O}_{10})(\text{F},\text{OH})_2$	mono- clinic	1.595	1.640	1.640
mica, muscovite $\text{KAl}_2(\text{AlSi}_3\text{O}_{10})(\text{F},\text{OH})_2$	mono- clinic	1.563	1.596	1.601
olivine $(\text{Mg},\text{Fe})_2\text{SiO}_4$	ortho- rhombic	1.640	1.660	1.680
perovskite CaTiO_3	ortho- rhombic	2.300	2.340	2.380
topaz $\text{Al}_2\text{SiO}_4(\text{F},\text{OH})_2$	ortho- rhombic	1.618	1.620	1.627
ulexite $\text{NaCaB}_5\text{O}_6(\text{OH})_6 \cdot 5\text{H}_2\text{O}$	triclinic	1.490	1.510	1.520

8.6.26. Metamaterials

Metamaterials are manufactured as periodic arrays of LC circuit resonators.

Ray diagram for a typical medium into a negative-index metamaterial (NIM):



$$n_2 < 0 \text{ so } n_1 \sin \theta_i = |n_2| \sin \theta_t$$

$$\text{For the metamaterial, } n_2 = -\sqrt{\epsilon_r \mu_r}$$

where effective $\epsilon < 0$ and $\mu < 0$.

Frequency of radiation remains constant.

Transmission Line Model of Metamaterials: metamaterials are left-handed ($\mathbf{E} \times \mathbf{H}$ is antiparallel to the Poynting vector) and use opposite-signed reactances in their transmission line models i.e. they have series *capacitances* and shunt *inductances* (reverse to normal materials: see Section 8.5.7).

Metamaterials constructed from arrays of split-ring resonators and conducting wires exhibit negative-index behaviour only for wavelengths of similar order to the cell size. Microwave radiation can be used with cells of ~ 1 cm. Metamaterial antennas are used for radio waves. Nanomaterials are required for visible wavelengths. Broadband metamaterials are currently under research development.

Reverse Cherenkov Radiation: when charged particles (e.g. electrons) pass through a metamaterial at speed $v > c/|n_2|$, the particle emits radiation directed *behind* it.

8.6.27. Liquid Crystals

A liquid crystal is a fluid of rod shaped molecules in which the molecules align locally along a direction vector field $\mathbf{n}(\mathbf{x})$. Examples of materials forming LCs include cholesteryl benzoate and *N*-(4-methoxybenzylidene)-4-butylaniline. Some biomolecules such as proteins and cell membranes act as LCs.

LCs may be thermotropic, lyotropic or metallotropic.

Distorsion free energy (Frank elastic energy) density for a non-chiral nematic liquid crystal:

$$\mathcal{F}_d = \frac{1}{2}K_1(\nabla \cdot \hat{\mathbf{n}})^2 + \frac{1}{2}K_2(\hat{\mathbf{n}} \cdot \nabla \times \hat{\mathbf{n}})^2 + \frac{1}{2}K_3(\hat{\mathbf{n}} \times \nabla \times \hat{\mathbf{n}})^2$$

($K_{1,2,3}$: Frank constants)

8.6.27. Summary of the Classes of Self-Powered and Functional Materials

Responsive / Functional Materials: conversion between forms of energy

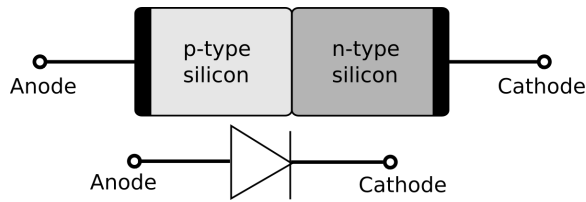
Effect	Applied stimulus	Resulting effect
Piezoelectric	Mechanical stress	Potential difference
	Potential difference	Mechanical strain
Pyroelectric	Temperature gradient (in time)	Potential difference
Thermoelectric	Temperature gradient (in space)	
Triboelectric	Friction	
Magnetoresistance	Magnetic field	Resistivity change
Photoelectric	Light	Electron radiation
Electro-optic	Electric field	Refractive index change (birefringence)
Magneto-optic	Magnetic field	
Photoelastic	Mechanical stress	
Magnetoelastic	Mechanical stress	Magnetic susceptibility change
Electrostriction	Electric field	Mechanical strain
Magnetostriction	Magnetic field	

Interactions with Electric and Magnetic Fields:

		Characteristics
Electrically conducting materials	Conductor	Carries a current proportional to the applied potential difference . Low resistivity, increases with temperature (Joule heating).
	Semiconductor	Conducts electricity above a threshold voltage . Resistivity decreases with temperature (thermal excitation of carriers into conduction band).
	Superconductor	Carries constant current when potential difference is applied once, below a critical temperature. Zero resistivity and zero magnetic permeability (fully diamagnetic).
Electrically insulating materials	Insulator	Ideally infinite resistivity, below a breakdown voltage .
	Linear polar dielectric	Has an electric polarisation proportional to the applied electric field . Constant permittivity.
	Paraelectric	Electric polarisation is nonlinearly dependent on the applied electric field with no hysteresis .
	Ferroelectric	Permanent electric polarisation with hysteresis depending on the applied electric field.
Magnetic materials	Diamagnetic	Has a magnetisation proportional to the applied magnetic field, in the same direction. Constant permeability.
	Paramagnetic	Has a magnetisation proportional to the applied magnetic field, in the opposite direction. Constant permeability.
	Ferromagnetic	Permanent magnetisation with hysteresis depending on the applied magnetic field.

8.7. Semiconductor Devices and Transistor Circuits

8.7.1. p-n Junction Representation of a Diode

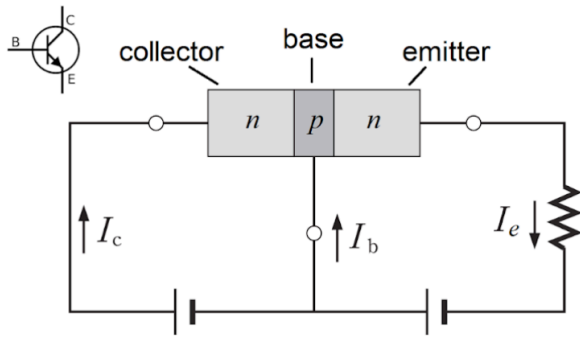


(Measurements at 25 °C.)

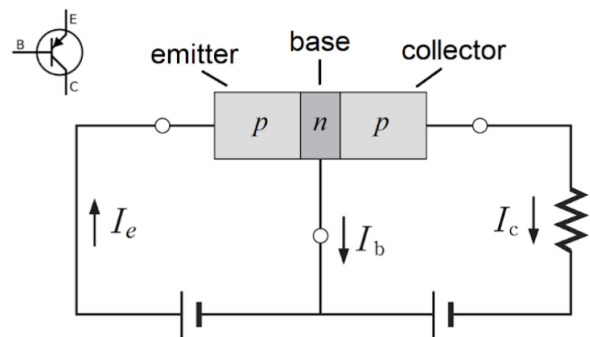
Semiconductor		Threshold voltage / V	Band gap / eV	Electron mobility / $\text{m}^2 \text{V}^{-1} \text{s}^{-1}$	Hole mobility / $\text{m}^2 \text{V}^{-1} \text{s}^{-1}$	Relative permittivity
Silicon	Si	0.7	1.12	0.16	0.05	12
Germanium	Ge	0.3	0.67	0.39	0.19	16
Gallium arsenide	GaAs	1.2	1.40	0.9	0.04	12.5
Indium antimonide	InSb	-	0.16	7.0	0.07	17

Values of the mobilities vary with temperature proportional to $T^{5/2}$ (in Kelvins).

8.7.2. p-n Junction Representation of a Bipolar Junction Transistor (BJT)



npn-type BJT



pnp-type BJT

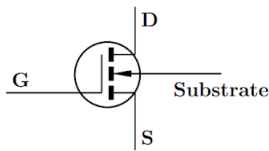
8.7.3. Modes of Operation for Insulated Gate Field-Effect Transistors (MOSFETs)

In enhancement mode, the transistor is 'off' (non-conducting) by default ($V_{GS} = 0 \rightarrow I_{DS} = 0$).

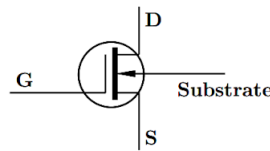
In depletion mode, the transistor is 'on' (conducting) by default ($V_{GS} = 0 \rightarrow I_{DS} \neq 0$).

In a p-channel, holes (current) flow from source to drain when on ($V_{GS} < V_{th}$)

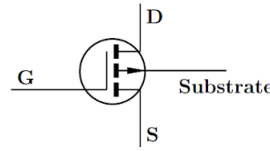
In an n-channel, electrons flow from source to drain when on ($V_{GS} > V_{th}$).



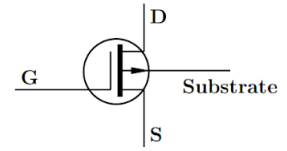
**n channel
enhancement mode**



**n channel
depletion mode**



**p channel
enhancement mode**



**p channel
depletion mode**

The circuit model is equivalent to that of the BJT (Section 8.7.2.) with

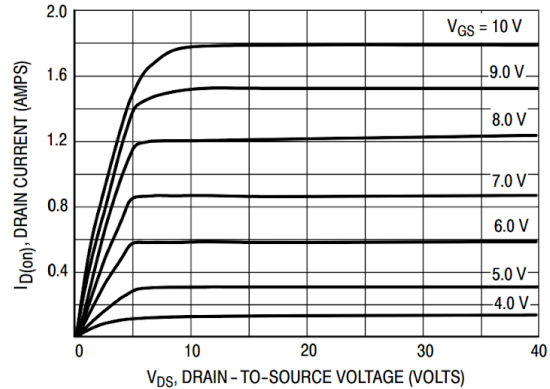
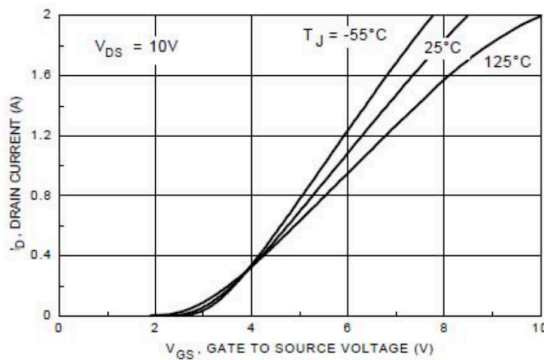
G: gate ↔ B: base; S: source ↔ E: emitter, D: drain ↔ C: collector

In many cases, the substrate is internally connected to the source electrode and is shown on the circuit symbol as such.

For the detailed structure (materials and solid state physics) of p-n junctions and related semiconductor fundamentals, see Section 8.6.5.

8.7.4. Discrete Semiconductor Devices and Characteristic Datasheets

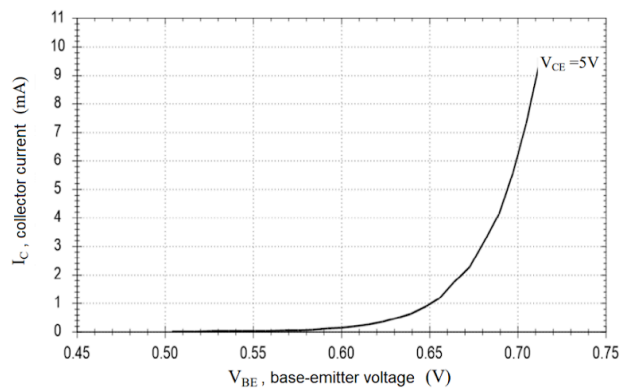
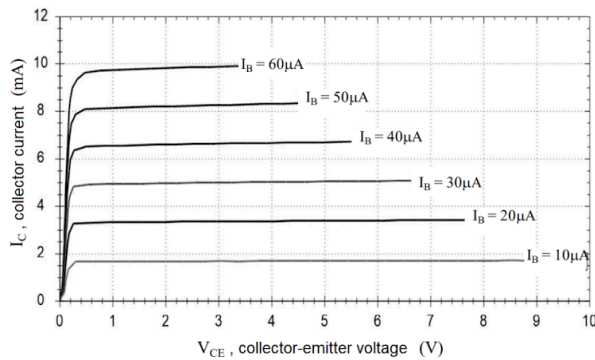
BS170 (n-Channel Enhancement Mode MOSFET): Input-Output Characteristics



Representative parameters (at 25 °C):

- Gate-source threshold voltage (pinch-off), V_{th} : 2.1 V
- Zero Gate Voltage Drain Current, I_{DSS} : 500 nA
- Mutual conductance, g_m : 370 mS
- Drain resistance, r_d : 350 Ω
- Gate-drain parasitic capacitance, C_{DG} : 30 pF
- Dissipative thermal resistance, R_{TH} : 150 K W⁻¹

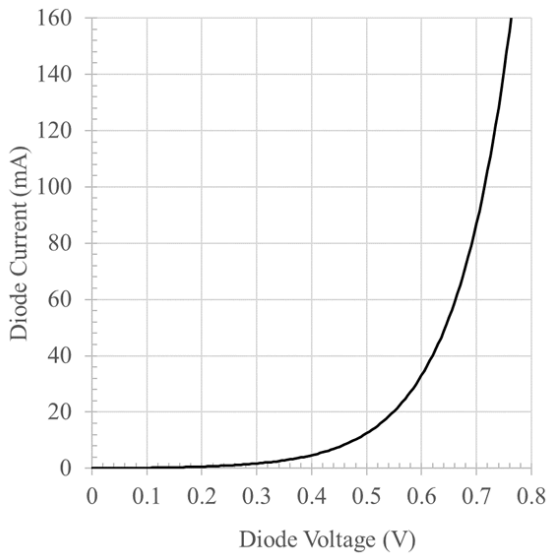
BC182L (npn-Type BJT): Input-Output Characteristics



Representative parameters (25 °C, a.c. characteristics at 1 k, $I_C = 2$ mA, $V_{CE} = 5$ V):

- Base-emitter threshold voltage (forward-bias voltage), V_{th} : 0.7 V
- Current gain, h_{FE} (DC) and h_{fe} (AC small signal): $h_{FE} = 170$, $h_{fe} = 250$
- Input impedance, h_{ie} (AC): 5 k Ω
- Output conductance, h_{oe} (AC): 50 μS
- Base-collector parasitic capacitance, C_{CB} : 8 pF

1N4001 (Silicon Diode): Voltage-Current Characteristic

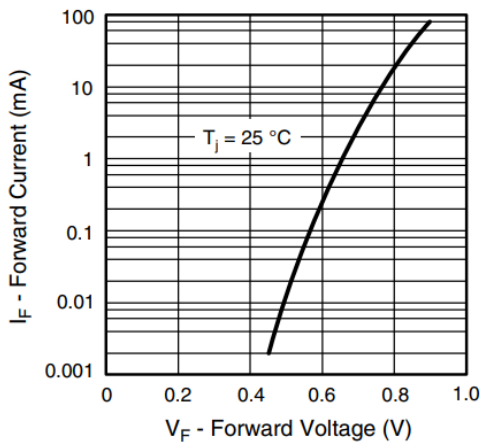


The forward-bias behaviour of a diode is modelled by the Shockley equation:

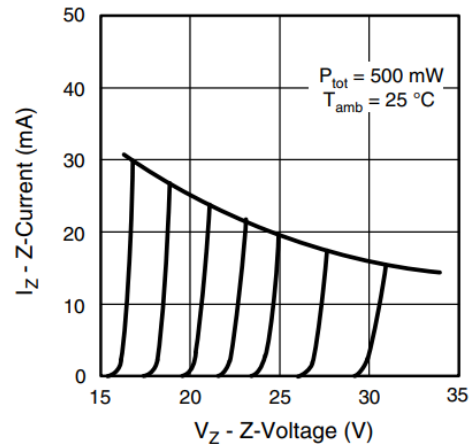
$$I = I_S \left(\exp \left(\frac{V_D}{nV_T} \right) - 1 \right)$$

(I_S : reverse bias saturation current,
 V_D : diode voltage; n : emission coefficient
 $V_T = \frac{k_B T}{|e|}$: thermal voltage)

BZX55 (Zener Diode): Voltage-Current Characteristic

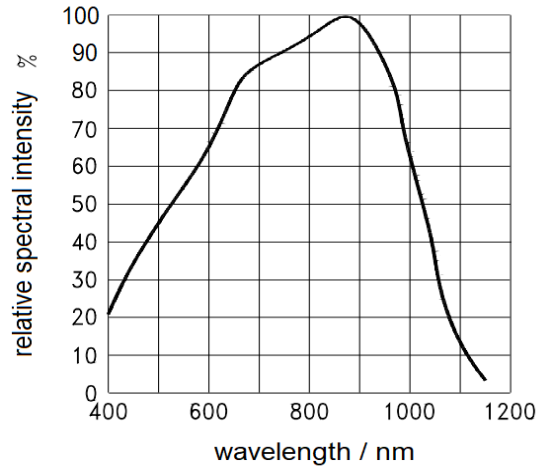
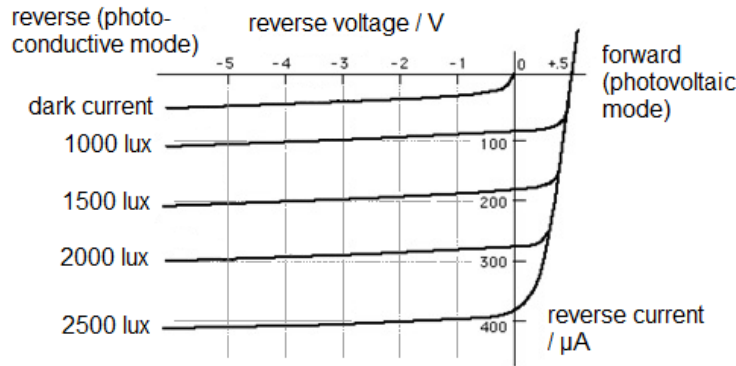


Forward bias mode



Zener (reverse bias) mode
 (rated voltages at $I_Z = 5 \text{ mA}$)

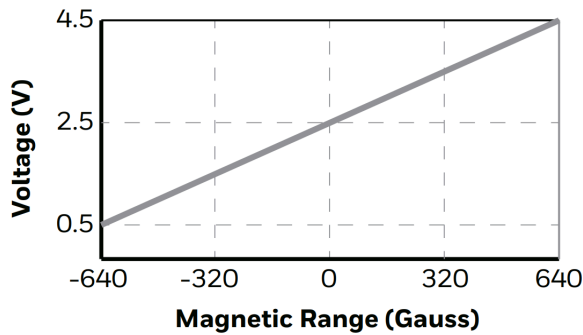
BPX65 (Photodiode): Light-Current Characteristic



(1 lux = 1 cd sr m⁻² = 7.9 mW m⁻² for sunlight)

Peak spectral sensitivity: 550 μA mW⁻¹, at 850 nm.

SS490 (Hall Effect Sensor): Field-Voltage Characteristic

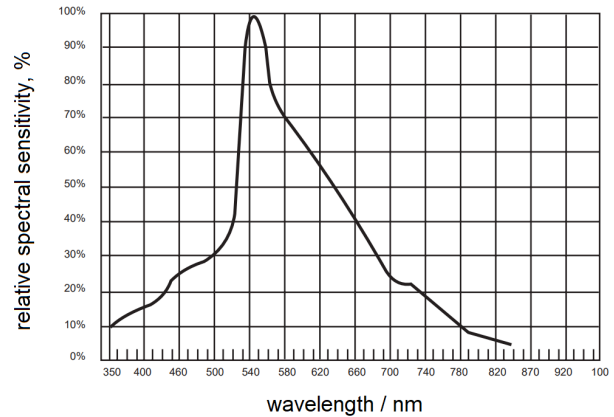
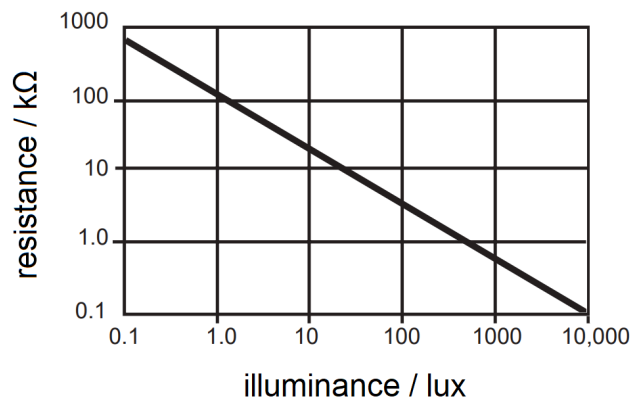


Gradient:

$$3.125 \text{ mV / Gauss} = 31.25 \text{ mV / mT}$$

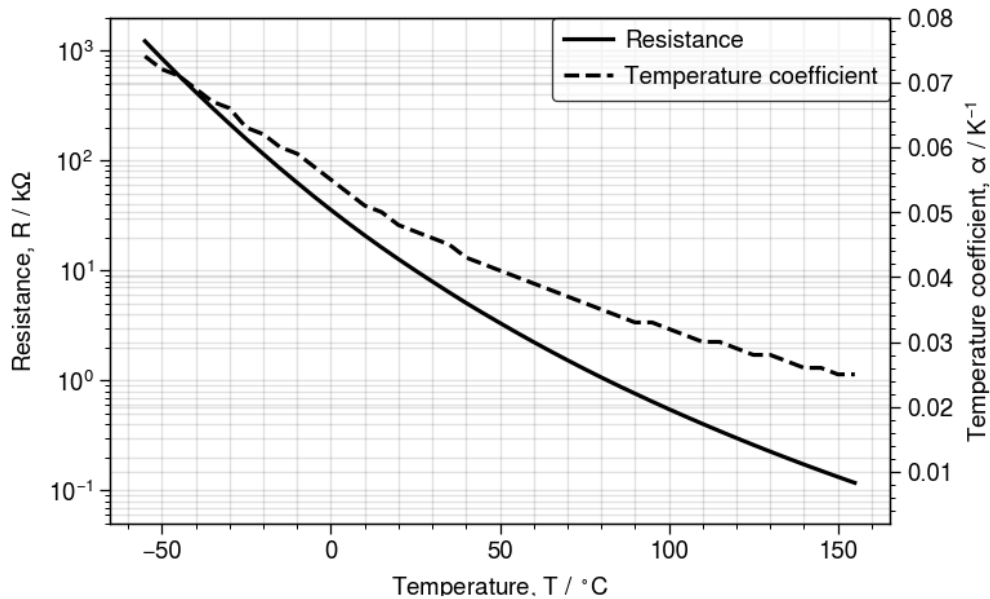
(1 Gauss = 100 microteslas (μT))

NORP12 (LDR): Light-Resistance Characteristic



$$\text{Power-law curve: } R [k\Omega] = 104.7 e^{-0.755 E_v [lux]}$$

Peak sensitivity: 550 nm.

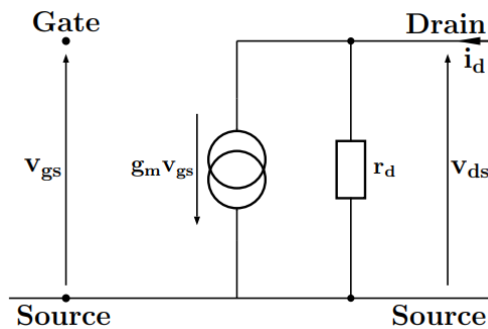
B57164K (10 kΩ NTC Thermistor): Temperature-Resistance Characteristic

$$R = R_0 \exp\left(\frac{B}{T} - \frac{B}{T_0}\right) \text{ where } (R_0, T_0) = (10 \text{ k}\Omega, 298 \text{ K}) \quad (\text{Steinhart-Hart equation})$$

At 25 °C: $R = 10 \text{ k}\Omega$, $\alpha = 0.047 \text{ K}^{-1}$, $B = 4300 \text{ K}$ ($\pm 3\%$) (B can be considered constant).

The temperature coefficient is defined as $\alpha = -\frac{1}{R} \frac{dR}{dT}$ (locally, $R = R_0(1 + \alpha \Delta T)$.)

8.7.5. AC Small-Signal Model for JFETs and MOSFETs (Hybrid-Pi Model)



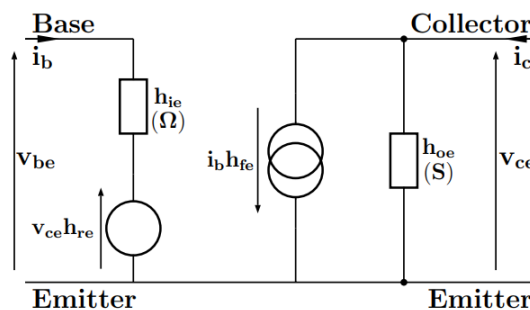
The small-signal drain current is $i_d = g_m v_{gs} + \frac{v_{ds}}{r_d}$ i.e. $g_m = \frac{\partial i_d}{\partial v_{gs}}$ and $\frac{1}{r_d} = \frac{\partial i_d}{\partial v_{ds}}$.

(g_m : mutual conductance/transconductance, r_d : drain resistance)

- To find the **input** impedance, short the **output** and find $\frac{v_x}{i_x}$ for a test **input** v_x & i_x .
- To find the **output** impedance, short the **input** and find $\frac{v_x}{i_x}$ for a test **output** v_x & i_x .
- To find the **gain**, find $\frac{v_{out}}{v_{in}}$.

It is commonly assumed that $r_d \rightarrow \infty$ (no current through it) to simplify the circuit analysis.

8.7.6. AC Small-Signal Model for BJTs (h -parameter Model)



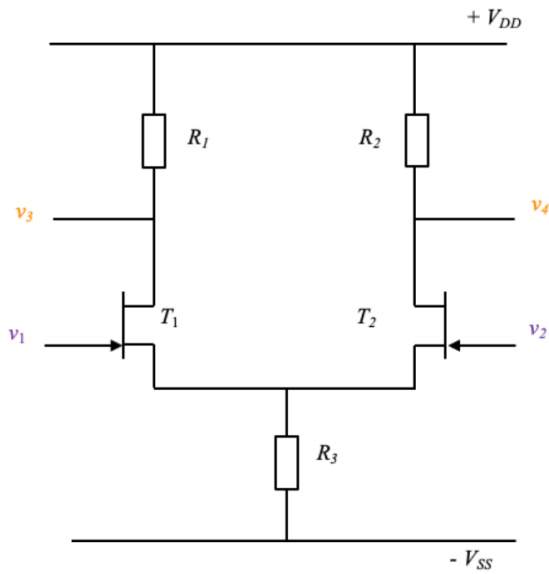
The small-signal voltages and currents are $v_{be} = h_{ie} i_b + h_{re} v_{ce}$ and $i_c = h_{fe} i_b + h_{oe} v_{ce}$

i.e. $h_{ie} = \frac{\partial v_{be}}{\partial i_b}$, $h_{re} = \frac{\partial v_{be}}{\partial v_{ce}}$, $h_{fe} = \frac{\partial i_c}{\partial i_b}$, $h_{oe} = \frac{\partial i_c}{\partial v_{ce}}$.

(h_{ie} : input resistance, h_{re} : reverse voltage transfer ratio, $h_{fe} = \beta$: forward current gain, h_{oe} : output conductance)

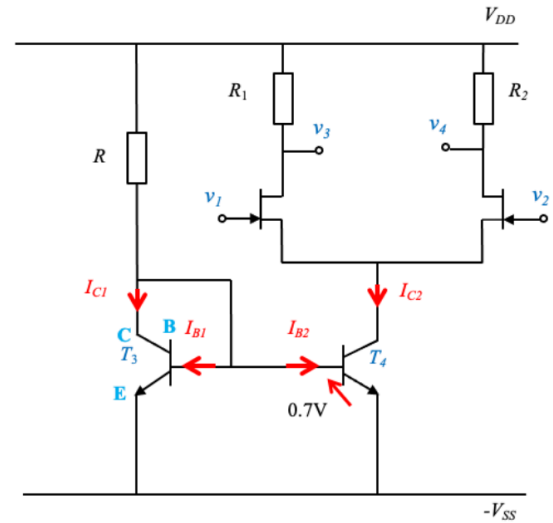
It is commonly assumed that $h_{re} \rightarrow 0$ and $h_{oe} \rightarrow 0$ to simplify the circuit analysis.

8.7.7. FET-Based Differential Amplifier and Current Mirror



Long-tailed pair:

$$v_3 - v_4 = A(v_1 - v_2)$$



R_3 replaced by current mirror:

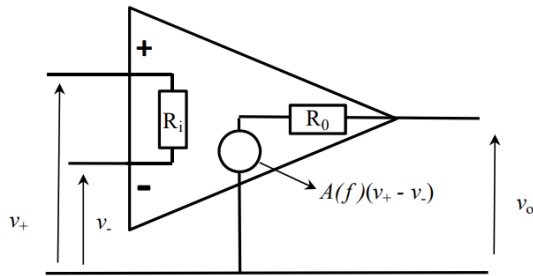
$$I_C = h_{FE} I_{B1} = h_{FE} I_{B2} \text{ and } I_{C1} = I_{C2} = \frac{V_{DD} - V_{SS} - 0.7}{R}$$

$$\text{Common Mode Rejection Ratio, CMRR} = \frac{\text{differential mode gain}}{\text{common mode gain}} = \frac{1 + 2g_m R_3 + \frac{2R_3}{r_d} + \frac{R_1}{r_d}}{1 + \frac{R_3}{r_d}}$$

which is approximately $CMRR \approx 2g_m R_3$ if $r_d \gg R_1$ and R_3 .

- In common mode, $v_1 = v_2$ and R_3 can be split into $2R_3 \parallel 2R_3$ by symmetry.
- In differential mode, $v_1 = -v_2$ and the FET sources are small-signal grounded.

8.7.8. Operational Amplifier (Op-Amp) Circuits



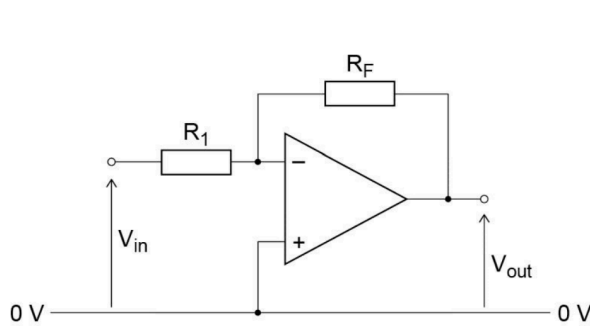
Input resistance: R_i Output resistance: R_o
 Open-loop gain: A (ideally infinite)

Ideal Comparator (without hysteresis):

$$V_{out} = \begin{cases} V_{--}, & \text{if } V_+ > V_- \\ V_{++}, & \text{if } V_+ < V_- \end{cases}$$

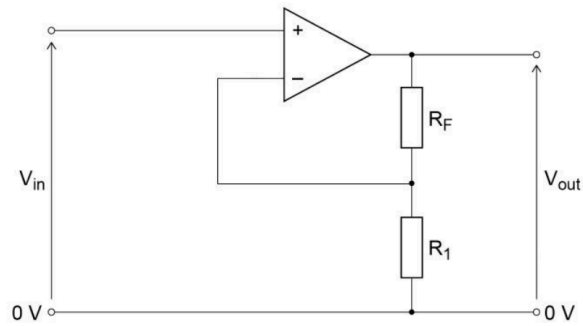
(The power supply rails, V_{--} and V_{++} are omitted.)

Some common op-amp circuits with resistive feedback are:



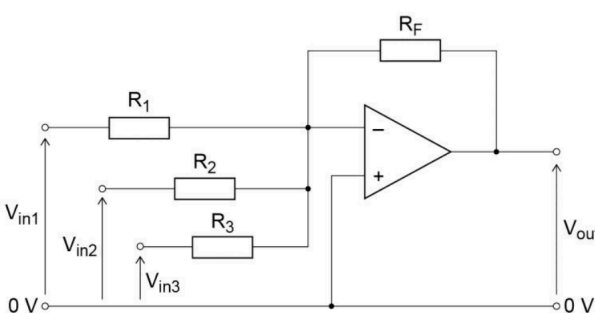
Inverting Amplifier

$$\frac{V_{out}}{V_{in}} = - \frac{R_F}{R_1}$$



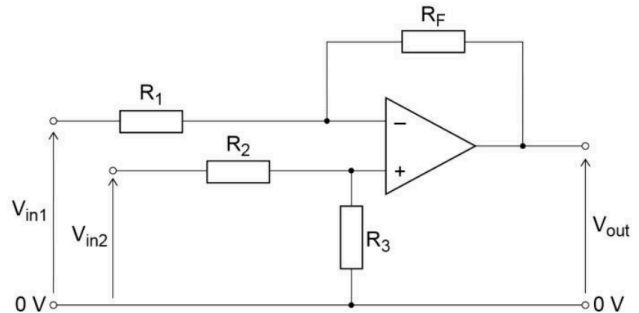
Non-Inverting Amplifier

$$\frac{V_{out}}{V_{in}} = 1 + \frac{R_F}{R_1}$$



Summing Amplifier

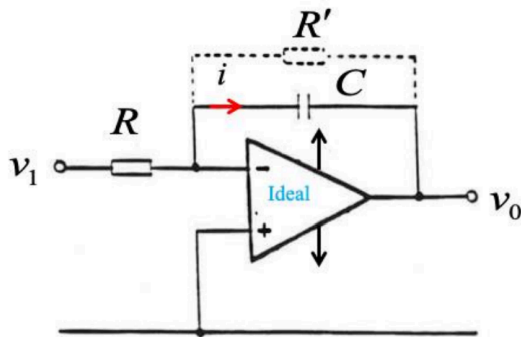
$$V_{out} = - R_F \left(\frac{V_{in1}}{R_1} + \frac{V_{in2}}{R_2} + \frac{V_{in3}}{R_3} \right)$$



Difference Amplifier

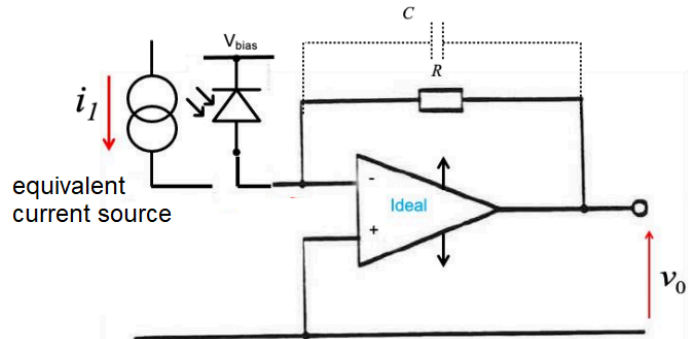
$$V_{out} = \frac{R_3}{R_2} V_{in2} - \frac{R_F}{R_1} V_{in1}$$

Some common op-amp circuits with more complex feedback are:



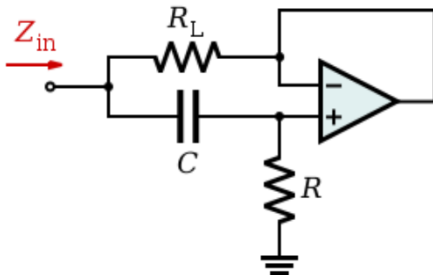
Integrator

$$v_o = \frac{-1}{RC} \int_0^t v_{in} dt$$



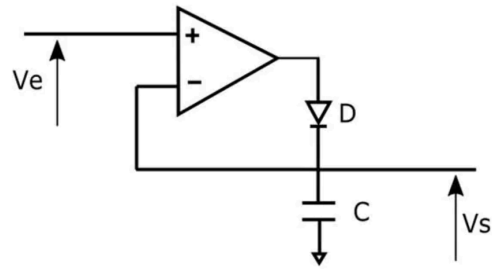
Transimpedance Amplifier

$$\frac{v_o}{i_1} = -R$$



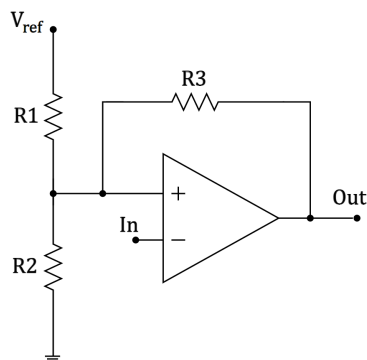
Gyrator

$$Z_{in} = R_L || j\omega R R_L C$$



Peak Detector

$$V_s = \max \{V_e\}$$

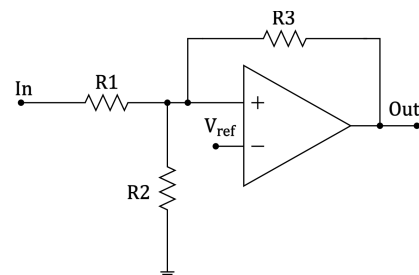


Schmitt Trigger (inverting)

Inverting comparator with hysteresis

$$V_{\text{thresh}}^{(\text{high})} = \frac{R_2(R_3 V_{\text{ref}} + R_1 V_{\text{out}}^{(\text{high})})}{R_2 R_3 + R_1 R_2 + R_1 R_3},$$

$$V_{\text{thresh}}^{(\text{low})} = \frac{R_2(R_3 V_{\text{ref}} + R_1 V_{\text{out}}^{(\text{low})})}{R_2 R_3 + R_1 R_2 + R_1 R_3}$$



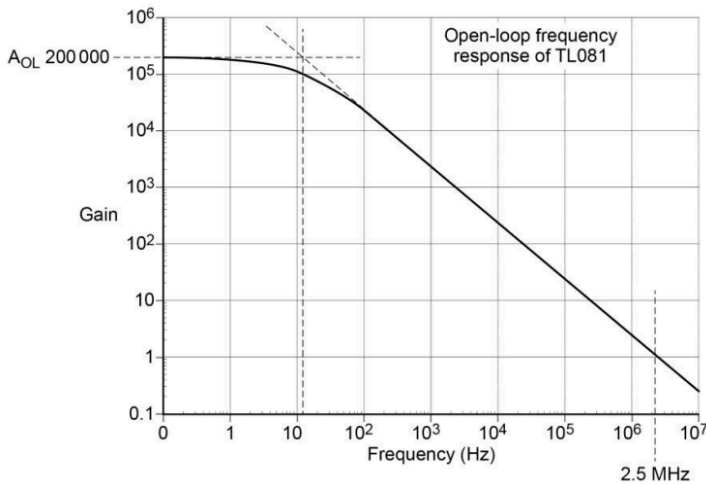
Schmitt Trigger (non-inverting)

Comparator with hysteresis

$$V_{\text{thresh}}^{(\text{high})} = V_{\text{ref}} + R_1 \left(\frac{V_{\text{ref}} - V_{\text{out}}^{(\text{low})}}{R_3} + \frac{V_{\text{ref}}}{R_2} \right)$$

$$V_{\text{thresh}}^{(\text{low})} = V_{\text{ref}} - R_1 \left(\frac{V_{\text{out}}^{(\text{high})} - V_{\text{ref}}}{R_3} - \frac{V_{\text{ref}}}{R_2} \right)$$

TL081 (Op-Amp) Open-Loop Frequency Response



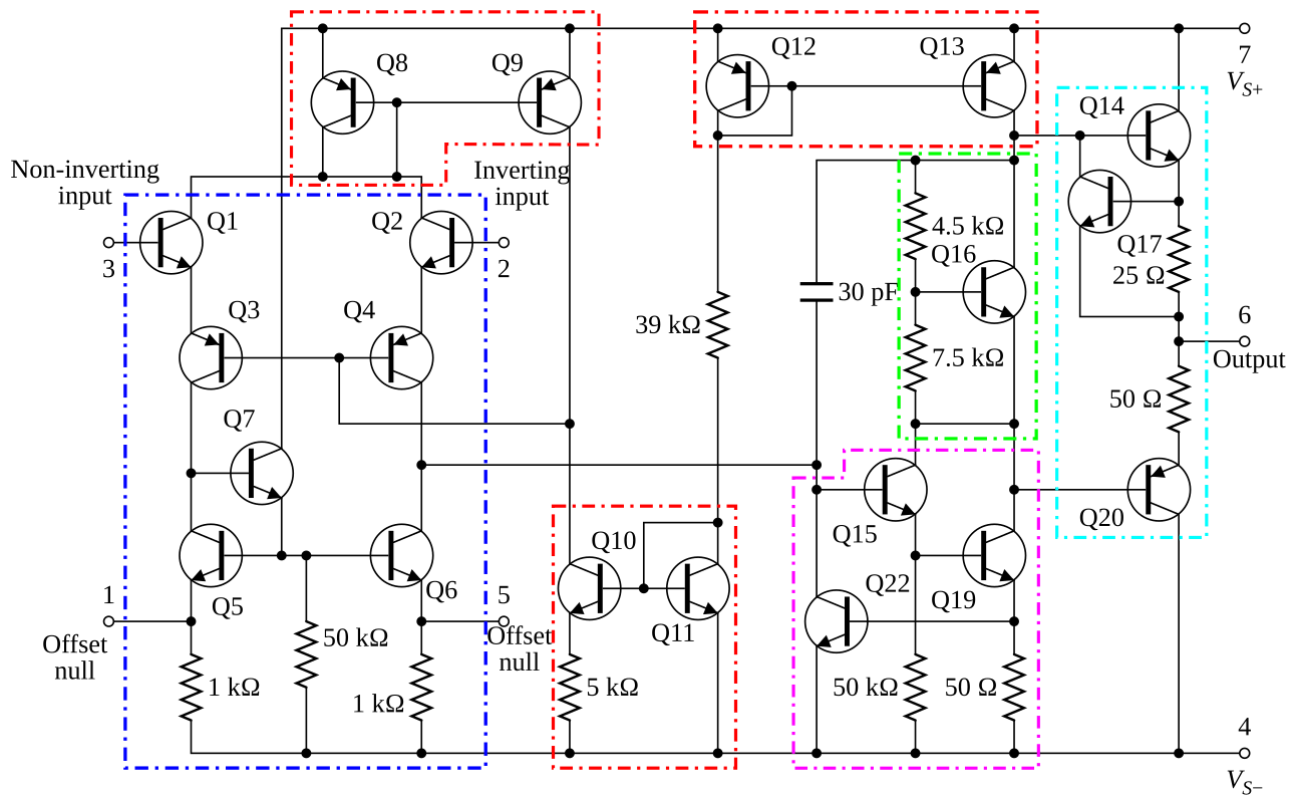
For finite gain amplifiers, $V_{out} = A(V_+ - V_-)$

Gain-Bandwidth product: $A(f) \times f_2 = constant$

$A(f) = (low\ freq.\ cut\ off, f_1) \times A_o \times (high\ freq.\ cut\ off, f_2)$

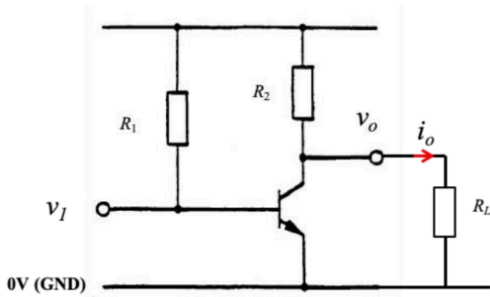
$$A(f) = \left(\frac{1}{1 + \frac{f_1}{jf}} \right) A_o \left(\frac{1}{1 + \frac{jf}{f_2}} \right)$$

Component-Level Diagram of 741 Op-Amp (LM741) Integrated Circuit



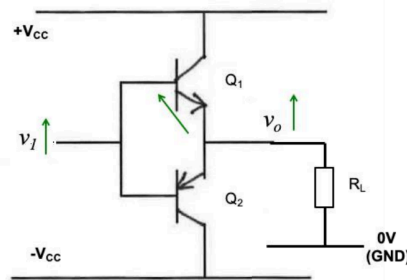
current mirrors differential amplifier class A gain stage
voltage level shifter output level stage

8.7.9. Power Amplifiers and CMOS Logic



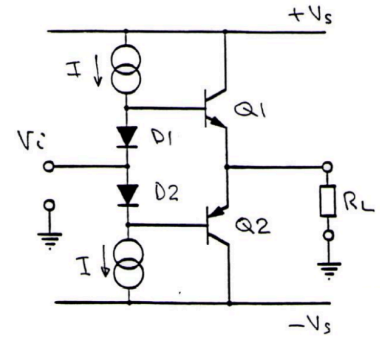
Class A

Common Source
Amplifier



Class B

Complementary
Emitter Follower



Class AB

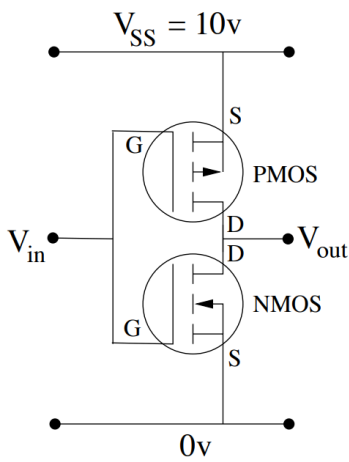
Biased Complementary
Emitter Follower

For the logic applications of complementary metal-oxide semiconductors (CMOS), see Section 9.1.1.

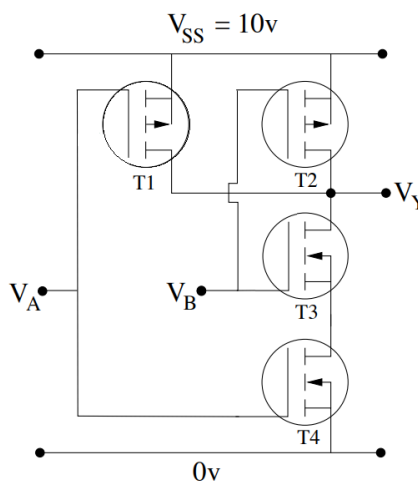
P9. DIGITAL ELECTRONICS, INSTRUMENTATION AND CONTROL

9.1. Digital Electronics

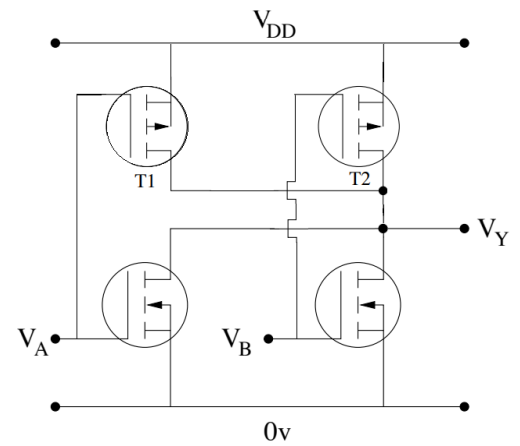
9.1.1. CMOS Circuits for Logic Gates



CMOS NOT Gate
(Inverter)



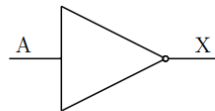
CMOS NAND Gate



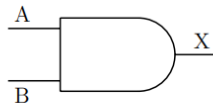
CMOS NOR Gate

9.1.2. Logic Gate Notation

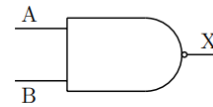
Logic gates:



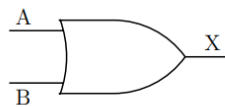
NOT: $X = \bar{A}$



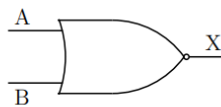
AND: $X = A \cdot B$



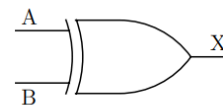
NAND: $X = \overline{A \cdot B}$



OR: $X = A + B$



NOR: $X = \overline{A + B}$



EXCLUSIVE OR: $X = A\bar{B} + \bar{A}B$

9.1.3. Boolean Algebra Identities and Combinational Logic Design

Simple identities: $A \cdot \bar{A} = 0$, $A \cdot A = A$, $A \cdot 0 = 0$, $A \cdot 1 = A$
 $A + \bar{A} = 1$, $A + A = A$, $A + 0 = A$, $A + 1 = 1$

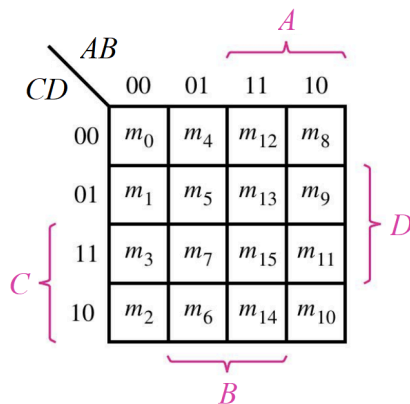
De Morgan's theorems: $\overline{A + B} = \bar{A} \cdot \bar{B}$ $\overline{A \cdot B} = \bar{A} + \bar{B}$

Inversion from NAND / NOR: $\bar{A} = \overline{A \cdot A} = \overline{A + A}$

XOR: $A \oplus B = A \cdot \bar{B} + \bar{A} \cdot B$

XNOR: $A \odot B = \overline{A \oplus B} = A \cdot B + \bar{A} + \bar{B}$

Karnaugh maps (K-maps): enumerated input states form a Gray code



← Typical 4-variable Karnaugh map for $m = f(A, B, C, D)$

For a NAND circuit, find a sum-of-products expression for the output (covering all **1**'s in the map), then apply De Morgan's theorem. Use $\bar{A} = \overline{A \cdot A}$ for inverters.

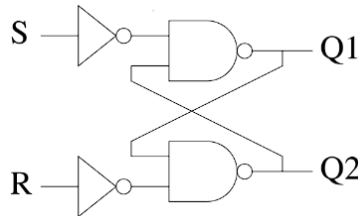
For a NOR circuit, find a sum-of-products expression for the **inverse** of the output (covering all **0**'s in the map), then apply De Morgan's theorem. Use $\bar{A} = \overline{A + A}$ for inverters.

Hazards:

- **Static 1-hazard:** a momentary single erroneous $1 \rightarrow 0 \rightarrow 1$ transition, occurring when sum-of-products terms for the **output** (1) do not overlap.
- **Static 0-hazard:** a momentary single erroneous $0 \rightarrow 1 \rightarrow 0$ transition, occurring when sum-of-products terms for the **inverse** (0) of the output do not overlap.
- **Dynamic hazard:** twice-repeated static hazards within the same transition period, resulting in an incorrect final state.
- Propagation delay: equal to the delay of a single gate times the maximum number of nested logic gate operations.
- Static hazards can be removed by ensuring all sum-of-products overlap on the Karnaugh map.
- If there are no static hazards, then there can be no dynamic hazards.

9.1.4. Bistable Circuits

Set-Reset Bistable (SR Flip-Flop): S turns Q_1 on (and Q_2 off); R turns Q_1 off (and Q_2 on).



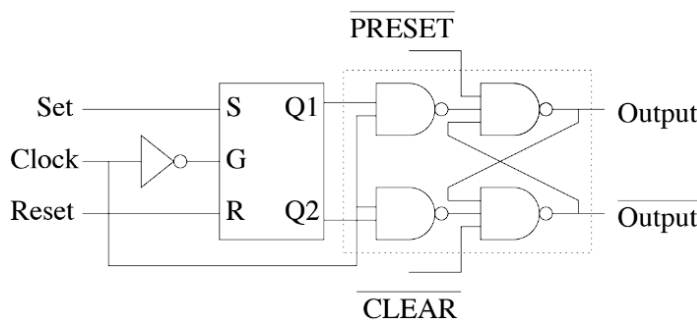
The outputs remain even when inputs return to $S = 0$ and/or $R = 0$. State $S = R = 1$ is not allowed (race condition).

Outputs: $Q_1 = \overline{\overline{S} \cdot Q_2} = S + \overline{Q_2}$ and $Q_2 = \overline{\overline{R} \cdot Q_1} = R + \overline{Q_1}$.

The SR-bistable can be used to mitigate contact debouncing from mechanical switches.

The **gated SR bistable** has inputs $\overline{S} = \overline{S \cdot G}$ and $\overline{R} = \overline{R \cdot G}$ where G is a clock (CLK), where the output can only change when the CLK is high (synchronous circuit).

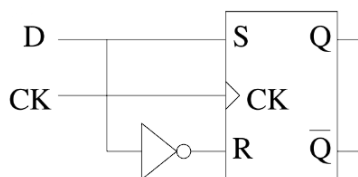
Master-Slave Bistable: two clock-gated SR bistables in series with manual override



The 'master' (first) bistable is synchronous and controls the 'slave' (second) bistable.

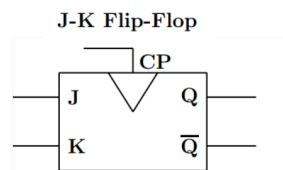
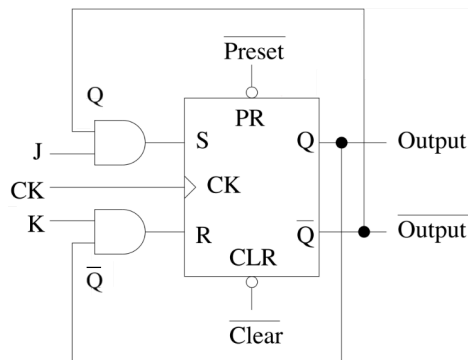
Preset and clear inputs in the slave SR bistable allow for asynchronous override. These are 'active low' signals.

D-type Latch (Data Latch; Delay Latch): output Q follows D , synchronised to a clock



Single-input clocked SR bistable, $Q = D$ when the clock rises.

JK-Bistable (JK Flip Flop): same function as SR, but now $J = K = 1$ swaps the outputs.



Excitation table			
Q_n	Q_{n+1}	J	K
0	0	0	X
0	1	1	X
1	1	X	0
1	0	X	1

Truth table		
J_n	K_n	Q_{n+1}
0	0	Q_n
0	1	0
1	0	1
1	1	$\overline{Q_n}$

Constructed using a master-slave SR bistable with output feedback.

(J : 'set' input, K : 'reset' input, CP: clock pulse, Q_n : current state, Q_{n+1} : next state, X: 'don't care' state)

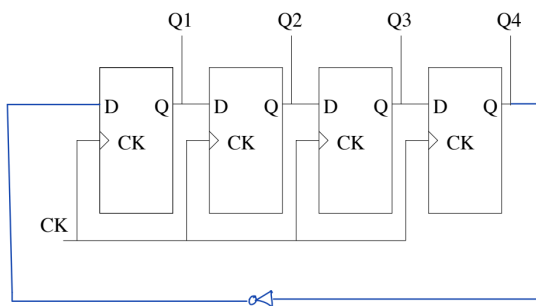
9.1.5. Sequential Logic Design using JK Bistables

General procedure for synchronous logic design using J-K flip-flops (bistables) and logic gates:

($J/K_i^{(n)}$: i th bistable input J/K at time step n , $Q_i^{(n)}$: i th bistable output at time step n ,
 A_i : input variable i , P_i : output variable i .)

1. Draw the **State Transition Diagram**, for each state identifying the output variables, input variables, and transitions.
2. Enumerate the states and allocate JK bistables to each state.
3. Draw the **State Transition Table**, consisting of the current bistable outputs $Q_i^{(n)}$, the current input variables A_i and the resulting next state $Q_i^{(n+1)}$. Use the excitation table to find the required bistable inputs, $J_i^{(n+1)}$ and $K_i^{(n+1)}$ to change $Q_i^{(n)}$ into $Q_i^{(n+1)}$.
4. Determine the input circuit logic for each input J_i and K_i as functions of the bistable outputs $Q_i^{(n)}$ and the inputs A_i , using **Karnaugh maps**.
5. Determine the output circuit logic to convert bistable outputs $Q_i^{(n)}$ to the outputs P_i .

9.1.6. Counting Circuits Using D-Type Latches

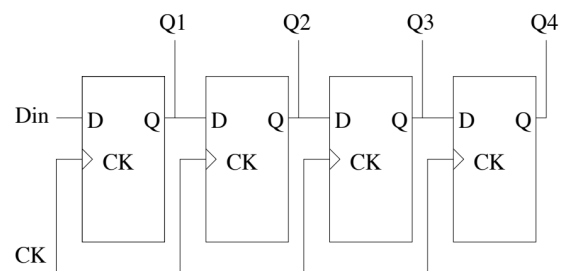


Johnson Counter

The number $Q_4Q_3Q_2Q_1$ increments in binary at every clock cycle.

Can also be made with JK bistables (**ripple counter**).

Additional logic can result in modulo n counters.



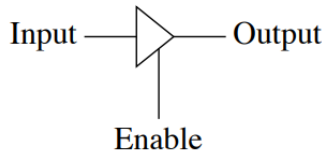
Shift Register

Each output is sequentially retimed and delayed.

Used for parallel loading to a serial data stream (serial data link).

9.1.7. Tri-State Buffer

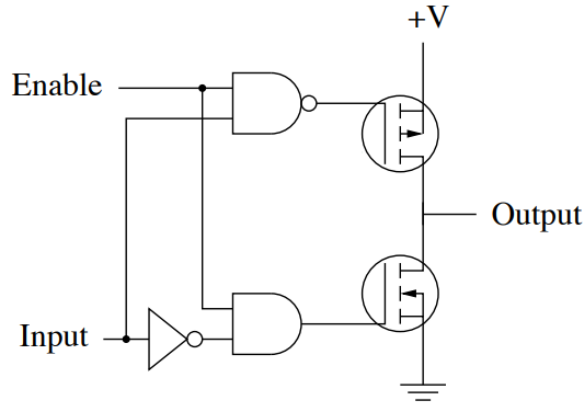
Symbol:



Truth Table:

Enable	Input	Output
0	0	floating
0	1	floating
1	0	0
1	1	1

CMOS circuitry implementation of tri-state buffer:



Note that some tri-state buffers may be 'active low' on the enable pin, which are indicated with a small circle.

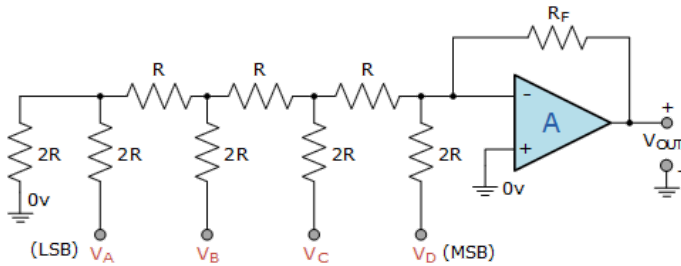
9.1.8. Full Adder

If S is the result bit and C_{in} is the input carry bit (initialised to 0), then $A + B$ is computed by

- $S = A \oplus B \oplus C_{in}$
- $C_{out} = A \cdot B + (A \oplus B) \cdot C_{in}$

If the remaining (most significant) carry bit is ignored, then these expressions are also valid for two's complement representations of negative numbers (Section 8.8.2.), which can compute effective subtraction.

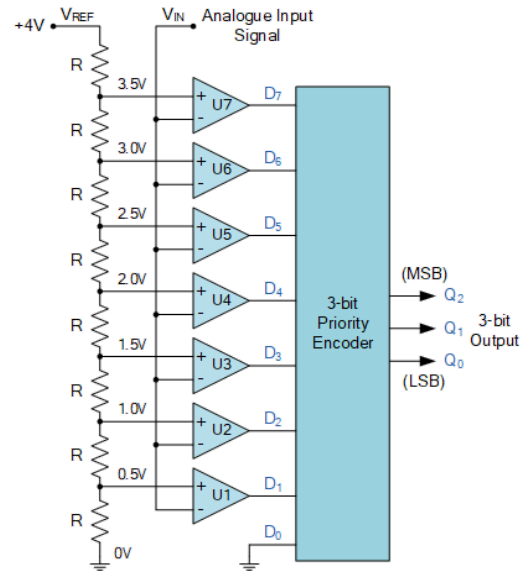
9.1.9. Digital and Analogue Conversion



Digital to Analogue

4-bit R - $2R$ ladder DAC

$$V_{out} = \frac{-R_F}{R} \times \frac{1}{2^n} \sum_{i=1}^n 2^i V_i$$



Analogue to Digital

3-bit flash ADC

Maximum input voltage V_{REF}

The flash ADC requires large numbers of comparators and resistors for high-bit resolution. An alternative is the 'stair-step ADC', which uses a divide by 2^n counter, DAC and Schmitt trigger, but is slower.

9.2. Computer Engineering and Communications

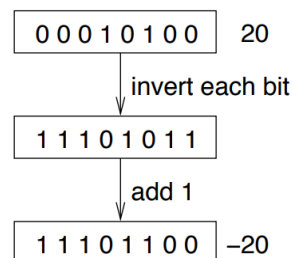
9.2.1. Decimal - Hexadecimal - ASCII Character Conversion

DEC	HEX	ASCII	DEC	HEX	ASCII	DEC	HEX	ASCII	DEC	HEX	ASCII
0	00	^@	32	20	SPACE	64	40	@	96	60	`
1	01	^A	33	21	!	65	41	A	97	61	a
2	02	^B	34	22	"	66	42	B	98	62	b
3	03	^C	35	23	#	67	43	C	99	63	c
4	04	^D	36	24	\$	68	44	D	100	64	d
5	05	^E	37	25	%	69	45	E	101	65	e
6	06	^F	38	26	&	70	46	F	102	66	f
7	07	^G	39	27	'	71	47	G	103	67	g
8	08	^H	40	28	(72	48	H	104	68	h
9	09	^I	41	29)	73	49	I	105	69	i
10	0A	^J	42	2A	*	74	4A	J	106	6A	j
11	0B	^K	43	2B	+	75	4B	K	107	6B	k
12	0C	^L	44	2C	,	76	4C	L	108	6C	l
13	0D	^M	45	2D	-	77	4D	M	109	6D	m
14	0E	^N	46	2E	.	78	4E	N	110	6E	n
15	0F	^O	47	2F	/	79	4F	O	111	6F	o
16	10	^P	48	30	0	80	50	P	112	70	p
17	11	^Q	49	31	1	81	51	Q	113	71	q
18	12	^R	50	32	2	82	52	R	114	72	r
19	13	^S	51	33	3	83	53	S	115	73	s
20	14	^T	52	34	4	84	54	T	116	74	t
21	15	^U	53	35	5	85	55	U	117	75	u
22	16	^V	54	36	6	86	56	V	118	76	v
23	17	^W	55	37	7	87	57	W	119	77	w
24	18	^X	56	38	8	88	58	X	120	78	x
25	19	^Y	57	39	9	89	59	Y	121	79	y
26	1A	^Z	58	3A	:	90	5A	Z	122	7A	z
27	1B	^[59	3B	;	91	5B	[123	7B	{
28	1C	^\	60	3C	<	92	5C	\	124	7C	
29	1D	^]	61	3D	=	93	5D]	125	7D	}
30	1E	^^	62	3E	>	94	5E	^	126	7E	~
31	1F	^_	63	3F	?	95	5F	_	127	7F	DEL

9.2.2. Binary Representation of Negative Numbers - Two's Complement

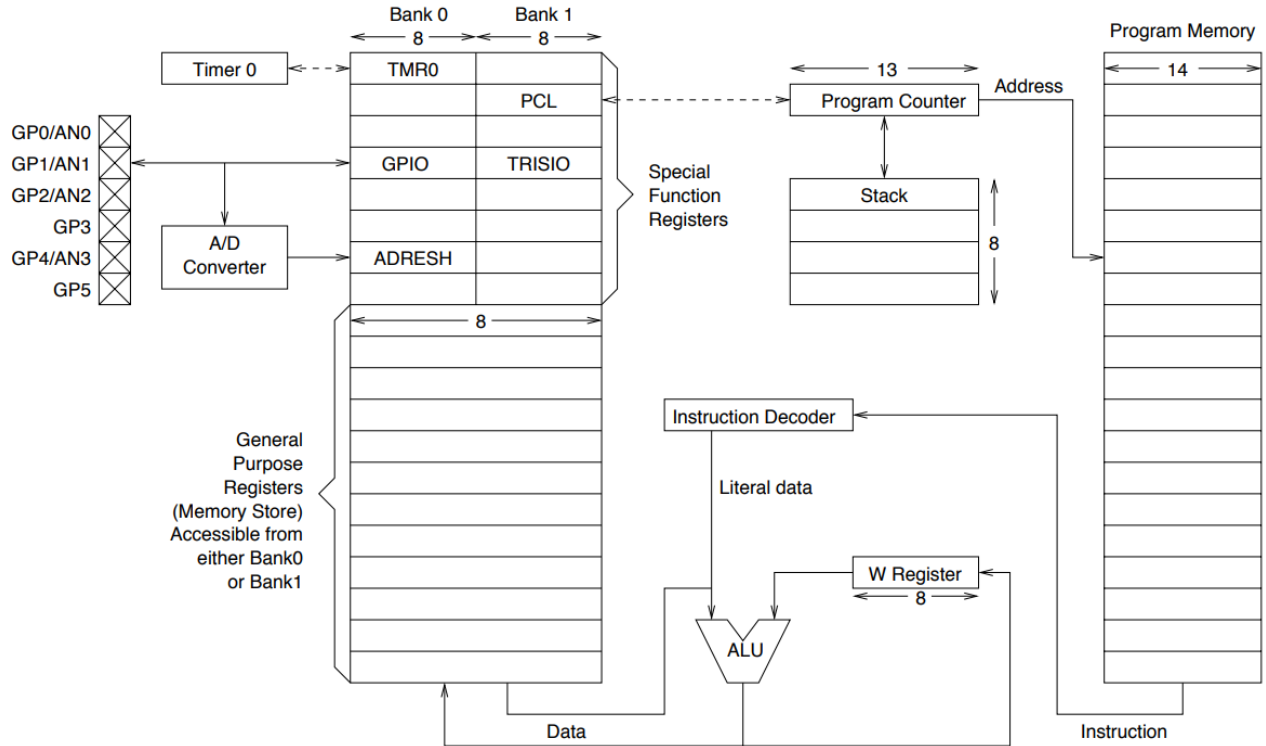
00000011	3
00000010	2
00000001	1
00000000	0
11111111	-1
11111110	-2
11111101	-3

To obtain a negative number:



9.2.3. Schematic of PIC Microprocessor

The PIC microprocessor is based on a Harvard architecture.



Special registers:

<p>GPIO Register (register location 0x05, bank 0)</p> <table border="1" style="width: 100%; text-align: center;"> <tr> <td style="width: 10%;">U-0</td> <td style="width: 10%;">U-0</td> <td style="width: 10%;">R/W-x</td> <td style="width: 10%;">R/W-x</td> <td style="width: 10%;">R/W-x</td> <td style="width: 10%;">R/W-x</td> <td style="width: 10%;">R/W-x</td> <td style="width: 10%;">R/W-x</td> </tr> <tr> <td style="border: none;">---</td> <td style="border: none;">---</td> <td>GPIO5</td> <td>GPIO4</td> <td>GPIO3</td> <td>GPIO2</td> <td>GPIO1</td> <td>GPIO0</td> </tr> <tr> <td colspan="2">bit 7</td> <td colspan="4"></td> <td colspan="2">bit 0</td> </tr> </table> <p>Bits 0-5 General purpose input or outputs (NB GPIO3 can only be an input) Bit 6-7 Unimplemented (read as 0)</p>	U-0	U-0	R/W-x	R/W-x	R/W-x	R/W-x	R/W-x	R/W-x	---	---	GPIO5	GPIO4	GPIO3	GPIO2	GPIO1	GPIO0	bit 7						bit 0		<p>TRISIO Register (register location 0x85, bank 1)</p> <table border="1" style="width: 100%; text-align: center;"> <tr> <td style="width: 10%;">U-0</td> <td style="width: 10%;">U-0</td> <td style="width: 10%;">R/W-x</td> <td style="width: 10%;">R/W-x</td> <td style="width: 10%;">R-1</td> <td style="width: 10%;">R/W-x</td> <td style="width: 10%;">R/W-x</td> <td style="width: 10%;">R/W-x</td> </tr> <tr> <td style="border: none;">---</td> <td style="border: none;">---</td> <td>TRISIO5</td> <td>TRISIO4</td> <td>TRISIO3</td> <td>TRISIO2</td> <td>TRISIO1</td> <td>TRISIO0</td> </tr> <tr> <td colspan="2">bit 7</td> <td colspan="4"></td> <td colspan="2">bit 0</td> </tr> </table> <p>Bits 0-5 Set (=1) means equivalent GPIO pin is input Clear (=0) means equivalent GPIO pin is output NB TRISIO3 is always 1 Bit 6-7 Unimplemented (read as 0)</p>	U-0	U-0	R/W-x	R/W-x	R-1	R/W-x	R/W-x	R/W-x	---	---	TRISIO5	TRISIO4	TRISIO3	TRISIO2	TRISIO1	TRISIO0	bit 7						bit 0	
U-0	U-0	R/W-x	R/W-x	R/W-x	R/W-x	R/W-x	R/W-x																																										
---	---	GPIO5	GPIO4	GPIO3	GPIO2	GPIO1	GPIO0																																										
bit 7						bit 0																																											
U-0	U-0	R/W-x	R/W-x	R-1	R/W-x	R/W-x	R/W-x																																										
---	---	TRISIO5	TRISIO4	TRISIO3	TRISIO2	TRISIO1	TRISIO0																																										
bit 7						bit 0																																											
<p>STATUS Register (register location 0x03, bank 0)</p> <table border="1" style="width: 100%; text-align: center;"> <tr> <td style="width: 10%;">IRP</td> <td style="width: 10%;">RP1</td> <td style="width: 10%;">RP0</td> <td style="width: 10%;">TO</td> <td style="width: 10%;">PD</td> <td style="width: 10%;">Z</td> <td style="width: 10%;">DC</td> <td style="width: 10%;">C</td> </tr> <tr> <td colspan="2">bit 7</td> <td colspan="4"></td> <td colspan="2">bit 0</td> </tr> </table> <p>C Carry Flag DC Digital Carry Flag Z Zero Flag PD Power Down TO Time Out RP0 Register Bank (0 sets bank 0, 1 sets bank 1) RP1 Not Used IRP Not Used</p>	IRP	RP1	RP0	TO	PD	Z	DC	C	bit 7						bit 0		<p>Other Registers</p> <p>W Working register PC Programme Counter (13 bits, using PCL, 0x02, for lower 8 bits and PCLATH, 0x0A, for upper 5 bits) FSR File select register (0x04, bank 0) INDF Indirect file register (used for indirect addressing) - doesn't have a physical address</p>																																
IRP	RP1	RP0	TO	PD	Z	DC	C																																										
bit 7						bit 0																																											

9.2.4. PIC Microprocessor Instruction Set

File Register Instructions that operate with whole bytes:

mnemonic	args	Description	Cycles	Opcode			
addwf	F,d	Add W and F and store the result in <i>d</i>	1	00	0111	dfff	ffff
andwf	F,d	AND W and F and store the result in <i>d</i>	1	00	0101	dfff	ffff
clrf	F	Clear F	1	00	0001	1fff	ffff
comf	F,d	Complement F and store the result in <i>d</i>	1	00	1001	dfff	ffff
decf	F,d	Decrement F and store the result in <i>d</i>	1	00	0011	dfff	ffff
decfsz	F,d	Decrement F and store the result in <i>d</i> , if the result is zero then skip the next instruction	1(2)	00	1011	dfff	ffff
incf	F,d	Increment F and store the result in <i>d</i>	1	00	1010	dfff	ffff
incfsz	F,d	Increment F and store the result in <i>d</i> , if the result is zero then skip the next instruction	1(2)	00	1111	dfff	ffff
iorwf	F,d	Inclusive OR W with F and store the result in <i>d</i>	1	00	0100	dfff	ffff
movf	F,d	Copy F to <i>d</i> (<i>d</i> = F)	1	00	1000	dfff	ffff
movwf	F	Copy W to F (F = W)	1	00	0000	1fff	ffff
rlf	F,d	Rotate F left through Carry and store the result in <i>d</i>	1	00	1101	dfff	ffff
rrf	F,d	Rotate F right through Carry and store the result in <i>d</i>	1	00	1100	dfff	ffff
subwf	F,d	Subtract W from F and store the result in <i>d</i>	1	00	0010	dfff	ffff
swapf	F,d	Swap low and high 4 bits of F and store the result in <i>d</i>	1	00	1110	dfff	ffff
xorwf	F,d	Exclusive OR W with F and store the result in <i>d</i>	1	00	0110	dfff	ffff

File Register Instructions that operate with bits:

addlw	Q	Add Q to W and store the result in W	1	11	111x	qqqq	qqqq
andlw	Q	AND Q with W and store the result in W	1	11	1001	qqqq	qqqq
iorlw	Q	Inclusive OR Q with W and store the result in W	1	11	1000	qqqq	qqqq
movlw	Q	Copy Q to W (W=Q)	1	11	00xx	qqqq	qqqq
retlw	Q	Return from Subroutine (Pull program counter from stack and Copy Q to W (W=Q))	2	11	01xx	qqqq	qqqq
sublw	Q	Subtract W from Q and store the result in W	1	11	110x	qqqq	qqqq
xorlw	Q	Exclusive OR Q with W and store the result in W	1	11	1010	qqqq	qqqq

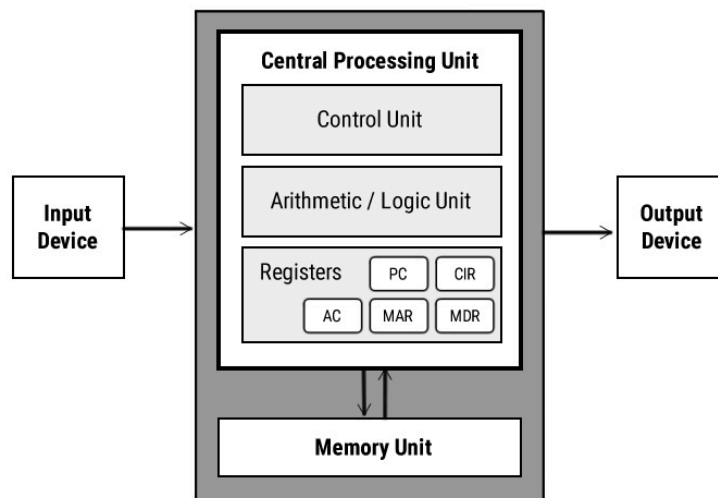
Call and Goto:

call	P	Push program counter onto the stack and Jump to program location P	2	10	0ppp	pppp	pppp
goto	P	Jump to program location P	2	10	1ppp	pppp	pppp

Instructions with no arguments:

clrw		Clear W (W=0)	1	00	0001	0xxx	xxxx
clrwtd		Clear Watchdog timer (if the watchdog timer overflows, the PIC is reset)	1	00	0000	0110	0100
nop		No operation	1	00	0000	0xx0	0000
retfie		Return from interrupt (Pull program counter from stack and enable interrupts)	2	00	0000	0000	1001
return		Return from subroutine (Pull program counter from stack)	2	00	0000	0000	1000
sleep		Go into standby mode	1	00	0000	0110	0011

9.2.5. Von Neumann Architecture



Components of the CPU (Central Processing Unit):

- CU (Control Unit): receives input from the CIR, flags and clock, and sends appropriate control signals to the control bus.
- ALU (Arithmetic and Logic Unit): performs binary mathematical and bitwise logical operations.
- Registers: high-speed storage for recording temporary data.

Registers in the CPU:

- MAR (Memory Address Register): points to the address of data that needs to be accessed
- MDR (Memory Data Register): holds data that is being transferred to or from memory
- AC (Accumulator): where intermediate arithmetic and logic results are stored
- PC (Program Counter): points to the address of the next instruction to be executed
- CIR (Current Instruction Register): contains the current instruction code during processing

Buses:

- Address bus: carries the **addresses** of data from the processor to the memory
- Data bus: carries data between the processor, the memory unit and the I/O devices
- Control bus: carries control signals/commands from the CPU (and status signals from other devices) in order to control and coordinate all the activities within the computer

9.2.6. Fetch-Execute-Decode Cycle

Every instruction cycle, the following sequence of microinstructions are executed:

1. The address in the PC is copied to the MAR.
2. The PC is incremented, to point at the next instruction.
3. The MAR address is read and the instruction is copied to the MDR.
4. The instruction is copied to the CIR.
5. The instruction in the CIR is decoded by the CU.
6. The CU sends signals to relevant components e.g. ALU.

9.2.7. OSI Model for Network Communication Protocols

A general protocol can operate at one or more of a series of layers:

(Lowest layer, most hardware-dependent)

1. Physical layer: transmits the raw bitstream over a medium (channel)
2. Data link layer: defines the format of the data. In computers, the OS drivers and NIC (Network Interface Card) operate here.
3. Network layer: decides which physical path the data will take (in a given topology)
4. Transport layer: decides on settings such as 'language' and size of packets
5. Session layer: maintains connections and controls ports and sessions
6. Presentation layer: ensures usability of data and applies encryption/decryption
7. Application layer: the human-computer interaction, where apps access the network

(Highest layer, most software-dependent)

Ethernet: a family of wired communication protocols at the physical and data link layers.

The access method is CSMA/CD (Carrier Sense Multiple Access with Collision Detection).

Coaxial cables are slower with ~10 Mbps. Twisted pair and fibre cables are used for Fast Ethernet and Gigabit Ethernet (~100-1000 Mbps).

Bluetooth: a family of IEEE 802.15 wireless communication protocols at the data link layer.

Bluetooth networks (piconets) use a controller/peripheral (master/slave) model to control which devices can send and receive data. Creating a Bluetooth connection requires inquiry (acquiring the address of the target) and paging (establishing a connection).

The carrier frequency is 2.4 G. Bluetooth uses AFH (Adaptive Frequency Hopping) to identify specific carrier frequencies (channels) not in use to minimise interference.

The bit rate is lower than Wi-Fi (<1 Mbps) and the range is lower but also has low latency. BLE (Bluetooth 4.0 Low Energy) is a variation using less power. It is best suited for replacing short-cable interactions.

Wi-Fi: a family of IEEE 802.11 wireless communication protocols at the data link layer.

This is the most common protocol in a WLAN (Wireless Local Access Network).

The carrier frequency is either 2.4 G or 5 G and the modulation method is QAM (using either 64-bit, 256-bit, or 1024-bit constellations; see Section 9.2.11.)

TCP/IP (Transmission Control Protocol / Internet Protocol):

A broad set of protocols spanning the application layer, transport layer (TCP), internet layer (IP), and data link layer.

UDP (User Datagram Protocol):

UDP packets are called 'datagrams'. Unlike TCP, there is no 'handshake' process before data transmission begins. The response is sent as soon as the request is received.

UDP can encapsulate IPv4 or IPv6. In IPv6, a checksum with error correction bits are included in the header.

The UDP is used by many internet applications including DNS (Domain Name Service) and DHCP (Dynamic Host Configuration Protocol).

HTTPS (Hypertext Transfer Protocol Secure): an encrypted extension of HTTP

The communication is encrypted with either TLS (Transport Layer Security) or SSL (Secure Sockets Layer).

A URL (Uniform Resource Locator) starting with `https://www.` denotes a HTTPS-secured website using the WWW (World Wide Web) domain name.

Web browsers trust HTTPS websites based on certificates.

FTP (File Transport Protocol): Client-server interaction for downloading/uploading files.

SMTP (Simple Mail Transfer Protocol): Transfers text-only (ASCII) emails.

IMAP (Internet Message Access Protocol): Transfers emails containing MIME (multimedia: images, videos, sound, files, typical attachments).

9.2.8. Distributed Systems

In a distributed system, computing resources are spread across wide distances, typically connected via the internet, and may be accessed from any connected device. Resource allocation techniques (concurrency, synchronisation / asynchronous programming, threading, multiprocessing, scheduling, load balancing) are essential to ensure reliability of service.

Cloud Computing: delivery of computing resources (storage, processing power, and services) over the internet instead of owning and maintaining physical hardware and software. Users use resources on-demand from remote data centres. Service models include:

- **Infrastructure as a Service (IaaS):** Provides virtualized computing resources e.g. virtual machines, storage, and networking. Users have control over the operating systems and applications they run.
- **Platform as a Service (PaaS):** Offers a platform that includes the infrastructure and tools for building, deploying, and managing applications. Developers can focus on coding without worrying about underlying infrastructure.
- **Software as a Service (SaaS):** Delivers fully developed software applications over the internet. Users access these applications through a web browser without the need for installation or maintenance.

Serverless and Edge Computing: cloud providers automatically manage the infrastructure, scaling, and provisioning of resources. Developers write code in the form of functions that are executed on-demand. Serverless architectures are event-driven, and developers are billed based on the actual compute resources used, rather than pre-provisioned instances.

Edge computing involves processing data closer to its source, reducing latency and improving response times. Instead of sending all data to centralised cloud servers, edge devices (like IoT devices) process data locally or in nearby edge servers (beneficial for applications that require real-time processing or work in environments with limited connectivity).

Blockchain: a decentralised digital ledger technology that records transactions across multiple computers in a secure and immutable manner. It enables secure and transparent data storage and transfer without the need for intermediaries. Most well-known is its application to cryptocurrencies, although the future of these instruments is uncertain.

9.2.9. Analogue Communications

Analogue communications: used by radios, television video (AM) and audio (FM).

Amplitude Modulation (AM): the modulated signal $s(t)$ is related to the source signal $x(t)$ by

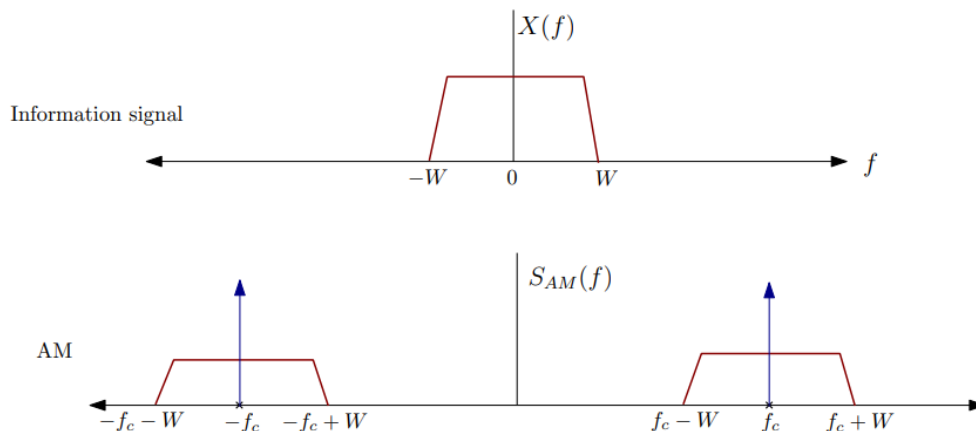
$$s(t) = (a_0 + x(t)) \cos 2\pi f_c t$$

The modulation index is $m_A = \frac{\max\{x(t)\}}{a_0}$ and f_c is the carrier frequency.

$$\text{AM signal power} = \frac{1}{2}a_0^2 + \frac{1}{2}P_x.$$

If $a_0 = 0$ then this is Double Sideband Suppressed Carrier (DSB-SC). Receiver (RX) uses a product modulator (multiply with $\cos 2\pi f_c t$) and low-pass filter.

The frequency spectrum of the AM signal is:



Frequency Modulation (FM): the modulated signal $s(t)$ is related to the information signal $x(t)$ by

$$s(t) = a_0 \cos \left(2\pi f_c t + 2\pi k_F \int_0^t x(\tau) d\tau \right)$$

The frequency deviation is $\Delta f = k_F \max \{ x(t) \}$.

If the information signal is $x(t) = a_x \cos 2\pi f_x t$, then the modulation index is $m_F = \frac{\Delta f}{f_x} = \frac{k_F a_x}{f_x}$.

Carson's rule for FM signals: If the information signal has bandwidth W and the frequency deviation is Δf , then the modulated signal bandwidth is approximately $2W + 2\Delta f$.

9.2.10. Digital Communications

- Quantisation noise: if quantisation step size is $\Delta = \frac{2V}{2^n}$ then the noise is assumed to be uniformly distributed on $[-\frac{\Delta}{2}, \frac{\Delta}{2}]$. The noise power is $\frac{\Delta^2}{12}$ (RMS power = $\frac{\Delta}{2\sqrt{3}}$).
- If a sinusoidal signal is quantised with an n -bit quantiser, the signal-to-quantisation noise ratio is $\text{SNR} = 1.76 + 6.02n$ dB.
- Non-uniform quantisation (companding) can reduce data rate.
- In baseband Pulse Amplitude Modulation (PAM: digital carrier, analogue data), the modulated signal is

$$x(t) = \sum_k X_k p(t - kT)$$

where X_k are information symbols drawn from a real-valued constellation, $p(t)$ is a unit-energy baseband pulse waveform, and T is the symbol period.

- In a constellation with M symbols, each symbol represents $\log_2 M$ bits.
The transmission rate is $\frac{1}{T}$ symbols per second or $\frac{\log_2 M}{T}$ bits per second (bps).
1 byte (B) = 8 bits (b); 1 kilobyte = 1000 bytes etc. “-ibi” prefix indicates powers of 1024 instead of 1000 e.g. 1 kibibyte (KiB) = 1024 bytes, 1 mibibit (Mib) = 1048576 bits.
- In Quadrature Amplitude Modulation (QAM: analogue carrier, digital data), the modulated signal is

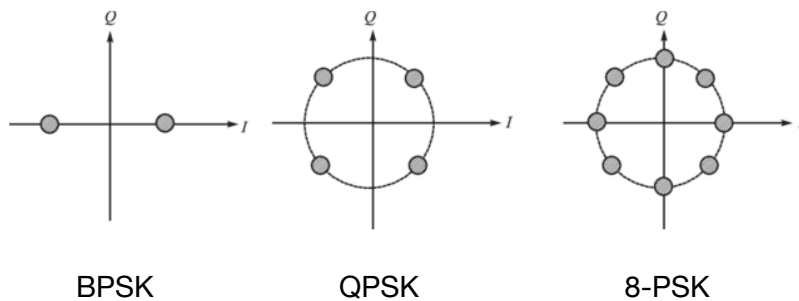
$$\begin{aligned} x(t) &= \sum_k \text{Re} [X_k e^{j2\pi f_c t}] p(t - kT) \\ &= \sum_k [\text{Re}[X_k] \cos(2\pi f_c t) - \text{Im}[X_k] \sin(2\pi f_c t)] p(t - kT) \\ &= \sum_k |X_k| \cos(2\pi f_c t + \arg(X_k)) p(t - kT). \end{aligned}$$

where X_k are information symbols drawn from a constellation (that can be complex valued), $p(t)$ is a unit-energy baseband pulse waveform, and T is the symbol period.

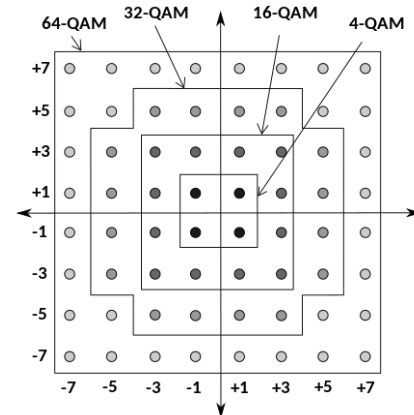
9.2.11. Constellations for Common Digital Modulation Schemes

Constellation: shows the set of symbols on a phasor plot. Each symbol is mapped to a unit of data e.g. $\{-A, A\} \rightarrow \{0, 1\}$ in BPSK. In a constellation with M symbols, each symbol represents $\log_2 M$ bits.

Phase Shift Keying (PSK):



Quadrature Amplitude Modulation (QAM):



The most modern WiFi standard (WiFi 6: 802.11ax) uses 1024-QAM. Mobile data uses 16-QAM (3G) up to 1024-QAM (5G).

9.2.12. Channel Model for Wireless Communications

- **Complex Gaussians:** $h \sim \text{CN}(0, \sigma^2)$ means that h is a complex random variable whose real and imaginary parts are independent Gaussian random variables, each distributed as $\text{N}(0, \frac{1}{2}\sigma^2)$.
- If $h \sim \text{CN}(0, \sigma^2)$, then the squared-magnitude $|h|^2$ is exponentially distributed, i.e., if $X = |h|^2$, the pdf of X is $f_X(x) = \frac{1}{\sigma^2} \exp\left(-\frac{x}{\sigma^2}\right)$ (see Section 5.2.2. for details)
- The Delay Spread T_d of a multipath fading channel is the maximum difference between delays of the paths from transmitter to receiver. The number of channel taps is $\text{ceil}(2WT_d)$, where W is the one-sided baseband bandwidth of the signal.
- If $T_d \ll \frac{1}{2W}$, the channel is said to have flat fading (no inter-symbol interference).
If $T_d > \frac{1}{2W}$, the fading channel has multiple taps (frequency selective).
- The coherence bandwidth of the channel is $\frac{1}{2T_d}$. If the one-sided baseband bandwidth of the transmitted signal is less than the coherence bandwidth, there will be only one channel tap, i.e., flat fading.

9.2.13. Multiplexing and Cellular Networks

Techniques for Multiple Access:

- **TDMA** (Time Division Multiple Access): each of K users gets one slot in a frame of duration $T_f = KT_u$, where T_u is the individual transmission window. Used by 2G.
- **FDMA** (Frequency Division Multiple Access): each of K users gets a non-overlapping frequency band of the total bandwidth $B > KB_u$, where B_u is the individual bandwidth allocation. Orthogonal FDMA (OFDM) is a combination of TDMA and FDMA, and is used by 4G LTE and 5G.
- **CDMA** (Code Division Multiple Access): each of K users gets a unique signature function (spreading code) $c_i(t)$, all of which are orthogonal ($\int c_i(t) c_j(t) dt = 1$ if $i = j$ else 0) over the symbol period T , so that each user transmits the signal $\sum c_i(t) x_i(t)$ (before upconversion by multiplying with $\cos(2\pi f_c t)$). At the RX, after downconverting (product modulator \rightarrow low pass filter), correlating the signal with each signature produces the data for that signature. Used by 3G.

Cellular Networks:

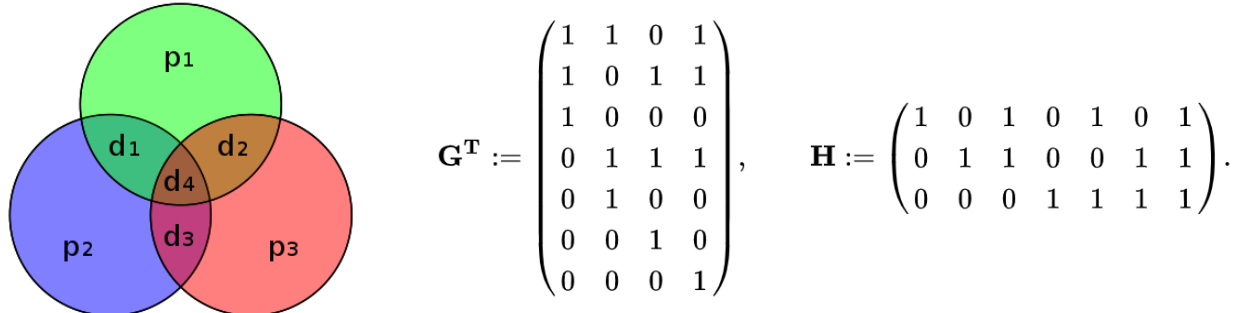
A network is divided into cells, with one base station per cell with users within each cell using a multiple access scheme to communicate simultaneously. Different telecommunications companies (cellular providers) typically place their antennas on the same tower in a given cellular region as they are assigned different frequency bands. Hand-off occurs when users move between cells, as the mobile automatically seeks the strongest signal. Adjacent cells must use different frequency bands to prevent interference.

The cell tower receives the sum of the modulated signals from its users. After demodulation, decorrelation and denoising, the data signals are recovered. The tower then forwards the data to the telecomms company's core network, and is then routed through the carrier's network to its destination.

For antenna design, see Section 8.5.13.

9.2.14. Hamming(7, 4) Code for Error Correction

The code generator matrix \mathbf{G} and the parity-check matrix \mathbf{H} for the (7, 4) Hamming code:



The data bits are $\{d_1, d_2, d_3, d_4\}$ and the parity bits are $\{p_1, p_2, p_3\}$, which are set to

$$p_1 = d_1 \oplus d_2 \oplus d_3; \quad p_2 = d_2 \oplus d_3 \oplus d_4; \quad p_3 = d_1 \oplus d_3 \oplus d_4$$

so that the transmitted codeword is $\{d_1, d_2, d_3, d_4, p_1, p_2, p_3\}$. The parity of each circle in the figure above must be even. (\oplus : bitwise addition)

9.2.15. General Linear Block Codes

- A k -dimensional linear block code of codeword length n (an (n, k) linear code) has encoder matrices of size $k \times n$, parity-check matrices of size $(n - k) \times n$, and rate $R = k/n$.
- An (n, k) linear block code has a systematic encoder matrix of the form $\mathbf{G} = [\mathbf{I}_k, \mathbf{P}]$, to which corresponds to a parity-check matrix of the form $\mathbf{H} = [-\mathbf{P}^T, \mathbf{I}_{n-k}]$.
- Singleton Bound: The minimum distance of any (n, k) block code satisfies $d_{min} \leq n - k + 1$, with equality for Maximum Distance Separable (MDS) codes.
- A block code with minimum distance d_{min} is guaranteed to correct any pattern of up to $\text{ceil}((d_{min} - 1)/2)$ errors. It can recover up to $d_{min} - 1$ erasures.
- The minimum distance d_{min} of a linear block code is the minimum Hamming weight of any nonzero codeword. For binary codes, it is also the minimum number of columns of \mathbf{H} that add up to the all-zero vector.

9.2.16. Binary LDPC Codes and Message Passing Algorithms

- Degree polynomials from a node perspective: $L(x) = \sum_{i=1}^{d_v^{\max}} L_i x^i$, $R(x) = \sum_{i=1}^{d_c^{\max}} R_i x^i$.
- Degree polynomials from an edge perspective: $\lambda(x) = \sum_{i=1}^{d_v^{\max}} \lambda_i x^{i-1}$, $\rho(x) = \sum_{i=1}^{d_c^{\max}} \rho_i x^{i-1}$.
- Average degrees: $\bar{d}_v = L'(1) = \left(\int_0^1 \lambda(x) dx \right)^{-1}$ and $\bar{d}_c = R'(1) = \left(\int_0^1 \rho(x) dx \right)^{-1}$.

- Design rate of an LDPC code is

$$R = 1 - \frac{\bar{d}_v}{\bar{d}_c} = 1 - \frac{L'(1)}{R'(1)} = 1 - \frac{\int_0^1 \rho(x) dx}{\int_0^1 \lambda(x) dx}.$$

- Density evolution for binary erasure channels with erasure probability ε : The probability p_t of a variable-to-check message along a (randomly picked) edge remaining erased after $t \geq 1$ steps of message passing is (Initialise with $p_0 = \varepsilon$.)

$$p_t = \varepsilon \lambda(1 - \rho(1 - p_{t-1})).$$

- Log-likelihood ratios for $j = 1, \dots, n$ are $L(y_j) = \ln \frac{P(y_j|c_j=0)}{P(y_j|c_j=1)}$.
- Log-likelihood ratio for a binary-input AWGN channel with inputs $\{+1, -1\}$ and noise variance σ^2 , for an output value y is $L(y) = \frac{2}{\sigma^2} y$.
- Log-likelihood ratio based decoding rules (for sum-product/belief propagation algorithm), with a check node denoted by i and a variable node by j :

The variable-to-check messages are

$$L_{ji} = L(y_j) + \sum_{i' \setminus i} L_{j i'}.$$

and the check-to-variable messages are

$$L_{ij} = 2 \tanh^{-1} \left[\prod_{j' \setminus j} \tanh \left(\frac{L_{j' i}}{2} \right) \right].$$

where $i' \setminus i$ denotes all the check nodes i' connected to j except i , and conversely for $j' \setminus j$.

- Min-sum simplified decoding rule for a check node:

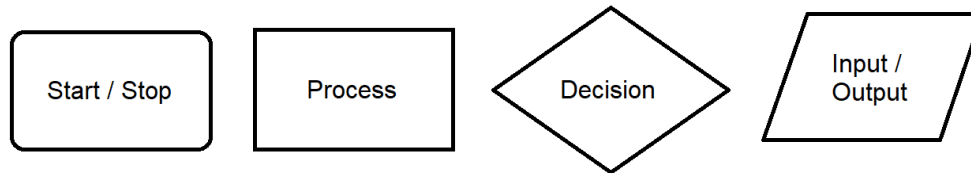
$$\text{sign}(L_{ij}) = \prod_{j' \setminus j} \text{sign}(L_{j' i}) \quad \text{and} \quad |L_{ij}| = \min_{j' \setminus j} (|L_{j' i}|).$$

9.2.17. Finite Fields for Cryptography and Reed-Solomon Codes

- A Galois Field $GF(q)$ for $q = p^m$ where p is any prime number consists of a multiplicative group of order $q - 1$ and an additive group of order q .
- The order of an element α in a group is the smallest power l such that $\alpha^l = 1$, where 1 is the neutral element of the group.
- Lagrange Theorem: The order of a subgroup (and thus the order of any element in a group) divides the order of the group.
- The Discrete Fourier Transform (DFT) of a vector $\mathbf{x} = [x_0, \dots, x_{n-1}]$ with elements over a finite field F is defined by $X_k = \sum_{m=0}^{n-1} x_m \alpha^{mk}$ for $k = 0, \dots, (n - 1)$. Here α must be an element of multiplicative order n in F .
- The inverse DFT is $x_m = \frac{1}{n^*} \sum_{k=0}^{n-1} X_k \alpha^{-mk}$ for $m = 0, \dots, (n - 1)$. Here $n^* = \sum_{j=1}^n 1$, where the sum is taken in F .
- Blahut's theorem: The linear complexity of the DFT of a sequence of length n equals the Hamming weight of the sequence, provided the Hamming weight is less than $n/2$.
- Reed-Solomon code: An (n, k) linear code over $GF(q)$ with a parity-check matrix $\mathbf{H} = [\alpha^{ij}]$ for $i = 0, \dots, (n - k - 1)$, and $j = 0, \dots, (n - 1)$, where α is an element of multiplicative order n in $GF(q)$.
- A Reed-Solomon code has rate $R = k/n$, has minimum distance $d_{\min} = n - k + 1$ and hence satisfies the singleton bound with equality, i.e., it is Maximum Distance Separable (MDS).

9.3. Data Structures, Algorithms and Programming

9.3.1. Algorithm Flowchart Notation



9.3.2. Algorithmic Complexity

The time (number of operations T) complexity or space (amount of memory S) complexity of an algorithm can be represented as a function of the input size n , as n approaches infinity. Proportionality constants are omitted.

Big-O notation: $O(f(n))$ indicates that $T(n) \leq k f(n)$ for all n above some finite value, for **some** positive constant k (an upper bound).

Little-o notation: $o(f(n))$ indicates that $T(n) \leq k f(n)$ for all n above some finite value, for **all** positive values of k (a weak upper bound).

Omega notation: $\Omega(f(n))$ indicates that $T(n) \geq k f(n)$ for all n above some finite value, for **some** positive constant k (a lower bound).

Theta notation: $\Theta(f(n))$ indicates both $O(f(n))$ and $\Omega(f(n))$ simultaneously.

Growth rates follow $n^n \gg n! \gg a^n \gg P(n) \gg n \log n \gg n \gg P(\log n) \gg \log^* n \gg 1$.

(red: non-polynomial time complexity class (NP), green: polynomial time complexity class (P), $\log^* n = \text{ceil}(1 + \log(1 + \log(1 + \dots (n \text{ times } n)))$) the iterated logarithm (inverse tetration: $n = {}^T T$)).

Master Theorem: typically used for evaluating complexities of recursive algorithms.

If $T(n) = a T\left(\frac{n}{b}\right) + g(n)$ for any $a \geq 1$ and $b > 1$ and function $g(n)$, then:

- If $g(n) = O(n^{\log_b a - \epsilon})$ for some positive ϵ , then $T(n) = \Theta(n^{\log_b a})$.
- If $g(n) = \Theta(n^{\log_b a})$, then $T(n) = \Theta(n^{\log_b a} \log n)$.
- If $g(n) = \Omega(n^{\log_b a + \epsilon})$ for some positive ϵ , and if $a g\left(\frac{n}{b}\right) \leq c g(n)$ for some $c < 1$ and all sufficiently large n , then $T(n) = \Theta(g(n))$.

9.3.3. Data Types

Many programming languages provide default implementations of common data types.

- **Integer:** a whole number, typically in base 10.
- **Floating-point Number:** a number with a decimal part, typically in base 10.
- **Character string:** one or more characters (letters, numbers, etc).
- **Boolean:** a value representing 'True' or 'False', typically as a single bit '1' or '0'.
- **Array:** an ordered sequence of elements.
- **Linked list:** a type of array in which each element has associated data and a pointer to the next (and previous in a doubly-linked list) element in the list.
- **Set:** an unordered collection of elements. The implementation is optimised for membership access in $O(1)$ time by hashing the elements.
- **Hashmap:** an associative array in which keys are mapped to values. The implementation is optimised for membership access in $O(1)$ time by hashing the elements.
- **Queue:** a sequence of elements in which operations are performed FIFO (first in first out).
- **Tree:** each node element has associated data and pointers to 'child' nodes.
 - Binary search tree: at each node: all left values $<$ node value $<$ all right values.
 - Heap: at each node: left child node value \leq node value \leq right child node value.
 - Trie (prefix tree): node values are strings. Each child value starts with the parent value, with one additional character appended.
 - k -D tree: a decision tree to partition k -dimensional search space into subspaces. The nodes represent subspaces and the decisions represent hyperplane cuts, so that the child nodes are the spaces on the 'left' and 'right' of the cut.
- **Graph:** each node element has pointers to other data and connection elements ('branches') which may have associated data ('weights').
- **Function:** in first-class programming languages, functions are objects like any other, which input and output other data types.

9.3.9. Algorithms on Arrays (Lists)

Binary Search: finds the index of an item in an array in $O(\log n)$ time.

Recursive algorithm:

```
def binary_search(arr: list, x, low: int = 0, high: int = float('inf')) -> int:
    high = len(arr) - 1 if high == float('inf') else high # default: last index
    if high >= low:
        mid = (high + low) // 2
        if arr[mid] == x: # found: return index
            return mid
        elif arr[mid] > x: # x is in left half, reject right half
            return binary_search(arr, x, low, mid - 1)
        else: # x is in right half, reject left half
            return binary_search(arr, x, mid + 1, high)
    else: # not found
        return None
```

Iterative algorithm:

```
def binary_search(arr: list, x) -> int:
    low = 0; high = len(arr) - 1; mid = 0
    while low <= high:
        mid = (high + low) // 2
        if arr[mid] < x: # x is in right half, reject left half
            low = mid + 1
        elif arr[mid] > x: # x is in left half, reject right half
            high = mid - 1
        else: # found: return index
            return mid
    return None # not found
```

Examples:

```
print(binary_search([1, 2, 6, 7, 10], 6)) # returns 2
print(binary_search([1, 2, 6, 7, 10], 5)) # returns None
```


Two Pointer Algorithm: a general technique to iterate through an array in a single pass.

Example: given an array of stock value data, find the maximum profit that can be achieved by buying then selling. (*LeetCode #121: Best Time to Buy and Sell Stock*)

```
def maxProfit(prices: list[float]) -> float:
    left = 0; right = 1 # main idea: left < right, always
    max_profit = 0 # track the variable of interest so far
    while right < len(prices): # loop until the right pointer reaches the end
        if prices[left] < prices[right]: # if there is potential profit here...
            profit = prices[right] - prices[left]
            max_profit = max(max_profit, profit) # update with observed profit
        else:
            left = right # no profit here - skip this whole window and start over
            right += 1 # keep the buy point, shift the sell point over by 1 to iterate
    return max_profit

maxProfit([7, 1, 5, 3, 6, 4]) # returns 5: buy at 1, sell at 6
```

Hashmaps: can be used to cache values, reducing $O(n)$ lookups to $O(1)$.

Example: given an array of distinct numbers, find the indices of the two numbers in the array which add up to a given target value. (*LeetCode #1: Two Sum*)

```
def twoSum(nums: list[int], target: int) -> tuple[int]:
    mapping = {} # maps required remainders to indices where they were seen
    for i in range(len(nums)):
        remainder = target - nums[i]
        if nums[i] in mapping: # we have seen the required remainder before
            return (mapping[nums[i]], i)
        else:
            mapping[remainder] = i # store the required remainder and its index

twoSum([2, -1, 8, 15, 10], 7) # returns (1, 2) because -1 + 8 = 7
```

9.3.10. Algorithms on Undirected Graphs

Dijkstra's Shortest Path Algorithm

It is a greedy algorithm. Each stage the visited set contains nodes closest to the destination and all the shortest paths. The set of shortest paths form a tree.

- Mark all nodes unvisited, and assign to every node a tentative distance value: zero for the destination node and infinity for all nodes.
- Set the destination node to the current node.
- While the current node is not the initial node:
 - Consider all unvisited neighbours of the current node and calculate their distances to the destination node through the current node. Compare this distance to the current assigned tentative distance for that node and assign the smaller one as the new tentative distance.
 - Mark the current node as visited.
 - Set the new current node to be the unvisited node with the smallest tentative distance.

A* Shortest Path Algorithm

Dijkstra's algorithm plus heuristic $h(x)$: distance from initial node to x is at least $h(x)$.

Last step: Set the new current node to be the unvisited node x with the smallest sum of tentative distance and heuristic $h(x)$.

Prim's Algorithm for Minimum Spanning Tree Generation

Bellman-Ford Algorithm for Shortest Path

9.3.11. Algorithms on Singly-Linked Lists (Directed Graphs)

A linked list contains Node objects, starting with a head node each of which have a value attribute and a next attribute, which points at the next node in the list, ending with a null pointer.

Implementation of a Linked List:

```
from __future__ import annotations # allows type hinting before type definition
class ListNode:
    def __init__(self, x, next: ListNode = None):
        self.val = x
        self.next = next
```

Reversing a Linked List

- Initialise the 'current' node at the head, the 'previous' node is null, the 'next' node is head.next.
- While the 'current' node is not null:
 - Set the current.next pointer to the 'previous' node.
 - Set the 'previous' node to the 'current' node.
 - Set the 'current' node to the 'next' node.
 - Set the 'next' node to the node pointed to by current.next.

Cycle Detection

To detect whether a linked list contains a cycle or not, and if so where it starts, use Floyd's tortoise-and-hare algorithm:

- Initialise a 'fast' pointer (the 'hare') and a 'slow' pointer (the 'tortoise') at the head.
- Do while the fast/slow pointers are different (and not at the start):
 - Move the fast pointer by two nodes and the slow pointer by one node.
 - If the fast pointer reaches the end at any point, there is **no** cycle.
- If the pointers have met, there **is** a cycle. Now initialise a second 'slow' pointer at the head.
- While the two slow pointers are different:
 - Move the slow pointers each by one node.
- The two slow pointers are now both at the start of a cycle.

Example: given the head of a linked list, determine whether or not it contains a cycle, and if so, return the value of its starting node. (*LeetCode #141: Linked List Cycle*)

```
def hasCycle(head: ListNode):
    i_slow = head; i_fast = head
    while True:
        if i_fast is not None and i_fast.next is not None:
            i_slow = i_slow.next
            i_fast = i_fast.next.next
        else:
            return False # pointer reached the end: there is no cycle
    if i_slow == i_fast:
        i_slow_2 = head
        while i_slow_2 != i_slow:
            i_slow_2 = i_slow_2.next
            i_slow = i_slow.next
        return i_slow.val
```

Example: given an array of $N + 1$ integers such that each and every integer in $[1, N]$ is in the array, find the duplicate integer in $O(1)$ space without modifying the array. (*LeetCode #287: Find Duplicate Number*)

By the pigeonhole principle, there is exactly one such integer. Consider forming a linked list from the array such that the head is the first item in the array, and the next item of any node is the value at this index of the array. Then there will be a cycle at the repeated integer.

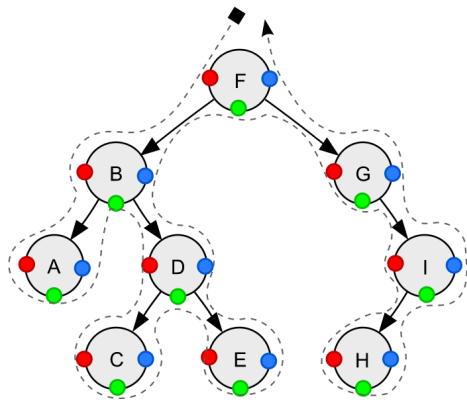
```
def findDuplicate(nums: list[int]) -> int:
    slow_i = nums[0]
    fast_i = nums[0]
    while True:
        slow_i = nums[slow_i]
        fast_i = nums[nums[fast_i]]
        if slow_i == fast_i:
            break
    slow_i_2 = nums[0]
    while slow_i != slow_i_2:
        slow_i = nums[slow_i]
        slow_i_2 = nums[slow_i_2]
    return slow_i
```

9.3.12. Algorithms on Binary Search Trees (BSTs)

Implementation of a BST

```
from __future__ import annotations # allows type hinting before type definition
class TreeNode:
    def __init__(self, val, left: TreeNode = None, right: TreeNode = None):
        self.val = val
        self.left = left
        self.right = right
```

Traversal of a BST: can be done depth-first (in-/pre-/post-order) or breadth-first (level-order).



In-order traversal: starting with the root,

- If this node is the root:
 - Recursively traverse the left node.
 - Visit the root.
 - Recursively traverse the right node.

For **pre-order** traversal or **post-order** traversal, visit the root **before** or **after** both traversals respectively.

Depth-First Search (DFS):

In-order traversal: A → B → C → D → E → F → G...

```
def traverseInOrder(root):
    if root:
        traverseInOrder(root.left)
        print(root.val) # visit the node
        traverseInOrder(root.right)
```

Pre-order traversal: F → B → A → D → C → E → G...

```
def traversePreOrder(root):
    if root:
        print(root.val) # visit the node
        traversePreOrder(root.left)
        traversePreOrder(root.right)
```

Post-order traversal: A → C → E → D → B → H → I...

```
def traversePostOrder(root):
    if root:
        traversePostOrder(root.left)
        traversePostOrder(root.right)
        print(root.val) # visit the node
```

Breadth-First Search (BFS):

Level-order traversal: F → B → G → A → D → I → C...

```
def traverseLevelOrder(root):
    h = height(root)
    for i in range(1, h + 1):
        traverseCurrentLevel(root, i)

def traverseCurrentLevel(root, level):
    if root is None:
        return None
    if level == 1:
        print(root.val) # visit the node
    elif level > 1:
        traverseCurrentLevel(root.left, level - 1)
        traverseCurrentLevel(root.right, level - 1)

def height(node):
    if node is None:
        return 0
    else:
        lheight = height(node.left)
        rheight = height(node.right)
        return lheight + 1 if lheight > rheight else rheight + 1
```

9.3.12. Dynamic Programming

Dynamic programming (DP) involves recognising that a problem can be written in terms of the answer to the same problem on subdivisions of the input, forming a decision tree.

The solution to a dynamic programming problem can be written in terms of the solution to the same problem (subproblems) of a smaller input.

Fibonacci-like Recurrence Relations: common in combinatorics questions (“how many ways...”)

Simple Fibonacci: $f(n) = f(n - 1) + f(n - 2)$

Generalised Fibonacci: $f(n) = \sum_{k=1}^N a_k f(n - k)$

2D Fibonacci: $f(m, n) = a_1 f(m - 1, n) + a_2 f(m, n - 1)$

All Fibonacci relations have a closed form ($O(1)$ evaluation time) by solving the corresponding difference equation (Section 3.4.15)

- Top-down traversal by DFS (backtracking: recursion with memoisation), or
- Bottom-up solution (tabulation).

Example: Given an array of reusable positive integer coin values c and a total amount value v to be made, find the minimum number of coins needed to make up the amount. (*LeetCode #322: Coin Change*)

Let $f(v)$ be the number of ways to make a value of v from the available selection of coins.

Observe that
$$f(v) = \min_{c_i \in c} \left\{ \underbrace{1}_{\text{chosen coin}} + \underbrace{f(v - c_i)}_{\text{ways to make remaining amount}} \right\}.$$

Using a top-down approach:

```
def coinChange(coins, amount, memo={}) -> int:
    if amount < 0: # amount cannot be made - set to negative to fail check
        return -1
    if amount == 0: # base case
        return 0
    if amount in memo:
        return memo[amount]
    min_count = float('inf')
    for c in coins:
        if 0 <= (f := coinChange(coins, amount - c, memo)) < min_count:
            min_count = 1 + f
    memo[amount] = min_count if min_count != float('inf') else -1
    return memo[amount]
```

Using a bottom-up approach:

```
def coinChange(coins: list[int], amount: int) -> int:
    dp = {0: 0} # Base case. dp maps amounts to number of ways {v: f(v)}
    for v in range(1, amount + 1): # starting from v = 1, build upwards
        # float('inf') is used to ignore all cases where v - c cannot be made
        dp[v] = min(1 + dp.get(v - c, float('inf')) for c in coins)
    return dp[amount] if dp[amount] != float('inf') else -1
```


Example: Given an integer array `nums`, return the length of the longest strictly increasing subsequence. (*LeetCode #300: Longest Increasing Subsequence*)

Let $f(i)$ be the maximum length of a subsequence ending at position i .

Observe that
$$\underbrace{f(i)}_{\text{longest subsequence ending at } i} = \max_{0 \leq j < i: x_i > x_j} \left\{ \underbrace{1}_{\text{including } x_i} + \underbrace{f(j)}_{\text{longest subsequence ending at } j < i} \right\}.$$

```
def lengthOfLIS(nums: list[int]) -> int:
    dp = {0: 1} # base case: {end index: longest increasing subsequence}
    for i in range(1, len(nums)):
        dp[i] = max((1 + dp[j]) if nums[i] > nums[j] else 1 for j in range(i))
    return max(dp.values())
```

Example: Given an array of houses each containing value x_i , find the maximum value that can be robbed from the houses if no two neighbouring houses can be robbed. (*LeetCode #198: House Robber*)

Let $f(i)$ be the amount that can be robbed from the houses up to index i (i.e. $x[0 : i + 1]$).

Observe that
$$\underbrace{f(i)}_{\text{amount that can be robbed from houses up to index } i} = \max \left\{ \underbrace{x_i + f(i - 2)}_{\text{choose to rob house } i}, \underbrace{f(i - 1)}_{\text{choose to not rob house } i} \right\}$$

```
def rob(self, nums: List[int]) -> int:
    dp = {0: nums[0]} # base case: {end index -> max amount robbable}
    for i in range(1, len(nums)):
        dp[i] = max(nums[i] + dp.get(i - 2, 0), dp.get(i - 1, 0))
    return dp[len(nums) - 1]
```

9.3.13. Python Cheat Sheet

Keywords		
Keyword	Description	Code Examples
False, True	Boolean data type	False == (1 > 2) True == (2 > 1)
and, or, not	Logical operators → Both are true → Either is true → Flips Boolean	True and True # True True or False # True not False # True
break	Ends loop prematurely	while True: break # finite loop
continue	Finishes current loop iteration	while True: continue print("42") # dead code
class	Defines new class	class Coffee: # Define your class
def	Defines a new function or class method.	def say_hi(): print('hi')
if, elif, else	Conditional execution: - "if" condition == True? - "elif" condition == True? - Fallback: else branch	x = int(input("ur val:")) if x > 3: print("Big") elif x == 3: print("3") else: print("Small")
for, while	# For loop for i in [0,1,2]: print(i)	# While loop does same j = 0 while j < 3: print(j); j = j + 1
in	Sequence membership	42 in [2, 39, 42] # True
is	Same object memory location	y = x = 3 x is y # True [3] is [3] # False
None	Empty value constant	print() is None # True
lambda	Anonymous function	(lambda x: x+3)(3) # 6
return	Terminates function. Optional return value defines function result.	def increment(x): return x + 1 increment(4) # returns 5

Basic Data Structures		
Type	Description	Code Examples
Boolean	The Boolean data type is either True or False. Boolean operators are ordered by priority: not → and → or	## Evaluates to True: 1<2 and 0<=1 and 3>2 and 2>=2 and 1==1 and 1!=0 ## Evaluates to False: bool(None or 0 or 0.0 or '' or [] or {} or set()) Rule: None, 0, 0.0, empty strings, or empty container types evaluate to False
Integer, Float	An Integer is a positive or negative number without decimal point such as 3. A float is a positive or negative number with floating point precision such as 3.1415926. Integer division rounds toward the smaller integer (example: 3//2==1).	## Arithmetic Operations x, y = 3, 2 print(x + y) # = 5 print(x - y) # = 1 print(x * y) # = 6 print(x / y) # = 1.5 print(x // y) # = 1 print(x % y) # = 1 print(-x) # = -3 print(abs(-x)) # = 3 print(int(3.9)) # = 3 print(float(3)) # = 3.0 print(x ** y) # = 9
String	Python Strings are sequences of characters. String Creation Methods: 1. Single quotes >>> 'Yes' 2. Double quotes >>> "Yes" 3. Triple quotes (multi-line) >>> """Yes We Can""" 4. String method >>> str(5) -- '5' True 5. Concatenation >>> "Ma" + "hatma" 'Mahatma'	## Indexing and Slicing s = "The youngest pope was 11 years" s[0] # 'T' s[1:3] # 'he' s[-3:-1] # 'ar' s[-3:] # 'ars' Slice [::2] x = s.split() x[-2] + " " + x[2] + "s" # '11 popes' ## String Methods y = " Hello world\t\n " y.strip() # Remove Whitespace "HI".lower() # Lowercase: 'hi' "hi".upper() # Uppercase: 'HI' "hello".startswith("he") # True "hello".endswith("lo") # True "hello".find("ll") # Match at 2 "cheat".replace("ch", "m") # 'meat' ''.join(["F", "B", "I"]) # 'FBI' len("hello world") # Length: 15 "ear" in "earth" # True

Complex Data Structures		
Type	Description	Example
List	Stores a sequence of elements. Unlike strings, you can modify list objects (they're mutable).	l = [1, 2, 2] print(len(l)) # 3
Adding elements	Add elements to a list with (i) append, (ii) insert, or (iii) list concatenation.	[1, 2].append(4) # [1, 2, 4] [1, 4].insert(1,9) # [1, 9, 4] [1, 2] + [4] # [1, 2, 4]
Removal	Slow for lists	[1, 2, 2, 4].remove(1) # [2, 2, 4]
Reversing	Reverses list order	[1, 2, 3].reverse() # [3, 2, 1]
Sorting	Sorts list using fast Timsort	[2, 4, 2].sort() # [2, 2, 4]
Indexing	Finds the first occurrence of an element & returns index. Slow worst case for whole list traversal.	[2, 2, 4].index(2) # index of item 2 is 0 [2, 2, 4].index(2,1) # index of item 2 after pos 1 is 1
Stack	Use Python lists via the list operations append() and pop()	stack = [3] stack.append(42) # [3, 42] stack.pop() # 42 (stack: [3]) stack.pop() # 3 (stack: [])
Set	An unordered collection of unique elements (at-most-once) → fast membership O(1)	basket = {'apple', 'eggs', 'banana', 'orange'} same = set(['apple', 'eggs', 'banana', 'orange'])
Dictionary	Useful data structure for storing (key, value) pairs	cal = {'apple': 52, 'banana': 89, 'choco': 546} # calories
Reading and writing elements	Read and write elements by specifying the key within the brackets. Use the keys() and values() functions to access all keys and values of the dictionary	print(cal['apple'] < cal['choco']) # True cal['cappu'] = 74 print(cal['banana'] < cal['cappu']) # False print('apple' in cal.keys()) # True print(52 in cal.values()) # True
Dictionary Iteration	You can access the (key, value) pairs of a dictionary with the items() method.	for k, v in cal.items(): print(k) if v > 500 else '' # 'choco'
Membership operator	Check with the in keyword if set, list, or dictionary contains an element. Set membership is faster than list membership.	basket = {'apple', 'eggs', 'banana', 'orange'} print('eggs' in basket) # True print('mushroom' in basket) # False
List & set comprehension	List comprehension is the concise Python way to create lists. Use brackets plus an expression, followed by a for clause. Close with zero or more for or if clauses. Set comprehension works similar to list comprehension.	l = ['hi' + x for x in ['Alice', 'Bob', 'Pete']] # ['Hi Alice', 'Hi Bob', 'Hi Pete'] l2 = [x * y for x in range(3) for y in range(3) if x>y] # [0, 0, 2] squares = {x**2 for x in [0,2,4] if x < 4} # {0, 4}

9.3.14. C/C++ Cheat Sheet

Include Headers

```
#include <headerfile>
```

Common Headers

```
iostream, fstream, math, ctype, string
```

Namespace

```
using namespace std;
```

Data Types

```
int, char, float, double, void, bool
```

Comments

```
// Comment text
/* Multi-line comment text */
```

Arithmetic Operators

```
+ (Addition), - (Subtraction), * (Multiplication), / (Division), % (Modulus)
```

Relational Operators

```
< (Less Than), <= (Less Than or Equal To), > (Greater Than),
>= (Greater Than or Equal To), == (Equal To), != (Not Equal To)
```

Logical Operators

```
|| (logical OR), && (logical AND), ! (logical NOT)
```

Pointers

```
int *ptr; //Define pointer
ptr = &var //ptr set to address of var
var2 = *ptr //Set var2, to value of var1
```

If Else

```
if(<condition>)
{ <statement 1>; }
else
{ <statement 2>; }
```

For Loop

```
for(<initialize>;<condition>;<update>)
{ <statement>; }
```

While Loop

```
while (<condition>)
{ <statement>; }
```

Do-While Loop

```
do { <statement>; }
while (<condition>;);
```

Switch Statement

```
switch(<expression>)
{
case <constant1>:
<statement sequence 1>;
break;
case <constant2>:
<statement sequence 2>;
break;

case <constantn+1>:
<statement sequence n+1>;
break;
[ default:
<statement sequence n>;
break;]
}
```

Arrays

```
//New 5 element array
int myArray[5];
//Array index starts at 0
//Access 3rd Element
myArray[2]=var;
```

I/O Operators

```
>> //Input Operator
<< //Output Operator
cin >> var1, var2, var3;
cout << "TEXT: " << var1 << endl;
cin.get(char* buffer, streamsize num, char delim );
```

File I/O

```
fstream file;
file.open("filename", <file mode constant>);
//Reads and Writes like cin and cout
file >> var;
file << "Text: " << var << endl;
// Read Entire Line
getline (file,line);
//Reading Writing Binary Data
file.read(memory_block, size);
file.write(memory_block, size);
file.close();
```

File Mode Constants

```
ios::in //Opens file for reading
ios::out //Opens file for writing
ios::ate //Seeks the EOF.I/O operations can occur anywhere
ios::app //Causes output to be appended at EOF
ios::trunc //Destroys the previous contents
ios::nocreate //Causes open() to fail if file doesnt already exist
ios::noreplace //Causes open() to fail if file already exists
```

Function Prototype

```
<return_data_type> <function_name> (parameter list)
{ body of the function }
```

Class Prototype

```
class <class_name>
{
public:
//method_prototypes
protected:
//method_prototypes
private:
//method_prototypes
//data_attributes
};
```

Structure Prototype

```
struct <structure_name> {
member_type1 member_name1;
member_type2 member_name2;
} <object_name>;
```

Accessing Data Structures

```
//Access member variable from Struct/Class
myStruct.membervar1 = var;
//Call Class Method
myClass.method1(args);
//Pointer to Struct/Class
myStructType *ptr;
ptr = &myStruct;
ptr->membervar1 = var;
```

9.3.15. Classes and Object-Oriented Programming (OOP)

Instantiation:	objects are instances of classes, which are created at runtime.
Inheritance:	a class (child) may derive its methods and attributes from another (parent).
Polymorphism:	a class or function which can inherit or take objects of multiple types.
Method:	a function associated with an object.
Attribute:	a variable associated with an object.
Encapsulation:	restriction of the scope of attributes to e.g. within the class or method.
Metaclass:	a class whose instances are classes.
Abstract class:	a class whose methods and attributes can be overwritten by its children.

Python example: Note: true private attributes are not available in Python. A more accurate term is 'protected'.

```

class Animal: pass # parent class not implemented

class Dog(Animal): # Dog inherits from Animal
    known_owners = ['Ross', 'James'] # class attribute
    def __init__(self, age, **kwargs): # initialisation and parameters
        self.age = age # setting an attribute
    def human_years(self): # method
        return self.age * 7 # referencing an attribute
    @staticmethod # static decorator
    def is_hungry(time, last_fed): # utility method with no self
        return (time.hour - last_fed.hour) > 5
    @classmethod # class decorator passes the class
    def create_puppy(cls, age=0): # instantiating with keywords
        return cls(age, puppy=True) # property decorator
    @property # property decorator
    def owner(self): # replace with private attribute
        return self._owner # encapsulation of attribute owner
    @owner.setter # encapsulation of attribute owner
    def owner(self, name): # referencing a class attribute
        if name not in Dog.known_owners: # entry validation
            raise ValueError # update private (internal) attribute
        self._owner = name

my_dog = Dog(5) # instantiation, creating an object
print(my_dog.human_years()) # calling a method

my_puppy = my_dog.create_puppy() # create a new Dog using the classmethod
while not hasattr(my_dog, 'owner'): # check if object has an attribute
    try:
        owner_name = input('Who owns this dog? ') # take input from STDIN
        my_dog.owner = owner_name # attempt to set attribute
    except ValueError: # blocked due to encapsulation
        print(f'{owner_name} cannot own a dog.') # simple error to STDOUT
print(f'{my_dog.owner} now owns this dog.') # print attr once allowed

```

9.3.16. Memory and File Access

9.3.17. Version Control

9.3.18. Unit Testing

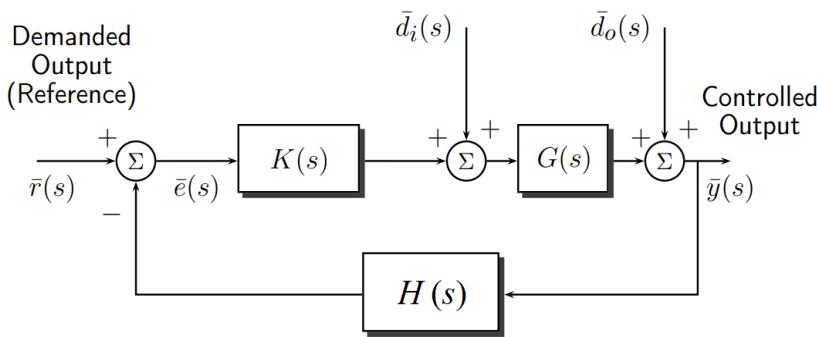
9.4. Control Theory

9.4.1. Principles of Classical Control Theory for a Negative Feedback Loop

Laplace Domain: classical control theory performs analysis in the complex frequency domain via the Laplace transform of all time-dependent signals (Section 3.4.12).

For digital control (discrete time), use the Z-transform.

Block Diagram: controllers, systems and observers represented as transfer functions



y : output

u : controlled input (computed as $u = K\bar{e}$)

d_i : input disturbance

d_o : output disturbance

e : output error

r : demanded steady-state (set-point) for y

$K(s)$: controller (compensator)

$G(s)$: plant (process dynamics)

$H(s)$: observer (sensors, filters)

- Error signal: $\bar{e}(s) = \bar{r}(s) - \bar{z}(s)$.
- Control signal: $\bar{u}(s) = K(s) \bar{e}(s)$
- Feedback signal: $\bar{z}(s) = H(s) \bar{y}(s) = H(s) G(s) K(s) \bar{e}(s) = L(s) \bar{e}(s)$.
- Open loop transfer function (OLTF, return ratio): $\frac{H(s) \bar{y}}{e} = L(s) = H(s) G(s) K(s)$.
- Sensitivity function: $\frac{\bar{y}}{d_o} = S(s) = \frac{1}{1 + L(s)}$ for $r = d_i = 0$
- Complementary sensitivity function: $T(s) = 1 - S(s) = \frac{L(s)}{1 + L(s)}$
- Closed-loop transfer function (CLTF): $\frac{\bar{y}}{r} = \frac{G(s) K(s)}{1 + L(s)}$ for $d_i = d_o = 0$ (same as $T(s)$ if $H = 1$)

Mason's Gain Rule: technique for quickly calculating transfer functions from block diagrams

To find the transfer function G mapping y_{in} to y_{out} , find $G(s) = \frac{y_{out}}{y_{in}} = \frac{\sum_{paths\ i} G_i \Delta_i}{\Delta}$ where

G_i is the product of TFs along forward paths i from y_{in} to y_{out} , Δ is the 'graph determinant' given by

$$\Delta = 1 - \sum_{(1)} L(s) + \sum_{(2)} L_i(s) L_j(s) - \sum_{(3)} L_i(s) L_j(s) L_k(s) \dots$$

and Δ_i is Δ for the graph excluding path i .

The summation over '(2)' is the sum over all (i, j) loop gain pairs $L_i L_j$ of non-touching loops, and similarly triples for '(3)' etc.

9.4.2. Analysis of Transfer Functions

In MATLAB, proper rational TFs such as $L(s) = k \frac{As^2 + Bs + C}{Ds^3 + Es^2 + Fs + G}$ can be represented using `sys = tf([A, B, C], [D, E, F, G]);` where k is a free parameter.

Stability: the ‘poles’ of the transfer function must be in the left half plane

For single input single output (SISO) systems, the closed-loop system, is stable if the roots of the characteristic equation, $1 + L(s) = 0$, have negative real parts ($\text{Re}(s) < 0$).

From the Routh-Hurwitz stability criteria (see also Section 6.2.11.), the roots of the polynomial equation $a_n s^n + a_{n-1} s^{n-1} + a_{n-2} s^{n-2} + \dots + a_1 s + a_0 = 0$, with $a_0 > 0$, must all have $\text{Re}(s) < 0$ if:

- for $n = 2$, if and only if all $a_i > 0$;
- for $n = 3$, if and only if all $a_i > 0$ and $a_1 a_2 > a_0 a_3$;
- for $n = 4$, if and only if all $a_i > 0$ and $a_1 a_2 a_3 > a_0 a_3^2 + a_4 a_1^2$.

Frequency Response:

Considering a feedback control system with unit-gain feedback ($H(s) = 1$), then $L(s) = K(s) G(s)$. If $e(t) = -\cos \omega t$ then the open-loop response at steady state is $y_{ss}(t) = A \cos(\omega t - \varphi)$, where gain $A = |L(j\omega)|$, phase $\varphi = \arg L(j\omega)$. In the Laplace domain, $\bar{y}(s) = L(s) \bar{e}(s)$.

A pole at $s = \sigma + \omega j$ represents a transfer function factor of $\frac{\omega}{(s - \sigma)^2 + \omega^2}$ with ILT $\exp(\sigma t) \sin(\omega t)$. Therefore when $\sigma < 0$, the signal decays and does not contribute to the steady-state signal.

The frequency response from $e(t)$ to $y(t)$ can be represented graphically in terms of $L(s)$:

Bode Plot: two plots, of $|L(s)|$ (gain) and $\arg L(s) = \angle L(s)$ (phase) against real ω where $s = j\omega$.

The Bode plot represents the gain $|L(j\omega)|$ in decibels (dB) as $20 \log_{10} |L(j\omega)|$. The phase $\angle L(j\omega)$ is typically given in degrees. Frequency ω is plotted logarithmically in ‘decades’. For rational TFs, the Bode plot can be estimated by hand by adding together the plots for each factor, given in Section 5.4.5. MATLAB command: `bode(sys);`

- **Gain margin:** measures how much the gain of the return ratio can be increased before the closed-loop system becomes unstable.
The **gain margin** is the value of $|L(j\omega)|$ in dB for the ω at which $\angle L(s) = -180^\circ$.
- **Phase margin:** measures how much phase shift lag can be added to the return ratio before the closed-loop system becomes unstable.
The **phase margin** is the value of $\angle L(j\omega) - (-180^\circ)$ for the ω at which $20 \log_{10} |L(j\omega)| = 0$.

Nyquist Plot: plot $L(s)$ in the complex plane parameterised by real ω where $s = j\omega$

It is often useful to let $L(s) = k g(s)$, where k is the gain and $g(s)$ is the normalised return ratio, and then make a Nyquist plot of $g(s)$ instead. MATLAB command: `nyquist(sys)`;

Nyquist stability criterion: for a stable closed-loop system, the full Nyquist plot of $g(s)$, for $s = j\omega$ and $-\infty < \omega < \infty$, should encircle the $(-1/k, 0j)$ point as many times as there are poles of $g(s)$ (i.e. open-loop poles) in the right half of the s -plane. The encirclements, for the path traced by increasing ω , are counted positive in an anticlockwise direction.

Bode's sensitivity integral:
$$\frac{1}{\pi} \int_0^{\infty} \ln |S(j\omega)| d\omega = \frac{1}{\pi} \int_0^{\infty} \ln \left| \frac{1}{1 + L(j\omega)} \right| d\omega = \sum_k \operatorname{Re}\{p_k\} - \frac{1}{2} \lim_{s \rightarrow \infty} s L(s)$$

(sum over the **unstable** poles of $L(s)$: all p_k with $\operatorname{Re}\{p_k\} > 0$)

The integral places constraints on the designer's ability to modify the control system loop-shape by simply re-tuning the parameters in the controller transfer function or by changing its basic form.

- The **gain margin** is the value of $\frac{1}{\alpha}$ where $L(j\omega)$ crosses the negative real axis at $s = -\alpha$.
- The **phase margin** is the value of $\angle L(j\omega) - (-180^\circ)$ for the ω at which $L(j\omega)$ intersects the unit circle.

Nichols Plot: plot $|L(s)|$ in dB against $\angle L(s)$ parameterised by real ω where $s = j\omega$.

The Nichols chart is used in robust control for quantitative feedback theory to assist with loop-shaping. MATLAB: `nichols(sys)`;

Root-Locus Plot: trace the poles in the complex plane as components of $L(s)$ are varied

For rational L , let $L(s) = k g(s) = k \frac{(s - z_1) \dots (s - z_z)}{(s - p_1) \dots (s - p_p)}$ (k : controller gain, $g(s)$: normalised CLTF)

The roots of $1 + k g(s) = 0$, the closed loop poles, trace loci as k varies from 0 to ∞ , starting at the open-loop poles ($k \rightarrow 0$) and ending at the open-loop zeros ($k \rightarrow \infty$) or at infinite distances. All sections of the real axis with an odd number of poles and zeros to their right are sections of the root locus (even number of poles and zeros to their right if $k < 0$). MATLAB: `rlocus(sys)`;

- $P > Z \rightarrow$ TF is strictly proper; $P = Z \rightarrow$ TF is bi-proper; $P \geq Z \rightarrow$ TF is proper; $P < Z \rightarrow$ TF is improper.
- At the breakaway points (coincident roots): $\frac{dg}{ds} = 0$.
- Angle condition: $\angle g(s) = (2m + 1)\pi$ if $k > 0$; $\angle g(s) = 2m\pi$ if $k < 0$, for integers m .
- Magnitude condition: $|g(s)| = \frac{1}{k}$.
- Asymptotes: If $g(s)$ has P poles and Z zeros, the asymptotes of the loci as $k \rightarrow \infty$ are straight lines at angles $\frac{(2m + 1)\pi}{P - Z}$ to the real axis if $k > 0$ and angles $\frac{2m\pi}{P - Z}$ if $k < 0$.

Their point of intersection σ with the real axis is given by:
$$\sigma = \frac{\sum(\text{poles of } g(s)) - \sum(\text{zeros of } g(s))}{P - Z}$$

9.4.3. Bode Diagrams for Common Factors in Rational Transfer Functions

Bode plot for K : (constant gain factor)

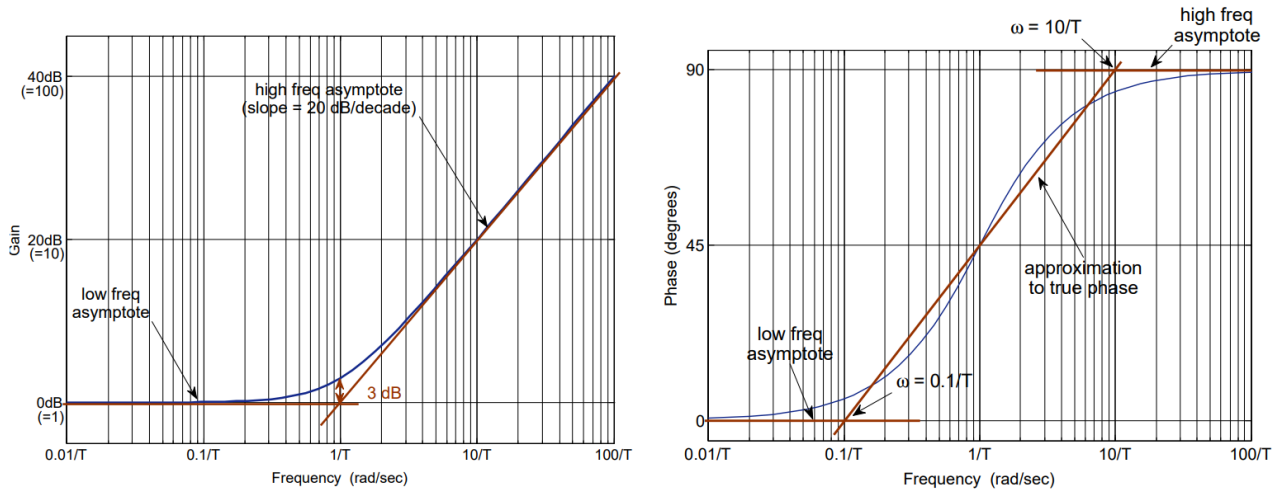
- gain is $20 \log_{10} |K|$ for all ω .
- Phase is 0° if $K > 0$; -180° if $K < 0$, for all ω .

Bode plot for s^n : ($n > 0 \rightarrow$ origin zero, differentiator; $n < 0 \rightarrow$ origin pole, integrator)

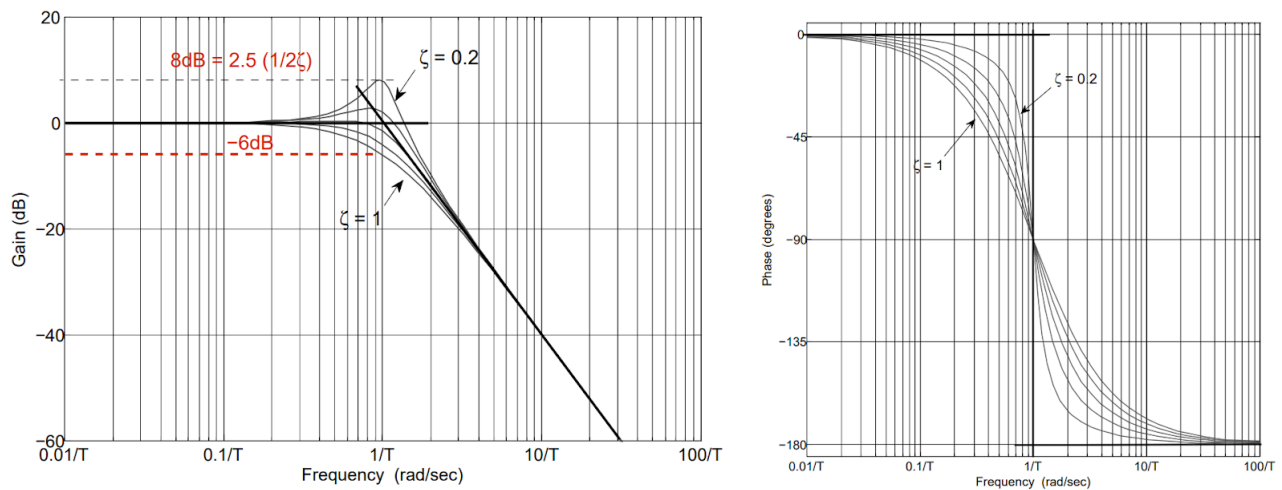
- gain is a straight line with slope $+20n$ dB/decade, passing 0 dB at $\omega = 1 \text{ rad s}^{-1}$.
- phase is $90n^\circ$ for all ω .

Bode plots for $1 + Ts$:

Phase reflected if $T < 0$. Gradient of phase at $1/T = 66^\circ$ per decade



Bode plots for $\frac{1}{1 + 2\zeta Ts + T^2 s^2}$:



More information on the step response, impulse response and harmonic response of first-order and second-order systems can be found in Section 6.2.

9.4.4. Model Linearisation, Reduction and System Identification

Model Linearisation: approximate a system as linear in the vicinity of an operating point

For a general nonlinear state space model of the form $\dot{x} = f(x, u, w)$, $y = g(x, v)$, the model can be linearised by substituting $\tilde{x} = x - x_0$, $\tilde{u} = u - u_0$, $\tilde{y} = y - y_0$, ..., $\tilde{\dot{x}} = \dot{\tilde{x}}$.

The linearised model is then $\tilde{\dot{x}} = A\tilde{x} + B\tilde{u} + B_w\tilde{w}$, $\tilde{y} = C\tilde{x} + B_v\tilde{v}$

where the state matrices are $A = J_{f,x}$, $B = J_{f,u}$, $B_w = J_{f,w}$, $C = J_{g,x}$, $B_v = J_{g,v}$

(all Jacobians J evaluated at the operating point to be linearised about, $(x_0, u_0, y_0, w_0, v_0)$. It is common to choose y_0 as the set point r , let $w_0 = v_0 = 0$, solve $r = g(x_0, v_0)$ for x_0 , then solve $0 = f(x_0, u_0, w_0)$ for u_0 . If y has lower dimension than x , then optimisation approach is necessary to solve for $x_0 = x_0^*$.)

For transfer functions, using $e^{-Ts} \approx 1 - Ts \approx (1 + Ts)^{-1}$, small poles can be exchanged with delays.

Model Order Reduction and System Identification: simplify models with high-order derivatives

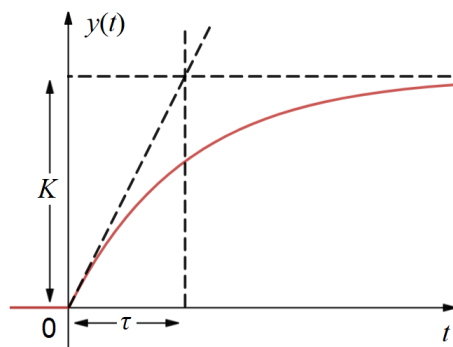
To approximate a high-order system as an n order system with a time delay (NOPDT), apply Skogestad's Half Rule: for a numerator of the form $K e^{-\theta s}$ and a denominator of the form $(1 + T_1s)(1 + T_2s)(1 + T_3s)...$ where $T_1 > T_2 > T_3 > ...$, the new model transfer function is

$$G(s) \approx \frac{K e^{-(\theta + \frac{1}{2}T_{n+1})s}}{(1 + T_1s)(1 + T_2s)...(1 + T_{n-1}s)(1 + (T_n + \frac{1}{2}T_{n+1})s)}$$

i.e. only the n most dominant time constants are retained, with the next most dominant being absorbed half-and-half into the delay and least dominant retained constant. Common process models are

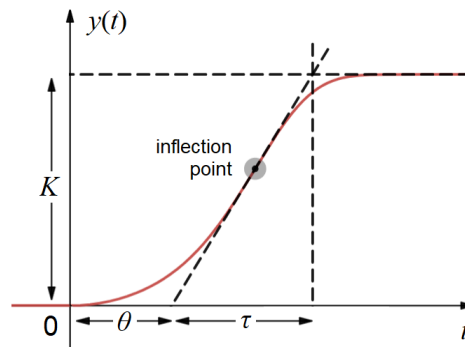
- P1D (first-order plus dead time, FOPDT): $n = 1$ $G(s) = \frac{K \exp(-\theta s)}{1 + T_{p1}s}$
- P2D (second-order plus dead time, SOPDT): $n = 2$ $G(s) = \frac{K \exp(-\theta s)}{(1 + T_{p1}s)(1 + T_{p2}s)}$
- P2DU (2nd-order underdamped plus time delay): $G(s) = \frac{K \exp(-\theta s)}{1 + 2\zeta T_w s + T_w^2 s^2}$

The MATLAB System Identification Toolbox can be used to fit the unknown parameters to given input and output data arrays. For an overdamped response, the following reference curves fit to first-order step responses (r : set point for y)



First Order:

$$\frac{y}{r} = \frac{K}{1 + \tau s} \leftrightarrow y = K(1 - e^{-t/\tau})$$



FOPDT (inflection point on t -axis if exact)

$$\frac{y}{r} = \frac{K e^{-\theta s}}{1 + \tau s} \leftrightarrow y = K H(t - \theta)(1 - e^{-t/\tau})$$

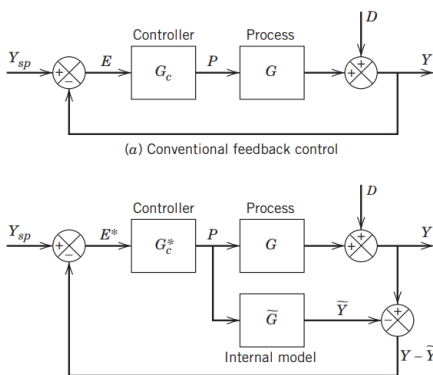
9.4.5. Direct Synthesis and Internal Model Methods for Controller Specification

Direct Synthesis: a target (controlled) transfer function is pre-specified and the required controller terms are solved for algebraically. For an open-loop system, let

\hat{G} : return ratio (OLTF) **without** controller, $\frac{Y}{Y_{sp}}$: desired CLTF; $\hat{L} = \frac{Y/Y_{sp}}{1 - Y/Y_{sp}}$: desired OLTF

Then the desired controller is given by $G_c = \hat{L}/\hat{G}$. Equate the found G_c with the coefficients of a known controller type e.g. PI. Taylor approximation is needed if desired CLTF has a delay (let $e^{-\theta s} = 1 - \theta s$).

Internal Model Control (IMC) Tuning:



Let the internal model \bar{G} be an approximation of the process G , and factor as $\bar{G} = \bar{G}_- \bar{G}_+$ where \bar{G}_+ contains all time delays and right-half plane zeros and has unit steady-state gain. Then:

$$f = \frac{1}{1 + \tau_c s}; \quad G_c^* = \frac{1}{\bar{G}_-} f; \quad G_c = \frac{G_c^*}{1 - G_c^* \bar{G}}; \quad \frac{Y}{Y_{sp}} = \bar{G}_+ f$$

(τ_c : desired closed loop time constant, f : unit-gain low-pass filter)

For a given model \bar{G} , the table gives the corresponding controller G_c expanded to fit a PI or PID controller $G_c \approx K_c(1 + (\tau_I s)^{-1} + (\tau_D s))$.

Model	$K_c K$	τ_I	τ_D
$\frac{K}{\tau s + 1}$	$\frac{\tau}{\tau_c}$	τ	-
$\frac{K}{(\tau_1 s + 1)(\tau_2 s + 1)}$	$\frac{\tau_1 + \tau_2}{\tau_c}$	$\tau_1 + \tau_2$	$\frac{\tau_1 \tau_2}{\tau_1 + \tau_2}$
$\frac{K}{\tau^2 s^2 + 2\zeta \tau s + 1}$	$\frac{2\zeta \tau}{\tau_c}$	$2\zeta \tau$	$\frac{\tau}{2\zeta}$
$\frac{K(-\beta s + 1)}{\tau^2 s^2 + 2\zeta \tau s + 1}, \beta > 0$	$\frac{2\zeta \tau}{\tau_c + \beta}$	$2\zeta \tau$	$\frac{\tau}{2\zeta}$
$\frac{K}{s}$	$\frac{2}{\tau_c}$	$2\tau_c$	-
$\frac{K}{s(\tau s + 1)}$	$\frac{2\tau_c + \tau}{\tau_c^2}$	$2\tau_c + \tau$	$\frac{2\tau_c \tau}{2\tau_c + \tau}$
$\frac{K e^{-\theta s}}{\tau s + 1}$	$\frac{\tau}{\tau_c + \theta}$	τ	-
$\frac{K e^{-\theta s}}{\tau s + 1}$	$\frac{\tau + \frac{\theta}{2}}{\tau_c + \frac{\theta}{2}}$	$\tau + \frac{\theta}{2}$	$\frac{\tau \theta}{2\tau + \theta}$
$\frac{K(\tau_3 s + 1)e^{-\theta s}}{(\tau_1 s + 1)(\tau_2 s + 1)}$	$\frac{\tau_1 + \tau_2 - \tau_3}{\tau_c + \theta}$	$\tau_1 + \tau_2 - \tau_3$	$\frac{\tau_1 \tau_2 - (\tau_1 + \tau_2 - \tau_3)\tau_3}{\tau_1 + \tau_2 - \tau_3}$
$\frac{K(\tau_3 s + 1)e^{-\theta s}}{\tau^2 s^2 + 2\zeta \tau s + 1}$	$\frac{2\zeta \tau - \tau_3}{\tau_c + \theta}$	$2\zeta \tau - \tau_3$	$\frac{\tau^2 - (2\zeta \tau - \tau_3)\tau_3}{2\zeta \tau - \tau_3}$
$\frac{K(-\tau_3 s + 1)e^{-\theta s}}{(\tau_1 s + 1)(\tau_2 s + 1)}$	$\frac{\tau_1 + \tau_2 + \frac{\tau_3 \theta}{\tau_c + \tau_3 + \theta}}{\tau_c + \tau_3 + \theta}$	$\tau_1 + \tau_2 + \frac{\tau_3 \theta}{\tau_c + \tau_3 + \theta}$	$\frac{\tau_3 \theta}{\tau_c + \tau_3 + \theta} + \frac{\tau_1 \tau_2}{\tau_1 + \tau_2 + \frac{\tau_3 \theta}{\tau_c + \tau_3 + \theta}}$
$\frac{K(-\tau_3 s + 1)e^{-\theta s}}{\tau^2 s^2 + 2\zeta \tau s + 1}$	$\frac{2\zeta \tau + \frac{\tau_3 \theta}{\tau_c + \tau_3 + \theta}}{\tau_c + \tau_3 + \theta}$	$2\zeta \tau + \frac{\tau_3 \theta}{\tau_c + \tau_3 + \theta}$	$\frac{\tau_3 \theta}{\tau_c + \tau_3 + \theta} + \frac{\tau^2}{2\zeta \tau + \frac{\tau_3 \theta}{\tau_c + \tau_3 + \theta}}$
$\frac{K e^{-\theta s}}{s}$	$\frac{2\tau_c + \theta}{(\tau_c + \theta)^2}$	$2\tau_c + \theta$	-
$\frac{K e^{-\theta s}}{s}$	$\frac{2\tau_c + \theta}{(\tau_c + \frac{\theta}{2})^2}$	$2\tau_c + \theta$	$\frac{\tau_c \theta + \frac{\theta^2}{4}}{2\tau_c + \theta}$
$\frac{K e^{-\theta s}}{s(\tau s + 1)}$	$\frac{2\tau_c + \tau + \theta}{(\tau_c + \theta)^2}$	$2\tau_c + \tau + \theta$	$\frac{(2\tau_c + \theta)\tau}{2\tau_c + \tau + \theta}$

Note that for models with integrated elements, the following alternative expression for f is used:

$$f = \frac{(2\tau_c - C)s + 1}{(\tau_c s + 1)^2}$$

where $C = \left. \frac{d\bar{G}_+}{ds} \right|_{s=0}$

9.4.6. PID Controller Tuning for FOPDT Processes

Controller tuning aims to optimise closed-loop responses by minimising an error criterion:

$$\begin{matrix} \text{Absolute error} & \text{Squared error} & \text{Time-weighted IAE} & \text{Error} \\ IAE = \int_0^{\infty} |e(t)| dt; & ISE = \int_0^{\infty} e(t)^2 dt; & ITAE = \int_0^{\infty} t |e(t)| dt; & IE = \int_0^{\infty} e(t) dt. \end{matrix}$$

where $e(t) = y(t) - y_{sp}(t)$. Controller: $G_c(s) = K_c \left(1 + \frac{1}{T_i s} + T_d s \right)$. Process: $G(s) = \frac{K e^{-\theta s}}{1 + \tau s}$.

The controller terms can be found using the expression $\kappa = A (\theta / \tau)^B$, where $\kappa = KK_c$ for P, $\kappa = \tau/T_i$ for I, and $\kappa = \tau/T_d$ for D (θ : pure delay time, τ : first-order time constant).

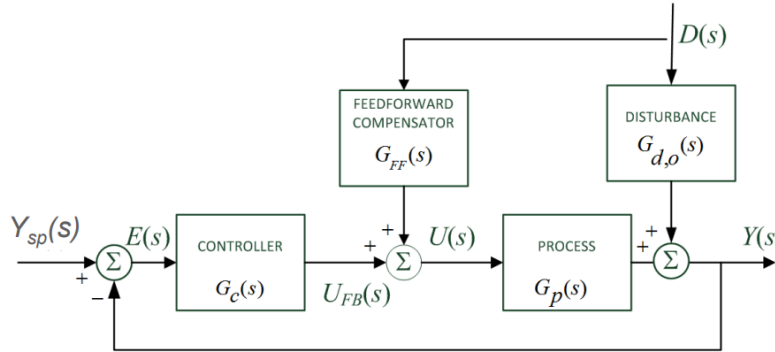
Controller	Criterion	Term	A	B
PI	IAE	P	0.758	-0.861
		I	1.02	-0.323
	ITAE	P	0.586	-0.916
		I	1.03*	-0.165*
PID	IAE	P	1.086	-0.869
		I	0.740	-0.130
		D	0.348	0.914
	ITAE	P	0.965	-0.855
		I	0.796*	-0.1465*
		D	0.308	0.929

Alternative tuning methods are: *: for ITAE integrators on **set-point** changes, use $Y = A + B(\theta / \tau)$.

Controller	Ziegler-Nichols (ZN)	Cohen-Coon (CC)
P	$KK_c = (\theta / \tau)^{-1}$	$KK_c = (\theta / \tau)^{-1} + 0.333$
PI	$KK_c = 0.9 (\theta / \tau)^{-1}$	$KK_c = 0.9 (\theta / \tau)^{-1} + 0.082$
	$\frac{T_i}{\tau} = 3.33 (\theta / \tau)$	$\frac{T_i}{\tau} = \frac{3.33 (\theta / \tau) \left[1 + \frac{1}{11} (\theta / \tau) \right]}{1 + 2.2 (\theta / \tau)}$
PID	$KK_c = 1.2 (\theta / \tau)^{-1}$	$KK_c = (\theta / \tau)^{-1} + 0.27$
	$\frac{T_i}{\tau} = 2 (\theta / \tau)$	$\frac{T_i}{\tau} = \frac{2.5 (\theta / \tau) \left[1 + \frac{1}{5} (\theta / \tau) \right]}{1 + 0.6 (\theta / \tau)}$
	$\frac{T_d}{\tau} = 0.5 (\theta / \tau)$	$\frac{T_d}{\tau} = \frac{0.37 (\theta / \tau)}{1 + 0.2 (\theta / \tau)}$

9.4.7. Practical Control Implementations

Feedforward Control: often used to compensate for a known measurable output disturbance.



Ideal compensator: $G_{FF} = -\frac{G_{d,o}}{G_p}$ (if delays present, requires $\theta_d \geq \theta_p$)

Transfer function: $Y = \frac{G_{d,o} + G_p G_{FF}}{1 + G_p G_c} D + \frac{G_p G_c}{1 + G_p G_c} Y_{sp}$

If $\theta_d < \theta_p$ then the ideal compensator will not be realisable, and a reduced model in which time delays are neglected (a lead-lag unit) is used, or alternatively ignore all dynamic terms (static compensation).

Loop Shaping and the Lead/Lag Compensator: a generalised PID controller

The loop shaping strategy involves choosing the controller $G_c(s)$ to shape $L(s) = G_c(s) G_p(s)$ such that

- $|G_c(j\omega)G_p(j\omega)| \gg 1$ for all $\omega < \omega_c$ i.e. get the benefits of feedback for low frequencies $\rightarrow |S(j\omega)| \ll 1$.
- $|G_c(j\omega)G_p(j\omega)| \ll 1$ for all $\omega > \omega_c$ i.e. suppress high frequency noise $\rightarrow |T(j\omega)| \ll 1$.
- $G_c(j\omega)G_p(j\omega)$ satisfies the Nyquist stability criterion, with adequate gain and phase margins. (ensuring that neither $S(j\omega)$ or $T(j\omega)$ have a large peak in the crossover region in between)

Choose the poles β and zeros α (all are negative) to shape the loop using compensators:

- Phase **lead** compensator: $G_c(s) = \frac{s - \alpha_1}{s - \beta_1}$ for $|\alpha_1| < \omega_c < |\beta_1|$, generalised PD controller

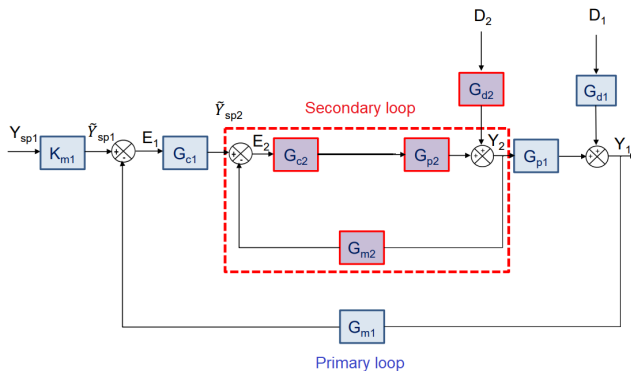
The lead compensator has zero gain for $\omega < |\alpha_1|$ and rises to unit gain for $\omega > |\beta_1|$ (bad), but introduces a phase lead for $|\alpha_1| < \omega < |\beta_1|$ (good - but only beneficial if $|\alpha_1| < \omega_c < |\beta_1|$).

- Phase **lag** compensator: $G_c(s) = \frac{s - \alpha_2}{s - \beta_2}$ for $|\beta_2| < |\alpha_2| < \omega_c$, reduces to a PI controller if $\beta_2 = 0$.

The lag compensator has unit gain for $\omega < |\beta_2|$ and drops to zero gain for $\omega > |\alpha_2|$ (good), but introduces a phase lag for $|\beta_2| < \omega < |\alpha_2|$ (bad - but ok if $\omega_c \gg |\alpha_2|$).

- Lead-lag compensator: $G_c(s) = \frac{(s - \alpha_1)(s - \alpha_2)}{(s - \beta_1)(s - \beta_2)}$ for $|\beta_2| < |\alpha_2| < |\alpha_1| < \omega_c < |\beta_1|$.

Cascade Control: often used to control a secondary variable whose disturbances lead to noise in the main controlled variable.



Transfer function (the secondary loop gain is

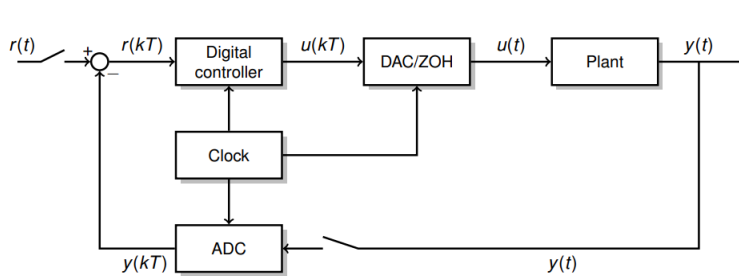
$$\frac{Y_2}{\bar{Y}_{sp2}} = \frac{G_{c2}G_{p2}}{1 + G_{c2}G_{p2}G_{m2}};$$

$$Y_1 = \frac{G_{c1}G_{c2}G_{p1}G_{p2}K_{m1}}{1 + G_{c2}G_{p2}G_{m2} + G_{c1}G_{c2}G_{p1}G_{p2}G_{m1}} Y_{sp} + \frac{G_{d1}(1 + G_{c2}G_{p2}G_{m2})}{1 + G_{c2}G_{p2}G_{m2} + G_{c1}G_{c2}G_{p1}G_{p2}G_{m1}} D_1 + \frac{G_{p1}G_{d2}}{1 + G_{c2}G_{p2}G_{m2} + G_{c1}G_{c2}G_{p1}G_{p2}G_{m1}} D_2$$

Centralised and Decentralised Control: for MIMO systems, it is the designer’s choice whether to make several independent SISO controllers from each output variable to each control input, or to use a single MIMO controller, or to group some of the variables together.

Input and Output Constraints: all physical systems have some limits on the control inputs, reference, state and measured variables, either due to physical constraints (e.g. actuator limits), safety constraints (e.g. temperature/pressure limits) or performance constraints (e.g. overshooting a reference). Optimal operating points (e.g. for optimal profit) are often near or at the limits of one constraint. Most control methods address constraints either a posteriori (e.g. anti-windup methods) or by including constraints in the cost (e.g. H_∞, H_2, L_1).

Computer Control Hardware



(DAC: digital-to-analog converter, ZOH: zero-order hold, ADC: analog-to-digital converter.

T : sample period, k : sample index $x(kT) = x_k = "x(k)":$ discrete signal.)

Full-State Feedback (Pole Placement)

For a controllable state-space model $\{ \dot{x} = Ax + Bu, y = Cx + Du \}$, where the control inputs u , state x and measured output y may be multivariable (vectors):

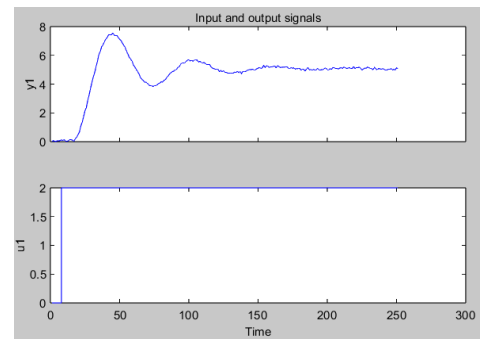
- Transfer function from $u \rightarrow y$: $G(s) = C(sI - A)^{-1} + D$
- Full state feedback: controller $u(s) = -K(s)x(s)$ ($x_{sp} = 0$) $\rightarrow \{ \dot{x} = (A - BK)x, y = (C - DK)x \}$
- Closed-loop poles s : $\det [sI - (A - BK)] = 0$

If the desired closed-loop poles are at known $s_1, s_2 \dots s_n$, form the desired characteristic equation $P(s) = (s - s_1)(s - s_2) \dots (s - s_n)$. By writing K as a matrix of unknowns, the above determinant can be expanded algebraically to match coefficients of the characteristic equations, solving for the required entries in K to give the desired pole placement.

9.4.10. Practical Examples of MATLAB and Simulink for Control System Design

Using the System Identification Toolbox

```
% import data into arrays from Excel file
data = xlsread('StepTestingData.xlsx');
t = data(:,1); % first column
u = data(:,2); % second column
y = data(:,3); % third column
% subtract initial values of u and y
u = u - u(1);
y = y - y(1);
```



With these variables in the workspace, open Apps > System Identification.

Import time domain data > input u, output y, start time 1, sample time 1. Then:

- View important plots: time plot, data spectra, frequency function (Bode plot)
- Estimate transfer function models: choose # poles, # zeros, delay and estimate. Right-click on tf1 and export to MATLAB to make the tf1 object in the workspace.
- Estimate state space model: choose delay in u by inspection, model order. Right click on ss1 and export to MATLAB and make the ss1 object in the workspace.
- Estimate process model: best-fit for a transfer function with given structure.
- Frequency domain analysis: drag a model to the LTI Viewer, right-click in the plot and click Plot types to choose Step response, Impulse response, Linear simulation (another input signal), Bode/Nyquist/Nichols/pole-zero plots.

Tuning a PID controller

Open Apps > PID Tuner and import a plant or transfer function from the workspace.

Choose type PID, add Time domain plot (for a step change) and view the tuned controller responses. When ready, show the parameters and export to a zpk object in the workspace.

9.4.11. Optimal Discrete-Time MIMO State Feedback Control

Denote the n states of a system $\mathbf{x}_k \in \mathbb{R}^n$ and m control inputs $\mathbf{u}_k \in \mathbb{R}^m$ at integer time steps $k \in \mathbb{N}$. For a given initial state \mathbf{x}_0 and a set of control inputs $\mathbf{u}_k \in \mathbb{R}^m$, a trajectory \mathbf{x}_k is generated:

- State-space dynamic model: $\mathbf{x}_{k+1} = \mathbf{f}(\mathbf{x}_k, \mathbf{u}_k)$, for $0 \leq k \leq h$ (h : finite horizon time)

In an optimal control problem, \mathbf{u}_k is to be chosen such that a cost function J is minimised:

- Finite horizon cost function: $J(\mathbf{x}, \mathbf{u}) = \sum_{k=0}^{h-1} c(\mathbf{x}_k, \mathbf{u}_k) + J_h(\mathbf{x}_h)$ (c : stage cost, J_h : terminal cost)
- Objective: find sequence \mathbf{u}_k^* such that J is minimised over all \mathbf{u}_k .

Discrete-Time Dynamic Programming: allows for a recursive approach to find the optimal \mathbf{u}_k^*

- Bellman's Principle of Optimality: the optimal \mathbf{u}^* also minimises $\sum_{i=k}^{h-1} c(\mathbf{x}_i, \mathbf{u}_i) + J_h(\mathbf{x}_h)$.
- Value function (cost to go): $V(\mathbf{x}, k) = \min_{\mathbf{u}_k, \dots, \mathbf{u}_{h-1}} \left(\sum_{i=k}^{h-1} c(\mathbf{x}_i, \mathbf{u}_i) + J_h(\mathbf{x}_h) \right)$, $V(\mathbf{x}, h) = J_h(\mathbf{x})$, $V(\mathbf{x}, 0) = J(\mathbf{x}, \mathbf{u}_k^*)$
- Dynamic programming solution: $V(\mathbf{x}, k) = \min_{\mathbf{u}_k} (c(\mathbf{x}, \mathbf{u}_k) + V(\mathbf{x}_{k+1}, k+1))$
(backwards recursion from $k = h$ to $k = 0$)
 $\mathbf{u}_k^* = \arg \min_{\mathbf{u}} (c(\mathbf{x}_k, \mathbf{u}) + V(\mathbf{f}(\mathbf{x}_k, \mathbf{u}), k+1))$

Discrete-Time Finite Horizon Linear Quadratic Regulator (LQR): quadratic cost and $\mathbf{x}_{k+1} = \mathbf{A}\mathbf{x}_k + \mathbf{B}\mathbf{u}_k$

- LQR cost function: $J(\mathbf{x}, \mathbf{u}) = \sum_{k=0}^{h-1} (\mathbf{x}_k^T \mathbf{Q} \mathbf{x}_k + \mathbf{u}_k^T \mathbf{R} \mathbf{u}_k) + \mathbf{x}_h^T \mathbf{X}_h \mathbf{x}_h$ for $\mathbf{Q} \geq 0$, $\mathbf{R} > 0$, $\mathbf{X}_h \geq 0$

Diagonal entries in \mathbf{Q} and \mathbf{R} represent multipliers on the signal energy $\|\mathbf{x}\|_2^2$ and $\|\mathbf{u}\|_2^2$.

- Minimisation of quadratic forms lemma: $\min_{\mathbf{u} \in \mathbb{R}^m} \begin{bmatrix} \mathbf{x}^T & \mathbf{u}^T \end{bmatrix} \begin{bmatrix} \mathbf{Q} & \mathbf{S}^T \\ \mathbf{S} & \mathbf{R} \end{bmatrix} \begin{bmatrix} \mathbf{x} \\ \mathbf{u} \end{bmatrix} = \mathbf{x}^T (\mathbf{Q} - \mathbf{S}^T \mathbf{R}^{-1} \mathbf{S}) \mathbf{x}$,

achieved when $\mathbf{u}^* = -\mathbf{R}^{-1} \mathbf{S} \mathbf{x}$. The LHS expands to $\mathbf{x}^T \mathbf{Q} \mathbf{x} + \mathbf{u}^T \mathbf{S} \mathbf{x} + \mathbf{x}^T \mathbf{S}^T \mathbf{u} + \mathbf{u}^T \mathbf{R} \mathbf{u}$.

- DP solution: $\mathbf{X}_{k-1} = \mathbf{Q} + \mathbf{A}^T \mathbf{X}_k \mathbf{A} - \mathbf{A}^T \mathbf{X}_k \mathbf{B} (\mathbf{R} + \mathbf{B}^T \mathbf{X}_k \mathbf{B})^{-1} \mathbf{B}^T \mathbf{X}_k \mathbf{A}$ where $V(\mathbf{x}, k) = \mathbf{x}^T \mathbf{X}_k \mathbf{x}$ for any $0 \leq k \leq h$.
- Optimal cost: $\mathbf{x}_0^T \mathbf{X}_0 \mathbf{x}_0$; Optimal controls: $\mathbf{u}_k^* = \mathbf{K} \mathbf{x}_k$ where $\mathbf{K} = -(\mathbf{R} + \mathbf{B}^T \mathbf{X}_{k+1} \mathbf{B})^{-1} \mathbf{B}^T \mathbf{X}_{k+1} \mathbf{A}$.
- Stability: controller $\mathbf{u}_k^* = \mathbf{K} \mathbf{x}_k$ is stabilising if $\rho(\mathbf{A} + \mathbf{B} \mathbf{K}) < 1$. (ρ : spectral radius, Section 4.1.7)

Discrete-Time Infinite Horizon LQR: solving $\mathbf{x}_{k+1} = \mathbf{A}\mathbf{x}_k + \mathbf{B}\mathbf{u}_k$ with horizon as $h \rightarrow \infty$

- Infinite horizon LQR cost function: $J(\mathbf{x}, \mathbf{u}) = \sum_{k=0}^{\infty} (\mathbf{x}_k^T \mathbf{Q} \mathbf{x}_k + \mathbf{u}_k^T \mathbf{R} \mathbf{u}_k)$
- Optimal cost: $\mathbf{x}_0^T \mathbf{X}_0 \mathbf{x}_0$; Optimal controls: $\mathbf{u}_k^* = -(\mathbf{R} + \mathbf{B}^T \mathbf{X} \mathbf{B})^{-1} \mathbf{B}^T \mathbf{X} \mathbf{A} \mathbf{x}_k$
where $\mathbf{X} = \mathbf{X}^T > 0$ is the solution to the discrete algebraic Riccati equation (DARE):

$$\mathbf{X} = \mathbf{Q} + \mathbf{A}^T \mathbf{X} \mathbf{A} - \mathbf{A}^T \mathbf{X} \mathbf{B} (\mathbf{R} + \mathbf{B}^T \mathbf{X} \mathbf{B})^{-1} \mathbf{B}^T \mathbf{X} \mathbf{A}.$$

- To solve the DARE numerically:
 - Python: `X = scipy.linalg.solve_discrete_are(A, B, Q, R)`
 - MATLAB: `[X, K, L, info] = idare(A, B, Q, R, [], [])`

9.4.12. Optimal Continuous-Time MIMO State Feedback Control

Denote the n states of a system $\mathbf{x} \in \mathbb{R}^n$ and m control inputs $\mathbf{u} \in \mathbb{R}^m$ at real time $t \in \mathbb{R}$.

For a given initial state $\mathbf{x}_0 = \mathbf{x}(0)$ and a control input $\mathbf{u} \in \mathbb{R}^m$, a trajectory $\mathbf{x}(t)$ is generated:

- State-space dynamic model: $\dot{\mathbf{x}} = \mathbf{f}(\mathbf{x}, \mathbf{u})$, for $0 \leq t \leq T$ (T : finite horizon time)

In an optimal control problem, $\mathbf{u}(t)$ is chosen such that a cost function J_h is minimised:

- Finite horizon cost function: $J(\mathbf{x}, \mathbf{u}) = \int_0^T c(\mathbf{x}, \mathbf{u}) dt + J_T(\mathbf{x}_T)$ (c : stage cost, J_T : terminal cost)
- Objective: find function $\mathbf{u}^*(t)$ such that J is minimised over all $\mathbf{u}(t)$.

Continuous-Time Dynamic Programming

- Bellman's Principle of Optimality: the optimal \mathbf{u}^* also minimises $\int_t^T c(\mathbf{x}_t, \mathbf{u}_t) dt + J_T(\mathbf{x}_T)$.
- Value function (cost to go): $V(\mathbf{x}, t) = \min_{\mathbf{u}} \int_t^T c(\mathbf{x}, \mathbf{u}) d\tau + J_T(\mathbf{x}_T)$, $V(\mathbf{x}, T) = J_T(\mathbf{x})$, $V(\mathbf{x}, 0) = J(\mathbf{x}, \mathbf{u}_k^*)$
- Discretised model: $\mathbf{x}(t+h) = \mathbf{x}(t) + \mathbf{f}(\mathbf{x}(t), \mathbf{u}(t))h + O(h^2)$ and $\int_t^{t+h} c(\mathbf{x}, \mathbf{u}) d\tau = c(\mathbf{x}, \mathbf{u})h$
- Solution: $-\frac{\partial V}{\partial t} = \min_{\mathbf{u}} \left(c(\mathbf{x}, \mathbf{u}) + \frac{\partial V}{\partial \mathbf{x}} \mathbf{f}(\mathbf{x}, \mathbf{u}) \right)$ (boundary condition: $(V(\mathbf{x}, T) = J_T(\mathbf{x}))$)

(the Hamilton-Jacobi-Bellman partial differential equation, HJB PDE).

The quantity being minimised is the system Hamiltonian H and can also be written as

$$-\frac{\partial V}{\partial t} = \min_{\mathbf{u}} H(\mathbf{x}, \mathbf{u}, \nabla V(\mathbf{x})) \text{ where } H(\mathbf{x}, \mathbf{u}, \lambda) = c(\mathbf{x}, \mathbf{u}) + \lambda^T \mathbf{f}(\mathbf{x}, \mathbf{u}) \quad (\text{Pontryagin's principle}).$$

λ is the Lagrange multiplier (costate vector for Lagrangian c) for the optimisation problem.

- Optimal cost: $V(\mathbf{x}_0, 0)$; Optimal controls: $\mathbf{u}^*(t) = \arg \min_{\mathbf{u}} \left(c(\mathbf{x}, \mathbf{u}) + \frac{\partial V}{\partial \mathbf{x}} \mathbf{f}(\mathbf{x}, \mathbf{u}) \right)$

Continuous-Time Linear Quadratic Regulator (LQR): for a linearised system, $\dot{\mathbf{x}} = \mathbf{A}\mathbf{x} + \mathbf{B}\mathbf{u}$:

- LQR cost function: $J(\mathbf{x}, \mathbf{u}) = \int_0^{t_1} (\mathbf{x}^T \mathbf{Q} \mathbf{x} + \mathbf{u}^T \mathbf{R} \mathbf{u}) dt + \mathbf{x}^T \mathbf{X}_{t_1} \mathbf{x}$ for $\mathbf{Q} \geq 0$, $\mathbf{R} > 0$, $\mathbf{X}_{t_1} \geq 0$
- Derivatives of value function: $V(\mathbf{x}, t) = \mathbf{x}^T \mathbf{X}(t) \mathbf{x} \rightarrow \frac{\partial V}{\partial \mathbf{x}} = \nabla V = 2\mathbf{x}^T \mathbf{X}(t)$; $\frac{\partial V}{\partial t} = \mathbf{x}^T \dot{\mathbf{X}}(t) \mathbf{x}$
- DP solution: $-\dot{\mathbf{X}}(t) = \mathbf{Q} + \mathbf{X}\mathbf{A} + \mathbf{A}^T \mathbf{X} - \mathbf{X}\mathbf{B}\mathbf{R}^{-1}\mathbf{B}^T \mathbf{X}$
- Optimal cost: $\mathbf{x}_0^T \mathbf{X}(0) \mathbf{x}_0$; Optimal controls: $\mathbf{u}^*(t) = -\mathbf{R}^{-1}\mathbf{B}^T \mathbf{X}(t) \mathbf{x}(t)$.

Continuous-Time Infinite Horizon LQR: solving $\dot{\mathbf{x}} = \mathbf{A}\mathbf{x} + \mathbf{B}\mathbf{u}$ with horizon as $T \rightarrow \infty$

- A convenient formulation is to use $\mathbf{z} = \begin{bmatrix} \mathbf{C}\mathbf{x} \\ \mathbf{u} \end{bmatrix}$ (solution \mathbf{X} is constant so 1 less dof)
- Infinite horizon LQR cost function: $J(\mathbf{x}, \mathbf{u}) = \|\mathbf{z}(t)\|_2^2 = \int_0^{\infty} \mathbf{z}^T \mathbf{z} dt = \int_0^{\infty} (\mathbf{x}^T \mathbf{C}^T \mathbf{C} \mathbf{x} + \mathbf{u}^T \mathbf{u}) dt$ for $\mathbf{C} \geq 0$
- Optimal cost: $\mathbf{x}_0^T \mathbf{X}(0) \mathbf{x}_0$; Optimal controls: $\mathbf{u}^*(t) = -\mathbf{B}^T \mathbf{X} \mathbf{x}(t)$, where \mathbf{X} is the stabilising solution ($\dot{\mathbf{X}}(t) = 0$ as $t \rightarrow \infty$, (\mathbf{A}, \mathbf{B}) controllable and (\mathbf{A}, \mathbf{C}) observable): $\mathbf{X} > 0$ to the control algebraic Riccati equation (CARE): $\mathbf{C}^T \mathbf{C} + \mathbf{X}\mathbf{A} + \mathbf{A}^T \mathbf{X} - \mathbf{X}\mathbf{B}\mathbf{B}^T \mathbf{X} = 0$. To solve the CARE numerically:
 - Python: `X = scipy.linalg.solve_continuous_are(A, B, C.T @ C, np.eye(1))`
 - MATLAB: `[X, K, L] = icare(A, [], C'*C, [], [], [], -B*B')`

9.4.13. Multivariable Observable Systems

For a system with internal states $\mathbf{x} \in \mathbb{R}^n$, control inputs $\mathbf{u} \in \mathbb{R}^p$ and measured output $\mathbf{y} \in \mathbb{R}^q$:

- State space dynamic model: $\dot{\mathbf{x}} = \mathbf{A}\mathbf{x} + \mathbf{B}\mathbf{u}$ and $\mathbf{y} = \mathbf{C}\mathbf{x}$ (continuous time)
($\mathbf{A} \in \mathbb{R}^{n \times n}$: state transition matrix, $\mathbf{B} \in \mathbb{R}^{n \times p}$: control input matrix, $\mathbf{C} \in \mathbb{R}^{q \times n}$: output matrix describing observation)
- Time-domain solution: $\mathbf{x}(t) = \exp(\mathbf{A}(t - t_0)) \mathbf{x}(t_0) + \int_{t_0}^t \exp(\mathbf{A}(t - \tau)) \mathbf{B} \mathbf{u}(\tau) d\tau$
- Transfer function: $\hat{\mathbf{Y}}(s) = \mathbf{G} \hat{\mathbf{u}}(s)$ where $\mathbf{G}(s) = \mathbf{C}(s\mathbf{I} - \mathbf{A})^{-1} \mathbf{B}$ (from state space realisation)
- Impulse responses: if $u_j(t) = \delta(t)$ then $y_i(t) = g_{ij}(t)$, where $\mathbf{g}(t) = L^{-1}\{\mathbf{G}(s)\} = \mathbf{C} \exp(\mathbf{A}t) \mathbf{B}$
- Open loop stability: all eigenvalues of \mathbf{A} have negative real part, so $\exp(\mathbf{A}t) \rightarrow 0$ as $t \rightarrow \infty$.
- Closed loop stability: if $\mathbf{u}(t) = \mathbf{K}\mathbf{x}(t)$ then all eigenvalues of $\mathbf{A} + \mathbf{BK}$ have negative real part.
- Observability: the ability to recover the unique \mathbf{x} from a given \mathbf{y} .
It is said that (\mathbf{A}, \mathbf{C}) is 'observable' if: (these two conditions are equivalent)
 - the $nq \times n$ observability matrix $[\mathbf{C}, \mathbf{C}\mathbf{A}, \mathbf{C}\mathbf{A}^2, \mathbf{C}\mathbf{A}^3, \dots, \mathbf{C}\mathbf{A}^{n-1}]^T$ has rank n
 - the observability Gramian $\mathbf{W}_o = \int_0^t \exp(\mathbf{A}^T \tau) \mathbf{C}^T \mathbf{C} \exp(\mathbf{A} \tau) d\tau$, which solves the Lyapunov equation $\mathbf{A}^T \mathbf{W}_o + \mathbf{W}_o \mathbf{A} + \mathbf{C}^T \mathbf{C} = 0$, is nonsingular for all $t > 0$. To solve this numerically,
Python: `W_o = scipy.linalg.solve_continuous_lyapunov(A.T, -C.T @ C)`
MATLAB: `W_o = lyap(A', -C'*C)`
- Controllability: the ability to choose some $\mathbf{u}(t)$ such that \mathbf{x} moves **from** any given initial state \mathbf{x}_0 to all final states $\mathbf{x}(T)$ within a finite time period T .
It is said that (\mathbf{A}, \mathbf{B}) is 'controllable' if: (these two conditions are equivalent)
 - the $n \times np$ controllability matrix $[\mathbf{B}, \mathbf{A}\mathbf{B}, \mathbf{A}^2\mathbf{B}, \mathbf{A}^3\mathbf{B}, \dots, \mathbf{A}^{n-1}\mathbf{B}]$ has rank n
 - the controllability Gramian $\mathbf{W}_c = \int_0^t \exp(\mathbf{A} \tau) \mathbf{B} \mathbf{B}^T \exp(\mathbf{A}^T \tau) d\tau$, which solves the Lyapunov equation $\mathbf{A} \mathbf{W}_c + \mathbf{W}_c \mathbf{A}^T + \mathbf{B} \mathbf{B}^T = 0$, is nonsingular for all $t > 0$.
- Balanced realisation: a state space model such that the Gramians \mathbf{W}_o and \mathbf{W}_c are equal and diagonal matrices. The entries of the diagonal are the Hankel singular values σ_i ordered descending. Can be used for model order reduction (retain only top σ).
Maximum reduction error for order k : $\sigma_{k+1} \leq \|\mathbf{G}(s) - \mathbf{G}_k(s)\|_\infty \leq 2 \sum_{i=k+1}^n \sigma_i$
- State transformation: if $\mathbf{x} = \mathbf{T}\mathbf{z}$ then the system $\{\dot{\mathbf{z}} = \mathbf{A}'\mathbf{z} + \mathbf{B}'\mathbf{u}, \mathbf{y} = \mathbf{C}'\mathbf{z}\}$ has $\mathbf{A}' = \mathbf{T}^{-1}\mathbf{A}\mathbf{T}$, $\mathbf{B}' = \mathbf{T}^{-1}\mathbf{B}$, $\mathbf{C}' = \mathbf{C}\mathbf{T}$ (\mathbf{D} is unchanged if present). Controllability and observability are conserved under \mathbf{T} . In modal coordinates, \mathbf{A}' is a block-diagonal matrix.
- Reachability: the ability to choose some $\mathbf{u}(t)$ such that \mathbf{x} moves **to** any given final state $\mathbf{x}(T)$ from all initial states \mathbf{x}_0 within a finite time period T . Equivalent to controllability for continuous LTI systems, but is not always preserved when a system is discretised.
- Stabilisability: a weaker form of reachability.
It is said that (\mathbf{A}, \mathbf{B}) is 'stabilisable' if there exists \mathbf{K} such that $\mathbf{A} + \mathbf{BK}$ is stable.
- Detectability: a weaker form of observability.
It is said that (\mathbf{C}, \mathbf{A}) is 'detectable' if there exists \mathbf{L} such that $\mathbf{A} + \mathbf{LC}$ is stable.

9.4.14. Kalman Filter: Linear Quadratic Estimator

For an **observable** system with disturbances realised by a discrete state space model

$$\mathbf{x}_{k+1} = \mathbf{A}\mathbf{x}_k + \mathbf{B}\mathbf{u}_k + \mathbf{w}_k; \quad \mathbf{y}_k = \mathbf{C}\mathbf{x}_k + \mathbf{v}_k$$

where the noise signals are assumed to be Gaussian with $\mathbf{w}_k \sim \mathcal{N}(\mathbf{0}, \mathbf{Q})$ and with $\mathbf{v}_k \sim \mathcal{N}(\mathbf{0}, \mathbf{R})$, the optimal observer when state feedback is unavailable is achieved with the Kalman filter. (\mathbf{Q} : covariance matrix of the process noise, \mathbf{R} : covariance matrix of the measurement noise)

The Kalman filter is the optimal Wiener filter (Section 5.4.13), making it highly robust to noise. To compute an optimal estimate $\hat{\mathbf{x}}_{k|k}$ of the state \mathbf{x} at time k using measured \mathbf{y}_k :

($\hat{\mathbf{x}}_{k|k-1}$: *a priori* estimate of state \mathbf{x}_k , $\mathbf{P}_{k|k-1}$: *a priori* covariance matrix of \mathbf{x}_k ;

$\hat{\mathbf{x}}_{k|k}$: *a posteriori* estimate of state \mathbf{x}_k , $\mathbf{P}_{k|k}$: *a posteriori* covariance matrix of \mathbf{x}_k)

- Prediction: $\hat{\mathbf{x}}_{k|k-1} = \mathbf{A}\hat{\mathbf{x}}_{k-1|k-1} + \mathbf{B}\mathbf{u}_{k-1}$ and $\mathbf{P}_{k|k-1} = \mathbf{A}\mathbf{P}_{k-1|k-1}\mathbf{A}^T + \mathbf{Q}$
- Optimal Kalman Gain: $\mathbf{K}_k = \mathbf{P}_{k|k-1}\mathbf{C}^T(\mathbf{C}\mathbf{P}_{k|k-1}\mathbf{C}^T + \mathbf{R})^{-1}$, then take measurement \mathbf{y}_k
- State/uncertainty update: $\hat{\mathbf{x}}_{k|k} = \hat{\mathbf{x}}_{k|k-1} + \mathbf{K}_k(\mathbf{y}_k - \mathbf{C}\hat{\mathbf{x}}_{k|k-1})$ and $\mathbf{P}_{k|k} = (\mathbf{I} - \mathbf{K}_k\mathbf{C})\mathbf{P}_{k|k-1}$

Note that the matrices \mathbf{A} , \mathbf{B} , \mathbf{C} , \mathbf{Q} , \mathbf{R} do not need to be constant in time, and should be evaluated at time step k . A model-free version of the Kalman filter is the ‘alpha-beta(-gamma) filter’, however it is typically less precise and suboptimal.

A common application of the Kalman filter is for filtering kinematics data, where the state space is [position, velocity, acceleration]. The filter is used to combine multiple sensor readings (e.g. attitude, accelerometer, rotary encoder) to produce a reliable state estimate (sensor fusion).

Linear Quadratic Gaussian (LQG) Control: LQR controller with Kalman filter observer

LQG is the optimal control policy for an LQR cost function (Section 9.4.12) when the input and output disturbances are assumed to be Gaussian. This is equivalent to static H_2 optimal control (Section 9.4.16).

9.4.15. Nonlinear Kalman Filters

Extended Kalman Filter (EKF): can use a nonlinear model $\mathbf{x}_{k+1} = \mathbf{f}(\mathbf{x}_k, \mathbf{u}_k) + \mathbf{w}_k$; $\mathbf{y}_k = \mathbf{h}(\mathbf{x}_k) + \mathbf{v}_k$

The Jacobians $\mathbf{J}_f(\hat{\mathbf{x}}_{k-1|k-1}, \mathbf{u}_k) = \partial \mathbf{f} / \partial \mathbf{x}$ and $\mathbf{J}_h(\hat{\mathbf{x}}_{k|k-1}) = \partial \mathbf{h} / \partial \mathbf{x}$ computed to linearise the model about the current state.

- Prediction: $\hat{\mathbf{x}}_{k|k-1} = \mathbf{f}(\hat{\mathbf{x}}_{k-1|k-1}, \mathbf{u}_{k-1})$ and $\mathbf{P}_{k|k-1} = \mathbf{J}_f \mathbf{P}_{k-1|k-1} \mathbf{J}_f^T + \mathbf{Q}$
- Optimal Kalman Gain: $\mathbf{K}_k = \mathbf{P}_{k|k-1} \mathbf{J}_h^T (\mathbf{J}_h \mathbf{P}_{k|k-1} \mathbf{J}_h^T + \mathbf{R})^{-1}$
- State/uncertainty update: $\hat{\mathbf{x}}_{k|k} = \hat{\mathbf{x}}_{k|k-1} + \mathbf{K}_k (\mathbf{y}_k - \mathbf{h}(\hat{\mathbf{x}}_{k|k-1}))$ and $\mathbf{P}_{k|k} = (\mathbf{I} - \mathbf{K}_k \mathbf{J}_h) \mathbf{P}_{k|k-1}$

Unscented Kalman Filter (UKF): uses deterministic sampling to estimate covariances

Using an ‘unscented transformation’, the covariance is propagated correctly, accounting for the nonlinear model. The UKF performs significantly better than the EKF for nonlinear models.

Unscented Transformation: produces a minimal set of sigma points \mathbf{s} that represent \mathbf{x}

Using preset parameters (α, β, κ) : α is typically set to a small positive number (e.g. $\alpha = 10^{-3}$). $\beta = 2$ is optimal when the distribution of \mathbf{x} is known to be Gaussian. κ is an additional scaling degree of freedom but often $\kappa = 0$ is used. For a given $\hat{\mathbf{x}}$ and \mathbf{P} :

- First sigma point and weights: $\mathbf{s}_0 = \hat{\mathbf{x}}$, $W_0^{(a)} = \frac{\alpha^2 \kappa - L}{\alpha^2 \kappa}$, $W_0^{(c)} = W_0^{(a)} + 1 - \alpha^2 + \beta$
- For j in range $[1, \dots, L]$: $\mathbf{s}_j = \hat{\mathbf{x}} + \alpha \kappa^{1/2} \mathbf{A}_j$, $\mathbf{s}_{L+j} = \hat{\mathbf{x}} - \alpha \kappa^{1/2} \mathbf{A}_j$
- For j in range $[1, \dots, 2L]$: $W_j^{(c)} = W_j^{(a)} = \frac{1}{2\alpha^2 \kappa}$

The weights are constrained to satisfy $E[x_i] = \sum_{j=0}^N W_j^{(a)} s_{j,i}$ and $E[x_i x_l] = \sum_{j=0}^N W_j^{(c)} s_{j,i} s_{j,l}$.

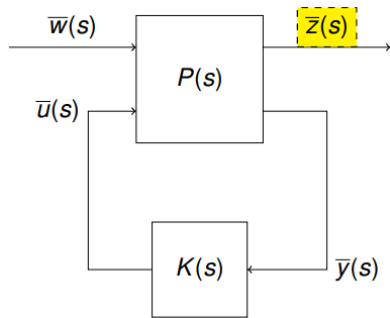
(L : dimension of state vector \mathbf{x} , $N = 2L + 1$: number of sigma points, \mathbf{A}_j : j th column of \mathbf{A} , where $\mathbf{P} = \mathbf{A}\mathbf{A}^T$ is the Cholesky decomposition (Section 4.3.4) of the covariance matrix.)

Unscented Kalman Filter Algorithm:

- Generate a set of sigma points \mathbf{s} and weights ($\mathbf{W}^{(a)}$, $\mathbf{W}^{(c)}$) using $\hat{\mathbf{x}}_{k-1|k-1}$ and $\mathbf{P}_{k-1|k-1}$.
- Propagate: $\mathbf{x}_j = \mathbf{f}(\mathbf{s}_j, \mathbf{u}_{k-1})$ for $0 \leq j \leq 2L$
- Predict: $\hat{\mathbf{x}}_{k|k-1} = \sum_{j=0}^{2L} W_j^{(a)} \mathbf{x}_j$ and $\mathbf{P}_{k|k-1} = \sum_{j=0}^{2L} W_j^{(c)} (\mathbf{x}_j - \hat{\mathbf{x}}_{k|k-1})(\mathbf{x}_j - \hat{\mathbf{x}}_{k|k-1})^T + \mathbf{Q}$
- Generate a **new** set of sigma points \mathbf{s} and weights ($\mathbf{W}^{(a)}$, $\mathbf{W}^{(c)}$) using $\hat{\mathbf{x}}_{k|k-1}$ and $\mathbf{P}_{k|k-1}$.
- Propagate: $\mathbf{y}_j = \mathbf{h}(\mathbf{s}_j)$ for $0 \leq j \leq 2L$
- Compute $\hat{\mathbf{y}} = \sum_{j=0}^{2L} W_j^{(a)} \mathbf{y}_j$, $\hat{\mathbf{S}}_k = \sum_{j=0}^{2L} W_j^{(c)} (\mathbf{y}_j - \hat{\mathbf{y}})(\mathbf{y}_j - \hat{\mathbf{y}})^T + \mathbf{R}$, $\mathbf{C}_{xy} = \sum_{j=0}^{2L} W_j^{(c)} (\mathbf{x}_j - \hat{\mathbf{x}}_{k|k-1})(\mathbf{y}_j - \hat{\mathbf{y}})^T$
- Optimal Kalman gain: $\mathbf{K}_k = \mathbf{C}_{xy} \hat{\mathbf{S}}_k^{-1}$ ($\hat{\mathbf{y}}$: mean, $\hat{\mathbf{S}}$: covariance, \mathbf{C}_{xy} : cross-covariance)
- State/uncertainty update: $\hat{\mathbf{x}}_{k|k} = \hat{\mathbf{x}}_{k|k-1} + \mathbf{K}_k (\mathbf{y}_k - \hat{\mathbf{y}})$ and $\mathbf{P}_{k|k} = \mathbf{P}_{k|k-1} - \mathbf{K}_k \hat{\mathbf{S}}_k \mathbf{K}_k^T$

9.4.16. H_2 Optimal Control

Linear Fractional Transformations (LFTs): useful formulation of noisy MIMO system



(w : input disturbance, x : state, y : measured output, z : performance output, u : control input, P : generalised plant, K : controller)

Lower LFT: TF from w to z : $\mathcal{F}_l(P(s), K(s)) = T_{\hat{w}(s) \rightarrow \hat{z}(s)}$

From generalised plant: $z = \mathcal{F}_l(P(s), K(s)) w = (P_{11} + P_{12}(I - KP_{22})^{-1}KP_{21})w$

$$\begin{bmatrix} \bar{z}(s) \\ \bar{y}(s) \end{bmatrix} = \underbrace{\begin{bmatrix} P_{11}(s) & P_{12}(s) \\ P_{21}(s) & P_{22}(s) \end{bmatrix}}_{P(s)} \begin{bmatrix} \bar{w}(s) \\ \bar{u}(s) \end{bmatrix}$$

$$\bar{z}(s) = P_{11}(s)\bar{w}(s) + P_{12}(s)\bar{u}(s)$$

$$\bar{y}(s) = P_{21}(s)\bar{w}(s) + P_{22}(s)\bar{u}(s)$$

$$\bar{u}(s) = K(s)\bar{y}(s).$$

For a stable system $\{\dot{x} = Ax + Bu; y = Cx\}$ with transfer function $\hat{Y}(s) = G\hat{u}(s)$ ($G(s) = C(sI - A)^{-1}B$):

- System \mathcal{H}_2 norm: $\|G\|_2^2 = \int_{-\infty}^{\infty} \text{trace}\{G(j\omega)^* G(j\omega)\} d\omega = \sum_{i,j} \|G_{ij}\|_2^2 \hat{y}_i(s) = G_{ij}(s)\hat{u}_j(s)$

- Lemma: $\|y\|_{\infty} \leq \frac{1}{\sqrt{2\pi}} \|G\|_2 \|u\|_2$ where $\|y\|_{\infty} = \sup \{y^T(t) y(t)\}^{1/2}$ and $\|u\|_2^2 = \int_{-\infty}^{\infty} u^T(t) u(t) dt$

Using Parseval's theorem, $\|g(t)\|_2 = \frac{1}{\sqrt{2\pi}} \|G(s)\|_2 = (\text{trace}\{B^T W_o B\})^{1/2}$

($g(t) = L^{-1}\{G(s)\} = C e^{At} B$: impulse response matrix, W_o : observability Gramian)

- The objective of \mathcal{H}_2 optimal control is to achieve $\min_{K(s) \text{ stabilising}} \|\mathcal{F}_l(P(s), K(s))\|_2^2$.
- Generalised state space model:

$$\begin{bmatrix} \dot{x} \\ z \\ y \end{bmatrix} = \begin{bmatrix} A & [B_1 \ 0] & B_2 \\ [C_1 \\ 0] & \begin{bmatrix} 0 & 0 \\ 0 & 0 \end{bmatrix} & [0 \\ I] \\ C_2 & [0 \ I] & 0 \end{bmatrix} \begin{bmatrix} x \\ w \\ u \end{bmatrix} \quad \text{where} \quad \begin{cases} (A, B_2) & \text{controllable} \\ (A, C_1) & \text{observable} \\ (A, B_1) & \text{controllable} \\ (A, C_2) & \text{observable} \end{cases}$$

\mathcal{H}_2 Optimal Control with State Feedback: case when $C_2 = I$

- Optimal \mathcal{H}_2 controller: $u = Fx$ where $F = B_2^T X$, and $X > 0$ is the stabilising solution to the CARE, $0 = XA + A^T X + C_1^T C_1 - X B_2 B_2^T X$.
- Optimal H_2 norm: $\min \|\mathcal{F}_l(P, K)\|_2^2 = 2\pi \times \text{trace}\{B_1^T X B_1\}$ (note: MATLAB omits the 2π factor)

H_2 Optimal Control with Output Feedback: assume optimal estimate $\hat{x} = x_k$ (Kalman \rightarrow LQG problem)

$$\text{Optimal } \mathcal{H}_2 \text{ controller: } \begin{bmatrix} \dot{x}_k \\ u \end{bmatrix} = \begin{bmatrix} A - B_2 F - H C_2 & -H \\ F & 0 \end{bmatrix} \begin{bmatrix} x_k \\ y \end{bmatrix}$$

where $F = B_2^T X$, $H = Y C_2^T$, and $X > 0$, $Y > 0$ are the stabilising solutions to

$0 = XA + A^T X + C_1^T C_1 - X B_2 B_2^T X$ (CARE) and $0 = YA^T + AY + B_1 B_1^T - Y C_2^T C_2 Y$ (FARE)

- Optimal \mathcal{H}_2 norm: $\min \|\mathcal{F}_l(P, K)\|_2^2 = 2\pi \times (\text{trace}\{B_1^T X B_1\} + \text{trace}\{Y F Y^T\})$

MATLAB: `[K, CL, gamma] = h2syn(P, nmeas, ncont)`

9.4.17. H_∞ Optimal Control

For a stable system $\{\dot{x} = Ax + Bu; y = Cx; x(0) = 0\}$ with transfer function $G(s) = C(sI - A)^{-1}B$:

- System \mathcal{H}_∞ norm: $\|G\|_\infty = \sup_\omega \{\text{largest singular value of } G(j\omega)\} = \sup \left\{ \frac{\|y\|_2}{\|u\|_2} \right\}$
- Boundedness: iff $A^T X + XA + C^T C + \gamma^{-2} X B B^T X = 0$ (CARE) has a solution $X > 0$ then $\|G\|_\infty \leq \gamma$.

With noise, so that $\dot{x} = Ax + B_1 w_1 + B_2 u$, $z = [C_1 x; u]$ and $y = C_2 x + w_2$,

- Objective: find stabilising K such that $\|\mathcal{F}_l(P(s), K(s))\|_\infty \leq \gamma$ (\mathcal{F}_l : lower LFT, Section 9.4.12)
 - Let the value function be $V = x^T X x$ for some $X = X^T$. For suitable X ,
 - the Riccati equation $A^T X + XA + C_1^T C_1 - X(B_2 B_2^T - \gamma^{-2} B_1 B_1^T) X = 0$, and
 - $A - B_2 B_2^T X$ is stable when $u = -B_2^T X x$ and $w = 0$ (best disturbance), and
 - $A - B_2 B_2^T X - \gamma^{-2} B_1 B_1^T X$ is stable when $u = -B_2^T X x$ and $w = \gamma^{-2} [B_1^T; 0] X x$ (worst disturbance), then with state feedback $u = -B_2^T X x$, we have $\|z\|_2^2 \leq \gamma^2 \|w\|_2^2$ so $\|T_{w \rightarrow z}\|_\infty \leq \gamma$.
- The smallest γ for which the above Riccati equation has a solution can be found by bisection.

\mathcal{H}_∞ Optimal Control with State Feedback

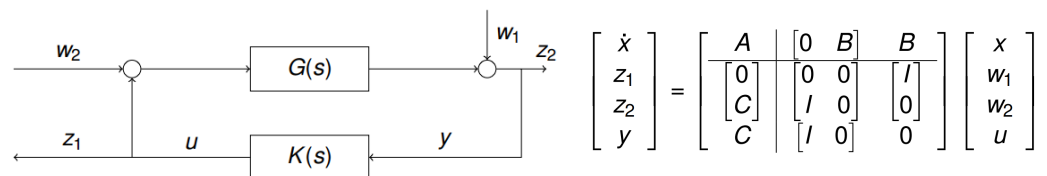
- Optimal \mathcal{H}_∞ controller: $u = -F x$ where $F = B_2^T X$, and $X > 0$ is the stabilising solution to the CARE $0 = A^T X + XA + C_1^T C_1 - X(B_2 B_2^T - \gamma^{-2} B_1 B_1^T) X$

\mathcal{H}_∞ Optimal Control with Output Feedback

- Optimal \mathcal{H}_∞ controller: $\begin{bmatrix} \dot{x}_k \\ u \end{bmatrix} = \begin{bmatrix} \hat{A} - B_2 F - H C_2 & -H \\ F & 0 \end{bmatrix} \begin{bmatrix} x_k \\ y \end{bmatrix}$

where $F = B_2^T X$, $H = Y C_2^T$, $\hat{A} = A + \gamma^{-2} B_1 B_1^T X$, and $X > 0$, $Y > 0$ are the stabilising solutions to $0 = XA + A^T X + C_1^T C_1 - X(B_2 B_2^T - \gamma^{-2} B_1 B_1^T) X$ (CARE) and $0 = Y \hat{A}^T + \hat{A} Y + B_1 B_1^T - Y(C_2^T C_2 - \gamma^{-2} F^T F) Y$ (FARE)

\mathcal{H}_∞ Loop-Shaping:



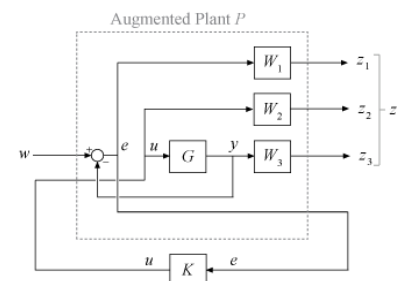
- Loop-Shifting Transformation: let

Then $\|\mathcal{F}_l(P, K)\|_\infty < \gamma \Leftrightarrow \|\mathcal{F}_l(\tilde{P}, \tilde{K})\|_\infty < \gamma$ for $\tilde{K} = \frac{1}{\beta} K$. $\tilde{P} \triangleq \begin{bmatrix} A & | & [0 & \frac{1}{\beta} B] & \frac{1}{\beta} B \\ \hline [0 & 0] & | & [I & 0] \\ [C] & | & [I & 0] & 0 \end{bmatrix}$ where $\beta^2 = 1 - \gamma^{-2}$.

- Solution: X and Y solve their CARE and FARE above for the transformed system iff
 - $X = X^T$ solves the CARE $XA + A^T X + C^T C - X B B^T X = 0 \rightarrow F = B_2^T X$,
 - $Z = Z^T$ ($A - Z C^T C$ stable) solves the FARE $Z A^T + A Z + B B^T - Z C^T C Z = 0$, and
 - $\gamma^2 - 1 > \max\{\text{eig}\{X Z\}\}$.

MATLAB: `K, CL, gamma = hinfsyn(P, nmeas, ncont, gam)`

Mixed-sensitivity H_∞ loop shaping can be achieved by introducing weighting transfer functions at the performance outputs to form an augmented plant P to be used in synthesis.



9.4.18. Convex Optimisation and Linear Matrix Inequalities for Control Design

For a stable linear system $\{\dot{\mathbf{x}} = \mathbf{A}\mathbf{x} + \mathbf{B}\mathbf{u}; \mathbf{y} = \mathbf{C}\mathbf{x}\}$ with transfer function $\mathbf{G}(s)$:

- Stability occurs if there exists $\mathbf{X} = \mathbf{X}^T > 0$ such that $\dot{V} < 0$ for $\mathbf{u} = 0$ (where $V = \mathbf{x}^T \mathbf{X} \mathbf{x}$)
- Solving $\dot{V} = \mathbf{x}^T (\mathbf{A}^T \mathbf{X} + \mathbf{X} \mathbf{A}) \mathbf{x} < 0$ is equivalent to finding $\mathbf{X} = \mathbf{X}^T > 0$ such that $\mathbf{A}^T \mathbf{X} + \mathbf{X} \mathbf{A} < 0$, which is an LMI in \mathbf{X} .

Useful identities:

- **Positive semi-definiteness:** iff $\mathbf{Q} \geq 0$ then $\mathbf{R}^T \mathbf{Q} \mathbf{R} \geq 0$ for any invertible \mathbf{R} .
- **Schur complement:** given $\mathbf{Q} = \mathbf{Q}^T$ and $\mathbf{R} = \mathbf{R}^T$ is invertible,
 iff
$$\begin{bmatrix} \mathbf{Q} & \mathbf{S} \\ \mathbf{S}^T & \mathbf{R} \end{bmatrix} \geq 0 \quad \text{then } \mathbf{R} \geq 0 \text{ and } \mathbf{Q} - \mathbf{S} \mathbf{R}^{-1} \mathbf{S}^T \geq 0$$
- **Kalman-Yakubovich-Popov (KYP) lemma:** given $\gamma > 0$, (\mathbf{A}, \mathbf{B}) controllable, $\text{Re}\{\text{eig}(\mathbf{A})\} < 0$,
 iff $\mathbf{P} = \mathbf{P}^T$ and \mathbf{Q} satisfying $\{\mathbf{A}^T \mathbf{P} + \mathbf{P} \mathbf{A} + \mathbf{Q} \mathbf{Q}^T; \mathbf{P} \mathbf{B} - \mathbf{C} = \gamma^{1/2} \mathbf{Q}\}$ exist
 then $\gamma + 2 \text{Re}\{\mathbf{C}^T (j\omega \mathbf{I} - \mathbf{A})^{-1} \mathbf{B}\} \geq 0$
 and $\{\mathbf{x}; \mathbf{x}^T \mathbf{P} \mathbf{x} = 0\}$ is the unobservable subspace for (\mathbf{C}, \mathbf{A}) .

For a stabilising feedback controller $\mathbf{u} = \mathbf{K}\mathbf{x}$, let $\mathbf{Y} = \mathbf{X}^{-1}$ and $\mathbf{Z} = \mathbf{K}\mathbf{Y}$ so that the LMI is $\mathbf{Y} \mathbf{A}^T + \mathbf{Z}^T \mathbf{B}^T + \mathbf{A} \mathbf{Y} + \mathbf{B} \mathbf{Z} \leq 0$, which can be solved for \mathbf{Y} and \mathbf{Z} ; then $\mathbf{X} = \mathbf{Y}^{-1}$ and $\mathbf{K} = \mathbf{Z} \mathbf{X}$.

The **state feedback \mathcal{H}_∞ control problem** can also be written in terms of an LMI using the KYP lemma: for $\{\dot{\mathbf{x}} = \mathbf{A}\mathbf{x} + \mathbf{B}\mathbf{u} + \mathbf{B}_w \mathbf{w}; \mathbf{z} = \mathbf{C}\mathbf{x} + \mathbf{D}\mathbf{u}\}$, find stabilising $\mathbf{u} = \mathbf{K}\mathbf{x}$ to minimise $\|T_{w \rightarrow z}\|_\infty \leq \gamma$.

With $\mathbf{Z} = \mathbf{K}\mathbf{Y}$, this translates to solving $dV/dt \leq -\mathbf{z}^T \mathbf{z} + \gamma^2 \mathbf{w}^T \mathbf{w}$, represented as an LMI with:

$$\begin{bmatrix} \mathbf{Y} \mathbf{A}^T + \mathbf{Z}^T \mathbf{B}^T + \mathbf{A} \mathbf{Y} + \mathbf{B} \mathbf{Z} & \mathbf{Y} \mathbf{C}^T + \mathbf{Z}^T \mathbf{D}^T & \mathbf{B}_w \\ \mathbf{C} \mathbf{Y} + \mathbf{D} \mathbf{Z} & -\mathbf{I} & \mathbf{0} \\ \mathbf{B}_w^T & \mathbf{0} & -\gamma^2 \mathbf{I} \end{bmatrix} \leq 0$$

Solve for \mathbf{Y} and \mathbf{Z} , minimising γ ; then $\mathbf{X} := \mathbf{Y}^{-1}$ and $\mathbf{K} = \mathbf{Z} \mathbf{X}$.

The library CVX can be used to solve LMIs, available in Python (cvxpy) and MATLAB (cvx).

9.4.19. Robust Control

Robust controllers are designed to accommodate uncertainties in plant models, due to e.g. neglecting complex higher order dynamics, manufacturing variations between systems, uncertain driving forces, stochastic noise inputs or drift of the system properties.

Disk Margin: generalised combined gain and phase margin

Enforcing gain/phase margins (Section 9.4.2) allows the inputs to vary in magnitude or phase at critical frequencies without losing closed-loop stability. However, this does **not** guarantee stability against simultaneous variation in gain and phase (even within their respective margins). It also does not guarantee performance across ranges of frequencies.

Gain and phase variation are encapsulated in a complex number $f = |f| \exp(j\theta)$ ($|f|$: gain multiplier, θ : phase shift). f can be plotted in the complex plane. $f = 1$ represents the original system. The modified loop gain $fL(s)$ is stable if it satisfies the Nyquist stability criterion (Section 9.4.2).

- Stability map: locus of all $f \in \mathbb{C}$ such that $fL(s)$ is stable.
- Disk margin: the radius of the largest circle in the stability map that encloses $z = 1$.

Disk Margin for MIMO Systems:

The ‘multi-loop I/O disk margin’ is the radius of the largest circle in the stability map

MATLAB: for transfer functions of the plant K and controller C :

- Disk margins for input variations: `[dmi, mmi] = diskmargin(C*G);`
- Disk margins for output variations: `[dmo, mmo] = diskmargin(G*C);`
- Disk margin for input and output variations: `mmio = diskmargin(G, C);`

Parameter Uncertainty: represent physical parameters as ranges of possible values

MATLAB: uncertain parameters can be defined by e.g. `p = ureal('p', 5, 'percent', 20)`, which defines a variable p having nominal (mean) value 5 and varying by up to $\pm 20\%$.

Robust analysis is then performed with `[stabilityMargin, wcu] = robstab(G_cl, ...)`

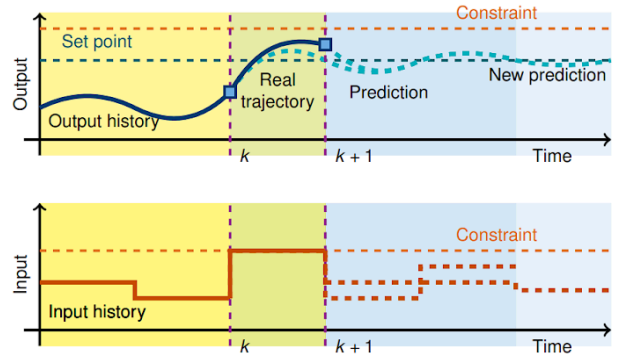
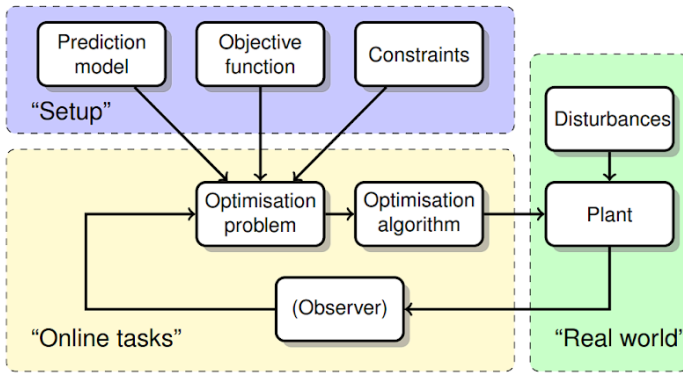
Robust \mathcal{H}_∞ Control (Mu Synthesis): accounts for uncertainty in model parameters

For imperfect models, the entries of \mathbf{P} are subject to some unknown variation. By minimising $\|\mathcal{F}_i(\mathbf{P}, \mathbf{K})\|_\infty$ (Section 9.4.17) over all possible uncertainties in a given range of models, robust performance is guaranteed. This can be done algorithmically by mu synthesis, in which a D-K iteration scheme runs \mathcal{H}_∞ control design, checks robustness, scales the \mathcal{H}_∞ norm appropriately and recomputes the \mathcal{H}_∞ controller until convergence (μ : structured singular value).

MATLAB: `[K, CLperf] = musyn(P, nmeas, ncont)`

9.4.20. Predictive Control

Predictive control is an alternative approach to optimal control that performs the optimisation on-line (in the loop, at each time step) as opposed to off-line (during setup of the controller).



Loop diagram: control input \mathbf{u} determined by optimisation algorithm

Receding Horizon:

Compute optimal trajectory and take only the **first** control input

Notation: \mathbf{x}_i is the **prediction** of $\mathbf{x}(k+i)$ (i time steps into the future), given the current state $\mathbf{x}_0 = \mathbf{x}(k)$, computed optimal controls $\mathbf{u}(k+i) = \mathbf{u}_i$ for $i \in \{0, 1, \dots, N-1\}$ and state space model $\{\mathbf{x}_{i+1} = \mathbf{A}\mathbf{x}_i + \mathbf{B}\mathbf{u}_i, \mathbf{y}_i = \mathbf{C}\mathbf{x}_i\}$ (N : finite time horizon for receding horizon control (RHC)).

At a given time step k , starting with a given (or estimated) current state $\mathbf{x}_0 = \mathbf{x}(k)$, compute a sequence $\mathbf{u} = \{\mathbf{u}_0, \mathbf{u}_1, \dots, \mathbf{u}_{N-1}\}$ such that:

- the value function $V(\mathbf{x}, \mathbf{u}) = \mathbf{x}_N^T \mathbf{P} \mathbf{x}_N + \sum_{i=0}^{N-1} (\mathbf{x}_i^T \mathbf{Q} \mathbf{x}_i + \mathbf{u}_i^T \mathbf{R} \mathbf{u}_i)$ is minimised
- subject to the sets of linear constraints $\mathbf{M}_i \mathbf{x}_i + \mathbf{E}_i \mathbf{u}_i \leq \mathbf{b}_i$ for $i \in \{0, 1, \dots, N-1\}$ and $\mathbf{M}_N \mathbf{x}_N \leq \mathbf{b}_N$.

If all $\mathbf{M}_i = \mathbf{0}$ the constraints are on the admissible inputs \mathbf{u} .

If all $\mathbf{E}_i = \mathbf{0}$ the constraints are on the admissible states \mathbf{x} .

Time-independent constraints (very common simplification) have all $\mathbf{M}_i = \mathbf{M}$ and all $\mathbf{E}_i = \mathbf{E}$.

If no constraints are applied, the controller is linear. Otherwise, the controller is nonlinear.

Once the optimisation problem has been solved for an optimal sequence $\mathbf{u} = \{\mathbf{u}_0, \mathbf{u}_1, \dots, \mathbf{u}_{N-1}\}$, the controller selects only the first input: $\boldsymbol{\kappa}_{\text{RHC}} = \mathbf{u}_0 = [\mathbf{I}, 0, 0, \dots, 0]^T [\mathbf{u}_0, \mathbf{u}_1, \dots, \mathbf{u}_{N-1}]$.

The closed loop dynamics are then given by $\mathbf{x}(k+1) = \mathbf{A}\mathbf{x}(k) + \mathbf{B}\boldsymbol{\kappa}_{\text{RHC}}(\mathbf{x})$.

The feasible region in state space will often be partitioned into subregions, within which the control law is linear, but is overall piecewise due to differences across subregion boundaries.

9.4.21. Matrix Formulation of the Predictive Control Problem

Define the horizon state vector $\theta = [u_0; x_1; u_1; x_2; u_2; \dots; x_{N-1}; u_{N-1}; x_N]$. The optimal control problem can be stated compactly as

$$\text{Find } \theta \text{ to minimise } V(x, u) = x_0^T Q x_0 + \theta^T \Omega \theta \text{ subject to } G\theta \leq h \text{ and } \Lambda\theta = b.$$

where $V(x, u)$ contains the value function, $G\theta \leq h$ contains the constraints and $\Lambda\theta = b$ acts as another constraint containing the prediction model.

Value function:

Prediction (using state space model):

$$V(x, u) = \underbrace{x_0^T}_{\theta} Q x_0 + \underbrace{\begin{bmatrix} R & 0 & 0 & 0 & \dots & 0 & 0 \\ 0 & Q & 0 & 0 & \dots & 0 & 0 \\ 0 & 0 & R & 0 & \dots & 0 & 0 \\ 0 & 0 & 0 & Q & \dots & 0 & 0 \\ \vdots & \vdots & \vdots & \vdots & \ddots & \vdots & \vdots \\ 0 & 0 & 0 & 0 & \dots & R & 0 \\ 0 & 0 & 0 & 0 & \dots & 0 & P \end{bmatrix}}_{\Omega} \underbrace{\begin{bmatrix} u_0 \\ x_1 \\ u_1 \\ x_2 \\ \vdots \\ u_{N-1} \\ x_N \end{bmatrix}}_{\theta}$$

$$\underbrace{\begin{bmatrix} B & -I & 0 & 0 & \dots & 0 & 0 \\ 0 & A & B & -I & \dots & 0 & 0 \\ 0 & 0 & 0 & A & \dots & 0 & 0 \\ \vdots & \vdots & \vdots & \vdots & \ddots & \vdots & \vdots \\ 0 & 0 & 0 & 0 & \dots & B & -I \end{bmatrix}}_{\Lambda} \underbrace{\begin{bmatrix} u_0 \\ x_1 \\ u_1 \\ x_2 \\ \vdots \\ u_{N-1} \\ x_N \end{bmatrix}}_{\theta} = \underbrace{\begin{bmatrix} -A x_0 \\ 0 \\ 0 \\ \vdots \\ 0 \end{bmatrix}}_b$$

Constraints: for example, for saturation constraints i.e. $u_{low} \leq u \leq u_{high}$, $y_{low} \leq y \leq y_{high}$, the optimisation problem constraints can be written as $G\theta \leq h$, where θ contains x and u over the horizon period:

$$M_i \triangleq \begin{bmatrix} 0 \\ 0 \\ -C \\ +C \end{bmatrix}, E_i \triangleq \begin{bmatrix} -I \\ +I \\ 0 \\ 0 \end{bmatrix}, b_i \triangleq \begin{bmatrix} -u_{low} \\ +u_{high} \\ -y_{low} \\ +y_{high} \end{bmatrix}$$

$$M_N \triangleq \begin{bmatrix} -C \\ +C \end{bmatrix}, b_N \triangleq \begin{bmatrix} -y_{low} \\ +y_{high} \end{bmatrix}$$

$$\underbrace{\begin{bmatrix} E_0 & 0 & 0 & 0 & \dots & 0 & 0 \\ 0 & M_1 & E_1 & 0 & \dots & 0 & 0 \\ 0 & 0 & 0 & M_2 & \dots & 0 & 0 \\ \vdots & \vdots & \vdots & \vdots & \ddots & \vdots & \vdots \\ 0 & 0 & 0 & 0 & \dots & E_{N-1} & 0 \\ 0 & 0 & 0 & 0 & \dots & 0 & M_N \end{bmatrix}}_G \underbrace{\begin{bmatrix} u_0 \\ x_1 \\ u_1 \\ x_2 \\ \vdots \\ u_{N-1} \\ x_N \end{bmatrix}}_{\theta} \leq \underbrace{\begin{bmatrix} -M_0 x_0 + b_0 \\ b_1 \\ b_2 \\ \vdots \\ b_{N-1} \\ b_N \end{bmatrix}}_b$$

Quadratic Programming: value function of the form $V(x, u) = \frac{1}{2} \theta^T Q \theta + c^T \theta$ (s.t. $G\theta \leq h, \Lambda\theta = b$)

If $Q > 0$ then the optimisation problem is convex, and a unique global minima exists.

QPs such as the above can be solved using the OSQP library, which is available in Python, MATLAB, C/C++, R and Julia. The sparsity of the matrices involved can be exploited (e.g. in Python, use the `scipy.sparse.csc_matrix` class) to improve computation speed. If nonzero set points and disturbances are used, the value function to be used is

$$V(x, u) = \sum_{i=0}^{N-1} [(y_i - y_s)^T Q (y_i - y_s) + \Delta u_i^T R \Delta u_i + (x_N - x_s)^T P (x_N - x_s)]$$

$$= \sum_{i=0}^{N-1} [(x_i - x_s)^T (C^T Q C) (x_i - x_s) + \Delta u_i^T R \Delta u_i + (x_N - x_s)^T P (x_N - x_s)]$$

where $\Delta u_i = u_i - u_{i-1}$ and $y_s = C x_s$. Let $y(k) = y_0 + d_0$ and $d_i = d_0$ (constant disturbance). See the [OSQP documentation](#) for an example of the above predictive control QP. Other problems can be cast as QPs:

Piecewise linear constraint: $\min V$ subject to $\max\{e^T \theta, f^T \theta\} \leq b \rightarrow \min V$ subject to $e^T \theta \leq b, f^T \theta \leq b$.

Piecewise linear cost: $\min |c^T \theta|$ subject to $G\theta \leq h \rightarrow \min \delta$ subject to $G\theta \leq h, c^T \theta - \delta \leq 0, -c^T \theta - \delta \leq 0$.

9.4.22. Stability of Constrained Predictive Control

Definitions:

- Set S is '**invariant**' if, for a given system $\mathbf{x}(k+1) = \mathbf{f}(\mathbf{x}(k))$, starting at any $\mathbf{x}(0) \in S$ implies $\mathbf{x}(k) \in S$ for all subsequent k .
- Set S is '**constraint admissible**' if, for a given control law $\mathbf{u} = \kappa(\mathbf{x})$, $(\mathbf{x}, \kappa(\mathbf{x})) \in \{(\mathbf{x}, \mathbf{u}) : \mathbf{M}\mathbf{x} + \mathbf{E}\mathbf{u} \leq \mathbf{b}\}$ for all $\mathbf{x} \in S$.
- The origin is a '**stable**' equilibrium point if, for any $\varepsilon > 0$ there exists $\delta > 0$ such that $\|\mathbf{x}(0)\| < \delta \Rightarrow \|\mathbf{x}(k)\| < \varepsilon$ for all $k > 0$. The origin is '**asymptotically stable**' if $\lim_{k \rightarrow \infty} \|\mathbf{x}(k)\| = 0$.
- $V : S \rightarrow \mathbb{R}$ is a '**Lyapunov function**' if 1) $V(\mathbf{0}) = 0$, 2) $V(\mathbf{x}) > 0$ for all $\mathbf{x} \in S \setminus \mathbf{0}$ and 3) $V(\mathbf{f}(\mathbf{x})) \leq V(\mathbf{x})$ for all $\mathbf{x} \in S$ (in continuous time, condition (3) is instead $dV/dt \leq 0$).

Conditions for Stability:

Consider the system $\mathbf{x}(k+1) = \mathbf{A}\mathbf{x}(k) + \mathbf{B}\mathbf{u}(k)$ with state and input constraints $\mathbf{M}\mathbf{x} + \mathbf{E}\mathbf{u} \leq \mathbf{b}$. Let $\mathbf{P} > 0$ and \mathbf{K} satisfy $\rho(\mathbf{A} + \mathbf{B}\mathbf{K}) < 1$ and $(\mathbf{A} + \mathbf{B}\mathbf{K})^T \mathbf{P} (\mathbf{A} + \mathbf{B}\mathbf{K}) - \mathbf{P} \leq -\mathbf{Q} - \mathbf{K}^T \mathbf{R} \mathbf{K}$. If the terminal constraint $\mathbf{M}_N \mathbf{x}_N \leq \mathbf{b}_N$ is chosen to be a constraint admissible invariant set for the closed loop system $\mathbf{x}(k+1) = (\mathbf{A} + \mathbf{B}\mathbf{K})\mathbf{x}(k)$ for some \mathbf{K} and the constrained finite horizon control problem is feasible at time $k=0$, then it is feasible for all $k \geq 1$ if the control input is given by the receding horizon control law $\mathbf{u}(k) = \mathbf{u}_0^*(\mathbf{x}(k))$, and **the resulting closed loop system is asymptotically stable**.

If there exists a Lyapunov function such that $V(\mathbf{f}(\mathbf{x})) < V(\mathbf{x})$ for all $\mathbf{x} \in S \setminus \mathbf{0}$ then the origin is an asymptotically stable equilibrium point for $\mathbf{x}(k+1) = \mathbf{f}(\mathbf{x}(k))$ with region of attraction S . If S is the whole space and $V(\mathbf{x}) \rightarrow \infty$ as $\|\mathbf{x}\| \rightarrow \infty$ then it is **globally asymptotically stable**.

For the constrained **infinite horizon** predictive control problem, the value function

$$V(\mathbf{x}, \mathbf{u}) = \sum_{k=0}^{\infty} (\mathbf{x}(k)^T \mathbf{Q} \mathbf{x}(k) + \mathbf{u}(k)^T \mathbf{R} \mathbf{u}(k))$$

is to be minimised while obeying constraints for all times k . Let $\mathbf{P} \geq 0$ be the solution to the DARE $\mathbf{P} = \mathbf{Q} + \mathbf{A}^T \mathbf{P} \mathbf{A} - \mathbf{A}^T \mathbf{P} \mathbf{B} (\mathbf{R} + \mathbf{B}^T \mathbf{P} \mathbf{B})^{-1} \mathbf{B}^T \mathbf{P} \mathbf{A}$ and let $\mathbf{K} = -(\mathbf{R} + \mathbf{B}^T \mathbf{P} \mathbf{B})^{-1} \mathbf{B}^T \mathbf{P} \mathbf{A}$. At each time step k , let $\mathbf{x} = \mathbf{x}(k)$ and compute a finite horizon input sequence that minimises the finite horizon cost function

$$V(\mathbf{x}, \mathbf{u}) = \mathbf{x}_N^T \mathbf{P} \mathbf{x}_N + \sum_{i=0}^{N-1} (\mathbf{x}_i^T \mathbf{Q} \mathbf{x}_i + \mathbf{u}_i^T \mathbf{R} \mathbf{u}_i)$$

where $\mathbf{x}_0 = \mathbf{x}$, $\mathbf{x}_{i+1} = \mathbf{A}\mathbf{x}_i + \mathbf{B}\mathbf{u}_i$, subject to $\mathbf{M}\mathbf{x}_i + \mathbf{E}\mathbf{u}_i \leq \mathbf{b}_i$ and $\mathbf{M}_N \mathbf{x}_N \leq \mathbf{b}_N$ for $i \in \{0, 1, \dots, N-1\}$, where the set $\{\mathbf{x} : \mathbf{M}_N \mathbf{x} \leq \mathbf{b}_N\}$ is constraint admissible and invariant for the closed loop system with control law $\mathbf{u}(k) = \mathbf{K}\mathbf{x}(k)$, and apply the control $\mathbf{u}(k) = \mathbf{u}_0^*$. This controller is stable.

9.4.23. Model-Based Reinforcement Learning (RL)

Reinforcement learning is a model-free approach to optimal control i.e. the ‘plant’ is unknowable. It is most practically useful when the sets of states and control inputs are discrete and **finite**.

At each time step $t \in \{0, 1, 2, \dots\}$, the **agent (controller)** takes **actions (inputs)** $a \in \mathcal{A}(s)$ which cause the **environment (plant)** to feed back to the agent with a new **state** $s \in \mathcal{S}$ and a **reward** $r \in \mathcal{R} \subset \mathbb{R}$.

Setup: the random variables $\{S, A, R\}$ are sampled at each iteration (finite Markov decision process, MDP).

- State transition model: $p(s', r | s, a) = \mathbb{P}(S_{t+1} = s', r_{t+1} = r | S_t = s, A_t = a)$.
- Agent policy: $p(a | s) = \pi(a | s)$, or if deterministic then can be written as $a = \pi(s)$
- Return (discounted reward): $G_t = \sum_{k=t+1}^T \gamma^{k-t-1} R_k = R_{t+1} + \gamma R_{t+2} + \gamma^2 R_{t+3} + \dots + \gamma^{T-t+1} R_T$ ($0 \leq \gamma \leq 1$)

If $\gamma = 1$ then this is an ‘episodic’ (non-continuing) case, eventually entering a terminal state $s \in \mathcal{S}^+ \subset \mathcal{S}$ at time $t = T$. This indicates the end of an ‘episode’.

- Objective: find policy $\pi = \pi^*$ that maximises $E_{\pi^*}[G_t]$ (under policy π^*).
Optimal policy π^* satisfies $v_{\pi^*}(s) \geq v_{\pi}(s)$ and $q_{\pi^*}(s, a) \geq q_{\pi}(s, a)$.

Useful constructs in solving this problem are:

- **Action-value function:** $q_{\pi}(s, a) = E_{\pi}[G_t | S_t = s, A_t = a]$ (expected return given current state/action)
- **State-value function:** $v_{\pi}(s) = E_{\pi}[G_t | S_t = s] = \sum_{a \in A} \pi(a | s) q_{\pi}(s, a)$ (policy weighted average q)

If a model is available (full access to $p(s', r | s, a)$), then a DP solution gives the optimal policy, using the Bellman equation (Section 9.4.8).

Since $v_{\pi}(s) = \sum_{a \in A} \pi(a | s) q_{\pi}(s, a)$ and $G_t = R_{t+1} + \gamma G_{t+1} \rightarrow q_{\pi}(s, a) = \sum_{r \in \mathcal{R}} \sum_{s' \in \mathcal{S}} p(s', r | s, a) (r + \gamma v_{\pi}(s'))$.

Policy Evaluation: iterate the Bellman equations to find the value function of the current policy π

- $v_{\pi}(s) = \sum_{a \in A} \pi(a | s) \sum_{r \in \mathcal{R}} \sum_{s' \in \mathcal{S}} p(s', r | s, a) (r + \gamma v_{\pi}(s'))$ (Bellman Equation for v)
- $q_{\pi}(s, a) = \sum_{r \in \mathcal{R}} \sum_{s' \in \mathcal{S}} p(s', r | s, a) (r + \gamma \sum_{a \in A} \pi(a | s) q_{\pi}(s, a))$ (Bellman Equation for q)

Policy Improvement: converges to the optimal policy $v_{\pi^*}(s) = \max_a q_{\pi^*}(s, a)$ over all a

- Using deterministic $a = \pi(s)$, choose the new policy as $\pi'(s) = \arg \max_a q_{\pi}(s, a)$ over all a (greedy wrt $v_{\pi}(s)$).
By the policy improvement theorem, $v_{\pi'}(s) \geq v_{\pi}(s)$. $q_{\pi}(s, a)$ is found from its Bellman Equation.

Policy Iteration: to find $\pi^*(s)$ and $v_{\pi^*}(s)$: compute $\{\pi_0, v_{\pi_0}, \pi_1, v_{\pi_1}, \pi_2, v_{\pi_2}, \dots, \pi^*, v_{\pi^*}\}$.

- Start from an initial policy $\pi_0(s)$, then iterate ... until optimal $\pi^*(s)$ and $v_{\pi^*}(s)$.
 - Use **Policy Evaluation (to convergence)** to find its value $v_{\pi_0}(s)$.
 - Use **Policy Improvement** to find a new policy $\pi_1(s)$.

Value Iteration: same as policy iteration but only using **one step** during the policy evaluation part.

9.4.24 Model-Free Reinforcement Learning (RL)

In model-free RL, the environment model $p(s', r | s, a)$ is unavailable, so policy iteration / value iteration cannot be used. Instead, only a finite sample of trajectories $\{S_0, A_0, R_1, S_1, A_1, R_2, S_2, A_2, \dots, R_T, A_T\}$ is available, found by running a policy through the MDP.

Monte-Carlo Evaluation: given M samples under π , estimate q_π , updating once per episode

Expand the new set of states to include actions as $S_t^{\text{new}} = \{S_t, A_t\}$, so that $v_\pi(S_t^{\text{new}}) = q_\pi(s, a)$, and the new 'Markov reward process' (MRP) is the trajectory $\{S_0, R_1, S_1, R_2, S_2, \dots, R_T, S_T\}^{(m)}$ (trajectories $m = 1, 2, \dots, M$).

The Monte-Carlo estimate is then $V(s) = E_\pi[G_t | S_t = s] \approx \frac{1}{C(s)} \sum_{m=1}^M \sum_{\tau=0}^{T_m-1} \mathbf{I}\{s_\tau^{(m)} = s\} g_\tau^{(m)}$, or as an update rule:

$$V(s_t^{(m)}) \leftarrow V(s_t^{(m)}) + \alpha(g_t^{(m)} - V(s_t^{(m)}))$$

($g_\tau^{(m)}$: evaluated return, $\mathbf{I} \in \{0, 1\}$: indicator, $C(s)$: number of times state s visited overall, α : step size hyperparameter replacing $1/C(s_t^{(m)})$ in constant-MC)

Monte-Carlo Control: allow for some exploration instead of greedily optimising q_π

- ϵ -greedy policy: with probability ϵ , act randomly; else, choose a to optimise q_π .

Off-Policy Method:

Monte-Carlo Exploring Starts:

Simulating an Episode

Initialisation: at $t = 0$, let $\pi(a | s)$ be uniform across all $a \in \mathcal{A}(s)$ (random action) and let $p_0(s)$ be uniform across all $s \in \mathcal{S}$ (random starting state).

Iteration:

- Draw from $p_0(s)$ to find the starting state s .
- Draw from $\pi(a | s)$ to find the action a .
- Draw from $p(s', r | s, a)$ to find the next state s' and reward r .

This generates a trajectory of $\{s_0, a_0, r_1, s_1, a_1, r_2, s_2, a_2, r_3, s_3, a_3, \dots, r_{T-1}, s_{T-1}, a_{T-1}, r_T, s_T\}^{(m)}$

The objective is to use a policy that maximises $g_0 = r_1 + \gamma r_2 + \gamma^2 r_3 + \dots + \gamma^{T-1} r_T$.

9.4.30. Practical Examples of Control System Implementations

Example 1: LSTM-based MPC for a corn-to-sugar process

Chemical engineering applications operate on ‘slower’ time scales than mechanical systems so the computational complexity of using neural network models is less important.

[Reference](#): Meng *et al.* RNN-LSTM-Based Model Predictive Control for a Corn-to-Sugar Process. *Processes* 2023, 11, 1080.

Example 2: 3D Kinematics Data Fusion with a Mahony Filter

A magnetic and inertial measurement unit (MIMU) consists of a 3-axis MEMS gyroscope, accelerometer and magnetometer. MIMUs are widely used in many applications of attitude determination (e.g. human motion tracking, unmanned aerial vehicles (UAV), mobile navigation).

An embedded MEMS chip contains an on-board 3-axis accelerometer, gyroscope and magnetometer to measure acceleration, attitude (orientation) and magnetic field strength

Example 3: Optimal Control of an Insulin Pump with a Glucose Biosensor

[Robust \$H_2\$ Glucose Control in Diabetes Using a Physiological Model](#)

Example 4: [Optimal Control of VTOL Drone](#)

State variables: $\mathbf{x} = [x_1, x_2, x_3, x_4, x_5, x_6]$ (x_1 : yaw angle, x_2 : yaw rate, x_3 : pitch angle, x_4 : pitch rate, x_5 : roll angle, x_6 : roll rate)

Control variables: $\mathbf{u} = [u_1, u_2, u_3]$ (u_1 : yawing torque, u_2 : pitching torque, u_3 : rolling torque)

Output variables: $\mathbf{y} = [y_1, y_2, y_3]$ (y_1 : yaw angle, y_2 : pitch angle, y_3 : roll angle)

P10. ASTROPHYSICS AND COSMOLOGY

10.1. Aerospace Engineering and Orbital Mechanics

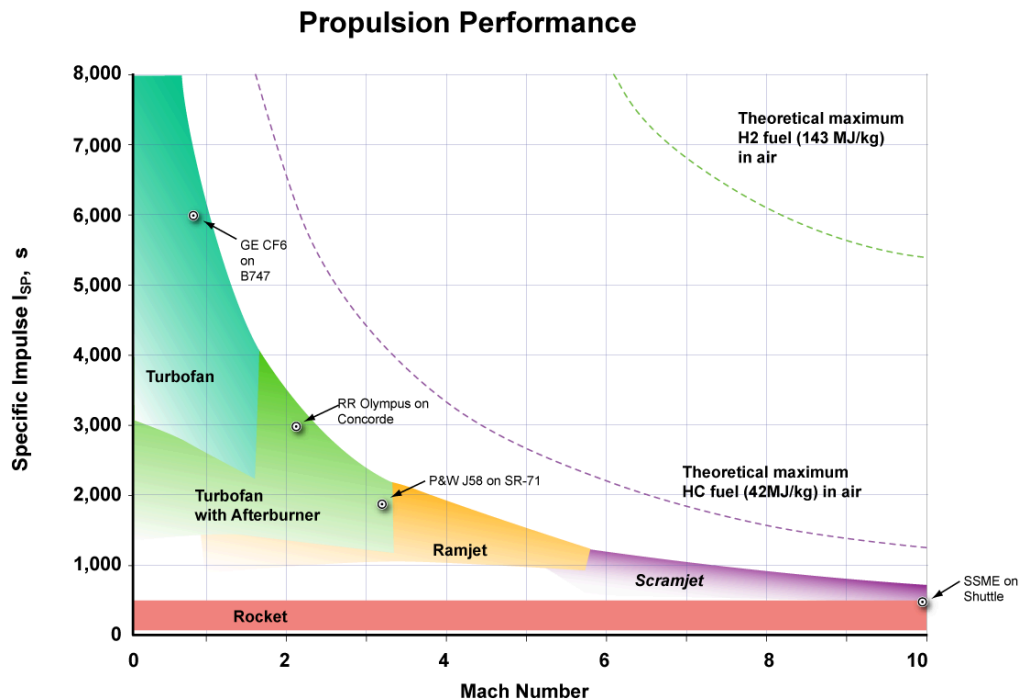
10.1.1. Ideal (Tsiolkovsky) Rocket Equation and Specific Impulse

The maximum possible delta-v with no drag is given by

$$\Delta v = v_e \ln \frac{m_0}{m_f} = I_{sp} g_0 \ln \frac{m_0}{m_f},$$

($v_e = I_{sp} g_0$: effective exhaust velocity (assumed constant), I_{sp} : specific impulse (dimensions of time), g_0 : standard surface gravity = 9.81 ms^{-2} , m_0 : wet mass (initial), m_f : dry mass.)

Typical values of I_{sp} are given below:



10.1.2. Breguet Range Equation for Aeronautical Vehicles

10.1.3. Kinematics and Geometry of Elliptical Orbits

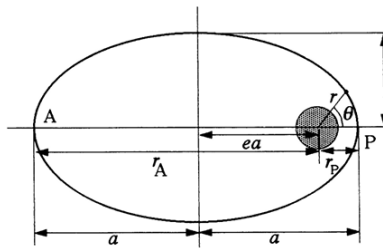
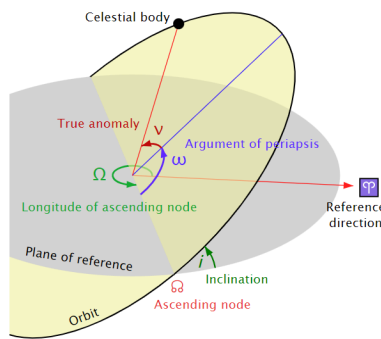
Satellites in a central gravitational potential follow trajectories of conic sections (circle: $e = 0$, ellipse: $0 < e < 1$, parabola: $e = 1$, hyperbola, $e > 1$), with the central body (e.g. a planet's COM) as one of its foci. Long-range, zero-drag projectile motion also follows this type of trajectory.

Circular Orbits: satellite maintains a constant distance above the primary.

Centripetal-gravitational force balance: $v = \sqrt{\mu/r}$ (v : satellite speed, r : radius)

Geosynchronous orbit: $r^3 = \frac{\mu P^2}{4\pi^2}$ (P : rotational period of primary)

Elliptical Orbits: satellite follows an ellipse with one focus at the primary's COM.



Polar equation: $\frac{l}{r} = 1 + e \cos \theta$
 where $\frac{1}{l} = \frac{a}{b^2} = \frac{GM}{h^2}$ and $e^2 = 1 - \left(\frac{b}{a}\right)^2$.

Periaapsis: $\theta = 0 \rightarrow r_p = (1 - e)a$
 Apoaapsis: $\theta = \pi \rightarrow r_p = (1 + e)a$

(a : semi-major axis, e : eccentricity, i : inclination, ω : argument of periaapsis, T : time of periaapsis passage, Ω : celestial longitude of ascending node, v : true anomaly, P : orbital period, N_1 : ascending node, N_2 : descending node, $\mu = GM$: gravitational parameter, γ : zenith angle (between \mathbf{r} and \mathbf{v}), $h = rv \sin \gamma$: specific angular momentum)

Kepler's third law: P^2 is proportional to a^3 ; specifically, $P^2 = \frac{4\pi^2}{G(M+m)} a^3$.

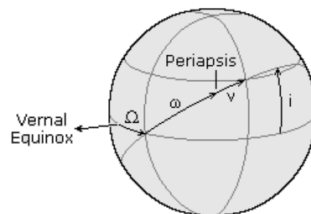
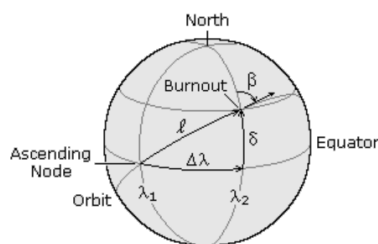
Launch of a Space Vehicle: given a vehicle entering free-fall after burnout at state $\{r_0, v_0, \gamma_0\}$:

Apoapsis and Periaapsis: $\frac{r_{A,P}}{r_0} = \frac{-C \pm \sqrt{C^2 + 4(1-C) \sin^2 \gamma_0}}{2(1-C)}$ where $C = \frac{2\mu}{hv_0} = \frac{2GM}{r_0 v_0^2}$.

Eccentricity: $e^2 = \left(\frac{hv_0}{\mu} - 1\right)^2 \cos^2 \phi + \sin^2 \phi$ where $\phi = \frac{\pi}{2} - \gamma$ (flight path angle).

True anomaly: $\tan v = \frac{\sin \gamma_0 \cos \gamma_0}{\sin^2 \gamma_0 - \frac{\mu}{hv_0}}$. Semi-major axis: $\frac{1}{a} = \frac{2}{r} - \frac{v^2}{\mu}$ (vis-viva equation)

Termination launch at apogee/perigee ($\gamma = 90^\circ$) results in minimum propellant consumption.

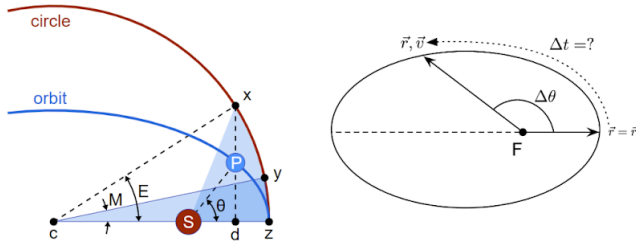


Given β, δ and λ_2 : $\tan l = \frac{\tan \delta}{\cos \beta}$;
 $\cos i = \cos \delta \sin \beta$; $\omega = l - v$;
 $\tan \Delta \lambda = \sin \delta \tan \beta$; $\lambda_1 = \lambda_2 - \Delta \lambda$

(β : azimuth heading, δ : geocentric latitude / declination, $\Delta \lambda$: angular distance between ascending node and burnout point in equatorial plane, λ_1 : geographic longitude of ascending node, λ_2 : geographic longitude of burnout)

10.1.4. Time Evolution of an Orbit

Given an initial state $\mathbf{r}_0 = (r_0, \theta_0)$ and $\mathbf{v}_0 = (v_{r0}, v_{t0})$ (in 2D polar coordinates), the state at a time Δt later can be found using the methods below.



$$r = \frac{h^2}{\mu} \frac{1}{1 + \left(\frac{h^2}{\mu r_0} - 1\right) \cos \Delta\theta - \frac{h v_{r0}}{\mu} \sin \Delta\theta}$$

Lagrange coefficients: defined such that $\vec{r} = f\vec{r}_0 + g\vec{v}_0$ and $\vec{v} = \dot{f}\vec{r}_0 + \dot{g}\vec{v}_0$:

$$f = 1 - \frac{\mu r}{h^2} (1 - \cos \Delta\theta) \quad \dot{f} = \frac{\mu}{h} \frac{1 - \cos \Delta\theta}{\sin \Delta\theta} \left[\frac{\mu}{h^2} (1 - \cos \Delta\theta) - \frac{1}{r_0} - \frac{1}{r} \right]$$

$$g = \frac{r r_0}{h} \sin \Delta\theta \quad \dot{g} = 1 - \frac{\mu r_0}{h^2} (1 - \cos \Delta\theta) , \quad f\dot{g} - g\dot{f} = 1$$

Kepler problems: given change in true anomaly $\Delta\theta$, find flight time Δt .

(M_e : mean anomaly, E : eccentric anomaly)

$$\int_{\theta_0=0}^{\theta=\Delta\theta} \left(\frac{1}{1 + e \cos \theta} \right)^2 d\theta = \int_0^t \frac{\mu^2}{h^3} dt$$

$$\frac{2\pi}{T} t = M_e = E - e \sin E$$

$$\tan \frac{E}{2} = \sqrt{\frac{1-e}{1+e}} \tan \frac{\Delta\theta}{2} ,$$

Inverse Kepler problems: given travel time Δt , find the change in true anomaly $\Delta\theta$.

The equation above has no closed form in E (it is transcendental) so must be solved numerically.

To help with numerical stability in this calculation, the Universal variable method is used:

Universal anomaly: $\chi \equiv \frac{\sqrt{\mu}}{r}$ (the Sundman transformation; χ_0 : initial guess (Chobotov approximation))

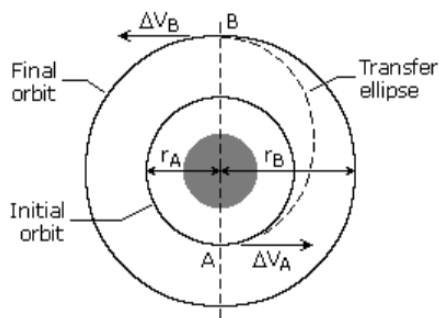
Kepler's equation: $\sqrt{\mu} \Delta t = \frac{r_0 v_{r0}}{\sqrt{\mu}} \chi^2 C(\alpha \chi^2) + (1 - \alpha r_0) \chi^3 S(\alpha \chi^2) + r_0 \chi$, $\alpha = \frac{1}{a} = \frac{2}{r_0} - \frac{v_0^2}{\mu}$, $\chi_0 = \frac{\sqrt{\mu}}{|a|} \Delta t$.
 $z = \alpha \chi^2$.

Stumpff functions: $S(x) = \begin{cases} (\sqrt{x} - \sin(\sqrt{x}))/\sqrt{x^3} & \text{if } x > 0 \\ 1/6 & \text{if } x = 0, \\ (\sinh(\sqrt{-x}) - \sqrt{-x})/\sqrt{(-x)^3} & \text{if } x < 0 \end{cases}$, $C(x) = \begin{cases} (1 - \cos \sqrt{x})/x & \text{if } x > 0 \\ 1/2 & \text{if } x = 0, \\ (1 - \cosh \sqrt{-x})/x & \text{if } x < 0 \end{cases}$, $S'(z) = \frac{1}{2z}(C - 3S)$
 $C'(z) = \frac{1}{2z}(1 - 2C - zS)$

Lagrange coefficients: $f = 1 - \frac{\chi^2}{r_0} C(\alpha \chi^2)$, $\dot{f} = \frac{\sqrt{\mu}}{r r_0} [\alpha \chi^3 S(\alpha \chi^2) - \chi]$, $\vec{r} = f\vec{r}_0 + g\vec{v}_0$.
 $g = \Delta t - \frac{1}{\sqrt{\mu}} \chi^3 S(\alpha \chi^2)$, $\dot{g} = 1 - \frac{\chi^2}{r} C(\alpha \chi^2)$, $\vec{v} = \dot{f}\vec{r}_0 + \dot{g}\vec{v}_0$.

10.1.5. The Hohmann Transfer

The ideal Hohmann transfer orbit is elliptical, initiated by a short-burst impulse tangent to the starting circular orbit (A) and ending with a second impulse on the opposite side (B) to fall into a second circular orbit.



- Impulse at A and B:

$$J_A = m \Delta V_A \quad J_B = m \Delta V_B$$

- Velocity on transfer orbit at A and B:

$$V_t = \sqrt{\mu \left(\frac{2}{r} - \frac{1}{a} \right)} \quad \left(a = \frac{r_A + r_B}{2} \right)$$

- Eccentricity of transfer ellipse:

$$e = 1 - \frac{r_A}{a}$$

10.1.6. Radiation Pressure

Solar radiation pressure is exerted on an object in space due to the change in momentum of incident photons.

- Radiation pressure by reflection: $p = (1 + \rho) \frac{I}{c} \cos^2 \theta$
- Radiation force (parallel component): $F = (1 + \rho) \frac{P}{c} \quad (P = IA, F = pA)$
- Radiation pressure by absorption / emission: $p = \varepsilon \frac{I}{c} \cos^2 \theta$

(ρ : surface reflectivity, ε : surface emissivity, θ : angle of incidence, I : irradiant intensity, P : radiant power, c : speed of light, A : projected area normal to incident radiation)

The irradiant intensity due to a star follows an inverse-square law with distance:

$$I \sim d^{-2} \Rightarrow I = I_0 \left(\frac{d_0}{d} \right)^2 \quad (I_0: \text{intensity measured at distance } d_0)$$

For the Sun, the irradiance at a distance of 1 A.U. is $I_0 = 1.361 \text{ kW m}^{-2}$.

Solar Sails: a solar sail is a spacecraft with a large planar reflector (up to 1 km in size) which is pushed (propelled) by radiation pressure. The point at which the radiation pressure balances the gravitational pull is the heliocentric equilibrium point.

Diffraction-based solar sails have also been developed, which use metamaterial gratings to diffract incoming radiation, allowing photons to be reused in e.g. solar panels.

10.1.7. Potential Futures of Space Travel and Space Civilisations

Kardashev Scale: classification of civilisations by magnitude of energy consumption

Assuming that all potential civilisations are expansionist and require resources, like humanity:

- **Type 0:** incomplete utilisation of the available energy in its home planet.
- **Type 1:** fully utilise the available energy in its home planet ($\sim 10^{16}$ W); start interplanetary travel.
- **Type 2:** fully utilise the available energy in its star ($\sim 10^{26}$ W); start interstellar travel.
- **Type 3:** fully utilise the available energy in its galaxy ($\sim 10^{36}$ W); start intergalactic travel.
- **Type 4:** fully utilise the available energy in the whole universe.

Humanity is a Type 0 civilisation, and is $\sim 75\%$ the way to becoming a Type 1 civilisation, which may occur at some point in the next ~ 200 years.

Dyson Sphere: extracts energy from a star, feasible for a type 2 civilisation




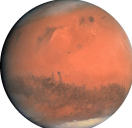

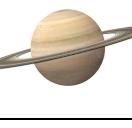


An orbiting swarm of satellites carrying reflective mirrors or solar panels. Acquiring the materials for constructing these satellites would require planet-scale mining.

Penrose Sphere: extracts energy from a rotating black hole, feasible for a type 3 civilisation

Frame dragging around the 'ringularity' of a rapidly rotating black hole leads to the formation of an ergosphere outside the event horizon. With a giant spherical mirror surrounding the black hole, radiation can be beamed into the black hole to be partially absorbed in the event horizon while the remainder is amplified in energy by superradiant scattering in the ergosphere (the Penrose process), extracting some of the black hole's angular momentum.

10.2. Astronomy

10.2.1. Planets in the Solar System

(not to scale)	Planet	Mass / kg	Mean Radius / km	Semi-major Axis / AU	Orbital Eccentricity	Orbital Period (Sidereal, Earth years)	Rotational Period (Sidereal, Earth days)	Structure
	Mercury	3.285×10^{23}	2439.7	0.387	0.205	0.241	58.6462	Solid rock; no atmosphere
	Venus	4.867×10^{24}	6051.8	0.723	0.007	0.615	-243.02 (retrograde)	Semi-solid Fe/Ni core; supercritical CO ₂ + H ₂ SO ₄ atmosphere
	Earth	5.972×10^{24} (M_{\oplus})	6371.0	1.000	0.0167	1.000	0.99727	Fe/Ni core; N ₂ + O ₂ atmosphere (See Section 14.2 for more)
	Mars	6.390×10^{23}	3389.5	1.52	0.093	1.881	1.0259	Liquid Fe core; thin CO ₂ atmosphere
	Jupiter	1.898×10^{27}	69911	5.20	0.0488	11.86	0.41354	Solid core; metallic hydrogen mantle;
	Saturn	5.683×10^{26}	58232	9.58	0.0565	29.46	0.44002	H ₂ + He atmosphere
	Uranus	8.681×10^{25}	25362	19.2	0.0472	84.01	-0.71833 (retrograde)	Solid rock core; water + ammonia + methane ice mantle;
	Neptune	1.024×10^{26}	24622	30.1	0.0086	164.8	0.67125	H ₂ + He + methane atmos.

10.2.2. Telescopes and Stellar Luminosity

Angular magnification in normal adjustment: $M = \frac{\text{angle subtended by image at an eye}}{\text{angle subtended by object at a naked eye}}$

Reflecting telescopes can be made using a Cassegrain arrangement of a parabolic concave primary mirror and convex secondary mirror.

Hipparcos scale: ranked from 1-6 (brightest to dimmest).

Apparent magnitude m : A difference of 1 on the magnitude scale is equal to an intensity ratio of 2.51.

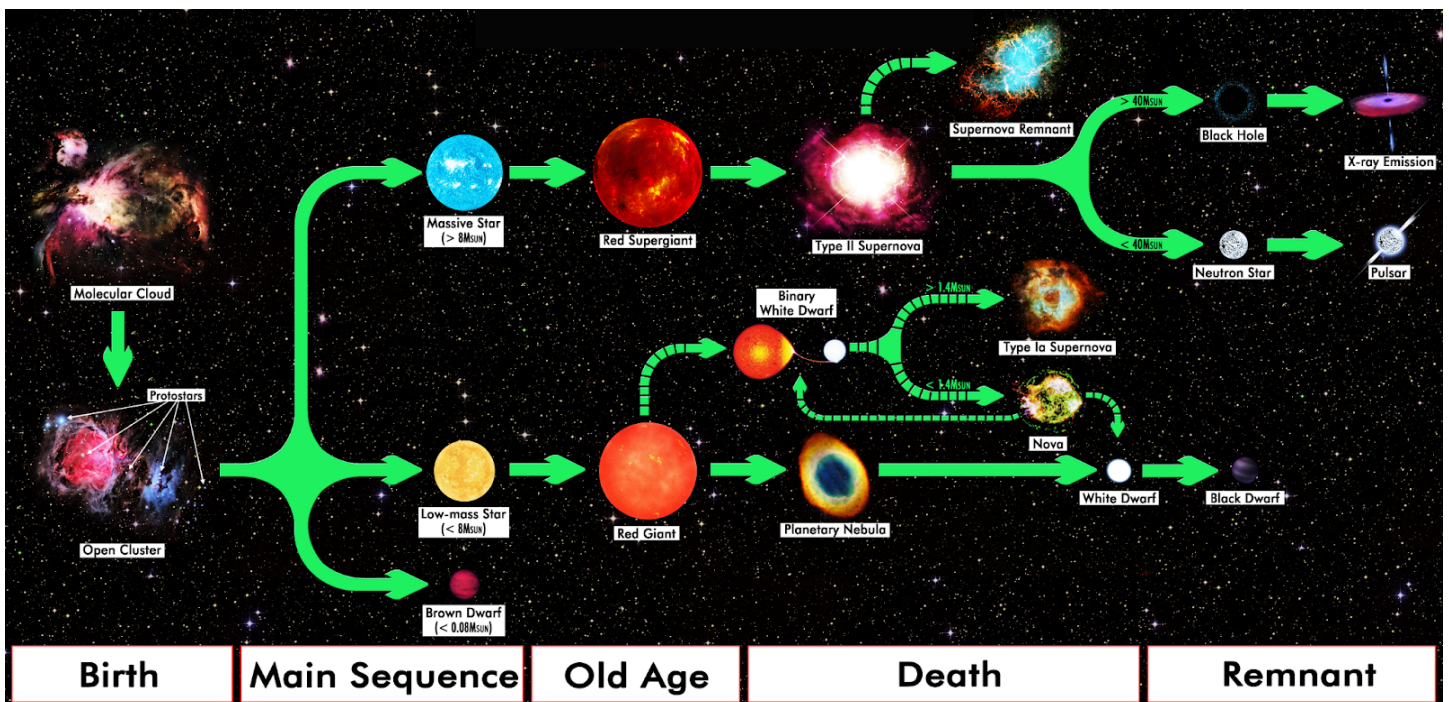
Minimum angular resolution of telescope (Rayleigh criterion): $\theta = 1.22 \times \frac{\lambda}{D}$.

Collecting power is proportional to diameter squared.

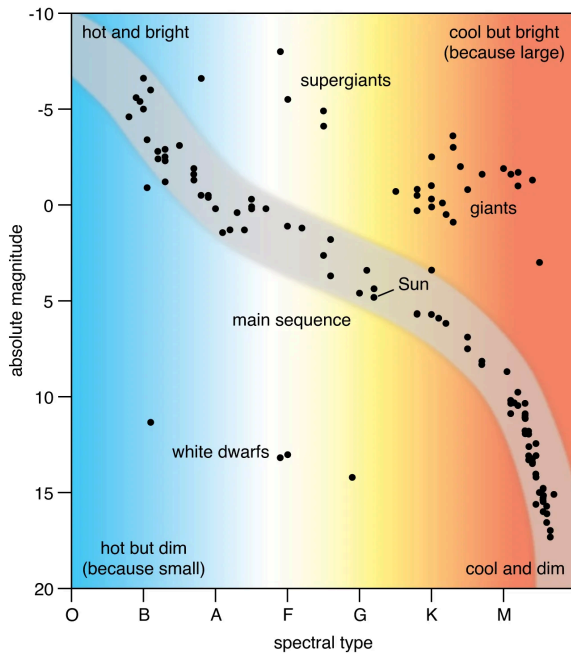
Absolute magnitude M : equal to the apparent magnitude at a distance of 10 parsecs.

Conversion: $m - M = 5 \log_{10} \frac{d [pc]}{10}$. Neglects extinction due to interstellar or cosmic dust.

10.2.3. Stellar Evolution

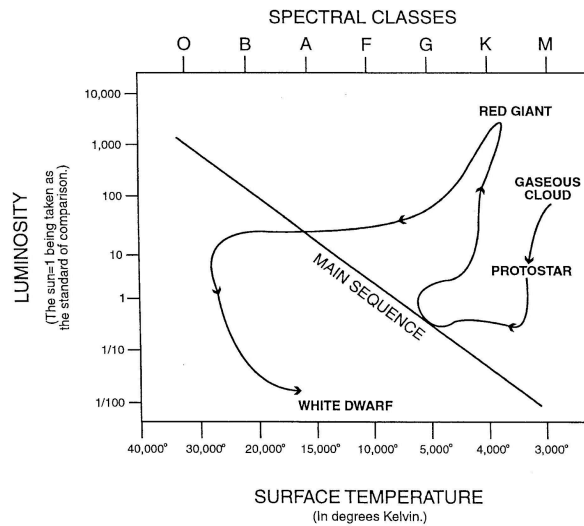


10.2.4. Stellar Spectral Classes and the Hertzsprung-Russell Diagram



Spectral Class	Intrinsic Colour	Temperature / K	Prominent Absorption Lines
O	blue	25000 - 50000	He ⁺ , He, H
B	blue	11000 - 25000	He, H
A	blue-white	7500 - 11000	H (strongest), ionised metals
F	white	6000 - 7500	Ionised metals
G	yellow-white	5000 - 6000	Ionised and neutral metals
K	orange	3500 - 5000	Neutral metals
M	red	< 3500	Neutral atoms, TiO

Stellar evolution of Sun-like stars:



10.2.5. Degenerate Matter

Electron degeneracy pressure: repulsive force arising from the Pauli exclusion principle of electrons. It supports the white dwarf state against further gravitational collapse in low-mass stars (below the Chandrasekhar limit: $M < 1.44 M_{\odot}$). Stars exceeding this mass will collapse to a neutron star.

Neutron degeneracy pressure: repulsive force arising from the Pauli exclusion principle of neutrons. It supports the neutron star state against further gravitational collapse in medium and high-mass stars (below the Tolman-Oppenheimer-Volkoff limit (TOV limit): $M \lesssim 2.1 M_{\odot}$). Stars exceeding this mass will collapse to a black hole (or, hypothetically, a quark star).

10.2.6. Formation of Stellar Remnants

Brown dwarf: a 'failed star', too light to sustain ^1H -fusion. They still produce a little light due to a small amount of deuterium fusion.

White dwarf: at the end of a red dwarf's life, the lighter outer layers of the star are ejected as a planetary nebula (nova) due to heat from core fusion, leaving behind a dense carbon-oxygen rich core (the white dwarf). It is hypothesised that the white dwarf will burn out to become a black dwarf (cold and inert) over an extremely long period of time.

Neutron star: at the end of a red supergiant's life, the iron core formed from fusion cannot fuse any further and cannot support the gravitational pull of the star. Once a critical mass of iron is attained, the core is rapidly compressed into neutron degenerate matter while the remainder of the star is ejected as a supernova. Their formation is accompanied by a gamma ray burst (GRB).

Pulsar: a rapidly rotating neutron star which expels electromagnetic radiation (typically radio waves) from its poles which sweep across observable space.

Magnetar: a neutron star with extremely strong magnetic fields at their poles, emitting energetic X-rays and gamma rays.

10.2.7. Supernovas

Classification:

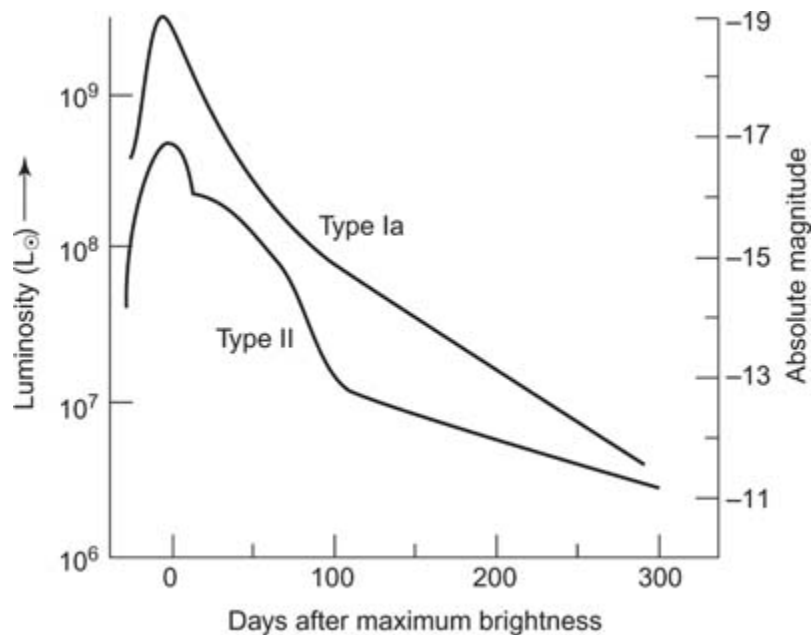
Type I - When a star accumulates matter from its companion star in a binary system and explodes after reaching a critical mass. Emission spectra has no hydrogen Balmer lines.

Type Ia - a Type I supernova with a white dwarf. When the companion star in the binary system runs out of hydrogen, it expands, allowing the white dwarf to begin accumulating some of its mass. When the white dwarf star reaches a critical mass, fusion begins and becomes unstoppable as the mass continues to increase, eventually causing the white dwarf to explode in a supernova.

Type II - The death of a high-mass star after it runs out of fuel.

Light Curves:

All types of supernovae occur at the same critical mass, meaning they all have a very similar peak absolute magnitude (about -19.3) and produce very consistent light curves, allowing astronomers to use them as standard candles to calculate distances to far-off galaxies (they can be seen up to 1000Mpc away).



Other important sources for standard candles are the Cepheid Variable stars, whose apparent magnitude fluctuates with a time period proportional to its absolute magnitude (Leavitt's law).

10.3. Cosmology and Relativity

10.3.1. Doppler Effect for Electromagnetic Waves

10.3.2. Hubble's Law and Redshift

10.3.3. Quasars and Galactic Structures

Quasars are extremely distant, luminous active galactic nuclei (AGN) that contain a rapidly accreting supermassive black hole at their core.

Quasars are observed with cosmological redshift, indicative of extreme distances. The most distant quasars formed only a few hundred million years after the Big Bang.

Large quasar groups (LQGs) are collections of quasars.

Galaxies consist of millions of stars in an elliptical, spiral or irregular shape. Most (but not all) galaxies have a large black hole in the centre.

Galaxies located together form a galaxy cluster (e.g. the Local Group).

Galaxy clusters located together form a galaxy supercluster (e.g. Virgo supercluster).

Galaxy superclusters located together form a galactic filament (e.g. Sloan Great Wall).

Galactic filaments surround sparse regions of space known as voids (e.g. Boötes Void).

Our galaxy, the Milky Way, may have been a 'Seyfert galaxy' in the past, in which the supermassive black hole Sagittarius A* emitted polar jets, at a lower intensity than a typical quasar.

A 'blazar' is a quasar whose polar jet is directed at observers on Earth, in which the jet energy is amplified by relativistic beaming (length contraction to higher intensity).

The Blandford–Znajek process provides the power for quasar extragalactic jets.

10.3.4. Michelson-Morley Interferometer

10.3.5. Special Relativity

Profound consequences:

- The speed of light c is constant in all inertial reference frames.
- The passage of time, including simultaneity, depends on the reference frame.
- It is impossible to distinguish between absolute and relative motion.

A relativistic body moving relative to an inertial observer frame will experience both time dilation (the body experiences time passing slower) and length contraction (the frame coordinates are compressed parallel to its motion).

The following are valid for motion in a straight line at constant speed.

Lorentz factor:
$$\gamma = \frac{1}{\sqrt{1 - v^2/c^2}} \quad (\gamma \geq 1, 0 \leq v \leq c)$$

Length contraction:
$$L' = \frac{L_0}{\gamma} = L_0 \sqrt{1 - v^2/c^2} \quad (L_0: \text{proper length})$$

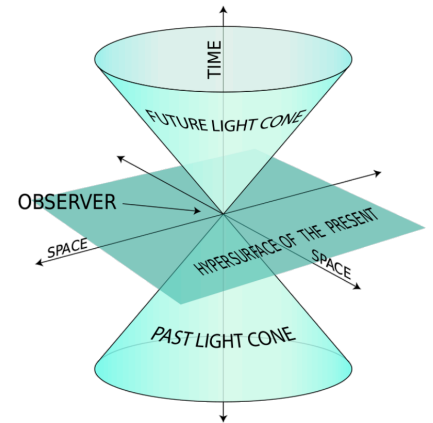
Time dilation:
$$\Delta t' = \gamma \Delta t_0 = \frac{\Delta t_0}{\sqrt{1 - v^2/c^2}} \quad (\Delta t_0: \text{proper time})$$

Mass increase:
$$m' = \gamma m_0 = \frac{m_0}{\sqrt{1 - v^2/c^2}} \quad (m_0: \text{rest mass})$$

Special relativity is a particular case of general relativity in the Minkowski metric tensor (flat spacetime). Accelerations and forces are more complicated in SR.

10.3.7. General Relativity

A particle in 3D space, observed with coordinate time t , moving with three-velocity $\mathbf{v} = \frac{dx}{dt} \mathbf{i} + \frac{dy}{dt} \mathbf{j} + \frac{dz}{dt} \mathbf{k}$, constitutes a world line in 4D space time, in which it experiences proper time τ . The dilation factor is $\gamma = \frac{d\tau}{dt} = \frac{1}{\sqrt{1-v^2}} \geq 1$ where v is normalised such that $c = 1$.



Einstein notation: $v^\alpha u_\alpha = \sum_i v^i u_i$, a summation over variables.

The Christoffel symbols Γ_{ij} denote the rate of change of basis vector e_i along a coordinate x^j , and depend only on the choice of coordinate system.

Geodesic equation: $\frac{dv}{d\tau} = 0 \Leftrightarrow \frac{dv^\alpha}{d\tau} = -\Gamma^\alpha_{\mu\nu} v^\mu v^\nu$ Metric tensor: $|v|^2 = (ds)^2 = g_{\mu\nu} dx^\mu dx^\nu = c^2$

In general, $\Gamma^\gamma_{\alpha\beta} = \frac{g^{\gamma\sigma}}{2} \left(\frac{dg_{\sigma\alpha}}{dx^\beta} + \frac{dg_{\sigma\beta}}{dx^\alpha} - \frac{dg_{\alpha\beta}}{dx^\sigma} \right)$, but in orthogonal coordinates, $\Gamma^\gamma_{\alpha\beta} = \frac{1}{2g_{\gamma\gamma}} \left(\frac{dg_{\gamma\alpha}}{dx^\beta} + \frac{dg_{\gamma\beta}}{dx^\alpha} - \frac{dg_{\alpha\beta}}{dx^\gamma} \right)$

$(g^{\gamma\sigma}$: inverse of $g_{\gamma\sigma}$)

Minkowski metric tensor (pseudo-Riemannian metric, $(-, +, +, +)$ signature): $\eta = \begin{pmatrix} -1 & 0 & 0 & 0 \\ 0 & 1 & 0 & 0 \\ 0 & 0 & 1 & 0 \\ 0 & 0 & 0 & 1 \end{pmatrix}$

This metric tensor has zero curvature (flat spacetime).

Riemann curvature tensor of spacetime: $R^\alpha_{\beta\mu\nu} = \frac{d\Gamma^\alpha_{\beta\nu}}{dx^\mu} + \Gamma^\lambda_{\beta\nu} \Gamma^\alpha_{\lambda\mu} - \frac{d\Gamma^\alpha_{\beta\mu}}{dx^\nu} - \Gamma^\lambda_{\beta\mu} \Gamma^\alpha_{\lambda\nu}$. Ricci tensor: $R_{\mu\nu} = R^\lambda_{\mu\lambda\nu}$

Ricci scalar: for orthogonal coordinates, $R = g^{\mu\nu} R_{\mu\nu}$ (average curvature in all directions)

If $R > 0$, parallel lines converge. If $R < 0$, parallel lines diverge.

Energy-momentum tensor: T_{tt} (energy density), $T_{xt} = T_{tx}$ (momentum density), T_{xx} (pressure).

In 4D spacetime, cross-terms in space arise, which are the viscosities.

Einstein field equation: $R_{\mu\nu} - \frac{1}{2}Rg_{\mu\nu} + \Lambda g_{\mu\nu} = \frac{8\pi G}{c^4} T_{\mu\nu}$ ($\Lambda \approx 1.1 \times 10^{-52} \text{ m}^2$: cosmological constant)

For a 1-body (mass M) problem in spherical coordinates (t, r, θ, ϕ) ,

(the Schwarzschild metric). Schwarzschild radius: $r = \frac{2GM}{c^2}$

(temporal term becomes zero \rightarrow black hole horizon radius:).

$$g_{\mu\nu} = \begin{bmatrix} c^2 - \frac{2GM}{r} & 0 & 0 & 0 \\ 0 & \frac{1}{\frac{2GM}{rc^2} - 1} & 0 & 0 \\ 0 & 0 & -r^2 & 0 \\ 0 & 0 & 0 & -r^2 \sin^2 \theta \end{bmatrix}$$

10.3.8. Hawking Model of Black Holes

The Kerr metric describes the geometry around a rotating mass.

The Morris-Thorne metric describes the geometry of non-gravitating wormholes.

10.3.9. The Big Bang Theory and the Λ CDM Model (Dark Matter and Dark Energy)

Λ CDM (lambda-cold dark matter) is the standard model of big bang cosmology. Based on general relativity, it explains the anisotropy of the cosmic microwave background (CMB) radiation, the large-scale structure of galaxy clusters, the observed abundances of H, He and Li, and the accelerating expansion of the universe from distant starlight.

The observed mass-energy density balance is made up of ~68% dark energy, ~27% dark matter and ~5% ordinary matter.

Evidence for the Accelerating Expansion of the Universe

- Spectral lines from distant galaxies are redshifted.
- Supernova luminosity curves decay with distance in accordance with time dilation.

Properties of Dark Matter: in Λ CDM, dark matter:

- cannot consist of any matter made from protons, neutrons, electrons or neutrinos
- has a velocity far less than the speed of light (cold)
- does not cool by radiative emission of photons
- interacts with itself and ordinary matter only by gravity (and possibly by the weak force)

Friedmann Equations

Λ CDM uses the Friedmann-Lemaître-Robertson-Walker (FLRW) metric to describe the observable universe from approximately 0.1 ms after the Big Bang to the present.

10.3.10. Mechanisms of Redshift

Sunyaev-Zel'dovich Effect: CMB photons are shifted to higher frequency due to an inverse Compton effect interaction with relativistic electrons in the corona of a black hole.

Integrated Sachs-Wolfe Effect: Photons lose less energy when emerging from a potential well than the energy gained when entering due to the presence of **dark energy** causing the expansion of spacetime, flattening the potential well.

P11. NUCLEAR, QUANTUM AND MEDICAL PHYSICS

11.1. Quantum Physics and The Standard Model

11.1.1. Standard Model of Elementary Particles

Quarks

Leptons

Gauge (Vector) Bosons

Scalar Bosons

Generations of matter (fermions)			Force carriers / interactions (bosons)	
I	II	III		
Up quark (u) $m = 2.2 \text{ MeV}/c^2$ $q = \frac{2}{3}$, spin = $\frac{1}{2}$	Charm quark (c) $m = 1.28 \text{ GeV}/c^2$ $q = \frac{2}{3}$, spin = $\frac{1}{2}$	Top quark (t) $m = 173.1 \text{ GeV}/c^2$ $q = \frac{2}{3}$, spin = $\frac{1}{2}$	Gluon (g) strong nuclear force $m = 0$ $q = 0$, spin = 1	Higgs boson (H) $m = 124.97 \text{ GeV}/c^2$ $q = 0$, spin = 0
Down quark (d) $m = 4.7 \text{ MeV}/c^2$ $q = -\frac{1}{3}$, spin = $-\frac{1}{2}$	Strange quark (s) $m = 96 \text{ MeV}/c^2$ $q = -\frac{1}{3}$, spin = $-\frac{1}{2}$	Bottom quark (b) $m = 4.18 \text{ GeV}/c^2$ $q = -\frac{1}{3}$, spin = $-\frac{1}{2}$	Photon (γ) electromagnetic force $m = 0$ $q = 0$, spin = 1	
Electron (e) $m = 0.511 \text{ MeV}/c^2$ $q = -1$, spin = $\frac{1}{2}$	Muon (μ) $m = 105.66 \text{ MeV}/c^2$ $q = -1$, spin = $\frac{1}{2}$	Tauon (τ) $m = 1.7768 \text{ GeV}/c^2$ $q = -1$, spin = $\frac{1}{2}$	Z boson (Z) weak nuclear force $m = 91.19 \text{ GeV}/c^2$ $q = 0$, spin = 1	
Electron neutrino (ν_e) $m = 0.07 \text{ eV}/c^2$ $q = 0$, spin = $\frac{1}{2}$	Muon neutrino (ν_μ) $m < 0.17 \text{ MeV}/c^2$ $q = 0$, spin = $\frac{1}{2}$	Tauon neutrino (ν_τ) $m < 18.2 \text{ MeV}/c^2$ $q = 0$, spin = $\frac{1}{2}$	W boson (W) weak nuclear force $m = 80.433 \text{ GeV}/c^2$ $q = \pm 1$, spin = 1	

Mass m conversion: $1 \text{ MeV}/c^2 = 1.7827 \times 10^{-30} \text{ kg}$

Charge q is given as a multiple of the elementary charge $e = 1.602 \times 10^{-19} \text{ C}$.

- The W boson exists as either W^+ or W^- , with the corresponding charge.
- Gluons have colour charge and anticolour charge (red / green / blue), with 8 different types.
- Gravitons (G) are hypothetical tensor bosons (spin = 2), predicted by theories in quantum gravity. If they exist, they are difficult to detect due to being extremely low energy ($m < 10^{-22} \text{ eV}/c^2$, $q = 0$). They may be the quanta of the gravitational field comprising gravitational waves (which have been detected).
- Anti-electrons are commonly called positrons (e^+).

11.1.2. Composite Particles (Hadrons)

Baryons (composed of three quarks):

Proton (p): uud Antiproton (\bar{p}): $\bar{u}\bar{u}\bar{d}$ Delta baryons (Δ): uuu / uud / udd / ddd
 Neutron (n): udd Antineutron (\bar{n}): $\bar{u}\bar{d}\bar{d}$ Lambda baryons (Λ): uds / udc / udb

Tetraquarks and pentaquarks are exotic baryons with 4 and 5 quarks respectively.

Mesons (composed of one quark and one antiquark):

Pion (π): $u\bar{d}$ / $u\bar{u}$ / $d\bar{d}$ / $\bar{u}d$ Kaon (K): $u\bar{s}$ / $d\bar{s}$ / $s\bar{u}$ Rho meson (ρ): $u\bar{d}$

11.1.3. Heisenberg Uncertainty Principles

Strictly, these uncertainties are standard deviations, but can also be interpreted qualitatively with less rigorous bounds.

Uncertainties in position and momentum: $\Delta x \Delta p_x \geq \frac{\hbar}{2}$

Uncertainties in time and energy: $\Delta t \Delta E \geq \frac{\hbar}{2}$

11.1.5. Wave-Particle Duality

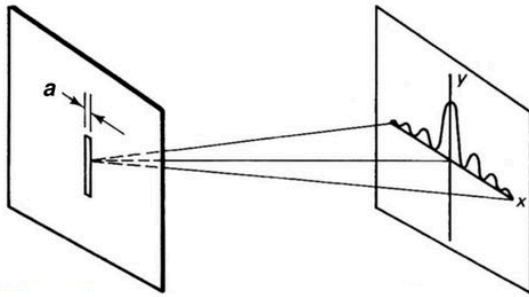
De Broglie wavelength: $\lambda = \frac{h}{p}$

Quantisation: $E = n\hbar\omega$ $p = n\hbar k$ ($\omega = 2\pi f$, $k = \frac{2\pi}{\lambda}$) n : integer

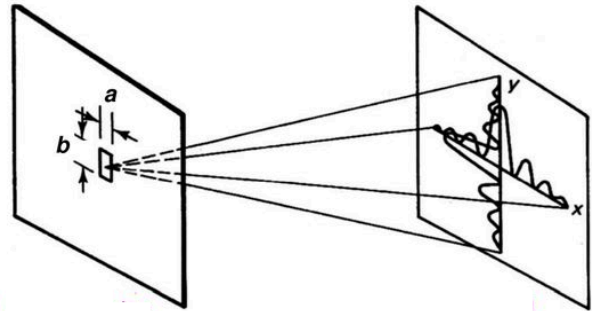
Dispersion relation: $\omega = \frac{\hbar k^2}{2m}$

11.1.6. Single-Slit Diffraction

Collinear and coherent quantum particles incident on a single slit undergo diffraction in a plane spanned by the momentum vector of the particle and the direction of the slit whose dimension a is similar to the (De Broglie) wavelength λ of the particle.



1D diffraction: $a \sim \lambda$



2D diffraction: $a \sim b \sim \lambda$

Angles of diffraction for **minima**: $\sin \theta_n = \frac{n\lambda}{a}$
 ($n = 1, 2, \dots$: order of diffraction, $x_n \approx D \sin \theta_n$ for flat screen)

At $\theta = 0$, there is the zero-order **maxima**, of intensity I_0 .

Angles of diffraction for **maxima**: solutions to $\tan u_n = u_n$ where $u_n = \frac{a\pi}{\lambda} \sin \theta_n$ ($n = 0, 1, 2, \dots$)
 ($u_n = 0, 4.493, 7.725, 10.904, 14.066, 17.221, 20.371, \dots$)

Fraunhofer diffraction intensity:

$$I(\theta) = I_0 \operatorname{sinc}^2\left(\frac{a\pi}{\lambda} \sin \theta\right) = I_0 \frac{\lambda^2 \sin^2\left(\frac{a\pi}{\lambda} \sin \theta\right)}{\pi^2 a^2 \sin^2 \theta} \quad \text{or} \quad I(x) = I_0 \operatorname{sinc}^2\left(\frac{\pi ax}{\lambda D}\right) = I_0 \frac{\lambda^2 D^2 \sin^2\left(\frac{\pi ax}{\lambda D}\right)}{\pi^2 a^2 x^2}$$

Diffraction of X-rays or electrons on polycrystalline graphite leads to a radially-symmetric circular diffraction pattern due to the random orientation of the splitting direction.

11.1.7. Double-Slit Diffraction and Interference

11.1.8. Quantum Mechanical Operators

Dirac's 'bra-ket' notation:

- 'Bra' operator: $\langle \Psi | = \int d\mathbf{x} \Psi^*(\mathbf{x})$ and 'Ket' operator: $|\Phi\rangle = \Phi(\mathbf{x})$
- Bra-ket inner product: $\langle \Psi | \hat{C} | \Phi \rangle = \int \Psi^*(\mathbf{x}) \hat{C} \Phi(\mathbf{x}) d\mathbf{x}$ (in a Hilbert space)

($\{\Psi, \Phi\}$: wavefunctions, \mathbf{x} : position vector, \hat{C} : operator, integrals taken over all space ($\mathbf{x} \in \mathbb{R}^3$))

- Quantum superposition: $|\psi\rangle = \alpha|\psi_1\rangle + \beta|\psi_2\rangle$ ($\{\alpha, \beta\} \in \mathbb{C}$: state coefficients)
- Expectation of an observable: $\langle C \rangle = \langle \psi | \hat{C} | \psi \rangle$
- Hermitian adjoint: $\langle \phi | \hat{C} \psi \rangle = \langle \hat{C}^\dagger \phi | \psi \rangle$ (\hat{C}^\dagger exists for any linear \hat{C})
- Hermitian operator \hat{C} (self-adjoint): $\langle \phi | \hat{C} | \psi \rangle = \langle \psi | \hat{C} | \phi \rangle^*$ (ψ^* : complex conjugate)
- Eigenstates of an operator: $\hat{C} f_i = \lambda_i f_i$ (f_i : eigenfunctions, λ_i : eigenvalues)
All Hermitian operators have real eigenvalues.
- Probability density function: $p(\mathbf{x}) = \psi(\mathbf{x})^* \psi(\mathbf{x}) = |\psi(\mathbf{x})|^2$

Operators representing physical observables (energy, momentum) are Hermitian as they have real expected values. Their eigenfunctions form an orthonormal basis.

- Position operator: $\hat{\mathbf{x}} = \mathbf{x}$
- Energy operator: $\hat{E} = -i\hbar \frac{\partial}{\partial t}$
- Momentum operator: $\hat{\mathbf{p}} = -i\hbar \nabla$
- Kinetic energy operator: $\hat{T} = -\frac{\hbar^2}{2m} \nabla^2$
- Potential energy operator: $\hat{V} = V(\mathbf{x})$
- Hamiltonian operator: $\hat{H} = \hat{T} + \hat{V}$
- Time evolution operator: $\hat{U} = \exp(-i\hat{H}t/\hbar)$

Schrödinger's equation (general time-dependent): $\hat{H}\Psi = \hat{E}\Psi$

Schrödinger's equation (time-independent): $\hat{H}\Psi = E\Psi$ (E : energy eigenvalues)

Probability current:
$$\mathbf{j} = \frac{1}{2m} (\Psi^* \hat{\mathbf{p}} \Psi - \Psi \hat{\mathbf{p}} \Psi^*) = -\frac{i\hbar}{2m} (\psi^* \nabla \psi - \psi \nabla \psi^*) = \frac{\hbar}{m} \text{Im}(\psi^* \nabla \psi)$$

Probability conservation law: for any control volume V and control surface S ,

$$\int_V \left(\frac{\partial p}{\partial t} + \nabla \cdot \mathbf{j} \right) dV = 0 \quad \Leftrightarrow \quad \frac{\partial}{\partial t} \int_V p dV + \oint_S \mathbf{j} \cdot d\mathbf{S} = 0$$

(divergence form) (flux form)

The 3D plane wave solution $\psi(\mathbf{x}) = A \exp(i(\mathbf{k} \cdot \mathbf{x} - \omega t))$ (\mathbf{k} : wavevector, ω : angular frequency) has a probability density $p(\mathbf{x}) = |A|^2$ and probability current $\mathbf{j}(\mathbf{x}) = |A|^2 \frac{\hbar}{m} \mathbf{k} = p\mathbf{v}$ (since $\mathbf{p} = \hbar\mathbf{k}$).

Stationary states (e.g. standing waves) have $\mathbf{j} = \mathbf{0}$ everywhere.

Transmission and reflection coefficients: $T + R = 1$ where $T = \left| \frac{\mathbf{j}_{\text{trans}} \cdot \mathbf{n}}{\mathbf{j}_{\text{inc}} \cdot \mathbf{n}} \right|$, $R = \left| \frac{\mathbf{j}_{\text{ref}} \cdot \mathbf{n}}{\mathbf{j}_{\text{inc}} \cdot \mathbf{n}} \right|$
 (\mathbf{n} : normal vector to barrier, $\mathbf{j}_{\text{trans}}$: transmission current, \mathbf{j}_{inc} : incident current, \mathbf{j}_{ref} : reflected current)

In an external electromagnetic field,
$$\mathbf{j} = \frac{1}{2m} \left[(\Psi^* \hat{\mathbf{p}} \Psi - \Psi \hat{\mathbf{p}} \Psi^*) - 2q\mathbf{A}|\Psi|^2 \right]$$

 (\mathbf{A} : magnetic vector potential)

For a spin- s particle without internal structure (e.g. electron),

$$\mathbf{j} = \mathbf{j}_e/q = \frac{1}{2m} \left[(\Psi^* \hat{\mathbf{p}} \Psi - \Psi \hat{\mathbf{p}} \Psi^*) - 2q\mathbf{A}|\Psi|^2 \right] + \frac{\mu_s}{qs\hbar} \nabla \times (\Psi^* \mathbf{S} \Psi)$$

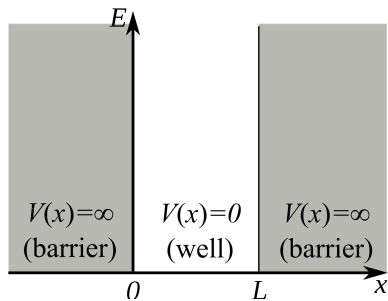
(\mathbf{j}_e : electric current density, q : charge, μ_s : spin magnetic moment, \mathbf{S} : spin vector)

Ladder Operators (Dirac Creation-Annihilation Operators)

$$\hat{J}_{\pm} \equiv \hat{J}_x \pm i\hat{J}_y; \quad \hat{J}_{\pm} |J, M\rangle = \sqrt{J(J+1) - M(M \pm 1)} |J, M \pm 1\rangle$$

where $| \cdot \rangle$ is bra-ket notation for a quantum superposition of states.

11.1.9. 1D Infinite Potential Well (Particle in a Box)



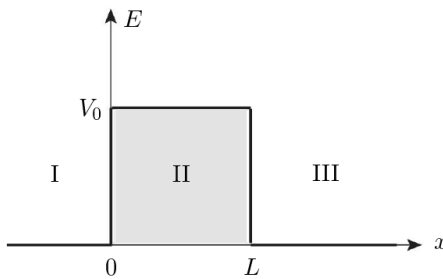
Potential: $V(x) = 0$ if $0 < x < L$ else ∞

Eigenfunctions: $\psi_n = \sqrt{\frac{2}{L}} \sin k_n x$ where $k_n = \frac{n\pi}{L}$

Eigenenergies: $E_n = \frac{\hbar^2 n^2}{8mL^2}$

Momentum: $\langle \psi | \hat{p} | \psi \rangle = 0$ Kinetic energy: $\langle \psi | \hat{T} | \psi \rangle = \frac{\hbar^2 n^2}{8mL^2}$

11.1.10. 1D Finite Barrier Potential



Potential: $V(x) = V_0$ if $0 < x < L$ else 0

Eigenfunctions:
$$\begin{cases} \psi_I = A_r e^{ik_0 x} + A_l e^{-ik_0 x} & x < 0 \\ \psi_{II} = B_r e^{ik_1 x} + B_l e^{-ik_1 x} & 0 \leq x \leq L \\ \psi_{III} = C_r e^{ik_0 x} + C_l e^{-ik_0 x} & x > L \end{cases}$$

Wavenumbers: $k_0 = \sqrt{\frac{2mE}{\hbar^2}}$, $k_1 = \sqrt{\frac{2m(E - V_0)}{\hbar^2}}$

$$A_r + A_l = B_r + B_l$$

$$ik_0(A_r - A_l) = ik_1(B_r - B_l)$$

Coefficients are constrained by: $B_r e^{ik_1 L} + B_l e^{-ik_1 L} = C_r e^{ik_0 L} + C_l e^{-ik_0 L}$

$$ik_1(B_r e^{ik_1 L} - B_l e^{-ik_1 L}) = ik_0(C_r e^{ik_0 L} - C_l e^{-ik_0 L})$$

Transmission coefficient:

Reflection coefficient:

$$t = \frac{4k_0 k_1 e^{-iL(k_0 - k_1)}}{(k_0 + k_1)^2 - e^{2iLk_1}(k_0 - k_1)^2} \quad r = \frac{(k_0 - k_1)^2 \sin k_1 L}{2ik_0 k_1 \cos k_1 L + (k_0^2 + k_1^2) \sin k_1 L}$$

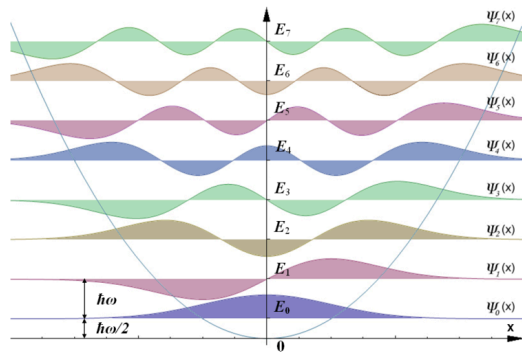
Transmission probability (quantum tunnelling from I to III):

$$\text{If } E < V_0 : T = |t|^2 = \left(1 + \frac{V_0^2 \sinh^2 k_1 L}{4E(V_0 - E)}\right)^{-1}$$

$$\text{If } E > V_0 : T = |t|^2 = \left(1 + \frac{V_0^2 \sin^2 k_1 L}{4E(E - V_0)}\right)^{-1}$$

$$\text{If } E = V_0 : T = \left(1 + \frac{2mL^2 V_0}{\hbar^2}\right)^{-1}$$

11.1.11. 1D Quadratic Potential (Quantum Harmonic Oscillator)



Potential: $V(x) = \frac{1}{2} kx^2$

Eigenfunctions:

$$\psi_n = \frac{1}{\sqrt{2^n n!}} \left(\frac{m\omega}{\pi \hbar} \right)^{1/4} \exp\left(-\frac{m\omega x^2}{2\hbar}\right) H_n\left(\sqrt{\frac{m\omega}{\hbar}} x\right)$$

(H_n : Hermite polynomials (Section 1.7.12), $\omega = \sqrt{\frac{k}{m}}$)

Eigenenergies: $E_n = (2n + 1) \frac{\hbar\omega}{2}$

The zero point (ground state) energy is non-zero and is given by $E_0 = \frac{h}{4\pi} \sqrt{\frac{m}{k}}$.

11.1.12. 3D Quadratic Potential (Spherically Symmetric Quantum Harmonic Oscillator)

Potential: $V(r) = \frac{1}{2} kr^2$ (μ : particle mass; $\omega = \sqrt{\frac{k}{\mu}}$)

Wavefunctions (in spherical coordinates):

$$\psi_{klm} = \sqrt{\left(\frac{2}{\pi}\right)^{1/2} \left(\frac{\mu\omega}{2\hbar}\right)^{l+3/2} \frac{2^{k+2l+3} k!}{(2k+2l+1)!!}} \times r^l \exp\left(-\frac{\mu\omega}{2\hbar} r^2\right) L_k^{(l+1/2)}\left(\frac{\mu\omega}{\hbar} r^2\right) Y_{lm}(\theta, \phi)$$

(L_k^n : generalised Laguerre polynomials, Y_{lm} : spherical harmonics, Section 1.7.13-14.)

Eigenenergies: $E_n = \hbar\omega \left(2k + l + \frac{3}{2}\right)$ where $n = 2k + l$.

For the **inverse** square potential, see the quantum model of hydrogenic atoms (Section 13.1.2).

11.1.13. Casimir Forces due to Vacuum Fluctuations

For two parallel, perfectly conducting plates separated by a submicron distance d , long-wave virtual bosons (primarily photons) are excluded from the region between them, exerting a Casimir pressure (force per unit area) pushing the plates together given by

$$\frac{F}{A} = \frac{\pi^2 \hbar c}{240 d^4} = \frac{1.302 \times 10^{-27}}{d^4}$$

The Casimir force can also be interpreted as a generalisation of the Van der Waals' force.

11.1.14. Quantum Electrodynamics (Special Relativistic Quantum Mechanics)

Klein-Gordon Equation: describes bosons (e.g. Higgs boson) ($\Psi: \mathbb{R}^{1,3} \rightarrow \mathbb{C}$).

$$\left(\frac{1}{c^2} \frac{\partial^2}{\partial t^2} - \nabla^2 + \frac{m^2 c^2}{\hbar^2} \right) \Psi(t, \mathbf{x}) = 0 \quad \text{or with the wave operator } \square^2 = \frac{1}{c^2} \frac{\partial^2}{\partial t^2} - \nabla^2$$

Dirac Equation: describes fermions (e.g. electrons) ($\Phi: \mathbb{R}^{1,3} \rightarrow \mathbb{C}^4$ (spinor)).

$$\left(i\hbar \gamma^\mu \partial_\mu - mc \right) \Phi(t, \mathbf{x}) = 0$$

where the contravariant Dirac matrices are

$$\gamma^0 = \begin{pmatrix} 1 & 0 & 0 & 0 \\ 0 & 1 & 0 & 0 \\ 0 & 0 & -1 & 0 \\ 0 & 0 & 0 & -1 \end{pmatrix}, \quad \gamma^1 = \begin{pmatrix} 0 & 0 & 0 & 1 \\ 0 & 0 & 1 & 0 \\ 0 & -1 & 0 & 0 \\ -1 & 0 & 0 & 0 \end{pmatrix},$$

$$\gamma^2 = \begin{pmatrix} 0 & 0 & 0 & -i \\ 0 & 0 & i & 0 \\ 0 & i & 0 & 0 \\ -i & 0 & 0 & 0 \end{pmatrix}, \quad \gamma^3 = \begin{pmatrix} 0 & 0 & 1 & 0 \\ 0 & 0 & 0 & -1 \\ -1 & 0 & 0 & 0 \\ 0 & 1 & 0 & 0 \end{pmatrix}.$$

11.2. Radioactivity and Nuclear Power Engineering

11.2.1. Radioactive Decay

Modes of Radioactive Decay

- **Alpha decay:** an alpha particle (${}^4\text{He}$ nucleus) escapes from the nucleus. ${}^A_Z X \rightarrow {}^{A-4}_{Z-2} Y + {}^4_2 \alpha$
- **Beta-minus decay:** a neutron becomes a proton. ${}^A_Z X \rightarrow {}^A_{Z+1} Y + {}^0_{-1} \beta^- + {}^0_0 \bar{\nu}_e$
- **Beta-plus decay:** a proton becomes a neutron. ${}^A_Z X \rightarrow {}^A_{Z-1} Y + {}^0_1 \beta^+ + {}^0_0 \nu_e$
- **Gamma decay:** an excited nucleus reduces in energy: ${}^A_Z X^* \rightarrow {}^A_Z X + {}^0_0 \gamma$
- **Electron capture:** a proton becomes a neutron: ${}^A_Z X + {}^0_{-1} e \rightarrow {}^A_{Z-1} Y + {}^0_0 \gamma + {}^0_0 \nu_e$
- **Internal Conversion:** orbital electron ejected: ${}^A_Z X^* \rightarrow {}^A_Z X + {}^0_{-1} e$
- **Cluster decay:** nucleus releases small nucleus e.g. ${}^{14}\text{C}$: ${}^A_Z X \rightarrow {}^{A-N}_{Z-M} Y + {}^N_M C$
- **Spontaneous fission:** nucleus breaks into smaller nuclei: ${}^A_Z X \rightarrow {}^{A-N-k}_{Z-M} Y + {}^N_M C + k {}^1_0 n$

Radius of nucleon: $r \approx r_0 A^{1/3}$ ($r_0 \sim 1.2$ fm, A : mass number) (sphere packing model)

Liquid Drop Model: estimates the binding energy of a nucleus

- Nuclear mass: $m_X = Zm_p + (A - Z)m_n - E_b/c^2$ (E_b : binding energy, E_b/c^2 : mass defect)

- Semi-empirical mass formula:

$$E_b = \underbrace{a_V A}_{\text{volume}} - \underbrace{a_S A^{2/3}}_{\text{surface}} - \underbrace{a_C Z(Z-1)A^{-1/3}}_{\text{Coulomb}} - \underbrace{a_A (A-2Z)^2 A^{-1}}_{\text{asymmetry}} \pm \underbrace{a_P A^{k_P}}_{\text{pairing}}$$

($a_V \approx 15.75$ MeV, $a_S \approx 17.8$ MeV, $a_C \approx 0.711$ MeV, $a_A \approx 23.7$ MeV, $a_P \approx 11.18$ MeV, $k_P \approx -0.5$. Pairing term is **zero** if A is odd; else, pairing term sign is + if Z is even and – if Z is odd.)

- Most stable neutron-proton ratio: $\max E_b(A) \rightarrow N/Z \approx 1 + \frac{a_C}{2a_A} A^{2/3}$.

In this model, binding energy per nucleon $\frac{E_b(A)}{A}$ is achieved at $A = 63$ (Cu).

This neglects the nuclear shells - magic nucleon numbers.

The nucleus with the true highest binding energy per nucleon is ^{62}Ni . It does **not** have the lowest mass per nucleon (most efficient binding), which is ^{56}Fe . Nuclei below ^{56}Fe release nuclear energy by fusion. Nuclei above ^{56}Fe release nuclear energy by fission.

The magic nucleon numbers are 2, 8, 20, 28, 50, 82, 126, which correspond to filled nuclear shells. Nuclei with proton or neutron counts equal to these magic numbers are especially stable. ^4He and ^{16}O are exceptionally stable (higher than usual binding energy per nucleon) due to being 'doubly magic' - both their protons and neutrons fill their nuclear shells.

Decay Rates and Activity: a random process following an exponential distribution

- Activity (decays per second): $A = \lambda N = A_0 e^{-\lambda t}$ (λ : decay constant, units: s^{-1})
- Mean lifetime: $\tau = 1/\lambda$.
- Median lifetime (half-life): $t_{1/2} = \frac{\ln 2}{\lambda} = \tau \ln 2$

Units of A : Becquerels (Bq), Curies (Ci) where 1 Bq = 1 disintegration per second; 1 Ci = 37 GBq.

Conservation of Energy and Momentum

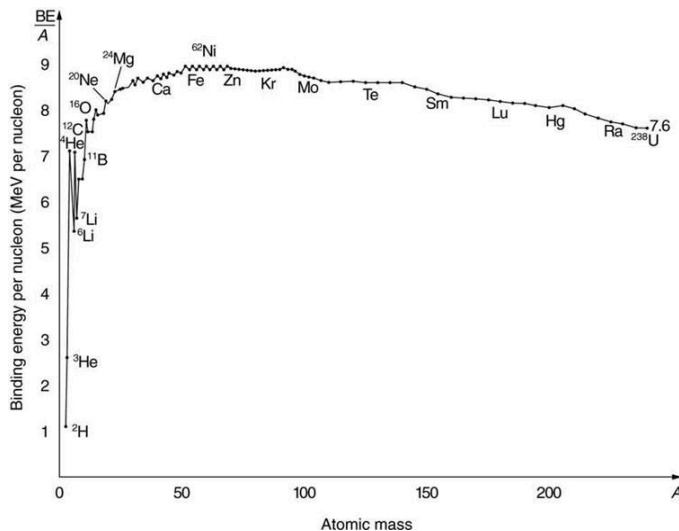
Considering a general nuclear reaction, $A \rightarrow M + m + \gamma$ (speed of M : V , speed of m : v)

- Kinetic energy: $KE_{products} [\text{MeV}] = \frac{1}{2}mv^2 + \frac{1}{2}MV^2 = 931.37 \times (A - M - m) [\text{amu}] - E_\gamma - KE_{A,0}$
 Q -value (disintegration energy released): $931.37 \text{ MeV} \times (m_r - m_p) [\text{amu}]$
- Momentum: since $p_\gamma \approx 0$ and $M \gg m$ then $MV = mv \rightarrow \frac{1}{2}mv^2 \approx KE_{products}$, $\frac{1}{2}MV^2 = \frac{KE_{products}}{1 + \frac{M}{m}}$.

(A : mass number, Z : charge number, neutron count = $A - Z$, in units of amu)

(1 amu = 1 u = 1/12 of ^{12}C atom mass = $1.6605 \times 10^{-27} \text{ kg} = 931.37 \text{ MeV}$ via $\Delta E = \Delta m c^2$.)

Proton mass: 1.007277 u. Neutron mass: 1.008665 u. ^1H mass: 1.007825 u.



Binding Energy per Nucleon

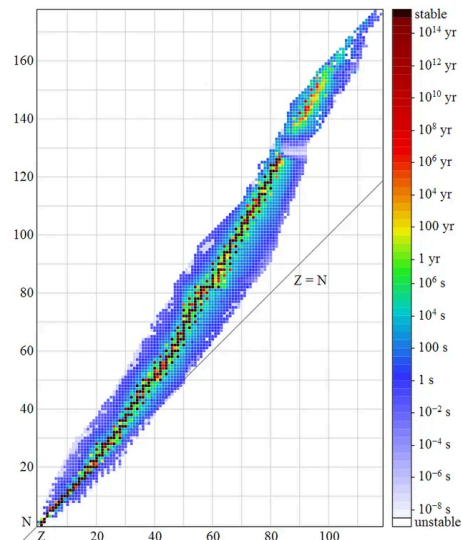


Chart of Nuclides (half-lives)

11.2.2. Alpha Decay

Alpha decay releases an α -particle from a neutron-deficient nucleus: ${}^A_Z X \rightarrow {}^{A-4}_{Z-2} Y + {}^4_2 \alpha$

Energy balance: $m_X c^2 = m_Y c^2 + \frac{1}{2} m_Y v_Y^2 + m_\alpha c^2 + \frac{1}{2} m_\alpha v_\alpha^2$ (parent X at rest)

Momentum balance: $m_Y v_Y = m_\alpha v_\alpha$

Geiger-Nuttall Law: short-lived isotopes emit more energetic alpha particles

Geiger-Nuttall law: $\log_{10} t_{1/2} = a E^{-1/2} + b$ ($t_{1/2}$: half life, E : α -particle energy, a, b : depend on Z)

Gamow Theory: alpha particles can quantum tunnel out of a strong nuclear force potential well

This model can derive the semi-empirical Geiger-Nuttall law.

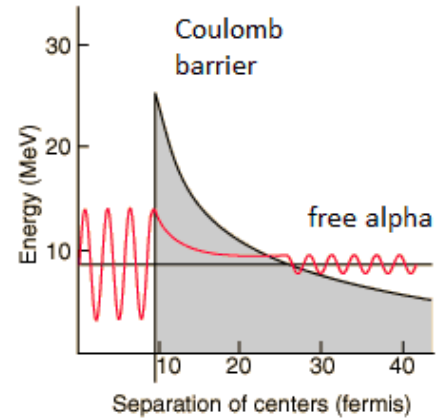
- Potential energy: $V(r) = \begin{cases} r < r_1: U; & r \geq r_1: \frac{2Ze^2}{4\pi\epsilon_0 r} \end{cases}$
(r_1 : radius of X , U : strong potential energy)

- Alpha particle mean lifetime: $\frac{1}{\lambda} = \frac{2r_1}{v} e^{2\gamma}$
($e^{2\gamma} \sim$ transmission coefficient, v : alpha velocity,

$$\gamma = \frac{\sqrt{2mE}}{\hbar} \int_{r_1}^{r_2} \sqrt{\frac{r_2}{r} - 1} dr, \quad r_2: \text{position such that } V(r_2) = E$$

- If $r_2 \gg r_1$, then $\gamma = \frac{K_1 Z}{\sqrt{E}} - K_2 \sqrt{Z r_1}$ ($K_1 = 1.980 \text{ MeV}^{1/2}$, $K_2 = 1.85 \text{ fm}^{-1/2}$)

- Gamow factor: $P(E) = e^{-\sqrt{E_G/E}}$ ($E_G = 2\mu_{12}(\pi\alpha c Z_1 Z_2)^2$, $\mu_{12} = \frac{m_1 m_2}{m_1 + m_2}$, $\alpha = \frac{e^2}{4\pi\epsilon_0 \hbar c}$)



11.2.3. Beta Decay, Electron Capture, Gamma Decay and Internal Conversion

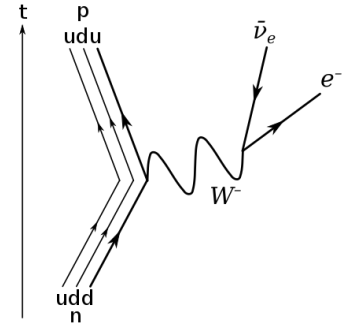
Beta Decay: change in one nucleon by releasing leptons

The W -boson mediates the weak nuclear force, changing the flavour of one quark in a nucleon (neutron: udd , proton: udu).

- β^- decay: $d \rightarrow u + W^-$ ($n \rightarrow p + W^-$) and $W^- \rightarrow e^- + \bar{\nu}_e$
- β^+ decay: $u \rightarrow d + W^+$ ($p \rightarrow n + W^+$) and $W^+ \rightarrow e^+ + \nu_e$

The Feynman diagram for β^- decay is shown on the right.

β^- decay is favoured in neutron-rich nuclei. β^+ decay is favoured in neutron-poor nuclei. β^+ decay can only occur when the daughter binding energy is higher than the parent.



The released energy is distributed among the lepton and the neutrino on a spectrum. The interaction breaks chiral symmetry (alignment of spin and momentum). All observed ν_e have left-handed chirality; all observed $\bar{\nu}_e$ have right-handed chirality. The beta particle is released with the opposite chirality.

Bound state decay: for highly ionised radioisotopes, the emitted electron may be released at an energy lower than the ion's ionisation energy, allowing it to enter an atomic orbital. This can result in a faster rate of beta decay, though this is only significant for total ionisation (bare nuclei: e^- into 1s).

Electron Capture: absorption of shell electron to mediate the weak interaction

If the wavefunction of an electron orbital is found to be within the nucleus, it can interact with the weak nuclear force. It is similar to β^+ decay in effect:

- EC decay: $u \rightarrow d + W^+$ ($p \rightarrow n + W^+$) and $e^- + W^+ \rightarrow \nu_e$, or
 $u + W^- \rightarrow d$ ($p + W^- \rightarrow n$) and $e^- \rightarrow \nu_e + W^-$

EC may occur whenever β^+ decay is possible. The electron may be sourced from any shell (K: $n = 1$, L: $n = 2$, M: $n = 3...$) but K -electron capture is most common. Radioisotopes that are fully ionised (no electrons) will not undergo electron capture.

Gamma Decay: emission of a photon from an excited state (isomeric transition)

Beta decays may result in an excited daughter nucleus, which then decay by gamma decay. Multiple gamma emissions may be required to fall down the nuclear energy levels to reach the ground state.

The energy of the nucleus decreases by hf , where f is the frequency of the photon. The photon is typically in the gamma ray region of the EM spectrum.

Internal Conversion: shell electron interacts with an excited nucleus and is ejected

IC is possible whenever gamma decay is possible. The inner shell electron is ejected, forming a hole, from which a cascade of higher shell electrons can fall, releasing characteristic X-rays. These X-rays can hit other electrons in the same atom, releasing them as Auger electrons.

11.2.3. Radiometric Dating

Carbon Dating: used on organic material and bones. Half-life of $^{14}\text{C} = 5740$ years.

Living organisms take in carbon from the atmosphere at a constant $^{14}\text{C} : ^{12}\text{C}$ isotopic ratio during their lifetime. After death, the ^{14}C within them decays and the resulting ratio can be used to determine the time since death.

Uranium-Lead Dating: used on rocks and minerals. Half-life of $^{235}\text{U} = 704$ million years.

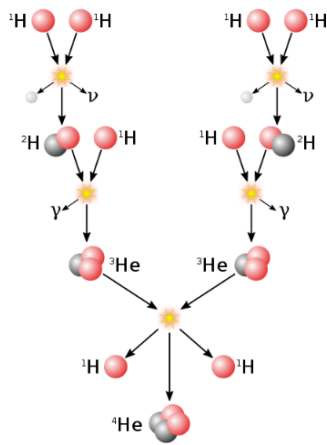
When rocks crystallise, they incorporate uranium which decays into lead. The ratio of lead to uranium indicates the time since crystallisation. With multiple samples, this can be done with the isochron method (plotting a 'concordia' curve).

11.2.4. Nuclear Weapons

History of Nuclear Weapons:

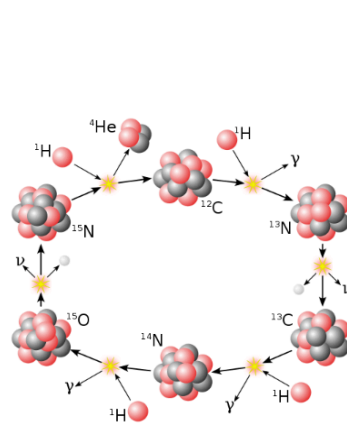
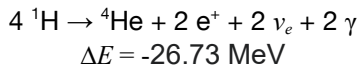
- Before World War 2 (1930s), scientists understood the potential of nuclear weapons, and Allied forces feared that Axis (Nazi) powers would develop weapons of mass destruction.
- Trinity test (June 1945): the first test of an atomic bomb, using plutonium fission.
- Hiroshima (Little Boy, Uranium) and Nagasaki (Fat Man, Plutonium) bombings (August 1945) forced the surrender of Imperial Japan and decisively ended WW2.
- Ivy Mike (1952): the first test of a thermonuclear bomb (hydrogen bomb), using plutonium for fission and deuterium for fusion. Start of the nuclear arms race between the USSR and USA.
- Tsar Bomba (1961): the most powerful bomb ever made, developed by the Soviets.

11.2.4. Stellar Nucleosynthesis



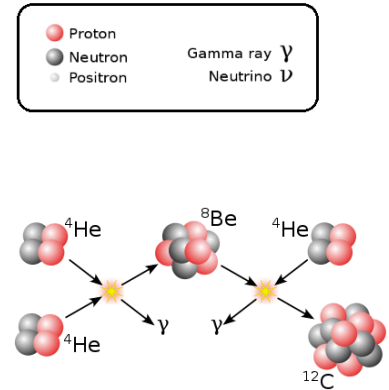
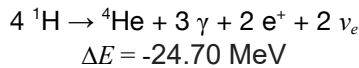
PP Chain:

Hydrogen is fused to helium.
Low-mass stars (incl. the Sun).



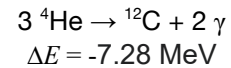
CNO Cycle (CNO-I):

Catalytic formation of helium.
High-mass stars.

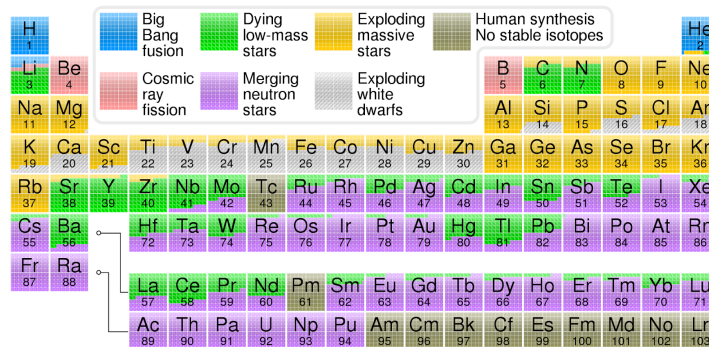


Triple Alpha Process:

Helium is fused to carbon.
Late-stage stellar evolution.



The emitted positrons from these processes annihilate 1:1 with electrons in the environment, releasing two photons and an additional $2m_e c^2 = 1.02 \text{ MeV}$ per positron emitted.



Heavier elements (up to Fe/Ni) are synthesised towards the end of a star's life, after nuclei like C, O, Ne, Si have been burned.

For elements heavier than iron, two processes dominate, which occur during and after supernova:

- *r*-process: rapid multiple neutron capture by ^{56}Fe (up to the neutron 'drip line': size for which the nuclear strong force can retain the neutron), followed by β -decay to form elements with higher proton numbers and also typically large neutron numbers.
- *s*-process: slow (one by one) neutron capture by ^{56}Fe , the products of which may undergo either α or β decay at each stage depending on stability, producing a wider range of products.

The *r*-process also occurs inside thermonuclear warheads to a limited extent, which produce synthetic transuranic elements (e.g. ^{252}Es , ^{257}Fm) in nuclear fallout.

11.2.5. Cosmic Ray Spallation (The x-process)

Cosmic Rays (Astroparticles): near-light speed massive particles travelling across space

Primary cosmic rays consist of stable atomic nuclei (fully ionised: mostly protons and alpha particles) and beta particles (electrons, e^-), as well as a small fraction of antiparticles. On Earth, they can originate from the Sun's solar wind, or from deep space (supernovas and active galactic nuclei/blazars).

When these particles interact with atoms such as in the upper atmosphere of Earth, they form secondary cosmic rays, consisting of pions (π^0, π^\pm), muons ($\pi^\pm \rightarrow \mu^\pm$), neutrons and muon neutrinos. The muons produced by the weak interaction are spin-polarised, do not interact strongly with matter, and persist down to Earth's surface due to relativistic time dilation before decaying to Michel electrons: $\mu^\pm \rightarrow e^\pm$.

Cosmic Ray Spallation:

Cosmic rays form the majority of ${}^7\text{Li}$, ${}^9\text{Be}$ and ${}^{10}\text{B}$, as well as some of the ${}^3\text{He}$.

Typical reactions: ${}^{14}\text{N} + {}^1_0n \rightarrow {}^{10}\text{Be} + {}^4_2\alpha + {}^1_1p$ and ${}^{16}\text{O} + {}^1_1p \rightarrow {}^{10}\text{Be} + {}^4_2\alpha + 2 {}^1_1p + {}^1_0n$

11.2.5. Principles of Nuclear Fusion Power

Important nuclides for synthetic nuclear fusion:

Nuclide	Natural abundance on Earth	Decay and Half-life	Sources
Deuterium (D = ^2H)	156 ppm	(stable)	Can be extracted readily from seawater.
Tritium (T = ^3H)	trace	β^- : $\text{T} \rightarrow ^3\text{He}^+$ $t_{1/2} = 12.32$ years $\Delta E = -18.6$ keV	Must be produced from neutron bombardment of lithium: $^6\text{Li} + \text{n} \rightarrow \text{T} + ^4\text{He} + 4.8$ MeV $^7\text{Li} + \text{n} \rightarrow \text{T} + ^4\text{He} + \text{n} - 2.5$ MeV
Helium-3 (^3He)	1.37 ppm	(stable)	Helium is rare on Earth but known to be present (especially ^3He) on the Moon (suitable for lunar mining).

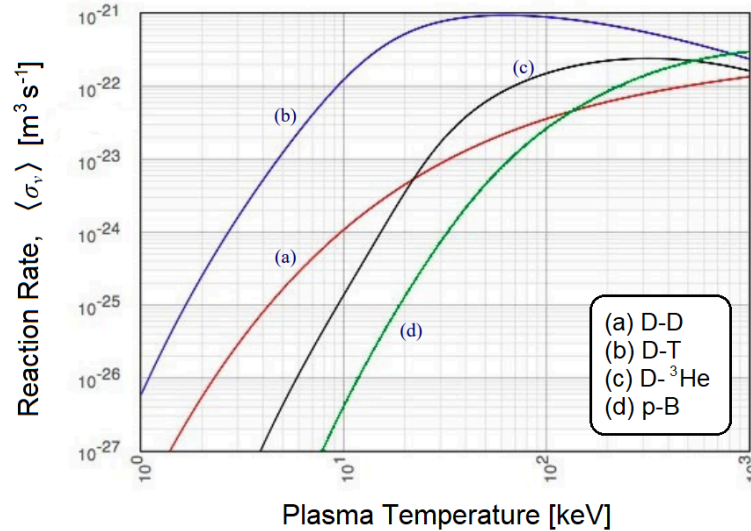
Popular fusion reactions include:

- $2 \text{D} \rightarrow \text{T} + ^1\text{H} + 4.02$ MeV and $2 \text{D} \rightarrow ^3\text{He} + \text{n} + 3.25$ MeV
- $^{11}\text{B} + ^1\text{H} \rightarrow 3 ^4\text{He} + 8.7$ MeV
- $\text{D} + \text{T} \rightarrow ^4\text{He} + \text{n} + 17.6$ MeV
- $\text{D} + ^3\text{He} \rightarrow ^4\text{He} + ^1\text{H} + 18.3$ MeV

The source of tritium is a concern since it is non-existent on Earth. Its production from lithium is also a concern since lithium is also somewhat rare and is already a critical material (used for e.g. batteries).

11.2.6. Nuclear Fusion Reactor Physics

Reaction rate as a function of temperature for important fusion reactions:

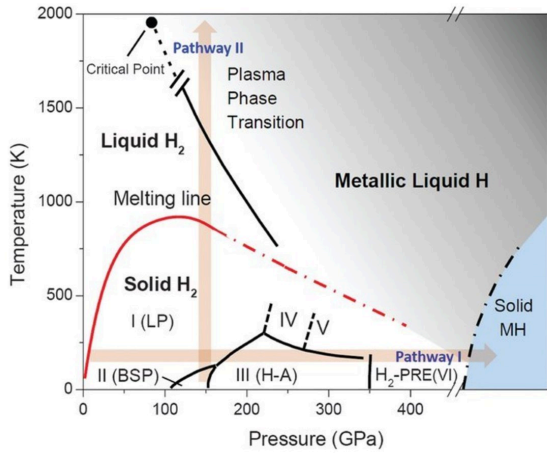


Plasma parameters and correlations:

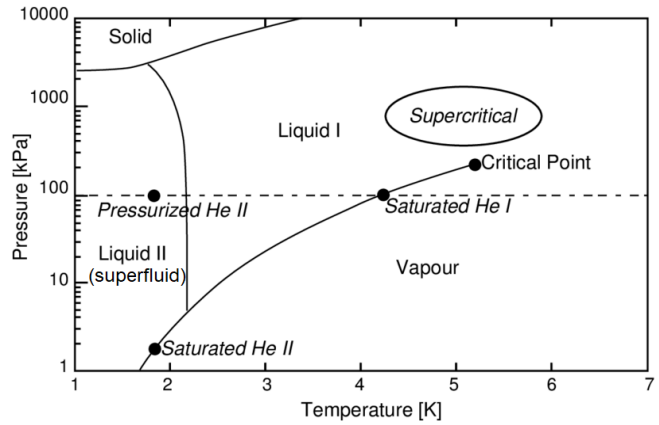
- Beta: $\beta = \frac{\text{plasma pressure: } \langle P \rangle = nk_B T}{\text{magnetic pressure: } p_{mag} = B^2 / (2\mu_0)} = \frac{2nk_B \mu_0 T}{B^2} \quad \beta \gtrsim 5\% \text{ for viable reactor}$
- Normalised beta: $\bar{\beta} = \frac{aB_T}{I_p} \times \beta \quad (I_p \text{ [MA]: plasma current, } a \text{ [m]: radius})$
- Greenwald density limit: $n_G = \frac{I_p}{\pi a^2} [10^{20} \text{ m}^3 \text{ s}^{-1}]$
- Plasma parameter $\Lambda_D = \frac{4\pi\epsilon_0 T_e^{3/2}}{3e^3 n_e^{1/2}} \gg 1$
- Confinement time scaling law: $\tau_e = H \times 0.145 I^{0.93} R_0^{1.39} a^{0.58} \kappa^{0.78} n_{20}^{0.41} B_0^{0.15} A^{0.19} P^{-0.69}$
(R_0 [m]: major radius, n_{20} [10^{23} m^{-3}]: density, B_0 [T]: magnetic flux density, P [MW]: power)
(Tokamak ELMy H-mode correlation, IPB98(y,2))
- Lawson criteria: $n_e \tau_E \geq \frac{12k_B T}{E \langle \sigma_v \rangle} (\approx 1.5 \times 10^{20} \text{ s m}^{-3} \text{ for D-T})$
- Triple product: $n_e \tau_E T_e \geq \frac{12k_B T^2}{E \langle \sigma_v \rangle} (\approx 10^{21} \text{ keV s m}^{-3} \text{ for D-T})$
- Bremsstrahlung radiation: $P_{brem} = 0.85 Pr^2 \frac{Z_{eff}^2}{T_{10keV}^{3/2}} [\text{MW m}^{-3}]$
- Effective plasma ion charge: $Z_{eff} = \frac{\sum Z_i^2 n_i}{\sum Z_i n_i}$
- Larmor gyromagnetic radius: $\rho_L = \frac{v_{th}}{\omega_{cy}} = \frac{(2mT)^{1/2}}{ZeB}$

11.2.7. Phase Diagrams of Hydrogen and Helium

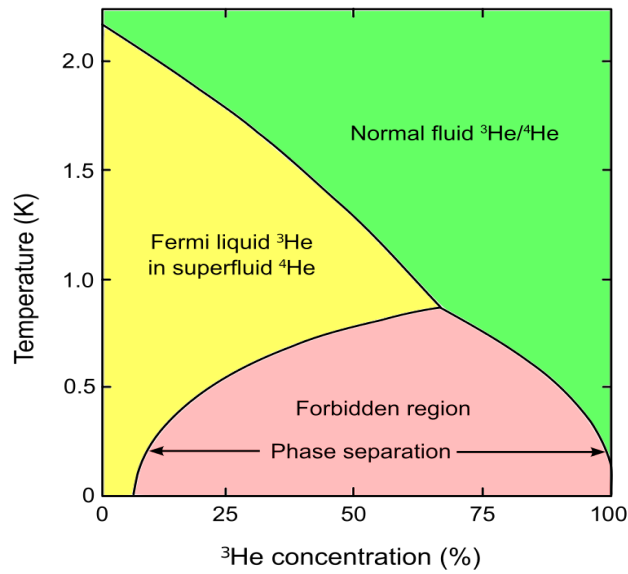
Hydrogen, high p and T



Helium (^4He), low T



^4He - ^3He mixture (low T , 1 bar, no magnetic field)



11.3. Acoustics and Medical Imaging

11.3.1. Acoustic Waves, the Doppler Effect and Beats

Sound is a longitudinal wave of pressure P and displacement s in a medium of density ρ .

Amplitude of pressure and displacement variations are related by $\Delta P_{max} = \rho c \omega \Delta s_{max}$ ($\omega = 2\pi f$).

Intensity: $I = \frac{\text{sound power}}{\text{area}} = \frac{1}{2} \rho c \omega^2 (\Delta s_{max})^2$; $\text{dB} = 10 \log_{10} \frac{I}{I_{ref}}$ where $I_{ref} = 10^{-12} \text{ W m}^{-2} = 1 \text{ pW m}^{-2}$.

General Equation of Travelling Waves and Stationary Waves:

Travelling right: $y_R(x, t) = A \cos(kx - \omega t + \phi_1)$; Travelling left: $y_L(x, t) = A \cos(kx + \omega t + \phi_2)$

Standing wave: $y_s(x, t) = y_L + y_R = 2A \cos\left(kx + \frac{\phi_1 + \phi_2}{2}\right) \cos\left(\omega t - \frac{\phi_1 - \phi_2}{2}\right)$

Wave PDE: $\frac{\partial^2 y}{\partial t^2} = c^2 \frac{\partial^2 y}{\partial x^2}$; Wave speed $c = \frac{\omega}{k}$; $y(x, t)$: pressure P or displacement s

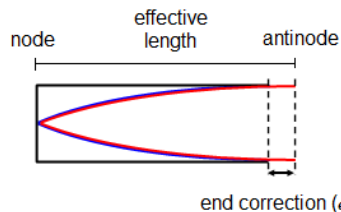
Resonance tube: for a tube of length L , mode shapes of the displacement waves are (n : n th harmonic)

$$L = \frac{2n-1}{4} \lambda = \frac{\lambda}{4}, \frac{3\lambda}{4}, \frac{5\lambda}{4}, \dots \text{ (one end open)}$$

$$L = \frac{n}{2} \lambda = \frac{\lambda}{2}, \lambda, \frac{3\lambda}{2}, \dots \text{ (both ends closed or both ends open)}$$

Closed end: node, reflection has no phase shift. Open end: antinode, reflection has 180° shift

Standing wave representation of the particle displacement:



End effect correction: e is independent of mode number.

For each open end, $e \approx 0.31 d$ (d : tube diameter)

Fundamental frequency: $f_0 = \frac{c}{\lambda_0} = \frac{c}{4(L+e)}$ (decreases due to e)

Pressure variation has a 90° phase lead relative to the displacement variation. Pressure wave has a node at **both** the closed and open end.

Doppler reflection: $\frac{f'}{f_0} = \frac{c + v_{obs}}{c + v_{src}}$

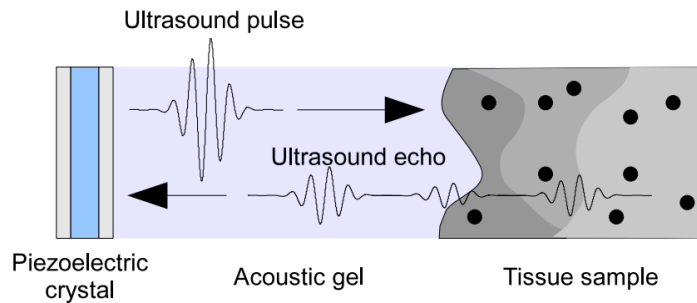
(f' : observed frequency, f_0 : source frequency, c : wave speed, v_{obs} , v_{src} : observer and source speed)

Sign conventions: observed frequency increases when the source is moving away from the observer, and vice versa for moving towards.

Oblique incidence of pulses (e.g. on a bloodstream): $\frac{\Delta f}{f_0} = \frac{2v}{c} \cos \theta$ (θ : angle of incidence)

Beats: when two acoustic waves of frequency f_1 and f_2 are superposed such that $f_1 \approx f_2$, the resultant sound contains beats of frequency $|f_1 - f_2|$.

11.3.3. Ultrasound



A broadband (high bandwidth) acoustic wave is generated by applying a short duration voltage to a piezoelectric crystal, causing it to vibrate. The pulse travels into the tissue, reflects at boundaries and is scattered by very small objects in the tissue. The ultrasound echo from the tissue in turn causes the piezoelectric crystal to vibrate, which generates an electrical signal.

- Acoustic impedance: $Z = \rho c$ (ρ : medium mass density, c : speed of ultrasound)
- Reflection coefficient: $\frac{I_r}{I_0} = \left(\frac{Z_2 - Z_1}{Z_1 + Z_2}\right)^2$
- Attenuation within matter: $I(x) = I_0 e^{-\mu x}$ (μ : attenuation coefficient)

The acoustic gel is used for impedance matching, minimising reflections away from the interface.

Medium	Density ρ (kg m ⁻³)	Speed of ultrasound c (ms ⁻¹)	Acoustic impedance Z (kg m ⁻² s ⁻¹)
air	1.3	330	429
water	1000	1500	1.5×10^6
fat	925	1450	1.34×10^6
muscle	1075	1590	1.70×10^6
bone	1400 - 1900	4080	$5.7 - 7.8 \times 10^6$

Ultrasound A-Scan (Amplitude Scan): short-pulse ultrasound waves are transmitted into the body, and the electron beam on a cathode ray oscilloscope (CRO) begins to move across the screen. The piezo transducer generates a pd on reflection and is displayed on the CRO. This type of scan is used to measure distances in the eye and the bi-parietal diameter of a foetus to measure its development.

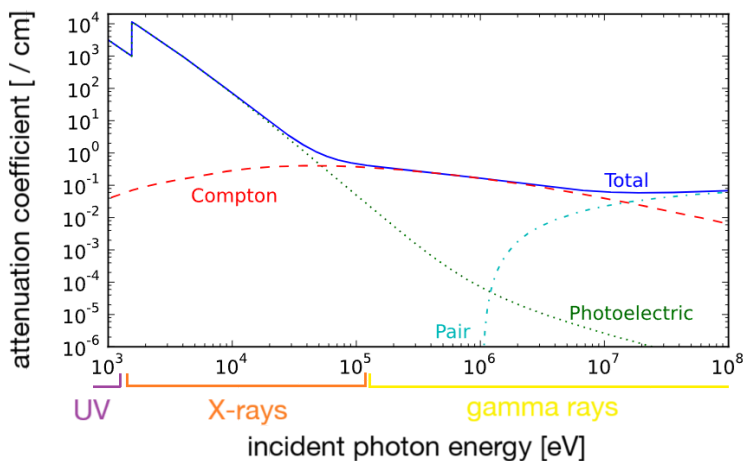
Ultrasound B-Scan (Brightness Scan): forms an image by moving the ultrasound beam across the patient, this is done because reflected signals can only be received if the transducer is normal to the reflected beam. A 2D image of a section of the body can be formed. This type of scan is used to find the midline structure of the brain in a foetus in order to know in which region an A-scan can be used to measure bi-parietal diameter, it is also used to determine the position of the placenta so that it can be determined whether a baby will have a safe delivery or if it will need to be delivered by C-section. It is also used in order to perform genetic testing on a foetus by imaging the position of the placenta and foetus accurately.

11.3.4. Mechanisms of Interactions of High-Energy Photons with Matter

The four mechanisms of high energy (above UV) photon-matter interactions:

- **Simple (Rayleigh, elastic) scattering:** photon interacts with electron, scattered with same energy. Most common in ~keV range (high energy UV / low energy X-ray). Does not contribute to attenuation. Higher energy radiation is scattered more.
- **Photoelectric effect:** photon absorbed completely by electron, electron is ejected. Dominates in ~keV range (high energy UV and X-rays).
- **Compton (inelastic) scattering:** electron in an atom ejected by photon (ionisation); photon is then scattered to lower energy. Dominates in ~100 keV range (low energy gamma rays).
- **Pair production:** photon spontaneously splits into electron and positron in the strong E-field near the nucleus of an atom. The positron rapidly annihilates with an electron, releasing a photon at half energy. Dominates in ~MeV range (energy $> 2m_e c^2 = 1.022$ MeV, high energy gamma rays).

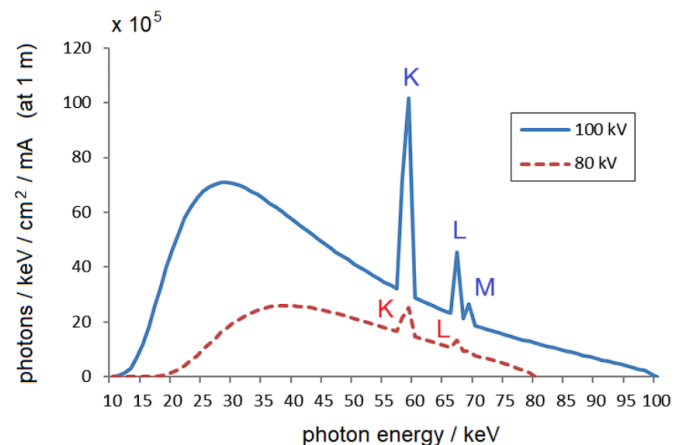
High-energy radiation (typically X-rays) are easily produced as *bremstrahlung* (braking radiation) by 'boiling' electrons from a hot cathode, accelerated into an anode. About 1% of the electron energy is converted to X-rays on a spectrum (with characteristic peaks due to ionisation of shell electrons). The rest of the collisions heat the anode.



Total attenuation coefficient: the value of μ for aluminium, by contribution from each mechanism of dissipative interaction.

K-absorption edge at 1.566 keV.

Attenuated intensity: $I(x) = I_0 e^{-\mu x}$



X-ray Tube Spectrum: the bremsstrahlung photon count for a tungsten anode, for tube voltages of 100 kV and 80 kV. K, L, M characteristic peaks shown.

11.3.5. X-Ray Imaging

An X-ray tube emits photons of a range of different energies, with maximum energy $E \leq eV$ (V : X-ray tube pd). This results in a variation in penetrating power into body tissue.

X-Ray Filters: lower-energy X-rays can damage tissue as they are absorbed, so X-ray filters are applied to the beam to reduce low-energy X-ray photon intensity ('beam hardening'). X-ray filters are made of metals to selectively absorb low-energy radiation by photoelectric effect (copper for therapy, aluminium for radiography).

The **sharpness and contrast** of an X-ray image is dependent on competing factors:

- For geometric sharpness, the distance between the focal spot and the film should be large (~1 m), while the distance of the film from the object should be small.
- A smaller focal spot can improve sharpness, but too small a spot can cause a concentration of energy in the target, which can lead to harmful heating effects.
- The exposure time determines the density/blackening of the film, so should be relatively long, however it is often determined by the amount of movement of the body part being imaged.
- Ideally, voltage and exposure would be set, and then the tube current would be chosen to produce the desired density, however this current level is often too high for the tube's rating and so the focal spot size would have to increase.
- Poor-contrast regions can be enhanced using contrast media e.g. barium sulfate for the GI tract and organic iodine compounds for the bloodstream.

The **beam size** must be controlled to minimise the radiation that the patient receives:

- A diaphragm consisting of two perpendicular pairs of metal sheets is used.
- Beam size is determined by the diaphragm aperture and its distances to the film & target.
- The diaphragm is close to the target, so the edge of the beam is less sharp.
- In therapeutic work a sharp edge is required so collimators are used.

An **X-ray film** is irradiated by primary photons (passing directly through the body, producing the image) and secondary photons (scattering, irradiating the whole film almost evenly). To reduce the amount of secondary photons reaching the film, a grid of fine strips of lead is used. However, this grid also absorbs small amounts of primary photons and so to counteract this, a longer exposure is used. This helps to maintain a suitable film density.

Intensifying screens can be used to increase the resulting exposure of the film. This allows a shorter X-ray exposure time to be used, whilst achieving the same density. They consist of a stiff ~1 mm thick cardboard sheet, a fluorescent layer of crystals e.g. CaWO_4 , a white material e.g. MgO sandwiched between them (redirects visible light towards film), and a tough waterproof material. Intensifying screens are placed either side of the film in a cassette. A pair of screens positioned like this, can result in an intensification factor of around 30 times. A metal cassette back is added behind the back screen to reduce radiation scattering back, which would result in a reduction of the film contrast.

Image Intensifiers are another method to intensify X-ray images, which increases the light output while maintaining a low X-ray dose. The X-ray pattern is directed onto a fluorescent screen and a corresponding pattern of light is emitted from this screen. The light pattern is incident on a photocathode emitting electrons, which are accelerated by a pd of around 25kV towards another fluorescent screen, which produce a much brighter image due to their higher energy. The brightness is increased by an order of around 5000 times, although the electron lens decreases the size of the pattern in the process. The viewing screen is viewed through a lead glass window. The image can also be photographed.

Indirect Flat Panel Detectors are a faster and more sensitive method of producing an X-ray image, than using a traditional film method. A scintillator converts X-ray photons into visible light photons which are directed at a low-noise photodiode (CCD) array. Each diode acts as a pixel. The stored charge is read by electronic scanning, producing digital signals used to form a digital image. The high sensitivity level means that a lower dose of radiation is required to achieve a given image quality. The digital image that is produced is also more transportable.

11.3.7. MRI Scan (Magnetic Resonance Imaging)

An MRI scanner consists of a circular superconducting magnet, enclosing a gradient coil and an RF (radio frequency) coil. The RF coil emits a radio pulse, causing proton spins to precess about the magnetic field, re-emitting during relaxation, which is received and measured using Fourier transform spectroscopy. Relaxation rates are tissue-dependent, which leads to a contrast in the signal received, represented as image voxel brightness.

Mechanism of Nuclear Magnetic Resonance

When exposed to strong external magnetic fields, nuclei with spin (primarily ¹H protons) have their spin vectors **s** precess about the external field vector **B** at a certain frequency ω .

Larmor equation: $\omega = \gamma \mathbf{B}$ (ω : precession angular velocity, γ : gyromagnetic ratio)

Bloch equation: $\dot{\mathbf{M}} = \gamma (\mathbf{M} \times \mathbf{B})$

¹H proton gyromagnetic ratio: $\gamma = 2.675 \times 10^8 \text{ rad T}^{-1} \text{ s}^{-1} = 42.58 \text{ M T}^{-1}$

Detected signal: $S = \frac{N\gamma^3 \hbar^2 B_0^2}{4kT}$ (at thermal equilibrium) Spin polarisation: $P = \frac{\gamma \hbar B_0}{2kT}$

Signal at measurement: $S = M_0 \underbrace{(1 - e^{-TR/T_1})}_{\text{longitudinal magnetisation}} \underbrace{e^{-TE/T_2}}_{\text{transverse magnetisation}}$

Boltzmann magnetisation: $\mathbf{M}_0 = \chi_0 \mathbf{B}_0$ (Curie's law) ($\chi_0 = \frac{N\gamma^2 \hbar^2}{16\pi^2 kT}$: static nuclear susceptibility)

(N : total number of nuclei, T_1 and T_2 are tissue-dependent time constants representing rates of spin realignment (relaxation) and proton spin decoherence (dephasing) respectively.)

Time constants for tissues:

Tissue (at $B_0 = 1 \text{ T}$)	T_1 (ms)	T_2 (ms)
water	2500	2500
fat	240	90
spleen	460	80
white matter	680	90
grey matter	810	100
CSF	2500	1400
liver	490	40
blood	800	180
muscle	730	40
bone	210	5.6

Types of scan by contrasting time constants:

	TR $\sim T_1$ (short TR)	TR $\gg T_1$ (long TR)
TE $\sim T_2$ (short TE)	not used	T_2 weighted image
TE $\gg T_2$ (long TE)	T_1 weighted image	M_0 weighted image

Some nuclei (³He, ¹³C, ¹²⁹Xe) may be hyperpolarised up to $P \sim 0.5$, allowing for inhalation of e.g. xenon-129 gas to image the lungs.

11.3.8. CAT Scan (CT Scan, Computed Axial Tomography)

CT scans are used to produce cross-sectional images of the body by taking a **continuous X-ray rotated** around the region being scanned. The X-ray beam is collimated and monochromatic. A circular ring of detectors records the intensity transmitted over the required cross-section. A computer algorithm (inverse Radon transform) reconstructs the 2D attenuation image, and these can be stacked across multiple cross-sections to develop a 3D model.

It can produce good images of bone fractures, organ calcification, the brain and abdominal organs, and it has high resolution. However, it is highly ionising, produces low contrast between similar-density tissues and requires the patient to hold their breath.

11.3.9. PET Scan (Positron Emission Tomography)

PET scanning produces 3D and cross-sectional images of the body.

- Patient is injected with a radionuclide e.g. FDG-18 (fluorodeoxyglucose, using ^{18}F)
- The patient lies on an examination table which is moved into the scanning machine. Throughout the scanning process, the patient must remain as stationary as possible.
- The radionuclide is metabolised in the imaged body part.
- ^{18}F atoms emit positrons due to β^+ decay. These positrons annihilate with electrons in the tissue to release gamma photons.
- Gamma cameras detect the gamma photons to produce 3D images.

Gamma cameras: used to detect the gamma radiation emitted by the radiopharmaceutical

- Gamma photons from the patient pass through a lead collimator
- They travel through to a large diameter crystal of sodium iodide
- Due to the collimator, each photon reaching the crystal has come from a position in the body that is directly below where it is incident on the crystal
- Scintillation occurs in the crystal and light photons are produced
- The light photons then pass into photomultiplier tubes for amplification.

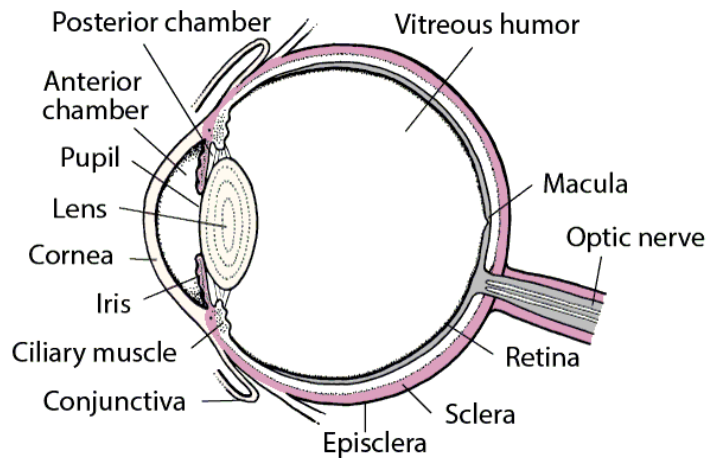
The output pulses from these tubes are used to form an image. The pulses are produced by:

- Light is incident on a photocathode resulting in electrons being emitted
- The electrons are accelerated to a series of electrodes known as dynodes
- Each dynode is more positive than the previous, until the electrons reach the anode
- The electron beam reaching the anode outputs an electrical pulse

SPECT (Single Photon Emission Computed Tomography): positron-free 3D imaging

In SPECT, a radioactive tracer (e.g. $^{99\text{m}}\text{Tc}$ as NaTcO_4 or organic chelating agents) is injected into the patient, with its pharmacokinetics designed to accumulate in a specific organ (e.g. bone, heart, brain). $^{99\text{m}}\text{Tc}$ undergoes gamma decay with half life ~6 hours into ^{99}Tc (half life 211,000 years), emitting photons in all directions from the targeted organ, detected with rotating gamma cameras, and the image is reconstructed by tomography techniques. The remaining ^{99}Tc in the body is eliminated through the kidneys.

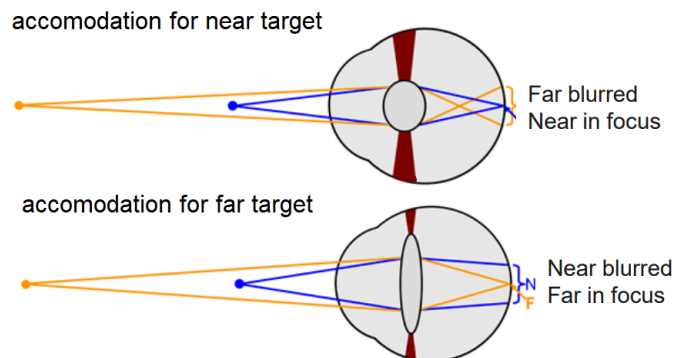
11.3.10. Parts of the Eye



11.3.11. Lens Accommodation and Optometry

The transparent biconvex lens structure changes shape to change focus. Lens curvature is controlled by ciliary muscles – by changing curvature, the eye focuses on objects at different distances. This process is called accommodation.

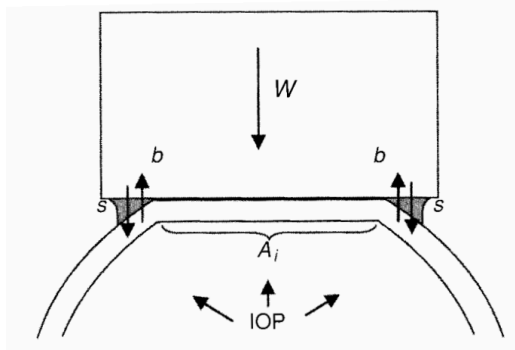
“Amplitude of accommodation” is the max amount that the lens can accommodate (diopters).



- Myopia: nearsightedness, an inability to view distant objects in focus; this is corrected with **concave** lenses.
- Hyperopia and Presbyopia: farsightedness, an inability to view close-up objects in focus; this is corrected with **convex** lenses.

The lens continually grows throughout life, laying new cells over the old cells. There appears to be no protein turnover in the lens nucleus throughout lifespan. The lens is thus prone to age-related changes, in particular stiffening, making near-field accommodation impossible.

11.3.12. Measurements of Intraocular Pressure

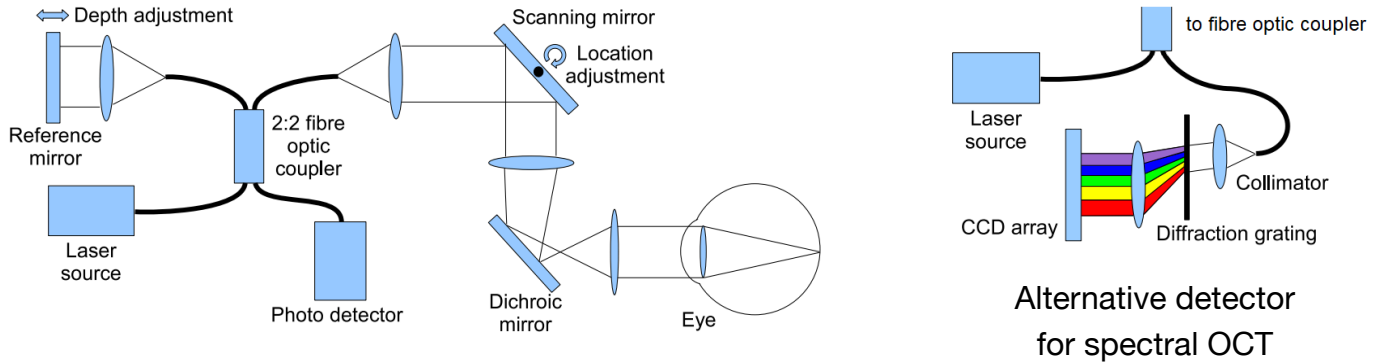


Goldmann tonometry: The intraocular pressure (IOP) is given by $p_{IOP} = W/A$, where A is the flattened area of the cornea, calibrated to be exactly 7.35 mm^2 (empirically found to eliminate tear film and bending stress effects), and W is the applied load. Further correction needed for abnormal corneal thickness.

The coefficient of rigidity is $\frac{dp_{IOP}}{dV} \approx \frac{2hE}{3RV(1-\nu)}$, where V is the eyeball volume, h is average cornea and sclera thickness, R is the radius of the eyeball, and (E, ν) are the Young's modulus and Poisson's ratio of the eyeball structure.

11.3.14. Optical Coherence Tomography (OCT) for Ophthalmological Retinal Imaging

Setup: the fibre optic coupler acts as a Michelson-Morley interferometer.



Interferometer Signal

In an ideal OCT system with no dispersion, the intensity I at the output of the interferometer, as a function of frequency ω , is given by:

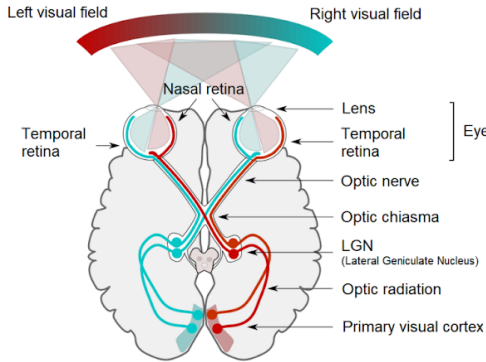
$$I(\omega) = \underbrace{S(\omega)}_{\text{detected}} + \underbrace{S(\omega)}_{\text{input pulse}} \underbrace{\left| \int_{-\infty}^{\infty} r_s(l_s) e^{j\frac{\omega}{c} l_s} dl_s \right|^2}_{\text{scattered}} + 2\Re \left\{ \underbrace{S(\omega) \int_{-\infty}^{\infty} r_s(l_s) e^{j\frac{\omega}{c} (l_r - l_s)} dl_s}_{\text{interference}} \right\}$$

(S : laser pulse power spectrum, r_s : tissue reflectivity density function, l_r : round-trip distance from the laser source to the reference mirror and back to the photodetector, l_s : round-trip distance from the laser source to a scatterer at a particular depth and back to the photodetector, c : average speed of light through the media in its path.)

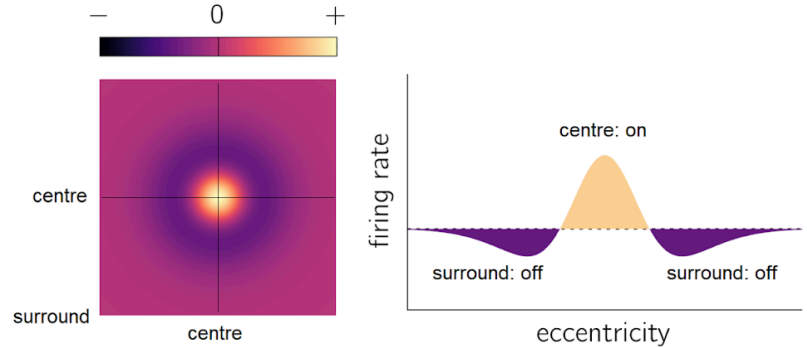
The quantity $\frac{l_r - l_s}{c}$ represents time t . In time-domain OCT, the singular photodiode detects $I = \int_{-\infty}^{\infty} I(\omega) d\omega$. In spectral OCT, $I(\omega)$ is detected directly due to the diffraction grating and CCD array.

11.3.15. Neuroscience of Vision and Visual Processing

The Visual Pathway



On-Centre Ganglion Cell Receptive Field: Difference of Gaussians



Receptive Fields: the variables (spatial position etc) which determine when a neuron will fire.

- Photoreceptor: the small angular position on the retina.
- Retinal ganglion cell (GC) and LGN neurons: the angular positions of nearby photoreceptors, with feedback from the centre of the field and opposing feedback from the surroundings. This approximates a difference of Gaussians (DoG) filter which acts as a contrast (edge) detector:

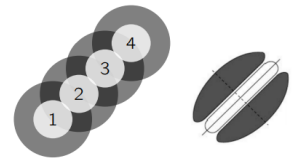
$$G(x, y, \sigma) = \frac{1}{2\pi\sigma^2} \exp\left(-\frac{x^2 + y^2}{2\sigma^2}\right)$$

is the 2D Gaussian blob detector kernel.

$$G(x, y, k\sigma) - G(x, y, \sigma) \approx (k - 1)\sigma^2 \nabla^2 G(x, y, \sigma)$$

- ‘Simple’ neurons: oriented, edge/line-like stimulus. Hubel-Wiesel’s feedforward model: the V1 neurons are fed by a line of GCs. Found in Brodmann area 17 (V1: primary visual cortex). Approximates a Gabor filter:

$$f(x, y) = \exp\left(-\frac{x^2 + (yy)^2}{2\sigma^2}\right) \cos(\omega x + \phi) \quad (y: \text{line axis})$$

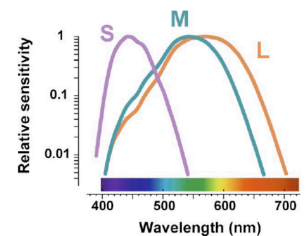


- ‘Complex’ neurons: nonlinear summation, motion sensitive along an axis, less specific to retinal location. Found in areas 17 (V1) and 18 (V2). Note: ‘hypercomplex’ neurons have end-stopped receptive fields, inhibiting after a certain length. Both simple and complex neurons can have this property. Found in areas 18 (V2) and 19 (V3) and **not** in V1.

Spatial Organisation: V1 is highly nonlinear, as shown by cortical maps (retinotopy). Cortical columns are block regions with similar stimuli (but have a range of spatial frequencies). Cortical hypercolumns combine nearby columns to include all orientations, with long-range connections encompassing multiple blobs.

Channel theory: different features of the visual scene (colour, orientation, spatial frequency, direction of motion) are represented in independent channels (merged in later processing stages). Evidence: contrast sensitivity function, neural fatigue/after-effects on over-exposure.

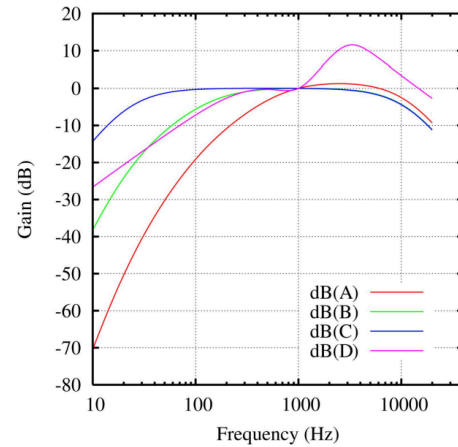
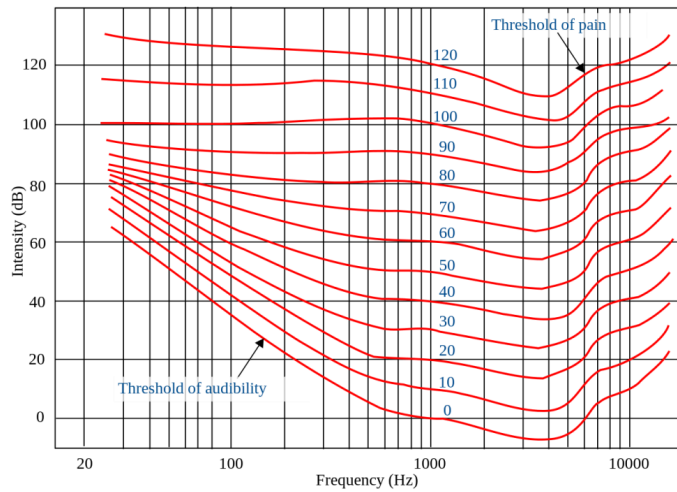
Colour vision: three channels of cones (S, M, L) in the fovea respond to wavelength bands. The colour-opponent channels are L+M+εS (achromatic), L-M (red-green) and L+M-S (yellow-blue). It is thought that these evolved to be the optimal way of coding (i.e. principal components) of the reflectance spectra for typical natural materials.



11.3.16. Parts of the Ear

11.3.17. Audiogram and Weighting Filter for Human Sensitivity to Frequency

Audible range: approximately 20 - 20 k.

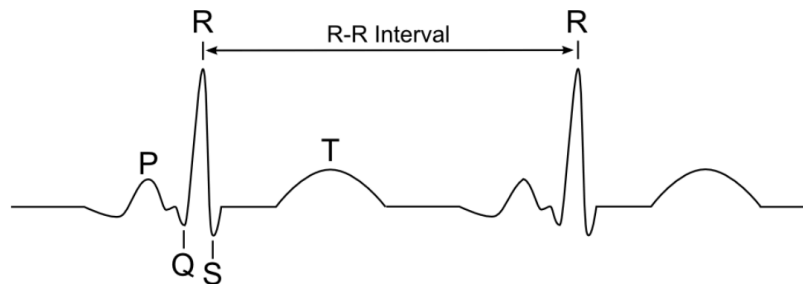


An A-weighting filter (red curve on the right) is applied to loudspeakers to compensate for the equal-loudness curves of human hearing (left).

Damage to hearing: hearing loss due to age raises the equal-loudness curves across all frequencies. Hearing loss due to an injury raises the curves more around one (over-exposed) frequency.

11.3.19. ECG (Electrocardiogram) Waveform

The contractions of the atria and ventricles are controlled by electrical signals produced by the heart in the sinoatrial (S-A) node, which firstly move across the atria, then after a short delay of the signal in the atrioventricular (A-V) node, the signal moves across the ventricles causing them to contract. These electrical signals can be measured using an electrocardiograph, which forms an ECG (electrocardiogram: voltage-time plot).



- P wave - this is when the electrical signal is first produced in the sinoatrial (S-A) node and causes the atria to contract (depolarisation).
- QRS wave - this occurs around 0.2 s later and this is where the electrical signal leaves the atrioventricular (A-V) node and causes the ventricles to contract (depolarisation) (The relaxation/repolarisation of this atria is masked by the large spike caused by the contraction of the ventricles).
- T wave - this occurs around 0.2 s later again and is where the ventricles relax and are repolarised in preparation for a second heartbeat.

C12. CHEMICAL DATA AND STANDARDS

12.1. Practical Chemistry in the Laboratory

12.1.1. Hazard Pictograms

GHS hazard symbols found on chemical substance containers include:



Toxic



Health Hazard



Flammable



Irritant



Oxidising Agent

Compressed
Gas

Explosive

Environmental
Hazard

Corrosive

Common symbols for other hazards include:



Biohazard



Radioactive

Non-ionising
Radiation

Electrocution



Lasers

Chemical
Weapon

Hot Surface



Forklifts



Trip Hazard

Explosive
AtmosphereEntrapment by
MachineryMagnetic
Fields

12.1.2. Risk Assessments

Regulations regarding workplace safety are location dependent. In the UK, the HSE (Health and Safety Executive) sets the regulations. The most important laws for substances are the **CoSHH** (Control of Substances Hazardous to Health) regulations.

Evaluating Risks: determine the extent to which a risk needs to be mitigated

		Severity of potential harm		
		Slightly harmful	Harmful	Extremely harmful
Likelihood of harm occurring	Highly unlikely	Trivial	Tolerable	Moderate
	Unlikely	Tolerable	Moderate	Substantial
	Likely	Moderate	Substantial	Intolerable

Mitigating Risks: the hierarchy of controls. From 'most effective' to 'least effective', consider, in order:

<p>1. Elimination Remove the hazard entirely by redesigning the activity or experiment</p>	<ul style="list-style-type: none"> Work at height eliminated for window cleaning by using long-handled cleaning equipment used from the ground
<p>2. Substitution Replace the hazard with a safer alternative</p>	<ul style="list-style-type: none"> Nanoparticles bought in paste form rather than powder to prevent exposure by inhalation Lower power of laser used Lower concentration of hazardous substance bought to reduce severity Less harmful pesticide used
<p>3. Engineering Controls Use of physical guards to separate people from the hazards</p>	<ul style="list-style-type: none"> Fixed guards for moving parts of machinery (lathes) Trip guards over cables on the floor, handrails and footplates on stairs Screens for lasers and radioactive substance use Remote operation (other room) for X-ray generators Fume cupboards, glove boxes and general ventilation Isolators for electrical safety Pressure relief valves on pressure vessels (to avoid explosion) Sprinklers in place to deal with fires (reduce consequences)
<p>4. Administrative Controls Use of regulations and training to change the way people work around the hazard</p>	<ul style="list-style-type: none"> Access to high-risk rooms or machinery restricted to people with training Standard operating/safe working procedure put in place Permit to work issued for high-risk work (e.g. on roofs) Emergency response plan in place (e.g. for spillages or fires) Validation protocols used for biological safety cabinets/autoclaves Maintenance, examination and testing of equipment in place to ensure all working to correct safety standards (e.g. fume cupboard testing) Exposure time restricted (e.g. work with noisy machinery)
<p>5. Personal Protective Equipment (PPE)</p>	<ul style="list-style-type: none"> Eye protection when using chemicals even in a fume cupboard, because splashes to the eye cannot be entirely ruled out Cotton lab coat with poppers (not buttons) and nitrile gloves when using chemicals – special gloves for use with hydrofluoric acid

12.1.3. Chemical Safety in Chemistry Laboratories

All chemicals have some degree of risk attached to their use. It is important that before any work is started a risk assessment is carried out.

Assessing Risk of Chemical Substances

All chemicals have a CAS number (e.g. acetone: #67-64-1), which can be searched to find its material safety data sheet (MSDS). The MSDS contains useful information for compiling a risk assessment, including sections **2) hazard precautionary statements** (including GHS pictograms, signal words 'Warning' or 'Danger', and H&P statements found online [here](#) and [here](#)), 4) first-aid measures, 5) fire-fighting measures, 6) accidental release measures, 8) occupational exposure limits, 9) physical and chemical properties, 10) stability/reactivity and compatibility, and 11) toxicological data including carcinogenicity and mutagenicity.

Control Measures in the Chemistry Lab

Best practices: always keep your work area(s) clean and tidy, clean up spills immediately, ensure all eyewash stations, emergency showers, fire extinguishers and exits are unobstructed and accessible, keep only materials you require for your work in your work area (everything else should be stored safely out of the way and not on the floor), any equipment that requires air flow or ventilation to prevent overheating should always be kept clear, handle glassware with caution, never eat or drink in the lab, do not apply cosmetics or touch your face, mouth or eyes, wear lab coat, safety glasses, long hair tied back, gloves, long trousers and enclosed shoes, avoid lone working, report near-misses and accidents to appropriate personnel immediately.

Fume cupboards: a partial containment enclosure designed to protect against airborne contaminants (chemical fumes, gases, chemical aerosols). The fume cupboard is ventilated by an induced flow of air through an adjustable working opening (the sash) which also offers the user some degree of mechanical protection against splashes of substances and flying particles.

DSEAR (Dangerous Substances and Explosive Atmosphere Regulations): risk assessments for solvents, paints, varnishes, flammable gases and LPG, dusts from machining, sanding, foodstuffs, pressurised gases and substances corrosive to metals. Ensure at least one element in the 'fire triangle' is eliminated: fuel, oxygen and heat.

Chemical storage and disposal: pay attention to shelf life, store in cupboards below head height, use drip trays, use vented caps, minimise exposure to heat/light, and check that existing waste disposal streams are suitable for each chemical used.

Emergencies: fire alarms, fire drills, carbon monoxide alarms, evacuation procedures, first-aid kits, spill kits, eye-wash stations, burn kits.

SOPs (Safe Operating Procedures): specialised protocols for particularly hazardous chemicals or activities e.g. hydrofluoric acid, piranha solution, fuming nitric acid.

12.1.4. Biological Safety in Biolabs

Biological agents are microorganisms (e.g. bacteria, viruses, moulds), cell cultures, or human endoparasites which may cause infection, allergy, toxicity or any other hazard to human health. Routes of infection can include ingestion, inhalation, instillation (eyes) or percutaneous (skin). Biohazards differ from chemical hazards in that there is no 'dose-response' relationship: even a tiny amount of contact can have serious consequences. Therefore, containment procedures are stricter when working with biological agents.

Biohazards are classed into the following hazard groups (1-4). An appropriate containment level (CL) for the biolab is required to handle such a hazard e.g. CL2 can handle groups 1 and 2.

1. Unlikely to cause disease to humans e.g. disabled *E. Coli*.
2. Potential to cause disease and spread, prophylaxis/treatment available e.g. *Streptococcus*.
3. Severe risk of disease and spreading, prophylaxis/treatment available e.g. Hepatitis B.
4. Severe risk of disease and spreading, prophylaxis/treatment **not** available e.g. Ebola.

Containment level	Cell line types	Facilities
CL1	<ul style="list-style-type: none"> well characterised, authenticated cell lines of human or primate origin low risk of endogenous infection with a biological agent presenting no apparent harm to laboratory tested for the most serious pathogens. 	<ul style="list-style-type: none"> impervious & resistant surfaces, easy to clean autoclave on site door closed during work observation window disinfection stations dedicated bins for contaminated solid waste sharps bins validated inactivation of liquid waste
CL2	<ul style="list-style-type: none"> finite or continuous cell lines/strains of human or primate origin not fully characterised or authenticated, except where there is a high risk of endogenous biological agents, e.g. blood-borne viruses. 	<ul style="list-style-type: none"> negative pressure if possible, microbiological safety cabinet (class II MSC with HEPA filter) access restricted side or back fastening lab coats, appropriate gloves, spill trays specified decontamination procedures control aerosol dissemination safe storage of biological agents

Higher CL biolabs (CL3, CL4) work with cell lines with endogenous biological agents or cells that have been deliberately infected, or primary cells from blood or lymphoid cells of human or simian origin, and have highly specialised working procedures.

Special facilities are required for working with live animals, which is prohibited entirely for great apes (human subjects are out of scope, requiring informed consent), and with restrictions for cats, dogs, fetuses and embryos. Ethical approval is required for working with human or animal tissue (surgical specimens or cadavers). Special risk assessments are required for working with genetically modified organisms (GMOs), where the recipient organism, inserted gene, donor and vector must be documented.

12.1.5. Common Equipment used in Chemistry

Glassware:

- **Small solutions:** test tube, boiling tube, Thiele tube
- **Large solutions:** beaker, graduated cylinder, conical/Erlenmeyer flask, volumetric flask, round-bottomed flask, Florence flask, Kjeldahl flask, pear-shaped flask, retort flask, Schlenk flask, Straus flask, Buchner flask
- **Funnels:** separating funnel, dropping funnel, filter funnel, thistle funnel
- **Columns and condensers:** burette, Liebig condenser, Graham condenser, Friedrichs condenser, distilling column, Claisen flask, Soxhlet extractor, chromatography column
- **Transferring solutions:** pipette, micropipette, capillary tube/melting point tube, gas syringe, graduated pipette, volumetric pipette

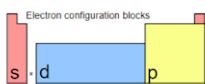
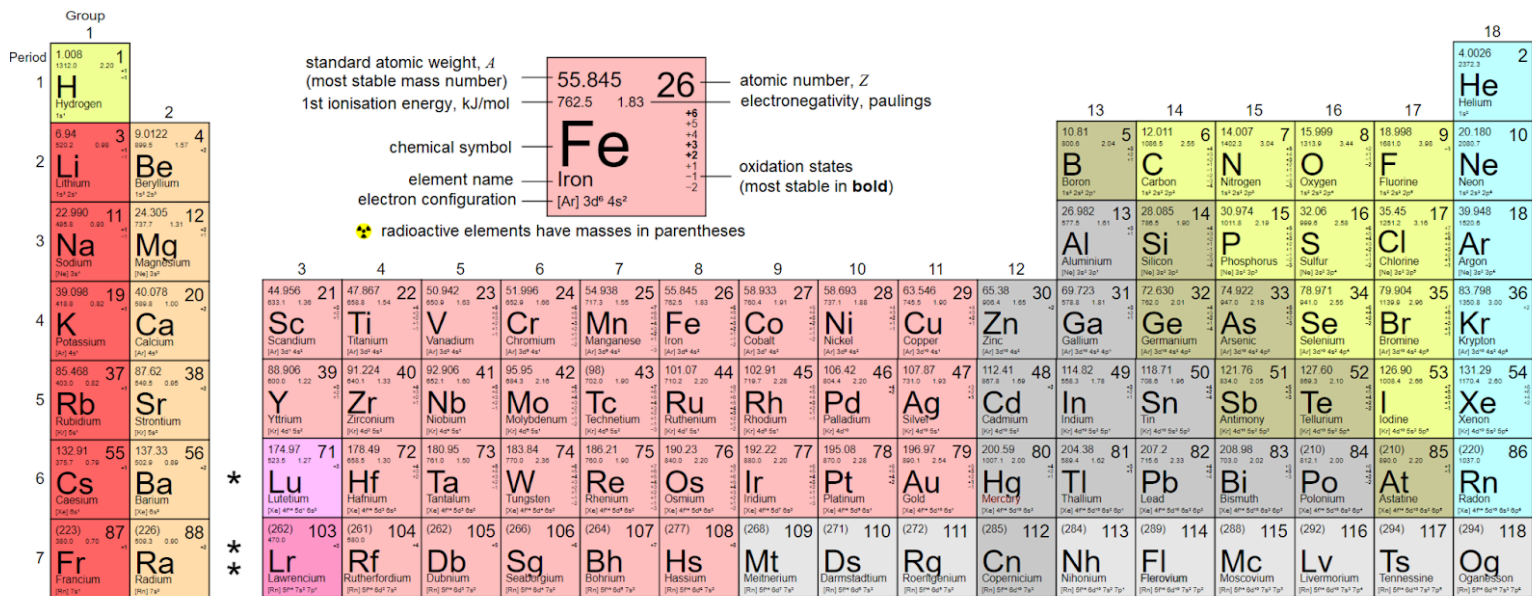
Apparatus:

- **Heating:** Bunsen burner, water bath
- **Holding:** retort stand (clamp, stand and boss), test tube rack

12.1.6. Common Experimental Procedures used in Chemistry

12.2. Chemical Data

12.2.1. The Periodic Table of Elements



Notes
 1 kJ/mol = 0.1013636 eV
 all elements are implied to have an oxidation state of zero.
 data as of 2018

139.91 57 Lanthanum ([Xe] 5d ¹ 6s ²)	140.12 58 Cerium ([Xe] 4f ¹ 5d ¹ 6s ²)	140.91 59 Praseodymium ([Xe] 4f ³ 6s ²)	144.24 60 Neodymium ([Xe] 4f ⁴ 6s ²)	(145) 61 Promethium ([Xe] 4f ⁵ 6s ²)	150.36 62 Samarium ([Xe] 4f ⁶ 6s ²)	151.96 63 Europium ([Xe] 4f ⁷ 6s ²)	157.25 64 Gadolinium ([Xe] 4f ⁷ 5d ¹ 6s ²)	158.93 65 Terbium ([Xe] 4f ⁹ 6s ²)	162.50 66 Dysprosium ([Xe] 4f ¹⁰ 6s ²)	164.93 67 Holmium ([Xe] 4f ¹¹ 6s ²)	167.25 68 Erbium ([Xe] 4f ¹² 6s ²)	168.93 69 Thulium ([Xe] 4f ¹³ 6s ²)	173.05 70 Ytterbium ([Xe] 4f ¹⁴ 6s ²)
(227) 89 Actinium ([Rn] 5f ⁷ 7s ²)	232.04 90 Thorium ([Rn] 6s ²)	231.04 91 Protactinium ([Rn] 5f ² 6d ¹ 7s ²)	238.03 92 Uranium ([Rn] 5f ³ 6d ¹ 7s ²)	(237) 93 Neptunium ([Rn] 5f ⁴ 6d ¹ 7s ²)	(244) 94 Plutonium ([Rn] 5f ⁶ 6d ¹ 7s ²)	(243) 95 Americium ([Rn] 5f ⁷ 7s ²)	(247) 96 Curium ([Rn] 5f ⁸ 7s ²)	(247) 97 Berkelium ([Rn] 5f ⁹ 7s ²)	(251) 98 Californium ([Rn] 5f ¹⁰ 7s ²)	(252) 99 Einsteinium ([Rn] 5f ¹¹ 7s ²)	(257) 100 Fermium ([Rn] 5f ¹² 7s ²)	(258) 101 Mendelevium ([Rn] 5f ¹³ 7s ²)	(259) 102 Nobelium ([Rn] 5f ¹⁴ 7s ²)

- alkali metals
- alkaline earth metals
- lanthanides
- transition metals
- unknown properties
- post-transition metals
- metalloids
- reactive nonmetals
- noble gases
- actinides

Groupings and Classification of Elements

- Group 1 (1): Alkali Metals (Li, Na, K, Rb, Cs, Fr)
- Group 2 (2): Alkaline Earth Metals (Be, Mg, Ca, Sr, Ba, Ra)
- Groups (3)-(12): Transition Metals (excludes lanthanides and actinides)
- Group 5 (15): Pnictogens (N, P, As, Sb, Bi, Mc)
- Group 6 (16): Chalcogens (O, S, Se, Te, Po, Lv)
- Group 7 (17): Halogens (F, Cl, Br, I, At, Ts)
- Group 0 (18): Noble Gases (He, Ne, Ar, Kr, Xe, Rn, Og)

- Period 6, f-block: lanthanides
- Period 7, f-block: actinides
- Period 7, d/p-block: transactinides

- Platinoids (noble metals): Ru, Rh, Pd, Os, Ir, Pt
- Metalloids (semimetals): B, Si, Ge, As, Sb, Te, Po, At
- Poor metals: Al, Ga, In, Sn, Tl, Pb, Bi

12.2.2. Chemical Properties of Elements

Z		Electron Configuration	Atomic Radius (pm)	1st Ionisation Energy (kJ mol ⁻¹)	1st Electron Affinity (kJ mol ⁻¹)	Electronegativity (Paulings)
1	H	1s ¹	25	1312.0	72.769	3.04
2	He	1s ²	120	2372.3	-48	-
3	Li	[He] 2s ¹	145	520.2	59.632	2.17
4	Be	[He] 2s ²	105	899.5	-48	2.42
5	B	[He] 2s ² 2p ¹	85	800.6	26.989	3.04
6	C	[He] 2s ² 2p ²	70	1086.5	121.776	3.15
7	N	[He] 2s ² 2p ³	65	1402.3	-6.8	3.56
8	O	[He] 2s ² 2p ⁴	60	1313.9	140.976	3.78
9	F	[He] 2s ² 2p ⁵	50	1681.0	328.165	4.00
10	Ne	[He] 2s ² 2p ⁶	160	2080.7	-116	-
11	Na	[Ne] 3s ¹	180	495.8	52.867	2.15
12	Mg	[Ne] 3s ²	150	737.7	-40	2.39
13	Al	[Ne] 3s ² 3p ¹	125	577.5	41.762	2.52
14	Si	[Ne] 3s ² 3p ²	110	786.5	134.0684	2.82
15	P	[Ne] 3s ² 3p ³	100	1011.8	72.037	3.16
16	S	[Ne] 3s ² 3p ⁴	100	999.6	200.4101	3.44
17	Cl	[Ne] 3s ² 3p ⁵	100	1251.2	348.575	3.50
18	Ar	[Ne] 3s ² 3p ⁶	71	1520.6	-96	-
19	K	[Ar] 4s ¹	220	418.8	48.383	2.07
20	Ca	[Ar] 4s ²	180	589.8	2.37	2.20
21	Sc	[Ar] 4s ² 3d ¹	160	633.1	17.3076	2.35
22	Ti	[Ar] 4s ² 3d ²	140	658.8	7.289	2.23
23	V	[Ar] 4s ² 3d ³	135	650.9	50.911	2.08
24	Cr	[Ar] 4s ¹ 3d ⁵	140	652.9	65.217 2	2.12
25	Mn	[Ar] 4s ² 3d ⁵	140	717.3	-50	2.20
26	Fe	[Ar] 4s ² 3d ⁶	140	762.5	14.785	2.32
27	Co	[Ar] 4s ² 3d ⁷	135	760.4	63.8979	2.34
28	Ni	[Ar] 4s ² 3d ⁸	135	737.1	111.65	2.32
29	Cu	[Ar] 4s ¹ 3d ¹⁰	135	745.5	119.235	2.86
30	Zn	[Ar] 4s ² 3d ¹⁰	135	906.4	-58	2.26
31	Ga	[Ar] 4s ² 3d ¹⁰ 3p ¹	130	578.8	29.0581	2.43
32	Ge	[Ar] 4s ² 3d ¹⁰ 3p ²	125	762	118.9352	2.79
33	As	[Ar] 4s ² 3d ¹⁰ 3p ³	115	947.0	77.65	3.15
34	Se	[Ar] 4s ² 3d ¹⁰ 3p ⁴	115	941.0	194.9587	3.37
35	Br	[Ar] 4s ² 3d ¹⁰ 3p ⁵	115	1139.9	324.5369	3.45
36	Kr	[Ar] 4s ² 3d ¹⁰ 3p ⁶		1350.8	-96	-

Continued:

Z		Electron Configuration	Atomic Radius (pm)	1st Ionisation Energy (kJ mol ⁻¹)	1st Electron Affinity (kJ mol ⁻¹)	Electronegativity (Paulings)
37	Rb	[Kr] 5s ¹	235	403	46.884	2.07
38	Sr	[Kr] 5s ²	200	549.5	5.023	2.13
39	Y	[Kr] 5s ² 4d ¹	180	600	30.035	2.52
40	Zr	[Kr] 5s ² 4d ²	155	640.1	41.806	2.05
41	Nb	[Kr] 5s ¹ 4d ⁴	145	652.1	88.516	2.59
42	Mo	[Kr] 5s ¹ 4d ⁵	145	684.3	72.097	2.47
43	Tc	[Kr] 5s ² 4d ⁵	135	702	53	2.82
44	Ru	[Kr] 5s ¹ 4d ⁷	130	710.2	100.950	2.68
45	Rh	[Kr] 5s ¹ 4d ⁸	135	719.7	110.27	2.65
46	Pd	[Kr] 4d ¹⁰	140	804.4	54.24	2.70
47	Ag	[Kr] 5s ¹ 4d ¹⁰	160	731	125.862	2.88
48	Cd	[Kr] 5s ² 4d ¹⁰	155	867.8	-68	2.36
49	In	[Kr] 5s ² 4d ¹⁰ 4p ¹	155	558.3	37.043	2.29
50	Sn	[Kr] 5s ² 4d ¹⁰ 4p ²	145	708.6	107.298 4	2.68
51	Sb	[Kr] 5s ² 4d ¹⁰ 4p ³	145	834	101.059	3.05
52	Te	[Kr] 5s ² 4d ¹⁰ 4p ⁴	140	869.3	190.161	3.14
53	I	[Kr] 5s ² 4d ¹⁰ 4p ⁵	140	1008.4	295.1531	3.20
54	Xe	[Kr] 5s ² 4d ¹⁰ 4p ⁶		1170.4	-77	-
55	Cs	[Xe] 6s ¹	260	375.7	45.505	1.97
56	Ba	[Xe] 6s ²	215	502.9	13.954	2.02
57	La	[Xe] 6s ² 5d ¹	195	538.1	53.795	2.49
58	Ce	[Xe] 6s ² 5d ¹ 4f ¹	185	534.4	57.9067	2.61
59	Pr	[Xe] 6s ² 4f ³	185	527	10.539	2.24
60	Nd	[Xe] 6s ² 4f ⁴	185	533.1	9.406	2.11
61	Pm	[Xe] 6s ² 4f ⁵	185	540	12.45	2.24
62	Sm	[Xe] 6s ² 4f ⁶	185	544.5	15.63	1.90
63	Eu	[Xe] 6s ² 4f ⁷	185	547.1	11.2	1.81
64	Gd	[Xe] 6s ² 5d ¹ 4f ⁷	180	593.4	20.5	2.40
65	Tb	[Xe] 6s ² 4f ⁹	175	565.8	12.670	2.29
66	Dy	[Xe] 6s ² 4f ¹⁰	175	573	1.45	2.07
67	Ho	[Xe] 6s ² 4f ¹¹	175	581	32.61	2.12
68	Er	[Xe] 6s ² 4f ¹²	175	589.3	30.10	2.02
69	Tm	[Xe] 6s ² 4f ¹³	175	596.7	99	2.03
70	Yb	[Xe] 6s ² 4f ¹⁴	175	603.4	-1.93	1.78
71	Lu	[Xe] 6s ² 4f ¹⁴ 5d ¹	175	523.5	23.04	2.68

Continued:

Z		Electron Configuration	Atomic Radius (pm)	1st Ionisation Energy (kJ mol ⁻¹)	1st Electron Affinity (kJ mol ⁻¹)	Electronegativity (Paulings)
72	Hf	[Xe] 6s ² 4f ¹⁴ 5d ²	155	658.5	17.18	2.01
73	Ta	[Xe] 6s ² 4f ¹⁴ 5d ³	145	761	31.7301	2.32
74	W	[Xe] 6s ² 4f ¹⁴ 5d ⁴	135	770	78.76	2.42
75	Re	[Xe] 6s ² 4f ¹⁴ 5d ⁵	135	760	5.8273	2.59
76	Os	[Xe] 6s ² 4f ¹⁴ 5d ⁶	130	840	104.0	2.72
77	Ir	[Xe] 6s ² 4f ¹⁴ 5d ⁷	135	880	150.9	2.79
78	Pt	[Xe] 6s ¹ 4f ¹⁴ 5d ⁹	135	870	205.041	2.98
79	Au	[Xe] 6s ¹ 4f ¹⁴ 5d ¹⁰	135	890.1	222.747	2.81
80	Hg	[Xe] 6s ² 4f ¹⁴ 5d ¹⁰	150	1007.1	-48	2.92
81	Tl	[Xe] 6s ² 4f ¹⁴ 5d ¹⁰ 6p ¹	190	589.4	30.8804	2.26
82	Pb	[Xe] 6s ² 4f ¹⁴ 5d ¹⁰ 6p ²	180	715.6	34.4183	2.62
83	Bi	[Xe] 6s ² 4f ¹⁴ 5d ¹⁰ 6p ³	160	703	90.924	2.69
84	Po	[Xe] 6s ² 4f ¹⁴ 5d ¹⁰ 6p ⁴	190	812.1	136	2.85
85	At	[Xe] 6s ² 4f ¹⁴ 5d ¹⁰ 6p ⁵	202	899	233.087	3.04
86	Rn	[Xe] 6s ² 4f ¹⁴ 5d ¹⁰ 6p ⁶	200	1037	-68	-
87	Fr	[Rn] 7s ¹	270	393	46.89	2.01
88	Ra	[Rn] 7s ²	215	509.3	9.648 5	2.15
89	Ac	[Rn] 7s ² 6d ¹	195	499	33.77	2.22
90	Th	[Rn] 7s ² 6d ²	180	587	58.633	2.62
91	Pa	[Rn] 7s ² 6d ¹ 5f ²	180	568	53.03	2.33
92	U	[Rn] 7s ² 6d ¹ 5f ³	175	597.6	30.390	2.45
93	Np	[Rn] 7s ² 6d ¹ 5f ⁴	175	604.5	45.85	2.35
94	Pu	[Rn] 7s ² 5f ⁶	175	584.7	-48.33	2.22
95	Am	[Rn] 7s ² 5f ⁷	175	578	9.93	2.28
96	Cm	[Rn] 7s ² 6d ¹ 5f ⁷	176	581	27.17	2.31
97	Bk	[Rn] 7s ² 5f ⁹		598	-165.24	2.08
98	Cf	[Rn] 7s ² 5f ¹⁰		608	-97.31	2.18
99	Es	[Rn] 7s ² 5f ¹¹		619	-28.60	2.29
100	Fm	[Rn] 7s ² 5f ¹²		629	33.96	2.38
101	Md	[Rn] 7s ² 5f ¹³		636	93.91	2.47
102	No	[Rn] 7s ² 5f ¹⁴		639	-223.22	2.06
103	Lr	[Rn] 7s ² 5f ¹⁴ 7p ¹		479	-30.04	2.10

Properties of transactinide elements are not well established and are primarily theoretical.

12.2.3. Bond Enthalpy and Bond Length Data

Bond enthalpies (energies) E [kJ mol^{-1}] and bond lengths L [$\text{pm} = 0.001 \text{ nm}$] are given. Values are averaged over a large number of chemical compounds.

Hydrogen Boron Carbon Metalloids N, P, As, Sb O, S, Se Halogens Noble Gases

Bond	E	L	Bond	E	L	Bond	E	L	Bond	E	L	Bond	E	L
H-H	432	74	C-C	346	154	Si-Si	222	233	N-N	167	145	O-O	142	148
H-B	389	119	C=C	602	134	Si-N	355		N=N	418	125	O=O	494	121
H-C	411	109	C≡C	835	120	Si-O	452	163	N≡N	942	110	O-F	190	142
H-Si	318	148	C-Si	318	185	Si-S	293	200	N-O	201	140	S=O	522	143
H-Ge	288	153	C-Ge	238	195	Si-F	565	160	N=O	607	121	S-S (S_8)	226	205
H-Sn	251	170	C-Sn	192	216	Si-Cl	381	202	N-F	283	136	S=S	425	149
H-N	386	101	C-Pb	130	230	Si-Br	310	215	N-Cl	313	175	S-F	284	156
H-P	322	144	C-N	305	147	Si-I	234	243	P-P	201	221	S-Cl	255	207
H-As	247	152	C=N	615	129	Ge-Ge	188	241	P-O	335	163	Se-Se	172	
H-O	459	96	C≡N	887	116	Ge-N	257		P=O	544	150	Se=Se	272	215
H-S	363	134	C-P	264	184	Ge-F	470	168	P=S	335	186	F-F	155	142
H-Se	276	146	C-O	358	143	Ge-Cl	349	210	P-F	490	154	Cl-Cl	240	199
H-Te	238	170	C=O	799	120	Ge-Br	276	230	P-Cl	326	203	Br-Br	190	228
H-F	565	92	C=O	1072	113	Ge-I	212		P-Br	264		I-I	148	267
H-Cl	428	127	C-B	356	160	Sn-F	414		P-I	184		At-At	116	
H-Br	362	141	C-S	272	182	Sn-Cl	323	233	As-As	146	243	I-O	201	
H-I	295	161	C=S	573	160	Sn-Br	273	250	As-O	301	178	I-F	273	191
B-B	293		C-F	485	135	Sn-I	205	270	As-F	484	171	I-Cl	208	232
B-O	536		C-Cl	327	177	Pb-F	331		As-Cl	322	216	I-Br	175	
B-F	613		C-Br	285	194	Pb-Cl	243	242	As-Br	458	233	Kr-F (KrF_2)	50	190
B-Cl	456	175	C-I	240	228	Pb-Br	201		As-I	200	254	Xe-O	84	175
B-Br	377					Pb-I	142	279	Sb-Sb	121		Xe-F	130	195
B-B	293								Sb-F	440				
									Sb-Cl (SbCl_5)	248				
									Sb-Cl (SbCl_3)	315	232			

12.2.4. Thermochemical Data

Standard Enthalpy of Formation and Standard Entropy

($\Delta_f H^\ominus$ [kJ mol⁻¹]: standard enthalpy of formation, S^\ominus [J mol⁻¹ K⁻¹]: standard entropy)

Solids				Solids			
Substance	Formula	$\Delta_f H^\ominus$	S^\ominus	Substance	Formula	$\Delta_f H^\ominus$	S^\ominus
carbon (diamond)	C (s)	1.90	2.4	potassium	K (s)	0	64.7
carbon (graphite)	C (s)	0	5.7	sodium chloride	NaCl (s)	-411.1	72.1
polystyrene*	(CH ₂) _n (s)	-28.5	25	potassium chloride	KCl (s)	-436.7	82.6
lithium fluoride	LiF (s)	-146.2	35.7	iodine	I ₂ (s)	0	116.1
silicon dioxide	SiO ₂ (s)	-911	41.5	glucose	C ₆ H ₁₂ O ₆ (s)	-1273.3	209.2
calcium	Ca (s)	0	41.6	xenon hexafluoride	XeF ₆ (s)	-294	210.4
sodium	Na (s)	0	51.5	sucrose	C ₁₂ H ₂₂ O ₁₁ (s)	-2221.2	392.4
magnesium fluoride	MgF ₂ (s)	-1124.2	57.2				
Liquids				Liquids			
Substance	Formula	$\Delta_f H^\ominus$	S^\ominus	Substance	Formula	$\Delta_f H^\ominus$	S^\ominus
water	H ₂ O (l)	-285.8	70.0	ethanoyl chloride	CH ₃ COCl (l)	-272	200.8
mercury	Hg (l)	0	75.9	cyclohexane	C ₆ H ₁₂ (l)	-157.7	204.0
hydrogen peroxide	H ₂ O ₂ (l)	-187.8	109.6	carbon tetrachloride	CCl ₄ (l)	-95.6	214.4
methanol	CH ₃ OH (l)	-238.4	127.2	silicon tetrachloride	SiCl ₄ (l)	-687.0	239.7
bromine	Br ₂ (l)	0	152.2	sulfur trioxide	SO ₃ (l)	-395.8	256.8
ethanoic acid	CH ₃ COOH (l)	-483.5	158.0	<i>n</i> -hexane	C ₆ H ₁₄ (l)	-198.7	296.1
ethanol	C ₂ H ₅ OH (l)	-276.2	159.9	isooctane**	C ₈ H ₁₈ (l)	-259.3	328.0
benzene	C ₆ H ₆ (l)	49.0	173.3	<i>n</i> -heptane	C ₇ H ₁₆ (l)	-224.4	328.6
Gases				Gases			
Substance	Formula	$\Delta_f H^\ominus$	S^\ominus	Substance	Formula	$\Delta_f H^\ominus$	S^\ominus
helium	He (g)	0	126.2	phosphine	PH ₃ (g)	5	210
hydrogen	H ₂ (g)	0	130.7	nitric oxide	NO (g)	90.3	210.8
hydrogen chloride	HCl (g)	-92.3	186.9	carbon dioxide	CO ₂ (g)	-393.5	213.8
methane	CH ₄ (g)	-74.9	188.7	ethene	C ₂ H ₄ (g)	52.5	219.3
water	H ₂ O (g)	-241.8	188.8	chlorine	Cl ₂ (g)	0	223.1
nitrogen	N ₂ (g)	0	191.6	ethane	C ₂ H ₆ (g)	-84.0	229.6
ammonia	NH ₃ (g)	-45.9	192.8	sulfur dioxide	SO ₂ (g)	-296.8	248.2
carbon monoxide	CO (g)	-110.5	197.7	iodine	I ₂ (g)	62.4	260.7
fluorine	F ₂ (g)	0	202.8	propane	C ₃ H ₈ (g)	-104.7	269.9
oxygen	O ₂ (g)	0	205.2	butane	C ₄ H ₁₀ (g)	-125.6	310.2

* polystyrene: value per (CH₂) monomer. $\Delta_f H^\ominus$ varies up to $\pm 2\%$ due to crystallinity (HDPE has the slightly more exothermic $\Delta_f H^\ominus$).

** isooctane = 2,2,4-trimethylpentane.

Standard Enthalpy of Combustion

($\Delta_c H^\ominus$ [kJ mol⁻¹]: standard enthalpy of combustion, per mole of fuel, dry basis)

Fuel	Combusted Product	$\Delta_c H^\ominus$ [kJ mol ⁻¹]
hydrogen	H ₂ O (l)	-285.8
carbon monoxide	CO ₂ (g)	-283.0
carbon (graphite)	CO ₂ (g)	-292.5
sulfur	SO ₂ (g)	-296.8
magnesium	MgO (s)	-601.6
polyethylene*	n CO ₂ (g) + n H ₂ O (l)	-651
methanol	CO ₂ (g) + 2 H ₂ O (l)	-726.1
methane	CO ₂ (g) + 2 H ₂ O (l)	-890.7
acetylene	2 CO ₂ (g) + H ₂ O (l)	-1301.1
ethanol	CO ₂ (g) + 3 H ₂ O (l)	-1366.8
ethene	2 CO ₂ (g) + 2 H ₂ O (l)	-1411.2
ethane	2 CO ₂ (g) + 3 H ₂ O (l)	-1560.7
glucose	6 CO ₂ (g) + 6 H ₂ O (l)	-2840
phosphorus (red)	P ₄ O ₁₀ (s)	-2967
phosphorus (white)	P ₄ O ₁₀ (s)	-2984
benzene	6 CO ₂ (g) + 3 H ₂ O (l)	-3267
trinitrotoluene	7 CO ₂ (g) + 5/2 H ₂ O (l) + 3/2 N ₂ (g)	-3406
cyclohexane	6 CO ₂ (g) + 6 H ₂ O (l)	-3930
isooctane	8 CO ₂ (g) + 9 H ₂ O (l)	-5461

* polystyrene: value per (CH₂) monomer. $\Delta_c H^\ominus$ varies up to $\pm 0.1\%$ due to crystallinity (LDPE has the slightly more exothermic $\Delta_c H^\ominus$).

Phase Change Enthalpy and Entropy

(T_m [K]: melting point or freezing point,

T_b [K]: boiling point,

$\Delta_{fus} H^\ominus$ [kJ mol⁻¹]: molar latent heat of fusion,

$\Delta_{vap} H^\ominus$ [kJ mol⁻¹]: molar latent heat of vaporisation,

$\Delta_{fus} S^\ominus$ [J mol⁻¹ K⁻¹]: molar entropy change of fusion,

$\Delta_{vap} S^\ominus$ [J mol⁻¹ K⁻¹]: molar entropy change of vaporisation)

Substance	Formula	T_m	T_b	$\Delta_{fus} H^\ominus$	$\Delta_{vap} H^\ominus$	$\Delta_{fus} S^\ominus$	$\Delta_{vap} S^\ominus$
water	H ₂ O	273.2	373.2	6.01	40.68	22.0	118.89
ethanol	C ₂ H ₅ OH	159.1	351.5	4.9	42.3	31	109.67
ammonia	NH ₃	195.3	239.7	5.65	23.35	29.83	97.41
propene	C ₃ H ₆	88.0	225.6	3.0	18.4	34.2	81.7
aluminium	Al	933.5	2473	8.66	307.6	9.28	124.4
xenon hexafluoride	XeF ₆	322.4	348.8	5.74	47.75	17.8	136.9

$$\text{Specific latent heat of phase change, } L \text{ [J g}^{-1}\text{]} = \frac{\text{Molar latent heat } \Delta H^\ominus = T \Delta S^\ominus \text{ [J mol}^{-1}\text{]}}{\text{Molar mass } M_r \text{ [g mol}^{-1}\text{]}}$$

'Trouton's Rule': $\Delta_{vap} S^\ominus$ is typically 85-88 J K⁻¹ mol⁻¹ for a wide range of liquids.

Hydrogen-bonded liquids have higher values.

Enthalpy of Hydration of Ions: $X^+(g) \rightarrow X^+(aq)$ $(\Delta_{hyd}H^\ominus [\text{kJ mol}^{-1}]$: standard enthalpy of hydration)

Cations:

Anions:

	$\Delta_{hyd}H^\ominus$		$\Delta_{hyd}H^\ominus$		$\Delta_{hyd}H^\ominus$		$\Delta_{hyd}H^\ominus$		$\Delta_{hyd}H^\ominus$		$\Delta_{hyd}H^\ominus$
H ⁺	-1091	Cu ⁺	-593	Ba ²⁺	-1309	Pt ²⁺	-2100	Y ³⁺	-4105	F ⁻	-524
Li ⁺	-520	Ag ⁺	-473	Ti ²⁺	1862	Zn ²⁺	-2047	Ga ³⁺	-4701	Cl ⁻	-378
Na ⁺	-406	Au ⁺	-615	Cr ²⁺	-1908	Cd ²⁺	-1809	In ³⁺	-4118	Br ⁻	-348
K ⁺	-320	NH ₄ ⁺	-307	Mn ²⁺	-1851	Hg ²⁺	-1829	Tl ³⁺	-4108	I ⁻	-308
Rb ⁺	-296	Be ²⁺	-2484	Fe ²⁺	-1950	Sn ²⁺	-1554	Cr ³⁺	-4563	NO ₃ ⁻	-314
Cs ⁺	-264	Mg ²⁺	-1926	Co ²⁺	-2010	Pb ²⁺	-1485	Fe ³⁺	-4429	OH ⁻	-460
In ⁺	-344	Ca ²⁺	-1579	Ni ²⁺	-2096	Al ³⁺	-4680	Co ³⁺	-4653		
Tl ⁺	-328	Sr ²⁺	-1446	Cu ²⁺	-2099	Sc ³⁺	-3930				

Enthalpy of Solution of Ionic Substances: $X_aY_b(s) \rightarrow aX^+(aq) + bY^-(aq)$ $(\Delta_{sol}H^\ominus [\text{kJ mol}^{-1}]$: standard enthalpy of solution)

Cation	Anion				
	fluoride (F ⁻)	chloride (Cl ⁻)	bromide (Br ⁻)	iodide (I ⁻)	hydroxide (OH ⁻)
lithium (Li ⁺)	4.7	-37.0	-48.8	-63.3	-23.6
sodium (Na ⁺)	0.9	3.9	-0.6	-7.5	-44.5
potassium (K ⁺)	-17.7	17.2	19.9	20.3	-57.6
ammonium (NH ₄ ⁺)	-1.2	14.8	16.8	13.7	—
silver (Ag ⁺)	-22.5	65.5	84.4	112.2	—
magnesium (Mg ²⁺)	-17.7	-160.0	-185.6	-213.2	2.3
calcium (Ca ²⁺)	11.5	-81.3	-103.1	-119.7	-16.7

Cation	Anion			
	nitrate (NO ₃ ⁻)	acetate (CH ₃ COO ⁻)	carbonate (CO ₃ ²⁻)	sulfate (SO ₄ ²⁻)
lithium (Li ⁺)	-2.5	—	-18.2	-29.8
sodium (Na ⁺)	20.5	-17.3	-26.7	2.4
potassium (K ⁺)	34.9	-15.3	-30.9	23.8
ammonium (NH ₄ ⁺)	25.7	-2.4	—	6.6
silver (Ag ⁺)	22.6	—	22.6	17.8
magnesium (Mg ²⁺)	-90.9	—	-25.3	-91.2
calcium (Ca ²⁺)	-19.2	—	-13.1	-18.0

12.2.5. Higher Ionisation Energies (up to Krypton): $X^{(n-1)+}(\text{g}) \rightarrow X^{n+}(\text{g}) + e^{-}$ [kJ mol⁻¹]

Z	Atom	1st	2nd	3rd	4th	5th	6th	7th	8th
1	H	1312.0							
2	He	2372.3	5250.5						
3	Li	520.2	7298.1	11,815.0					
4	Be	899.5	1757.1	14,848.7	21,006.6				
5	B	800.6	2427.1	3659.7	25,025.8	32,826.7			
6	C	1086.5	2352.6	4620.5	6222.7	37,831	47,277.0		
7	N	1402.3	2856	4578.1	7475.0	9444.9	53,266.6	64,360	
8	O	1313.9	3388.3	5300.5	7469.2	10,989.5	13,326.5	71,330	84,078.0
9	F	1681.0	3374.2	6050.4	8407.7	11,022.7	15,164.1	17,868	92,038.1
10	Ne	2080.7	3952.3	6122	9371	12,177	15,238.90	19,999.0	23,069.5
11	Na	495.8	4562	6910.3	9543	13,354	16,613	20,117	25,496
12	Mg	737.7	1450.7	7732.7	10,542.5	13,630	18,020	21,711	25,661
13	Al	577.5	1816.7	2744.8	11,577	14,842	18,379	23,326	27,465
14	Si	786.5	1577.1	3231.6	4355.5	16,091	19,805	23,780	29,287
15	P	1011.8	1907	2914.1	4963.6	6273.9	21,267	25,431	29,872
16	S	999.6	2252	3357	4556	7004.3	8495.8	27,107	31,719
17	Cl	1251.2	2298	3822	5158.6	6542	9362	11,018	33,604
18	Ar	1520.6	2665.8	3931	5771	7238	8781	11,995	13,842
19	K	418.8	3052	4420	5877	7975	9590	11,343	14,944
20	Ca	589.8	1145.4	4912.4	6491	8153	10,496	12,270	14,206
21	Sc	633.1	1235.0	2388.6	7090.6	8843	10,679	13,310	15,250
22	Ti	658.8	1309.8	2652.5	4174.6	9581	11,533	13,590	16,440
23	V	650.9	1414	2830	4507	6298.7	12,363	14,530	16,730
24	Cr	652.9	1590.6	2987	4743	6702	8744.9	15,455	17,820
25	Mn	717.3	1509.0	3248	4940	6990	9220	11,500	18,770
26	Fe	762.5	1561.9	2957	5290	7240	9560	12,060	14,580
27	Co	760.4	1648	3232	4950	7670	9840	12,440	15,230
28	Ni	737.1	1753.0	3395	5300	7339	10,400	12,800	15,600
29	Cu	745.5	1957.9	3555	5536	7700	9900	13,400	16,000
30	Zn	906.4	1733.3	3833	5731	7970	10,400	12,900	16,800
31	Ga	578.8	1979.3	2963	6180				
32	Ge	762	1537.5	3302.1	4411	9020			
33	As	947.0	1798	2735	4837	6043	12,310		
34	Se	941.0	2045	2973.7	4144	6590	7880	14,990	
35	Br	1139.9	2103	3470	4560	5760	8550	9940	18,600
36	Kr	1350.8	2350.4	3565	5070	6240	7570	10,710	12,138

12.3. General Nomenclature of Organic Compounds

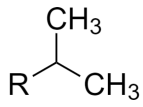
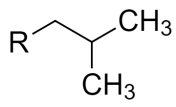
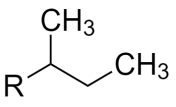
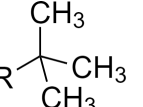
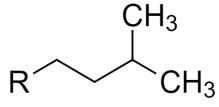
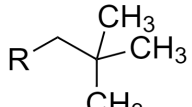
12.3.1. Alkane Chain Names

Prefixes for straight chains:

- Add -yl for an alkane substituent.
- Add -ane for the longest alkane chain with no other substituents.

<i>n</i>	1	2	3	4	5	6	7
	meth- (Me)	eth- (Et)	prop- (Pr)	but- (Bu)	pent-	hex-	hept-
<i>n</i>	8	9	10	11	12	13	14
	oct-	non-	dec-	undec-	dodec-	tridec-	tetradec-
<i>n</i>	15	16	17	18	19	20	21
	pentadec-	hexadec-	heptadec-	octadec-	nonadec-	icos-	unicos-

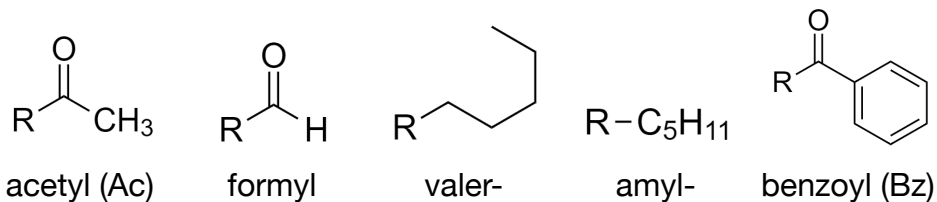
Common prefixes and IUPAC equivalents for branched chains:

					
isoprop- (iPr)	isobut- (iBu)	sec-but- (sBu)	tert-but- (tBu)	isopent-	neopent-
isoprop-	2-methylprop-	butan-2-	tert-but-	3-methylbut-	2,2-dimethylprop-

When ordering substituent names alphabetically,

- iso and cyclo prefixes **are** included.
- all other prefixes (*sec*, *tert*, *neo*, *di*, *tri*, *tetra*...) are **not** included; order by the base name.

Other unofficial names:



12.3.2. Functional Group Names and Priorities

Colour key: hydrocarbon, halogen, oxygen, nitrogen, sulfur, phosphorus

Naming key (top to bottom): functional group name; suffix (highest priority); prefix (lower priority)

Alkane -ane	Alkene -ene	Alkyne -yne	Arene -yl benzene phenyl-	Haloalkane halo-	Alcohol -ol hydroxy-	Aldehyde -al oxo-	Ketone -one oxo-	Carboxylic Acid -oic acid carboxy-	Acid Anhydride -oic anhydride alkyloxycarbonyl-
Acyl Halide -oyl halide chlorocarbonyl-	Ester -yl -oate alkoxycarbonyl-	Ether -oxy -ane -oxy -yl-	Epoxide -ene oxide oxiranyl-	Amine -amine amino-	Amide -amide carbamoyl-	Nitrate -nitrate nitrooxy-	Nitrite -nitrite nitrosooxy-	Nitrile -nitrile cyano-	Nitro nitro-
Nitroso nitroso-	Imine -imine alkylimino-	Imide -imide alkylcarbonyl-	Azide azido-	Cyanate -yl cyanate cyanato-	Isocyanate -yl isocyanate isocyanato-	Azo Compound azo-	Thiol -thiol mercapto-	Sulfide -yl sulfane alkylthio-	Disulfide disulfide alkyldisulfanyl-
Sulfoxide sulfoxide -ylsulfinyl-	Sulfone sulfone -ylsulfonyl-	Sulfinic Acid -sulfinic acid sulfino-	Sulfonic Acid -sulfonic acid sulfo-	Sulfonate -yl sulfonate oxysulfonyl-	Thiocyanate thiocyanate thiocyanato-	Isothiocyanate isothiocyanate isothiocyanato-	Thial thial thioformyl-	Thioketone thione thioyl-	Phosphine -yl phosphine phosphanyl
Oxime -one oxime hydroxyimino-	Hydrazone -ylidene hydrazine hydrazineylidene-	Acetal -oxy-	Hemiacetal -oxy -ol -oxy- hydroxy-	Ketal -oxy -alkoxy -oxy-	Hemiketal -oxy -ol -oxy- hydroxy-	Phosphonic Acid -phosphonic acid phospho-	Phosphinic Acid -phosphinic acid phosphino-	Phosphonate -yl phosphonate -oxyphosphonyl-	Sulfonamide N-alkyl -sulfonamide N- -sulfamoyl-

Naming priority order (not exhaustive):

(Highest priority: suffix) Carboxylic Acid > Sulfonic Acid > Ester > Acyl Halide > Amide > Nitrile > Aldehyde > Ketone > Alcohol > Thiol > Amine > Arene > Alkene > Alkyne > **Alkane** > Haloalkane > Ether > Azide > Nitro (Lowest priority: prefix)

C13. PHYSICAL CHEMISTRY

13.1. Atomic Structure and Quantum Chemistry

13.1.1. History of Molecular Theory and Atomic Theory

- In ~450 BC (Ancient Greece), Empedocles claimed all matter was composed of four **fundamental elements** (earth, fire, air, water) as continuous substances, as well as a fifth element permeating the space outside of Earth (quintessence; the luminiferous aether). There were also similar ideas in ancient China and India regarding fundamental elements.
- In ~400 BC, Democritus proposed '**atomism**', the concept that every substance is made of indivisible parts ('atomos'). The concept of the aether was retained, passed on by Aristotle. Atomism was developed further in ~300 BC by Epicurus. In ~50 BC (Ancient Rome), Lucretius brought back atomism. After the fall of the Roman Empire, Western thought on matter regressed and did not develop in any significant way until the late Renaissance.

During the Islamic Golden Age, alchemy (mysticism and proto-chemistry) was developed, with the fundamental 'principles' including sulfur, mercury and salt. Alchemy was considered more an art than a science, and was widely practised throughout Asia and spread to Europe in the late Middle Ages under scholasticism. The majority of thought in these times concerned metaphysics (e.g. souls, existence) and not matter. Many writers (Dante, Chaucer) considered alchemy to be fraudulent and/or nonsensical. In the 17th century (the Scientific Revolution), Newton, Gassendi, Boyle, Descartes and Lemery tried to rationalise properties of matter. They considered atoms to have different shapes and hook together, modifying Democritus' atomism to create corpuscular theory, which considered light to be made of particles (corpuscles). In the 18th century, the phlogiston theory was created to explain combustion and corrosion, and disproved in the 1770s with the discovery of oxygen by Lavoisier.

- **1803: Dalton's model** considered atoms as hard spheres in different forms (elements), that atoms can join together to form compounds, and that chemical reactions involve rearranging the atoms. In 1811, Avogadro considered gases as lots of molecules made of small numbers of atoms, building on Bernoulli's kinetic theory of gases, reconciling it with Gay-Lussac's law. By the 1830s, the molecular formulas of many simple molecules had been correctly identified. In 1871, Mendeleev's periodic table of elements was published, recognising periodicity and predicting properties. In 1887, the Michelson-Morley experiment disproved the existence of the luminiferous aether.
- **1904: Thompson's 'plum pudding' model**, proposed after his discovery of the electron with cathode ray tube experiments in 1897, with atoms as a large positively charged body with small negative electrons distributed inside.
- **1911: Rutherford's 'nuclear' model**, proposed after his discovery of the proton with his alpha particle scattering experiment, with a small positive nucleus and electrons around.
- **1913: Bohr's 'planetary model'**, proposed the electrons orbit in shells.

- **1916: Lewis' octet rule**, provided a rationale for the Lewis structure of covalent molecules.
- **1926: Quantum mechanics**, developed by de Broglie, Heisenberg, Schrödinger and Born, gave rise to the quantum model of the atom, with electrons as probability density clouds occupying orbitals around the nucleus.
- **1928: Dirac** formulated **quantum electrodynamics**, combining the quantum model with Einstein's special relativity, describing electrons as fundamental particles with **spin**.
- **1929:** Bethe and van Vleck developed **crystal field theory** to describe bonding in metal-inorganic complexes using the concepts of atomic orbital theory.
- **1931:** Pauling developed **hybridisation theory** to describe bonding in molecules.
- **1932:** Hund, Mulliken and Hückel developed **molecular orbital theory**, describing covalent bonds as in-phase and antiphase overlaps between atomic or hybridised orbitals. In the same year, Chadwick discovered neutrons in the nucleus, completing the nuclear model.
- **1933:** Pauling developed **resonance bonding** in terms of quantum superposition. Soviet scientists rejected this theory until the late 1950s due to their Marxist-Leninist philosophy, seeing resonance and quantum phenomena as anti-materialist and anti-deterministic, criticising it as metaphysical.
- **1957:** Griffith and Orgel developed **ligand field theory**, applying the techniques of molecular orbital theory to crystal field theory, accurately describing the bonding in organometallic compounds.
- **1964:** Gell-Mann and Zweig proposed that protons and neutrons are composed of **quarks** with deep inelastic scattering experiments. The quark model was incorporated into Dirac's quantum field theory.

13.1.1. Types of Structures due to Bonding

	Ionic	Covalent	Metallic
Solid	<ul style="list-style-type: none"> • Regular ion lattice with a repeating unit cell containing ions of opposite charges. • High melting point, electrical insulator, often soluble in water. 	<ul style="list-style-type: none"> • Simple molecular (e.g. CO₂ (s), H₂O (s)): low melting point, weak VdW intermolecular forces. • Giant covalent (e.g. diamond (C), SiO₂ (s)): very high melting point, electrical insulator or semiconductor. • Polymer (e.g. polyethylene, BeCl₂ (s)): medium melting point, strong VdW IMFs. 	<ul style="list-style-type: none"> • Regular ion lattice surrounded by a sea of delocalised electrons. • High electrical and thermal conductivity, variable melting point, high density, shiny (lustrous), sonorous.
Liquid	<ul style="list-style-type: none"> • Freely moving ions with strong IMFs. • Electrical conductor. 	<ul style="list-style-type: none"> • Freely moving molecules with strong IMFs. 	<ul style="list-style-type: none"> • Freely moving ions with delocalised electrons. • Electrical conductor.
Gas	<ul style="list-style-type: none"> • Single neutral molecules and small clusters. • All ionic properties lost. 	<ul style="list-style-type: none"> • Freely moving molecules with weak IMFs. • No distinctive properties. 	<ul style="list-style-type: none"> • Single neutral atoms and small molecule clusters. • All metallic properties lost.

13.1.2. Lewis Dot Structures

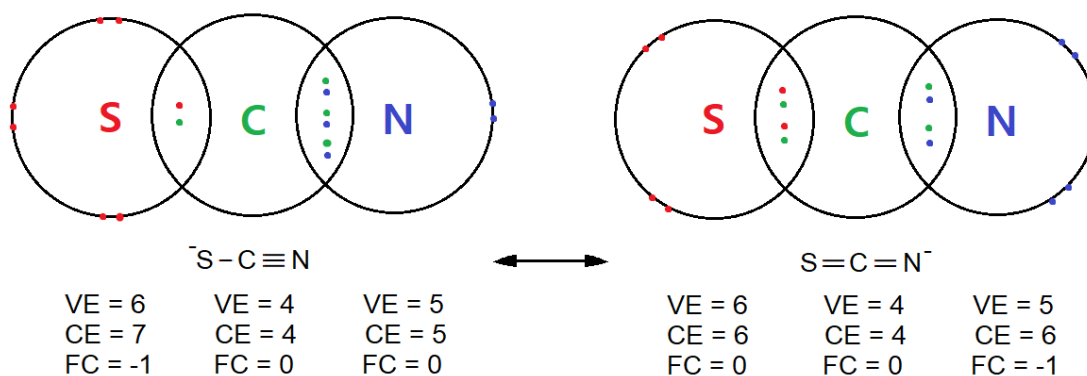
Valence electrons: $VE = \text{group number of atom}$

Contributed electrons: $CE = \text{nonbonding electrons} + \text{donated electrons}$

Donated electrons: 1 per single bond, 2 per double bond, 2 per dative covalent bond

Formal charge: $FC = VE - CE$

Lewis Dot example: the resonance forms of the thiocyanate anion (SCN^-)

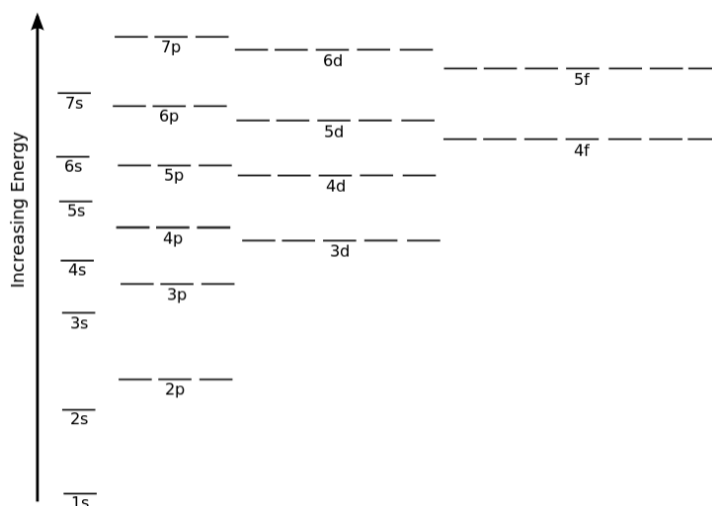


Lewis dot structures are usually only valid for atoms up to Period 3 (allowing for expanded octets in e.g. P (10 e⁻) and S (12 e⁻)), and are a highly simplified depiction of bonding.

13.1.3. Predicted Ground-State Electron Configurations

- **Aufbau principle:** electrons occupy the orbitals with the lowest energy before the orbitals with higher energy. The usual order is:
 $1s \rightarrow 2s \rightarrow 2p \rightarrow 3s \rightarrow 3p \rightarrow 4s \rightarrow 3d \rightarrow 4p \rightarrow 5s \rightarrow 4d \rightarrow 5p \rightarrow 6s \rightarrow 4f \rightarrow 5d \rightarrow 6p \rightarrow 7s \rightarrow 5f \rightarrow 6d \rightarrow 7p$.
- **Hund's rule:** every suborbital is singly occupied before any orbital in the sublevel is doubly occupied.
- **Pauli exclusion principle:** two electrons with the same spin cannot occupy the same suborbital.

From these three observations, the ground-state electron configurations of neutral atoms follows from the lowest unoccupied energy level in the following diagram:



The main exceptions to this rule are neutral Cu, Cr, Ag, Au, Pd and Mo atoms: see Section 11.2.1. for the electron configurations of all atoms. This is often due to the additional exchange energy of a half-full or full d orbital.

The noble gases [He], [Ne], [Ar], [Kr], [Xe], [Rn] end in $1s^2$, $2p^6$, $3p^6$, $4p^6$, $5p^6$, $6p^6$ respectively.

When a transition metal is ionised, electrons are removed from the valence s orbital before the valence d orbital.

13.1.4. Quantum Numbers

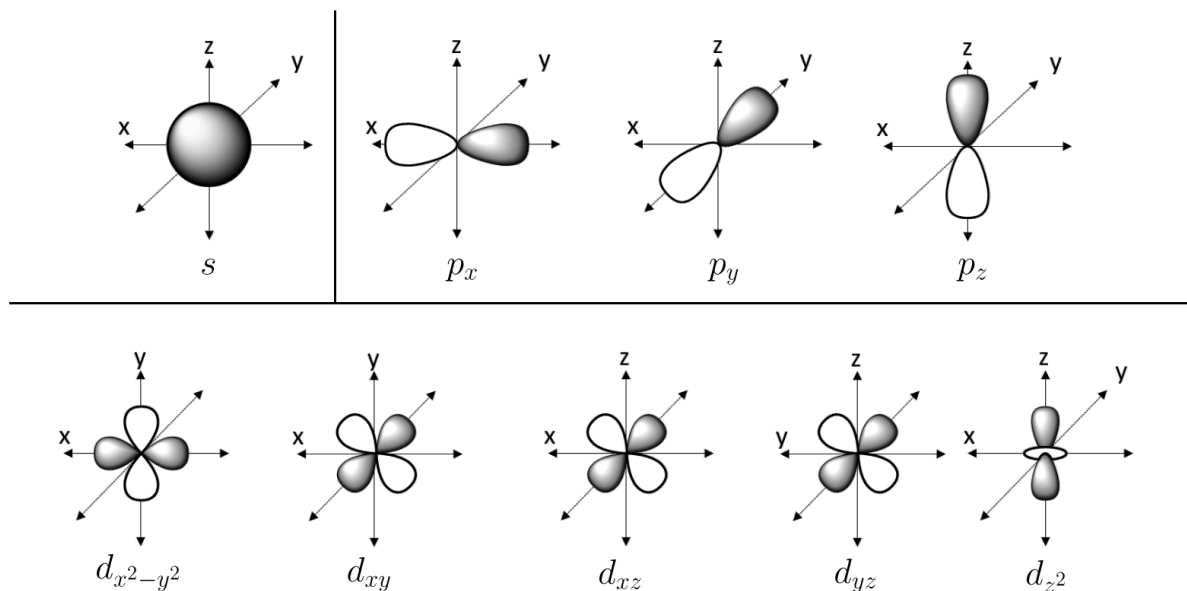
An electron can be described with four quantum numbers (n, l, m_l, m_s):

- Principal quantum number, n : the period, or equivalent Bohr model orbit.
- Azimuthal (angular momentum) quantum number, l : the type of orbital.
 $l = 0$ is an s -orbital, $l = 1$ is a p -orbital, $l = 2$ is a d -orbital, $l = 3$ is an f -orbital.
- Magnetic quantum number, m_l or m : the sub-orbital, with $-l \leq m_l \leq l$.
- Spin quantum number, m_s : represents spin-up or spin-down, with $m_s = \pm \frac{1}{2}$.

12.1.5. Shapes and Designations of Atomic s, p and d -orbitals

The shades represent opposing phases of the wavefunction for the atomic orbital.

The z -axis is taken as the internuclear axis when bond formation occurs.




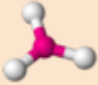
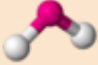
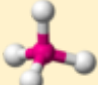
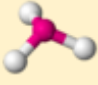
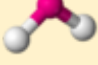
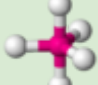
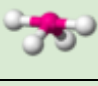
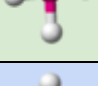
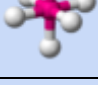
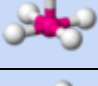
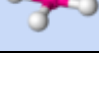
The magnetic quantum numbers of these orbitals are

$$\begin{array}{cccccc}
 p_z: m_l = 0, & p_x: m_l = 1, & p_y: m_l = -1 & & & \\
 d_{z^2}: m_l = 0, & d_{xz}: m_l = 1, & d_{yz}: m_l = -1, & d_{xy}: m_l = 2, & d_{x^2-y^2}: m_l = -2 &
 \end{array}$$


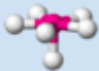
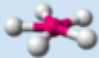


For the field splitting of d -orbitals in transition metal complexes, see Section 15.4.1.

13.1.6. Molecular Geometry, Hybridisation and the VSEPR Theory

The bonding in covalent molecules is predicted by VSEPR (valence shell electron pair repulsion) theory. Some of the valence atomic orbitals (s , p , d) on a single atom can be combined into a set of degenerate hybrid atomic orbitals (sp , sp^2 , ...), which can then form covalent bonds with other orbitals.

Atoms	Lone pairs	Electron domains (hybridisation)	Shape (point group)	Ideal bond angles	Examples	Image
2	0	2 (sp)	linear ($D_{\infty h}$)	180°	CO_2 , BeF_2	
3	0	3 (sp^2)	trigonal planar (D_{3h})	120°	BF_3 , SO_3	
2	1		bent (C_{2v})	120° (119°)	SO_2	
4	0	4 (sp^3)	tetrahedral (T_d)	109.47°	CH_4 , MnO_4^-	
3	1		trigonal pyramidal (C_{3v})	109.47° (106.8°)	NH_3 , ClO_3^-	
2	2		bent (C_{2v})	109.47° (104.48°)	H_2O	
5	0	5 (sp^3d)	trigonal bipyramidal (D_{3h})	90° , 120°	PCl_5 , $\text{Fe}(\text{CO})_5$	
4	1		seesaw (C_{2v})	180° , 120° , 90°	SF_4 , AsF_4^-	
3	2		T-shaped (C_{2v})	90° , 180°	ClF_3	
6	0	6 (sp^3d^2)	octahedral (O_h)	90° , 180°	SF_6 , $\text{Mo}(\text{CO})_6$	
5	1		square pyramidal (C_{4v})	90°	BrF_5 , MnCl_5^{2-}	
4	2		square planar (D_{4h})	90° , 180°	XeF_4 , PtCl_4^{2-}	

For higher numbers of atoms, more complex geometries are:

Atoms	Lone pairs	Electron domains (hybridisation)	Shape (point group)	Ideal bond angles	Examples	Image
7	0	7 (sp^3d^3)	pentagonal bipyramidal (D_{5h})	$90^\circ, 72^\circ, 180^\circ$	IF_7, ZrF_7^{3-}	
6	1		pentagonal pyramidal (C_{5v})	$72^\circ, 90^\circ, 144^\circ$	$XeOF_5^-, IOF_5^{2-}$	
5	2		pentagonal planar (D_{5h})	$72^\circ, 144^\circ$	IF_5^{2-}	
8	0	8 (sp^3d^4)	square antiprismatic (D_{4d})	$70.5^\circ, 99.6^\circ, 109.5^\circ$	TaF_8^{3-}	
9	0	9 (sp^3d^5)	tricapped trigonal prismatic (D_{3h})	$90^\circ, 120^\circ$	$ReH_9^{2-}, Th(H_2O)_9^{4+}$	

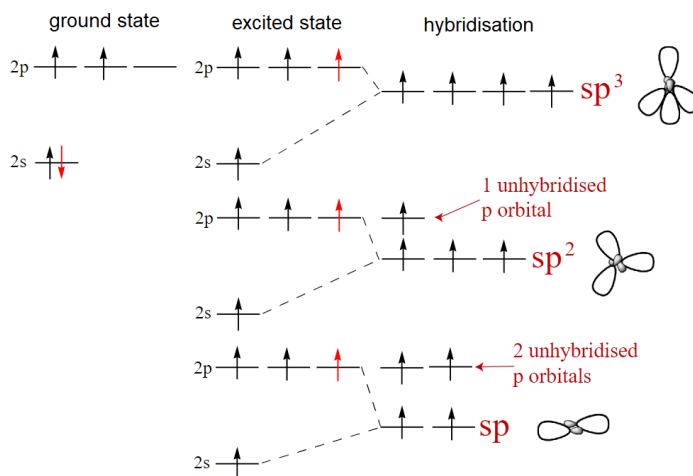
The presence of lone pairs on an atom reduces the bond angles. Bonding pairs repel less strongly:

$$LP-LP > LP-BP > BP-BP$$

There is a reduction in bond angle by about 2.5° per lone pair (very approximate).

Note: the point groups are not unique to a particular geometry and are only true when the groups surrounding the central atom are identical.

Conceptual Formation of sp , sp^2 and sp^3 Hybrid Atomic Orbitals: e.g. for carbon.



13.1.7. Bohr Model for Hydrogenic Atoms

The Bohr model has electrons in orbits around the nucleus analogous to planets around the Sun.

- Orbit radius, $r_n = \frac{a_0 n^2}{Z}$
- Orbit speed, $v_n = \frac{e^2}{2\epsilon_0 \hbar} \frac{Z}{n}$
- Orbit angular momentum, $L_n = \frac{nh}{2\pi} = \hbar n$
- Kinetic energy, $T_n = \frac{Z^2 e^2}{8\pi\epsilon_0 a_0 n^2}$
- Potential energy, $V_n = -\frac{Z^2 e^2}{4\pi\epsilon_0 a_0 n^2}$
- Total energy, $E_n = -\frac{Z^2 e^2}{8\pi\epsilon_0 a_0 n^2}$

(Z : nuclear charge (H = 1, He⁺ = 2, Li²⁺ = 3...), $m_e = 9.109 \times 10^{-31}$ kg: electron rest mass, $h = 6.63 \times 10^{-34}$ J s: Planck's constant, $\hbar = 1.06 \times 10^{-34}$: reduced Planck's constant, $|e| = 1.61 \times 10^{-19}$ C: electron charge, $a_0 = 5.292 \times 10^{-11}$ m: Bohr radius, $\epsilon_0 = 8.854 \times 10^{-12}$ C N⁻¹ m⁻²: vacuum permittivity.)

Line spectrum of hydrogen: the lines in the emission spectra can be divided into the Lyman series ($n \rightarrow 1$), Balmer series ($n \rightarrow 2$), Paschen series ($n \rightarrow 3$), Brackett series ($n \rightarrow 4$), Pfund series ($n \rightarrow 5$) and Humphreys series ($n \rightarrow 6$), in which the electron falls from a higher state to the state shown.

Direct de-excitation from state n_2 to state n_1 shows at line wavelength (Rydberg's formula):

$$\frac{1}{\lambda} = \frac{\Delta E}{hc} = Z^2 R_\infty \left(\frac{1}{n_1^2} - \frac{1}{n_2^2} \right) \quad (R_\infty = 1.097 \times 10^7 \text{ m}^{-1}: \text{Rydberg constant})$$

When an electron in the excited state n_2 de-excites to state n_1 , there are a maximum of $\frac{\Delta n (\Delta n + 1)}{2}$ emission lines due to intermediate transitions (where $\Delta n = n_2 - n_1$).

In X-ray experiments, the shells $n = 1, 2, 3$ are denoted K, L, M respectively.

The Bohr model is a significant oversimplification for multi-electron atoms. The electron shells are considered to have 2, 8, 8, 18, 18, 32, 32... electrons, in that order.

13.1.8. Quantum Model for Hydrogenic Atoms

The time-independent Schrodinger equation (TISE) for a one-electron atom (hydrogen-like) is:

$$\hat{H}\Psi = E\Psi, \quad \hat{H} = -\frac{\hbar^2}{2\mu}\nabla^2 + V, \quad V = \frac{Ze^2}{4\pi\epsilon_0 r}, \quad \mu = \frac{m_e m_{nucleus}}{m_e + m_{nucleus}}$$

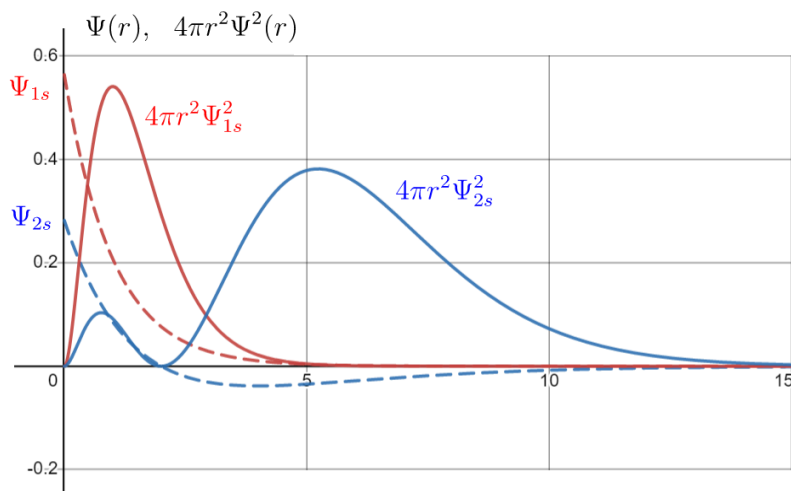
(E : energy of a state, $\Psi(\mathbf{r})$: wavefunction of a state.) The solution for Ψ with \mathbf{r} in spherical coordinates (r, θ, ϕ) is separable (radial: polynomial with exponential decay; angular: spherical harmonic) and is given by:

$$\Psi_{nlm}(r, \theta, \phi) = \underbrace{\sqrt{\frac{4(n-l-1)!}{(a_0^*)^3 n^4 (n+l)!}}}_{\text{normalisation constant}} \times \underbrace{\rho^l e^{-\frac{1}{2}\rho} L_{n-l-1}^{2l+1}(\rho)}_{\text{radial dependence}} \times \underbrace{Y_l^m(\theta, \phi)}_{\text{angular dependence}}$$

($a_0^* = m_e a_0 / \mu$: reduced Bohr radius, $\rho = 2r / n a_0^*$: dimensionless radial coordinate, L : generalised Laguerre polynomial (Section 1.7.12), Y_l^m : spherical harmonic (Section 1.7.17).)

The corresponding energy eigenvalues (energy levels) are $E_n = \frac{-m_e e^4}{32\pi^2 \epsilon_0^2 \hbar^2} \frac{1}{n^2} \approx \frac{-13.6 \text{ eV}}{n^2}$.

Plots of the 1s and 2s Wavefunctions for Hydrogenic Atoms



The quantity $4\pi r^2 |\Psi|^2$ is the radial probability density function.

$$1s : \Psi_{1,0,0} = \pi^{-1/2} a_0^{-3/2} e^{-r/a_0}$$

Maximum of $4\pi r^2 \Psi_{1s}^2$ is at $r = a_0$.

$$\frac{r}{a_0} \quad 2s : \Psi_{2,0,0} = \frac{1}{4} \pi^{-1/2} a_0^{-3/2} \left(2 - \frac{r}{a_0} \right) e^{-r/(2a_0)}$$

Node of $4\pi r^2 \Psi_{2s}^2$ is at $r = 2a_0$.

- The s orbitals ($l = 0$) are spherical, with radial nodes and alternating phases between them.
- The p orbitals ($l = 1$) are axial, with one nodal plane and opposite phases on each side of the plane.
- Number of radial nodes = $n - l - 1$. Number of angular nodes (nodal planes) = l .
- The higher orbitals have more complex geometries.

13.1.9. Quantum Model for Multi-Electron Atoms

For a system of n electrons, the wavefunction is a function of $3n$ spatial variables e.g. the spherical coordinates $(r_1, \theta_1, \phi_1, r_2, \theta_2, \phi_2, \dots, r_n, \theta_n, \phi_n)$. The Hamiltonian is

$$\hat{H} = \underbrace{-\frac{\hbar^2}{2\mu} \sum_{i=1}^n \nabla_i^2}_{\text{kinetic energy}} - \underbrace{\sum_{i=1}^n \frac{Ze^2}{4\pi\epsilon_0 r_i}}_{\text{nuclear attraction potential energy}} + \underbrace{\sum_{i=1}^{n-1} \sum_{j=i+1}^n \frac{e^2}{4\pi\epsilon_0 r_{ij}}}_{\text{mutual repulsion potential energy}}$$

∇_i^2 is the Laplacian operator with respect to only the coordinates of electron i :

$$\nabla_i^2 = \frac{1}{r_i^2 \sin \theta_i} \left[\sin \theta_i \frac{\partial}{\partial r_i} \left(r_i^2 \frac{\partial}{\partial r_i} \right) + \frac{\partial}{\partial \theta_i} \left(\sin \theta_i \frac{\partial}{\partial \theta_i} \right) + \frac{1}{\sin \theta_i} \frac{\partial^2}{\partial \phi_i^2} \right]$$

and r_{ij} is the distance between electron i and electron j :

$$r_{ij} = \sqrt{r_i^2 + r_j^2 - 2r_i r_j (\cos \theta_i \cos \theta_j + \sin \theta_i \sin \theta_j \cos(\phi_i - \phi_j))}$$

13.1.10. Linear Combinations of Atomic Orbitals (LCAO)

A common simplification to multi-electron or polynuclear species is the LCAO approximation. Under this assumption, a molecular orbital (MO) can be formed by combining atomic orbitals (AOs) in either constructive or destructive interference:

$$\Psi^{(MO)} = \sum_n c_n \psi^{(AO)} \quad \text{i.e. a linear superposition of atomic orbitals.}$$

The collection of AOs used to form an MO is the 'basis set'. The coefficients c_n can be found by variational methods to minimise the energy of each electron. Hybridised atomic orbitals can also be expressed in this way (e.g. $\Psi^{(sp^3)} = \frac{1}{2}(\psi^{(s)} \pm \psi^{(p_x)} \pm \psi^{(p_y)} \pm \psi^{(p_z)})$).

For binary homonuclear species, $|c_1| = |c_2|$ (equal sharing of electrons):

$$\Psi_{MO} = \frac{1}{\sqrt{2(1+S)}} \left(\psi_1^{(AO)} + \psi_2^{(AO)} \right) \quad \text{and} \quad \Psi_{MO^*} = \frac{1}{\sqrt{2(1-S)}} \left(\psi_1^{(AO)} - \psi_2^{(AO)} \right)$$

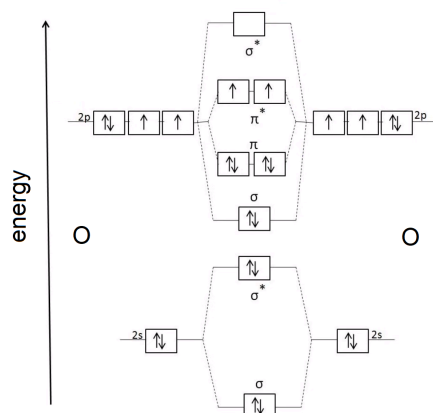
(bonding: constructive interference) (anti-bonding: destructive interference)

where $S = \int_V \psi_1^{(AO)} \psi_2^{(AO)} dV$ is the overlap integral, bounded by $0 \leq S \leq 1$.

13.1.11. Molecular Orbital Theory

Atomic orbitals (AOs, potentially hybridised) on two nearby atoms can interact. The resulting molecular orbital (MO) can be considered a linear superposition of a bonding MO and an antibonding MO, where the AOs interfere constructively and destructively respectively.

- When AOs interact directly (e.g. s orbitals, sp^n hybrid orbitals, axial p orbitals), the resulting MOs are sigma (σ and σ^*)
- When AOs interact laterally (e.g. lateral p orbitals), the resulting MOs are pi (π and π^*).



Example: MO diagram for diatomic oxygen (O_2)

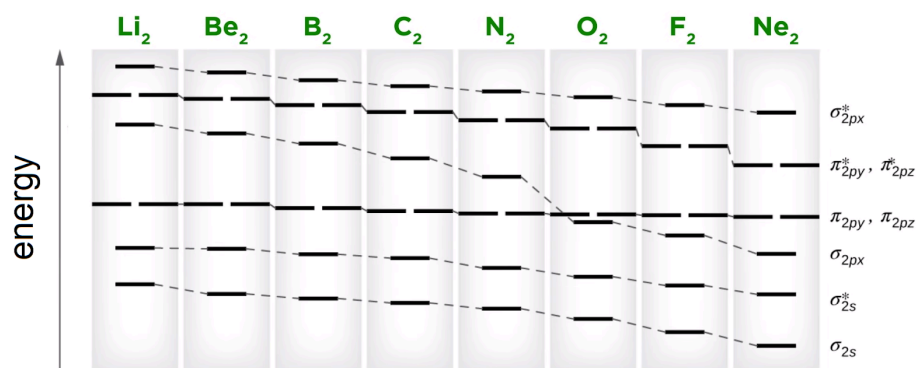
Each O atom has valence configuration $2s^2 2p^4$.

The $2p_z$ AOs interfere directly to form σ_{2p} and σ_{2p}^* .

The $2p_x$ and $2p_y$ AOs interfere laterally to form π_{2p} and π_{2p}^* .

(The $2s$ AOs also form σ_{2s} and σ_{2s}^* , but these are both fully filled and so cancel out i.e. do not contribute to bond order.)

s - p Mixing in Period 2 Homonuclear Diatomic Molecules



When the s and p AOs have similar energies, the resulting σ_{2s} and σ_{2p} interfere such that σ_{2p} becomes less stable.

For less electronegative atoms (Li...N), the resulting $\sigma_{2p} > \pi_{2p}$, leading to a different order of MO filling.

$$\text{Bond order} = \frac{\# \text{ bonding } e^- - \# \text{ antibonding } e^-}{2} \quad (1: \text{ single, } 2: \text{ double, } 3: \text{ triple})$$

For the application of MO theory to d orbitals, see Ligand Field Theory (LFT, Section 15.5.14.)

13.1.12. Magnetic Properties of Matter

Materials may respond to external magnetic field \mathbf{B} by creating an internal magnetisation \mathbf{M} which may act in the same or opposite direction.

- If $\mathbf{B} = 0$ produces $\mathbf{M} = 0$, then the material is an induced magnet.
- If $\mathbf{B} = 0$ produces $\mathbf{M} > 0$, then the material is a permanent magnet (ferromagnetic).

Iron, cobalt, nickel, ruthenium and many rare-earth alloys are ferromagnetic at room temperature. These elements have a microstructure of magnetic domains in which all electron spins are aligned to produce a large unidirectional magnetisation (below the Curie temperature). For more information / data on magnetic materials, see Section 8.6.

For the relationships between \mathbf{B} , \mathbf{H} , \mathbf{M} and μ , see Section 8.1.1. The two modes of induced magnetism are:

	Diamagnetic	Paramagnetic
Electron configuration	No unpaired electrons	At least one unpaired electron
Spin alignment with external magnetic field \mathbf{B}	Anti-parallel to \mathbf{B} ($-1 \leq \chi_v < 0$)	Parallel to \mathbf{B} ($\chi_v > 0$)
Reaction to magnets	Weakly repelled	Attracted
Effect on field lines of \mathbf{B}	Field bends away from material	Field bends towards material

Magnetic susceptibility: $\chi_v = \frac{\text{internal magnetisation}}{\text{applied magnetic field}} = \frac{M}{H} = \mu_r - 1.$

Molar susceptibility: $\chi_m = \frac{M_r}{\rho} \chi_v$

Superconductors are perfectly diamagnetic with $\chi = -1$ below the critical temperature and expel the magnetic field completely (Meissner effect).

13.1.13. Symmetry Adapted Linear Combinations (SALCs) of Atomic Orbitals

Molecular orbitals for polyatomic molecules can be deduced using projection operators to account for the symmetry about a central atom. For the character tables of point groups, see Section 13.2.10.

1. Determine the point group. (If linear, use D_{2h} / C_{2v} instead as it is simpler.)
2. Assign the x - y - z axes. z is the principal axis. If nonlinear, y points to the outer atom.
3. Find reducible representation Γ of outer atom orbitals (moves: 0, symmetric: +1, antisymmetric: -1)
4. Use the character table to find the irreducible representation Γ of outer atom orbitals (SALCs).

Example: SALCs of the water molecule (H_2O). H_2O belongs to the C_{2v} point group. Assign the z -axis as principal axis (C_2 symmetry) so that the molecule lies in the x - z plane. The character table for C_{2v} contains the symmetries $\{E, C_2^z, \sigma^{xz}, \sigma^{yz}\}$. Consider the counts of each symmetry applied to each atomic orbital:

Hydrogen $1s$ orbital:

Reducible representation:

$$\Gamma = \{E: 2, C_2: 0, \sigma^{xz}: 2, \sigma^{yz}: 0\}$$

Irreducible representation:

$$\Gamma_{2\text{H},1s} = 1 A_1 \oplus 1 B_1.$$

Oxygen $2s$ orbital:

Reducible representation

$$\Gamma = \{E: 1, C_2: 1, \sigma^{xz}: 1, \sigma^{yz}: 1\}$$

Irreducible representation

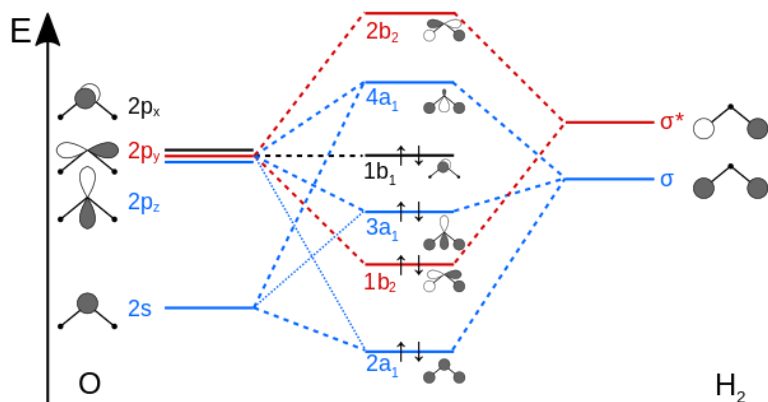
$$\Gamma_{\text{O},2s} = 1 A_1.$$

Oxygen $2p$ orbital:

From the character table, these are by definition:

$$A_1 (p_z), B_1 (p_x), B_2 (p_y).$$

Orbitals with the same symmetry now interact, splitting into bonding and antibonding to form the MO diagram.

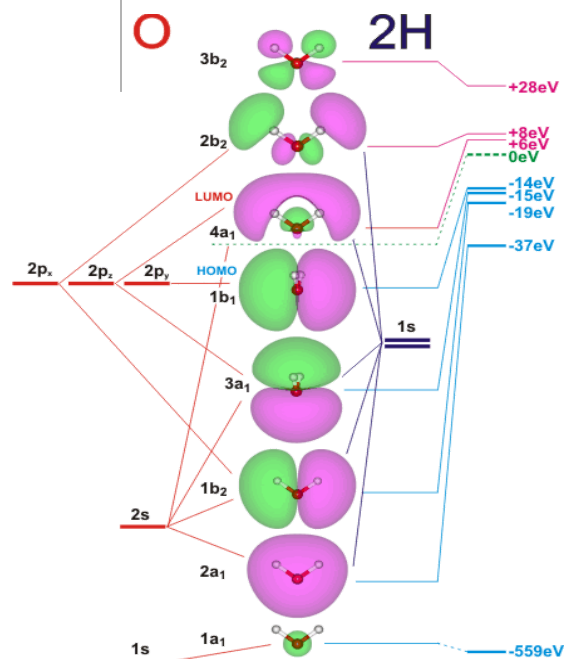


SALC-predicted MO diagram of water

(HOMO: $1b_1$, nonbonding; LUMO: $4a_1$, anti-bonding)

$1b_1$ acts as the main 'lone pair' (hydrogen bond acceptor) can be considered the second lone pair.

This applies in the ideal gas phase (energies are shifted and broadened slightly into bands in liquid water/ice).



True MOs and energy levels of water (computed with Hartree-Fock DFT)

but $2a_1$

13.1.14. Huckel's Method

13.1.15. Angular Overlap Method

13.1.15. Density Functional Theory (DFT)

DFT is a computational algorithm used to determine the electron density of a system across space. It effectively approximates the solution to the Schrodinger equation for large quantum systems e.g. interacting molecules, large molecules, nanoparticles, network solids, for which molecular dynamics simulations are prohibitively computationally expensive.

Hohenberg-Kohn Theorems:

1. The external potential and total energy are unique functionals of electron density.
2. The functional corresponding to the system's ground state energy gives the lowest energy if and only if the input density is the true ground-state density.

Kohn-Sham Equations: the electrons are approximated as non-interacting, instead modifying the potential function to account for the changes. The equations modelling the fictitious system are:

$$\left(-\frac{\hbar^2}{2m} \nabla^2 + v_{\text{eff}}(\mathbf{r}) \right) \varphi_i(\mathbf{r}) = \varepsilon_i \varphi_i(\mathbf{r}).$$

Schrodinger equation

$$\rho(\mathbf{r}) = \sum_i^N |\varphi_i(\mathbf{r})|^2.$$

Electron density

($\varphi_i(\mathbf{r})$): wavefunction for Kohn-Sham orbital, given by a Slater determinant)

Exchange-correlation functional: used to approximate the $E'_{xc}[n]$ term in the energy density functional (n : electron density per unit volume).

$$\begin{aligned} E[n] &= E_{\text{kin,KS}}[n] + E_{\text{Coul}}[n] + E_{\text{ext}}[n] + (E_{\text{kin}}[n] - E_{\text{kin,KS}}[n]) + E_{\text{xc}}[n] \\ &= 2 \sum_{i=1}^{N_{\text{el}}/2} \int \psi_i^*(\mathbf{r}) \left(-\frac{1}{2} \nabla^2 \right) \psi_i(\mathbf{r}) d\mathbf{r} + E_{\text{Coul}}[n] + E_{\text{ext}}[n] + E'_{\text{xc}}[n] \end{aligned}$$

The EC functionals can be written in terms of the energy per electron, $E'_{xc}[n] = \int n(\mathbf{r}) \varepsilon_{xc}[n(\mathbf{r})] d\mathbf{r}$.

Local density approximation (LDA): $E'_{xc}[n] = E_x[n] + E_c[n]$, where $E_x[n] = C \int n(\mathbf{r})^{4/3} d\mathbf{r}$.

A variety of expressions for $E_c[n]$ exist (e.g. VWN, VWN5, CAPZ), and should be chosen suitably depending on the type of computation, which may contain empirically-derived parameters.

13.1.16. Classical Computational Chemistry (Molecular Dynamics)

While quantum mechanics must be considered for atomic-scale simulation, for larger systems this is typically infeasible. A classical alternative to DFT is molecular dynamics.

A molecular dynamics simulation produces a trajectory of states \mathbf{x} at time steps t . Useful information is obtained by computing an observable quantity $A(\mathbf{x})$.

Monte Carlo Simulation

In Monte Carlo simulation, the aim is to create a stochastic process that tends to the Boltzmann distribution, as fast as possible and compute observables as averages over phase space. Dynamical evolution of system variables does not correspond to real dynamics in any way. It is not suitable for studying non-equilibrium and other time-dependent phenomena.

- Transition probability: $p(j \rightarrow i) = \min\{1, e^{-\frac{E_i - E_j}{kT}}\}$, then apply the Metropolis-Hastings algorithm (Section 5.4.10).
- Time-averaged value of an observable A : $\bar{A} \approx \frac{1}{Z} \int A(x) e^{-\frac{E(x)}{kT}} dx \approx \int_0^\tau A(x_{Langevin}(t)) dt$

Error Analysis in Correlated Time Series of Observables

- Time-averaged value of an observable A : $\bar{A} = \frac{1}{\tau} \int_0^\tau A(x(t)) dt = \frac{1}{N} \sum_{i=1}^N A(x(t_i))$
- Normalised autocorrelation: $\rho(\tau) = C(\tau)/C(0)$, where C is the autocorrelation of A given by $C(\tau) = E[(A(t) - \bar{A})(A(t + \tau) - \bar{A})]$, and $C(0) = \text{Var}[A]$.
- Exponential autocorrelation time: if $|\rho(\tau)| \leq e^{-\tau/\tau_0}$ then $\tau_0^{exp} = \lim_{\tau \rightarrow \infty} \sup\{\frac{-\tau}{\ln|\rho(\tau)|}\}$.

Measurements separated by at least $\sim 10 \tau_0^{exp}$ are uncorrelated (independent). This can be used to set a **'burn-in'** period of a simulation after setting initial conditions, where the system equilibrates before collecting data.

- Variance of mean observable: $\text{Var}[\bar{A}] = 2\tau_0^{int} \times \frac{C(0)}{N}$, where $\tau_0^{int} = \frac{1}{2} + \sum_{k=1}^{\infty} \rho(\tau_k)$.

To reduce noise effects, compute smallest M such that $M \geq 10 \hat{\tau}_0^{int}$ ($\hat{\tau}_0^{int} = \frac{1}{2} + \sum_{k=1}^M \rho(\tau_k)$).

LAMMPS is a package written in C++ that can use an OPLS force model (bond stretching + bending + torsion + electrostatics + Lennard-Jones VdW), commonly used for high-speed classical molecular dynamics.

13.2. Crystallography and Solid State Chemistry

13.2.1. Unit Cells of Some Simple Crystal Structures

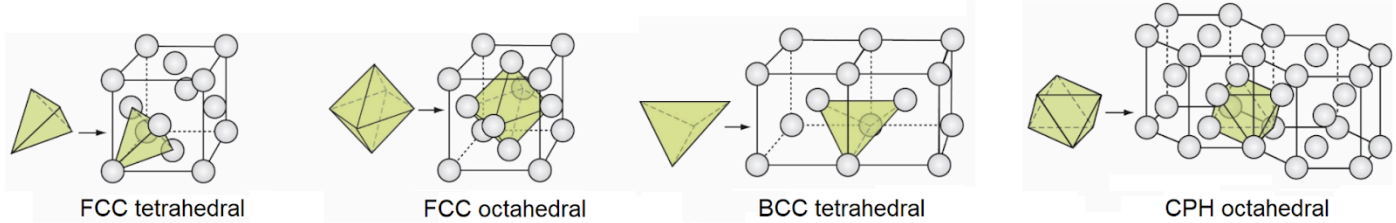
Unit Cell (green: close-packed planes)			
Name	FCC Face-Centred Cubic	BCC Body-Centred Cubic	CPH (HCP) Close-Packed Hexagonal
Atoms	4	2	6
Coordination Number	12	8	12
Packing Fraction	$\frac{\sqrt{2}\pi}{6} \approx 74\%$	$\frac{\sqrt{3}\pi}{8} \approx 68\%$	$\frac{\sqrt{2}\pi}{6} \approx 74\%$
Atomic radius in terms of lattice constant(s)	$r = \frac{\sqrt{2}}{4} a \approx 0.354a$	$r = \frac{\sqrt{3}}{4} a \approx 0.433a$	$r = \frac{1}{2} a = \frac{\sqrt{6}}{8} c \approx 0.306c$
Cell Volume	$V = 16\sqrt{2} r^3$	$V = \frac{64\sqrt{3}}{9} r^3$	$V = 24\sqrt{2} r^3$

Some common particular structures are:

- **Diamond Cubic (DC):** an FCC lattice with either four (1:1) or eight (1:2) of the tetrahedral voids occupied. Notable cases: zinc blende / sphalerite (ZnS), fluorites (CaF₂), antifluorites (Na₂O, Li₂O), Si and Ge, diamond (C), silicon carbide (SiC).
- **Corundum:** a CPH lattice with four (2:3) of the octahedral voids occupied. Notable cases: metal(III) oxides (Al₂O₃, Fe₂O₃, Cr₂O₃)
- **Halite:** two FCC lattices of each atom (1:1), alternating along any edge. Notable cases: rock salt (NaCl).
- **Primitive Cubic BCC:** a simple cubic structure with the single body-centre position occupied (1:1). Notable cases: caesium chloride (CsCl).

13.2.2. Voids in Simple Lattices

Only FCC, BCC and CPH are given here. For other lattices, see Section 12.2.7.



Voids in an FCC Lattice, per unit cell with monatomic radius R :

- 8 regular tetrahedral voids, with $\frac{r}{R} = \sqrt{\frac{3}{2}} - 1 \approx 0.225$, coordination number 4, with centroids at $\{\frac{1}{2} \pm \frac{1}{4}, \frac{1}{2} \pm \frac{1}{4}, \frac{1}{2} \pm \frac{1}{4}\}$.
- 4 regular octahedral voids, with $\frac{r}{R} = \sqrt{2} - 1 \approx 0.414$, coordination number 6, with centroids at $\{\frac{1}{2}, \frac{1}{2}, \frac{1}{2}\}, \{0, 0, \frac{1}{2}\}$, etc.

Voids in a BCC lattice, per unit cell with monatomic radius R :

- 12 irregular (distorted) tetrahedral voids, with $\frac{r}{R} = \sqrt{\frac{5}{3}} - 1 \approx 0.290$, coordination number 2, with a centroid at $\{\frac{1}{2}, 0, \frac{1}{4}\}$, etc.
- 6 irregular (distorted) octahedral voids, with $\frac{r}{R} = \frac{2\sqrt{3}-3}{3} \approx 0.155$, coordination number 2, with a centroids at $\{\frac{1}{2}, \frac{1}{2}, 0\}$ and $\{\frac{1}{2}, 0, 0\}$ (among others).

Voids in a CPH lattice, per unit cell with monatomic radius R :

- 12 regular tetrahedral voids, with $\frac{r}{R} = \sqrt{\frac{3}{2}} - 1 \approx 0.225$, coordination number 4, with centroids at $\{0, 0, \frac{3}{8}\}, \{0, 0, \frac{5}{8}\}, \{\frac{2}{3}, \frac{1}{3}, \frac{1}{8}\}$ and $\{\frac{2}{3}, \frac{1}{3}, \frac{7}{8}\}$ (among others).
- 6 regular octahedral voids, with $\frac{r}{R} = \sqrt{2} - 1 \approx 0.414$, coordination number 6, with centroids at $\{\frac{1}{3}, \frac{2}{3}, \frac{1}{4}\}$ and $\{\frac{1}{3}, \frac{2}{3}, \frac{3}{4}\}$ (among others).

13.2.3. Crystallographic Defects

Point Defects:

- **Schottky defect:** vacancy of equal numbers of cation and anion lattice positions.
- **Frenkel defect:** displacement of an ion at a lattice position to an interstitial position.
- **Metal excess defect:** replacement of an anion lattice position with an unpaired electron (F-centre). The electron absorbs light in the visible spectrum, giving colour.
- **Metal deficiency defect:** vacancy of a cation lattice position, balanced by cations in higher oxidation states.

Line Defects:

- **Edge dislocation:** an extra half-plane of atoms.
The line vector is perpendicular to the Burgers vector.
- **Screw dislocation:** a fork in the lattice.
The line vector is parallel to the Burgers vector.
- **Mixed dislocation:** a combination of edge and screw dislocations.
The line vector is at an acute angle to the Burgers vector.

Plane and Bulk Defects:

- Areas: Grain boundaries, Twin boundaries,
- Volumes: Cracks, Pores, Precipitates.

13.2.4. Defect Reactions

Kröger-Vink notation for point defects: A_S^C where

- A is the entity symbol (atomic element symbol, or v = vacancy, e = electron, h = hole),
- S is the substituted entity symbol (atomic element symbol, or i = interstitial site),
- C is the real or effective charge (\bullet = positive, $/$ = negative, \times = zero)

Defect reactions for fully ionised point defects of metal oxides M_aO_b are:

Schottky disorder	$0 \Rightarrow v_M^{\frac{2b}{a}/} + \frac{b}{a} v_O^{\bullet\bullet}$ balanced = metal vacancy + oxygen vacancy
Frenkel disorder	$M_M^{\times} + v_i^{\times} \Rightarrow v_M^{\frac{2b}{a}/} + M_i^{\frac{2b}{a}\bullet}$ metal atom + interstitial void = metal vacancy + interstitial metal
Anti-Frenkel disorder	$O_O^{\times} + v_i^{\times} \Rightarrow v_O^{\bullet\bullet} + O_i^{//}$ oxygen atom + interstitial void = oxygen vacancy + interstitial oxygen
Intrinsic electronic ionisation	$0 \Rightarrow e' + h^{\bullet}$ balanced = conduction band electron + valence band hole
Oxygen excess	$\frac{1}{2} O_2(g) + v_i^{\times} \Rightarrow O_i^{//} + 2 h^{\bullet}$ $O_2(g) + \text{interstitial void} = \text{interstitial oxygen} + \text{valence holes}$
Oxygen deficiency	$O_O^{\times} \Rightarrow v_O^{\bullet\bullet} + 2 e' + \frac{1}{2} O_2(g)$ oxygen atom = oxygen vacancy + conduction electrons + $O_2(g)$
Metal excess	$M_M^{\times} + \frac{b}{a} O_O^{\times} + v_i^{\times} \Rightarrow M_i^{\frac{2b}{a}\bullet} + \frac{2b}{a} e' + \frac{b}{2a} O_2(g)$ metal atom + oxygen atom + interstitial void = interstitial metal + conduction electrons + $O_2(g)$
Metal deficiency	$\frac{b}{2a} O_2(g) \Rightarrow v_M^{\frac{2b}{a}/} + \frac{b}{a} O_O^{\times} + \frac{2b}{a} h^{\bullet}$ $O_2(g) = \text{metal vacancy} + \text{oxygen atom} + \text{valence hole}$

Doping of ionic compounds: either form defects with opposite effective charge, or consume defects of same effective charge. Examples:

- Doping of $Ni_{1-x}O$ with Li_2O :

$$Li_2O(s) + 2 v_{Ni}^{//} \Rightarrow 2 Li_{Ni}' + O_O^{\times}$$
 or, in the presence of oxygen:

$$Li_2O(s) + \frac{1}{2} O_2(g) \Rightarrow 2 Li_{Ni}' + 2 O_O^{\times} + 2 h^{\bullet}$$
- Doping of ZrO_{2-y} with Y_2O_3 :

$$Y_2O_3(s) \Rightarrow 2 Y_{Zr}' + v_O^{\bullet\bullet} + 3 O_O^{\times}$$
- Doping of $LaScO_3$ with CaO :

$$CaO(s) + \frac{1}{2} Sc_2O_3 \Rightarrow Ca_{La}' + Sc_{Sc}^{\times} + \frac{5}{2} O_O^{\times} + \frac{1}{2} v_O^{\bullet\bullet}$$
- Doping of LaF_{3-x} with EuF_2 :

$$EuF_2(s) \Rightarrow Eu_{La}' + v_F^{\bullet} + F^-$$

13.2.5. Kinetics and Thermodynamics of Defect Reactions

Defect activity (site fraction): $a_{A_S^c} = \frac{[A_S^c]}{[S]}$. Equilibrium constant, $K = \prod_i a_i^{v_i}$.

Note that terms such as $a_{Zn_{Zn}^x} = \frac{[Zn_{Zn}^x]}{[Zn]} \approx 1$ and can be neglected from the expression.

For electronic defects, use $a_{e'} = \frac{n}{N_C}$ and $a_{h\cdot} = \frac{p}{N_V}$ (N : state density in conduction / valence bands)

Thermodynamics: $K = \exp\left(\frac{-\Delta G^\ominus}{RT}\right) = \exp\left(\frac{\Delta S_{vib}^\ominus}{R}\right) \exp\left(\frac{-\Delta H^\ominus}{RT}\right)$

Conventional electronic 'equilibrium' constant: $K' = [e'] [h\cdot] = np = N_C N_V \exp\left(\frac{-E_g}{RT}\right)$.

Other common conventional simplifications: scale $a_{O_2(g)}$ as $\frac{p_{O_2}}{1 \text{ bar}}$, scale $a_{e'}$, $a_{h\cdot} = n, p$.

Brouwer diagram: plot of $\log n$ against $\log p_{O_2}$, typically a straight line.

Example reaction: $0 \Rightarrow v_M^{2n/} + n v_O^{\bullet\bullet}$, activities are constrained by:

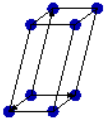
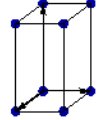
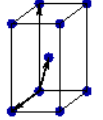
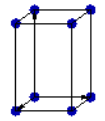
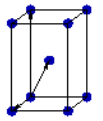
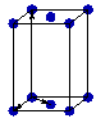
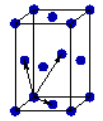
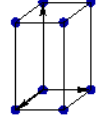
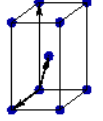
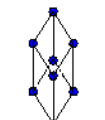
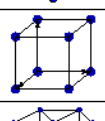
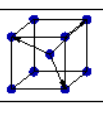
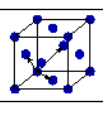
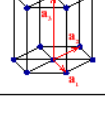
Electroneutrality: $n [v_O^{\bullet\bullet}] = [v_M^{2n/}]$ since net charge remains constant

Site balance: $[v_M^{2n/}] + [M_M^x] = [M] = \text{const.}$ and $[v_O^{\bullet\bullet}] + [O_O^x] = [O] = \text{const.}$

Therefore $K = [v_M^{2n/}] [v_O^{\bullet\bullet}]^n \Rightarrow K = n [v_O^{\bullet\bullet}]^{n+1} \Rightarrow [v_O^{\bullet\bullet}] = \left(\frac{K}{n}\right)^{1/(n+1)}$.

13.2.6. Bravais Lattices

The Bravais lattices fall into seven main classes:

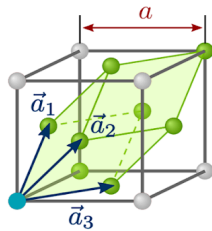
	Sides, Angles	Simple (Primitive, P)	Body Centred (I)	Base Centred (C)	Face Centred (F)
Triclinic	$a \neq b \neq c$ $\alpha \neq \beta \neq \gamma$				
Monoclinic	$a \neq b \neq c$ $\beta = \gamma = 90^\circ$, $\alpha \neq 90^\circ$				
Orthorhombic	$a \neq b \neq c$ $\alpha = \beta = \gamma = 90^\circ$				
Tetragonal	$a = b \neq c$ $\alpha = \beta = \gamma = 90^\circ$				
Trigonal	$a = b = c$ $\alpha = \beta = \gamma < 120^\circ$				
Cubic	$a = b = c$ $\alpha = \beta = \gamma = 90^\circ$				
Hexagonal	$a = b \neq c$ $\alpha = 120^\circ$ $\beta = \gamma = 90^\circ$				

13.2.7. Reciprocal Lattices and Brillouin Zones

Wigner-Seitz Primitive Unit Cell: a new unit cell with reduced size based on Voronoi partitioning. The Wigner-Seitz primitive unit cell is the Voronoi tessellation (regions closest to each lattice point: Section 2.3.15) of a given set of lattice points. It is the smallest possible unit cell choice. It can be constructed as the region enclosed by the perpendicular bisector planes to all nearest-neighbour lattice points. Primitive cubic → cubic; BCC → truncated octahedron; FCC → rhombic dodecahedron.

Reciprocal space (k-space): for a given Bravais lattice, define a set of primitive translation vectors $\{\mathbf{a}_1, \mathbf{a}_2, \mathbf{a}_3\}$ such that any lattice point in the Bravais lattice can be written in the form $\mathbf{r} = m\mathbf{a}_1 + n\mathbf{a}_2 + o\mathbf{a}_3$ where (m, n, o) are integers. The corresponding reciprocal lattice is composed of translation vectors $\{\mathbf{b}_1, \mathbf{b}_2, \mathbf{b}_3\}$ (or labelled $\{\mathbf{k}_x, \mathbf{k}_y, \mathbf{k}_z\}$ in quantum mechanics with spatial frequency and momentum as the Fourier transform of position), where:

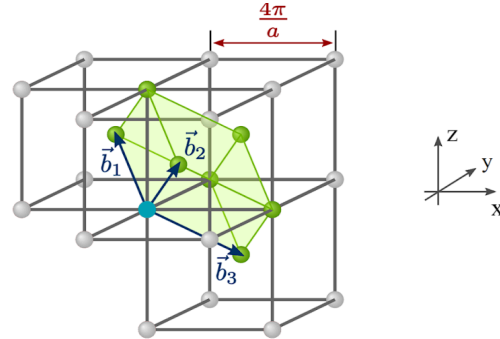
$$\mathbf{b}_1 = \frac{2\pi}{V}(\mathbf{a}_2 \times \mathbf{a}_3), \quad \mathbf{b}_2 = \frac{2\pi}{V}(\mathbf{a}_3 \times \mathbf{a}_1), \quad \mathbf{b}_3 = \frac{2\pi}{V}(\mathbf{a}_1 \times \mathbf{a}_2), \quad V = |\mathbf{a}_1 \cdot (\mathbf{a}_2 \times \mathbf{a}_3)|: \text{unit cell volume}$$



Bravais lattice:

FCC, lattice spacing a

Primitive translation vectors: $\{\mathbf{a}_1, \mathbf{a}_2, \mathbf{a}_3\}$

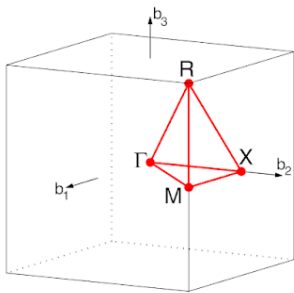


Reciprocal lattice:

BCC, lattice spacing $4\pi/a$

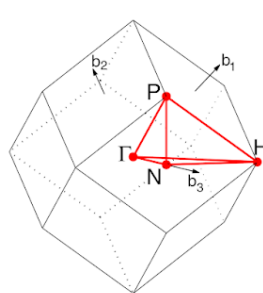
Primitive translation vectors: $\{\mathbf{b}_1, \mathbf{b}_2, \mathbf{b}_3\}$

First Brillouin Zones: Wigner-Seitz unit cell of the **reciprocal** (wavenumber) lattice unit cell. The Brillouin zone indicates the periodicity of the lattice as a function of direction. More isotropic lattices have more spherical Brillouin zones. The **irreducible Brillouin zone (IBZ)** is a smaller unit cell that exploits more symmetries, shown in red below. The n th Brillouin zone is constructed using the n th nearest neighbours in constructing the WS unit cell instead of the nearest.



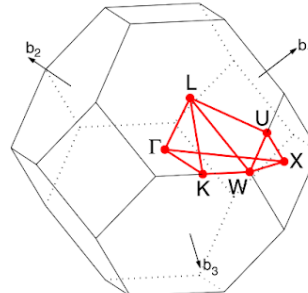
Primitive Cubic

Reciprocal lattice: cubic
First Brillouin zone: cube



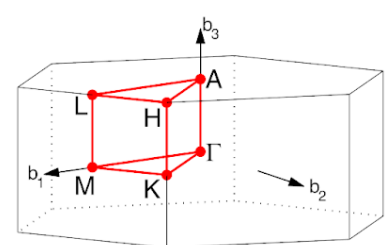
Body-centred Cubic (BCC)

Reciprocal lattice: FCC
First Brillouin zone: rhombic dodecahedron



Face-centred Cubic (FCC)

Reciprocal lattice: BCC
First Brillouin zone: truncated octahedron



Primitive Hexagonal (HCP)

Reciprocal lattice: HCP
First Brillouin zone: hexagonal prism

13.2.8. Miller Indices, k -Space and X-ray Diffraction of Lattices

Consider a coordinate system with axes parallel to the basis vectors $\{\mathbf{a}_1, \mathbf{a}_2, \mathbf{a}_3\}$ of a Bravais lattice. Let the lengths of a unit cell along these directions be $\{a, b, c\}$.

Miller index notation: the notation $[hkl]$ can, depending on context, represent either:

- the **plane** intersecting the three axes at positions $\left[\frac{a}{h}, \frac{b}{k}, \frac{c}{l}\right]$ along each axis. A Miller index is taken as zero if the plane is parallel to the axis i.e. intersects at infinity. A Miller index is represented with an overbar if it intersects at a negative ordinate e.g. $-1 \rightarrow \bar{1}$.
- the **line** which passes through the origin and has direction vector $[h, k, l]$, which is a normal vector to the above plane.

Spacing between adjacent parallel planes $[hkl]$ in adjacent unit cells: $\frac{1}{d^2} = \frac{h^2}{a^2} + \frac{k^2}{b^2} + \frac{l^2}{c^2}$

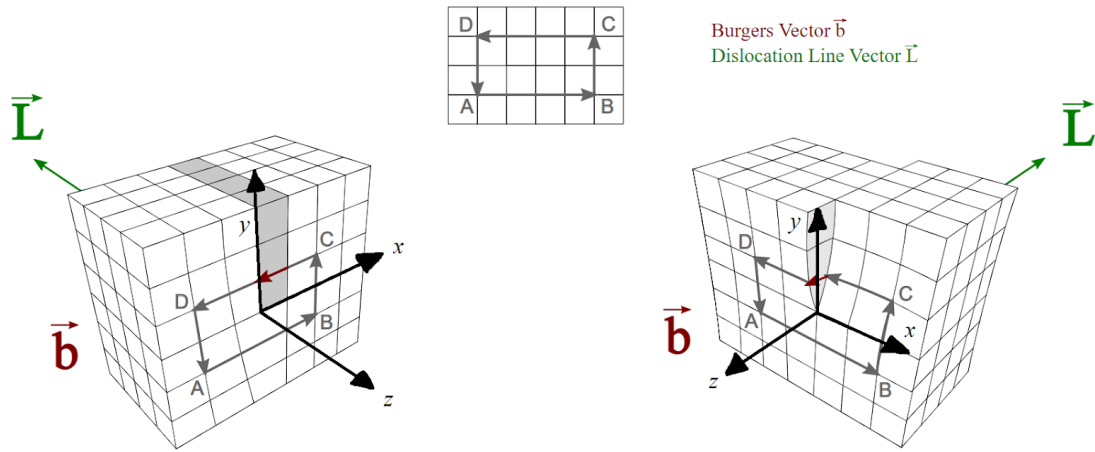
Vector equation of planes: $\mathbf{r} \cdot \left[\frac{h}{a}, \frac{k}{b}, \frac{l}{c}\right] = 1$. (see also Section 2.4.6.)

Symmetry-adapted extension to HCP lattices: use four basis vectors so that the plane $[hkl]$ in $\{\mathbf{a}, \mathbf{b}, \mathbf{d}\}$ space becomes $[hkil]$ in $\{\mathbf{a}, \mathbf{b}, \mathbf{c}, \mathbf{d}\}$ space, where $i = -(h + k)$, and \mathbf{c} is the third vector in the hexagonal plane such that $(\mathbf{a}, \mathbf{b}, \mathbf{c})$ are separated by 120° and $\mathbf{c} \perp \mathbf{d}$. In this new basis, all symmetry-related planes and lines have Miller indices which are permutations, like the cubic lattices.

X-Ray Diffractometry: diffraction pattern has peaks at the reciprocal lattice points

- Bragg's law of diffraction: $n\lambda = 2d \sin \theta$
(n : order of diffraction, λ : beam wavelength, θ : glancing angle of incidence)
- Laue equations: $\Delta \mathbf{k} \cdot \mathbf{a}_1 = 2\pi h$; $\Delta \mathbf{k} \cdot \mathbf{b}_2 = 2\pi k$; $\Delta \mathbf{k} \cdot \mathbf{c}_3 = 2\pi l$
($\Delta \mathbf{k} = \mathbf{k}_{\text{out}} - \mathbf{k}_{\text{in}}$: scattering vector / transferred wavevector, such that the X-ray can be represented as $\mathbf{E}(\mathbf{x}, t) = \mathbf{E}_0 \cos(\omega t - \mathbf{k} \cdot \mathbf{x} + \varphi)$.)

13.2.9. Stress Fields due to Dislocations



Edge Dislocation ($\mathbf{b} = -a \mathbf{i}$)

Screw Dislocation ($\mathbf{b} = a \mathbf{k}$)

$$\sigma_{xx} = - \frac{Gby(3x^2 + y^2)}{2\pi(1 - \nu)(x^2 + y^2)^2}$$

$$\sigma_{yy} = - \frac{Gby(x^2 - y^2)}{2\pi(1 - \nu)(x^2 + y^2)^2}$$

$$\sigma_{zz} = \frac{Gby}{\pi(1 - \nu)(x^2 + y^2)^2}$$

$$\tau_{xy} = \tau_{yx} = - \frac{Gbx(x^2 - y^2)}{2\pi(1 - \nu)(x^2 + y^2)^2}$$

$$\tau_{xz} = \tau_{zx} = \tau_{yz} = \tau_{zy} = 0$$

$$\tau_{xz} = \tau_{zx} = \frac{Gby}{2\pi(x^2 + y^2)} = \frac{Gb \sin \theta}{2\pi r}$$

$$\tau_{yz} = \tau_{zy} = \frac{Gbx}{2\pi(x^2 + y^2)} = \frac{Gb \cos \theta}{2\pi r}$$

$$\sigma_{xx} = \sigma_{yy} = \sigma_{zz} = \tau_{xy} = \tau_{yx} = 0$$

(ν : Poisson's ratio, G : shear modulus)

compressive stresses for $y > 0$ and
tensile stresses for $y < 0$

For macroscopic results involving dislocations, including external stress fields, see Section 6.6.1.

13.2.10. Crystallographic Point Group Notation (Schönflies Notation)

A point group identifies the ways to transform a molecule or crystal lattice such that the overall arrangement of the atoms is unchanged.

Symmetry elements and operations:

Element	Symbol	Operation
Identity (all space)	E	Do nothing
Mirror Plane (plane)	σ	Reflection (σ_h : plane of highest order rotation, σ_v : plane containing highest order rotational axis, σ_d : vertical plane cutting bonds only)
Proper Rotation Axis (line)	C_n	Proper Rotation (n : rotation by $360^\circ/n$)
Improper Rotation Axis (line)	S_n	Improper Rotation / Rotoinversion ($S_n^{(m)}$ rotation followed by reflection σ_h)
Inversion Centre (point)	i	Inversion (i.e. S_2)

Symmetry species (Γ)

Mulliken symbol	Description	Mulliken symbol	Description
A	Symmetric with respect to principal axis	g	Symmetric to inversion
B	Antisymmetric with respect to principal axis	u	Antisymmetric to inversion
E	Doubly degenerate	X'	Symmetric to σ_h
T	Triply degenerate	X''	Antisymmetric to σ_h
X_1	Symmetric to C_2 rotation perpendicular to principal axis		
X_2	Antisymmetric to the C_2 rotation perpendicular to principal axis		

13.2.11. Character Tables for Point Groups

The point groups are generated by the quotient of the space groups by the Bravais lattices.

$n = 2$ point groups:

C_i	E	i	
A_g	1	1	$R_x; R_y; R_z \quad x^2; y^2; z^2; xy; xz; yz$
A_u	1	-1	$x; y; z$

C_s	E	σ_h	
A'	1	1	$x; y \quad R_z \quad x^2; y^2; z^2; xy$
A''	1	-1	$z \quad R_x; R_y \quad xz; yz$

C_2	E	C_2^z	
A	1	1	$z \quad R_z \quad x^2; y^2; z^2; xy$
B	1	-1	$x; y \quad R_x; R_y \quad xz; yz$

C_{2v}	E	C_2^z	σ^{xz}	σ^{yz}	
A_1	1	1	1	1	$z \quad x^2; y^2; z^2$
A_2	1	1	-1	-1	$R_z \quad xy$
B_1	1	-1	1	-1	$x \quad R_y \quad xz$
B_2	1	-1	-1	1	$y \quad R_x \quad yz$

C_{2h}	E	C_2^z	i	σ^{xy}	
A_g	1	1	1	1	$R_z \quad x^2; y^2; z^2; xy$
B_g	1	-1	1	-1	$R_x; R_y \quad xz; yz$
A_u	1	1	-1	-1	z
B_u	1	-1	-1	1	$x; y$

D_2	E	C_2^z	C_2^y	C_2^x	
A	1	1	1	1	$x^2; y^2; z^2$
B_1	1	1	-1	-1	$z \quad R_z \quad xy$
B_2	1	-1	1	-1	$y \quad R_y \quad xz$
B_3	1	-1	-1	1	$x \quad R_x \quad yz$

D_{2d}	E	$2S_4$	C_2^z	$2C_2'$	$2\sigma_d$	
A_1	1	1	1	1	1	$x^2 + y^2; z^2$
A_2	1	1	1	-1	-1	R_z
B_1	1	-1	1	1	-1	$x^2 - y^2$
B_2	1	-1	1	-1	1	$z \quad xy$
E	2	0	-2	0	0	$(x, y) \quad (R_x, R_y) \quad (xz, yz)$

D_{2h}	E	C_2^z	C_2^y	C_2^x	i	σ^{xy}	σ^{xz}	σ^{yz}	
A_g	1	1	1	1	1	1	1	1	$x^2; y^2; z^2$
B_{1g}	1	1	-1	-1	1	1	-1	-1	$R_z \quad xy$
B_{2g}	1	-1	1	-1	1	-1	1	-1	$R_y \quad xz$
B_{3g}	1	-1	-1	1	1	-1	-1	1	$R_x \quad yz$
A_u	1	1	1	1	-1	-1	-1	-1	
B_{1u}	1	1	-1	-1	-1	-1	1	1	z
B_{2u}	1	-1	1	-1	-1	1	-1	1	y
B_{3u}	1	-1	-1	1	-1	1	1	-1	x

$n = 3$ point groups:

C_3	E	C_3	C_3^2	$\omega = \exp(2\pi i/3)$
A	1	1	1	$z \quad R_z \quad x^2 + y^2; z^2$
E	1	ω	ω^2	$x - iy \quad R_x - iR_y \quad xz - iy; z; x^2 + 2ixy - y^2$
	1	ω^2	ω	$x + iy \quad R_x + iR_y \quad xz + iy; z; x^2 - 2ixy - y^2$

C_{3v}	E	$2C_3$	$3\sigma_v$	
A_1	1	1	1	$z \quad x^2 + y^2; z^2$
A_2	1	1	-1	R_z
E	2	-1	0	$(x, y) \quad (R_x, R_y) \quad (xz, yz); (x^2 - y^2, 2xy)$

D_3	E	$2C_3$	$3C_2$	
A_1	1	1	1	$x^2 + y^2; z^2$
A_2	1	1	-1	$z \quad R_z$
E	2	-1	0	$(x, y) \quad (R_x, R_y) \quad (xz, yz); (x^2 - y^2, 2xy)$

D_{3d}	E	$2C_3$	$3C_2$	i	$2S_6$	$3\sigma_d$	
A_{1g}	1	1	1	1	1	1	$x^2 + y^2; z^2$
A_{2g}	1	1	-1	1	1	-1	R_z
E_g	2	-1	0	2	-1	0	$(R_x, R_y) \quad (xz, yz); (x^2 - y^2, 2xy)$
A_{1u}	1	1	1	-1	-1	-1	
A_{2u}	1	1	-1	-1	-1	1	z
E_u	2	-1	0	-2	1	0	(x, y)

D_{3h}	E	$2C_3$	$3C_2$	σ_h	$2S_3$	$3\sigma_v$	
A_1'	1	1	1	1	1	1	$x^2 + y^2; z^2$
A_2'	1	1	-1	1	1	-1	R_z
E'	2	-1	0	2	-1	0	$(x, y) \quad (x^2 - y^2, 2xy)$
A_1''	1	1	1	-1	-1	-1	
A_2''	1	1	-1	-1	-1	1	z
E''	2	-1	0	-2	1	0	$(R_x, R_y) \quad (xz, yz)$

$n = 4$ point groups:

C_{4v}	E	$2C_4$	C_4^2	$2\sigma_v$	$2\sigma_d$	
A_1	1	1	1	1	1	z $x^2 + y^2; z^2$
A_2	1	1	1	-1	-1	R_z
B_1	1	-1	1	1	-1	$x^2 - y^2$
B_2	1	-1	1	-1	1	xy
E	2	0	-2	0	0	(x, y) (R_x, R_y) (xz, yz)

Note: The σ_v planes in C_{4v} coincide with the xz and yz planes.

\mathcal{D}_{4h}	E	$2C_4$	C_4^2	$2C_2$	$2C_2'$	i	$2S_4$	σ_h	$2\sigma_v$	$2\sigma_d$	
A_{1g}	1	1	1	1	1	1	1	1	1	1	$x^2 + y^2; z^2$
A_{2g}	1	1	1	-1	-1	1	1	1	-1	-1	R_z
B_{1g}	1	-1	1	1	-1	1	-1	1	1	-1	$x^2 - y^2$
B_{2g}	1	-1	1	-1	1	1	-1	1	-1	1	xy
E_g	2	0	-2	0	0	2	0	-2	0	0	(R_x, R_y) (xz, yz)
A_{1u}	1	1	1	1	1	-1	-1	-1	-1	-1	
A_{2u}	1	1	1	-1	-1	-1	-1	-1	1	1	z
B_{1u}	1	-1	1	1	-1	-1	1	-1	-1	1	
B_{2u}	1	-1	1	-1	1	-1	1	-1	1	-1	
E_u	2	0	-2	0	0	-2	0	2	0	0	(x, y)

Note: The C_2 axes in \mathcal{D}_{4h} coincide with the x and y axes, and the σ_v planes with the xz and yz planes.

 $n = 5$ point groups:

Note that the quantities $\eta_{\pm} \equiv \frac{1}{2}(\sqrt{5} \pm 1)$ satisfy $\eta_{\pm}^2 = 1 \pm \eta_{\pm}$ and $\eta_+ \eta_- = 1$.

C_{5v}	E	$2C_5$	$2C_5^2$	$5\sigma_v$	$\eta_{\pm} = \frac{1}{2}(\sqrt{5} \pm 1)$
A_1	1	1	1	1	z $x^2 + y^2; z^2$
A_2	1	1	1	-1	R_z
E_1	2	η_-	$-\eta_+$	0	(x, y) (R_x, R_y) (xz, yz)
E_2	2	$-\eta_+$	η_-	0	$(x^2 - y^2, 2xy)$

\mathcal{D}_5	E	$2C_5$	$2C_5^2$	$5C_2$	$\eta_{\pm} = \frac{1}{2}(\sqrt{5} \pm 1)$
A_1	1	1	1	1	$x^2 + y^2; z^2$
A_2	1	1	1	-1	z R_z
E_1	2	η_-	$-\eta_+$	0	(x, y) (R_x, R_y) (xz, yz)
E_2	2	$-\eta_+$	η_-	0	$(x^2 - y^2, 2xy)$

\mathcal{D}_{5d}	E	$2C_5$	$2C_5^2$	$5C_2$	i	$2S_{10}^3$	$2S_{10}$	$5\sigma_d$	$\eta_{\pm} = \frac{1}{2}(\sqrt{5} \pm 1)$
A_{1g}	1	1	1	1	1	1	1	1	$x^2 + y^2; z^2$
A_{2g}	1	1	1	-1	1	1	1	-1	R_z
E_{1g}	2	η_-	$-\eta_+$	0	2	η_-	$-\eta_+$	0	(R_x, R_y) (xz, yz)
E_{2g}	2	$-\eta_+$	η_-	0	2	$-\eta_+$	η_-	0	$(x^2 - y^2, 2xy)$
A_{1u}	1	1	1	1	-1	-1	-1	-1	
A_{2u}	1	1	1	-1	-1	-1	-1	1	z
E_{1u}	2	η_-	$-\eta_+$	0	-2	$-\eta_-$	η_+	0	(x, y)
E_{2u}	2	$-\eta_+$	η_-	0	-2	η_+	$-\eta_-$	0	

\mathcal{D}_{5h}	E	$2C_5$	$2C_5^2$	$5C_2$	σ_h	$2S_5$	$2S_5^3$	$5\sigma_v$	$\eta_{\pm} = \frac{1}{2}(\sqrt{5} \pm 1)$
A_1'	1	1	1	1	1	1	1	1	$x^2 + y^2; z^2$
A_2'	1	1	1	-1	1	1	1	-1	R_z
E_1'	2	η_-	$-\eta_+$	0	2	η_-	$-\eta_+$	0	(x, y) (xz, yz)
E_2'	2	$-\eta_+$	η_-	0	2	$-\eta_+$	η_-	0	$(x^2 - y^2, 2xy)$
A_1''	1	1	1	1	-1	-1	-1	-1	
A_2''	1	1	1	-1	-1	-1	-1	1	z
E_1''	2	η_-	$-\eta_+$	0	-2	$-\eta_-$	η_+	0	(R_x, R_y) (xz, yz)
E_2''	2	$-\eta_+$	η_-	0	-2	η_+	$-\eta_-$	0	

$n = 6$ point groups:

C_{6v}	E	$2C_6$	$2C_6^2$	C_6^3	$3\sigma_v$	$3\sigma_d$	
A_1	1	1	1	1	1	1	z $x^2 + y^2; z^2$
A_2	1	1	1	1	-1	-1	R_z
B_1	1	-1	1	-1	1	-1	
B_2	1	-1	1	-1	-1	1	
E_1	2	1	-1	-2	0	0	(x,y) (R_x, R_y) (xz, yz)
E_2	2	-1	-1	2	0	0	$(x^2 - y^2, 2xy)$

D_6	E	$2C_6$	$2C_6^2$	C_6^3	$3C_2$	$3C_2'$	
A_1	1	1	1	1	1	1	$x^2 + y^2; z^2$
A_2	1	1	1	1	-1	-1	z R_z
B_1	1	-1	1	-1	1	-1	
B_2	1	-1	1	-1	-1	1	
E_1	2	1	-1	-2	0	0	(x,y) (R_x, R_y) (xz, yz)
E_2	2	-1	-1	2	0	0	$(x^2 - y^2, 2xy)$

D_{6h}	E	$2C_6$	$2C_6^2$	C_6^3	$3C_2$	$3C_2'$	i	$2S_3$	$2S_6$	σ_h	$3\sigma_d$	$3\sigma_v$	
A_{1g}	1	1	1	1	1	1	1	1	1	1	1	1	$x^2 + y^2; z^2$
A_{2g}	1	1	1	1	-1	-1	1	1	1	1	-1	-1	R_z
B_{1g}	1	-1	1	-1	1	-1	1	-1	1	-1	1	-1	
B_{2g}	1	-1	1	-1	-1	1	1	-1	1	-1	-1	1	
E_{1g}	2	1	-1	-2	0	0	2	1	-1	-2	0	0	(R_x, R_y) (xz, yz)
E_{2g}	2	-1	-1	2	0	0	2	-1	-1	2	0	0	$(x^2 - y^2, 2xy)$
A_{1u}	1	1	1	1	1	1	-1	-1	-1	-1	-1	-1	
A_{2u}	1	1	1	1	-1	-1	-1	-1	-1	-1	1	1	z
B_{1u}	1	-1	1	-1	1	-1	-1	1	-1	1	-1	1	
B_{2u}	1	-1	1	-1	-1	1	-1	1	-1	1	1	-1	
E_{1u}	2	1	-1	-2	0	0	-2	-1	1	2	0	0	(x,y)
E_{2u}	2	-1	-1	2	0	0	-2	1	1	-2	0	0	

Cubic symmetry:

T	E	$4C_3$	$4C_3^2$	$3C_2$	$\omega = \exp(2\pi i/3)$
A_1	1	1	1	1	$x^2 + y^2 + z^2$
E {	1	ω	ω^2	1	$z^2 + \omega^2 x^2 + \omega y^2$
	1	ω^2	ω	1	$z^2 + \omega x^2 + \omega^2 y^2$
T_2	3	0	0	-1	(x,y,z) (R_x, R_y, R_z) (yz, xz, xy)

T_d	E	$8C_3$	$3C_2$	$6S_4$	$6\sigma_d$	
A_1	1	1	1	1	1	$x^2 + y^2 + z^2$
A_2	1	1	1	-1	-1	
E	2	-1	2	0	0	$((2z^2 - x^2 - y^2), \sqrt{3}(x^2 - y^2))$
T_1	3	0	-1	1	-1	(R_x, R_y, R_z)
T_2	3	0	-1	-1	1	(x,y,z) (yz, xz, xy)

O	E	$8C_3$	$3C_2^2$	$6C_4$	$6C_2$	
A_1	1	1	1	1	1	$x^2 + y^2 + z^2$
A_2	1	1	1	-1	-1	
E	2	-1	2	0	0	$((2z^2 - x^2 - y^2), \sqrt{3}(x^2 - y^2))$
T_1	3	0	-1	1	-1	(x,y,z) (R_x, R_y, R_z)
T_2	3	0	-1	-1	1	(xz, xy, yz)

O_h	E	$8C_3$	$3C_2^2$	$6C_4$	$6C_2$	i	$8S_6$	$3\sigma_h$	$6S_4$	$6\sigma_d$	
A_{1g}	1	1	1	1	1	1	1	1	1	1	$x^2 + y^2 + z^2$
A_{2g}	1	1	1	-1	-1	1	1	1	-1	-1	
E_g	2	-1	2	0	0	2	-1	2	0	0	$((2z^2 - x^2 - y^2), \sqrt{3}(x^2 - y^2))$
T_{1g}	3	0	-1	1	-1	3	0	-1	1	-1	(R_x, R_y, R_z)
T_{2g}	3	0	-1	-1	1	3	0	-1	-1	1	(xz, xy, yz)
A_{1u}	1	1	1	1	1	-1	-1	-1	-1	-1	
A_{2u}	1	1	1	-1	-1	-1	-1	-1	1	1	
E_u	2	-1	2	0	0	-2	1	-2	0	0	
T_{1u}	3	0	-1	1	-1	-3	0	1	-1	1	(x,y,z)
T_{2u}	3	0	-1	-1	1	-3	0	1	1	-1	

Icosahedral symmetry:

I_h	E	$12C_5$	$12C_5^2$	$20C_3$	$15C_2$	i	$12S_{10}^3$	$12S_{10}$	$20S_6$	15σ	$\eta_{\pm} = \frac{1}{2}(\sqrt{5} \pm 1)$
A_g	1	1	1	1	1	1	1	1	1	1	$x^2 + y^2 + z^2$
T_{1g}	3	η_+	$-\eta_-$	0	-1	3	η_+	$-\eta_-$	0	-1	(R_x, R_y, R_z)
T_{2g}	3	$-\eta_-$	η_+	0	-1	3	$-\eta_-$	η_+	0	-1	
G_g	4	-1	-1	1	0	4	-1	-1	1	0	
H_g	5	0	0	-1	1	5	0	0	-1	1	$(\sqrt{\frac{1}{12}}(2z^2 - x^2 - y^2), \frac{1}{2}(x^2 - y^2), xz, xy, yz)$
A_u	1	1	1	1	1	-1	-1	-1	-1	-1	
T_{1u}	3	η_+	$-\eta_-$	0	-1	-3	$-\eta_+$	η_-	0	1	(x,y,z)
T_{2u}	3	$-\eta_-$	η_+	0	-1	-3	η_-	$-\eta_+$	0	1	
G_u	4	-1	-1	1	0	-4	1	1	-1	0	
H_u	5	0	0	-1	1	-5	0	0	1	-1	

Linear symmetry:

$C_{\infty v}$	E	$2C^z(\alpha)$	\dots	$\infty\sigma_v$	
$\Sigma^+ (A_1)$	1	1	\dots	1	z $x^2 + y^2; z^2$
$\Sigma^- (A_2)$	1	1	\dots	-1	R_z
$\Pi (E_1)$	2	$2\cos\alpha$	\dots	0	(x,y) (R_x, R_y) (xz, yz)
$\Delta (E_2)$	2	$2\cos 2\alpha$	\dots	0	$(x^2 - y^2, 2xy)$
$\Phi (E_3)$	2	$2\cos 3\alpha$	\dots	0	
\dots	\dots	\dots	\dots	\dots	

$D_{\infty h}$	E	$2C^z(\alpha)$	\dots	$\infty\sigma_v$	i	$2S^z(\alpha)$	\dots	∞C_2	
$\Sigma_g^+ (A_{1g})$	1	1	\dots	1	1	1	\dots	1	$x^2 + y^2; z^2$
$\Sigma_g^- (A_{2g})$	1	1	\dots	-1	1	1	\dots	-1	R_z
$\Pi_g (E_{1g})$	2	$2\cos\alpha$	\dots	0	2	$-2\cos\alpha$	\dots	0	(R_x, R_y) (xz, yz)
$\Delta_g (E_{2g})$	2	$2\cos 2\alpha$	\dots	0	2	$2\cos 2\alpha$	\dots	0	$(x^2 - y^2, 2xy)$
$\Phi_g (E_{3g})$	2	$2\cos 3\alpha$	\dots	0	2	$-2\cos 3\alpha$	\dots	0	
\dots	\dots	\dots	\dots	\dots	\dots	\dots	\dots	\dots	
$\Sigma_u^+ (A_{1u})$	1	1	\dots	1	-1	-1	\dots	-1	z
$\Sigma_u^- (A_{2u})$	1	1	\dots	-1	-1	-1	\dots	1	
$\Pi_u (E_{1u})$	2	$2\cos\alpha$	\dots	0	-2	$2\cos\alpha$	\dots	0	(x,y)
$\Delta_u (E_{2u})$	2	$2\cos 2\alpha$	\dots	0	-2	$-2\cos 2\alpha$	\dots	0	
$\Phi_u (E_{3u})$	2	$2\cos 3\alpha$	\dots	0	-2	$2\cos 3\alpha$	\dots	0	
\dots	\dots	\dots	\dots	\dots	\dots	\dots	\dots	\dots	

13.2.12. Tables for Descent in Symmetry

C_{2v}	C_2	C_s (E, σ^{xz})	C_s (E, σ^{yz})
A_1	A	A'	A'
A_2	A	A''	A''
B_1	B	A'	A''
B_2	B	A''	A'

D_{3h}	C_{3v}	C_{2v} ($\sigma_h \rightarrow \sigma^{xz}$)	C_s (E, σ_h)	C_s (E, σ_v)
A'_1	A_1	A_1	A'	A'
A'_2	A_2	B_2	A'	A''
E'	E	$A_1 \oplus B_2$	$2A'$	$A' \oplus A''$
A''_1	A_2	A_2	A''	A''
A''_2	A_1	B_1	A''	A'
E''	E	$A_2 \oplus B_1$	$2A''$	$A' \oplus A''$

$D_{\infty h}$ (x,y,z)	C_{2v} (x,z,y)
Σ_g^+	A_1
Σ_g^-	B_1
Π_g	$A_2 \oplus B_2$
Δ_g	$A_1 \oplus B_1$
\dots	\dots
Σ_u^+	B_2
Σ_u^-	A_2
Π_u	$A_1 \oplus B_1$
Δ_u	$A_2 \oplus B_2$
\dots	\dots

$O(3)$	O_h	T_d
S_g	A_{1g}	A_1
P_g	T_{1g}	T_1
D_g	$E_g \oplus T_{2g}$	$E \oplus T_2$
F_g	$A_{2g} \oplus T_{1g} \oplus T_{2g}$	$A_2 \oplus T_1 \oplus T_2$
G_g	$A_{1g} \oplus E_g \oplus T_{1g} \oplus T_{2g}$	$A_1 \oplus E \oplus T_1 \oplus T_2$
\dots	\dots	\dots
S_u	A_{1u}	A_2
P_u	T_{1u}	T_2
D_u	$E_u \oplus T_{2u}$	$E \oplus T_1$
F_u	$A_{2u} \oplus T_{1u} \oplus T_{2u}$	$A_1 \oplus T_2 \oplus T_1$
G_u	$A_{1u} \oplus E_u \oplus T_{1u} \oplus T_{2u}$	$A_2 \oplus E \oplus T_2 \oplus T_1$
\dots	\dots	\dots

13.2.13. Reduction of Representation and Products of Group Operations

Reduction of Representation: If $\Gamma = a_1\Gamma^{(1)} \oplus a_2\Gamma^{(2)} \oplus \dots \oplus a_n\Gamma^{(n)}$ then

$$a_k = \frac{1}{h} \sum_R \chi^{(k)}(R)^* \chi(R)$$

($\chi(R)$: character of the operation R in the representation Γ , $\chi^{(k)}(R)$: character of the operation R in the representation $\Gamma^{(k)}$, h : number of elements in the group)

Projection Operators: The projection operator for representation $\Gamma^{(k)}$ is

$$\mathcal{P}^{(k)} = \frac{n_k}{h} \sum_R \chi^{(k)}(R)^* R.$$

The projected function $\mathcal{P}^{(k)}f$ (obtained by applying $\mathcal{P}^{(k)}$ to any function f) is either zero or a component for the basis for $\Gamma^{(k)}$.

Direct Products: In general, $\chi^{\Gamma \otimes \Gamma'}(R) = \chi^\Gamma(R) \chi^{\Gamma'}(R)$ and if the resulting representation is reducible it can be reduced in the usual way. Alternatively the following rules can be applied:

- Treat g/u and $'/'$ symmetry separately. For groups with an inversion centre,

$$g \otimes g = u \otimes u = g \quad \text{and} \quad g \otimes u = u.$$

- For groups with a horizontal plane σ_h but no inversion centre, the notation $'$ and $''$ denotes symmetry and antisymmetry with respect to σ_h . Then,

$$' \otimes ' = '' \otimes '' = ' \quad \text{and} \quad ' \otimes '' = ''.$$

- Direct products involving non-degenerate representations are easily worked out from the character table. The product of any A or B with any E is an E , and likewise the product of any A or B with any T is a T . In the cubic groups T_d , O and O_h ,

$$E \otimes E = A_1 \oplus A_2 \oplus E$$

$$E \otimes T_1 = E \otimes T_2 = T_1 \oplus T_2$$

$$T_1 \otimes T_1 = T_2 \otimes T_2 = A_1 \oplus E \oplus T_1 \oplus T_2$$

$$T_1 \otimes T_2 = A_2 \oplus E \oplus T_1 \oplus T_2$$

See the next page for direct products in axial groups.

Direct Products in Axial Groups: For products of E_i with E_j in the axial groups, the rules are more complicated. If there is only one E representation, apart from g/u or $'/'$ labels, it should be considered as E_1 . The order n of the principal axis is usually obvious e.g. 5 for D_{5h} - **but** for D_{md} with m even, $n = 2m$ (because D_{md} has an S_{2m} axis when m is even).

- For $E_i \otimes E_i$:
 - If E_{2i} exists then $E_i \otimes E_i = A_1 \oplus A_2 \oplus E_{2i}$
 - Otherwise, if $4i = n$ then $E_i \otimes E_i = A_1 \oplus A_2 \oplus B_1 \oplus B_2$
 - Otherwise $E_i \otimes E_i = A_1 \oplus A_2 \oplus E_{|2i-n|}$

- For $E_i \otimes E_j$ with $i \neq j$:
 - If E_{i+j} exists then $E_i \otimes E_j = E_{|i-j|} \oplus E_{i+j}$
 - If $2(i+j) = n$ then $E_i \otimes E_j = E_{|i-j|} \oplus B_1 \oplus B_2$
 - Otherwise $E_i \otimes E_j = E_{|i-j|} \oplus E_{|i+j-n|}$

(If there is only one A representation, apart from g/u and $'/'$ labels, read A_1 and A_2 above as A , and likewise for B .)

Antisymmetrised Squares:

The antisymmetric component of $E \otimes E$ or $E_i \otimes E_i$ is always A_2 .

In the cubic groups, the antisymmetric component of $T_1 \otimes T_1$ and $T_2 \otimes T_2$ is always T_1 .

13.2.14. Identification of IR-active and Raman-active Bonds

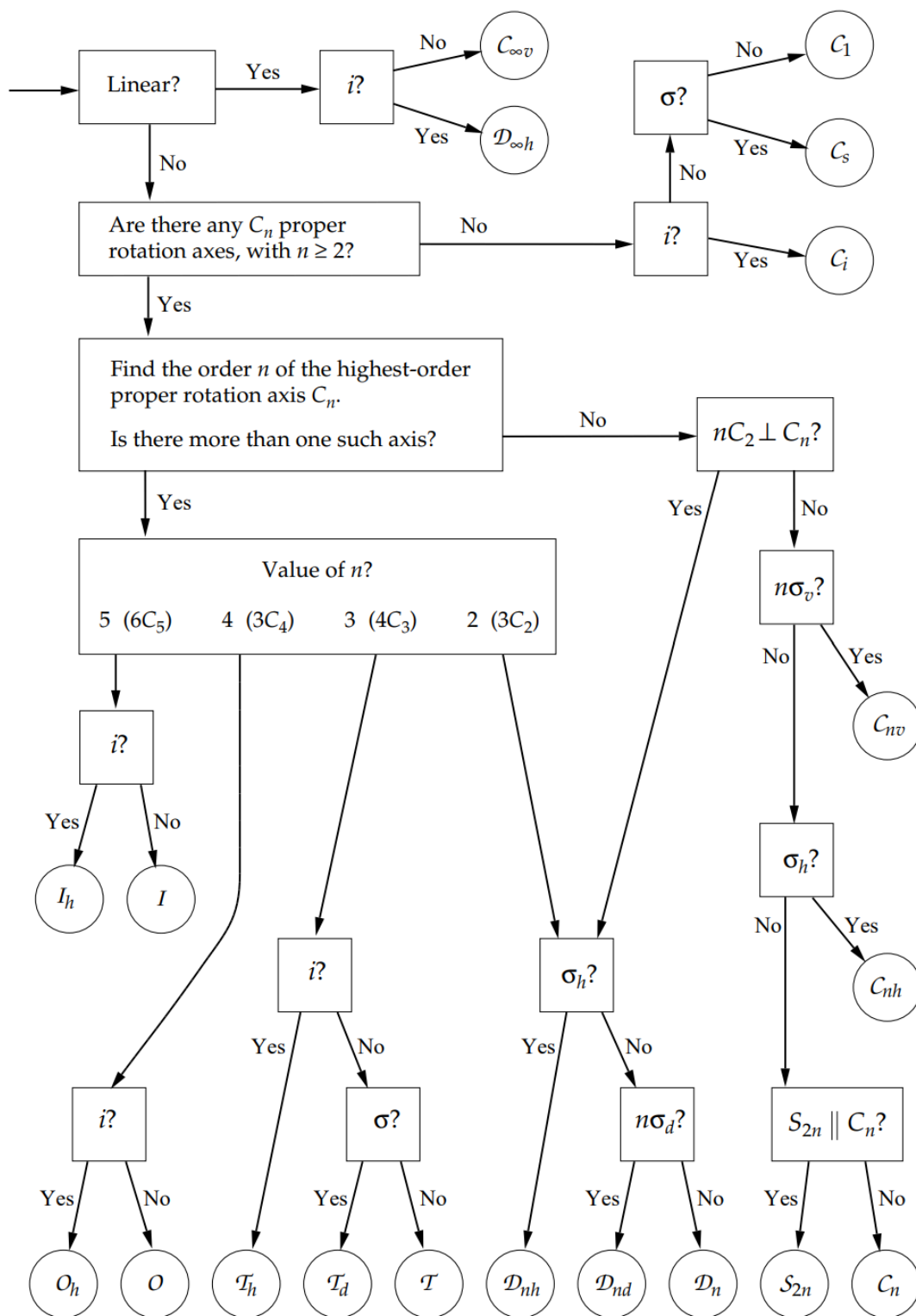
If a vibration results in the change in the molecular dipole moment, it is **IR-active**. In the character table, the vibrational modes that are IR-active are those with symmetry of the x , y and z axes (**linear terms**).

If a vibration results in a change in the molecular polarisability, it is **Raman active**. In the character table, the vibrational modes that are Raman-active are those with symmetry of any of the binary products xy , xz , yz , x^2 , y^2 , z^2 (**quadratic terms**) or a linear combination of binary products (e.g. $x^2 - y^2$).

For the IR absorbance wavenumber table, see Section 15.4.3.

13.2.15. Point Group Classification Flow Chart From Geometry

For the names of the common molecular geometries and their associated point groups, see Section 12.1.8.



13.2.16. Common Space Groups and their Equipoints

Graphic symbol	Num. symbol	Graphic symbol	Num. symbol
None	1		$\bar{1}$
	2		$2/m$
	2_1		$2_1/m$
	3		$\bar{3}$
	3_1		$\bar{4}$
	3_2		$4/m$
	4		$4_2/m$
	4_1		$\bar{6}$
	4_2		$6/m$
	4_3		$6_3/m$
	6		m
	6_1		a, b, c
	6_2		a, b, c
	6_3		n
	6_4		d
	6_5		d

The space groups comprise all rigid transformation operations, including translations. There are a total of 230 distinct space groups. The Hermann-Mauguin notation describes the lattices and some generators of the group.

Screw axis n_m : a symmetry group comprising C_n followed by a translation m/n of a unit cell parallel to the C_n axis. The rotation is defined anticlockwise when viewed down the screw axis (so that the translation moves the molecule towards the viewer).

Glide plane g : a symmetry group comprising σ followed by a translation by $1/2$ of a unit cell parallel to the plane

Enantiomorphs: screw axes with different handedness (e.g. 4_1 (right) and 4_3 (left)), which can occur when the individual species are enantiomers.

General Equivalent Positions (GEPs) and Special Equivalent Positions (SEPs)

Space Group $P2_1$: (primitive monoclinic, 2_1 screw axis along b)

- GEPs: 2, at (x_n, y_n, z_n) and $(-x_n, \frac{1}{2} + y_n, -z_n)$.
- SEPs: None.

Space Group $P2_1/c$: (with perpendicular c -glide)

- GEPs: 4, at (x_n, y_n, z_n) , $(-x_n, \frac{1}{2} + y_n, \frac{1}{2} - z_n)$, $(x_n, \frac{1}{2} - y_n, \frac{1}{2} + z_n)$, $(-x_n, -y_n, -z_n)$.
- SEPs: 4 pairs:

2 at $(0, 0, 0)$ and $(0, \frac{1}{2}, \frac{1}{2})$;	2 at $(0, 0, \frac{1}{2})$ and $(0, \frac{1}{2}, 0)$;
2 at $(\frac{1}{2}, 0, 0)$ and $(\frac{1}{2}, \frac{1}{2}, \frac{1}{2})$;	2 at $(\frac{1}{2}, \frac{1}{2}, 0)$ and $(\frac{1}{2}, 0, \frac{1}{2})$.

Space Group $P2_12_12_1$: (primitive orthorhombic, layers parallel to (010) planes)

- GEPs: 4, at (x_n, y_n, z_n) , $(-x_n, \frac{1}{2} + y_n, \frac{1}{2} - z_n)$, $(\frac{1}{2} + x_n, \frac{1}{2} - y_n, -z_n)$, $(\frac{1}{2} - x_n, -y_n, \frac{1}{2} + z_n)$.
- SEPs: None.

For the Bravais lattices and applications to XRD, see Sections 12.2.5-6.

13.3. Theory of Kinetics, Energetics and Thermodynamics

13.3.1. Macroscopic Kinetic Theory of Gases

Physical constants:

- Ideal gas constant: $\bar{R} = 8.314 \text{ J mol}^{-1} \text{ K}^{-1}$
- Avogadro's number: $N_A = 6.022 \times 10^{23} \text{ mol}^{-1}$
- Boltzmann constant: $k_B = \bar{R} / N_A = 1.3806 \times 10^{-23} \text{ J K}^{-1}$

Ideal Gases:

Macroscopic ideal gas law: $pV = n\bar{R}T$ or $pV = mRT$ or $pv = RT$ or $p = \rho RT$

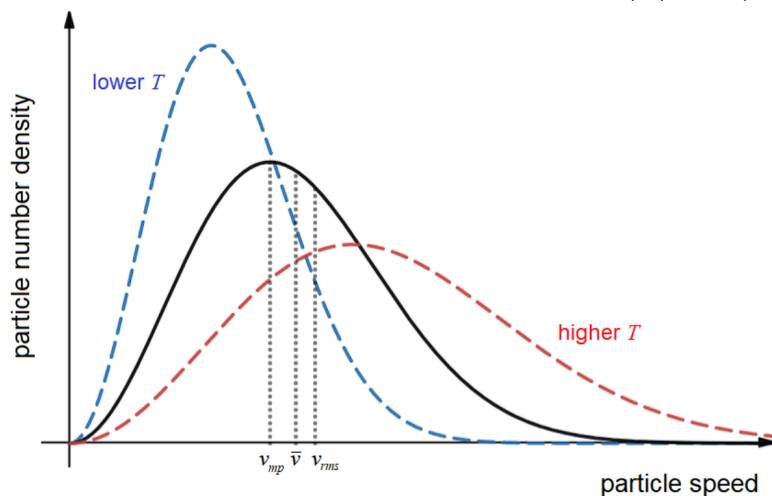
(p [Pa]: pressure, V [m^3]: volume, n [mol]: moles, T [K]: temperature, m [kg]: mass, R [$\text{J kg}^{-1} \text{ K}^{-1}$]
 $= \frac{\bar{R} [\text{J mol}^{-1} \text{ K}^{-1}]}{M_r [\text{kg mol}^{-1}]}$: mass gas constant, v [$\text{m}^3 \text{ kg}^{-1}$] = $\frac{V}{m} = \frac{1}{\rho}$: specific volume, ρ [kg m^{-3}]: density)

13.3.2. Microscopic Kinetic Theory of Gases

Microscopic ideal gas law: $pV = Nk_B T$ ($N = \frac{n}{N_A}$: number of particles)

Maxwell-Boltzmann Distribution: probabilistic distribution of particle speeds

Maxwell-Boltzmann distribution: $f_v(v) = \left(\frac{2}{\pi}\right)^{1/2} \left(\frac{m}{k_B T}\right)^{3/2} v^2 \exp\left(-\frac{mv^2}{2k_B T}\right)$ (m : particle mass)



Mode particle speed: $v_{mp} = \sqrt{\frac{2k_B T}{m}}$

Mean particle speed: $\bar{v} = \sqrt{\frac{8k_B T}{\pi m}}$

RMS particle speed: $v_{rms} = \sqrt{\frac{3k_B T}{m}}$

Macro RMS speed: $pV = \frac{1}{3}Nm(v_{rms})^2$

Mean particle kinetic energy \bar{E}_k :

$$\bar{E}_k = \frac{3}{2}k_B T = \frac{1}{2}m(v_{rms})^2 \quad (3 \text{ dof})$$

The x , y and z components of the particle velocities and momenta are all identical and independent Normal distributions: $v_x \sim N(0, k_B T / m)$.

13.3.3. Statistical Mechanics (Microscopic Thermodynamics)

Statistical mechanics assumes isolated ergodic systems at thermal equilibrium, for which each accessible microscopic state is equally likely (equipartition theorem). When two systems of different temperature are allowed to exchange energy (but not mass), they will reach the same temperature at thermal equilibrium.

- Number of microstates at a given energy: $\Omega(E)$
- For equilibrium systems A and B: $\Omega(E_A, E_B) = \Omega_A(E_A) \Omega_B(E_B)$
- Boltzmann configurational entropy: $\ln \Omega = \ln \Omega_A(E_A) + \ln \Omega_B(E - E_A)$
- Most likely state is observed:
$$\frac{\partial(\ln \Omega)}{\partial E_A} = 0 \Rightarrow \frac{\partial(\ln \Omega_A(E_A))}{\partial E_A} = \frac{\partial(\ln \Omega_B(E_B))}{\partial E_B} = \frac{1}{kT} = \beta$$

If the states of A are $\{x\}$ and the states of B are $\{y\}$ then

- The joint probability distribution $p(x, y)$ is uniform; $p(x) = \sum_y p(x, y)$ is proportional to $\Omega_B(E_B)$.
- For a large system B ($E_B \gg E_A$), it follows that $p(x) = \frac{1}{Z} e^{-\beta E_A}$ ($Z = \sum_x e^{-\beta E_A}$: partition function)
- Total internal energy: $U = \int E(x) p(x) dx = - \frac{\partial(\ln Z)}{\partial \beta}$.

13.3.3. Properties of Gases and Gas Mixtures

Assumptions in the ideal gas model: point gas particles, elastic collisions, no inter-particle forces, large separation between particles.

Special Cases of the Ideal Gas Law:

- Boyle's law: for constant T , pV is constant.
- Charles' law: for constant p , VT^{-1} is constant.
- Gay-Lussac's law: for constant V , pT^{-1} is constant.
- Avogadro's law: for constant p and T , nV^{-1} is constant.

Effusion of Ideal Gases: diffusional flux through a hole smaller than the mean free path

Relative rates of efflux: $\frac{r_1}{r_2} = \sqrt{\frac{\rho_2}{\rho_1}} = \sqrt{\frac{M_2}{M_1}} \Leftrightarrow \rho r^2$ and Mr^2 are constant (Graham's law)

(r [mol s^{-1}]: rate of diffusion out of hole, ρ [kg m^{-3}]: gas density, M [kg mol^{-1}]: gas molar mass.)

Partial Pressure in a Gas Mixture

For a mixture containing n_i moles of gaseous species i , with total pressure P and total moles of particles N , the partial pressure p_i of species i is

$$p_i = \frac{n_i}{N} \times P \quad \Leftrightarrow \quad \frac{p_i}{P} = \frac{n_i}{N} \quad (\text{Dalton's law})$$

Many other state variables of mixtures can be partitioned in this way e.g. enthalpy, entropy, internal energy.

Degrees of Freedom for Polyatomic Gases

	DOF, f (including vibrational)	
Monatomic (He, Ne, Ar, ...):	3	(3 translational, 0 rotational, 0 vibrational)
Diatomic (H_2 , O_2 , HCl):	6	(3 translational, 2 rotational, 1 vibrational)
Triatomic, linear (CO_2):	9	(3 translational, 2 rotational, 4 vibrational)
Triatomic, nonlinear (H_2O):	9	(3 translational, 3 rotational, 3 vibrational)

Mean energy per degree of freedom = $\frac{\bar{E}}{f} = \frac{1}{2}k_B T$ (equipartition theorem)

Isobaric specific heat capacity per degree of freedom = $\frac{c_p}{f} = \frac{1}{2}R$

Adiabatic constant = $\gamma = 1 + \frac{2}{f} = \frac{c_p}{c_v}$

Note: if $300 \text{ K} < T < 600 \text{ K}$, then the vibrational mode is inactive and should **not** be counted in per-degree-of-freedom basis calculations.

13.3.4. Non-Ideal Gases

Van der Waals equation of state for non-ideal gases: $\left(p + \frac{an^2}{V^2}\right)(V - bn) = n\bar{R}T$

a represents attractive forces. $b = \frac{16}{3}N_A n\pi r^3$ represents the volume occupied by the molecules (r : radius of molecules)

Compressibility factor: $Z = \frac{pV}{n\bar{R}T} = 1 + \left(b - \frac{a}{RT}\right)V^{-1} + b^2V^{-2} + b^3V^{-3} + \dots$ ($Z = 1$: ideal)

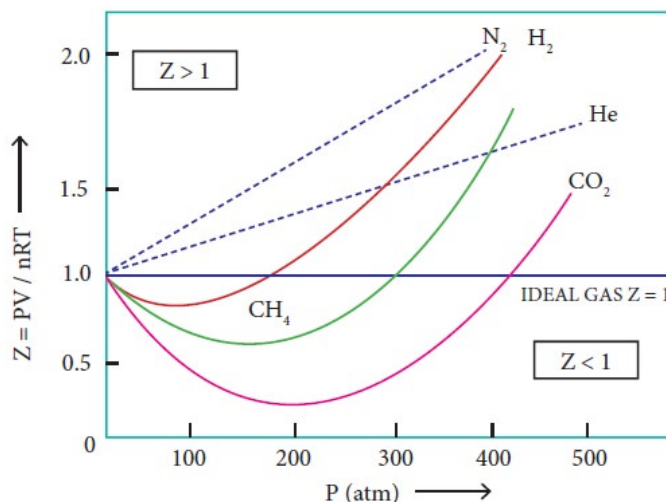
Fugacity: $f = p \exp\left(\frac{bp}{RT}\right) = p \exp\left(\frac{bnZ}{V}\right)$ ($f \rightarrow p$ as $Z \rightarrow 1$)

Activity coefficient: $\phi = \frac{f}{p} = e^{bp/\bar{R}T}$

Van der Waals constants for some gases. Note pressure units are in atm.

Substance	a [L ² atm / mol ²]	b [L / mol]	Substance	a [L ² atm / mol ²]	b [L / mol]
He	0.0341	0.02370	Cl ₂	6.49	0.0562
Ne	0.211	0.0171	H ₂ O	5.46	0.0305
Ar	1.34	0.0322	CH ₄	2.25	0.0428
Kr	2.32	0.0398	CO	1.51	0.0399
Xe	4.19	0.0510	CO ₂	3.59	0.0427
Rn	6.60	0.0624	CCl ₄	20.4	0.1383
N ₂	1.39	0.0391	NH ₃	4.23	0.0371
H ₂	0.244	0.0266	C ₂ H ₆	5.56	0.0638
O ₂	1.36	0.0318	C ₂ H ₄	4.61	0.0582

Variation of compressibility factor Z with pressure for some gases:

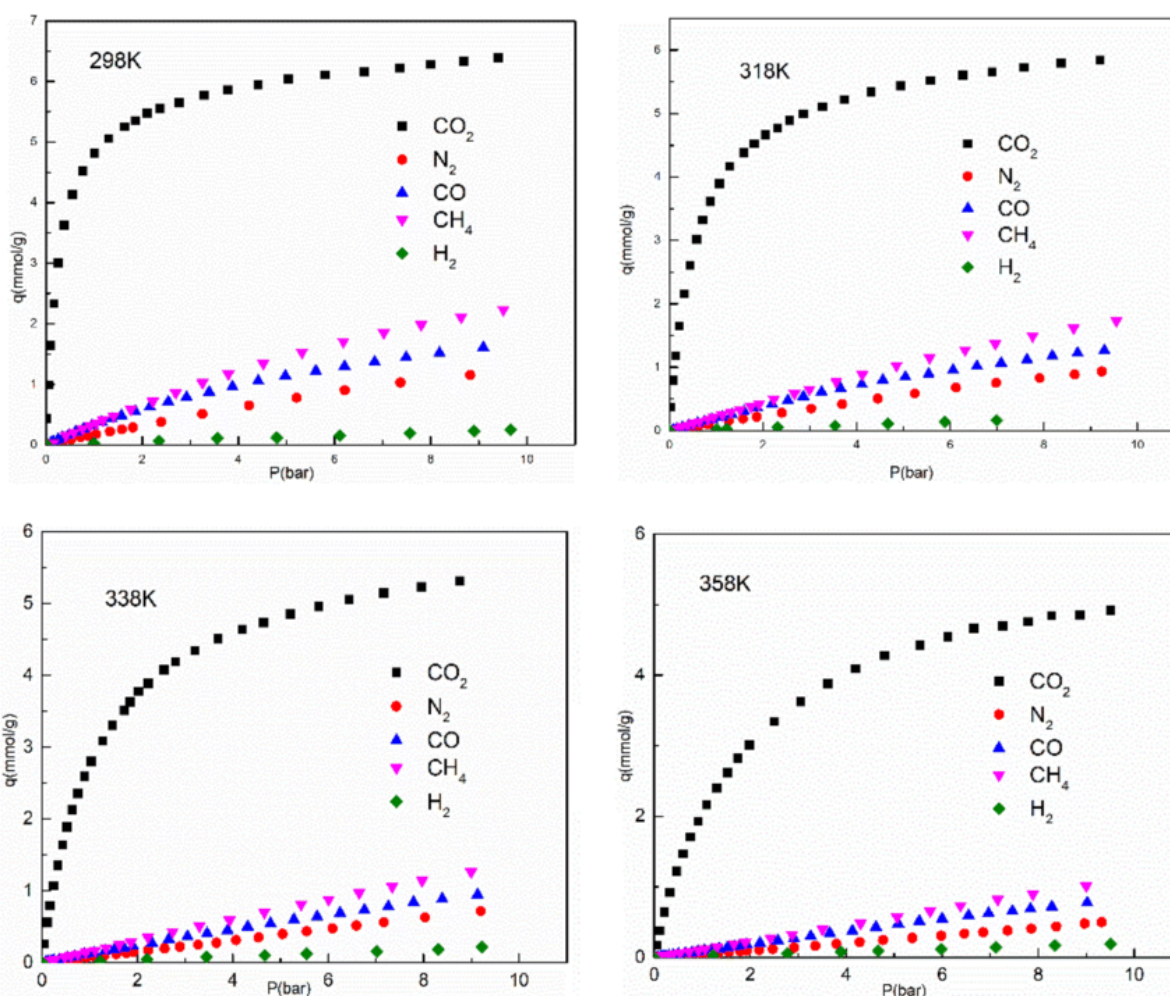


13.3.5. Freundlich Adsorption Isotherms

The extent of adsorption, $\frac{x}{m} = \frac{\text{mass (or moles) of adsorbate}}{\text{mass of adsorbent}}$, varies with pressure p at a particular temperature given by the power-law relationship:

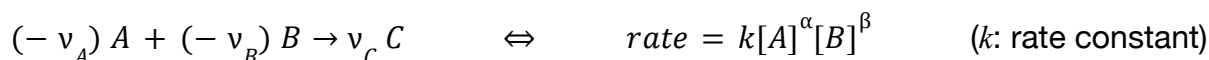
$$\frac{x}{m} = k p^{1/n} \quad n \approx 1 \text{ for } P \ll p_0; \quad n \rightarrow \infty \text{ for } P \gg p_0$$

Isotherms for adsorption of CO₂, N₂, CO, CH₄ and H₂ on NaY zeolite are shown at 298 K, 318 K, 338 K and 358 K, given in mmol adsorbate per gram adsorbent.



13.3.6. Rate Equations

Elementary reactions have rate equations in the form of a product of reactant concentrations:



Notes: (ν : stoichiometric coefficient, which is **negative** for reactants)

- For elementary reactions (single step mechanism), $\alpha = -\nu_A$ and $\beta = -\nu_B$ (law of mass action).
- The overall order of reaction is $\alpha + \beta$.
- For multistep reactions, the orders may differ from the stoichiometric ratios.
- Only species in the rate limiting step of the mechanism may appear in the rate equation.
- For a homogeneous catalyst, the catalyst may appear in the rate equation.
- Note that heterogeneous catalysts (and macromolecular e.g. enzyme-catalysed) do not obey a power-law expression: for details of their kinetics see Section 13.3.4.

In differential form, the rate equations form a system of first-order nonlinear ODEs:

$$r = \frac{d[C]}{dt} = k [A]^\alpha [B]^\beta = \frac{\nu_C}{\nu_A} \frac{d[A]}{dt} = \frac{\nu_C}{\nu_B} \frac{d[B]}{dt}, \quad \text{initial conditions } [A]_0, [B]_0 \text{ at } t = 0$$

The system can be uncoupled into an ODE in each species by substituting from the similarity

relation $\frac{[X] - [X]_0}{[Y] - [Y]_0} = \frac{\nu_X}{\nu_Y}$ where X and Y are any two species.

Order n	ODE	Solution (integrated rate law)	Half-life $t_{1/2}$	Characteristic kinetic plot	Slope of plot	Units of k
0	$\frac{d[A]}{dt} = -k$	$[A] = [A]_0 - kt$	$\frac{[A]_0}{2k}$	$[A]$ vs t	$-k$	$\text{mol dm}^{-3} \text{s}^{-1}$
1	$\frac{d[A]}{dt} = -k[A]$	$[A] = [A]_0 e^{-kt}$	$\frac{\ln 2}{k}$	$\ln [A]$ vs t	$-k$	s^{-1}
2	$\frac{d[A]}{dt} = -k[A]^2$	$[A] = \frac{[A]_0}{1 + k[A]_0 t}$	$\frac{1}{k[A]_0}$	$1/[A]$ vs t	k	$\text{mol}^{-1} \text{dm}^3 \text{s}^{-1}$
3	$\frac{d[A]}{dt} = -k[A]^3$	$[A] = \frac{[A]_0}{\sqrt{1 + 2k[A]_0^2 t}}$	$\frac{3}{2k[A]_0}$	$1/(2[A]^2)$ vs t	k	$\text{mol}^{-2} \text{dm}^6 \text{s}^{-1}$

13.3.7. Reaction Kinetics and Transition State Theory

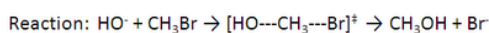
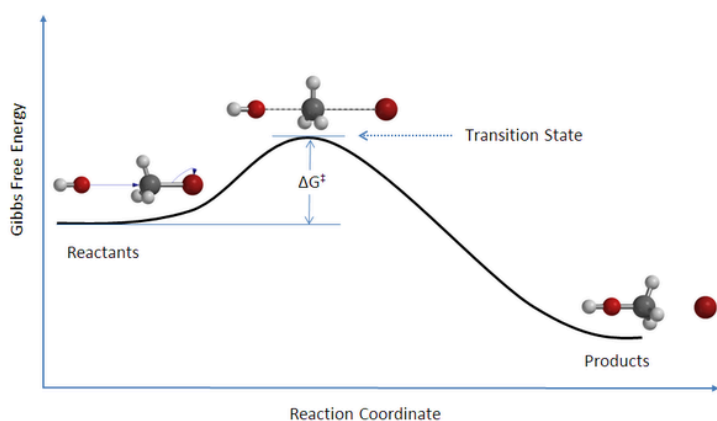
Arrhenius Equation: For a wide variety of physical and chemical processes (chemical reactions, diffusion, crystal nucleation rate, crystal growth rate, etc), the rate constant k is

$$\text{rate constant, } k = A \exp\left(-\frac{E_a}{RT}\right) \Leftrightarrow \ln k = \ln A - \frac{E_a}{RT}$$

(A : constant pre-exponential factor, E_a : activation energy, $\exp(-E_a/RT)$: fraction of the particle ensemble with the required activation energy.)

The A -factor accounts for steric effects (collision theory) and represents the rate which would occur if the kinetic barrier E_a was nonexistent.

Transition State Theory: quasi-equilibrium between reactants and intermediate state



Van 't Hoff equation: $\frac{d(\ln K)}{dT} = \frac{\Delta_r H^\ominus}{RT^2}$

Integrated: $K = K^\ominus \exp\left[\frac{\Delta_r H^\ominus}{R}\left(\frac{1}{T^\ominus} - \frac{1}{T}\right)\right]$

Transition thermodynamics:

$$\Delta G^\ddagger = \Delta H^\ddagger - T \Delta S^\ddagger \quad (\Delta H^\ddagger = E_a)$$

Eyring equation:

$$k = \frac{\kappa k_B T}{h} \exp\left(-\frac{\Delta G^\ddagger}{RT}\right)$$

(κ : transmission coefficient, $h = 6.63 \times 10^{-34}$ J s: Planck's constant)

13.3.8. Reaction Thermodynamics

Absolute values of thermodynamic potentials based on the state functions (Q : heat absorbed by the system, W : work done by the system, P : pressure, V : volume, S : entropy, T : temperature) are:

- Internal Energy: $U = Q - W$ (1st law of thermodynamics)
- Enthalpy: $H = U + PV$
- Gibbs Energy: $G = H - TS = U + PV - TS$
- Helmholtz Free Energy: $A = U - TS = G - PV$

Incremental changes are:

$$dU = T dS - P dV, \quad dH = T dS + V dP, \quad dG = V dP - S dT, \quad dA = -P dV - S dT$$

Isothermal $\rightarrow dT = 0$; isobaric $\rightarrow dP = 0$; isochoric $\rightarrow dV = 0$; adiabatic $\rightarrow dQ = 0$,
isentropic $\rightarrow dS = 0$; reversible $\rightarrow dG = 0$; isenthalpic $\rightarrow dH = 0$.

Under isobaric conditions, $W = P \Delta V$ and $Q = \Delta H$ ($\Delta H < 0$: exothermic; $\Delta H > 0$: endothermic)

Total entropy never decreases: $\Delta S_{\text{universe}} = \Delta S + \Delta S_{\text{surroundings}} \geq 0$ (2nd law of thermodynamics)

Entropy increase of the surroundings: $\Delta S_{\text{surroundings}} = -\frac{\Delta H}{T}$

Gibbs spontaneity criterion: $\Delta G = \Delta H - T \Delta S \leq 0$ (if isobaric and isothermal)

Helmholtz spontaneity criterion: $\Delta A = \Delta U - T \Delta S \leq 0$ (if isochoric and isothermal)

Gibbs Free Energy: for an isothermal, isobaric process (assumed in a reaction):

$$\Delta G = \Delta H - T \Delta S.$$

$\Delta G = 0 \rightarrow$ system at dynamic equilibrium (reversible).

$\Delta G < 0 \rightarrow$ spontaneous (exergonic); $\Delta G > 0 \rightarrow$ nonspontaneous (endergonic).

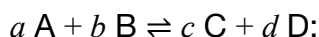
	$\Delta S > 0$	$\Delta S < 0$
$\Delta H > 0$	spontaneous only at high T	never spontaneous
$\Delta H < 0$	always spontaneous	spontaneous only at low T

Spontaneity temperature: $\Delta G = 0$ when $T = \frac{\Delta H}{\Delta S}$.

For Ellingham diagrams, see Section 15.1.3.

13.3.9. Equilibrium Thermodynamics

Basic Principles of Equilibria: for a reversible chemical system at dynamic equilibrium



- The forward rate is $r_1 = k_1[A]^p[B]^q$ (p, q : orders of reaction, k_1 : forward rate constant)
- The reverse rate is $r_{-1} = k_{-1}[C]^r[D]^s$ (r, s : orders of reaction, k_{-1} : reverse rate constant)
- The forward and reverse rates are equal: $r_1 = r_{-1}$.
- The amounts of each species remain constant in time.

Le Chatelier's principle: when conditions change, the equilibrium shifts to oppose the change.

Equilibrium Constant: defined as $K^\ominus = \frac{\{C\}^c\{D\}^d}{\{A\}^a\{B\}^b} = \frac{k_1}{k_{-1}}$ where $\{X\}$ is the activity of X.

In the strict sense, K and $\{X\}$ are all dimensionless. K is independent of pressure and reaction mechanism (e.g. use of catalyst). K_c uses concentrations. K_p uses partial pressures.

Activity of Species in Heterogeneous Media

Solutions: For a dissolved species X, the activity is $\{X\} = \frac{\gamma_X}{c^\ominus} [X]$, where:

- $[X]$ is the concentration of X in units of mol dm^{-3} , defined as $[X] = n_X / V$
- c^\ominus is the standard concentration, a constant ($c^\ominus = 1 \text{ mol dm}^{-3}$).
- γ_X is the activity coefficient (between 0 and 1). Often assumed that $\gamma_X \approx 1$ for $[X] \ll 1$.

Gases: For a gaseous species X, the activity (dimensionless fugacity) is $\{X\} = \frac{f_X}{p^\ominus} = \frac{\phi_X}{p^\ominus} p_X$, where:

- f_X is the fugacity of X in units of bar, defined as $d\mu_X = RT d(\ln f_X)$ (μ_X : chemical potential of X)
- p^\ominus is the standard pressure, a constant ($c^\ominus = 1 \text{ bar}$).
- ϕ_X is the fugacity coefficient (between 0 and 1). For ideal gases, $\phi_X = 1$.
- p_X is the partial pressure of X in units of bar, defined as $p_X = (n_X / n_{\text{tot,g}}) \times P_{\text{tot,g}}$

Pure liquids and undissolved solids: assumed to have $\{X\} = 1$ (exact at $p = 1 \text{ bar}$).

Free Energy at Equilibrium: net free energy change is zero at equilibrium

Standard Gibbs free energy change (for the forward reaction) is $\Delta G^\ominus = -RT \ln K$.

Non-equilibrium free energy change (for the forward reaction) is $\Delta G = \Delta G^\ominus + RT \ln \zeta$

(In general, the reaction quotient ζ (Section 13.3.10) is used. At equilibrium, $\zeta = K$, so $\Delta G = 0$.)

13.3.10. Chemical Potential and Reaction Quotient

Chemical Potential

The chemical potential μ is defined such that (N : number of particles):

$$dU = T dS - P dV + \sum \mu dN, \quad dG = -S dT + V dP + \sum \mu dN$$

For an isothermal and isobaric process, $dG = \sum \mu dN$.

For a binary mixture AB at equilibrium: $n_A d\mu_A + n_B d\mu_B = 0$ (Gibbs-Duhem equation)

Reaction Quotient

For a system of reactants and products $a A + b B \rightleftharpoons c C + d D$, **not** necessarily having reached equilibrium, the reaction quotient ξ is

$$\xi = \frac{\{C\}^c \{D\}^d}{\{A\}^a \{B\}^b} \quad \text{where } \{X\} = \text{activity of species X.}$$

- For solids and liquids, $\{X\} = 1$ i.e. can be omitted from the formula.
- For gases and aqueous phases, $\{X\}$ is as defined in Section 13.3.9.

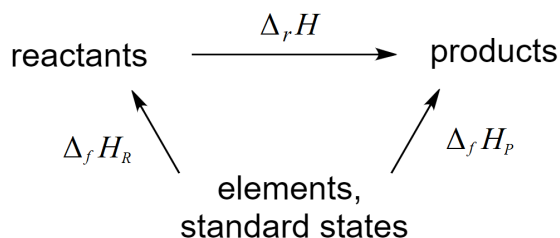
The equilibrium value of ξ is the (concentration) equilibrium constant K_c .

- If $\xi < K_c$ then the equilibrium shifts right.
- If $\xi > K_c$ then the equilibrium shifts left.

13.3.11. Hess's Law

Since enthalpy is a thermodynamic state function, the energy change in a chemical reaction is independent of the route taken. By drawing a 'Hess triangle', the energy changes can be considered like vectors: going along the arrow takes the value shown, while going against the arrow means the negative of the value shown. Values are added head to tail to find the total energy change for a given route.

Typical simple application: enthalpies of reaction given standard values.



Enthalpy of reaction: $\Delta_r H = \Delta_f H_P - \Delta_f H_R$ (change = products - reactants)

Entropy of reaction: $\Delta_r S = S_P - S_R$ (change = products - reactants)

Bond enthalpy: $\Delta_r H = \sum_R \Delta_{bond} H - \sum_P \Delta_{bond} H$ (change = bonds broken - bonds made)

Bond enthalpies, as listed in the table in Section 12.2.3, are positive for bond dissociation.

Enthalpies of reaction to non-standard states must account for enthalpies of vaporisation or fusion using additional steps.

13.3.12. Standard Enthalpy Changes and Experimental Lattice Enthalpies

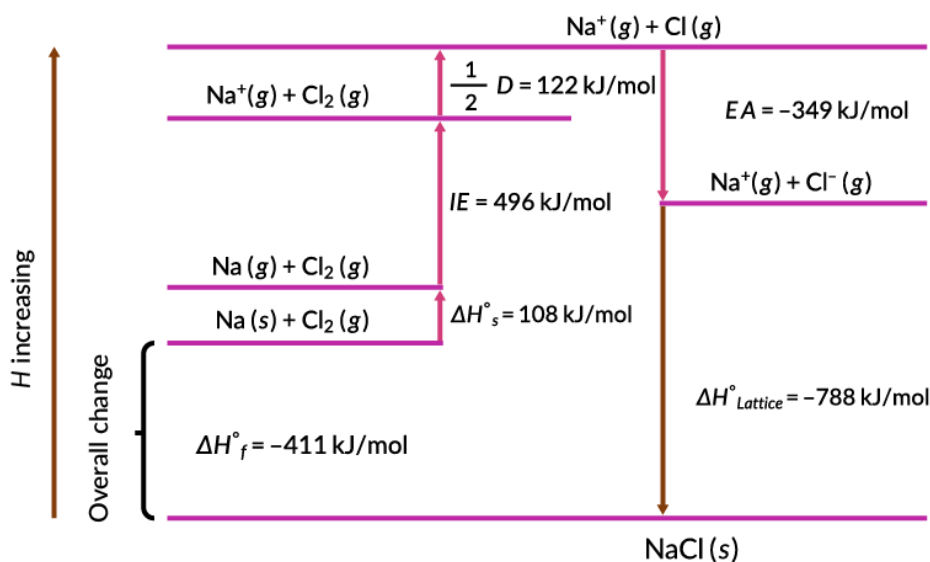
In the definitions, standard states are denoted with $^\ominus$. Standard enthalpies are defined as

- Enthalpy of Reaction ($\Delta_{rxn} H^\ominus$): reactants $^\ominus \rightarrow$ products $^\ominus$ (mole basis must be specified)
- Enthalpy of Formation ($\Delta_f H^\ominus$): elements $^\ominus \rightarrow$ substance $^\ominus$ (1 mole)
- Enthalpy of Solution ($\Delta_{sol} H^\ominus \approx 0$): substance $^\ominus$ (s) (1 mole) \rightarrow substance $^\ominus$ (aq)
- Enthalpy of Combustion ($\Delta_c H^\ominus < 0$): substance $^\ominus$ (1 mole) + x O₂ \rightarrow products $^\ominus$
- Enthalpy of Atomisation ($\Delta_{at} H^\ominus > 0$): substance $^\ominus \rightarrow$ atoms (g) (1 mole)
- Enthalpy of Sublimation ($\Delta_{sub} H^\ominus > 0$): substance $^\ominus \rightarrow$ substance (g) (1 mole)
- Enthalpy of Hydration ($\Delta_{hyd} H^\ominus < 0$): ions (g) (1 mole) \rightarrow ions (aq)
- (First) Enthalpy of Ionisation ($\Delta_{ion} H^\ominus > 0$): substance (g) (1 mole) \rightarrow cation (g) + e⁻
- Enthalpy of Bond Dissociation ($\Delta_{bond} H^\ominus > 0$): covalent bonds (g) (1mole) \rightarrow radicals or atoms
- (First) Electron affinity ($\Delta_{ea} H^\ominus > 0$): substance (g) (1 mole) + e⁻ \rightarrow anion (g)
- Enthalpy of Lattice formation ($\Delta_{lat} H^\ominus < 0$): ions (g) \rightarrow ionic solid $^\ominus$ (1 mole)

A Born-Haber cycle can be used to calculate unknown enthalpies from standard values.

Born-Haber cycles cannot be used to predict lattice enthalpies involving polyatomic ions.

Solution, Lattice formation and Hydration: $\Delta_{sol} H = \Delta_{hyd} H - \Delta_{lat} H$; see also Section 13.3.8.



Born-Haber Cycle for NaCl

Experimentally-determined lattice enthalpy of formation involves standard state formation, sublimation, ionisation, bond breaking, electron affinity

13.3.13. Theoretical Enthalpy of Lattice Dissociation from Perfect Ionic Model

The Born-Landé equation, based on assuming perfectly electrostatic interactions between point ions with complete lattice crystallinity, gives:

$$\Delta_{lat}H = \frac{N_A M z_1 z_2 e^2}{4\pi\epsilon_0 r_0} \left(1 - \frac{1}{n}\right) = \frac{1.389 \times 10^{-4} \times (1 - 1/n) M z_1 z_2}{r_1 + r_2} [\text{J mol}^{-1}]$$

(N_A : Avogadro's constant, M : Madelung constant, (z_1, z_2) : charge on ions, e : charge on electron, ϵ_0 : vacuum permittivity, r : inter-ionic (lattice) spacing, n : Born parameter)

The Madelung constant M is lattice geometry dependent (weighted distance to every ion):

lattice	ZnS	NaCl	CsCl	TiO ₂	CaF ₂	Al ₂ O ₃
M	1.64132	1.74756	1.76267	2.408	2.51939	4.17186

The Born parameter n represents repulsion. It can be estimated from the period of the ion:

Period	2 [He]	3 [Ne]	4 [Ar]	5 [Kr]	6 [Xe]	7 [Rn]
n	5	7	9	10	12	12

Differences between the theoretical and experimental lattice enthalpies indicate a degree of covalent character in the lattice (incomplete charge polarisation). This typically occurs when the constituent ions have 1) a small difference in electronegativity and/or 2) low polarising power (soft acids or soft bases; low charge density). The theoretical value typically underestimates the experimental value. The values are typically within 10% for an electronegativity difference of more than 1 Paulings, and within 1% for an electronegativity difference of more than 2 Paulings.

For a table of electronegativities, see Section 12.2.4. For HSAB theory, see Section 15.5.16.

13.4. Solutions and Heterogeneous Equilibria

13.4.1. Molarity, Molality and Normality

(m : mass of solute A, M : mass of solvent B, $M_{r(X)}$: relative molecular mass of X (g mol^{-1}), ρ : mass density, V : volume of solvent (dm^3), ν_A : stoichiometric coefficient when A reacts with 1 mole of a given substance)

- Moles: $n_A = \frac{m}{M_{r(A)}}$, $n_B = \frac{M}{M_{r(B)}}$ [mol]
- Molarity: $c = \frac{n_A}{V_B} = \frac{\rho_B n_A}{M}$ [$\text{mol dm}^{-3} = \text{M (molar)}$]
- Molality: $b = \frac{n_A}{M} = \frac{n_A}{\rho_B V_B}$ [mol kg^{-1} (molal)]
- Normality: $N = \frac{n_A \times (\text{reactive units of A})}{V_B}$ [$\text{Eq L}^{-1} = \text{N (equivalents per litre)}$]
- Weight and Volume fractions: $w/v \% = \frac{m [\text{g}]}{V_A + V_B [\text{ml}]} \times 100\%$ (grams of solute in 100 ml solution)
 $v/v \% = \frac{V_A}{V_A + V_B} \times 100\%$ (volume fraction)
 $w/w \% = \frac{m}{M + m} \times 100\%$ (mass fraction = weight fraction)

Conversion between b and c : $\frac{c}{b} = \rho_B - \frac{M_{r(A)}}{1000} c$ (further from proportional if M_r is large)

Note that $1 \text{ dm}^3 = 1 \text{ L} = 1000 \text{ ml} = 1000 \text{ cm}^3$. The density of water is $1 \text{ kg dm}^{-3} = 1 \text{ g ml}^{-1}$, so molarity and molality have approximately the same numerical value in the above units.

The product of moles of A with its number of reactive units is the 'mole equivalent' of A.

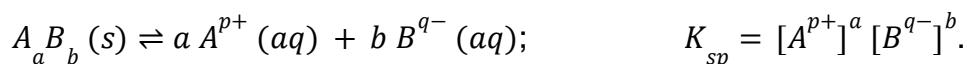
Making Solutions

Example: magnetic polymer solution of 10 wt% polystyrene and 30 wt% iron oxide in a 1000 μL binary solvent of (85 v/v% DMF + 15 v/v% acetone):

- To make the solvent, mix 850 μL DMF with 150 μL acetone in a glass vial.
- Measure the mass of the solvent. Suppose that the solvent mass is found to be 894 mg.
- The mass of polystyrene to be added is $\frac{0.1}{1 - (0.1 + 0.3)} \times 894 \text{ mg} = 149 \text{ mg}$.
- The mass of iron oxide to be added is $\frac{0.3}{1 - (0.1 + 0.3)} \times 894 \text{ mg} = 447 \text{ mg}$.
- The total mass of the system is then 1490 mg.

13.4.2. Ionic Solubility Products and Precipitation from Solution

A solute $A_a B_b$ dissolves in a solvent to give ions A^{p+} and B^{q-} in an equilibrium given by



For non-binary solutes, the solubility equilibrium constant is defined similarly: ignore solids, include only aqueous species. For strong (fully soluble) electrolytes, $K_{sp} \rightarrow \infty$.

For a pure solute, $\frac{[A^{p+}]}{[B^{q-}]} = \frac{a}{b}$. The limiting solubility is $[A_a B_b] = \left(a^a b^b \times K_{sp} \right)^{1/(a+b)}$.

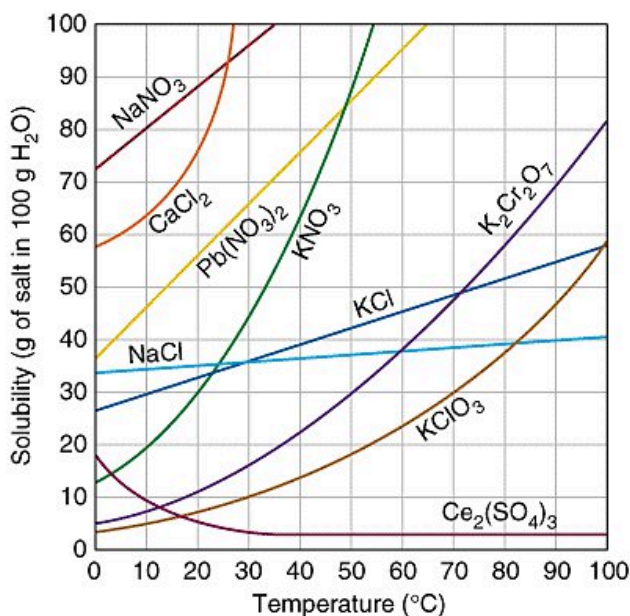
The solubility limit will be reached and precipitation will occur if the reaction quotient $Q \geq K_{sp}$.

Selective precipitation: in a saturated mixture, the least soluble precipitate will form predominantly.

Common ion effect: adding an ion to a solution promotes precipitation with that ion.

Relation to thermodynamics: $\Delta G_{sol}^{\ominus} = -RT \ln K_{sp}$ where $\Delta G_{sol}^{\ominus} = \Delta H_{sol}^{\ominus} - T \Delta S_{sol}^{\ominus}$.

Solubility Data for Soluble Ionic Substances



Solubility limit for salts in water at varying temperatures (x : g salt per 100 g water).

$$x \text{ [g salt per 100 g water]} = \frac{10x}{M_r \text{ [g/mol]}} \text{ mol dm}^{-3}$$

For an aqueous salt A_aB_b ,

$$\text{Solubility product: } K_{sp} = \frac{1}{a^a b^b} \left(\frac{\rho(T) \text{ [kg m}^{-3}\text{]} x}{100 M_r \text{ [g/mol]}} \right)^{(a+b)}$$

(M_r : salt molecular mass, $\rho(T)$: water density at temp)

Solubility Data for Sparingly Soluble Ionic Substances

Table of values of K_{sp} in $(\text{mol dm}^{-3})^{a+b}$ in water at 25 °C (listed in A-Z by compound name):

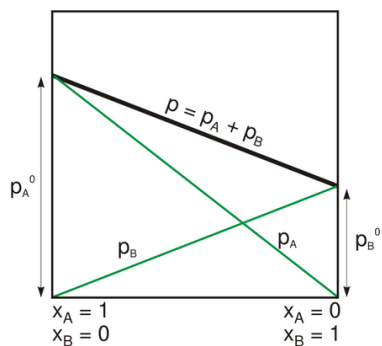
Al(OH) ₃	1.8×10^{-5}	CaC ₂ O ₄	2.7×10^{-9}	Fe(OH) ₂	8.0×10^{-16}	MgNH ₄ PO ₄	2.5×10^{-13}	Ag ₃ AsO ₄	1.0×10^{-22}	Tl(OH) ₃	6.3×10^{-46}
AlPO ₄	6.3×10^{-19}	Ca ₃ (PO ₄) ₂	2.0×10^{-29}	FeS*	6×10^{-19}	Mg ₃ (AsO ₄) ₂	2×10^{-20}	AgN ₃	2.8×10^{-9}	Sn(OH) ₂	1.4×10^{-28}
BaCO ₃	5.1×10^{-9}	CaSO ₄	9.1×10^{-6}	FeAsO ₄	5.7×10^{-21}	MgCO ₃	3.5×10^{-8}	AgBr	5.0×10^{-13}	SnS*	1×10^{-26}
BaCrO ₄	1.2×10^{-10}	CaSO ₃	6.8×10^{-8}	Fe ₄ [Fe(CN) ₆] ₃	3.3×10^{-41}	MgF ₂	3.7×10^{-8}	AgCl	1.8×10^{-10}	ZnCO ₃	1.4×10^{-11}
BaF ₂	1.0×10^{-6}	Cr(OH) ₂	2×10^{-16}	Fe(OH) ₃	4×10^{-38}	Mg(OH) ₂	1.8×10^{-11}	Ag ₂ CrO ₄	1.1×10^{-12}	Zn(OH) ₂	1.2×10^{-17}
Ba(OH) ₂	5×10^{-3}	Cr(OH) ₃	6.3×10^{-31}	FePO ₄	1.3×10^{-22}	MgC ₂ O ₄	8.5×10^{-5}	AgCN	1.2×10^{-16}	ZnC ₂ O ₄	2.7×10^{-8}
BaSO ₄	1.1×10^{-10}	CoCO ₃	1.4×10^{-13}	Pb ₃ (AsO ₄) ₂	4×10^{-36}	Mg ₃ (PO ₄) ₂	1×10^{-25}	AgIO ₃	3.0×10^{-8}	Zn ₃ (PO ₄) ₂	9.0×10^{-33}
BaSO ₃	8×10^{-7}	Co(OH) ₂	1.6×10^{-15}	Pb(N ₃) ₂	2.5×10^{-9}	MnCO ₃	1.8×10^{-11}	AgI	8.5×10^{-17}	ZnS*	2×10^{-25}
BaS ₂ O ₃	1.6×10^{-6}	Co(OH) ₃	1.6×10^{-44}	PbBr ₂	4.0×10^{-5}	Mn(OH) ₂	1.9×10^{-13}	AgNO ₂	6.0×10^{-4}		
BiOCl	1.8×10^{-31}	CoS*	4×10^{-21}	PbCO ₃	7.4×10^{-14}	MnS*	3×10^{-14}	Ag ₂ SO ₄	1.4×10^{-5}		
BiOOH	4×10^{-10}	CuCl	1.2×10^{-6}	PbCl ₂	1.6×10^{-5}	Hg ₂ Br ₂	5.6×10^{-23}	Ag ₂ S*	6×10^{-51}		
CdCO ₃	5.2×10^{-12}	CuCN	3.2×10^{-20}	PbCrO ₄	2.8×10^{-13}	Hg ₂ Cl ₂	1.3×10^{-18}	Ag ₂ SO ₃	1.5×10^{-14}		
Cd(OH) ₂	2.5×10^{-14}	CuI	1.1×10^{-12}	PbF ₂	2.7×10^{-8}	Hg ₂ I ₂	4.5×10^{-29}	AgSCN	1.0×10^{-2}		
CdC ₂ O ₄	1.5×10^{-8}	Cu ₃ (AsO ₄) ₂	7.6×10^{-36}	Pb(OH) ₂	1.2×10^{-15}	HgS*	2×10^{-53}	SrCO ₃	1.1×10^{-10}		
CdS*	8×10^{-28}	CuCO ₃	1.4×10^{-10}	PbI ₂	7.1×10^{-9}	NiCO ₃	6.6×10^{-9}	SrCrO ₄	2.2×10^{-5}		
CaCO ₃	2.8×10^{-9}	CuCrO ₄	3.6×10^{-6}	PbSO ₄	1.6×10^{-8}	Ni(OH) ₂	2.0×10^{-15}	SrF ₂	2.5×10^{-9}		
CaCrO ₄	7.1×10^{-4}	Cu[Fe(CN) ₆] ₃	1.3×10^{-16}	PbS*	3×10^{-28}	NiS*	3×10^{-19}	SrSO ₄	3.2×10^{-7}		
CaF ₂	5.3×10^{-9}	Cu(OH) ₂	2.2×10^{-20}	Li ₂ CO ₃	2.5×10^{-2}	ScF ₃	4.2×10^{-18}	TlBr	3.4×10^{-6}		
CaHPO ₄	1×10^{-7}	CuS*	6×10^{-37}	LiF	3.8×10^{-3}	Sc(OH) ₃	8.0×10^{-31}	TlCl	1.7×10^{-4}		
Ca(OH) ₂	5.5×10^{-6}	FeCO ₃	3.2×10^{-11}	Li ₃ PO ₄	3.2×10^{-9}	AgC ₂ H ₃ O ₂	2.0×10^{-3}	TlI	6.5×10^{-8}		

*: equilibrium for sulfides is $MS(s) + H_2O(l) \rightleftharpoons M^{2+}(aq) + HS^-(aq) + OH^-(aq)$ so K_{sp} has units $\text{mol}^3 \text{dm}^{-9}$.

13.4.3. Raoult's Law and Henry's Law for Ideal Liquid-Vapour Equilibria

Raoult's Law: in an ideal solution, vapour pressure decreases linearly with solute concentration:

$$p_S = x_S^{(L)} p_S^\ominus \quad (x_S: \text{mole fraction of solvent, } p_S^\ominus: \text{vapour pressure of pure solvent})$$



$$\text{For an ideal binary solution, } x = \frac{p - p_A^\ominus}{p_B^\ominus - p_A^\ominus}.$$

Most solutions are non-ideal, especially at higher concentrations.

Positive deviation: p is higher than predicted; cohesion > adhesion.

Negative deviation: p is lower than predicted; adhesion > cohesion.

Pressure curves with minima/maxima produce azeotropes.

$$\text{Entropy of mixing: } \Delta S_{mix}^\ominus = -nRT(x_1 \ln x_1 + x_2 \ln x_2).$$

Henry's Law: the solubility of a gas is directly proportional to its partial pressure:

$$b_S^{(L)} = K_H p_S \quad (b: \text{molality of dissolved gas, } p: \text{partial pressure of gas, } K_H: \text{Henry's law constant})$$

K_H is the solubility constant (equilibrium constant) for the equilibrium $A(g) \rightleftharpoons A(aq)$.

The Henry's law constant varies with temperature according to $K_H = K_H^\ominus \exp \left[\alpha \left(\frac{1}{T} - \frac{1}{T^\ominus} \right) \right]$ where α is the constant value of $\frac{d \ln K_H}{d \left(\frac{1}{T} \right)}$ and (T^\ominus, K_H^\ominus) is a standard measurement.

Values of K_H^\ominus and α are given in the table for some commonly soluble gases in a water solvent, with the standard measurement at $T^\ominus = 298 \text{ K}$.

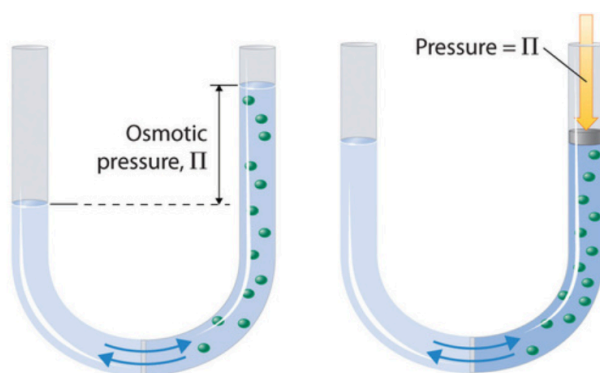
Gas	K_H^\ominus (mol kg ⁻¹ bar ⁻¹)	α (K)	Gas	K_H^\ominus (mol kg ⁻¹ bar ⁻¹)	α (K)
H ₂	0.00078	640	CO	0.0009	1600
He	0.00038	92	NO ₂	0.012	2500
N ₂	0.0006	1300	SO ₂	1.2	3100
O ₂	0.0013	1700	NH ₃	56	4200
Cl ₂	0.095	2100	PH ₃	0.0081	2000
Ar	0.00014	1500	CH ₄	0.0013	1900
CO ₂	0.034	2400	C ₂ H ₆	0.0019	2300

13.4.4. Osmotic Pressure

At the interface of two solutions with a **difference** in concentration c in a common solvent which can flow freely (semi-permeable membrane: ions cannot flow), solvent will flow into the more concentrated solution by osmosis, resulting in a net pressure gradient.

Van 't Hoff factor, i = moles of aqueous particles per mole of solute (ideal).

- Osmotic pressure: $\Pi = icRT$
For multiple species, the total concentration is used, so that ic is the moles of ions per unit volume.
- Force required for volume balance: $F = \Pi A$
- Moles of solute: $n = FL/(2iRT)$ ($c = n/V$, $V = AL/2$)
- Work done to compress by distance x : $W = \int_0^x F(x) dx = -nRT \ln\left(\frac{L}{2} - x\right)$



L : length of water in U-tube.

(minimum work: neglects enthalpy of mixing, neglects gravity, assumes slow compression (quasi-static), neglects hydrodynamic (drag) loss for pushing solvent through membrane, fouling of membrane).

Osmotic pressure is also generated at interfaces with ionic substances, with much higher magnitudes than with dissolved solutes. Poly-ionic nanoparticles with high surface areas are used to generate very high osmotic pressures in e.g. water desalination. The water molecules near the interface are associated (reduced activity) and expel solutes from the bound region (diffusioosmosis).

13.4.5. Boiling Point Elevation and Freezing Point Depression

Addition of a solute to a solvent results in an increase to the boiling point and a decrease to the freezing point of the system, proportional to the molality of the solute:

$$\Delta T_b = i K_b M \quad \text{and} \quad \Delta T_f = -i K_f M$$

(T_b : boiling point, T_f : freezing point, K_b : ebullioscopic constant, K_f : cryoscopic constant, M : molality, i : van 't Hoff factor)

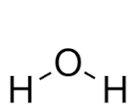
The van 't Hoff factor i is the number of moles of fully solvated particles formed per mole of dissolved solute. Incomplete dissociation (or re-association in solution) results in this being less than the number of constituent solute ions or particles.

Solvent	$T_b / ^\circ\text{C}$	$T_f / ^\circ\text{C}$	$K_b / ^\circ\text{C kg mol}^{-1}$	$K_f / ^\circ\text{C kg mol}^{-1}$
water	100	0	0.512	1.86
ethanol	78.4	-114.6	1.22	1.99
acetic acid	118	17	3.07	3.90
acetone	56	-95	1.71	0.850
ethylene glycol	197.5	-13.0	2.26	3.11
DMSO	191.9	18.52	3.22	3.85
pyridine	115.2	-41.63	2.83	4.26
phenol	181.8	40.89	3.55	6.84
aniline	184	-6	3.82	5.87
nitrobenzene	211	6	5.20	7.00
carbon tetrachloride	76.5	-22.99	5.03	30.0
chloroform	62.1	-63.5	3.63	4.70
benzene	80.1	5.49	2.53	5.12
cyclohexane	80.7	6.59	2.92	20.8
carbon disulfide	46.2	-111.5	2.34	3.83
diethyl ether	34.5	-116.2	2.02	1.79
camphor	208.0	179.8	5.95	40
naphthalene	218	80	5.80	6.94

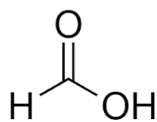
K_b and K_f can be considered the gradients of the liquidus and solidus lines on the phase diagram of the solvent-solute system, as linear approximations for dilute solutions.

13.4.5. Some Common Solvents

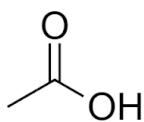
Polar Protic



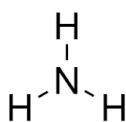
water



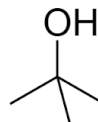
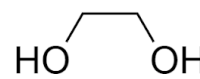
formic acid



acetic acid

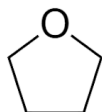


ammonia

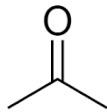
*tert*-butanol

ethylene glycol

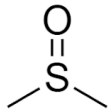
Polar Aprotic



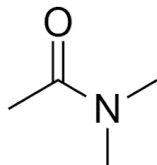
THF



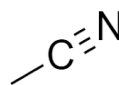
acetone



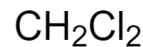
DMSO



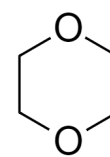
DMF



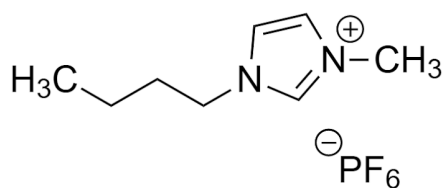
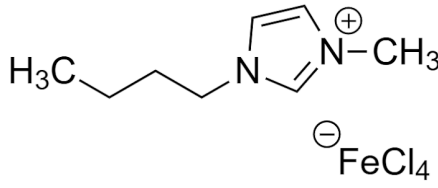
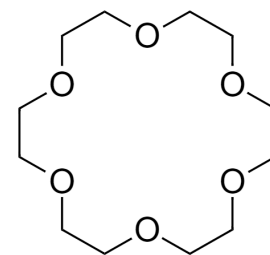
acetonitrile



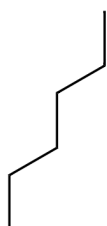
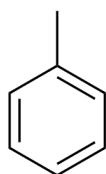
DCM



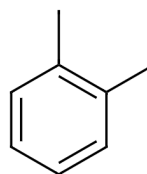
1,4-dioxane

BMIM- PF_6
(IL: ionic liquid)BMIM- FeCl_4
(MIL: magnetic ionic liquid)18-Crown-6
(Crown ether)

Nonpolar

*n*-hexane

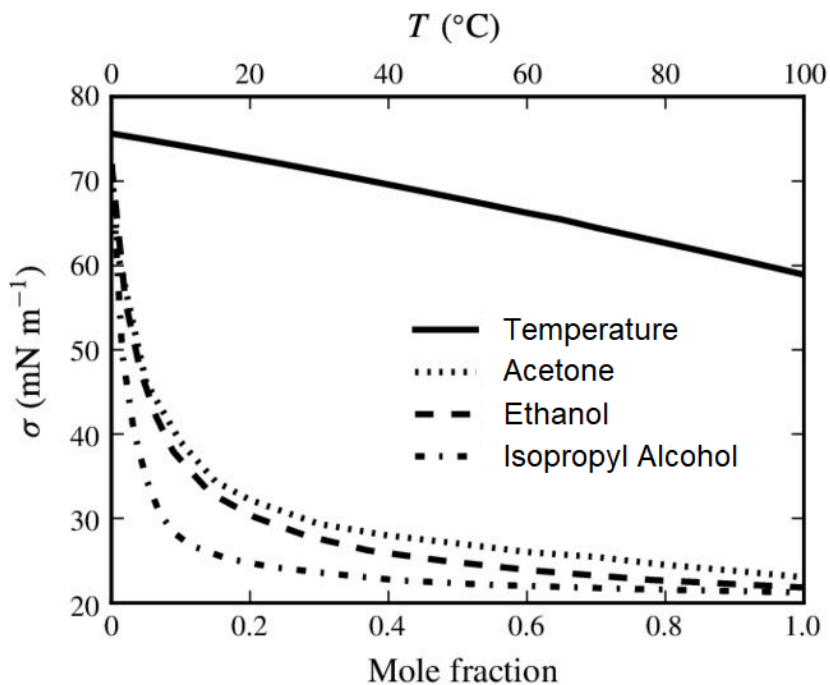
toluene

*o*-xylene

camphor

13.4.6. Surface Tensions of Some Liquid Mixtures

The surface tension σ of water-acetone, water-ethanol and water-isopropyl alcohol binary systems are shown, as well as the variation of σ for pure water with temperature.



13.4.7. Partition Coefficients for Common Solvents

For a binary system of two immiscible phases (one organic, one aqueous) with one solute:

Partition coefficient:
$$K_{ow} = P = \frac{[solute]_{organic}}{[solute]_{aqueous}} \quad \text{“Log P”} = \log_{10} K_{ow}$$

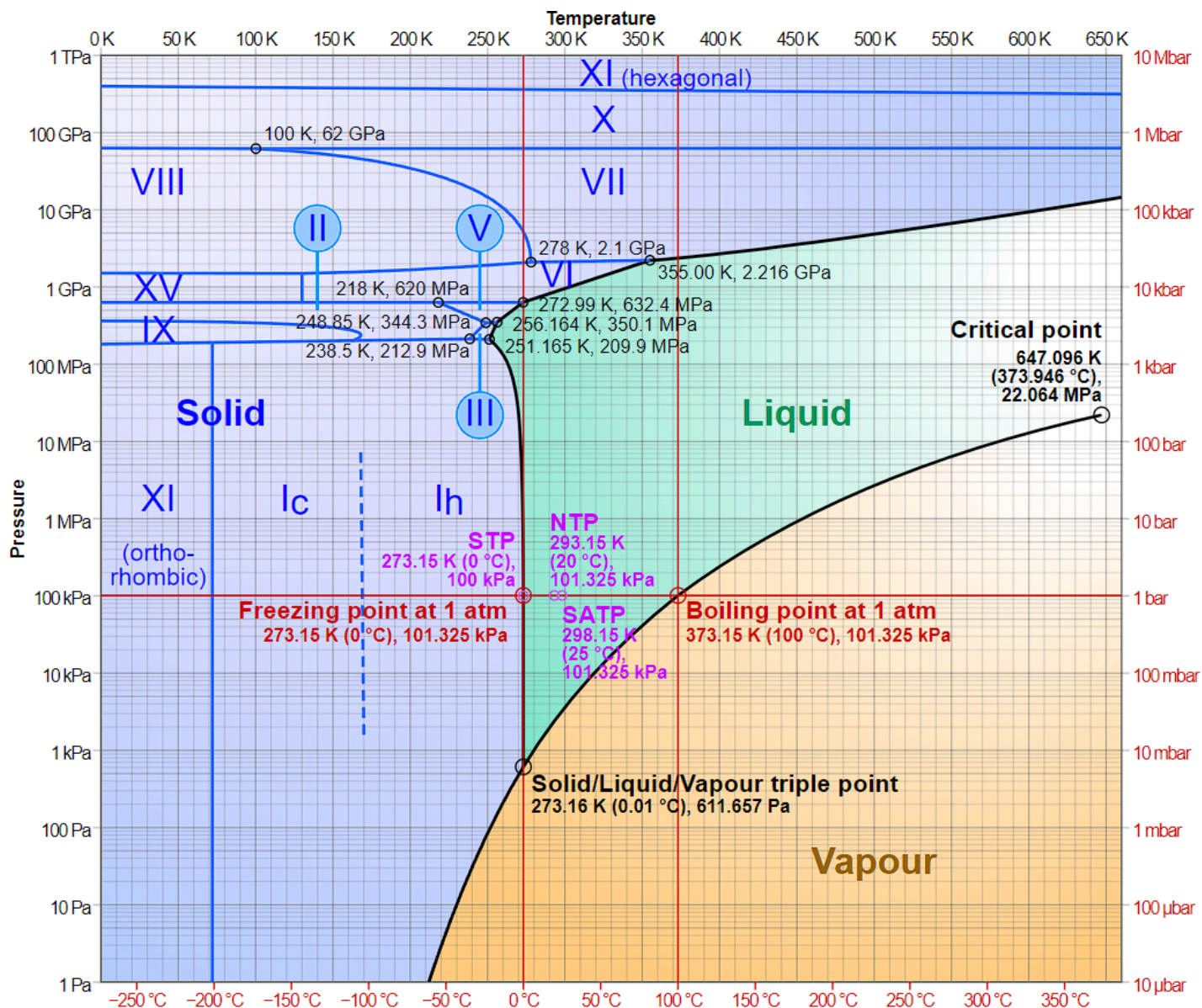
The organic phase is usually taken as octan-1-ol unless otherwise specified.

Fully miscible (hydrophilic, lipophobic)		Partially miscible		Immiscible (lipophilic, hydrophobic)	
Solute	Log P	Solute	Log P	Solute	Log P
dimethylsulfoxide	-1.3	propanol	0.28	diethyl ether	2.9
dioxane	-1.1	ethyl acetate	0.68	tetrachloromethane	3.0
<i>N,N</i> -dimethylformamide	-1.0	butanol	0.80	pentane	3.0
methanol	-0.76	diethyl ether	0.85	cyclohexane	3.2
acetonitrile	-0.33	butyl acetate	1.7	hexane	3.5
ethanol	-0.24	dipropyl ether	1.9	diphenyl ether	4.2
acetone	-0.23	chloroform	2.0	octane	4.5
		benzene	2.0	dodecanol	5.0
		toluene	2.5	hexyl ether	5.1
				dodecane	6.6
				dioctyl phthalate	9.6

13.4.8. Equilibrium Phase Diagrams of Solvents and Solid Solution Mixtures

For phase diagrams of metal alloys, see Section 6.7.13-14.

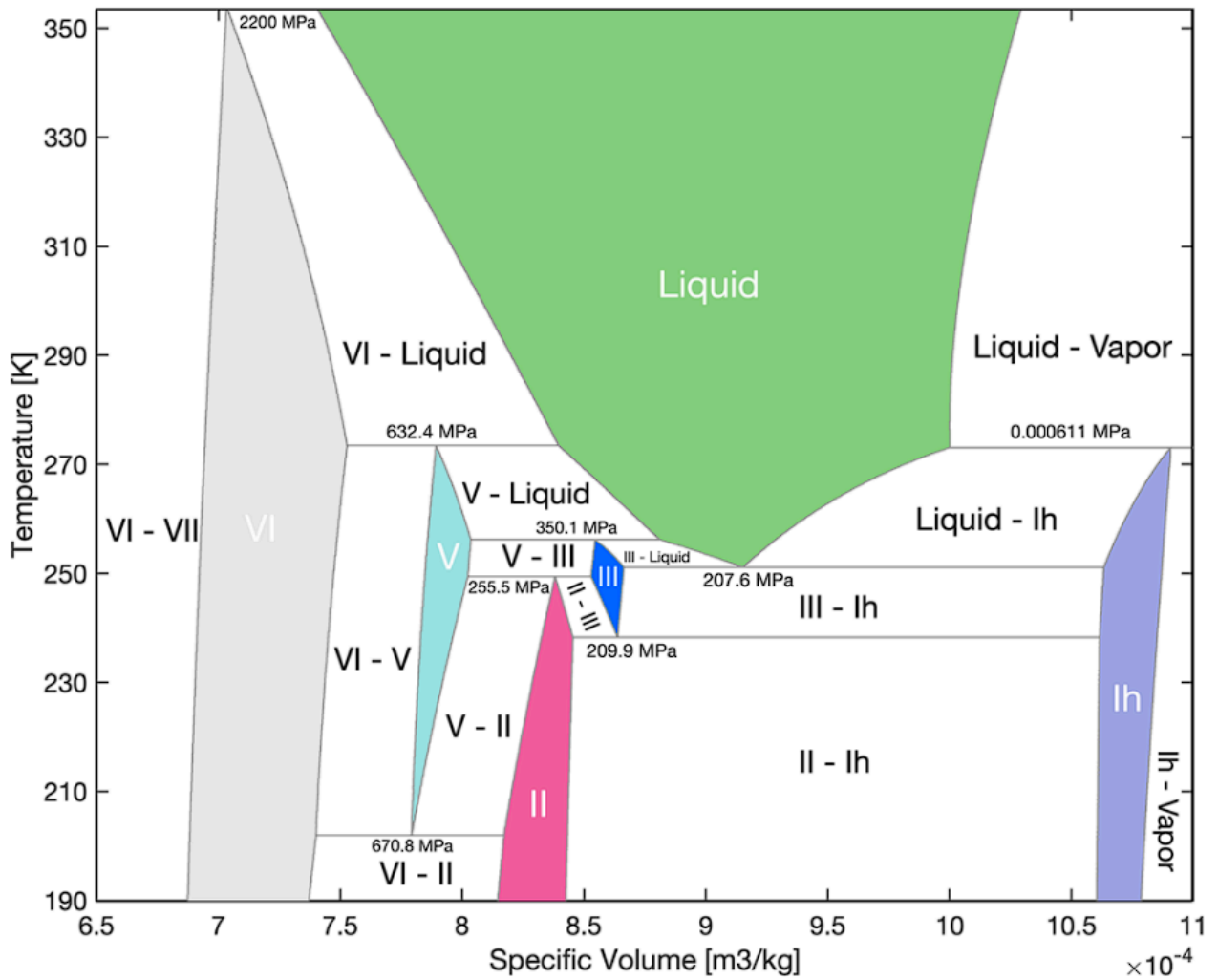
p - T , **Water (H₂O)**: state specified by pressure p and temperature T



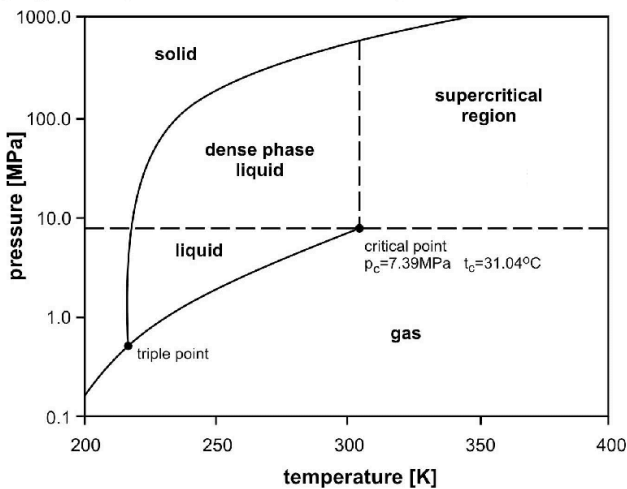
Notes:

- The phases ice I_h , ice I_c , ice II, ice III, etc are polymorphs of ice.
- At pressures below the triple point, sublimation/deposition is the only phase change.
- At temperatures and pressures above the critical point, water becomes supercritical.
- At pressures above 1 TPa, water enters a 'metallic' phase (C2/m).

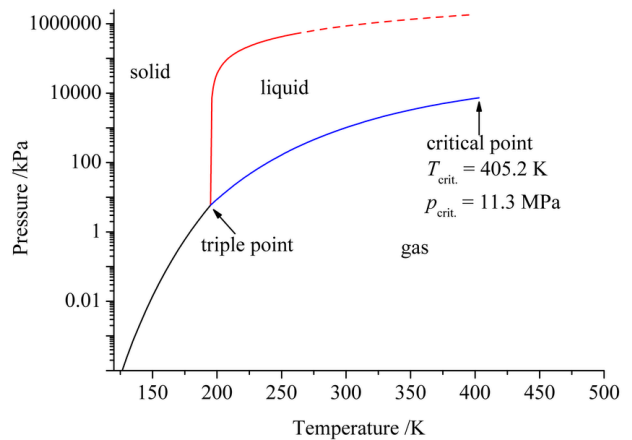
T - v , Water (H_2O): state specified by temperature T and specific volume v



p - T , Carbon Dioxide (CO_2)

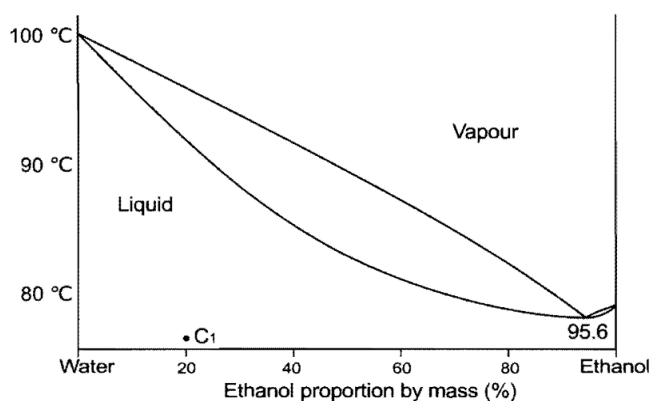


p - T , Ammonia (NH_3)

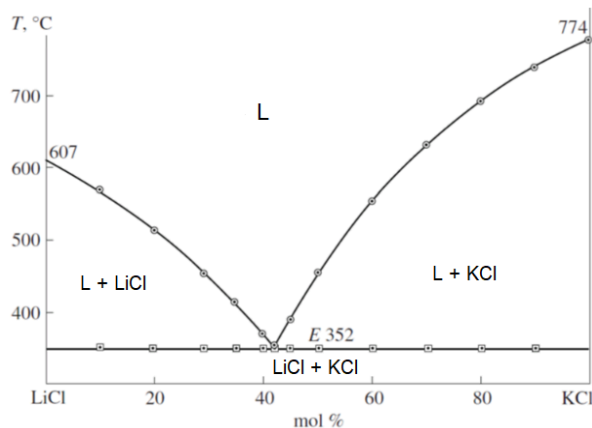


T-x Binary Phase Diagrams: The phase diagrams for some selected equilibria of solid, liquid and vapour phases recorded at a pressure of 1 bar are shown. Some azeotropes and eutectics (E) are indicated. L = liquid, V = vapour.

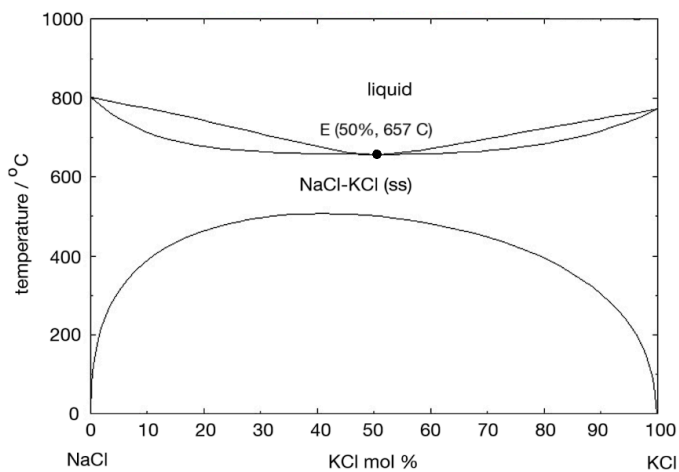
Water-Ethanol (L, V)



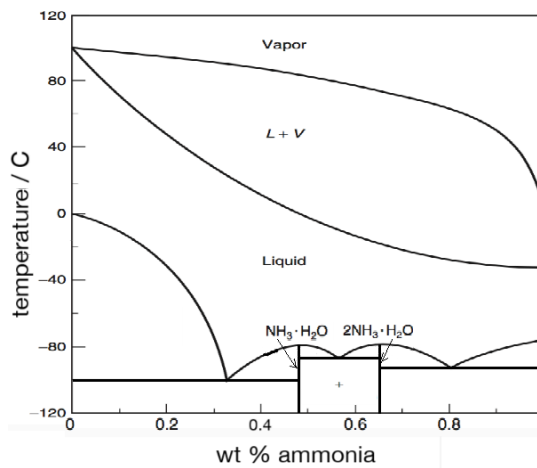
LiCl-KCl (S, L)



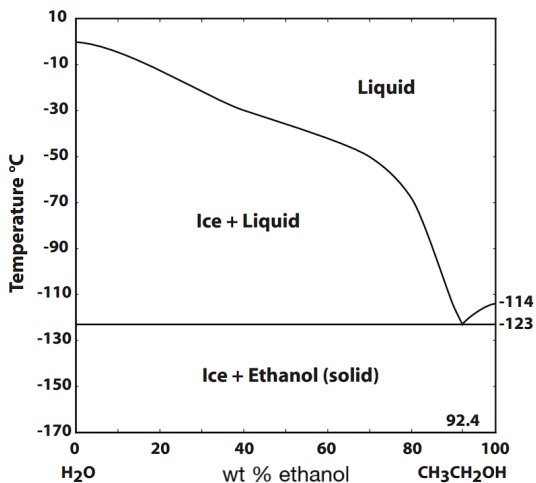
NaCl-KCl (S, L)



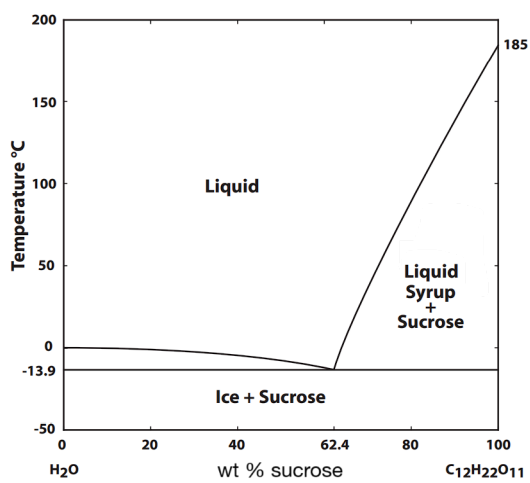
Water-Ammonia (S, L, V)



Water-Ethanol (S, L)



Water-Sucrose (S, L)

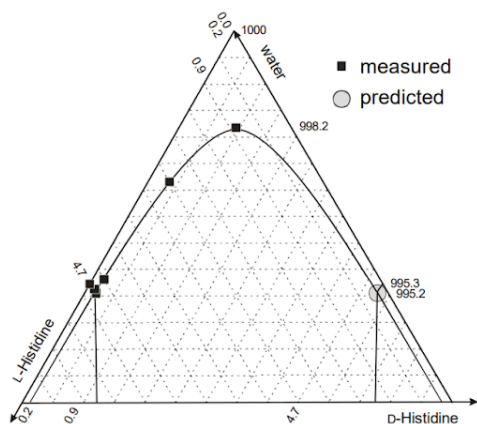


Enantioselective Crystallisation of Amino Acids and Catalysts (Ternary Phase Diagrams)

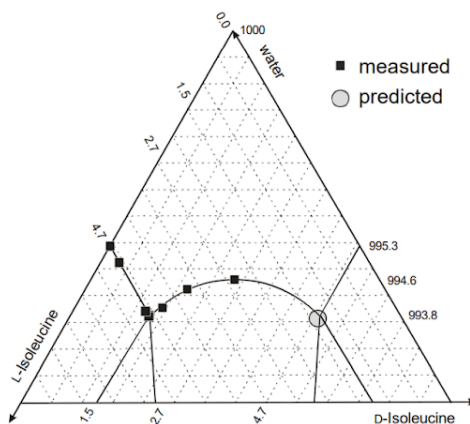
Compositions are given as 1000 × mole fraction. All data at 25 °C. The predicted eutectic composition is only shown on the minor enantiomer side of the phase diagram for clarity.

For amino acid biochemical data, see Section 16.5.10. For the catalyst structures, see Section 14.1.4.

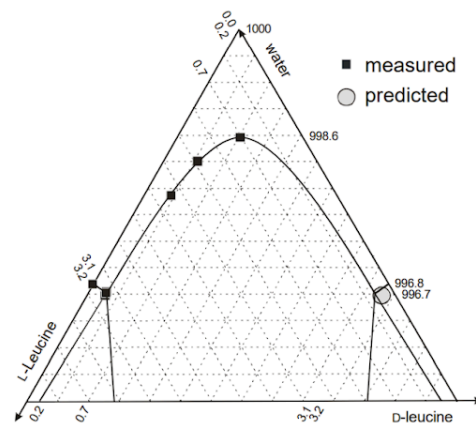
L-His - D-His - H₂O



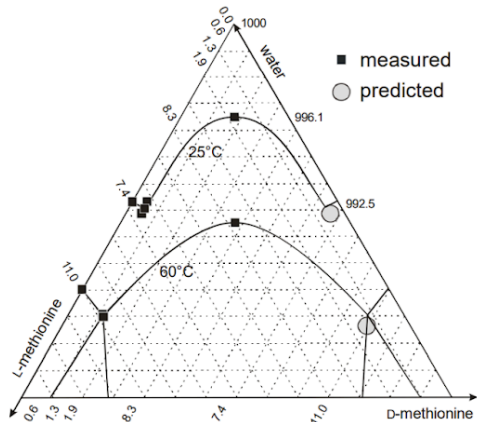
L-Ile - D-Ile - H₂O



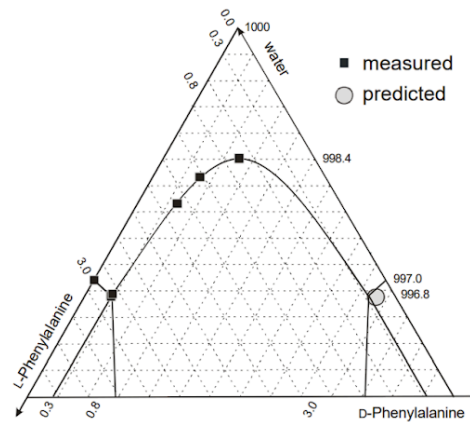
L-Leu - D-Leu - H₂O



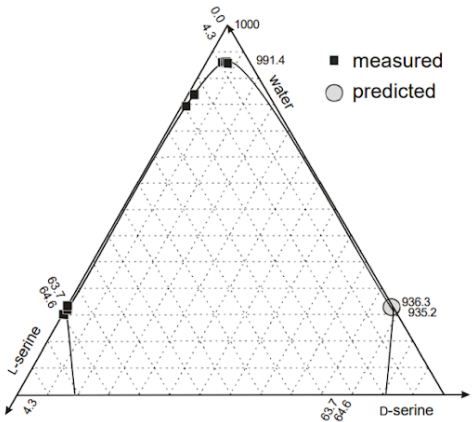
L-Met - D-Met - H₂O



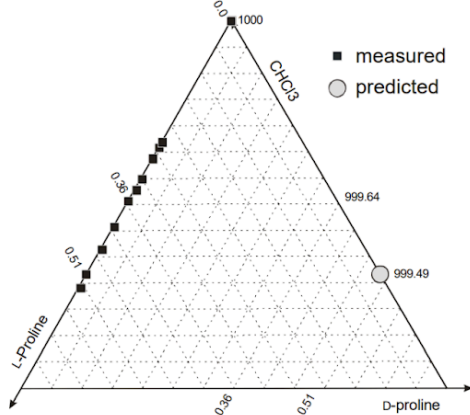
L-Phe - D-Phe - H₂O



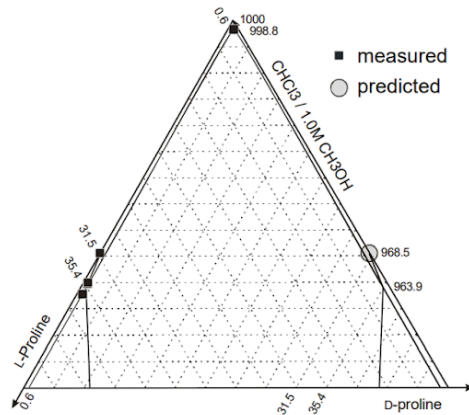
L-Ser - D-Ser - H₂O



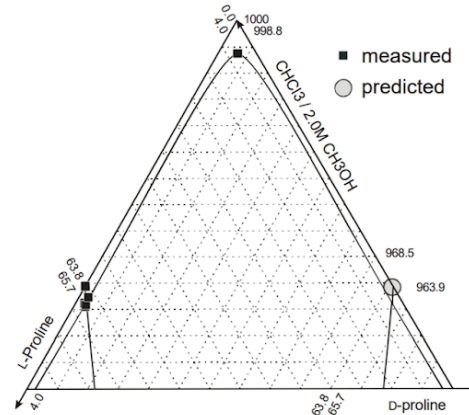
L-Pro - D-Pro - CHCl₃



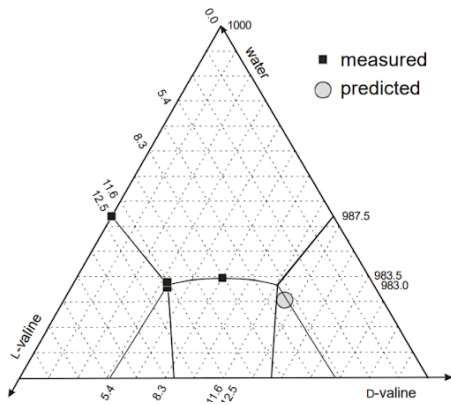
L-Pro - D-Pro - CHCl₃/1M MeOH



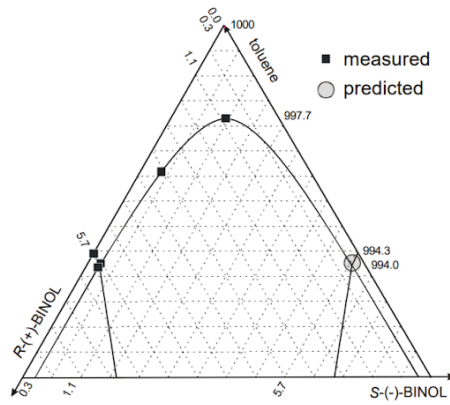
L-Pro - D-Pro - CHCl₃/2M MeOH



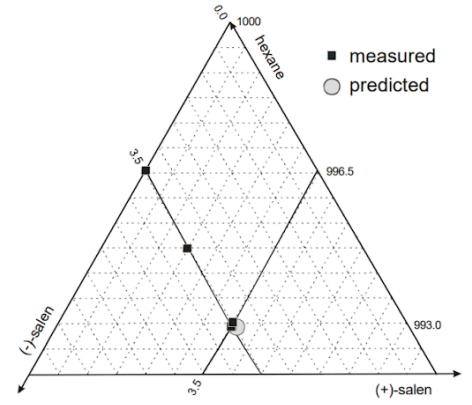
L-Val - D-Val - H₂O



R-BINOL - S-BINOL - toluene

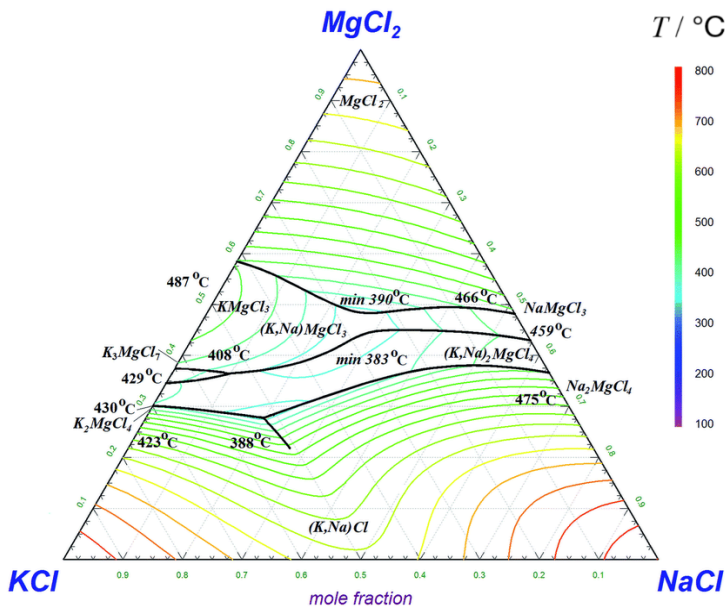


(-)-salen - (+)-salen - hexane

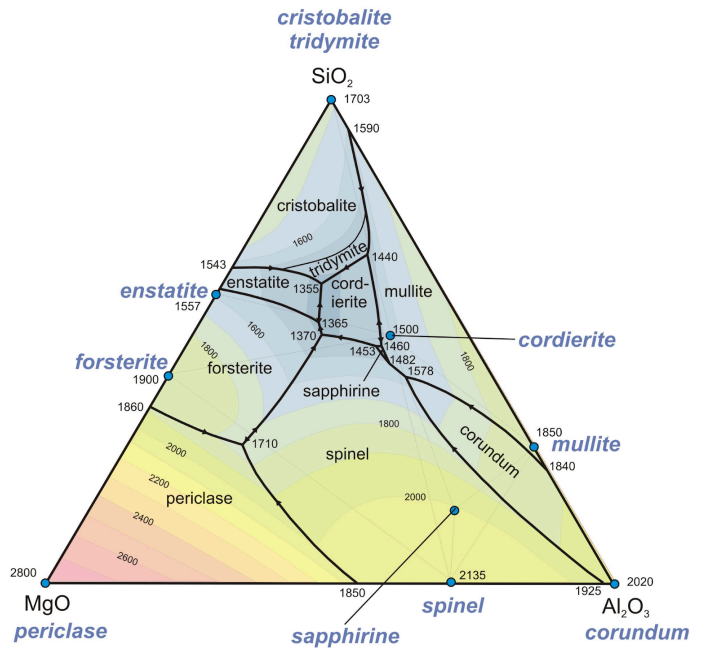


Temperature Dependence of Mineral Solid Solution Stability

MgCl₂ - KCl - NaCl



SiO₂ - MgO - Al₂O₃



13.5. Electrochemistry

13.5.1. Measurements of Electric Charge Flow

For an electrolyte with concentration c (consisting of n^+ moles of cations and n^- moles of anions per mole of dissolved electrolyte) with potential difference V between electrodes of effective area A , separated by distance L , with current flow I ,

- Resistance [Ω] and Resistivity [$\Omega \text{ m}$], $R = \frac{V}{I}$, $\rho = \frac{RA}{L}$ (cell constant: $\frac{L}{A}$)
- Conductance [S] and Conductivity [S m^{-1}] $G = \frac{1}{R} = \frac{I}{V}$, $\kappa = \frac{1}{\rho} = \frac{GL}{A} = \frac{L}{RA}$
- Molar conductivity [$\text{S cm}^2 \text{ mol}^{-1}$], $\Lambda_m = \frac{10^3 \times \kappa [\text{S cm}^{-1}]}{c [\text{mol dm}^{-3}]} = \frac{10^3 \times \frac{L}{A} [\text{cm}^{-1}]}{R [\Omega] \times c [\text{mol dm}^{-3}]}$
- Equivalent conductivity [$\text{S cm}^2 \text{ eq}^{-1}$], $\Lambda_{eq} = \frac{\Lambda_m}{n^+ + n^-}$

Kohlrausch's Law for Strong and Weak Electrolyte Conductivity

- At infinite dilution (as $c \rightarrow 0$), the molar conductivity of a **strong** electrolyte tends to a finite limiting conductivity, $\lim_{c \rightarrow 0} \Lambda_m = \Lambda_m^0$, while for **weak** electrolytes, Λ_m goes to a large but finite value.
- Kohlrausch's Law (independent ion migration): $\Lambda_m^0 = n^+ \lambda_+^0 + n^- \lambda_-^0$
- Ionic strength: $I = \frac{1}{2} \sum_{i=1}^n c_i z_i^2$ (c_i : concentration of ion i , z_i : charge on ion i)
- Debye-Hückel-Onsager equation (for **strong** electrolytes at dilute concentrations):

$$\Lambda_m = \Lambda_m^0 - (A + B\Lambda_m^0)\sqrt{c}, \quad \text{where } A = \frac{82.4}{(\epsilon_r T)^{1/2} \eta} \text{ and } B = \frac{8.2 \times 10^5}{(\epsilon_r T)^{3/2}}$$

- Temperature dependence: $\lambda^0(T) = \lambda_{298K}^0 (1 + \alpha \Delta T)$ where $\alpha \approx 0.02 \text{ K}^{-1}$ (0.0139 K^{-1} for H^+)
- Equivalent conductivity: $\Lambda_{eq} = \Lambda_m / |z|$ (z : ion charge, in units of e)
- Limiting conductivity (for **weak** electrolytes): $\Lambda_m^0(AB) := \Lambda_m^0(AX) + \Lambda_m^0(BY) - \Lambda_m^0(XY)$
- Degree of dissociation, $\alpha = \frac{\Lambda_m}{\Lambda_m^0}$; Dissociation constant, $K = \frac{c \alpha^2}{1 - \alpha} = \frac{c (\Lambda_m)^2}{\Lambda_m^0 (\Lambda_m^0 - \Lambda_m)}$.
- Diffusion coefficient: $D [\text{cm}^2 \text{ s}^{-1}] = \frac{RT \lambda^0}{|z| F^2}$ (Nernst-Einstein correlation).

13.5.2. Microscopic View of Electrode-Solution Interactions

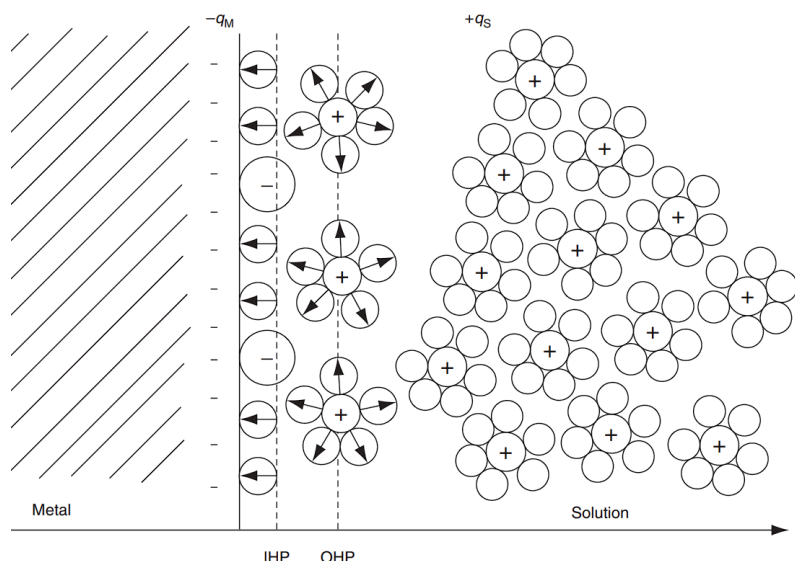
Anode: electrode in which conventional current leaves, associated with **oxidation**.

The anode is positively charged in an electrolytic cell and negatively charged in a galvanic cell.

Cathode: electrode in which conventional current enters, associated with **reduction**.

The cathode is negatively charged in an electrolytic cell and positively charged in a galvanic cell.

Electrical Double Layer (EDL, Helmholtz Layer) Formation at Electrode Interfaces



Within the inner Helmholtz plane (IHP), adsorbed ions and solvent molecules are in contact with the electrode surface. The outer Helmholtz plane (OHP) represents the furthest point at which solution counterions are interacting with the electrode; in the bulk solution, they are fully solvated and diffuse under the EMF.

Molecular Orbital Interactions

For band theory, see Section 8.6.1. For MO theory, see Section 13.1.11.

At an **inert (capacitive, polarisable), conducting** electrode (e.g. platinum or graphite):

- at **negative** potential ($-V$), the conduction band is partially filled, **raising** the Fermi level
- at **positive** potential ($+V$), the valence band is partially depleted, **lowering** the Fermi level

Interactions with nearby molecules in the solution can then occur:

- when the Fermi level is at or **above** the LUMO energy of a solution species, electron density can be accepted by the solution species from the electrode conduction band (**reduction**)
- when the Fermi level is at or **below** the HOMO energy of a solution species, electron density can be donated by the solution species into the electrode valence band (**oxidation**)

At a **reactive (Faradaic, non-polarisable), conducting** electrode (e.g. Cu, Zn, Ag, Au, Hg), the species may be the corresponding ion in solution (e.g. Ag^+ ions reacting with electrons in an Ag electrode at negative potential), leading to growth or depletion of the electrode metal.

13.5.3. Thermodynamics of Electrochemical Cells

Electrochemical reactions interconvert electrical and chemical energy of redox reactions.

- Anode half-reaction (oxidation): $a A \rightarrow c C + n e^-$
 - Cathode half-reaction (reduction): $b B + n e^- \rightarrow d D$
 - Overall reaction: $a A + b B \rightarrow c C + d D$ (n electrons transferred)
 - Standard electrode potential: E^\ominus at standard conditions ($c = 1 \text{ mol dm}^{-3}$, $T = 298 \text{ K}$, $p = 1 \text{ bar}$). For a table of E^\ominus values (relative to SHE), see Section 13.5.22.
 - Cell potential: $E_{\text{cell}} = E_{\text{cathode}} - E_{\text{anode}}$ (both taken as reduction potentials. Units: volts)
 - Ideal cell potential, non-standard conditions: $E_{\text{cell}} = E^\ominus - \frac{RT}{nF} \ln \xi$ (Nernst equation)
(E^\ominus : standard electrode potential, $R = 8.314 \text{ J mol}^{-1} \text{ K}^{-1}$: ideal gas constant, T : temperature, $F = 96486 \text{ C mol}^{-1}$: Faraday's constant (charge of mole of electrons), $\xi = (\{C\}^c \{D\}^d) / (\{A\}^a \{B\}^b)$: reaction quotient)
 - Equilibrium constant: $\ln K = \frac{nFE^\ominus}{RT}$ (equilibrium attained when $E = 0$, $\xi = K$)
 - Gibbs energy change (maximum reversible work): $\Delta_r G^\ominus = -nF E^\ominus$ and $\Delta_r G = -nF E$
($\Delta G \neq 0$: cells are inherently non-equilibrium processes due to external work)
 - Current drawn: $I(t) = nF r(t)$ (r [mol s^{-1}]: rate of reaction)
 - Charge transferred: $\Delta Q = \int_0^{\Delta t} I(t) dt = I_{\text{avg}} \Delta t = i_{\text{avg}} A \Delta t$ (Δt : time duration)
 - For a unimolecular E mechanism electrode process $O + n e^- \rightleftharpoons R$, current due to kinetic overpotential η :
(Butler-Volmer equation)
- $$i = i_0 \left(\underbrace{e^{\frac{\alpha n F}{RT} \eta}}_{\text{anodic}} - \underbrace{e^{-\frac{(1-\alpha) n F}{RT} \eta}}_{\text{cathodic}} \right) \xrightarrow[\alpha=1/2]{\text{reversible}} i = 2i_0 \sinh \left(\frac{nF}{2RT} \eta \right) \xrightarrow[\text{about } \eta=0]{\text{linearised}} i = \left(\frac{RT}{i_0 n F} \right)^{-1} \eta$$
- (i : current density [A cm^{-2}], i_0 : reversible current (at $\eta = 0 \text{ V}$ so $E = E_{\text{Nernst}}$),
 $\alpha = \frac{-1}{F} \frac{\partial(\Delta G_{ox}^\ddagger)}{\partial \phi}$: (anodic) charge transfer coefficient (fraction of current, equal to 0.5 if reversible),
 $\Delta G_{ox}^\ddagger = RT \ln \alpha$: Gibbs free activation energy of (anodic) reaction, $A_{TS} = \frac{2.303 RT}{\alpha n F}$: (anodic) Tafel slope
 (of η vs $\log_{10} i$ graph, equal to **reciprocal** of limiting slope of $\log_{10} \eta$ vs i graph), equal to 118 mV per decade for ($n = 1$, $T = 298 \text{ K}$, $\alpha = 0.5$))
- Approximation at high overpotentials: $\eta = \pm A_{TS} \log_{10} \frac{i}{i_0}$ (Tafel equation)

Note: n may be different in the anodic and cathodic branches if they have different mechanisms.

In addition to kinetic and Ohmic losses, there may also be concentration polarisation (back-diffusion due to concentration gradients during operation) and bubble overpotential (gas formation at the electrode decreases effective area) contributions to the overpotential. Typical ranges for electrolysis of water are $E_{\text{cell}} = 1.5 \text{ V}$, $E_{\text{Nernst}} = 1.29 \text{ V}$, $\eta = 10 \text{ mV}$, $IR = 300 \text{ mV}$.

Electrolytic cell: external electrical energy is supplied ($W < 0$) to an otherwise non-spontaneous chemical reaction to render it spontaneous. Typical application: chloralkali process.

For practical electrolytic cells, see Section 8.5.15.

- Non-ideal cell potential: $E_{\text{cell}} [\text{V}] = -E^{\ominus} + \frac{RT}{nF} \ln \xi + \eta_a + \eta_c + IR_{\Omega}$
(η : electrode kinetic overpotential for anode and cathode, I : current, R_{Ω} : electrolyte resistance)
- Loss of available power due to irreversibilities: $r\sigma [\text{W}] = rnF(\eta_a + \eta_c + iR_{\Omega})$
- Electrical power input: $P_{\text{in}} [\text{W}] = I E_{\text{cell}} = r(\Delta_r G + \sigma)$ (minimum input power: $P_{\text{in}} \geq r \Delta_r G$)
- Chemical energy output: $rQ_{\text{sys}} [\text{W}] = r\Delta_r H = r(\Delta_r G + T \Delta_r S)$; if $\sigma = -T \Delta_r S$ then cell is isothermal
- Coefficient of performance: $\eta = \frac{\text{chemical power output}}{\text{electrical power input}} = \frac{r \times \Delta_r H}{P_{\text{in}}}$ (maximum CoP: $\eta \leq \frac{\Delta_r H}{\Delta_r G}$)

Galvanic cell: energy from a spontaneous chemical reaction is converted to electrical energy ($W > 0$). Typical application: batteries and fuel cells.

For practical galvanic cells, see Section 8.5.8.

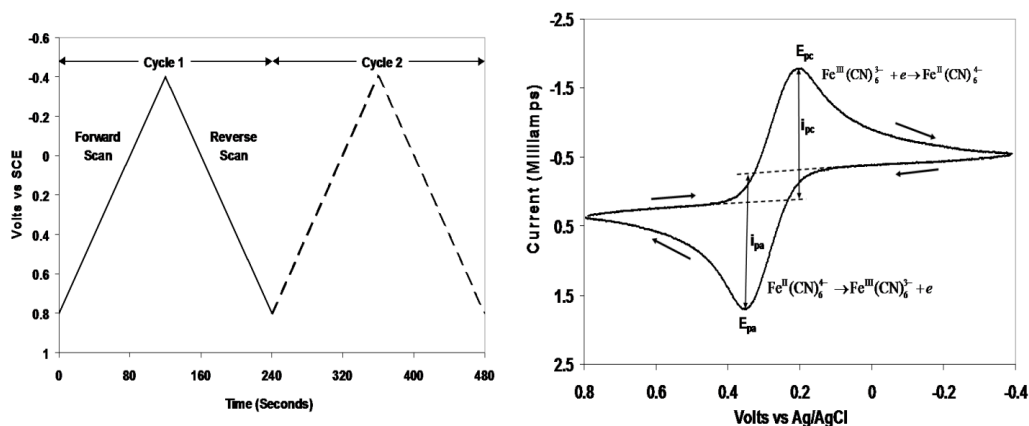
- Non-ideal cell potential: $E_{\text{cell}} [\text{V}] = E^{\ominus} - \frac{RT}{nF} \ln \xi - \eta_a - \eta_c - iR_{\Omega}$
(η : electrode kinetic overpotential for anode and cathode, I : current, R_{Ω} : electrolyte resistance)
- Loss of available power due to irreversibilities: $r\sigma [\text{W}] = rnF(\eta_a + \eta_c + iR_{\Omega})$
- Electrical power output: $P_{\text{out}} [\text{W}] = I E_{\text{cell}} = r(\Delta_r G - \sigma)$ (maximum output power: $P_{\text{out}} \leq r \Delta_r G$)
- Chemical energy input: $rQ_{\text{sys}} [\text{W}] = r\Delta_r H = r(\Delta_r G + T \Delta_r S)$; if $\sigma = -T \Delta_r S$ then cell is isothermal
- Efficiency: $\eta = \frac{\text{electrical power output}}{\text{chemical power input}} = \frac{P_{\text{out}}}{r \times \Delta_r H}$ (maximum efficiency: $\eta \leq \frac{\Delta_r G}{\Delta_r H} < 1$)

13.5.4. Charge Transfer Phenomena in Water

- **Solvation of ions:** aqueous cations are surrounded by a coordination sphere (primary solvation shell) of water molecules e.g. $\text{Na}^+ \rightarrow [\text{Na}(\text{H}_2\text{O})_6]^+$. Coordination numbers vary from 4 for Li^+ and Be^{2+} to 6 for most transition metals to 8-9 or higher for lanthanides / actinides. Additional water molecules (12 or more) associate with the metal ion through a secondary solvation shell by hydrogen bonding to coordinated water molecules.
- **Solvation of hydronium:** hydronium ions (H_3O^+) are solvated in water to form various associated species, including the Eigen cation H_9O_4^+ (hydronium with three hydrogen bonds to three water molecules) and the Zundel cation H_5O_2^+ (a proton forms a symmetric hydrogen bond to two water molecules).
- **Exclusion zone:** at the interface between water and hydrophilic solid (e.g. Nafion) or metal (e.g. electrodes), water molecules are more ordered and have reduced activity. Hydrophobic molecules, including microparticles, are expelled from this coherent region (diffusiophoresis, Section 13.4.4). Under intense IR radiation to ionise the coherent state, a current and p.d. is generated in pure water (oxhydroelectric effect).
- **Grotthuss proton-hopping mechanism:** hypothesised transfer of protons between water molecules through hydrogen bonds in a linear fashion, at a much higher rate than by diffusion in bulk solution. At low temperatures, quantum tunnelling of protons contributes to this effect.
- **Pines mechanism:** recent research indicates a well-supported alternative to the Grotthuss mechanism, where groups of three water molecules (H_7O_3^+) shuttle a proton between them, with new water molecules ahead joining the group to continue the conduction.
- **Special pair dance:** hydronium ions alternate between Eigen and Zundel states. Since the exchange can occur in any direction, this mechanism transfers protons at an overall rate even faster than the Grotthuss mechanism.

13.5.5. Cyclic Voltammetry (CV)

A slow periodic (shifted triangular wave) voltage is applied to a working electrode in a galvanic cell setup. The current through the counter electrode is measured. The working electrode is typically a glassy carbon electrode (GCE).



For reversible electrode reactions,

- Peak current: $i_p = 0.4463 \times (nF)^{3/2} Ac \left(\frac{D\dot{v}}{RT} \right)^{1/2}$ (Randles-Sevcik equation)
- Peak voltages: $E^\ominus = \frac{1}{2} (E_{pa} + E_{pc})$ and $E_{pa} - E_{pc} = \frac{0.059 [V]}{n}$

Reaction mechanisms (E: redox step, C: chemical step)

- E mechanism: $O + n e^- \rightleftharpoons R$: has $i_{pa} = i_{pc}$ (if reversible; diffusion controlled)
- EC mechanism: $O + n e^- + A \rightleftharpoons R + A \rightarrow Z$: has $i_{pc} > i_{pa}$. If $Z = O$ (catalytic regeneration) then acts as a simple E mechanism instead.
- CE mechanism: $Z \rightarrow O + n e^- \rightleftharpoons R$: has $i_{pa} > i_{pc}$. As scan rate decreases, ratio approaches 1.
- Adsorption process: $i_p = \frac{n^2 F^2 \Gamma A \dot{v}}{4RT}$; charge consumed = $Q = \int i dv = nFA\Gamma$.

(\dot{v} : voltage sweep rate [$V s^{-1}$], D : diffusion coefficient [$cm^2 s^{-1}$], A : working electrode surface area [cm^2], c : bulk concentration [$mol cm^{-3} = mM$], Γ : surface coverage fraction)

For irreversible reactions (charge transfer coefficient $\alpha \neq 0.5$):

- Peaks for a redox couple are more widely separated.
- Voltage: $E_p = E^\ominus - \frac{RT}{\alpha nF} \left(0.78 - \ln \frac{k^\ominus}{\sqrt{D}} + \ln \left(\frac{\alpha nF}{RT} \right)^{1/2} \right)$
- Current: $i_p = 2.99 \times 10^5 [C mol^{-1} V^{-1/2}] \times \alpha^{1/2} n^{3/2} Ac D^{1/2} \dot{v}$

13.5.6. Chronoamperometry

A step change in potential (external overpotential) is applied to a working electrode using a potentiostat. The resulting current through the working electrode is measured over time.

Diffusion-controlled Faradaic current: $i_d = nFAc\left(\frac{D}{\pi t}\right)^{1/2}$ (Cottrell equation)

(c : ion concentration in bulk solution, t : time since step applied, D : diffusion coefficient of ion in solution, $i_d(t)$: time-dependent step response in current)

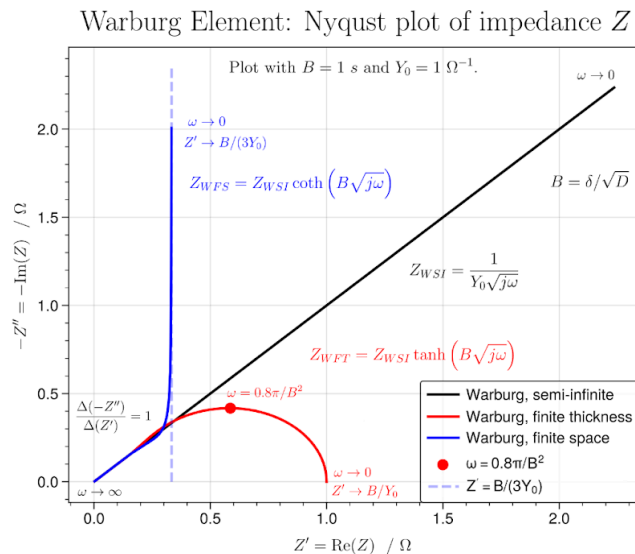
When the step is applied, ions in the immediate vicinity of the electrode are reacted and generate a high initial current. This current dissipates over time as the products form a diffusion layer, which ions from the bulk solution must traverse through before they can react at the electrode. The current decays to the equilibrium value.

The time-integrated current response over a period after the step yields the total charge transferred. A variation is to measure the charge transferred directly (chronocoulometry), which reduces the noise further by implicit integration (amplifier with capacitor)

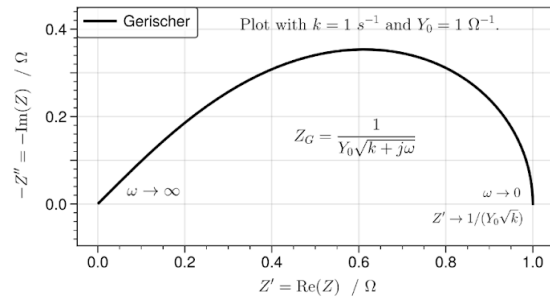
13.5.7. Electrical Impedance Spectroscopy (EIS)

The AC impedance of an electrode can be measured with electrical impedance spectroscopy (EIS). (Z : impedance, $Z' = \text{Re}(Z)$: resistance, $Z'' = \text{Im}(Z)$: reactance such that $Z = Z' + jZ''$)

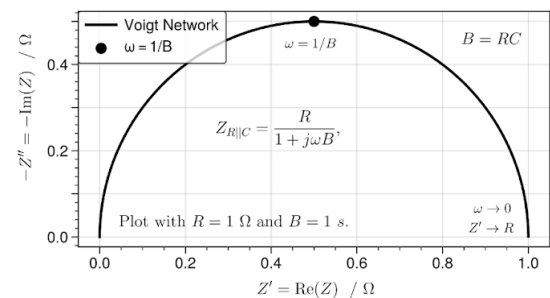
Nyquist Plots of Common Nonlinear Circuit Elements (Warburg, Gerischer, Voigt):



Gerischer Element: Nyquist Plot of Impedance Z



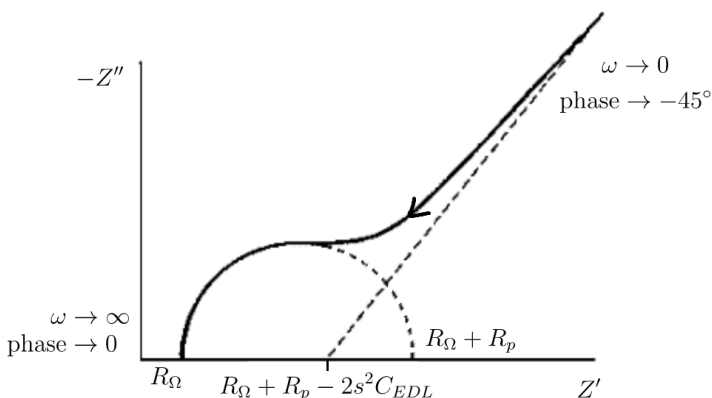
Voigt Network: Nyquist Plot of Impedance Z



(Y_0 : reference admittance ($1/Z$) at $\omega = 1 \text{ rad s}^{-1}$, B : time constant, k : rate constant for C step)

The constant-phase element (CPE) is also common, representing an imperfect double-layer capacitance: $Z_{CPE} = 1 / [(j\omega)^n C_{EDL}]$. Nyquist plot: straight line with $\theta = -\frac{\pi}{2}n$ ($n \leq 1$).

Randles cell: models a full single electrode: $Z_R = R_\Omega + [Z_{CPE} || (R_p + Z_{WSI})]$



(R_Ω : Ohmic resistance (electrolyte),
 Z_{CPE} : CPE representing electrical double layer,
 R_p : polarisation (charge transfer) resistance,
 Z_{WSI} : Warburg impedance (semi-infinite),
 s : Warburg constant, such that $Y_0 = (\sqrt{2} \text{ s})^{-1}$,

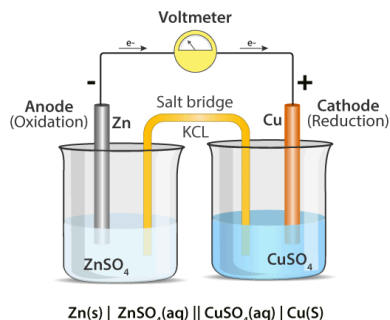
$$\text{also given by } s = \frac{RT}{\sqrt{2}n_e^2 F^2 A} \left(\frac{1}{\sqrt{D_{ox}} C_{ox}^*} + \frac{1}{\sqrt{D_{red}} C_{red}^*} \right)$$

(Nyquist plot shows $n = 1$ in the CPE; D : diffusion coefficient, c^* : surface concentration, n_e : moles of electrons)

13.5.8. Primary Galvanic Cells

Galvanic (voltaic) cell: a system which converts chemical energy to electrical energy.

Primary cell: a cell using irreversible reactions, so cannot be reused once fully discharged.



The half-reaction with the larger reduction potential E^{\ominus}_{red} will proceed as **reduction** (the **cathodic** reaction). The other half-reaction is an **oxidation** (the **anodic** reaction). From the salt bridge, anions flow to the anode solution, and cations flow to the cathode solution to maintain electroneutrality.

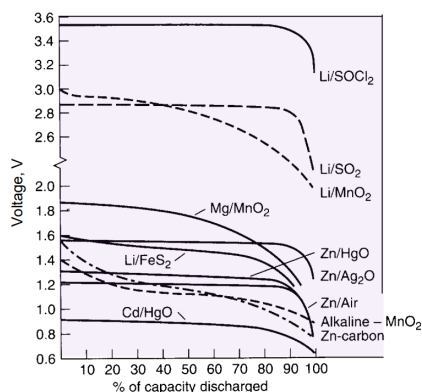
Left: Daniell cell, $\text{Zn} \mid \text{Zn}^{2+} \parallel \text{Cu}^{2+} \mid \text{Cu}$, with KCl salt bridge.

Reference Half-Cells (Standards and Secondary Standards): $(E^{\ominus}$ relative to SHE)

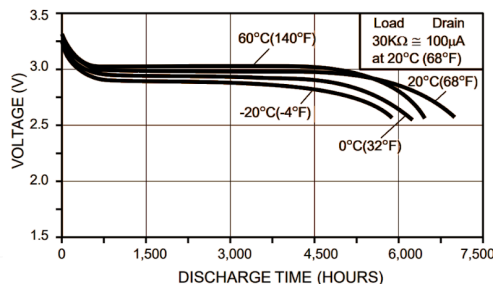
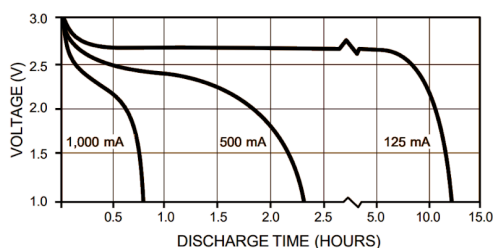
- Standard Hydrogen Electrode (SHE): H^+ (aq, 1 M) \mid H_2 (g, 1 bar) \mid Pt $E^{\ominus} \equiv 0.000$ V
- Silver Chloride Electrode: Ag (s) \mid AgCl (s) \mid KCl (aq, 3 M) $E^{\ominus} = 0.235$ V
- Saturated Calomel Electrode (SCE): Cl^- (aq, 4 M) \mid Hg_2Cl_2 (s) \mid Hg (l) \mid Pt $E^{\ominus} = 0.241$ V

Common Primary Cells: cell notation A \mid B \parallel C \mid D implies $\text{A} \rightarrow \text{B}$ (anode, -ve) and $\text{C} \rightarrow \text{D}$ (cathode, +ve)

Cell	Anodic reaction (-ve)	Cathodic reaction (+ve)	E^{\ominus}	Notes and common applications
Daniell cell	$\text{Zn (s)} \rightarrow \text{Zn}^{2+} \text{ (aq)} + 2 \text{ e}^-$	$\text{Cu}^{2+} \text{ (aq)} + 2 \text{ e}^- \rightarrow \text{Cu (s)}$	1.10 V	The first battery invented (the Voltaic pile).
zinc-carbon cell (Leclanché type)	$\text{Zn (s)} \rightarrow \text{Zn}^{2+} \text{ (aq)} + 2 \text{ e}^-$	$2 \text{ MnO}_2 \text{ (s)} + 2 \text{ NH}_4^+ \text{ (aq)} + 2 \text{ e}^- \rightarrow \text{Mn}_2\text{O}_3 \text{ (s)} + 2 \text{ NH}_3 \text{ (aq)} + \text{H}_2\text{O (l)}$ (also formed: MnOOH , Mn_3O_4)	1.43 V	Common, low-cost primary battery; available in a variety of sizes. Used for e.g. flashlights, portable radios, toys, novelties, instruments...
alkaline dry cell	$\text{Zn (s)} + 2 \text{ OH}^- \text{ (aq)} \rightarrow \text{ZnO (s)} + \text{H}_2\text{O (l)} + 2 \text{ e}^-$ (intermediate: $\text{Zn(OH)}_2 \text{ (aq)}$)	$2 \text{ MnO}_2 \text{ (s)} + \text{H}_2\text{O (l)} + 2 \text{ e}^- \rightarrow \text{Mn}_2\text{O}_3 \text{ (s)} + 2 \text{ OH}^- \text{ (aq)}$	1.43 V	Most popular general-purpose premium battery (Duracell AA / AAA); good low-temperature and high-rate performance; moderate cost.
soluble lithium cell	$\text{Li (s)} \rightarrow \text{Li}^+ \text{ (aq)} + \text{e}^-$	$2 \text{ SOCl}_2 \text{ (l)} + 4 \text{ e}^- \rightarrow \text{S (s)} + \text{SO}_2 \text{ (l)} + 4 \text{ Cl}^- \text{ (aq)}$	3.65 V	High energy density; long shelf life; good performance over wide temperature range.
lithium-manganese button cell	$\text{Li (s)} \rightarrow \text{Li}^+ \text{ (aq)} + \text{e}^-$	$\text{MnO}_2 \text{ (s)} + x \text{ Li}^+ \text{ (aq)} + \text{e}^- \rightarrow \text{Li}_x\text{MnO}_2 \text{ (s)}$	3.3 V	High energy density; good rate capability and low-temperature performance; long shelf life; competitive cost.



Characteristic discharge curves for Li/MnO₂ cell for various I and T



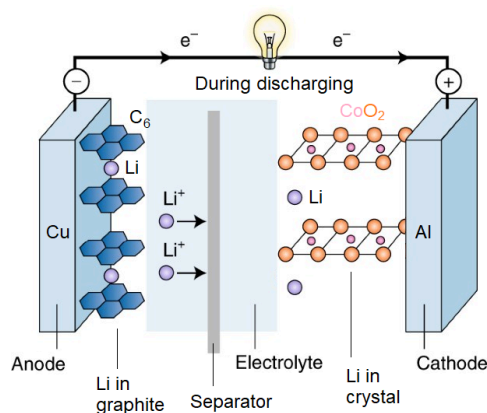
13.5.9. Secondary Galvanic Cells

Secondary cell: a cell using reversible reactions, so can be recharged after use and used again.

Cell	Anodic reaction (-) (forward is discharging)	Cathodic reaction (+) (forward is discharging)	Typical battery specifications	Notes and common applications
lead acid battery	$\text{PbO}_2 (\text{s}) + 4 \text{H}^+ (\text{aq}) + 2 \text{e}^- \rightleftharpoons \text{Pb}^{2+} (\text{aq}) + 2 \text{H}_2\text{O} (\text{l})$	$\text{Pb} (\text{s}) \rightleftharpoons \text{Pb}^{2+} (\text{aq}) + 2 \text{e}^-$	$E^\ominus = 2.1 \text{ V}$ $E_{\text{grav}} = 40 \text{ Wh kg}^{-1}$ $E_{\text{vol}} = 85 \text{ Wh L}^{-1}$ $P = 180 \text{ W kg}^{-1}$	<p>Dissolution-precipitation mechanism. Sulfuric acid at $0 < \text{pH} < 1$ is used, forming PbSO_4. The Pb is hardened by alloying with ~5% Sb, and shaped into a grid.</p> <p>Modifications include the SLI (Starting, Lighting, Ignition: cells stacked in series as planar grids), VRLA/SLA (valve regulated lead acid: less electrolyte), carbon-enhanced battery (a hybrid supercapacitor with one C cathode and twin PbO_2 anode).</p>
nickel-cadmium battery	$\text{Cd} + 2 \text{OH}^- \rightleftharpoons \text{Cd}(\text{OH})_2 + 2 \text{e}^-$	$\text{NiOOH} + \text{H}_2\text{O} + \text{e}^- \rightleftharpoons \text{Ni}(\text{OH})_2 + \text{OH}^-$	$E^\ominus = 1.2 \text{ V}$ $E_{\text{grav}} = 50 \text{ Wh kg}^{-1}$ $E_{\text{vol}} = 100 \text{ Wh L}^{-1}$ $P = 150 \text{ W kg}^{-1}$	<p>Long cycle life and fast recharging. However, has a memory effect (voltage depression) in some cases, due to physical changes in uncycled regions of the cathode.</p>
Ni-MH battery (metal hydride)	$\text{MH} + \text{OH}^- \rightleftharpoons \text{M} + \text{H}_2\text{O} + \text{e}^-$ <p>(M = alloy storing hydrogen)</p>	$\text{NiOOH} + \text{H}_2\text{O} + \text{e}^- \rightleftharpoons \text{Ni}(\text{OH})_2 + \text{OH}^-$	$E^\ominus = 1.2 \text{ V}$ $E_{\text{grav}} = 100 \text{ Wh kg}^{-1}$ $E_{\text{vol}} = 200 \text{ Wh L}^{-1}$ $P = 600 \text{ W kg}^{-1}$	<p>Oxygen recombination prevents gas build-up: Charged cathode: $4 \text{OH}^- \rightarrow 2 \text{H}_2\text{O} + \text{O}_2 + 4 \text{e}^-$ Charged anode: $4 \text{MH} + \text{O}_2 \rightarrow 4 \text{M} + 2 \text{H}_2\text{O}$</p>
Li-ion polymer battery (LiPo)	$\text{Li} \rightleftharpoons \text{Li}^+ + \text{e}^-$ <p>(Li is intercalated in graphite as LiC_6, between graphenes)</p>	$x \text{Li}^+ + \text{Li}_{1-x}\text{CoO}_2 + x \text{e}^- \rightleftharpoons \text{Li}^+[\text{CoO}_2]^-$ <p>(lithium-doped crystal substrate)</p>	$E^\ominus = 3.7 \text{ V}$ $E_{\text{grav}} = 200 \text{ Wh kg}^{-1}$ $E_{\text{vol}} = 500 \text{ Wh L}^{-1}$ $P = 300 \text{ W kg}^{-1}$	<p>Rechargeable ion battery, used in electric vehicles. Li^+ ions are exchanged between being intercalated in an anode (high energy state) and in a cathode (low energy state) to produce a voltage.</p> <p>See Section 13.5.10 for more info.</p>

13.5.10. Design of Rechargeable Ion Batteries

Principle of Operation: exchange of small cations from one intercalator to another of different energies to provide the cell EMF



Lithium-ion Cell: Anode intercalation prevents dendritic growth of solid lithium, which can puncture the electrolyte and cause the short-circuiting and breakdown of the cell. The electrolyte is a lithium salt e.g. LiPF_6 , which permits rapid diffusion of Li^+ . The separator is a nanoporous polymer structure e.g. PP, PE, which blocks electron diffusion while permitting Li^+ . When charging for the first time after the cell's construction, Li^+ ions are solvated by the electrolyte and react with the graphite to form a solid-electrolyte interface passivation layer (SEI layer), consuming about 5% of the lithium in the process. This prevents electrons contacting the electrolyte which would result in its degradation, and permits cycling.

Performance Metrics for Rechargeable Batteries

- Total charge capacity [A h]: $1 \text{ A h} = 3600 \text{ C}$
- Battery output: specific power [W kg^{-1}], power density [W L^{-1}]. A trade-off with battery capacity.
- Battery capacity: gravimetric energy density [W h kg^{-1}], volumetric energy density [W h L^{-1}]
- Discharge current: C-rate [h^{-1}] = $\frac{\text{output current required to fully discharge battery in one hour [A]}}{\text{charge capacity [A h]}}$
- Cycle life: number of charge-discharge cycles to lose performance. Depends on the depth of discharge and the quantitative metric used to assess extent of loss of performance.
- Cost: lifetime cost [$\$/\text{kWh/cycle}$], total per-unit cost [$\$$], material cost [$\$/\text{kg}^{-1}$]
- Self-discharge: voltage drop over time in open-circuit conditions, settling at the float voltage
- Reliability and safety: up-time, breakdown rate, maintenance costs, risk, hazard severity

Important performance metrics for EVs and grid-scale energy storage applications are:

- Electric sedan cars: per-unit cost > volumetric capacity > cycle life.
- Electric heavy vehicles (freight lorries, ships and planes): gravimetric capacity > cycle life > cost.
- Transmission load/frequency balancing: lifetime cost > safety and reliability > cycle life.
- Residential storage and smart grid: safety and reliability > lifetime cost > cycle life.

Battery Chemistry and Practicalities of Materials Selection

Many of the materials used in these batteries are critical materials (e.g. lithium, cobalt, manganese). Alternative battery chemistries are needed to alleviate strains on resources as batteries are crucial in sustainable energy technologies in the future. This is an active area of research, but technology readiness and maturity remains a hurdle.

The mining and refining of critical materials is subject to availability due to geopolitical and supply chain influences. As with most raw materials, mining companies have high leverage as they can sell their produce to refiners as commodities on the spot market, which is volatile. Battery companies with higher bargaining power may be able to negotiate fixed-price contracts to alleviate this uncertainty.

Variations in battery chemistry currently under research with potential applications include:

- High nickel, low cobalt cathode materials (e.g. $\text{LiNi}_{0.6}\text{Co}_{0.05}\text{Mn}_{0.35}\text{O}_2$), to reduce reliance on critical materials.
- Lithium iron phosphate (LFP, LiFePO_4) eliminates cobalt completely, as pursued by Tesla for use in EVs.
- Sodium ion cells, replacing Li^+ with Na^+ (eliminates Li). Less flammable but lower energy performance.
- Zinc ion cells, including the $\text{Na}_{0.12}\text{Zn}_{0.25}\text{V}_2\text{O}_5 \cdot 2.5 \text{H}_2\text{O}$ (NVZO) cathode. The NVZO battery uses water-based electrolyte to exploit the special pair dance mechanism (Section 13.5.4) giving exceptional kinetics and no flammability hazard. Challenges include hydrogen formation from electrolysis of water (requiring low operating voltage), and dendrite formation in the zinc anode.
- Solid state batteries (SSBs) use a solid phase electrolyte, allowing the use of metal anodes (lithium without graphite) as dendrite formation is no longer problematic for the cell.

Cathodes can be classed as layered (e.g. LiCoO_2), spinel (e.g. LiMn_2O_4), polyanionic (e.g. $\text{Li}_x\text{Fe}_2(\text{XO}_4)_3$, $\text{X} = \text{S} / \text{Mo} / \text{W}$) or olivine (e.g. LiFePO_4). Ion migration through the cathode lattice is dependent on the octahedral site stabilisation energy of a metal cation in interstitial voids, $\text{OSSE} = \text{CFSE}_{\text{octahedral}} - \text{CFSE}_{\text{tetrahedral}}$ (Section 15.5.8, crystal field theory).

Battery Engineering in Electric Vehicles (EVs)

EV technology is already widespread and growing in the automotive industry, for cars (e.g. Tesla Model Y, Hyundai Ioniq 6, Nissan Leaf) and many trains. EV adoption is less common for heavy-duty applications (trucks, planes, ships) due to the high power requirements.

Ion batteries are typically manufactured in a cylindrical geometry, in which thin-film intercalator and cathode materials are deposited onto metal electrode foils, placed in close contact with the electrolyte/separator between them and rolled up to save space. Current collectors are placed at the metal foils, and output current is used to power a brushless DC motor (for hybrid plug-in EVs) or induction motor (for high-performance pure EVs). Motors produce usable torque output across a wider band of speeds than internal combustion engines.

In an EV, ion cells are connected in series to increase the voltage, and these are stacked in parallel to increase the current, to form a single battery module. Several modules are further connected in series to form a battery pack, with typical ratings on the order of ~25 V and ~250 A (~6 kW, 200 Ah). The high cell density leads to heat production during operation, which can reduce the performance of the battery, and can be a fire hazard in defective assemblies.

A battery management system (BMS) is a digital system used to monitor the state of charge (SoC), temperature and voltage levels. Liquid-cooling (water with glycol for sub-freezing temperatures) is used to dissipate heat from the batteries, with the BMS setting the coolant flow rate using a control system to maintain optimal battery temperature. In some EVs (e.g. Tesla), BMS can also use cell balancing (voltage protection) to ensure all cells discharge at the same rate, preventing anomalous charging and discharging due to over/undervoltage.

13.5.11. Fuel Cell Batteries

Fuel cells: not rechargeable (primary), but never used up as long as reactants are supplied.

Cell	Anodic reaction (-) (forward is discharging)	Cathodic reaction (+) (forward is discharging)	E^\ominus	Notes and common applications
alkaline hydrogen fuel cell (AFC)	$\text{H}_2 + 2 \text{OH}^- \rightarrow 2 \text{H}_2\text{O} + 2 \text{e}^-$	$\text{O}_2 + 2 \text{H}_2\text{O} + 4 \text{e}^- \rightarrow 4 \text{OH}^-$	1.23 V	Maximum efficiency is ~70%. A recent development is the solid state alkaline fuel cell (SAFC) which prevents KOH being poisoned by CO_2 into K_2CO_3 .
proton exchange membrane (PEMFC)	$\text{H}_2 \rightarrow 2 \text{H}^+ + 2 \text{e}^-$	$\text{O}_2 + 4 \text{H}^+ + 4 \text{e}^- \rightarrow 2 \text{H}_2\text{O}$	1.23 V	The polyelectrolyte (ionomer) membrane conducts protons but blocks the gas fuels.
solid oxide fuel cell (SOFC)	$\text{H}_2 \rightarrow 2 \text{H}^+ + 2 \text{e}^-$; $2 \text{H}^+ + \text{O}^{2-} \rightarrow \text{H}_2\text{O}$	$\text{O}_2 + 4 \text{e}^- \rightarrow 2 \text{O}^{2-}$	1.23 V	High temperatures (600 - 1000 °C), no catalyst required. Oxide ions (O^{2-}) diffuse across the solid yttria-stabilised zirconia (YSZ) electrolyte. Requires fuel desulfurisation to avoid poisoning. They can be integrated in a gasification power plant for burning biomass/coal.
glucose biofuel cell (GBFC)	glucose ($\text{C}_6\text{H}_{12}\text{O}_6$) + 2OH^- \rightarrow gluconolactone ($\text{C}_6\text{H}_{10}\text{O}_6$) + $2 \text{H}_2\text{O} + 2 \text{e}^-$ (glucose oxidase enzyme catalysed)	$\text{O}_2 + 4 \text{H}^+ + 4 \text{e}^- \rightarrow 2 \text{H}_2\text{O}$ (laccase enzyme catalysed)	1.34 V	The enzymes require cofactors and very specific operating conditions to function. They are currently not as efficient as hydrogen fuel cells but are more sustainable. For more info, see Section 17.4.10.

13.5.12. Molten Salt Batteries and Liquid Metal Batteries

High-operating temperature batteries can be used to generate electricity from industrial waste heat, where chemical reactions are often much more efficient.

Molten salt batteries are the galvanic equivalent of molten salt electrolysis. The separator is a β -alumina solid electrolyte (BASE, sodium polyaluminate) which is a fast ion conductor. They typically use temperatures around $T = 300$ °C.

Established example: sodium-sulfur battery: $2 \text{Na} + 4 \text{S} \rightarrow \text{Na}_2\text{S}_4$. ($E = 2.0$ V)

Modern example: sodium-nickel chloride battery (NaNiCl_2 , ZEBRA battery).

Liquid metal batteries use molten metal electrodes, at very high temperatures ($T = 700$ °C).

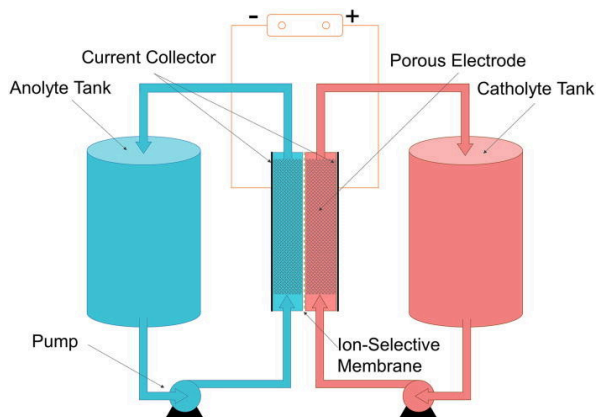
Example: a Mg (l) anode, Sb (l) cathode.

Anode: $\text{Mg}(\text{l}) \rightarrow \text{Mg}^{2+}(\text{l}) + 2 \text{e}^-$; Cathode: $\text{Mg}^{2+}(\text{l}) + 2 \text{e}^- \rightarrow \text{Mg}^{2+}(\text{in Sb})$

Mg^{2+} ions diffuse between the electrodes from the pure to the alloy state. Very high current densities are possible. At full charge, the cathode is pure Sb (l).

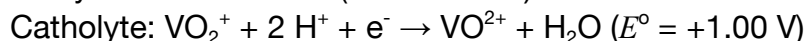
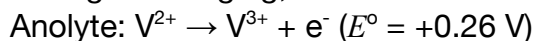
13.5.13. Redox Flow Batteries (RFBs, Redox Cells)

Redox flow batteries use continuous circulation of reactant solutions (anolyte/negolyte and catholyte/posolyte), like a rechargeable fuel cell. RFBs have been projected as useful for large grid-scale energy storage.



Vanadium Ion RFB (1.5 M VSO₄ in 2 M H₂SO₄: near pH 0)

During discharging,



Electrodes: porous carbon electrocatalysts
e.g. graphene, CNTs, WO₃-MWCNTs.

Separator: Nafion ionomer membrane (H⁺ exchange)
VO₂⁺ and VO²⁺ may be represented as V⁵⁺ and V⁴⁺.

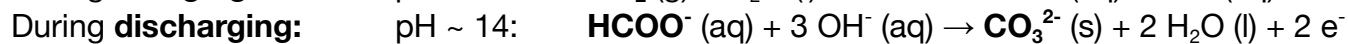
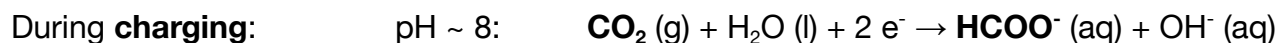
The volumetric flow rate sets the current and power output (up to a limit set by reaction kinetics). The volume of the supply tanks set the energy capacity, up to potentially very large sizes.

RFBs are typically constructed in stacks, with the tank feeding the electrolyte in series (high voltage) or in parallel (high current). Cell balancing by controlling the flow rate is necessary for safe and efficient operation, and state of charge (SoC) monitoring is done using an open-circuit test system to monitor open circuit voltage at the inlet and outlet of the electrolyte. Using a hybrid membrane of tungsten trioxide (WO₃) nanoparticles on graphene with teflon-reinforced Nafion, leakage of cations into the membrane is prevented.

Zinc-Bromine RFB: Zn/Zn²⁺ anolyte and Br₂/Br⁻ catholyte. During charging, zinc metal plates the anode and liquid bromine formation at the cathode. The bromine is corrosive and must be either stored in an organic complexed phase (e.g. *N*-methyl-*N*-ethylmorpholinium bromide, MEMBr), or using a porous monolithic carbon cryogel electrode to alleviate the high partial pressure of bromine. The catholyte flow contains additives to avoid zinc dendrite formation and facilitate uniform deposition.

Carbon Dioxide RFB: carbon negative generation of electricity

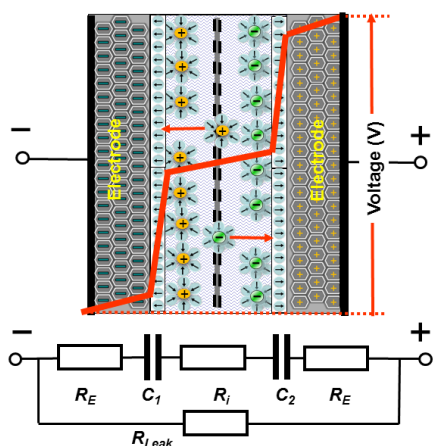
The anolyte reaction is run at different pH during charging/discharging to exploit the variable solubility of CO₂, cogenerating electricity and storing CO₂ as carbonate. The catholyte is Br₂/Br⁻.



The bifunctional anode electrocatalyst can be PdSn on LaCoO₃ perovskite. The high-pH conditions require NaOH which must be sourced sustainably (e.g. renewable chloro-alkali process: electrolysis of seawater desalination brine).

13.5.14. Supercapacitors

A capacitor consists of two high-surface-area inert electrodes separated by an ion-conducting electrolyte. There is a maximum allowable voltage between the electrodes in order to prevent 1) electrolysis and 2) breakdown from occurring, so the electrolyte behaves as a dielectric insulator (as in a regular capacitor) rather than an electrically-conductive medium.



Ions in the electrolyte are attracted to the electrodes, once they have been charged to some degree. The ions form an electrical double layer capacitance (EDLC), allowing the input charge to be stored in the electrodes.

Common electrolytes include salt water, salts in solid polymer matrices, quaternary ammonium salts in organic solvent, or ionic liquids.

Current leakage (self-discharge) can occur over long periods of time, in which charge is gradually depleted due to the finite resistance of the medium.

Energy density [J kg^{-1} or kWh kg^{-1}] depends on the geometry of the device, since the capacitance is dependent on shape and construction.

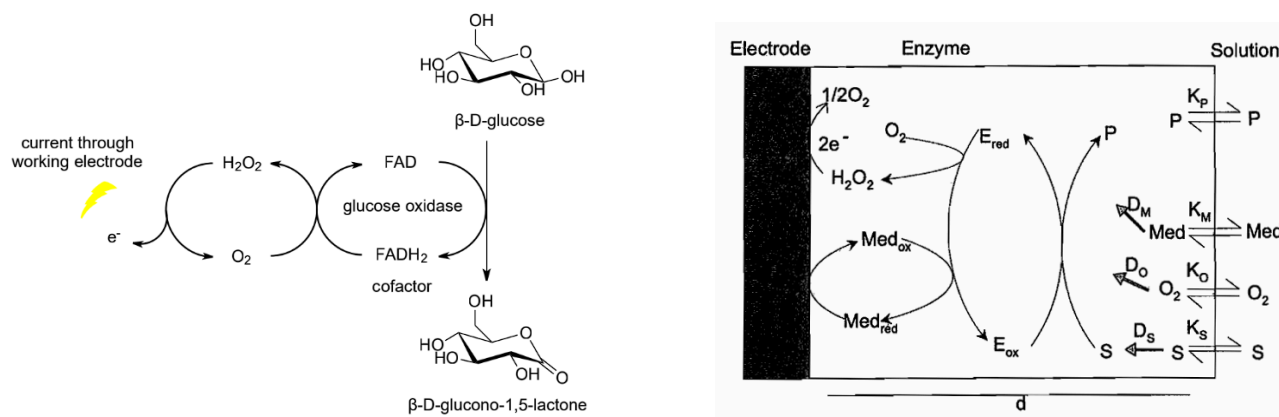
Power density [W kg^{-1}] depends on the impedance of the load it is connected to.

Supercapacitors are useful for energy storage, with high power density [W kg^{-1}] due to rapid charge exchange, but low energy density [$\text{kWh kg}^{-1} \sim \text{J kg}^{-1}$].

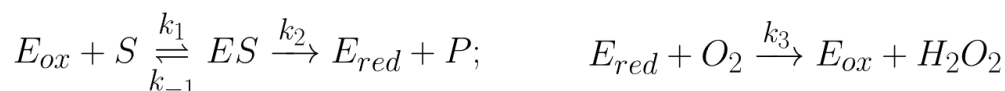
13.5.15. Bioelectrochemistry (Electrochemical Biosensors and Biofuel Cells)

Electrochemical Biosensors: current signal output indicates substrate concentration

An enzyme catalyses a redox reaction with a substrate using a cofactor, and the electrons are transferred to an electrode. The mechanism may involve electron transfer through a mediator molecule acting as a redox couple. Using chronoamperometry (Section 13.5.6), the substrate concentration can be estimated. Example: **glucose biosensor** (below).



For an oxidoreductase enzyme and cofactor (oxidised form: E_{ox} , reduced form: E_{red}) converting analyte/substrate S to product P via a simple oxygen mediator, reactions are:



Rate of oxidoreductase enzyme reaction: $r [\text{mol dm}^{-3} \text{ s}^{-1}] = -\frac{d[S]}{dt} = k_2[E_{total}] \frac{[S]}{K_M + [S]}$.

Enzyme current: $I_{enz} [\text{A cm}^{-2}] = nFd k_2 [E_{total}] \frac{[S]}{K_M + [S]}$ (d : enzyme layer thickness, n : electrons)

- For $[S] \gg K_M$, I_{enz} levels off to a maximum: $I_{max} = nFd k_2 [E_{total}]$
- For $[S] < K_M$, $I_{enz}([S])$ is approximately linear: $I_{enz}([S]) \approx \frac{I_{max}}{K_M} [S]$ (else: $\frac{I_{enz}}{I_{max}} = \frac{[S]}{K_M + [S]}$)

Under steady-state diffusion-limited conditions, $I_d = \frac{nFD[S]}{d}$ (linear).

For best calibration, set $\frac{D}{d^2} = \frac{k_2[E_{total}]}{K_M}$ so that I_d is linear with gradient equal to $\frac{dI_{enz}}{d[S]}$ at $[S] = 0$.

Under this constraint, $\frac{I_d}{I_{max}} = \frac{D}{d^2 k_2 [E_{total}]} [S]$ has a linear response.

The sensor is then linear for $[S] < K_M$. Too far outside this range would underestimate the concentration. The effective K_M can be tuned by diffusion-limiting membranes.

When a current is produced during operation in the working electrode, the biosensor circuitry detects the signal (transimpedance amplifier and ADC, Section 8.7.8), and after digital filtering (DSPs) the analyte concentration is computed (microcontroller).

Biosensors are used to detect e.g. glucose, lactate, cholesterol, urea and HbA1c (glycated haemoglobin) in biomedical diagnostics and monitoring. They can be coupled with control systems (e.g. insulin autoinjectors to treat type 1 diabetes).

Biofuel Cells: produced electricity is used as a power source

Biofuel cells are based on the same principle as the biosensor, with the aim of delivering high electrical power rather than linear responsiveness.

Organic fuel (e.g. glucose) can be oxidised in the enzymatic reaction to produce current through the electrode. Alternatively, the enzymatic reaction may be chosen to form a secondary fuel as a product from a substrate (e.g. hydrogen), which can be passed to a conventional fuel cell to cogenerate electricity. Microbial cells have also been used in this arrangement.

Performance Optimisation

Protein engineering techniques (Section 17.4.5) can be used to optimise the properties of the enzyme used in the device e.g. thermostabilisation, faster kinetics, higher specificity...

Using cofactors with lower reduction potentials (e.g. ferrocene/ferrocenium) helps to prevent unwanted oxidation of interferents in biofluids e.g. ascorbic acid in blood. Measuring from the blood requires diffusion coefficient correction due to hematocrit h : $D' = D_0 (1 - h) / (1 + 0.952h)$.

Mediators may have poor electron transfer kinetics and are often toxic, motivating the 'third generation biosensors', which do not use mediators, and electrons are directly transferred from the cofactor to a nanofunctionalised electrode (e.g. conducting polymer/CNT surface). These can be prepared using electrodeposition during cyclic voltammetry and can be used for continuous implantable *in vivo* blood glucose monitors.

Enzyme-free biosensors have also been developed using electro-oxidation to drive the reaction with a transition metal complex replacing the cofactor with direct electron transfer to a nanomaterial matrix. These are the 'fourth generation biosensors'. However, they have poor selectivity and can require unsuitable chemical conditions (e.g. high pH).

13.5.15. Electrolysis and Electrolytic Cells

Electrolysis with Inert Electrodes: ions in liquid or solution discharge at electrodes

Inert electrodes (e.g. graphite, platinum, carbon nanotubes) are conductive and polarisable. They develop static surface charges (like a capacitor) when an external DC EMF is applied. These charges are used as electron sources and sinks to facilitate redox reactions with the electrolyte, which results in a continuous current flow as the reactions proceed.

For the electrolysis of **molten** (pure anhydrous) ionic salts X^+Y^- (l),

- the **cation** X^+ is **reduced** to its elemental form at the **cathode** (-ve electrode)
- the **anion** Y^- is **oxidised** to its elemental form at the **anode** (+ve electrode)

For the electrolysis of **aqueous** ionic salts X^+Y^- (aq), neglecting overpotential effects:

- If $E^\ominus(X) < E^\ominus(H_2O)$ then **water is reduced** to H_2 and OH^- (X less reactive than H_2)
- If $E^\ominus(O_2) < E^\ominus(Y)$ then **water is oxidised** to O_2 and H^+ (typically: oxyanions)
- Otherwise, the same rules apply as in the electrolysis of molten X^+Y^- (l).

The reduction potentials of oxygen and water are $E^\ominus(H_2O) = -0.83$ V and $E^\ominus(O_2) = +1.23$ V.

Simple metal reactivity series: **K > Na > Li > Ca > Mg > Al > C > Zn > Fe > H₂ > Cu > Ag > Au > Pt**
(for aqueous electrolysis: **metal more reactive than H₂: produces H₂ (g) at the cathode; otherwise produces the metal**)

Quantitative electrolysis: $I = nrF$ (I : current [A], r : reaction rate [mol s⁻¹], $F = 96500$ C mol⁻¹)

Examples:

Electrolyte	Anode product	Cathode product
NaCl (l)	$2 Cl^- (l) \rightarrow Cl_2 (g) + 2 e^-$	$Na^+ (l) + e^- \rightarrow Na (s)$
NaCl (aq) or HCl (aq)	$2 Cl^- (l) \rightarrow Cl_2 (g) + 2 e^-$	$2 H_2O (l) + 2 e^- \rightarrow H_2 (g) + 2 OH^- (aq)$
CuBr ₂ (aq)	$2 Br^- (l) \rightarrow Br_2 (g) + 2 e^-$	$Cu^{2+} (aq) + 2 e^- \rightarrow Cu (s)$
H ₂ SO ₄ (aq)	$4 OH^- (aq) \rightarrow O_2 (g) + 2 H_2O (l) + 4 e^-$	$2 H^+ (aq) + 2 e^- \rightarrow H_2 (g)$

Electrolysis with Reactive Electrodes: ions compete with electrode to react

Examples:

Anode	Cathode	Electrolyte	Anode product	Cathode product
Cu	Cu	CuSO ₄ (aq)	$Cu \rightarrow Cu^{2+} + 2 e^-$	$Cu^{2+} + 2 e^- \rightarrow Cu$
Ag	any metal	AgNO ₃ (aq)	$Ag \rightarrow Ag^+ + e^-$	$Ag^+ + e^- \rightarrow Ag$

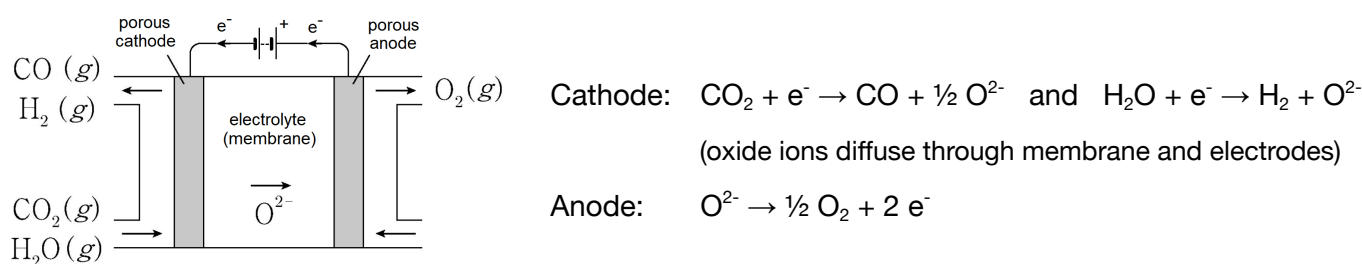
The silver nitrate with silver anode is used for electroplating, as the cathode is covered in silver.

13.5.16. Solid Oxide Electrolysis Cells (SOECs)

SOECs use a solid electrolyte instead of water. They allow for high current density, high efficiency and good stability. A common use is in high-temperature steam electrolysis (HTE), which performs the water-splitting reaction on steam at efficiencies of ~80%, higher than at room temperature.

To minimise energy input, the heat source to provide the temperature can come from the output of a suitably integrated system, such as the steam tube of a combined-cycle gas turbine (heat recovery, Section 7.2.13), cogeneration (CHP), or the water circuit of an LWR nuclear power plant.

Another application is the high-temperature co-electrolysis with carbon dioxide for its removal:



The CO_2 can be sourced from carbon capture schemes, while the $\text{H}_2 + \text{CO}$ product is syngas and can be converted to methane (synfuel) via Fischer-Tropsch synthesis (Section 14.2.1). In order to minimise net carbon emissions, the electrical power input as well as the heat source for the high temperature must be supplied from sustainable sources.

The electrodes are made of porous oxide composites. Common anode materials are nickel-YSZ (yttria stabilised zirconia, $\text{Ni-Y}_2\text{O}_3\text{-ZrO}_2$), or perovskites. A common cathode material is LSM (lanthanum strontium manganite, $\text{La}_{1-x}\text{Sr}_x\text{MnO}_3$). The high temperatures (~700 °C) can lead to degradation of the mechanical properties of these materials.

Solid oxide fuel cells (SOFCs) use similar materials for the reverse process, as a fuel cell.

Reversible solid oxide cells (rSOCs) use bifunctional electrolytes to allow fuel cell and electrolysis processes to take place in the same device, and are versatile load balancing components to achieve high energy efficiency in power plants.

13.5.17. Limiting Molar Ionic Conductivities Table

Cations: (values of λ^0 are given in $\text{S cm}^2 \text{ mol}^{-1}$, measured at 298 K (25 °C))

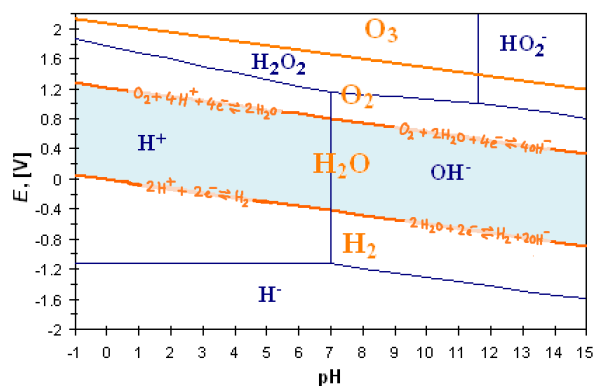
Ion (1+)	λ^0	Ion (1+)	λ^0	Ion (2+)	λ^0
H^+ (as H_3O^+)	349.6	$(\text{CH}_3)_3\text{NH}^+$	47.2	Zn^{2+}	108.6
Li^+	38.7	$(\text{CH}_3)_4\text{N}^+$	44.9	Pb^{2+}	142.0
Na^+	50.08	$\text{C}_5\text{H}_{12}\text{N}^+$	37.2	UO_2^{2+}	64
K^+	73.50	Ion (2+)	λ^0	Ion (3+)	λ^0
Rb^+	77.8	Be^{2+}	90	Al^{3+}	183
Cs^+	77.2	Mg^{2+}	106.0	Fe^{3+}	204
Ag^+	61.9	Ca^{2+}	119.0	La^{3+}	209.1
NH_4^+	73.5	Sr^{2+}	118.9	Ce^{3+}	209.4
$\text{CH}_3\text{CH}_2\text{NH}_3^+$	47.2	Ba^{2+}	127.2		
$(\text{CH}_3\text{CH}_2)_2\text{NH}_2^+$	42.0	Mn^{2+}	106.2		
$(\text{CH}_3\text{CH}_2)_3\text{NH}^+$	34.3	Fe^{2+}	108.0		
$(\text{CH}_3\text{CH}_2)_4\text{N}^+$	32.6	Co^{2+}	105.6		
$(\text{CH}_3\text{CH}_2\text{CH}_2\text{CH}_2)_4\text{N}^+$	19.5	Ni^{2+}	107.0		
$(\text{CH}_3)_2\text{NH}_2^+$	51.8	Cu^{2+}	107.2		

Anions: (values of λ^0 are given in $\text{S cm}^2 \text{ mol}^{-1}$, measured at 298 K (25 °C))

Ion (1-)	λ^0	Ion (1-)	λ^0	Ion (2-)	λ^0
OH^-	199.1	IO_4^-	54.5	CO_3^{2-}	138.6
F^-	55.4	HCO_3^-	44.5	HPO_4^{2-}	66
Cl^-	76.35	H_2PO_4^-	57	SO_4^{2-}	160.0
Br^-	78.1	HSO_4^-	50	$\text{C}_2\text{O}_4^{2-}$	148.2
I^-	76.8	HC_2O_4^-	40.2	Ion (3-)	λ^0
NO_2^-	71.8	HCOO^-	54.6	PO_4^{3-}	207
NO_3^-	71.46	CH_3COO^-	40.9	$\text{Fe}(\text{CN})_6^{3-}$	302.7
ClO_3^-	64.6	$\text{C}_6\text{H}_5\text{COO}^-$	32.4	Ion (4-)	λ^0
ClO_4^-	67.3			$\text{Fe}(\text{CN})_6^{4-}$	442.0

The values of λ for H^+ (aq) and OH^- (aq) are higher due to ion-hopping mechanisms (Section 13.5.4), in which solvent water molecule clusters exchange protons and hydroxyl groups.

13.5.18. Pourbaix Diagrams (Electrochemical Phase Diagrams)



Pourbaix diagram of water: all E against SHE

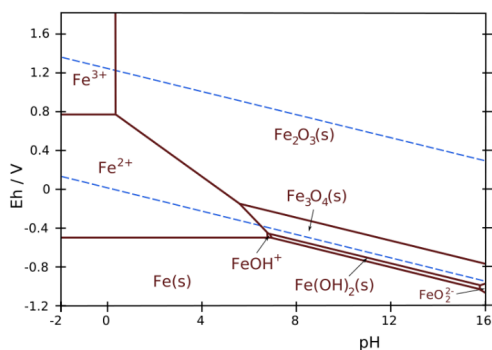
Thermodynamically stable products shown in orange.
Corresponding redox agents shown in blue.

Above the upper limit for H_2O , oxygen gas is formed.
Below the lower limit for H_2O , hydrogen gas is formed.

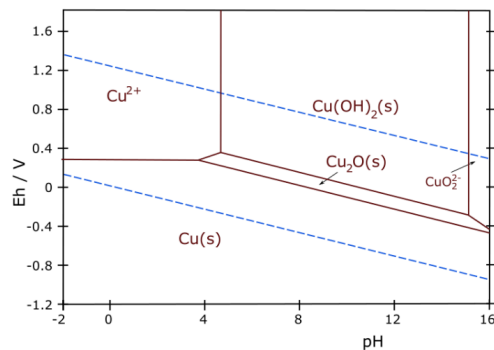
H_2O limit bounds: $0 < E + 0.0592 \text{ pH} < 1.229$.

Pourbaix diagrams for metals: upper (oxidation) and lower (reduction) H_2O limits in dotted lines.

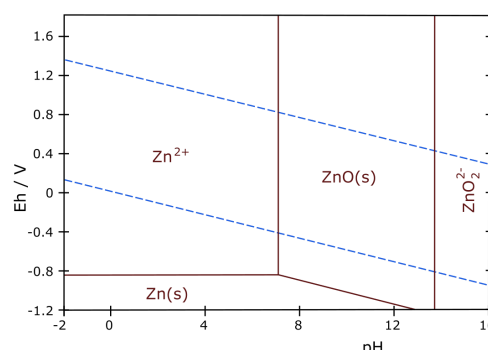
If the thermodynamically stable species is solid, then a film of this species plates the metal and renders it immune to further corrosion (i.e. the metal is passivated, Section 13.5.20). If the stable species is aqueous, the metal dissolves to form this ion, and the metal is corroded. Kinetics (solubility) may result in a thermodynamically stable oxide still failing to prevent corrosion.



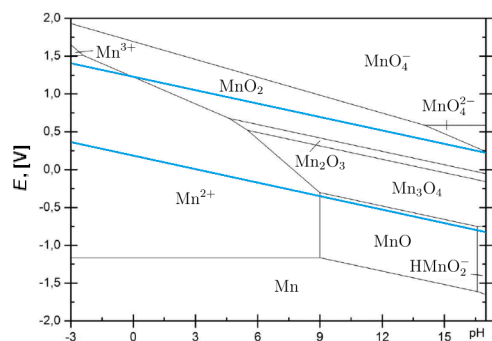
Iron (Fe)



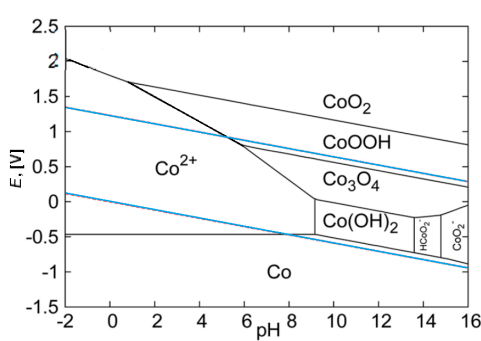
Copper (Cu)



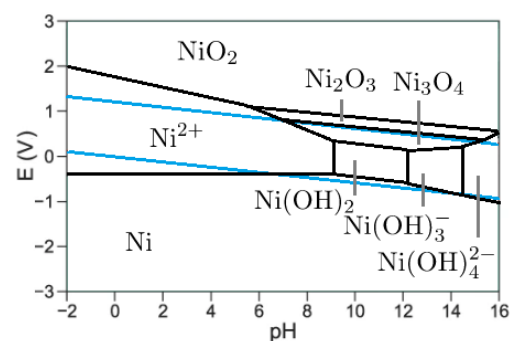
Zinc (Zn)



Manganese (Mn)



Cobalt (Co)



Nickel (Ni)

13.5.19. Standard Electrode Potentials (Reduction Potentials, E^\ominus , Relative to SHE)Sorted from highest to lowest E^\ominus :

$\text{H}_2\text{XeO}_6 + 2\text{H}^+ + 2\text{e}^- \rightarrow \text{XeO}_3 + 3\text{H}_2\text{O}$	+3.0	$\text{Hg}_2\text{SO}_4 + 2\text{e}^- \rightarrow 2\text{Hg} + \text{SO}_4^{2-}$	+0.62
$\text{F}_2 + 2\text{e}^- \rightarrow 2\text{F}^-$	+2.87	$\text{MnO}_4^{2-} + 2\text{H}_2\text{O} + 2\text{e}^- \rightarrow \text{MnO}_2 + 4\text{OH}^-$	+0.60
$\text{O}_3 + 2\text{H}^+ + 2\text{e}^- \rightarrow \text{O}_2 + \text{H}_2\text{O}$	+2.07	$\text{MnO}_4^- + \text{e}^- \rightarrow \text{MnO}_4^{2-}$	+0.56
$\text{S}_2\text{O}_8^{2-} + 2\text{e}^- \rightarrow 2\text{SO}_4^{2-}$	+2.05	$\text{I}_2 + 2\text{e}^- \rightarrow 2\text{I}^-$	+0.54
$\text{Ag}^+ + \text{e}^- \rightarrow \text{Ag}$	+1.98	$\text{Cu}^+ + \text{e}^- \rightarrow \text{Cu}$	+0.52
$\text{Co}^{3+} + \text{e}^- \rightarrow \text{Co}^{2+}$	+1.81	$\text{I}_3^- + 2\text{e}^- \rightarrow 3\text{I}^-$	+0.53
$\text{H}_2\text{O}_2 + 2\text{H}^+ + 2\text{e}^- \rightarrow 2\text{H}_2\text{O}$	+1.78	$\text{NiOOH} + \text{H}_2\text{O} + \text{e}^- \rightarrow \text{Ni(OH)}_2 + \text{OH}^-$	+0.49
$\text{Au}^+ + \text{e}^- \rightarrow \text{Au}$	+1.69	$\text{Ag}_2\text{CrO}_4 + 2\text{e}^- \rightarrow 2\text{Ag} + \text{CrO}_4^{2-}$	+0.45
$\text{Pb}^{4+} + 2\text{e}^- \rightarrow \text{Pb}^{2+}$	+1.67	$\text{O}_2 + 2\text{H}_2\text{O} + 4\text{e}^- \rightarrow 4\text{OH}^-$	+0.40
$2\text{HClO} + 2\text{H}^+ + 2\text{e}^- \rightarrow \text{Cl}_2 + 2\text{H}_2\text{O}$	+1.63	$\text{ClO}_4^- + \text{H}_2\text{O} + 2\text{e}^- \rightarrow \text{ClO}_3^- + 2\text{OH}^-$	+0.36
$\text{Ce}^{4+} + \text{e}^- \rightarrow \text{Ce}^{3+}$	+1.61	$[\text{Fe(CN)}_6]^{3+} + \text{e}^- \rightarrow [\text{Fe(CN)}_6]^{4-}$	+0.36
$2\text{HBrO} + 2\text{H}^+ + 2\text{e}^- \rightarrow \text{Br}_2 + 2\text{H}_2\text{O}$	+1.60	$\text{Cu}^{2+} + 2\text{e}^- \rightarrow \text{Cu}$	+0.34
$\text{MnO}_4^- + 8\text{H}^+ + 5\text{e}^- \rightarrow \text{Mn}^{2+} + 4\text{H}_2\text{O}$	+1.51	$\text{Hg}_2\text{Cl}_2 + 2\text{e}^- \rightarrow 2\text{Hg} + 2\text{Cl}^-$	+0.27
$\text{Mn}^{3+} + \text{e}^- \rightarrow \text{Mn}^{2+}$	+1.51	$\text{AgCl} + \text{e}^- \rightarrow \text{Ag} + \text{Cl}^-$	+0.22
$\text{Au}^{3+} + 3\text{e}^- \rightarrow \text{Au}$	+1.40	$\text{Bi} + 3\text{e}^- \rightarrow \text{Bi}$	+0.20
$\text{Cl}_2 + 2\text{e}^- \rightarrow 2\text{Cl}^-$	+1.36	$\text{Cu}^{2+} + \text{e}^- \rightarrow \text{Cu}^+$	+0.16
$\text{Cr}_2\text{O}_7^{2-} + 14\text{H}^+ + 6\text{e}^- \rightarrow 2\text{Cr}^{3+} + 7\text{H}_2\text{O}$	+1.33	$\text{Sn}^{4+} + 2\text{e}^- \rightarrow \text{Sn}^{2+}$	+0.15
$\text{O}_3 + \text{H}_2\text{O} + 2\text{e}^- \rightarrow \text{O}_2 + 2\text{OH}^-$	+1.24	$\text{AgBr} + \text{e}^- \rightarrow \text{Ag} + \text{Br}^-$	+0.07
$\text{O}_2 + 4\text{H}^+ + 4\text{e}^- \rightarrow 2\text{H}_2\text{O}$	+1.23	$\text{Ti}^{4+} + \text{e}^- \rightarrow \text{Ti}^{3+}$	0.00
$\text{ClO}_4^- + 2\text{H}^+ + 2\text{e}^- \rightarrow \text{ClO}_3^- + \text{H}_2\text{O}$	+1.23	$2\text{H}^+ + 2\text{e}^- \rightarrow \text{H}_2$	0, by definition
$\text{MnO}_2 + 4\text{H}^+ + 2\text{e}^- \rightarrow \text{Mn}^{2+} + 2\text{H}_2\text{O}$	+1.23	$\text{Fe}^{3+} + 3\text{e}^- \rightarrow \text{Fe}$	-0.04
$\text{Br}_2 + 2\text{e}^- \rightarrow 2\text{Br}^-$	+1.09	$\text{O}_2 + \text{H}_2\text{O} + 2\text{e}^- \rightarrow \text{HO}_2^- + \text{OH}^-$	-0.08
$\text{Pu}^{4+} + \text{e}^- \rightarrow \text{Pu}^{3+}$	+0.97	$\text{Pb}^{2+} + 2\text{e}^- \rightarrow \text{Pb}$	-0.13
$\text{NO}_3^- + 4\text{H}^+ + 3\text{e}^- \rightarrow \text{NO} + 2\text{H}_2\text{O}$	+0.96	$\text{In}^+ + \text{e}^- \rightarrow \text{In}$	-0.14
$2\text{Hg}_2^{2+} + 2\text{e}^- \rightarrow \text{Hg}_2^{2+}$	+0.92	$\text{Sn}^{2+} + 2\text{e}^- \rightarrow \text{Sn}$	-0.14
$\text{ClO}^- + \text{H}_2\text{O} + 2\text{e}^- \rightarrow \text{Cl}^- + 2\text{OH}^-$	+0.89	$\text{AgI} + \text{e}^- \rightarrow \text{Ag} + \text{I}^-$	-0.15
$\text{Hg}_2^{2+} + 2\text{e}^- \rightarrow \text{Hg}$	+0.86	$\text{Ni}^{2+} + 2\text{e}^- \rightarrow \text{Ni}$	-0.23
$\text{NO}_3^- + 2\text{H}^+ + \text{e}^- \rightarrow \text{NO}_2 + \text{H}_2\text{O}$	+0.80	$\text{Co}^{2+} + 2\text{e}^- \rightarrow \text{Co}$	-0.28
$\text{Ag}^+ + \text{e}^- \rightarrow \text{Ag}$	+0.80	$\text{In}^{3+} + 3\text{e}^- \rightarrow \text{In}$	-0.34
$\text{Hg}_2^{2+} + 2\text{e}^- \rightarrow 2\text{Hg}$	+0.79	$\text{Tl}^+ + \text{e}^- \rightarrow \text{Tl}$	-0.34
$\text{Fe}^{3+} + \text{e}^- \rightarrow \text{Fe}^{2+}$	+0.77	$\text{PbSO}_4 + 2\text{e}^- \rightarrow \text{Pb} + \text{SO}_4^{2-}$	-0.36
$\text{BrO}^- + \text{H}_2\text{O} + 2\text{e}^- \rightarrow \text{Br}^- + 2\text{OH}^-$	+0.76	$\text{V}^{2+} + 2\text{e}^- \rightarrow \text{V}$	-1.19
$\text{Ti}^{3+} + \text{e}^- \rightarrow \text{Ti}^{2+}$	-0.37	$\text{Ti}^{2+} + 2\text{e}^- \rightarrow \text{Ti}$	-1.63
$\text{Cd}^{2+} + 2\text{e}^- \rightarrow \text{Cd}$	-0.40	$\text{Al}^{3+} + 3\text{e}^- \rightarrow \text{Al}$	-1.66
$\text{In}^{2+} + \text{e}^- \rightarrow \text{In}^+$	-0.40	$\text{U}^{3+} + 3\text{e}^- \rightarrow \text{U}$	-1.79
$\text{Cr}^{3+} + \text{e}^- \rightarrow \text{Cr}^{2+}$	-0.41	$\text{Sc}^{3+} + 3\text{e}^- \rightarrow \text{Sc}$	-2.09
$\text{Fe}^{2+} + 2\text{e}^- \rightarrow \text{Fe}$	-0.44	$\text{Mg}^{2+} + 2\text{e}^- \rightarrow \text{Mg}$	-2.36
$\text{In}^{3+} + 2\text{e}^- \rightarrow \text{In}^+$	-0.44	$\text{Ce}^{3+} + 3\text{e}^- \rightarrow \text{Ce}$	-2.48
$\text{S} + 2\text{e}^- \rightarrow \text{S}^{2-}$	-0.48	$\text{La}^{3+} + 3\text{e}^- \rightarrow \text{La}$	-2.52
$\text{In}^{3+} + \text{e}^- \rightarrow \text{In}^{2+}$	-0.49	$\text{Na}^+ + \text{e}^- \rightarrow \text{Na}$	-2.71
$\text{U}^{4+} + \text{e}^- \rightarrow \text{U}^{3+}$	-0.61	$\text{Ca}^{2+} + 2\text{e}^- \rightarrow \text{Ca}$	-2.87
$\text{Cr}^{3+} + 3\text{e}^- \rightarrow \text{Cr}$	-0.74	$\text{Sr}^{2+} + 2\text{e}^- \rightarrow \text{Sr}$	-2.89
$\text{Zn}^{2+} + 2\text{e}^- \rightarrow \text{Zn}$	-0.76	$\text{Ba}^{2+} + 2\text{e}^- \rightarrow \text{Ba}$	-2.91
$\text{Cd(OH)}_2 + 2\text{e}^- \rightarrow \text{Cd} + 2\text{OH}^-$	-0.81	$\text{Ra}^{2+} + 2\text{e}^- \rightarrow \text{Ra}$	-2.92
$2\text{H}_2\text{O} + 2\text{e}^- \rightarrow \text{H}_2 + 2\text{OH}^-$	-0.83	$\text{Cs}^+ + \text{e}^- \rightarrow \text{Cs}$	-2.92
$\text{Cr}^{2+} + 2\text{e}^- \rightarrow \text{Cr}$	-0.91	$\text{Rb}^+ + \text{e}^- \rightarrow \text{Rb}$	-2.93
$\text{Mn}^{2+} + 2\text{e}^- \rightarrow \text{Mn}$	-1.18	$\text{K}^+ + \text{e}^- \rightarrow \text{K}$	-2.93
		$\text{Li}^+ + \text{e}^- \rightarrow \text{Li}$	-3.05

Sorted from A-Z:

$\text{Ag}^+ + \text{e}^- \rightarrow \text{Ag}$	+0.80	$\text{Ca}^{2+} + 2\text{e}^- \rightarrow \text{Ca}$	-2.87
$\text{Ag}^{2+} + \text{e}^- \rightarrow \text{Ag}^+$	+1.98	$\text{Cd(OH)}_2 + 2\text{e}^- \rightarrow \text{Cd} + 2\text{OH}^-$	-0.81
$\text{AgBr} + \text{e}^- \rightarrow \text{Ag} + \text{Br}^-$	+0.0713	$\text{Cd}^{2+} + 2\text{e}^- \rightarrow \text{Cd}$	-0.40
$\text{AgCl} + \text{e}^- \rightarrow \text{Ag} + \text{Cl}^-$	+0.22	$\text{Ce}^{3+} + 3\text{e}^- \rightarrow \text{Ce}$	-2.48
$\text{Ag}_2\text{CrO}_4 + 2\text{e}^- \rightarrow 2\text{Ag} + \text{CrO}_4^{2-}$	+0.45	$\text{Ce}^{4+} + \text{e}^- \rightarrow \text{Ce}^{3+}$	+1.61
$\text{AgF} + \text{e}^- \rightarrow \text{Ag} + \text{F}^-$	+0.78	$\text{Cl}_2 + 2\text{e}^- \rightarrow 2\text{Cl}^-$	+1.36
$\text{AgI} + \text{e}^- \rightarrow \text{Ag} + \text{I}^-$	-0.15	$\text{ClO}^- + \text{H}_2\text{O} + 2\text{e}^- \rightarrow \text{Cl}^- + 2\text{OH}^-$	+0.89
$\text{Al}^{3+} + 3\text{e}^- \rightarrow \text{Al}$	-1.66	$\text{ClO}_4^- + 2\text{H}^+ + 2\text{e}^- \rightarrow \text{ClO}_3^- + \text{H}_2\text{O}$	+1.23
$\text{Au}^+ + \text{e}^- \rightarrow \text{Au}$	+1.69	$\text{ClO}_4^- + \text{H}_2\text{O} + 2\text{e}^- \rightarrow \text{ClO}_3^- + 2\text{OH}^-$	+0.36
$\text{Au}^{3+} + 3\text{e}^- \rightarrow \text{Au}$	+1.40	$\text{Co}^{2+} + 2\text{e}^- \rightarrow \text{Co}$	-0.28
$\text{Ba}^{2+} + 2\text{e}^- \rightarrow \text{Ba}$	+2.91	$\text{Co}^{3+} + \text{e}^- \rightarrow \text{Co}^{2+}$	+1.81
$\text{Be}^{2+} + 2\text{e}^- \rightarrow \text{Be}$	-1.85	$\text{Cr}^{2+} + 2\text{e}^- \rightarrow \text{Cr}$	-0.91
$\text{Bi}^{3+} + 3\text{e}^- \rightarrow \text{Bi}$	+0.20	$\text{Cr}_2\text{O}_7^{2-} + 14\text{H}^+ + 6\text{e}^- \rightarrow 2\text{Cr}^{3+} + 7\text{H}_2\text{O}$	+1.33
$\text{Br}_2 + 2\text{e}^- \rightarrow 2\text{Br}^-$	+1.09	$\text{Cr}^{3+} + 3\text{e}^- \rightarrow \text{Cr}$	-0.74
$\text{BrO}^- + \text{H}_2\text{O} + 2\text{e}^- \rightarrow \text{Br}^- + 2\text{OH}^-$	+0.76	$\text{Cr}^{3+} + \text{e}^- \rightarrow \text{Cr}^{2+}$	-0.41
$\text{Cs}^+ + \text{e}^- \rightarrow \text{Cs}$	-2.92	$\text{MnO}_4^- + 2\text{H}_2\text{O} + 2\text{e}^- \rightarrow \text{MnO}_2 + 4\text{OH}^-$	+0.60
$\text{Cu}^+ + \text{e}^- \rightarrow \text{Cu}$	+0.52	$\text{Na}^+ + \text{e}^- \rightarrow \text{Na}$	-2.71
$\text{Cu}^{2+} + 2\text{e}^- \rightarrow \text{Cu}$	+0.34	$\text{Ni}^{2+} + 2\text{e}^- \rightarrow \text{Ni}$	-0.23
$\text{Cu}^{2+} + \text{e}^- \rightarrow \text{Cu}^+$	+0.16	$\text{NiOOH} + \text{H}_2\text{O} + \text{e}^- \rightarrow \text{Ni(OH)}_2 + \text{OH}^-$	+0.49
$\text{F}_2 + 2\text{e}^- \rightarrow 2\text{F}^-$	+2.87	$\text{NO}_3^- + 2\text{H}^+ + \text{e}^- \rightarrow \text{NO}_2 + \text{H}_2\text{O}$	-0.80
$\text{Fe}^{2+} + 2\text{e}^- \rightarrow \text{Fe}$	-0.44	$\text{NO}_3^- + 4\text{H}^+ + 3\text{e}^- \rightarrow \text{NO} + 2\text{H}_2\text{O}$	+0.96
$\text{Fe}^{3+} + 3\text{e}^- \rightarrow \text{Fe}$	-0.04	$\text{NO}_3^- + \text{H}_2\text{O} + 2\text{e}^- \rightarrow \text{NO}_2^- + 2\text{OH}^-$	+0.10
$\text{Fe}^{3+} + \text{e}^- \rightarrow \text{Fe}^{2+}$	+0.77	$\text{O}_2 + 2\text{H}_2\text{O} + 4\text{e}^- \rightarrow 4\text{OH}^-$	+0.40
$[\text{Fe(CN)}_6]^{3+} + \text{e}^- \rightarrow [\text{Fe(CN)}_6]^{4-}$	+0.36	$\text{O}_2 + 4\text{H}^+ + 4\text{e}^- \rightarrow 2\text{H}_2\text{O}$	+1.23
$2\text{H}^+ + 2\text{e}^- \rightarrow \text{H}_2$	0, by definition	$\text{O}_2 + \text{e}^- \rightarrow \text{O}_2^-$	-0.56
$2\text{H}_2\text{O} + 2\text{e}^- \rightarrow \text{H}_2 + 2\text{OH}^-$	-0.83	$\text{O}_2 + \text{H}_2\text{O} + 2\text{e}^- \rightarrow \text{HO}_2^- + \text{OH}^-$	-0.08
$2\text{HBrO} + 2\text{H}^+ + 2\text{e}^- \rightarrow \text{Br}_2 + 2\text{H}_2\text{O}$	+1.60	$\text{O}_3 + 2\text{H}^+ + 2\text{e}^- \rightarrow \text{O}_2 + \text{H}_2\text{O}$	+2.07
$2\text{HClO} + 2\text{H}^+ + 2\text{e}^- \rightarrow \text{Cl}_2 + 2\text{H}_2\text{O}$	+1.63	$\text{O}_3 + \text{H}_2\text{O} + 2\text{e}^- \rightarrow \text{O}_2 + 2\text{OH}^-$	+1.24
$\text{H}_2\text{O}_2 + 2\text{H}^+ + 2\text{e}^- \rightarrow 2\text{H}_2\text{O}$	+1.78	$\text{Pb}^{2+} + 2\text{e}^- \rightarrow \text{Pb}$	-0.13
$\text{H}_4\text{XeO}_6 + 2\text{H}^+ + 2\text{e}^- \rightarrow \text{XeO}_3 + 3\text{H}_2\text{O}$	+3.0	$\text{Pb}^{4+} + 2\text{e}^- \rightarrow \text{Pb}^{2+}$	+1.67
$\text{Hg}_2^{2+} + 2\text{e}^- \rightarrow 2\text{Hg}$	+0.79	$\text{PbSO}_4 + 2\text{e}^- \rightarrow \text{Pb} + \text{SO}_4^{2-}$	-0.36
$\text{Hg}_2\text{Cl}_2 + 2\text{e}^- \rightarrow 2\text{Hg} + 2\text{Cl}^-$	+0.27	$\text{Pt}^{2+} + 2\text{e}^- \rightarrow \text{Pt}$	+1.20
$\text{Hg}_2^{2+} + 2\text{e}^- \rightarrow \text{Hg}$	+0.86	$\text{Pu}^{4+} + \text{e}^- \rightarrow \text{Pu}^{3+}$	+0.97
$2\text{Hg}_2^{2+} + 2\text{e}^- \rightarrow \text{Hg}_2^{2+}$	+0.92	$\text{Ra}^{2+} + 2\text{e}^- \rightarrow \text{Ra}$	-2.92
$\text{Hg}_2\text{SO}_4 + 2\text{e}^- \rightarrow 2\text{Hg} + \text{SO}_4^{2-}$	+0.62	$\text{Rb}^+ + \text{e}^- \rightarrow \text{Rb}$	-2.93
$\text{I}_2 + 2\text{e}^- \rightarrow 2\text{I}^-$	+0.54	$\text{S} + 2\text{e}^- \rightarrow \text{S}^{2-}$	-0.48
$\text{I}_3^- + 2\text{e}^- \rightarrow 3\text{I}^-$	+0.53	$\text{S}_2\text{O}_8^{2-} + 2\text{e}^- \rightarrow 2\text{SO}_4^{2-}$	+2.05
$\text{In}^+ + \text{e}^- \rightarrow \text{In}$	-0.14	$\text{Sc}^{3+} + 3\text{e}^- \rightarrow \text{Sc}$	-2.09
$\text{In}^{2+} + \text{e}^- \rightarrow \text{In}^+$	-0.40	$\text{Sn}^{2+} + 2\text{e}^- \rightarrow \text{Sn}$	-0.14
$\text{In}^{3+} + 2\text{e}^- \rightarrow \text{In}^+$	-0.34	$\text{Sn}^{4+} + 2\text{e}^- \rightarrow \text{Sn}^{2+}$	+0.15
$\text{In}^{3+} + \text{e}^- \rightarrow \text{In}^{2+}$	-0.49	$\text{Sr}^{2+} + 2\text{e}^- \rightarrow \text{Sr}$	-2.89
$\text{K}^+ + \text{e}^- \rightarrow \text{K}$	-2.93	$\text{Ti}^{2+} + 2\text{e}^- \rightarrow \text{Ti}$	-1.63
$\text{La}^{3+} + 3\text{e}^- \rightarrow \text{La}$	-2.52	$\text{Ti}^{3+} + \text{e}^- \rightarrow \text{Ti}^{2+}$	-0.37
$\text{Li} + \text{e}^- \rightarrow \text{Li}$	-3.05	$\text{Ti}^{4+} + \text{e}^- \rightarrow \text{Ti}^{3+}$	0.00
$\text{Mg}^{2+} + 2\text{e}^- \rightarrow \text{Mg}$	-2.36	$\text{Tl}^+ + \text{e}^- \rightarrow \text{Tl}$	-0.34
$\text{Mn}^{2+} + 2\text{e}^- \rightarrow \text{Mn}$	-1.18	$\text{U}^{3+} + 3\text{e}^- \rightarrow \text{U}$	-1.79
$\text{Mn}^{3+} + \text{e}^- \rightarrow \text{Mn}^{2+}$	+1.51	$\text{U}^{4+} + \text{e}^- \rightarrow \text{U}^{3+}$	-0.61
$\text{MnO}_2 + 4\text{H}^+ + 2\text{e}^- \rightarrow \text{Mn}^{2+} + 2\text{H}_2\text{O}$	+1.23	$\text{V}^{2+} + 2\text{e}^- \rightarrow \text{V}$	-1.19
$\text{MnO}_4^- + 8\text{H}^+ + 5\text{e}^- \rightarrow \text{Mn}^{2+} + 4\text{H}_2\text{O}$	+1.51	$\text{V}^{3+} + \text{e}^- \rightarrow \text{V}^{2+}$	-0.26
$\text{MnO}_4^- + \text{e}^- \rightarrow \text{MnO}_4^{2-}$	+0.56	$\text{Zn}^{2+} + 2\text{e}^- \rightarrow \text{Zn}$	-0.76

13.6. Acid-Base Chemistry

13.6.1. Acids and Bases

Theory of acids and bases:

	Acid	Base
Lewis Theory	lone pair acceptor	lone pair donor
Brønsted-Lowry Theory	proton donor	proton acceptor

For a general Brønsted-Lowry acid-base equilibrium $HA + B \rightleftharpoons A^- + BH^+$,

- A^- is the conjugate base of HA
- BH^+ is the conjugate acid of B
- HA is reduced to A^-
- B is oxidised to BH^+

If HA and B are the same molecule then this is a self-ionisation reaction and the compound is said to be amphoteric (simultaneous oxidation and reduction).

Measures of acidity and basicity in aqueous solutions are:

- $pH = -\log_{10} [H^+]$ ('protons' are in fact hydronium ions, H_3O^+ (aq))
- $pOH = -\log_{10} [OH^-]$
- $pH + pOH = pK_w$ of water = 14 (for water at 25 °C)

Redox chemistry:

- Oxidation is gain of oxygen / loss of electrons / loss of hydrogen / gain of oxidation state
- Reduction is loss of oxygen / gain of electrons / gain of hydrogen / loss of oxidation state

Strong and weak acids and bases:

- Strong acids and strong bases dissociate completely into ions in aqueous solution.
- Weak acids and weak bases dissociate partially into ions in aqueous solution.

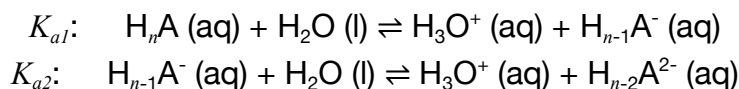
The main strong acids are HCl, HNO_3 , H_2SO_4 , HBr, HI, $HClO_4$, $HClO_3$.

The main strong bases are LiOH, NaOH, KOH, RbOH, CsOH, $Mg(OH)_2^*$, $Ca(OH)_2^*$, $Sr(OH)_2$, $Ba(OH)_2$.

* These substances are usually still considered strong bases despite being sparingly soluble in water. Up to the solubility limit, the compounds dissociate completely into ions (strong electrolyte), whereas a weak base (e.g. $Fe(OH)_3$) would primarily form molecular clusters (in this case, the complex $[Fe(OH)_3(H_2O)_3]$), preventing complete dissociation into free OH^- ions while remaining dissolved.

13.6.2. Dissociation Constants of Weak Acids

The dissociation constants K_a are defined as equilibrium constants for the reaction



...

$$\text{so that } K_{a1}[\text{H}_n\text{A}] = \frac{[\text{H}^+][\text{H}_{n-1}\text{A}^-]}{[\text{H}_n\text{A}]}, \quad K_{a2}[\text{HA}] = K_{a1}[\text{H}_{n-1}\text{A}^-] = \frac{[\text{H}^+][\text{H}_{n-2}\text{A}^{2-}]}{[\text{H}_{n-1}\text{A}^-]}, \dots$$

Values for weak acids (measured at 25 °C unless specified otherwise) are given below.

Name	Formula	K_{a1}	K_{a2}	K_{a3}
Acetic acid	CH ₃ COOH	1.75×10^{-5}	-	-
Arsenic acid	H ₃ AsO ₄	5.5×10^{-3}	1.7×10^{-7}	5.1×10^{-12}
Benzoic acid	C ₆ H ₅ COOH	6.25×10^{-5}	-	-
Boric acid	H ₃ BO ₃	$5.4 \times 10^{-10*}$	$>1 \times 10^{-14*}$	-
Bromoacetic acid	CH ₂ BrCOOH	1.3×10^{-3}	-	-
Carbonic acid	H ₂ CO ₃	4.5×10^{-7}	4.7×10^{-11}	-
Chloroacetic acid	CH ₂ ClCOOH	1.3×10^{-3}	-	-
Chlorous acid	HClO ₂	1.1×10^{-2}	-	-
Chromic acid	H ₂ CrO ₄	1.8×10^{-1}	3.2×10^{-7}	-
Citric acid	C ₆ H ₈ O ₇	7.4×10^{-4}	1.7×10^{-5}	4.0×10^{-7}
Cyanic acid	HCNO	3.5×10^{-4}	-	-
Dichloroacetic acid	CHCl ₂ COOH	4.5×10^{-2}	-	-
Fluoroacetic acid	CH ₂ FCOOH	2.6×10^{-3}	-	-
Formic acid	HCOOH	1.8×10^{-4}	-	-
Hydrazoic acid	HN ₃	2.5×10^{-5}	-	-
Hydrocyanic acid	HCN	6.2×10^{-10}	-	-
Hydrofluoric acid	HF	6.7×10^{-4}	-	-
Hydrogen selenide	H ₂ Se	1.3×10^{-4}	1.0×10^{-11}	-
Hydrogen sulfide	H ₂ S	8.9×10^{-8}	1×10^{-19}	-
Hydrogen telluride	H ₂ Te	$2.5 \times 10^{-3}‡$	1×10^{-11}	-

Dissociation constants of weak acids, continued

Name	Formula	K_{a1}	K_{a2}	K_{a3}
Hypobromous acid	HBrO	2.8×10^{-9}	-	-
Hypochlorous acid	HClO	4.0×10^{-8}	-	-
Hypoiodous acid	HIO	3.2×10^{-11}	-	-
Iodic acid	HIO ₃	1.7×10^{-1}	-	-
Iodoacetic acid	CH ₂ ICOOH	6.6×10^{-4}	-	-
Nitrous acid	HNO ₂	5.6×10^{-4}	-	-
Oxalic acid (ethanedioic acid)	HOOC-COOH	5.6×10^{-2}	1.5×10^{-4}	-
Periodic acid	HIO ₄	2.3×10^{-2}	-	-
Phenol	C ₆ H ₅ OH	1.0×10^{-10}	-	-
Phosphoric acid	H ₃ PO ₄	6.9×10^{-3}	6.2×10^{-8}	4.8×10^{-13}
Phosphorous acid	H ₃ PO ₃	$5.0 \times 10^{-2*}$	$2.0 \times 10^{-7*}$	-
Resorcinol (benzene-1,2-diol)	C ₆ H ₄ (OH) ₂	4.8×10^{-10}	7.9×10^{-12}	-
Selenic acid	H ₂ SeO ₄	(strong)	2.0×10^{-2}	-
Selenious acid	H ₂ SeO ₃	2.4×10^{-3}	4.8×10^{-9}	-
Sulfuric acid	H ₂ SO ₄	(strong)	1.0×10^{-2}	-
Sulfurous acid	H ₂ SO ₃	1.4×10^{-2}	6.3×10^{-8}	-
<i>meso</i> -Tartaric acid (2,3-dihydroxybutanedioic acid)	C ₄ H ₆ O ₆	6.0×10^{-4}	1.4×10^{-5}	-
L(+)-Tartaric acid	C ₄ H ₆ O ₆	1.3×10^{-3}	4.0×10^{-5}	-
Telluric acid	H ₂ TeO ₄	$2.1 \times 10^{-8}‡$	$1.0 \times 10^{-11}‡$	-
Tellurous acid	H ₂ TeO ₃	5.4×10^{-7}	3.7×10^{-9}	-
Trichloroacetic acid	CCl ₃ COOH	2.2×10^{-1}	-	-
Trifluoroacetic acid	CF ₃ COOH	3.0×10^{-1}	-	-

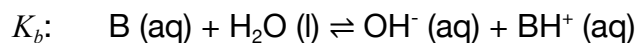
Table notes:

* values are measured at 20 °C. ‡ values are measured at 18 °C.

pK_a: $pK_a = -\log_{10} K_a$ so that acids approach 'strong' as $pK_a \rightarrow -\infty$.

13.6.3. Dissociation Constants of Weak Bases

The dissociation constants K_b are defined as equilibrium constants for the reaction



$$\text{so that } K_b[B] = \frac{[\text{OH}^-][\text{BH}^+]}{[B]}$$

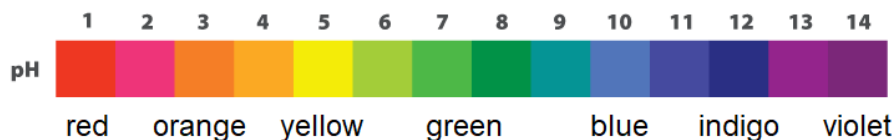
Values for weak bases (measured at 25 °C) are given below.

Name	Formula	K_b
Ammonia	NH_3	1.8×10^{-5}
Aniline	$\text{C}_6\text{H}_5\text{NH}_2$	7.4×10^{-10}
<i>n</i> -Butylamine	$\text{C}_4\text{H}_9\text{NH}_2$	4.0×10^{-4}
<i>sec</i> -Butylamine	$(\text{CH}_3)_2\text{CHCH}_2\text{NH}_2$	3.6×10^{-4}
<i>tert</i> -Butylamine	$(\text{CH}_3)_3\text{CNH}_2$	4.8×10^{-4}
Dimethylamine	$(\text{CH}_3)_2\text{NH}$	5.4×10^{-4}
Ethylamine	$\text{C}_2\text{H}_5\text{NH}_2$	4.5×10^{-4}
Hydrazine	N_2H_4	1.3×10^{-6}
Hydroxylamine	NH_2OH	8.7×10^{-9}
Methylamine	CH_3NH_2	4.6×10^{-4}
Propylamine	$\text{C}_3\text{H}_7\text{NH}_2$	3.5×10^{-4}
Pyridine	$\text{C}_5\text{H}_5\text{N}$	1.7×10^{-9}
Trimethylamine	$(\text{CH}_3)_3\text{N}$	6.3×10^{-5}

$$\text{p}K_b: \quad \text{p}K_b = -\log_{10} K_b$$

13.6.4. Colour Ranges of Indicators

Universal Indicator (Full Range)



Binary Indicators

Indicator	pH Range	Colour in Low pH	Colour in High pH
Thymol Blue	1.2 - 2.8	red	yellow
2,4-Dinitrophenol (2,4-DNP)	2.4 - 4.0	colourless	yellow
Methyl yellow	2.9 - 4.0	red	yellow
Methyl orange	3.1 - 4.4	red	orange
Bromophenol blue	3.0 - 4.6	yellow	indigo
α -Naphthyl red	3.7 - 5.0	red	yellow
Methyl red	4.4 - 6.2	red	yellow
<i>p</i> -Nitrophenol	5.0 - 7.0	colourless	yellow
Phenol red	6.4 - 8.0	yellow	red
α -Naphtholphthalein	7.3 - 8.7	pink	green
Thymol blue	8.0 - 9.6	yellow	blue
Phenolphthalein	8.0 - 10.0	colourless	red
Thymolphthalein	9.4 - 10.6	colourless	blue
Nile blue	10.1 - 11.1	blue	red
Trinitrobenzoic acid	12.0 - 13.4	colourless	orange-red

Indicators for Complexometric Titrations

Concentrations of metal cations (e.g. Ca^{2+}) can be determined using complexometric titrations, in which a chelating solution (e.g. EDTA) removes metal cations from solution. An indicator which changes colour in the presence of these cations can be used to indicate the endpoint, such as:

Indicator	Commonly used cations	Colour without cations	Colour with cations
Eriochrome Black T	Ca^{2+} , Mg^{2+}	blue	red
Calconcarboxylic acid	Ca^{2+} , Mg^{2+}	blue	red
Fast Sulphon Black F	Cu^{2+}	green	purple

13.6.5. Titration Curves

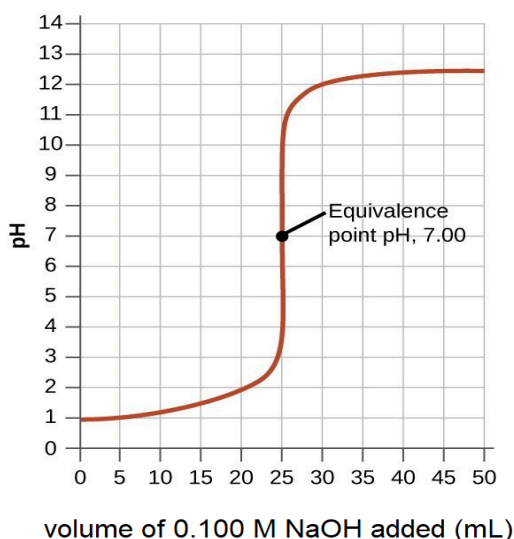
To set up a titration, put the standard solution (titrant, of known concentration) in the burette and the unknown solution (analyte) in the conical flask.

At the equivalence point, moles of acid = moles of base $\rightarrow c_{acid}V_{acid} = c_{base}V_{base}$.

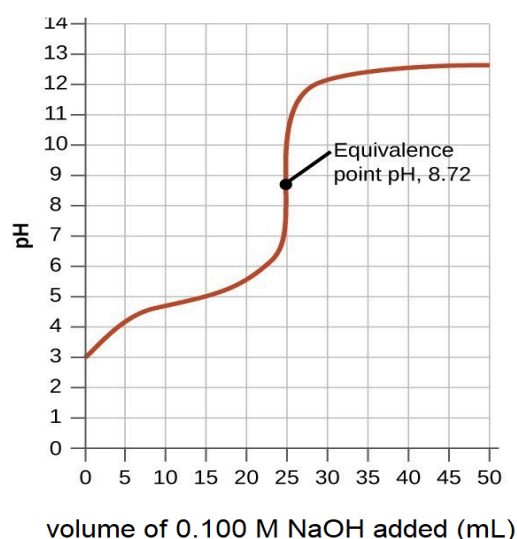
At the half-equivalence point ($V = \frac{V_{acid.eq}}{2}$) for a weak acid titration, $[HA] = [A^-] \rightarrow pH = pK_a$.

Titration curves with single equilibria:

Titration of HCl with NaOH
(strong acid + strong base)

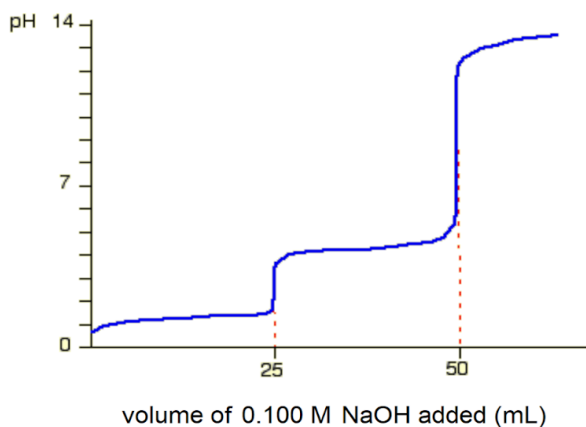


Titration of CH₃COOH with NaOH
(weak acid + strong base)

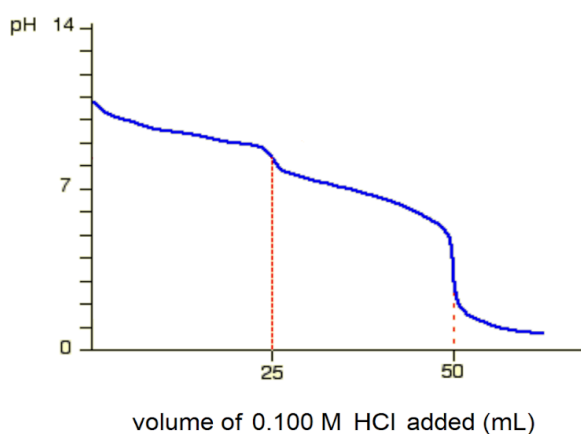


Titrations with multiple equilibria:

Titration of C₂H₄O₂ with NaOH
(weak acid + strong base)



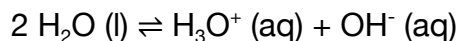
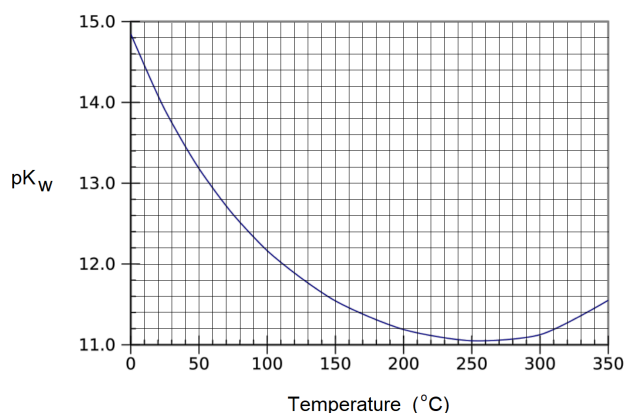
Titration of Na₂CO₃ with HCl
(strong acid + weak base)



13.6.6. Buffers and the Henderson-Hasselbalch Equations

Autoionisation Product of Water

Water is amphoteric: it partially self-ionises into protons and hydroxide ions:



The equilibrium constant (ionic product), $K_w = [\text{H}_3\text{O}^+][\text{OH}^-]$, varies with temperature:

$$pK_w = -\log_{10} K_w \quad \quad \quad pH + pOH = pK_w$$

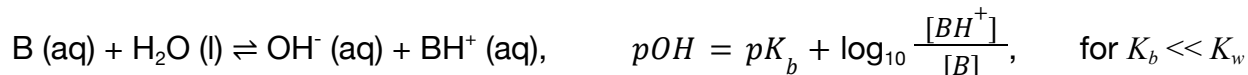
In pure water, $[\text{H}^+] = [\text{H}_3\text{O}^+] = [\text{OH}^-]$, so $K_w = [\text{H}^+]^2$.

At 25 °C, $pK_w = 14$, $K_w = 1 \times 10^{-14} \text{ mol}^2 \text{ dm}^{-6}$.

Weak Acid Buffer: when a weak acid HA is mixed with a salt of its conjugate base A^- , the equilibrium shifts to maintain the value of K_a for the weak acid:



Weak Base Buffer: when a weak base B is mixed with a salt of its conjugate acid BH^+ , the equilibrium shifts to maintain the value of K_b for the weak base.



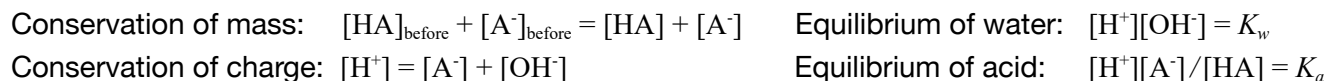
(These are the Henderson-Hasselbalch equations, and can be derived with an 'ICE' table.)

Degree of Dissociation / Ionisation: $\alpha = \frac{[\text{ion}]}{[\text{neutral, initial}]}$ so that $\frac{[\text{neutral}]}{[\text{neutral, initial}]} = 1 - \alpha$.

Percentage Ionisation: $\frac{[\text{ion}]}{[\text{neutral}]} = \frac{\alpha}{1 - \alpha}$ so $\% \text{ ionised} = \alpha = \left(1 + \left(\frac{[\text{ion}]}{[\text{neutral}]} \right)^{-1} \right)^{-1} \times 100\%$.

Calculations with Very Weak Acids or Very Weak Bases

If $pK_a \approx pK_w$, then the autoionisation of water will contribute a significant proportion of the protons to the final pH of the solution, and the above analysis (which typically assumes negligible change of water) is invalid. Therefore, both the equilibrium of the water and of the solute must be considered:



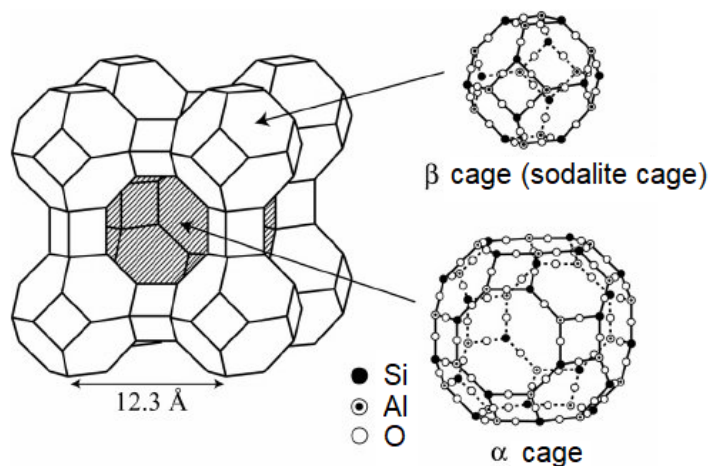
Note that equations are nonlinear (cubic in $[\text{H}^+]$) and therefore require numerical methods to solve.

C14. SURFACE AND PARTICLE CHEMISTRY

14.1. Catalysis

14.1.2. Structures and Applications of Some Inorganic Catalysts

Zeolites



Aluminosilicate Zeolite A

Typical applications of ZSM-5 (pentasil zeolite; zeolite sieve of molecular porosity 5):

- Isomerisation of *meta*-xylene to *para*-xylene.
- Vapour-phase alkylation of benzene with ethene into ethylbenzene.
- Dehydration of alcohols into alkanes.
- Hydrated zeolites are used as ion exchangers in the softening of hard water.

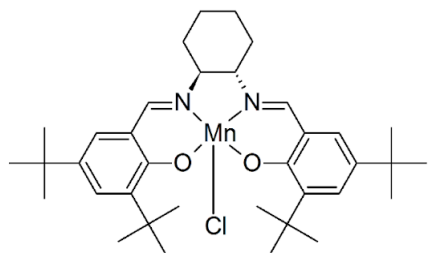
Alkali Metal Catalysts

- Soda lime ($\text{NaOH} + \text{CaO}$): for decarboxylation
- Ziegler-Natta Catalyst ($\text{TiCl}_4 + \text{Al}(\text{CH}_2\text{CH}_3)_3$): for addition polymerisation of ethene

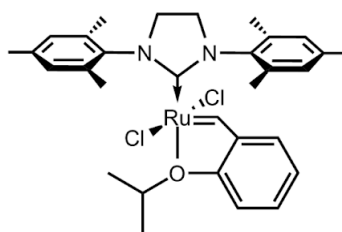
Transition Metal Catalysts

- Raney Nickel (Ra-Ni): for reducing C-S bonds to C-H bonds, or hydrogenation
- Lindlar Catalyst (Pd-BaSO_4 , quinoline): for partial hydrogenation of alkynes
- Palladium on charcoal (Pd-C): for hydrogenation of alkenes
- Sodium-ammonia electride salt ($\text{Na} + \text{NH}_3(l)$; $[\text{Na}(\text{NH}_3)_6]^+e^-$): for the Birch reduction

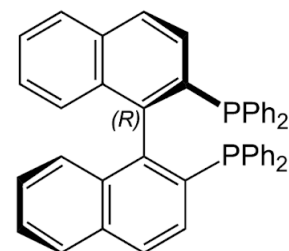
14.1.3. Structures and Applications of Some Organometallic Catalysts



Jacobsen's Salen Catalyst
(*S, S*) active

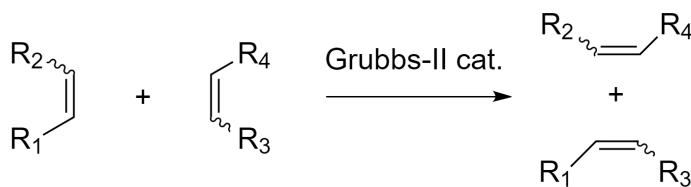


Grubbs II Catalyst



BINAP
(BINOL derivative)

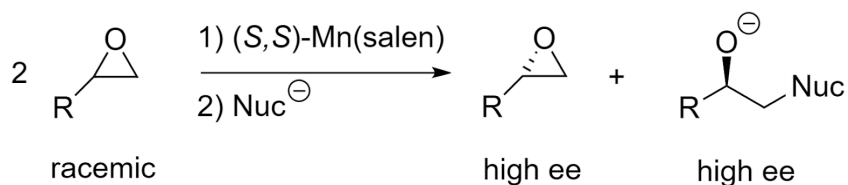
Typical application of the Grubbs II catalyst: alkene metathesis.



The Ru=CH-Ph group undergoes [2+2] cyclisation with an alkene bond, and is replaced in its future catalytic cycles.

In a ring-closing metathesis (RCM), an intramolecular reaction occurs between two alkene bonds separated by any number of carbons to form a ring.

Typical application of the Jacobsen catalyst: enantiomeric resolution of terminal epoxides.



In the Jacobsen HKR (hydrolytic kinetic resolution), the nucleophile is water, forming the vicinal diol as the second product.

14.1.4. Kinetics of Heterogeneous Catalysis

Heterogeneous catalysis requires adsorption at some point in the mechanism. The adsorption step can be written as $A + S \rightleftharpoons AS$ where A is a reactant, S is an adsorption site on the catalyst and AS is the adsorbed complex. The various types of mechanism are:

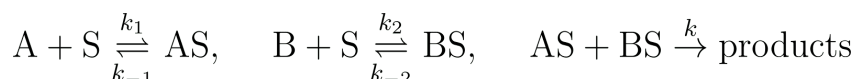
Simple Decomposition: $A + S \xrightleftharpoons[k_{-1}]{k_1} AS \xrightarrow{k_2} \text{products}$

The rate of product formation follows the Michaelis-Menten equation, most suitable for enzyme-substrate type reactions (see also Section 16.5.11):

$$r = \frac{k_1 k_2 [A][S]}{k_1 [A] + k_{-1} + k_2}; \quad \text{if } [S] \text{ is large, } r = r_{max} \frac{[A]}{[A] + K_m} \quad \text{where} \quad K_m = \frac{[A][S]}{[AS]} = \frac{k_{-1} + k_2}{k_1}.$$

- Adsorption equilibrium constant: $K = k_1/k_{-1}$.
- Surface coverage: $\theta = \frac{r}{k_2 [S]} = \frac{[AS]}{[S]}$
- If the rate-limiting step is adsorption, the equation is $r \approx k_1 [A][S]$ (second order)
- If the rate-limiting step is reaction, then $\theta \approx \frac{K[A]}{1 + K[A]} \rightarrow r \approx \frac{K k_2 [A][S]}{1 + K[A]}$ (Langmuir isotherm)

Bimolecular Langmuir-Hinshelwood Mechanism:



Two molecules A and B adsorb on neighbouring sites and react in their adsorbed state.

$$r = k[S]^2 \frac{K_1 K_2 [A][B]}{(1 + K_1 [A] + K_2 [B])^2}$$

where the equilibrium constants are $K_1 = k_1/k_{-1}$ and $K_2 = k_2/k_{-2}$.

Example: hydrogenation of ethene on metal catalysts.

Bimolecular Eley-Rideal Mechanism:



Only one reactant molecule A adsorbs, which then reacts directly with free molecules of B.

$$r = k[S][B] \frac{K[A]}{1 + K[A]}$$

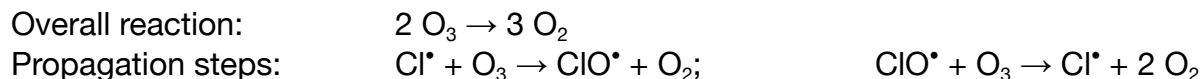
where the equilibrium constant is $K = k_1/k_{-1}$.

14.1.5. Photocatalytic Decomposition Reactions

High-energy radiation ($h\nu$) induces homolysis (homolytic fission) of weak chemical bonds, forming reactive free radicals.

Decomposition of Ozone

CFCs form radicals due to UV radiation in the stratosphere: $\text{R-Cl} + h\nu \rightarrow \text{R}^\bullet + \text{Cl}^\bullet$



Decomposition of Peroxides

The O-O bond is weak and gradually decomposes: $\text{HO-OH} + h\nu \rightarrow \text{HO}^\bullet + \text{}^\bullet\text{OH}$

14.1.6. Autocatalysis

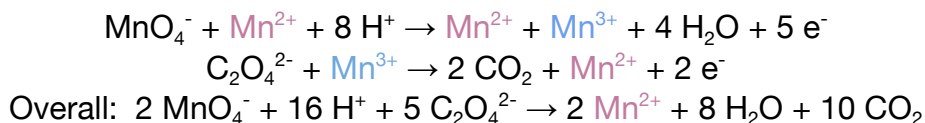
Autocatalysis: a reaction in which the product(s) act(s) as a catalyst for the reaction. The autocatalyst produces more of itself as the reaction proceeds. For $\text{A} + \text{B} \rightleftharpoons 2 \text{B}$, rates are

$$-\frac{d[\text{A}]}{dt} = \frac{d[\text{B}]}{dt} = k_+[\text{A}][\text{B}] - k_-[\text{B}]^2 \Rightarrow [\text{B}](t) = \frac{[\text{A}]_0 + [\text{B}]_0}{\left(\frac{[\text{A}]_0}{[\text{B}]_0} - \frac{k_-}{k_+}\right) e^{-k_+([\text{A}]_0 + [\text{B}]_0)t} + 1 + \frac{k_-}{k_+}}$$

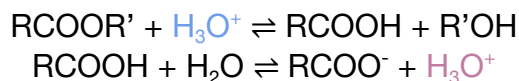
Autocatalytic set: a set of reactions in which the products of each reaction act as a catalyst for one or more other reactions in the set.

Examples of autocatalysis:

- Redox reaction of MnO_4^- (aq) with $\text{C}_2\text{O}_4^{2-}$ (aq) in acid, autocatalysed by Mn^{2+} (aq) product



- Hydrolysis of esters, autocatalysed by the carboxylic acid product



- Reduction of copper metal with nitric acid, autocatalysed by adsorbed NO (g) product
- Photopolymerisation, autocatalysed by the high-refractive index polymer regions
- Soai reaction of pyrimidine-5-carbaldehyde with diisopropylzinc, autocatalysed by the chiral product (asymmetric autocatalysis: amplifies the ee of the product).

14.2. Separation Processes and Chemical Engineering

14.2.1. Fossil Fuels

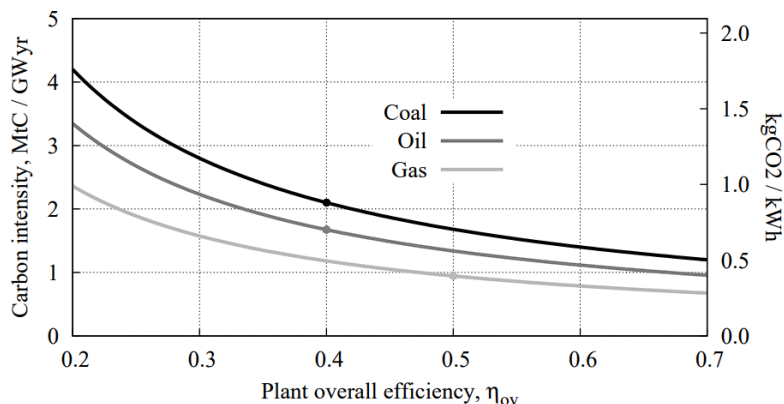
Fossil fuels are non-renewable energy sources found underground. There are three types:

Coal is formed from ancient dead plants on the ground, compacted and heated over millions of years to form **peat**, **lignite**, **bituminous coal** and **anthracite** (increasing time and carbon content). It is primarily found in the Carboniferous layer of the geologic column. It contains large heterocyclic organic molecules with some nitrogen and sulfur content. Distillation of coal without air forms coke (near pure carbon, porous), by removing tar (brown liquid of HCs).

Oil (crude oil, petroleum) is formed from ancient dead plants on the ocean floor, buried under layers of sediment. It is extracted using drilling or hydraulic fracturing (fracking). It is a highly variable liquid mixture of hydrocarbons (HCs) and polycyclic aromatic hydrocarbons (PAHs).

Gas (natural gas) is released during the decay process of ancient dead plants, trapped in underground reservoirs. It is extracted using drilling/fracking and is usually stored as liquefied natural gas (LNG). It is primarily composed of methane (CH_4) with some CO_2 , N_2 and H_2S .

Burning of fossil fuels is responsible for the majority of global anthropogenic greenhouse gas emissions and directly contributes to global warming. For this reason, fossil fuels are being phased out across the developed world in favour of cleaner energy sources, although economic competition of new technologies can be challenging, as fossil fuel economies are mature, optimised and often subsidised.



Carbon and CO_2 emissions for:

- Coal-fired ($\eta \sim 40\%$)
- Oil-fired ($\eta \sim 40\%$)
- Gas-fired (CCGT: $\eta \sim 50\text{-}60\%$)

Emissions follows

coal > oil > natural gas

14.2.2. Feedstock Processing

Fractionation (Fractional Distillation): physical separation of crude oil into components by molecular weight (boiling point). The fractions are bitumen (bottom: $>C_{70}$, $>400\text{ }^{\circ}\text{C}$), fuel oil (C_{21-70} , $\sim 370\text{ }^{\circ}\text{C}$), diesel oil (C_{15-20} , $\sim 300\text{ }^{\circ}\text{C}$), kerosene/paraffin (C_{10-14} , $\sim 200\text{ }^{\circ}\text{C}$), gasoline/petrol (C_{5-9} , $\sim 70\text{ }^{\circ}\text{C}$), and natural gas (top: C_{1-4} , $\sim 20\text{ }^{\circ}\text{C}$).

Cracking: higher alkanes are broken down into smaller alkanes using one of:

Thermal cracking: free radical recombination at $700\text{ }^{\circ}\text{C}$ and 70 atm. Forms many alkenes.

Catalytic cracking: splitting at $500\text{ }^{\circ}\text{C}$ with zeolite catalyst. Forms branched and aromatics.

Steam cracking: rapid high pressure steam flow at $850\text{ }^{\circ}\text{C}$. Forms many alkenes.

Flue Gas Desulfurisation (FGD): sulfur impurities (SO_2) in burned fuels can be removed (scrubbed) from smoke stacks using a CaO/CaCO_3 slurry, forming solid CaSO_4 (plaster of Paris). Wet scrubbers can also remove soluble gases (HCl , NH_3). This has helped prevent acid rain.

Catalytic Converter: the catalytic converter in cars consists of a Pt/Pd/Rh metal painted onto a ceramic honeycomb support. Exhaust toxins (NO_x , CO , C_xH_y) are converted to less harmful products (N_2 , CO_2 , $\text{H}_2\text{O} + \text{CO}_2$, respectively). Sulfur oxides can poison the catalyst over time. Nitrogen oxides react with a urea solution, $\text{CO}(\text{NH}_2)_2$ (diesel exhaust fluid e.g. AdBlue)

Gasification: uses coal / biomass / hydrocarbons to form syngas ($\text{H}_2 + \text{CO}$) by pyrolysis.

Biogasification: uses organic waste to form biogas ($\text{CH}_4 + \text{CO}_2$) by pyrolysis.

14.2.3. Petrochemical Reactions and Transformations

Addition Polymerisation: conversion of small alkene monomers to polymers (often plastics).

Conditions: radical initiator, high pressure. Common products: polyethylene (PE), polypropylene (PP), polyvinyl chloride (PVC), polystyrene (PS).

Condensation Polymerisation: conversion of difunctional monomers to polymers.

Conditions depend on the chemistry. Common products: nylon, polyesters, polyurethanes.

Vulcanisation of Natural Rubber: cross-linking of natural rubber (polyisoprene) by heating with elemental sulfur, forming polysulfide bridges between chains, improving its elastomeric properties.

Fermentation: conversion of glucose to ethanol using yeast and/or enzymes.

Isomerisation: conversion of straight-chained alkanes to branched alkanes.

Conditions: $\text{AlCl}_3 + \text{HCl}$ catalyst, 200 °C, 35 atm.

Alkylation: addition of hydrocarbons (often alkenes) to produce higher alkanes.

Conditions: HF catalyst (or more recently: BMIM-PF₆ ionic liquid catalyst).

Common applications: 2-methylpropene + 2-methylpropane → 2,2,4-trimethylpentane (petrol).

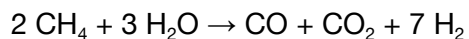
Aromatisation (Reforming): dehydrogenation of aliphatic hydrocarbons to give aromatics.

Conditions: 500 °C, Pt catalyst. Common application: *n*-heptane → toluene + 3 H₂.

Hydrogenation: addition of H₂ to alkenes to give the alkane. Uses Raney Ni catalyst.

Controlled Oxidation: catalytic oxidation of organic molecules at moderate temperatures can lead to formation of other useful chemicals instead of combustion e.g. toluene → benzyl hydroperoxide / benzaldehyde, methane → methanol, depending on conditions and catalysts.

Steam-Methane Reforming (SMR): forms syngas from methane:



Water Gas Shift Reaction (WGSR): purifies syngas to hydrogen: $\text{CO} + \text{H}_2\text{O} \rightleftharpoons \text{CO}_2 + \text{H}_2$

Boudouard reaction: a relevant equilibrium occurring in many processes: $2 \text{CO} \rightleftharpoons \text{CO}_2 + \text{C}$

Sabatier Process: forms methane: $\text{CO}_2 + 4 \text{H}_2 \rightarrow \text{CH}_4 + 2 \text{H}_2\text{O}$.

Conditions: 350 °C, 3 MPa, Ni/Ru cat.

Fischer-Tropsch Synthesis (FT): uses syngas (H₂ + CO) to form higher alkanes (often liquids i.e. as part of a coal liquefaction process after gasification). Conditions: 200 °C, 1 MPa.

Wacker Process: uses ethylene to form acetaldehyde (ethanal): $\text{CH}_2\text{CH}_2 + \frac{1}{2} \text{O}_2 \rightarrow \text{CH}_3\text{CHO}$
Conditions: PdCl_2 and CuCl_2 catalysts.

Hydroformylation (Oxo Process): uses syngas and alkenes to form aldehydes.
Conditions: $\text{CO} + \text{H}_2$, 100 °C, 50 atm, Rh/Co-based catalyst.

Haber Process: uses hydrogen and nitrogen to form ammonia: $\text{N}_2 + 3 \text{H}_2 \rightleftharpoons 2 \text{NH}_3$
Conditions: 450 °C, 200 atm, Fe catalyst.

Cumene Process: uses benzene and propene to form phenol and propanone:

1) $\text{C}_6\text{H}_6 + \text{C}_3\text{H}_6 \rightarrow \text{C}_6\text{H}_5\text{iPr}$; 2) $\text{C}_6\text{H}_5\text{iPr} + \text{O}_2 \rightarrow \text{C}_6\text{H}_5\text{OH} + \text{CH}_3\text{COCH}_3$.

Conditions: 250° C, 30 atm, phosphoric acid, oxidation in air.

14.2.4. Separation and Purification Techniques

Packed Bed / Adsorbent Column: batchwise filling of a packed column of adsorbent beads, purifying the liquid over time as impurities become stuck to the column. The purified liquid falls out at the bottom for collection, and can be sent to the top again for multiple passes of purification.

Gravity Separation: a variety of methods where denser matter falls to the bottom of a mixture, such as by shaking, vibrating or sedimentation.

Centrifugation: high-speed rotation of a mixture, with separation to the edges occurring due to different densities.

Cake Filtration: cyclical fluid flow through a porous adsorbent, which removes particulate matter from the stream, growing the 'cake filter' in the process.

Solvent Extraction: addition of a specific solvent to solubilise the desired target, leaving the remainder in its own phase, so that the solvent phase can be extracted easily.

Chromatography: a variety of methods are possible. Allows for separation by exploiting differential adsorption to a stationary phase and a solvent (mobile phase), as well as characterisation and identification based on residence times.

Magnetic Separation: uses magnets to remove magnetic impurities e.g. metals from a slurry.

Pressure-Swing Adsorption: used to extract a specific component of a gas mixture. High pressure and an adsorbent is used to fix the desired gas, leaving the rest free to be removed. When the pressure is released, the desired gas desorbs and can be extracted.

Cryogenic Distillation: liquefaction of a gas mixture followed by fractional distillation to extract the different gases as they boil separately.

Membrane Separation / Gas Permeation: uses semi-permeable membranes to separate gases by particle size and permeability.

Cyclones: impure gas carrying particulate matter flows down a spiral rapidly and is sucked back up in the middle, leaving the particles on the bottom edge of the cyclone. The outlet air is purified.

14.2.5. Hydrogen as Fuel

An alternative to burning natural gas as fuel is to use hydrogen (H_2). Depending on the implementation, this can be far more sustainable than using fossil fuels and may be on par with renewables.

Hydrogen Fuel Cells for Hydrogen-Powered Vehicles

Hydrogen is used as an input to fuel cells (see Section 13.5.11). Currently, fuel cells are somewhat inefficient (~50%) and are one of the key bottlenecks in a hydrogen economy. The primary application is fuel cell vehicles (FCVs), a type of electric vehicle (EV), although there are competing approaches for this and related sectors e.g. electric road systems (ERS), especially for heavy vehicles (public transport, long-haul road and rail freight).

Hydrogen Production: sustainability depends on how it was produced, which can vary significantly:

- **Green Hydrogen:** electrolysis of water using renewable electricity from solar/wind
- **Pink Hydrogen:** electrolysis of water using renewable electricity from nuclear
- **Turquoise Hydrogen:** pyrolysis of natural gas using renewable electricity, releasing solid carbon
- **Blue Hydrogen:** methane reforming of natural gas and carbon capture and storage.
- **Grey Hydrogen:** methane reforming of natural gas (no CCS).
- **Black / Brown Hydrogen:** gasification of coal (black: bituminous, brown: lignite) with no CCS.

Green Hydrogen: Renewable electricity (green: solar/wind, pink: nuclear) powers an electrolysis system to split water into hydrogen and oxygen. The hydrogen is compressed and stored in tanks for transport. Since the hydrogen becomes water again when burned, this is a circular reaction and is effectively a form of energy storage (with inefficiencies) rather than an energy source.

Blue Hydrogen: Oil and gas (fossil fuels) are extracted from the Earth by drilling/fracking. The methane is converted to syngas using steam-methane reforming (SMR) or autothermal reforming (ATR), and then to purer H_2/CO_2 using the water-gas shift reaction (WGSR). The CO_2 side product is removed from the stream into a carbon capture and storage (CCS) facility, leaving pure H_2 . The hydrogen is, as before, compressed and bottled for transport.

14.2.6. General Continuously Stirred Tank Reactor (CSTR)

For a single non-steady, non-isothermal homogeneous CSTR with negligible shaft work:

- dependent variables: volume V , concentrations of species $c_A \dots$, temperature T
- controlled variables: volumetric flow rates Q_{in} and $Q_{out} = Q$, concentration in $c_{A,in}$
- independent variable: time t

Considering a control volume (CV) around the reactor contents:

Mass balance on a species A (each term has units of kg s^{-1} or mol s^{-1} depending on choice):

$$\underbrace{\frac{d}{dt}(Vc_A)}_{\substack{\text{net change in} \\ \text{moles of A} \\ \text{in CV}}} = \underbrace{Q_{in}c_{A,in}}_{\text{mole flux in}} - \underbrace{Qc_A}_{\text{mole flux out}} + \underbrace{\nu_A k V c_A^n}_{\text{rate of reaction}}$$

Energy balance (each term has units of $\text{J s}^{-1} = \text{W}$): assuming enthalpy $h = c_p T$:

$$\underbrace{\frac{d}{dt}(\rho V c_p T)}_{\text{net change in energy in CV}} = \underbrace{\rho_{in} Q_{in} \left(c_{p,in} T_{in} + \frac{1}{2} v_{in}^2 + g z_{in} \right)}_{\text{enthalpy flux in}} - \underbrace{\rho Q \left(c_p T + \frac{1}{2} v_{out}^2 + g z_{out} \right)}_{\text{enthalpy flow out}} + \underbrace{\nu_A k V (\Delta H) c_A^n}_{\text{heat generated by reaction}} + \underbrace{\dot{Q} - \dot{W}}_{\text{external heat and work transferred into CV}}$$

(ν_A : stoichiometric coefficient, k : reaction rate constant, n : order of reaction wrt A, ρ : density of flow, c_p : specific heat capacity of flow, T : temperature, v : flow speed, g : acceleration due to gravity, z : elevation, ΔH : specific enthalpy change for the reaction, \dot{Q} : heat transferred into CV (e.g. steam tube heater, coolant flow, conduction through vessel walls), \dot{W} : work done by CV (e.g. hydrodynamic impeller shaft work))

These equations are often simplified e.g. LHS = 0 (steady state), fluid properties are constant and independent of temperature, neglect kinetic/gravitational contributions to enthalpy flux, assume temperature-independent rate constant.

14.2.7. Two-Dimensional Cylindrical Plug Flow Reactor (PFR)

For a cylindrical, laminar flow, diffusive, non-isothermal homogeneous PFR with no gravitational effects, sedimentation or mixing,

- dependent variables: concentrations of species $c_A \dots$, temperature T
- controlled variables: axial velocity profile $u(r)$
- independent variables: axial position x , radial position r , time t .

Considering an annular control volume at position (x, r) with axial thickness dx and radial thickness dr :

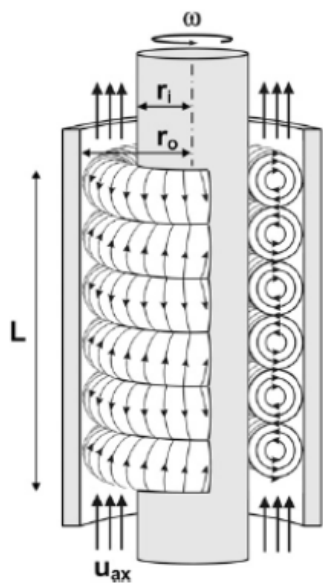
Mass balance on a reactant species A (each term has units concentration per time)

$$\underbrace{\frac{\partial c_A}{\partial t}}_{\text{net concentration change}} = \underbrace{-u \frac{\partial c_A}{\partial x}}_{\text{axial convective flux}} + \underbrace{\nu_A k c_A^n}_{\text{rate of reaction}} + \underbrace{D \left(\frac{\partial^2 c_A}{\partial r^2} + \frac{1}{r} \frac{\partial c_A}{\partial r} + \frac{\partial^2 c_A}{\partial x^2} \right)}_{D \nabla^2 c_A: \text{diffusive flux}}$$

Energy balance (each term has units temperature per unit time)

$$\underbrace{\frac{\partial T}{\partial t}}_{\text{temperature change}} = \underbrace{-u \frac{\partial T}{\partial x}}_{\text{axial convective flux}} + \underbrace{\frac{\nu_A k \Delta H}{\rho c_p} c_A^n}_{\text{rate of reaction}} + \underbrace{\frac{\lambda}{\rho c_p} \left(\frac{\partial^2 T}{\partial r^2} + \frac{1}{r} \frac{\partial T}{\partial r} + \frac{\partial^2 T}{\partial x^2} \right)}_{\alpha \nabla^2 T: \text{diffusive flux}}$$

14.2.8. Taylor-Couette Reactor (TCR)



The Taylor number is the cylindrical Reynolds number,

$$Ta = \frac{\rho^2 \omega^2 r_i (r_o - r_i)^3}{\mu^2}$$

For $Ta > Ta_c$, axisymmetric vortices form, where

$$Ta_c = 41.3 \times \frac{(1 + \Lambda)^2}{2\Lambda \sqrt{(1 - \Lambda)(3 + \Lambda)}}; \quad \Lambda = \frac{r_i}{r_o}$$

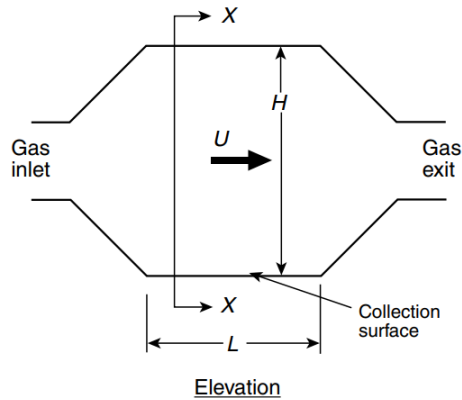
The Péclet number, $Pe = \frac{u_{ax} L}{D}$ describes the ratio of advection to diffusion.

When $Pe \rightarrow 0$, the TCR approaches a CSTR.

When $Pe \rightarrow \infty$, the TCR approaches a PFR.

14.2.9. Settling Chamber for Gravity Separation

For a gas flow of speed U (defined such that the flow rate is $Q = HW \times U$ in the below geometry) and density ρ_f containing particles of diameter x and density ρ_p to be removed:



If Stokes' law applies to the particle flow regime ($Re_p < 0.3$):

Terminal velocity:

$$U_T = \frac{x^2 g (\rho_p - \rho_f)}{18\mu}$$

Collection efficiency:

$$\eta = \frac{U_T L}{HU}$$

14.2.10. Fluid Flow Through a Packed Bed

For a packed column of height L , area A , fluid density ρ_f and particle density ρ_p and (mean surface-volume) particle diameter x :

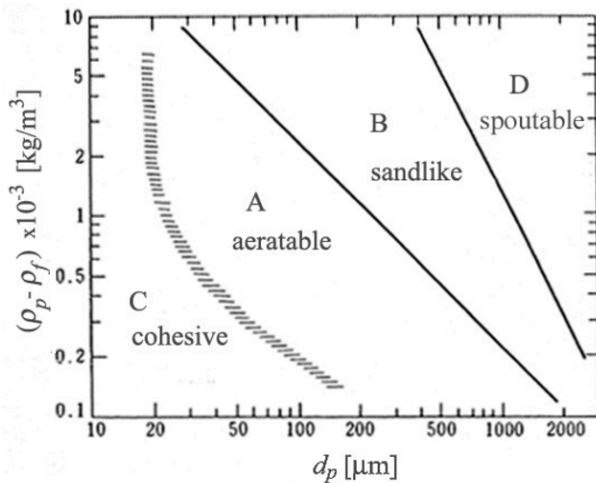
- Porosity (voidage ratio) $\varepsilon = \frac{V_{void}}{V_{total}} = 1 - \frac{M_p}{\rho_p AL}$
- Superficial velocity (through the packed region): $U_i = \frac{U}{\varepsilon}$
- Pressure drop in laminar flow: $\frac{-\Delta p}{L} = 180 \frac{\mu U}{x^2} \frac{(1-\varepsilon)^2}{\varepsilon^3}$ (Carman-Kozeny equation)
- Pressure drop in turbulent flow: $\frac{-\Delta p}{L} = 150 \frac{\mu U}{x^2} \frac{(1-\varepsilon)^2}{\varepsilon^3} + 1.75 \frac{\rho_f U^2}{x} \frac{1-\varepsilon}{\varepsilon^3}$ (Ergun equation)
- Pressure drop in a fluidised bed: $-\Delta p = (1 - \varepsilon)(\rho_p - \rho_f)gL$
- Modified Reynolds number: $Re^* = \frac{xU \rho_f}{\mu(1-\varepsilon)} = \frac{Re_x}{1-\varepsilon}$
- Modified friction factor: $f^* = \frac{-\Delta p}{L} \frac{x}{\rho_f U^2} \frac{\varepsilon^3}{1-\varepsilon} = 1.75 + \frac{150}{Re^*}$

14.2.11. Cake Filtration

- For an incompressible cake, cake resistance $r_c = \frac{-\Delta p}{\mu UL} = \frac{150}{x^2} \frac{(1 - \epsilon)^2}{\epsilon^3}$.
- Volume of cake formed per unit volume of passing filtrate: $\phi = \frac{LA}{V}$
- Instantaneous filtrate volumetric flow rate (no medium resistance): $\frac{dV}{dt} = \frac{A^2(-\Delta p)}{r_c \mu \phi V}$.
- If Δp is constant then $\frac{dV}{dt}$ is inversely proportional to V and $t = \frac{r_c \mu \phi}{2A^2(-\Delta p)} V^2$.
- If $\frac{dV}{dt}$ is constant then Δp is proportional to V .

14.2.12. Geldart Groupings of Powders and Minimum Bubbling Velocity

Fluidisation behaviour can be predicted by classification based on density relative to the fluidisation medium and size.



	Group C	Group A	Group B	Group D
Most obvious characteristic	Cohesive, difficult to fluidize	Ideal for fluidization. Exhibits range of non-bubbling fluidization	Starts bubbling at U_{mf}	Coarse solids
Typical solids	Flour, cement	Cracking catalyst	Building sand	Gravel, coffee beans
Property				
Bed expansion	Low because of channelling	High	Moderate	Low
De-aeration rate	Initially fast, then exponential	Slow, linear	Fast	Fast
Bubble properties	No bubbles—only channels	Bubbles split and coalesce. Maximum bubble size	No limit to size	No limit to size
Solids mixing	Very low	High	Moderate	Low
Gas backmixing	Very low	High	Moderate	Low
Spouting	No	No	Only in shallow beds	Yes, even in deep beds

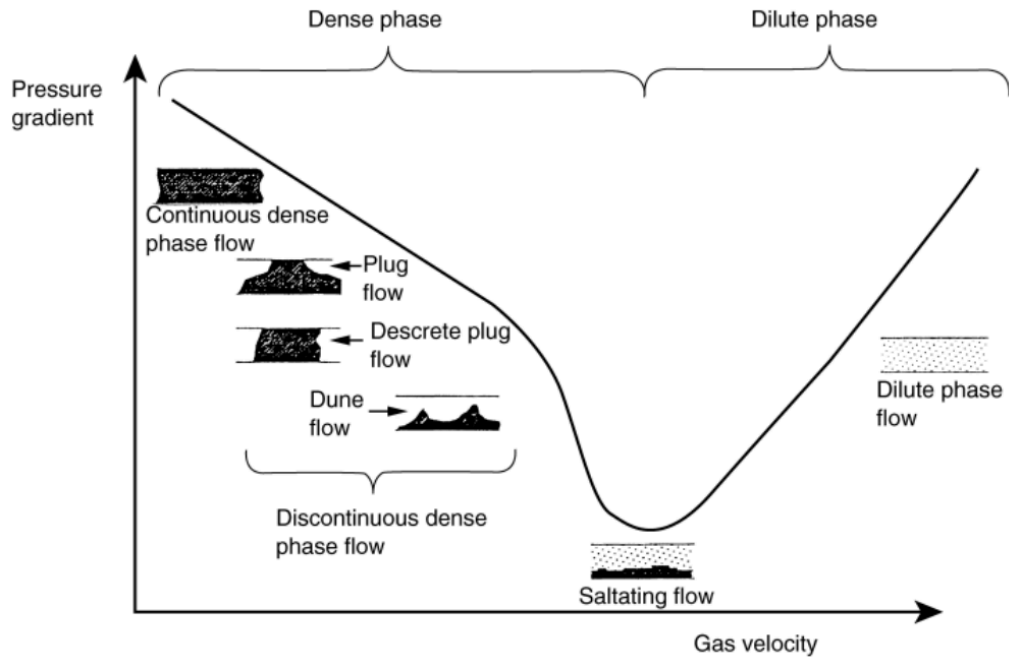
Correlation for minimum bubbling velocity: $U_{mb} = 2.07 e^{0.716 F} \frac{x_p \rho_g^{0.06}}{\mu^{0.347}}$

where F is the fraction of powder less than 45 μm in size.

Group A: $U_{mb} > U_{mf}$, Group B, D: $U_{mb} = U_{mf}$.

14.2.13. Phases of Pneumatic Transport

When a solid phase is dispersed in a flowing gas phase, the mode of transport and pressure drop depends on the gas velocity.

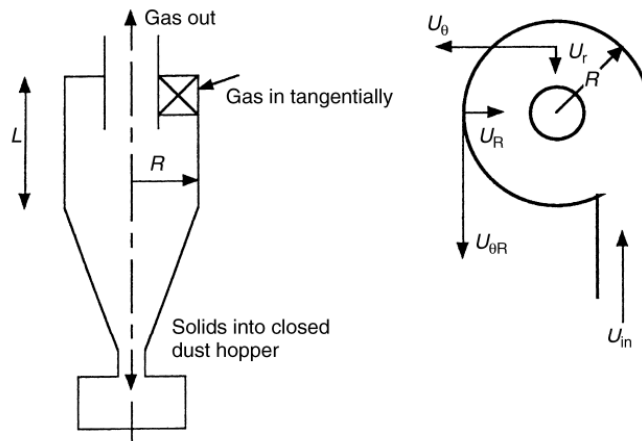


The overall pressure drop consists of inertial, frictional and static head effects:

$$\Delta p = \underbrace{\frac{1}{2}\epsilon\rho_f U_f^2}_{\text{fluid acceleration}} + \underbrace{\frac{1}{2}(1-\epsilon)\rho_p U_p^2}_{\text{particle acceleration}} + \underbrace{\bar{F}_{fw}L}_{\text{fluid-wall friction}} + \underbrace{\bar{F}_{pw}L}_{\text{particle-wall friction}} + \underbrace{\rho_f L \epsilon g \sin \theta}_{\text{fluid head}} + \underbrace{\rho_p L (1-\epsilon) g \sin \theta}_{\text{particle head}}$$

(U_f : gas velocity, ρ_f : gas density, U_p : particle velocity, ρ_p : particle density, ϵ : porosity, L : length of tube, \bar{F}_{fw} : gas-wall friction per unit volume, \bar{F}_{pw} : particle-wall friction per unit volume, g : gravitational acceleration, θ : angle of inclination of tube to horizontal)

14.2.14. Gas Cyclone Separators



Pressure drop between gas inlet and gas outlet (Euler number):

$$Eu = \frac{\Delta p}{\frac{1}{2}\rho_f U^2}$$

Azimuthal velocity distribution:

$$U_\theta(r) \times r^{1/2} = \text{constant}$$

Critical particle diameter for separation:

$$x_{50}^2 \approx \frac{18\mu}{\rho_p - \rho_f} \frac{U_R}{U_{\theta R}^2} R$$

Performance of geometrically similar cyclones (Stokes number):

$$Stk_{50} = \frac{x_{50}^2 \rho_p U}{36 \mu R}$$

Grade efficiency:

$$\eta = \frac{(x/x_{50})^2}{1 + (x/x_{50})^2}$$

Euler-Stokes correlation:

$$Eu = \sqrt{\frac{12}{Stk_{50}}}$$

14.2.15. Particle Size Reduction in Ball Milling

Breakage energy per unit mass of feed: $\frac{dE}{dx} = -\frac{k}{x^n}$

Kick's law: $n = 1$ (by mass), Rittinger's law: $n = 2$ (by surface area), Bond's law: $n = 1.5$ (by $\sqrt{\frac{S}{V}}$)

Product size distribution: $\frac{dm_i}{dt} = \sum_{j=1}^{i-1} (b(i,j)S_j m_j) - S_i m_i$

(m_i : mass fraction of particles in size interval i ,

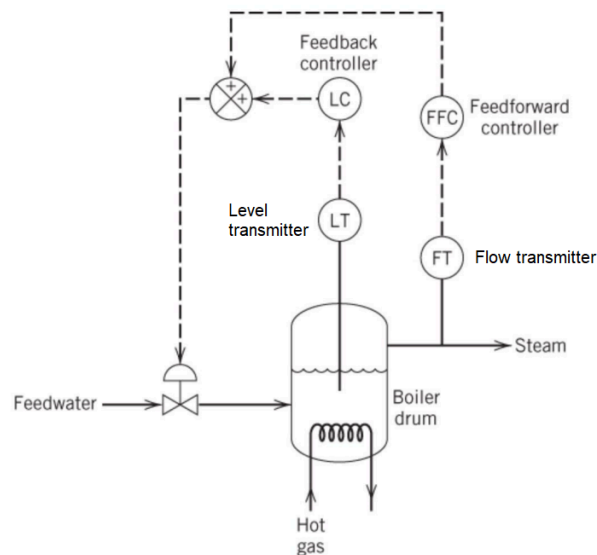
$b(i,j)$: fraction of breakage product from size interval j which falls into size interval i ,

S_j : probability of a particle of size j being broken in unit time.)

14.2.16. Process and Instrumentation Diagram (P&ID) Abbreviations

	Locally mounted instrument		Flow alarm		Unit shut down
	Board mounted instrument		Flow element		Position/unit switch closed
	Pressure controller		Flow indicator		Shut down valve relay
	Pressure indicator		Flow recorder		Shut down valve
	Pressure recording		Flow recording controller		Position/limit indicator open
	Pressure indicating controller		Temperature alarm		Temperature relay
	Pressure recording controller		Temperature indicator		Spectacle blind open
	Pressure safety valve		Temperature recorder		Spectacle blind closed
	Relief valve		Temperature recording controller		Orifice flanges
	Level alarm		Temperature well		Piping speciality item
	Level alarm high		Gate valve		Instrument air line
	Level alarm low		Globe valve		Instrument electrical
	Level controller		Check valve		Instrument capillary tubing
	Level glass		Control valve		Pipe
	Level indicator		Plug valve		Transmitter
	Level indicating controller		Ball valve		Hand control valve
	Level recording controller		Butterfly valve		

Example: water boiler with feedforward and feedback control (see Section 9.4.10):



14.3. Colloids and Nanoparticle Chemistry

14.3.1. Classification of Colloidal Systems

Dispersed phase	Dispersion medium	Colloid type	Examples
Solid	Solid	Solid sol	ruby glass, alloys
Solid	Liquid	Sol	paint, starch, proteins, ink
Solid	Gas	Solid aerosol	smoke, volcanic dust
Liquid	Solid	Gel	cheese, butter, agar, gelatin
Liquid	Liquid	Emulsion / Liquid crystal	milk, mayonnaise, latex
Liquid	Gas	Liquid aerosol	fog, cloud, hair spray
Gas	Solid	Solid foam	aerogel, rubber, styrofoam, pumice
Gas	Liquid	Foam	foam, whipped cream, soda water
Gas	Gas	–	none at standard conditions

14.3.2. Preparation and Purification of Colloids

Lyophilic colloids form readily by simply mixing the two phases.

Lyophobic colloids require input work, and can be formed by:

- Oxidation: e.g. $2 \text{H}_2\text{S} (\text{aq}) + \text{O}_2 (\text{bubbled through}) \rightarrow 2 \text{H}_2\text{O} + 2 \text{S} (\text{colloidal})$
- Reduction: e.g. $2 \text{AuCl}_3 (\text{aq}) + 3 \text{SnCl}_2 \rightarrow 3 \text{SnCl}_4 + 2 \text{Au} (\text{gold sol; 'Purple of Cassius'})$
- Hydrolysis: e.g. $\text{FeCl}_3 (\text{aq}) + \text{H}_2\text{O} (\text{boiling}) \rightarrow 3 \text{HCl} + \text{Fe}(\text{OH})_3 (\text{colloidal})$
- Decomposition: e.g. $\text{As}_2\text{O}_3 + 3 \text{H}_2\text{S} \rightarrow 3 \text{H}_2 + \text{As}_2\text{S}_3 (\text{sol})$
- Mechanical dispersion: grind particles, form suspension, use colloidal mill (rapidly rotating disks shear the particles into microparticles)
- Electrical dispersion (Bredig's arc method): for sols of Pt, Ag, Au, Cu; a high-voltage electrical discharge is struck between metal electrodes in an ice bath, releasing metal microparticles. Add KOH as a stabiliser.
- Peptisation: addition of an electrolyte to a precipitate reforms the colloid.
- Supercritical antisolvent precipitation (SAS, Section 14.2.11) and electrohydrodynamic atomisation (EHDA, Section 14.2.10), are modern methods for colloid synthesis.

Colloids can be purified using electrodialysis, ultrafiltration and ultracentrifugation.

14.3.3. Micellisation of Surfactants

- Gibbs free energy change for micellization: $\Delta G = RT \ln c_{CMC}$
- Ionic surfactants typically have a 'Krafft temperature', T_K , where micellisation occurs for $T > T_K$.
- Nonionic surfactants typically have a 'cloud point', T_c , where micellisation occurs for $T < T_c$.
- Micelle aggregation number, N : number of surfactant molecules per micelle.
- Phillips criterion for the CMC: $\left[\frac{d^3\phi}{dc} \right]_{c=c_{CMC}} = 0$ (ϕ is a property in Section 14.4.4.)

The CMC for some common surfactants in aqueous solution (in mM) are shown below.

Surfactant	Type	$c_{CMC} / \text{mmol dm}^{-3}$
sodium lauryl sulfate (SLS)	anionic	9.95
sodium dodecyl sulfate (SDS)	anionic	8.099
sodium stearate (SS)	anionic	0.071
cetrimonium bromide (CTAB)	cationic	0.92
cetylpyridinium chloride (CPC)	cationic	1
lauryl betaine	zwitterionic	1.18
cocamidopropyl betaine	zwitterionic	0.974
penta(ethyleneglycol)-monododecyl ether (C12E5)	nonionic	0.065
poloxamer L35 (Pluronic L35, PEO ₁₁ PPO ₁₆ PEO ₁₁)	nonionic	5.3
poloxamer L121 (Pluronic L121, PEO ₅ PPO ₆₈ PEO ₅)	nonionic	0.001
polysorbate 80 (E433)	nonionic	0.012
nonylphenol ethoxylate-9 (NP-9)	nonionic	0.097
Triton X-100	nonionic	0.22

Surfactant micellisation is influenced by various factors:

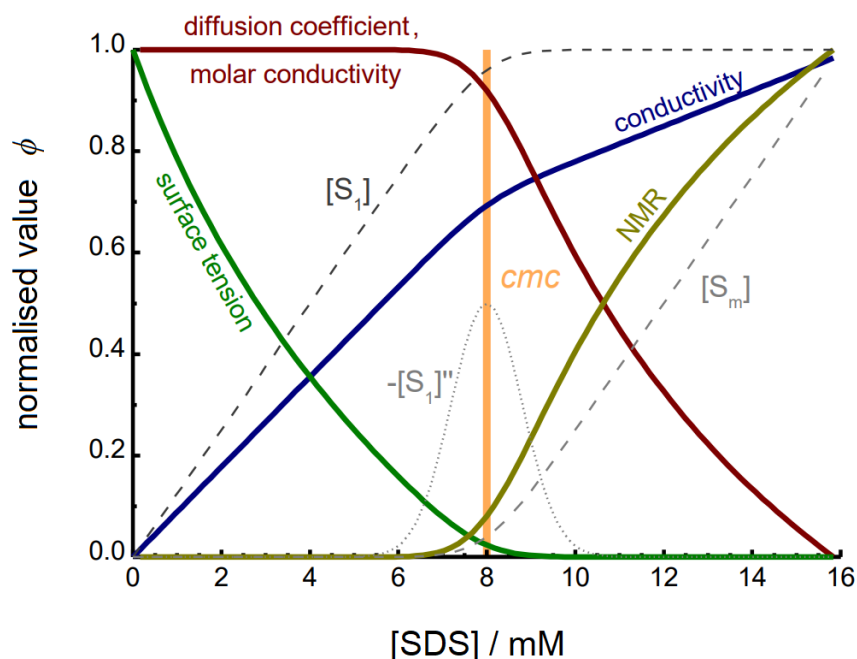
- Addition of salts containing kosmotropic anions decreases the CMC and forms larger micelles. Addition of salts containing chaotropic anions increases the CMC and forms smaller micelles. These effects are more significant in ionic surfactants than nonionic surfactants.
- Surfactant molecules with longer hydrophobic chains have smaller CMC.
- Increasing the temperature decreases the CMC.

14.3.4. Isothermal Physical Properties of Amphiphilic Colloids (Surfactant Solutions)

The graph shows normalised values of:

- electrical conductivity σ (normalised to $\sigma_\infty = 71.8 \text{ mS m}^{-1}$)
- molar conductivity Λ_m (normalised to $\Lambda_m^0 = 72 \text{ S cm}^2 \text{ mol}^{-1}$)
- self-diffusion coefficient D (normalised to $D_0 = 5.04 \times 10^{-10} \text{ m}^2 \text{ s}^{-1}$)
- surface tension γ (normalised to $\gamma_0 = 71.8 \text{ mN m}^{-1}$)
- NMR chemical shift δ (measured in D_2O) (normalised to $\delta_{16\text{mM}}^{(\text{H}^1)} = 0.97 \text{ ppm}$)
- monomer phase concentration $[S_1]$, (normalised to $[S_1]_\infty = 8 \text{ mM}$)
- micelle phase concentration $[S_m]$ (normalised to $[S_m]_\infty = 8 \text{ mM}$)

against the concentration of SDS (sodium dodecyl sulfate) in water (in mmol dm^{-3}) at 25°C .



Other properties include:

- In a lyophilic colloid (suspension in water), viscosity is higher and surface tension is lower than the bulk solvent.
- In associated colloids, deviations of colligative properties are smaller than in the bulk solvent due to lower Van 't Hoff factor (lower particle count).

14.3.5. DLVO Theory and the Electrical Double Layer of Colloidal Particles

For colloidal particles of diameter x separated by closest-distance D ,

- Van der Waals cohesive force: $V_{vdW}(D) = \frac{-Ax}{24D}$ $F_{vdW}(D) = \frac{-Ax}{24D^2}$
- Electrical double layer repulsive force: $V_{EDL}(D) = \pi\epsilon x \Psi_0^2 e^{-\kappa D}$ $F_{EDL}(D) = \pi\epsilon x \Psi_0^2 \kappa e^{-\kappa D}$
- Overall force: $F = F_{vdW} + F_{EDL} = \pi\epsilon x \Psi_0^2 \kappa e^{-\kappa D} - \frac{Ax}{24D^2}$.

(A : Hamaker constant, Ψ_0 : surface potential, κ : Debye screening parameter, ϵ : permittivity of medium. The zeta potential ζ approximates Ψ_0 .)

An excluded volume with additional radius approximately equal to the the Debye length $\lambda = \frac{1}{\kappa}$ is formed around the solid particle, representing the extent of the diffuse layer of the EDL.

- Debye constant variation with salt concentration: $\kappa [nm^{-1}] = 3.29 \sqrt{I}$, $\lambda [nm] = \frac{0.304 nm}{\sqrt{I}}$
(I [$mol\ dm^{-3}$]: ionic strength)
- Surface charge on colloidal particle: $\sigma [C\ m^{-2}] = \epsilon \zeta \kappa$ (Gouy-Chapman equation)

Nanobubbles in water (gaseous cavities) also acquire surface charge like colloidal particles.

14.3.6. Surface Electrostatic Data for Common Particulate Materials

Isoelectric Point (IEP) and Hamaker Constants for Interfaces

The isoelectric point (IEP) and Hamaker constant A for the force between particles of (Material 1) and (Material 3), through a medium of (Material 2), are given in the tables.

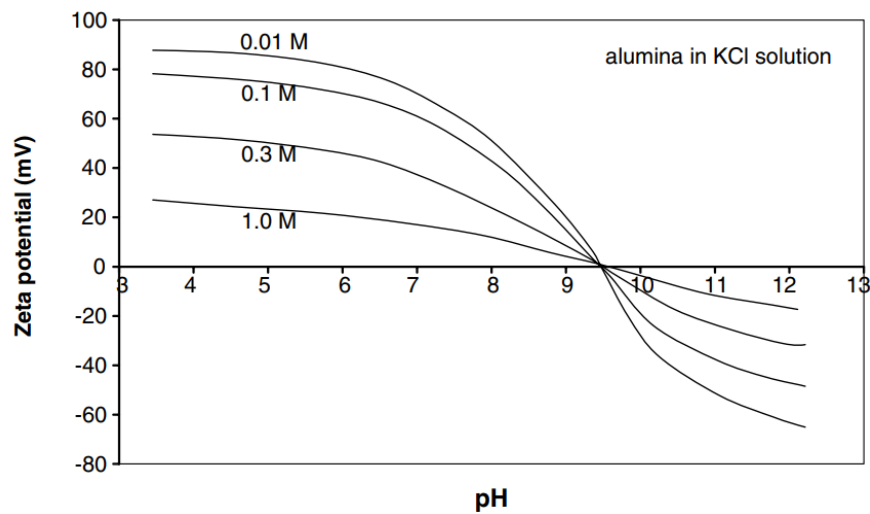
Material	pH of IEP
Silica	2–3
Alumina	8.5–9.5
Titania	5–7
Zirconia	7–8
Hematite	7–9
Calcite	8
Oil	3–4
Air	3–4

Material 1	Material 2	Material 3	Hamaker constant (approximate) (J)
Alumina	Air	Alumina	15×10^{-20}
Silica	Air	Silica	6.5×10^{-20}
Zirconia	Air	Zirconia	20×10^{-20}
Titania	Air	Titania	15×10^{-20}
Alumina	Water	Alumina	5.0×10^{-20}
Silica	Water	Silica	0.7×10^{-20}
Zirconia	Water	Zirconia	8.0×10^{-20}
Titania	Water	Titania	5.5×10^{-20}
Metals	Water	Metals	40×10^{-20}
Air	Water	Air	3.7×10^{-20}
Octane	Water	Octane	0.4×10^{-20}
Water	Octane	Water	0.4×10^{-20}
Silica	Water	Air	-0.9×10^{-20}

(silica: SiO_2 , alumina: Al_2O_3 , titania: TiO_2 , zirconia: ZrO_2 , hematite: Fe_2O_3 , calcite: CaCO_3 , oil: liquid hydrocarbons, air: air microbubbles.)

Zeta Potential for Alumina Particles in Strong Electrolyte

Zeta potential ζ of alumina particles as a function of pH and salt concentration. (Data from Johnson et al., 2000)



14.3.8. Non-Newtonian Fluid Viscosity

Newtonian fluid: μ is independent of shear rate and time. For non-Newtonian fluids:

Shear rate dependence:

- Shear-thinning (pseudoplastic): μ decreases with shear rate
e.g. molten polymers, ketchup, whipped cream, blood, paint, nail polish.
- Shear-thickening (dilatant): μ increases with shear rate
e.g. cornstarch suspensions in water.

Time dependence:

- Thixotropic: μ decreases with time (under a constant shear rate)
e.g. ketchup, toothpaste, shaving cream.
- Rheopectic: μ increases with time (under a constant shear rate)
e.g. printer inks, synovial fluid, gypsum paste.

Most gels, colloids and biofluids are thixotropic while rheopexy is rarer. They may be shear-thinning or thickening.

14.3.9. Flory-Huggins Solution Theory of Polymeric Colloids

Brownian Motion of Colloidal Particles

Mean Free Path:
$$\bar{L} = \frac{1}{\sqrt{2}n_v \pi d^2} = \frac{RT}{N_A P} \frac{1}{\sqrt{2} \pi d^2} = \frac{\mu}{P} \sqrt{\frac{\pi k_B T}{2m}}$$

Mean Squared Displacement:
$$\overline{x^2} = 2Dt \text{ (in 1D); } \overline{x^2} = 4Dt \text{ (in 2D); } \overline{x^2} = 6Dt \text{ (in 3D)}$$

Diffusion coefficient:
$$D = \frac{kT}{3\pi\eta\mu} \text{ (Stokes-Einstein relation)}$$

($n_v = \frac{n}{N_A V}$: number of particles per unit volume, d : diameter of particles, μ : viscosity of medium, P : pressure, M_r : relative molecular mass of particle (per mole))

Forces between hard colloidal particles with a polymeric surface:

- Bridging flocculation: attractive, maximised when surface coverage is ~50%.
- Steric repulsion: repulsive, maximised when surface coverage is ~100%.

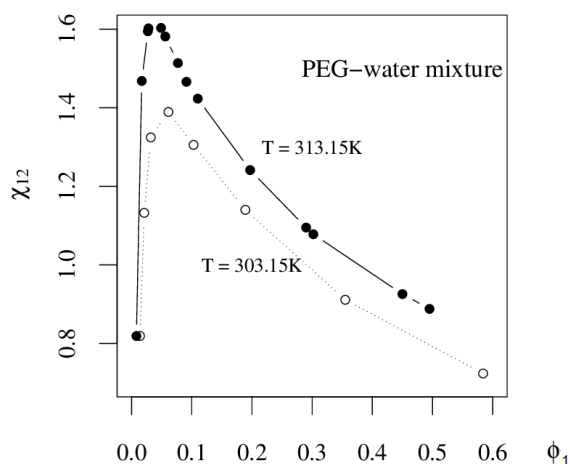
The Gibbs free energy of mixing between solvent (n_1 moles, volume fraction ϕ_1) and polymer (n_2 moles, volume fraction ϕ_2) is $\Delta G_m = RT[n_1 \ln \phi_1 + n_2 \ln \phi_2 + n_1 \phi_2 \chi_{12}]$

(T : temperature, R : gas constant, χ_{12} : polymer-solvent interaction parameter, $V_{m,s}$: actual volume of a polymer segment.)

Interaction parameter:
$$\chi_{12} = \frac{V_{seg}(\delta_a - \delta_b)^2}{RT} \text{ } (\delta: \text{Hildebrand solubility parameter})$$

Dimensionless free energy per unit volume:
$$f = \frac{\phi}{N} \ln \phi + (1 - \phi) \ln(1 - \phi) + \chi\phi(1 - \phi)$$

The value of χ_{12} for some polymer-solvent systems (varying with solvent fraction ϕ_1) are given below. PEG-water varies with solvent fraction and its variation is shown in the graph.



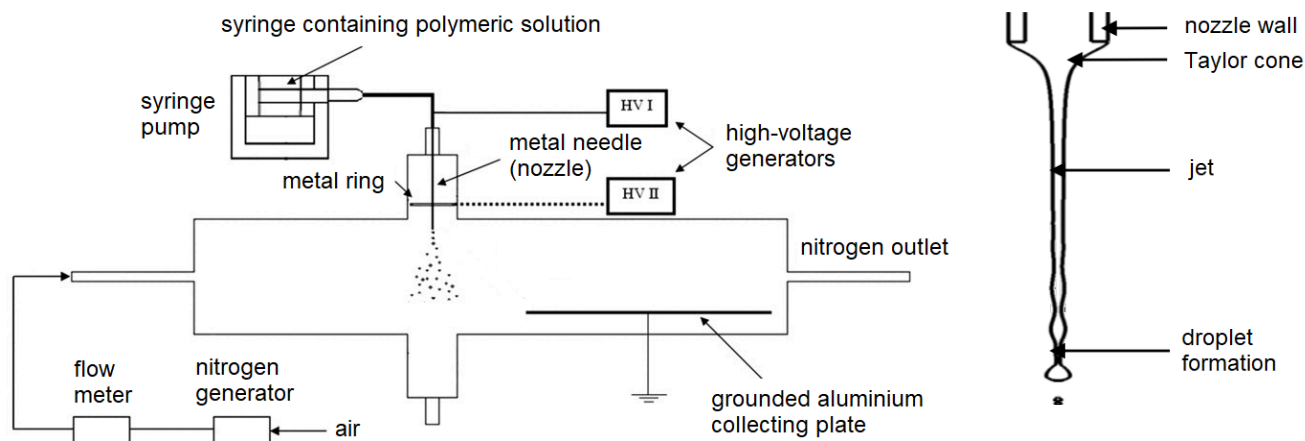
Polymer	Solvent	χ_{12}	Temp / °C
EVA	cyclohexane	0.490	30
EVA	THF	0.411	30
carbosilane dendrimer	benzene	0.85	35
PCL	ethyl acetate	1.466	25

14.3.10. Electro spraying and Electrohydrodynamic Atomisation (EHDA)

EHDA is a modern technique for synthesising loaded microparticles.

General flow diagram of EHDA:

Close-up of nozzle tip:

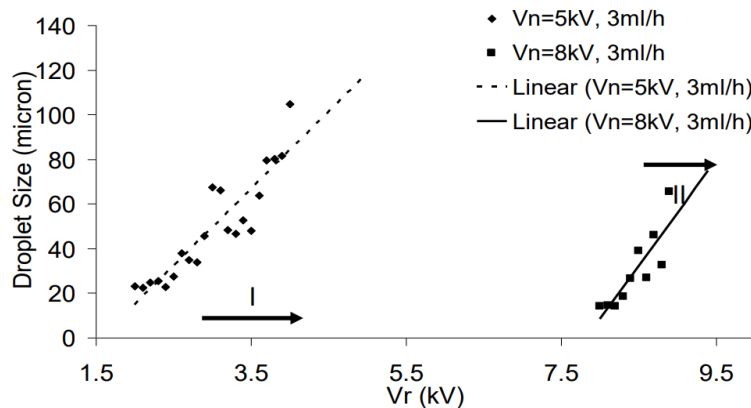


Droplet size variation with different ring electrical potential (V_r)

Nozzle potentials

I: $V_n = 5 \text{ kV}$

II: $V_n = 8 \text{ kV}$



The cone-jet model for the Taylor cone formed at the nozzle tip implies that

$$I \propto \sqrt{\gamma \kappa Q} \quad \text{and} \quad d \propto \left(\frac{\rho \varepsilon_0 Q^4}{I^2} \right)^{1/6} \propto \sqrt{Q}$$

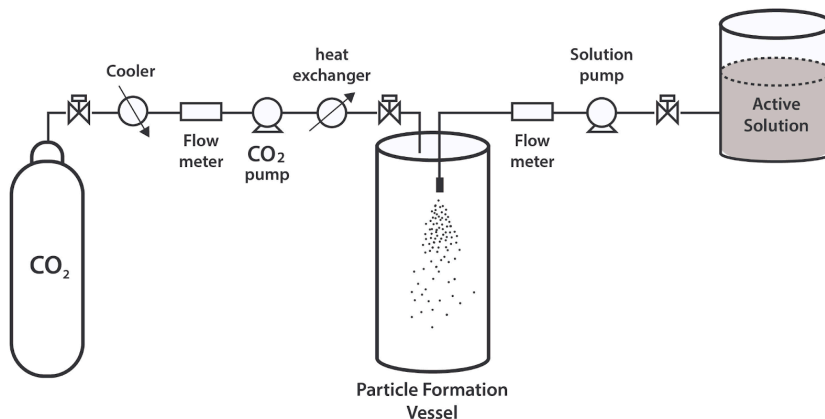
(d : droplet diameter, c : constant, Q : volumetric flow rate, ρ : liquid density, γ : liquid surface tension, κ : liquid electrical conductivity, I : current, ε_0 : vacuum permittivity.)

Modifications to EDHA include coaxial EDHA (CEDHA): two polymer flows in the nozzle, in coflow.

14.3.11. Supercritical Antisolvent Precipitation (SAS)

SAS is a modern technique for synthesising loaded nanoparticles.

General flow diagram of SAS (using sCO₂ as the antisolvent):



$$\text{Encapsulation Efficiency (EE)} = \frac{\text{amount of active compound in nanovesicle suspension}}{\text{total amount of active compound initially in solution}} (\times 100\%)$$

Important parameters affecting the particle size distribution, EE and particle morphology, are the sCO₂ pressure, temperature and flow rate, the physical and chemical properties of the active compound and the encapsulant, and the nozzle geometry.

Modifications to SAS include:

- SAS with enhanced mass transfer (SAS-EM): uses ultrasonication, typically decreasing particle size further, and can be used to control particle morphology.
- Atomised Rapid Injection for Solvent Extraction (ARISE): removes the capillary injector, allowing for higher throughput.

For the phase diagram of CO₂, see Section 14.4.7.

14.3.12. Applications of Nanoparticles and Nanostructures

Well-established nanotechnologies include:

- **Titanium dioxide and/or zinc oxide** (TiO_2 -NPs / ZnO -NPs): used in sunscreen to reflect and scatter UVA and UVB radiation.
- **Silver (Ag-NPs)**: used in textiles for their antimicrobial properties. When these textiles are washed however, Ag-NPs can be released into rivers which are toxic to fish.
- **Graphene**: used in thin-film electronics as an excellent conductor.
- **Graphene oxide**: graphene with -OH pairs, epoxide bridges and -COOH groups. Used in fast-switching electronics and photonics/optoelectronics.
- **Tungsten trioxide graphene composite**: used for energy storage, gas sensors and heterogeneous or photocatalysis.
- **Carbon nanotubes**: extremely high tensile strength along the fibre direction.
- **Buckyballs** (buckminsterfullerene, C_{60}): used as a model for drug delivery by encapsulation.
- **Quantum dots**: made of semiconductors e.g. C, Si, Ge, PbS, CdSe, CdTe, InAs, InP. Used in photonics, quantum information processing and medical diagnostics.

C15. INORGANIC AND ENVIRONMENTAL CHEMISTRY

15.1. Metallurgy

15.1.1. Common Names and Formulas of Ores and Minerals

Metal	Ores	Composition	Metal	Ores	Composition
aluminium (Al)	bauxite	$\text{Al}_2\text{O}_3 \cdot 2 \text{H}_2\text{O}$	zinc (Zn)	sphalerite	ZnS
	diaspore	$\text{Al}_2\text{O}_3 \cdot \text{H}_2\text{O}$		calamine	ZnCO_3
	corundum (ruby: with Cr, sapphire: with Fe, Ti)	Al_2O_3		zincite	ZnO
iron (Fe)	haematite	Fe_2O_3	lead (Pb)	galena	PbS
	magnetite	Fe_3O_4		anglesite	PbSO_4
	siderite	FeCO_3		cerussite	PbCO_3
	iron pyrite	FeS_2	magnesium (Mg)	carnallite	$\text{K}_2\text{MgCl}_4 \cdot 6 \text{H}_2\text{O}$
	limonite	$\text{FeO}(\text{OH})$		magnesite	MgCO_3
copper (Cu)	chalcopyrite	CuFeS_2		dolomite	$\text{MgCO}_3 \cdot \text{CaCO}_3$
	copper glance	CuS_2		olivine	$\text{Mg}_2\text{SiO}_4 \cdot \text{Fe}_2\text{SiO}_4$
	cuprite	Cu_2O	epsom salt	$\text{MgSO}_4 \cdot 7 \text{H}_2\text{O}$	
	malachite	$\text{CuCO}_3 \cdot \text{Cu}(\text{OH})_2$	tin (Sn)	cassiterite	SnO_2
	azurite	$2 \text{CuCO}_3 \cdot \text{Cu}(\text{OH})_2$		silver (Ag)	argentite
beryllium (Be)	beryl / emerald	$\text{Be}_3\text{Al}_2(\text{SiO}_3)_6$	pyrargyrite		Ag_3SbS_3
mercury (Hg)	cinnabar	HgS	cobalt (Co)	cobaltite	CoAsS
uranium (U)	pitchblende	$\text{UO}_2 + \text{U}_3\text{O}_8$	tungsten (W)	scheelite	CaWO_4
silicon* (Si)	quartz	SiO_2		wolframite	$(\text{Fe}, \text{Mn})\text{WO}_4$
cerium** (Ce)	monazite	$(\text{Ce}, \text{La}, \text{Nd}, \text{Th})\text{PO}_4$	chromium (Cr)	chromite	FeCr_2O_4

* silicon is a metalloid so quartz does not qualify as an ore. It is a common gangue mineral.

** monazite often contains a wide variety of lanthanides and actinides (rare-earths).

15.1.2. Classification of Elements by Ore Type

Elements are classified according to their most abundant type of ore in Earth's crust.

1 H																	2 He
3 Li	4 Be											5 B	6 C	7 N	8 O	9 F	10 Ne
11 Na	12 Mg											13 Al	14 Si	15 P	16 S	17 Cl	18 Ar
19 K	20 Ca	21 Sc	22 Ti	23 V	24 Cr	25 Mn	26 Fe	27 Co	28 Ni	29 Cu	30 Zn	31 Ga	32 Ge	33 As	34 Se	35 Br	36 Kr
37 Rb	38 Sr	39 Y	40 Zr	41 Nb	42 Mo	43 Tc	44 Ru	45 Rh	46 Pd	47 Ag	48 Cd	49 In	50 Sn	51 Sb	52 Te	53 I	54 Xe
55 Cs	56 Ba	* 71 Lu	* 72 Hf	* 73 Ta	* 74 W	* 75 Re	* 76 Os	* 77 Ir	* 78 Pt	* 79 Au	* 80 Hg	* 81 Tl	* 82 Pb	* 83 Bi	* 84 Po	* 85 At	* 86 Rn
87 Fr	88 Ra	** 103 Lr	** 104 Rf	** 105 Db	** 106 Sg	** 107 Bh	** 108 Hs	** 109 Mt	** 110 Ds	** 111 Rg	** 112 Cn	** 113 Nh	** 114 Fl	** 115 Mc	** 116 Lv	** 117 Ts	** 118 Og
		* 57 La	* 58 Ce	* 59 Pr	* 60 Nd	* 61 Pm	* 62 Sm	* 63 Eu	* 64 Gd	* 65 Tb	* 66 Dy	* 67 Ho	* 68 Er	* 69 Tm	* 70 Yb		
		** 89 Ac	** 90 Th	** 91 Pa	** 92 U	** 93 Np	** 94 Pu	** 95 Am	** 96 Cm	** 97 Bk	** 98 Cf	** 99 Es	** 100 Fm	** 101 Md	** 102 No		

Lithophiles (oxides, silicates)

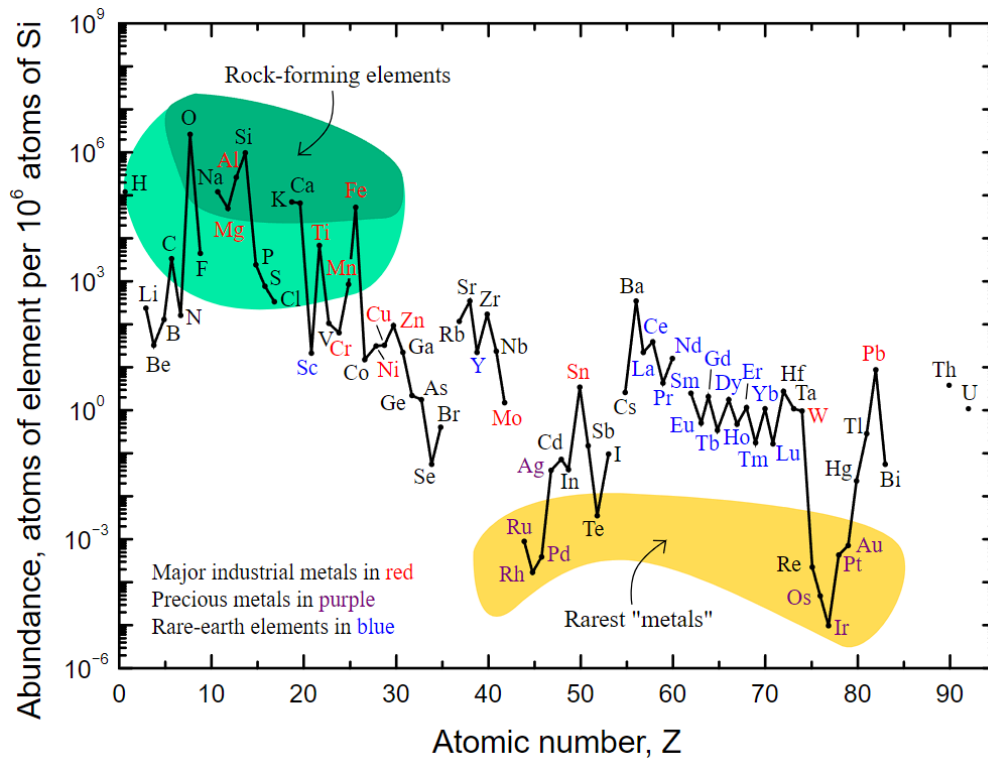
Siderophiles (iron solid solution)

Chalcophiles (sulfides)

Atmophiles (volatile, atmospheric)

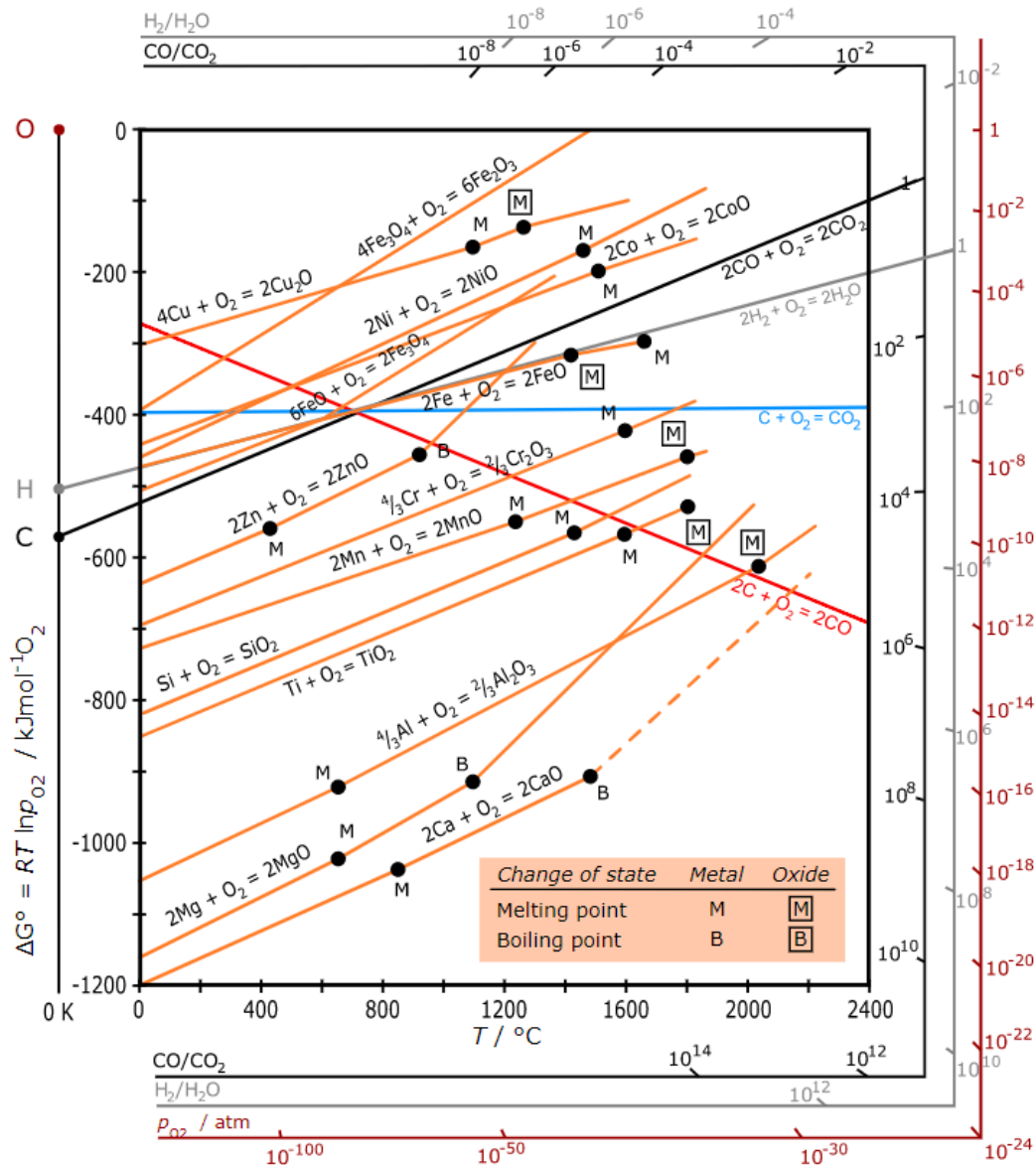
Not found in nature

Elemental abundance: molar abundance in crust, relative to silicon (Si)



15.1.3. Ellingham Diagram for Oxidation Reactions

The lower the position of a metal's line in the Ellingham diagram, the greater is the stability of its oxide. If the curves for two metals at a given temperature are compared, the metal with the **lower** Gibbs free energy of oxidation on the diagram **will reduce the oxide with the higher** Gibbs free energy of formation e.g. carbon can reduce Cr_2O_3 to Cr above 1200°C by oxidation to CO.



(The dotted line for forming CaO (g) indicates hypothetical (experimentally unknown) values).

Contours of p_{O_2} , $\frac{p_{\text{H}_2}}{p_{\text{H}_2\text{O}}}$ and $\frac{p_{\text{CO}}}{p_{\text{CO}_2}}$ (partial pressures at equilibrium) are shown on the sides, which each point to the **O**, **H** and **C** points respectively on $T = 0\text{ K}$.

15.1.4. Metal Extraction Techniques

The typical processes for metal extraction from ores are:

1. **Pulverisation:** the ore is mechanically crushed and ground into a powder by e.g. ball milling, stamp milling.
2. **Dressing:** impurities in the ore are removed, concentrating the desired product.
3. **Extraction:** the crude metal is chemically extracted by converting the ore to a compound which is more suitable for reduction, often an oxide, then reduced to the metal.
4. **Refining:** the metal is purified using a technique specific to the desired application.

Methods of dressing (mineral processing) include hydraulic washing (gravity separation), electromagnetic separation, froth flotation processes and base leaching processes (hydrometallurgy).

Methods of pre-conversion of concentrated ores to their oxide (pyrometallurgy):

- Calcination (carbonate \rightarrow oxide + CO_2 , by thermolysis without oxygen)
- Roasting (sulfide + $\text{O}_2 \rightarrow$ oxide + SO_2 , by heating with oxygen); may include self-reduction e.g. Cu_2S , PbS due to reaction with its own oxide to form the metal.

Methods of reduction of the to the metal:

- Smelting: heating of the oxide with coal or coke (C) or aluminium powder (thermite) in a blast furnace, with addition of flux (acidic flux e.g. borax, SiO_2 to remove basic impurities, basic flux e.g. MgO , CaCO_3 to remove acidic impurities), which converts gangue to easily-removable slag.
- Metal displacement: e.g. sulfide + $\text{O}_2 \rightarrow$ sulfate, or sulfide + $\text{NaCN} \rightarrow$ metallic cyanide complex, which reacts with electropositive metals e.g. Cu to give the pure metal by a displacement reaction.
- Electrolysis: molten salt (electrometallurgy) or aqueous salt (electrowinning) electrolysis using a graphite anode and a metal cathode.

Methods of refining to a pure metal:

- Liquefaction: readily fusible metals can be melted at a temperature where the impurities remain solid.
- Distillation: volatile metals can be vaporised at a temperature where the impurities remain solid.
- Zone refining (fractional crystallisation): segregation of impurities from the liquid state forms ultrapure grains on recrystallisation. Used for pure semiconductors.
- Column chromatography: the mixture is put in a liquid or gaseous medium which is moved through an adsorbent, which adsorbs at different levels, and can be eluted once adsorption has finished.
- Vapour phase refining: the metal is converted to a volatile compound, then heated to decompose from the gas phase to the pure metal, which deposits.
- Electrorefining: aqueous or molten electrolysis using a solution of the metal as the electrolyte. The anode is the impure metal, depositing its insoluble inert impurities ('anode mud': often containing precious metals), while the cathode accumulates pure metal.

15.1.5. Industrial Metal Extraction Processes

Lithium

- **Ore processing:** spodumene ($\text{LiAl}(\text{SiO}_3)_2$) is mined from Li-rich pegmatite deposits, crushed and gravity separated. It is then roasted to convert it to lithium carbonate or lithium hydroxide, which may be used as chemicals or converted to metallic lithium by electrolytic refining.
- **Brine extraction:** brine deposits in salt flats or underground reservoirs are pumped to the surface and evaporated to concentrate the salts. Lithium is selectively precipitated from the solution using soda ash or sodium hydroxide (e.g. $2 \text{Li}^+ + \text{Na}_2\text{CO}_3 \rightarrow \text{Li}_2\text{CO}_3 + 2 \text{Na}^+$) to form Li_2CO_3 or LiOH , which is filtered, washed and dried.

Sodium, Potassium

- **Downs process** (1923): electrolysis of the molten sodium chloride using a graphite anode and iron cathode: e.g. $2 \text{NaCl} \rightarrow 2 \text{Na} + \text{Cl}_2$
- **Solvay process** (1863): produces soda ash (Na_2CO_3) from brine (NaCl) and limestone (CaCO_3) solutions, catalysed by ammonia in several chemical reactions.

Magnesium

- **Molten electrolysis:** anhydrous magnesium chloride is fused with NaCl and CaCl_2 to lower the melting point and electrolysed. The chloride can be made by either heating carnallite ($\text{MgCl}_2 \cdot 6 \text{H}_2\text{O}$) in catalytic HCl gas or smelting the oxide via $\text{MgO} + \text{C} + \text{Cl}_2 \rightarrow \text{MgCl}_2 + \text{CO}$.

Chromium, Vanadium, Niobium, Molybdenum

- **Goldschmidt aluminothermic process** (1895): smelting of the oxide using powdered aluminium (thermite): e.g. $3 \text{V}_2\text{O}_5 + 10 \text{Al} \rightarrow 5 \text{Al}_2\text{O}_3 + 6 \text{V}$

Aluminium

- **Bayer process** (1888): bauxite ore is roasted to oxidise ferric oxide impurities (FeO) to Fe_2O_3 . The roasted ore is then base-hydrolysed and the hydroxide is calcined:
 $\text{Al}_2\text{O}_3 + \text{NaOH} \rightarrow \text{NaAlO}_2 + \text{H}_2\text{O} \rightarrow \text{Al}(\text{OH})_3 (+ \text{NaOH}) \rightarrow \text{Al}_2\text{O}_3$.
- **Serpuk process** (1903): bauxite ore with silica impurities is smelted at 2000°C in air with coke to give the nitride, which is readily hydrolysed to give the hydroxide and ammonia, which is calcined: $\text{Al}_2\text{O}_3 + \text{N}_2 + \text{C} \rightarrow \text{AlN}$; $\text{AlN} + \text{H}_2\text{O} \rightarrow \text{Al}(\text{OH})_3 + \text{NH}_3$; $\text{Al}(\text{OH})_3 \rightarrow \text{Al}_2\text{O}_3$.
- **Hall-Héroult process** (1886): electrolysis of a fused matrix of Al_2O_3 and cryolite (Na_3AlF_6) or fluorspar (CaF_2), which are added to lower melting point and increase conductivity, using a graphite anode and steel cathode: $2 \text{Al}_2\text{O}_3 + 3 \text{C} \rightarrow 4 \text{Al} + 3 \text{CO}_2$.
- **Hoopès process** (1925): electrolytic refining of Al to very high purity (~99.98%).

Copper, Zinc

- **Froth floatation** (1905): copper pyrites (CuFeS_2) are crushed into the powdered ore and sieved into a water-pine oil mixture and roasted in air to give the sulfide ore (Cu_2S)
- **Bessemerisation** (1856): smelting with O_2 and SiO_2 converts FeS impurities to FeSiO_3 (slag). The Cu_2S self-reduces with CuO to give Cu (blister copper, ~99% pure) and SO_2 .
- **Electrolytic refining** to ~99.9% purity using Cu electrodes in acidic CuSO_4 electrolyte, with inert impurities such as Sb , Se , Te , Ag dropping out in the anode mud.
- **Phytomining** (1998): hyperaccumulator plants are grown to high biomass density in soil with copper ore (bioleaching), then dried and incinerated in air to produce copper-rich ash (phytoextraction). The copper ash is displaced by scrap iron in sulfuric acid.

Gold, Silver

- **MacArthur-Forrest cyanide process** (1887): the ore is leached with dilute NaCN in air to form $\text{Na}[\text{Au}(\text{CN})_2]$, and then displaced by scrap zinc powder to precipitate Au .
- **Ziervogel process** (1885): argentite (Ag_2S) is oxidised to silver sulfate at 85°C , which is reacted with scrap copper or iron metal to precipitate silver metal:

$$\text{Ag}_2\text{S} + 2 \text{O}_2 \rightarrow \text{Ag}_2\text{SO}_4; \quad \text{Ag}_2\text{SO}_4 + \text{Cu} \rightarrow \text{CuSO}_4 + 2 \text{Ag}$$
- **Patio process** (1557): mercury and magistral (burnt pyrites - sulphates and oxides of copper and iron) are added to the powdered mineral containing saline. The mixture is kept for several days. An amalgam of silver (mercurial silver) is formed. On washing, drying and subsequent distillation, silver metal is obtained.
- **Parkes process** (1850): a liquid-liquid extraction of silver from lead to produce bullion. Zinc is added to the molten lead, in which silver is much more soluble. The $\text{Zn}(\text{Ag})$ phase separates and the zinc can be boiled away to leave pure silver.

Lead

- **Froth floatation process**: galena is concentrated as PbS .
- **Betts process** (1904): electrolytic refining in molten fluorosilicates ($\text{H}_2\text{SiF}_6 + \text{PbSiF}_6$). Uses a pure lead cathode and an impure lead anode. Pure lead plates the cathode.
- **Betterton-Kroll process** (1922): add Ca-Mg alloy to remove Bi and Sb impurities at 350°C . Skim off the dross (surface layer film) containing $\text{CaMgBi}_2 + \text{CaMgSb}_2$, passing it through a hydraulic press to recover molten lead in this layer leaving ~99.99% pure lead in the bulk.
- **Air reduction**: PbS is fused in a reverberatory furnace in air to give PbO and PbSO_4 , which self-reduce more PbS into crude lead metal. Carbon reduction: PbS is mixed with lime and heated in a sinterer to give PbO , then mixed with coke and smelted in a blast furnace to form crude lead metal.

Titanium, Zirconium

- **Kroll process** (1940): TiCl_4 or ZrCl_4 is reduced by liquid magnesium metal at $825\text{ }^\circ\text{C}$ to give MgCl_2 and porous spongy Ti or Zr, which is purified by leaching or vacuum distillation. The sponge is crushed, pressed and melted in a consumable carbon electrode vacuum arc furnace. The melted ingot solidifies under vacuum, and can be remelted to remove inclusions and ensure uniformity.

Uranium

- **Milling:** ore is extracted from underground shafts, transported to mills and crushed. The pulped ore is leached with acid/base/peroxide, where uranium oxides are converted to uranyl complexes (UO_2^{2+}) which form yellowcake (mainly U_3O_8).
- **In situ leaching:** if processing on-site, the leaching solution is injected through drill holes into the ore. The leachate is pumped to the surface and recovered.
- **Smelting:** yellowcake is smelted into purified UO_2 .
- **Enrichment:** uranium oxides are reacted with fluorine to form uranium hexafluoride gas (UF_6). The gas is spun in a centrifuge so that the fissile lighter isotope (^{235}U) accumulates in the centre at elevated concentration (low enriched uranium: $<20\%$ ^{235}U , highly enriched uranium: $>20\%$ ^{235}U , weapons-grade uranium: $>90\%$ ^{235}U).

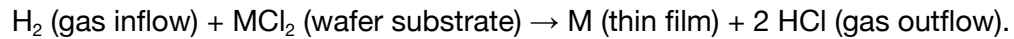
Iron and Steel

- Iron ores (magnetite, haematite and limonite) are concentrated by **gravity separation** followed by **electromagnetic separation**. The ore is then **calcined and roasted in air** to remove moisture and impurities as CO_2 , SO_2 and As_2O_3 , while oxidising FeO to Fe_2O_3 . This is then **smelted** in a blast furnace (with coke and limestone) to form sponge iron, then to pig iron (impure iron with C, Mn and Si). Pig iron can be remelted and cooled to form cast iron, with $\sim 5\%$ carbon.
- **Duplex process for steelmaking** (1930): molten pig iron is first treated in an acid-lined Bessemer converter to remove Si, Mn and a part of C. The molten pig iron is then transferred to a base-lined (calcined dolomite) open-hearth furnace to remove P and remaining C to the desired carbon content, with small amounts of alloy metals e.g. Mn, Cr, V, Co, Ni, Mo, W being added to improve mechanical, thermal and electrochemical properties.

15.1.6. Specialised Manufacturing Methods for Single Crystal Materials

These are materials consisting of a single macroscopic grain (i.e. all atoms are fully aligned across the bulk structure with no grain boundaries). Useful in the semiconductor industry (silicon), optoelectronics (graphene, sapphires, InP, CdTe), high-performance electrical conductors (copper, silver), and single crystal turbine blades (SX nickel superalloys). Methods include:

- Czochralski method: nucleation with a small crystal, slowly pulled up and out of the melt.
- Liquid phase electroepitaxy (LPEE): electrochemical deposition onto a substrate.
- Chemical vapour deposition (CVD): used for semiconductors and nanomaterials. Formation of thin films on a hot substrate by chemical reaction e.g.



- Investment casting: used for metals. A helical 'pigtail' is used to cull unwanted crystal growth orientations from a cooling melt.

15.2. Earth Science, Geochemistry and Physical Geography

15.2.1. Properties of the Earth's Atmosphere

Components of the Atmosphere:

The 'dry' atmosphere is (by moles): 78.08% N₂, 20.95% O₂, 0.93% Ar and ~0.04% CO₂ (as of 2022). Water vapour can also be present (up to 3%). Trace gases include Ne, He, CH₄, Kr, Xe, H₂, N₂O, CO, O₃, HCHO, NO_x, NH₃, SO₂, present at ppb levels, and sometimes variable due to environmental factors.

Troposphere (up to 6 - 18 km):

- All common weather occurs in the troposphere, including the three-cell circulation (Section 15.2.2).
- It extends highest over the tropics, and lowest over the poles.
- Hurricanes occupy the whole vertical extent, flattening out at the tropopause.
- The 'planetary boundary layer', where flow is influenced by landscape, extends to ~0.1-2 km.

Stratosphere (up to 50 km):

- The ozone layer is at ~15 - 40 km, which absorbs all high energy radiation (UVC and above).
- Temperature increases towards the stratopause.
- Some military aircraft fly in the stratosphere.
- The Armstrong limit, above which humans require a pressurised suit to survive, is at 19 km.

Mesosphere (up to 85 km):

- Temperature decreases towards the mesopause, cooling to around -143 °C.
- Meteors burn up in the mesosphere. Very bright meteors are called bolides.

Thermosphere (up to 690 km):

- High energy UV causes photoionisation to a plasma state (ionosphere), with temperatures reaching 2000 °C dependent on solar activity.

Exosphere (beyond 690 km and up to ~100,000 km):

- Highly rarefied gas gravitationally bound by Earth's gravity, consisting mainly of hydrogen.

15.2.2. Electromagnetism in Geophysics

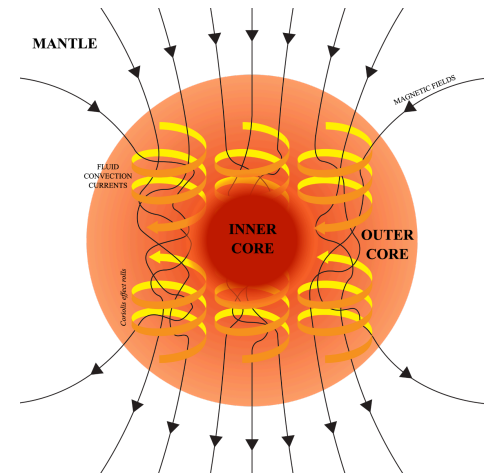
For the theories of electromagnetism, plasma physics and magnetohydrodynamics, see Section 8.5.

Dynamo Theory: a rotating, convecting, electrically-conducting fluid sustains a magnetic field.

The liquid iron-nickel outer core is conductive and is organised into vortices by the Coriolis force (Taylor columns). The initial weak magnetic field at Earth's formation was primordial, but is then amplified and sustained by magnetic induction and thermal convection in the outer core. Only ~1% of the field intensity extends out of the surface of the Earth.

Magnetic field evolution is described by the MHD induction equation: $\partial \mathbf{B} / \partial t = \eta \nabla^2 \mathbf{B} + \nabla \times (\mathbf{v} \times \mathbf{B})$.

To sustain a planetary dynamo, the magnetic Reynolds number must be $Re_m > 100$.



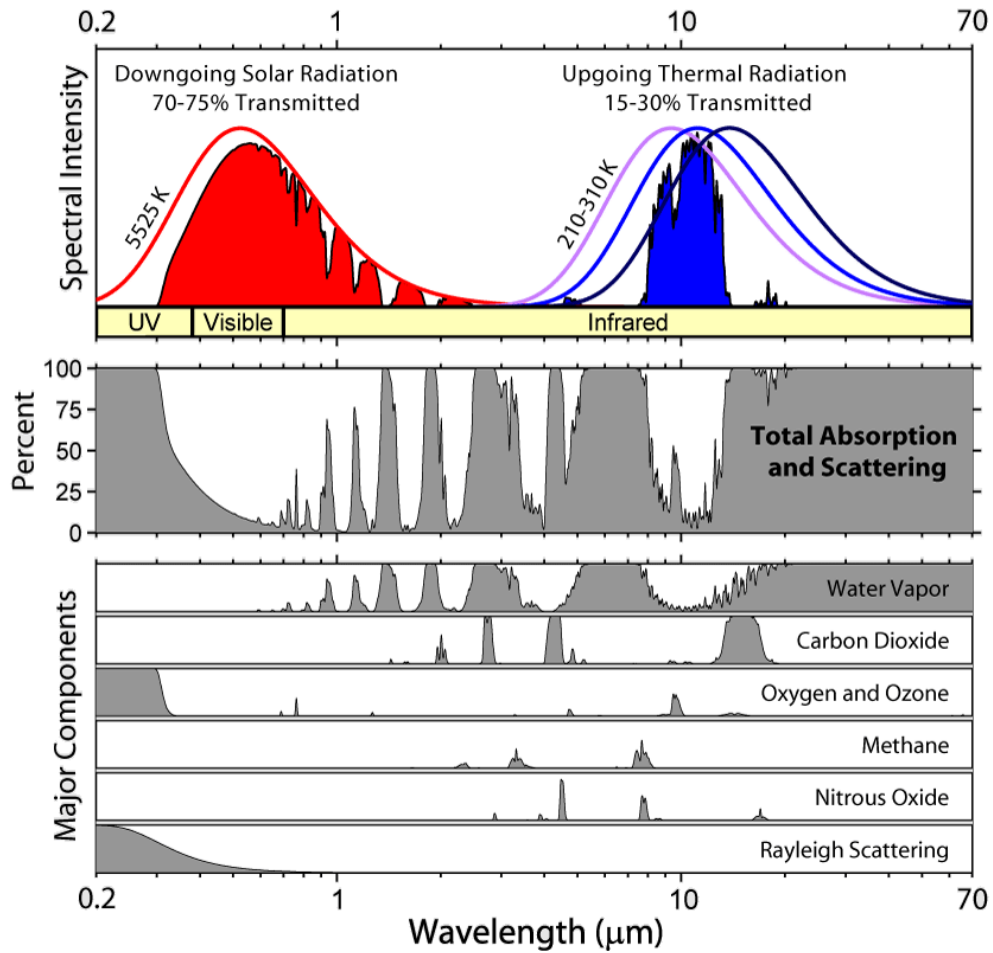
Electromagnetic Phenomena in the Earth's Atmosphere: ionosphere as an RF waveguide

- Auroras occur in geomagnetic storms (from coronal mass ejections), when incoming high-energy electrons accelerated by magnetic reconnection collide with plasma ions, emitting light by fluorescence.
- Radio waves from below are reflected and refracted by the plasma, enabling radio transmission. The natural frequency of standing radio waves due to reflection causes Schumann resonances at ~8 , which can be excited by RF emission from lightning strikes. Oscillations from strong radio waves can cause interference by cross-modulation (Luxembourg effect).
- Residual atmospheric gases are free from turbulence and stratify by molecular mass (turbosphere).
- The Karman line, an arbitrary line designating 'outer space', is at 100 km.
- The International Space Station (ISS) orbits at ~400 km.
- The anacoustic zone, where the atmosphere is rarified enough to prevent audible sound propagation, begins at 160 km (higher frequencies are attenuated first).

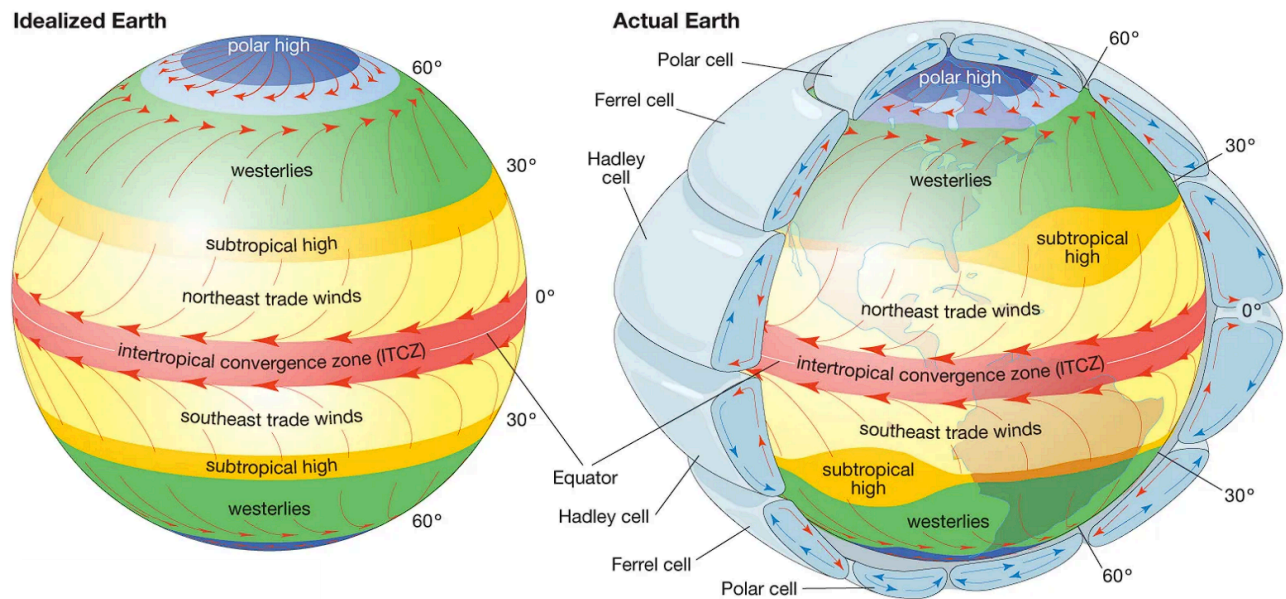
The outer magnetosphere deflects solar wind up to ~60,000 km (magnetopause).

Transmission Spectrum of the Atmosphere to Insolation and Radiant Heat

The Sun emits radiation (insolation) at a near-black body spectrum with $T = 5525\text{ K}$, of which ~75% (mainly wavelengths at UVB and longer) is transmitted to the ground. The Earth's own thermal emission spectrum emits IR radiation which is partially absorbed and reflected back to the surface by greenhouse gases in the atmosphere.



15.2.2. Three-Cell General Atmospheric Circulation Model



Surface winds circulate by natural convection within cells due to variation in temperature.

- **Hadley cells:** between 30° N/S (the Tropic of Cancer and Tropic of Capricorn, respectively). Carries the trade winds from the subtropical highs to the intertropical convergence zone (ITCZ, near-equator).
- **Ferrel cells:** between 30° N/S and 60° N/S. Carries the westerly jet streams from the subtropical highs to the subpolar lows in Rossby waves (high wind shear, large-scale undulations due to Coriolis forces).
- **Polar cells:** between 60° N/S and 90° N/S (the North pole and South pole respectively). Carries the polar easterlies from the poles to the subpolar lows.

15.2.3. Continents and Oceans on Earth



15.2.6. Natural Causes for Changes in Earth's Climate

The Earth's climate depends broadly on its temperature, which is influenced by the amount of solar insolation (radiant power) received from the Sun. Changes in orientation of the Earth relative to the Sun, as well as changes in the output of the Sun, produce natural climate variation.

Milankovitch cycles: changes in the orbit of the Earth over long periods of time. Equatorial regions are more affected by variation in eccentricity/precession. Polar regions are more affected by variation in obliquity.

- Eccentricity: Earth's elliptical orbit varies in eccentricity from 0.005 (low eccentricity → more climate stability) to 0.058 (high eccentricity → less climate stability) with period 100,000 years.
- Obliquity: Earth's axial tilt relative to the ecliptic varies from 22.1° (less tilt → less extreme seasons) to 24.5° (more tilt → more extreme seasons) with period 41,000 years.
- Precession: Earth's axis precesses about the ecliptic plane normal with period 25,700 years.

Solar cycles: changes in the magnetic activity and total radiant power of the Sun over time.

- Sunspots (regions of high coronal temperature and strong magnetic field, associated with more solar flares and coronal mass ejections (CMEs)) appear with fluctuating counts with period 11 years.
- The variation in solar irradiance over a sunspot cycle is small (~0.1%).
- Other (irregular) variations can have a stronger effect on the climate.

Seasons: depends on the part of the Earth facing direct sunlight

- June/Northern Solstice: the Sun is directly overhead on the Tropic of Capricorn (23.3° N).
- December/Southern Solstice: the Sun is directly overhead on the Tropic of Cancer (23.3° S).
- Equinoxes (Spring, Autumn): the Sun is directly overhead on the Equator (0° N).

Above the Arctic Circle (66.3° N), the Sun never sets around the June solstice, and never rises around the December solstice, and vice versa for below the Antarctic Circle (66.3° S).

Eclipses and Tides: depends on the relative locations of the Sun and the Moon.

The Moon is tidally locked with the Earth (same face points towards Earth). It orbits with inclination 5.14° to the ecliptic, with negligible axial tilt and eccentricity 0.05.

- Solar Eclipse: when the moon falls between the Sun and the Earth, obscuring the Sun.
- Lunar Eclipse: when the Earth falls between the Sun and the moon, obscuring the moon.
- High tide: when and where the Moon is directly overhead (neglecting phase lag)
- Low tide: occurs between the points facing and antipodal to the moon (neglecting phase lag)
- Spring tide: more extreme tides in which the Sun and the Moon are aligned (New Moon, Full Moon)
- Neap tide: less extreme tides in which the Sun and the Moon are perpendicular (1st/3rd quarter)

The El Niño Southern Oscillation (ENSO): the most significant global climate fluctuation

Changes to the temperature gradients in the equatorial Pacific Ocean can affect the nominally East-to-West trade winds, causing severe weather in tropical regions e.g. floods in Peru, droughts in India. The oscillations are irregular: the warming phase is called an 'El Niño year' and the cooling phase is called a 'La Niña year'.

15.2.7. Properties of the Earth's Crust

Elemental Composition of the Crust

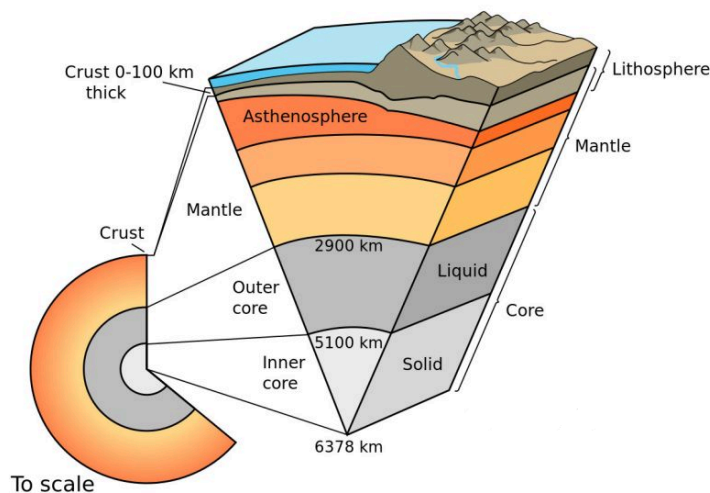
Component	wt. %
Oxygen, O	46.60%
Silicon, Si	27.72%
Aluminium, Al	8.13%
Iron, Fe	5.00%

Component	wt. %
Calcium, Ca	3.63%
Sodium, Na	2.83%
Potassium, K	2.59%
Magnesium, Mg	2.09%

The mantle is mainly peridotite (such as olivine, MgFeSiO_4)

The core is mainly iron (85.5%) as well as nickel.

Layers of the Earth



Oceanic crust: thin, high-density basalt

Continental crust: thick, low-density granite rocks

Mohorovičić discontinuity (Moho): separates the oceanic crust from the asthenosphere near an oceanic ridge.

Lithosphere: the crust and the uppermost solid mantle

Asthenosphere: the hot fluid mantle in which convection currents flow

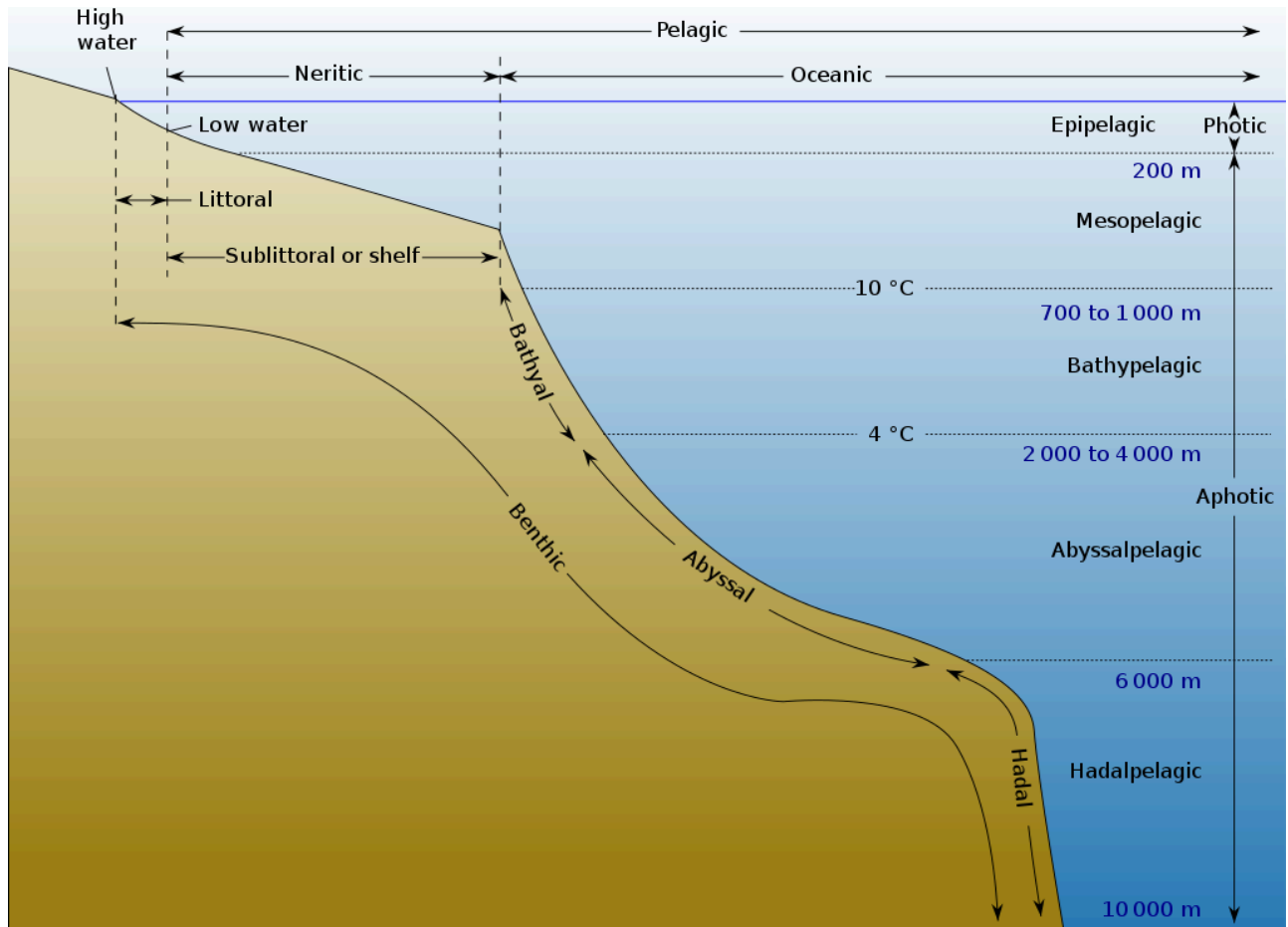
Mesosphere: the rigid lower mantle, made of ultramafic peridotites

D" layer: a heterogeneous layer between the lower mantle and outer core with a large temperature gradient.

Outer core: liquid iron and nickel at $T \sim 5500 \text{ }^\circ\text{C}$ and $p \sim 3 \times 10^8 \text{ atm} = 30 \text{ TPa}$.

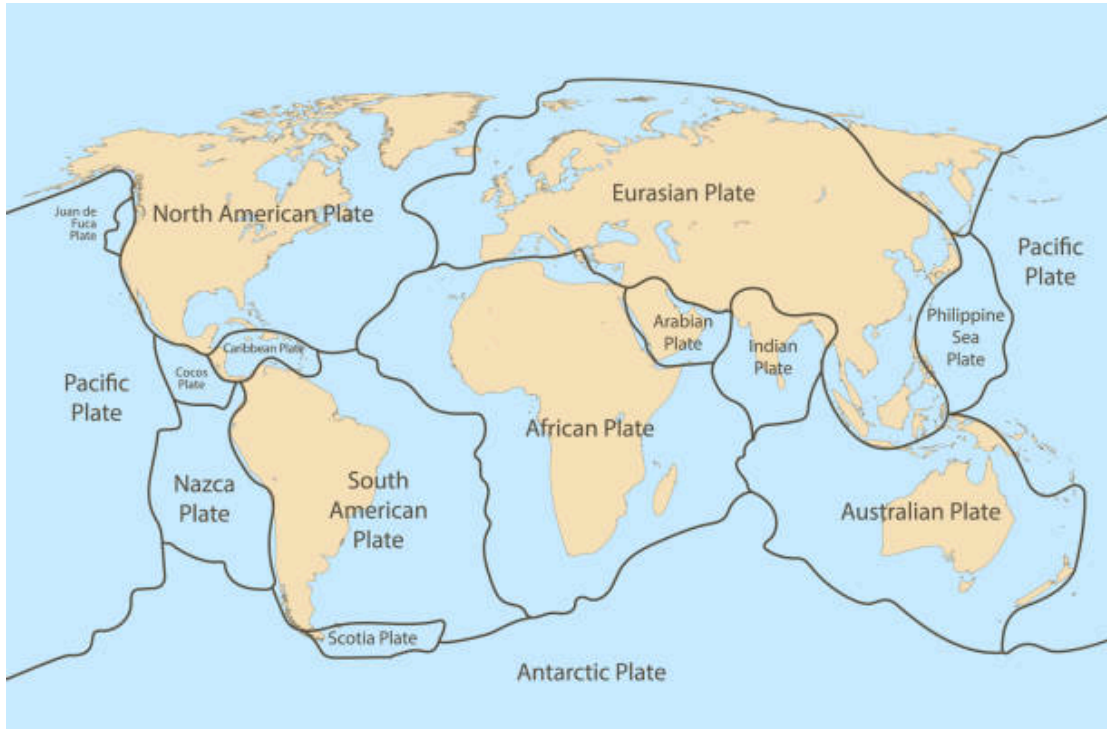
Inner core: solid iron and nickel, rotating faster than the outer core (superrotation). The motion of molten metal is equivalent to an electric current, which generates a circulating magnetic field (magnetohydrodynamics). This creates a dynamo effect by driving a current through the outer core, which is thought to create the Earth's magnetic field (the dynamo theory).

15.2.9. Layers of the Ocean and Oceanic Crust



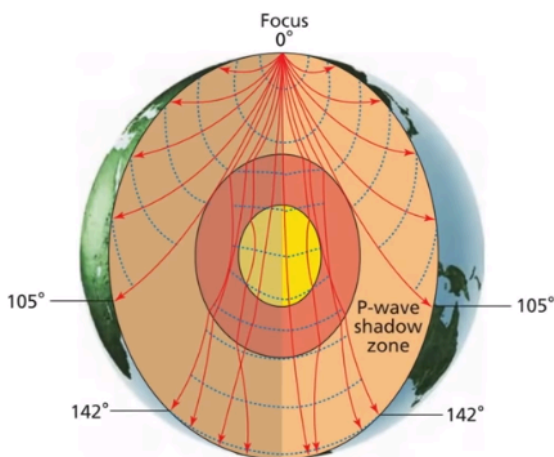
15.2.10. Current Boundary Locations of the Earth's Tectonic Plates

Tectonic plates drift on the mantle over time, colliding and causing various geological activity (earthquakes, tsunamis, volcanoes, mountains) at and around their boundaries.

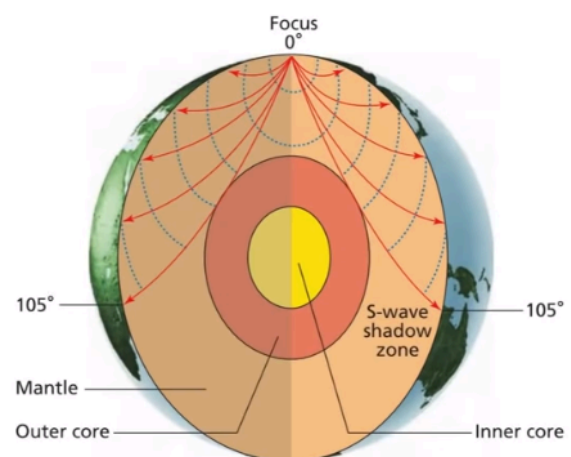


15.2.11. Trajectories of Primary (P) and Secondary (S) Waves Through Earth

During an earthquake, P-waves (faster, longitudinal) and S-waves (slower, transverse) propagate from the focus (hypocentre).



P-waves: refracted at phase boundaries.

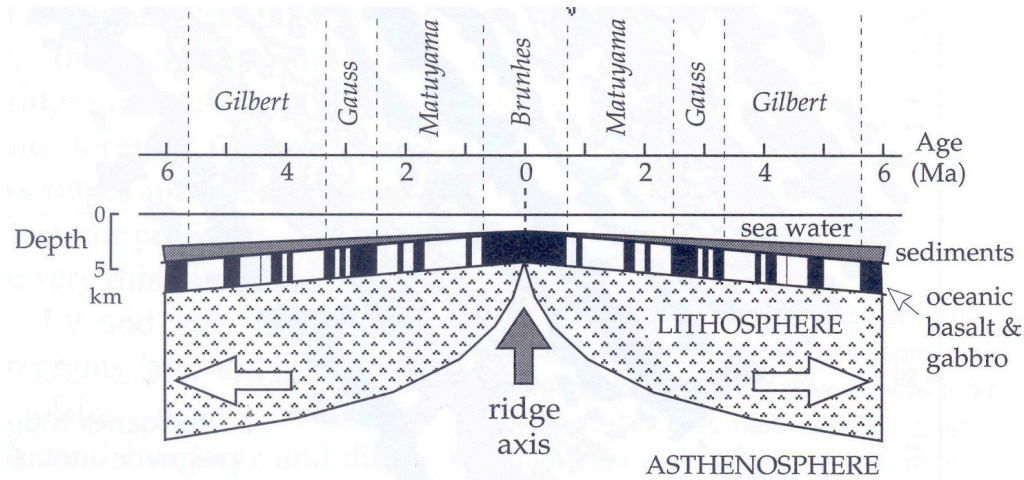


S-waves: absorbed (blocked) by liquid.

15.2.12. Evidence for Tectonic Theory: Vine-Matthews Hypothesis and The Wilson Cycle

Vine-Matthews Hypothesis: at a mid-oceanic ridge, the rate of seafloor spreading is linked to geomagnetic reversals due to magnetic striping. This is observed at the mid-Atlantic ridge.

The most recent chrons are named Brunhes, Matuyama, Gauss, Gilbert...



Wilson Cycle: volcanism on plates induced by stationary vertical 'hotspots' (mantle plumes) leads to the formation of chains of volcanoes (a seamount) as the plate moves, which are then gradually eroded.

15.2.13. Geological Classification of Rocks

Rocks within the Earth can be classified as:

- **Igneous** rock (e.g. granite, basalt, obsidian): formed from crystallisation of magma.
- **Sedimentary** rock (e.g. sandstone, limestone, shale): formed from lithification of sediment by compaction and cementing.
- **Metamorphic** rock (e.g. gneiss, schist, slate): formed by metamorphism of sedimentary or igneous rocks under high pressure and temperature.

15.2.14. Biomes and The Characteristics of Deserts and Rainforests

Biomes are described by the unique interdependence of climate, water (or permafrost in the case of tundra and polar regions), soils, plants, animals and the actions of people who live within them.

Desert environments:

- Causes of desertification: climate change, population growth, removal of fuel wood, overgrazing, over-cultivation and soil erosion.
- Strategies used to reduce the risk of desertification: water and soil management, tree planting and use of appropriate technology.

Rainforest environments:

- Causes of deforestation: subsistence and commercial farming, logging, road building, mineral extraction, energy development, settlement, population growth.
- Impacts of deforestation – economic development, soil erosion, contribution to climate change.

15.2.15. Protection of Natural Landscapes

Landscapes may be protected by:

- Hard engineering – (coastal) sea walls, rock armour, gabions and groynes; (rivers) dams and reservoirs, straightening, embankments, flood relief channels.
- Soft engineering – (coastal) beach nourishment and reprofiling, dune regeneration, coastal realignment (managed retreat); (rivers) flood warnings and preparation, flood plain zoning, planting trees and river restoration.

15.2.16. Transport Phenomena in Coastal, River, Glacial and Urban Environments**Coastal processes** and landforms:

- Weathering – mechanical, chemical.
- Mass movement – sliding, slumping and rock falls.
- Erosion – hydraulic power, abrasion and attrition. Forms landscapes such as headlands and bays, cliffs and wave cut platforms, caves, arches, stacks and stumps.
- Transportation – longshore drift.
- Deposition – forms landscapes such as beaches, sand dunes, spits and bars.

Fluvial processes and landforms:

- erosion – hydraulic action, abrasion, attrition, solution, vertical and lateral erosion. Forms landscapes such as V-shaped valleys, interlocking spurs, waterfalls, gorges, meanders and ox-bow lakes.
- transportation – traction (rolling), saltation (bouncing), suspension and solution.
- deposition – forms landscapes such as levées, flood plains and estuaries.

Glacial processes and landforms:

- freeze-thaw weathering
- erosion – abrasion and plucking. Forms landscapes such as corries, arêtes, pyramidal peaks, truncated spurs, glacial troughs, ribbon lakes and hanging valleys.
- movement and transportation – rotational slip and bulldozing.
- deposition – till and outwash. Forms landscapes such as erratics, drumlins, and types of moraine (lateral, ground, terminal, recessional, medial, supraglacial).

Urban environments typically do not permit water infiltration due to the low permeability of paving materials e.g. concrete / tarmac. Instead, surface runoff occurs. Freeze-thaw cycling may lead to erosive damage e.g. potholes. Sustainable drainage systems (SuDS) may be used to avoid excess runoff. For information on geotechnical engineering of water and drainage systems, see Section 6.5.3.

Changes to natural environments can have a significant impact on the local wildlife. Over longer periods of time, environmental changes can lead to speciation (evolution by diversification).

15.2.17. Natural Hazards

Natural hazards and extreme adverse weather events can cause extensive damage through mass transport in a variety of ways.

- **Volcanic eruptions:** upthrust of magma through a vent and surface flows of lava. Volcanic ash (tephra; particulate matter e.g. PM10) is also released into the atmosphere which can cause widespread pollution, acid rain and cooling due to albedo decrease. Especially explosive eruptions can cause pyroclastic flows (hot fast gas streams) and/or lahars (dense mudslides) down the volcano cone.

Volcanic activity often occurs near tectonic plate subduction zones, or above mantle hotspots.

Volcanoes can be classed as shield volcanoes (gentle slope, small crater) or composite cone volcanoes (steep slope, large crater (caldera), viscous lava).

- **Earthquakes:** rapid shaking or vibration (tremors) of land due to tectonic plates shearing on a fault line. If an earthquake occurs near the ocean floor, the impulse may trigger formation of large waves which accumulate and rush towards shores (tsunamis).
- **Landslides:** mass movement of land down a slope, such as lahars (mud down a volcano), avalanches (snow down a mountain).
- **Geysers:** a hot spring with a high-pressure reservoir. Violently discharges boiling water and steam from fissures in the surface of rocks. Usually found near volcanoes, with heat provided by magma. Geysers do not typically cause widespread damage, but can harm individuals local to them.
- **Tropical Storms:** high-speed circular winds forming over warm oceans which spin due to Coriolis forces and migrate due to the global wind currents (usually the trade winds). Named cyclones (South Pacific/Indian ocean), hurricanes (Atlantic/north-eastern Pacific ocean) or typhoons (north-western Pacific ocean). Summer (wet) monsoons are larger-scale seasonal wind patterns accompanied by persistent torrential rain.
- **Extreme weather:** e.g. drought (extended periods of dryness and low cloud cover, common in arid climates), flash floods (powerful water flows, often due to torrential rain on a large drainage basin), sandstorms (transport of sand in wind currents in deserts), blizzards (transport of precipitation (sleet), ice (hail) and snow in wind currents in cold climates). There has been a recent increase in adverse weather events, with the evidence pointing to global warming as the main driving factor, as more energy in the climate allows for more chaotic weather patterns.

15.2.18. Water Chemistry

Natural water sources contain a range of ions: Ca^{2+} , Mg^{2+} , Na^+ , K^+ , HCO_3^- , CO_3^{2-} , Cl^- , SO_4^{2-} , PO_4^{3-} , NO_3^- . These can be influenced by local geology, soil, hydrology and nearby human activity.

Concentration

Normality of an ion [milliequivalents, mEq] = $\frac{\text{concentration [mg / L]}}{\text{ion molecular mass [mol / g]}} \times \text{ion charge}$

Parts per million [ppm] = concentration [mg / L] (since density of water $\approx 10^6$ mg / L)

Alkalinity and Corrosivity: buffering capacity of water against acids

Water alkalinity is due to CO_3^{2-} , HCO_3^- and OH^- ions. Water acidity is due to dissolved CO_2 (carbonic acid equilibrium).

- “P alkalinity”: titrate using phenolphthalein.
- “M alkalinity”: titrate using methyl orange.
- “T alkalinity”: total alkalinity. Measured in ppm.

Carbonate scale (e.g. limescale, CaCO_3) can form on surfaces at high pH. Corrosion (weathering) can occur at low pH.

Langelier saturation index (LSI): the difference between the water pH and the pH at CaCO_3 saturation. $\text{LSI} > 0 \rightarrow$ scale-forming. $\text{LSI} < 0 \rightarrow$ corrosive. $\text{LSI} = 0 \rightarrow$ balanced.

Water Fluoridation and Chlorination: sanitation of bodies of water used by people.

Fluoride (F^-) is supplied to public drinking water sources as hexafluorosilicic acid (H_2SiF_6 , $[\text{F}^-] \sim 1$ ppm). It helps to combat tooth decay by forming fluorapatite ($\text{Ca}_{10}(\text{PO}_4)_6\text{F}_2$) in the enamel, which dissolves less readily than the naturally present hydroxyapatite ($\text{Ca}_{10}(\text{PO}_4)_6(\text{OH})_2$). This baseline intake of fluoride is helped by brushing teeth with fluoride toothpaste (contains NaF , $[\text{F}^-] \sim 1000$ ppm).

Chlorine (Cl_2) can be added to water as an antibacterial agent, typically in swimming pools. However, due to its equilibrium with hypochlorous acid (HClO), its effectiveness is strongly dependent on pH. It is typically supplied in solid form (calcium hypochlorite, $\text{Ca}(\text{ClO})_2$). Stabilisers such as cyanuric acid ($(\text{CONH})_3$) can be added, which also protects the chlorine from UV degradation by converting it to trichloroisocyanuric acid.

Water bromination is a more stable and less irritating alternative to chlorination.

15.3. Reactions of Inorganic Compounds

15.3.1. Reactions Involving Group 1 Metals

Reactions of pure Group 1 metals: (M = {Li, Na, K, Rb, Cs})

- $M(s) + H_2O(l) \rightarrow MOH(aq) + \frac{1}{2} H_2(g)$ hydroxide formation
- $M(s) + H_2(g) \rightarrow MH(s)$ hydride formation
- $M(s) + \frac{1}{2} S(s) \rightarrow \frac{1}{2} M_2S(s)$ sulfide formation
- $M(s) + \frac{1}{2} X_2 \rightarrow MX(s)$ halide: X = {F₂, Cl₂, Br₂, I₂}
- $M(s) + NH_3(g) \rightarrow MNH_2(s) + \frac{1}{2} H_2(g)$ amide formation
- $M(s) + 2 NH_3(l) \rightarrow [M(NH_3)]^+ + e^-(NH_3)$ solubility in liquid ammonia

Formation of oxides, peroxides and superoxides:

- $Li(s) + \frac{1}{4} O_2(g) \rightarrow \frac{1}{2} Li_2O(s)$ lithium oxide
- $Na(s) + \frac{1}{2} O_2(g) \rightarrow \frac{1}{2} Na_2O_2(s)$ sodium peroxide
- $K(s) + O_2(g) \rightarrow KO_2(s)$ also {Rb, Cs} superoxide

Reactions of Group 1 metal hydroxides, monoxides, peroxides and superoxides:

- $MOH(aq) + NH_4Cl(s) \rightarrow NH_3(g) + MCl(aq) + H_2O(l)$
- $M_2O(s) + H_2O(l) \rightarrow MOH(aq)$
- $M_2O_2(s) + 2 H_2O(l) \rightarrow 2 MOH(aq) + H_2O_2(l)$
- $M_2O_2(aq) + 2 CO_2(g) \rightarrow M_2CO_3(aq) + O_2(g)$

Acid-base reactions of metal hydroxides, oxides and carbonates:

- $MOH(aq) + H^+(aq) \rightarrow M^+(aq) + H_2O(l)$
- $MOH(aq) + \frac{1}{2} CO_2(g) \rightarrow \frac{1}{2} M_2CO_3(s) + \frac{1}{2} H_2O(l)$ carbonate formation
- $M_2O_2(s) + H_2SO_4(aq) \rightarrow M_2SO_4(aq) + H_2O_2(l)$ at ~ 0 °C
- $M_2CO_3(aq) + HNO_3(aq) \rightarrow 2 MNO_3(aq) + CO_2(g) + H_2O(l)$

Thermal decomposition of metal oxyanions:

- $M_2CO_3(s) \rightarrow M_2O(s) + CO_2(g)$
- $MHCO_3(s) \rightarrow M_2CO_3(s) + H_2O(g) + CO_2(g)$
- $LiNO_3(s) \rightarrow \frac{1}{2} Li_2O(s) + NO_2(g) + \frac{1}{4} O_2(g)$
- $NaNO_3(s) \rightarrow NaNO_2(s) + \frac{1}{2} O_2(g)$ other nitrates are stable
- $Li_2SO_4(s) \rightarrow Li_2O(s) + SO_2(g) + \frac{1}{2} O_2(g)$ other sulfates are stable
- $MClO(s) \rightarrow MCl(s) + \frac{1}{2} O_2(g)$
- $LiClO_3(s) \rightarrow LiCl(s) + \frac{3}{2} O_2(g)$ all other chlorites are stable

15.3.2. Reactions of Group 2 Metals

Reactions of pure Group 2 metals: (M = {Be, Mg, Ca, Sr, Ba})

- $M(s) + 2 H_2O(l) \rightarrow M(OH)_2(aq) + H_2(g)$ except Mg (forms oxide)
- $M(s) + \frac{1}{2} X_2 \rightarrow MX(s)$ halide: X = {F₂, Cl₂, Br₂, I₂}
- $M(s) + 2 NH_3(g) \rightarrow M(NH_2)_2(s) + H_2(g)$ amide formation
- $M(s) + 2 NH_3(l) \rightarrow [M(NH_3)]^+ + e^-(NH_3)$ solubility in liquid ammonia

Formation of oxides and peroxides:

- $Be(s) + \frac{1}{2} O_2(g) \rightarrow BeO(s)$ {Be, Mg, Ca} oxide
- $Sr(s) + O_2(g) \rightarrow SrO_2(s)$ {Sr, Ba} peroxide
- $Mg(s) + H_2O(l) \rightarrow MgO(s) + H_2(l)$

Reactions of Group 2 metal oxides, hydroxides and sulfates:

- $MO(s) + H_2O(l) \rightarrow M(OH)_2$ {Be, Mg}(OH)₂ are insoluble
- $M(OH)_2 + \frac{1}{2} NH_4Cl(aq) \rightarrow MCl_2(aq) + 2 NH_4OH(aq)$
- $MSO_4(aq) + NaOH(aq) \rightarrow M(OH)_2 + Na_2SO_4(aq)$ {Sr, Ba}SO₄ are insoluble

Acid-base reactions of metal hydroxides, oxides and carbonates:

- $M(OH)_2(aq) + 2 H^+(aq) \rightarrow M^{2+}(aq) + 2 H_2O(l)$
- $MO(aq) + CO_2(g) \rightarrow MCO_3(aq)$ using SiO₂ gives MSiO₃ (silicate)
- $M_2CO_3(aq) + HNO_3(aq) \rightarrow 2 MNO_3(aq) + CO_2(g) + H_2O(l)$

Thermal decomposition of carbonates:

- $MCO_3(s) \rightarrow MO(s) + CO_2(g)$ stability increases going down the group

15.3.3. Reactions Involving Boron

Formation of boron:

- $\text{Na}_2\text{B}_4\text{O}_7$ (borax) + 2 HCl + 5 H₂O → 4 H₃BO₃ (orthoboric acid) + 2 NaCl;
2 H₃BO₃ → B₂O₃ (boric oxide) + 3 H₂O;
B₂O₃ + 3 Mg → 2 B + 3 MgO
- KBF₄ (potassium tetrafluoroborate) + 3 K → 4 KF + B

Reactions of boron:

- 4 B + 3 O₂ → 2 B₂O₃
- 2 B + N₂ → 2 BN (boron nitride)
- 2 B + 2 NaOH + 2 H₂O → 2 NaBO₂ (sodium metaborate) + 3 H₂
- 2 B + 3 H₂SO₄ → 2 H₃BO₃ (orthoboric acid) + 3 SO₂
- 2 B + 3 H₂S → B₂S₃ (boron sulfide) + 3 H₂

Formation and reactions of B₂H₆ (diborane): (contains 3c-2e bonds)

- 2 BF₃ + 6 LiH → B₂H₆ + 6 LiF
- Mg₃B₂ (magnesium boride) + 6 HCl (aq) → 3 MgCl₂ + B₂H₆
- B₂H₆ + 3 H₂O → H₃BO₃ + 3 H₂
- B₂H₆ + 3 O₂ → B₂O₃ + 3 H₂O
- 3 B₂H₆ + 6 NH₃ → 2 B₃N₃H₆ (borazine / borazole) + 12 H₂ (isoelectronic to benzene)
- B₂H₆ + 2 NaH → 2 NaBH₄ (sodium borohydride)

Reactions of boron compounds:

- 2 B₂O₃ + 7 C → B₄C (boron carbide) + 6 CO (electric arc furnace)
- B₂O₃ + 2 NH₃ → 2 BN (boron nitride) + 3 H₂O (forms amorphous BN)
- BN + Li₃N → Li₃BN₂ (lithium nitridoborate)
- 2 BCl₃ + 2 Hg → Hg₂Cl₂ + B₂Cl₄
- 6 NaBH₄ + 3 (NH₄)₂SO₄ → 2 B₃N₃H₆ + 3 Na₂SO₄ + 18 H₂ (intermediate: B₃N₃H₃Cl₃)

Reactions of orthoboric acid and borax:

- 2 H₃BO₃ → B₂O₃ + 3 H₂O (thermal decomposition)
- H₃BO₃ + H₂O ⇌ B(OH)₄⁻ + H⁺
- Na₂B₄O₇ + H₂SO₄ + 5 H₂O → Na₂SO₄ + 4 H₃BO₃
- Na₂B₄O₇ → NaBO₂ + B₂O₃

15.3.4. Reactions Involving Carbon

For combustion reactions, see Section 15.3.6.

Industrial reactions of carbon compounds: (syngas: CO + H₂ mixture)

- $\text{CO}_2 + 2 \text{H}_2 \rightarrow \text{C (graphite)} + 2 \text{H}_2\text{O}$ (Bosch reaction; Fe catalyst, 600 °C)
- $\text{CO} + \text{H}_2\text{O} \rightleftharpoons \text{CO}_2 + \text{H}_2$ (Water-gas shift reaction (WGSR))
- $\text{CH}_4 + \text{H}_2\text{O} \rightleftharpoons \text{CO} + 3 \text{H}_2$ (Steam-methane reforming (SMR))
- $n \text{CO} + (2n + 1) \text{H}_2 \rightarrow \text{C}_n\text{H}_{2n+2} + n \text{H}_2\text{O}$ (Fischer-Tropsch synthesis (FTS))
- $\text{CH}_4 + \text{CO}_2 \rightarrow 2 \text{CO} + 2 \text{H}_2$ (dry reforming)

Hydration of inorganic carbides forms organic gases:

- $\text{CaC}_2 + 2 \text{H}_2\text{O} \rightarrow \text{C}_2\text{H}_2 \text{ (acetylene)} + \text{Ca(OH)}_2$ (also Mg₂C)
- $\text{BeC}_2 + 4 \text{H}_2\text{O} \rightarrow \text{CH}_4 \text{ (methane)} + 2 \text{Be(OH)}_2$ (very slow)
- $\text{SiC} + 2 \text{H}_2\text{O} \rightarrow \text{CH}_4 + \text{SiO}_2$
- $\text{Al}_4\text{C}_3 + 12 \text{H}_2\text{O} \rightarrow 3 \text{CH}_4 + 4 \text{Al(OH)}_3$
- $\text{Mg}_2\text{C}_3 \text{ (magnesium allylenide)} + 4 \text{H}_2\text{O} \rightarrow \text{C}_3\text{H}_4 \text{ (propyne)} + \text{Mg(OH)}_2$

Other reactions of metal carbides:

- $\text{CaC}_2 + \text{N}_2 \rightarrow \text{CaNCN (calcium cyanamide; nitrolime)} + \text{C}$ (Frank-Caro process)
- $\text{BaC}_2 + \text{N}_2 \rightarrow \text{Ba(CN)}_2 \text{ (barium cyanide)}$

15.3.5. Reactions Involving Nitrogen

Formation of nitrogen:

- $\text{NH}_4\text{Cl (aq)} + \text{NaNO}_2 \text{ (aq)} \rightarrow \text{N}_2 + \text{H}_2\text{O} + \text{NaCl}$
- $(\text{NH}_4)_2\text{Cr}_2\text{O}_7$ (ammonium dichromate) $\rightarrow \text{N}_2 + 4 \text{H}_2\text{O} + \text{Cr}_2\text{O}_3$ (thermal decomp.)
- $4 \text{NH}_3 + 6 \text{NO} \rightarrow 5 \text{N}_2 + 6 \text{H}_2\text{O}$
- $\text{Ba(N}_3)_2$ (barium azide) $\rightarrow \text{Ba} + 3 \text{N}_2$
- NH_2NH_2 (hydrazine) + $2 \text{H}_2\text{O}_2$ (hydrogen peroxide) $\rightarrow \text{N}_2 + 4 \text{H}_2\text{O}$

Formation of nitrogen oxides:

- $4 \text{NH}_3 + 5 \text{O}_2 \rightarrow 4 \text{NO}$ (nitric oxide) + $6 \text{H}_2\text{O}$
- $2 \text{NO} + \text{O}_2 \rightarrow 2 \text{NO}_2$ (nitrogen dioxide)
- $2 \text{NO}_2 \rightleftharpoons \text{N}_2\text{O}_4$ (dinitrogen tetroxide) (dimerisation)
- $3 \text{NO}_2 + \text{H}_2\text{O} \rightarrow 2 \text{HNO}_3 + \text{NO}$ (Ostwald process, V_2O_5 cat.)
- $2 \text{NaNO}_2 + 2 \text{FeSO}_4 + 3 \text{H}_2\text{SO}_4 \rightarrow \text{Fe}_2(\text{SO}_4)_3 + 2 \text{NaHSO}_4 + 2 \text{H}_2\text{O} + 2 \text{NO}$
- $\text{NH}_4\text{NO}_3 \rightarrow \text{N}_2\text{O}$ (nitrous oxide) + $2 \text{H}_2\text{O}$
- $\text{NO} + \text{NO}_2 \rightarrow \text{N}_2\text{O}_3$

Reactions of nitric acid:

- $\text{HNO}_3 + 2 \text{H}_2\text{SO}_4 \rightarrow \text{NO}_2^+$ (nitronium ion) + $\text{H}_3\text{O}^+ + 2 \text{HSO}_4^-$
- $8 \text{HNO}_3 + 3 \text{Cu} \rightarrow 3 \text{Cu}(\text{NO}_3)_2 + 2 \text{NO} + 4 \text{H}_2\text{O}$
- $\text{HNO}_3 + 3 \text{HCl} \rightarrow \text{NOCl} + \text{Cl}_2 + 2 \text{H}_2\text{O}$ (aqua regia formation)
- $\text{Au (s)} + \text{HNO}_3 + 4 \text{HCl} \rightarrow \text{HAuCl}_4$ (chloroauric acid) + $\text{NO} + \text{H}_2\text{O}$

Formation and reactions of ammonia and ammonium compounds:

- $\text{N}_2 + 3 \text{H}_2 \rightarrow 2 \text{NH}_3$ (Haber-Bosch process)
- $\text{NH}_4\text{Cl} + \text{NaOH} \rightarrow \text{NH}_3 + \text{NaCl} + \text{H}_2\text{O}$
- $8 \text{NH}_3 + 3 \text{Cl}_2 \rightarrow 6 \text{NH}_4\text{Cl} + \text{N}_2$ (excess Cl_2 forms NCl_3 and HCl instead)
- $\text{NH}_3 \text{ (aq)} + \text{NaClO} \rightarrow \text{NH}_2\text{Cl}$ (chloramine) + $\text{NaCl} + \text{H}_2\text{O}$ (also forms NHCl_2 , NCl_3)

Formation and reaction of metal nitrides, azides and amides:

- $3 \text{Mg} + \text{N}_2 \rightarrow \text{Mg}_3\text{N}_2$ (magnesium nitride)
- $\text{Mg}_3\text{N}_2 + 6 \text{H}_2\text{O} \rightarrow 3 \text{Mg}(\text{OH})_2 + 2 \text{NH}_3$
- $2 \text{Na} + 2 \text{NH}_3 \text{ (l)} \rightarrow 2 \text{NaNH}_2$ (sodium amide) + H_2
- $2 \text{NaNH}_2 + \text{N}_2\text{O} \rightarrow \text{NaN}_3$ (sodium azide) + $\text{NaOH} + \text{NH}_3$
- $\text{NaNO}_3 + 3 \text{NaNH}_2 \rightarrow \text{NaN}_3 + 3 \text{NaOH} + \text{NH}_3$
- $\text{NaN}_3 + \text{HCl} \rightarrow \text{HN}_3$ (hydrazoic acid) + NaCl
- $2 \text{NaN}_3 + 2 \text{HNO}_2$ (nitrous acid) $\rightarrow 3 \text{N}_2 + 2 \text{NO} + 2 \text{NaOH}$

15.3.6. Reactions Involving Oxygen

General hydrocarbon combustion reactions:

- $C_xH_y + \left(x + \frac{y}{4}\right)O_2 \rightarrow x CO_2 + \frac{y}{2} H_2O$ (complete)
- $C_xH_y + \left(x + \frac{y}{4} - a - \frac{b}{2}\right)O_2 \rightarrow a C + b CO + (x - a - b) CO_2 + \frac{y}{2} H_2O$ (incomplete)
(undetermined coefficients satisfy $a \geq 0, b \geq 0, 0 \leq a + b \leq x$)

Aliphatic hydrocarbon C_xH_y has $x + 1 - \frac{y}{2}$ (C=C) bonds, $\frac{y}{2} - 2$ (C-C) bonds and y (C-H) bonds.

The maximum enthalpy of combustion is achieved for complete combustion ($a = b = 0$).

Reactions of oxygen:

- $H_2 + O_2 \rightarrow H_2O$ (combustion of hydrogen forms water)
- $2 SbF_5(l) + 2 O_2(g) + F_2(g) \rightarrow 2 [O_2]^+[SbF_6]^-$ (oxidation by strong Lewis acid)

15.3.7. Reactions Involving Aluminium

Reactions of aluminium:

- $4 Al + 3 O_2 \rightarrow 2 Al_2O_3$ (nanoscopic oxide surface layer impermeable to O_2)
- $2 Al + 3 Cl_2 \rightarrow 2 AlCl_3$ (forms Al_2Cl_6 dimers only in the liquid/vapour state)
- $2 Al + 3 Br_2 \rightarrow Al_2Br_6$ (dimer is stable at lower temperatures)
- $2 Al + 3 H_2SO_4 \rightarrow Al_2(SO_4)_3 + 3 H_2$
- $2 Al + 2 NaOH + 6 H_2O \rightarrow 2 NaAl(OH)_4$ (sodium aluminate hydrate) + $3 H_2$
- $Al + Fe_2O_3 \rightarrow Al_2O_3 + Fe$ (thermite reaction)

Reactions of aluminium oxides:

- $Al_2O_3 + 6 HCl \rightarrow 2 AlCl_3 + 3 H_2O$
- $Al_2O_3 + 6 NaOH \rightarrow 2 NaAlO_2$ (sodium aluminate) + H_2O

15.3.7. Reactions Involving Silicon

Formation of silicon:

- $\text{SiO}_2 + 2 \text{C} \rightarrow \text{Si} + 2 \text{CO}$
- $\text{SiC} + \text{SiO}_2 \rightarrow \text{Si (s)} + \text{SiO (g)} + \text{CO (g)}$ (ultrapure silicon for semiconductors)
- $\text{SiO}_2 + 2 \text{Mg} \rightarrow \text{MgO} + \text{Si}$

Reactions of silicon:

- $\text{Si} + \text{O}_2 \rightarrow \text{SiO}_2$
- $\text{Si} + 2 \text{F}_2 \rightarrow \text{SiF}_4 \text{ (g)}$
- $\text{Si} + 2 \text{Cl}_2 \rightarrow \text{SiCl}_4 \text{ (l)}$
- $\text{Si} + 2 \text{Mg} \rightarrow \text{Mg}_2\text{Si}$ (magnesium silicide) (n-type semiconductor)

Reactions of silicon compounds:

- $\text{SiCl}_4 + 2 \text{H}_2\text{O} \rightarrow \text{SiO}_2 + 4 \text{HCl}$
- $\text{SiO}_2 + 6 \text{HF} \rightarrow \text{H}_2\text{SiF}_6$ (hexafluorosilicic acid) (used in water fluoridation)
- $4 \text{SiH}_4 \text{ (silane) (g)} + 3 \text{O}_2 \rightarrow 2 \text{Si}_2\text{O}_3 + 6 \text{H}_2\text{O}$

Reactions of metal silicides:

- $\text{Mg}_2\text{Si} + 4 \text{HCl (aq)} \rightarrow 2 \text{MgCl}_2 \text{ (aq)} + \text{SiH}_4 \text{ (g)}$ (thermally decomposes to $\text{Si} + 2 \text{H}_2$)

15.3.8. Reactions Involving Phosphorus

Formation of phosphorus (white phosphorus):

- $2 \text{Ca}_3(\text{PO}_4)_2 + 10 \text{C} + 6 \text{SiO}_2 \rightarrow 6 \text{CaSiO}_3 + 10 \text{CO} + \text{P}_4$ (white phosphorus)

Allotrope formation of phosphorus:

- white P (tetrahedral P_4 molecules) \rightarrow red P (polymeric P_4 units) (heating in CO_2)
- red P \rightarrow α -black P (amorphous) (heating in insulated tube)
- white P \rightarrow β -black P (graphite-like P_6 units) (heat at high pressure)

Reactions of phosphorus:

- $\text{P}_4 + 5 \text{O}_2 \rightarrow \text{P}_4\text{O}_{10}$ (yellow phosphorus: oxide impurities)
- $\text{P}_4 + 10 \text{Cl}_2 \rightarrow 4 \text{PCl}_5$ (s) (excess, otherwise forms PCl_3)
- $\text{P}_4 + 3 \text{NaOH} + 3 \text{H}_2\text{O} \rightarrow \text{PH}_3$ (phosphine) + $3 \text{NaH}_2\text{PO}_2$
- $\text{P}_4 + 20 \text{HNO}_3 \rightarrow 4 \text{H}_3\text{PO}_4 + 20 \text{NO}_2 + 4 \text{H}_2\text{O}$
- $\text{P} + 5 \text{HNO}_3 \rightarrow \text{H}_3\text{PO}_4 + 5 \text{NO}_2 + \text{H}_2\text{O}$

Formation of metal phosphides:

- P (white) + $3 \text{Na} \rightarrow \text{Na}_3\text{P}$
- P_4 (white) + $3 \text{CuSO}_4 + 6 \text{H}_2\text{O} \rightarrow \text{Cu}_3\text{P}_2 + 2 \text{H}_3\text{PO}_3 + 3 \text{H}_2\text{SO}_4$
- $\text{Ca}_3(\text{PO}_4)_2 + 8 \text{C} \rightarrow \text{Ca}_3\text{P}_2 + 8 \text{CO}$ (carbothermal reduction)

Reactions of metal phosphides:

- $\text{Na}_3\text{P} + 3 \text{H}_2\text{O} \rightarrow 3 \text{NaOH} + \text{PH}_3$ (also Li_3P)
- $\text{Cu}_3\text{P}_2 + 5 \text{CuSO}_4 + 8 \text{H}_2\text{O} \rightarrow 8 \text{Cu} + 5 \text{H}_2\text{SO}_4 + 2 \text{H}_3\text{PO}_4$

Reactions of phosphorus oxides:

- $\text{P}_4\text{O}_6 + 6 \text{H}_2\text{O} \rightarrow 4 \text{H}_3\text{PO}_3$ (phosphonic acid)
- $\text{P}_4\text{O}_{10} + 6 \text{H}_2\text{O} \rightarrow 4 \text{H}_3\text{PO}_4$ (phosphoric acid)
- $\text{P}_4\text{O}_{10} + 4 \text{HNO}_3 \rightarrow 2 \text{N}_2\text{O}_5 + 4 \text{HPO}_3$

Acid-base reactions of phosphorus oxides:

- H_3PO_3 (phosphorous acid) + $\text{NaOH} \rightarrow \text{NaH}_2\text{PO}_3$ (Na dihydrogen phosphite) + H_2O
- $\text{P}_4\text{O}_6 + 8 \text{NaOH} \rightarrow 4 \text{Na}_2\text{HPO}_3$ (Na hydrogen phosphite) + H_2O

15.3.9. Reactions Involving Sulfur

Reactions of sulfur:

- $S + O_2 \rightarrow SO_2$
- $2 S + Cl_2 \rightarrow S_2Cl_2$ (disulfur dichloride)
- $S + Na_2SO_3$ (sodium sulfite) $\rightarrow Na_2S_2O_3$ (sodium thiosulfate) (boil in absence of air)

Reactions of sulfur oxides:

- $SO_2 + CaO \rightarrow CaSO_3$
- $SO_3 + CaO \rightarrow CaSO_4$
- $SO_2 + H_2O \rightleftharpoons H_2SO_3$ (sulfurous acid)
- $SO_3 + H_2O \rightarrow H_2SO_4$
- $Na_2S_2O_3 + HCl \rightarrow 2 NaCl + SO_2 + S + H_2O$
- $2 SO_2 + O_2 \rightleftharpoons 2 SO_3$ (Contact process, step 1)
- $SO_3 + H_2SO_4 \rightarrow H_2S_2O_7$ (oleum) (Contact process, step 2, V_2O_5 cat., 450 °C)

Reactions of sulfuric acids:

- $H_2SO_4 + 2 Br^- + 2 H^+ \rightarrow Br_2 + SO_2 + 2 H_2O$ (H_2SO_4 is an oxidising agent)
- $H_2SO_4 + 8 I^- + 8 H^+ \rightarrow 4 I_2 + H_2S + 4 H_2O$ (I^- is a stronger reducing agent than Br^-)
- $2 H_2SO_4 + HNO_3 \rightarrow NO_2^+$ (nitronium ion) + H_3O^+ + $2 HSO_4^-$
- $H_2SO_4 + 2 NH_3 \rightarrow (NH_4)_2SO_4$
- $H_2SO_4 + H_2O_2 \rightarrow H_2SO_5$ (persulfuric acid) + H_2O (piranha solution formation)
- $2 H_2SO_4 + C \rightarrow CO_2 + 2 H_2O + 2 SO_2$ (carbon from e.g. dehydration of sucrose)
- $H_2S_2O_7 + H_2O \rightarrow 2 H_2SO_4$ (Contact process, step 3)

Acid-base reactions:

- $SO_2 + 2 NaOH \rightarrow Na_2SO_3$ (sodium sulfite) + H_2O
- $Na_2SO_3 + H_2O + SO_2 \rightarrow 2 NaHSO_3$ (sodium bisulfite)

15.3.10. Reactions Involving Chlorine

Formation of chlorine:

- $2 \text{NaCl} + 3 \text{H}_2\text{SO}_4 + \text{MnO}_2 \rightarrow \text{Cl}_2 + \text{MnSO}_4 + 2 \text{NaHSO}_4 + 2 \text{H}_2\text{O}$ (also Br_2 , I_2)
- $4 \text{HCl} + \text{O}_2 \rightarrow 2 \text{Cl}_2 + 2 \text{H}_2\text{O}$ (Deacon's process)

Reactions of chlorine:

- $\text{Cl}_2 + \text{H}_2 \rightarrow 2 \text{HCl}$
- $3 \text{Cl}_2 + 2 \text{Fe} \rightarrow 2 \text{FeCl}_3$ (also F_2 , Br_2 : using I_2 forms FeI_2)
- $\text{Cl}_2 + \text{Be} \rightarrow \text{BeCl}_2$ (BeCl_2 forms polymeric chains in the solid state)
- $\text{Cl}_2 + \text{H}_2\text{O} \rightleftharpoons \text{HCl} + \text{HClO}$ (hypochlorous acid)
- $2 \text{Cl}_2 + 2 \text{H}_2\text{O} \rightarrow 4 \text{HCl} + \text{O}_2$ (HClO undergoes photolysis in sunlight)
- $\text{Cl}_2 + 2 \text{NaOH} \rightarrow \text{NaClO}$ (sodium hypochlorite) + $\text{NaCl} + \text{H}_2\text{O}$ (cold, dilute NaOH)
- $3 \text{Cl}_2 + 6 \text{NaOH} \rightarrow \text{NaClO}_3$ (sodium chlorate) + $5 \text{NaCl} + 3 \text{H}_2\text{O}$ (hot, concentrated NaOH)

Reactions of chlorine oxides:

- Cl_2O_7 (dichlorine heptoxide) + $\text{H}_2\text{O} \rightarrow \text{HClO}_4$ (perchloric acid)
- Cl_2O (chlorine monoxide) + $\text{H}_2\text{O} \rightleftharpoons 2 \text{HClO}$

Acid-base reactions:

- $\text{HClO}_4 + \text{NaOH} \rightarrow \text{NaClO}_4$ (sodium perchlorate) + H_2O
- $\text{NaClO} + \text{HCl} \rightarrow \text{Cl}_2 + \text{H}_2\text{O} + \text{NaCl}$
- $\text{Cl}_2\text{O}_7 + 2 \text{NaOH} \rightarrow 2 \text{NaClO}_4 + \text{H}_2\text{O}$

Reactions of chlorates:

- $\text{NaClO} + \text{C}_3\text{H}_6\text{O}$ (propanone) $\rightarrow \text{CHCl}_3$ (chloroform) + CH_3COONa (haloform rxn)
- $\text{NaClO} + \text{H}_2\text{O}_2 \rightarrow \text{NaCl} + \text{H}_2\text{O} + \text{O}_2^*$ (reactive singlet oxygen, O_2 ($^1\Delta_g$) is produced)

15.3.11. Reactions Involving Noble Gases

Noble gases are inert to most reactions, but under harsh and/or specialised conditions can react to form binary compounds and complexes.

Helium and neon do not form any stable chemical compounds under any laboratory conditions. Argon, krypton, xenon and radon can react in some extreme cases.

Reactions Involving Argon:

- $\text{Ar} + \text{HF} \rightarrow \text{HArF}$ (argon fluorohydride) (stable below $-246\text{ }^\circ\text{C}$)

Reactions Involving Krypton:

- $\text{Kr} + \text{F}_2 \rightarrow \text{KrF}_2$ (UV light, stable below $-78\text{ }^\circ\text{C}$)
- $3 \text{KrF}_2 + \text{Xe} \rightarrow \text{XeF}_6 + 3 \text{Kr}$

Reactions Involving Xenon:

- $\text{Xe} + \text{F}_2 \rightarrow \text{XeF}_2$ (s) (UV light)
- $\text{XeF}_2 + 2 \text{F}_2 \rightarrow \text{XeF}_6$ (120 $^\circ\text{C}$ with NiF_2 cat.)
- $\text{XeF}_6 \rightarrow \text{XeF}_4 + \text{F}_2$ (pyrolysis, NaF cat.)
- $\text{XeF}_6 + 3 \text{H}_2\text{O} \rightarrow \text{XeO}_3 + 6 \text{HF}$ (hydrolysis)
- $2 \text{XeO}_3 + 2 \text{Ba}(\text{OH})_2 \rightarrow \text{Xe} + \text{Ba}_2\text{XeO}_6$ (barium perxenate) + $\text{O}_2 + 2 \text{H}_2\text{O}$

Reactions Involving Radon:

- $\text{Rn} + \text{F}_2 \rightarrow \text{RnF}_2$ (stable below $250\text{ }^\circ\text{C}$)
- $2 \text{Rn} + 3 \text{O}_2 \rightarrow 2 \text{RnO}_3$ (above $500\text{ }^\circ\text{C}$)
- $\text{Rn} + 2 [\text{O}_2]^+[\text{SbF}_6]^- \rightarrow [\text{RnF}]^+[\text{Sb}_2\text{F}_{11}]^- + 2 \text{O}_2$ (room temperature)

For chemical reactions, radon can be generated from the decay of thorium-228 or radium-224. The radon compounds then decay into lead-208.

15.4. Periodicity Trends

15.4.1. Trends in Physical Properties of the Elements

Property	→ Trend along period(s)	↓ Trend down group(s)
Atomic radius	decreases	increases
Electronegativity, ionisation energy and electron affinity	increases	decreases
Effective nuclear charge	increases	
Halide covalent character	increases	decreases
Group 2 hydroxide and nitrate solubility in water		increases
Group 2 sulfate and carbonate solubility in water		decreases
Group 7 ion (halides) solubility in water and ammonia		decreases
Group 1 and 2 hydroxide, carbonate, sulfate and nitrate thermal stability		increases
Group 7 boiling point		increases
Oxidising power	increases	decreases
Anion reducing power	decreases	increases
Metal oxide, hydroxide and hydride basicity	decreases	increases
Transition metal melting point	decreases	
Metal electrical conductivity	increases	increases

15.4.2. Inert Pair Effect and the Lanthanide Contraction

Poor shielding (by inner d and f shells) and relativistic stabilisation (contraction of s orbitals) makes **outer 5s and 6s electrons less likely to participate in bonding**. This results in large cations being stable in lower oxidation state than expected e.g. In^+ , Tl^+ , Sn^{2+} , Pb^{2+} , Sb^{3+} , Bi^{3+} , Te^{4+} , Po^{4+} , I^{5+} : in these ions, the $5s^2$ and $6s^2$ pairs are inert. As a result, 6s electrons are drawn closer to the nucleus, decreasing the atomic radius of the lanthanides and post-lanthanide elements (including the actinides and transactinides).

These ions may mimic smaller ions, such as Na^+ or Ca^{2+} in biological organisms, while disrupting their usual functions, causing heavy metal poisoning.

The very low melting point of mercury ($[\text{Xe}] 4f^{14} 5d^{10} 6s^2$) is fundamentally due to the contracted 6s orbital and the inert pair effect. The $6s^2$ electrons in Hg are localised and do not contribute significantly to the metal's conduction band, significantly weakening the metallic bonds such that Hg is a liquid at room temperature.

15.4.3. Electron Deficient and Hypervalent Molecules (Octet Rule Exceptions)

Electron-deficient molecules contain atoms with less than 8 valence electrons.

Hypervalent molecules contain atoms with more than 8 valence electrons.

Examples of electron-deficient species: BF_3 , BeH_2 , AlCl_3 , B_2H_6 , carbenes ($\text{R}-\text{C}:-\text{R}'$)

Examples of hypervalent species ('expanded octets'): PCl_5 , SF_6 , ClF_3 , ClO_2^- , I_3^- , XeF_4

Electron deficient species often contain 3c-2e bonds.

Hypervalent species often contain 3c-4e bonds.

15.5. Coordination and Organometallic Chemistry

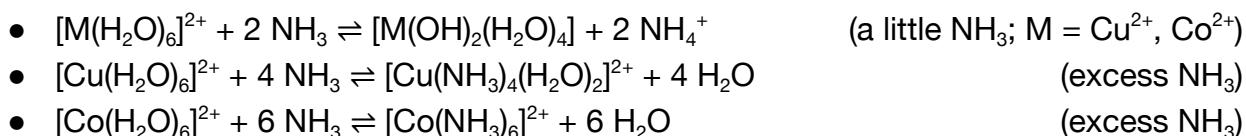
15.5.1. Reactions of Aqueous Ions (Metal Aquo Complexes)

Metal ions M^{n+} are coordinated to water molecules in aqueous solution (primary solvation).

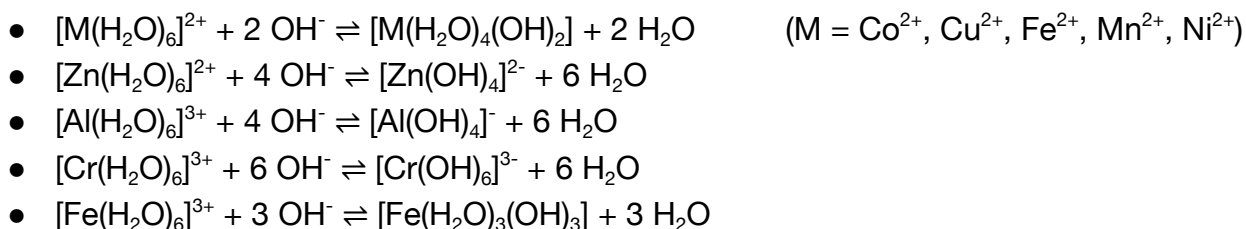
Reactions with HCl:



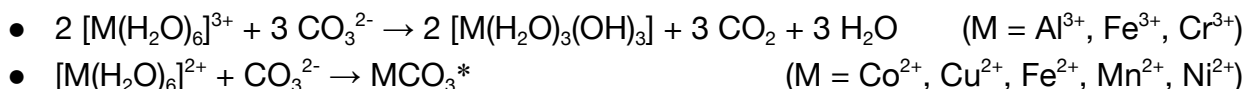
Reactions with NH_3 :



Reactions with NaOH:



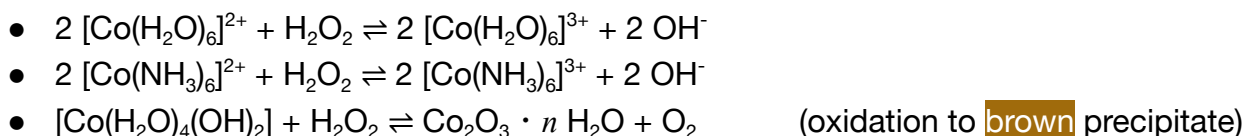
Reactions with Na_2CO_3 :



* the "basic carbonate" is of the form $x MCO_3 \cdot y M(OH)_2 \cdot z H_2O$.

The M^{3+} aqueous ions are more acidic than the M^{2+} ions due to its higher polarising power (Section 15.5.10).

Reactions with H_2O_2 :



Other reactions:



15.5.2. Colours of Common Aqueous Metal Complexes

The colours of some compounds differ to the colours given in Section 15.4.5. This is due to alterations of the central metal ion HOMO-LUMO gap due to the presence of e.g. hydration spheres, strong-field ligands (Section 15.5.8.), etc.

$[\text{Cr}(\text{H}_2\text{O})_6]^{3+}$ violet-blue-grey	$[\text{Fe}(\text{H}_2\text{O})_6]^{2+}$ pale green	$[\text{Co}(\text{H}_2\text{O})_6]^{2+}$ pink	$[\text{Ni}(\text{H}_2\text{O})_6]^{2+}$ green	$[\text{Cu}(\text{H}_2\text{O})_6]^{2+}$ light blue	$[\text{CuCl}_4]^{2-}$ yellow-green
$[\text{Cr}(\text{OH})_6]^{3-}$ green	$[\text{Cr}(\text{NH}_3)_6]^{3+}$ purple	$[\text{Cu}(\text{NH}_3)_4(\text{H}_2\text{O})_2]^{2+}$ very dark blue	$[\text{CoCl}_4]^{2-}$ deep blue	$[\text{Co}(\text{NH}_3)_6]^{2+}$ dirty yellow	$[\text{Fe}(\text{H}_2\text{O})_6]^{3+}$ pale yellow
		$[\text{Cr}(\text{H}_2\text{O})_5\text{SO}_4]^+$ green	$[\text{Fe}(\text{H}_2\text{O})_5\text{SCN}]^{2+}$ deep red		

15.5.3. Naming of Mononuclear Complex Salts

The cation is named before the anion. The metal oxidation state is given in Roman numerals. The ligands are given before the metal ion, in alphabetical order (**not** including prefixes).

Rename:

- Anion ligands: 'ide' → 'o' (exception: Cl⁻ is chlorido); 'ite' → 'ito'; 'ate' → 'ato'
- Positive groups: 'ine' / 'ia' → 'ium'
- Multiple groups if ligand already includes: 'di' → 'bis'; 'tri' → 'tris'; 'tetra' → 'tetrakis'
- Complex anion: '(metal)ium/um' → '(metal)ate', (with exceptions below)

For complex anions, non-trivial names are:

lead → plumbate; gold → aurate; tin → stannate; silver → argentate; iron → ferrate;
aluminium → aluminate; manganese → manganate; copper → cuprate; nickel → nickelate;
antimony → antimonate; arsenic → arsenate; bismuth → bismuthate; tungsten → tungstate;
tantalum → tantalate; mercury → mercurate.

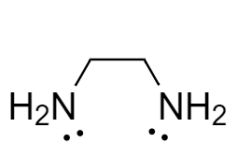
Common ligand names: Cl⁻ = chlorido; NH₃ = ammine; OH⁻ = hydroxy; H₂O = aqua.

Examples:

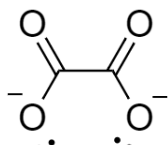
- $[\text{CoSO}_4(\text{NH}_3)_4]\text{NO}_3$ is sulfatotetraamminecobalt(III) nitrate
- $(\text{NH}_2\text{NH}_3)[\text{NiCl}_3(\text{OH})]$ is hydrazinium hydroxytrichloridonickelate(II)
- $[\text{Cr}(\text{en})_3][\text{V}(\text{H}_2\text{O})(\text{CN})_5]_2$ is trikis(ethylenediamine)chromium(IV) di(aquapentacyanovanadate(III))

15.5.4. Abbreviations for Common Large Ligands

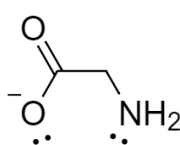
In the structures below, only the lone pairs which form dative bonds are shown.



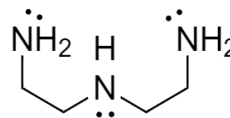
en
(ethylenediamine)



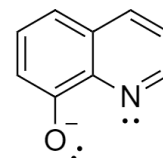
ox
(oxalato)



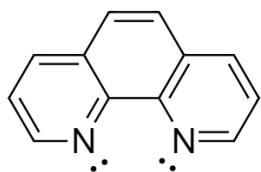
gly
(glycinato)



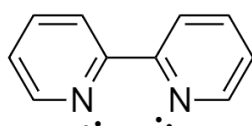
dien
(diethylenetriamine)



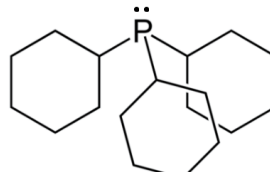
oxine
(8-hydroxyquinolinato)



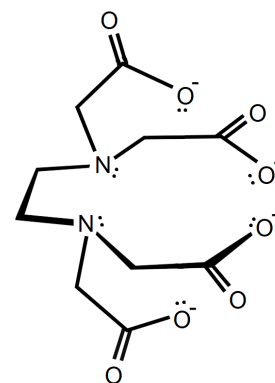
phen
(1,10-phenanthroline)



bipy
(2,2'-bipyridine)



P(Cy)₃
(tricyclohexylphosphine)



EDTA
(ethylenediaminetetraacetic acid)

15.5.5. Bonding in Coordination Complexes

Ligands form coordinate (dative) covalent bonds to metal ion centres.

Polydentate Ligands:

- **Denticity** (κ): number of sites of electron density used for covalent bonding
- Ligands may be monodentate (κ^1), bidentate (κ^2), tridentate (κ^3), hexadentate (κ^6) etc.
- **Bite angle**: the L-M-L bond angle on a bidentate ligand L-R-L.
- **Chelate effect**: ligand substitution to higher denticity is entropically favourable.
- Examples of polydentate ligands are given in Section 15.5.4 (e.g. ethylenediamine, κ^2).

Multiple Bonding Ligands:

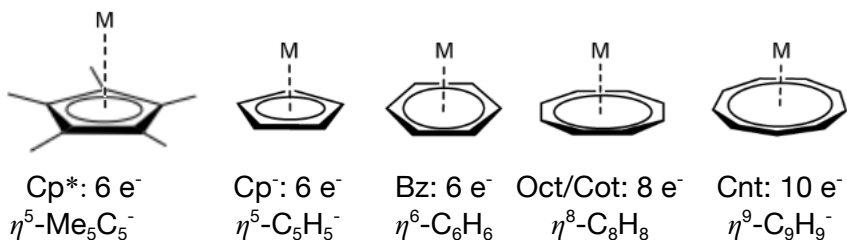
- Ligands with multiple lone pairs can form multiple dative bonds e.g. M=O (oxide), M=S (sulfide), M≡N (nitride), M=NR (imide)
- **Backbonding**: ligands with empty π^* LUMOs can accept $d-\pi^*$ backbonding, stabilising the complex e.g. M-NO⁺ (nitrosyl), M-CO (carbonyl).
- **Alkylidenes** (CR₂): forms M=C double bonds. **Fischer (singlet)** carbenes have σ (sp^2-d) dative bonding and π ($d-p$) backbonding. **Schrock (triplet)** carbenes have double σ bonding.
- **Alkylidynes** (CR): forms M≡C triple bonds. **Fischer (doublet)** carbynes have σ ($sp-d$) dative bonding, σ ($p-d$) covalent bonding and σ ($d-p$) dative bonding. **Schrock (quartet)** carbynes have triple σ bonding.

Bridging Ligands:

- Bridging ligands are named with the symbol μ to indicate the bridges in polynuclear complexes.
- sp^3 -hybridised oxide (O²⁻), sulfide (S²⁻) or halide (Cl⁻, Br⁻) ions can act as bridging ligands.
- Hydride (H⁻) can act as a 3c-2e bridge, donating 1 e⁻ in each bond.
- Peroxide (O₂²⁻) can act as either a bidentate ligand (3 membered ring) or a bridging ligand.

Polyhapto Ligands:

- **Hapticity** (η): number of delocalised electrons in a ligand that coordinates to the metal centre
- In **metal-alkene complexes** (e.g. Zeise's salt, [PtCl₃(η^2 -C₂H₄)]), the π HOMO of the alkene donates electrons into the empty metal d orbital. $d-\pi^*$ backbonding can also occur, indicated by drawing the complex as a 3 membered ring (the Dewar-Chatt-Duncanson model).
- **Aromatic polyhapto ligands** and their hapticity and electron counts (also: Cp' = MeCp, Cp'' = Me₂Cp)

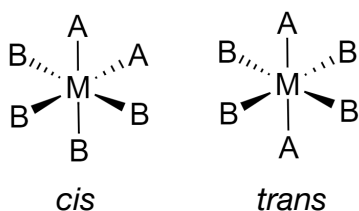


- The hapticity η of many ligands may vary. **Alkynes** may be either η^4 or η^2 . **Allylic** carbanions (e.g. C₃H₅⁻) may be η^3 or η^1 . Aromatic polyhapto ligands can shift coordination numbers by a slippage or folding mechanism, e.g. Cp⁻ may slip from η^5 to η^3 .
- **Sandwich complex**: two polyhapto ligands. May be homoleptic (same η) or heteroleptic (different η).

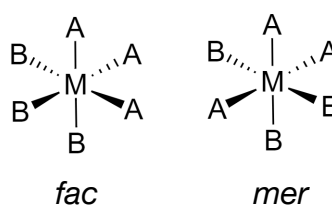
15.5.6. Stereoisomerism of Heteroleptic Complexes

Geometric Isomerism: complexes are *cis* when similar ligands are adjacent (90° bond angle) and *trans* when similar ligands are opposite (180° bond angle).

Octahedral complex of form MA_2B_4 :

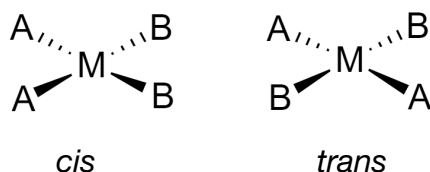


Octahedral complex of form MA_3B_3 :

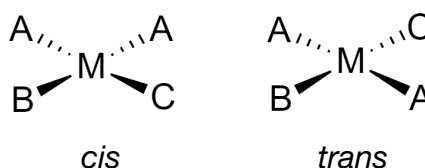


Octahedral complexes of form $M(ABCDEF)$ in general have 15 isomers.

Square planar complex of form MA_2B_2 :

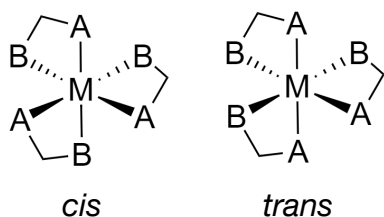


Square planar complex of form MA_2BC :

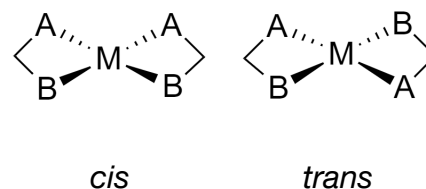


Square planar complexes of form $M(ABCD)$ in general have 3 isomers.

Octahedral, bidentate ligands:



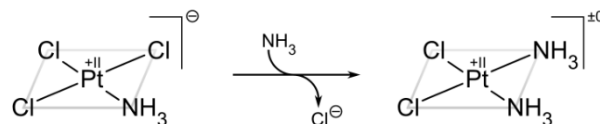
Square planar, bidentate ligands:



Kinetic Trans Effect: existing ligands are *trans*-directing to incoming substituent ligands

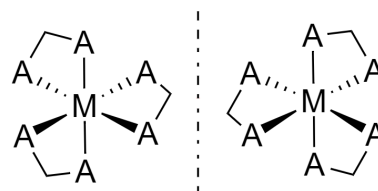
(Weak, directs *cis*) F^- , H_2O , OH^- < NH_3 < py < Cl^- < Br^- < I^- , SCN^- , NO_2^- , $SC(NH_2)_2$, Ph^- < SO_3^{2-} < PR_3 , AsR_3 , SR_2 , CH_3^- < H^- , NO , CO , CN^- , C_2H_4 (Strong, directs *trans*)

For example, $[PtCl_3NH_3]^- + NH_3 \rightarrow cis-[PtCl_2(NH_3)_2]$ (cisplatin) since $Cl^- > NH_3$ directs the incoming NH_3 *trans* to a Cl^- (overall *cis* square planar).



Optical Isomerism in Homoleptic Complexes

E.g. for three identical symmetric bidentate ligands:



15.5.7. Valence Bond Theory for Correlating Spin State with Hybridisation

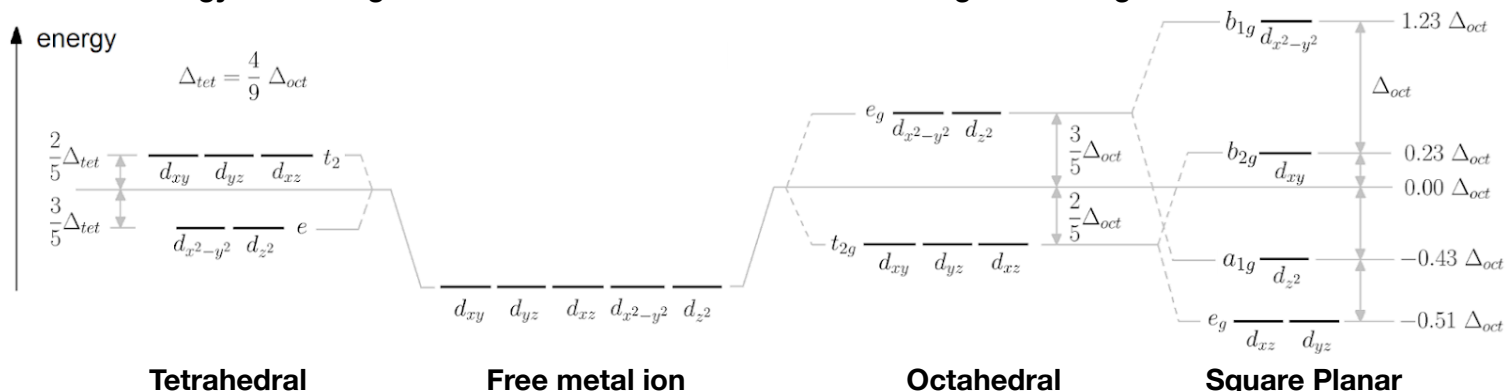
Hybridised VBT is a basic (often insufficient) model for bonding in complexes.

- A high-spin complex uses sp^3d^2 hybridisation with its outer (4d) orbital.
- A low-spin complex uses sp^2d^3 hybridisation with its inner (3d) orbital.

15.5.8. Crystal Field Theory (CFT)

CFT is an ionic bonding model in which ligands split the d orbital of a transition metal ion into non-degenerate sets of orbitals, occupied by the metal ion's valence electrons. Ligands may be strong field (low spin, e^- are filled by Aufbau/Hund rules) or weak field (high spin, orbitals are filled unpaired-first) (the spectrochemical series, Section 15.5.9).

Energy Level Diagrams for Metal Ions in a Field of Point Negative Charges:



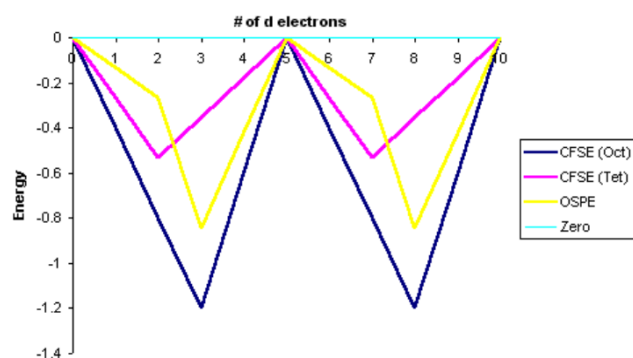
For other geometries, the splitting patterns are, in ascending energy order:

Square Pyramidal ($\{d_{xz}, d_{yz}\}, d_{xy}, d_{z^2}, d_{x^2-y^2}$); Trigonal/Pentagonal Bipyramidal ($\{d_{xz}, d_{yz}\}, \{d_{xy}, d_{x^2-y^2}\}, d_{z^2}$); Square Antiprismatic ($d_{z^2}, \{d_{xy}, d_{x^2-y^2}\}, \{d_{xz}, d_{yz}\}$).

The energy levels are related (for oct and tet) by ($P > 0$: pairing energy for mutual repulsion)

$$E_{\text{ligand}} = \underbrace{n_{t_{2g}} \left(-\frac{2}{5} \Delta \right) + n_{e_g} \left(\frac{3}{5} \Delta \right)}_{\text{energy relative to barycentre}} + \underbrace{\left(n_{\text{pairs}}^{t_{2g}} + n_{\text{pairs}}^{e_g} \right) P}_{\text{pairing energy}} \quad E_{\text{isotropic}} = \underbrace{n_{\text{pairs}}^d P}_{\text{pairing energy in degenerate d orbital}}$$

- Crystal field stabilisation energy, $CFSE = E_{\text{ligand}} - E_{\text{isotropic}}$
- Octahedral site preference energy, $OSPE = CFSE_{(\text{oct})} - CFSE_{(\text{tet})}$



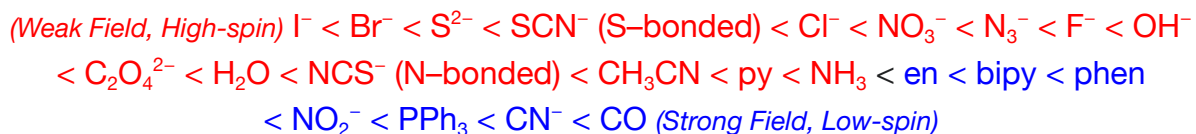
CFSE and OSPE for high-spin complexes (shown left) depend only on the number of d electrons, in units of Δ_{oct} .

- d^3 and d^8 strongly favour octahedral.

Low-spin complexes depend on P .

15.5.9. Spectrochemical Series and Spin States

In order of ligand strength i.e. increasing values of Δ :



15.5.10. Magnetic Moment due to Electron Configuration

The total magnetic moment of a compound (atom, ion, molecule or complex) is due to the contribution of unpaired electrons (possessing spin) and electrons in orbitals with non-zero angular momentum.

Quantisation of magnetic moment (Bohr magneton): $\mu_B = \frac{e\hbar}{2m_e} = 9.274 \times 10^{-24} \text{ A m}^2$

Spin-only magnetic moment: $\mu_s = g\sqrt{S(S+1)}\mu_B = \sqrt{n(n+2)}\mu_B$ ($g = 2.0023$: e^- g-factor)

Orbital magnetic moment: $\mu_l = \sqrt{L(L+1)}\mu_B$ (z-component has $\mu_l^{(z)} = m_l\mu_B$)

Total magnetic moment: $\mu = \mu_s + \mu_l$

(n : number of unpaired electrons, S : sum of the spin quantum numbers and L : sum of all angular momentum quantum numbers of all electrons (d , e_g , t_{2g} etc all have $l = 2$).

For low-spin complexes, $\mu_s = 0$ since all electrons are paired in the t_{2g} orbital.

The contribution to the magnetic moment from the nuclear spin is negligible in size compared to the electrons, although the interactions have significance in e.g. NMR. The nuclear contribution is responsible for the slight diamagnetism of e.g. hydrogen.

If both spin and orbital contributions to μ are present, the resulting magnetic fields interact (spin-orbit coupling, fine structure splitting, Zeeman effect). Interaction with the nuclear magnetic moment produces further slight interactions (hyperfine structure splitting).

Bulk Magnetisation: may occur spontaneously in ferromagnets (domain regions)

Theoretical bulk saturation magnetisation, $M_{\max} [\text{A m}^{-1}] = \frac{n_{\text{atoms/cell}}}{V_{\text{cell}}} \times \mu = \frac{\rho N_A \mu}{M_r}$.

Theoretical bulk saturation magnetic flux density, $B_{\max} [\text{T}] = \mu_0 M_{\max}$

(n_a : number of atoms or complexes per unit cell, V_{cell} : volume of unit cell, μ : magnetic moment, $\mu_0 = 4\pi \times 10^{-7} \text{ T m}^2 \text{ A}^{-1}$: permeability of vacuum, ρ : mass density, $N_A = 6.022 \times 10^{23} \text{ mol}^{-1}$: Avogadro's number, M_r : molar mass (in kg mol^{-1}). For unit cell counts, see Section 13.2.1.)

15.5.11. Electron Counting of Complexes

To determine the total number of electrons a central metal ion's valence shell:

1. Calculate the oxidation state of the metal ion, its electron configuration and valence electrons.
2. Calculate the number of electrons donated by each ligand to the metal; add together.

18 electron rule: neglecting valence *f* orbitals, a complex is usually most stable with 18 e⁻ valence electrons. Some tetravalent complexes may also be stable with 16 e⁻, in which case:

- Tetrahedral (16 e⁻, high spin d⁸ complexes): [CuCl₄]²⁻, [CoCl₄]²⁻, [Zn(CO)₄]²⁻
- Square planar (16 e⁻, low spin d⁸ complexes): [NiCl₂(NH₃)₂], [PtCl₄]²⁻, [PtCl₃(η²-C₂H₄)]⁻

Example: [W(PMe₃)₃Cl₂(η⁵-Cp)]⁺. The ligands have charges Cl⁻ and Cp⁻, so the metal centre is W⁴⁺. Normally, tungsten has configuration [Xe] 6s² 4f¹⁴ 5d⁴ so W⁴⁺ is [Xe] 4f¹⁴ 5d². The ligands PMe₃ (2 e⁻), Cl⁻ (2 e⁻) and η⁵-Cp⁻ (6 e⁻) provide 16 valence electrons. The total number of non-*f*-orbital valence electrons on the metal centre is then 2 + 16 = 18 e⁻ (stable for an octahedral complex).

The number of electrons donated by the various ligands are (using the ionic counting convention)

Ligand	# e ⁻	Ligand	# e ⁻	Ligand	# e ⁻
H ⁻ (hydro)	2	NR ²⁻ (imido), PR ²⁻	4 or 6	NO ⁺ (nitrosyl)	2
X ⁻ (halido)	2	N ³⁻ (nitride), P ³⁻	6	NO ₂ ⁻ (nitrito)	2
OH ⁻ (hydroxo), RO ⁻ (alkoxo)	2	CO (carbonyl)	2	CNR (isociano)	2
H ₂ O (aqua)	2	CR ₃ ⁻ (carbanion)	2	η ³ -C ₃ H ₅ ⁻ (allyl)	4
O ²⁻ (oxido), S ²⁻ (sulfo)	4 or 6	CR ₂ (alkylidene)*	2	η ⁵ -C ₅ H ₅ ⁻ (Cp)	6
O ₂ ²⁻ (peroxo)	4	CR ⁻ (alkylidyne)*	4	η ³ -C ₅ H ₅ ⁻ (Cp)	4
NR ₃ (ammine), PR ₃	2	C ₂ R ₄ (alkene)	2	η ⁶ -C ₆ H ₆ (Bz)	6
NR ₂ ⁻ (amido), PR ₂ ⁻	2 or 4	C ₂ R ₂ (alkyne)	2 or 4	η ¹ -C ₆ H ₅ ⁻	2

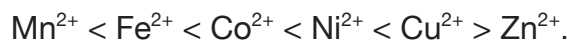
Electron counting conventions: in the above table, the ionic convention is used.

- **Ionic convention:** number of e⁻ donated = hapticity + negative formal charge
- **Covalent / neutral convention:** formal charges omitted; number of e⁻ donated = hapticity
- The convention affects the oxidation state of the metal ion, but if used consistently, does not affect the overall electron count.
- *In the ionic scheme, alkylidenes may be Fischer-type carbenes (singlet: CR₂, 2 e⁻) or Schrock-type carbenes (triplet: CR₂²⁻, 4 e⁻). In the covalent scheme, they are always CR₂, 2 e⁻. Similarly, alkylidynes may be CR³⁻, 6 e⁻ or CR⁻, 4 e⁻.

15.5.12. Irving-William Series of Divalent Complex Stability

The complexes of divalent cations (M^{2+}) of late 3d transition metals show increasing stability with decreasing atomic radius due to higher charge density.

The first stepwise stability constants ($\log K_1$) follows the trend

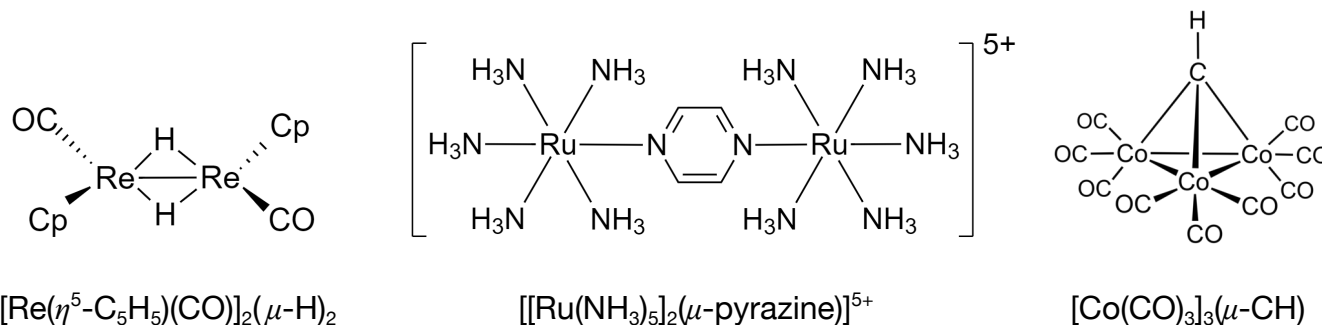


The maximal stability of Cu^{2+} is not predicted by CFT, and is due to formation of Jahn-Teller distorted octahedral complexes (Section 15.5.15).

15.5.13. Polynuclear Complexes

Ligands may donate their lone pair(s) to multiple metal centres. These are known as bridging ligands. Each metal ion is most stable at its full electron count, and there may be metal-metal bonds present.

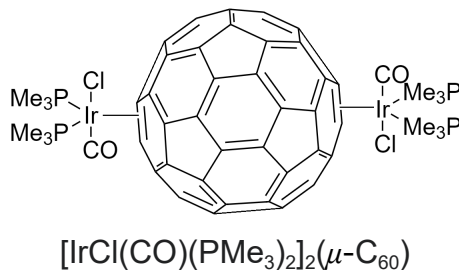
Formulas of polynuclear complexes are written with μ to indicate the bridging ligand:



Hydride ligands donate $1 e^-$ into each metal-hydride bond, for its normal total of $2 e^-$.

Halide ligands may donate multiple lone pairs.

Buckminsterfullerene (C_{60}) can act as a π ligand:

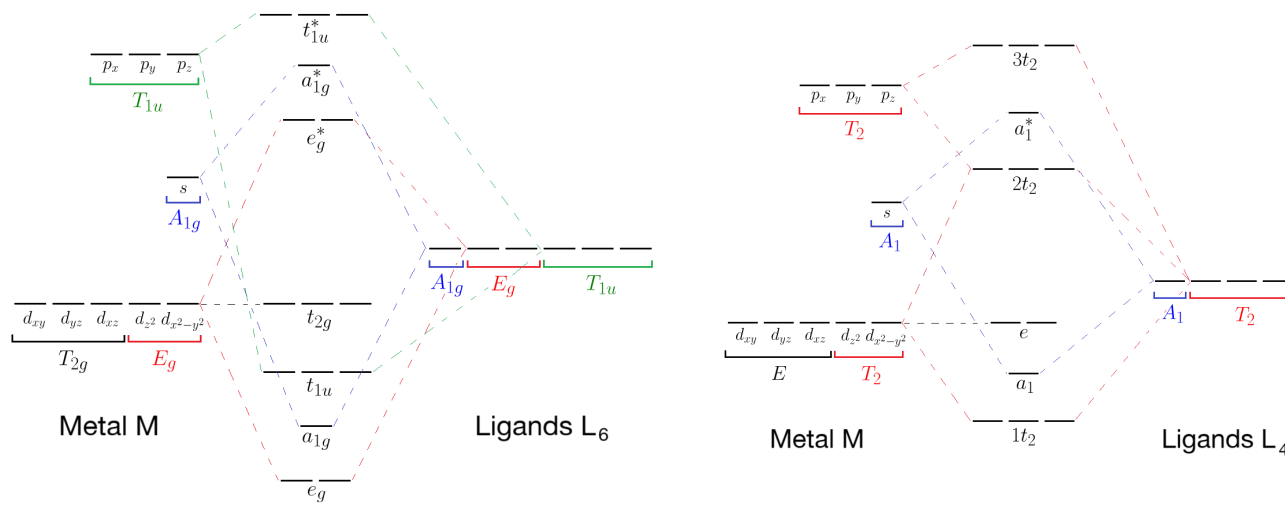


Some solid state complexes can form polymer-like chains e.g. $BeCl_2$.

15.5.14. Ligand Field Theory

Ligand Field Theory (LFT) applies MO theory to CFT, allowing it to be used for metal complexes which are not perfectly ionic e.g. organometallic complexes.

The frontier (valence) orbitals of a period n metal ion are $\{(n-1)d, ns, np\}$. These split into orbitals given by their irreducible representations under the point group of the molecular geometry.



Octahedral (O_h): ML_6

$$\Delta_{\text{oct}} = \text{energy of } e_g^* - \text{energy of } t_{2g}$$

Tetrahedral (T_d): ML_4

$$\Delta_{\text{tet}} = \text{energy of } 2t_2 - \text{energy of } e$$

If π back-bonding occurs, e and $2t_2$ can drop in energy.

Ligand contributions can be determined with projection operators (Section 13.2.10).

Total electron pairing energy: $\Pi_{\text{total}} = \Pi_c + \Pi_e$

Π_c is the Coulombic repulsion term due to two electrons present in the same sub-orbital.

Π_e is the stabilising exchange energy of electrons in degenerate orbitals with the same spin.

For $n e^-$ in a degenerate set of n orbitals with same spin, there are ${}^nC_2 = \frac{n(n-1)}{2}$ multiples of Π_e .

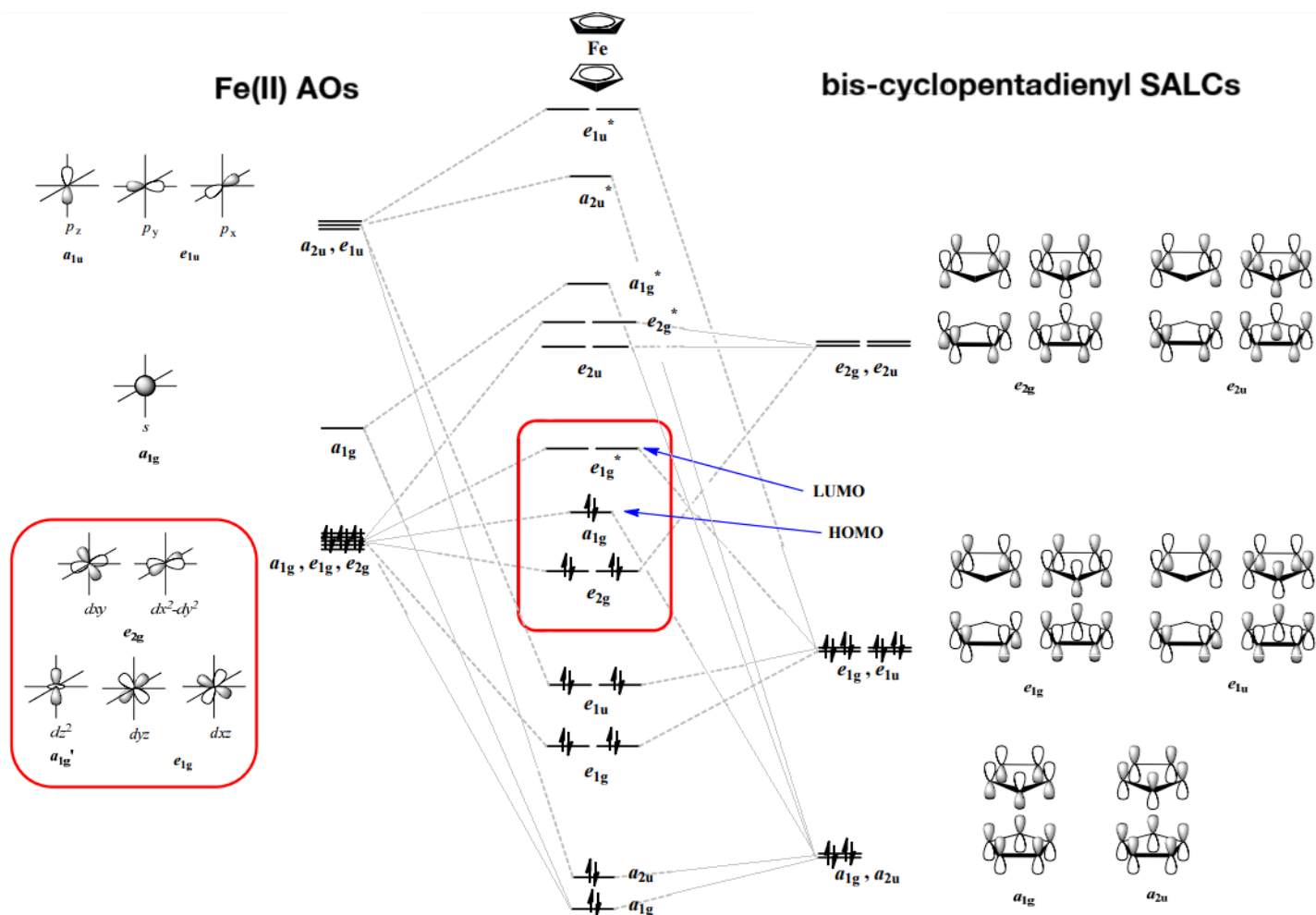
π -acceptor ligands (CO, NO, CN^- , pyridine) have empty π^* orbitals that accept electrons from metal T_{2g} d -orbitals. This backbonding effect strengthens the metal-ligand bond but weakens ligand multiple bonds. In the spectrochemical series (Section 15.5.9), π -donors are towards the small Δ_o end while π -acceptors are towards the large Δ_o end. σ -only ligands are intermediate.

4d and 5d metals are usually low spin due to stronger σ bonds and also due to decreased electron repulsion in their larger d orbitals.

Example: molecular orbitals of ferrocene $[\text{Fe}(\eta^5\text{-C}_5\text{H}_5)_2]$ using SALCs

The frontier orbitals of the cyclopentadienyl anion Cp^- (C_5H_5^-) are 5 sets of delocalised p orbitals totalling 6 electrons. Each ring is in the D_{5h} point group. The staggered conformation of bis-cyclopentadienyl has 10 sets of p orbitals with 12 electrons in the D_{5d} point group. The reducible representation is $\Gamma = \{E: 10, 5\sigma_d: 2\}$. The irreducible representation in D_{5d} is $\Gamma = A_{1g} \oplus E_{1g} \oplus E_{2g} \oplus A_{2u} \oplus E_{1u} \oplus E_{2u}$.

The bonding $\text{Fe}^{2+} = [\text{Ar}] 3d^6$ atomic orbitals transform in D_{5d} as $\{A_{1g}: (s, d_z), E_{1g}: (d_{yz}, d_{xz}), E_{2g}: (d_{x^2-y^2}, d_{xy}), A_{2u}: (p_z), E_{1u}: (p_x, p_y)\}$



15.5.15. Jahn-Teller Effect

Nonlinear molecules may distort their geometry to remove the degeneracy (equality of energy) of unequally occupied orbitals. This lowers the energy of the complex as a whole.

- e_g orbitals split into d_{z^2} and $d_{x^2-y^2}$ orbitals.
- t_{2g} orbitals split into d_{xz} , d_{yz} and d_{xy} orbitals.

Asymmetry in e_g causes a strong Jahn-Teller effect (e.g. low-spin d^7 or d^9 , high-spin d^4), while asymmetry in t_{2g} causes a weak Jahn-Teller effect.

- If $d_{x^2-y^2} > d_{z^2}$ (i.e. d_{z^2} is **occupied**) then there is tetragonal **elongation** along the z -axis.
- If $d_{x^2-y^2} < d_{z^2}$ (i.e. d_{z^2} is **vacant**) then there is tetragonal **compression** along the z -axis.

Jahn-Teller theory cannot predict the direction, only its presence and strength.

Jahn-Teller distortion is a permanent effect, occurring in the aqueous and pure (solid/liquid/gas) states.

15.5.16. Polarisability of Ligands

Transition metal centres (M) act as Lewis acids. Ligands (L) act as Lewis bases. The formation of the transition metal complex (ML) is considered an acid-base reaction.

Hard-Soft Acid Base Theory (HSAB theory)

	thermodynamics	ionic radius	charge	charge density	polarisability	MO energy
Hard acid	$\Delta_f G^\ominus_{M^{n+}} < 0$	small	high +ve	high	low	high LUMO
Soft acid	$\Delta_f G^\ominus_{M^{n+}} > 0$	large	high -ve	low	high	low LUMO
Hard base	$\alpha_{ML}^* < 0$	small	high -ve	high	low	high HOMO
Soft base	$\alpha_{ML}^* > 0$	large	low -ve	low	high	low HOMO

For a given base (ligand), $RT \ln K_{ML} = \alpha_{ML}^* \Delta_f G^\ominus_{M^{n+}} - \beta_{ML}^* r_{M^{n+}} + \gamma_{ML}^* \Delta_{hyd} G^\ominus_{M^{n+}} - \delta_{ML}^*$, where (α_{ML}^* , β_{ML}^* , γ_{ML}^* , δ_{ML}^*) are constants fit across a range of metal ions M^{n+} . Hard acid-hard base (more ionic) and soft acid-soft base (more covalent) interactions are more favourable - the interaction energy term $\alpha_{ML}^* \Delta_f G^\ominus_{M^{n+}} > 0$, as species which are α more 'polarisable' have **less** 'polarising power'.

(K_{ML} : stability constant of ML, $\Delta_f G^\ominus_{M^{n+}}$: Gibbs free energy of formation for M^{n+} , $\Delta_{hyd} G^\ominus_{M^{n+}}$: Gibbs free energy of hydration for M^{n+} (solvation energy), $r_{M^{n+}}$: effective ionic radius of M^{n+})

Classification of Metals and Ligands:

<p>Hard Bases F^-, Cl^-, H_2O, OH^-, O^{2-}, ROH, RO^-, R_2O, CH_3COO^-, NO_3^-, ClO_4^-, CO_3^{2-}, SO_4^{2-}, PO_4^{3-}, IO_3^-, NH_3, RNH_2, N_2H_4, Glu, ADP, ATP, AMP-5'</p>	<p>Intermediate Bases Br^-, NO_2^-, N_3^-, N_2, SO_3^{2-}, $C_6H_5NH_2$, C_5H_5N, His, Asp</p>	<p>Soft Bases H^-, I^-, H_2S, SH^-, S^{2-}, RSH, RS^-, R_2S, SCN^-, CN^-, RNC, CO, $S_2O_3^{2-}$, R_3P, $(RO)_3P$, R_3As, C_2H_4, C_6H_6, en, $EDTA^{4-}$, Cys, Gly</p>
<p>Hard Acids HX, $*H^+$, Li^+, Na^+, K^+, Rb^+, Cs^+, $*Be^{2+}$, Mg^{2+}, Ca^{2+}, Sr^{2+}, Ba^{2+}, BF_3, BCl_3, $B(OR)_3$, Al^{3+}, Ga^{3+}, $Al(CH_3)_3$, $AlCl_3$, Ti^{3+}, V^{3+}, Cr^{3+}, Mn^{2+}, Fe^{3+}, Co^{3+}, Eu^{2+}, U^{3+}, Np^{3+}</p>	<p>Intermediate Acids $B(CH_3)_3$, NH_4^+, Fe^{2+}, Co^{2+}, Ni^{2+}, Zn^{2+}, Rh^{3+}, Cd^{2+}, Ir^{3+}, Os^{2+}, Sn^{2+}, Pb^{2+}, Tl^+</p>	<p>Soft Acids BH_3, $Tl(CH_3)_3$, Bi^{3+}, Cu^+, Ag^+, Au^+, Cu^{2+}, Hg_2^{2+}, Hg^{2+}, CH_3Hg^+, Pd^{2+}, Pt^{2+}, Pt^{4+}, Au^{3+}, Ru^{3+}, Br_2, I_2, all π acceptors</p>

15.5.17. Organometallic Reactions

M-L bond strength increases down the group ($5d > 4d > 3d$).

Ligand Substitution: $ML_x + n L' \rightarrow ML_{x-n}L'_n + n L$

Associative (S_NAc -like): $ML_x + L' \rightarrow ML_xL' \rightarrow ML_{x-1}L' + L$. Preferred by $16 e^-$ uncrowded complexes.

Dissociative (S_N1 -like): $ML_x \rightarrow ML_{x-1} + L$, $ML_{x-1} + L' \rightarrow ML_{x-1}L'$. Preferred by $18 e^-$ crowded complexes.

Interchange (S_N2 -like): $ML_x + L' \rightarrow ML_{x-1}L' + L$. Preferred by $18 e^-$ complexes.

Reductive activation (R): $ML_x + e^- \rightarrow ML_x^-$. Preferred when the LUMO is nonbonding / antibonding.

Oxidative activation (O): $ML_x \rightarrow ML_x^+ + e^-$. Preferred when the HOMO is nonbonding / antibonding.

The regioselectivity of substitution is subject to the trans effect (Section 15.5.6).

Oxidative Addition and Reductive Elimination: $M^{(n)} + A-B \rightleftharpoons A-M^{(n+2)}-B$

Preferred with metals with stable oxidation states separated by $2 e^-$. Common substrates:

H-H, Si-H, B-B, B-H, Sn-H, Sn-Sn, N-H, O-H, S-H, C-X, C-H (in e.g. CH_4 , C_6H_6).

Concerted oxidative addition: The σ_{A-B} bond donates electron density into the empty M d_{z^2} orbital, and may also accept backbonding from M d orbitals into the σ_{A-B}^* bond. The result is *cis* addition of A and B into the complex, pushing one ligand into an alternate position.

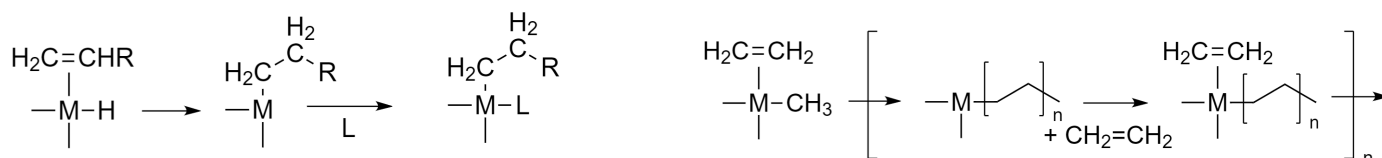
Stepwise oxidative addition: electrophilic addition-like mechanism.

Reductive elimination: the reverse of oxidative addition. The leaving bonds M-A and M-B must be *cis* to each other. A common pattern is reduction followed by oxidation with a different substrate (effectively a redox substitution).

Migratory Insertion: $L_n-\overset{\overset{X}{|}}{M}-Y \rightleftharpoons L_n-M-X-Y \longrightarrow L_n-\overset{\overset{L'}{|}}{M}-X-Y$

Ligand insertion is reversible. There is no change in the oxidation state of M. To interchange, X and Y must be *cis* to each other. The ligands must contain π bonds (e.g. CO).

Hydrometalation (reverse β -hydride elimination): Carbometalation (Ziegler-Natta addition polymerisation):



Ligand Attack

Metathesis

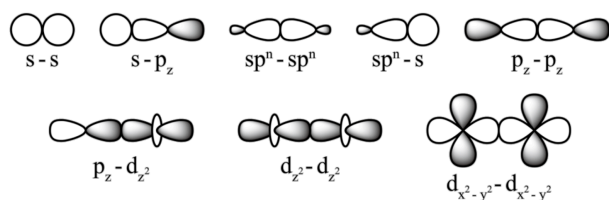
C16. ORGANIC AND BIOCHEMISTRY

16.1. Bonding and Forces in Organic Molecules

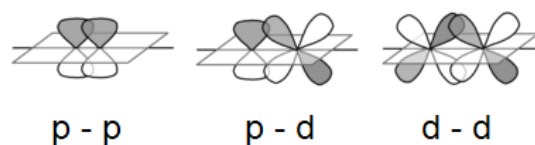
16.1.1. Sigma and Pi Bonding Between Atomic and Hybridised Orbitals

Bonding occurs when orbital wavefunctions superpose in-phase (represented as same shade).

Sigma (σ) bonds:



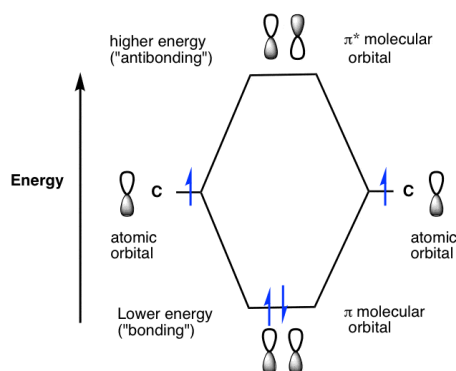
Pi (π) bonds:



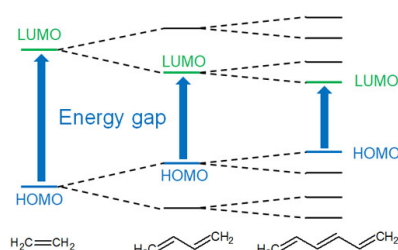
16.1.2. Carbon-Carbon Pi Bonding and Resonance

A pi bonding orbital (π) has neighbouring p-orbitals in phase, while a pi antibonding orbital (π^*) has neighbouring p-orbitals in antiphase.

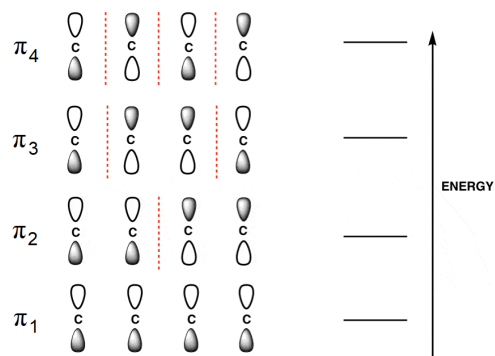
Two neighbouring p-orbitals in antiphase will have a nodal plane between them. There are no transverse nodes at the lowest level, above which they are distributed symmetrically in the system. The HOMO-LUMO gap decreases with the extent of conjugation.



MO diagram for a $C=C$ π bond



MOs of conjugated alkenes



Nodal planes for buta-1,3-diene

Huckel's rule for aromatic conjugation: $(4n + 2) e^-$ for aromaticity, $4n e^-$ for antiaromaticity.

16.1.3. Mechanisms of Bond-Mediated Electron Density Redistribution

- **Inductive effect (I):** electron density is pushed/pulled through sigma bonds, due to electronegativity differences. This is a permanent effect.
- **Mesomeric effect (M):** electron density is delocalised through pi bonds, due to electronic **resonance**. This is a permanent effect, in which the molecular orbitals are a quantum superposition of contributing classical resonance structures.
- **Electromeric effect (E):** electron density is pushed/pulled through pi bonds, due to the presence of an nearby electrophile or nucleophile. This is a temporary effect.

16.1.4. Tautomerism

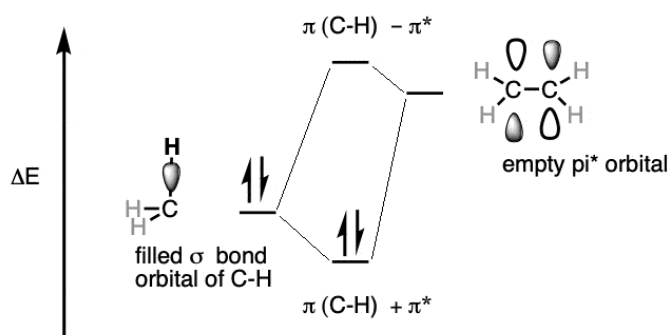
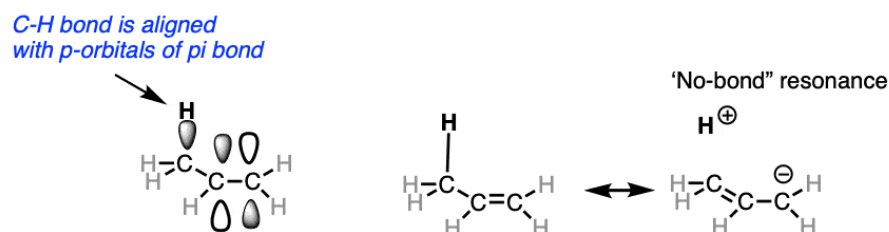
Tautomerism occurs in molecules with rapidly interconverting states, through intermolecular reactions with the solvent, typically proton transfers to and from water molecules.

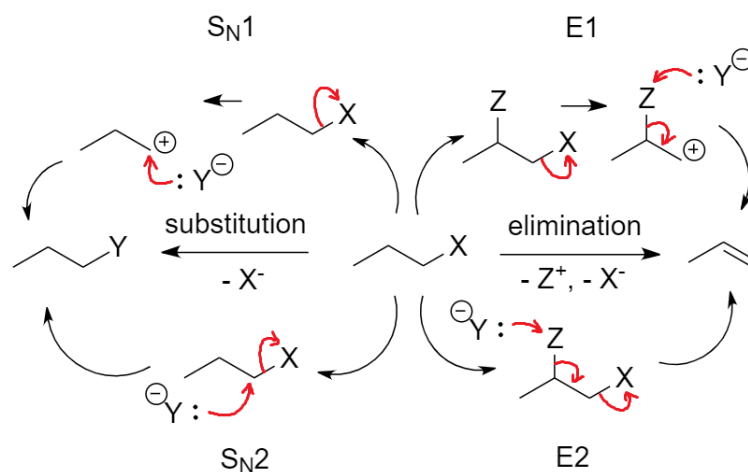
- **Keto-enol tautomerism:** $\text{RCOCH}_2\text{R}'$ (**ketone**) \rightleftharpoons RC(OH)=CH-R (enol). The keto form predominates in most cases, but the enol form is stabilised when conjugating C=C bonds are present in R e.g. phenols, or in 1,3-diketones.
- **Amide-imidic acid tautomerism:** RCONHR' (**amide**) \rightleftharpoons $\text{RC(OH)NR}'$ (imidic acid). The amide form predominates in water or oxygen, while the imidic acid form predominates in ammonia or methane. In cyclic amides (lactams), the corresponding imidic acid is a lactim, important for tautomerism in DNA and RNA nucleobases.
- **Enamine-imine tautomerism:** $\text{R}_2\text{C(NH}_2\text{)CR}'$ (enamine) \rightleftharpoons $\text{R}_2\text{C(NH)CHR}'$ (imine). The imine is stabilised in acid, the enamine is stabilised in base. Imine (Schiff base) formation is important in many biochemical pathways.

Others include oxime-nitroso, amino acid-ammonium carboxylate (zwitterion formation), ketene-ynol, tetrazole-azide, nitro-nitronic acid and phosphite-phosphonic acid tautomerism.

16.1.4. σ - π^* Hyperconjugation (No-Bond Resonance)

For a C-H σ -bond to be eligible for hyperconjugation, the α C must be sp^3 hybridised. The C-H σ -bonds can then be conjugated with an adjacent C=C π -bond by interaction with an empty π^* antibonding orbital. A resonance structure is formed, weakening the C-H bonds.



16.1.5. Nucleophilic Substitution (S_N) and Elimination (E)

(X: leaving group, Y: nucleophile (S_N) or base (E), Z: acidic group (often a proton).)

Note that if Y is added in a polar solvent, a molecule of solvent may take the role of Y.

Conditions for favouring mechanisms:

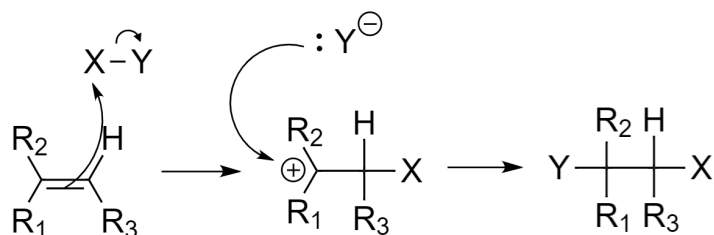
- Substrate R: Steric hindrance on the substrate RX promotes S_N1 . Sterically open substrates promote S_N2 and $E2$.
- Reactant Y: Strong bases / charged nucleophiles (e.g. NaOH , Cl^-) promote S_N2 and $E2$. Weak bases / neutral nucleophiles (e.g. EtOH , NH_3), as well as strong acids (e.g. H_2SO_4), promote S_N1 and $E1$.
- Solvent: Polar protic solvents (e.g. H_2O , EtOH) promote $E2$ and inhibit S_N2 by solvating Y with hydrogen bonding. Polar aprotic solvents (e.g. DMSO , acetone) promote S_N2 and inhibit $E2$ by replacing Y as a less effective base.
- Temperature: High temperatures promote $E1$. Low temperatures promote S_N1 .

Note that:

- A strong base in an alcohol solvent will favour E over S_N (alkoxide is strong & bulky base)
- S_N1 , $E1$ are unimolecular, with 1st-order rate kinetics: $r = k [Y]$
- S_N2 , $E2$ are bimolecular (concerted; concurrent), with 2nd-order rate kinetics: $r = k [Y][RX]$
- S_N reactions involve an inversion of stereochemistry.
- S_N1 and $E1$ allow for proton transfers (1,2-hydride shifts) if an adjacent carbocation is more stable, and 1,2-methyl shifts if a neighbouring carbon is 4° (forming a 3° carbocation).

16.1.6. Electrophilic Addition

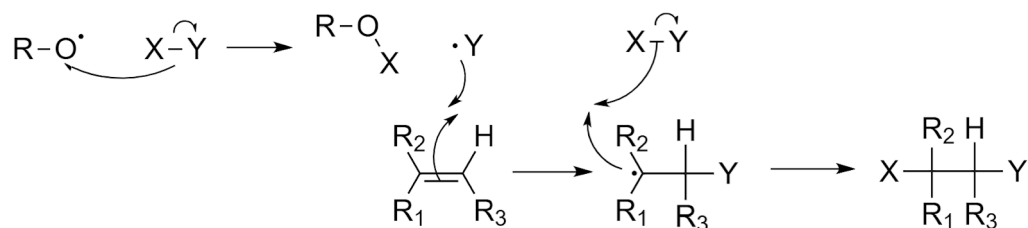
Markovnikov addition: the carbocation resides on the highest-order carbon.



(X-Y: electrophile, X: more electropositive, Y: more electronegative)

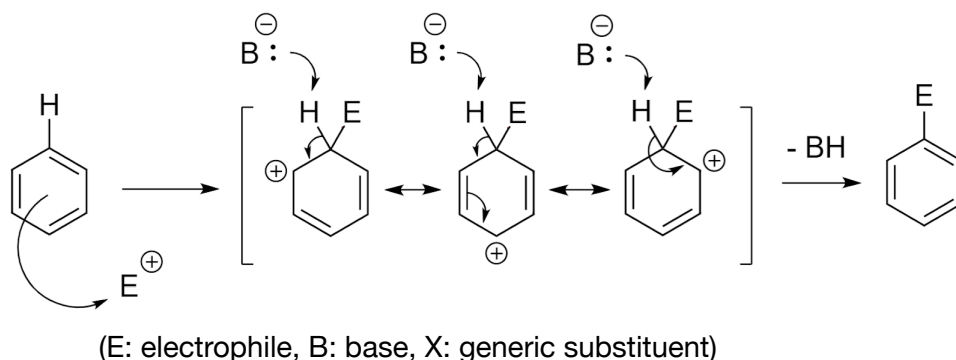
Anti-Markovnikov addition: the radical lies on the highest-order carbon.

In the presence of free radicals generated by e.g. R-O-O-R peroxide decomposition,

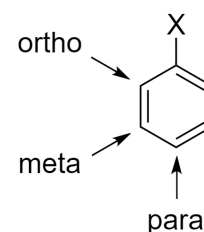


Rearrangements may occur to stabilise the transition state. In order of migratory aptitude,

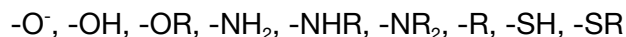
hydride shift > methyl shift > alkyl shift

16.1.7. Electrophilic Aromatic Substitution (EAS, S_NAr)

Substituents on an aromatic system influence the stability of the intermediate carbocation formed when an electrophile attacks. The stability of the carbocation is increased by resonance, hyperconjugation and positive inductive effects, in decreasing order of significance. A more stable carbocation indicates a higher regioselectivity towards substitution at the cationic position.

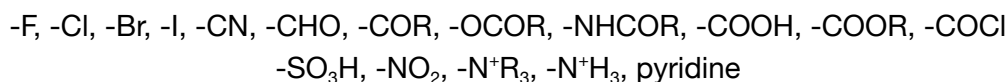


- **Electron-Releasing Groups (ERGs)** exhibit **positive** mesomeric and inductive effects (+M, +I). They decrease acidic strength. When present in an aromatic system, they favour substitution at the **ortho** and **para** positions, and are typically **activating** groups, increasing the rate of electrophilic substitution, **except** the halogens, which are deactivating. Examples of ERGs are:



Alkyl groups exhibit +I effects, with magnitude $3^\circ > 2^\circ > 1^\circ > -CH_3 > -H$, and increasing with the number of carbon atoms in the group e.g. *tert*-butyl \gg methyl.

- **Electron-Withdrawing Groups (EWGs)** exhibit **negative** mesomeric and inductive effects (-M, -I). They increase acidic strength. When present in an aromatic system, they favour substitution at the **meta** positions, and are typically **deactivating** groups, decreasing the rate of electrophilic substitution. Examples of EWGs are:

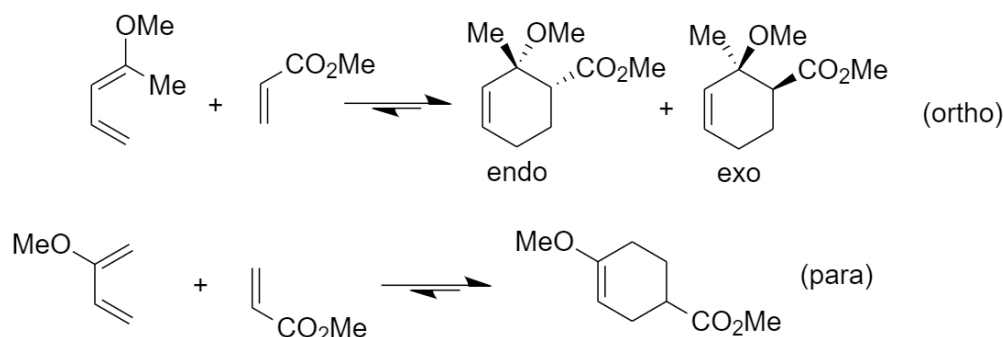


If multiple aromatic systems are present in a molecule, substitution will favour the one which is more activating, with the other being treated as a substituent e.g. 2-phenylpyridine can be mononitrated at the *meta* position on the benzene ring.

16.1.8. Pericyclic Reactions and Rearrangements

In a pericyclic reaction, π electrons move to form σ bonds in concerted fashion.

Diels-Alder Reaction: when an *s-cis*-diene reacts with a dienophile, two diastereomers form due to the different orientations in which the molecules may react:



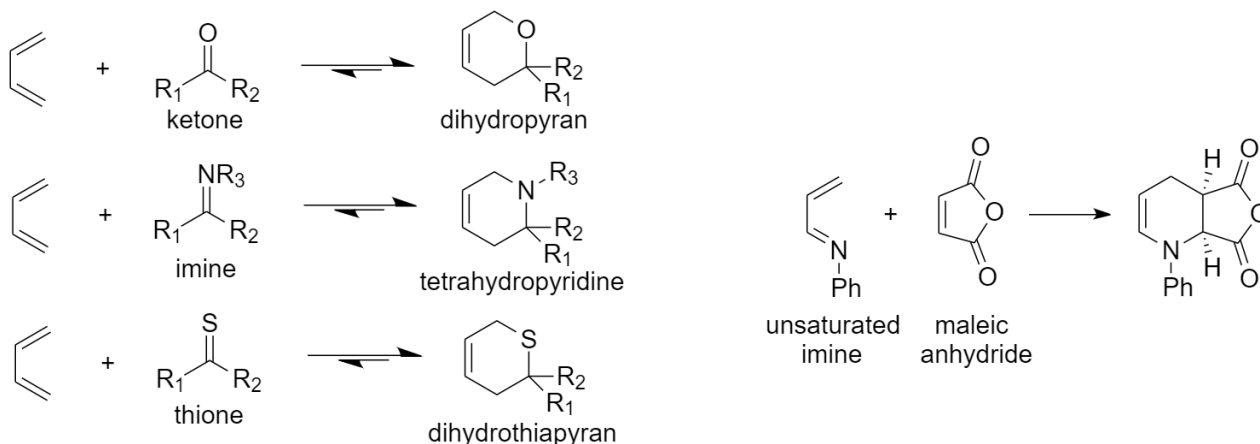
The enantiomers of each form will also be produced if they are not *meso* compounds.

- The *endo* form is the kinetically favoured product.
- The *exo* form is the thermodynamically favoured product.

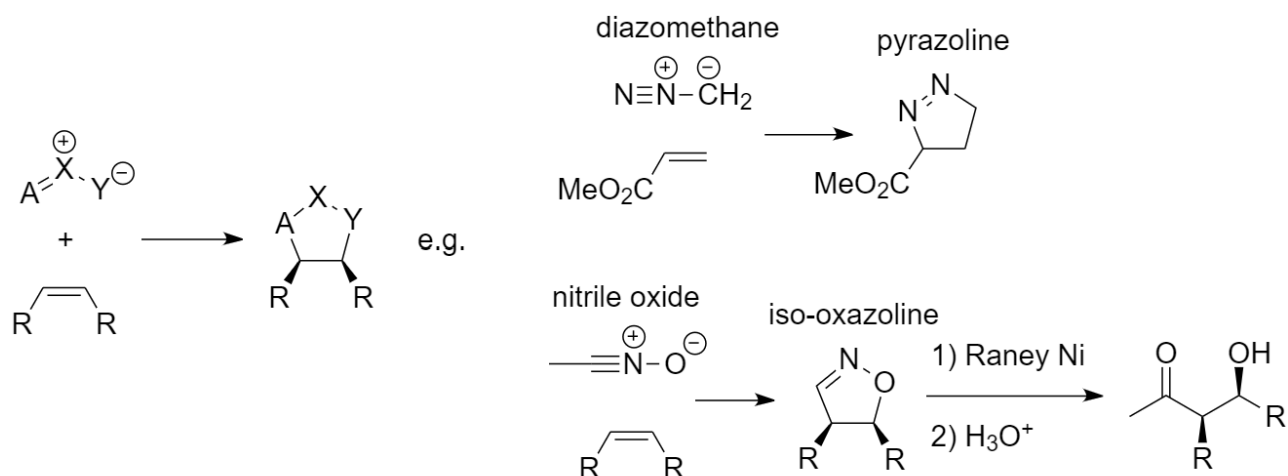
Rate increases with EWGs on dienophile and ERGs on the diene.

The two forms exist due to the fact that the diene can 'descend' onto the dienophile with the C group oriented in the same (*exo*) or opposite (*endo*) direction as the B group.

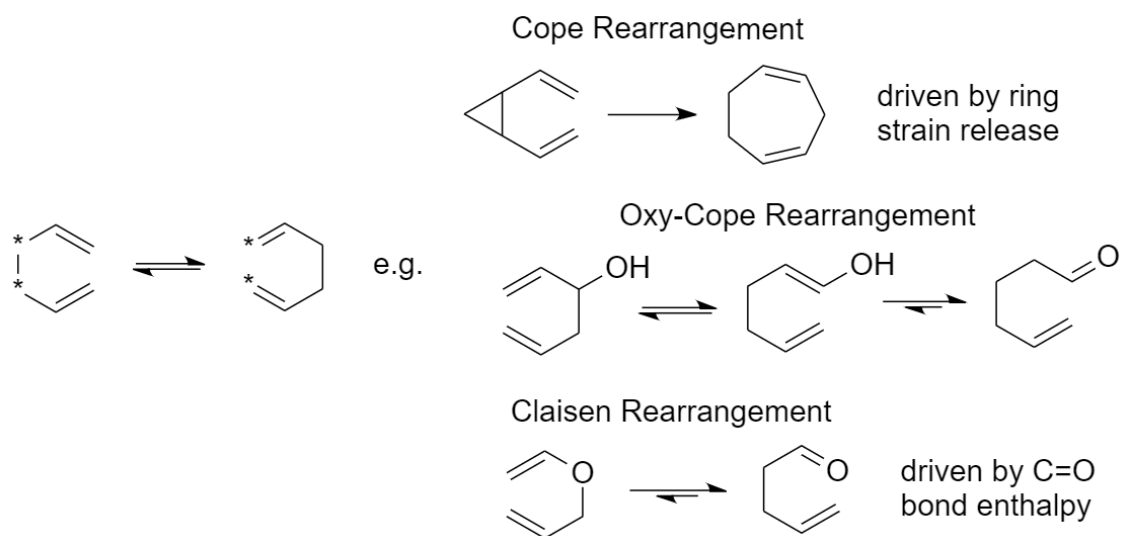
Heteroatomic Diels-Alder Reaction: atoms on the diene or dienophile can be replaced with e.g. O, N, S, as long as the dienophile remains electron-withdrawing and the diene remains electron-releasing, to form e.g. dihydropyran, tetrahydropyridines, dihydrothiapyran.



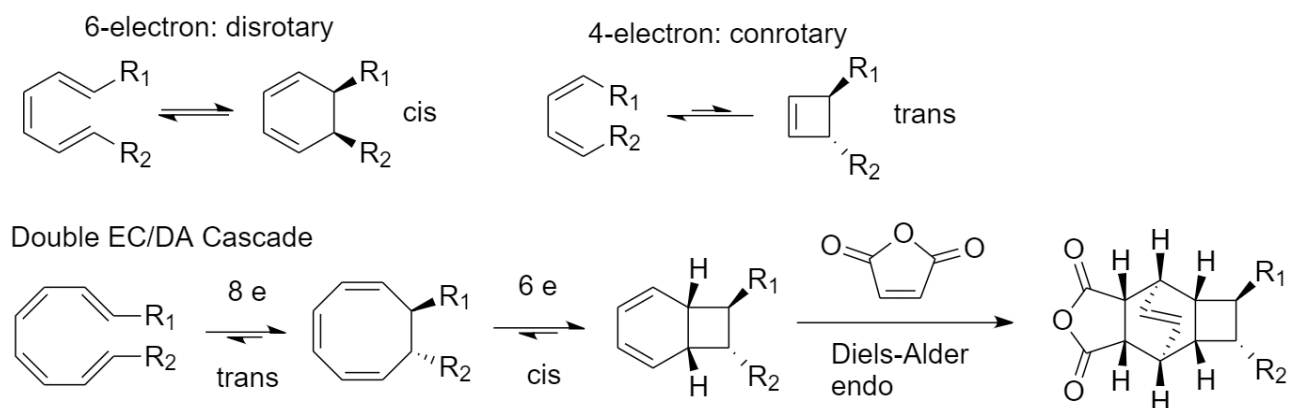
1,3-Dipolar Cycloadditions: unsaturated ylides react with alkenes to form a 5-membered ring in similar concerted [4+2] cycloaddition.



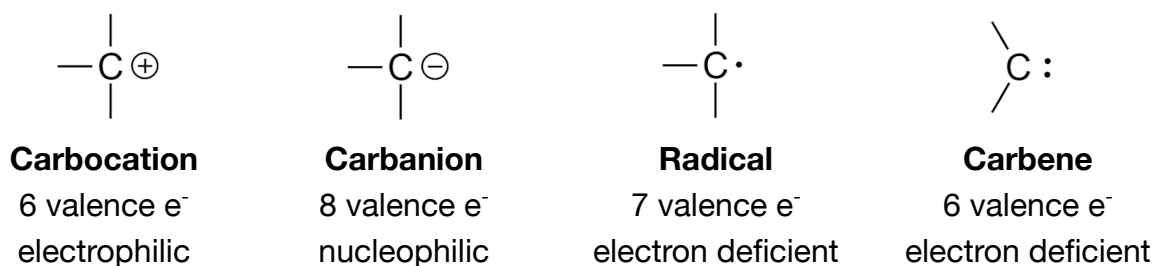
Sigmatropic Shifts: a [3+3] shift to form γ - δ unsaturated compounds.



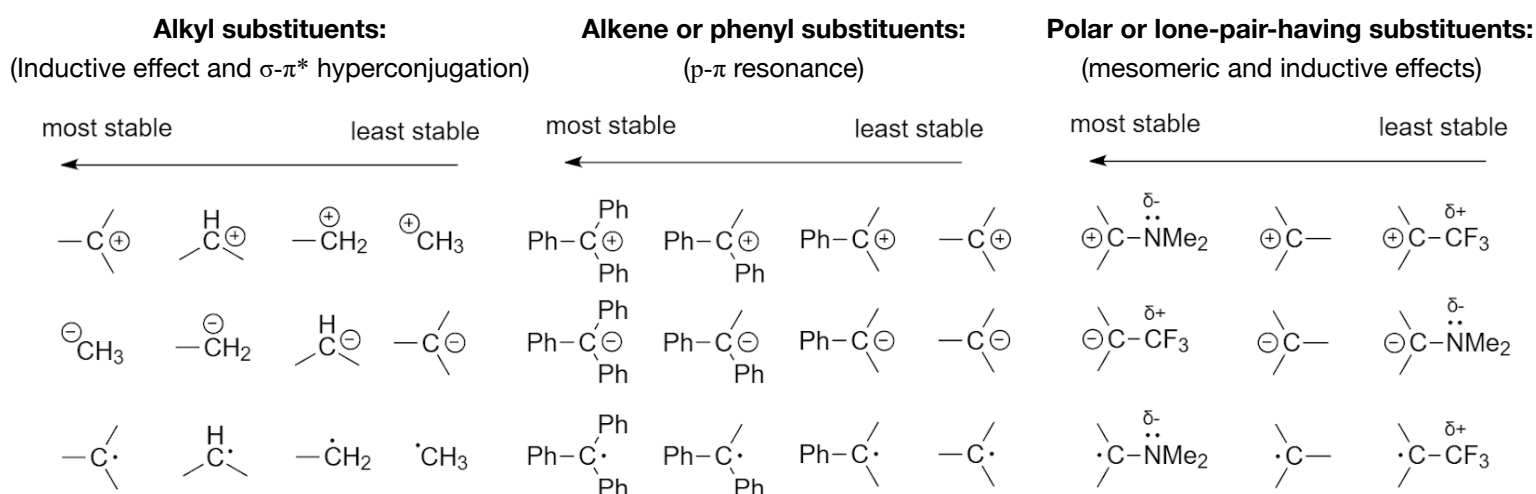
Electrocyclisation: formation of a σ bond to close a ring.



16.1.9. Types of Carbon Species (Carbocations, Carbanions, Radicals, Carbenes)



Carbocations, Carbanions and Radicals vary in stability depending on substituents:



Carbenes: reactive sp² hybridised carbons.

- **Triplet carbene:** diradical. One unpaired e⁻ in an sp² orbital and one unpaired e⁻ in a p orbital.
- **Singlet carbene:** paired electrons in an sp² orbital, empty p orbital.

Most chemical reactions which form carbenes (e.g. RCN₂ → RC:, CHCl₃ + NaOH → :CCl₂) result in the singlet state unless light is used to excite the electrons (photochemistry).

Addition of singlet carbenes onto π bonds is concerted with simultaneous sp² → π^* donation and π → p acceptance to form a cyclopropane ring. Stereochemistry is preserved.

Addition of triplet carbenes does not preserve stereochemistry since the process is stepwise. After the first bond formation, the remaining unpaired electron must change spin to form, which takes time (phosphorescence / spin-orbit coupling) so bonds may rotate.

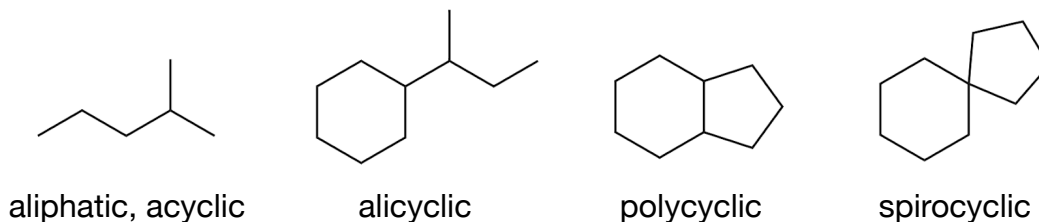
16.1.10. Woodward-Hoffmann Rules and Frontier Molecular Orbital Theory

16.1.11. Felkin-Ahn Model of Asymmetric Induction

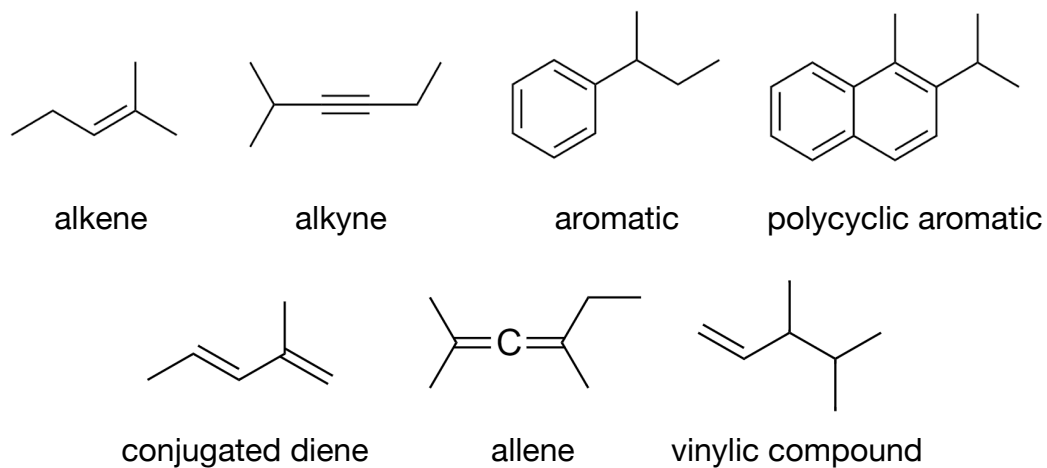
16.2. Structure of Organic Molecules

16.2.1. Classification of Hydrocarbons

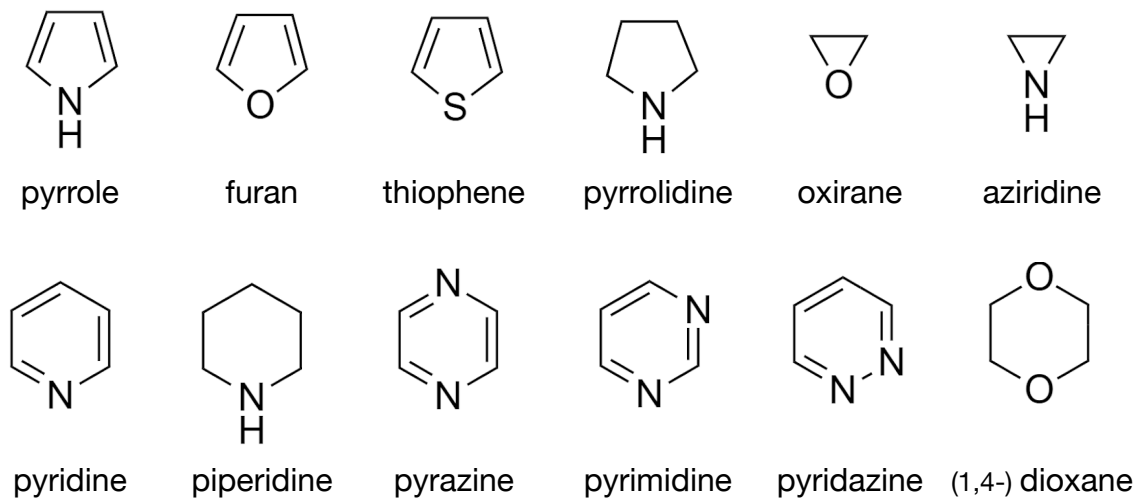
Saturated



Unsaturated



16.2.2. Heterocyclic Compounds



16.2.3. Nomenclature of Stereoisomerism Using Cahn-Ingold-Prelog (CIP) Convention

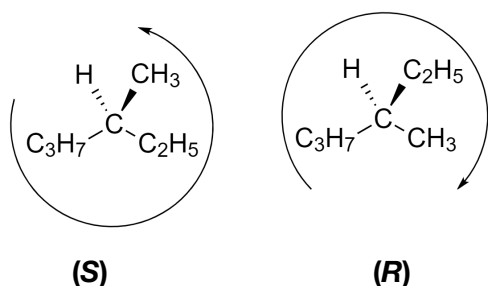
Geometric Isomerism



When alkenes are hetero-substituted, priority is assigned by the highest atomic number of the nearest neighbouring atom (**not** the group as a whole).

- The *trans* isomer is more stable than the *cis* isomer. They do not interconvert.
- The *s-trans* isomer is more stable than the *s-cis* isomer. They may interconvert.

Optical Isomerism



For chiral centres with four different substituents in sp^3 (tetrahedral) geometry, where the priority is assigned by the highest atomic number of the nearest neighbouring atom (**not** the group as a whole) when the lowest substituent (H in above example) is facing directly away from view.

anticlockwise priority

clockwise priority

Other conventions include:

- **D/L**: similarity to glyceraldehyde. D: anomeric hydroxyl group on the right of Fischer projection.
- **+/-**: + slows down right-handed (clockwise, from receiver) circularly polarised light, and vice versa.

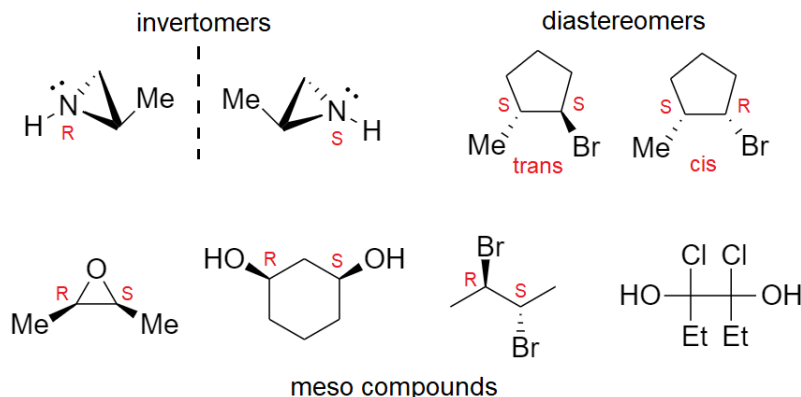
Specific optical rotation, $\alpha_{\lambda}^{(T)}$ [$\text{deg ml g}^{-1} \text{dm}^{-1}$] = $\frac{\Delta\theta [\text{deg}]}{c [\text{g ml}^{-1}] \times L [\text{dm}]}$, depends on temperature and wavelength.

Enantiomers rotate plane-polarised light in opposite directions (optically active).

Diastereomers: multiple stereocenters.

cis: same stereochemistry; *trans*: opposite stereochemistry.

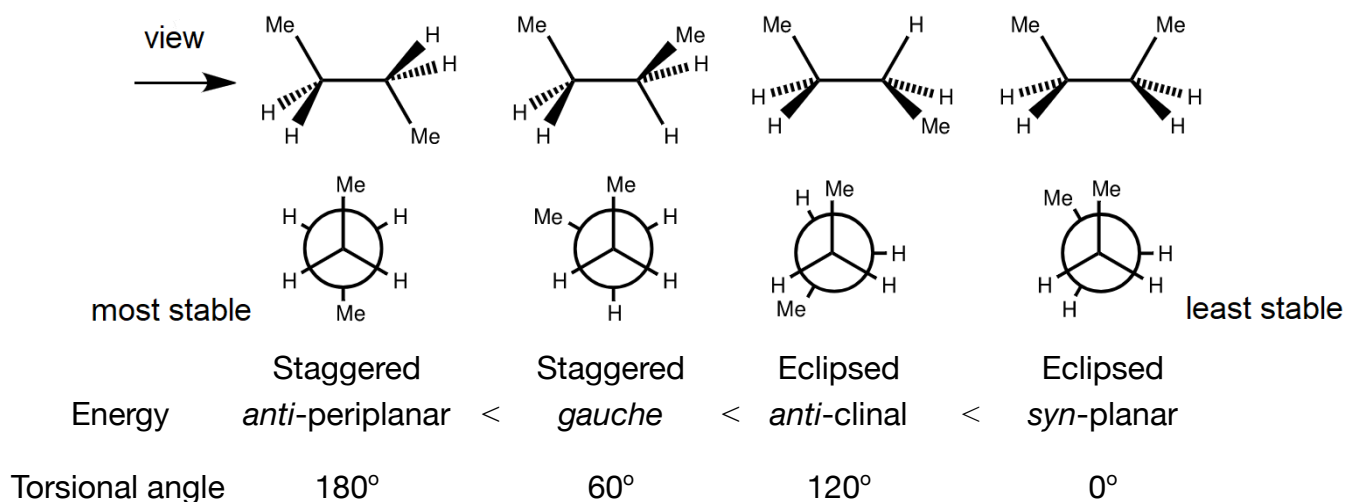
Invertomers: constrained N-centres.



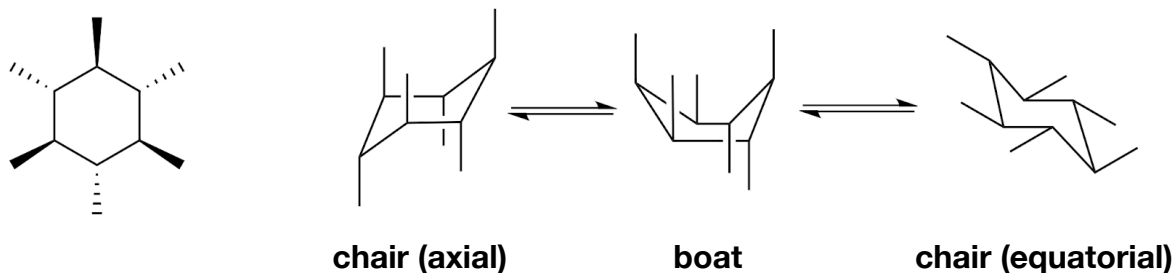
Meso compounds: both *R* and *S*, with a plane of symmetry (not chiral; inactive).

16.2.4. Nomenclature of Conformational Stereoisomerism

Newman Projections of the Rotamers of Butane



Bond-Line Structures of the Conformations of Cyclohexane

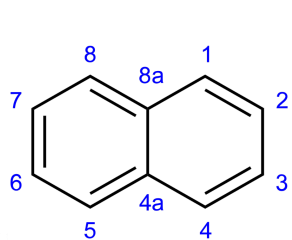


Hashed bonds are drawn downwards. Wedged bonds are drawn upwards.

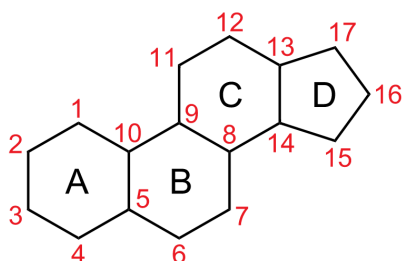
The relative position (axial / equatorial) of all substituents is swapped in a chair ring flip.

The stability of the three conformations depend on substituents: the more stable conformation minimises axial-axial interactions.

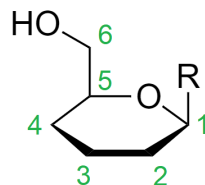
16.2.5. Numbering System for Specific Cyclic and Polycyclic Compounds



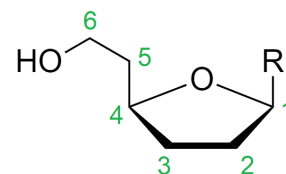
naphthalene



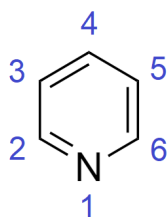
steroid



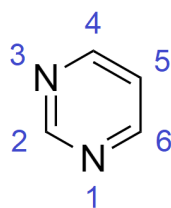
pyranose sugar



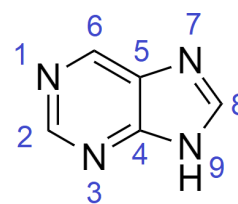
furanose sugar



pyridine



pyrimidine base



purine base

16.2.6. Nomenclature of Bicyclic and Spiro Compounds

Numbering of Bicyclic Compounds:

- Begin numbering from one bridgehead along the **longest** path to the 'other' bridgehead.
- Continue numbering from the 'other' bridgehead along the next longest paths.

Numbering of Spiro Compounds:

- Begin numbering in the smaller ring, adjacent to (not at) the spiro carbon.
- Continue numbering around the other ring.

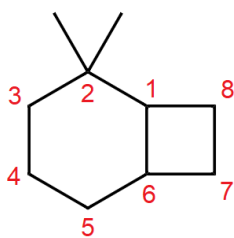
Naming:

- Count the total number of carbon atoms in the ring system, giving the root name.
- Find all unique paths between the bridgeheads, counting the number of carbons (x, y, z) between the bridgeheads.
- The name is then either

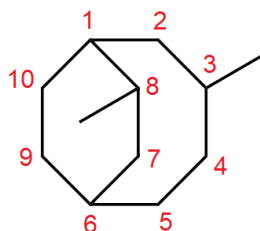
“bicyclo[$x.y.z$]alkane” (where $x \geq y \geq z \geq 0$)

or “spiro[$x.y$]alkane” (where $2 \leq x \leq y$)

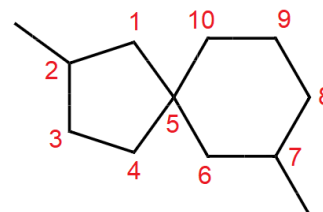
Examples:



2,2-dimethyl-
bicyclo[4.2.0]octane



3,8-dimethyl-
bicyclo[4.2.2]decane

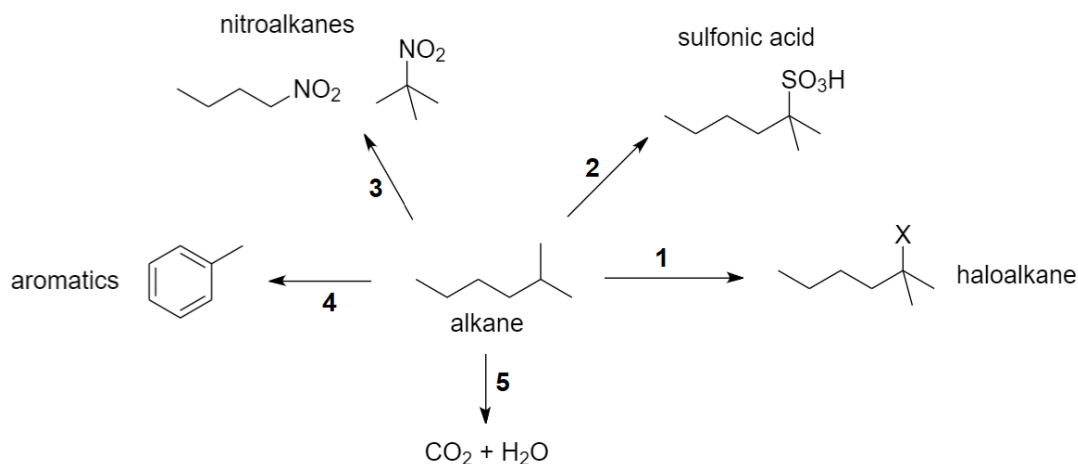


2,7-dimethyl-
spiro[4.5]nonane

16.3. Synthetic Organic Chemistry

16.3.1. Reactions of Hydrocarbons and Aliphatic Haloalkanes

Alkanes:



1: Halogenation. Reagents: X_2 (Cl₂ or Br₂), UV light (hv). Mechanism: free radical substitution. Regioselectivity: 3° > 2° > 1°. Rate: Br > Cl.

2: Sulfonation. Reagents: oleum (conc. H₂SO₄ (g), *in situ* H₂S₂O₇), 400 °C. Regioselectivity: 3° > 2° > 1°. Only used for higher alkanes (carbon numbers $n \geq 6$).

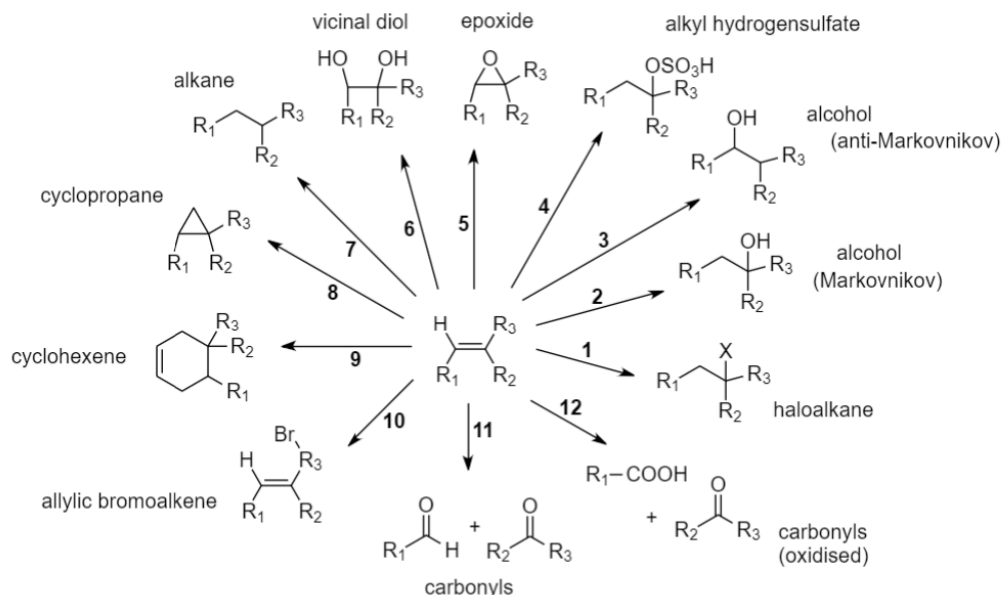
3: Nitration. Reagents: HNO₃ (g), 400 °C. Forms a mixture of products by breaking all combinations of C-C and C-H bonds and replacing them with C-NO₂.

4: Aromatisation. Reagents: Cr₂O₃, Al₂O₃ cat, 600 °C. Mechanism: cyclisation (reforming) then dehydrogenation. *n*-hexane → benzene; *n*-heptane → toluene.

5: Combustion (complete oxidation). Heat in air. Excess O₂ gives pure CO₂ and H₂O. Limiting O₂ gives incomplete combustion to C, CO, CO₂, H₂O and some amount of the unburned hydrocarbons.

For reactions on alkanes used in the petrochemical industry, see Section 14.4.1.

Alkenes:



1: Hydrohalogenation or Dihalogenation. Reagents: **HX or X₂ in dry ether.** Mechanism: electrophilic addition. Rate: HI > HBr > HCl. Follows Markovnikov and peroxide rules.

2: (a) Acid catalysed hydration or (b) oxymercuration-demercuration. Reagents: **(a) H₂O, H₂SO₄ (aq) cat. or (b) 1) Hg(OAc)₂ (aq); 2) NaBH₄, NaOH.** Mechanism: electrophilic addition.

3: Hydroboration-oxidation. Reagents: **1) BH₃ or Sia₂BH or 9-borabicyclo(3.3.1)nonane (9-BBN), tetrahydrofuran (THF); 2) H₂O₂, NaOH, H₂O.** Mechanism: Step 1 involves addition of H and BHR' across the C=C bond. Regioselectivity: Anti-Markovnikov. Stereoselectivity: *syn* addition of H and OH.

4: Hydrogen sulfate formation. Reagents: **conc H₂SO₄.** Mechanism: electrophilic addition. Can be hydrolysed to the alcohol when heated. Regioselectivity: Markovnikov's rule. Stereoselectivity: *anti* addition of H and OSO₃H.

5: Epoxidation ((b): Prilezhaev reaction). Reagents: **(a) 1) Cl₂ + H₂O (in situ HClO); 2) NaOH or (b) RCO₃H (peroxy acid), dichloromethane or (c) for ethene only: O₂, Ag cat.** Mechanism: intramolecular S_N2. **(a)** forms a chlorohydrin intermediate. **(b)** also produces the carboxylic acid RCOOH.

6: Syn oxidation. Reagents: **(a) KMnO₄, cold NaOH (aq) (Baeyer's reagent) or (b) OsO₄, N-methylmorpholine N-oxide (NMO), NaHSO₄.**

7: Syn hydrogenation. Reagents: **H₂ (g), Ni / Pt / Pd-C cat, 50 °C.** Mechanism: heterogeneous catalysis.

8: Simmons-Smith cyclopropanation. Reagents: **Zn(Cu), CH₂I₂.** Mechanism: I-CH₂-ZnI carbenoid. Releases ZnI₂.

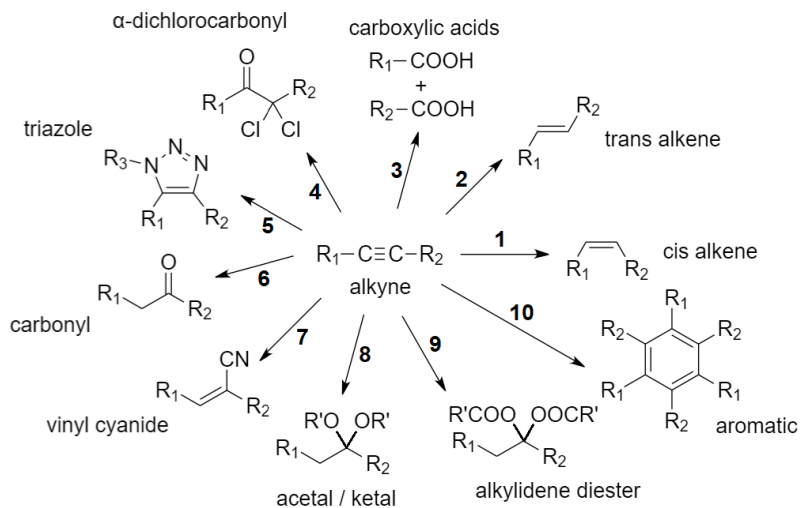
9: Diels-Alder cycloaddition. Reagents: **buta-1,3-diene, heat.** For more information, see Section 16.3.13.

10: Wohl-Ziegler reaction (allylic bromination). Reagents: **N-bromosuccinimide (NBS), (PhCOO)₂, CCl₄.**

11: Ozonolysis. Reagents: **1) O₃ (CCl₄); 2) Zn or dimethyl sulfide (DMS), H₂O.** Using H₂O₂ in step 2) gives R-COOH instead of R-CHO.

12: Oxidative cleavage. Reagents: **KMnO₄, hot conc H₂SO₄.**

Alkynes:



1: Partial syn hydrogenation. Reagents: H_2 (g), Pd-CaSO_4 cat., quinoline (Lindlar's catalyst).

Mechanism: poisoned heterogeneous catalysis.

2: Birch reduction (partial anti hydrogenation). Reagents: Na (s), NH_3 (l) (in situ NaNH_2). Terminal alkynes ($\text{R}_2 = \text{H}$) stop at $\text{R}_1\text{-C}\equiv\text{C}^- \text{Na}^+$, which can undergo C-C bond-forming S_{N} reactions. Using Cu^+ or Ag^+ in this case forms similar alkynide salts.

3: Oxidative cleavage. Reagents: O_3 / KMnO_4 . Terminal alkynes ($\text{R}_2 = \text{H}$) give $\text{H}_2 + \text{CO}_2$ due to decomposition of formic acid (HCOOH).

4: Condensation. Reagents: $\text{HCl} + \text{H}_2\text{O}$ (in situ HClO). Regioselectivity: R_1 more sterically bulky than R_2 .

5: Huisgen cycloaddition (Click chemistry). Reagents: $\text{R}_3\text{-N}_3$ (azide), copper(I) cat e.g. Cu_2O .

Mechanism: [3+2] cycloaddition. Also forms the other isomer. Faster rate of reaction when alkyne is strained (SPAAC) e.g. cyclooctyne or benzyne.

6: Oxymercuration. Reagents: H_2O , HgSO_4 , H_2SO_4 . Mechanism: nucleophilic addition. Keto-enol tautomerism occurs. If terminal alkyne, ketone is favoured. Alkynes form π compounds with heavy metal ions (Hg^{2+} , Pb^{2+} , Ba^{2+}).

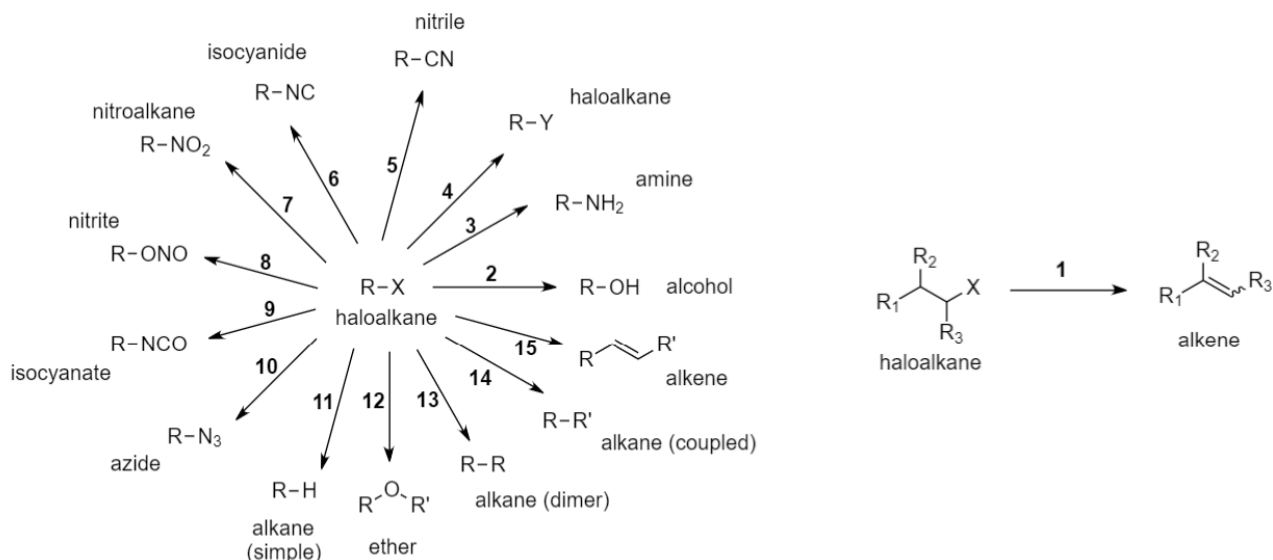
7: Nitrile addition. Reagents: $\text{Ba}(\text{CN})_2$. Mechanism: nucleophilic addition.

8: Acetal formation. Reagents: 1) $\text{R}'\text{-OH}$ (2 mol eq), HgSO_4 , heat; 2) H_2O ; 3) heat. Mechanism: 1) forms a vinyl ether. 2) hydrolyses to an alcohol and aldehyde. 3) forms the acetal.

9: Ester formation. Reagents: $\text{R}'\text{-COOH}$ (2 mol eq), HgSO_4 . Mechanism: nucleophilic addition. Using 1 mol eq $\text{R}'\text{-COOH}$ gives the vinyl (mono)ester.

10: Aromatisation (Alkyne trimerisation). Reagents: red hot iron tube, 600°C or rhodium(I) catalyst e.g. $\text{RhCl}(\text{PPh}_3)_3$ for intramolecular aromatisation. Mechanism: [2+2+2] cycloaddition. Acetylene \rightarrow benzene; propyne \rightarrow 1,3,5-methylbenzene. Impractical as shown due to excessive side reactions. Can be done using a compound with three alkyne bonds separated by 3-4 C's intramolecularly to form polycyclic compounds.

Haloalkanes:



1: Elimination. Reagents: **conc. NaOH, ethanol, heat**. Mechanism: elimination. Rate: $I > Br > Cl > F$; $3^\circ > 2^\circ > 1^\circ$.

2: Alcohol formation. Reagents: **dil NaOH (aq)**. Mechanism: nucleophilic substitution. Regioselectivity: Markovnikov's rule. Stereoselectivity: *Anti*-addition of H and OH. Rate: $I > Br > Cl > F$.

3: Hoffman ammonolysis. Reagents: **NH₃, ethanol, heat in sealed tube**. Mechanism: nucleophilic substitution. Forms 2°, 3° and 4° ammonium salt if haloalkane is in excess.

4: (a) Finkelstein reaction (Y = I > Br > Cl) or (b) Swartz fluorination (Y = F). Reagents: **(a) HY, acetone or (b) AgF / SbF₃, dimethylsulfoxide (DMSO)**.

5: Nitrile formation. Reagents: **KCN, ethanol, heat**. Mechanism: nucleophilic substitution.

6: Isocyanide formation. Reagents: **AgCN**. Mechanism: nucleophilic substitution (AgCN more covalent than KCN).

7: Nitroalkane formation. Reagents: **AgNO₂**. Mechanism: nucleophilic substitution.

8: Alkyl nitrite formation. Reagents: **NaNO₂**. Mechanism: nucleophilic substitution.

9: Isocyanate formation. Reagents: **NaOCN**. Mechanism: nucleophilic substitution.

10: Azide formation. Reagents: **NaN₃**. Mechanism: nucleophilic substitution.

11: Reduction. Reagents: **LiAlH₄ in dry ether**. Non-selective.

12: Williamson ether synthesis. Reagents: **R'OH + Na (in situ R'ONa)**. Mechanism: nucleophilic substitution.

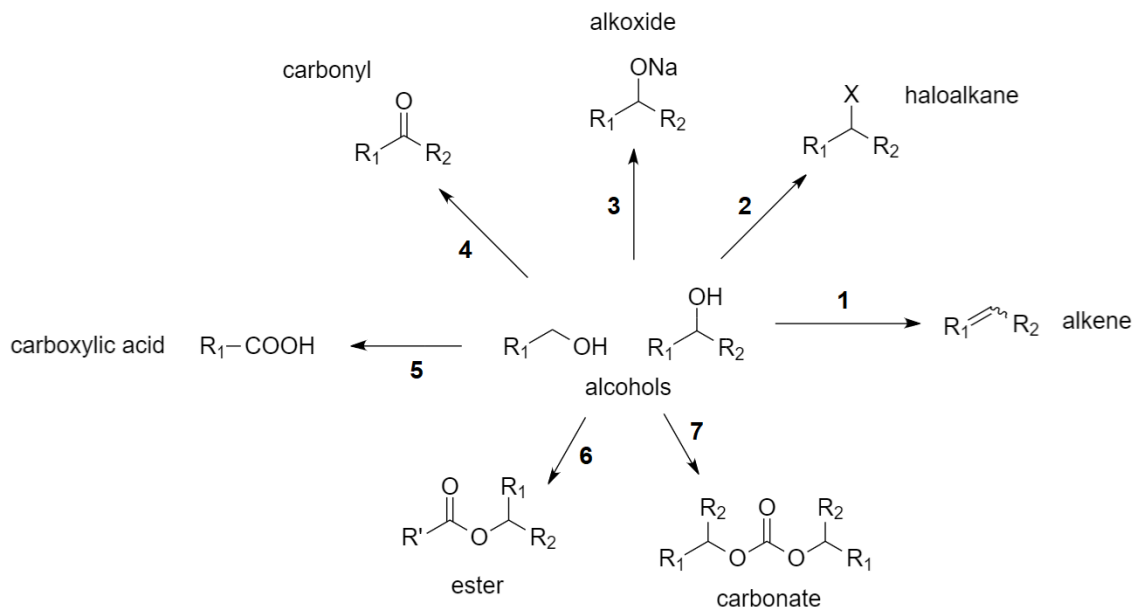
13: Wurtz coupling. Reagents: **Na, ether**.

14. (a) Corey-House synthesis or (b) Grignard reaction or (c) Alkynide coupling or (d) Suzuki reaction or (e) Stille cross-coupling. Reagents: **(a) 1) Li + CuI; 2) R'-X (organic pseudohalide) or (b) R'-MgBr (Grignard reagent) or (c) R''-C≡C-Na (alkynide salt, where R'' = R''-C≡C-) or (d) R'-BY₂, Pd⁰ cat or (e) R'-SnBu₃, Pd cat**. Mechanism: **(a)** 1) forms the complex Gilman reagent Li⁺ [R-Cu-R]⁻. 2) also forms RCu and LiX; **(b)** Releases MgBrX; **(c)** R''-C≡C-Na can be made from terminal alkynes with NaNH₂.

15. Heck reaction. Reagents: **Pd⁰ cat, base**. Releases HX. Mechanism: palladium cross-coupling catalytic cycle.

16.3.2. Reactions of Oxygen-Containing Organic Compounds

Alcohols:



1: Dehydration. Reagents: **conc. H_2SO_4 / $POCl_3$ / Al_2O_3 / P_2O_5 / ThO_2 / MoO_3 / Cu cat, heat.** Mechanism: elimination. Follows Zaitsev's rule. Stereoselectivity: trans alkenes favoured.

2: Halogenation. Reagents: **HX / PX_3 / PX_5 / $SOCl_2$, pyridine.** Mechanism: nucleophilic substitution. Forms a carbanion intermediate.

3: Neutralisation. Reagents: **Na (s).** Mechanism: Lewis acid-base reaction. Releases H_2 (g) as effervescence.

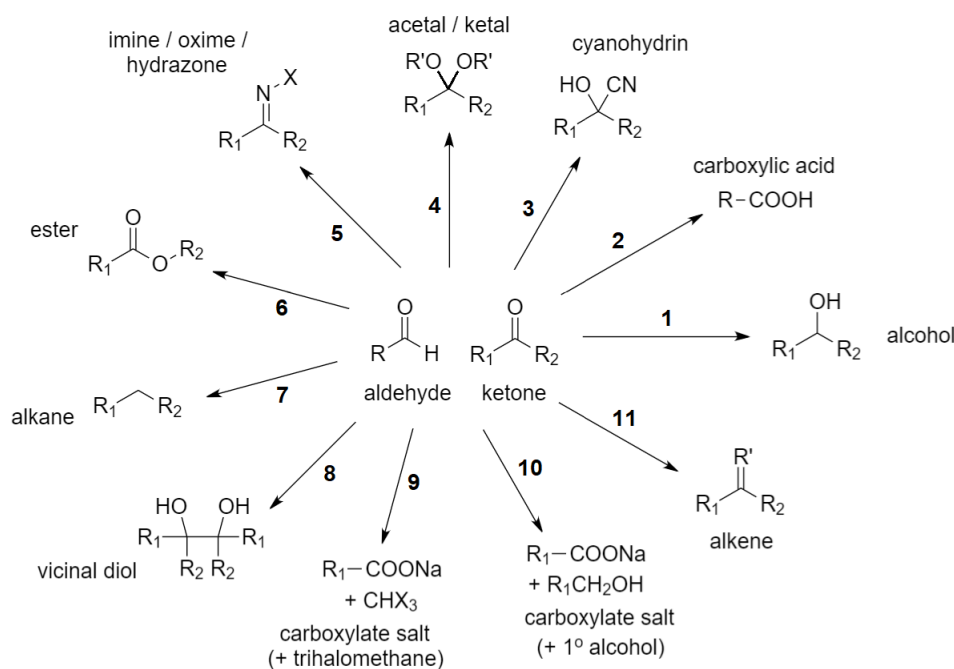
4: (a) Jones oxidation or (b) Oppenhour oxidation or (c) Dess-Martin oxidation or (d) Swern oxidation. Reagents: **(a) CrO_3 or $K_2Cr_2O_7$, H_2SO_4 (Jones reagent or similar chromates) / PCC (pyridinium chlorochromate) / PDC (pyridinium dichromate) or (b) Cu , $300\text{ }^\circ C$ / $(iPrO)_3Al$, heat or (c) DMP (Dess-Martin periodinane) or (d) 1) $(COCl)_2$ (oxalyl chloride), $DMSO$; 2) Et_3N .** Produces: 1° : aldehyde, requires distillation. 2° : ketone. 3° : unreactive without harsh oxidative cleavage. Partial oxidation; avoids complete oxidation of aldehydes.

5: Complete oxidation. Reagents: **excess $K_2Cr_2O_7$ + conc. H_2SO_4 / $KMnO_4$ / CrO_3 + H_2O , heat.** 1° only, requires reflux to oxidised intermediate aldehyde.

6: Fischer esterification. Reagents: **$R'-COOH$, H_3O^+ cat.** Releases H_2O by condensation.

7: Phosgenation. Reagents: **$COCl_2$ (phosgene).** Releases HCl . Forms chloroformate intermediate ($ROCOCl$).

Carbonyls (Aldehydes and Ketones):



1: (a) Non-selective reduction or (b) Grignard reaction or (c) Meerwein-Ponndorf-Verley reduction (MPV reduction). Reagents: **(a)** $NaBH_4$ / $LiAlH_4$ (less selective), **dry ether then NaOH**, or **(b)** R_3-MgBr , or **(c)** $(iPrO)_3Al$, **heat**. Reaction **(a)** can form 1° / 2° alcohols, **(b)** can form 3° alcohols.

2: Oxidation. Reagents: $K_2Cr_2O_7$, **conc. H_2SO_4** or $CrO_3 + H_2O$ (Jones reagent), **heat** or $KMnO_4$, or $AgNO_3$, NH_4OH (Tollen's reagent). Oxidises aldehydes only.

3: Cyanohydrin formation. Reagents: $NaCN$, HCl (aq) (in situ HCN). Mechanism: nucleophilic addition. Alternatively, using $NaHSO_3$ gives a bisulfite ($HO-C-SO_3Na$). Variation: α -aminonitrile formation, using NH_3 and HCN , which can be used to form amino acids by acid hydrolysis (Strecker amino acid synthesis).

4: Acetal / ketal formation. Reagents: $R'-OH$. 1 mol eq \rightarrow hemiacetal/hemiketal; 2 mol eq \rightarrow acetal/ketal; $R' = H$ (water) \rightarrow hydrate (geminal diol). Cyclic acetals form with diols. Mechanism: nucleophilic addition.

5: (a) Imine or (b) oxime or (c) hydrazone formation. Reagents: **(a)** $R-NH_2$ or **(b)** hydroxylamine (NH_2OH) or **(c)** hydrazine (N_2H_4). Mechanism: nucleophilic addition.

6: Baeyer-Villiger oxidation. Reagents: $R'CO_3H$ (peroxy acid: e.g. *meta*-chloroperoxybenzoic acid (m-CPBA)). Forms lactones (cyclic esters if using a cyclic ketone). Regioselectivity: R_2 more sterically bulky than R_1 .

7: (a) Wolff-Kishner reaction or (b) Clemmensen reduction or (c) Mozingo reaction. Reagents: **(a)** N_2H_4 , KOH or **(b)** $Zn(Hg)$ (zinc amalgam), **conc. HCl** or **(c)** 1) dithiol e.g. propane-1,3-thiol; 2) H_2 , Raney Ni. Mechanism: **(a)** hydrazone intermediate; **(b)** carbenoid mechanism; **(c)** 1) forms the cyclic dithioacetal. 2) $Ra-Ni$ irreversibly becomes nickel sulfide.

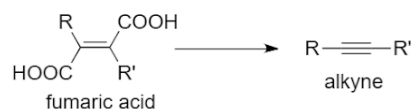
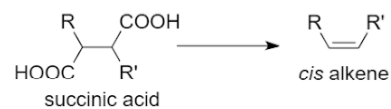
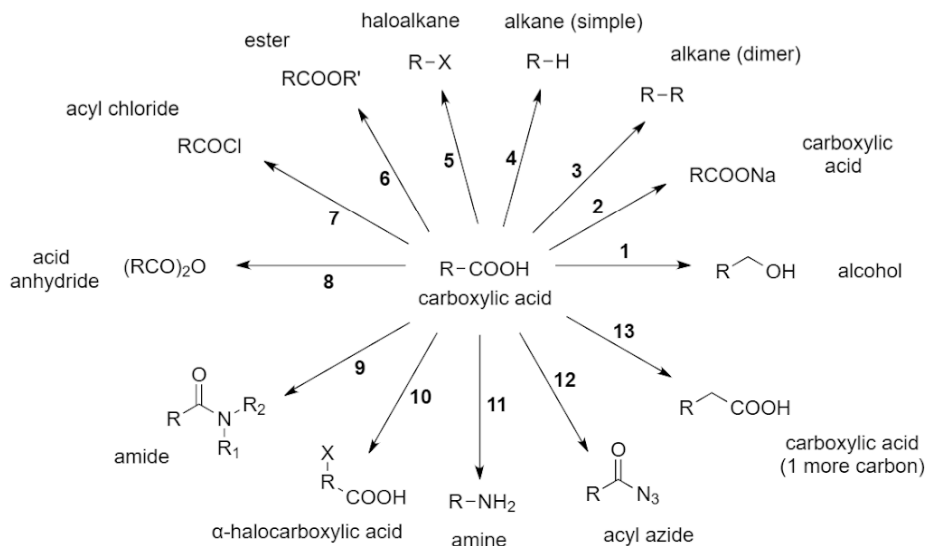
8: Pinacol radical coupling. Reagents: Mg (s) then H_3O^+ . Stereoselectivity: the two $-OH$ groups end up *syn* to each other. Mechanism: the intermediate complex has $C^*-O-Mg-O-C^*$.

9: Haloform reaction. Reagents: X_2 , $NaOH$ (in situ $NaXO$) ($X = Cl, Br, I$). Methyl ketones only. Releases CHX_3 .

10: Cannizzaro reaction. Reagents: $NaOH$. Non-enolisable aldehydes only. Mechanism: nucleophilic acyl substitution.

11: (a) Wittig reaction or (b) McMurry reaction ($R' = R_1-C-R_2$) or (c) Peterson olefination ($R' = R_3-C-H$). Reagents: **(a)** $Ph_3P + R'-Br$ (haloalkane) then base (Wittig reagent) or **(b)** $TiCl_4$, THF , $LiAlH_4$ (Ti^{2+} intermediate) or **(c)** 1) $Me_3Si-C(X)-R_3 + Mg/Li$; 2) acid or base. In **(a)**, R' must be 1° or 2° . In **(b)**, R' is identical to R_1-C-R_2 (the alkene is coupled). Stereoselectivity: **(a)** If $R' =$ alkyl, alkene is *cis*. If $R' =$ ester/ketone, alkene is *trans*. Mechanism: The Wittig reagent is an ylide (1,2-dipolar zwitterion), whose carbanion attacks the carbonyl; **(b)** uncontrolled (sterics). **(b)** can also work intramolecularly with amides or esters to form heterocycles; **(c)** In Step 2, acid yields *cis*, while base yields *trans*.

Carboxylic Acids:



1: Reduction. Reagents: NaBH_4 then NaOH or LiAlH_4 in dry ether (less selective).

2: Neutralisation. Reagents: NaOH / KOH .

3: Kolbe electrolysis. Reagents: 1) NaOH (aq); 2) electrolysis, collect at anode. Mechanism: decarboxylates to release CO_2 then fuses the α C in two alkyl radicals together. Forms the higher alkane at the anode. Variation:

3': Biradical Kolbe electrolysis of dicarboxylic acids. Reagents: 1) NaOH , 2 eq., 2) electrolysis with (a) for cis: Ni or (b) for trans: Na (s) + NH_3 (l) (in situ NaNH_2 ; Birch conditions). If the dicarboxylic acid has $\text{C}2=\text{C}3$ (e.g. fumaric acid, $\text{HOOC}-\text{C}=\text{C}-\text{COOH}$) then the alkyne is formed.

4: Decarboxylation. Reagents: soda lime (CaO , NaOH), heat. Releases CO_2 .

5: (a) Hunsdiecker reaction or (b) Kochi reaction. Reagents: (a) 1) AgF ; 2) X_2 , CCl_4 or (b) $\text{Pb}(\text{OAc})_4$, LiX .

6: Fischer esterification. Reagents: $\text{R}'\text{OH}$, H_3O^+ cat. Using $\text{R}'\text{-SH}$ (thiol) instead gives a thioester (RCOSR').

7: Acyl chloride formation. Reagents: SOCl_2 (thionyl chloride) or PCl_3 or PCl_5 , pyridine solvent.

8: Acid anhydride formation. Reagents: R-COCl or P_2O_5 . Mechanism: S_N then elimination.

9: Amide formation. Reagents: $\text{R}_1\text{-NH-R}_2$, heat or dicyclohexylcarbodiimide (DCC). Mechanism: S_N then E.

10: Hell-Volhard-Zelinsky reaction (HVZ reaction). Reagents: 1) $\text{P} + \text{X}_2$; 2) H_2O . Can react with ammonia to form amino acids.

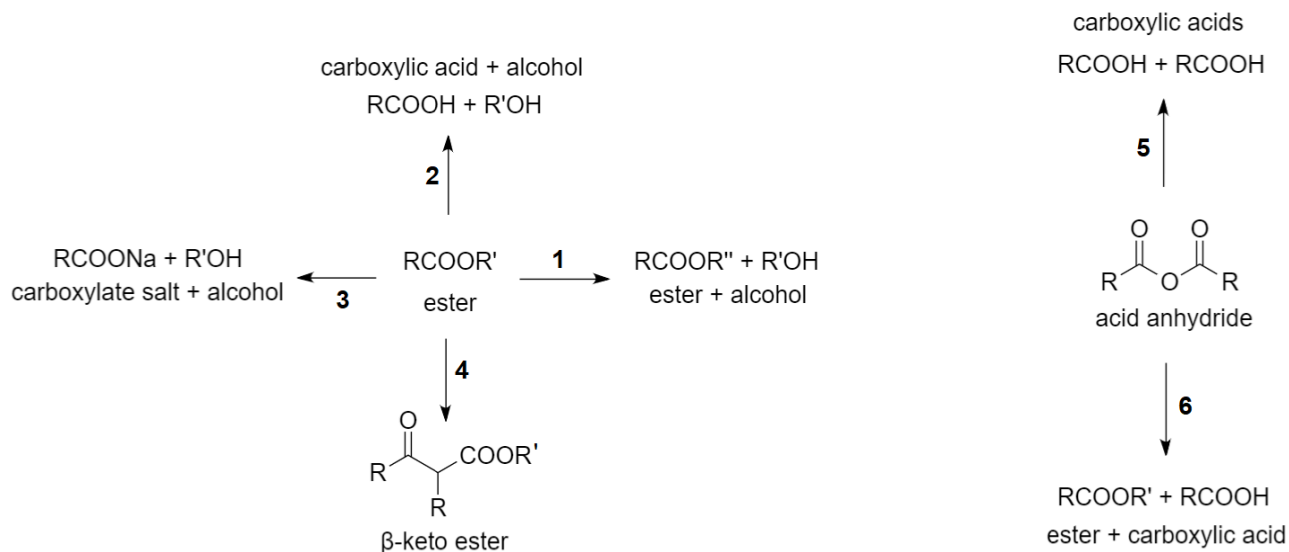
11: Schmidt reaction. Reagents: hydrazoic acid (HN_3), cold conc H_2SO_4 . Releases CO_2 and N_2 .

Mechanism: forms an isocyanate intermediate.

12: Acyl azide formation. Reagents: 1) N_2H_4 (hydrazine); 2) HNO_2 (nitrous acid) or diphenylphosphoryl azide (DPPA). Mechanism: 1) forms the acyl hydrazine (R-CO-NH-NH_2). 2) forms the acyl azide. DPPA forms the acyl azide directly.

13: Arndt-Eistert reaction (homologation). Reagents: 1) SOCl_2 ; 2) CH_2N_2 (diazomethane), ether; 3) Ag^+ cat, H_2O , dioxane. Mechanism: Wolff rearrangement of the intermediate diazoketone via the ketene. Using $\text{R}'\text{OH}$ or $\text{R}'\text{NH}_2$ in Step 3 results in the ester $\text{RCH}_2\text{COOR}'$ or amide $\text{RCH}_2\text{CONHR}'$ respectively. Can be used to convert α -amino acids to β -amino acids with protection.

Esters and Acid Anhydrides:



1: Transesterification. Reagents: $\text{R}''\text{-OH}$.

2: Acid hydrolysis. Reagents: H_2O , HCl (aq) cat. Equilibrium.

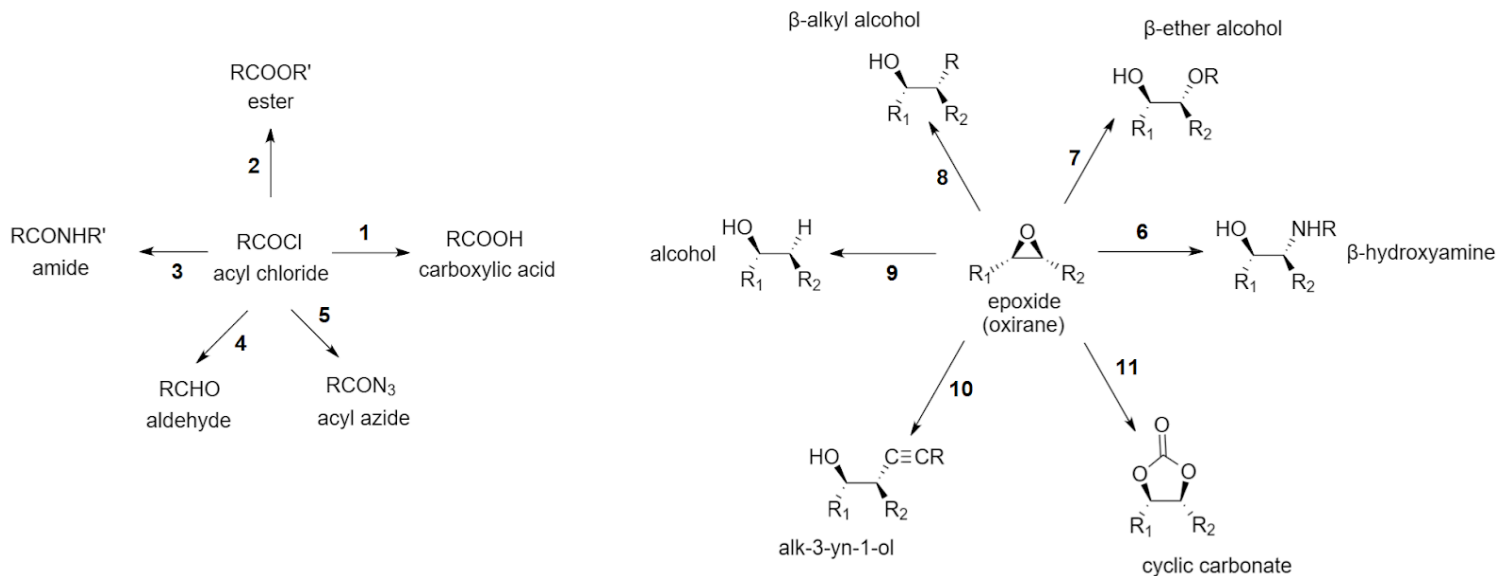
3: Base hydrolysis / saponification. Reagents: H_2O , NaOH (aq).

4: (a) Claisen condensation or (b) Dieckmann rearrangement (intramolecular). Reagents: **1) $\text{R}'\text{ONa}$, ethanol;** **2) H_3O^+ .** Mechanism: enolate chemistry. Can use two different esters for cross-Claisen condensation. The $\text{R}'\text{ONa}$ alkoxide base must match the R' group in the ester to avoid product mixtures due to trans esterification.

5: Hydrolysis. Reagents: H_2O , **pyridine solvent.** Using H_2O_2 instead forms a peroxy acid $\text{RCO}_3\text{H} + \text{RCO}_2\text{H}$.

6: Esterification. Reagents: $\text{R}'\text{OH}$.

Acyl Chlorides (Acid Chlorides) and Epoxides



1: Hydration. Reagents: H_2O . Releases HCl as effervescence.

2: Esterification. Reagents: $\text{R}'\text{OH}$, pyridine solvent. The pyridine neutralises the acid.

3: Schotten-Baumann reaction (amidation). Reagents: $\text{R}'\text{NH}_2$, H_2O , Et_2O .

4: Rosenmund reduction. Reagents: H_2 (g), Pd-BaSO₄ cat, quinoline (Rosenmund catalyst). Mechanism: poisoned heterogeneous catalysis. Selective for acyl chlorides.

5: Acyl azide formation. Reagents: NaN_3 or Me_3SiN_3 .

6: Amine addition by (a) Acid or (b) base catalysed epoxide ring opening. Reagents: RNH_2 (amine), CH_3NO_2 solvent, (a) acid or (b) base. Stereoselectivity: Anti-addition of -OH and -NHR. Regioselectivity: (a) steric hindrance $\text{R}_2 > \text{R}_1$; (b) steric hindrance $\text{R}_1 > \text{R}_2$.

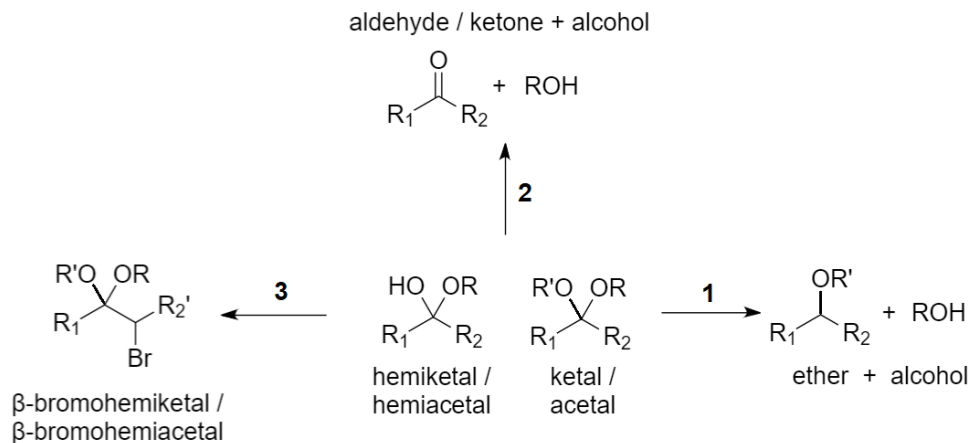
7: Alcohol addition by base catalysed epoxide ring opening. Reagents: ROH , base. Anti addition of -OH and -OR.

8: Grignard reaction. Reagents: R-MgBr , H_3O^+ . Anti addition of -OH and -R.

9: Reduction. Reagents: LiAlH_4 , dry ether, H_3O^+ . Anti addition of -OH and -H.

10: Alkylidene addition. Reagents: $\text{R}'\text{-C}\equiv\text{C}^- \text{Li}^+$ (alkylidyne), H_3O^+ . Mechanism: nucleophilic addition. Anti addition of -OH and -C-C \equiv C-R.

11: Cyclic carbonate formation. Reagents: CO_2 , Zn / Al / ammonium-based catalyst. Organic carbonates are useful for carbon storage (green chemistry) and as electrolytes in LiPo batteries.

Acetals and Ketals:

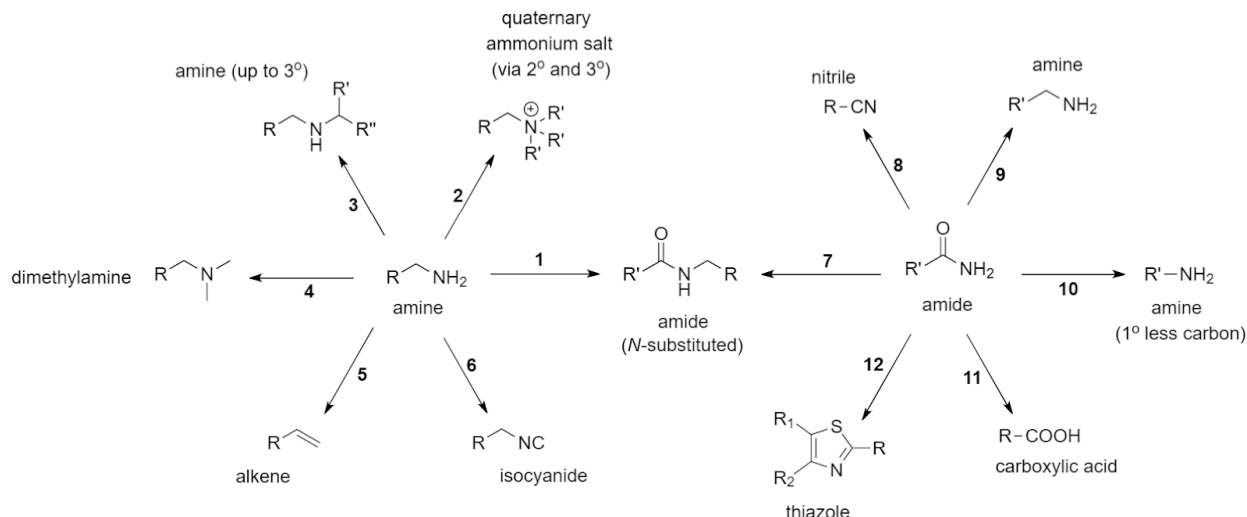
1: Reduction. Reagents: **diisobutylaluminium hydride (DIBAL-H)**. Note that LiAlH_4 does **not** reduce acetals/ketals, allowing e.g. ethane-1,2-diol to be used to protect aldehydes/ketones during reduction (forms a cyclic acetal).

2: Acid hydrolysis. Reagents: H_3O^+ . Used for de-protecting.

3: β -Halogenation ($\text{R}_2 = \text{R}_2' - \text{CH}_2 -$). Reagents: $\text{Br}_2 (\text{l})$. Mechanism: protons adjacent to acetal are slightly acidic.

16.3.3. Reactions of Nitrogen-Containing Organic Compounds

Amines and Amides:



1: Amidation. Reagents: **(a) R'COOH, heat** or **(b) R'COCl, pyridine** or **(c) (R'CO)₂O, pyridine**.

Mechanism: nucleophilic addition-elimination.

2: Hoffman ammonolysis / alkylation. Reagents: **excess R'-X**, via the 2° and 3° amines.

3: Reductive amination. Reagents: **R'-CO-R'' (carbonyl), NaBH₃CN**. Mechanism: imine/iminium intermediate.

4: Eschweiler-Clarke reaction. Reagents: **CH₂O, HCOOH**. Mechanism: imine/iminium intermediate. Releases CO₂.

5: Hoffman elimination. Reagents: **1) excess MeI; 2) Ag₂O, H₂O, heat, vacuum**. Mechanism: Step 1 forms the quaternary trimethylammonium salt, Step 2 is thermal decomposition of the hydroxide salt. Regioselectivity: anti-Zaitsev (forms the **least** substituted alkene).

6: Carbylamine reaction. Reagents: **CHCl₃, KOH (ethanolic chloroform)**. Mechanism: dichlorocarbene (:CCl₂) forms as an intermediate.

7: Alkylation. Reagents: **R'-X**.

8: Dehydration. Reagents: **SOCl₂ or POCl₃ or P₂O₅, pyridine, distil**. Requires primary amide. Releases SO₂ + HCl.

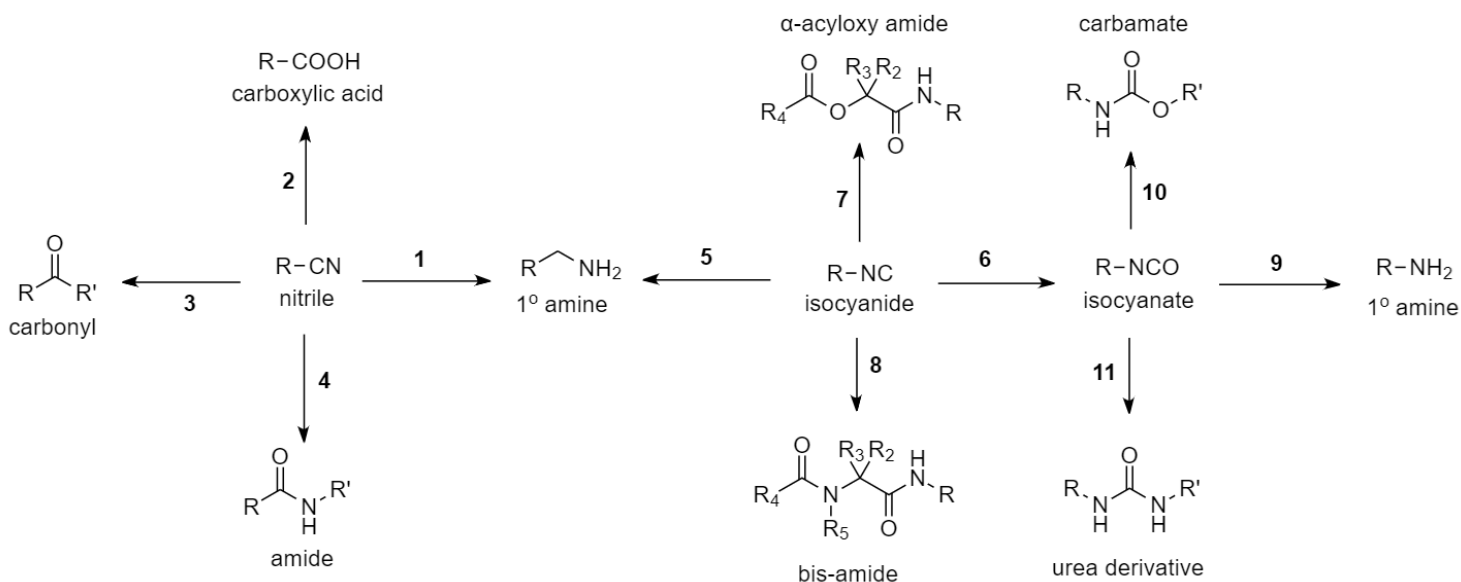
9: Reduction. Reagents: **LiAlH₄, dry ether**. Can be used to form 3° amines from *N,N*-disubstituted amides.

10: Hoffman degradation / rearrangement / bromoamide synthesis. Reagents: **1) Br₂ + NaOH (in situ NaBrO); 2) H₂O**. Mechanism: 1) generates NaBrO, which forms the intermediate isocyanate. 2) adds water to give a carbamic acid which loses CO₂ to give the amine.

11: Acid hydrolysis. Reagents: **H₂O, H₂SO₄**. Releases NH₃ (or amine if substituted).

12: Hantzsch thiazole synthesis. Reagents: **1) anisole (CH₃-O-C₆H₅; methoxybenzene) + P₂S₅ (Lawesson's reagent); 2) α-haloketone (R₁-CHX-CO-R₂), heat**. Mechanism: Lawesson's reagent converts C=O to C=S (thioamide). 2) forms the ring, releasing HX and H₂O. For other heterocycles, see Section 16.3.9.

Nitriles, Isocyanides and Isocyanates:



1: Reduction. Reagents: LiAlH_4 then H_2O . Mechanism: LiAlH_4 forms the dianion $[\text{R}-\text{C}-\text{N}]^{2-}$. Water forms the primary amine. Also can be used with nitroalkanes i.e. $\text{R}-\text{CH}_2\text{NO}_2 \rightarrow \text{R}-\text{CH}_2\text{NH}_2$.

2: Oxidation. Reagents: H_2SO_4 (aq), heat. Mechanism: forms an amide intermediate.

3: Grignard reaction. Reagents: $\text{R}'\text{MgX}$, H_3O^+ . Also works with HCN to form aldehydes.

4: Ritter reaction. Reagents: $\text{R}'\text{OH}$ (alcohol), H_3O^+ . Works best for 3° alcohols. Mechanism: alcohol is eliminated to give the carbocation, which is attacked by the nitrile. Any species which generates a carbocation can be used e.g. alkenes, epoxides. Stereoselectivity: *syn* addition. Extensions can be used in enantioselective organocatalysis.

5: Reduction. Reagents: LiAlH_4 then H_2O . Mechanism: LiAlH_4 forms the dianion $[\text{R}-\text{C}-\text{N}]^{2-}$. Water forms the primary amine.

6: Oxidation. Reagents: HgCl_2 , H_2O . Releases Hg (l) and HCl. Forms the isocyanate.

7: Passerini reaction. Reagents: R_4-COOH (carboxylic acid), $\text{R}_2-\text{C}(\text{O})-\text{R}_3$ (ketone).

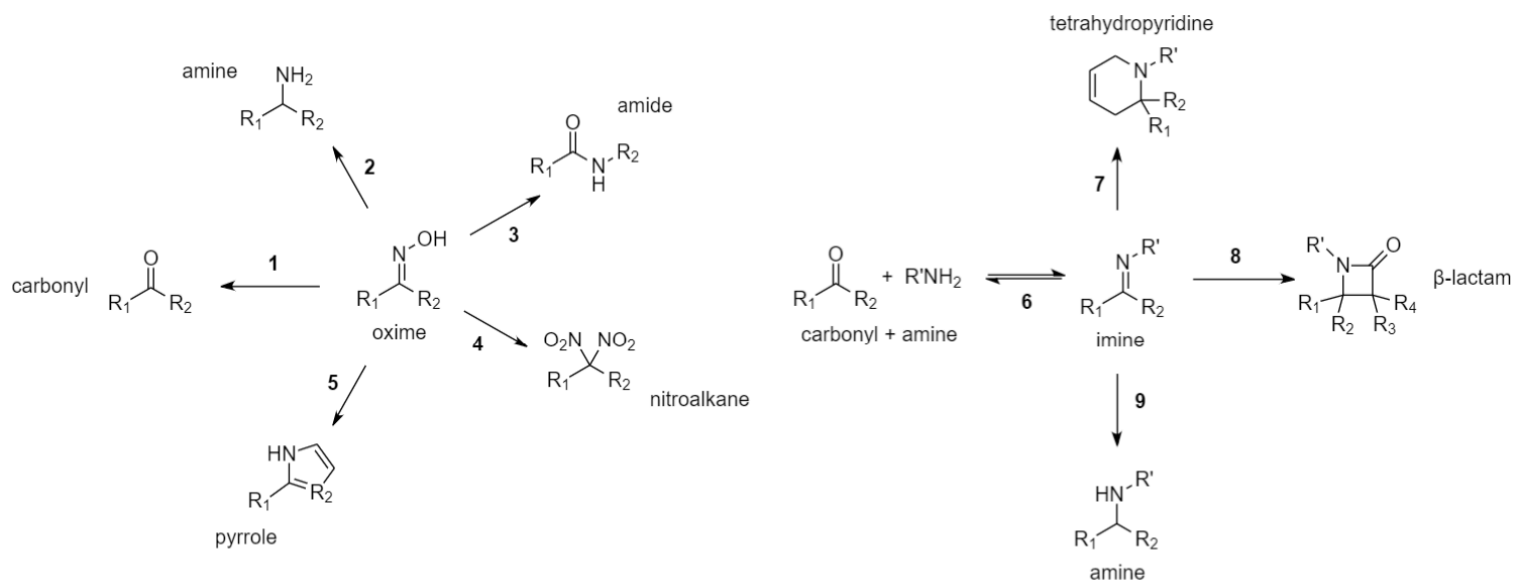
8: Ugi reaction. Reagents: R_4-COOH (carboxylic acid), $\text{R}_2-\text{C}(\text{O})-\text{R}_3$ (ketone), R_5-NH_2 (amine).

9: Hydration. Reagents: H_2O . Mechanism: nucleophilic addition.

10: Alcoholysis. Reagents: $\text{R}'\text{OH}$. Mechanism: nucleophilic addition.

11: Ammonolysis. Reagents: $\text{R}'\text{NH}_2$. Mechanism: nucleophilic addition. Forms a urea derivative.

Oximes, Imines and Hydrazones:



1: Hydrolysis. Reagents: H_2O . Occurs naturally (equilibrium).

2: Reduction. Reagents: NaBH_4 or LiAlH_4 or H_2 / Ni .

3: Beckmann rearrangement. Reagents: H_2SO_4 or SOCl_2 or PCl_5 (aq) cat.
Cyclic oximes give lactams with +1 ring number. Orientation depends on oxime E/Z.

4: Ponzio reaction. Reagents: N_2O_4 .

5: Cyclisation. Reagents: C_2H_2 (acetylene).

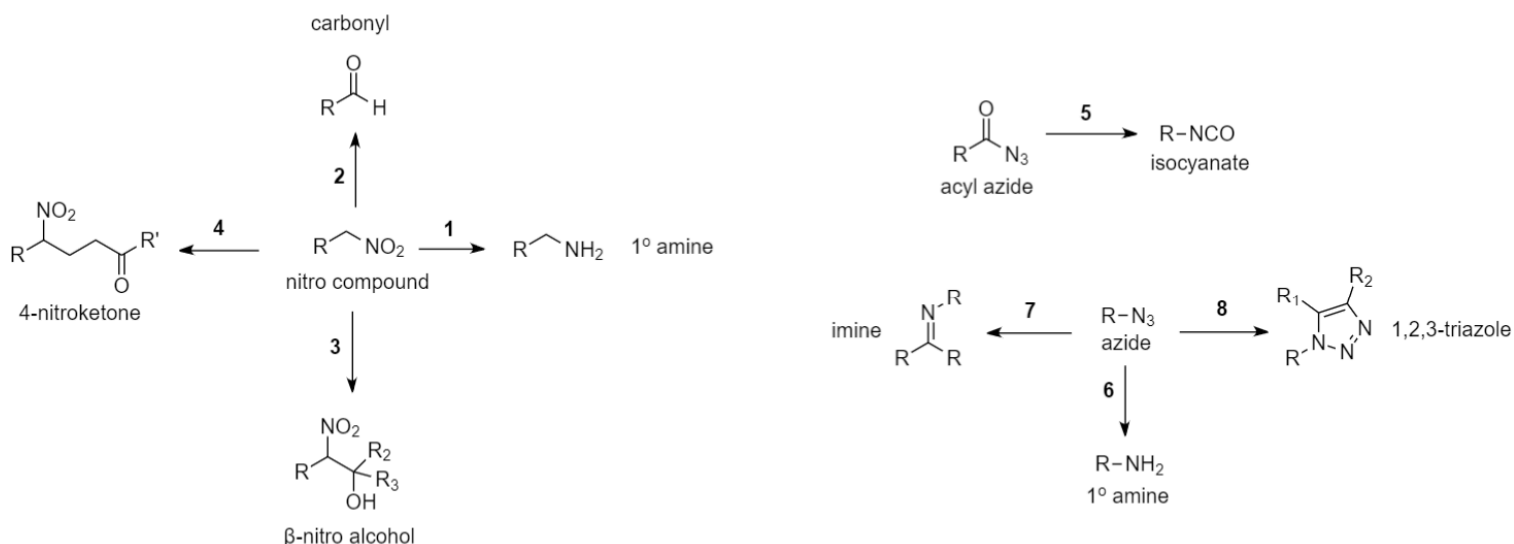
6: Hydrolysis. Reagents: H_2O . Occurs naturally (equilibrium).

7: Hetero Diels-Alder reaction. Reagents: buta-1,3-diene. Mechanism: [4+2] cycloaddition.

8: Staudinger synthesis of β -lactams. Reagents: $\text{R}_3\text{-C(=C=O)-R}_4$ (ketene). Mechanism: [2+2] cycloaddition.

9: Reductive amination. Reagents: H_2 (high pressure) / Pd.

Nitroalkanes, Azides and Acyl Azides:

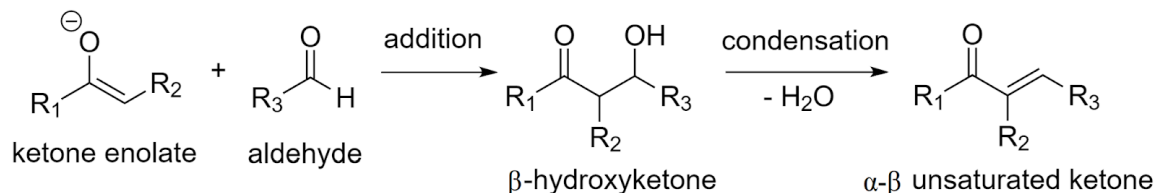


- 1: Reduction.** Reagents: H_2 / Pd or Sn / HCl or LiAlH_4 (non-selective, forms azo compound with nitrobenzene).
- 2: Nef reaction.** Reagents: 1) OH^- ; 2) H_3O^+ . Releases N_2O . Mechanism: Step 1 forms a nitronate salt intermediate.
- 3: Henry reaction (nitroaldol reaction).** Reagents: OH^- . This product can be eliminated to a nitroalkene, reduced to a β -amino alcohol or oxidised to an α -nitro carbonyl.
- 4: Michael addition (umpolung).** Reagents: $\text{CH}_2=\text{CH}-\text{C}(\text{O})\text{R}'$ (α - β unsaturated ketone), base then acid. The nitro compound acts as the Michael donor, with a carbanion at the α position. If R is an acidic and base is in excess then the product can undergo intramolecular aldol reaction to a cyclopentenone (like a Robinson annulation).
- 5: Curtius rearrangement.** Reagents: heat (thermal decomposition).
- 6: Staudinger reaction.** Reagents: 1) PPh_3 ; 2) H_2O . Mechanism: Step 1 forms the ylide $\text{Ph}_3\text{P}=\text{NR}$.
- 7: Aza-Wittig reaction.** Reagents: 1) PPh_3 ; 2) R_2CO (ketone).
- 8: Huisgen cycloaddition.** Reagents: $\text{R}_1-\text{C}\equiv\text{C}-\text{R}_2$ (alkyne), heat or Cu or Ru cat. A good click reaction.

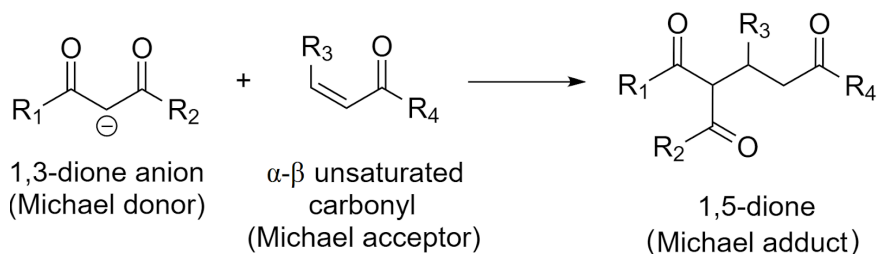
16.3.4. Reactions Involving Enolate Chemistry

Some reactions of carbonyls proceed via enol (carbonyl + acid) or enolate (carbonyl + base) chemistry. Common bases are NaOH, KOH, Ba(OH)₂.

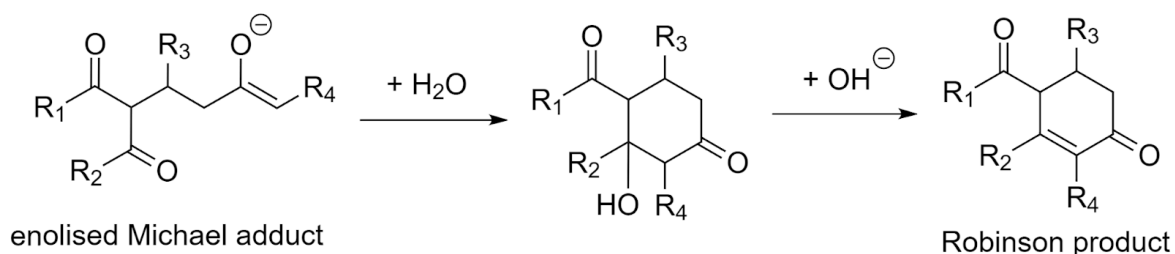
Aldol Reaction: using enolate form (if enol form, aldehyde is protonated; same products):
Cross-aldol products may form with multiple reacting carbonyls, such as in:



Michael Addition: the dione anion can be formed with 1,3-dione + base:

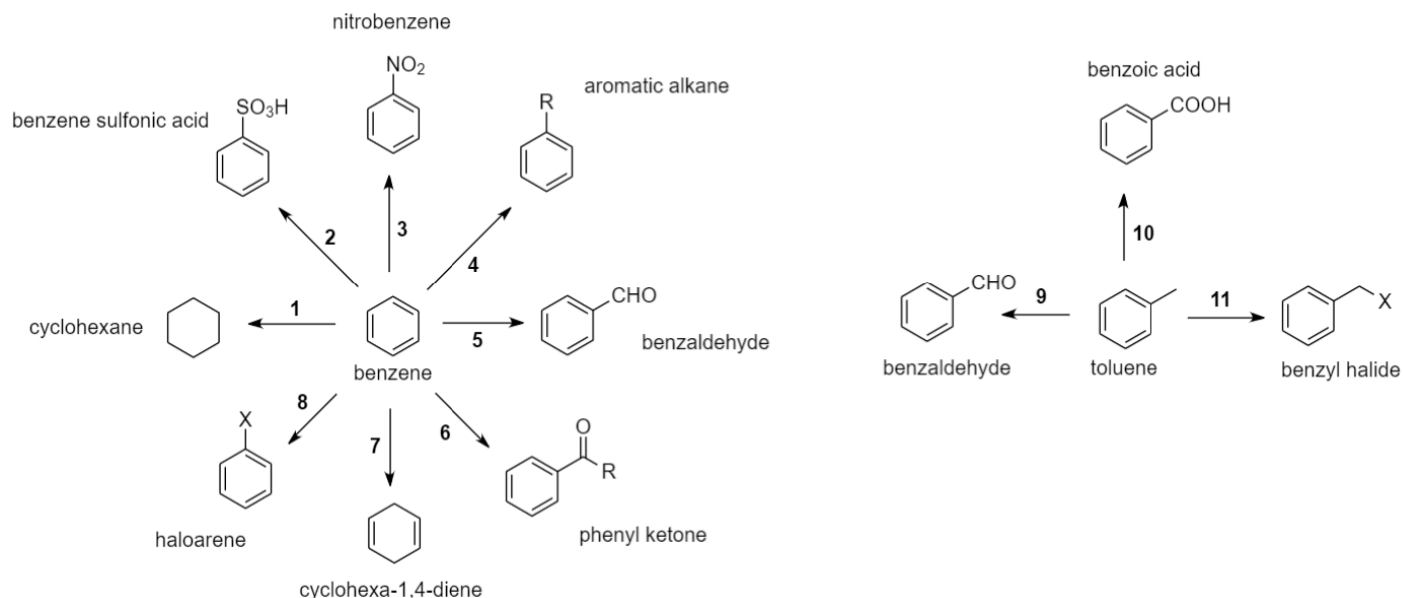


Robinson Annulation: a Michael addition followed by an intramolecular aldol reaction, possible if excess base is present:



16.3.5. Reactions of Aromatic Compounds

Benzene and Toluene:



1: Hydrogenation. Reagents: H_2 (3 mol eq.), Ni cat, $300\text{ }^\circ\text{C}$, 30 atm. Requires harsher conditions than regular hydrogenation since benzene is resonance stabilised.

2: Sulfonation. Reagents: SO_3 , conc H_2SO_4 , reflux.

3: Nitration. Reagents: conc HNO_3 and H_2SO_4 (aq), $30\text{ }^\circ\text{C}$. At higher temps, 1,3- and 1,3,5- compounds form.

4: Friedel-Crafts alkylation. Reagents: R-Cl (haloalkane) + AlCl_3 cat.

5: Gatterman-Koch reaction. Reagents: $(\text{CO or HCN}) + \text{HCl}$.

6: Friedel-Crafts acylation. Reagents: R-COCl (acyl chloride) + AlCl_3 cat.

7: Birch reduction. Reagents: Na, NH_3 , EtOH solvent. Mechanism involves radical anion formation due to presence of the electride salt $[\text{Na}(\text{NH}_3)_x]^+ \text{e}^-$. Regioselectivity: protonation occurs at the *ortho* and *para* positions, with ERGs favouring the *ortho* position and EWGs favouring the *para* position.

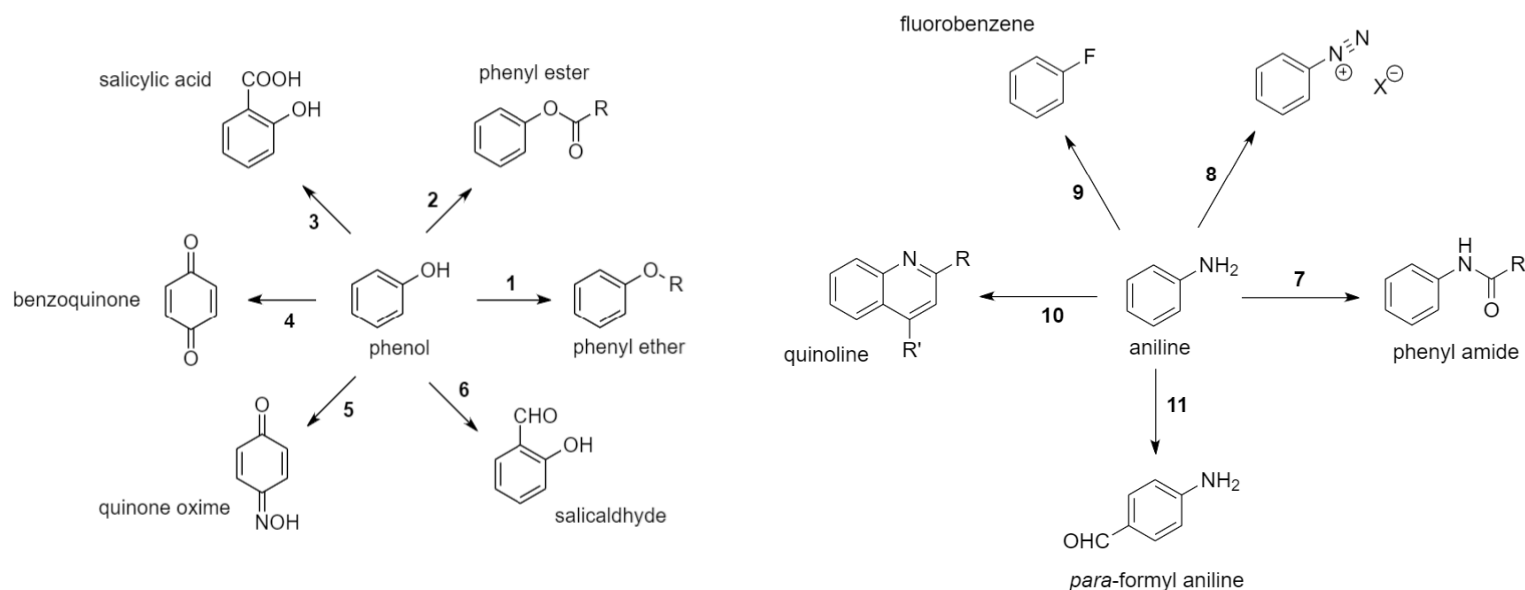
8: Halogenation. Reagents: X_2 , FeX_3 (X = Cl / Br) or I_2 , CuBr_2 (X = I). Fluorination (X = F) is uncommon.

9: Étard reaction. Reagents: CrO_2Cl_2 (chromyl chloride).

10: Oxidation. Reagents: KMnO_4 . Requires at least one C-H bond on the sp^3 carbon. Will break off any further C-C bonds to give the benzoic acid.

11: Aliphatic halogenation. Reagents: X_2 , UV. Mechanism: free-radical substitution.

Phenol and Aniline:



1: Williamson synthesis. Reagents: **1) Na or OH⁻; 2) RX**. For anisole (PhOMe), use **2) DMS (dimethyl sulfate)**, which releases phenyl hydrogensulfate.

2: Esterification. Reagents: **RCOOH** or **RCOCl** or **(RCO)₂O**, **pyridine** or **NaOH**.

3: Kolbe reaction (ortho carboxylation). Reagents: **1) Na; 2) CO₂, high pressure; 3) H₃O⁺**.

4: Oxidation. Reagents: **Na₂Cr₂O₇**. The quinones can be reduced back to the hydroquinones with **SnCl₂**.

5: Nitrosation. Reagents: **HNO₂, 0 °C**. Mechanism: the oxime tautomerises with the nitroso phenol (HO-Ar-N=O) via proton transfer.

6: Reimer-Tiemann reaction. Reagents: **CHCl₃, NaOH**. Mechanism: carbylamine mechanism, forms dichlorocarbene (:CCl₂) as an intermediate.

7: Amidation. Reagents: **RCOOH** or **RCOCl** or **(RCO)₂O**, **NaOH** or **pyridine**.

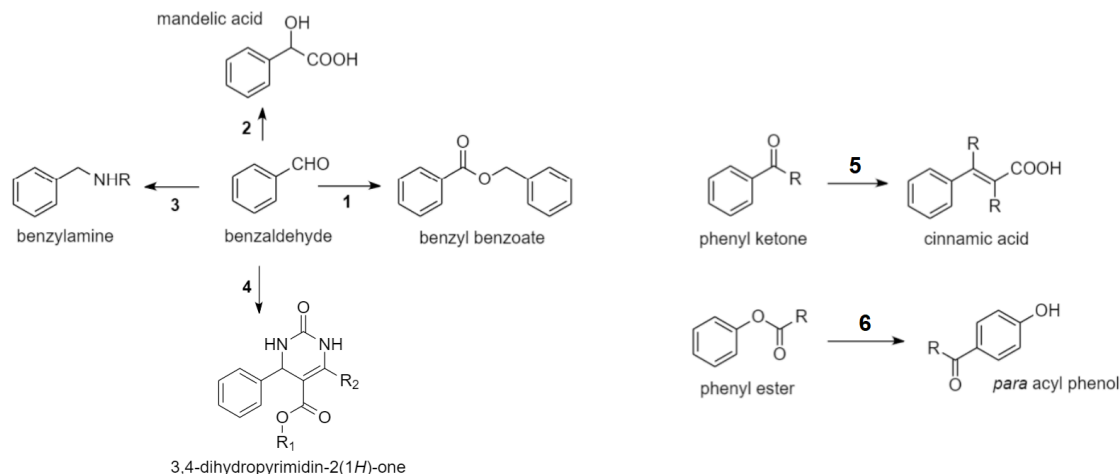
8: Diazotisation. Reagents: **NaNO₂, H₃O⁺, 0 °C**. The resonance structure (Ph-N=N⁺) may bond to neighbouring rings by **S_NAr**.

9: Balz-Schiemann reaction. Reagents: **1) NaNO₂, H₃O⁺; 2) HBF₄ or HPF₆ or HSbF₆, heat**. Mechanism: 1) forms the diazonium salt. 2) displaces the counter anion which thermally decomposes.

10: Combes quinoline synthesis. Reagents: **R-CO-CH₂-CO-R' (1,3-diketone) then H₃O⁺**. Mechanism: First, N: attacks a carbonyl, which rearranges by proton transfers. The C=O⁺H carbocation is attacked by the benzene ring.

11: Vilsmeier-Haack reaction. Reagents: **1) DMF, POCl₂; 2) H₂O**. Can also start with various other electron-rich species e.g. alkenes (styrene → cinnamaldehyde) or α -methylene groups.

Benzaldehyde, Phenyl Ketones and Phenyl Esters:



1: Cannizzaro reaction. Reagents: **conc NaOH (aq)**. Mechanism: disproportionation to benzyl alcohol and benzoic acid which then react in esterification.

2: Mandelic acid synthesis. Reagents: **1) HCN; 2) H₂O (2 mol eq)**. Mechanism: Step 1 forms the hydroxynitrile which is hydrolysed in Step 2 to the carboxylic acid. Forms a α -hydroxycarboxylic acid.

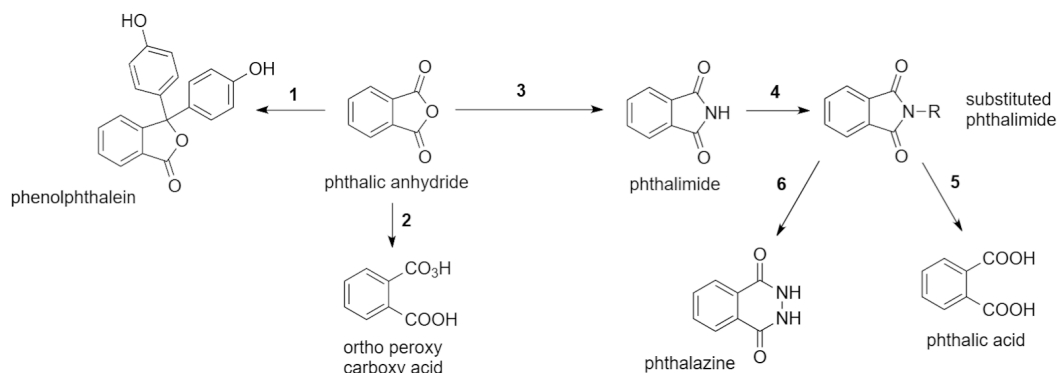
3: Reductive amination. Reagents: **RNH₂, H₂ / Ni cat.**

4: Biginelli reaction. Reagents: **R₂-C(O)-CH₂-COOR₁ (β -keto ester), CO(NH₂)₂ (urea)**. Forms a dihydropyrimidinone. Enantioselectivity at C4 can be induced using a chiral proline catalyst.

5: Perkin condensation. Reagents: **(R'Ac)₂O (acid anhydride), NaOAc**. Mechanism: aldol condensation. Also forms the carboxylic acid R'-CH₂-COOH. If reagent is Ac₂O (acetic anhydride) then R = R' = H.

6: Fries rearrangement. Reagents: **HF or AlCl₃ or BF₃ or TiCl₄ (CS₂)**. Regioselectivity: kinetic product (< 60 °C) \rightarrow *para*; thermodynamic product (> 160 °C) \rightarrow *ortho*.

Phthalic Anhydride and Phthalimide:



1: Phenolphthalein synthesis. Reagents: **phenol (2 mol eq)**;

2: Ring-opening with peroxide. Reagents: **H₂O₂**.

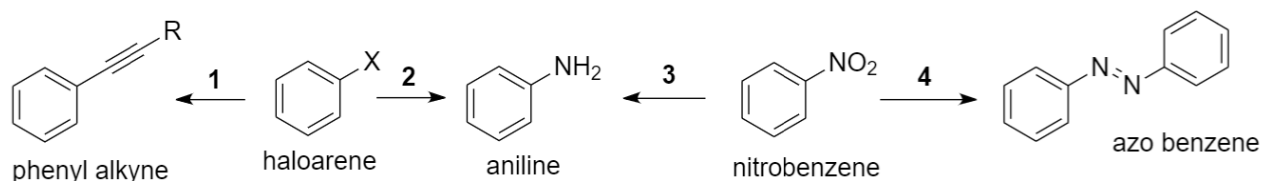
3: Phthalimide synthesis. Reagents: **NH₃ or (NH₃)₂CO₃ or urea**;

4: Gabriel's phthalimide synthesis. Reagents: **KOH, RI**;

5: Hydrolysis of phthalimide. Reagents: **H₂O**.

6: Gabriel's amine synthesis. Reagents: **N₂H₄ (hydrazine)**. Releases the amine R-NH₂.

Haloarenes and Nitrobenzene:



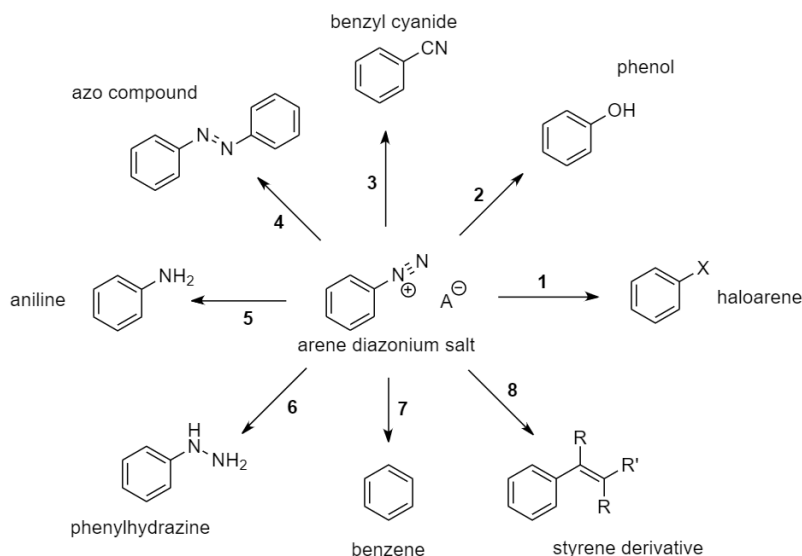
1: Sonogashira reaction. Reagents: $\text{R}-\text{C}\equiv\text{CH}$ (terminal alkyne), $\text{Pd}(\text{PPh}_3)_4$ cat., CuI , Et_3N , THF.
Can also start with a vinylic haloalkene.

2: Aniline formation. Reagents: Na , NH_3 (l), $-30\text{ }^\circ\text{C}$. Benzyne mechanism ($\text{S}_{\text{N}}\text{Ar}$).
Elimination gives an aryne intermediate.

3: Reduction. Reagents: H_2 , Pd-C or Zn / Sn / Fe.

4: Azo coupling. Reagents: Zn, NaOH (MeOH).

Arenediazonium Salts:



1: Sandmeyer reaction to haloarene. Reagents: HBF_4 , heat (X = F), CuCl (X = Cl) or CuBr (X = Br) or KI (X = I).

2: Sandmeyer reaction to phenol. Reagents: H_2O , (H_2SO_4 or Cu_2O), heat

3: Sandmeyer reaction to benzonitrile. Reagents: CuCN .

4: Azo coupling. Reagents: benzene (or other aromatics), NaOH. Azobenzenes can photoisomerise, with higher frequency (UV) light favouring *cis*, lower frequencies (light) favouring *trans*. Substituted benzenes are *para*-directed. Larger aromatics (e.g. 2-naphthol) give colourful dyes.

5: Reverse diazotisation. Reagents: Zn, HCl.

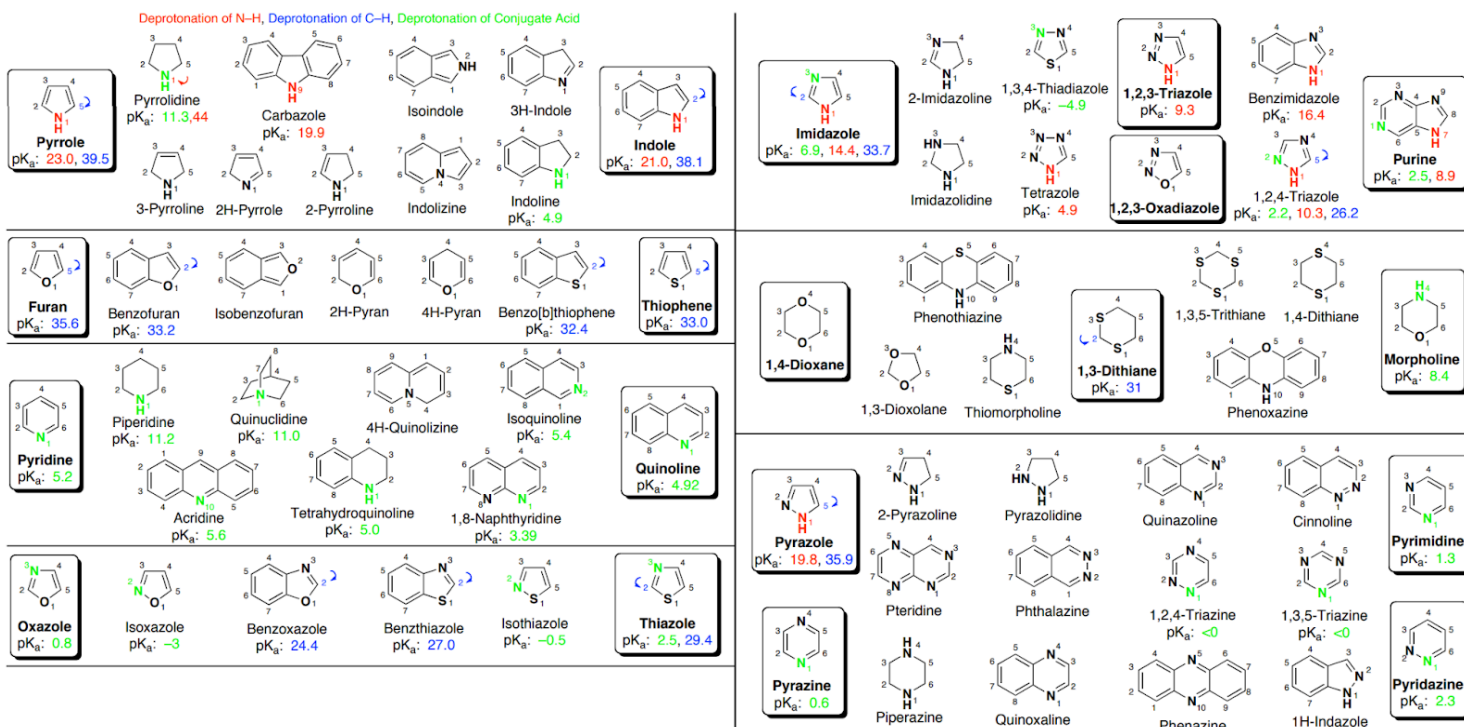
6: Phenylhydrazine formation. Reagents: SnCl_2 , HCl or NaSO_3 , NaOH (aq)

7: Reduction. Reagents: H_3PO_2 .

8: Meerwein arylation. Reagents: $\text{R}-\text{CH}=\text{CRR}'$ (alkene). R' is an EWG.

16.3.6. Heterocyclic Aromatic Compounds

Names, numbering and ionisation of heterocyclic organic compounds:

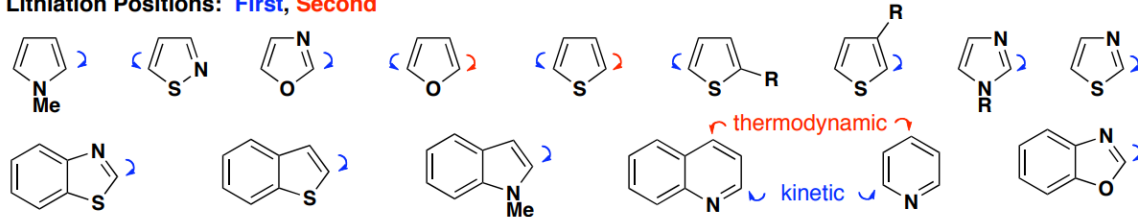


Regioselectivity in heterocyclic systems: sites of lithiation and electrophilic substitution

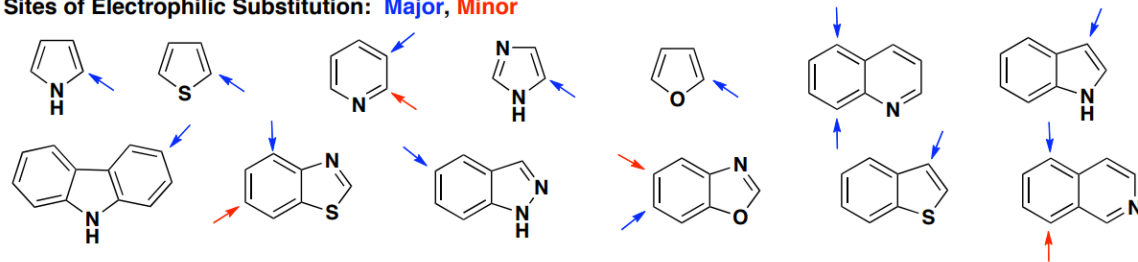
Effects of Substitution on Pyridine Basicity:

		Me	^t Bu	NH ₂	NHAc	OMe	SMe	Cl	Ph	vinyl	CN	NO ₂	CH(OH) ₂
	2-position	6.0	5.8	6.9	4.1	3.3	3.6	0.7	4.5	4.8	-0.3	-2.6	3.8
	3-position	5.7	5.9	6.1	4.5	4.9	4.4	2.8	4.8	4.8	1.4	0.6	3.8
	4-position	6.0	6.0	9.2	5.9	6.6	6.0	3.8	5.5	5.5	1.9	1.6	4.7

Lithiation Positions: First, Second



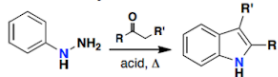
Sites of Electrophilic Substitution: Major, Minor



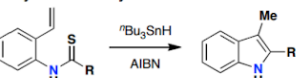
Synthesis of Heterocycles (Indoles, Carbazoles, Pyrroles, Thiophenes, Oxazoles and Isoxazoles):

Synthesis of Indoles and Carbazoles:

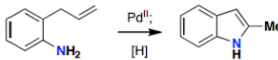
Fischer Indole Synthesis



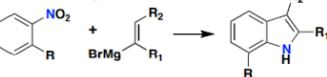
Fukuyama Indole Synthesis



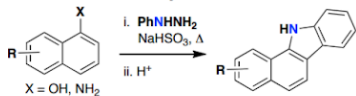
Hegedus Indole Synthesis



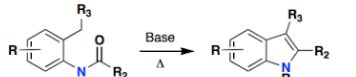
Bartoli Indole Synthesis



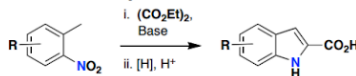
Bucherer Carbazole Synthesis



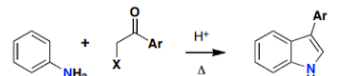
Madelung Indole Synthesis



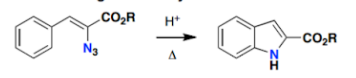
Reisser Indole Synthesis



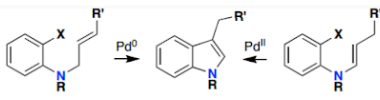
Bischler Indole Synthesis



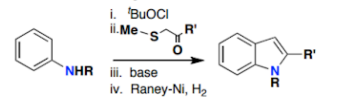
Hemetsberger Indole Synthesis



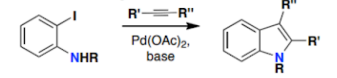
Heck Reaction



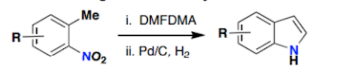
Gassman Indole Synthesis



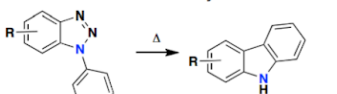
Larock Indole Synthesis



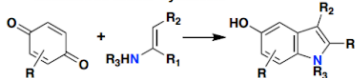
Batcho-Leimgruber Indole Synthesis



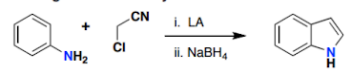
Graebe-Ullmann Carbazole Synthesis



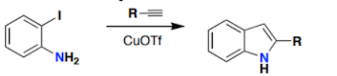
Nenitzescu Indole Synthesis



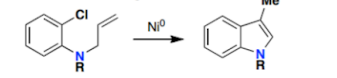
Sugasawa Indole Synthesis



Castro Indole Synthesis

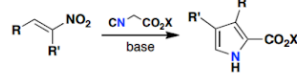


Mori-Ban Indole Synthesis

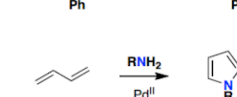
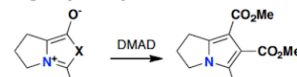


Synthesis of Pyrroles:

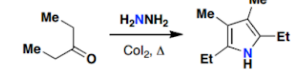
Barton-Zard Pyrrole Synthesis



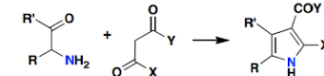
Huisgen Pyrrole Synthesis



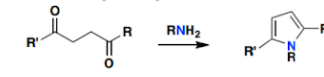
Piloty Pyrrole Synthesis



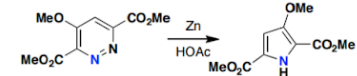
Knorr Pyrrole Synthesis



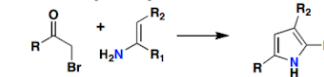
Paal-Knorr Pyrrole Synthesis



Boger Pyrrole Synthesis

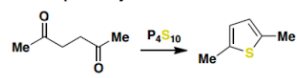


Hantzsch Pyrrole Synthesis

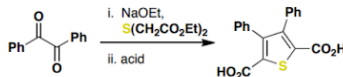


Synthesis of Thiophenes:

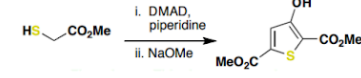
Paal Thiophene Synthesis



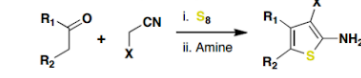
Hinsberg Thiophene Synthesis



Fieselmann Thiophene Synthesis

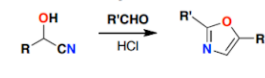


Gewald Aminothiophene Synthesis

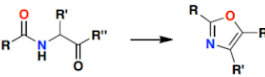


Synthesis of Oxazoles and Isoxazoles:

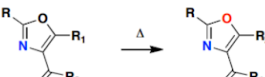
Fisher Oxazole Synthesis



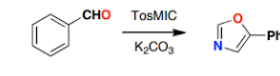
Robinson-Gabriel Oxazole Synthesis



Cornforth Rearrangement



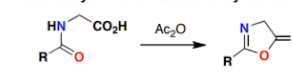
van Leusen Oxazole Synthesis



Claisen Isoxazole Synthesis



Erlenmeyer-Plöchl Azlactone Synthesis

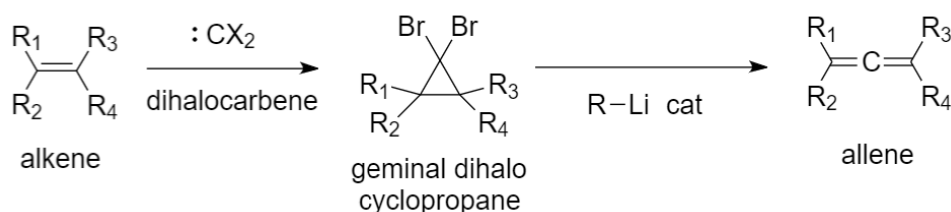


16.3.7. Other Miscellaneous Reactions

This section outlines reactions which cannot be easily classed as converting a single functional group into another. For pericyclic reactions such as the heteroatomic Diels-Alder reaction, the Cope rearrangement, the oxy-Cope rearrangement, the Claisen rearrangement, and more, see Section 16.1.8.

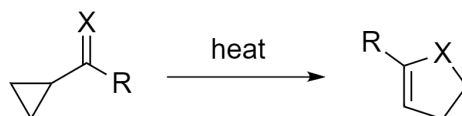
Doering-LaFlamme allene synthesis: forms cumulated dienes (allenes).

The second step is called the Skattebøl rearrangement.

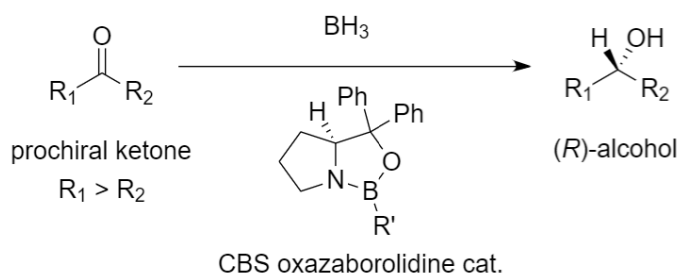


Vinylcyclopropane Rearrangement: forms cyclopentenes or heterocycles.

X = CH₂ / O / NH.

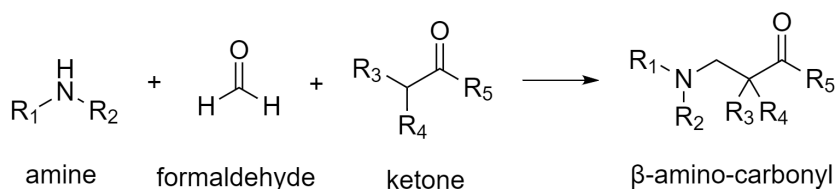


Corey-Itsuno Reduction (CBS Reduction): enantioselective reduction of prochiral ketones.



Mannich Reaction: multi-component addition.

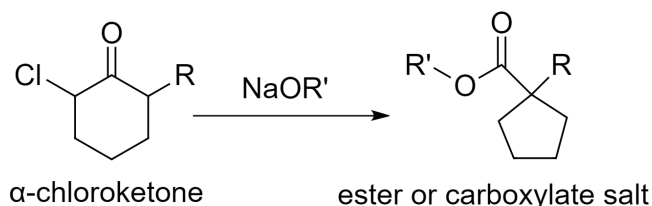
Can use a chiral proline catalyst to carry out an asymmetric transformation.



Favorskii Rearrangement: ring contraction.

Using NaOH instead of NaOR' gives the carboxylate salt instead.

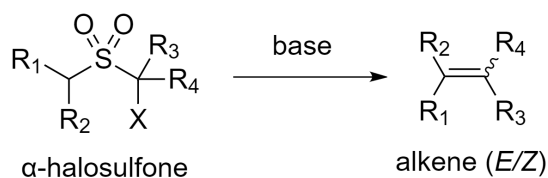
Forms a spiro or bicyclic cyclopropanone intermediate.



Peterson Olefination: alkene formation from α -halosulfones.

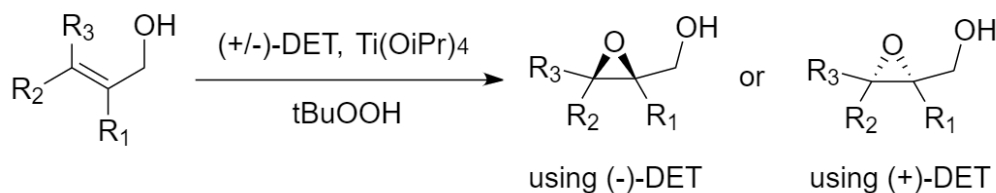
Forms a thiirane dioxide intermediate which extrudes SO_2 by cheletropic reaction.

The α -halosulfone can be made by α -halogenating an organic sulfide (thioether) (e.g. with NBS) followed by oxidation with mCPBA. Often used in cyclic systems (e.g. tetrahydrothiophene dioxides) to enforce stereoselectivity by ring strain (e.g. to form cyclobutenes).



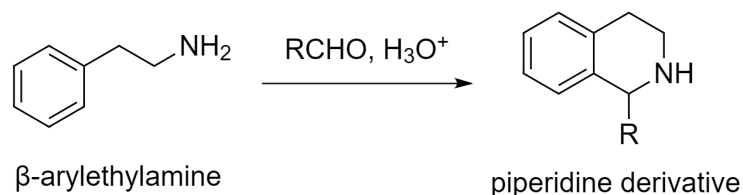
Sharpless Epoxidation: enantioselective epoxide formation from α -hydroxyalkenes.

DET is diethyltartrate, using either (*S,S*) = (-) or (*R,R*) = (+). tBuOOH is *tert*-butyl hydroperoxide, the oxidising agent.

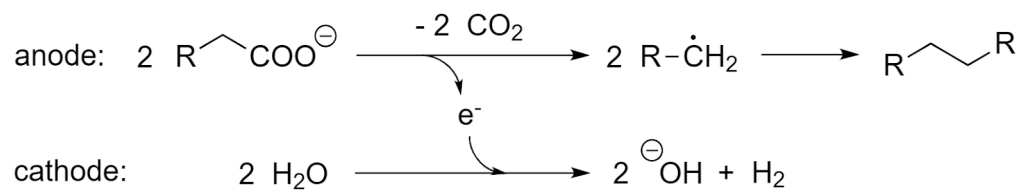


Pictet-Spengler Reaction: ring closure of β -arylethylamines with aldehydes.

Electron-rich aromatic rings work best e.g. indoles, pyrroles, 3,4-dimethoxyphenyls.



Kolbe Electrolysis: an electrosynthesis reaction. Electrolysis of aqueous carboxylate salts forms free radicals at the anode after decarboxylation, which can react to form either dimer or intramolecular C-C bonds.



For 1,4-dicarboxylates, the radical termination step is intramolecular and forms an alkene.

16.4. Analytical Methods in Chemistry and Molecular Biology

16.4.1. Flame Tests for Metals in Inorganic Compounds

Metals can be identified by dipping a nichrome wire (e.g. an inoculation loop) into an aqueous solution of their salt and holding it into a Bunsen burner flame on high heat.

The electrons in heated metal ions are thermally excited to higher orbitals, which then undergo relaxation, releasing light at characteristic wavelengths (colours). This is applied quantitatively in **flame emission spectroscopy** to identify the ions from their line spectrum.

Li^+ lithium deep brick-red	Na^+ sodium intense yellow	K^+ potassium lilac	Rb^+ rubidium red-violet	Cs^+ caesium blue-violet		
Ca^{2+} calcium orange-red	Sr^{2+} strontium red	Ba^{2+} barium pale green	Ra^{2+} radium crimson	Cu^{2+} copper blue-green	$\text{Fe}^{2+}/\text{Fe}^{3+}$ iron yellow-orange	Zn^{2+} zinc light blue-green
B^{3+} boron bright green	In^{3+} indium indigo	Pb^{2+} lead blue-white	As^{3+} arsenic light blue	$\text{Sb}^{3+}/\text{Sb}^{5+}$ antimony light green	$\text{Se}^{2+}/\text{Se}^{4+}$ selenium blue	

Some metals which produce white (or silvery) flame tests such as magnesium (very bright), aluminium, beryllium, cobalt, chromium, hafnium, nickel, tin (blue-white), and titanium. Zinc and lead are also sometimes reported as white.

Flame tests may alternatively be carried out using the borax bead test (see Section 15.4.3).

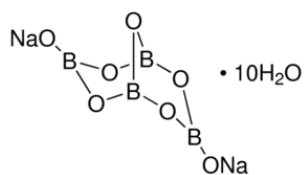
The variation in the colours of fireworks is based on the same principle as the flame test. In a firework, a fuel (black gunpowder: 75% KNO_3 + 15% charcoal + 10% sulfur) and oxidiser (chlorates and nitrates) are used with a dextrin binder to heat the powdered metal salt and produce coloured light.

16.4.2. Test-Tube Reactions for Inorganic Compounds

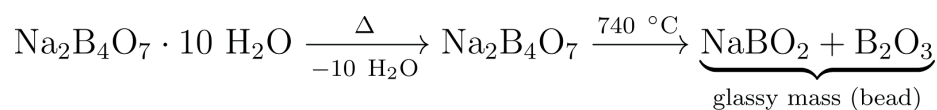
Analyte (testing for)	Procedure	Positive result	Notes
hydrogen (H ₂)	Hold a lit splint into a test tube.	'Squeaky pop' sound heard.	Hydrogen is combusted in air.
carbon dioxide (CO ₂)	Bubble through limewater (Ca(OH) ₂ (aq)).	Limewater turns cloudy (increased turbidity).	Cloudiness is due to formation of a solid suspension of CaCO ₃ .
ammonia (NH ₃)	Hold damp red litmus paper into the test tube.	Litmus paper turns blue.	Ammonia is alkaline.
chlorine (Cl ₂)	Hold damp blue litmus paper into the test tube.	Litmus paper bleached to white.	HCl + HClO bleach mixture formed.
sulfates (SO ₄ ²⁻)	Add dilute HCl (aq) then barium chloride solution (BaCl ₂ (aq)).	White precipitate of insoluble BaSO ₄ formed.	The acid neutralises carbonate ion impurities which would give false positive.
carbonates (CO ₃ ²⁻)	Add dilute HCl, collect gas and pump into limewater.	Limewater turns cloudy (increased turbidity) due to release of CO ₂ .	HCl liberates CO ₂ from carbonates.
chlorides (Cl ⁻)	Add dilute nitric acid (HNO ₃) then silver nitrate solution (AgNO ₃ (aq)).	White precipitate formed, soluble in dilute ammonia.	The acid neutralises ions which could give false positives. Forms AgCl; dissolves in NH ₃ .
bromides (Br ⁻)	Confirm colour by testing solubility in dilute and concentrated ammonia (NH ₃).	Cream precipitate formed, soluble in concentrated NH ₃ .	Forms AgBr; dissolves only in concentrated NH ₃ .
iodides (I ⁻)	(Note: AgF is water soluble so it gives no precipitate).	Yellow precipitate formed, insoluble in concentrated NH ₃ .	Forms AgI; insoluble in NH ₃ .
ammonium ions (NH ₄ ⁺)	Add dilute NaOH and warm gently. Hold in damp red litmus paper.	Litmus paper turns blue.	Reaction forms ammonia and water.

16.4.3. Borax Bead Test for Identification of Metals

Boric anhydride reacts with many metal salts to form coloured metaborates.



The beads are formed by holding borax into a Bunsen flame:



The bead (on the end of an inert metal wire) is then dipped into a sample, which partially adheres to the bead. The bead is then held in the **reducing (lower)** part and then in the **oxidising (upper)** part of the Bunsen flame, and the colours are observed in each case.

Element	Oxidising flame		Reducing flame
	Hot	Cold	Hot / Cold
Chromium	yellow-red	green	green
Manganese	violet	violet	colourless
Nickel	yellow-brown	red-brown	grey
Copper	green-blue	green-blue	red-brown
Cobalt	blue	blue	blue
Iron	yellow-red	pale yellow	green

16.4.4. Colours of Common Period 3 Transition Metal Ion Solutions

Aqueous ions (metal-aquo complexes) $[\text{M}(\text{H}_2\text{O})_6]^{a+}$ in various oxidation states:

Sc	Ti	V	Cr	Mn	Fe	Co	Ni	Cu	Zn
	+2	+2	+2	+2	+2	+2	+2	+2	+2
+3	+3	+3	+3	+3	+3	+3	+3	+3	
	+4	+4	+4	+4	+4	+4	+4		
	+5	+5	+5	+5	+5	+5			
			+6	+6	+6				
				+7					

Some of these may be reported differently.

Solid phase compounds often have different colours to their aqueous phases. Most salts are colourless when anhydrous, only showing colour in aqueous solution.

Some compounds may also differ in colour to those shown above due to field splitting by ligands (see CFT in Section 15.4.4).

(Ti^{3+} : lilac, V^{2+} : lilac, V^{3+} : green, V^{4+} : light blue, V^{5+} : yellow, Cr^{2+} : dark blue, Cr^{3+} : green, Cr^{6+} : orange, Mn^{2+} : very pale pink, Mn^{7+} : deep purple, Fe^{2+} : pale green, Fe^{3+} : pale yellow, Co^{2+} : pink, Co^{3+} : dark yellow, Ni^{2+} : green, Cu^{2+} : dark blue, all others are colourless.)

16.4.5. Qualitative Determination of Organic Compounds by Test-Tube Reactions

Analyte (testing for)	Procedure	Positive result	Notes
Alkenes	Add bromine water.	Bromine water decolourised.	Br ₂ is removed from the water by reaction to form dibromoalkanes.
Haloalkanes	Warm with NaOH in 1:1 water-ethanol, test for halide ion using AgNO ₃ / HNO ₃ (aq) then NH ₃ .	White (Cl) / Cream (Br) / Yellow (I) ppt formed.	NaOH converts to alcohol and releases the halide ion.
Alcohols (1° and 2°)	Mix with acidified potassium dichromate (K ₂ Cr ₂ O ₇ / H ⁺). Heat and distil products.	Colour changes from orange to green.	Cr ⁶⁺ reduced to Cr ³⁺ .
Alcohols (all)	Add ceric ammonium nitrate solution [Ce(NH ₄) ₂ (NO ₃) ₆].	Colour changes from amber to red.	Ligand substitution: forms [Ce(NO ₃) ₄ (ROH) ₃].
Aldehydes (also: α-hydroxyketones, hemiacetals and all reducing sugars)	Add Tollens' reagent.	Silver mirror formed.	Ag ⁺ reduced to Ag.
	Add Fehling's solution or Add Benedict's reagent.	Blue solution turns to brick-red precipitate.	Cu ²⁺ reduced to Cu ⁺ .
Carbonyls (aldehydes and ketones)	Add Brady's reagent (methanol + acidic 2,4-DNPH; 2,4-dinitrophenylhydrazine)	Forms orange precipitate.	
Carboxylic acid	Add NaHCO ₃ or Na ₂ CO ₃ .	Effervescence.	Acid liberates CO ₂ .
1° amines	Add dilute NaOH and benzene sulfonyl chloride (PhSO ₂ Cl). Observe reaction then add HCl. (Hinsberg's test)	No initial change; insoluble precipitate forms with HCl.	Sulfonamide product has acidic hydrogen so soluble only in alkali.
2° amines		Precipitate forms; does not dissolve in HCl.	Sulfonamide product has no acidic hydrogen so insoluble in alkali.
3° amines		Precipitate forms; dissolves in HCl.	No reaction; forms soluble ammonium salt.
Aromatic amines	Add NaNO ₂ + HCl then 2-naphthol.	Bright red-orange insoluble precipitate formed.	Diazonium salt undergoes diazotisation.

16.4.6. Qualitative Determination of Biochemical Compounds by Test-Tube Reactions

Analyte (testing for)	Procedure	Positive result	Notes
Reducing sugars as α -hydroxyketones	Tollens' test Add Tollens' reagent.	Silver mirror formed.	Ag^+ reduced to Ag.
	Fehling's test or Benedict's test Add Fehling's solution or Add Benedict's reagent.	Blue solution turns to brick-red precipitate.	Cu^{2+} reduced to Cu^+ .
Carbohydrates	Molisch's test Add 1% alcoholic solution of 1-naphthol, then add conc H_2SO_4 .	Violet ring forms at the interface of the two layers.	The carbohydrate is dehydrated to an aldehyde by the acid, which reacts with the phenol to form the coloured product.
Starch	Iodine starch test Stain with iodine.	Turns dark blue / black.	I_3^- (triiodide) complexes in amylose helices.
Proteins	Biuret test Add alkaline CuSO_4 (aq).	Turns from pale blue to violet.	Cu^{2+} complexes with peptide CONH bonds.
	Ninhydrin test Boil with aqueous ninhydrin (2,2-dihydroxyindane-1,3-dione).	Turns blue-violet.	Protein is hydrolysed, amino acids react.
	Xanthoproteic test Add concentrated HNO_3 .	Turns yellow.	Benzene rings on aromatic groups (Tyr, Trp or Phe) are nitrated.
	Millon's test Add mercuric nitrate in nitric acid (HgNO_3 , HNO_3).	White precipitate forms.	Reacts with the phenolic group in tyrosine.
Glycosamino-glycans	Use Alcian blue stain.	Stains blue.	Often used to test cell tissues.

For spectrometric methods, see Section 16.4.5.

16.4.7. Infrared (IR) Spectroscopy

IR spectroscopy involves recording the transmittance of infrared radiation through a sample. Molecular bonds have characteristic absorbance 'peaks' at corresponding energies.

- Wavenumber k [cm^{-1}] = $\frac{10^4}{\text{wavelength } [\mu\text{m}]}$,
- Energy E [eV] = 1.9662×10^{-5} [eV cm] $\times k$ [cm^{-1}]

Bond	Wavenumber / cm^{-1}
N – H (amines)	3300 – 3500
O – H (alcohols)	3230 – 3550
C – H	2850 – 3300
O – H (acids)	2500 – 3000
C \equiv N	2220 – 2260
C = O	1680 – 1750
C = C	1620 – 1680
C – O	1000 – 1300
C – C	750 – 1100

16.4.8. Fourier Transform IR and Raman Band Correlation Data (Sorted Ascending)

In case of disagreement between the here and the IR table in Section 16.4.1, the table below should be considered more accurate.

Wave-number (cm ⁻¹)	Assignment	Intensity	Wave-number (cm ⁻¹)	Assignment	Intensity
100 - 210	lattice vibrations	strong	1625 - 1680	C=C	very strong
150 - 430	metal-O	strong	1630 - 1665	C=N	very strong
250 - 400	C-C (aliphatic)	strong	1690 - 1720	urethane	moderate
295 - 340	Se-Se	strong	1710 - 1725	aldehyde	moderate
425 - 550	S-S	strong	1710 - 1745	ester	moderate
460 - 550	Si-O-Si	strong	1730 - 1750	aliphatic ester	moderate
490 - 550	C-I	strong	1735 - 1790	lactone	moderate
505 - 700	C-Br	strong	1740 - 1830	acid anhydride	moderate
550 - 790	C-Cl	strong	1745 - 1780	acyl chloride	moderate
580 - 680	C=S	strong	2020 - 2100	isothiocyanate	moderate
630 - 1250	C-C (aliphatic)	moderate	2070 - 2250	alkyne	strong
670 - 780	C-S	strong	2080 - 2150	Si-H	moderate
720 - 800	C-F	strong	2090 - 2170	isonitrile	moderate
800 - 950	C-O-C	weak	2100 - 2170	thiocyanate	very weak
910 - 960	COOH acid dimer	weak	2110 - 2160	azide	moderate
990 - 1100	aromatic rings	strong	2200 - 2230	aromatic nitrile	moderate
1010 - 1095	Si-O-C	weak	2200 - 2280	diazonium salt	moderate
1010 - 1095	Si-O-Si	weak	2220 - 2260	nitrile	moderate
1020 - 1225	C=S	strong	2230 - 2270	isocyanate	very weak
1025 - 1060	sulfonic acid	very weak	2290 - 2420	P-H	very weak
1050 - 1210	sulfonamide	moderate	2530 - 2610	thiol	strong
1050 - 1210	sulfone	moderate	2680 - 2740	aldehyde	weak
1120 - 1190	Si-O-C	weak	2750 - 2800	N-CH ₃	weak
1145 - 1240	sulfonic acid	very weak	2770 - 2830	CH ₂	strong
1315 - 1435	carboxylate salt	moderate	2780 - 2830	aldehyde	weak
1320 - 1350	nitro	very strong	2790 - 2850	O-CH ₃	weak
1355 - 1385	C-CH ₃	weak	2810 - 2960	C-CH ₃	strong
1365 - 1450	aromatic azo	very strong	2870 - 3100	aromatic C-H	strong
1405 - 1455	CH ₂	weak	2880 - 3530	OH	weak
1405 - 1455	CH ₃	weak	2900 - 2940	CH ₂	strong
1450 - 1505	aromatic ring	moderate	2980 - 3020	CH=CH	strong
1535 - 1600	nitro	moderate	3010 - 3080	terminal =CH ₂	strong
1540 - 1590	aliphatic azo	moderate	3150 - 3480	amide	moderate
1550 - 1610	heteroatomic ring	strong	3150 - 3480	amine	moderate
1550 - 1700	amide	strong	3200 - 3400	phenol	weak
1600 - 1710	ketone	moderate	3210 - 3250	alcohol	weak
1610 - 1740	carboxylic acid	moderate	3250 - 3300	alkyne	very weak

16.4.9. ^{13}C NMR Spectroscopy

NMR provides information on molecular structure and connectivity by analysing the relaxation of spin- $\frac{1}{2}$ nuclei, which possess an intrinsic magnetic moment, in the presence of a magnetic field.

General Principle of Nuclear Magnetic Resonance (NMR) Spectroscopy

- In the presence of an external magnetic field, spin $\frac{1}{2}$ nuclei align with or against the field. These two alignments have different nuclear energy levels.
- When RF (radio wave, M range) electromagnetic radiation is incident on the nuclei, they undergo transitions between the two states at resonant frequencies.
- The difference in resonant frequencies between a given nucleus and a standard is dependent on interactions in the chemical environment, and is reported as the chemical shift δ in ppm.

Organic molecules contain ^{13}C at an average abundance of 1.1%. In proton-decoupled ^{13}C NMR spectra, splitting does **not** occur, and the integration ratio does **not** indicate atom count. In very high resolution ^{13}C NMR, splitting can be observed ($n + 1$, where n is the number of attached hydrogens to the carbon).

Type of carbon	Group	δ (ppm)	Type of carbon	Group	δ (ppm)
$\text{R}_3\text{-C-C-R}_3$	alkyl	5 - 40	$\text{R}_2\text{C=CR}_2$	alkene	90 - 150
R-C-Cl or Br	haloalkane	10 - 70	RCN	nitrile	110 - 125
RCOCR_3	carbonyl	20 - 50	C_6H_6	benzene / aryl	110 - 160
RCNR_2	amine	25 - 60	RCOR	ester, carboxylic acid	160 - 185
R_3COR	alcohol, ether, ester	50 - 90	RCOR	aldehydes, ketones	190 - 220

16.4.10. Proton (^1H) NMR Spectroscopy

The compound under study is immersed in a deuterated solvent (e.g. heavy water (D_2O), deuterated chloroform (CDCl_3) or CD_3CN) as the $\text{D} = ^2\text{H}$ nucleus has no spin, or proton-free solvent (e.g. CCl_4), and the NMR is conducted against a TMS standard.

Proton NMR Chemical Shifts

Type of proton	Group	δ (ppm)	Type of proton	Group	δ (ppm)
RCH_3	methyl	0.7 - 1.2	ROCHR_2	ether	3.1 - 3.9
RNH_2	amine	1.0 - 4.5	RCH_2Cl or Br	haloalkane	3.1 - 4.2
ROH	alcohol	1.0 - 5.0	RCOOCHR_2	ester	3.7 - 4.1
RSH	thiol	1.0 - 5.0	$\text{R}_2\text{C}=\text{CHR}$	alkene	4.5 - 6.0
R_2CH_2	alkyl (2°)	1.2 - 1.4	C_6H_6	aryl / benzene	6.5 - 8.0
R_3CH	alkyl (3°)	1.4 - 1.6	RCHO	aldehyde	9.0 - 10.0
RCOCHR_2	carbonyl	2.1 - 2.6	RCOOH	carboxylic acid	10.0 - 12.0

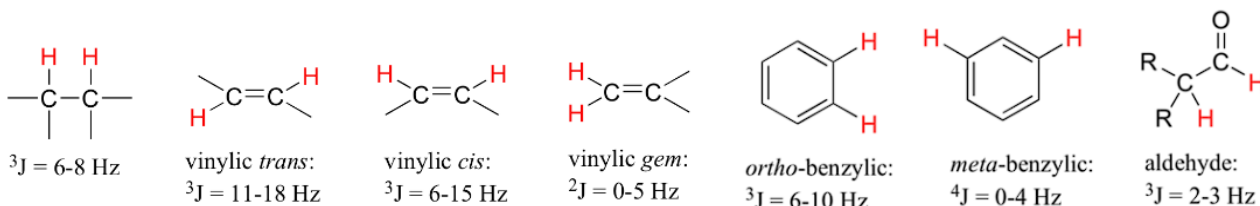
NH, OH and SH peaks are often broad and the sample must be very dry for them to show. Chemical shifts of groups near electronegative atoms are shifted downfield (larger δ) due to deshielding.

Integration Ratio: peak area is proportional to number of H-atoms in an identical environment. This is sometimes shown on the spectrum as an accumulating curve (integration ratio = step size).

Splitting: high-resolution NMR can show peak splitting when H-atoms on adjacent atoms are present

Number of peaks in a split = $n + 1$ (n : number of H atoms bonded to adjacent atoms). Types of peaks: Singlet ($n = 0$), doublet ($n = 1$; 1:1), triplet ($n = 2$; 1:2:1), quartet ($n = 3$; 1:3:3:1), quintet ($n = 4$, 1:4:6:4:1), etc.

J -coupling constant, $^mJ_{ab}$: difference in frequency (in Hz) between peaks due to proton environments a and b , separated by m bonds. The values of J for some proton configurations are:



H atoms bonded to O, N, etc typically do **not** split due to proton exchange through hydrogen bonds, unless the temperature is low (e.g. if $T \lesssim 0^\circ\text{C}$ then O-H **does** contribute to splitting).

Species undergoing dynamic equilibrium on the NMR frequency timescale will display noisy spectra due to the Heisenberg uncertainty principle, as well as exchange peak broadening.

The protons on benzene rings are shifted further ($\delta \sim 7.3 \text{ ppm}$) than on vinyl alkenes due to aromatic ring current deshielding.

16.4.11. NMR Spectroscopy with Other Nuclei (^{15}N , ^{19}F , ^{31}P , ^{129}Xe)

16.4.12. Advanced NMR Spectroscopy (DEPT, COSY, HSQC and HMBC)

16.4.13. UV/Vis Spectrophotometry

Absorbance: $A = -\log_{10} \frac{I}{I_0}$ (I : initial intensity, I_0 : measured intensity)

Beer-Lambert law: $A = \epsilon bc$ and $I = I_0 e^{-\epsilon bc}$ half intensity at $bc = \frac{\ln 2}{\epsilon}$

(ϵ : solvent molar absorptivity (molar extinction coefficient), b : path length, c : concentration)

The molar absorptivity varies significantly with wavelength, so the wavelength must be specified when reporting (e.g. $A_{240} \rightarrow \lambda = 240 \text{ nm}$). In the visible range, the technique is called colourimetry.

Protein Assays: spectrophotometry is often used for quantitative determination of proteins (e.g. enzymes, antibodies, antigens) by addition of a colourimetric reagent and measuring UV/Vis absorbance at a fixed wavelength:

- **Biuret Assay:** add Biuret's reagent. The solution turns violet as Cu^{2+} in the reagent complexes with peptide bonds. Measure A_{540} .
- **Lowry Assay:** add alkaline CuSO_4 (aq) followed by the Folin-Ciocalteu reagent. The solution turns blue. Measure A_{750} .
- **Bradford Assay:** add the dye 'Coomassie brilliant blue G-250'. The solution turns blue. Measure A_{600} .
- **BCA Assay / Smith Assay:** add Biuret's reagent followed by bicinchoninic acid (BCA). The solution turns violet. Measure A_{560} .

Cofactor Assays: Enzymatic reaction kinetics can be assessed by tracking the concentration of a cofactor (e.g. NADH: A_{260} or A_{340}) over time.

16.4.14. Immunological Assays for Selective Quantitative Determination of Proteins

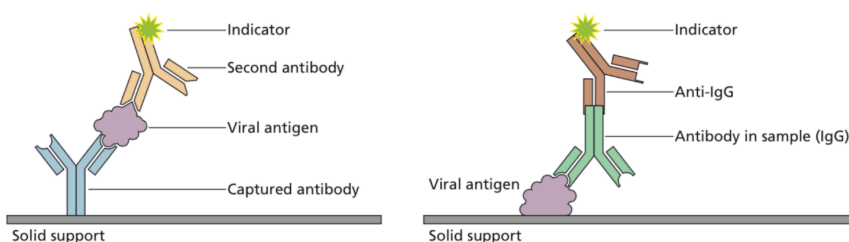
Immunological assays are used to determine the amount of a specific protein present in a sample, typically applied to antibodies, antigens or hormones in biofluids.

Enzyme-Linked Immunosorbent Assay (ELISA): detects antibodies or antigens

(A) Sandwich ELISA for antigen (Ag) detection: 1) Ag-specific mAbs are immobilised on a solid support. 2) Ag-containing solution is added. 3) After washing, a second (detection, enzyme-conjugated) mAb specific to a different Ag epitope is added.

(B) Indirect ELISA for antibody (Ab) detection: 1) Antigens for the target antibody are immobilised on a solid support. 2) Ab-containing solution is added. 3) After washing, a second (detection, enzyme-conjugated) mAb specific to the constant region of the target Ab is added.

Then, a chromogenic/fluorogenic enzyme-specific substrate is added, which is cleaved by the conjugated enzyme to produce a colorimetric or fluorescent signal.



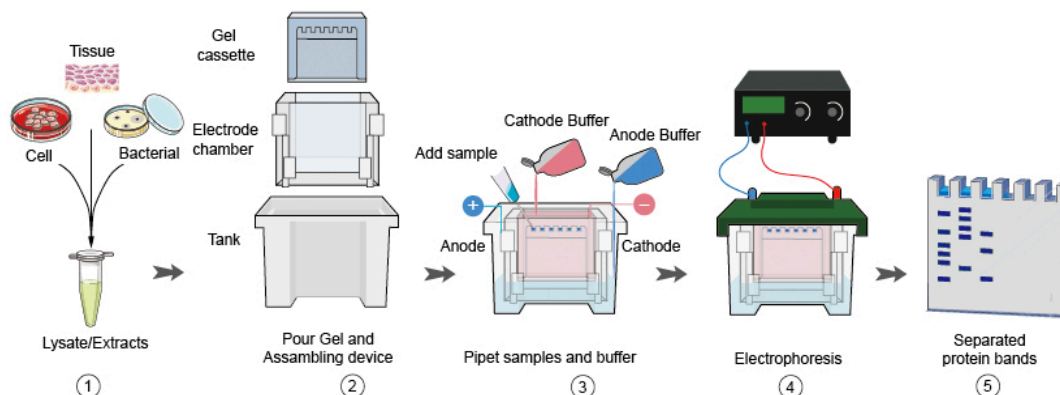
(A) Detecting antigens (e.g. viral) **(B) Detecting antibodies (e.g. IgG)**

Western Blotting (Immunoblotting): separates mixtures of proteins

First, 2D gel electrophoresis (carried out in two steps) produces the electropherogram:

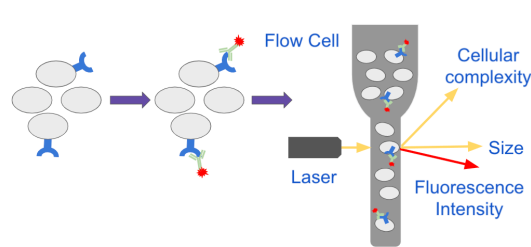
- **Isoelectric Focussing (IEF):** pH gradient and electric field applied in one direction, giving separation by isoelectric point.
- **SDS-PAGE:** proteins are denatured with surfactant (SDS), and migration by applied electric current applied in perpendicular direction in polyacrylamide gel gives separation by molecular weight.

The protein spots are then transferred to a gel, and the sandwich ELISA principle is applied.



Flow Cytometry: measures antigen expression on cells

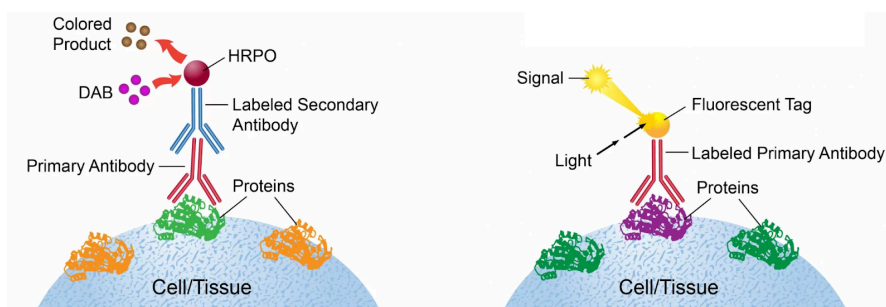
Cells expressing a particular antigen (Ag) are suspended in PBS (phosphate-buffered saline) and labelled with fluorophore-conjugated antibodies (Ab) for the target Ag. The cell solution is loaded into a flow cytometer where it passes a laser in a single-file stream. The detector measures the fluorescent response from cells with the Ag.



Immunocytochemistry (ICC) / Immunofluorescence (IF): identifies intracellular proteins.

Cells containing a particular protein are immobilised and permeabilised with Triton X-100. To prevent non-specific antibody binding, a solution of bovine serum albumin (BSA) is added to bind all surface antigens, and washed. A primary antibody for the target protein is added, and a secondary indicator antibody (binds to the constant region of the primary Ab) is added.

The indicator Ab is conjugated to a fluorophore (for IF: fluorescent microscopy) or enzyme (for ICC: chromogenic staining, by adding DAB substrate (3,3'-diaminobenzidine) to form a coloured product).



Immunocytochemistry (ICC)

Immunofluorescence (IF)

Immunohistochemistry (IHC) uses the same method as ICC, but is applied to a whole biological tissue rather than a cellular solution.

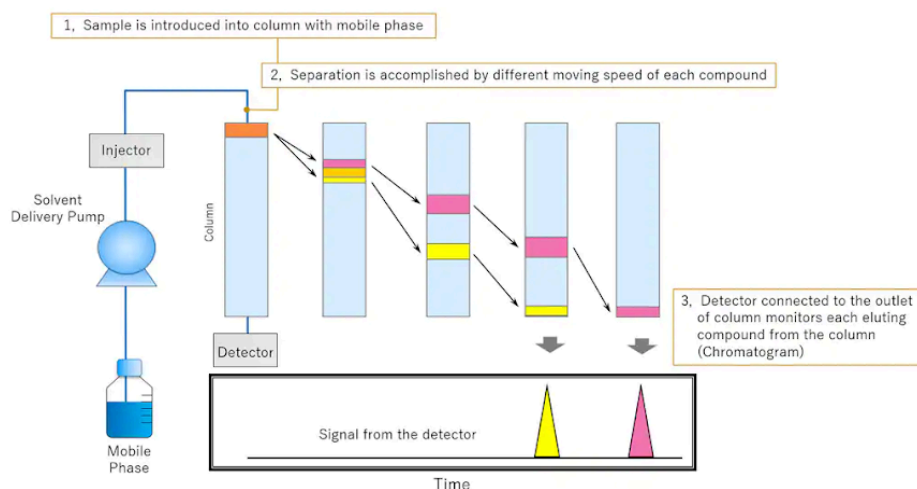
16.4.15. Chromatography for Simple Organic Molecules

Thin-layer chromatography (TLC): separation is based on relative affinity to a mobile phase (solvent) and a stationary phase (adsorbate/substrate).

The analyte can be located by spraying the chromatogram with a developing agent (e.g. ninhydrin) or viewing under blacklight (UVA light). The retention factor R_f is the ratio of the distance travelled by an analyte to the distance travelled by the solvent front.

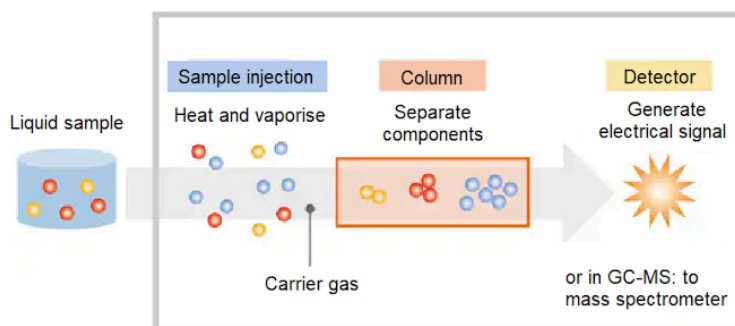
High-Performance Liquid Chromatography (HPLC):

A column is packed with porous silica beads. Analytes adhere to the silica to different extents resulting in different retention times. Automated systems for column chromatography enable high precision and quantitative determination of the components of a mixture. A variation is supercritical fluid chromatography (SCF), which uses supercritical CO_2 as the solvent.



Gas Chromatography (GC):

A liquid mixture is evaporated in an oven and injected into a carrier gas which acts as the solvent, and is transported through a long coil-shaped pipe. The separated components arrive at the detector and can be analysed for their mass (GC-MS).



Dead time (holdup time): time taken for the eluent (unretained solvent) to reach the detector.

16.4.16. Chromatography for Protein Separation and Purification

Ion Exchange Chromatography (IEC): separates proteins by isoelectric point

The chromatography column is chosen to be either:

- Anionic exchanger: uses a positive (cationic) column (e.g. DEAE-C, diethylaminoethyl cellulose) to bind negatively charged proteins ($\text{pH} \gg \text{pI}$).
- Cationic exchanger: uses a negative (anionic) column (e.g. CMC, carboxymethyl cellulose) to bind positively charged proteins ($\text{pH} \ll \text{pI}$).

For further separation, a pH gradient over time (anionic: high \rightarrow low pH; cationic: low \rightarrow high pH), or a salt (NaCl or Na_2SO_4) concentration gradient over time (R_f increases with concentration and charge) can be applied to the eluent. As elution occurs, determination of protein concentration is recorded in real-time by UV/Vis spectrophotometry.

Hydrophobic Interaction Chromatography (HIC): separates proteins by hydrophobicity.

Addition of salt exposes hydrophobic sections of the protein (salting out) which can bind to the hydrophobic column.

Affinity Chromatography: separates recombinant (tagged) proteins.

The column contains adsorbent ligands for affinity tags that can be added to recombinant proteins. Common fusion tags, corresponding column adsorbents and eluents include:

Fusion tag	Affinity adsorbent	Elution with
glutathione-S-transferase (GST)	glutathione	glutathione
protein A	IgG	free IgG (competitive elution; cleaves the tag)
maltose binding protein	amylose	maltose
6xHis tag	nickel-NTA agarose (immobilised metal affinity chromatography, IMAC)	imidazole or histidine
epitope tag (e.g. FLAG tag)	anti-FLAG mAbs	free FLAG
strep-II tag	streptavidin	biotin (vitamin B ₇)
CBD intein	chitin	DTT (cleaves the tag)

Tags can also be cleaved by engineering the protein with a protease recognition site upstream of the tag, then adding the protease to the eluted protein.

Size Exclusion Chromatography (SEC) / Gel Filtration (GF): separates proteins by size.

Large molecules (proteins) run through the column without fractionation, while smaller molecules are adsorbed more. This can also be used to separate salts from protein (desalting), or as a final 'polish' step in purifying a protein solution.

16.4.17. Mobility of Amino Acids in Thin-Layer Chromatography (TLC)

The table shows the R_f values of some amino acids for TLC with a silica stationary phase and a variety of polar mobile phases. Solvent compositions are given in v/v %.

M_1 : ethylene glycol

M_2 : ethanol

M_3 : acetone

M_4 : ethanol/ethylene glycol (1:1)

M_5 : ethanol/ethylene glycol (7:3)

M_6 : ethanol/ethylene glycol (3:7)

M_7 : ethanol/ethylene glycol/acetone (5:3:2)

M_8 : ethanol/30% aq. ethylene glycol/acetone (5:3:2)

M_9 : ethanol/50% aq. ethylene glycol/acetone (5:3:2)

M_{10} : ethanol/70% aq. ethylene glycol/acetone (5:3:2)

M_{11} : ethanol/70% aq. ethylene glycol/acetone (5:3:1)

M_{12} : ethanol/70% aq. ethylene glycol/ethyl acetate (5:3:3)

Amino acids	Mobile phases (M)											
	M_1	M_2	M_3	M_4	M_5	M_6	M_7	M_8	M_9	M_{10}	M_{11}	M_{12}
Leucine	0.98	0.14	0.01	0.91	0.71	0.92	0.77	0.82	0.82	0.75	0.87	0.87
Isoleucine	0.97	0.21	0.01	0.92	0.72	0.92	0.76	0.81	0.81	0.77	0.85	0.81
Phenyl alanine	0.99	0.26	0.01	0.90	0.74	0.90	0.78	0.81	0.88	0.78	0.88	0.89
Tyrosine	0.97	0.22	0.02	0.92	0.75	0.91	0.80	0.83	0.86	0.77	0.90	0.88
Alanine	0.93	0.14	0.01	0.90	0.54	0.91	0.66	0.67	0.70	0.70	0.77	0.68
Lysine	0.97	0.06	0.01	0.27	0.07	0.31	0.60	0.10	0.08	0.11	0.08	0.07
Proline	0.92	0.10	0.01	0.75	0.47	0.76	0.36	0.45	0.46	0.53	0.58	0.58
Serine	0.94	0.14	0.01	0.88	0.61	0.91	0.59	0.65	0.70	0.71	0.75	0.68
Glutamic acid	0.95	0.17	0.01	0.70	0.68	0.77	0.54	0.47	0.41	0.58	0.64	0.49
Methionine	0.92	0.10	0.01	0.84	0.68	0.89	0.69	0.72	0.75	0.66	0.85	0.81
Arginine	0.92	0.07	0.01	0.24	0.05	0.28	0.09	0.10	0.06	0.05	0.07	0.05
Histidine	0.92	0.11	0.01	0.79	0.40	0.85	0.55	0.64	0.48	0.16	0.66	0.54
Tryptophan	0.99	0.14	0.01	0.83	0.77	0.89	0.63	0.83	0.88	0.78	0.88	0.83

16.5. Polymers and Biochemistry

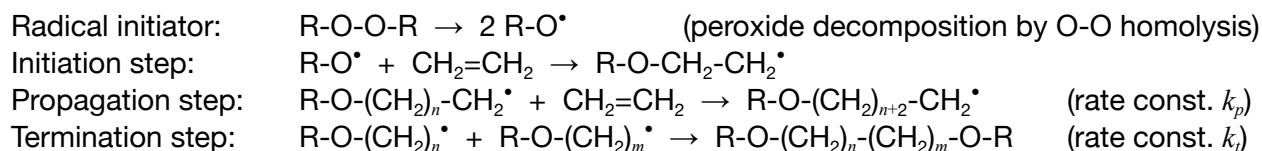
16.5.2. Addition Polymerisation

Addition polymerisation typically proceeds by a free-radical mechanism. The initiator may be a radical (e.g. from homolysis of a peroxide), an ion (superacids / alkyllithium), or an organometallic complex (coordination polymerisation: Ziegler-Natta catalysts).

Free Radical Initiators: produces free radicals used to carry out the initiation step

- Peroxides ($R-O-O-R \rightarrow 2 R-O^\bullet$): e.g. hydrogen peroxide (H_2O_2), benzoyl peroxide ($(PhCOO)_2$, BPO)
- Azo compounds ($R-C-N=N-C-R \rightarrow 2 R-C^\bullet + N_2$): e.g. α, α' -azobis(isobutyronitrile) (AIBN)
- Redox initiators: e.g. $R-C-OOH + Fe^{2+} \rightarrow R-C-O^\bullet + OH^- + Fe^{3+}$
- UV light (photolysis) and/or heat (thermolysis) can also induce radical initiator breakdown.

Free-Radical Polymerisation: using ethene \rightarrow polyethene as an example



Total number of molecules: $N = N_0(1 - p)$ (p : conversion ratio)

Mean degree of polymerisation (mean chain length): $\overline{DP} = \frac{N_0}{N} = \frac{1}{1-p}$

Conditions of Free-Radical Polymerisation Reactions

Polymerisation can be done in bulk (no contamination), in suspension (e.g. water with stabiliser), in solution (e.g. $scCO_2$) or in emulsion (micelles act as microvesicles). Bulk polymerisation results in an increased viscosity with chain growth. Due to decreased Brownian motion, the termination step can become kinetically impeded, leading to rapid reaction rate increase, temperature rise and gelation (autoacceleration; Trommsdorff effect):

$$r_p = k_p [M] \left(\frac{f k_d [I]}{k_t} \right)^{1/2} \quad (M: \text{monomer}, I: \text{initiator}, f: \text{radical formation efficiency of initiator})$$

During the propagation steps, head-to-tail orientation is most common due to steric effects (single repeating unit). Stereochemistry is typically random (atactic) unless temperature is low. Chain transfer reactions, in which the oligomer radical moves, can create branched polymers. Disproportionation or reaction with initiators will produce side product impurities.

Monomers with allylic hydrogens (e.g. propene, isobutene) are unable to undergo free-radical polymerisation due to chain transfer of the allylic H. Polymerisation of dienes can form cyclic repeating units or crosslinks (for thermosets). Conjugated dienes can form 1,2-, *cis*-1,4- or *trans*-1,4- polymers.

16.5.3. Condensation Polymers, Photopolymers and Copolymers

Condensation Polymerisation

Condensation polymerisation involves the joining of different monomers and the elimination of a small molecule (e.g. H₂O, HCl).

Common pairs of functional groups: di(acyl chloride) + dicarboxylic acid → polyester, dicarboxylic acid + diol → polyester, diamine + di(acyl chloride) → polyamide.

Typical reaction: $n \text{HOOC-R}_1\text{-COOH} + n \text{HO-R}_2\text{-OH} \rightarrow [-\text{OOC-R}_1\text{-COO-R}_2-]_n + (2n - 1) \text{H}_2\text{O}$

Photopolymerisation

Photopolymerisation typically proceeds as free-radical addition polymerisation, although the free-radical initiator is generated using ultraviolet radiation ($h\nu$). Photopolymerisation is often autocatalytic, since the resulting polymeric regions of the reacting mixture have higher refractive index, which in turn guides more light into the region, amplifying the rate of polymerisation in those regions.

Stereolithography (vat photopolymerisation; 3D inkjet printing) uses lasers of UV radiation to cure sections of a liquid photosensitive monomer-oligomer mixture (SLA resin) into the solid polymer state. It can also be used to induce cross-linking of reactive side groups or terminal groups.

Copolymerisation

The use of multiple monomers to generate a polymer with variation in the chain structure (a copolymer, as opposed to a homopolymer). In a block copolymer, monomer types are the same for large sections of the polymer, but alternate. Copolymers may also be branched (graft polymers, dendrimers).

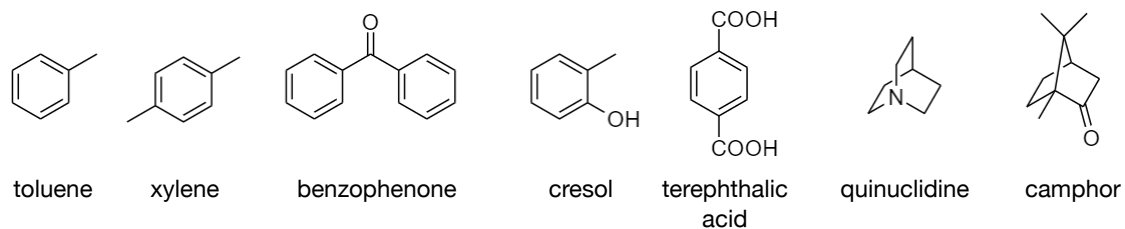
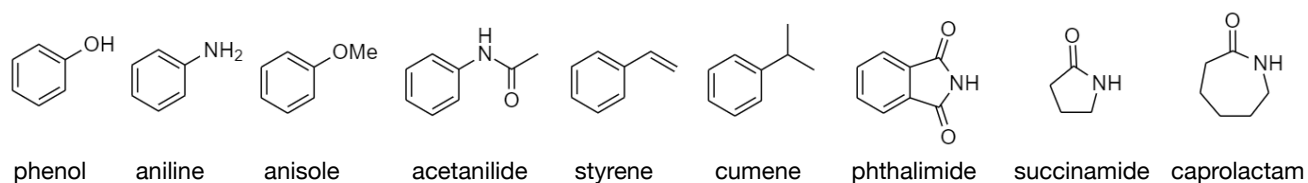
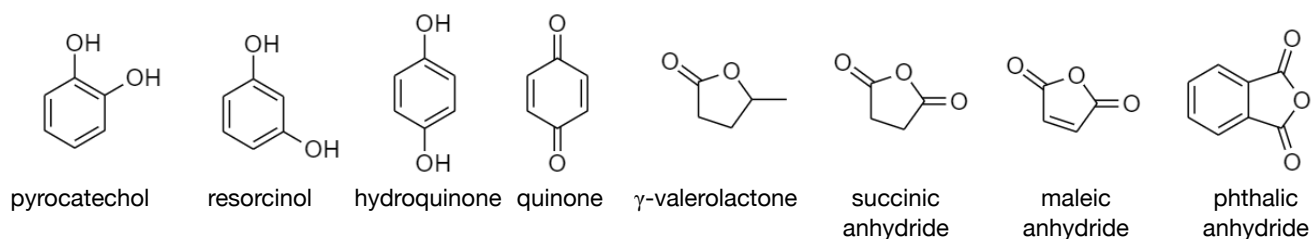
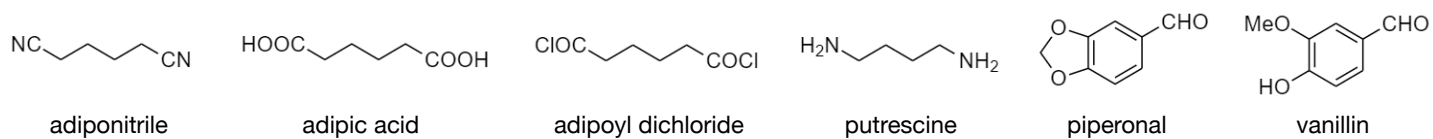
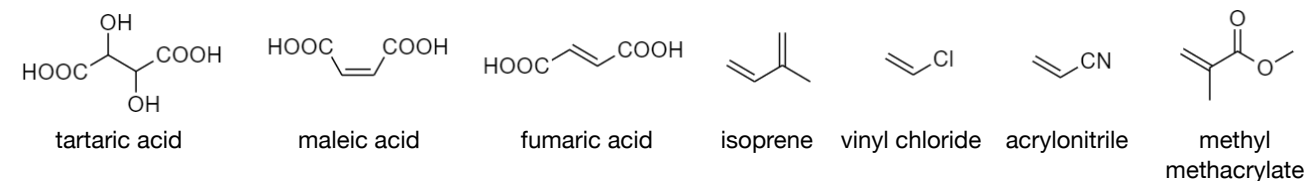
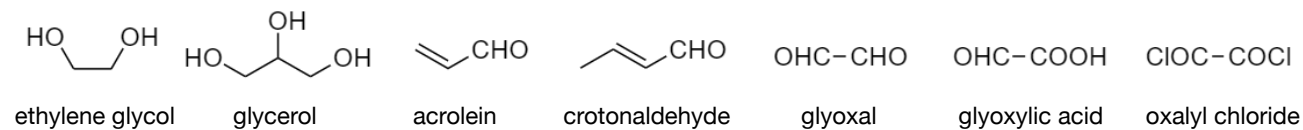
Synthetic Biopolymers

Bacteria can be gene-edited to secrete useful polymers (bioplastics) e.g. polyhydroxybutyrate (PHB) and polydiketoenamine (PDK), or to synthesise enzymes that can synthesise the monomers for a new polymer. These polymers are also typically biodegradable and highly recyclable, although their mechanical properties are typically less optimal than those derived from traditional methods.

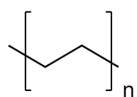
Enzymes have also been found to degrade synthetic plastics into monomers (e.g. PETase into ethylene glycol and terephthalic acid). These enzymes are often mutations of e.g. cutin hydrolases, where the active site is enlarged to permit hydrolysis of bulky condensation polymers. The metabolites can be used to make new materials (upcycled plastics) or degraded further into useful chemicals.

16.5.4. Common Names of Synthetic Precursors and Reagents

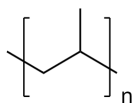
Small molecule alcohols, aldehydes and carboxylic acids:



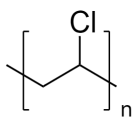
16.5.5. Structures of Some Common Polymers



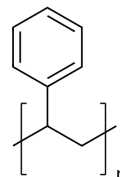
polyethylene (PE)



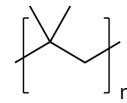
polypropylene (PP)



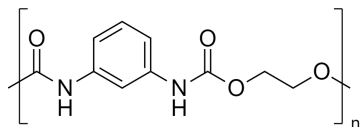
polyvinyl chloride (PVC)



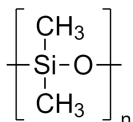
polystyrene (PS)



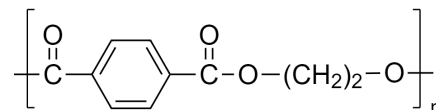
polyisobutylene



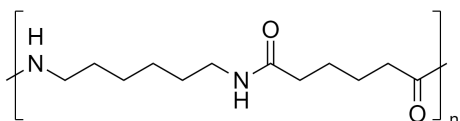
polyurethane



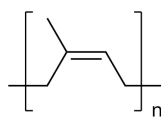
silicone



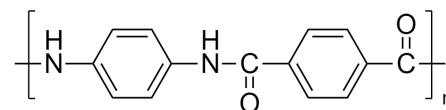
polyethylene terephthalate (PET) / terylene / dacron



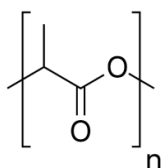
Nylon 6,6



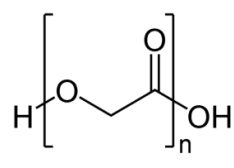
natural rubber (polyisoprene)



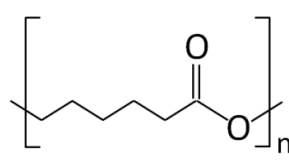
kevlar



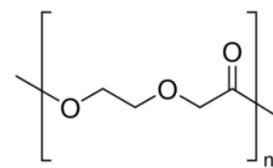
poly(lactic acid) (PLA)



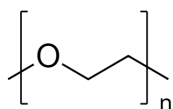
poly(glycolic acid) (PGA)



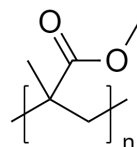
polycaprolactone (PCL)



poly trimethyl carbonate (PTMC)



poly(ethylene glycol) (PEG)



poly(methyl methacrylate) (PMMA)

16.5.6. Sugars and Carbohydrates

Monosaccharides: consists of one sugar unit (no glycosidic bonds: cannot be hydrolysed).

Sugars based on open-chain group (C_n epi- means the epimer (opposite stereochemistry) at carbon n)

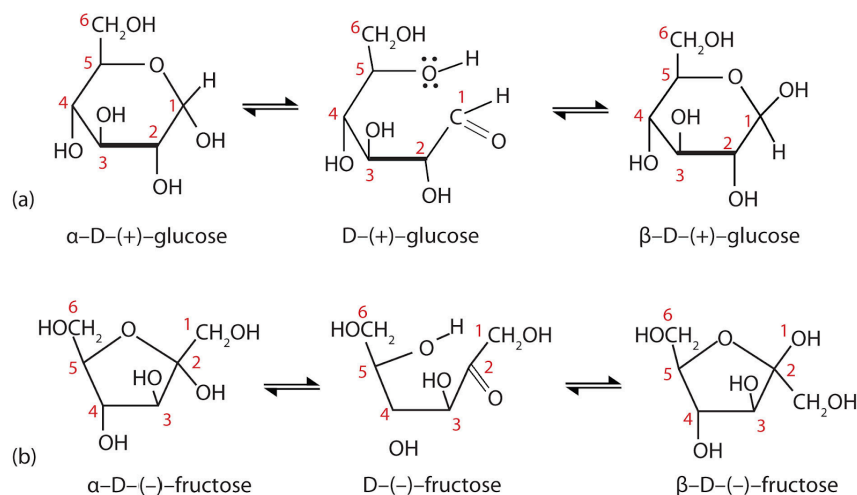
- Trioses (3 C): glyceraldehyde, dihydroxyacetone
- Tetroses (4 C): threose (Thr), erythrose (C_2 epi-Thr)
- Aldopentoses (5 C): ribose (Rib), arabinose (C_2 epi-Rib), xylose (C_3 epi-Rib), lyxose (C_2 epi-Xyl)
- Ketopentoses (5 C): ribulose (Rbu), xylulose (C_3 epi-Rbu)
- Aldohexose (6 C): glucose (Glu), mannose (C_2 epi-Glu), allose (C_3 epi-Glu), galactose (C_4 epi-Glu)
- Ketohexose (6 C): fructose (Fru), psicose (C_3 epi-Fru), sorbose (C_5 epi-Fru)

Monosaccharides exist in two different crystalline forms, α and β (anomers), which differ in stereochemistry at C_1 (the anomeric carbon). There is an equilibrium between the cyclic hemiacetal/hemiketal forms with the open-chain forms, with the ring typically being predominant.

The D and L convention refers to chemical similarity with glyceraldehyde, while the + and - convention shows the direction of specific optical rotation. These may differ from each other, as well as from the standard *R* and *S* convention.

Deoxy sugars have carbon atoms with no hydroxyl groups e.g. 2-deoxyribose (Section 16.5.9).

Macrolides are biomolecules composed of a ~15-membered lactone ring with deoxy sugars bonded to it by glycosidic bonds, and are used as bacteriostatic antibiotics.



Monosaccharides undergo various reactions due to their aldehyde/ketone and alcohol groups:

- Oxidation with e.g. Tollens' reagent, Fehling's solution (forms brick-red ppt), Br_2 (aq) ($CHO \rightarrow COOH$) or conc. HNO_3 ($-CH_2OH$ and $-CHO \rightarrow 2 -COOH$)
- Reduction with e.g. HI ($-CHO \rightarrow -CH_3$, $-OH \rightarrow -H$) or $Na(Hg) + H_2O$ ($-CHO \rightarrow -CHOH$)
- Sugar oxime formation with NH_2OH (hydroxylamine) or sugar cyanohydrin formation with HCN
- Acetylation with e.g. CH_3COCl ($-COH \rightarrow -OOCCH_3$)
- Osazone formation with e.g. $PhNHNH_2$ (phenylhydrazine) ($CHO, 1^\circ -COH \rightarrow -C=NNHPh$)

Oligosaccharides

Oligosaccharides can be disaccharides (2 sugars), oligosaccharides (3-10 sugars). Monosaccharides can form oligosaccharides by condensation reactions at C1 and C4 (forming glycosidic C-O-C bonds). They can be acid-hydrolysed to the constituent monosaccharides by boiling in acidified alcoholic solution.

- **Sucrose:** α -glucose + β -fructose with (Glu C1 - Fru C4)
- **Maltose:** α -glucose + α -glucose with (Glu C1 - Glu C4)
- **Lactose:** β -galactose + β -glucose with (Gal C1 - Glu C4)
- **Raffinose:** α -galactose + α -glucose + α -fructose (Gal C1 - Glu C6; Glu C1 - Fru C4)

Polysaccharides (glycans)

Polysaccharides are longer and are not considered sugars (they are not sweet in taste).

Particular polysaccharides and derivatives:

- **Starch:** polymer of α -glucose with 1,4 links (**amylose**) and 1,6 crosslinks (**amylopectin**)
- **Cellulose:** polymer of β -glucose with 1,4 links
- **Xanthan gum:** cellulose with C3-substituted trisaccharide of β -glucose derivatives
- **Glycogen:** same as starch with more crosslinks (like amylopectin, with even more branching)
- **Dietary Fibre:** carbohydrates which cannot be absorbed or metabolised in the body
- **Glycosaminoglycans:** repeating disaccharides with carboxylic acid/sulfate/ether/amine/amide/phosphate at the C2, C4 and/or C5 positions. Examples: heparin, chondroitin, keratan (sulfates), hyaluronic acid.
- **Lipopolysaccharides:** glycans substituted with fatty acids ('lipid A') and O-linked oligosaccharides (antigen).

These derivative polysaccharides are often important components of biological cell walls/organelle membranes and can form complex structures in solution (Section 16.5.7, Section 17.2.1.)

Iodine starch test: stain with iodine. In the presence of starch, it will turn dark blue/black, due to the complexing of I_3^- (triiodide) in amylose helices.

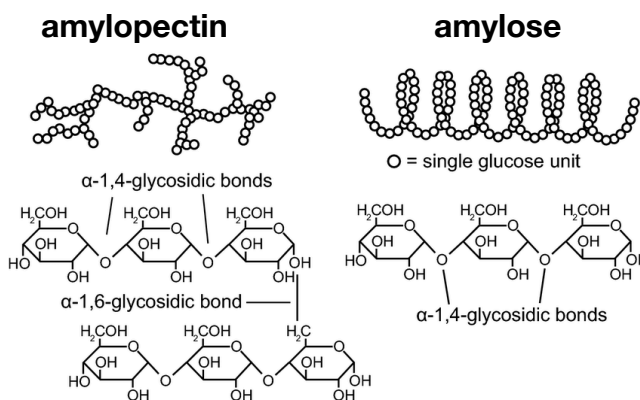
Reducing and Non-Reducing Sugars

All reducing sugars undergo mutarotation (anomers interconvert to an equilibrium mixture) in aqueous solution (but not in the solid state) due to formation of the open-chain structure.

- All monosaccharides are reducing.
- Free reducing groups (aldehyde, α -hydroxyketone or hemiacetals) also indicate reducing sugars.
- If reducing groups are bonded, then the resulting disaccharide is non-reducing.

Tests for reducing sugars: Tollens' / Fehling's / Benedict's reagents (Section 15.4.3).

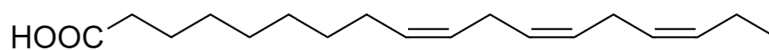
Test for any carbohydrate: Molisch's test (add 1-naphthol, H_2SO_4 : purple ring forms at interface)



16.5.7. Lipids (Fats and Oils)

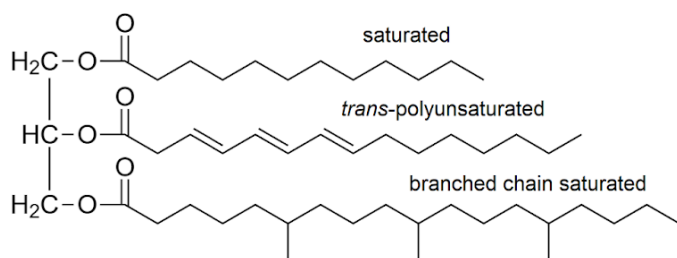
Lipids are typically amphiphilic long-chain molecules. Fats are solid lipids, oils are liquid lipids, at room temperature. The chain of a lipid may be saturated (C-C bonds only) or unsaturated (has C=C bonds: mono = 1, poly = more); which in turn may be *cis* or *trans*.

Fatty acids: a single hydrophilic -COOH head with an alkyl tail.

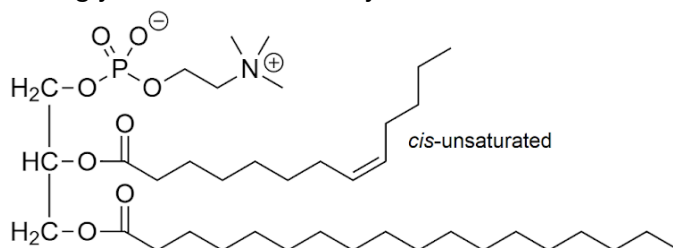


- Omega-3 fatty acid: a polyunsaturated *cis*-fat with a C₃=C₄ bond (counting from the end), with various beneficial health effects including supporting growth of the brain.

Triglycerides and Phospholipids: the ester product of glycerol with three fatty acids.



Triglyceride

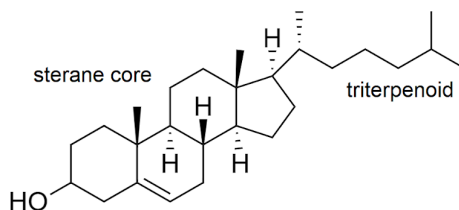


Phospholipid

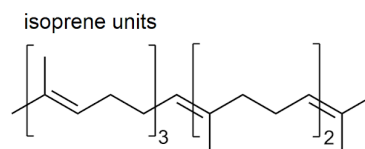
- Saponification: base hydrolysis of triglycerides to fatty carboxylate salts and glycerol. Fatty carboxylate salts form micelles in solution and can be used as anionic surfactants.
- Transesterification with methanol produces methyl esters (biodiesel) and glycerol.
- Monounsaturated fat: a chain with only one C=C bond.
- Partial hydrogenation of vegetable oils can convert *cis* bonds to *trans*, producing *trans*-fats.
- *Trans*-fats are harder to break down due to denser intermolecular packing, as well as promoting accumulation of low-density lipoprotein (LDL, 'bad') cholesterol in the body.
- Phospholipid: one chain is replaced by a substituted phosphate. Can form micelles in water and inverse micelles in organic solvent, and together can form phospholipid bilayers and/or liposomes.

Other Types of Lipids:

- Steroids, sterols and steranes: four fused rings with alkyl side chains, e.g. cholesterol, gonane.
- Triterpenoids: hydrocarbons of repeating isoprene units e.g. squalene, squalane.
- Sphingolipids: long-chain aliphatic amino alcohols. e.g. sphingosine, sphingomyelin, ceramide.



Cholesterol: a triterpenoid steroid.



Squalene: a triterpenoid hydrocarbon oil.

For the carbon numbering convention of the polycyclic steroid system, see Section 16.2.5.

16.5.8. Proteins

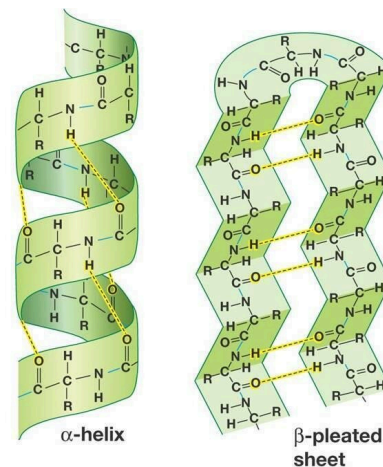
Proteins are linear sequences of amino acid residues, linked by peptide (-CONH-) bonds. Smaller units may be dipeptides (two linked amino acids), oligopeptides (less than ~10 linked amino acids) or polypeptides (a larger chain, ~100 linked amino acids). Amino acids may also form cyclic oligopeptides which is a common motif for antibiotics.

Primary Structure: the amino acid sequence comprising the protein.

- The C-terminus (end with the -COOH group) corresponds to the 5' end of RNA.
- The N-terminus (end with the -NH₂ group) corresponds to the 3' end of RNA.
- In biology, proteins are formed by translation of RNA from 5' to 3'.
- The peptide bonds are planar, delocalised and resist hydrolysis at pH 7 / 25 °C ($k \sim 10^{-10} \text{ s}^{-1}$)

Secondary Structure: the localised structures which arise due to interactions (typically hydrogen bonds) between the backbones of amino acid residues.

- **α -helix:** a right-handed spiral formed due to backbone coaxial C=O...H-N bonds.
- **β -pleated sheet:** a folded sheet formed due to backbone transverse C=O...H-N bonds.
- **Turns:** β -turns, γ -turns and β -hairpins.



Tertiary Structure: the wider-range structures which arise due to interactions between the side chains of primarily-distant amino acid residues which determine the folding pattern.

- **Disulfide bridge:** a covalent -S-S- bond formed due to oxidative folding of cysteine. These may also form when thiol side groups (in antioxidants e.g. glutathione) neutralise reactive oxygen species (ROS: e.g. peroxides) and free radicals in the body. Releases H₂.
- Ionic bonds / Salt bridge: ionic attractions between formally charged side chains.
- Lactam bridge (synthetic only): intramolecular amide bond formation between adjacent residues containing -COOH and -NH₂ side chains. Can stabilise α -helices.

Quaternary Structure: the assembled form of a protein in its biophysiological environment.

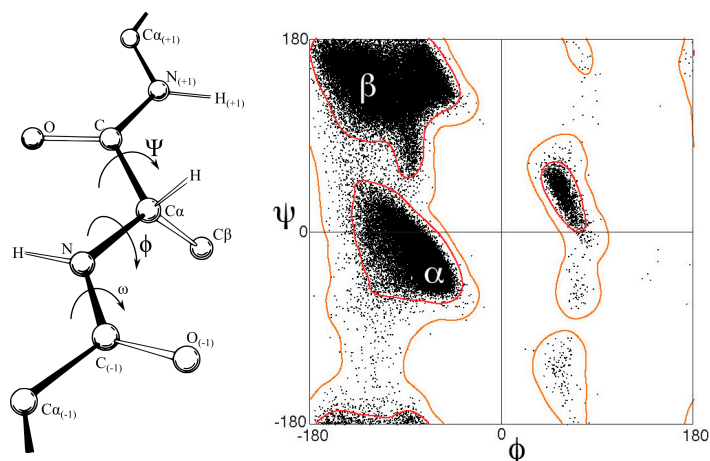
- Complexes: interactions with cofactors such as nucleic acids and prosthetic groups.
- Oligomers: interactions with protein chains on a different protein subunit.

Protein shape: proteins may be globular (round) or fibrous (elongated). Only globular proteins have functional (enzymatic) roles, while fibrous proteins are typically structural (e.g. keratin, collagen for connective tissue and actin, myosin for muscle fibres).

Anfinsen's dogma: the hypothesis/postulate that the tertiary structure of small polypeptides depends only on the primary structure, independent of environment conditions. In general, proteins have several free energy minima across a range of conformational folding patterns, but the equilibrium conformation is the unique lowest energy thermodynamically stable form. Exceptions include the 'intrinsically disordered proteins' and 'circadian oscillator proteins'.

Ramachandran plot: shows the energetically feasible regions of folding conformations (in terms of the amino acid backbone dihedral torsional angles (ψ , ϕ) due to steric effects. Angle ω is always 180° due to the planarity of the amide bond. Analysis of 3D protein structure yields a kernel density plot in (ψ , ϕ) space.

The dihedral angles of amino acid residues in right-handed α -helices (α) and beta-sheets (β) occupy different regions in the Ramachandran plot. Left-handed α -helices occupy the island region with $\phi > 0$.



Protein water solubility: when in water, hydrophobic residues tend to be found closer to the centre of the protein, while polar and/or charged residues are found interacting with water on the surface. The presence of salt ions in the water influences the stability (solubility) of the secondary and tertiary structures of the protein according to the Hofmeister series (lyotropic series). From **promoting salting out** (decreases solubility, strengthens solute-solute interactions) to **promoting salting in** (increases solubility, weakens solute-solute interactions):

Salt anions:

$\text{Cit}^{3-} > \text{PO}_4^{3-} > \text{SO}_4^{2-} > \text{Tar}^{2-} > \text{HPO}_4^{2-} > \text{CrO}_4^{2-} > \text{Ac}^- > \text{OH}^- > \text{HCO}_3^- > \text{F}^- > \text{Cl}^- > \text{Br}^- > \text{NO}_3^- > \text{I}^- > \text{SCN}^- > \text{ClO}_4^- > \text{ClO}_3^-$

Salt cations:

$\text{Al}^{3+} > \text{Mg}^{2+} > \text{Ca}^{2+} > \text{Ba}^{2+} > \text{Li}^+ > \text{Na}^+ > \text{K}^+ > \text{NH}_4^+ > \text{Rb}^+ > \text{Cs}^+ > \text{Gua}^+$

(Cit: citrate, Tar: tartrate, Ac: acetate, Gua: guanidium)

The effect of the anion typically dominates over the effect of the cation, if they compete.

It is generally observed that **kosmotropic ions** (promote ordering of the water structure) and **chaotropic ions** (promote disordering of the water structure) correlate with **salting out** and **salting in** respectively, but the predictive power and underlying mechanistic validity of making this connection is uncertain. 'Hydrotropic ions' can solubilise proteins even more than chaotropic ions, and using surfactants more still, by unfolding (destabilising, and often denaturing) the protein to break up aggregate particles and form a stabilised colloid (Section 14.3.9). At high protein content, the solution may form a hydrogel (Section 16.5.11).

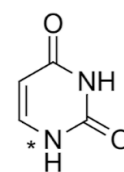
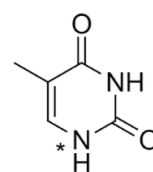
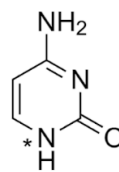
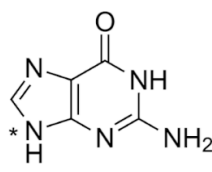
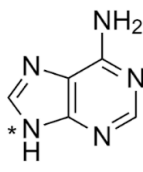
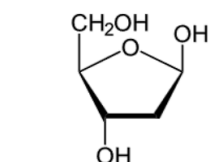
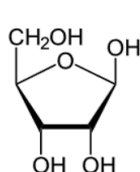
Glycoconjugation of Proteins (Glycosylation): addition of polysaccharide chains to proteins

Glycoproteins are made of proteins and carbohydrates, in which amino acid side chains form either glycosidic bonds (O-linkage, e.g. from Ser, Thr, Tyr) or peptide bonds (N-linkage, e.g. from Asn, Arg) with the C1 position on a sugar (forming an oligosaccharide / polysaccharide side chain). The glycan chains are typically relatively short and branched.

Proteoglycans are made of proteins and glycosaminoglycans (GAGs: Section 16.5.7, 16.5.9), again using either glycosidic (O-linkage) or amide bonds (N-linkage) to attach them to the protein structure. Enzymes can also substitute -OH groups for -OSO₃H (sulfate, by sulfonation) on the GAG chain. There are typically multiple GAG chains per protein, and they are long and linear.

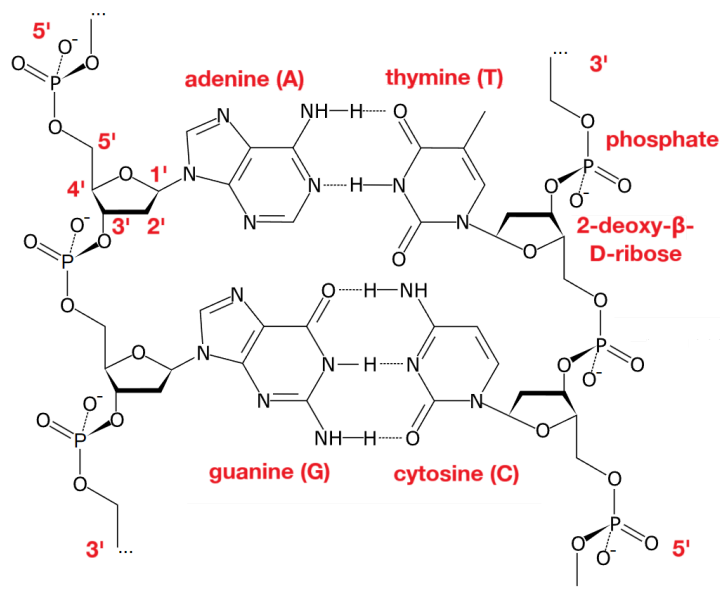
Biuret test for proteins: add alkaline CuSO₄ → turns **violet** due to Cu²⁺-CONH complexing.

16.5.9. Nucleobases, Nucleotides, DNA and RNA

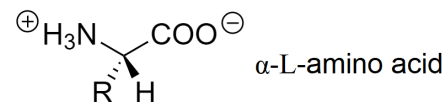


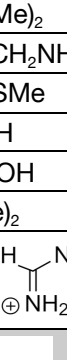
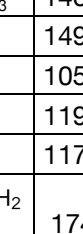
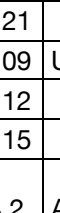
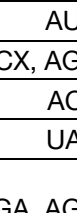
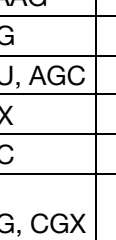
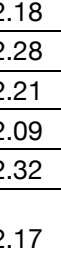
β -D-ribose β -D-2-deoxyribose adenine (A) guanine (G) cytosine (C) thymine (T) uracil (U)
(furanose sugars, Haworth projection) (purine nucleobases) (pyrimidine nucleobases)

- In DNA (shown right) and RNA, nucleobases are bound to sugars by a bond at the anomeric carbon, in which the 1-hydroxyl group (on the sugar) and the amino group (shown above with the starred *N) condense to lose H₂O.
- Sugars are bound to phosphate groups at the 3'- and 5'-hydroxyl groups, forming condensation polymers.
- A single nucleotide consists of a phosphate, pentose sugar, and a nucleobase. A nucleoside is a sugar and nucleobase.
- In life, the negative charges due to the phosphate groups are balanced by counterions (e.g. Mg²⁺) in transport and by protonated amino groups in lysine side chains on histone proteins in chromosomes (Section 17.2.2).
- DNA is a right-handed double helix of paired nucleotides. β -D-2-deoxyribose is the sugar. Complementary base pairings are A-T (2 H-bonds) and G-C (3 H-bonds).
- RNA is a right-handed single helix of nucleotides. β -D-ribose is the sugar. Base conversions in the transcription of DNA to RNA are A \rightarrow U, T \rightarrow A, G \rightarrow C, C \rightarrow G.



16.5.10. Amino Acids: Structures and Biochemical Data



Amino Acid (A-Z)			Side group, R	M_r	RNA codons	pK_a	pK_b	pK_x	pI
Alanine	Ala	A	-Me	89.1	GCX	2.34	9.69	-	6.00
Asparagine	Asn	N	-CH ₂ CONH ₂	132.12	AAU, AAC	2.02	8.80	-	5.41
Aspartic acid	Asp	D	-CH ₂ COO ⁻	133.11	GAU, GAC	1.88	9.60	3.65	2.77
Cysteine	Cys	C	-CH ₂ SH	121.16	UGU, UGC	1.96	10.28	8.18	5.07
Glutamic acid	Glu	E	-CH ₂ CH ₂ COO ⁻	147.13	GAA, GAG	2.19	9.67	4.25	3.22
Glutamine	Gln	Q	-CH ₂ CH ₂ CONH ₂	146.15	CAA, CAG	2.17	9.13	-	5.65
Glycine	Gly	G	-H	75.07	GGX	2.34	9.60	-	5.97
Isoleucine	Ile	I	-CH(Me)CH ₂ Me	131.18	AUU, AUC, AUA	2.36	9.60	-	6.02
Leucine	Leu	L	-CH ₂ CH(Me) ₂	131.18	UUA, UUG, CUX	2.36	9.60	-	5.98
Lysine	Lys	K	-CH ₂ CH ₂ CH ₂ CH ₂ NH ₃ ⁺	146.19	AAA, AAG	2.18	8.95	10.53	9.74
Methionine	Met	M	-CH ₂ CH ₂ SMe	149.21	AUG	2.28	9.21	-	5.74
Serine	Ser	S	-CH ₂ OH	105.09	UCX, AGU, AGC	2.21	9.15	-	5.68
Threonine	Thr	T	-CH(Me)OH	119.12	ACX	2.09	9.10	-	5.60
Valine	Val	V	-CH(Me) ₂	117.15	UAC	2.32	9.62	-	5.96
Arginine	Arg	R	-CH ₂ CH ₂ CH ₂ NH ₂ 	174.2	AGA, AGG, CGX	2.17	9.04	12.48	10.76
Histidine	His	H		155.16	CAU, CAC	1.82	9.17	6.00	7.59
Phenylalanine	Phe	F		165.19	UUU, UUC	1.83	9.13	-	5.48
Proline	Pro	P		115.13	CCX	1.99	10.6	-	6.30
Tryptophan	Trp	W		204.23	UGG	2.83	9.39	-	5.89
Tyrosine	Tyr	Y		181.19	UAU	2.20	9.11	10.07	5.66

Red: positively charged; **Blue:** negatively charged; **Orange:** uncharged polar; **Black:** hydrophobic non-polar; Essential amino acid; Aromatic side group.

- M_r values are given in the neutral (zwitterionic) state, in g mol⁻¹.
- In the RNA codon table, 'X' represents **any** of A, U, G or C.
- At low pH, -COO⁻ is protonated, giving net +ve charge. At high pH, -NH₃⁺ is deprotonated, giving net -ve charge.
- pK_a and pK_b are dissociation constants for the main -COOH and -NH₂ groups respectively.
- pK_x is the dissociation constant for any ionisable side groups (-OH, -SH, -COOH, -NH, -NH₂).
- pI is the isoelectric point, given by $pI \approx (pK_a + pK_b) / 2$ (assumes equal acid and base strengths).
- Selenocysteine (R = -CH₂SeH) and pyrrolysine are special amino acids sometimes incorporated at stop codons.

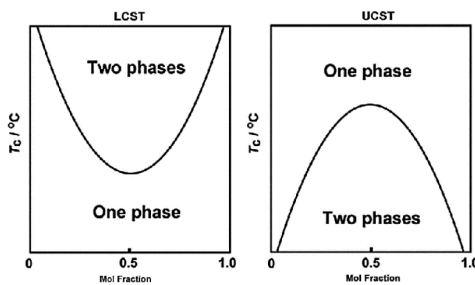
16.5.11. Polyelectrolytes and Hydrogels

Polyelectrolyte: a polymer in which the polymer chains contain formally charged groups, with counterions present in the interstitial medium. Most biopolymers (e.g. proteins, glycosaminoglycans, DNA & RNA) are polyelectrolytes.

- Polyanions ($-\text{COO}^-$, $-\text{SO}_3^-$, $-\text{OSO}_3^-$, $-\text{CSS}^-$, $-\text{OPO}_3^{2-}$): anions on the polymer chain.
- Polycations ($-\text{NH}_3^+$, $=\text{NH}_2^+$, $-\text{NR}_3^+$, $-\text{PR}_3^+$): cations on the polymer chain.
- Polyampholytes: the polymer chain is zwitterionic (both anionic and cationic).

If the number of charged groups is low, there may be microphase separation in which hydrophobic sections of the polymer cluster between regions of high charge density.

Responsive materials: polyelectrolytes conformation is sensitive to the environment.



Temperature changes: induces a phase change between the sol (two-phase, liquid) and gel (one-phase, solid, cross-linked).

Lower critical solution temperature hydrogels (LCST) and upper critical solution temperature hydrogels (UCST) have different phase diagrams in water (shown left), with the type depending on the hydrophobicity/hydrophilicity.

pH changes: presence of H^+ or OH^- can neutralise chain groups and cause aggregation.

- **Anionic** hydrogels swell in basic conditions ($\text{pH} > \text{pK}_b$)
- **Cationic** hydrogels swell in acidic conditions ($\text{pH} < \text{pK}_a$)

Light intensity changes: may induce conformational change e.g. azo compound *trans* \rightarrow *cis*, acting like a switch. Use of light can also induce cross linking (in e.g. methacrylates with an initiator), solidifying the gel state into a more rigid structure.

Hydrogels: a solid network of hydrophilic crosslinked polymer chains in water. Hydrogels applied in technology (e.g. bioinks for 3D printing, Section 17.4.17) are often derived from biopolymers. Hydrogels swell in water but do not dissolve. Hydrocolloids do dissolve and form a gel, independent of temperature. Some polymers commonly used in hydrogels are: (UCST, LCST, variable, anionic, cationic, nonionic)

- **Natural:** agarose, alginate, chitosan, gelatin, collagen, hyaluronan, fibrin, matrigel
- **Synthetic:** PEG diacrylate (PEGDA), modified cellulose, methacrylated gelatin (GelMA), pluronic F127

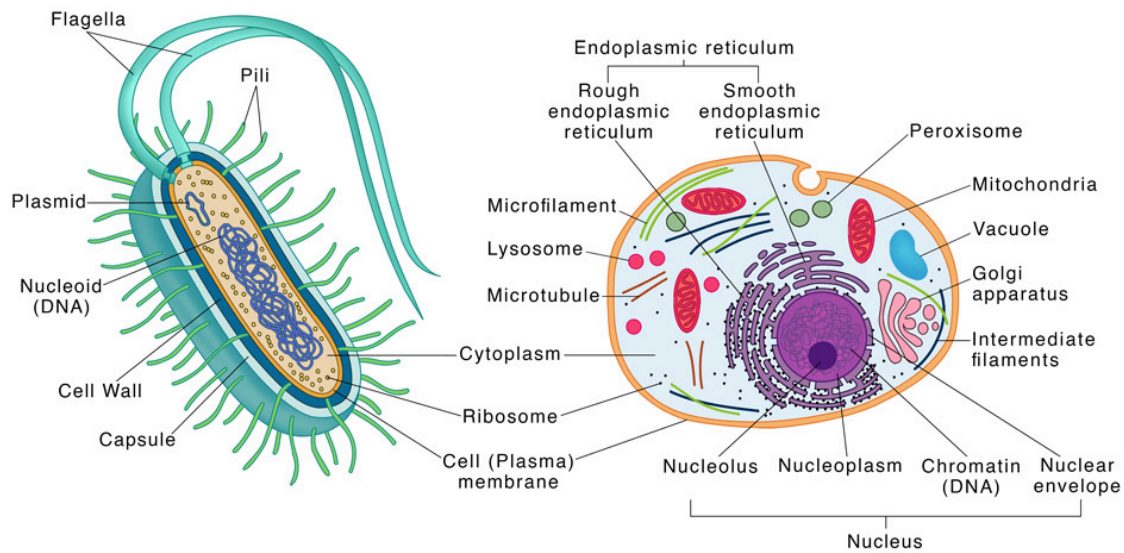
Protein-based hydrogels (e.g. gelatin) can be made mechanically stiffer by addition of kosmotropic anions (e.g. citrate) (Section 16.5.8) during gel formation, due to promoted protein agglomeration.

By combining responsive hydrogels with functional materials (e.g. MoS_2 monolayers, Section 8.6.6), mechanical responses (actuation) can be induced from a variety of stimuli (e.g. light, pH, heat).

B17. MOLECULAR BIOLOGY

17.1. Cellular Biology and Metabolism

17.1.1. Generalised Structure of Cells



Prokaryotic Cell

(Bacteria, Archaea)

Eukaryotic Cell

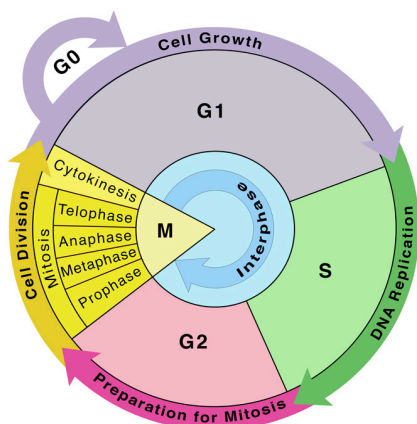
(Protists, Fungi, Animals, Plants)

- **Plant cells additionally include a cellulose cell wall and chloroplasts** (not shown).
- Gram-positive bacteria (shown left) have a thick peptidoglycan cell wall and a thin inner cell membrane.
- Gram-negative bacteria (e.g. *E. Coli*) have a thin cell wall and two cell membranes inside and outside.
- The capsule (slime layer) on a bacteria (shown above) is not always present.
- Hypertonic (concentrated) media lead to plasmolysis (shrinking). Hypotonic (dilute) media lead to cytolysis (swelling).

Structure and Functions of the Main Components and Organelles:

- **Cell membrane:** a phospholipid bilayer bounding the cytoplasm.
- **Cell wall:** a cellulose barrier giving plant and algal cells structure.
- **Cytoplasm:** the interior of the cell, composed of the organelles in an aqueous solution (cytosol).
- **Ribosome:** contains the cell machinery to synthesise proteins from mRNA (translation).
- **Mitochondria:** where respiration occurs to release energy for the cell.
- **Vacuole:** stores water and nutrients as cell sap to maintain the cell's turgor pressure.
- **Nucleus:** contains chromosomes (bundled DNA as chromatin). The nucleolus synthesises ribosomes.
- **Plasmid:** bacterial circular DNA, which can be exchanged with other bacterial cells to pass along genes.
- **Endoplasmic reticulum:** the RER is a ribosome-dense region where proteins are modified for their function.

17.1.2. The Cell Cycle



Healthy, non-stem, somatic cells can undergo ~50 cell divisions before entering cell senescence (the Hayflick limit) due to telomere attrition (Section 17.2.3). Stem cells and gamete cells have much longer replication limits, and cancer cells can divide forever (immortality).

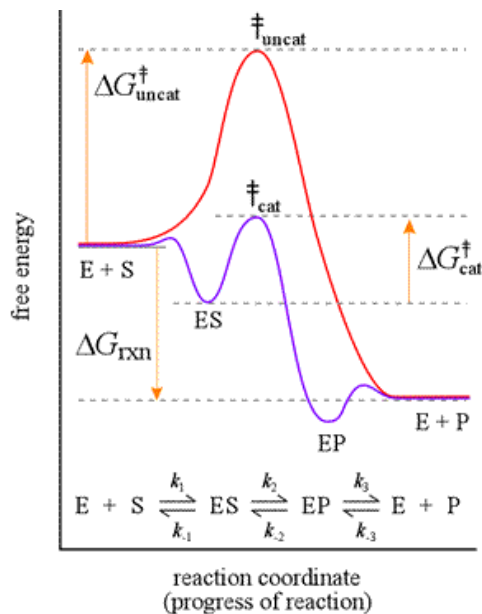
17.1.3. Basic Functions of Common Enzymes

Enzymes are biologically-derived proteins with the ability to act as enantioselective, stereospecific, homogeneous catalysts.

Enzyme name	Biotransformation typically catalysed <i>in vivo</i>
Invertase (sucrase)	sucrose → glucose + fructose
Maltase	maltose → 2 glucose
Lactase	lactose → glucose + galactose
Amylase	starch → <i>n</i> glucose
Emulsin	cellulose → <i>n</i> glucose
Lipase	triglyceride (lipids) + H ₂ O → triol + carboxylic acid
Urease	NH ₂ CONH ₂ → CO ₂ + 2 NH ₃
Carbonic anhydrase	H ₂ CO ₃ → CO ₂ + H ₂ O
Pepsin	proteins → α amino acids (acidic conditions)
Trypsin	proteins → α amino acids (basic conditions)
Nucleases	DNA or RNA → nucleotides
DNA or RNA polymerase	nucleotide phosphates → DNA or RNA
Reverse transcriptase	RNA → DNA

For more on enzymes, including their use in biotechnology, see Section 17.1.11-15. For the chemical structures of enzymes and other biomolecules, see Section 16.5.

17.1.4. Thermodynamics of Enzymatic Metabolic Reactions



Thermodynamics of the Enzyme-Substrate Binding Model

The binding step $E + S \rightarrow ES$ is entropically unfavourable but exothermic due to the electrostatic stabilisation in the active site, so is exergonic.

The reaction $ES \rightarrow EP$ is then performed in the active site, with lower activation energy and so at much higher rate:

$$\Delta G_{cat}^{\ddagger} < \Delta G_{uncat}^{\ddagger} \Rightarrow k_2 \gg k_{uncat}$$

The product then dissociates, which may be either exergonic or endergonic (entropy and enthalpy effects compete).

Catabolic processes (bond breaking) are net **exergonic**.

Anabolic processes (bond forming) are net **endergonic**.

Non-Spontaneous Enzymatic Reactions: when $\Delta G_{rxn} > 0$

If the reaction to be catalysed is endergonic, free energy must be supplied to the system in order to render it spontaneous. Most bond-forming reactions (e.g. DNA replication, protein translation, photosynthesis) are endergonic. The energy may be provided from various sources depending on the reaction and context, such as light, a proton gradient or chemical energy (e.g. ATP). In DNA synthesis, DNA polymerase reacts deoxyribonucleotide triphosphates (dNTPs) with the DNA chain, forming the bond and releasing inorganic pyrophosphate (PP_i).

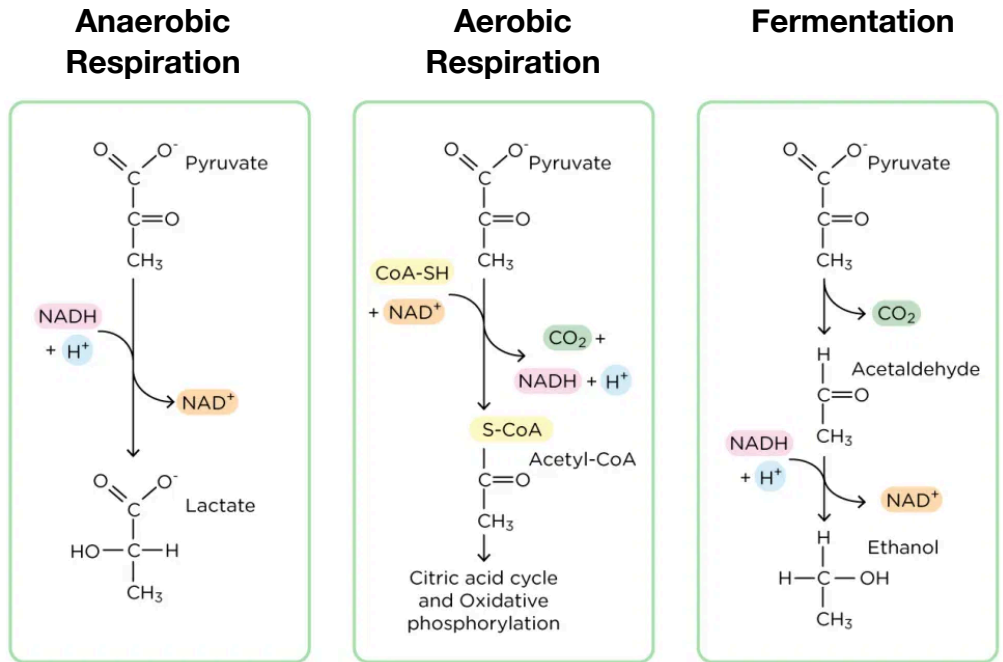
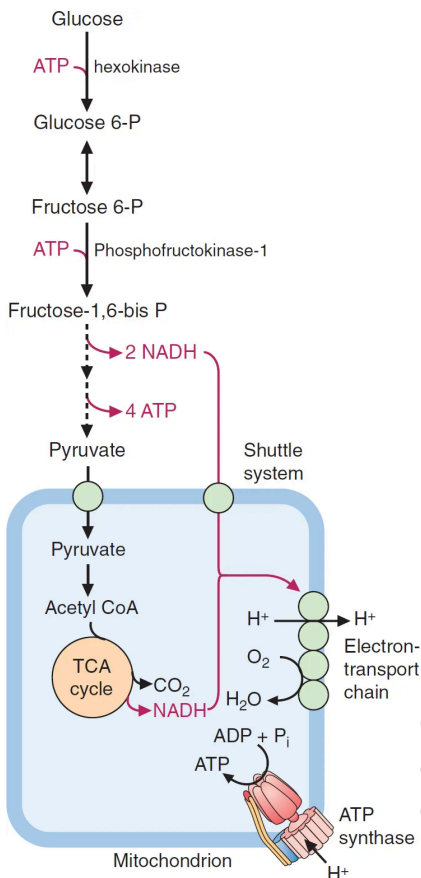
Cells as Open Systems: non-equilibrium allows for spontaneous local structural organisation

- A cell maintains low-entropy homeostasis by increasing the entropy of its surroundings by release of heat to the environment.
- A cell uses available energy sources to drive endergonic reactions away from equilibrium.
- Any cell or organism in equilibrium with its environment is dead.

Thermodynamics of Photosynthesis: $Q < 0$: heat absorbed by system, $W > 0$: work done by system

The reaction $6 \text{CO}_2 + 6 \text{H}_2\text{O} \rightarrow \text{C}_6\text{H}_{12}\text{O}_6 + 6 \text{O}_2$ has $\Delta G > \Delta H > 0$, $\Delta S < 0$. The available non- pV work supplied by the sunlight is $W_{\max} = \Delta G$, and $\Delta H = Q + W$ ($W \leq W_{\max}$). The reaction releases heat $Q \geq T \Delta S$ to the environment, increasing its entropy as $\Delta S_{\text{surr}} = -Q / T \geq -\Delta S$, so overall entropy $\Delta S + \Delta S_{\text{surr}} \geq 0$. Real photon absorption is irreversible, leading to faster entropy generation and lower exergy efficiency ($W = \eta W_{\max} \rightarrow -\Delta S / \Delta S_{\text{surr}} = \eta$ where $\eta \approx 0.35$).

17.1.5. Respiration

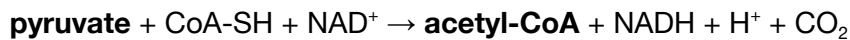


Glycolysis is the conversion of glucose (sugar from foods) to pyruvate. It is the common first part of respiration in all life. It is a 10-step enzymatic process with overall reaction:



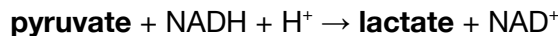
The pyruvate can then be metabolised in different ways: (P_i = PO₄³⁻: inorganic phosphate)

Aerobic Respiration: in mitochondria, with oxygen present, pyruvate is converted to acetyl-CoA:



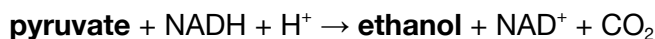
The acetyl-CoA is then used in the citric acid cycle (Section 17.1.4) and then to the electron transport chain (Section 17.1.5), which produces a total of up to 38 ATP per glucose.

Anaerobic Respiration: in the cytoplasm, pyruvate is converted to lactate:



Lactate is typically oxidised to lactic acid, yielding no further ATP, but can also be used to regenerate glucose by gluconeogenesis in the liver (reverse glycolysis, consuming 6 ATP).

Fermentation: in both prokaryotes and eukaryotes, pyruvate is converted to ethanol:

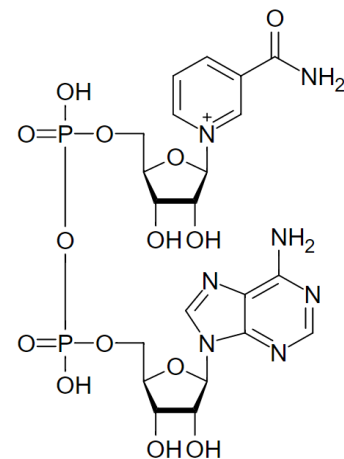
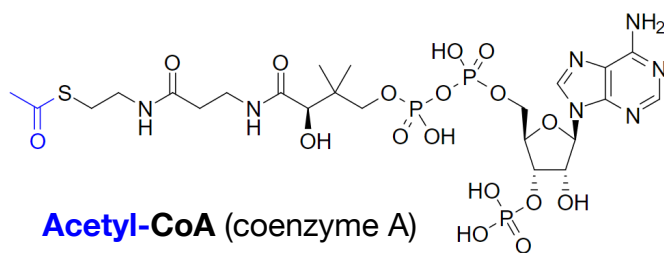
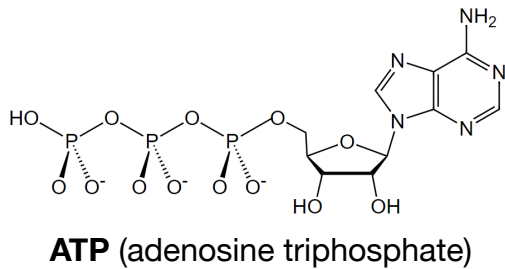
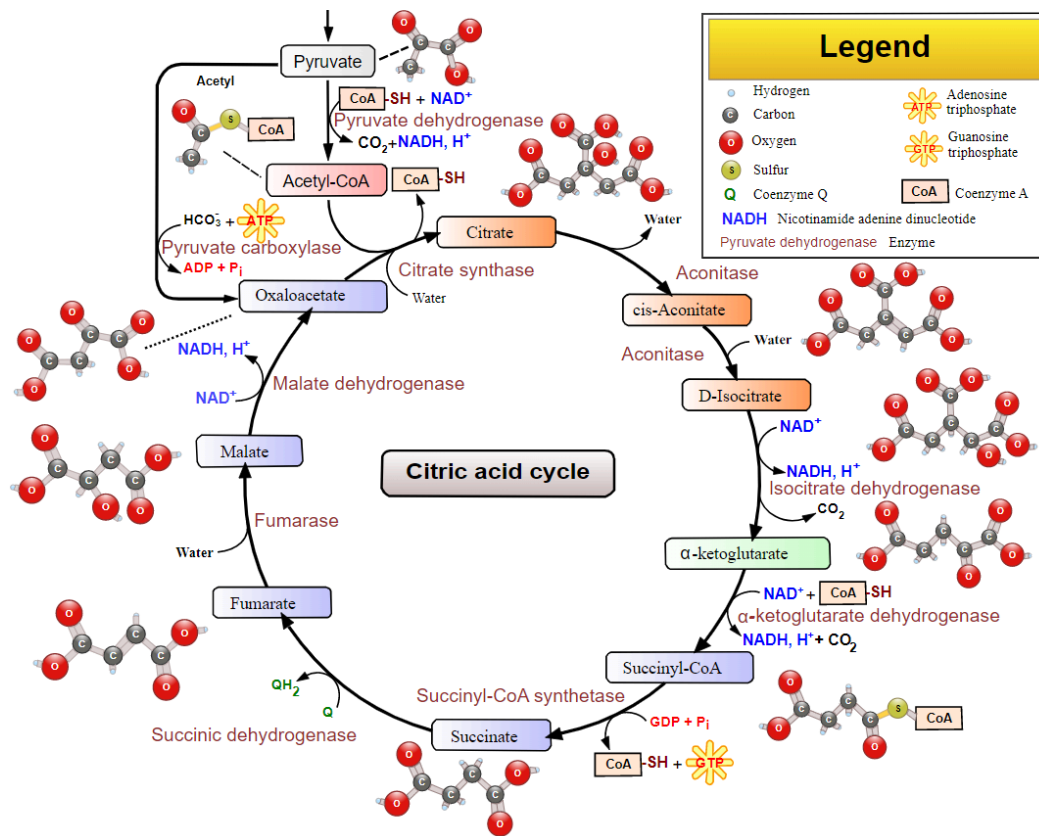


17.1.6. Citric Acid Cycle (Krebs Cycle; TCA Cycle) for Aerobic Respiration

The citric acid cycle phosphorylates GDP to GTP (guanosine triphosphate) from pyruvate (from glycolysis). On a per-cycle basis, the overall reaction is:



GTP can then be converted to ATP via nucleoside-diphosphate kinase: $\text{GTP} + \text{ADP} \rightarrow \text{ATP} + \text{GDP}$.



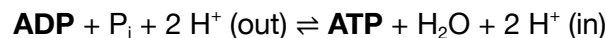
17.1.7. Oxidative Phosphorylation and the Electron Transport Chain

Mitochondria convert ADP to ATP, which provides the necessary chemical energy to carry out a wide range of catabolic reactions.

Electron Transport Chain: sets up and maintains a proton-motive force gradient across the inner mitochondrial membrane (or the plasma membrane in prokaryotes).

- 1. Delivery of electrons by NADH and FADH₂.** Reduced electron carrier cofactors (NADH and FADH₂) from glycolysis/aerobic respiration/citric acid cycle transfer their electrons to molecules near the beginning of the transport chain. In the process, they turn back into NAD⁺ and FAD, which can be reused in other steps of cellular respiration.
- 2. Electron transfer and proton pumping.** As electrons are passed down the chain, they move from a higher to a lower energy level, releasing energy. Some of the energy is used to pump protons, moving them out of the matrix and into the intermembrane space. This pumping establishes an electrochemical proton gradient across the membrane (outside: high H⁺, inside: low H⁺).
- 3. Splitting of oxygen to form water.** At the end of the electron transport chain, molecular oxygen is the electron acceptor, which splits and takes up H⁺ to form water: $\frac{1}{2} \text{O}_2 + 2 \text{e}^- + 2 \text{H}^+ \rightarrow \text{H}_2\text{O}$.

Chemiosmosis-driven synthesis of ATP: as protons flow down their gradient from the intermembrane space back into the mitochondrial matrix, they pass through the molecular machine enzyme ATP synthase, which harnesses the proton flux to synthesise ATP.



ATP synthase consists of two main parts: the F_o proton channel embedded in the membrane and the F₁ catalytic domain extending inside the matrix. F_o consists of the c-ring ('rotor/turbine') and γ subunit ('axle'), while F₁ ('stator') is an assembly of alternating nucleotide (ADP)-binding proteins (α and β) whose conformations are changed between 'closed' and 'opened' by the continuously-rotating γ subunit, permitting reaction with ADP and dissociation of ATP. Two of the proteins in the c-ring are encoded in the mtDNA genome (Section 17.2.4).

The same process occurs in chloroplasts through the thylakoid membrane, with the electron transport chain being initiated by photochemical oxidation (photosynthesis) rather than NADH. The resulting ATP is used by plants in the light-independent reactions of photosynthesis (Calvin cycle, Section 17.3.4). In vacuoles, this system works in reverse, acting as 'V-ATPase', creating a proton gradient by consuming ATP (active transport).

In prokaryotes, these processes all occur across the cell membrane and are used for chemotaxis (Section 17.3.6) via the molecular motor at the base of their flagella.

17.1.8. Glucose Transport and Metabolism in Animals

When a meal is eaten, a series of events allows for the energy to be released in the body:

- 1. Digestion:** salivary amylase enzymes in the mouth partially breaks down starch (more complete for soluble starch) into oligosaccharides (e.g. maltotriose, dextrans) and disaccharides (e.g. maltose). On entering the small intestine, pancreatic amylase, as well as maltase, lactase and sucrase break these down completely into simple sugars (e.g. glucose).
- 2. Transport:** Glucose undergoes active transport into enterocytes lining the small intestines, through a sodium-ion symport transporter protein SGLT1. Glucose then leaves the cells into the hepatic portal vein through GLUT2 (a glucose transporter protein) by facilitated diffusion, **entering the bloodstream**. This occurs within ~1 hour of eating.
- 3. Glucose sensing:** In the islets of Langerhans of the pancreas, glucose enters beta cells via GLUT2, undergoes metabolism to produce ATP. An ion channel cascade leads to exocytosis of vesicles containing insulin, **releasing insulin hormone** into the bloodstream.
- 4. Insulin action:** Insulin binds to its receptor (IR) on muscle cells, fat cells and liver cells, where they induce production of vesicles containing GLUT4, which anchor within the cell membrane (through the cascade: phosphodiesterase activation → cAMP levels drop → activation of protein kinase B (Akt) → translocation of GLUT4). The increased number of cells expressing GLUT4 transporters allow for **more glucose uptake** by muscle and fat cells.
- 5. Respiration:** Intracellular glucose rapidly undergoes glycolysis to pyruvate in the cytosol, then is transported into the mitochondria to undergo the citric acid cycle, which drives the electron transport chain, which in turn drives ATP synthase to generate ATP (Section 17.1.5-7). The ATP is used as chemical energy in a wide variety of metabolic processes.

Glycogenesis: glucose-rich blood enters hepatocytes in the liver via GLUT2. Excess glucose can then be stored as glycogen (glycogenesis), which requires signalling from insulin.

When blood glucose is low, pancreatic alpha cells release **glucagon** hormone. Glucagon acts to raise blood glucose by 1) stimulating **glycogenolysis**, 2) promoting **gluconeogenesis**, 3) inhibiting glycolysis, 4) promoting **lipolysis**. Insulin and glucagon together form a negative feedback control system by which dietary variations in glucose are smoothed out over time, maintaining cellular homeostasis.

Type 1 Diabetes: an autoimmune disease in which pancreatic beta cells are attacked, blocking insulin production, leading to insufficient glucose uptake by cells in the body. Glucose therefore remains at high levels in the bloodstream (hyperglycemia). This promotes lipolysis, from which ketone metabolites accumulate leading to metabolic acidosis. Type 1 diabetes requires regular insulin injection.

Type 2 Diabetes: cells become resistant to the presence of insulin, rendering it ineffective at releasing GLUT4 transporters, leading to insufficient glucose uptake by cells in the body. The mechanism by which GLUT4 production is impaired in type 2 diabetes is not fully understood. Type 2 diabetes is generally associated with obesity; losing visceral fat and eating less sugar often resolves type 2 diabetes by increasing insulin sensitivity.

17.1.9. Gas Exchange in Animals

Nonpolar gas molecules such as O_2 and CO_2 are soluble in lipids and can freely cross cell membranes by diffusion. Oxygen gas is inhaled from the atmosphere into the lungs, through the bronchioles and diffuses through alveoli into capillaries. In the bloodstream, oxygen binds to haemoglobin proteins in erythrocytes (red blood cells) for transport, forming oxyhaemoglobin.

In **oxyhaemoglobin**, the haem B cofactor complexes with an iron ion centre, which is also bound to oxygen and a proximal histidine residue on the polypeptide. A distal His also stabilises the oxygen by hydrogen bonding. There is a resonance structure between Fe^{2+}/O_2 (ferrous, oxygen) and Fe^{3+}/O_2^- (ferric, superoxide). The electronic properties of the iron ion and the porphyrin ring contribute to blood's red colour. The iron ion may also occur purely in the Fe^{3+} oxidation state (methemoglobin), which has reduced oxygen-carrying capacity.

In **deoxyhemoglobin**, the haemoglobin complex dissociates, and the Fe^{2+} ion lies just outside of the conjugated porphyrin plane, broadening the band structure and making deoxygenated blood a slightly darker red than oxygenated blood. This releases free O_2 into the blood plasma, diffusing through the interstitial fluid, across cell membranes and into mitochondria, where it is consumed in aerobic respiration (the electron transport chain, powers ATP synthase (Section 17.1.7)). Oxygen is also used in gluconeogenesis (rev. glycolysis) in the liver to convert lactate (product of anaerobic respiration) to glucose.

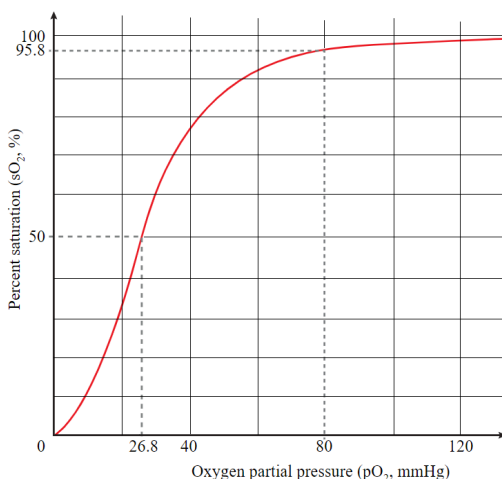
Aerobic respiration generates CO_2 , which is dissolved in the bloodstream by the carbonate buffer, with some gaseous CO_2 remaining dissolved in the plasma. It is transported through alveoli to the lungs where it is exhaled.

Blood contents: ~55% plasma (low-density pale yellow fluid containing water, proteins, nutrients and hormones), ~44% red blood cells (erythrocytes: most dense) and ~1% white blood cells (basophils, neutrophils, eosinophils, monocytes, lymphocytes) and platelets (thrombocytes).

Blood pH buffers: the pH of the blood plasma must be 7.40 ± 0.05 to prevent acidemia/alkalemia.

- Carbonate buffer: $CO_2 + H_2O \rightleftharpoons H_2CO_3 \rightleftharpoons HCO_3^- + H^+ \rightleftharpoons CO_3^{2-} + 2 H^+$
- Phosphate buffer: $H_2PO_4^- \rightleftharpoons HPO_4^{2-} + H^+$

Oxygen-haemoglobin dissociation curve (1 mmHg = 133.322 Pa)



The pH of blood is controlled by the carbonic anhydrase enzyme, which catalyses the reaction

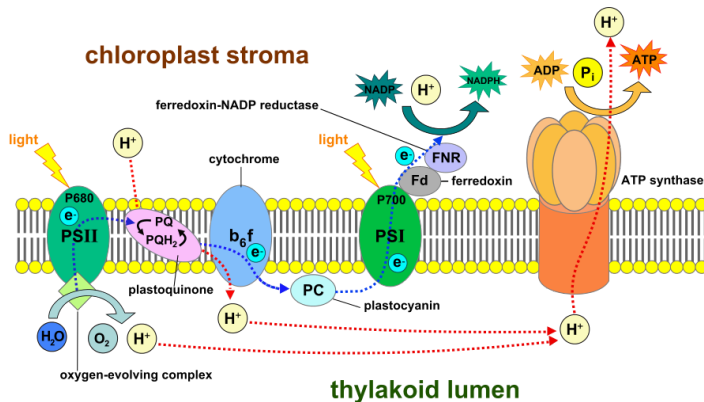


Bohr effect: an increase in blood CO_2 causes a decrease in pH, which induces a conformational change in haemoglobin proteins (relaxed; high-affinity \rightarrow taut; low-affinity) which makes it more difficult to bind O_2 .

Carbon monoxide (CO) severely inhibits O_2 transport by binding ~250 times more efficiently. CO also triggers the Bohr effect, further enhancing CO uptake by other haem sites.

17.1.10. The Calvin Cycle and Photosynthesis in Plants

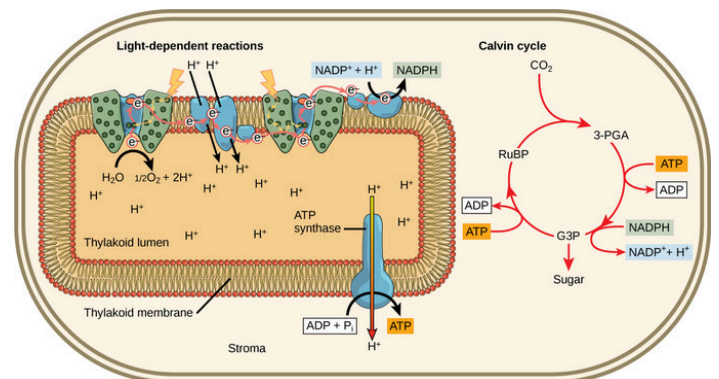
Photosynthesis occurs in chloroplasts (and cyanobacteria). It consists of two reaction sequences (light dependent set in the thylakoid lumen and light independent set in the stroma) which overall generate glucose ($C_6H_{12}O_6$) and oxygen from CO_2 , water, and light.



Light-dependent reactions

- 1. Photosystem II:** photons incident on the fully-conjugated porphyrin ring of a chlorophyll molecule form polarons (excited resonance electrons), which via carotenoids conjugate to two chlorophyll molecules (P680). The electron is passed on to pheophytin, leaving a hole that induces oxidation of water at the oxygen-evolving complex (a Mn_4CaO_5 complex).
- 2. Electron transport chain:** the passed electron is shuttled through a series of other membrane-bound proteins (plastoquinone, cytochrome b_6f , plastocyanin). Photosystem I (P700) re-energises the electrons. The energy of the electron is used to form a proton gradient which converts NADP to NADPH.
- 3. ATP production:** the proton gradient is used to drive ATP synthase, forming ATP in the stroma, used to power the Calvin cycle.

The Calvin cycle is the only mechanism of photosynthesis in C_3 plants. In **C_4 plants**, CO_2 is fixed into malic acid in the mesophyll as an intermediate before being converted back into CO_2 to enter the Calvin cycle in the bundle sheath, as a defence against photorespiration. In **CAM plants**, the malic acid intermediate step occurs only in the dark. In cyanobacteria, photosynthesis occurs directly on free chlorophyll A molecules in the cytoplasm.

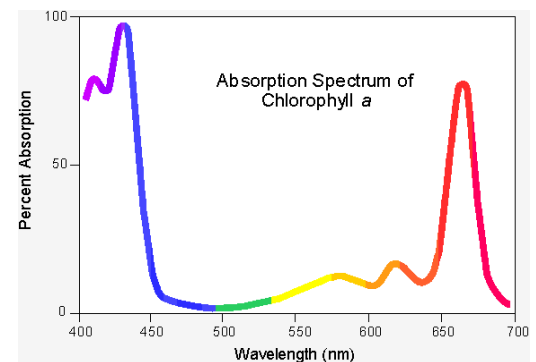


Light-independent reactions (Calvin cycle; shown on right)

- 1. CO_2 fixation:** $3 CO_2 + 3 RuBP \rightarrow 3 \text{ 3-PGA}$, via RuBisCO.
- 2. Reduction:** $6 \text{ 3-PGA} + 6 ATP + 6 NADPH \rightarrow 6 G3P + 6 ADP + 6 NADP^+$.
- 3. Regeneration:** $5 G3P + 3 ATP \rightarrow 3 RuBP + 3 ADP + 2 P_i$, via several sugar intermediates.

Glucose formation: G3P is converted to fructose-1,6-bisphosphate via aldolase, which is used to make glucose via gluconeogenesis.

(RuBP: ribulose-1,5-bisphosphate,
3-PGA: 3-phosphoglycolic acid,
G3P: glyceraldehyde 3-phosphate.)



17.1.11. Chemosynthesis and Nitrogen Fixation in Prokaryotes

Chemosynthesis and nitrogen fixation are some of the most primitive metabolic processes evolved by early life, as a method of deriving energy from the few consistent chemical sources available on early Earth (see Section 17.5).

Chemosynthesis: conversion of inorganic chemicals to organic chemicals without light

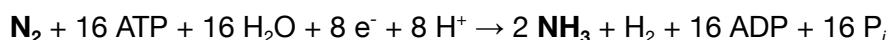
Some extremophile deep-sea microorganisms (chemolithotrophs), including bacteria and archaea, can derive energy from chemicals released from hot hydrothermal vents and cold seeps (seafloor fissures). There are a range of possible pathways, including sulfur, iron pyrites and methane, such as:



The carbon products can then be converted to glucose by carbon fixation processes. Sulfides and sulfates can be reduced to elemental sulfur. Some chemosynthetic organisms are hosted as internal endosymbionts within deep-sea tubeworms, clams and mussels.

Nitrogen Fixation: conversion of nitrogen into ammonia

Some bacteria, including cyanobacteria and green sulfur bacteria, can metabolise nitrogen into ammonia with a high ATP cost via the nitrogenase enzyme complex with overall reaction:



Nitrogenase is composed of an iron protein (Fe) reductase and an iron-molybdenum (FeMo) protein. The Fe protein binds ATP, pumping electrons and protons into the FeMo cofactor ($\text{Fe}_7\text{MoS}_9\text{C}$) over a P-cluster between the two to form the 'Janus intermediate'. With further proton addition, this can progressively reduce a molecule of nitrogen (N_2) bound to the FeMo cofactor into hydrazine (N_2H_4) then ammonia (2NH_3). The precise mechanism varies by circumstances and is not fully understood.

Molecular O_2 inhibits nitrogenase, so cyanobacteria must isolate photosynthesis from nitrogen fixation, either by only nitrogen-fixing at night, or in communities of cyanobacteria, by nitrogen-fixing only in specialised cells (heterocysts) that are impermeable to O_2 and that degrade photosystem II prevent local oxygen production.

Recently, the geometry of the FeMo cofactor has inspired a synthetic iron complex catalyst used in the Haber process for synthetic ammonia production from nitrogen, and an alternative approach of directed evolution on synthetic nitrogenase enzymes has given way to a route to agricultural fertiliser synthesis without relying on fossil-fuel-derived hydrogen.

The resulting ammonia is used in various reactions, such as amino acid synthesis, nucleotide synthesis, glutamate metabolism and the urea cycle. Nitrogen-fixing bacteria in soils are a key part of the nitrogen cycle in plants (Section 19.2.7), where they can release ammonium into the soil for uptake as nitrates by plants.

17.2. Genetics and Evolutionary Developmental Biology

17.2.1. Mendelian Genetics and Inheritance

Types of Reproduction

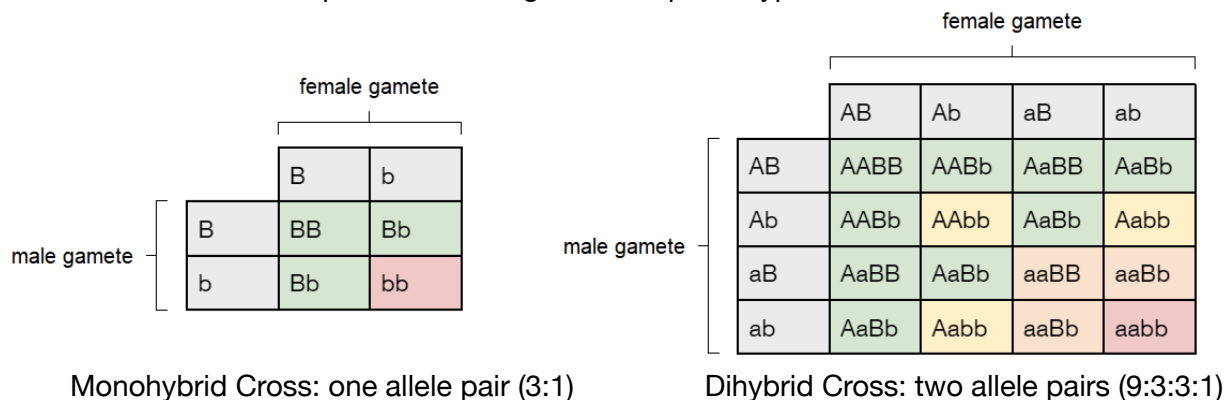
Sexual reproduction involves the joining (fusion) of male and female gametes (sperm and egg cells in animals; pollen and egg cells in flowering plants). There is mixing of genetic information (gamete formation uses meiosis: spermatocyte → 4 spermatozoa, oocyte → 1 ovum + 3 nonfunctional eggs, then gamete fusion at fertilisation to form the zygote) which leads to variety in the offspring.

Asexual reproduction involves only one parent and no fusion of gametes. There is no mixing of genetic information (mitosis), producing genetically identical offspring (clones).

Both Types: e.g. malarial parasites (asexually in human host, sexually in mosquito), many fungi (asexually by spores, sexually to give variation), many plants (sexually by seeds, asexually by runners such as strawberry plants, or bulb division such as daffodils).

Gametes (sex cells) are haploid (n chromosomes; $n = 23$ in humans = 22 autosomes + X or Y)
 Somatic cells are diploid ($2n$ chromosomes; $2n = 46$ in humans = 22 autosome pairs + XX or XY)

Alleles: different sequences of a gene at a given locus on a chromosome. A pair of chromosomes may have the same (homozygous) or different (heterozygous) alleles of a given gene: in the simplified model, the genotype is written e.g. “BB / Bb / bb”. The phenotype (presenting trait) for the dominant “B” is expressed unless both gametes provide the recessive “b”. Heterozygous alleles are ‘carriers’ of the recessive trait despite not showing it in their phenotype.



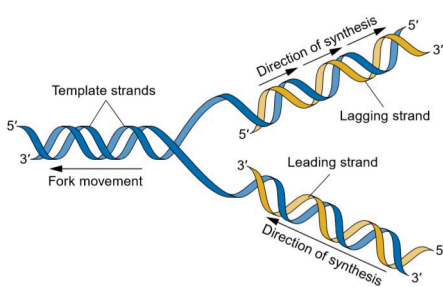
Most traits are not controlled by a single gene. Simplifications are often made to allow for probabilistic analysis of Punnett squares, such as from inherited disorders (e.g. polydactyly, cystic fibrosis, alopecia). The sex chromosomes X and Y can be treated as codominant ‘alleles’.

Mendelian genetics provided a biological mechanism for Darwin’s theory of evolution by natural selection, with their combination forming the ‘modern synthesis’ (‘neo-Darwinism’). Evolution is therefore defined as the variation of allele frequency in a given population.

17.2.2. DNA: Replication, Transcription and Translation

DNA semiconservative replication occurs in the S phase of the cell cycle, in the nucleus (in eukaryotes). DNA transcription and RNA translation occur in the G₁ and G₂ phases. For the structures of DNA and RNA, see Section 16.5.7.

The 'central dogma of molecular biology': **DNA** → **RNA** → **Protein**. (exception: reverse transcription)

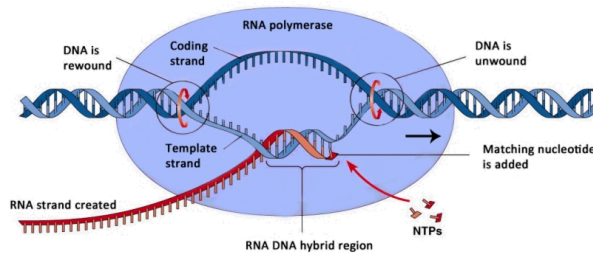


DNA Replication

Initiation: helicase unwinds the helix by disrupting the hydrogen bonds. This creates a replication fork. Topoisomerase relieves torsional strain ahead of the replication fork by breaking, untwisting, and reconnecting the DNA. SSB proteins stabilise the separated strands.

Leading Replication: primase anneals a short RNA sequence (primer) to each half of the DNA. DNA can only be synthesised in the 5' → 3' direction, so only one strand can anneal free dNTPs (deoxynucleotide triphosphates) continuously (the leading strand), using DNA polymerase III in prokaryotes (different in eukaryotes).

Lagging Replication: short 'Okazaki fragments' on the 5' to 3' strand (lagging strand) are formed, one at a time, requiring a primer for each. DNA polymerase I (in prokaryotes) replaces the RNA primers with DNA nucleotides. In eukaryotes, several enzymes fulfil this role together. Ligase joins fragments of DNA together on the lagging strand.



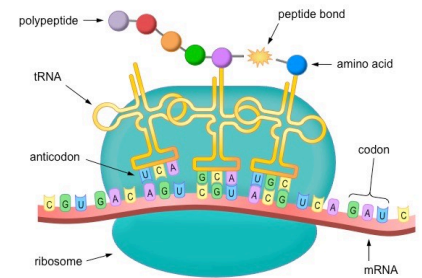
DNA Transcription

Initiation: RNA polymerase binds with various transcription factors to a promoter sequence (e.g. TATA box in eukaryotes) of DNA near the beginning of a gene. The two strands (coding, template) of DNA are separated, forming a replication bubble.

Elongation: RNA polymerase adds complementary ribonucleotides of the template strand, building in the RNA 5' → 3' direction, with the synthesised strand of RNA being released continuously.

Termination: a termination sequence (AAUAAA) is recognised near the 3' end of the pre-mRNA once the full gene has been transcribed. The DNA is returned to its original state.

Post-Transcriptional Modification: A 5' cap (single modified G nucleotide) and a 3' tail (poly-A sequence) are added to each end of the pre-mRNA. A spliceosome enzyme cuts out non-coding intron sections. The remaining coding exon sections are combined. The 5' cap is recognised by a nuclear pore complex, allowing the mRNA to leave the nucleus.



RNA Translation

The small ribosomal subunit (**rRNA**) binds to the start of the mRNA.

Aminoacyl-tRNA synthetases (ARSs) attach amino acids to one end of tRNA molecules. A tRNA molecule carrying methionine binds to the start codon of the mRNA.

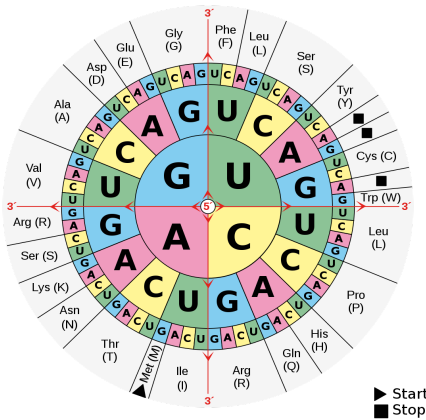
The large ribosomal subunit binds to form the complete initiation complex.

During the elongation stage, new tRNA molecules corresponding to the next codon triplet enter the ribosome, binding, and resulting in the carried amino acids becoming linked by a peptide bond, forming a polypeptide.

When a stop codon is encountered, there exists no corresponding tRNA carrier, so termination occurs. The complex dissociates and the amino acid sequence detaches.

The polypeptide enters the rough endoplasmic reticulum for folding and the Golgi apparatus for further modification (e.g. to form a proteoglycan), assisted by chaperone proteins, to form the final protein.

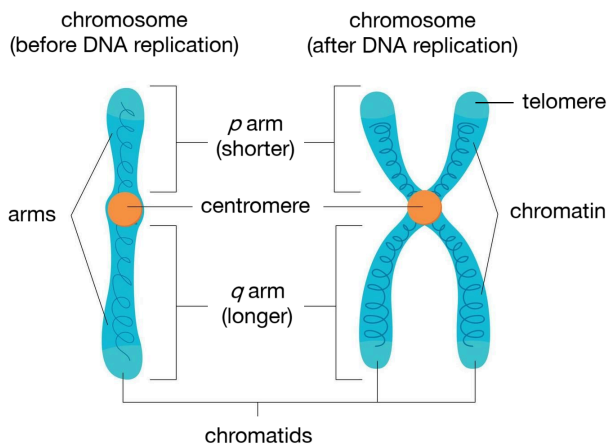
17.2.3. RNA to Amino Acid Inverse Codon Mappings



The genetic code conversion process is highly conserved throughout evolution, in most organisms.

In a coding section of a gene, each consecutive triplet of mRNA codons (directed from 5' to 3') forms a single amino acid, as determined from the chart. The **start codon** is methionine (in eukaryotes) or formyl methionine (in prokaryotes). The **stop codons** are sometimes called amber (UAG), opal/umber (UGA), ochre (UAA). In some cases, these serve other functions, and can incorporate special amino acids instead.

17.2.4. Nuclear DNA (Chromosomes)



In eukaryotes, the main component of the genome is the chromosomes, which are found inside the nucleus of most cells. The nucleus is surrounded by the nuclear envelope (with an inner and outer membrane) which has nuclear pores to protect the chromosomes from chemical damage while allowing controlled access across the membrane. Diploid cells have $2n$ chromosomes, with chromosomes coming in pairs (one maternal, one paternal). The two chromosomes are homologous (contain the same genes) but are not identical due to natural variation in the population. During the interphase of a cell cycle, each chromosome duplicates into two identical sister chromatids, conjoined at the centromere.

Chromosomal Origins of Mendelian Genetics: the 'law of segregation' is accounted for by the fact that during meiosis I, the maternal and paternal chromosomes are separated into each new cell, so only one allele is carried forward; the 'law of independent assortment' is accounted for by the fact that different traits arise from genes on different chromosomes, which are arranged randomly when meiosis occurs.

Centromere: the site where the two sister chromatids bind together. The centromere DNA sequence contains groups of long repeating sequences (such as α -satellite DNA; alphoid repeats). The identity of the centromere sequence varies between species.

Telomeres: the telomere sequence 'TTAGGG' is repeated several hundreds of times on the ends of the arms of each chromosome. The RNA primers for the last Okazaki fragment at the end of a DNA strand cannot be removed during DNA replication, resulting in slight chromosome shortening at each cell cycle. In gametes, telomerase is responsible for gradually regenerating the telomere sequences, but it is marginally too slow to keep up with the rate of cell replication, leading to gradual information loss (telomere attrition; replicative senescence), which is the main biomarker for cell ageing. Telomerase is activated in cancerous somatic cells, contributing to their immortality.

17.2.5. Non-Nuclear DNA and Ribosomal RNA

Mitochondria and chloroplasts inside eukaryotic cells originate as endosymbionts and share many similarities with prokaryotes.

Mitochondrial DNA (mtDNA)

- **Structure:** animal mtDNA is a singular circular chromosome, with a 'heavy' (H) strand and a 'light' (L) strand, no introns, of size 11-28 kbp. Arrangements differ in other kingdoms.
- **Transcription:** mitochondria undergo their own cell cycle, independently of the host cell, using binary fission for replication. Many components required for mtDNA replication, including subunits of DNA polymerase and helicase, must be sourced from the host cell as they are encoded in nuclear DNA. mtDNA uses single gene promoters, not operons.
- **Translation:** The mt-mRNA is translated in mitochondrial ribosomes. Vertebrate mtDNA uses different start/stop codons than nuclear DNA, and also has some differences in the codon table.
- **Mitoeptigenetics:** mtDNA methylation is observed as a mode of mitochondrial gene regulation.
- **Human mtDNA genes:** human mtDNA is 16,569 bp long, with genes primarily responsible for respiration, including for subunits of ATP synthase, subunits for cytochrome c oxidase, NADH dehydrogenase, humanin micropeptide, as well as 22 tRNAs and 2 rRNAs. Transpositions from mtDNA into nuclear DNA (NUMTs, nuclear-mitochondrial segments) happen often. Mutations in either the main nuclear DNA or mtDNA can cause a variety of mitochondrial diseases, limiting the energy availability from respiration for the host cell/organism.
- **Human Haplogroups:** mtDNA is maternally conserved (matrilineal), since the mitochondria-containing midpieces of sperm fall away when they fertilise the egg. It is subject to a slow and steady mutation rate (the human mtDNA molecular clock). Variations in mtDNA can be grouped by single nucleotide polymorphisms (SNPs) and microsatellite DNAs (STRs) and are indicative of broad human communities, useful for tracing migration patterns in recent evolutionary history (paleogenomics). The patrilineal equivalent is obtained by similar analysis of the Y-chromosomal DNA (Y-DNA).

Chloroplast DNA (cpDNA)

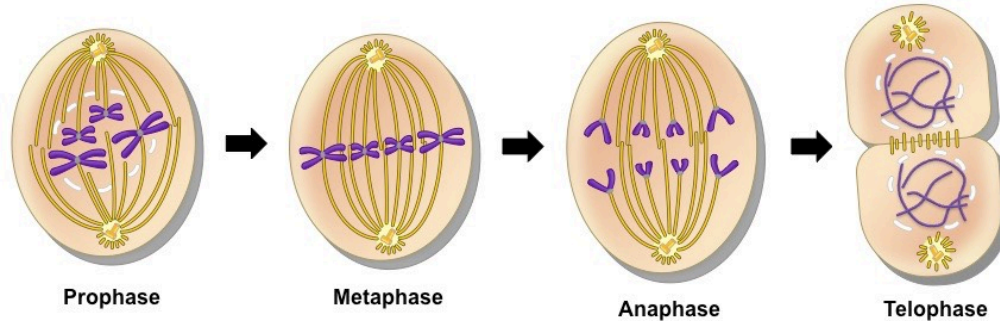
- Plant cpDNA is a singular circular chromosome of size 120-170 kbp.
- Some cpDNA genes have introns and are typically organised into operons.
- cpDNA genes are primarily responsible for photosynthesis, including RuBisCo, photosystem I and II, and ATP synthase, as well as components for replication, including subunits of RNA polymerase, ~30 tRNAs and 4 rRNAs.

Ribosomal RNA (rRNA)

- Ribosome synthesis: nuclear genes for the rRNA precursors are transcribed and ligated to form the small and large ribosomal subunits in the nucleolus.
- Small and large subunits bind with ribosomal proteins to form the ribosome with stem-loop motifs.
- Most of the rRNA genes are highly conserved across all three domains of life.

17.2.6. Mitosis (Somatic Cell Division)

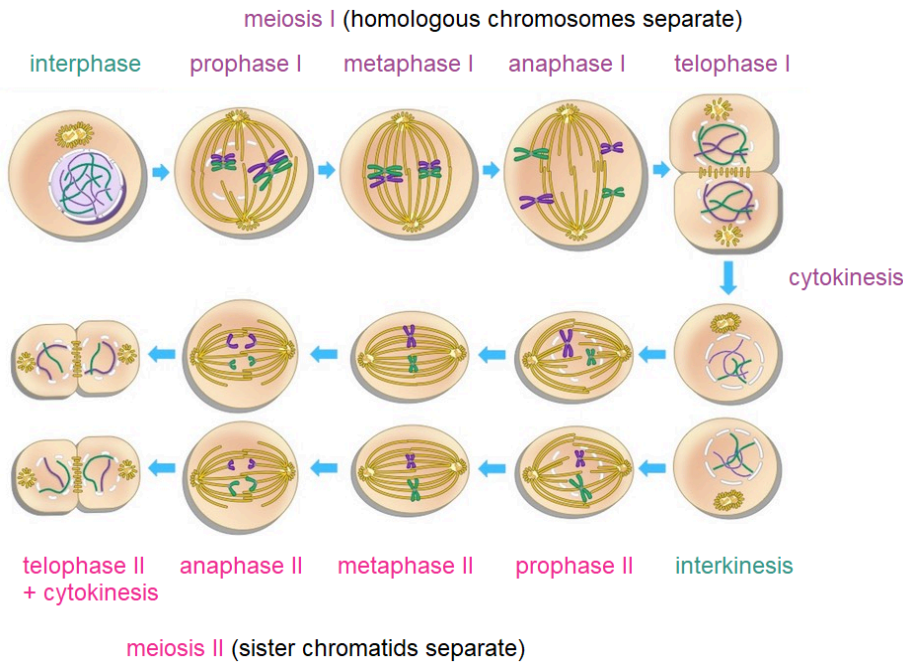
Mitosis involves the copying of genetic material to produce identical cells (barring mutations).



- 1) **Prophase:** chromosomes assemble, centrosome duplicates, spindle fibres form. The microtubules between the centrosomes extend in length.
- 2) **Prometaphase:** nucleus breaks apart, kinetochores attach at the centromeres of the pairs.
- 3) **Metaphase:** chromosomes aligned in the centre, the two centrosomes are at the poles of the cell.
- 4) **Anaphase:** separase enzyme cleaves the cohesins of the centrioles, then the kinetochores pull the chromatids apart by motor proteins, cell elongates.
- 5) **Telophase:** two new nuclei form around each set of chromosomes.
- 6) **Cytokinesis:** the cytoplasm will continue to divide, pinching off in two.

17.2.7. Meiosis (Gametic Division)

Meiosis involves mixing of genetic material in a diploid cell to produce four identical haploid cells.



1) Meiosis I, interphase: DNA replication to form a diploid cell.

2) Meiosis I, prophase I: pairs of chromosomes may exchange fragments of themselves by 'crossing over'.

3) The remainder of meiosis I is similar to mitosis, with each chromosome being pulled randomly to a pole.

4) Meiosis II: functionally identical to mitosis in each cell.

Anisogamy: the difference in size and form between the two sexes of gametes.

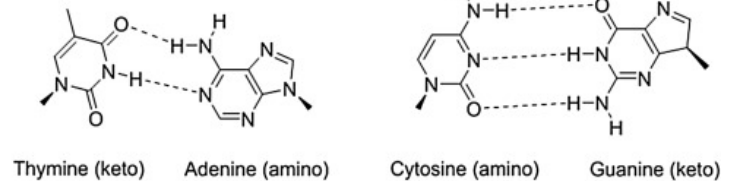
17.2.8. Genetic Mutations

For the structure of DNA and nucleobases, see Section 16.5.9.

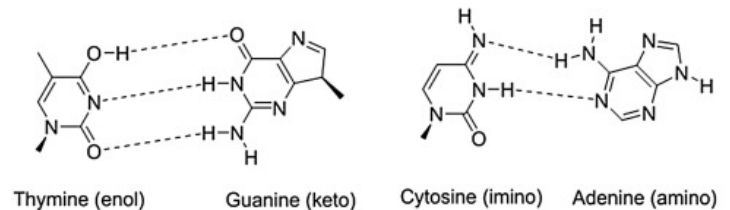
Sources of DNA Mutations

- Tautomerism** of nucleobases (shown right), where ketone/amine groups on bases are in chemical equilibrium with their rarer enol/imine groups respectively (Section 16.1.4), which have different hydrogen bonding environments, prompting DNA polymerase to insert the wrong base. Fixed by other DNA polymerases (proofreading / DNA repair).
- Deamination** of 5-methylcytosine (epigenetically marked C) to thymine, and of cytosine to uracil. These hydrolysis reactions occur spontaneously. Fixed by nucleases and glycosylases (base excision repair).
- High energy radiation (e.g. UVB, X-rays)** can cause bonding between adjacent T or C bases on the same strand (pyrimidine dimer) to form a cyclobutane ring between them, causing a kink in the DNA helix. Fixed by photolyases (nucleotide excision repair).
- Chemical mutagens** such as oxidising agents can oxidise nucleobases, changing their structure and identity of the corresponding base. Fixed by nucleases and glycosylases (base excision repair).

(A) Standard base pairing arrangements



(B) Anomalous base pairing arrangements



DNA Repair: DNA damage can be fixed, but occasionally a mistake will occur (mutation).

- 3' (to 5') exonuclease activity (proofreading):** nucleotides at 3'-OH termini can be removed, allowing for in-place correction during replication before continuing. Exhibited by DNA polymerase I and III.
- 5' (to 3') exonuclease activity (DNA repair):** nucleotides at 5'-P termini can be removed, allowing for removal of existing DNA nucleotides. Exhibited by DNA polymerase I.
- Nucleotide excision repair (NER):** replacement of a short single strand of nucleotides.
- Base excision repair (BER):** replacement of oxidised, alkylated or deaminated bases.
- Double-stranded break repair (DSBR):** includes homologous recombination (copying from undamaged sister chromatid) and non-homologous end-joining (NHEJ, deliberate indel formation).

Point mutation: a change in a single nucleotide in the template strand of DNA (a missense mutation). Can be benign if no change in the resulting amino acid, or if in an intron section. Point mutations can be written in terms of the amino acids: e.g. Glu346Lys (glutamic acid at protein position 346 becomes lysine). If the new mRNA triplet is a stop codon, the resulting incomplete protein is usually non-functional (a nonsense mutation).

RNA mutations can also occur (post-transcriptional modification of mRNA). The main mechanism is by adenosine-to-inosine RNA editing, in which an adenine nucleoside (adenosine) is deaminated by an ADAR enzyme to form inosine, which mimics a guanine nucleobase instead (a point mutation).

This mode of mutation does not affect the genome, but can increase the diversity of the 'transcriptome'. It occurs at high rates in cephalopods (a class of molluscs: octopuses, squid, cuttlefish), potentially as a method of rapid environmental adaptation.

Other types of mutations: often having larger influence than point mutations

- **Frame shift mutation:** single insertions or deletions (indels) in DNA, resulting in a change in the reading frame (large number of mutations). This can significantly change the tertiary structure and size of the encoded protein, making the protein non-functional or of alternative function.
- **Transposons:** movement of a section of DNA. Can lead to **gene/chromosomal duplication, inversion or translocation**, which allow for significant diversification of the genome (neofunctionalisation). If the transposon contained *cis*-regulatory elements e.g. a promoter region, an adjacent non-coding section may become coding (*de novo* genes).

If a mutation occurs in gametes or their stem cell progenitors, it can be passed to the next generation, as the alleles have the chance to form the offspring's genome at fertilisation.

Gene flow and horizontal gene transfer: exchange of genetic material between cells or populations e.g. plasmid conjugation: bacterial plasmids are transferred from one bacterium to another, conferring e.g. antibiotic resistance. This forms one of the mechanisms of evolution.

17.2.9. Gene Regulation in Eukaryotes (Epigenetics)

The majority of the genetic information in a eukaryotic cell is found in the chromosomes, in the nucleus of eukaryotic cells. Histones are octamer protein particles around which DNA coils to form nucleosomes, which in turn supercoils to form chromatin which comprises the chromosomes. DNA may be accessible (euchromatin) or inaccessible (heterochromatin) to transcription factor enzymes, altering gene activity.

Mechanisms of Regulation

- **DNA methylation:** DNA methyltransferases (DNMT) add a CH₃ group to cytosine bases to form 5-methylcytosine. Results in **gene silencing** due to inhibition of transcription proteins and recruitment of methyl-cytosine-binding proteins (MeCPs) and is associated with increased cell specialisation. Demethylation results in a reversal towards the pluripotent stem cell state. During DNA replication, methylation can be produced (by e.g. DNMT1) on the new strand at CpG dinucleotides (CG islands) to produce methylated bases at adjacent positions on each strand. 5-methylcytosine can spontaneously deaminate to thymine, causing a point mutation (C → T).
- **Histone acetylation and deacetylation:** histone acetyltransferases (HAT) adds and histone deacetylases (HDAC) remove COCH₃ groups to and from N-terminal tails of core histone subunit proteins. Acetylation results in **gene expression** due to the loose packing of histones. This can also induce histone remodelling (euchromatin formation) due to the conformational changes, which can further increase DNA availability. This can also be caused by ATP-driven complexes which eject nucleosomes from the histones.
- **Other histone modifications:** histone methyltransferases add a CH₃ group to lysine side chains (**histone methylation**); protein kinases add a phosphate group to serine side chains (**histone phosphorylation**); core histone subunits can bind to ubiquitin or SUMO proteins, which in turn bind lysine side chains (**histone ubiquitination / SUMOylation**). Depending on the site targeted, these can result in **either silencing or expression** by inducing chromatin remodelling.
- **Non-Coding RNA:** micro-RNA (miRNA) and short-interfering-RNA (siRNA) can bind or cleave newly-transcribed mRNA to prevent its translation, resulting in **gene silencing**.
- **Positive Gene Regulation:** a signalling molecule (e.g. cAMP) can bind to an activator protein, which can bind to DNA near the promoter sequence, enhancing the affinity of RNA polymerase for the promoter, resulting in **gene expression**. This can also occur in operons (Section 17.2.5).
- **Cis-Regulatory Elements (Promoters, Enhancers, Silencers, Operators):** transcription factors can bind to specific intron (non-coding) regions of DNA, which then recruit other activator proteins associated with the promoter region (e.g. TATA box) of a given gene (a protein-DNA interaction). This results in the DNA bending and looping around to bring the two regions close together, which recruits RNA polymerase to the developing transcription-initiation complex.

Example: Human lactose tolerance. The *LCT* gene codes for lactase (breaks lactose into glucose and galactose). A regulatory region on the intron of the *MCM6* gene, which typically codes for a helicase, functions as an enhancer for an *LCT* promoter. Recently in human evolution (~10 kYA), for Western populations, a mutation in *MCM6* has increased its regulatory activity further, enabling 'lactase persistence', in which *LCT* is expressed at high levels throughout adult life rather than only in the first few years of life, allowing lactose to be metabolised, naturally selected for as these societies farmed dairy. Those without the mutation (~75% of humans worldwide) remain 'lactose intolerant': the absence of lactase in the small intestine leaves the lactose available for the bacteria in the large intestine, which ferment it, leading to fatty acid and gas production, causing symptoms.

Epigenetic Inheritance

In some organisms, some regulatory signals can be inherited from one generation to another, if they occur in gametes (epimutations). This can lead to a change in phenotype in the offspring.

Epigenetic inheritance is not 'Lamarckism', which was the pre-Darwinian idea that organisms inherit traits based on the parents' behaviours during their life.

Intergenerational epigenetic inheritance: epigenetic marks are inherited up to one generation. This is common for most epigenetic markers expressed in gametes at fertilisation.

Transgenerational epigenetic inheritance: epigenetic marks are inherited through multiple generations, potentially forever. TEI is well studied in plants, occurring alongside polyploidy to provide significant capacity for rapid adaptation, but may also happen in animals to a lesser degree.

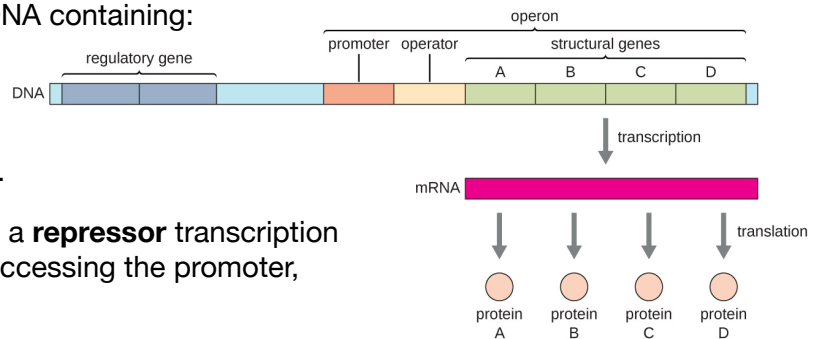
There is disputed evidence of TEI in humans, from 'foetal programming' after environmental stressors induced by famines, in which babies born to malnourished mothers in the famine exhibit phenotypic changes.

17.2.10. Gene Regulation in Prokaryotes (Operons)

Modulation of plasmid gene expression is based on negative feedback from the surrounding chemical environment: if there is a high concentration of a particular metabolite in the cell, this will act as an inhibitor for its own production, helping to reduce its level and prevent accumulation of toxins.

An **operon** is a sequence of prokaryotic DNA containing:

- Genes** coding for proteins.
- Promoter** sequence, signalling the start region of a gene to be transcribed.
- Operator** sequence, which can bind to a **repressor** transcription factor to block RNA polymerase from accessing the promoter, effectively turning the gene **off**.



In operons synthesising amino acids Trp, His, Phe, Thr only, a **leader** sequence is found between operator and first gene, which encodes for a **leader peptide** and an **attenuator**. The leader peptide contains several of the target amino acid residues. The attenuator mRNA has self-complementary regions which form hairpins. When RNA polymerase transcribes the operon, ribosomes can begin translating the growing mRNA. Negative feedback (**attenuation**) is established as the ribosome can stall if the target amino acid tRNAs are absent. If present, translation occurs quickly and the ribosome detaches, forming the terminator which blocks operon transcription.

- The repressor protein is synthesised by a repressor gene elsewhere (typically upstream).
- The repressor may be either **active** or **inactive** when it is newly transcribed - presence of a molecule can switch the repressor's state (**metabolite: to active, inducer: to inactive**), switching the operator's state, turning the gene **on** or **off**.
- If the gene codes for the metabolite, then a negative (inhibitory) feedback loop is established.
- The genes on the operon are all adjacent to a single promoter, so are all transcribed at the same time.
- Operons can be monocistronic (1 gene), bicistronic (2 genes), tricistronic (3 genes), polycistronic (more).
- Operons are rare in eukaryotes. Some are known in model organisms *D. melanogaster* and *C. elegans*.

Tryptophan synthesis: the *trp* operon, found in *E. coli*. Negative feedback regulation of tryptophan (Trp).

- *trp* has five genes: *trpE*, *trpD*, *trpC*, *trpB*, *trpA*.
- When Trp is **absent**, the *trp* repressor (encoded by *trpR*) is **inactive** (operon **on**).
- When Trp is **present**, Trp acts as a metabolite for the *trp* repressor, making it **active** (operon **off**).
- Attenuation mechanism: when Trp is **absent**, leader translation is slow, antiterminator hairpin forms, transcription continues (operon **on**). When Trp is **present**, leader translation is fast, terminator hairpin forms, transcription ends (operon **off**).

Lactose metabolism: the *lac* operon, found in *E. coli*. Digest lactose (Lac) when glucose (Glu) is absent.

- *lac* has three genes: *lacZ* (β -galactosidase), *lacY* (permease), *lacA* (acetyltransferase).
- When Lac is **absent**, the *lac* repressor (encoded by *lacR*) is active (operon **off**).
- When Lac is **present**, (allo)lactose is the metabolite for the *lac* repressor, making it inactive (operon **on**).
- Positive gene regulation mechanism: when Glu is **absent**, cAMP is present, attaches to CAP, allowing it to bind the upstream CAP site of DNA. Bound CAP **helps** RNA polymerase bind to the promoter (operon **strongly on**). When Glu is **present**, cAMP is absent, CAP is unbound and **cannot help** RNA polymerase (operon is **weakly on**).

17.2.11. Stochastic Modelling of Genetic Regulatory Networks (Systems Biology)

Interactions within genetic circuits yield time-varying concentrations of molecular species (mRNAs, proteins, signalling molecules etc).

Master Equation: models the joint probability density function of a given state

(n_i : number of molecules of species i (mRNAs, proteins etc), k_j : rate constant for reaction j , $p(n_1, \dots, n_N)$: joint PDF of number of molecules.) p varies over time according to a Poissonian discrete state space Markov chain model (Section 4.4.8): the current state $\mathbf{x} = [n_1, \dots, n_N]^T$ can evolve over time due to reactions changing each n_i .

Rate equations: e.g. if $A \rightarrow A + B$ (rate k), then $dp/dt = -kn_A p(n_A, n_B) + kn_A p(n_A, n_B - 1)$ (first term: transition from $[n_A, n_B]^T \rightarrow [n_A, n_B + 1]^T$, second term: transition from $[n_A, n_B - 1]^T \rightarrow [n_A, n_B]^T$).

Moment generating function (MGF, Section 5.2.8) of p : $F(z_1, \dots, z_N) = \sum_{n_i} (z_1^{n_1} \dots z_N^{n_N}) p(n_1, \dots, n_N)$.

Reaction type	Reaction	Time Evolution of MGF, dF/dt
Synthesis from a template (e.g. transcription, translation)	$A \xrightarrow{k} A + B$	$\dot{F} = kz_A(z_B - 1) \frac{\partial F}{\partial z_A}$
Degradation (e.g. removal of mRNA, protein)	$B \xrightarrow{\gamma} 0$	$\dot{F} = -\gamma(z_B - 1) \frac{\partial F}{\partial z_B}$
Forward irreversible reaction ($n_A + n_B = n$, a constant)	$A \xrightarrow{k} B$	$\dot{F} = kn(z_B - 1)F - kz_B(z_B - 1) \frac{\partial F}{\partial z_B}$
Dynamic equilibrium (e.g. enzyme or receptor process)	$A \xrightleftharpoons[k_{-1}]{k_1} B$	$\dot{F} = k_1(z_B - z_A) \frac{\partial F}{\partial z_A} + k_{-1}(z_A - z_B) \frac{\partial F}{\partial z_B}$

Combinations of these terms yield more complete models of genetic cascades. Statistical moments (mean, variance) can be easily found from the MGF at **steady state**: $dF/dt = 0$.

Under the condition $\{z_1, \dots, z_N\} = \{1, \dots, 1\}$, at which $F(1, \dots, 1) = 1$, important statistics are:

$$E[n_i] = \frac{\partial F}{\partial z_i}, \quad E[n_i(n_i - 1)] = \frac{\partial^2 F}{\partial z_i^2}, \quad E[n_i n_j] = \frac{\partial^2 F}{\partial z_i \partial z_j} \quad (i \neq j), \quad \text{Var}[n_i] = \frac{\partial^2 F}{\partial z_i^2} - \left(\frac{\partial F}{\partial z_i} \right)^2 + \frac{\partial F}{\partial z_i}.$$

For systems of interactions, the equations are typically nonlinear, and a matrix formulation can be written, linearising about the steady state i.e. $d\mathbf{x}/dt = (\mathbf{K} - \mathbf{\Gamma})\mathbf{x}$ (can be extended with control inputs \mathbf{u} and outputs \mathbf{y} , see Section 5.4.11), with $E[\mathbf{x}] = \nabla F(\mathbf{1})$ etc. The ‘Langevin approach’ is another method, starting with the deterministic rate equations and adding a stochastic noise term, solving to find the resulting output disturbance by Fourier transforms (Section 3.6.4).

17.2.12. Composition of Genomes

Only a small proportion of the genome is for protein-coding genes. Organisms with larger genome sizes tend to have smaller protein-coding fractions:

Organism	Genome size (bp)	Proportion protein coding
Humans (<i>Homo sapiens</i>)	3.2 billion	1.5%
Fruit fly (<i>Drosophila melanogaster</i>)	180 million	20%
Nematode (<i>Caenorhabditis elegans</i>)	100 million	25%
Yeast (<i>Saccharomyces cerevisiae</i>)	12 million	70%

The non-coding section of the genome contains mobile genetic elements, introns, repetitive/duplicate elements and entirely non-functional DNA ('junk DNA').

Mobile genetic elements: variable loci in the genome; forms ~50% of the human genome.

- **Transposons:**

- Retrotransposons (Class I): 'copy and paste': transcribed to mRNA, then reverse transcribed back into DNA and re-integrated into the genome at another position, using the encoded reverse transcriptase (RT) and integrase enzymes.
 - LTR retrotransposons: commonly encodes the genes *gag* and *pol*. The *gag* protein assembles a virus-like particle (VLP) to protect the mRNA from degradation. The *pol* gene has four proteins: protease, reverse transcriptase, RNase H and integrase.
 - Endogenous retroviruses (ERVs): benign retroviruses, permanently incorporated.
 - Short/long interspersed retrotransposable elements (SINEs and LINEs): common are the *Alu* and SVA SINEs and the LINE1 gene, highly conserved in primate genomes.
- DNA transposons (Class II): 'cut and paste' by transposase enzymes.

- **Viral agents:**

- Viruses and viroids: free viral DNA or RNA transcribed within the cell during a viral infection.
- Endogenous viral elements: proviral sequences in the genome during a retroviral infection.

- **Plasmids:** circular chromosomes found in prokaryotes and some fungi (e.g. yeast).

17.2.13. Comparative Genomics and Bioinformatics

Metrics of Distance: compute a difference score between sequences

- **Hamming distance:** number of positions at which the corresponding symbols in two strings of **equal length** are different.
- **Edit distance (Levenshtein distance):** minimum number of single-character edits (insertions, deletions, or substitutions) required to change one sequence into the other.

Smith-Waterman Local Alignment Algorithm: compute a similarity score between sequences

- Initialise a $(m + 1) \times (n + 1)$ matrix of zeros. (m, n : sequence lengths)
- Define the scoring scheme e.g. match: +1, mismatch: -1, gap penalty: -2.
- For each cell (i, j) in the matrix:
 - Calculate the score for extending the alignment ending here by considering **1)** extending from the diagonal (match/mismatch), **2)** extending from the left (gap in sequence 1), **3)** extending from above (gap in sequence 2).
 - Let this cell in the matrix be the maximum score among these (or zero: local alignment).
- Traceback: starting with the maximum cell in the matrix, follow the decreasing values to reach the cell with score zero. This forms the optimal alignment path.

This is an $O(mn)$ algorithm (quadratic), so heuristics are necessary for practical applications, where seed strings are used to find diagonal banded matches. FASTA and BLAST are popular heuristic-assisted algorithms for efficient comparison. Repeats in vertebrate genomes can make alignments easier by providing conserved anchors. However, when the repeats are variable (e.g. transposons, microsatellites/STRs), alignment is complicated and gaps (indels) must be accounted for suitably (such as in whole-genome comparisons).

Phylogenetic Analysis: infer evolutionary relationships among taxa from genetic similarity.

While evolution is not necessarily parsimonious (due to e.g. variable mutation rates, selection pressures, genetic drift, gene flow, horizontal gene transfer), it is often a strong indicator of relatedness, especially at and above the taxonomic genus level.

- **Fitch algorithm:** minimise the number of character state changes.
- **Sankoff algorithm:** minimise the costs associated with different types of evolutionary events.

Clustering methods can be used to generate a phylogenetic tree from the distance matrix, by iteratively starting with a star topology (all equally related) and merging nearest neighbours.

17.2.14. Experimental Analysis of Gene Expression

***In vitro* microarray analysis techniques** are used in interpreting the data generated from experiments on DNA (gene chip), RNA, and protein microarrays. After isolation:

1. Solvent separation: move mRNA into aqueous phase, protein and DNA into phenol phase.
2. Reverse transcription (RT) is used to convert mRNAs into cDNA.
3. Coupling: fluorescent cyanine (Cy) dyes used to label the cDNA targets (single channel).
For two-colour arrays, Cy3 and Cy5 are used to distinguish control and test groups.
4. Hybridisation: the labelled cDNAs bind with complementary probes in the array wells.
5. Scanning: fluorescence microscopy is used to record which array wells responded.
6. Analysis: plotting to calculate RNA abundance across the array, normalising the intensity against control spots.

Statistical rank products analysis: used to identify differentially expressed genes. The significance is assessed by bootstrapping (comparing with a null RP population from a large random set of permutations) to estimate the false discovery rate. Hierarchical clustering groups genes on their similarity of expression pattern (either by gene or by sample) by constructing a dendrogram (tree structure) and applying clustering algorithms.

Serial analysis of gene expression (SAGE): a high-throughput assay for quantifying gene expression, used to analyse whole transcriptomes with SAGE libraries of tags. Robust variants include RL-SAGE and SuperSAGE. It has been expanded with **massively parallel signature sequencing (MPSS)**, which forms part of modern **next-generation sequencing (NGS)**, a much higher throughput method than the traditional Sanger sequencing and shotgun assembly methods, making rapid whole genome accession viable.

Chromatin immunoprecipitation (ChIP): used to investigate protein-DNA interactions. Cells are crosslinked with formaldehyde to preserve protein-DNA bonds. After lysis, and shearing of the chromatin, an antibody for the protein of interest is added to precipitate selected protein-DNA complexes, isolated with protein A/G beads (binds IgA/IgG) or magnetic beads. The DNA can then be sequenced (ChIP-Seq: 'ChIP on chip').

***In vivo* morpholino knockdown tests** can be done with morpholino oligomers (synthetic RNA analogs) which can be designed to bind specific mRNA sequences to form a morpholino-RNA heteroduplex, preventing their expression. Analysis of the resulting phenotype in animal models informs on the function of the gene.

17.2.15. Homeotic Genes and Body Plan Development

Homeotic genes regulate morphogenesis (changing the shape of an organism), which are active during embryonic development of multicellular eukaryotes. They encode the body plan in plants, animals, fungi and some protists. Homeotic mutations can cause serious developmental defects and are often fatal. Homeotic genes can exhibit:

- Heterochrony: time-dependent expression during development.
- Heterotopy: space-dependent expression during development.

Homeobox genes are homeotic genes that contain a conserved 180 bp sequence (homeobox) within them. The homeobox gene translates into a transcription factor protein, with the homeobox region translating into a constant 60 amino acid sequence (homeodomain: three α -helices folded around a hydrophobic core and a flexible N-terminal arm). The helix-turn-helix motif can bind DNA, epigenetically up/downregulating transcription. The homeodomain can recruit histone-modifying enzymes and interact with chromatin-remodelling complexes and microRNAs.

Hox genes: the main class of homeobox genes in bilaterian animals, originally discovered in *Drosophila* (fruit flies). They are found arranged in clusters on chromosomes. In some lineages, including vertebrates, Hox genes have been duplicated, giving four clusters across multiple chromosomes. The ordering of the genes along the chromosome corresponds to the order of phenotypic expression along an anterior-posterior axis (spatial collinearity).

Pax genes (paired box genes): another class of homeobox genes.

Gap genes demarcate the boundaries between body segments, and are activated through interactions between the protein products of MEGs (maternal effect genes, Section 17.2.11), and they also regulate each other. This allows for space-dependent control of mitosis, apoptosis and cell differentiation, forming different segments of the body.

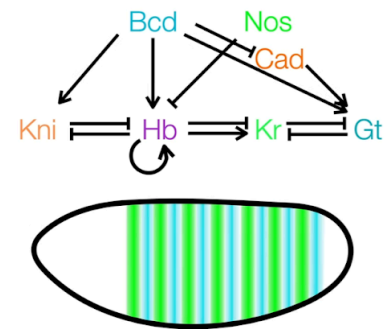
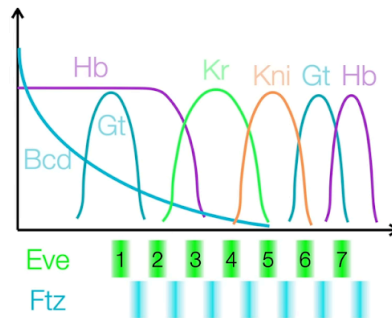
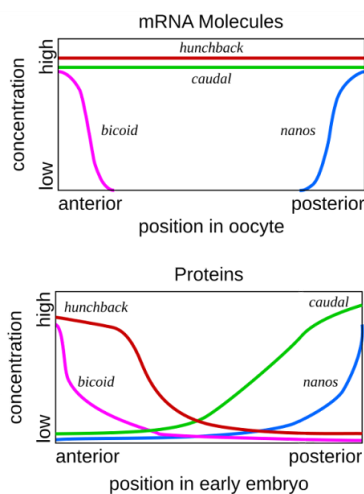
17.2.16. Embryonic Development

Morphogenesis: the progressive developmental organisation in a growing embryo

- Haeckel: development follows evolutionary history ('ontogeny recapitulates phylogeny').
- Von Baer: development diversification reflects evolutionary diversification (no recapping).

Von Baer's concept (while not perfect), is the more accurate summary for evo-devo biology.

Maternal Localisation: At fertilisation, maternal effect genes (MEGs) encode factors (e.g. mRNAs) that are present in the oocyte (egg cell), and are bound to the poles of the cell (maternal localisation), which initialises the head-tail axis. The cascade following MEG expression in *Drosophila* are shown:



Initial mRNA concentration and resulting protein distribution due to diffusion

Second cascade layer forming segments (*Eve*, *Ftz*: pair-rule genes)

Regulatory network for cascade layers 1 and 2, and resulting embryo segments

The third cascade layer sets up the polarity within each segment using 'segment polarity genes'. The fourth cascade is the spatially dependent activation of the homeotic selector genes (Section 17.2.10). These cascades can be modelled as bistable oscillators using systems of ODEs (Section 17.2.7).

17.2.17. Sexual Dimorphism and X-linked Genes

During embryonic development of biologically female organisms (XX chromosomes), one of the X-chromosomes in each diploid cell is randomly permanently inactivated (lyonisation), in order for X-linked gene expression to equalise in males and females. For heterozygous females, neighbouring cell clusters may express different alleles of X-linked genes (mosaicism). X-linked recessive inheritance causes various disorders in homozygous XX females.

17.2.18. Organogenesis and Stem Cell Differentiation**The Hedgehog Signalling Pathway**

Embryonic stem cell differentiation is controlled by spatial expression of hedgehog (*hh*) genes. Mammals have three hedgehog homologues, 'desert' (DHH), 'indian' (IHH), and 'sonic' (SHH).

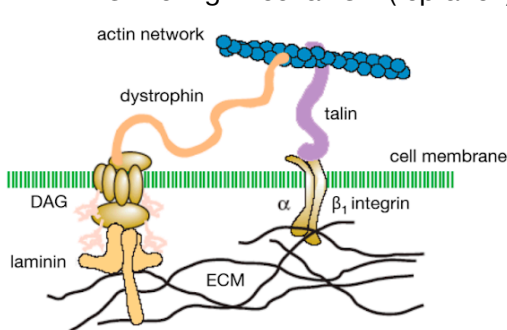
When SHH is translated, the protein is processed by forming an N-terminal domain and O-linkage with a cholesterol molecule for lipid transport out of the cell membrane. By paracrine signalling, a DISP protein

17.3. Biomechanics

17.3.1. Cytoskeleton and Cellular Biomechanics

The cytoskeleton is a protein scaffold. The overall mechanical rigidity of a eukaryotic cell is dominated by the cytoskeleton, since the lipid membrane is compliant and the cytoplasm is primarily viscous only.

The **persistence length** of a rubber-like polymeric fibre is the length scale over which the curvature of the fibre remains correlated before the effect of random thermal Brownian motion ‘scrambles’ the structure. Persistence length of a fibre: $l_p = EI / k_B T$ (EI : flexural rigidity, $k_B T$: thermal energy). Sections of polymer shorter than l_p can be modelled as elastic beams, while for sections longer than l_p , an ‘entropic spring’ statistical model (like natural rubber) is more appropriate. Flexible polymer chains can migrate by a ‘slithering’ mechanism (reptation). The cytoskeleton has three main parts at different scales of l_p :

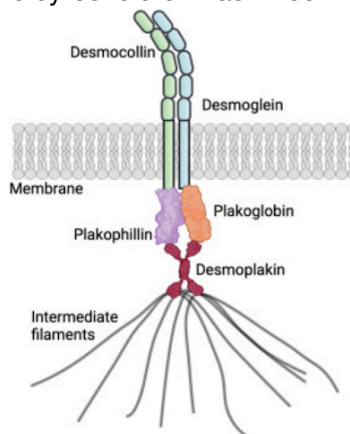


Actin Filament

thin strands linked to cell membrane

$t = 7-9 \text{ nm}$, $l_p = 15 \text{ }\mu\text{m}$, $E = 1.3-2.5 \text{ GPa}$

- In ‘**actin networks**’, filaments form loosely crosslinked 3D meshes near the cell membrane, bound to integrins/laminins by dystrophin and talin.
- In ‘**actin bundles**’, filaments form tightly-bound parallel arrays, cross-linked by actin-bundling proteins with Ca^{2+} -binding domains.

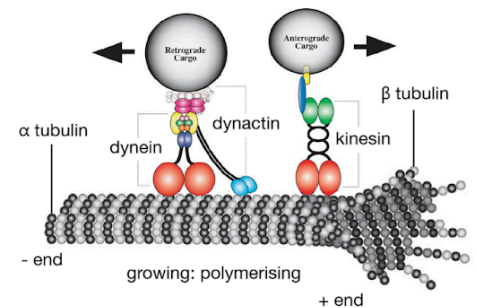


Intermediate Filament

bundles of twisted-coil chains

$t = 12 \text{ nm}$, $l_p = 1-3 \text{ }\mu\text{m}$, $E = 2-5 \text{ MPa}$ $d_o = 25 \text{ nm}$, $d_i = 14 \text{ }\mu\text{m}$, $l_p = 5200 \text{ }\mu\text{m}$, $E = 1.9 \text{ GPa}$

- Made of fibrous proteins (in the cytoplasm: keratin, vimentin, neurofilament).
- **Cytoplasmic IFs** are **passive** elements, providing elasticity.
- **Nuclear lamins** form square lattices and support the inner nuclear membrane. It also helps anchor heterochromatin to the nuclear membrane and can indirectly affect gene expression via epigenetics.
- **Spectrin** (α and β) forms a triangulated lattice on inner cell membranes with flexible hinge proteins, providing high compliance, high ultimate tensile strength and high lock-up strain (until filaments straighten out).



Microtubule

rigid hollow cylindrical tubes

- Made of helical globular tubulin heterodimer proteins (α and β). These blocks can have post-translational modifications (e.g. phosphorylation) to influence microtubule functionality (the tubulin code)
- Microtubules are used as a ‘**molecular highway**’ by motor proteins (dynein and kinesin).
- The mitotic spindle organises the chromatids during mitosis.
- The ‘-’ end is anchored at the cell centrosomes, adjacent to the Golgi apparatus, where modified proteins in vesicles are collected by kinesin. The ‘+’ protrudes freely into the cytoplasm and has a ‘**dynamic instability**’.

17.3.2. Mechanobiology and Mechanotransduction

Cells respond to mechanical and osmotic forces in their environment, as well as use enzyme-catalysed reactions to perform mechanical work at the molecular level.

Mammalian cells are ~70% water by mass. Their dry mass (without water) is composed of 60% protein, 13% lipids, 4% RNA (ribosomes), 1% DNA (remaining 22% polysaccharides, metabolites, ions etc). The overall cell mass is approximately 10^{-12} g = 1 pg.

Experiments find that various gene expression pathways are epigenetically inhibited in microgravity (μ g), suggesting that mechanotransduction is fundamentally an adaptation to the presence of gravity on life.

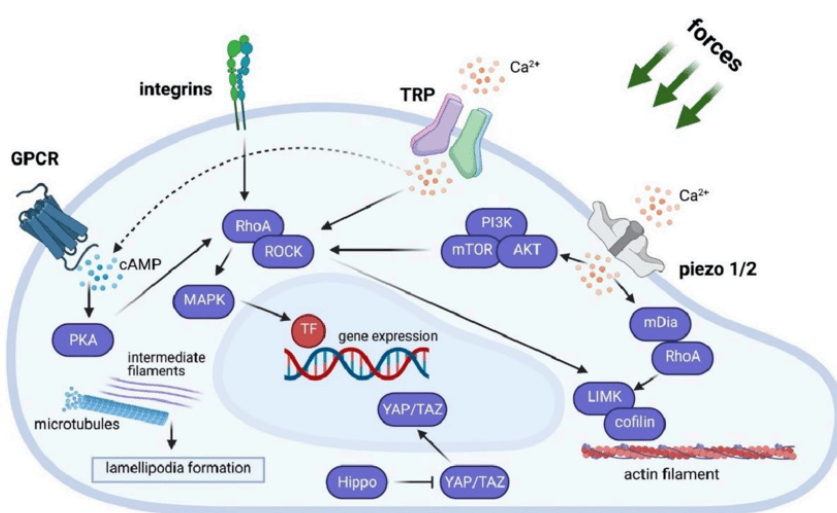
Cell migration can be influenced by molecules (chemotaxis) or stressors (mechanotaxis):

- Durotaxis: migration up gradients in ECM substrate mechanical rigidity
- Plithotaxis: cells migrate in-plane along axes of principal stresses (minimal shear stress)
- Haptotaxis: directional outgrowth up gradients of adhesion sites and chemoattractants
- Gravitropism: plant cell growth in the directions aligned with self-weight (roots: with, shoots: against)

Mechanisms of Mechanotransduction

- Stretch-activated ion channels (SACs)
- Contact with fibronectin in the ECM promotes focal adhesions via vinculin, talin, integrins
- Shear forces cause glycocalyx deformation with coupling to the cytoskeleton

Signalling Cascades Associated following Mechanical Stimulation



Ca²⁺ is transported through mechanosensitive ion channels such as Piezo1 and Piezo2 (biologically analogous to the piezoelectric effect).

Integrins bind cells to the ECM signalled by RGD sequences, and the focal adhesions are matured by vinculin, promoting stability.

Mechanical forces can influence gene expression via pathways to mechanotransducers (e.g. YAP/TAZ) and transcription factors (e.g. NF-κB).

(GPCR: G-protein coupled receptor, PKA: protein kinase A, TRP: transient receptor potential)

Together with chemical signals, mechanical signals also control cell growth, differentiation and fate switching in developing embryos, giving rise to 'evo-devo mechanobiology'.

17.3.3. Photoreception (The Eye)

17.3.4. Phonoreception and Bioacoustics

The Ear

Vocalisation

Echolocation

17.3.5. Olfactory Reception (The Nose)

17.3.6. Mechanoreception

17.3.7. Thermoreception (Response to Temperature)

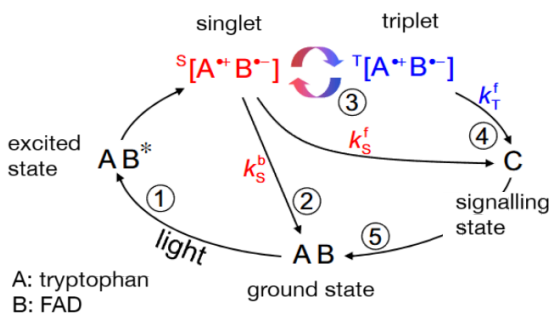
17.3.8. Electroreception and Electrogenesis

17.3.7. Magnetoreception (Response to Magnetic Fields)

Many animals (some arthropods, molluscs, and vertebrates) use magnetoreception for navigation by orienting with Earth's magnetic field. Several independently evolved mechanisms exist.

Cryptochrome: a flavoprotein in retinal rod cells in the eyes of some animals.

In plants, cryptochromes mediate phototropism. In animals, type 1 cryptochromes regulate the circadian rhythm while type 2 cryptochromes can sometimes be used for magnetoreception via the quantum mechanical 'radical pair mechanism', modelled as follows:



- ① Cryptochrome has a FAD chromophore cofactor absorbing at ~465 nm (blue light), forming an exciton FAD* with ~50% quantum yield.
- ② FAD* dissociates by charge transfer with a tryptophan residue in cryptochrome. The radical spins are correlated in the singlet state ($\uparrow\downarrow$).
- ③ Intersystem crossing to the triplet state ($\uparrow\uparrow$). When a magnetic field aligns with the spins, the triplet state is stabilised (Zeeman effect).
- ④ H⁺ transfer to FAD* induces conformational change in the signalling state of the complex, with field-dependent formation kinetics ($k_t^f \ll k_s^f$). A downstream neurotransmitter cascade is therefore field-dependent.

In birds, the magnetoreception signal activates 'cluster N' in the forebrain of the bird brain. Low-intensity stray radio-frequency electromagnetic fields can disorient migratory birds by interfering with the geomagnetic field at the cryptochrome complexes. This biological compass is likely noisy and requires signal integration over several seconds to improve the fidelity.

Cryptochrome has high DNA sequence homology with the DNA repair protein (6-4) photolyase, sharing high-energy photon sensitivity due to the FAD cofactor. Molecular clock phylogenies indicate that animal and plant cryptochromes both evolved in the late Precambrian, ~1000-541 MYA.

Magnetosome: liposomal superparamagnetic particles (magnetite (Fe₃O₄) / greigite (Fe₃S₄), ~100 nm).

Magnetosomes are found in the polyphyletic group of magnetotactic bacteria (MTB), most being in phylum *Pseudomonadota*, with some horizontal gene transfer. MTBs are found in anoxic waters and sediment and are often anaerobic. The magnetosome crystals are produced by biomineralisation, arranged in a linear chain inside the cell membrane as their total magnetic moment produces the least demagnetizing field when aligned parallel to the field. The chains are also bound to the actin filament cytoskeleton and so passively orient the cell.

The core genes and operons for magnetotaxis are conserved across all MTBs. The selective pressure for the magnetosome is unknown, but it may relate to the Great Oxidation event in the Archaeal promoting the storage of reduced iron (Fe⁰) to defend against reactive oxygen species (ROS).

Eukaryotic magnetosomes are rare, only occurring with functionality in some aquatic unicellular protists (euglenids and algae). Free magnetite particles are known in many animals but their mechanism of action is unclear, and they may be serving as stores of iron. Sea turtles migrate with an unknown mode of magnetoreception, hypothesised to be due to symbiotic MTBs in the lacrimal glands of the eyes, potentially transported by macrophages, with connections to the ophthalmic nerve.

17.3.3. Structural Analysis of Biomaterials and Cellular Tissue

Periodic Stiff Lattices (Rigid Biopolymer Foam Model)

Structural biopolymer networks can be modelled as 3D frameworks of elastic-perfectly plastic ‘bars’ with plastic hinge joints to model frictional torques at cross-links. The mechanical properties of a rigid-jointed truss are similar to the equivalent pin-jointed truss, but:

- The rigid-jointed truss will have a weak **bending** mode if the pin-jointed truss is mechanistic.
- The rigidity of the truss depends on the lattice connectivity, Z (average number of bars per joint).

Connectivity Criteria for Rigidity of Periodic Lattices

	Stiff Stretching dominated	Compliant Bending dominated
2D	$Z \geq 4$	$Z < 4$
3D	$Z \geq 6$	$Z < 6$

Effective Properties of Anisotropic Lattices in 2D (Prismatic) and 3D (Foams)

Direction	Modulus reduction factor	Strength reduction factor
Transverse (weak)	2D $\bar{E} / E_s \sim \bar{\rho}^3$	2D $\bar{\sigma}_y / \sigma_y \sim \bar{\rho}^2$
	3D $\bar{E} / E_s \sim \bar{\rho}^2$	3D $\bar{\sigma}_y / \sigma_y \sim \bar{\rho}^{3/2}$
Axial (strong)	$\bar{E} / E_s \sim \bar{\rho}$	$\bar{\sigma}_y / \sigma_y \sim \bar{\rho}$

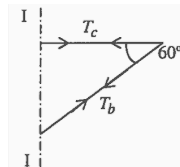
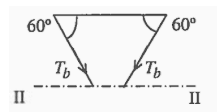
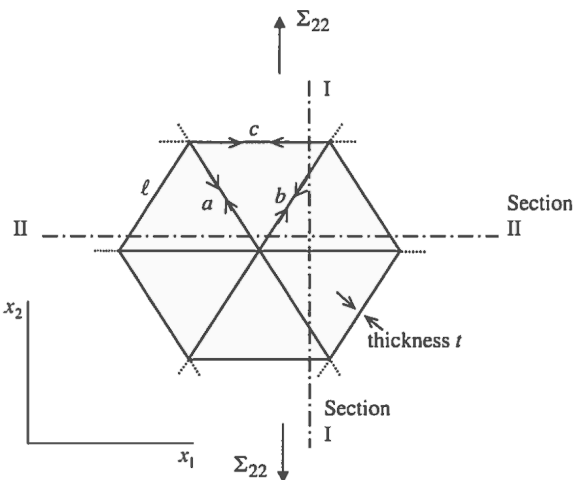
Notable points:

- Any 2D lattice with 120° rotational (C_3) symmetry has an isotropic in-plane modulus.
- Irregular/random polygons in the lattice do not significantly affect the structural properties (~3%).
- For a 3D foam topology to be rigid, its unit cell must tessellate and be rigid ($Z \geq 6$). None of the platonic solids achieve this, so combinations are necessary (e.g. FCC octet truss).

Example: for the stiff 2D triangulated lattice shown, what is the effective Young’s modulus and yield stress?

(Σ_{22} : macroscopic applied axial stress, ϵ_{22} : axial strain, E_s : link elastic modulus l : cross-linker length, $\{a, b, c\}$: link tensions. Unit cell: equilateral triangle with thickness $t/2$.)

Elastic Analysis: consider **free-body cuts** of the unit cell



$$\bar{\rho} = \frac{\text{unit cell solid area}}{\text{unit cell total area}} = 2\sqrt{3} \frac{t}{l}$$

$$A = \frac{\sqrt{3}}{4} l^2$$

By symmetry, $T_a = T_b$

$$\leftrightarrow: (T_a + T_b) \cos 30^\circ = \Sigma_{22} l$$

$$T_a = T_b = \Sigma_{22} l / \sqrt{3}$$

$$\leftrightarrow: T_c + T_b \cos 30^\circ = 0$$

$$T_c = -1/2 T_b = -\Sigma_{22} l / 2\sqrt{3}$$

Virtual work (per unit depth): $\Sigma_{22} \epsilon_{22} A = \frac{1}{2} (T_a e_a + T_b e_b + T_c e_c)$; (factor $\frac{1}{2}$ as bar forces are shared per cell)

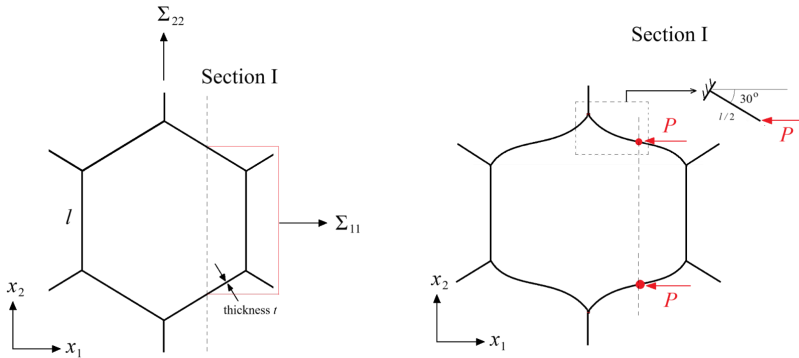
$$\text{Elastic law: } e = \frac{Tl}{E_s t} \rightarrow \frac{\Sigma_{22}}{\epsilon_{22}} = \bar{E} = \frac{1}{3} \bar{\rho} E_s$$

Plastic Analysis: assume bars a, b attain yield (perfectly plastic) while c remains rigid. Let $T_a = T_b = \sigma_y t$.

The FBD cut at Section II-II shows that $\sigma_y t = \Sigma_{22} l / \sqrt{3} \rightarrow$ therefore $\Sigma_{22} = \bar{\sigma}_y = \sqrt{3} \sigma_y t / l = \frac{1}{2} \bar{\rho} \sigma_y$.

Periodic Compliant Lattices (Honeycomb Biopolymer Foam Model)

Example: for the compliant 2D hexagonal foam shown, what is the effective modulus and yield stress?



Imagine pulling the lattice in each direction. Place Section I at the inflection point of a beam.

Relative density: $\bar{\rho} = \frac{2}{\sqrt{3}} \frac{t}{l}$

Elastic analysis: at Section I, curvature $\kappa = 0$
 → bending moment $M = 0$ → only a force exists.

By force balance on Section I, per unit depth,
 $P = \Sigma_{11} l(1 + \sin 30^\circ) \rightarrow P = \frac{3}{2} \Sigma_{11} l$.

Consider a half-section of the beam anchored at the joint, which can be modelled as a cantilever.

- Force P has transverse component $\frac{1}{2}P$, which causes transverse tip deflection by $u = \frac{Pl^3}{48 E_s I}$.
- The strain $\epsilon_{11} = \frac{2(u \sin 30^\circ)}{l \cos 30^\circ} = \frac{2\sqrt{3}}{3} \frac{u}{l}$. ($I = \frac{1}{12}t^3$: second moment of area per unit depth)
- The effective modulus is then $E_{11} = \frac{\Sigma_{11}}{\epsilon_{11}} = \frac{3}{2} E_s \bar{\rho}^{-3}$. This modulus is isotropic.

Plastic analysis: assume plastic hinge formation (Section 6.3.22) at the cantilever roots (top, bottom joints).

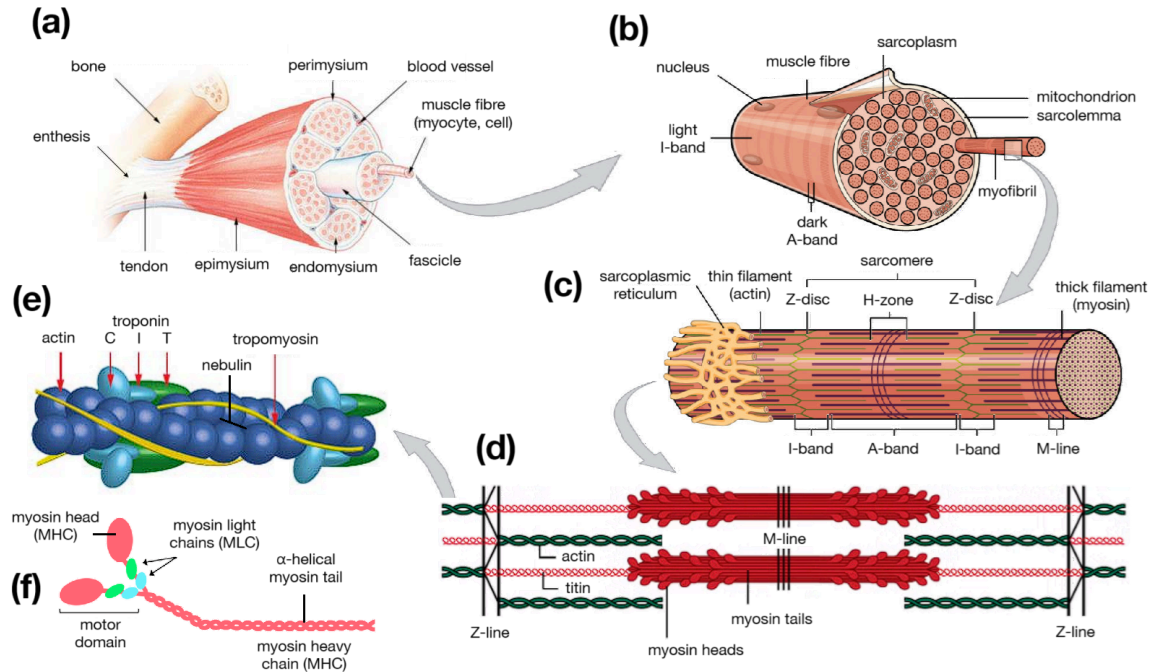
- External work = internal dissipation : $\Sigma_{11} \epsilon_{11} \times \frac{3\sqrt{3}}{2} l^2 = \frac{1}{2} M_p \times (4\theta \times 2)$ (θ : hinge rotation)
- Plastic modulus per unit depth: $Z_p = \frac{1}{4} t^2 \Rightarrow$ plastic moment capacity: $M_p = \frac{1}{4} t^2 \sigma_y$ (Section 6.3.21)
- Deformation geometry: $\epsilon_{11} = \frac{l\theta \sin 30^\circ}{l \sin 60^\circ} = \frac{\theta}{\sqrt{3}}$. At yield, let $\Sigma_{11} = \bar{\sigma}_y$. Then $\bar{\sigma}_y = \frac{2}{3} \sigma_y \frac{t^2}{l^2} = \frac{1}{2} \sigma_y \bar{\rho}^{-2}$.

Examples of Biological Structures as Lattice Models

- Square lattice (2D, $Z = 4$): nuclear lamins supporting the inner nuclear membrane of eukaryotic cells.
- Hexagonal lattice (2D, $Z = 3$): cellulose and lignin honeycomb cell walls in xylem tubes and wood.
- Triangulated lattice (2D, $Z = 6$): spectrin fibres supporting the cell membrane of erythrocytes.
- Amorphous network (2D): wavy collagen fibres in skin giving very low elastic modulus.

17.3.4. Muscle Anatomy and Physiology

Muscle Anatomy: a hierarchical arrangement of parallel fibrous structures



(a) Macroscopic skeletal muscle anatomy. **(b)** A single muscle fibre (cell). **(c)** A single myofibril. **(d)** A single sarcomere lengthwise unit of myofibril. **(e)** A single actin filament. **(f)** A single myosin unit.

Muscle Signalling: pathway for a conscious striated muscle contraction

1. **Motor cortex** (part of the cerebral cortex) of the brain generates a signal from conscious inputs.
2. **Motor neurons** in the CNS (spinal cord) propagate the action potential to the PNS.
3. Exocytosis of **acetylcholine (ACh)** into synaptic cleft of motor unit neuromuscular junction.
4. Binding of ACh to receptors on sarcolemma, inducing **Na⁺ uptake** into the muscle cell.
5. An **action potential** propagates along the **sarcolemma** and into T-tubules.
6. Voltage-gated dihydropyridine receptors are activated, mechanically linked to ryanodine receptors, which induce **Ca²⁺ ion release** from the sarcoplasmic reticulum into the sarcoplasm.

Muscle Function: Lymn-Taylor crossbridge cycle / sliding filament theory for **striated muscle** contractions

1. **Calcium binding:** Ca²⁺ binds to troponin C, displacing tropomyosin, exposing actin binding sites.
2. **Hydrolysis:** a myosin head containing ATP is hydrolysed to ADP and P_i, retaining them and changing the conformation of the myosin head to the 'cocked' state.
3. **Cross-bridge formation:** cocked myosin head (holding ADP + P_i) binds to actin sites.
4. **Power stroke:** the P_i is released, causing the myosin head to pull the whole actin filament towards the centre of the sarcomere (power stroke). The ADP is then also released.
5. **Dissociation:** a new ATP binds to myosin, breaking the cross-bridges and returning the myosin to the 'cocked' state, ready to release the conformational strain energy again.

This is the basis of the **sliding filament theory**: myosin thick fibres are fixed in place, and their heads continuously bind actin filaments and pull it towards the M-line (sarcomere centre). The sarcomere length (between Z-discs) decreases, so the muscle experiences contraction.

Muscle **relaxation** is the reverse process, with Ca^{2+} being actively transported **out** of the sarcoplasm back into the sarcoplasmic reticulum by calcium pump ATPases.

All skeletal muscles act in **antagonistic pairs** (one shortens, one lengthens). The striated muscles are attached to bones in the skeleton by **tendons** (made of collagen and proteoglycans), so the contractions exert forces and torques on the rigid skeleton, which induce translational and rotational motion.

Muscle fibres can be **slow twitch or fast twitch**. These use different isoforms of myosin heavy chain (slow: MHC I, fast: MHC IIa) to achieve differences in cross-bridge cycling rate. Fast twitch muscle fibres are suited for short bursts of force with high maximum mechanical power output, while slow twitch muscle fibres are suited for long-lasting low force production.

Smooth Muscles

In **smooth muscles**, Ca^{2+} instead acts via binding to calmodulin and phosphorylation of myosin light-chain (MLC) starts the cross-bridge cycle. Smooth muscles are involuntary muscles (stimulated by unconscious nerve impulses), found near soft organ tissue (except the heart cardiac muscle) and do not actuate the skeleton.

Muscles in Other Animals (comparative biomechanics)

Muscles are highly evolutionarily conserved from around ~600 MYA (Precambrian; Ediacaran), appearing in all but the most basal animal phyla (e.g. *Porifera*: sea sponges) as smooth muscle cells. Phylum *Cnidaria* (e.g. jellyfish) have the most primitive of muscle apparatus, lacking the embryonic mesoderm layer that all other phyla develop muscles (and the heart and circulatory system) from but having striated cells in its reproductive stage.

In **small animals** (e.g. insects, arthropods and some amphibians), very rapid movements can be generated despite tiny muscle masses, due to 'latch-mediated spring actuation' (LaMSA). The muscle fibres contract and store elastic energy in tendons or specialised structures, and a latch mechanically holds the tendon in place without expending further energy. On release of the latch, the stored energy is released as kinetic energy. This exploits passive elasticity to amplify the mechanical power significantly.

In **apes**, muscularity varies due to evolutionary adaptation. Humans have on average ~70% slow and ~30% fast twitch muscle fibres, giving us relatively high endurance and manual dexterity but low overall muscle strength. The other great apes (e.g. gorillas, chimpanzees) possess higher fast-twitch muscle fibre content as well as increased overall muscle mass due to decreased myostatin expression.

Muscle Energy Sources

Striated muscles are specialised for respiration. Oxygen gas binds to myoglobin for facilitated diffusion, ensuring a plentiful supply for mitochondrial respiration. Slow-twitch muscle fibres have many mitochondria for aerobic respiration to generate ATP. Fast-twitch muscle fibres have few mitochondria, performing glycolysis and anaerobic respiration to form lactic acid, which must be cleared by transport to the liver, and the oxygen must be replenished by panting (oxygen debt).

The ATP required for the myosin crossbridge cycle is sourced from existing ATP stores, as well as the on-demand **Lohmann reaction** ($\text{phosphocreatine} + \text{ADP} \rightleftharpoons \text{creatine} + \text{ATP}$, via creatine phosphokinase) in the sarcoplasm.

Muscle Growth and Repair

Muscles grow primarily by hypertrophy (myocyte size) rather than hyperplasia (myocyte count). During **strenuous exercise**, minor damage to muscles can result from increased metabolic reactive oxygen species (ROS) production, leading to inflammation which triggers a local innate immune response. Satellite cells (muscle stem cells) undergo **myogenesis** to produce new muscle myofibrils. Microtears occurring from mechanical stress trigger nuclear migration to the site to deliver mRNA for **protein synthesis** to fill in the microtears. The mTOR pathway also promotes muscle growth by upregulating protein synthesis in myocytes.

Muscle injuries and soreness is often caused by eccentric contractions (muscle lengthening) since high tensile forces are developed even for small extensions. A careful balance in resistance training intensity and protein intake is required to promote muscle growth without damage.

Abnormal Muscle Function: disruptions at any point in the muscle signalling cascade. Examples:

When an organism **dies**, the calcium pumps are shut down and Ca^{2+} diffuses into the sarcoplasm, causing contraction and the diminished ATP stores cannot break the myosin crossbridges, so the muscle remains firmly contracted for ~12 hours (*rigor mortis*), only breaking when the proteins themselves begin to degrade by action of free proteases and microorganisms.

Nerve agents inhibit acetylcholinesterase in the synaptic cleft, leading to ACh accumulation and uncontrolled muscle contractions.

Botulinum toxin (botox) from the bacteria *Clostridium botulinum* blocks ACh exocytosis, promoting muscle relaxation (paralysis / botulism), used by cosmetic surgeons to relax facial muscles, reducing wrinkles. The toxin from *Clostridium tetani* has the opposite effect, causing tetanus disease (forced contractions).

17.3.5. Experimental Muscle Mechanics

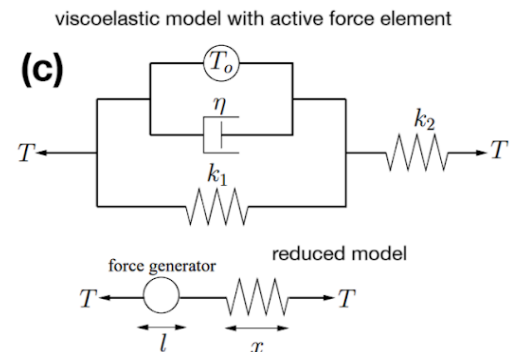
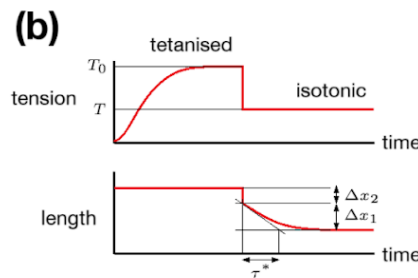
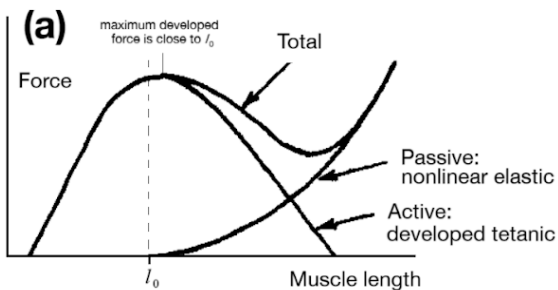
Isometric Stimulation of Muscles: hold at constant length L , stimulate, measure force $T(x)$.

A muscle removed from an animal and kept in a cold sterile isosmotic solution can be studied *ex vivo* for its response to stimuli. On electrical stimulus (applied voltage), a muscle held isometrically (constant length) responds with a tensile force depending on the applied stimulus:

- **Twitch:** single impulse stimuli → transient decaying response. The tension rises and falls back to zero within about one second.
- **Unfused tetanus (clonus):** low-frequency impulse train → superposition of twitches. The tension reaches a moderate steady-state value with small oscillations.
- **Fused tetanus:** high-frequency (>50 in mammalian muscles) impulse train → tension rises to maximum steady-state value with no oscillations.

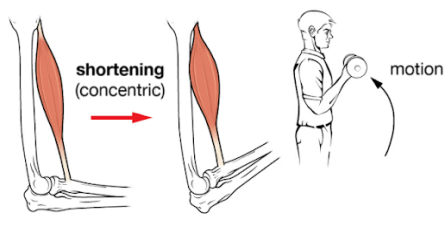
Total muscle force $T(x, t) = \text{Tetanic (Active) force } T_a(x, t) + \text{Passive Elastic force } P(x)$.

Isotonic Stimulation of Muscles: tetanise to tension T_0 , stop and apply step tension $T < T_0$, measure length response $L(t)$. The negative creep response resembles a viscoelastic standard linear solid model (Section 6.2.9) with an additional active force component. The initial gradient of the relaxation curve $x(t)$ is the ‘shortening velocity’, $v = \Delta x_1 / \tau^*$.

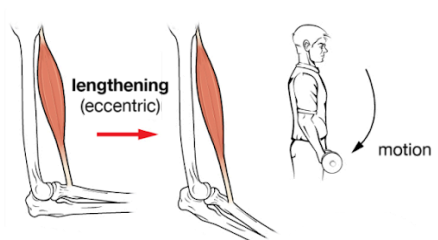


(a) Isometric force-length characteristic. **(b)** Hill’s step drop experiment. **(c)** Active standard linear solid model (Section 6.2.9) and reduced model to explain the isotonic experimental data.

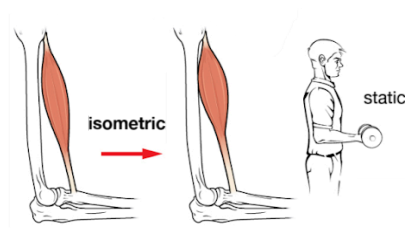
Types of Active Muscle Contractions in Exercise: muscle is usually in unfused tetanus state



Isotonic Shortening (concentric)
bicep shortens, tricep lengthens



Isotonic Lengthening (eccentric)
bicep lengthens, tricep shortens

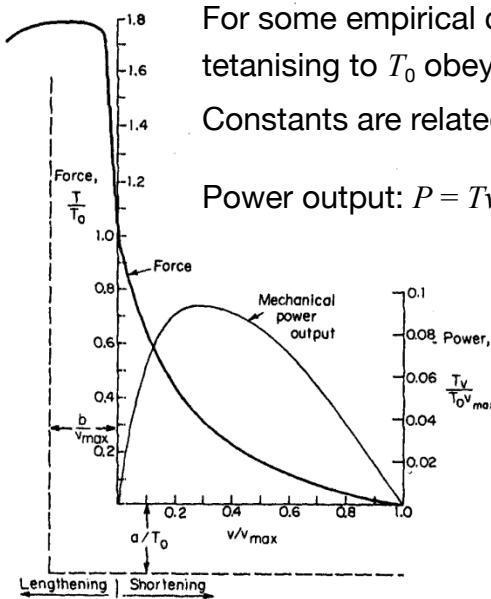


Isometric Contraction
neither changes length

Note: bicep curls as shown are not truly isotonic due to time-varying torque demand (‘auxotonic’).

17.3.6. Modelling of Muscle Mechanics

Hill's Active State Model: relates T and v from **isotonic** tetanising experiments.



For some empirical constants (a, b), the tension T and shortening velocity v after tetanising to T_0 obeys the **Hill equation**, $(T + a)v = b(T_0 - T)$.

Constants are related by $v_{max} = \frac{b}{k}$ where $k = \frac{a}{T_0}$. Typically, $4 < \frac{1}{k} < 6$.

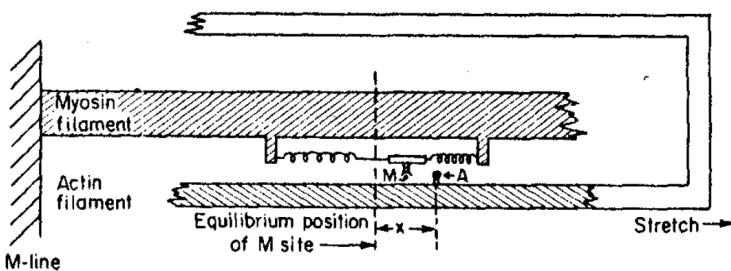
Power output: $P = Tv$, normalised as $\hat{P} = \hat{T} \hat{v}$ where $\hat{T} = \frac{T}{T_0}$, $\hat{v} = \frac{v}{v_{max}}$, $\hat{P} = \frac{P}{T_0 v_{max}}$

Maximum power output occurs at $\hat{v} = k(\sqrt{1 + 1/k} - 1) \sim 0.3$.

Fenn's energy balance: the total heat developed by a muscle is $Q = -(T + a) \Delta x$ (work done + additional heat). Experiments find strong agreement with the Hill model, with $a = a$ and $d/dt \Delta x = -v$.

Forces above isometric in lengthening can cause yielding (failure), experienced as 'pulling' the muscle.

Huxley's Crossbridge Dynamics Model: explains the T - v characteristic considering a sarcomere.



Assume 1) only active contractile components (neglect passive parallel elastic elements), 2) peak of the tension- length curve (all available cross-bridges will attach), 3) full tetanisation, 4) velocity and tension are constant, 5) each attached cross-bridge undergoes the full ATP reaction cycle.

(x : instantaneous displacement of an actin active site A from the equilibrium position of a myosin head M . $n(x, t)$: proportion (i.e. probability) of attached cross-bridges at position x and time t .)

- Isotonic cross-bridge kinetics: $dn/dt = -V dn/dx = (1 - n(x))f(x) - n(x)g(x) \rightarrow -V dn/dx + (f + g)n = f(x)$. ($V = -dx/dt$, f : attaching rate const: 'desire to contract', g : detaching rate const: 'desire to relax'). Let $f(x) = \{x < 0: 0; 0 < x < h: (f_1/h)x; x > h: 0\}$ and $g(x) = \{x < 0: g_2; x > 0: (g_1/h)x\}$ to fit data well. (h : bridge maximum reach)
For $x > 0$, attached bridges act to shorten. For $x < 0$, attached bridges act to lengthen.
- Boundary conditions:
if isotonic shortening ($V > 0$), $n(x) = 0$ for $x \geq h$; if isotonic lengthening ($V < 0$), $n(x) = 0$ for $x \leq 0$.
Solve the DE for a piecewise continuous pdf $n(x)$.

To find the tension-velocity relationship $T(V)$, consider an energy balance on a half-sarcomere:

- Total work done: $T \times l = \frac{mAs}{2} \int_{-\infty}^{\infty} n(x, V) kx dx$ ($l \gg h$: contraction distance, m : crossbridges per unit volume, A : area of muscle, s : sarcomere length, k : myosin filament spring constant).

Unlike Hill's model, Huxley's model additionally predicts accurate lengthening behaviour:

- Discontinuous slope: $\frac{\lim_{v \rightarrow 0^-} dT/dV}{\lim_{v \rightarrow 0^+} dT/dV} = \frac{f_1}{g_1} > 1$.
- Yielding: $\lim_{V \rightarrow -\infty} T(V) = T_0 \frac{f_1 + g_1}{g_1}$ where $T_0 = T(0)$ (isometric tension).
- Total rate of energy release (work + heat): $E' = \frac{mAs e}{2l} \int_{-\infty}^{\infty} (1 - n(x)) f(x) dx$ (e : energy per contraction site per cycle), matching Fenn's experiment with suitable choice of constants.
- Overall muscle efficiency: $\eta = \frac{TV}{E'}$ (mechanical power output / total energy)

At $V = V_{max}$, equal numbers of bridges pull in opposite directions, generating no overall force but consuming energy nonetheless. This corroborates Hill's model, which predicts zero efficiency at both $V = 0$ (isometric) and $V = V_{max}$, and by choosing the constants suitably, very close agreement can be found with Hill's experimental T - v data. By fitting a value for the energy released per ATP cycle, strong agreement with Fenn's heat experiments is found as well. Huxley's model additionally predicts the yielding phenomenon for moderate negative v (lengthening).

- At isometric conditions ($V = 0$), $E'_0 = \frac{mAsh}{4l} \left(\frac{f_1 g_1}{f_1 + g_1} \right)$ and $\eta = 0$.

Huxley-Simmons Kinetic Model: explains the transient effects of Hill's experiments.

The force response of a step-strain applied to Hill's T - v model does not fit experimental data, which sees a 'fast' partial development of force followed by a 'slow' continuation to the required force.

The **change in configuration** of the myosin motors represents the '**fast**' process.

The **crossbridge cycling** of the myosin motors represents the '**slow**' process.

The 'fast' rate constant (reciprocal time constant) is $r = \frac{1}{2} r_0 (1 + e^{-\gamma y})$ (y : step change in length). This can be derived by considering Arrhenius equations / Boltzmann statistics for the equilibrium between the (assumed) two starting and ending crossbridge states. The myosin head 'rocks' around, changing the force suddenly.

Further adjustments include modifying the myosin head potential energy wells.

17.3.6. Modelling Diffusion-Controlled Homeostasis

Mechanisms by which a cell can achieve chemical homeostasis include:

- **Passive carrier diffusion** of small hydrophilic molecules through porins (water-filled channel proteins in the cell membrane) or ion channels, or hydrophobic molecules through the cell membrane directly.
- Passive osmosis of water through aquaporins (water-selective channel proteins).
- **Facilitated diffusion** of sugars and amino acids by mobile protein mediators (carriers; ionophores) which pass through the cell membrane. This is also passive.
- **Active transport** via ATP-powered pumps e.g. Na^+/K^+ -ATPase and Ca^{2+} -ATPase (Section 17.3.7).

Modelling Diffusion Across Membranes (L : membrane width)

1D Reaction-diffusion equation: $\frac{\partial c}{\partial t} = D \frac{\partial^2 c}{\partial x^2} + r(c)$ (c : concentration, r : reaction rate to form c)

At steady state, $\frac{\partial c}{\partial t} = 0$; boundary conditions $[c_0, c_L]$ with solution $c(x) = c_0 + (c_L - c_0) \frac{x}{L}$

By Fick's law, flux $J = -D \frac{\partial c}{\partial x} = \frac{D}{L} (c_0 - c_L)$, so the 'diffusion resistance' is $\frac{L}{D}$ (per unit area).

Passive Carrier Diffusion (Slab Reactor): substrate S, enzyme carrier E, bound complex ES

- Equilibrium: $E + S \xrightleftharpoons[k_-]{k_+} ES$ with kinetics $r = k_+[E][S] - k_-[ES]$.
- Conservation of enzyme amount: $[E] + [ES] = [E]_{\text{total}} = \text{constant} \rightarrow \frac{\partial [E]}{\partial t} + \frac{\partial [ES]}{\partial t} = 0$.
- Diffusion: $\frac{\partial [S]}{\partial t} = D_S \frac{\partial^2 [S]}{\partial x^2} - r$, $\frac{\partial [E]}{\partial t} = D_E \frac{\partial^2 [E]}{\partial x^2} - r$, $\frac{\partial [ES]}{\partial t} = D_{ES} \frac{\partial^2 [ES]}{\partial x^2} + r$.
with boundary conditions $\{x=0: [S] = s_0; x=L: [S] = s_L\}$ and $\{(x=0, x=L): \frac{\partial [E]}{\partial x} = 0, \frac{\partial [ES]}{\partial x} = 0\}$.
- Total substrate flux: $J = J_S + J_{ES} = -\left(D_S \frac{\partial [S]}{\partial x} + D_{ES} \frac{\partial [ES]}{\partial x}\right)$ at steady state ($\frac{\partial [S]}{\partial t} = \frac{\partial [ES]}{\partial t} = \frac{\partial [E]}{\partial t} = 0$)
- Solution: $J = \frac{D_S}{L} (1 + \mu\rho)(s_0 - s_L)$ where $\rho = \frac{D_{ES}}{D_S} \frac{[E]_{\text{total}}}{K}$ and $\mu = \frac{K^2}{(s_0 + K)(s_L + K)}$ ($K = k_+/k_-$)
assuming $r \approx 0$, which is larger than unaided diffusion by an increase of $\mu\rho > 0$.

Facilitated Transport: carrier E conformation switches S between 'in' to 'out'. x is irrelevant.

- Equilibria: $E_{in} + S_{in} \xrightleftharpoons[k_-]{k_+} ES_{in} \xrightleftharpoons[k_+]{k} ES_{out} \xrightleftharpoons[k_+]{k_-} E_{out} + S_{out}$; $E_{in} \xrightleftharpoons[k_+]{k} E_{out}$ constant influx of S = J
with kinetics $\frac{d[S_{in}]}{dt} = k_-[ES_{in}] - k_+[E_{in}][S_{in}] - J$ and $\frac{d[E_{in}]}{dt} = k_-[ES_{in}] + k[E_{out}] - k_+[E_{in}][S_{in}] - k[E_{in}]$, etc.
- Conservation of S and E: $[S_{in}] + [S_{out}] + [ES_{in}] + [ES_{out}] = [S]_{\text{total}}$ and $[E_{in}] + [E_{out}] + [ES_{in}] + [ES_{out}] = [E]_{\text{total}}$
- At steady state, $\frac{d[E_{in}]}{dt} = \frac{d[E_{out}]}{dt} = \frac{d[ES_{in}]}{dt} = \frac{d[ES_{out}]}{dt} = 0$
- Solution: $J = \frac{1}{2} K_d K_m k_+ [E]_{\text{total}} \frac{s_{out} - s_{in}}{(s_{in} + K_m + K_d)(s_{out} + K_m + K_d) - K_d^2}$ where $K_m = \frac{k_-}{k_+}$, $K_d = \frac{k}{k_+}$.
- Symport vs antiport ionophore: two different substrates move in the same vs opposite directions.

17.3.7. Modelling Active Transport-Controlled Homeostasis

ATP-powered pumps use an ATPase to pump chemical species across a membrane against their concentration gradient by hydrolysing ATP into ADP and P_i. They are responsible for maintaining the difference in conditions between the cytosol (inside) and extracellular fluid (ECF, outside).

- P-type pump: cell membrane active transport of **ions**: H⁺ (bacteria), Na⁺/K⁺ (animals) or Ca²⁺ (sarcoplasm)
- ABC transporter: cell membrane active transport of **small molecules** (amino acids, sugars, cholesterol etc)
- V-type pump: organelle (vacuole, lysosome) membrane active transport of **protons**: H⁺ (eukaryotes)
- F-type ATP synthase: mitochondrial and chloroplast membrane, **passive proton-powered ATP synthase**.

Cytosolic conditions must be maintained independent of the ECF conditions. This includes pH 7.2, **high [K⁺], low [Na⁺], low [Ca²⁺] and low [Cl⁻]** (relative to the ECF e.g. blood).

Calcium Pumps: removes Ca²⁺ from the muscle cell cytosol to enable muscle relaxation

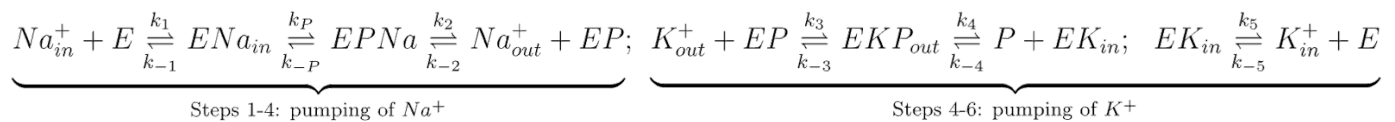
In muscles, Ca²⁺ is stored in the sarcoplasmic reticulum. When a muscle relaxes, P-type Ca²⁺ pumps (SERCAs) actively transport Ca²⁺ from the muscle cell cytosol (deactivating the contraction due to tropomyosin) back into storage.

The action of the Ca²⁺ pump involves 1) binding of cytosolic Ca²⁺ and ATP, 2) Mg²⁺-facilitated ATP hydrolysis to ADP and P_i, 3) P_i transfer by phosphorylation of a distal Asp residue, 4) conformational change, 5) dissociation of Ca²⁺ due to lower affinity, now on the sarcoplasmic reticulum side, 6) hydrolysis of Asp-P_i bond and returning to original conformation.

Sodium-Potassium Pumps: removes 3 Na⁺ from the cell and brings 2 K⁺ into the cell, maintaining the membrane resting potential in neurons after an action potential floods the neuron with Na⁺ (high *I*)

The Na⁺/K⁺ pump is a tetramer (α₂β₂), whose action is similar to the calcium pump. It involves 1) binding of cytosolic Na⁺ and ATP, 2) Mg²⁺-facilitated ATP hydrolysis to ADP and P_i, 3) P_i transfer by phosphorylation of a distal Asp residue, 4) dissociation of Na⁺ due to lower affinity, now on the outside, and binding of outside K⁺, 5) hydrolysis of the Asp-P_i bond and returning to original conformation, 6) dissociation of K⁺ due to lower affinity, now on the inside.

Na⁺/K⁺ pump equilibria (using simplified 1:1 Na:K binding model instead of 3:2): (E: pump enzyme)



Steady-state Na⁺/K⁺ flux: $J = [E]_{total} \frac{[Na_{in}^+][K_{out}^+]K_1K_2 - [Na_{out}^+][K_{in}^+]K_{-1}K_{-2}[P_i]}{([K_{out}^+]K_2 + [K_{in}^+]K_{-2})K_n + ([Na_{in}^+]K_1 + [Na_{out}^+]K_{-1})K_k}$

($K_1 = k_1k_2k_P$; $K_{-1} = k_{-1}k_{-2}k_{-P}$; $K_2 = k_3k_4k_5$; $K_{-2} = k_{-3}k_{-4}k_{-5}$; $K_n = k_{-1}k_{-P} + k_2k_{-1} + k_2k_P$; $K_k = k_3k_4[P_i] + k_3k_5 + k_4k_5$. k_P and k_{-P} are the forward and reverse rate constants for Mg²⁺-facilitated ATP ⇌ ADP + P_i.)

Goldman-Hodgkin-Katz (GHK) equation for membrane potential: $V = \frac{RT}{F} \ln \frac{\sum_{\text{cations } i} p_i [i_{out}^+] + \sum_{\text{anions } j} p_j [i_{in}^-]}{\sum_{\text{cations } i} p_i [i_{in}^+] + \sum_{\text{anions } j} p_j [i_{out}^-]}$

17.3.8. Biofluid Mechanics

Biofluids (e.g. blood, urine, synovial fluid, sweat, cerebrospinal fluid (CSF), saliva, cytosol, interstitial fluid) are a chemically diverse range of water-based solutions. They can transport ions, dissolved gases, organic molecules and whole cells by advection in internal flows. For the theory of fluid mechanics and thermofluid dynamics, see Sections 7.1 and 7.2. Biofluids may be:

- Non-Newtonian: shear and/or time-dependent viscosity (Section 14.3.8)
- Viscoelastic or Bingham plastic: interstitial fluids provide biopolymers in tissues with viscosity in addition to elasticity (Section 6.2.9).
- Water-based colloids: proteins agglomerate in water (Section 14.3), providing oncotic pressure (colloid-osmotic pressure). Starling equation: $Q = L_p S (p_c - p_i - \sigma(\pi_p - \pi_g))$ (Q : volumetric flow rate, L_p : hydraulic conductivity, S : surface area, p_c : capillary/interstitial hydrostatic pressure, π_p : plasma protein/subglycocalyx oncotic pressure, σ : Staverman's reflection coefficient)
- Cell suspensions: transport properties affected when cell size is comparable to pipe diameter, e.g. blood viscosity increases for $d \sim 10 \mu\text{m}$ (Fåhræus-Lindqvist effect / sigma effect)

Haemodynamics and Pulsatile blood flow: oscillating pressure gradients due to heart contractions
Consider laminar axisymmetric homogeneous incompressible Newtonian pipe flow.

If the pressure gradient $\frac{\partial p}{\partial x}$ oscillates as described by its complex Fourier series $\frac{\partial p}{\partial x}(t) = \sum_{n=0}^{\infty} P'_n e^{in\omega t}$:

Analytical solution (velocity field): $u(r, t) = \text{Re} \left\{ \sum_{n=0}^{\infty} \frac{i P'_n}{\rho n \omega} \left(1 - \frac{J_0(\alpha n^{1/2} i^{3/2} r/R)}{J_0(\alpha n^{1/2} i^{3/2})} \right) e^{in\omega t} \right\}$, for $0 \leq r \leq R$

(J_0 : Bessel function (Section 1.7.9), $\alpha = R \sqrt{\frac{\omega \rho}{\mu}}$: Womersley number.)

The zeroth harmonic in the Fourier series of $u(t)$ corresponds to Poiseuille flow (Section 7.1.9).

The walls of the blood vessels are subject to stresses (like pressure vessels, Section

17.4. Biotechnology and Bioengineering

17.4.1. Enzyme Classification

Enzyme database available [here](#).

EC 1: oxidoreductases; $A^- + B \rightarrow A + B^-$; $AH + B \rightarrow A + BH$ or $A + O \rightarrow AO$; uses NADH / NADPH / FAD cofactor

- | | |
|--|--|
| EC 1.1. dehydrogenases; acting on alcohols | EC 1.10. acting on diphenols or quinones |
| EC 1.2. acting on aldehydes or oxo groups | EC 1.11. peroxidases; acting on peroxides |
| EC 1.3. acting on CH-CH bonds | EC 1.12. hydrogenases; acting on molecular hydrogen |
| EC 1.4. acting on 1° amines | EC 1.13. dioxygenases; acting on two oxygen atoms |
| EC 1.5. acting on 2° amines | EC 1.14. monooxygenases; acting on paired donors, with O ₂ addition |
| EC 1.6. acting on NADH or NADPH | EC 1.15. acting on superoxides as acceptors |
| EC 1.7. acting on other nitrogen-containing groups | EC 1.16. oxidising metal ions |
| EC 1.8. acting on sulfur-containing groups | EC 1.17. acting on CH or CH ₂ groups |
| EC 1.9. acting on a haem group | EC 1.18. acting on iron-sulfur proteins as donors |

EC 2: transferases; $AB + C \rightarrow AC + B$; can use pyridoxal 5'-phosphate cofactor

- | | |
|---|---|
| EC 2.1. methyltransferases; moving 1 C groups | EC 2.6. transaminases; moving nitrogen groups |
| EC 2.2. transketolases/transaldolases; moving C=O | EC 2.7. phosphotransferases; moving P _i groups |
| EC 2.3. acyltransferases; moving COO groups | EC 2.8. sulfur/sulfo/CoA transferases; moving sulfur groups |
| EC 2.4. glycosyltransferases; moving sugars | EC 2.9. selenotransferases; moving selenium groups |
| EC 2.5. moving alkyl or aryl groups other than methyl | EC 2.10. molybdenum/tungstentransferases; moving Mo or W |

EC 3: hydrolases; $AB + H_2O \rightarrow AOH + BH$; no cofactor required

- | | | |
|--|-----------------------------------|------------------------------|
| EC 3.1. acting on ester bonds | EC 3.5. acting on other C-N bonds | EC 3.9. acting on P-N bonds |
| EC 3.2. glycosylases; acting on sugars | EC 3.6. acting on acid anhydrides | EC 3.10. acting on S-N bonds |
| EC 3.3. acting on ether bonds | EC 3.7. acting on C-C bonds | EC 3.11. acting on C-P bonds |
| EC 3.4. acting on peptide bonds | EC 3.8. acting on halide bonds | EC 3.12. acting on S-S bonds |
| | | EC 3.13. acting on C-S bonds |

EC 4: lyases; $X-A-B-Y \rightarrow A=B + X-Y$;

- | | |
|--|----------------------------------|
| EC 4.1. carboxylase/aldolases; acting on C-C bonds | EC 4.5. acting on C-halide bonds |
| EC 4.2. hydratases; acting on C-O bonds | EC 4.6. acting on P-O bonds |
| EC 4.3. acting on C-N bonds | EC 4.7. acting on C-P bonds |
| EC 4.4. acting on C-S bonds | EC 4.8. acting on N-O bonds |

EC 5: isomerases; $ABC \rightarrow BCA$

- | | |
|---|---|
| EC 5.1. epimerases/racemases; affecting R/S | EC 5.4. intramolecular transferases |
| EC 5.2. <i>cis/trans</i> -isomerases; affecting E/Z | EC 5.5. intramolecular lyases |
| EC 5.3. intramolecular oxidoreductases | EC 5.6. affecting macromolecular conformation |

EC 6: ligases; $X + Y + ATP \rightarrow XY + ADP + P_i$

- | | | |
|---------------------------|---------------------------|-----------------------------------|
| EC 6.1. forming C-O bonds | EC 6.3. forming C-N bonds | EC 6.5. forming phosphoric esters |
| EC 6.2. forming C-S bonds | EC 6.4. forming C-C bonds | EC 6.6. forming N-metal bonds |
| | | EC 6.7. forming N-N bonds |

EC 7: translocases; $AX + B_{\text{side 1}} \parallel \rightarrow A + X + \parallel B_{\text{side 2}}$

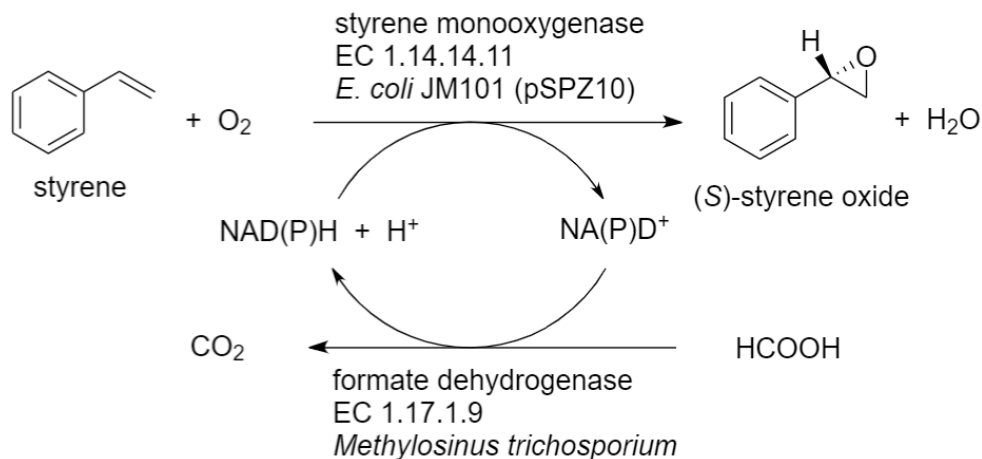
- | | | |
|-------------------------------------|--|---------------------------------|
| EC 7.1. acting on hydrons | EC 7.3. acting on inorganic anions | EC 7.5. acting on carbohydrates |
| EC 7.2. acting on inorganic cations | EC 7.4. acting on amino acids/peptides | EC 7.6. acting on nucleosides |

17.4.2. Enzymatic Biotransformations

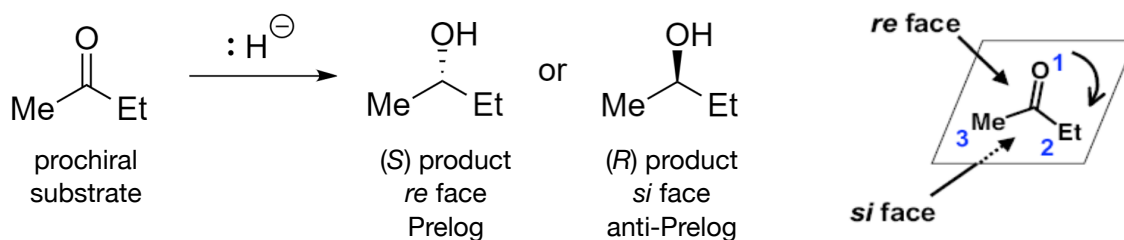
Common synthetic enzymatic reactions applied in biotechnology / biotransformations:

Enzyme class	Reactions (not complete; small molecules such as H ₂ O, O ₂ , H ⁺ , NH ₃ omitted)	Cofactors (for forward reaction)	Notes
Mono-oxygenase (MO) (uses O ₂) EC 1	alkane ⇌ alcohol alkane ⇌ 1,2-diol (dioxygenase) arene ⇌ phenol sulfide ⇌ thioketone ketone ⇌ ester alkene ⇌ epoxide alkene ⇌ peroxide (dioxygenase, no NADH)	NAD(P)H ⇌ NAD(P) ⁺ (balance with H ⁺ + O ₂ ⇌ H ₂ O)	High enantioselectivity and regioselectivity. Equilibrium favours the alcohol In cytochrome P450 monooxygenases, O ₂ is activated by Fe ²⁺ in haem. Iron must be added if using cell-free systems. FAD / FMN is an alternative cofactor which activates O ₂ into O.
Dehydrogenase (DH) EC 1	alcohol ⇌ ketone aldehyde ⇌ carboxylic acid amine ⇌ ketone α-amino acid ⇌ α-oxocarboxylic acid alkane ⇌ alkene	NAD(P) ⁺ ⇌ NAD(P)H (balance with ~ ⇌ H ⁺)	Equilibrium favours the alcohol or α-amino acid . Can also use FAD ⇌ FADH ₂ . Equilibrium favours the carboxylic acid. Prelog's rule: the S enantiomer is favoured (e.g. R ₁ -C(⋯OH)-R ₂ where R ₂ > R ₁)
Oxidase EC 1	amine ⇌ ketone α-amino acid ⇌ α-oxocarboxylic acid alcohol ⇌ ketone	None	Often FADH ₂ dependent. Equilibrium favours carbonyl compounds, no net consumption of cofactors (easier to use in cell-free systems).
Reductase EC 1	alkene ⇌ alkane	None	Best enantioselectivity when EWGs present on C=C. Enantiomer depends on E / Z.
Transaminase EC 2	R ₁ -CH(NH ₂)-COOH + R ₂ -COCOOH ⇌ R ₂ -CH(NH ₂)-COOH + R ₁ -COCOOH (amine + ketone ⇌ ketone + amine)	None	Often dependent on pyridoxal 5'-phosphate (P5P).
Hydrolase (uses H ₂ O) EC 3	ester ⇌ acid + alcohol amide ⇌ acid + amine epoxide ⇌ 1,2-diol	None (balance with H ₂ O ⇌ ~)	Esterase, lipase: in organic solvent for reverse Amidase, protease Epoxide hydrolase
Lyase EC 4	alkene ⇌ amine alkene ⇌ alcohol α-oxocarboxylic acid ⇌ aldehyde nitrile ⇌ amide aldehyde ⇌ α-hydroxynitrile	None	Ammonia lyase Hydratase Decarboxylase: uses thiamine pyrophosphate Nitrile hydratase Hydroxynitrile lyase
Isomerase EC 5	glucose ⇌ fructose (aldohexose ⇌ ketohexose) cis-alkene ⇌ trans-alkene	None	Important in resolutions
Ligase EC 6	glutamate ⇌ glutamine (carboxylic acid ⇌ amide)	ATP or GTP	Glutamine synthetase: uses ATP and NH ₄ ⁺

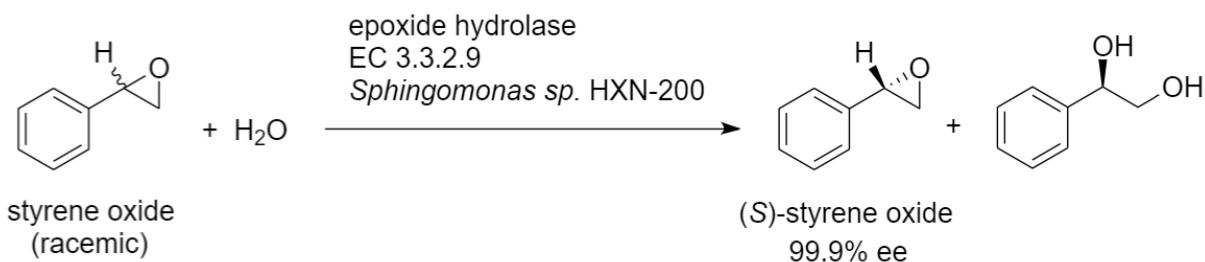
Example Biotransformation with Cofactor Recycling: enzymes which use opposing cofactors can be coupled together to exchange cofactors (catalytic cycle).



Prelog's Rule for Enantioselectivity in Asymmetric Catalysis: nucleophilic additions are carried out by delivering nucleophiles (e.g. hydride) onto the *re* face of planar prochiral substrates. (The *re* face is the front when there is more steric hindrance on the right-hand side i.e. Et > Me.) Enzymes can be classified as being enantioselective towards Prelog or anti-Prelog.



Kinetic Resolution: enzymes only react with one enantiomer, purifying the other.



Curves can be plotted of ee against % conversion for different enantiomeric ratios *E*. An enzyme is said to be 'enantiospecific' if it leads to 100% ee (perfect enantioselectivity).

Enzyme Cascades: a reaction scheme with multiple enzymatic reactions.

- Rate-limiting step: the step setting the overall steady-state rate i.e. maximum flux control coefficient $C = \frac{dJ}{J} / \frac{d[E]}{[E]} = \frac{d(\ln J)}{d(\ln [E])}$. (*J*: product flux, [*E*]: concentration or activity)
- Committed step: a near-irreversible step which, once occurred, ensures the target will form.

17.4.3. Purification and Identification of Enzymes

Separation: remove the solution containing the enzyme from the cells.

1. **Cell lysis** (not required if enzyme is extracellular): osmotic shock / homogeniser / blender / grinding / French pressure cell press / ball mill / ultrasonication
2. **Separation:** filtration / centrifugation / two-phase aqueous liquid-liquid extraction, to produce the cell-free extract (CFE) in the supernatant (contains the proteins of interest).

Concentration: starting with the enzyme solution, increase its concentration.

1. **Precipitation:** salting out with $(\text{NH}_4)_2\text{SO}_4$ / adding organic solvent / precipitate at $\text{pH} = \text{pI}$ / heat treatment / add polyvalent cations / add hydrophilic polymer e.g. PEG
2. **Stabilisation:** use buffer at optimal pH / work at low temperature / exclude O_2 to avoid free radical formation / avoid foaming to limit mechanical stress / use DTT or 2-mercaptoethanol to stabilise labile thiol groups / add BSA as a dilution standard / add protease inhibitors to prevent proteolysis

Chromatography: starting with a concentrated enzyme solution, separate the desired one while retaining biological activity.

A variety of selective chromatography methods are available (Section 16.4.7), based on isoelectric point (IEC), hydrophobicity (HIC), fusion tag affinity (IMAC) and size (SEC).

Automated UV/Vis spectrophotometry at a wavelength calibrated to the target enzyme can be used to record elution concentration in real time.

SEC / gel filtration is often used as a final polishing or desalting step, purifying the enzyme.

Quality Control and Characterisation: various assays can be used to investigate the enzyme:

- SDS-PAGE (Section 16.4.6): check for molecular mass and purity
- Electrospray mass spectrometry: determine precise molecular mass in kilodaltons (kDa)
- Isoelectric focussing (IEF): determine isoelectric point.
- Edman degradation: obtain the amino acid sequence of the protein.
- UV/Vis spectrophotometry: cofactor determination (holoenzyme or apoenzyme).
- X-ray crystallography / cryo-electron microscopy / 3D NMR: 3D structure determination
- Kinetic studies: calculate enzyme K_m , k_{cat} , K_i , proficiency, productivity (IU), etc.
- Chiral column chromatography with supercritical fluid: record enzyme enantioselectivity.
- HPLC with circular dichroism (CD) / optical rotation (OR) / refractive index (RIU) detection.
- Peptide mass fingerprinting and identification by e.g. MOWSE score.

17.4.4. Quantitative Analysis of Enzymatic Reactions

Enzyme Kinetics: rates of reaction of enzymatic biotransformations, accounting for saturation.

Typical enzyme-substrate (induced fit model) kinetics: $E + S \xrightleftharpoons[k_{-1}]{k_1} ES \xrightarrow{k_{cat}} E + P$

Michaelis-Menten equation: $r = \frac{r_{max} [S]}{K_M + [S]}$ ($r_{max} = V_{max}$ = maximum reaction velocity)

($r = k_{cat}[ES]$; $r_{max} = k_{cat}[E]_{tot}$; $[E]_{tot} = [E] + [ES]$; $K_M = \frac{\text{loss rate of } ES}{\text{gain rate of } ES} = \frac{k_{-1} + k_{cat}}{k_1}$)

Lineweaver-Burk plot: plot $\frac{1}{r}$ against $\frac{1}{[S]}$. x -intercept is $-\frac{1}{K_M}$; y -intercept is $\frac{1}{r_{max}}$; gradient is $\frac{K_M}{r_{max}}$.

Eadie-Hofstee plot: plot r against $\frac{r}{[S]}$. x -intercept is $\frac{r_{max}}{K_M}$; y -intercept is r_{max} ; gradient is $-K_M$.

Second-order rate constant (specificity constant): $\frac{k_{cat}}{K_M}$; Enzyme proficiency = $\frac{k_{cat} / K_M}{k_{non-cat}}$.

Enzyme Productivity: quantities of product formed.

Enzyme activity [symbol: U or IU = $\mu\text{mol min}^{-1}$] = $\frac{\text{quantity of product formed } [\mu\text{mol}]}{\text{time duration } [\text{min}]}$

Specific activity may be measured in IU g^{-1} , (per unit mass of enzyme **or** the cell dry weight (cdw)).

Space-time yield: tons of product per year per m^3

(1 ton $yr^{-1} m^{-3} \approx 2 \text{ mg min}^{-1} L^{-1}$; 1 op. year = 500,000 min).

Enzyme Inhibition: there may be additional $E + I \rightleftharpoons EI$ (competitive, equilibrium constant K_i) or $ES + I \rightleftharpoons ESI$ (uncompetitive, equilibrium constant K_i') reactions.

Let $\alpha = 1 + \frac{[I]}{K_i}$ and $\alpha' = 1 + \frac{[I]}{K_i'}$. Then the kinetics of the formation of the product are:

	Type of inhibition	Apparent K_M	Apparent r_{max}
K_i only ($\alpha' = 1$)	Competitive	$K_M \alpha$	r_{max}
K_i' only ($\alpha = 1$)	Uncompetitive	K_M / α'	r_{max} / α'
$K_i = K_i'$ ($\alpha = \alpha'$)	Non-competitive	K_M	r_{max} / α'
$K_i \neq K_i'$ ($\alpha \neq \alpha'$)	Mixed	$K_M (\alpha / \alpha')$	r_{max} / α'

Enzyme Enantioselectivity: extent of specificity towards chiral substrates and/or products.

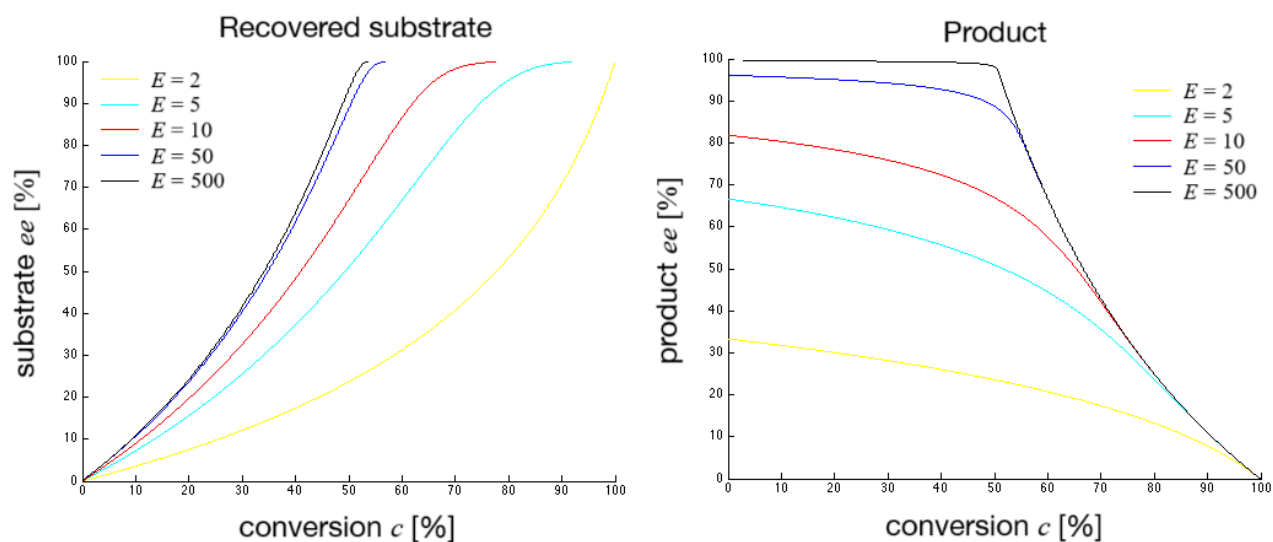
Kinetic resolution is used to convert a chiral racemic substrate A ($A_R : A_S = 1 : 1$) into a product B (ee_{product} , yield c), leaving enantioenriched substrate A ($ee_{\text{substrate}}$, yield $1 - c$).

Enzyme E catalyses $A_R \rightarrow B_R$ with rate constant k_R and $A_S \rightarrow B_S$ with rate constant k_S .

If E is enantiospecific then one of k_R or k_S is zero and the corresponding [B] is zero for all t .

- Enantiomeric excess (for R): if the concentrations (or molar ratio) is R : S then $ee = \frac{R - S}{R + S}$, as %.
- Conversion (percentage yield of product): $c = 1 - \frac{[A_R] + [A_S]}{[A_R]_{t=0} + [A_S]_{t=0}} = \frac{ee_{\text{substrate}}}{ee_{\text{substrate}} + ee_{\text{product}}}$.
- Mole fractions: $A_R = \frac{(1 + ee_{\text{substrate}})(1 - c)}{2}$, $A_S = \frac{(1 - ee_{\text{substrate}})(1 - c)}{2}$, $B_R = \frac{(1 + ee_{\text{product}})c}{2}$, $B_S = \frac{(1 - ee_{\text{product}})c}{2}$
such that $A_R + A_S = 1 - c$, $B_R + B_S = c$ and $A_R + A_S + B_R + B_S = 1$.
- Enantiomeric ratio E (for R) (aka selectivity factor s): $E = s = \frac{k_R}{k_S} = \frac{[k_{\text{cat}} / K_M]_R}{[k_{\text{cat}} / K_M]_S} = \frac{\ln\left(\frac{[A_R]_{t=0}}{[A_R]_{t=0}}\right)}{\ln\left(\frac{[A_S]_{t=0}}{[A_S]_{t=0}}\right)}$.
In terms of ee and c , $E = s = \frac{\ln\left[1 - c(1 + ee_{\text{products}})\right]}{\ln\left[1 - c(1 - ee_{\text{products}})\right]} = \frac{\ln\left[(1 - c)(1 - ee_{\text{substrates}})\right]}{\ln\left[(1 - c)(1 + ee_{\text{substrates}})\right]}$.
- Prochiral substrates: for asymmetric transformations ($A_R, A_S = A$), $E = s = \frac{1 + ee_{\text{product}}}{1 - ee_{\text{product}}}$.

Kinetic resolutions typically have a maximum of $c < 50\%$, since one enantiomer of A cannot react. However, if the substrates can interconvert and racemise (epimerise) spontaneously ($A_R \rightleftharpoons A_S$), then greater product yields (up to 100%) can be attained (dynamic kinetic resolution), though there is a trade-off due to lower ee in the product: likewise, there is higher ee in the substrate but less of it in total. Characteristic curves for attainable ee against conversion (yield) for different enantiomeric ratios E are shown.



17.4.5. Protein Engineering and Directed Enzyme Evolution

Mutagenesis can be used to improve enzymes' thermostability, enantioselectivity, yield, rate etc.

Protein engineering procedure: molecular modelling → predictions → sequence → mutagenesis → expression → purify protein → test properties → repeat with new information.

Site-directed mutagenesis: use a cloned gene for the protein and introduce mutations. Selecting the target position requires knowing the 3D structure as well as having good information about how it relates to its function (i.e. mechanisms at active site).

Mutations can be introduced using error-prone PCR (in the presence of e.g. UV light, mutagens (MNNG, MMS, 2-AP, AFB), or host mutations (uvrABC (UV lesion repair), phr (pyrimidine dimers), dnaQ (proofreading))). Also use low $[Mg^{2+}]$ and high $[Mn^{2+}]$, aiming for only 1-2 base changes per gene.

- Point mutation notation: e.g. 'D256A' means the amino acid D (aspartic acid) at position 256 counting from the N-terminus was replaced with the amino acid A (alanine).
- Thermostability: increased by having fewer heat-sensitive amino acids (Asn, Gln: deamination; Cys: disulfide bond cleavage; Asp: peptide bond hydrolysis), and a more densely packed hydrophobic interior.
- Applications: subtilisin (used in detergents, engineered to remove dependence on Ca^{2+}); glucose isomerase (used to make high-fructose corn syrup (HFCS) by the Maillard reaction, engineered to have a more suitable optimum pH and increased thermostability).

Directed Enzyme Evolution: use a sequential or combinational approach:

Number of possible variants by M simultaneous mutations over N amino acids = $19^M \times {}^N C_M$.

Starting with the wild-type enzyme performing its natural function, perform either sequential (amplify with mutations → test → select single best → repeat) or combinational (amplify with mutations → test → select top K best → cross with DNaseI for recombinant genes → repeat)

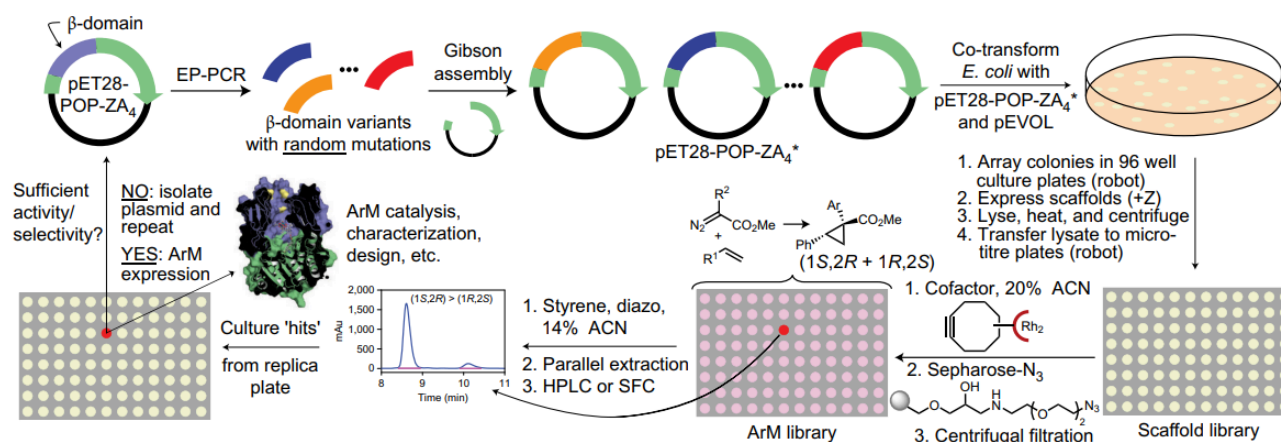
Applications: novel biotransformations, computational drug design...

Depending on the active site geometry, slight modifications to the substrate may still allow a reaction to proceed, allowing for another degree of freedom to investigate when designing an enzyme for the purpose of carrying out a new reaction. This is known as 'enzyme promiscuity'. Advances in protein folding prediction with machine learning algorithms (e.g. Google's AlphaFold 3) have allowed for such modifications to be simulated, which can reduce the need for extensive experiments and significantly speed up design/discovery of new enzymes.

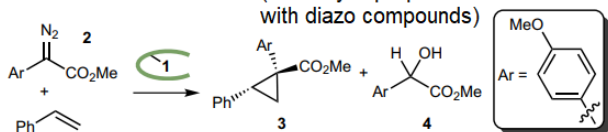
Example: Designing Artificial Metalloenzymes and Evolving by Random Mutagenesis

An artificial metalloenzyme (ArM) based on the POP (prolyl oligopeptidase, a natural serine protease) enzyme chain is designed. An azide group was genetically encoded into the protein chain by mutating an active site Ser residue, incorporated using bioorthogonal tRNA/synthetase pair (reassigns the amber stop codon), which then reacts with a metal-containing linker (**c**) to form the metalloenzyme (**b**) by a click reaction. The goal is to improve the enantioselectivity of this enzyme by referring to a model reaction (**a**) and using random mutagenesis (error-prone PCR) to vary the composition near the active site (the β -domain).

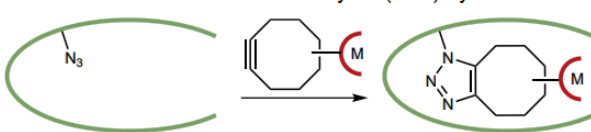
Procedure for carrying out mutagenesis:



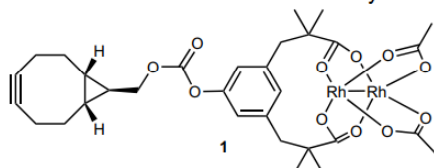
a: reaction to be carried out (olefin cyclopropanation with diazo compounds)



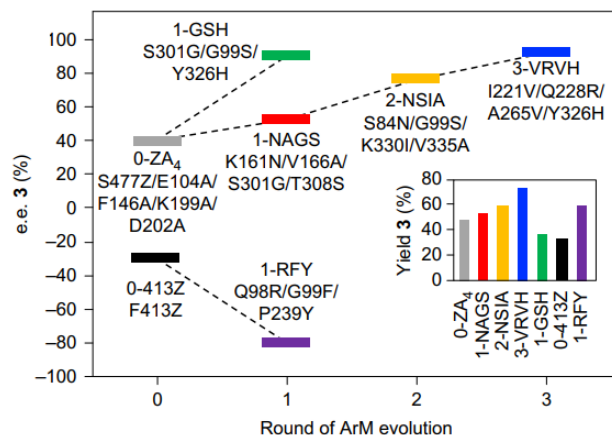
b: formation of the artificial metalloenzyme (ArM) by click chemistry



c: full structure of metal cofactor with linker to alkyne



Results: e.e. of product 3 after several rounds of ArM evolution



(Source: Yang *et al.*, 2018, *Evolving artificial metalloenzymes via random mutagenesis*)

17.4.6. Industrial Biotransformations

The main classes of bioprocesses are:

- Fermentation of bulk chemicals (e.g. ethanol, citric acid, lactate)
- Bioproduction (e.g. indigo, penicillin G, vitamin B₁₂, mABs, enzymes)
- Bioconversion with whole cells (free or immobilised, for e.g. corticosteroids, acrylamide)
- Bioconversion with isolated enzymes (free or immobilised, for e.g. aspartate, HFCS, 6-APA. Materials used for immobilisation include Sepharose beads and magnetic nanobiocatalysts.)

Cofactor Recycling: cofactors are expensive, so recycling significantly helps reduce material costs
Common enzymes used for cofactor regeneration (coupled enzymes):

NAD ⁺ regeneration	NADP ⁺ regeneration	NADH regeneration	NADPH regeneration
<ul style="list-style-type: none"> • Lactate dehydrogenase (NADH + pyruvate + H⁺ → NAD⁺ + lactate) • Glutamic dehydrogenase (NADH + 2-oxoglutarate + NH₃ + H⁺ → NAD⁺ + glutamate + H₂O) • Alcohol dehydrogenase (NADH + acetaldehyde + H⁺ → NAD⁺ + ethanol) 	<ul style="list-style-type: none"> • Glutamic dehydrogenase (NADPH + 2-oxoglutarate + NH₃ + H⁺ → NADP⁺ + glutamate + H₂O) • Alcohol dehydrogenase (NADPH + acetone + H⁺ → NADP⁺ + isopropanol) 	<ul style="list-style-type: none"> • Alcohol dehydrogenase (NAD⁺ + ethanol → NADH + acetaldehyde + H⁺) • Formate dehydrogenase (NAD⁺ + formic acid → NADH + CO₂ + H⁺) • Glucose dehydrogenase (NAD⁺ + glucose → NADH + gluconolactone + H⁺) • Hydrogenase (NAD⁺ + H₂ → NADH + H⁺) 	<ul style="list-style-type: none"> • Glucose dehydrogenase (NADP⁺ + glucose → NADPH + gluconolactone + H⁺)

Alternatively, the same enzyme can be used to carry out two reversible reactions (coupled substrates).

Use of Organic Solvents

Hydrophilic solvents can be used to solubilise lipophilic substrates without deactivating the enzymes. Partially miscible solvents ($0 < \log P < 4$) are typically not used as they cause enzyme distortion, decreasing activity, while lipophilic solvents cause no distortion and retain high activity. For a table of partition coefficients (miscibility), see Section 13.4.7.

Klibanov rules: requirements for an enzyme to perform well in an organic solvent.

- Specific enzyme conformations can be attained by adding a specific ligand and lyophilising (freeze, remove water under vacuum, anhydrous extraction of the ligand). Adding water reforms the natural conformation; adding anhydrous solvent retains the conformation.
- Enzyme conformations are more 'rigid' in organic solvents and more flexible in water, so activities of optical catalytic conformations are diminished in water and improved in solvent.
- Lyoprotectants (glycerol, sugars, salts) can be used to block these changes if needed.

Organic solvents are typically used to sterilise the biotransformation environment, although some strains of bacteria can survive in miscible organic solvents, by releasing emulsifier (lipopolysaccharide) micelles from their cell membrane to dissolve the organic phase into the aqueous phase, away from the bacterium.

Use of Microbial Cells

Bacteria can be gene edited to express specific enzymes by splicing in a plasmid coding for the required protein, or by deactivating proteins which inhibit the desired activity. Bacteria benefit from having 'built-in' cofactor recycling as part of their natural metabolism. However, product extraction is complicated by additional purification/separation steps.

Bacteria can also be immobilised on an adhesive surface for easier re-use, but with lower activity.

Bacterial growth phases: lag (adjustment to conditions) → exponential growth → growth plateau (nutrients are depleted) → death (accumulation of toxic byproducts).

Growth in the presence of a limiting substrate of concentration [S]:

$$\mu = \mu_{max} \frac{[S]}{K_s + [S]} \quad (\text{proportional growth rate: such that } \frac{dN}{dt} = \mu N) \quad (\text{Monod equation})$$

Enzyme synthesis rate, r_e [IU L⁻¹ hr⁻¹] = Specific synthesis rate, q_e [IU g_{cell}⁻¹ hr⁻¹] × Biomass, c_x [g_{cell} L⁻¹]

Enzyme productivity, P_e [IU L⁻¹ hr⁻¹] = $\frac{1}{T} \int_0^{t_e} q_e(t) c_x(t) dt$ (T = fermentation time t_e + turnaround time)

Product Recovery

The stages of recovering product from a bioreactor with microbial cells include:

Disruption of microbe cell wall: release the cytoplasm, generating cell debris.

- Chemical methods (can inactivate/denature the enzyme).
Can use alkali, detergents or organic solvents.
- Enzymatic methods (specific, mild). Can use lysozymes (for Gram-positive bacteria), lysozymes with EDTA (for Gram-negative bacteria) or β-glucanases/mannanase/chitinase (for yeast and fungi).
- Physical methods. Can use freeze-thaw, sonicator, pressure bomb, wet milling, French press/homogeniser.

Removal of cells or other particles: cake filtration / cross-flow filtration / centrifugation.

Primary isolation of dissolved compounds: solvent extraction / sorption with ion exchanger or hydrophobic resin / adsorption chromatography / precipitation / membrane filtration (ultrafiltration, composite membranes) / reverse osmosis / pervaporation (permeation then evaporation) / perstraction (permeation then solvent extraction (dialysis))

Purification and final product isolation: chromatography, crystallisation, concentration, centrifugation and drying, distillation.

Bioprocess Economics

Costs can be broken down as being associated with 1) running the fermentor, 2) product recovery, 3) raw materials for cell growth, 4) substrate for reaction.

Approximate correlations for startup and operating costs are:

- Fermentor costs [US \$] $\approx 40,000 \times V^{0.6}$ (includes cell recovery) (V : fermentor volume [m³])
- Cost per unit product [US \$ kg⁻¹] = $\frac{31250}{M_w [g \text{ mol}^{-1}] \times P_e [IU L^{-1} \text{ min}^{-1}]}$ where $P_e = \frac{t_{\text{cycle}}}{t_{\text{turnaround}}} \times q_e c_x$

Raw materials: carbon sources (e.g. whey: \$ 0.1 kg⁻¹, molasse: \$ 0.2 kg⁻¹, glucose: \$ 0.38 kg⁻¹), nitrogen sources (e.g. ammonium sulfate: \$ 1.8 kg⁻¹), phosphate/magnesium/trace sources (e.g. as salts: approx \$ 0.5 kg_{cdw}⁻¹)

- Source costs [\$ kg_{cdw}⁻¹] = $\frac{\text{cost of source } [\$ \text{ kg}_{\text{source}}^{-1}]}{\text{yield } [kg_{\text{cdw}} \text{ kg}_{\text{source}}^{-1}]}$, where $\text{yield} = \frac{\text{mass fraction of atoms in cells}}{\text{mass fraction of atoms in source}}$
- Cost per unit product [US \$ kg⁻¹] = $\frac{\text{source costs } [US \$ \text{ kg}_{\text{cdw}}^{-1}]}{\text{productivity } [kg \text{ kg}_{\text{cdw}}^{-1}]}$ = $\frac{\text{source costs } [US \$ \text{ kg}_{\text{cdw}}^{-1}] \times 10^6}{\text{activity } [IU \text{ g}_{\text{cdw}}^{-1}] \times M_w [g \text{ mol}^{-1}] \times t_{\text{turnaround}} [\text{min}]}$
- Substrate costs [\$ kg⁻¹] = $\frac{\text{substrate cost } [\$ \text{ kg}_{\text{substrate}}^{-1}] \times M_w [g \text{ mol}^{-1}]_{\text{substrate}}}{\text{yield } [mol \text{ mol}_{\text{substrate}}^{-1}] \times M_w [g \text{ mol}^{-1}]_{\text{product}}}$
- Product recovery costs [\$ kg⁻¹] $\approx k \times (\text{product concentration } [M])^{-0.75}$ (k : method dependent)

17.4.7. Bioremediation and Genetic Engineering of Bacteria

Bioremediation involves the use of microorganisms (usually bacteria or fungi) to remove pollutants from, or provide nutrients to, a region of a biome in the natural environment.

Genetic engineering can be used to deploy GMOs with the genes coding for proteins which can degrade harmful compounds. However, there are concerns about the possibility of horizontal gene transfer with other organisms.

Bacteria can accept exogenous plasmids. If a plasmid containing a gene for a desired protein is synthesised (a recombinant plasmid), it will be expressed and secreted by the bacteria. A wide range of synthetically useful proteins can be produced directly in this way (e.g. enzymes: Section 17.4.6, but also peptide hormones e.g. insulin to be used as medicine for diabetes). Enzymes can also be designed and optimised to carry out a new biotransformation on native metabolites into a useful product (Section 17.4.5) e.g. monomers for bioplastics.

17.4.8. Reproductive Cloning of Organisms

Somatic Cell Nuclear Transfer (SCNT) can be used to clone a living organism. A somatic cell is extracted and its nucleus is isolated. An egg cell is taken and its nucleus is removed and replaced with the somatic nucleus. With an electric shock, the egg now behaves as if it were newly fertilised, and develops into an embryo. The embryo is transplanted into a surrogate mother and carried to term, where it is born as a clone of the original organism.

In 1996, 'Dolly' became the first mammal (a sheep) to be created as a cloned organism. Dolly lived for 7 years, appearing to age faster than usual, as well as having various health complications.

This cloning procedure could hypothetically be applied to humans, but is currently far too uncertain and unethical for such an experiment to be performed in the foreseeable future.

17.4.9. Polymerase Chain Reaction (PCR)

PCR is a synthetic technique to amplify a given sequence of DNA. It can be considered *in vitro* DNA replication, using a polymerase enzyme (Taq polymerase, a thermostable polymerase I), 3' end complementary primer sequences, and a source of nucleotides (supplied as deoxynucleoside triphosphates, dNTPs).

Thermal cycling is used to carry out the following steps repeatedly:

1. Denaturation at 95 °C: the DNA is unravelled by melting the hydrogen bonds.
2. Annealing at 55 °C: primers anneal to the 3' ends of each open strand.
3. Extension at 70 °C: Taq polymerase builds the complementary strand from the template.

A pH buffer is used for optimal activity. A solution of Mg^{2+} (or other divalent cations) is used to provide the metal cofactors for the polymerase enzymes. If mutations are desired (PCR-mediated DNA mutagenesis), Mn^{2+} can be used instead, which displaces Mg^{2+} polymerase cofactors and are less specific to nucleotide pairing, increasing the rate of errors.

PCR can be used to test for the presence of specific viruses. Once the genome of the virus has been sequenced, its primers can be developed. For RNA viruses, the RNA must be converted to cDNA (with reverse transcriptase) first. Fluorescent DNA probes (nucleic acid stains e.g. SYBR green) are used to indicate the presence of the viral cDNA. This is the basis for the COVID-19 PCR test.

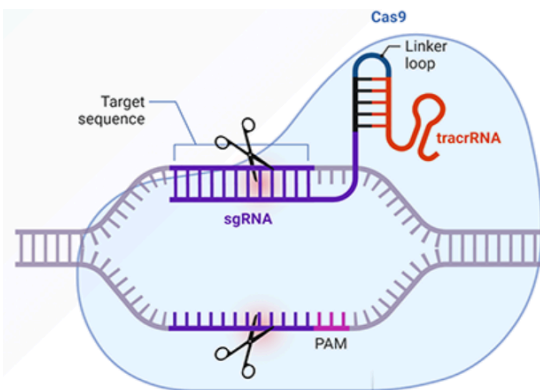
17.4.10. Gene Editing with CRISPR

CRISPR (Clustered Regularly Interspaced Short Palindromic Repeats) is a naturally-occurring component of the adaptive immune systems of prokaryotes (bacteria and archaea / extremophiles) to defend against bacteriophages and plasmids. It can be employed to edit genomes with high precision.

Natural CRISPR Mechanism (*in vivo*: in a living organism)

When viral DNA is injected into the bacteria, it can be inserted between palindromic sequences in the CRISPR locus to form a CRISPR array. This DNA can be transcribed into pre-crRNA. Effector complexes are Cas9 (nuclease) proteins bound to tracrRNA strands. If the complex encounters viral DNA complementary to its crRNA, it will cleave the DNA at the end of the protospacer adjacent motif (PAM) sequence, preventing its transcription and therefore preventing viral replication.

Artificially Engineered CRISPR Mechanism (initially *in vitro*: in a laboratory)



crRNA and tracrRNA can be linked to form a single molecule, sgRNA. When combined with Cas9, this system will read DNA until the pre-specified complementary strand is found. It will cleave the DNA after the PAM sequence.

For **gene knock-out**, the non-homologous end-joining (NHEJ) repair pathway rejoins the two sections of DNA. For **gene knock-in**, the homology-directed repair (HDR) repair pathway fills the gap by replicating from a template DNA. This can be used for transfection.

Gene therapy: the gene-edited cells can then be used appropriately (*in vitro*: e.g. CAR T-cell therapy for anticancer antibody production, viral vector vaccine production, etc).

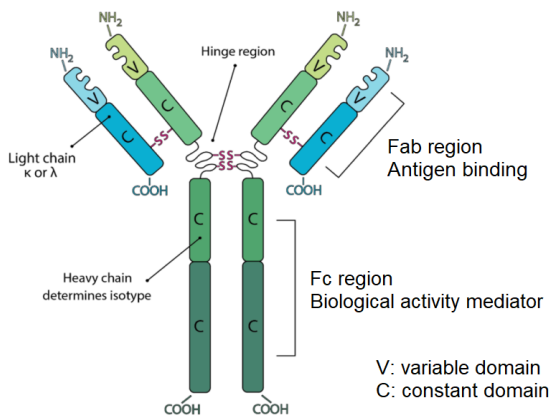
In vivo usage of CRISPR/Cas9 is currently underway (as of 2021) which could edit the genomes of live adult cells in an organism. Such a usage is limited to adult somatic cells: extension to gene editing of human embryos remains extremely controversial and unethical. In 2019, a Chinese scientist was imprisoned for conducting such an experiment in which two human twins were equipped with a gene intended to protect against HIV. As of 2023, they are alive and remain healthy, although long-term effects are highly uncertain as their natural development continues.

17.4.11. Monoclonal Antibodies

Antibodies are immunoglobulin proteins which are freely circulating in the blood plasma. They bind to matching antigens on cells, which are then recognised by macrophages. Polyclonal antibodies (pAbs) can bind to multiple epitopes (regions; antigenic determinants) of the same type of antigen. Monoclonal antibodies (mAbs) are specific to a single epitope of a single antigen.

IgG: monomer, activates phagocytosis; IgM: pentamer, activates complement

Manufacture of Murine Antibodies



- An animal (e.g. mouse) is vaccinated with the target antigen
- The immune response generates pAbs for this antigen
- B cell antiserum is extracted from the spleen
- Myelomas (cancerous white blood cells) are grown in 8-azaguanine
- The B cells are fused with the myelomas in a PEG medium
- The resulting hybridomas are immortal, divide fast, and generate pAbs.

The cells are cultured in a HAT medium. Aminopterin (A) inhibits the folate pathway of new DNA synthesis while hypoxanthine (H) and thymidine (T) provide raw materials for the salvage pathway (in order to do this, they must have the HGPRT gene, which B cells have but myelomas do not). The result is purification of only hybridomas (B cells die naturally over time).

To obtain mAbs from the pAb product, isolate individual cells by 'infinite dilution' (1 cell per well). Screen using ELISA (Section 16.6.17) with target antigen, then scale up for mass production.

Second Generation Antibodies: Murine (mouse-derived, suffix: -momab) antibodies are typically not used when immunocompatibility in humans is important. By making the antibody structure more similar to those found in humans, antibodies can be administered more safely.

- Chimeric: the constant domain of the antibody is human. Suffix: -ximab.
- Humanised: the constant domain, and most of the variable domain, is human. Suffix: -zumab.
- Human: the whole antibody is human. Suffix: -umab.

Production: *in vitro* immunisation / SCID mice / phage display / transgenic mice.

Common Applications of mAbs:

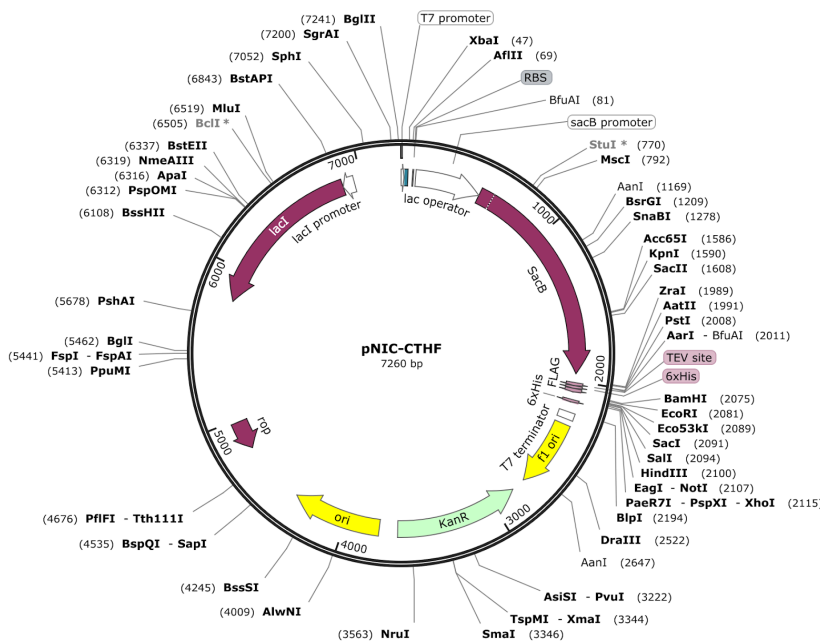
- Pregnancy test kits: based on an ELISA test strip for hCG hormone antigen with fluorescent markers.
- Lateral flow tests: same principle, testing for presence of viral antigens
- Allergen detection in foods: tests for the presence of common allergens e.g. gluten protein.
- Radiopharmaceuticals: mAbs for cancer cell antigens bonded by a linker to a chelated radioactive atom (e.g. ^{131}I , ^{90}Y , ^{177}Lu), which kills the targeted cell by emitting β radiation
- Bioassays: various methods of identifying, separating and/or characterising proteins e.g. ELISA, Western blotting, flow cytometry, immunohistochemistry, affinity chromatography

17.4.12. DNA Sequencing, Cloning and Synthesis Technology

DNA Synthesis

DNA Cloning: plasmids are used to carry genes, amplify and express in bacteria

Artificial plasmids are available to molecular biologists for cloning purposes. For example, pNIC-CTHF is a bacterial plasmid (expression vector) designed to inducibly express genes in *E. coli*. It contains:



T7 promoter: the main driver of gene expression.

Lac operator: typically binds to the repressor *lacI* (encoded by *lacI* regulator gene) preventing transcription, but when IPTG (isopropyl β-D-1-thiogalactopyranoside), which mimics allolactose, is added to the culture, it deactivates the repressor and permits transcription (inductive gene expression).

RBS: ribosome binding site, for protein production.

SacB gene: confers sensitivity to sucrose, such that expression in 5% sucrose prevents growth (negative selection marker).

XbaI, PstI and EcoRI: restriction enzyme sites.

TEV site: protease recognition site.

6xHis and FLAG: protein tags useful for purification and identification.

KanR: gene for kanamycin antibiotic resistance.

The plasmid pNIC-CTHF can be linearised with the restriction enzymes *XbaI* and *PstI*, resulting in excision of *SacB*, to be replaced with a suitable DNA fragment containing the new gene. The new DNA fragment must contain a ribosome-binding site downstream of *XbaI*, a start codon for the open reading frame, and ending with a *PstI* site. It is common to obtain the DNA fragments via PCR amplification. The primers used in the PCR must be designed carefully to ensure that the resulting DNA is in the same phase (reading frame) as the adjacent sequences in the plasmid, using additional sequences if needed.

Example Workflow using Plasmid Engineering: testing of a modern protein subunit vaccine

Novel gene design and synthesis:

- Obtain the DNA sequence of a spike protein on the virus using next-generation sequencing.
- To the designed sequence, add a His-tag, RBS and TEV protease recognition site. Optimise the codons for the spike protein if necessary.
- Synthesise the designed DNA sequence using e.g. phosphoramidite method, Klenow/Gibson assembly.
- Design and synthesise PCR primers for the DNA sequence, containing *XbaI* and *PstI* restriction sites.
- Carry out PCR on the template DNA using the designed PCR primers, amplifying the DNA. Purify the DNA.

Cloning process:

- Obtain bacterial plasmid pNIC-CTHF, suitable for inductive gene expression, and linearise using restriction enzymes *XbaI* and *PstI*, resulting in excision of the *SacB* gene from the plasmid.
- Use DNA ligase to splice the PCR-amplified DNA into the plasmid, forming the recombinant plasmid.
- Transform *E. Coli* with the plasmids and culture on a multiwell microtiter plate containing kanamycin antibiotic and 5% sucrose to kill cells which did not take up the plasmid, or took up an unmodified/self-ligated plasmid (no spike protein gene), respectively.
- Inoculate a culture of the transformed cells in growth medium (e.g. lysogeny broth) and culture to the mid-log phase of cell growth to produce recombinant clones.
- Induce protein expression by adding IPTG and continue to culture for some time period.

Product extraction:

- Extract the protein by cell lysis and centrifugation, and isolate by affinity chromatography (IMAC: nickel-agarose column to bind with the His-tagged protein, then elution with imidazole).
- Digest the His-tags with TEV protease solution to remove the tags, yielding the free protein.
- Purify the protein product by gel filtration chromatography.
- Analyse the protein for purity by 2D gel electrophoresis (using isoelectric focussing and SDS-PAGE), and Western blotting with anti-FLAG antibodies.
- For the purposes of protein subunit vaccine development, suspend the proteins (either freely or in liposomes) in a suitable buffer and formulate with adjuvants.
- Store the solution, typically at -80 °C for long-term storage or distribution.

17.4.13. Vaccines

Vaccines can 'simulate' a viral infection without a real infection, priming the body's immune system and allowing it to respond quickly, significantly increasing the chance of recovery. They work by causing the characteristic biomarkers belonging to the pathogen responsible for the disease to be presented on host cells, allowing for the immune system to recognise them and proceed with the innate immune response. Once immunity is achieved, subsequent exposure with the same pathogen will immediately stimulate a strong immune reaction, preventing infection.

Types of vaccines: different ways of inducing antigen presentation in the host cells

- **Live attenuated virus:** a live virus which has acquired mutations that severely reduce its toxicity.
- **Inactivated virus:** a virus that has been 'killed' using chemicals/heat to break the virus into pieces.
- **Toxoid:** used for anti-bacterial vaccines, containing inactivated toxins released by the bacteria.
- **Protein subunit:** a component of the virus (antigen; spike protein) or bacteria (cell wall polysaccharide)
- **Viral vector vaccine:** a replication-deficient adenovirus with DNA coding for the target antigen.
- **mRNA vaccine:** lipid nanoparticle containing mRNA coding for the antigen.
- **Dendritic cell vaccine:** personalised dendritic cells already presenting neoantigens, for cancers.

Adjuvants: compounds that stimulate the immune response

For non-live vaccines, adjuvants accompany the vaccine load in small quantities to increase the sensitivity of the immune system. These work by (directly or indirectly) increasing the number of pro-inflammatory cytokines (interleukins) in the blood plasma, which attract immune cells. Common adjuvants include aluminium hydroxide nanoparticles, squalene emulsion, emulsifiers (e.g. polysorbate 80) or Toll-like receptor (TLR) agonists. Some adjuvants also promote the initial endocytosis of the vaccine payload into host cells by increasing the affinity for cell receptors.

Vaccines may be monovalent (targets only one serotype) or multivalent (targeting multiple serotypes). The serotype targeted is dependent on the identity of the surface antigens.

17.4.15. Gene Transfection

HEK-293 cells (human embryonic kidney cells) are an immortalised cell line commonly used as a common eukaryotic target for gene transfection.

17.4.16. Stem Cell Bioengineering

Stem cell potential to undergo further differentiation: Totipotent (e.g. zygote) > pluripotent (e.g. embryonic stem cells (ESCs)) > multipotent (e.g. adult stem cells: hematopoietic stem cells (HSCs), mesenchymal stem cells (MSCs)).

Induced pluripotent cells (iPSCs): treatment with the Yamanaka reprogramming factors (Oct4, Sox2, Klf4, C-Myc) leads to reversion of cells to the pluripotent state. Conditions can then be tuned to favour differentiation to a desired cell type.

Tissue engineering (Section 17.4.17) with stem cells has several applications in regenerative and personalised medicine, as well as in sustainable agriculture:

- Osteoblasts (bone stem cells) → bone regeneration.
- Myoblasts (muscle stem cells) → cultured meat (“lab-grown meat”).

Stem Cell Culture Media

A culture medium must maintain the self-renewal and pluripotency of stem cells, as well as the growth of the cells themselves. Modern growth media are xeno-free (no animal components; human-derived only) chemically-defined medium with recombinant growth factors and small molecules.

17.4.17. Tissue Engineering and Bioprinting

Regenerative medicine is an emerging field in biomedical science, involving the *in vivo* formation of personalised tissues (e.g. skin, bone, organ tissue). In order to successfully integrate with the host tissue, implanted tissues must contain:

- Matrix / scaffold: polymeric 3D structure mimicking the extracellular matrix (ECM).
- Signalling molecules: various biomolecules e.g. growth factors, Yamanaka factors
- Cells: live cells, depending on the type of tissue to be regenerated e.g. stem cells.

An alternative cell-free approach to tissue engineering involves removing cells from the formulation, and instead using ‘homing’ of host cells into the new scaffold, promoted by the biomolecules.

Scaffold: typically made of synthetic resorbable aliphatic polyesters (e.g. PCL, PTMC). It must have a porous interconnected structure (to allow nutrient flow), be biodegradable/bioresorbable at a rate matching the cell proliferation rate, have suitable surface chemistry to permit cell attachment and proliferation, have matching mechanical properties and be easily processed into various shapes.

The scaffold geometry must have very high surface area. For this purpose, geometries using triply periodic minimal implicit surfaces (e.g. Schwarz “P” unit cell) or space-filling curves can be used. Scaffolds can also be made by decellularising tissue *ex vivo*, leaving a natural matrix.

Bioprinting: automated and controllable deposition of matrix-cell-biomolecule bioinks.

Bioink contains live cells in a hydrogel-biomolecule formulation. The bioink may contain the fully-formed scaffold, or its precursors (controlled induced cross-linking). Bioprinting can be done by various methods, adapted from and inspired by the approaches in conventional 3D printing.

- Extrusion: continuous deposition of a viscous bioink stream from a syringe.
- Inkjet: directed emission of bioink droplets from a piezoelectric nozzle.
- Projection: UV-initiated cross-linking of photosensitive hydrogels (**not** polymerisation like photolithography).

The rheological properties of the bioink (gelation kinetics, surface tension, viscoelasticity, shear-dependent and time-dependent viscosity) are important design parameters, depending on the printing method. The addition of cross-linkers into the bioink allows the solidification of the hydrogel in the scaffold once deposited. Depending on whether the hydrogel is UCST or LCST (Section 16.5.11), either the syringe or stage must be heated to form the gel before deposition.

The cells can be supported on microcarriers suspended in the bioink, which are made of either natural (cellulose, gelatin, collagen) or synthetic (e.g. dextran, plastic, glass) hard materials. This arrangement permits high cell counts to be used without compromising viability, as well as improved nutrient exchange. Some types of cell e.g. chondrocytes can help to replace the scaffold with new ECM tissue if rigidity is desired. Functional materials (e.g. graphene, magnetic fibres, metal nanoparticles) can also be supplied in the bioink with careful control of suspension rheology and biocompatibility.

Like other CAM hardware, bioprinters can be designed to print from inputs given by parametric equations for the toolpath, G-code (low-level language), CAD models or images (by segmentation).

17.5. Systems Chemistry, Origin of Life and Astrobiology

17.1.1. Driving Forces for Systems Chemistry on the Prebiotic Earth

Systems chemistry is the study of networks of interacting molecules, forming highly dynamic systems.

Life is suspected to have begun in either the late Hadean or early Archaean eon (~4.1 - 3.8 BYA), approximately 500 million years after Earth's formation (4.55 BYA).

- **High temperatures:** the Earth's surface was ~70 °C throughout the late Hadean, allowing hot liquid water oceans across the surface.
- **Lunar tides:** the moon formed 4.527 BYA, and orbited ~17 times closer in the Hadean than today, amplifying the strength of lunar tides, allowing cyclic forcing of lava flows and generating heat due to tidal friction.
- **Radiation:** the Sun was more intense in the high energy UV and X-ray wavelengths, although was ~30% less intense overall. A hot greenhouse layer of CO₂ insulated the Earth. Earth's magnetic field was only beginning to start in the late Hadean, allowing a larger flux of cosmic rays and ions from the solar wind to reach the Earth.
- **Impact events:** a large influx of meteorites led to regular redistribution of land mass, including ejection to space. The meteorites delivered highly reduced minerals to the surface (e.g. metallic iron). The Late Heavy Bombardment, occurring at ~3.8 BYA,
- **Weakly reducing atmosphere:** the Hadean's thick, hydride-rich, oxygen-poor atmosphere resembling the solar nebula slowly gave way to the 'prebiotic atmosphere', containing methane (CH₄), ammonia (NH₃), hydrogen (H₂), carbon dioxide (CO₂) as well as nitrogen (N₂) and some noble gases (He, Ne, Ar...).

17.1.1. Organic Molecules on the Early Earth

Abiogenesis describes the naturalistic origin of life on Earth from abiotic matter (chemicals) in several stages. This is an active area of research and these stages have varying degrees of supporting evidence. The early atmosphere had no oxygen, but was rich in nitrogen and carbon dioxide, as well as various other gases (methane, hydrogen, water vapour). The Hadean eon (up to about 4 billion years ago) was highly energetic, with extremely high temperatures ($>100\text{ }^{\circ}\text{C}$), frequent lightning, volcanic eruptions, UV radiation and asteroid impacts. The Archean eon thereafter was less violent, though still with lots of geothermal activity providing a rich source of chemicals. Fossil evidence of microorganisms are known as early as 3.7 billion years ago, suggesting that abiogenesis occurred on the order of ~ 100 million years in between these two geologic eons.

Amino Acids: precursors to proteins.

In the presence of heat and electrical sparks, small molecules assumed present on early Earth's atmosphere such as H_2O , NH_3 , CH_4 , H_2 can form racemic amino acids and also some nucleobases. Intermediates in this reaction include formaldehyde, hydrogen cyanide, acetylene, cyanoacetylene among others (the Miller-Urey experiment). A 'prebiotic soup' containing these chemicals, potentially found near hydrothermal vents or hot springs, could have permitted this reaction to occur on early Earth, forming amino acids. Amino acids have also been observed on meteorites in space, which may have been delivered to Earth during its formation. The conditions during protoplanetary disc formation may have allowed for the formation of amino acids in space (astrochemistry). Many samples e.g. the Murchison meteorite contain enantioenriched amino acids, contributing to the symmetry breaking of L over D observed in biology (homochirality).

Monosaccharides: components of nucleosides and precursors to carbohydrates

Simple sugars can be made by the formose reaction (Butlerov reaction), in which small molecules such as formaldehyde and glyceraldehyde (which are known to form from CO_2 and H_2O) can react under alkaline conditions in an autocatalytic cycle to form a range of monosaccharides. By varying the conditions, such as with borate minerals or chiral amino acids (e.g. proline), product specificity (e.g. forming ribose) can be increased significantly, as well as the yield. Under strongly alkaline conditions, the competing Cannizzaro reaction may disrupt this process, so the milder pathways are considered more prebiotically relevant.

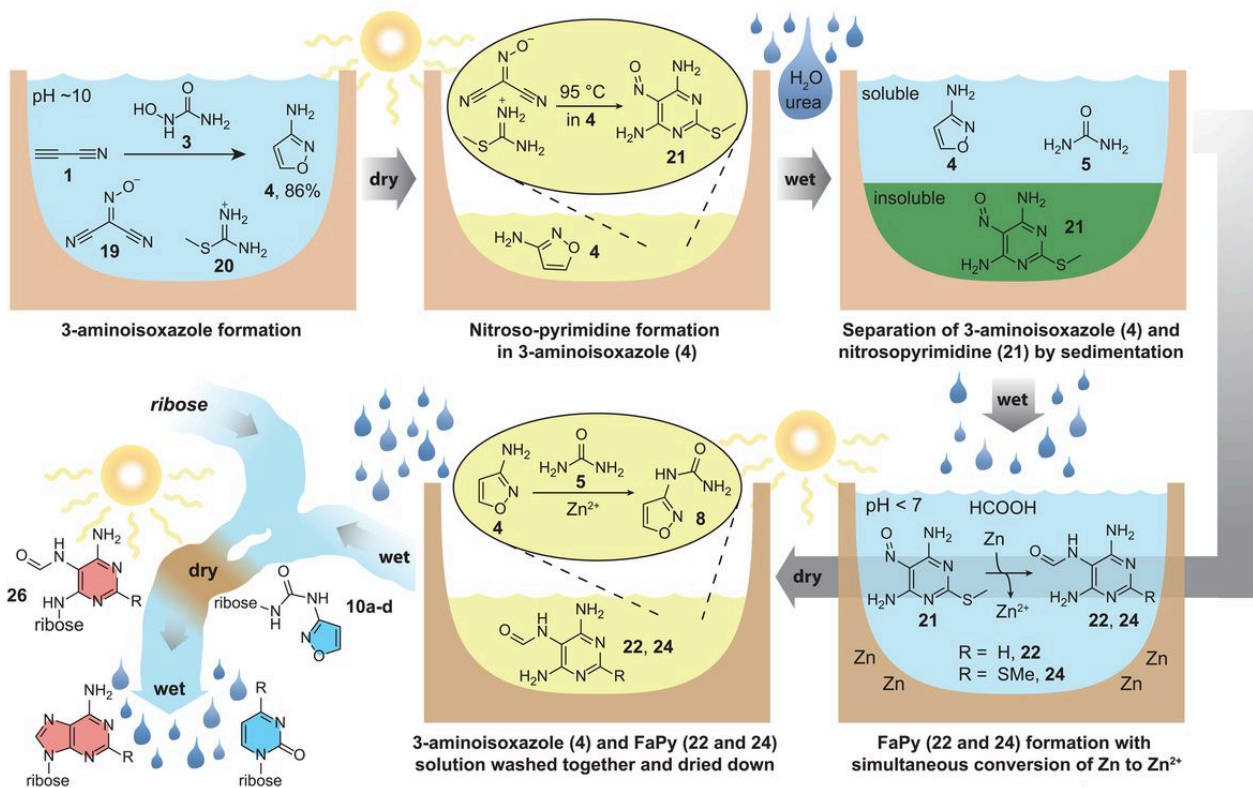
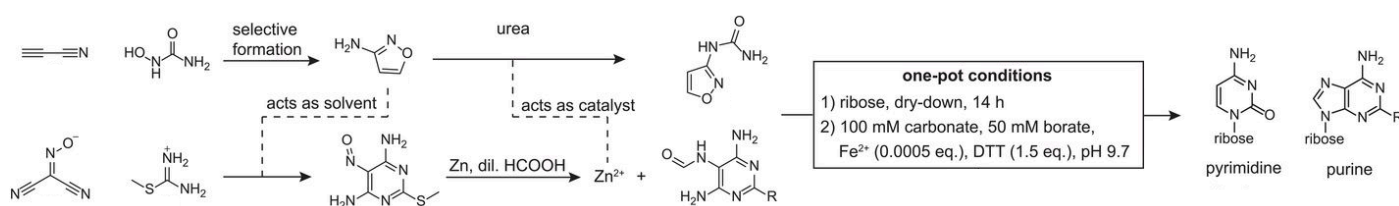
Lipids: precursors to cell membranes and other compartmentalised systems

The acylation and phosphorylation of glycerol are both condensation reactions, with possible condensing agents being urea, cyanamide and imidazole. Lipid mixtures (mono/di/triglycerides) can be formed from ammonium salts of fatty acid and glycerol on hot kaolinite clay. Glycerol can also be phosphorylated by inorganic phosphate sources which react with fatty acid salts, and then further with cyanamide and difunctional hydroxy-amines to form phospholipid esters.

Nucleobases, Nucleosides and Nucleotides: precursors to genetic material (RNA, DNA).

The purine and pyrimidine nucleobases are known to be able to form from oxazole or iso-oxazole derivative precursors and glyceraldehyde. The products are chiral in high e.e. when small amounts of near-racemic (low e.e.) proline catalyst is present. Cyanoacetylene (C_2HCN) can be formed from nitrogen and methane. Hydroxyurea ($HONHCONH_2$) can be formed from hydroxylamine (NH_2OH) and isocyanic acid ($HNCO$). Malononitrile ($CH_2(CN)_2$) can also be generated from cyanoacetylene.

Once these are made, a prebiotically plausible synthesis of the four nucleosides is as follows, using wet-dry cycling, in which consecutive periods of hot and cold cause repeated precipitation and solution:



A variety of prebiotically plausible pathways for phosphorylation exist, such as via pyrophosphate ($PP_i = P_2O_7^{4-}$, a possible chemical ancestor of ATP), trimetaphosphate ($P_3m = P_3O_9^{3-}$), phosphorylated amino acids, diamidophosphate ($DAP = P(NH_2)_2O_2$), hydroxyapatite ($Ca_5(PO_4)_3OH$) and phosphide minerals (Fe_3P). The regioselectivity at the 5' position is promoted in the presence of borate minerals, which can stabilise the ribose by forming 2'-3' cyclic dimers. Nucleoside phosphorimidazolides are an alternative.

17.5.2. Homochirality and Symmetry Breaking

All biomolecules today are 'homochiral', in which their polymers contain residues of enantiomerically pure monomers. This requires explanation, since almost all familiar chemistry typically produces racemic molecules. Depending on the molecule class, homochirality may have occurred either at the monomer level (enantiopure monomers → homochiral polymers) or at the polymer level (racemic polymers → homochiral polymers).

Monomer level:

- Chiral amino acids have been observed in outer space, suggesting an extraterrestrial mechanism of symmetry breaking. It is known that circularly polarised light can selectively break bonds in chiral amino acids (photolysis), permitting only one enantiomer of a given sample to survive. These polarised light sources could have come from the synchrotron radiation emitted by pulsars in deep space.
- Chiral mineral surfaces may have been the key to 'asymmetric catalysis', in which one enantiomer of a monomer reacts or polymerises by selective adsorption more rapidly than the other in the presence of the chiral catalyst.
- Asymmetric autocatalysis is an unusual type of reaction in which racemic starting materials react in the presence of a small amount of product with low e.e. to significantly increase the e.e. of the product. A well-established example is the Soai reaction, although this is not presumed to be prebiotic.
- Aqueous amino acids can crystallise into separate enantiopure conglomerates. Two amino acids (Thr, Asn) do this spontaneously, and others can do the same if given a small chiral nucleation point with any amino acid crystal.

Polymer level:

- Kinetic resolution can occur during polymerisation, in which current homochiral oligomers will react faster with monomers of the matching enantiomer than the opposite, forming longer homochiral polymers more rapidly.
- Polymers with self-replicating capabilities e.g. ribozymes (RNA) can perform autocatalysis faster when they are homochiral, allowing them to outcompete other polymers over time with many cycles of replication.

17.5.3. Systems Chemistry, Catalytic Cycles and Chemical Evolution**17.5.4. Formation of Proteins****17.5.5. Formation of Carbohydrates****17.5.6. Formation of Membranes from Lipids**

Amphiphilic molecules such as fatty acids and phospholipids form micelles spontaneously in aqueous solution. The rate of micelle formation has been shown to increase in the presence of mineral clays (e.g. montmorillonite).

17.5.7. Hypotheses of Macromolecule Replication: RNA and Proteins

RNA World Hypothesis:

Metabolism First Hypothesis:

Amyloid World Hypothesis:

17.5.8. Other Hypotheses of Abiogenesis

Iron-Sulfur World:

PAH World:

Panspermia:

Lipid World:

Hydrothermal Vent Hypothesis:

Lukewarm Universe Hypothesis:

17.5.9. Formation of Protocells and FUCA

Progenotes (ribocells)

17.5.10. Origin of Viruses**Giant Viruses****17.5.11. Origin of LUCA (~4.1 BYA)**

LUCA is expected to be a unicellular prokaryote that lived around 4.1 billion years ago, very simple compared to life today but nonetheless complex in chemical structure. It was not the first life, but is the earliest life from which all extant life is derived. It must have had an irreducible set of several hundred DNA-based genes which took over 100 million years to form. Synthetically developing a LUCA-like organism is unfeasible on experimental time-scales, and is outside the scope of origin of life research (creating life *in vitro* is the study of synthetic biology, which primarily uses material derived from existing life).

LUCA is the root of the evolutionary tree of life, marking a reference point in the transition from chemical to biological evolution. LUCA represents an individual cell within a community of primitive cells, which exchange genetic material with each other by horizontal gene transfer. At this stage, heredity occurred both horizontally and vertically, so the tree of life more resembles an interrelated web, which stabilises into two domains: bacteria and archaea.

17.5.12. Origin of Bacteria and Archaea (4 - 3 BYA)

During the Archean era (4 - 2.5 billion years ago (Ga)), while surviving geologic formations from this era are rare, rocks from this time contain some of the oldest evidence of life. Carbonaceous matter has been identified in rocks as old as 3.95 Ga, but the oldest forms may be abiogenic (not produced by living organisms). Metamorphism has altered the molecular composition of Archean organic matter, making it challenging to distinguish between biological and non-biological carbonaceous compounds, such as those that could have formed in seafloor hydrothermal systems.

Benthic microbial mats, dating back to 3.47 Ga, are supported by the presence of organic laminae in stromatolitic carbonates, siliceous sinters, and siliciclastic sediments. However, the organic matter in these deposits rarely preserves fossil cellular structures, making it difficult to attribute the simple textures to microfossils or mineral templates.

Filamentous-sheath microfossils are found in rocks from 2.52 Ga, and there are indications of altered counterparts as old as 3.47 Ga. Spheres and complex organic lenses in rocks as old as 3.22 Ga and ~3.4 Ga, respectively, are considered strong candidates for the oldest microfossils.

Titaniferous microtubes previously thought to be microbial trace fossils have been reevaluated as metamorphic or magmatic textures. Microbially-induced mineralization is supported by CaCO_3 nanostructures in 2.72 Ga stromatolites. Sulfides from 3.48 Ga and younger rocks bear S-isotope ratios indicative of microbial sulfate reduction. Ferruginous conditions, suggested by Fe-isotope ratios, may have fueled primary production via anoxygenic photosynthesis, potentially as early as 3.77 Ga. Microbial methanogenesis and methane oxidation, both likely anaerobic processes, are indicated by C-isotope ratios as early as 3.0 Ga and ~2.72 Ga, respectively.

Photosynthetic production of O_2 is inferred to have started between 3.2 and 2.8 Ga, well before the Great Oxidation Event (2.45–2.31 Ga). This is supported by various inorganic tracers of oxidation reactions, the morphology of benthic deposits, and evidence for aerobic nitrogen metabolism in N-isotope ratios at ~2.7 Ga.

17.5.13. Origin of Eukaryotes and Protists (2.6 BYA)

Today, eukaryotes are much more complex than prokaryotes, but they are thought to have split off from archaea via recombination with bacterial DNA when they were still relatively similar. The microfossil evidence suggests that early eukarya was as simple as other life at the time, and only later complexified through a series of one-off events.

The endosymbiotic theory states that about around this time, one archaean prokaryote engulfed a small bacterial prokaryote of the phylum *Alphaproteobacteria* without destroying it, which would specialise to become the eukaryotic cell's mitochondria. Extant eukaryotic cell's mitochondria have numerous features indicative of this theory: having their own highly maternally-conserved mtDNA in the form of plasmids, a cell cycle based on binary fission that operates independently of the host cell's, and are specialised into a specific niche of energy production.

17.5.14. Origin of Multicellular Protists**17.5.15. Diversification of Multicellular Eukaryotes**

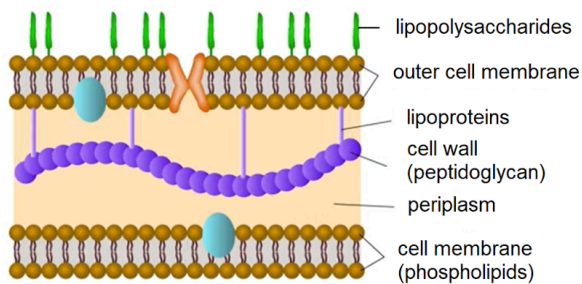
- Amorphea (1400 MYA: early Ectasian)
 - Amoebazoa (800 MYA: middle Tonian)
 - Obazoa (1030 MYA: late Stenian)
 - Opisthokonts
 - Fungi
 - Animals
 - Choanoflagellates

B18. MICROBIOLOGY

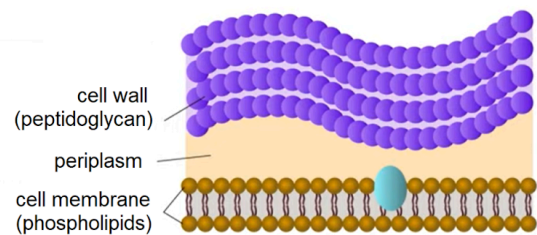
18.1. Bacteria and Archaea

18.1.1. Bacterial Structure and Organelles

Bacterial Cell Walls: contains different amounts of peptidoglycan.



Gram-negative Cell Wall
(stains pink)

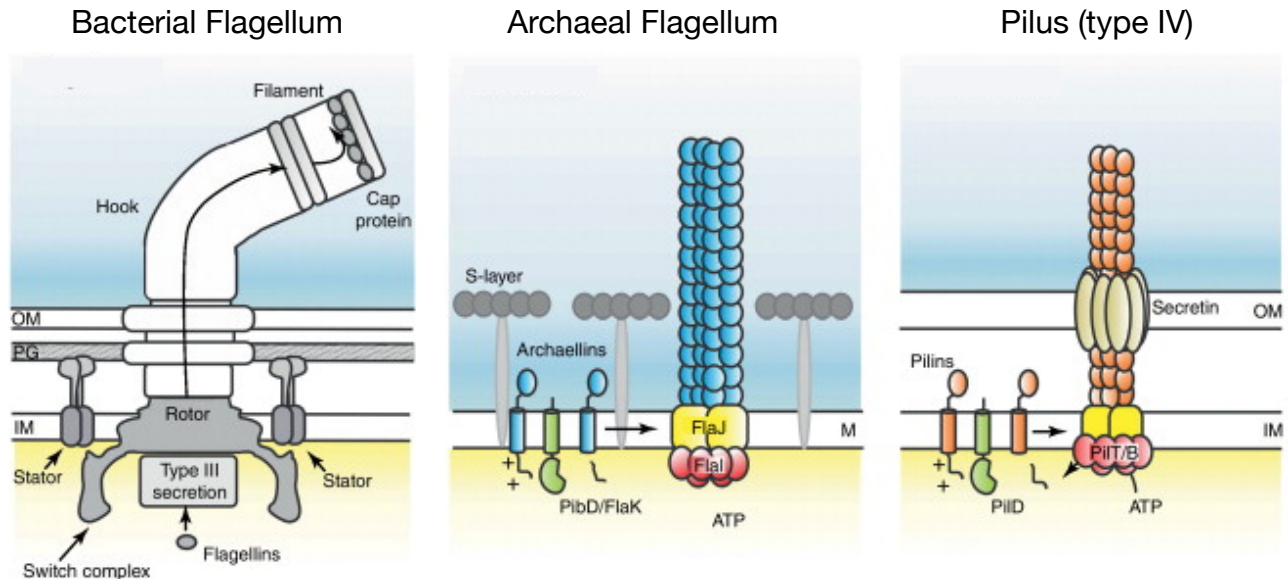


Gram-positive Cell Wall
(stains purple)

The Gram stain test (crystal violet stain to turn all cells purple → add iodine to trap crystal violet in the peptidoglycan layer of the bacteria → add decolouriser and counterstain (e.g. basic fuchsin)) can be used to discriminate between the types of cell wall.

18.1.2. Motility in Prokaryotes

Taxis: directional movement in response to a stimulus (as opposed to kinesis; no stimulus). Prokaryotes primarily use a flagellum for chemotaxis, and pili for inter-cell communication.



Abbreviations: OM: outer membrane; IM: inner membrane; PG: peptidoglycan; M: membrane.

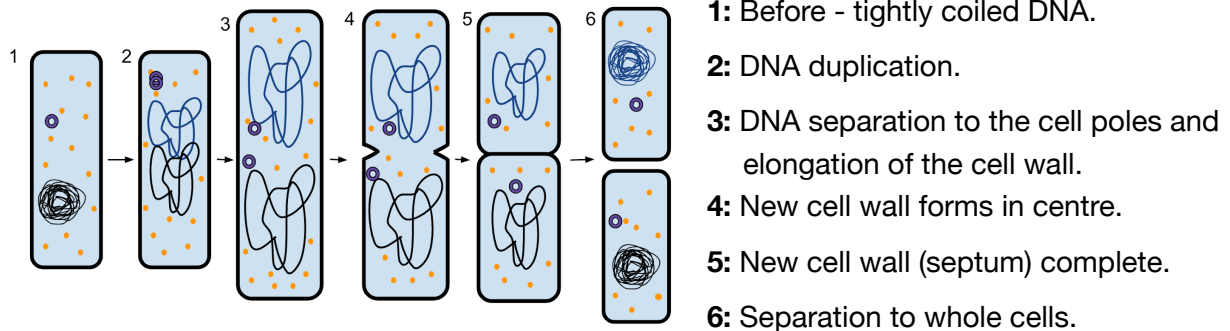
Other features found protruding from the cell membrane include the cilia and injectisome, many of which comprise similar protein subunits but with the overall organelle serving different functions.

18.1.3. Morphological Classification of Bacteria

- **Coccus (spherical):** unicellular. Plural: cocci.
 - Diplococci: two cocci.
 - Tetrads: four cocci, in a square configuration.
 - Streptococci: a long chain of cocci.
 - Staphylococci: a cluster of cocci.
 - Sarcina: a 3D compact cluster of cocci.
- **Bacillus (rod-shaped):** unicellular. Plural: bacilli.
 - Diplobacilli: two bacilli.
 - Streptobacilli: a long chain of bacilli.
- **Spiral-shaped bacteria:**
 - Spirillum: rigid, external flagella.
 - Spirochete: internal flagella.

18.1.4. Bacterial Replication: Binary Fission

Prokaryotes replicate exclusively by binary fission, a form of asexual reproduction. Mitochondria and chloroplasts within eukaryotes also use this method, and their cell cycle is timed independently of the host, supporting the endosymbiotic theory for their evolutionary origin from ancient prokaryotes. Many protists can also undergo fission, sometimes to multiple (more than 2) daughter cells.



The resulting cells are identical (with random mutations). Bacterial binary fission occurs quickly (doubling time ~30 minutes at 37 °C), allowing populations to proliferate rapidly.

18.1.5. Infectious Bacteria

Bacteria evolved the ability to infect host organisms as a side effect of exploiting their resources. Bacteria can enter a host's body through inhalation, ingestion, open wounds, by sexual transmission or by being bitten from a vector. Once inside, bacteria can cause disease by:

- Adhering to cells in the body and colonising (multiplying), occurring in the incubation period.
- Biofilm formation (sticky webs of polysaccharides supporting a community of microorganisms) by quorum sensing (population-controlled gene expression), when a critical number of bacteria are present in one area. Biofilms commonly form on dental plaque or on implanted foreign bodies (microplastics, catheters, stents, pacemakers etc) and can impede the immune response.
- In Gram-positive bacteria, the peptidoglycan cell wall can stimulate fever/inflammation.
- In Gram-negative bacteria, the surface lipopolysaccharides can be recognised as an endotoxin by the immune system.
- Exotoxin release, which can interfere with a wide variety of host bodily functions, in addition to causing cytolysis. These exotoxins can be encoded either on the bacterial plasmid or present in a phage in the bacteria.
- Superantigen release, which trigger a strong immune response (toxic shock syndrome).

Bacteria can also evade host defences by changing their surface proteins, hiding within host cells, inactivating host defences (e.g. complement). Some bacteria have a capsule (slime layer) which mimics host cells, and some can form physical barriers using enzymes.

18.1.6. Archaea

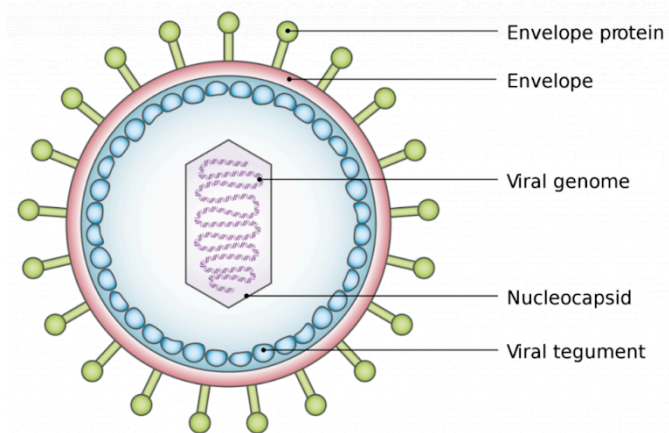
Archaea are single-celled prokaryotes. They are visually similar to bacteria: their genetics is based on plasmids with operon-based gene transcription and have no nucleus or membrane-bound organelles, but in fact are a completely different kingdom of life. They have cell walls and cell membranes (phospholipid monolayers based on ether-linked L-glycerol and terpenoid chains) with different compositions to bacteria, and can sometimes incorporate hard particles of inorganic minerals into their structure. They also use biomolecules not common in other organisms (e.g. heptose sugars). Archaea are often extremophiles, and were more prevalent on early Earth when life was far more primitive and conditions were harsher.

Unlike bacteria, archaea do not cause any known diseases in humans. In the large intestines of mammals, methanogenic archaea constitute about 1% of the gut microbiome, where they remove the hydrogen gas byproduct of early digestion and convert it to methane.

18.2. Virology and Parasitic Agents

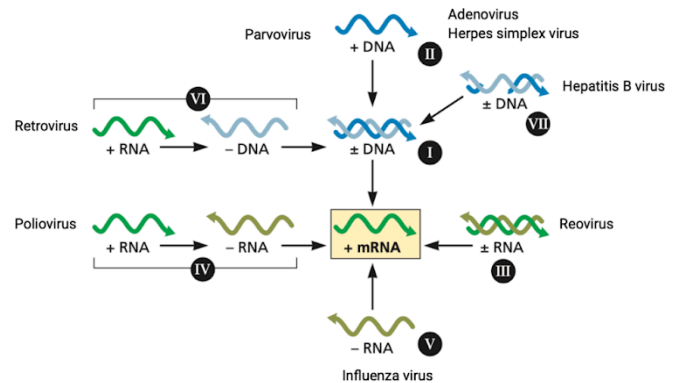
18.2.1. Structure of Viruses

Viruses: obligate intracellular parasites containing genetic material to be injected into and expressed by a cell.



Virus structure:

capsid around genome, in envelope with spike proteins



Viral genome types:

I: dsDNA, II: ssDNA, III: dsRNA, IV: ss(+) RNA, V: ss(-) RNA, VI: SS(+) RNA with DNA intermediate, VII: gapped dsDNA. Only +mRNA is 'ribosome ready'.

Virus Life Cycle: after attachment to a cell and release:

- Lytic cycle: synthesis of protein → reassembly → lysis
- Lysogenic cycle: incorporation of DNA (prophage) → cell replication → lysis on trigger

The genetic material inside a virus contains genes coding for most of the proteins contained within it (*gag* gene: capsid, *env* gene: envelope, as well as genes for various enzymes e.g. polymerase for replication). The envelope may also contain some of these enzymes already.

Viruses may exit cells via viroporins (protein ion channels) created by the viral genome.

18.2.2. Retroviruses

Retroviruses are ssRNA viruses. Within their envelope, they also carry a reverse transcriptase (RT) enzyme and an integrase enzyme, which are also encoded by its genome. They act by:

1. Fusion with the host cell membrane, release of viral RNA and enzymes into host cytoplasm.
2. A host cell tRNA primer binds to a specific sequence at the 5' end of the viral ssRNA.
3. Using host cell dNTPs, RT builds cDNA from the viral RNA while degrading the RNA template. RT then synthesises a complementary DNA strand to form dsDNA.
4. The pre-integration complex (PIC), including viral integrase with nuclear localisation signals (NLS), transports the dsDNA through a nuclear pore into the host nucleus.
5. Integrase interacts with host nuclear proteins to cut host DNA and insert the viral DNA. The integration site is somewhat random but often targets euchromatin.
6. The viral DNA has long terminal repeat (LTR) sequences at each end, which promote its transcription into new viral RNA and proteins. New viruses are assembled and can leave the cell to infect more cells.

Types of Retroviruses

- **Oncoviruses:** viruses that directly or indirectly contribute to cancer development.
- **Lentiviruses:** slow-acting retroviruses, which go 'dormant' (chronic; lysogenic cycle) for a long period of time once integrated by suppressing their transcription by various mechanisms (e.g. epigenetics). Includes HIV which causes AIDS by infecting CD4⁺ T-lymphocytes. When the host cell undergoes mitosis, the new cells retain the proviral DNA.
- **Endogenous retroviruses (ERVs):** retroviruses infecting gametes can be incorporated into the organism's whole line of surviving descendants. These are used to study evolutionary relatedness (paleovirology). Due to mutations over time, they are now harmless and are unable to reform as viruses anymore due to being epigenetically marked as non-coding DNA. A small proportion of ERVs have been turned into useful genes by this process.

Some viruses replicate with similar characteristics as retroviruses (e.g. SV40, a DNA virus using large T antigen instead of integrase). The SV40 virus has a strong promoter sequence making it a useful vector in gene transfection.

Antiretroviral drugs e.g. azidothymidine can inhibit reverse transcriptase. Azidothymidine is a nucleoside with a substituted 3' azide group, which (after conversion to the dNTP form) blocks polymerisation on the DNA chain, terminating the reverse transcription process. The incomplete DNA fragments cannot be incorporated into the host genome. This can also hinder host cell DNA (including mtDNA) replication to some extent, causing side effects.

18.2.3. Prions

Prions are mutated endogenous lone proteins which, due to having a different folding pattern, are infectious agents. Prions replicate by coming into contact with normal proteins, and can induce their misfolded conformation onto these proteins.

The misfolded proteins do not perform any useful functions, leading to the progressive destruction of tissues within the host. The change in shape can also cause proteins to aggregate, causing e.g. brain shrinkage.

Prions typically have many β -sheets while the healthy proteins have many α -helices. The β -sheets in prions can polymerize to form aggregated amyloid fibril structures that are insoluble and protease-resistant. The structures responsible for propagation can be studied using high-intensity X-rays to mutate the structures in various ways and test for replicative ability.

Prions are known to be responsible for some neurodegenerative diseases in humans, such as Creutzfeldt-Jakob disease (CJD) and bovine spongiform encephalopathy (BSE or 'mad cow disease' - affects cattle and can be transmitted to humans causing variant CJD) as well as scrapie in sheep and chronic wasting disease (CWD) in goats. These diseases have a very high fatality rate. Recently, Alzheimers' disease was shown to be indirectly caused by two slow-acting prions.

18.2.4. Viroids

18.2.5. Bacteriophages

18.2.6. Protists

Protists are a diverse set of single-celled eukaryotes with a wide range of characteristics. They include algae, flagellates, amoebas and slime moulds. There are also fungi-like protists. Protists primarily reproduce by binary fission, but some can also use meiosis (sexual).

Some common phyla of protists:

- **Euglenids** have flagella, can perform photosynthesis, and have photoreceptors (eyespot).
- **Diatoms** are unicellular algae, with a hard silica cell wall for surviving high pressures.
- **Dinoflagellates** have hard cellulose cell walls and flagella that cause rotational motion only.
- **Ciliates** have many cilia, an oral groove for eating, as well as trichocysts (spikes) for defence.
- **Radiolarians** have silicate internal skeletons and have a high degree of symmetry.
- **Amoebas** have pseudopod protrusions that can capture unicellular prey.

18.3. Mycology

18.3.1. Characteristics of Fungi

Fungi are small but larger-than-microscopic organisms such as mushrooms, yeasts and moulds. They reproduce both sexually and asexually, involving germination of spores (similar to how plants grow from seeds). Many fungi form large networks (hyphae) of mycelium fibres (like roots) for nutrient acquisition. Often, these filaments attach to roots of plants and trees in symbiotic relationships to form mycorrhizae, but may also be parasitic depending on the fungal phylum.

B19. ANIMALS AND PLANTS

19.1. Ecology and Evolutionary Biology

19.1.1. Foundations of Evolution

Observations leading to the formation of evolutionary theory (Darwin in *Origin of Species*, 1859)

- Organisms are well suited (adapted) for their environment.
- Life shares many characteristics (traits) despite rich variation in form and function.
- Populations can only expand to sizes sustainable by the available resources.
- Populations are naturally generally stable in size (resources are the limiting factor).
- Variation between individuals affects access to resources, influencing their reproduction rates.
- Variation is heritable from parent to offspring.
- The environment (and therefore what is beneficial to organisms) is constantly changing.

Darwin's Theory of Evolution: common descent with modification.

Selective pressures lead to competition creating differential reproductive success (**natural selection**).

The 'fitness' (conceptualised as a fitness landscape) is context-dependent for every population.

Neo-Darwinian Evolution: the 'modern synthesis', defined as variation in the allele frequency in a population over generations. Mendelian inheritance states **mutations** are the mechanism of variation that drives Darwinian natural selection. For Mendelian genetics, see Section 17.2.1.

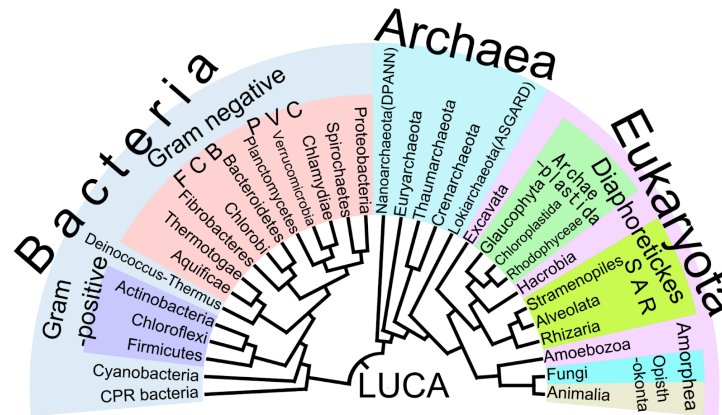
Additional mechanisms in the propagation of genetic variation:

- **Gene flow (migration):** movement of individuals between populations.
 - **Sexual selection:** preferential mating of individuals with particular heritable traits, possibly without an intrinsic survival advantage.
- **Genetic drift:** variation in allele frequency due random chance.
 - **Population bottleneck:** extinction events leave much smaller populations, whose new allele distribution may not represent the previous distribution.
 - **Founder effect:** the first individuals to occupy a new niche or habitat will set the allele frequency in the resulting population if they remain isolated.

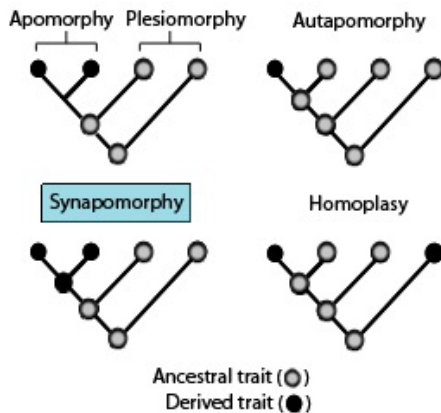
Neo-Darwinian evolution was the basis of the **extended evolutionary synthesis** (EES), including:

19.1.2. Phylogeny and Cladistics

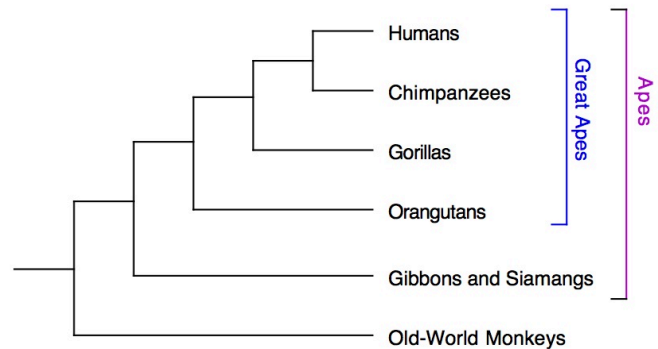
Phylogenetic tree: shows evolutionary diversification of life scaled in time, anywhere between the Last Universal Common Ancestor (LUCA) and extant life.



Cladograms: shows diversifications without considering the time taken.



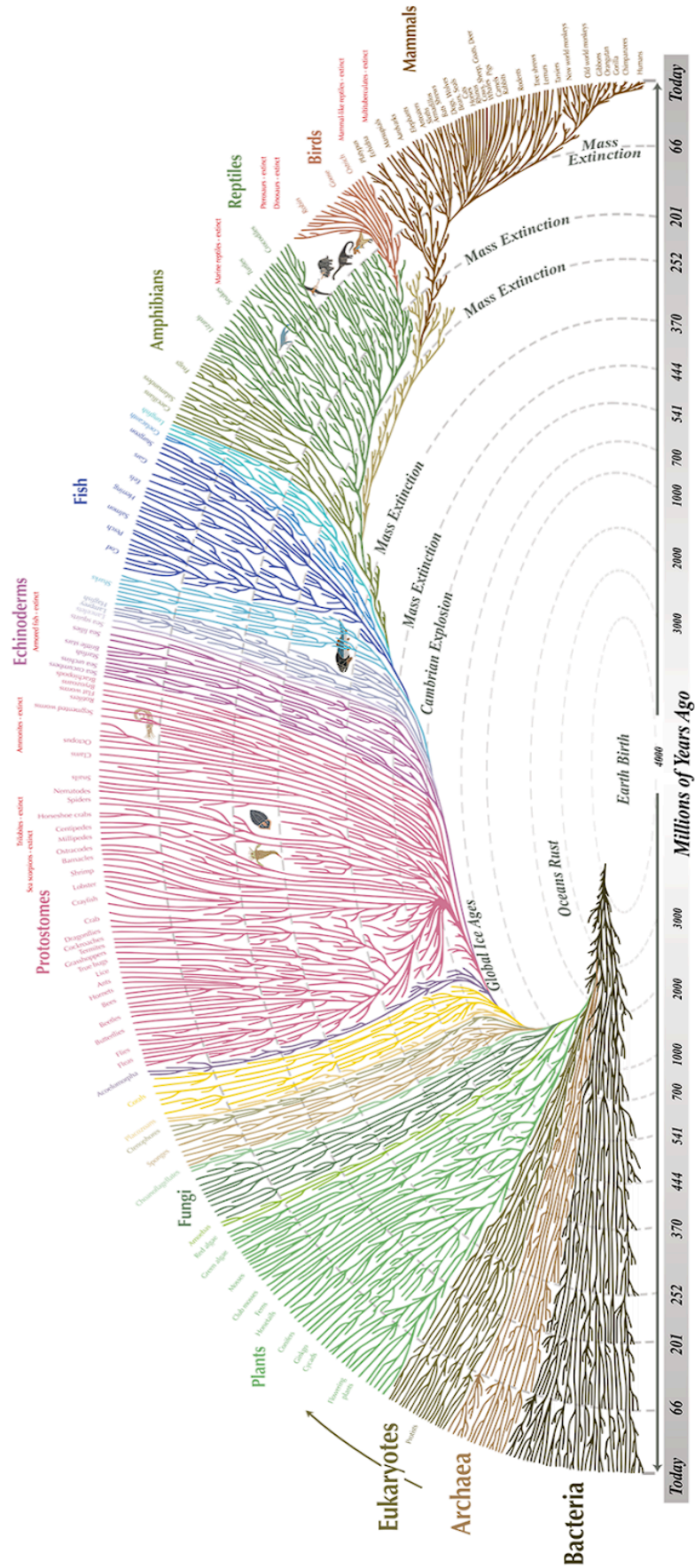
Variation in traits represented on a cladogram



Cladogram of extant New World monkeys showing the clades of Great Apes and Apes

- Apomorphy: a specialised (derived) trait unique to a clade.
- (Sym)plesiomorphy: a primitive (ancestral) trait inherited by a common ancestor.
- Autapomorphy:** a trait **unique** to a single species or taxon within a larger group.
- Synapomorphy:** a specialised (derived) trait **inherited from** a common ancestor.
- Homoplasy: a common trait of unrelated species e.g. due to convergent evolution.

19.1.3. Tree of Life



19.1.4. Taxonomy

The Linnaean classification system defined hierarchical tiers of organisms with similar characteristics. The precise tier system can change over time.

Life \supset Domain \supset Kingdom \supset Phylum \supset Class \supset Order \supset Family \supset Genus \supset Species

A common system used today, listed to the phylum level, is: Binomial name: *Genus species*

Domain *Bacteria*: unicellular prokaryotes (no nucleus or membrane-bound organelles), rigid peptidoglycan cell wall, circular chromosome.

Kingdom *Eubacteria*:

Phyla: *Acidobacteriota, Actinomycetota, Aquificota, Armatimonadota, Atribacterota, Bacillota, Bacteroidota, Balneolota, Bdellovibrionota, Caldiseicota, Calditrichota, Campylobacterota, Chlamydiota, Chlorobiota, Chloroflexota, Chrysiogenota, Coprothermobacterota, Deferribacterota, Deinococcota, Dictyoglomota, Elusimicrobiota, Fibrobacterota, Fusobacteriota, Gemmatimonadota, Ignavibacteriota, Kiritimatiellota, Lentisphaerota, Mycoplasmatota, Myxococcota, Nitrospinota, Nitrospirota, Planctomycetota, Pseudomonadota, Rhodothermota, Spirochaetota, Synergistota, Thermodesulfobacteriota, Thermomicrobiota, Thermotogota, Verrucomicrobiota.*

Domain *Archaea*: unicellular prokaryotes, rigid non-peptidoglycan cell walls, unique rRNA genes/polymerases.

Kingdom *Archaea*:

Phyla: *Nitrososphaera, Thermoproteota, Euryarchaeota, Thorarchaeota, Methanobacteriota*, as well as many other candidate phyla

Domain *Eukarya*: eukaryotes (nucleus, membrane-bound organelles)

Kingdom *Protista*: a polyphyletic clade for any eukaryote not fitting into the below three (may be unicellular or multicellular, may or may not have cell walls).

Phyla: *Amoebozoa, Apusozoa, Bigyra, Cercozoa, Choanozoa, Ciliophora, Cryptistanas, Eolouka, Euglenozoa, Gyrista, Haptista, Malawimonada, Metamonada, Miozoa, Opisthosporidia, Percolozoa, Retaria.*

Kingdom *Fungi*: multicellular, chitin cell walls, heterotrophic

Phyla: *Ascomycota, Basidiomycota, Blastocladiomycota, Chytridiomycota, Glomeromycota, Microsporidia, Neocallimastigomycota, Zygomycota.*

Kingdom *Plantae*: multicellular, cellulose cell walls, autotrophic

Phyla: *Anthocerotophyta, Bryophyta, Charophyta, Chlorophyta, Cycadophyta, Ginkgophyta, Glaucophyta, Gnetophyta, Lycopodiophyta, Magnoliophyta, Marchantiophyta, Polypodiophyta, Coniferophyta, Rhodophyta.*

Kingdom *Animalia*: multicellular, no cell walls, heterotrophic

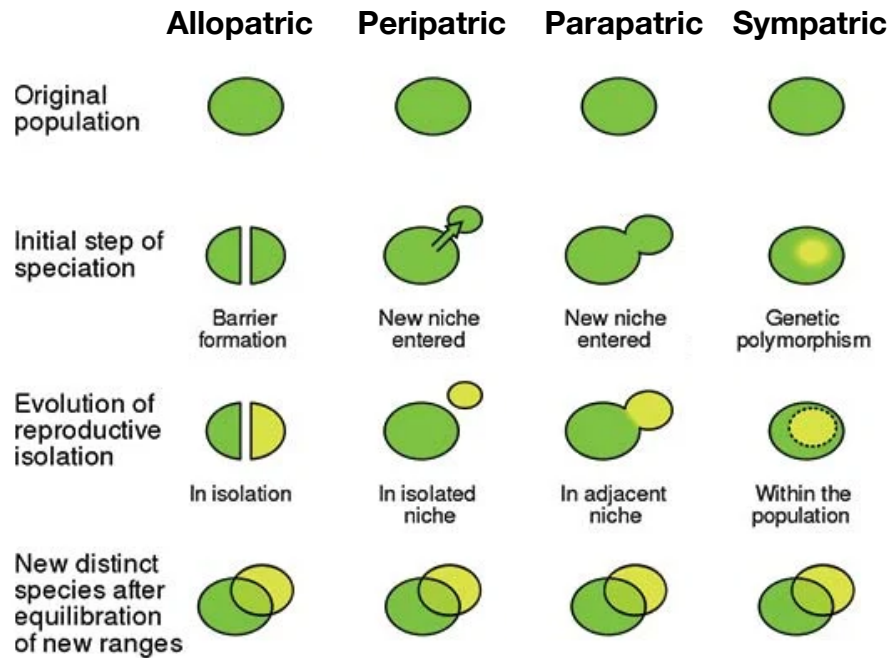
Phyla: *Annelida, Agmata, Archaeocyatha, Arthropoda, Brachiopoda, Bryozoa (Ectoprocta), Chaetognatha, Chordata, Cnidaria, Ctenophora, Cyclophora, Echinodermata, Entoprocta, Gastrotricha, Gnathostomulida, Hemichordata, Kinorhyncha, Loricifera, Micrognathozoa, Mollusca, Nematoda, Nematomorpha, Nemertea, Onychophora, Petalonamae, Phoronida, Placozoa, Platyhelminthes, Porifera, Priapulida, Proarticulata, Rhombozoa (Dicyemida), Rotifera, Saccorhytida, Tardigrada, Trilobozoa, Vetulicolia, Xenacoelomorpha.*

19.1.5. Evolution

Causes of Speciations

- **Natural Selection:** the ongoing process by which genes which produce useful adaptations to an organism’s current environment can proliferate, while the others die off. The small changes caused by natural selection can lead to speciation over time, and are amplified/accelerated by other mechanisms.
- **Genetic Drift:** change in the allele frequencies in a population as a result of “sampling error” while selecting the alleles for the next generation from the gene pool of the current population. It is debated whether genetic drift contributes to speciation directly or only to evolution in general.

Modes of Speciation



19.1.6. Principles of Evolution

Species: a set of similar individual organisms capable of interbreeding or exchanging DNA (the 'biological species concept').

Adaptation: a beneficial characteristic to a species in its environment.

Variation: the diversity in the genes carried by a single species, caused by natural mutations.

Natural selection: the ongoing process by which genes which produce useful adaptations to an organism's current environment can proliferate, while the others die off.

Selective pressure: an external factor that influences the survivability of a species, potentially accelerating the process of natural selection towards adapting to the pressure.

Speciation: the diversification of a species into multiple species, often due to geographic separation into different environments (allopatric speciation).

Fitness landscape: the suitability of a gene as a function of its many possible mutations, which varies with time and environment. Natural selection can be thought of as moving towards the peaks of the fitness landscape at all times.

Rate of evolution: phyletic gradualism is the idea that evolution occurs slowly in a population, while punctuated equilibrium claims that populations are relatively stagnant most of the time, but abruptly diversify over short periods occasionally. Both models contribute to evolution, as the rate of evolution is indicative of the strength of the selective pressures acting in a given context.

19.1.7. Evidence for Evolution

Direct observation: the basic principles of evolution by natural selection are well-established scientific facts and are easily observed in organisms with short life cycles e.g. antibiotic resistance, seasonal viral infections, domestication of animals, as well as larger animals (including humans) over historical time scales.

Homology and embryology: similarity of a structure or function of body parts with different origins, implying descent from a common evolutionary ancestor. For very distant species, these similarities are only present in the embryo stage of development, before significant differentiation takes place. This is studied from the genetics perspective in evolutionary developmental biology.

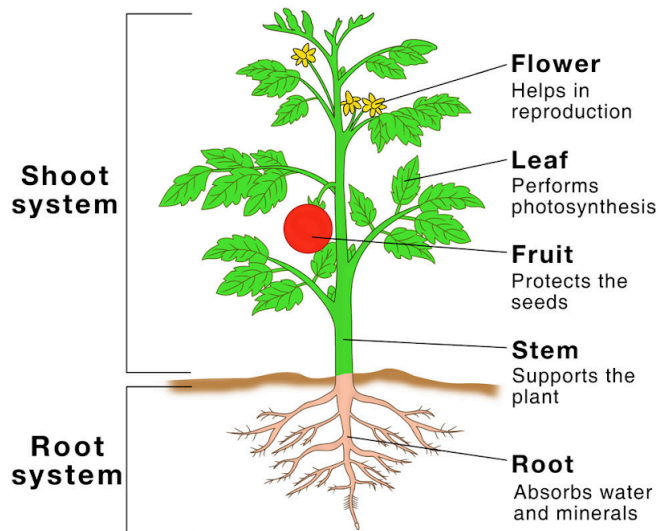
Genetics: DNA sequencing of extant life reveals a hierarchical similarity, implying common descent. Endogenous retroviruses (ERVs) are especially strong indicators of relatedness.

Transitional fossils: the fossil record contains various examples of organisms with clearly intermediate morphologies (e.g. *Archaeopteryx*, *Ichthyostega*) between distinct extant species, including those on and around the human lineage.

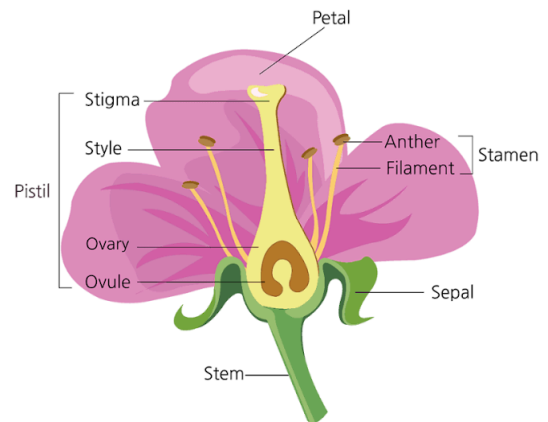
Stratigraphy and the geologic column: there is a strong correlation between the depth at which fossils are found and the age of the fossils, allowing trends over geologic timescales to be identified.

19.2. Botany and Agriculture

19.2.1. Structure of Flowering Plants (Angiosperms)



Parts and functions of a plant



Parts of a flower

Functions of the parts of a plant:

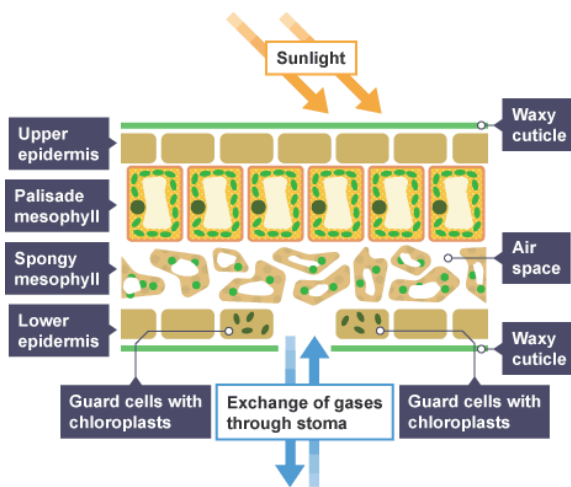
- **Stem:** provides structural support and allows for food, water and nutrient exchange.
- **Roots:** ingrain into soil. Made of root hair cells which absorb water by osmosis and minerals by active transport.
- **Leaves:** captures oxygen and performs photosynthesis (in the chloroplasts of palisade cells).
- **Sex Organs:** forms the reproductive system of the plant (pollen + ovule → seeds → plant).
 - **Sepal:** protects a developing flower bud.
 - **Stamen:** male reproductive organ. The anther produces and holds pollen grains (contains male gametes). The filament supports the anther and permits pollen dispersal.
 - **Petal:** brightly coloured to attract pollinators (bees, insects).
 - **Stigma:** female reproductive organ. Captures pollen grains (pollination).
 - **Ovule:** matures into a seed (fertilisation). Contains female gametes.
 - **Ovary:** matures into a fruit (which protects the seeds) after fertilisation. The seeds are to be dispersed and grow into new plants (germination).

Most plants are monoecious (shown above: contain both male and female reproductive organs). Some are dioecious, where individual plants have separate sexes.

Life cycle: pollination → fertilisation → seed dispersal → germination.

19.2.2. Plant Organisation and Tissues

Layers of a Leaf: permits transport of gases.



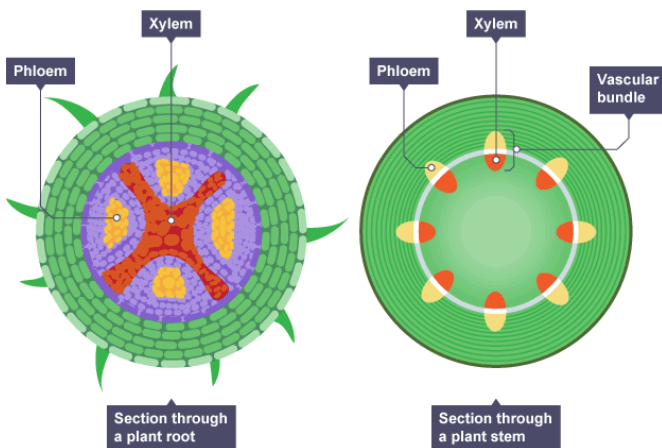
Waxy cuticle: a transparent layer which prevents water loss from the leaf in dry conditions.

Upper/Lower epidermis: protects from damage and infection. Contains stomata surrounded by guard cells to allow gas exchange (oxygen out, CO₂ in, water vapour in/out).

Palisade mesophyll: palisade cells contain lots of chloroplasts to generate glucose by photosynthesis.

Spongy mesophyll: loose-packed surrounded by water in which gases can dissolve.

Cross-Section of a Stem: permits transport of food and water.



Xylem: hollow tube of dead cells strengthened by lignin (primary component of wood). One-way (roots → leaves) transport of liquid water and minerals (the transpiration stream) by capillary action (cohesion-tension theory).

Phloem: Two-way (roots ↔ leaves) transport of cell sap (dissolved sugars and amino acids) (translocation), with porous sieve tube plates at regular lengthwise intervals.

The xylem and phloem are paired in vascular bundles running along the stem.

Rate of transpiration (volumetric flow rate of water) is set by the rate of evaporation: variations in temperature (hotter → faster), humidity (humid → slower: higher vapour pressure gradient), air movement (windy → faster: humid air is removed) and light intensity (brighter → faster: stomata open to increase oxygen uptake for photosynthesis).

Meristem tissue: exists at roots and shoots. Contains undifferentiated (totipotent; unspecialised) cells which serve to grow into the various parts of the plant.

19.2.3. Respiration and Photosynthesis

For the detailed molecular biology of respiration and photosynthesis, see Section 17.3.1-4.

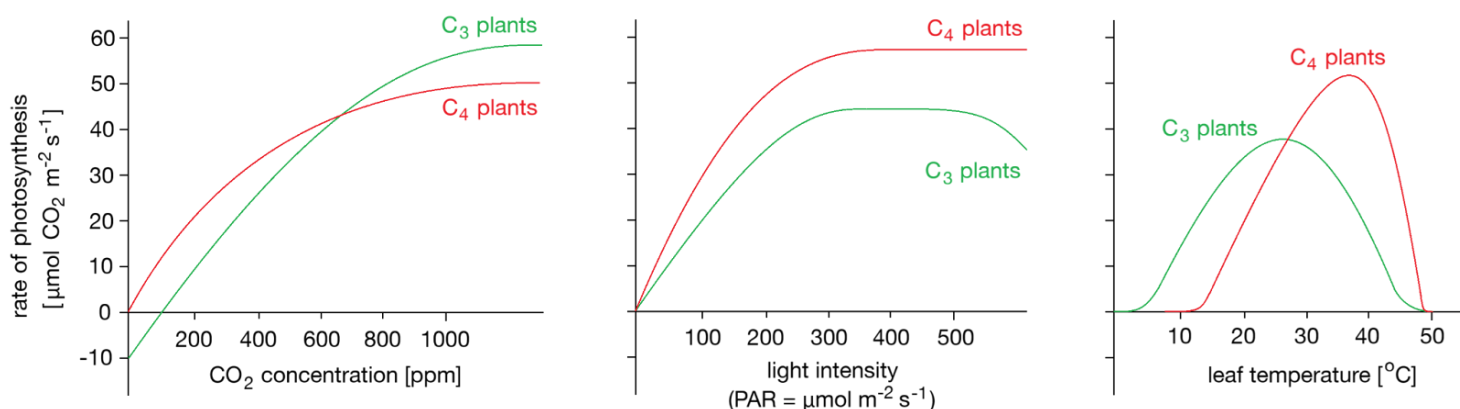
Aerobic Respiration: $C_6H_{12}O_6 + 6 O_2 \rightarrow 6 CO_2 + 6 H_2O$ (releases energy as ATP)

Anaerobic Respiration: $C_6H_{12}O_6 \rightarrow 2 C_2H_5OH + 2 CO_2$ (releases energy as ATP)

Photosynthesis: $6 CO_2 + 6 H_2O \rightarrow C_6H_{12}O_6 + 6 O_2$ (absorbs energy as light)

Plants are a key step in the carbon cycle: atmospheric carbon dioxide is fixed into glucose, which is metabolised in animals when they eat the plants, and mineralises the soil when they/the plants die. Fossil fuel usage puts the carbon back into the atmosphere.

Rate of photosynthesis: usually measured by volumetric flow rate of CO_2 [$\mu\text{mol m}^{-2} \text{s}^{-1}$]



- **CO₂ concentration:** rate increases with concentration up to saturation at around 0.1% (1000 ppm). At $[CO_2] < 100$ ppm, photosynthesis may be reversed (photorespiration) in C₃ plants. Under atmospheric conditions, CO₂ is typically the limiting factor (diffusion controlled).
- **Light intensity:** rate increases with light intensity up to saturation (depending on chlorophyll content). At very high intensity, photoinhibition can reduce the rate in C₃ plants. The light intensity can be measured in lux or 'photosynthetically active radiation' (PAR = $\mu\text{mol m}^{-2} \text{ s}^{-1}$ of photons for wavelengths $400 \text{ nm} < \lambda < 700 \text{ nm}$). For sunlight, $1 \mu\text{mol m}^{-2} \text{ s}^{-1} = 45 \text{ lux}$.
- **Temperature:** enzyme kinetics favours an optimal temperature. The optimal temperature increases with CO₂ concentration: 25 °C at 325 ppm to 35 °C at 1900 ppm for C₃ plants. C₄ plants have a narrower tolerance than C₃ plants, with a higher optimal temperature.

The glucose produced in photosynthesis may be used for respiration, converted into insoluble **starch** for storage, used to produce **fat or oil** for storage, used to produce **cellulose** (strengthens the cell wall), and used to produce **amino acids** for protein synthesis. To produce proteins, plants also use nitrate ions that are absorbed from the soil.

19.2.4. Plant Hormones and Homeostasis

Plant Hormones: natural signalling molecules, also used in agriculture / horticulture.

- **Gibberellins:** initiates seed germination. Artificially used to end seed dormancy, promote flowering and increase fruit size.
- **Auxin:** promotes cell growth/division. Artificially used as weed killer, rooting powder and promoting growth in tissue culture.
- **Ethene:** limits cell growth/division and promotes ripening of fruits. Artificially used to control ripening of fruit during storage and transport. The mechanism involves π -bonding of ethene to a Cu^+ centre in a transcription factor.

Overuse of artificially-distributed plant hormones can reduce biodiversity.

Plants produce hormones to coordinate and control growth and responses to light (phototropism) and gravity (gravitropism / geotropism). Unequal distributions of auxin cause unequal growth rates in plant roots and shoots.

19.2.5. Phytopathology and Plant Diseases

Plant diseases can be identified by stunted growth, spots on leaves, areas of decay (rot), abnormal growths, malformed stems or leaves, discolouration, and the presence of pests. Identification can be made by reference to a gardening manual or website, taking infected plants to a laboratory to identify the pathogen, and using monoclonal antibody testing kits.

Ion deficiency conditions: fix by using e.g. NPK fertiliser: nitrate, phosphate, potassium.

- Nitrate (NO_3^-) deficiency: stunted growth due to decreased amino acid synthesis.
- Magnesium (Mg^{2+}) deficiency: chlorosis due to decreased chlorophyll synthesis.
- Phosphate (PO_4^{3-}) deficiency: dark green/purple spots on leaf undersides.
- Potassium (K^+) deficiency: browning at the edges and yellowing between veins.

Common plant diseases: plants are often infected by viruses, fungi and pest insects.

- Tobacco mosaic virus (TMV) causes yellow mottling on leaves.
- *Diplocarpon rosae* (a fungus) causes rose black spot.
- Aphids (insects) eat through leaves.

Plant defences: adaptations include

- Physical (cellulose cell walls, tough waxy cuticle on leaves, layers of dead cells around stems (bark on trees) which fall off)
- Chemical (antibacterial chemicals, poisons to deter herbivores)
- Mechanical (thorns and hairs deter animals, sometimes with warning colouration (aposematism), leaves which droop or curl when touched, mimicry to trick animals)

19.2.6. Horticulture

Annual plant: lives for one year

Biennial plant: lives for two years

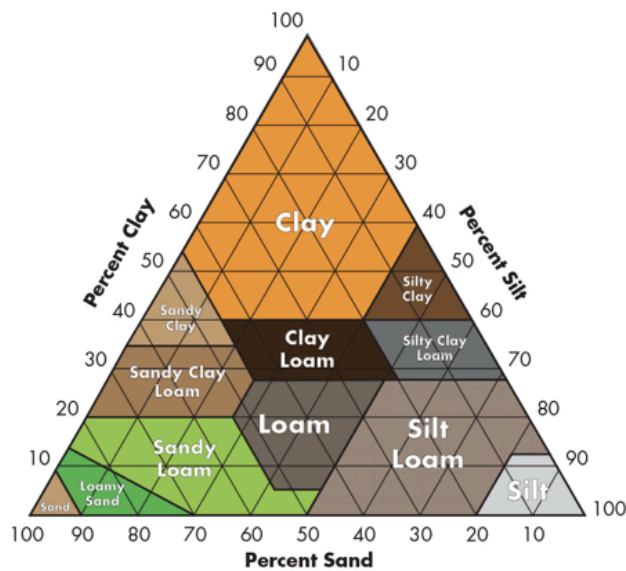
Perennial plant: lives for a longer period

Deciduous plants: leaves fall off once mature

Evergreen plants: leaves remain throughout life

Gardening

Soil Properties



The soil texture affects the levels of moisture, aeration and biological activity (microorganisms and earthworms), as well as the soil's mechanical workability (ease of digging and tilling).

The soil chemistry affects the ease of nutrient absorption, with most plants being optimally grown in soils of pH 6-7. Simple colourimetric soil pH test kits can be used to determine pH.

← Soil Texture Triangle

Greenhouses

19.2.7. Symbiotic and Synergistic Agriculture Techniques

Permaculture: a design philosophy that seeks to mimic natural ecosystems to create sustainable, self-sufficient, and regenerative agricultural systems, maximising biodiversity, and minimising waste.

Agroforestry (Afforestation, Rewilding): combines agricultural crops with trees and shrubs in the same farming area. Trees provide shade, windbreaks, nutrient cycling, and soil improvement. The combination of crops and trees enhances biodiversity, soil fertility, ecosystem resilience, and promotes environmental conservation. A traditional regenerative form of agroforestry is 'syntropic agriculture', in which whole communities live among the ecosystem, in which the natural progression of vegetation is followed: bare rocks → lichens → small annuals, grasses and perennials (pioneer species) → shrubs and shade intolerant species → shade tolerant trees (climax community).

Hydroponics: a soilless farming technique where plants are grown in nutrient-rich water solutions. This method allows for precise control of nutrients and water, leading to faster growth and higher yields compared to traditional soil-based farming. A variation is 'sandponics', where sand is used as a growth medium and filter instead of soil. It provides better root support and water retention, making it suitable for certain plant species, especially those in desert biomes.

Aquaponics: combines hydroponics with aquaculture (fish farming). Fish waste (ammonia) can be metabolised to nitrate by nitrifying bacteria in soil for plants, and the plants' roots help to filter the water, creating a closed-loop system. Variations include sandponics and aeroponics, suitable for different types of plants.

Agrivoltaics (dual-use farming): co-location of solar panels and agricultural crops on the same land. The panels provide shade for crops, reducing water evaporation and improving crop yields. Most suited for crops requiring low sunlight e.g. leafy greens, herbs.

Vertical Farming: stacking of plants in vertical layers, often indoors or in controlled environments. It minimises land use, optimises light exposure, and conserves water. LED lights can be used to provide optimal conditions, with different wavelengths for different stages of growth, useful for space-limited urban areas.

19.2.9. Issues in the Agriculture Industry

Food and Water Security: ensuring a stable and consistent supply of nutritious food and safe freshwater to all people is a global challenge. Population growth, climate change, and resource limitations can impact availability and affordability.

Genetically Modified Organisms (GMOs): use of organisms with altered genetic material for specific traits. They can enhance crop yields, nutritional content, and resistance to pests and diseases. While some people view GMOs as a way to address food security, others have concerns about potential environmental effects (e.g. horizontal gene transfer), human health impacts, and corporate control over the food supply.

Pesticides: used to control pests and increase agricultural yields. However, they can also have negative impacts on ecosystems, non-target organisms, and human health. Integrated Pest Management (IPM) strategies aim to minimise pesticide use by combining various techniques such as biological control and cultural practices.

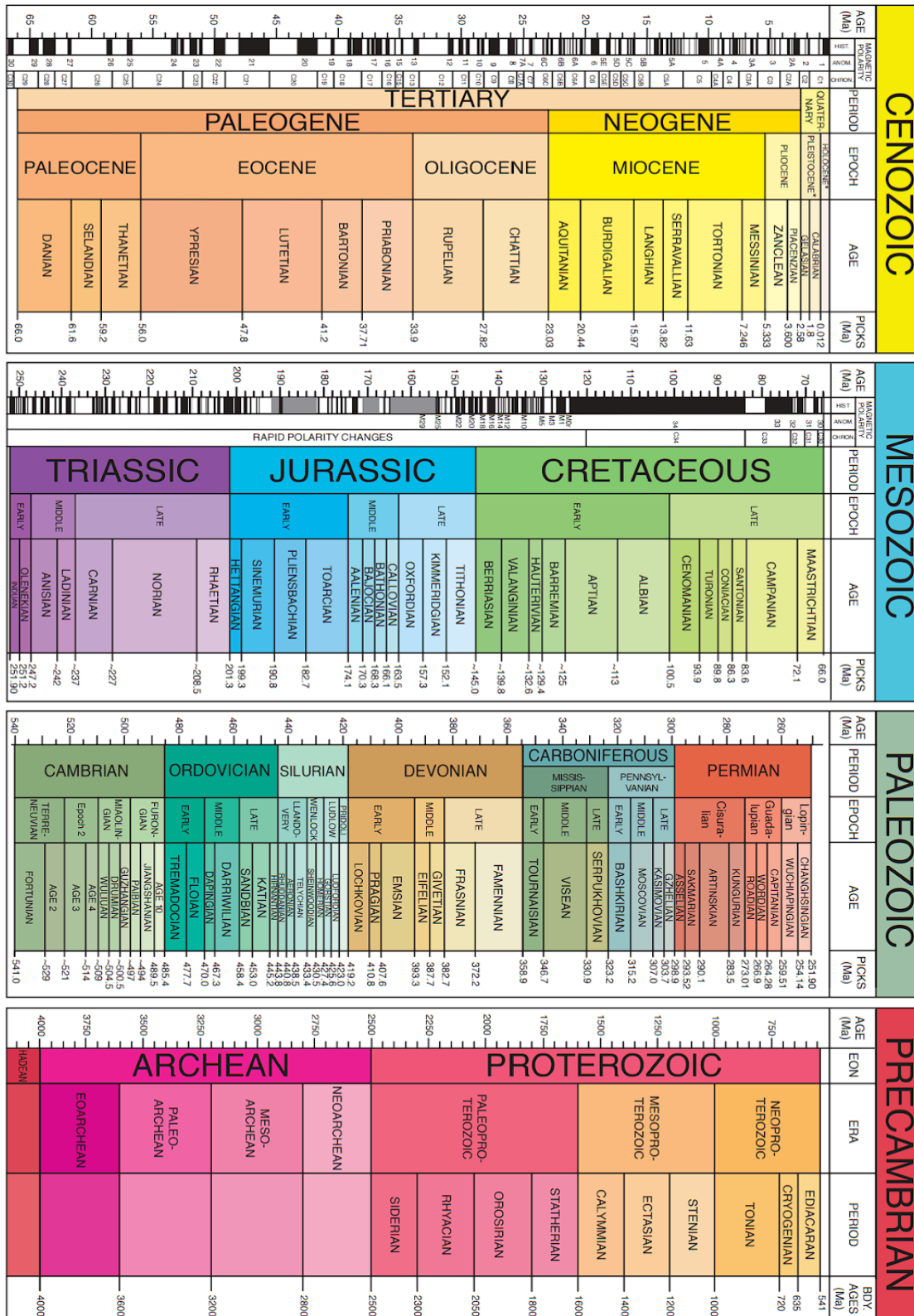
Lab-Grown Meat (Cellular Agriculture): involves producing meat from animal stem cells and an animal-free growth medium without traditional animal farming, providing a sustainable protein source with fewer ethical concerns. It is currently thought to be the best approach for widespread adoption of vegetarian or vegan diets among the general population, which could alleviate food security concerns significantly. However, challenges include scaling up production, addressing regulatory concerns, and public acceptance.

Sustainable Fisheries: overfishing and illegal, unreported, and unregulated (IUU) fishing threaten marine ecosystems and fish populations. Sustainable fisheries management involves setting catch limits, protecting vulnerable species, and implementing measures to prevent overfishing. Marine Protected Areas (MPAs) also contribute to ecosystem preservation.

Deforestation and Desertification: degradation of natural environments by overfarming (subsistence, 'slash and burn' or commercial) and overgrazing leads to infertile land and soil erosion. Widespread logging contributes to global warming due to the reduction in CO₂ storage.

19.3. Zoology and Paleontology

19.3.1. Geologic History of Earth



19.3.2. Significant Events in Evolutionary History

(ka: kilo-annum (thousand years ago), Ma: mega-annum (million years ago), Ga: giga-annum (billion years ago))

Mass Extinction Events: the 'Big Five'.

- **Ordovician mass extinction** (445 Ma).
- **Devonian extinctions** (372-359 Ma). A combination of the Kellwasser event and the Hangenberg event.
- **Permian extinction event** (The Great Dying) (252 Ma).
- **Triassic extinction event** (201 Ma)
- **Cretaceous (K-Pg) extinction event** (66 Ma). Caused the extinction of all non-avian dinosaurs, and the resulting open niches gave rise to the 'age of mammals', from which all primates arose.

Other Extinction Events:

- Great Oxidation Event (2.3 Ga).
- End-Ediacaran extinction event (550 Ma - 539 Ma).
- Capitanian mass extinction event (259 Ma).
- Pleistocene glaciation (2.58 Ma - 11.7 kA): the most recent ice age, out of five in history.
- Anthropocene extinction (100 ya - present): the ongoing rapid endangerment and extinction of many species due to human activity post-industrial revolution.

Biodiversification Events

- Avalon explosion (565 Ma):
- Cambrian explosion (540-515 Ma):
- Great Ordovician Biodiversification Event (GOBE) (497-467 Ma): It has been suggested that the Cambrian explosion and GOBE may have in fact been one long continuous radiation.

19.3.3. Taxonomic Classification of Animals

Appearance of Animals

Domain *Eukarya*:

- Clade *Parabasalia / Fornicata / Preaxostyla* [protists]
- Eukaryote host + α -proteobacterium [mitochondrial endosymbiont]
 - Clade *Discoba*
 - Clade *Jakobida / Heterolobosea / Euglenozoa* [protists]
 - Clade *Neokaryotes*
 - Clade *Harosa*
 - Clade *Archaeplastida*
 - **Kingdom *Plantae***
 - Clade *Amorphea*
 - Clade *Amoebozoa*
 - Clade *Obazoa*
 - Clade *Apusomonadida*
 - Clade *Opisthokonta*
 - Clade *Holomycota*
 - Clade *Nucleariiae*
 - **Kingdom *Fungi***
 - Clade *Holozoa*
 - Clade *Ichthyosporea*
 - Clade *Pluriformea*
 - Clade *Filozoa*
 - Clade *Filasterea*
 - Clade *Choanozoa*
 - Clade *Choanoflagellata*
 - **Kingdom *Animalia***

Diversification of Animals

There is some debate as to relationships between the most basal animal clades, with many other arrangements proposed. The phylogeny shown is due to Giribet and Edgecombe (2020).

Kingdom *Animalia*:

- Phylum *Porifera*
- Phylum *Ctenophora*
- Clade *Para-Hoxozoa*
 - Phylum *Placozoa*
 - Phylum *Cnidaria*
 - Clade *Bilateria*
 - Phylum *Xenacoelomorpha*
 - Clade *Nephrozoa*
 - Clade *Deuterostomia*
 - Clade *Ambulacraria*
 - Phylum *Chordata*
 - Clade *Protostomia*
 - Clade *Ecdysozoa*
 - Clade *Spiralia*

19.4. Primatology, Paleoanthropology and Archaeology

19.4.1. Taxonomic Classification of Extant Primates

Primates are a taxonomic order of class *Mammalia*, phylum *Chordata*, characterised by grasping hands, forward facing eyes (binocular vision), nails instead of claws, enlarged brains, diverse diets, reduced olfactory sense, social behaviours and flexible locomotion.

Order *Primates*:

- Suborder *Strepsirrhini* (lemurs)
 - Infraorder *Chiromyiformes*
 - Family *Daubentoniidae* (aye-ayes)
 - Infraorder *Lemuriformes*
 - Family *Cheirogaleidae*
 - Subfamily *Cheirogaleinae* (dwarf and mouse lemurs)
 - Subfamily *Phanerinae* (fork-crowned lemurs)
 - Family *Lemuridae* (true lemurs)
 - Family *Megaladapidae* (sportive and koala lemurs)
 - Family *Indridae* (indris, sifakas, and avahis)
 - Family *Palaeopropithecidae* (sloth lemurs)
 - Family *Archaeolemuridae* (baboon lemurs)
 - Infraorder *Lorisiformes*
 - Family *Lorisidae*
 - Subfamily *Lorinae* (lorises)
 - Subfamily *Perodicticinae* (pottos and angwantibos)
 - Family *Galagidae* (bush babies, or galagos)
- Suborder ***Haplorhini*** ('haplorhine')
 - Infraorder *Tarsiiformes*
 - Family *Tarsiidae* (tarsiers)
 - Infraorder ***Simiiformes*** ('simians'; 'anthropoids')
 - Parvorder *Platyrrhini* ('platyrrhines'; 'New World monkeys')
 - Family *Callitrichidae* (marmosets)
 - Family *Cebidae* (capuchins and squirrel monkeys)
 - Family *Aotidae* (durukulis, or night monkeys)
 - Family *Pitheciidae* (sakis, uakaris, and titis)
 - Family *Atelidae* (spider, woolly, and howler monkeys)
 - Parvorder ***Catarrhini*** ('catarrhine monkeys'; 'Old World monkeys')
 - Superfamily *Cercopithecoidea*
 - Family *Cercopithecidae*
 - Subfamily *Cercopithecinae* (macaques, baboons, geladas...)
 - Subfamily *Colobinae* ('leaf-eating monkeys'; langurs...)
 - Superfamily ***Hominoidea*** ('hominoids'; apes)
 - Family *Hylobatidae* (gibbons and siamangs)
 - Family ***Hominidae*** ('hominids'; great apes)
 - Subfamily *Ponginae* (orangutans)
 - Subfamily ***Homininae*** ('hominines'; African apes and humans)
 - Tribe *Gorillini* (gorillas)
 - Tribe ***Hominini*** ('hominins')
 - Genus *Pan*
 - Species *Pan troglodytes* (chimpanzees)
 - Species *Pan paniscus* (bonobos)
 - Genus ***Homo*** (humans)
 - Species ***Homo sapiens*** (extant humans)

19.4.3. Evolutionary History of Primates

Genera and Species of Extinct Primates: selected species are mostly (but not all) on the human lineage.

Southern Africa Eastern Africa Northern/Western Africa Europe Asia America Oceania

Paleogene (66 - 23.03 MYA)

- *Purgatorius* (66-63 MYA)
- *Altiatlasius* (58-55 MYA)
- *Cantius* (56-47.8 MYA)
- *Smilodectes* (50.3-46.2 MYA)
- *Notharctus* (54-38 MYA)
- *Parapithecus* (40-33 MYA)
- *Biretia fayumensis* (~37 MYA)
- *Aegyptopithecus zeuxis* (38-29 MYA)
- *Proteopithecus* (34-28 MYA)
- *Catopithecus* (32-31 MYA)
- *Apidium phiomense* (30-28 MYA)
- *Kamoyapithecus hamiltoni* (27.5-24.2 MYA)
- *Rukwapithecus fleaglei* (25.2 MYA)

Miocene (23.03 - 5.33 MYA)

- *Proconsul africanus* (23-14 MYA)
- *Morotopithecus* (21-20.6 MYA)
- *Rangwapithecus* (~20 MYA)
- *Ekembo nyanzae* (20-17 MYA)
- *Dendropithecus* (20-15 MYA)
- *Limnopithecus* (20-11.6 MYA)
- *Micropithecus clarki* (19-15 MYA)
- *Prohylobates* (18 MYA)
- *Afropithecus turkanensis* (18-16 MYA)
- *Heliopithecus* (~17 MYA)
- *Victoriapithecus macinnesi* (17-15 MYA)
- *Nyanzapithecus* (16-11.6 MYA)
- *Otavipithecus* (16-11.6 MYA)
- *Equatorius* (15.58-15.36 MYA)
- *Nacholapithecus* (15-14 MYA)
- *Kenyapithecus* (14 MYA)
- *Griphopithecus* (13.65-11.1 MYA)
- *Pierolapithecus* (13 MYA)
- *Dryopithecus* (12.5 MYA)
- *Sivapithecus* (12.5 MYA)
- *Danuvius* (11.6 MYA)
- *Hispanopithecus* (11.1-9.5 MYA)
- *Rudapithecus* (10 MYA)
- *Ankarapithecus* (10-9.8 MYA)
- *Nakalipithecus nakayamai* (9.9-9.8 MYA)

- *Khoratpithecus* (9-7 MYA)
- *Samburupithecus kiptalami* (9.5 MYA)
- *Ouranopithecus* (9.5-7.4 MYA)
- *Graecopithecus* (9-8 MYA)
- *Chororapithecus abyssinicus* (~8 MYA)
- *Yuanmoupithecus xiaoyuan* (8.2-7.1 MYA)
- *Oreopithecus* (7 MYA)
- *Sahelanthropus tchadensis* (7 MYA)
- *Lufengpithecus* (8-6 MYA)
- *Orrorin tugenensis* (6 MYA)
- *Ardipithecus kadabba* (5.8-5.2 MYA)

Pliocene (5.33 - 2.6 MYA)

- *Indopithecus giganteus* (5-4 MYA)
- *Ardipithecus ramidus* (4.4 MYA)
- *Australopithecus anamensis* (4.2-3.8 MYA)
- *Kenyanthropus platyops* (3.5 MYA)
- *Australopithecus afarensis* (3.6-2.9 MYA)
- *Australopithecus africanus* (3.3-2.1 MYA)

Pleistocene (2.58 MYA - 11.7 kYA)

- *Paranthropus aethiopicus* (2.7-2.3 MYA)
- *Homo habilis* (2.3-1.65 MYA)
- *Homo ergaster* (1.8-1.3 MYA)
- *Paranthropus boisei* (2.5-1.15 MYA)
- *Australopithecus sediba* (1.98 MYA)
- *Homo rudolfensis* (2 MYA)
- *Paranthropus robustus* (2.87-0.87 MYA)
- *Homo erectus** (1.89-0.11 MYA)
- *Homo antecessor* (1.2-0.8 MYA)
- *Gigantopithecus blacki* (1-0.1 MYA)
- *Bunopithecus sericus* (~700-130 kYA)
- *Homo heidelbergensis*** (700-200 kYA)
- *Homo floresiensis* (100-50 kYA)
- *Homo neanderthalensis* (400-40 kYA)
- *Homo naledi* (336-235 kYA)
- *Denisovans / Homo longi**** (285-51.6 kYA)

Holocene (11.7 kYA - present)

- *Homo sapiens* (300 kYA - present: extant)

* *H. erectus sensu lato* = {*H. georgicus*, *H. ergaster*, *H. erectus sensu stricto*}, a 'lumped' taxon.

* *H. habilis* = {*H. rudolfensis*, *H. gautengensis*}

Genus *Australopithecus* = {**A. africanus**, **A. afarensis**, **A. sediba**, **A. anamensis**, *A. deyiremeda*, *A. bahrelghazali*, *A. garhi*, *A. prometheus*} (**bold**: most commonly accepted taxa)

** wastebasket taxon ('muddle in the middle'). ***unofficial; *H. longi* is suggested by some to be a Denisovan.

Characteristics found in species **most closely related to humans** include bipedality, an anterior foramen magnum, parabolic palate of teeth, smaller canines and larger molars, larger brain size, opposable thumbs, grasping hands, nails instead of claws, shorter snout/nose, reduced olfactory sense, stereoscopic trichromatic vision, extended parental periods, complex social structures with advanced languages and behavioural traits.

Representative Skulls of Some Known Hominins (arranged by general morphologic similarity)



Binomial classification
(Specimen identifier), brain case size in cc, time period

- A** *Sahelanthropus tchadensis* (TM 266), 350 cc, 7-8 MYA
- B** *Ardipithecus ramidus* (ARA-VP-6), 300-350 cc, 4.4 MYA
- C** *Australopithecus afarensis* (multi-specimen cast), 350-500 cc, 2.95-3.24 MYA
- D** *Australopithecus africanus* (STS 5), 400-555 cc, 2-3 MYA
- E** *Australopithecus sediba* (MH1), 420-440 cc, 1.95-2 MYA
- F** *Homo habilis* (KNM ER 1813), 509-687 cc, 1.65-2.3 MYA
- G** *Homo rudolfensis* (KNM ER 1470), 750-825 cc, 2 MYA
- H** *Homo gautengensis* (STW 53), est. 500-700 cc, 1.5-1.8 MYA
- I** *Homo georgicus* (D2700), 600 cc, 1.7-1.8 MYA
- J** *Homo ergaster* (KNM ER 3733), 850 cc, 1.4-2.27 MYA
- K** *Homo erectus* (Tattersall-Sawyer cast), 600-1200 cc, 0.1-2 MYA
- L** *Homo heidelbergensis* (Rhodesian man), 1220-1300 cc, 0.2-0.6 MYA
- M** *Homo neanderthalensis* (La Chapelle), 1500-1700 cc, 0.044-0.4 MYA
- N** Archaic *Homo sapiens* (Cro Magnon 1), 1200-1600 cc, 0.3 MYA-present
- O** *Homo sapiens* (modern cast), 1200-1400 cc, 0.3 MYA-present

Compiled by Erika
(Gutsick Gibbon)

Locomotor Styles: main modes of movement across the ground or through the trees

- Bipedal (habitual / obligate): two limbs support the body weight, used primarily.
- Quadrupedal: movement with all four limbs supporting the body weight.
- Brachiator: swinging through trees by hanging from the arms.
- Pronograde: quadrupedal knuckle-walking with the body approximately horizontal.
- Palmigrade: walking with flat hands (open palms) or feet on the ground.
- Plantigrade: walking with the toes and metatarsals flat on the ground (done by humans).

Suite of Characteristics Indicative of Bipedalism: originated in late Miocene hominids

Morphology and biomechanics are linked by causal morphogenesis (Wolff's law).

- Anterior foramen magnum*: allows the skull to rest on the top of the spine.
- Sagittally-oriented iliac blades*: allows the pelvis to rest upright
- Valgus knee (bicondylar angle)*: the femur is angled to keep the knees in line.
- In-line hallux: the big toe is aligned with the other toes, aiding in walking.
- Bowl-shaped pelvis: supports the visceral organs around the abdomen.
- Lumbar lordosis (S-shaped vertebral column): supports an upright posture.
- Arched foot: three arches (medial, lateral, transverse) in the feet act as shock absorbers in walking.

* strongest indicators, since these biomechanically prevent quadrupedalism.

Sites of Interest to Paleoanthropology: significant hominin fossil finds and associated artefacts

- Lomekwi (Kenya): oldest stone tools, attributed to *Australopithecus* or *Kenyanthropus*.
- Koobi Fora (Kenya): *A. anamensis*, *P. boisei* and *H. habilis* discovered.
- Olduvai Gorge (Tanzania): many stone artefacts discovered with hominin remains around ~2 MYA.
- Hadar (Ethiopia): Lucy (*A. afarensis*) discovered.
- Laetoli (Tanzania): footprints of *Australopithecus* discovered, most likely *A. afarensis*.
- Cradle of Humankind (South Africa): Taung child, Little Foot, Mrs Ples and other australopithecines.
- Rising Star Cave (South Africa): *Homo naledi* discovered within.
- Liang Bua (Indonesia): *Homo floresiensis* discovered within.
- Jebel Irhoud (Morocco): archaic *Homo sapiens* discovered.
- Fertile Crescent (Middle East): neolithic farming, ancient cities and civilisations from ~12 kYA.

19.4.4. Genetic Mutations in Human Evolution

The full genomes of *Homo sapiens*, *Homo neanderthalensis* and Denisovans are available, as well as all extant primates.

Neurological development:

- **ARHGAP11**: the basal form, ARHGAP11A, encodes the protein RhoGAP with nuclear localisation, found in all extant non-human mammals. A partial duplication ~5 MYA seen in *Homo sapiens*, Neanderthals and Denisovans led to them additionally acquiring ARHGAP11B, which shows mitochondrial localisation instead. It promotes basal progenitor cells (BP cells) and increases the neocortex size significantly.
- **TKTL1 (transketolase-like 1)**: modern *Homo sapiens* has an arginine point mutation (K261R) while Neanderthals, Denisovans, archaic *Homo sapiens* and other extant primates have the lysine form. The human gene promotes production of basal radial glial cells (bRG cells, neural stem cells), significantly increasing upper-layer cortical neuron production and the size of the brain's gyri (ridges) in the frontal lobe.

Musculature and biomechanics:

- **PPARGC1A and promoters for MYH7**: promotes a higher proportion of slow-twitch muscle fibres rather than fast-twitch.
- **GDF8 (myostatin)**: negatively regulates skeletal muscle growth.

Metabolism:

- **GULO (L-gulonolactone oxidase)**: in mammals, encodes an enzyme for producing vitamin C, but is non-functional in haplorhines, occurring as the GULOP pseudogene.

19.4.4. Analytical Methods in Paleontology, Geology and Archaeology**Dating:**

- Radiometric dating:
 - Carbon dating (^{14}C)
 - Potassium-argon dating (^{40}K - ^{40}K)
 - Argon-argon dating (^{39}Ar - ^{40}Ar)
 - Uranium series dating (^{230}Th - ^{234}U , ^{234}U - ^{238}U , etc)
- Dendrochronology (tree ring dating)
- Aspartic acid racemisation
- Seafloor spreading (marine magnetic anomalies, Section 15.2.12)

Climate Analysis:

- Oxygen isotope ratio cycle ($\delta^{18}\text{O}/\delta^{16}\text{O}$)
- Ice cores
- Sediment analysis
- Pollen grains

Genetic Analysis:

Y chromosomal DNA has a faster mutation rate than other chromosomes, with significant degradation in humans. However, in recent times the mutations occurred primarily in non-coding regions and no genes have been lost for 7 MA, and only one gene lost for 25 MA.

19.4.5. Paleolithic Stone Age

The 'old' (paleolithic) stone age ranges from the earliest known stone tools used by many hominins, including those prior to genus *Homo*. It spans from ~3.3 MYA (middle Pliocene) to 11.65 kYA (end of the Pleistocene).

The domestication of dogs from wolves (*Canis lupus*) began approximately ~40 kYA.

19.4.6. Mesolithic Stone Age

The 'middle' (mesolithic) stone age ranges from ~15 kYA to 5 kYA in Europe, and from ~20 kYA to 10 kYA in the Middle East.

The domestication of cats from the African wildcat (*Felis silvestris*) began ~12 kYA.

'Cheddar Man' is a skeleton dated to 11 kYA, found in Britain. DNA analysis found that he was likely a hunter-gatherer with blue-green eyes and black skin, with no lactase persistence.

19.4.7. Neolithic Stone Age

The 'new' (neolithic) stone age ranges from ~12 kYA to ~4 kYA (10,000 BC to 2,000 BC).

The Neolithic Revolution (agricultural revolution) introduced subsistence farming and settlements developing in the Fertile Crescent.

19.4.8. Copper Age (Chalcolithic)

The Copper Age ranges from ~5,000 BC to ~3,000 BC, and it overlaps with the Neolithic stone age, as both copper and stone tools were used in this period.

The beginning of documented history, coinciding with the invention of writing, began around 4,000 BC.

'Ötzi the Iceman' is a naturally frozen mummy carbon dated to ~3,200 BC, found in the Alps.

19.4.9. Bronze Age

The Bronze Age ranges from 3,300 BC to 1,200 BC.

The Ancient Egyptians lived from ~3,100 BC to 332 BC.

19.4.10. Iron Age

The Iron Age ranges from ~1,300 BC to ~300 AD.

The Ancient Greeks lived from 1,200 BC to 323 BC.

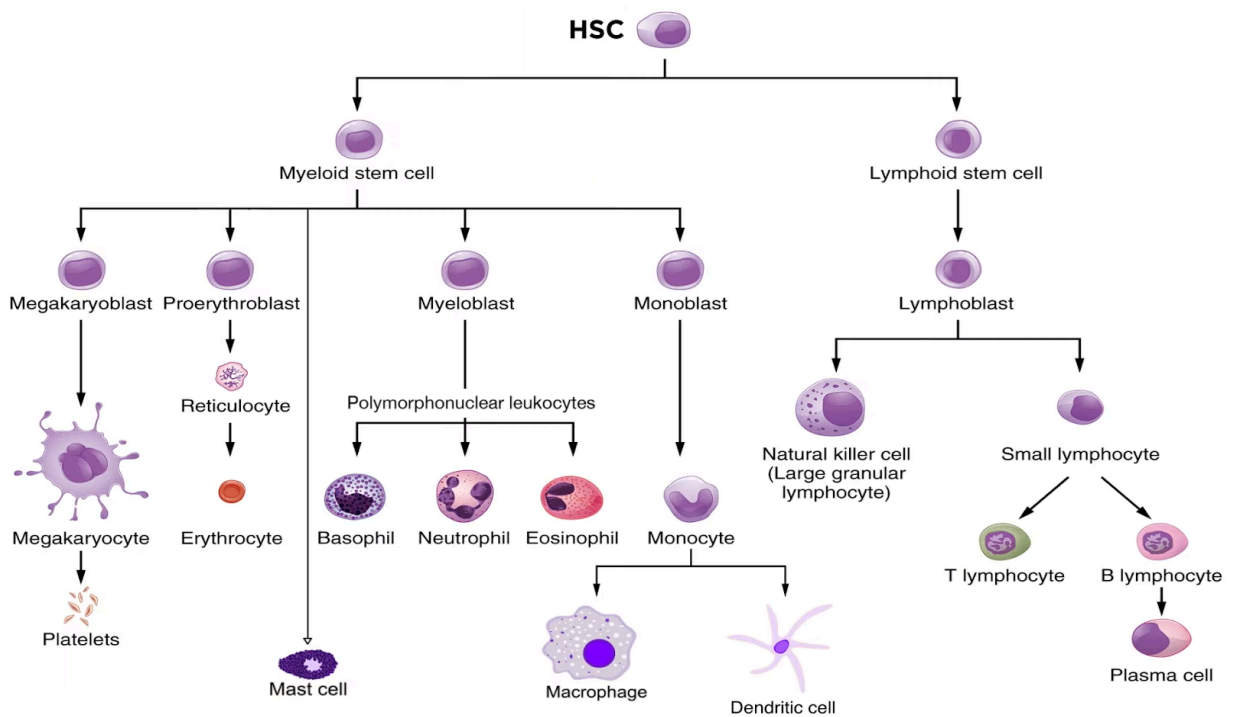
The Ancient Romans lived from 753 BC to 476 AD.

B20. MEDICAL BIOLOGY

20.1. Immunology

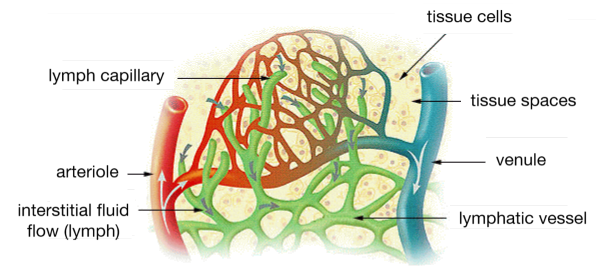
20.1.2. Production of Immune Cells

Haematopoiesis: differentiation from multipotent hematopoietic stem cells (HSCs) in bone marrow. HSCs form two separate lineages (myeloid and lymphoid) of stem cell progenitors.



20.1.3. The Lymphatic System

Interstitial fluid containing cellular waste products and dead cell debris from tissues around the body is pulled into the lumen of lymphatic capillaries by capillary exchange. The lymphatic vessels form a network between lymph nodes. There are ~600 lymph nodes in an adult human, distributed across the body, mostly around vital organs.



Immune cells congregate at lymph nodes to help organise an immune response. Lymph node sinuses are lined with macrophages and dendritic cells that sample lymph fluid for pathogens and debris that could trigger an immune reaction. Chemokines demarcate B cell zones (follicles) and T cell zones within the lymph nodes, housing each cell type. Once a naive lymphocyte has found its cognate antigen, it undergoes costimulation and activation, followed by cell division and migration to the site of infection.

- T-cell zone: antigen-presenting dendritic cells can find a T cell with the cognate antigen
- B-T zone margin: helper T cells find B cells with the cognate antigen, forming germinal centres
- Naive B/T cells circulate through their respective zones to try finding their cognate antigen.

The spleen acts as a single giant lymph node. Healthy red blood cells are able to re-enter the venous sinus by flexing through the inter-endothelial slit in the splenic cords / cords of Billroth in the 'red pulp' region. Old and damaged red blood cells are unable to pass and are phagocytosed. The iron from senescent red blood cell haemoglobin is also recycled into new haem cofactors. Other filtration processes of pathogens occur in the 'white pulp' region, in the PALS (periarteriolar lymphoid sheath) region, serving as the spleen's T cell zone, inside which is the marginal zone.

The thymus is a region of early T cell development after progenitor migration from the bone marrow, most active in infancy. Naive T cells leave the thymus to enter circulation through lymph nodes.

The mucosa-associated lymphatic tissues (MALTs) line the digestive tract, airways etc equip thin tissues with lymph-like structures, supplying them with antigens from microfold cells (M cells).

20.1.4. Signal Transduction in Immune Cells

Lymphocyte cell receptors are typically transmembrane proteins with an extracellular and intracellular domain. Ligand binding to the extracellular domain initiates a signalling cascade on the intracellular side.

Kinase enzymes (e.g. Lck: lymphocyte-specific protein tyrosine kinase) catalyse the phosphorylation of amino acid residues in proteins. Phosphatase enzymes reverse this process. The presence or absence of a phosphate group on a protein can promote or inhibit its activity due to conformational change, acting as protein-level regulation.

Another pathway starts via G-protein coupled receptors in the cell membrane; on ligand binding, a heterotrimeric complex ($\alpha\beta\gamma$) binds to the receptor. The inactive complex is bound to GDP, but on conversion to GTP (through e.g. guanine-nucleotide exchange factors (GEFs)), the active state forms, which can phosphorylate downstream. Large/small GTPase enzymes, which convert GTP to GDP (analogous to ATP/ADP), regulate this pathway. Ras, Rac and Rho are common small GTPases.

Types of Immune Cell Receptors

- **Antigen Receptors:** pattern recognition receptors (PRRs) (e.g. Toll-like receptors (TLRs), nucleotide-binding oligomerisation domain-like receptors (NOD-like, NLRs), C-type lectin receptors (CLRs), Rig-1-like receptors (RLRs)): PRRs recognise pathogen-associated molecular patterns (PAMPs) and damage-associated molecular patterns (DAMPs). Antigen-specific lymphocyte receptors are expressed in only one unique type per lymphocyte.
- **Costimulatory Receptors:** T-cells express CD28 which is costimulatory for CD80 and CD86 on antigen-presenting cells. T-cells also express ICOS (inducible costimulator), which binds to ICOS-L on antigen-presenting cells, which helps prepare CD4⁺ T cells. Antigen-presenting cells express CD40, which binds CD40L on T-cells, increasing CD80 expression on dendritic cells, sustaining a positive feedback loop.
- **Inhibitory Receptors:** receptor CTLA-4 (cytotoxic T-lymphocyte-associated protein 4) on T-cells binds and competitively inhibits CD80/CD86 on antigen-presenting cells, limiting CD28 effects. PD-1 binds PD-L1/L2, promoting T-cell apoptosis. Natural killer cells inhibitory receptors bind MHC class I molecules for healthy self cells, protecting them from attack.
- **Cytokine Receptors:** cytokines are soluble protein signalling molecules, determining immune cell development and inflammation vs repair.
- **Chemokine Receptors:** guides immune cells to the site of damage by chemotaxis. Most chemokine receptors are large G-protein coupled receptors, inducing changes in cell adhesion and motility (chemotaxis).

20.1.5. Cytokines and Chemokines

Cytokine families: interferons (IFN-), tumour necrosis factors (TNF-), transforming growth factors (TGF-), colony stimulating factors (-CSF), interleukins (IL-), lymphotoxins (LT-).

Types of Adaptive Immune Response: characterised by different **cytokine profiles** for fighting different types of pathogens. The immune response types are named after the type of helper T cell involved.

- **Type 1 Response (Th1 Cytokines, Th1 Helper T Cells):** promotes cellular **immunity** against intracellular pathogens (e.g. **viruses**, some bacteria) by activating CD8⁺ **T cells and NK cells**. Th1 cytokines include **IL-2** (critical for T cell growth and differentiation), **IL-12** (activates NK cells, polarises T cells to be more type 1-like), **TNF- α** (promotes apoptosis, broad pro-inflammatory effects), **LT- α** and **LT- β** (kills chronically infected cells, activates macrophages, promotes lymphoid tissue development), **IFN- γ** (antiviral by promoting cellular MHC class I expression, activates macrophages, inhibits polarisation to type 2-like T cells).
- **Type 2 Response (Th2 Cytokines, Th2 Helper T Cells):** activates humoral responses (**antibodies**) for destruction by **B cells**, with high presence of **eosinophils, basophils and mast cells**, common for fighting **parasitic worms** (helminths) and promote wound healing/tissue repair. Th2 cytokines include **IL-4** (polarises T cells to type 2-like, promotes mast cell growth in bone marrow, stimulates eosinophils, activates B cells), **IL-5** (eosinophil development in bone marrow), **IL-10** (enhances B cell activation and antibody production, suppresses Th1 cytokine expression), **IL-13** (signals B cells to make IgE antibodies), **IL-25** (amplifies response by inducing IL-4/5/13, activates type 2 innate lymphoid cells).
- **Type 17 Response (Th17 Cytokines, Th17 Helper T Cells):** fights **fungal** and large bacterial infections by recruiting **neutrophils**. Th17 cytokines include **IL-17** (increases production of chemokine IL-8 (CXCL8, a strong neutrophil chemoattractant), **IL-22** (promotes proliferation in epithelial barrier cells in the skin/lung/gut, production of antimicrobial peptides), **IL-23** (polarises helper T cell to type 17).
- **Regulatory Response (Treg Cytokines, Regulatory T Cells):** limits the effects of an immune response to prevent excessive damage and autoimmune diseases. Treg cytokines include **IL-10** and **TGF- β** (promotes tissue repair, wound healing, anti-inflammatory, promotes Treg development, inhibits B cell proliferation, inhibits activated macrophages).

Chemokines: induces chemotaxis in immune cells to guide them towards a stimulus. Chemokine families include CC (contains two adjacent Cys residues near N-terminus) and CXC (Cys residues separated by a variable residue). Names with 'L' indicate ligands (e.g. CCL2). Names with 'R' indicate receptors (e.g. CCR2 is a receptor for either a CC or CXC chemokine).

- **CC Chemokines:** induces migration in lymphocytes and monocytes. CC chemokines include **CCL2** (MCP-1) (promotes Th2 immunity and histamine release from basophils), **CCL3** (MIP-1 α) (recruits monocytes/macrophages/neutrophils, promotes Th2 immunity), **CCL4** (MIP-1 β) (recruits monocytes and NK cells), **CCL5** (RANTES) (recruits eosinophils/T cells/basophils, activates NK cells), **CCL18/19** (secreted by dendritic cells, recruit T/B cells to lymph node), **CCL21** (secreted by stromal cells in lymph node to recruit dendritic cells).
- **CXC Chemokines:** induces migration in neutrophils. CXC chemokines include **CXCL1/2/3** (released by endothelial cells/fibroblasts/monocytes, promotes angiogenesis (growth of new blood vessels), activates neutrophils, stimulates fibroblast proliferation), **CXCL7** (released from activated platelets, activates neutrophils, promotes angiogenesis), **CXCL8** (IL-8) (recruits neutrophils to infected tissues), **CXCL13** (secreted by follicular dendritic cells to recruit B cells to the B cell zone (binds CXCR5)).

20.1.6. Barrier Defences of the Innate Immune System

The innate immune system is the fast-acting, nonspecific, most evolutionarily conserved (~700 MYA: plants, invertebrates, single celled organisms) part of immunity, utilising Toll-like receptors (TLRs), the complement system, phagocytosis and antimicrobial peptides.

Barrier Defences: structural and biochemical obstructions to pathogens at the surface of tissues.

Barrier surfaces are lined with epithelial cells connected by tight junctions. Barriers also possess a microbiome with commensal microorganisms (prevents colonisation, helps train the immune system).

Surfaces produce antimicrobial enzymes such as lysozymes (lyses peptidoglycan cell walls), secretory phospholipase A₂ (hydrolyses membrane phospholipids), antimicrobial peptides (AMPs) (directly kills pathogens: defensins (hydrophobic insertion into cell membrane and charge disruption), cathelicidins (pro-peptides, C-terminus acts like a defensin), histatins (fights pathogenic fungi)).

Barrier surfaces include:

- **Skin** (~2 m² on adults): contains a Gram-positive bacterial microbiome, an acid mantle, and dead keratinocyte epithelial cells. Skin-resident dendritic cells (Langerhans cells) quickly help mobilise innate and adaptive immune responses.
- **Respiratory tract** (~100 m², exposed to ~10 m³ air per day): uses the mucociliary escalator to push mucus away from the lungs up to the larynx for coughing or swallowing. Airway epithelial cells produce lamellar bodies containing beta-defensins released into the pulmonary surfactant of alveoli, and these cells express a wide range of PRRs. The nasal microbiota is similar to that of the skin but diversified, and prevents infections spreading to the lower respiratory tract.
- **Gastrointestinal tract (GI tract):** saliva contains defensins and antimicrobial enzymes. The stomach produces gastric acid, proteases and lipases for destroying microbes. Peristalsis in the intestines forces a constant movement towards excretion, preventing colonisation. A lubricated mucus surface layer generated by goblet cells also nourishes gut microbiome commensals. The intestinal crypt contains Paneth cells, secreting antimicrobial peptides, lysozymes and cryptidins (alpha defensins).
- **Female reproductive tract:** vaginal microbiome (mainly *Lactobacillus*) prevents yeast infections and bacterial vaginosis, metabolising glycogen to lactic acid and producing hydrogen peroxide.

20.1.7. Complement System

Complement System: circulating protein effectors activated on binding to Ag/Ab complexes, a key part of the innate immune system.

Most complement proteins are zymogens (inactive enzymes, activated by cleavage of a precursor). There are 9 main complement proteins (C1-9). Cleaved products have suffix 'a' (smaller, anaphylatoxin) and 'b' (larger, binding portion) (exception: reverse convention in C2) e.g. C3 → C3a + C3b. Fragments complex together to form enzymes, e.g. C3 convertase = C4b2a = C4b + C2a; C5 convertase = C4b2a3b = C3b + C4b2a.

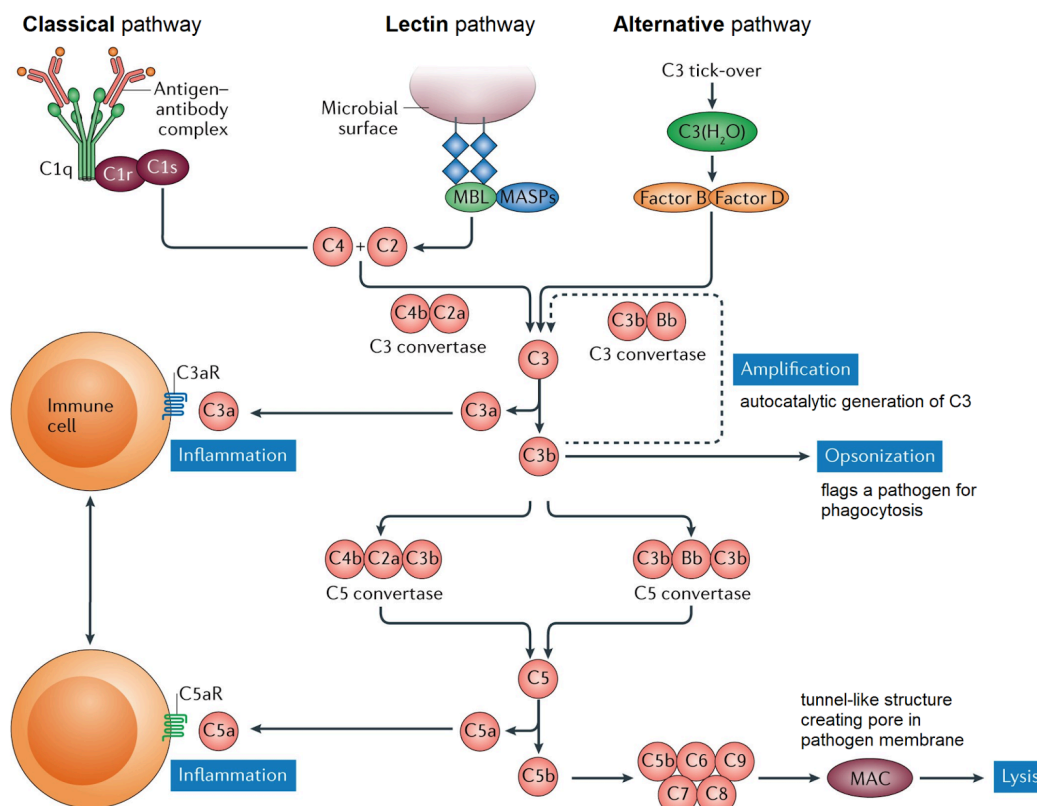
Complement is activated through classical, lectin or alternative pathways, converging at C3 cleavage:

- Classical:** antibody recognition, most evolutionarily recent (found in jawed vertebrates).
- Lectin:** acts as PRRs for binding pathogenic cell wall polysaccharides.
- Alternative:** uses a distinct C3 convertase (C3bBb), most evolutionarily conserved.

C3 is the most abundant complement protein (1.2 mg/ml in the serum), and is amplified autocatalytically by the alternative pathway. Downstream effects of C3 include:

- Inflammation:** C3a and C5a promotes inflammation and recruits neutrophils and monocytes.
- Opsonisation:** C3b coats pathogen surfaces and are recognised by phagocytes for phagocytosis. C3b has an exposed labile thioester for rapid attachment, but is inactivated by hydrolysis.
- Nucleation of membrane attack complex (MAC):** pore formation in a cell membrane.

Regulatory proteins (C1 inhibitor, decay-accelerating factor, C4 binding protein, CR1, factor H, vitronectin, protectin) limit complement overactivation and harming of host cells.



20.1.8. Inflammatory Response

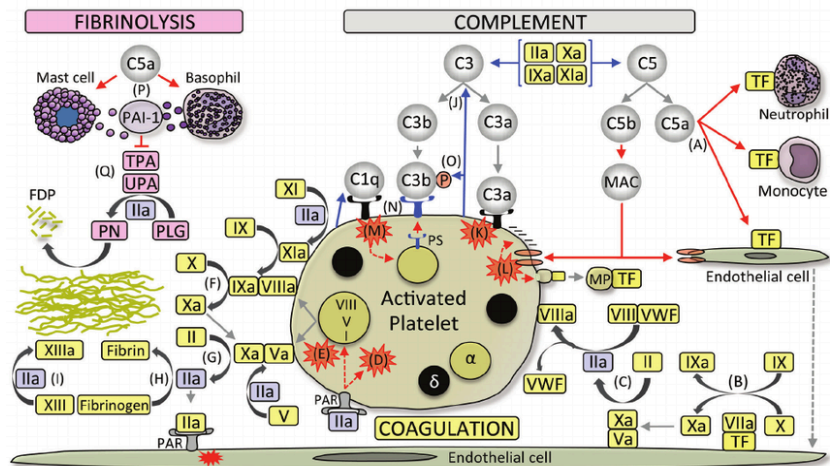
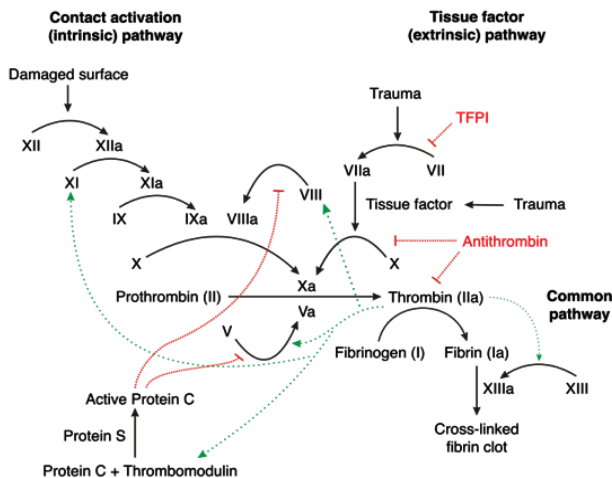
Inflammation is characterised by pain, redness, swelling, heat and loss of function. Acute inflammation is an evolutionary adaptation to contain and limit early spread of infectious microbes, by destroying invading microbes, inducing local blood clotting and repairing injured tissue.

Tissue-resident immune cell PRRs sense PAMPs and DAMPs indicative of tissue damage or microbial infection. Activated macrophages release inflammatory lipid mediators (leukotrienes, prostaglandins and platelet activating factor) and nitric oxide, acting on smooth muscle cells to induce vasodilation, slowing blood flow and increased vascular permeability for neutrophil, complement and antibody migration.

In endothelial activation, cell adhesion molecule (e.g. P-selectin) expression on the lumen is increased, facilitating immune cells leaving the bloodstream. P-selectin is expressed in response to cytokine TNF- α , bacterial endotoxin, leukotriene B4, histamine or complement protein C5a. E-selectins are also expressed, which bind glycoproteins on immune cells. The immune cells then slow to a roll along the lumen wall, express adhesion molecules LFA-1 and CR3, interacting with ICAM-1/2 on endothelial cells, promoted by chemokine CXCL8, where they leave the blood vessels (extravasation) by binding of PECAM-1 (CD31).

Coagulation Cascade: forms a fibrin blood clot, trapping pathogens.

Interactions between Coagulation and Complement:



Kinin System: another protease cascade, forming vasodilator oligopeptides bradykinin and kallidin from Factor XIIa, as well as plasmin ('PN' in fibrinolysis). Plasmin also amplifies complement C3 / C5 formation.

Resolution of inflammation: controls the immune response and promotes wound healing.

The short lifespan of neutrophils (efferocytosis: phagocytosis by infiltrating macrophages after ~3 days in the tissue) help to limit inflammation. Anti-inflammatory cytokines are then released from the macrophages. Lipid mediators for resolution (derived from polyunsaturated fatty acids: resolvins, protectins, lipoxins, maresins) promote production of anti-inflammatory IL-10, stimulates efferocytosis, inhibits neutrophil chemotaxis, decreases expression of endothelial cell adhesion molecules, decreases vascular permeability. Resolution also includes angiogenesis, epithelial cell proliferation and deposition of ECM proteins (collagen). Chronic inflammation results if resolution does not occur, with many serious side effects (no return to homeostasis, rheumatoid arthritis, autoimmune disease and cancer).

20.1.9. Pattern Recognition Receptors (PRRs) and the Inflammasome

Innate immune cells contain pattern recognition receptors (PRRs), that can bind to pathogen-associated molecular patterns (PAMPs) and damage-associated molecular patterns (DAMPs). PRRs can be found facing the extracellular space on the cell membrane, free in the cytosol, or facing endosomes of ingested pathogens.

PAMPs include bacterial cell wall lipids, peptidoglycans lipopolysaccharides, bacterial flagellin, lipoteichoic acid, fungal polysaccharides, viral endosomal ssDNA/dsRNA, and unmethylated CpG-rich DNA. PAMPs are highly conserved among pathogens and tend to be essential for their survival, preventing them from evolving away from innate immune defences. DAMPs are host cell molecules that should normally not be present outside of cells (e.g. ATP), indicative of leakage from damaged cells, or ROS (reactive oxygen species), amyloid beta (prion-like) and inorganic irritants (silica, asbestos).

PAMP Detection: PRR families that can detect PAMPs include

- **Toll-like receptors (TLRs)** are homologs of the *Drosophila* Toll protein found across mammals, invertebrates and plants. TLRs are transmembrane proteins with leucine-rich repeats at the extracellular side, forming a C-shape ligand-binding domain. The intracellular side contains a TIR domain used for signal transduction. On binding to a ligand, TLRs dimerise and bring together the tails on the intracellular side, allowing docking of adaptor proteins (MyD88, TRIF, Mal, TRAM). The MyD88 and TRIF pathways lead to release of NF- κ B which translocates to the nucleus, acting as a transcription factor for inflammatory cytokines (TNF- α , IL-6). The TRIF pathway also forms dimerised IRF3, a transcription factor for type 1 interferon cytokines.
- **NOD-like receptors (NLRs)** are similar to TLRs, often expressed in epithelial cells and are suited to detecting intracellular bacteria due to peptidoglycan recognition. The intracellular side contains an N-terminal CARD domain, which activates NF- κ B release (similar to TRIF pathway of TLRs).
- **Rig-I-like Receptors (RLRs):** contains a helicase-like domain for binding viral RNA with two CARD termini for signal transduction. RIG-I detects viral ssRNA, while MDA5 detects cytosolic dsDNA. Activation produces transcription factors (IRF3/7, NF- κ B) for type 1 interferons.

DAMP Detection using PRRs:

- **P2X7** senses extracellular ATP.
- **RAGE** senses the DNA-binding protein HMGB1 (typically found in the cytosol) and the S100 family of calcium-binding proteins.

DAMP recognition generally leads to pro-inflammatory cytokine production, like with PAMPs. Many PRRs that normally recognise PAMPs can also recognise DAMPs.

Inflammasome: a faster route of threat detection than through PRRs.

Inflammasomes are complex structures that sense threats and initiate inflammation directly. They contain sensors for a wide range of PAMPs and DAMPs (without direct binding necessary), a CARD domain, and caspase zymogens as effectors. After priming on sensing, pro-inflammatory IL-1 β and IL-18 are produced, and pyroptosis is induced (inflammation-associated cell death) through N-GSDMD. Well-studied inflammasomes include NLRP1, NLRP3 (cryopyrin), NLRC4, NLRP6 and AIM2.

20.1.10. Neutrophils

Neutrophils are the main **pathogen-fighting cell** of the **innate** immune system.

HSCs undergo granulopoiesis (differentiation through myelocytes and band cells) to form neutrophils in large numbers ($\sim 10^{11}$ produced in the bone marrow per day). Mature neutrophils are retained in the bone marrow due to their expression of chemokine receptors CXCR2/4, which are activated by CXCL12 released by osteoblasts and stromal cells. Growth factor G-CSF promotes neutrophil exit from the bone marrow by downregulating expression of these chemokines and receptors.

Neutrophils contain many granules (secretory vesicles containing antimicrobial chemicals) which can be exocytosed, and are polynuclear (3-5 lobules). Mature neutrophils express CD11b (Mac-1), CD15, CD16/ $Fc\gamma$ receptor III, CD33 and CD66b. They characteristically do not express CD14. Their cytokine, chemokine and growth factor secretion profile indicate a range of roles including hematopoiesis, angiogenesis and wound healing.

Under homeostatic conditions, neutrophils enter circulation, migrate to tissues and are eliminated by macrophages (short half-life \sim 6-8 hours) to form the viscous pus fluid after an infection. Neutrophil functions in tissues include:

- Phagocytosis: clears microbes and dead cells. Occurs by either a 'trigger' or 'zipper' mechanism, using lipid remodelling and the actin cytoskeleton to shape the cell membrane into engulfing and binding the target pathogen. The pathogen is internalised into a phagosome.
- Degranulation: sequential exocytosis of chemical-filled granules. Firstly, the 'tertiary' granules containing myeloperoxidase/lysozyme/cathepsin/gelatinase are released to facilitate extravasation. The 'secondary' granules contain lactoferrin/alkaline phosphatase/NADPH oxidase for neutrophil recruitment, chemotaxis receptor upregulation, bactericide and chemoattractant generation. Lastly, the 'primary' granules contain elastase/MPO/defensins/cathepsin/HNP-1/2/3 / BPI, which fuse with phagosomes to deliver the contents to kill ingested pathogens.
- NETosis (formation of neutrophil extracellular traps): the chromatin in neutrophil DNA loosens and is released to form complexes with histones as well as azurophilic granules (MPO/elastase/cathepsin G). These complexes accumulate concentrations of antimicrobial agents, and pathogens entering them will be immobilised for phagocytosis.

In a tumor microenvironment, neutrophils may become polarised to tumor-associated neutrophils (TANs). They may have N1 (anti-tumor, by $IFN-\beta$) or N2 (pro-tumor, by $TGF-\beta$) phenotypes.

20.1.11. Mast Cells, Basophils and Eosinophils

Mast cells play effector roles in both innate and adaptive immunity, as well as in allergic inflammation (hypersensitivity type 1) reactions and in fighting pathogens and parasites. Together with basophils and eosinophils, they form the granulocyte white blood cells.

Mast Cells

Mast cells leave the bone marrow as progenitors and mature in peripheral tissues (not in blood), while basophils and eosinophils remain in the bone marrow until maturation. Mast cells are typically first to recognise damage from the external environment due to being localised on barrier tissues. Activated mast cells coordinate the early innate immune response, recruiting basophils and eosinophils by providing inflammatory chemotactic stimuli.

Mast cells in humans are classed as MC_T (tryptase, found in mucosa of respiratory and GI tract) or MC_{TC} (chymase, found in connective tissues including dermis and heart). Mast cells express the stem cell factor receptor CD117 (KIT), FcεR1, the IgG receptor CD32a (FcγR2a), the IFN-γ receptor CD64 (FcγR1), the receptors for complement C3a and C5a, the nerve growth factor receptor, as well as various other interleukins and chemokines. Activation of mast cells occurs by aggregation of FcεR1 when allergens bind to IgE antibodies. Activation results in exocytosis of granules containing e.g. histamine, serine proteases.

Basophils

Basophils have fewer, larger granules than mast cells and reproduce less. They express receptors for cytokines (IL-3/5R, GM-CSFR), chemokines (CCR2/3), complement (CD11b/11c/35/88), prostaglandins (CRTH2), immunoglobulins (FcεR1, FcγR2b) and TLRs. Their activation is similar to mast cells. The gp120 protein from the virus HIV is a superantigen for basophil IgE.

Eosinophils

Eosinophils have a bi-lobed nucleus with condensed chromatin. They have two types of granules (specific: cationic proteins e.g. MBP, eosinophil peroxidase, ECP, EDN and primary: Charcot-Leyden crystal protein). They also contain lipid bodies with eicosanoid synthetic enzymes, formed only after eosinophil activation. They express a diverse receptor profile.

Eosinophil degranulation is tightly regulated, and they can form DNA traps similar to neutrophils, as well as phagocytosis and respiratory bursts.

20.1.12. Macrophages

Macrophages are long-lived innate immune cells for recognition and destruction of pathogens.

Macrophages are evolutionarily conserved phagocytes found in vertebrates, exhibiting tissue-specific phenotypic plasticity with different functions under pro/anti-inflammatory conditions. Tissue-resident macrophages are present from embryonic development of hematopoietic stem cells (HSCs) in the foetal yolk sac. They can be grouped as classically-activated (M1) macrophages and alternatively-activated (M2) macrophages, polarised by Th1 or Th2 cytokines. Unique phenotypes of macrophages include tumour-associated macrophages (TAMs) and adipose tissue macrophages (ATMs), with specific expression of cytokines, chemokines, TLRs and matrix metalloproteinases (MMPs).

M1 macrophages express high levels of MHC class II, CD68/80/86.

M2 macrophages express low levels of MHC class II, high CD163/200R and MGL1/2.

Phagocytosis cascades are diverse, starting with pathogen recognition by receptors on macrophages. The pathogen is endocytosed into a phagosome, where NADPH reacts with oxygen to release H^+ and superoxide free radical ($O_2^{\bullet -}$, an ROS), while phospholipase A_2 produces free fatty acids. Together with fusion with a lysosome, this creates a broad-spectrum fatal environment for pathogens, where they are lysed, degraded and recycled.

20.1.13. Natural Killer Cells

NK cells show spontaneous cytotoxic activity towards any physiologically-stressed cell (tumour cells and virally-infected cells). As a member of the group 1 innate lymphoid cells, they secrete $IFN-\gamma$ and are dependent on transcription factor Tbet. They develop from common lymphoid progenitor (CLP) cells in the bone marrow, liver and thymus. Most mature circulating NK cells are 'dim' for CD56 and NKp46 (low expression) and produce few cytokines/chemokines on activation, but can sometimes spontaneously lyse tumour cells. NK cells have both activating and inhibitory receptors, allowing a range of activity. The inhibitory receptors bind MHC class I molecules, present on healthy cells but can be absent in virus-infected cells, triggering activation. Tumour cells also tend to show upregulation of expression of ligands for the NK cell activating receptors.

One mechanism of cytotoxicity in active NK cells begins with the formation of an immunological synapse between the NK cell and the target cell, inducing cellular reorganisation of the NK cell's actin cytoskeleton. The microtubule-organising centre (MTOC) is polarised and secretory lysosome is prepared for degranulation into the target cell. An alternative mechanism is 'death receptor induced target cell apoptosis', in which the NK cells express FasL, TNF (tumour necrosis factor) and TRAIL receptors that bind to ligands on the target cell, triggering a caspase enzyme cascade for apoptosis within the target cell.

NK cells can acquire immunological memory, unlike the rest of the innate immune system. This may occur via either antigens or cytokines.

20.1.14. Innate Lymphoid Cells

Innate lymphoid cells share similar functionality with the T cells of the adaptive immune system, but lack antigen specificity. They develop from a common lymphoid progenitor before differentiating into either NK cells (without transcription factor GATA3) or ILCs (with GATA3).

The ILC groups 1, 2, 3 and LTi are the innate counterparts of the helper (CD4⁺) T cell groups Th1, Th2, Th17 and Treg, respectively. Similarly, NK cells mirror the killer (CD8⁺) T cells. These phenotypes show adaptive plasticity based on the microenvironment.

ILC1 cells (including NK cells) are weakly cytotoxic, producing IFN- γ via the Tbet transcription factor, for fighting viruses and bacteria. ILC2 cells produce type 2 cytokines (IL-4/5/13) via the GATA3 transcription factor, for fighting parasites e.g. helminths. ILC3 cells produce IL-22 via ROR γ t transcription factor, for fighting bacteria at mucosal sites.

20.1.15. Dendritic Cells

Dendritic cells help switch from an innate immune response to an adaptive immune response.

Immature dendritic cells (DCs) are produced from differentiation of CD34⁺ HSCs in the bone marrow. On antigen presentation to T cells, the DC may assume an immunity role (activating effector (CD4⁺/CD8⁺) T cells and B cell maturation) or a regulatory role (activates regulatory T cells for peripheral immune tolerance and homeostasis).

Types of DCs include: (some variations on whether human-derived or murine (mouse) derived)

- Classical / conventional / myeloid DCs (cDC): has dendrite extensions, CD11c/1a/14⁺, CD11b^{+/−}. cDCs patrol tissues for bacterial and viral antigens, then migrate to lymph nodes for antigen presentation to T cells, producing the stimulatory mediators TNF, nitric oxide and IL-12.
- Plasmacytoid cells (PC): expresses Siglec-H and Ly6c, CD4/123⁺, HLA-DR, BCDA-2, TLR-7/9. PCs also present antigens but mainly recognise viral antigens, entering the lymph nodes directly from the bloodstream. They secrete IL-12, IL-6, TNF- α and pro-inflammatory chemokines.
- Langerhans cells (LC): for immune surveillance (activation of T cells), expresses CD207⁺ (langerin)
- Monocyte-derived cells (MC): generated upon inflammation and prime T cells in adaptive immunity.

Genetic and environmental factors can alter the function of DCs, producing autoreactive killer T cells, leading to autoimmune diseases (e.g. rheumatoid arthritis, multiple sclerosis).

20.1.16. Development of Adaptive Immune Cells (T cells and B cells)

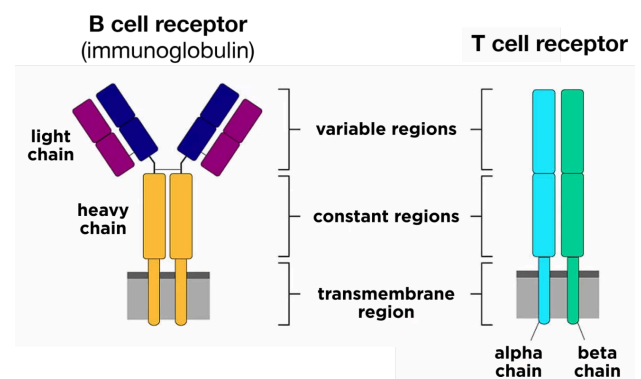
The adaptive immune system is the more advanced, evolutionarily recent (~450 MYA in jawed vertebrates) part of the immune system, responsible for antigen-specific targeting and production of long-lasting immunity against subsequent infection.

Adaptive immunity is driven by T cells (for cell-mediated immunity) and B cells (for antigenic/ humoral immunity). The B and T lymphocytes develop in the bone marrow from HSCs, with T cells migrating to the thymus, and then to the lymph nodes and spleen once matured, where they capture circulating antigens from the lymph and blood.

B-cells express both antigen receptors and antibodies on their surface, and secrete their Ag receptors into circulation where they can bind Abs. The isotypes of immunoglobulin Abs are IgM, IgD, IgA, IgE and IgG (classified by their constant domain).

V(D)J Recombination: allows complete antigen receptor diversity in lymphocytes

During the development of B and T cells, *de novo* BCR and TCR (B/T cell receptor) genes are created by recombining pre-existing gene segments, in order to translate into a huge range of combinations of receptors.



The variable (V), diversity (D) and joining (D) genes lie upstream of the constant region in the germline DNA. In humans, the loci for the heavy chain and the light chain lie on different chromosomes. Through somatic recombination, DNA is rearranged to form a VJ sequence (in light/alpha chains) or a VDJ sequence (in heavy/beta chains). A section of DNA is processed to join a random D to a random J, using RAG proteins to splice out a loop of the DJ sequence between recombination signal sequences (RSS) with 12 and 23 bp-length spacers, with the RSS orientation determining whether inversion or deletion is applied. Additional variation introduced by adding random nucleotides to the open ends. Rejoining occurs by the NHEJ pathway. The excised loops are closed and discarded on cell division. When transcribed, the mRNA introns code for a unique protein each time.

T Cell Receptor Selection and Activation:

Once a T cell has developed to express a unique receptor, they are filtered (selected) for self-antigen recognition in the thymus, with self-reactive and non-reactive receptors being eliminated by induced apoptosis. Surviving naive mature T cells exit the thymus and enter the peripheral lymphoid system, where they begin their life of being exposed to foreign peptides in MHC molecules of antigen-presenting cells (e.g. macrophages, dendritic cells, B cells) during an immune challenge (infection). Once the matching ligand has been found, they undergo clonal expansion in either the CD4⁺ (helper) or CD8⁺ (killer) phenotype, depending on whether the ligand was held by MHC class I (infected/cancer cell → CD8⁺) or MHC class II (macrophage → CD4⁺). The helper T cells activate naive B cells to produce antibodies and rejuvenate macrophages, while the killer T cells directly phagocytose infected target cells.

20.1.1. Summary of the Immune Responses

Innate Immune Response: non-specific and fast. Highly conserved evolutionarily (~700 MYA).

1. Damaged cells release signals (interferons: cytokines, histamine, bradykinin, prostaglandins) which initialises the immune system. Signals also increase MHC Class I production to increase cell transparency to immune cells.
2. **Macrophages consume bacteria by phagocytosis.**
3. Macrophages release messenger proteins to make blood vessels release water (inflammation: prostaglandin A's), bringing in complement proteins.
4. Macrophages signal for neutrophils (a type of white blood cell) to move to the site.
5. **Neutrophils release toxins** which obstruct and kill nearby pathogens and cells. Neutrophils have a short life to prevent excess damage.
6. If the pathogen persists, macrophages signal to dendritic cells to begin the adaptive immune response.

Adaptive Immune Response: specific and slow. Evolutionarily more advanced (~450 MYA).

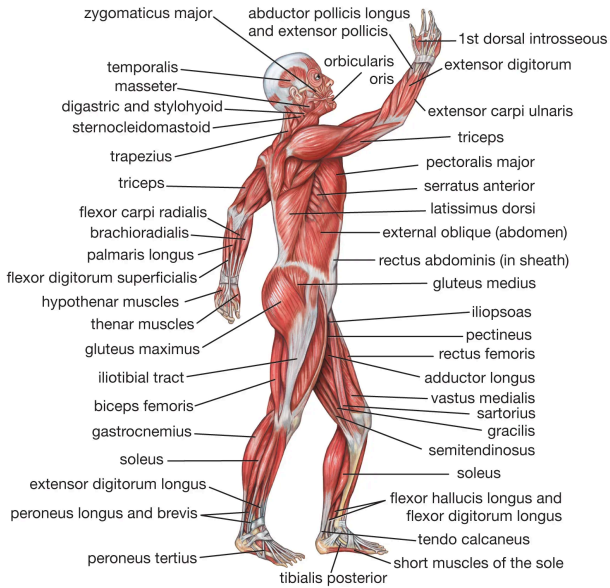
1. Dendritic cells retain the antigens of the pathogens they destroy and display them on their surface in their MHC class I windows.
2. The dendritic cells migrate to a lymph node.
3. The dendritic cell finds a (virgin / naive helper) CD8⁺ T cell with a matching receptor.
4. The **T cell becomes activated** and rapidly divides, creating clones of (effector) helper T cells which all recognise the correct antigen. Some of the T cells become memory T cells instead and remain in the lymph node.
5. Some of the helper T cells move to the site of infection and will revitalise macrophages to kill more vigorously. The rest activate (virgin / naive) B cells.
6. The **B cells produce large amounts of matching antibodies**, stimulated to persist by the T cells.

The large influx of antibodies bind to the pathogens, which impedes their motion, making it easy for killer cells e.g. macrophages to destroy them. Once the pathogens have cleared, remaining helper cells become memory cells, the B cells continuously produce antibodies for long-lasting immunity.

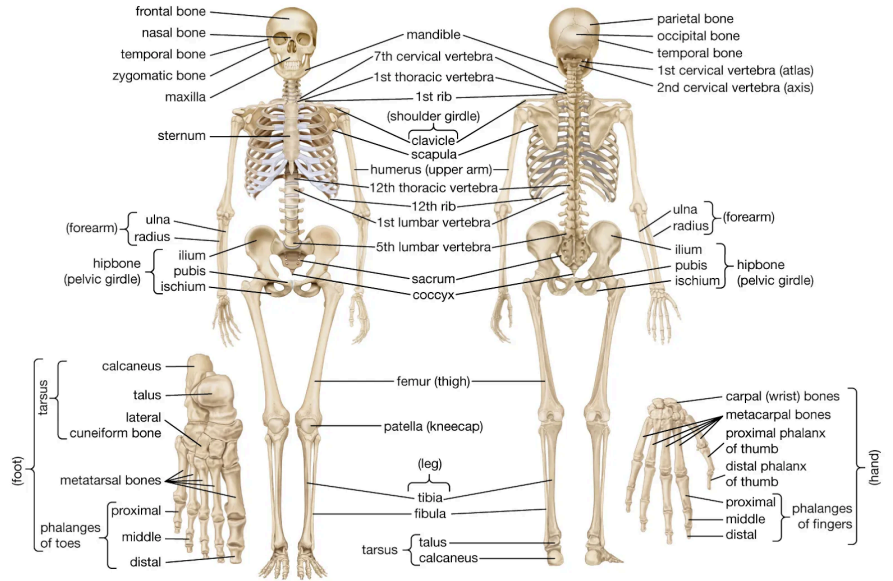
20.2. Human Anatomy and Physiology

20.2.1. Organ Systems and Their Parts

The Muscular System



The Skeletal System

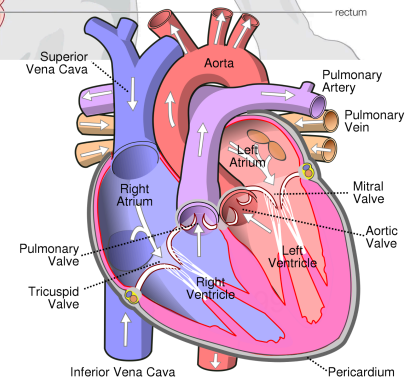
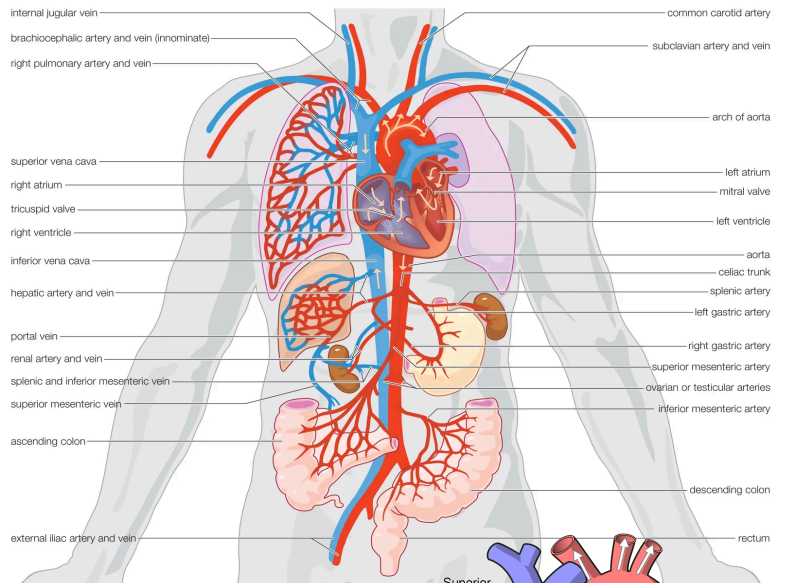
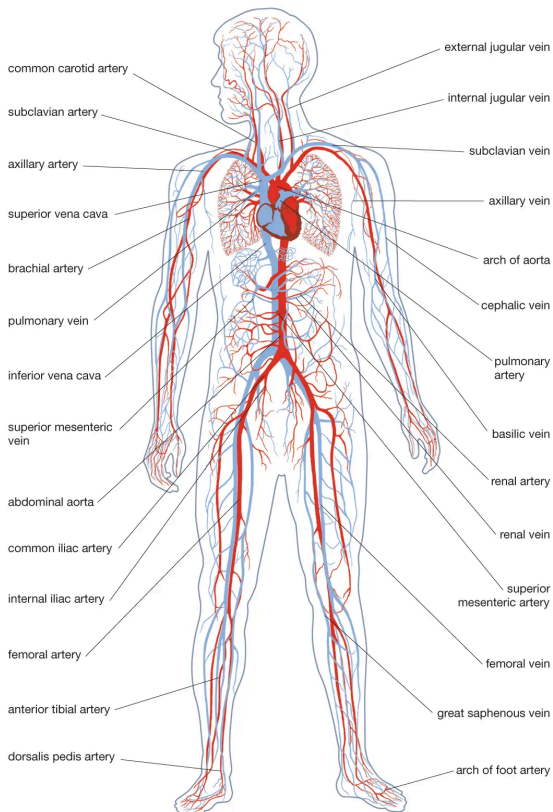


The Cardiovascular System

Arteries (carries blood away from the heart) and **Veins** (carries blood into the heart):

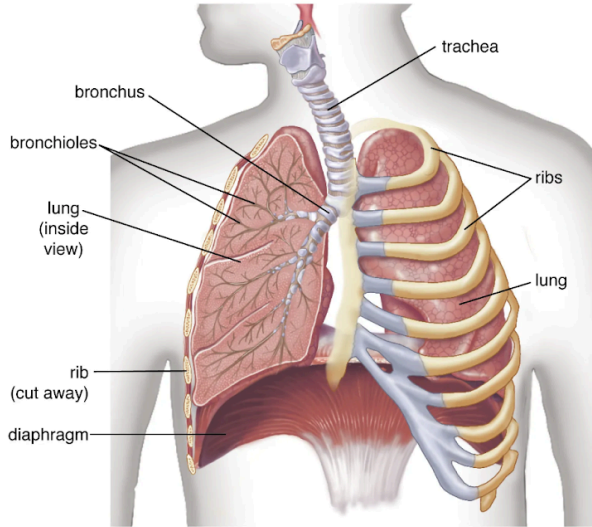
The Circulatory System and The Heart

blue: deoxygenated → lungs → **red:** oxygenated

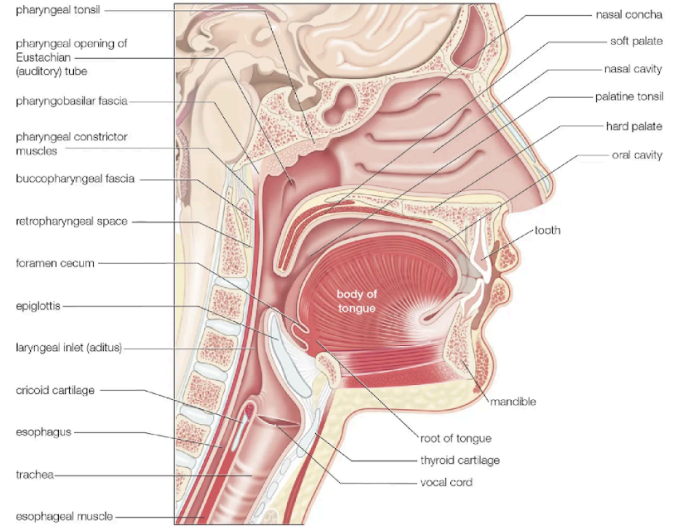


The Respiratory System

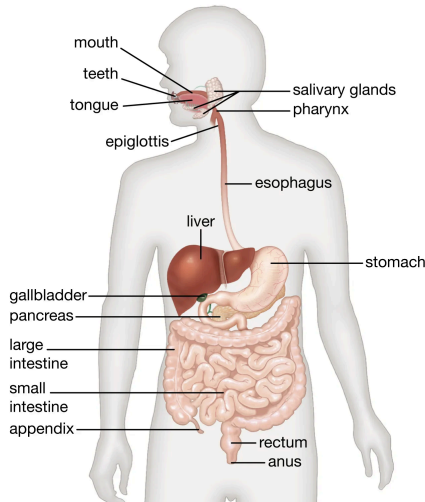
The Lungs



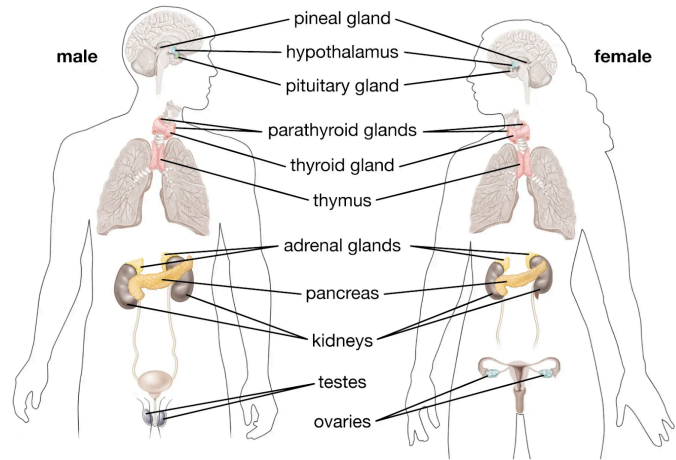
The Nose, Mouth and Throat



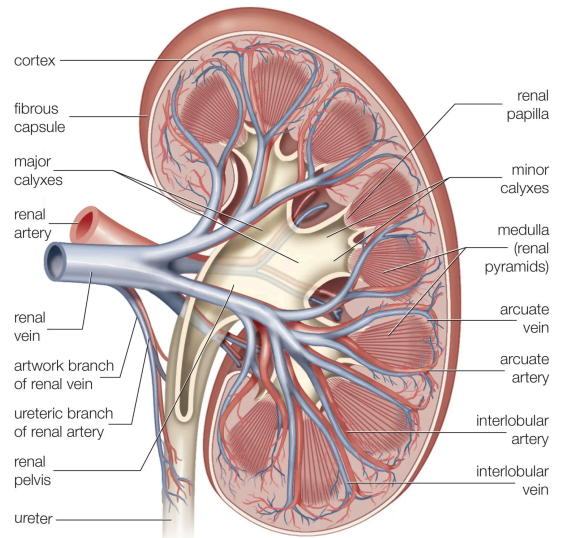
The Digestive System



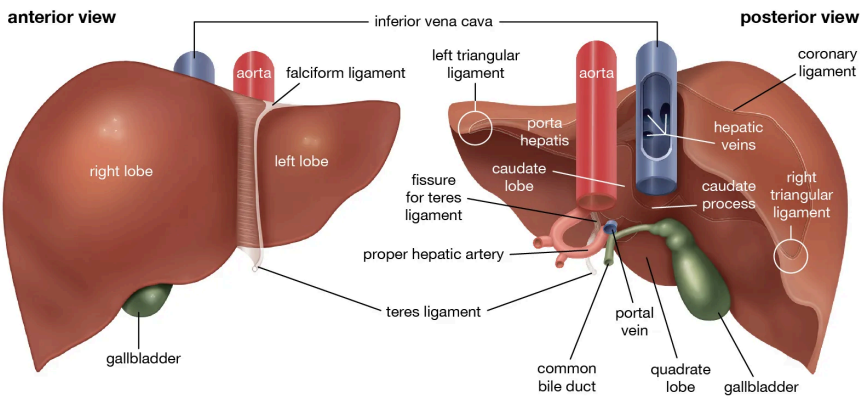
The Endocrine System



The Kidneys

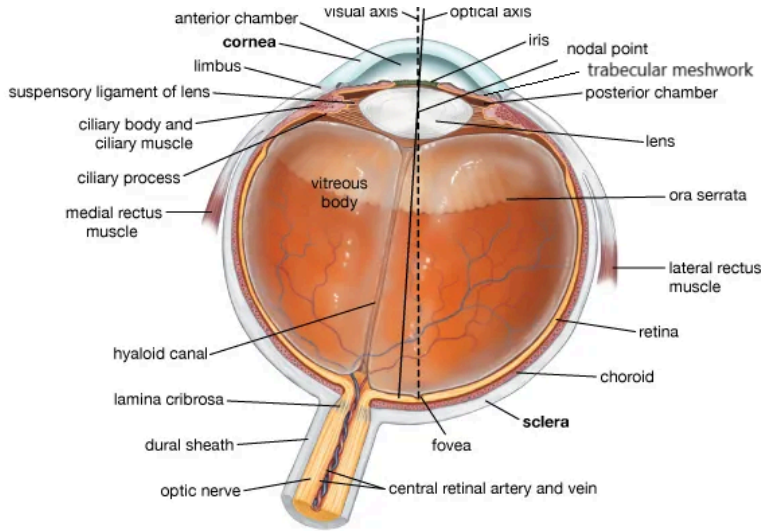


The Liver

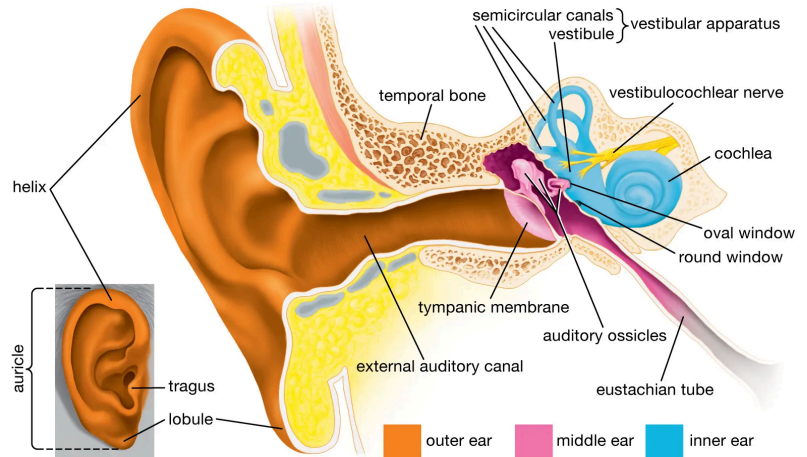


The Sensory Organs

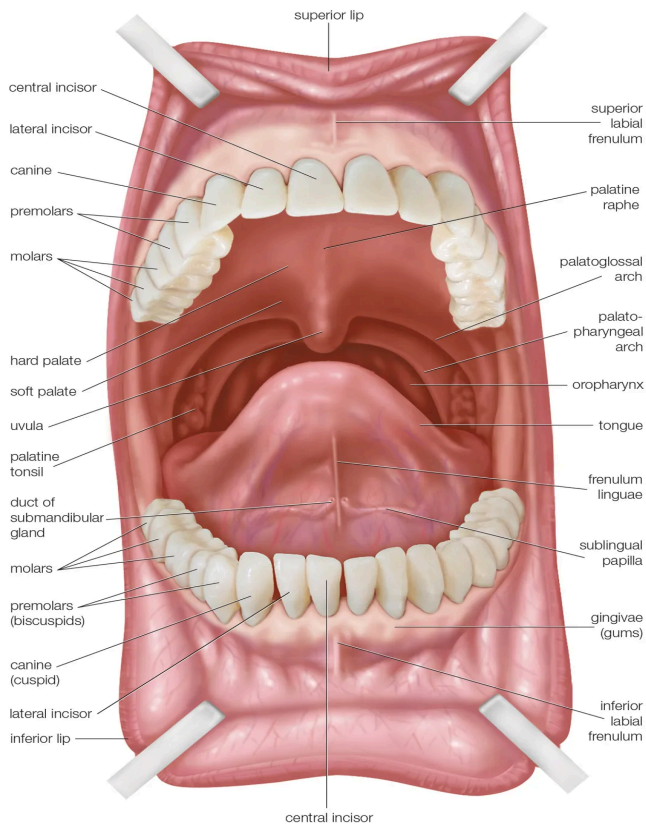
The Eye



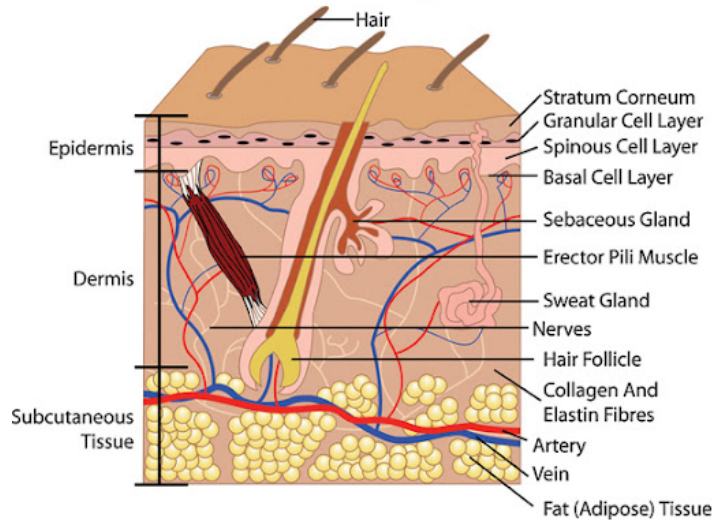
The Ear



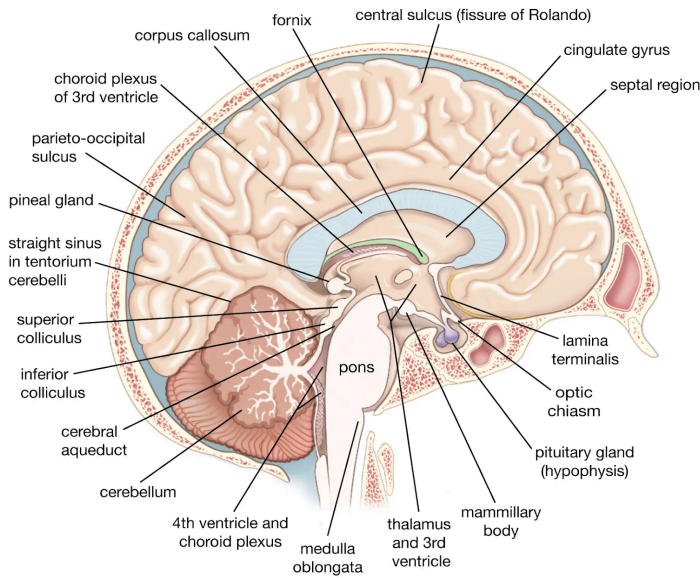
The Mouth and Teeth



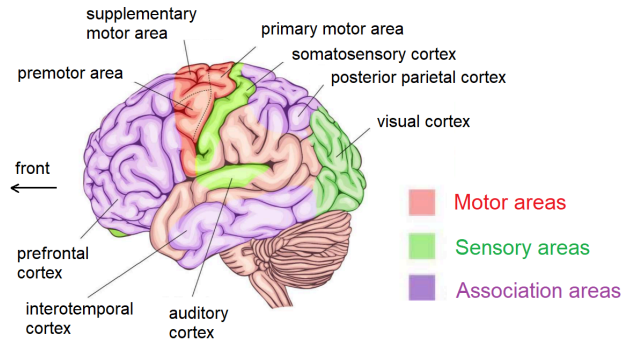
The Skin



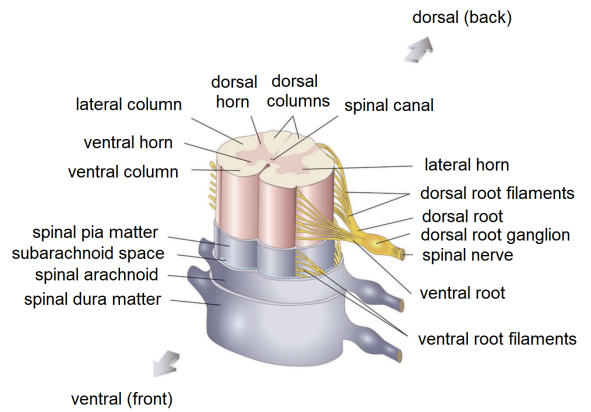
The Brain (By Structure)



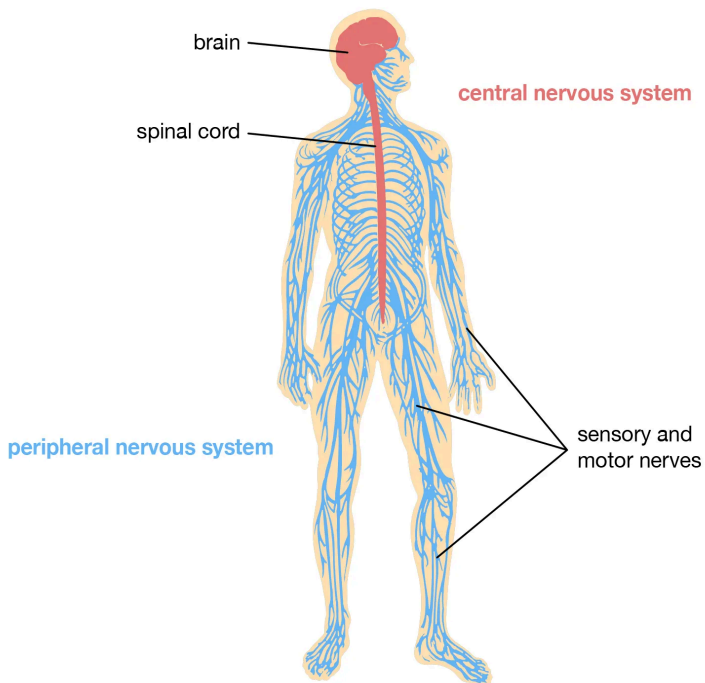
The Brain (By Function)



The Spinal Cord

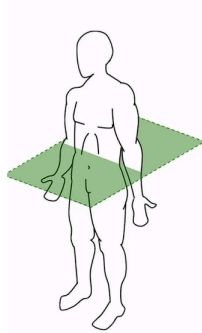


The Nervous System (CNS and PNS)



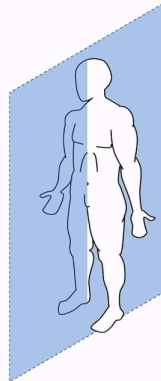
20.2.2. Terminology of Human Skeletal Anatomy

For labelled diagrams of bones in the skeleton, see Section 20.2.1.



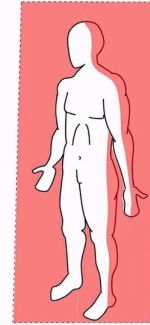
Transverse plane

superior: above
inferior: below



Sagittal plane

medial: closer to centre
lateral: further from centre



Coronal plane

anterior / ventral: front
posterior / dorsal: back

Axial skeleton: skull, rib cage and vertebral column.

The trunk includes the central parts of the body excluding the limbs. 'Proximal' refers to being connected closer to the trunk. 'Distal' refers to being connected further away from the trunk.

The **skull** contains 8 cranial bones fused together by sutures. The spinal cord exits through the foramen magnum. The paired **facial bones** are the nasals, lacrimals, palatines, inferior nasal concha, maxilla, zygomatics (cheek bones), while the mandible (houses the teeth) and vomer are unpaired. In each quadrant of the mouth, there are 2 incisors, 1 canine, 2 premolars and 3 molars (2:1:2:3 dental formula); the most posterior molars can cause crowding (the 'wisdom teeth').

The **vertebral column** protects the spinal cord and consists of cervical (C1-C7), thoracic (Th1-Th12), lumbar (L1-L5) and sacral vertebrae (5 fused vertebrae in the sacrum and 3-5 fused vertebrae in the coccyx/tailbone). Cervical discs C1 (atlas) and C2 (axis) permit movement of the head.

The paired **ribs** contain 7 'true ribs' (connected to the sternum), 2 'false ribs' (connected via cartilage) and 2 'floating ribs' (not connected to the sternum). The sternum is composed of the manubrium (most superior), body and xiphoid process.

Appendicular skeleton: limbs and pelvis. Fully symmetric about the sagittal plane.

The **pectoral girdle** (clavicle and scapula, articulated by the acromion process) connects the upper limbs (articulating with the humerus) to the axial skeleton.

The **forearms** contain two bones, the radius (distal) and the ulna (proximal). The hands, from proximal to distal, contain the carpals, metacarpals, phalanges (proximal, middle and distal phalanges). There are eight carpals (wrist bones).

The **pelvis** consists of three fused bones, the ilium, ischium and pubis. The pelvis articulates with the femur by the acetabulum (hip socket). The leg bones are the fibula and tibia.

20.2.3. Hormones

Hormones are signallers of the mammalian endocrine system.

Class	Hormone	Tissues secreting	Effects
amino acid derivative	adrenaline (epinephrine)	adrenal gland (near the kidneys)	<ul style="list-style-type: none"> Vasoconstriction, causing increase in blood pressure Increases heart rate and contraction force
	melatonin	pineal gland (near the brain centre)	<ul style="list-style-type: none"> Regulates the circadian rhythm (sleep-wake cycle)
	noradrenaline (norepinephrine)	adrenal gland (near the kidneys)	<ul style="list-style-type: none"> Vasoconstriction, causing increase in blood pressure Increases heart contraction force
	triiodothyronine (thyroid hormone)	thyroid gland (near the throat)	<ul style="list-style-type: none"> Increases metabolism
	dopamine	substantia nigra (in the midbrain)	<ul style="list-style-type: none"> Regulates cellular cAMP levels
eicosanoid	prostaglandins	from all cells with nuclei	<ul style="list-style-type: none"> Vasodilation, causing decrease in blood pressure
	leukotrienes	from white blood cells	<ul style="list-style-type: none"> Increases vascular permeability
	prostacyclins	from endothelial cells	<ul style="list-style-type: none"> Vasodilation Inhibits platelet production
	thromboxane	from platelets	<ul style="list-style-type: none"> Vasoconstriction Inhibits platelet aggregation
peptide	antidiuretic hormone (ADH, vasopressin)	pituitary gland (near the hypothalamus)	<ul style="list-style-type: none"> Water retention in kidneys Moderate vasoconstriction
	follicle-stimulating hormone (FSH)	pituitary gland (near the hypothalamus)	<ul style="list-style-type: none"> Promotes maturation in the ovary (females) Promotes production of sperm cells (males)
	glucagon	pancreas	<ul style="list-style-type: none"> Glycogenolysis, increasing blood glucose level
	human growth hormone (hGH)	pituitary gland (near the hypothalamus)	<ul style="list-style-type: none"> Cell growth and division
	insulin	pancreas	<ul style="list-style-type: none"> Glycogenesis and glycolysis, decreasing blood glucose level Synthesis of triglycerides from lipids in fat cells
	luteinising hormone (LH)	pituitary gland (near the hypothalamus)	<ul style="list-style-type: none"> Ovulation (females) Production of testosterone (males)
	oxytocin	pituitary gland (near the hypothalamus)	<ul style="list-style-type: none"> Lactation (release of breast milk) Cervix contraction (orgasm)
androgen steroid	testosterone	testes and ovaries	<ul style="list-style-type: none"> Libido and maturation of sex organs (males) Muscle mass gain
	dihydrotestosterone (DHT)	testes, ovaries and liver	<ul style="list-style-type: none"> Promotes cell growth and division in the penis Can miniaturise hair cells (usually a side effect as a metabolite of testosterone)
oestrogen steroid	estradiol	testes and ovaries	<ul style="list-style-type: none"> Maturation and release of an egg Promotes growth in the female sex organs
glucocorticoid steroid	cortisol	adrenal gland (near the kidneys)	<ul style="list-style-type: none"> Inhibits glucose uptake in muscle and fat cells
progestogen steroid	progesterone	ovaries, adrenal gland, placenta (when pregnant)	<ul style="list-style-type: none"> Prepares the uterus lining for a fertilised egg
secosteroid (vitamin D ₃)	calcitriol	skin, kidney tubule	<ul style="list-style-type: none"> Increase absorption of calcium and phosphate

20.2.4. Neurotransmitters

Neurotransmitters can induce or inhibit action potentials in neurons.

Class	Neurotransmitter	Effects
catecholamine	dopamine	<ul style="list-style-type: none"> Motivation, reward, pleasure, mood regulation, motor control
	epinephrine (adrenaline)	<ul style="list-style-type: none"> Increases heart rate and alertness, redirects blood flow to muscles
	norepinephrine (noradrenaline)	<ul style="list-style-type: none"> Constricts blood vessels, raises blood pressure With epinephrine, initiates the 'fight or flight' response
indolamine	serotonin (5-HT: 5-hydroxytryptamine)	<ul style="list-style-type: none"> Mood regulation, sleep, appetite
	melatonin	<ul style="list-style-type: none"> Sleep-wake cycle, circadian rhythm
	histamine	<ul style="list-style-type: none"> Immune response, alertness, wakefulness
trace amine	phenethylamine and <i>N</i> -methylphenethylamine	<ul style="list-style-type: none"> Mood regulation
	tyramine	<ul style="list-style-type: none"> Releases norepinephrine
	3-iodothyronamine	<ul style="list-style-type: none"> Thyroid hormone metabolism, thermoregulation
	octopamine	<ul style="list-style-type: none"> Arousal, movement
	tryptamine	<ul style="list-style-type: none"> Precursor to serotonin
amino acid	glutamate	<ul style="list-style-type: none"> Main excitatory neurotransmitter, all synaptic transmission
	aspartate	<ul style="list-style-type: none"> Excitatory neurotransmitter
	D-serine	<ul style="list-style-type: none"> NMDA glutamate receptor coagonist, synaptic plasticity, learning
	γ -aminobutyric acid (GABA)	<ul style="list-style-type: none"> Main inhibitory neurotransmitter
	glycine	<ul style="list-style-type: none"> Inhibitory neurotransmitter, motor/sensory functions (in spinal cord)
gastro-transmitter	nitric oxide (NO)	<ul style="list-style-type: none"> Cell signalling, regulation, vasodilation, anti-oxidant (in the GI tract)
	carbon monoxide (CO)	
	hydrogen sulfide (H ₂ S)	
neuropeptide	oxytocin	<ul style="list-style-type: none"> Love, emotional bonding
	somatostatin	<ul style="list-style-type: none"> Inhibits release of various hormones e.g. GH, TSH, insulin, glucagon
	substance P	<ul style="list-style-type: none"> Pain transmitter, neuroinflammation
	cocaine and amphetamine regulated transcript (CART)	<ul style="list-style-type: none"> Energy homeostasis, controls appetite, found in the reward system Mimics cocaine and amphetamine alone, but inhibits their effects when these substances are present Cocaine is an epigenetic promoter of CART gene transcription
	opioid peptides e.g. β -endorphin	<ul style="list-style-type: none"> Neuromodulators in the pain/reward system, Binds to opioid receptors
purine	adenosine triphosphate (ATP)	<ul style="list-style-type: none"> Pain signalling, synaptic plasticity, and neuroprotection
	adenosine	<ul style="list-style-type: none"> Reduces neural activity, promotes sleep
others	acetylcholine (ACh)	<ul style="list-style-type: none"> Released at neuromuscular junctions to effect motion In the CNS, promotes cognition, memory and learning
	anandamide	<ul style="list-style-type: none"> Binds to cannabinoid receptors to affect mood, pain perception, appetite, and neuroprotection

20.1.5. Blood Types

The ABO system: based on the presence of two common antigens, A and B.

Group	Antigens on erythrocytes	Antibodies flowing in the plasma	Can donate to:	Can receive from:
A	A	anti-B	A, AB	O, A
B	B	anti-A	B, AB	O, B
AB	none	anti-A and anti-B	AB	O, A, B, AB
O	A and B	none	O, A, B, AB	O

Blood can be donated only if the recipient does **not** have antibodies for the incoming (donor's) antigens, otherwise the antibodies will attack the corresponding blood cells. The genes for A and B antigens are codominant (so type O is recessive).

The Rh system: based on the presence of rhesus (Rh) antigens, primarily RhD.

If RhD antigens are present, then the blood type is positive (+).

If RhD antigens are absent, then the blood type is negative (-).

Recipients with Rh- blood can **only** receive blood from Rh- donors.

The gene for RhD+ is dominant (so Rh- is recessive).

Rare Blood Types: the ABO and Rh(+/-) make up 8 different types based on antigen composition, but some people may be missing Rh antigens other than RhD, which require special attention. In the most extreme case, a person's blood may contain no Rh antigens at all (Rh-null). Compatible blood donors are much more difficult to find due to their rarity.

20.3. Pharmacology

20.3.1. Some Important Receptors and Signalling Molecules

Toll-Like Receptors (TLRs)

Found on the surface of macrophages and dendritic cells.

NF- κ B (Nuclear Factor Kappa-light-chain-enhancer of Activated B Cells)

G-protein Coupled Receptors (GPCRs)

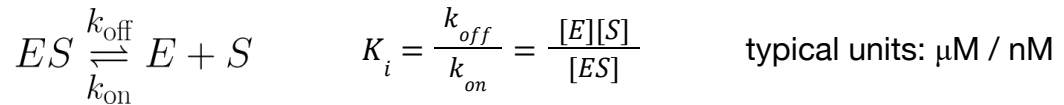
Adenylyl Cyclase, ATP and cAMP

Protein Kinases

PAMPs and DAMPs

20.3.2. Neurotransmitter Receptors

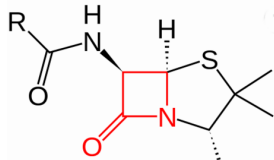
The binding affinity K_i of a substrate/ligand/drug S with respect to an enzyme/receptor E is the equilibrium constant for



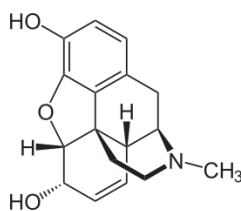
K_i is identical to the Michaelis-Menten constant (Section 17.4.4) for the system assuming no further reaction ($k_{cat} = 0$). When binding is stronger, K_i is smaller.

- Adrenergic receptors (α_{1A} , α_{1b} , α_{1c} , α_{1d} , α_{2a} , α_{2b} , α_{2c} , α_{2d} , β_1 , β_2 , β_3): targeted by catecholamines and beta-blockers.
- Muscarinic acetylcholine receptors (mAChRs) (M1, M2, M3, M4, M5).
- Dopaminergic receptors (D_1 , D_2 , D_3 , D_4 , D_5).
- GABAergic receptors ($GABA_A$, $GABA_{B1a}$, $GABA_{B1\delta}$, $GABA_{B2}$, $GABA_C$).
- Glutamatergic receptors (NMDA, AMPA, Kainate, $mGluR_1$, $mGluR_2$, $mGluR_3$, $mGluR_4$, $mGluR_5$, $mGluR_6$, $mGluR_7$)
- Glycine receptors: mediates inhibition in the spinal cord and brainstem.
- Histaminergic receptors (H_1 , H_2 , H_3).
- Opioidergic receptors (μ , δ_1 , δ_2 , κ).
- Serotonin receptors ($5-HT_{1A}$, $5-HT_{1B}$, $5-HT_{1D}$, $5-HT_{1E}$, $5-HT_{1F}$, $5-HT_{2A}$, $5-HT_{2B}$, $5-HT_{2C}$, $5-HT_3$, $5-HT_4$, $5-HT_5$, $5-HT_6$, $5-HT_7$)

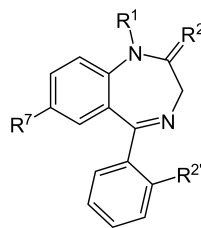
20.3.1. Some Common Drug Classes

**Beta-Lactams**

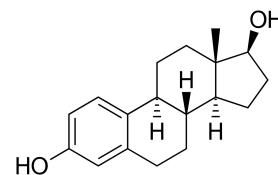
(Antibiotics:
penicillin, ampicillin...)

**Opioids**

(Potent analgesics:
oxycodone, morphine,
cocaine, heroin, fentanyl...)

**Benzodiazepines**

(Tranquilisers:
diazepam, oxazepam
alprazolam...)

**Steroids**

(Synthetic hormones:
cholesterol, estradiol,
cortisol, testosterone...)

Beta-lactam antibiotics bind to PBPs (penicillin binding proteins) and inhibit their usual enzymatic activity of peptidoglycan synthesis for building cell walls. The carbonyl group in the lactam ring undergoes nucleophilic attack by the hydroxyl group of the active site serine residue, forming a covalent bond. Antibiotic resistance can occur naturally when mutations produce beta-lactamase enzymes, which cleave the amide bond in e.g. penicillin, completely breaking its ring structure.

Opioids are agonists to opioid receptors, found on the surface of nerve cells. Inhibition of the release of certain neurotransmitters, such as 'substance P' (an 11-member neuropeptide pain signaller), occurs due to activation during binding to μ -opioid receptors. The 'morphine rule' is a rule of thumb for the pharmacophores (ligand motifs) to trigger this effect: (1) a benzene ring (2) attached to a 4° carbon connected by (3) an ethyl linker to (4) a tertiary amine. An exception is fentanyl (no 4° carbon) which still fits into the receptor. Opioids can produce intense psychoactive effects including euphoria and are addictive with high risk of dependency/abuse.

Benzodiazepines bind to GABA-A receptors in neural CNS synapses. This increases the activity of adjacent GABA receptors. The frequency of Cl⁻ ion channel opening increases while bound, increasing the hyperpolarisation potential of the cell and decreasing neuronal excitability. Some drugs also act directly on the Ca²⁺ voltage-gated ion channels. They are used to treat anxiety, insomnia and seizures by promoting a relaxed state of mind.

Steroids bind to steroid hormone receptors in various cell cytoplasm. A conformational change permits translocation to the nucleus where it binds to hormone response elements of DNA. The steroid then acts as a transcription factor for genes relating to metabolism. Steroids may be corticosteroids (anti-inflammatory) or anabolic (promoting muscle growth).

20.3.2. Naming and Regulation of Illicit Drugs

Drugs can be named using:

- Chemical name: the unique systematic IUPAC name of the drug, often long (and can induce chemophobia in the general public). e.g. 2,4-diamino-6-piperidinopyrimidine 3-oxide.
- Generic name: a trivial but unique name assigned to drugs, used as a practical substitute for the chemical name. e.g. minoxidil.
- Brand name: a trademarked name for use when sold by a pharmaceutical company, used for marketing e.g. *Regaine*. The same active ingredient can have different brand names, since it can be sold by different companies, and a brand name drug may also include multiple active ingredients (a combination drug). Often the most recognisable.
- Street name: illicit drugs may be given informal names by users to avoid disclosing their possession to law enforcement. e.g. 'Special K' for ketamine.

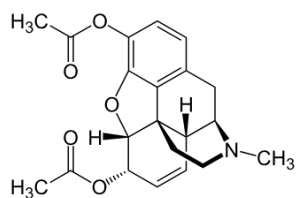
Drugs are often regulated in order to limit their availability to the general public. The methods of regulation vary by country and their legality is roughly (not always) determined by their potential to cause harm and induce dependency.

- In the USA, the DEA (Drug Enforcement Agency) sets five schedules, including Schedule I: no medical use (heroin, LSD, ecstasy/MDMA, marijuana/weed), Schedule II: limited medical use (cocaine, oxycodone, fentanyl, stimulants), down to Schedule V: negligible risk (cough medicines).
- In the UK, the Misuse of Drugs Act (1979) sets three classes. Class A (heroin, cocaine, ecstasy), Class B (cannabis/weed, amphetamine, ketamine) and Class C (steroids, benzodiazepines).

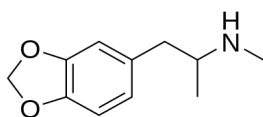
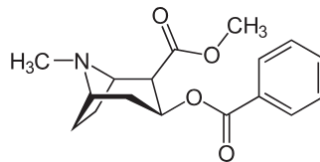
Different countries may restrict different substances, and there can be debate about the class status of certain substances (e.g. cannabis, alcohol, caffeine). Since studies on the long-term effects of drugs are often tentative and inconclusive, their interpretation and subsequent legislation is often subject to biased politics. For example, cannabis is widely considered to be minimally harmful despite being classed severely, while alcohol (which has various known health implications) is typically not classed as a controlled drug at all. Propaganda campaigns can seek to prohibit some drugs by creating and/or targeting stereotypes about the socioeconomic or racial groups that use them, a form of scientific racism (pseudoscience).

New psychoactive substances (NPS) are often derived from common drug motifs, with slight functional group or steric modifications (e.g. DMT → 5-MeO-DMT, 4-HO-MET; MDMA → synthetic cathinones), or to sidestep prohibitive laws by passing as 'research chemicals'. However, many countries have laws with "catch-all" clauses, outlawing drug-like substances with similar structure to known drugs, regardless of whether it is explicitly listed.

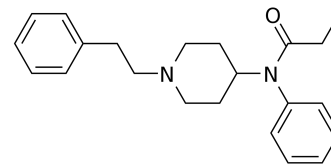
20.3.3. Illicit Recreational Drugs



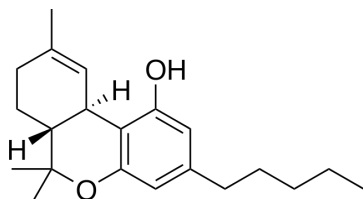
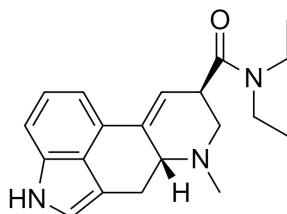
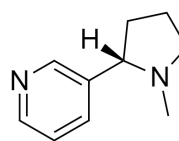
Heroin

3,4-methylenedioxy-
methamphetamine
(MDMA)

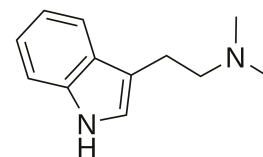
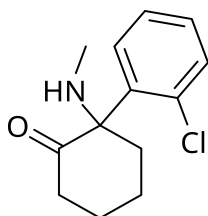
Cocaine



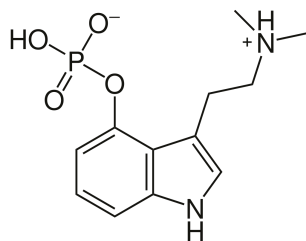
Fentanyl

Tetrahydrocannabinol
(THC)Lysergic acid diethylamide
(LSD)

Nicotine

Dimethyltryptamine
(DMT)

Ketamine



Psilocybin

20.3.3. Drug Administration, Pharmacokinetics and Pharmacodynamics

The 'Six Rights' of Drug Administration: principles to ensure safe usage of medical drugs.

1. **Right patient.**
2. **Right medication.**
3. **Right dose.**
4. **Right route of administration**, which may be:
 - enteral (into mouth/stomach e.g. sublingual (under tongue), buccal (against cheek))
 - topical (on the skin)
 - parenteral (through skin e.g. intravenous, intravenous, intradermal, subcutaneous).
5. **Right time of delivery.** May be at regular intervals or with meals.
6. **Right documentation.** Record the medication time, dosage, route and any observations.

Patients also have the 'Right to Refuse' any medication for any reason (best noted as 'declined at this time').

Pharmacokinetics: how the body impacts the drug's ability to deliver its effect.

ADME: absorption, distribution, metabolism, excretion. The kinetics of drug delivery depend on the diffusion into the bloodstream (bioavailability), distribution through the bloodstream (affinity for off-target receptors), resistance to degradation (in e.g. first pass through the liver) and ease of excretion once the drug has delivered its effect.

Lipinski's Rule of Five (RO5): a rule of thumb for the properties of most orally available drugs:

"No more than 5 H-bond donors; No more than 10 H-bond acceptors; $M_w < 500$ Da; $\log P_{oct} < 5$."

Pharmacodynamics: how the drug impacts the body once delivered.

Drugs interact with parts of proteins (active sites on receptors or enzymes). These sites typically accept a ligand in order to become activated and propagate a signal in some way. Drugs can be agonists (mimicking the native ligand) or antagonists (binds to and inhibits the receptor). Binding may be competitive, uncompetitive or noncompetitive (see Section 17.1.3).

The binding affinity is higher when the drug fits well into the active site and makes more electrostatic interactions. Drugs can be tailored to specific receptors if their structure is known by modelling their interactions (molecular docking) or testing variations (structural-activity relationship studies (SARs)). The mechanism of action concerns the way in which the receptor-ligand complex reacts, potentially involving a chemical reaction in which the drug is metabolised to other substances.

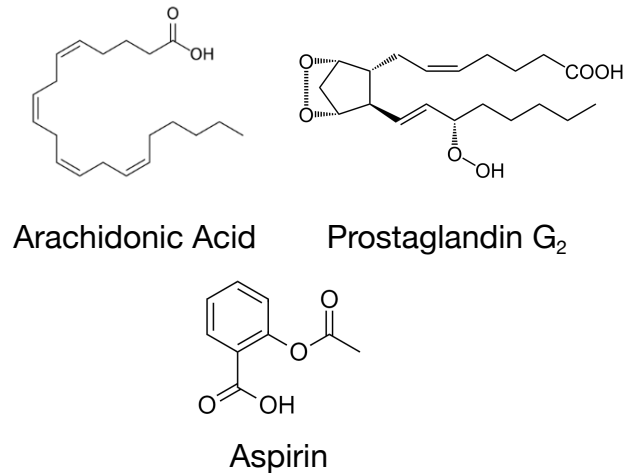
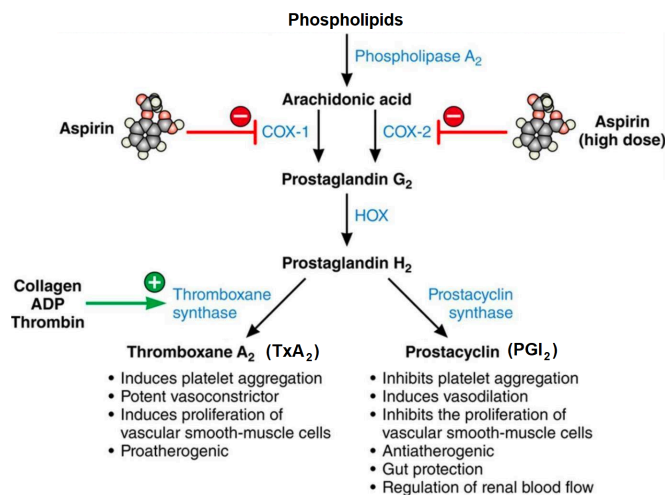
Measures of a drug's pharmacodynamic effects include:

- Drug efficacy: the maximum effect of a drug as the dose approaches infinity (often qualitative). Determined by the drug's ability to act as an agonist or antagonist.
- Drug potency (median effective dose, ED_{50}): concentration for it to produce 50% of the maximum effect. Determined by the drug's affinity for the target receptor.
- Drug lethality (median lethal dose, LD_{50}): concentration that kills 50% of a test population (animals in preclinical trials) exposed to it. Determined by the types of receptors targeted.
- Therapeutic index = LD_{50} / ED_{50} .

20.3.4. Pharmacodynamics of Common Drugs

NSAIDs (Non-Steroidal Anti-Inflammatory Drugs): aspirin, acetaminophen, ibuprofen, naproxen, celecoxib

NSAIDs are antipyretic (reduces fever), analgesic (reduces pain) and anti-inflammatory. They operate by inhibiting the cyclooxygenase (COX) enzymes, preventing synthesis of inflammatory prostaglandins.



Aspirin binds irreversibly, by acetylation of homologous Ser-529 in COX-1 and Ser-516 in COX-2, nullifying the nucleophilicity of the active site, while ibuprofen and naproxen bind reversibly. Celecoxib inhibits COX-2 selectively. Acetylated COX-2 retains some functionality and generates aspirin-triggered lipoxins (ATLs) such as 15-epi-lipoxin A₄ (an epimer of a natural lipoxin), a potent anti-inflammatory agent.

Antihistamines (Allergy-Alleviating Drugs)

Histamine is released by mast cells in tissues and by basophils in the blood. Its binding to the H₁ receptor triggers the inflammatory cascade and then an innate immune response. Antihistamines prevent these causes of allergies from occurring.

1st generation antihistamines cross the blood-brain barrier and have psychoactive side effects (sedation and anticholinergic effects). 2nd generation antihistamines do not cause these effects as they activate protein pumps which remove them from the brain space.

DMARDs (Disease-Modifying Antirheumatic Drugs): methotrexate, tofacitinib citrate, infliximab

DMARDs treat Rheumatoid arthritis (RA). They are classified as either small molecule (activate / deactivate proteins) or biologic (antibodies to target the proteins) DMARDs. Biologic DMARDs cause less side effects than small molecule DMARDs due to their higher specificity but are more complex to produce and require injection. They are both immunosuppressive.

Methotrexate is a prodrug, being modified *in vivo* by mimicking folic acid as a substrate to the FPGS enzyme, becoming activated to MTXPG. This inhibits the ATIC enzyme, leading to accumulation of adenosine, stimulating adenosine 2A receptors, providing anti-inflammatory effects, by reducing cytokine production and preventing activation of immune cells.

Glucocorticoids Immunosuppressants (Steroidal Drugs): hydrocortisone, dexamethasone

The glucocorticoid nuclear receptor NR3C1 is activated by glucocorticoids, and the complex is translocated into the nucleus through a nuclear pore. This complex has epigenetic activity. Gene expression of COX enzymes is decreased, reducing inflammation. Expression of transcription factor NF- κ B is also decreased, reducing cytokine production and suppressing immune activity. A wide range of other signalling pathways are also affected.

Non-Glucocorticoid Immunosuppressants: cyclosporin, tacrolimus, rapamycin (cyclic oligopeptides)

- **Immunophilin binding drugs:** immunophilin typically isomerises proline and are the receptor for these drugs, found in the cytosol of T-cells. The complex then binds to calcineurin (or mTORC1 in the case of rapamycin), preventing it from acting as a transcription factor for interleukin 2 (IL-2), impeding activity, maturation and differentiation of T cells.
- **Cytostatic drugs:** these drugs inhibit dihydrofolate reductase, preventing thymidine synthesis (required for *de novo* DNA synthesis), preventing cell division in immune cells.
- **Antilymphocyte antibodies:** these are specific antibodies for CD52 receptors on mature B/T cells, triggering their immediate apoptosis, preventing their function.
- **Monoclonal antibodies:** binds even more specifically, to CD3 receptors, similarly triggering apoptosis of T cells.

Immunostimulants:

- **Colony stimulating factors:** enhance production and release from the bone marrow of white blood cells.
- **Interleukins:** recombinant forms of immune-stimulating chemokines.
- **Interferons:** binds to interferon receptors on plasma membranes of white blood cells, activating transcription factors for immune stimulating proteins such as cytokines and growth factors for natural killer cells, B cells and T cells.
- **Vaccines:** triggers a slow immune response to an unfamiliar pathogen, priming the immune system for future attack by formation of memory cells.

Bronchodilators: salbutamol, levalbuterol, tiotropium bromide

Used to treat chronic breathing disorders such as asthma, emphysema, bronchitis by relaxing smooth muscle cells to increase the radius of the lumen.

- **β_2 adrenoreceptor agonism:** non-selectively activated by adrenaline/noradrenaline. The β_2 receptor is specifically activated via the $G_{\alpha s}$ pathway, in which a heterotrimer dissociates into $G_{\alpha s}$ and a $G\beta\gamma$ heterodimer. $G_{\alpha s}$ binds to adenylate cyclase and increases its conversion of ATP into cAMP, increasing binding to protein kinase A, activating myosin phosphatase, which phosphorylates the myosin light chain, preventing it binding to actin, reducing contractility. $G\beta\gamma$ also plays a role by activating K^+ channels to hyperpolarise (efflux K^+) the cells, reducing mobilisation of Ca^{2+} , reducing calmodulin activation, further inhibiting muscle cell contraction.
- **Muscarinic receptor antagonism:** non-selectively activated by acetylcholine. The M3 receptor is activated via the $G_{\alpha q}$ pathway, in which a heterotrimer dissociates into $G_{\alpha q}$ and a $G\beta\gamma$ heterodimer. $G_{\alpha q}$ binds to phospholipase C, which hydrolyses PIP_2 into DAG and IP_3 . DAG activates protein kinase C (acts similar to the above protein kinase A). IP_3 binds to its receptor on the endoplasmic reticulum, liberating Ca^{2+} from cell stores, increasing contractility.

Antitussives: codeine, dextromethorphan, benzonatate (tessalon)

Used to block the coughing reflex. They only treat the symptoms (not the root cause).

- **μ opioid receptor agonism:** codeine is a prodrug, metabolised by enzymes UGT2B7 and CYP2D6 to form codeine 6-glucuronide and morphine respectively, which together signal the μ opioid receptor on neurons in the GI tract via the $G_{\alpha i}$ pathway. The resulting K^+ efflux due to $G\beta\gamma$ release reduces neurotransmission in the reflex arc of the medulla. The risks of addiction mean that codeine is only administered in extreme cases.
- **Voltage-gated sodium channel blocking:** benzonatate blocks VGSCs in the bronchi and alveoli reducing action potential frequency output from the afferent cough pathway via the vagal fibres. It also blocks VGSCs in the medulla, affecting processing of the cough reflex.

Decongestants: phenylephrine, oxymetazoline, tramazoline, ephedrine

Used to relieve nasal congestion by restricting blood flow to the mucosal membranes of the nose.

- **α_1 adrenergic receptor agonism:** activates the $G_{\alpha q}$ pathway, which increases contractility.

Cannabinoids: tetrahydrocannabinol (THC), cannabidiol (CBD)

From the *Cannabis* plant, tetrahydrocannabinolic acid (THCA) is extracted and decarboxylated to THC.

- Δ^9 -tetrahydrocannabinol is a partial agonist to cannabinoid receptor CB_1 (a G-protein receptor).

20.4. Diseases

20.4.1. Bacterial Infections

Food Poisoning: *E. Coli*

Certain strains of *E. Coli* are enterohemorrhagic, releasing shiga toxin (Stx).

Cholera: *Vibrio cholerae*

Typhoid Fever: *Salmonella typhi*

Anthrax: *Bacillus anthracis*

Lyme Disease: *Borrelia burgdorferi*

The Plague: *Yersinia pestis*

Tuberculosis: *Mycobacterium tuberculosis*

Legionnaire's Disease: *Legionella pneumophila*

Gonorrhoea: *Neisseria gonorrhoeae*

Syphilis: *Treponema pallidum*

Whooping Cough: *Bordetella pertussis*

MRSA: *Staphylococcus Aureus*

Rocky Mountain Spotted Fever: *Rickettsia rickettsii*

20.4.2. Viral Infections**The Common Cold:** rhinovirus**Influenza:** the flu**Herpes:** herpes simplex virus**Chickenpox and Shingles:** Varicella-Zoster virus**Mononucleosis:** Epstein-Barr virus**Hepatitis A:** hepatovirus A**Poliomyelitis:** poliovirus**Smallpox:** variola virus**Measles:** morbillivirus**Rabies:** lyssavirus**West Nile Virus:** flavivirus**HPV:** human papillomavirus**AIDS:** human immunodeficiency virus (HIV)**Ebola:** ebolavirus (EVD)**Zika Virus Disease:** flavivirus (ZVD)**SARS, MERS and COVID-19:** coronavirus

20.4.3. Protist Infections

Malaria: *Plasmodium falciparum*

The protist parasite *Plasmodium falciparum* is responsible for causing malaria, using a mosquito host as its vector. When the mosquito bites a human or other animal, it injects sporozoites, which transform and multiply in the liver to form merozoites, before migrating into red blood cells, destroying them in the process. Gametocytes (male and female forms of the parasite) can develop at this stage. If another mosquito bites, it draws up some blood containing the gametocytes as part of its 'blood meal', which reproduce sexually inside the mosquito, completing the life cycle of the parasite.

Dysentery: *Entamoeba histolytica*

Giardiasis: *Giardia lamblia*

Toxoplasmosis: *Toxoplasma gondii*

Primary Amoebic Meningoencephalitis: *Naegleria fowleri*

20.4.4. Fungal Infections

Onychomycosis (nail infections)

Ringworm:

Vaginal Candidiasis (Thrush):

Athlete's Foot:

Dandruff: *Malassezia*

20.4.5. Non-Communicable Diseases of the Eyes

Glaucoma: the second most common form of blindness, after cataracts. Glaucoma causes loss of peripheral vision. If the trabecular meshwork is blocked, aqueous humour can no longer drain out, causing an increase in intraocular pressure (IOP), which exerts a stress on the porous connective tissue filling the optic nerve head (lamina cribrosa), damaging nearby retinal ganglion nerve cells.

20.4.6. Non-Communicable Diseases of the Ear, Nose and Throat

Ménière's disease:

Tinnitus:

20.4.7. Non-Communicable Diseases of the Circulatory System**20.4.8. Non-Communicable Diseases of the Nervous System**

Guillain-Barré syndrome:

20.5. Biopsychology, Health, Fitness and Nutrition

20.5.1. Sex Determination

Sex: the purely biological classification based on the reproductive functions of the organism.

Binary Model of Sex: humans are ~15% sexually dimorphic by weight: the body morphology of the two sexes is fundamentally different. In **most** humans, the sex chromosomes present in the cells determine the sex of the human: only X in gametes and **XX** in somatic cells indicates **female** sex, while either X or Y in gametes and **XY** in somatic cells indicates **male** sex. At fertilisation between a male and a female, the male gamete (sperm) fertilises the female gamete (egg) to form a zygote with either XX or XY sex chromosomes, which determines the sex of the resulting baby.

The binary model is a simplified view of sex and neglects cases where the most common route to forming a viable foetus is not followed. In these cases, alterations to anatomy and/or hormone profile may occur without impacting the viability of the foetus. In normal prenatal sex differentiation, the male and female embryos are anatomically identical until week 7 of the pregnancy, when the presence or the absence of various genes influences gonad development, for example:

- The SOX9 gene (chromosome 17) forms the testes by producing Sertoli cells.
- The NR0B1 gene (chromosome X) codes for protein DAX1 which inhibits SOX9.
- The SRY gene (chromosome Y) codes for a protein which inhibits transcription of NR0B1.

Differences in Sex Development (DSD) / Variations in Sex Characteristics (VSC) / Intersex: any atypical combination of sex chromosomes, gametes and gonads.

- **Aneuploid karyotypes:** any variation in sex chromosome number in somatic (diploid) cells. Examples: 47,XXY (Klinefelter syndrome); 47,XYY (Jacob's syndrome); 47,XXX (trisomy X syndrome); 45,X (Turner's syndrome). These are usually not considered a deviation from binary sex.
- **Gonadal dysgenesis:** genotype is the binary opposite of the phenotype.
 - Swyer syndrome: 46,XY but develops female gametes and reproductive organs.
 - De la Chapelle syndrome: 46,XX but develops male gametes and reproductive organs.
- **Sex chromosomal mosaicism:** different cells around the body have opposite genotypes.
- **Congenital adrenal hyperplasia:** virilised (masculinised) hormone profile and ambiguous genitalia, caused by mutations in the 21-hydroxylase enzyme, leading to accumulation of cortisol precursors, overstimulating the adrenal glands and producing an excess of androgens.
- **Androgen insensitivity syndrome:** entirely feminised development in karyotypic males, caused by mutations in the androgen receptor, rendering androgens an ineffective hormone.
- **Persistent Mullerian duct syndrome:** partial or complete female gonads in karyotypic males.

Cultural Variations: some communities have their own unique experiences of sex.

- **Guevedoces people:** a small Dominican community with a common mutation in 5-alpha-reductase, rendering testosterone in the foetal stage ineffective. They are karyotypic males who appear female until puberty when they develop male gonads. The study of this population in the 1970s led to the development of the DHT blocker medication finasteride.
- **Hijra people:** a community in India/Pakistan/Bangladesh who are sometimes intersex, but also have unique experiences of gender (often being transgender or a 'third gender').

20.5.2. Gender Identity

Gender encompasses various socially-constructed concepts relating to psychology and sociology, including gender roles and gender presentation (culture-dependent expectations about how people with a perceived biological sex should behave in society). Gender identity is a person's innate sense of what aspects of gender feel the most natural, and is generated by the brain.

Gender Identity: a person's internal and individual experience of gender.

Gender identity has its basis in brain structure, which in turn is influenced strongly by hormone exposure during development. All humans have varying amounts of testosterone and oestrogen, and the receptor proteins for these hormones are controlled by numerous separate gene pathways. Estradiol produces female secondary sex characteristics but male brain anatomy, and is typically blocked from crossing the blood-brain barrier in females by alpha-fetoprotein.

It is known that the human brain assumes a 'female' phenotype from conception, and differentiates to the 'male' phenotype only if exposed to the gonadal hormones, which operate by epigenetic mechanisms (inhibition of methyltransferase enzymes, reducing suppression of masculinising genes). When this process occurs, the person's gender identity matches their sex (a cisgender person) and when it does not, the gender identity may differ from the sex (a transgender person).

Sexually dimorphic regions of the brain include the SDN-POA (sexually dimorphic nucleus of the preoptic area), BsTC (bed nucleus of stria terminalis) and VIP-expressing neurons in the SCN (vasoactive intestinal polypeptide in the suprachiasmatic nucleus), which are small densely packed regions near the hypothalamus. In transgender individuals, these regions typically show structures skewed towards those resembling their gender identity rather than their sex.

- **Cis man:** assigned male at birth, has a male gender identity.
- **Cis woman:** assigned female at birth, has a female gender identity.
- **Trans man:** assigned female at birth (AFAB), has a male gender identity.
- **Trans woman:** assigned male at birth (AMAB), has a female gender identity.
- **Non-binary / Genderqueer:** any different, fluctuating and/or indeterminate gender identity.

Transgender people may (if possible and desirable) undergo 'gender affirming surgery' (top and bottom surgery) in which the external appearance of the body is changed to match those associated with their gender identity, as well as hormone therapy to adjust the endocrine profile and bring about changes in the secondary sexual characteristics. Neither the sex nor the gender identity changes in this process, but the resulting congruence between gender presentation and gender identity allows for the resolution of gender dysphoria in transgender people. Since transgender identities are rooted in brain structure, the organ that generates the sense of self, it is more practical and customary to treat transgender individuals according to their gender identity rather than their sex, unless there is good reason not to do so (e.g. physical capabilities in sports, which are segregated by sex).

20.5.3. Sexuality

Sexuality: a natural desire to be sexually or romantically attracted to members of a particular gender.

Some of the sexually dimorphic regions of the brain also show differences in homosexual and heterosexual people, e.g. the BsTC and SCN, indicating that sexuality can also be rooted in biology, like gender identity. However, the SDN does not show such changes, indicative of the difference between sexuality and gender identity. Sexuality is known to be influenced predominantly by genetic (deterministic) factors, but also by epigenetic (environmental) factors.

Sexualities can be classified into:

- Heterosexual (straight): a man or woman attracted to another of the opposite gender.
- Homosexual (gay / lesbian): a man or woman attracted to another of the same gender.
- Bisexual: being sexually attracted to both men and women, and potentially other genders.
- Asexual: not having strong sexual attractions towards anyone.
- Pansexual: being sexually attracted to all genders (gender is not a factor in determining attraction).
- Queer: usually describes any other sexuality that fluctuates or is not easily categorised.

Besides sexual attraction, individuals may also be independently 'romantically attracted' (can develop strong emotional bonds but may not have sexual desires) to people of certain gender(s). There are many other terms occasionally used to describe these groups, but most can be considered combinations (e.g. aro-ace = asexual + aromantic) or some point on a spectrum between those of the above.

Many aspects of gender identity and sexuality can also be considered a spectrum rather than discrete or binary classifications, owing to the complexity and potential for variation of the neurochemical profile responsible for creating these traits. This is an active area of research, and many of the sociocultural aspects fall outside the domain of 'hard' science.

LGBTQ+ Community: lesbian, gay, bisexual, transgender, queer, ...

Due to the historically dominant ideologies of heteronormativity and cisnormativity, LGBTQ+ individuals may face discrimination (homophobia, transphobia), and form a community to improve visibility and promote understanding. The LGBTQ+ acronym is sometimes extended to include other named groups (I: intersex, A: asexual, P: pansexual...).



Rainbow: Lesbian, Gay, Bisexual
Arrows: Transgender, ethnic minorities
Circle: Intersex



Bisexual
The most common
type of LGBT



Transgender

20.5.4. Neurodiversity

Neurodiversity refers to the range of brain functions and behavioural traits in a population.

Neurodivergence refers to deviations from the most common ('neurotypical') traits in the population, and includes the autism spectrum, ADHD, dyslexia, dyscalculia and dyspraxia.

Autistic Spectrum Disorder (ASD)

Autism is characterised by some degree of decreased social awareness and increased adherence to repetitive behaviour (DSM-5), with specifics varying by age, culture, gender, and co-occurrence of other intersectional mental conditions. The variations in brain structure associated with autism are subtle, primarily concerning neural connectivity, and cannot be reliably detected even in brain scans.

Autism may be 'low support needs' or 'high support needs', reflecting the spectrum of assistance required to comfortably navigate day-to-day life. Autistic individuals may learn to use behavioural management ('masking') to try suppressing expression of some autistic traits if they feel the social environment is unsupportive or hostile to their expression, especially in school children. This may contribute to developing social anxiety.

Issues with Reliable Diagnostics

Diagnostic data and guidelines for a variety of psychiatric, medical and wellness issues have historically been biased towards studies on White males, leading to a failure to account for the variation in the symptoms, risk factors and mode of expression in other populations. Disorders such as ASD are often misdiagnosed in girls and Western ethnic minorities.

20.5.4. Bioenergetics of Macronutrients for a Healthy Diet

- Food energy is measured using bomb calorimetry to determine the total enthalpy (heat) of combustion, and is displayed on food labels.
- Metabolisable (available) energy = Energy in food – Energy in excreted substances. The digestibility efficiency is usually very high (~97%).
- The brain consumes about 20% of the total energy intake.
- Basal metabolic rate (BMR): energy expenditure rate when at rest.
 Men: $BMR [kcal/day] \approx 10W [kg] + 6.25H [cm] - 5A [yr] + 5$
 Women: $BMR [kcal/day] \approx 10W [kg] + 6.25H [cm] - 5A [yr] - 161$
 (*W*: weight, *H*: height, *A*: age) (Harris-Benedict equations, rev. by Mifflin *et al*, 1990)
 Individuals with ‘fast’ or ‘slow’ metabolisms have larger or smaller BMR respectively, with deviations up to ±15% from the above average value.
- Recommended daily energy intakes, accounting for background thermogenic activity, are:
 Men: 2500 kcal (10.46 MJ); Women: 2000 kcal (8.34 MJ)

	Reference daily intake (adult RDI)	Energy content	Specific dynamic action (SDA, thermic effect, energy required for metabolism)
Protein	50 g	4 kcal/g	20-30% (net: 2.8-3.2 kcal/g)
Carbohydrates	260 g of which sugar: 90 g	4 kcal/g	5-10% (net: 3.6-3.8 kcal/g)
Fats	70 g of which saturated: 20 g	9 kcal/g	0-5% (net: 8.5-9.0 kcal/g)

- Net energy balance = Food energy × (1 – SDA) – BMR – Calories lost due to exercise
 An overall SDA of approximately 10% = 0.1 is a reasonable estimate (higher if protein-rich).
- If the net energy balance is negative, the body sources the missing energy from stored tissue: 1) liver glycogen, 2) blood glucose, 3) fat, 4) muscle protein (detrimental).
- If the net energy balance is positive, the body stores the excess energy by forming glycogen/fat/protein (anabolism).
- A calculator for recommended macronutrient intake is available [here](#).
- Body mass index: $BMI = Mass [kg] / (Height [m])^2$. Healthy range: $18 < BMI < 25$.
 BMI is an approximate indicator of body fat (not accounting for muscle mass) for adults.
- Somatotype model: three characteristic morphologies of the body (descriptive, not fixed for life)
 - Ectomorph: thinner body, lower muscle mass, faster metabolism
 - Mesomorph: average weight and build
 - Endomorph: broader body, slower metabolism

20.5.5. Vitamins and Minerals

Essential vitamins: these nutrients are not produced endogenously and must be obtained from food. The 'recommended daily intake' often represents a range and is quoted for healthy adults. Typically, children require less than these values, men require closer to the upper value, women require closer to the lower value except when pregnant or lactating.

Vitamin	Functions and Purposes	Food Sources	Symptoms of Deficiency	Recommended Daily Intake
Vitamin A (retinol, retinal, retinoic acid, β -carotene)	<ul style="list-style-type: none"> Vision: forms the rhodopsin pigment in rods on the retina Skin: promotes collagen growth Immune system: differentiation of B/T cells 	milk, cod liver oil, carrots, butter, green leaves, tomatoes, eggs	night blindness, xerophthalmia (hard cornea)	600 - 700 μ g
Vitamin B₁ (thiamine)	<ul style="list-style-type: none"> Metabolism of carbohydrates Digestion: helps produce HCl in the stomach Nerves: production of neurotransmitters Cardiovascularity: production of red blood cells 	nuts, green vegetables, yeast, egg yolk	beriberi	1.1 - 1.2 mg
Vitamin B₂ (riboflavin)	<ul style="list-style-type: none"> Metabolism of carbohydrates and proteins Cofactor for antioxidant enzymes Eye health: protects against cataract formation 	milk, meat, green vegetables, yeast	ariboflavinosis (tongue inflammation)	1.1 - 1.3 mg
Vitamin B₃ (niacin)	<ul style="list-style-type: none"> Cholesterol management Skin health: reduces inflammation, hyperpigmentation, rosacea DNA repair 	meat, fish, nuts, legumes; from tryptophan	pellagra (diarrhea, dermatitis, dementia)	13 - 16 mg
Vitamin B₅ (pantothenic acid)	<ul style="list-style-type: none"> Hormone production (testosterone, oestrogen, cortisol) 	meat, fish, eggs, whole grains	very uncommon	5 mg
Vitamin B₆ (pyridoxine)	<ul style="list-style-type: none"> Metabolism of proteins Neurotransmitter production (serotonin, dopamine, GABA) Antibody production Hormones: production of melatonin and cortisol; regulates oestrogen and testosterone 	meat, fish, nuts, legumes	various generic symptoms	1.2 - 1.4 mg
Vitamin B₇ (biotin)	<ul style="list-style-type: none"> Skin, hair and nail health Foetal development Blood sugar regulation 	egg yolks, liver, nuts, whole grains	hair loss, skin rash, brittle nails	30 - 100 μ g
Vitamin B₉ / B₁₁ (folate / folic acid / folacin)	<ul style="list-style-type: none"> DNA synthesis Foetal development in early stage of pregnancy Heart health: reduces homocysteine (heart disease) 	leafy green vegetables, citrus fruits, beans, fortified foods	fatigue, anaemia, birth defects	400 μ g
Vitamin B₁₂ (cobalamin)	<ul style="list-style-type: none"> Red blood cell production Nerves: produces myelin DNA synthesis 	meat, fish, eggs, dairy	fatigue, anaemia	2.4 μ g

Essential vitamins (continued)

Vitamin	Functions and Purposes	Sources	Deficiency	Recommended Daily Intake
Vitamin C (L-ascorbic acid)	<ul style="list-style-type: none"> • Antioxidant: protects against free radicals • Collagen synthesis for skin and bones • Immune system: produces white blood cells • Iron absorption • Wound healing: helps to form vascular tissue 	citrus fruits, strawberries, kiwi, papaya, bell peppers	scurvy (joint pains, bleeding gums)	75 - 90 mg
Vitamin D (calciferol)	<ul style="list-style-type: none"> • Calcium absorption • Cell growth and differentiation 	sunlight, fatty fish	osteoporosis, autoimmune disease	15 µg
Vitamin E (α-tocopherol)	<ul style="list-style-type: none"> • Antioxidant • Skin health: protects against UV damage 	nuts, seeds, vegetable oils	muscle weakness, vision problems	15 mg
Vitamin K (K ₁ : phyloquinone, K ₂ : menaquinone)	<ul style="list-style-type: none"> • Clotting factors in blood • Bone health: regulates calcium metabolism, bone mineralisation 	leafy greens, fermented foods	abnormal bleeding, bone fracture	90 - 120 µg
Choline	<ul style="list-style-type: none"> • Forms the neurotransmitter acetylcholine 	meat, broccoli	liver damage	425 - 550 mg
Ubiquinone (CoQ ₁₀)	<ul style="list-style-type: none"> • Energy production in mitochondria • Topically, reduces oxidative stress in skin 	fatty fish	fatigue	100 - 200 mg (not well established)

Essential Minerals: ions used for osmoregulation and metabolic processes (in metalloenzymes)

Essential in substantial quantities (> ~10 mg/day); Essential in trace quantities (< ~10 mg per day)

Mineral	Purposes	Recommended Daily Intake
chloride (Cl ⁻)	<ul style="list-style-type: none"> Production of stomach acid and pH regulation 	800 - 2000 mg
phosphorus (as phosphate, PO ₄ ³⁻)	<ul style="list-style-type: none"> As phosphate, forms hydroxyapatite for bone matrix including teeth Production of ATP for energy storage Backbone of DNA and RNA Phosphate buffer for pH regulation in the blood and intracellular fluid 	700 mg
sulfur (as sulfate, SO ₄ ²⁻)	<ul style="list-style-type: none"> Component of cysteine, methionine, biotin, thiamine, glutathione, taurine etc. As sulfate, forms sulfate ester bonds in glycosaminoglycans Sulfated steroids for cell signalling 	850 mg
calcium (Ca ²⁺)	<ul style="list-style-type: none"> Triggers release of neurotransmitters Required for muscle contraction and relaxation, and heartbeat Forms hydroxyapatite for bone matrix including teeth Cofactor for amylase 	700 mg
iron (Fe)	<ul style="list-style-type: none"> Cofactor for catalase, cytochrome and haemoglobin (in haem), nitrogenase, hydrogenase 	8.7 - 14.8 mg
magnesium (Mg ²⁺)	<ul style="list-style-type: none"> Cofactor for glucose 6-phosphatase, hexokinase, DNA polymerase In plants, used in chlorophyll as the initiator of photosynthesis 	270 - 300 mg
potassium (K ⁺)	<ul style="list-style-type: none"> Regulates blood pressure via osmotic pressure Nerve impulses: intracellular K⁺ exits the neuron while the action potential propagates 	2600 - 3400 mg
sodium (Na ⁺)	<ul style="list-style-type: none"> Regulates blood pressure via osmotic pressure Nerve impulses: extracellular Na⁺ enter the neuron while the action potential propagates 	1500 mg
zinc (Zn)	<ul style="list-style-type: none"> Development and function of immune cells Taste and smell receptors Cofactor for carbonic anhydrase, alcohol dehydrogenase, DNA/RNA polymerase, carboxypeptidase and zinc finger proteins 	8 - 11 mg
iodide (I ⁻)	<ul style="list-style-type: none"> Used by the thyroid gland to make hormones for growth and metabolism 	150 µg
chromium (Cr)	<ul style="list-style-type: none"> Regulation of blood sugar levels by enhancing insulin activity 	25 - 35 µg
cobalt (Co)	<ul style="list-style-type: none"> Cofactor for cobalamin (vitamin B₁₂), nitrile hydratase and carbon monoxide dehydrogenase 	5 - 8 µg
copper (Cu)	<ul style="list-style-type: none"> Cofactor for cytochrome oxidase and superoxide dismutase 	900 µg
manganese (Mn)	<ul style="list-style-type: none"> Cofactor for arginase 	1.8 - 2.3 µg
molybdenum (Mo)	<ul style="list-style-type: none"> Cofactor (in molybdopterin) for nitrate reductase, sulfite/xanthine oxidase and nitrogenase Prosthetic group (in molybdopterin) for formate dehydrogenase 	45 µg
nickel (Ni)	<ul style="list-style-type: none"> Cofactor in urease 	23 - 35 µg
selenium (Se)	<ul style="list-style-type: none"> Cofactor for glutathione peroxidase 	55 µg

The following minerals are essential in some organisms, but with little or no known use in humans:

Mineral	Potential Purposes
boron (B)	<ul style="list-style-type: none"> As inorganic borates, essential for plants and may be beneficial in maintaining healthy bones and joints.
silicon (Si)	<ul style="list-style-type: none"> May help to synthesise collagen for connective tissues e.g. bones, cartilage.
vanadium (V)	<ul style="list-style-type: none"> Cofactor for bromoperoxidase in marine algae Can mimic insulin signalling for glucose metabolism in some mammals, but less effective in humans
nitrate (NO ₃ ⁻)	<ul style="list-style-type: none"> In plants, used as an essential nitrogen source for growth and development. Not required for humans.
tungsten (W)	<ul style="list-style-type: none"> In some extremophiles, replaces molybdenum in molybdopterin cofactor. Toxic in many other organisms.
lanthanides (Ln ³⁺)	<ul style="list-style-type: none"> In some bacteria, La, Ce, Pr, Nd are used in some PQQ-dependent methanol dehydrogenase (MDH) enzymes

20.5.6. Metabolism of Proteins

Proteins: metabolised to amino acids

- **Essential amino acids:** of the 20 proteinogenic amino acids (Section 16.5.10), 9 are essential (not produced inside the body): histidine (His), isoleucine (Ile), leucine (Leu), lysine (Lys), methionine (Met), phenylalanine (Phe), threonine (Thr), tryptophan (Trp), and valine (Val).
- **'Complete proteins'** are sourced from foods containing all amino acids: all animal proteins, including eggs and fish, are complete, and some but not all plant proteins are also complete e.g. quinoa, whey, blue-green algae, soybeans.
- Protein deficiency rarely occurs as an isolated condition. It usually accompanies a deficiency of dietary energy and other nutrients resulting from insufficient food intake.
- Proteins are broken down into amino acids by proteases in the stomach and intestine (e.g. trypsin, pepsin, chymotrypsin), then used for cell growth and repair to build endogenous proteins from aminoacyl-tRNAs, or used for gluconeogenesis if blood sugar is low, or for biosynthesis of neurotransmitters and hormones.

20.5.7. Metabolism of Lipids

Lipids are hydrophobic molecules, including fatty acids, triglycerides, phospholipids, cholesterol and fat-soluble vitamins. Most lipid metabolism occurs in the small intestine.

Bile is produced by the liver and stored in the gallbladder, and contains bile salts, formed from the condensation of bile acids (steroid acids, e.g. cholic acid) with amino acids (e.g. glycine, taurine). These are bio-surfactants in the duodenum (upper small intestine) that emulsify fats and facilitate lipolysis by pancreatic lipase enzymes, breaking down triglycerides into free fatty acids.

The fatty acids are collected into water-soluble micelles by the bile salts, and are absorbed by enterocytes (intestinal epithelial cells). The triglycerides are then reassembled and packed into chylomicrons (lipoproteins) for transport via the lymphatic system, with further processing by the liver.

Types of lipoprotein (lipid microparticles produced by the body for transporting cholesterol and triglycerides) include:

- **Chylomicrons:** produced in the small intestine villi, transporting triglycerides to the liver, skeletal muscles and adipose tissues via the lacteal lymphatic vessels. Once emptied, the chylomicron remnants are cleared from the bloodstream by being consumed in the liver, where their lipids are used to synthesise VLDL, LDL and HDL.
- **Low density lipoproteins (LDL):** circulates fat around the bloodstream to the whole body. They carry ~60% cholesterol. High genetic expression of the **ApoB** protein increases the proportion of LDL in the body, and mutations in the LDL receptor (LRL-R) contribute to their slower removal from the bloodstream. It is considered '**bad** cholesterol', as it can deposit the cholesterol in arterial walls, narrowing the blood vessels (atherosclerosis) and increasing risk of heart attack, stroke and coronary artery disease.
- **High density lipoproteins (HDL):** collects fat from cells and tissues, returns it to the liver for conversion to steroid hormones. High genetic expression of the **ApoA1** protein increases the proportion of HDL in the body. The microRNA MiR-33 epigenetically inhibits ApoA1 production, reducing HDL. It is considered '**good** cholesterol', as it removes cholesterol from circulation.

Non-genetic factors associated with increased LDL proportion include high-calorie, high-saturated fat, smoking and binge drinking. Dietary cholesterol consumption only slightly increases LDL content, and is not considered a risk factor if part of a balanced diet and in moderation. Statins are drugs for inhibiting HMG-CoA reductase for liver LDL production.

Saturated Fats: straight-chain lipids with no C=C bonds. Consumption increases LDL content.

Unsaturated Fats: straight-chain lipids with C=C bonds.

- **Trans fats:** contain a *trans* C=C bond. Sharply raises LDL and lowers HDL. Processed foods containing partially hydrogenated vegetable oils are high in trans fats.
- **Omega-3 fatty acids:** helps lower triglyceride levels, aids in brain grey matter and heart health.

20.5.7. Food Ingredients and Processed Foods

Ingredients in Foods: ingredients that often appear in dietary headlines

- **High-fructose corn syrup (HFCS):** a sweetener used in processed foods, derived from corn starch. Indirectly associated with obesity, insulin resistance and some metabolic disorders.
- **Hybridised wheat / maize:** breeding of different plant species by cross-pollination.
- **Genetically modified organisms (GMOs):** direct genetic modification of plants or small animals, typically with the aim of increasing crop yields or resilience against pest insects.
- **Lab-grown meat (cultured meat):** meat grown from cultivated animal cells (satellite stem cells). As of 2024, lab-grown meat is legal in the US (chicken), UK (pet food), Singapore (chicken) and Israel (beef).
- **Nitrites:** sodium nitrite is a preservative and inhibitor of *Clostridium botulinum* used in cured meats (bacon, ham, sausages) that can react with creatine in the meat on cooking to form nanogram quantities of nitrosamines, which are carcinogenic and hepatotoxic.
- **Fortified foods:** addition of normally-absent nutrients to foods e.g. vitamin B₉/D in bread, iodine in salt, iron in wheat/maize flours.
- **Ultra-processed foods:** edible food-like products subjected to extensive processing including non-culinary ingredients. UPFs are designed to be addictive ('hyper-palatable').
- **Animal fats and vegetable fats:** animal fats are high in monounsaturated and saturated fats, while vegetable fats are high in omega/mono/polyunsaturated (oleic acid and linoleic acid).
- **Hydrogenated oils:** processing of vegetable oils forms saturated fats and trans fats in high proportions.
- **Refined oils:** volatile fatty acids removed from olive oils. Unrefined oils include 'extra virgin' olive oil.
- **Inverted sugar syrup:** an added sugar in honey, jam or chocolate, that crystallises less readily, consisting of hydrolysed sucrose (glucose and fructose), using citric acid or invertase enzyme catalyst.
- **Refined sugars:** processed sugar from sugarcane, found in sodas and sweets. Linked to obesity, type 2 diabetes and tooth decay.
- **Gluten:** a structural protein made of gliadin and glutenin, found in wheat grain, including bread. People with coeliac disease and other gluten-related disorders must avoid gluten.
- **Artificial sweeteners (aspartame, sucralose, saccharin, acesulfame K):** a sugar substitute in low-calorie diets. Sucralose, saccharin and acesulfame K are not metabolised in the body.
- **Artificial food colourings (Red 3/40, Yellow 5/6, Blue 1/2):** coloured compounds used in processed foods, with some associations with hyperactivity in children.
- **Monosodium glutamate (MSG):** a lower-sodium salt natural flavour enhancer, widely used in Asia.
- **Chlorinated chicken:** in the US, slaughtered chicken is routinely washed in chlorine to kill pathogens. Importing chlorinated chicken from the US is banned in the EU, due to concerns that it is used to conceal the effects of substandard animal welfare, or potentially for protectionism.

Organic Food: avoids the use of synthetic fertilisers, pesticides, growth regulators (hormones) and livestock feed additives, as well as avoiding irradiation and GMOs, in growing the food. Labels include:

- “100% Organic”: all ingredients in a food product are organic (meeting the above definition).
- “Organic”: at least 95% of the ingredients are organic. Up to 5% may be non-organic.
- “Made with Organic”: at least 70% of the ingredients are organic. Up to 30% may be non-organic.

Diets:

- **Pescatarian:** no eating red meat. Fish, eggs and dairy are allowed.
- **Plant-based:** prioritises eating foods from plants, minimising meat consumption.
- **Vegetarian:** no eating meat. Eggs and dairy are allowed.
- **Vegan:** no eating meat and no eating any product derived from animals (eggs, dairy).
- **Paleo:** non-processed foods diet. Organic meats, fruit and vegetables, nuts and seeds.
- **Keto:** low-carb, high-fat diet. Meat, dairy, seafood, nuts and seeds.
- **Halal:** Islamic diet. No pork or alcohol derived products, with additional religious facets.
- **Kosher:** Jewish diet. No pork, rabbit, crab, mollusc, among others, with additional religious facets.

20.5.6. Skincare

Components of the skin surface: forms the first barrier against pathogenic infection

- **Lipid layer:** the outermost physical barrier (the stratum corneum), made of ceramides, cholesterol and fatty acids.
- **Acid mantle:** the thin film of sebum and natural oils at pH 4.7-5.7, which inhibits pathogen colonisation. Skin pH influences cellular signalling pathways, skin pigmentation and epidermal stem cell differentiation.
- **Microbiome (skin flora):** the community of non-pathogenic bacteria, which competes for resources with potentially harmful bacteria. The microbiome is destroyed when the surface pH becomes alkaline.

Active ingredients in Skin Moisturisers:

- Polyelectrolytes: e.g. hyaluronic acid, chitosan, alginate
- Retinol (vitamin A), niacinamide (vitamin B₃) and ascorbic acid (vitamin C)
- Hydroxy acids: mild exfoliants (shedding of dead surface skin), with three types:
 - Alpha-hydroxy acids (AHAs): e.g. glycolic acid, lactic acid, mandelic acid
 - Beta-hydroxy acids (BHAs): e.g. salicylic acid, mild anti-inflammatory agent
 - Poly-hydroxy acids (PHAs): e.g. gluconolactone, lactobionic acid.
- Ceramides
- Probiotics

Other ingredients used in Cosmetics: used to optimise formulation properties

- Carbomer (polyacrylic acid): increases formulation viscosity
- Polyquaternium-*n*: range of 4^o ammonium polycations, holds active ingredients in place for longer

Sun Protection: the Sun emits UV radiation which can damage the skin

- UVA (lower energy) is responsible for tanning, hyperpigmentation and skin ageing.
- UVB (higher energy) is responsible for sunburn (erythema) and skin cancer (melanoma).
- Incident UV may be specular (direct sunlight) or diffuse (reflected from surfaces / scattered by clouds), so UV is still present when in the shade or on a cloudy day.
- Sunscreens may work by reflecting (physical e.g. ZnO/TiO₂ NPs) or absorbing (chemical e.g. oxybenzone, drometrizole trisiloxane) UV radiation.
- Sunscreens marked with 'SPF50+' indicate less than 2% of UVB radiation penetrates the skin when applied fully.
- Broad-spectrum sunscreens also block UVA, indicated by a PPD (persistent pigment darkening) score, with the best being 'PA++++'.
- Sunscreens only last ~6 hours before needing reapplication due to absorption into skin (even if not used in the sun) and UV degradation.
- Sunscreen is typically recommended when the outdoors UV index is 3 or above.
- When the UV index is low, sunscreen is not advised to allow the body to synthesise sufficient vitamin D₃ from 7-dehydrocholesterol in response to the UVB exposure.
- Sunscreen quantity and formulation must be suitable for one's skin tone, as melanin acts like a mild sunscreen: ~SPF 5 for Black people relative to White people, blocking ~80% of UV. This means that equal UV penetration (2%) occurs for a White person with SPF 50 and a Black person with SPF 10.
- When indoors, glass windows block diffuse UVB but allows UVA to pass.

20.5.7. Haircare

Head hair on the scalp grows in permanently from about 1 year after birth, with vellus hair (short, thin, light-coloured) occurring over the body. During puberty, vellus hair is converted to terminal hair (long, thick, melanated) by androgen hormones. In men, the extent and thickness of terminal hair is larger than in women.

The hair cell cycle: anagen (growth: 2-6 years) → catagen (pause) → telogen (shedding and rest). During the anagen phase, hair grows at 1-2 cm per month.

Hair colours and types:

- **Colours:** black, brown (more eumelanin), red (more pheomelanin), blonde (less melanin)
- **Shape:** frizzy, curly, wavy, straight. Determined genetically by asymmetry of the hair bulb.
- **Porosity:** high porosity (absorbs and releases moisture quickly), low porosity (does not absorb moisture). Determined by the openness of the cuticle surface. Intermediate porosity provides optimal moisturability, while high or low porosity hair tends to dry out easily.

Hair shampooing: cleans the scalp skin and hair

- A blend of surfactants remove contaminants in a manner similar to soap.
- Sulfate-free shampoos avoid using SLS as the surfactant, which reduces irritation and oil removal.
- Shampoo is usually applied less frequently than conditioner, as it can lead to drying and frizzing.

Hair conditioning: provides moisture to hair, increasing ease of brushing, shininess and smoothness.

- Protein-free conditioners are suitable for low porosity hair, as this tends to increase porosity.
- Leave-in conditioners with shea butter/argan oil/coconut oil are suitable for high porosity hair.
- Conditioner is usually applied after shampoo and rinsing, resupplying the lost moisture.

Chemical depilatory: used to remove hair from the skin. Thioglycolates cleave disulfide bridges in keratin and hydrolyse for easy removal. These are also used in perms for curly hair.

Hair follicle miniaturisation: in adult males, the enzyme 5α -reductase converts testosterone to dihydrotestosterone (DHT), which is a much more potent agonist of the androgen receptor (NR3C4), accelerating virilisation (masculinisation). DHT promotes pubic hair growth but also induces scalp recession (receding hairlines) and male pattern baldness (androgenic **alopecia** in men). Inhibitors of 5α -reductase such as **finasteride** or **dutasteride** can treat these conditions, as well as its use in hormone therapy as an androgen inhibitor for transgender women. The non-hormonal vasodilator **minoxidil** is also known to promote hair growth in ~60% of men by a not-fully-understood mechanism.

Greying of hair (canities): decreased melanin pigment production from the root hair cells leads to grey/white hair follicles. This occurs when the melanocyte stem cells at the root stop undergoing melanogenesis, beginning in early adulthood and progressing throughout later life, fundamentally due to a mixture of environmental (e.g. stress) and genetic factors.

20.5.8. Dental Care

Active ingredients in toothpastes:

Bacteria colonise on teeth, feeding on sugar deposits, forming dental plaque. These bacteria release acids as they metabolise the sugar, which dissolves the hydroxyapatite in the enamel, demineralising the enamel and forming caries and cavities.

- Fluoride: prevents cavities by remineralising enamel (converting hydroxyapatite to the less soluble fluorapatite), and also provides antimicrobial protection. Usually present as sodium fluoride (~1500 ppm), which is soluble and can wash away. It does not 'whiten' the teeth.
- NovaMin: a calcium phosphosilicate bioactive glass for steady hydroxycarbonate apatite formation in the presence of acid. It is the active ingredient in Sensodyne toothpaste. Does not contain fluoride.
- Nano-hydroxyapatite: nanoparticles of hydroxyapatite that deposit in cracks on teeth. Prevents cavities and also has a whitening effect, but not antimicrobial.
- BioMinF: a fluoro-calcium phosphosilicate bioactive glass for steady remineralisation by fluorapatite formation.

Drinking water, which is fluoridated at a low concentration, provides a baseline source of fluoride between meals to help when teeth brushing is missed. Fluoride operates by both a topical and a systemic mechanism. Excessive fluoride can result in fluorosis, a discolouration of the teeth due to CaF_2 formation.

Active ingredients in mouthwashes:

- Chlorhexidine: a disinfectant and antiseptic. Only recommended for short-term use due to binding with dietary tannins (polyphenols) to stain teeth.
- Cetylpyridinium chloride: a quaternary ammonium surfactant, anti-plaque and anti-tartar.
- Alcohol: people with dry mouths should not use alcoholic mouthwashes.
- Hydrogen peroxides: a bleaching agent with a teeth whitening effect.

20.5.9. Cosmetics

Deodorants: masks body odour

- Sold in roll-on (balm stick) or spray (liquid formulation in a pressurised canister) forms.
- May contain aerosolised fragrances, odour absorbers (e.g. zinc ricinoleate), antimicrobial agents (e.g. chlorhexidine gluconate), carrier fluid (propellants e.g. liquefied butane).
- Natural ingredients include baking soda (increases skin pH), coconut oil, shea butter, cocoa butter, essential oils (tea tree oil, lavender oil). Some of these are also moisturisers.

Anti-perspirants: inhibits sweating

- Sold in roll-on or spray forms.
- Some contain aluminium (as aluminium chlorohydrate), with some evidence of toxicity.

20.6. Medical Physics, Biointerfaces and Bioelectronics

20.6.1. Implantable Devices

Cardiac Pacemaker: to maintain a regular heart rate.

Fitted using local anaesthesia, for bradycardia, tachycardia, heart block and cardiac arrest, by delivering electrical signals to the heart muscles to modulate contraction and pumping. They can be single-chamber, dual-chamber, or biventricular. Most models pace only when needed and are rate responsive. Implantable cardioverter defibrillators (ICDs) can 'reboot' the heart.

Auditory Prostheses: to allow hearing in hearing-impaired or deaf people

A **hearing aid** is a simple amplifier with background noise filtering, fitted in the ear canal. It requires all parts of the ear to remain functional despite being reduced in sensitivity. A **cochlear implant** features a microphone, processor, transmitter (located on the scalp) and a receiver (located under the skin). Electrical signals from the receiver are conducted by an electrode threaded into the cochlea and stimulate the auditory nerve. Current spreading in the cochlea can result in decreased sound clarity, so configuration of electrodes (multipolar arrangement) and stimulation protocols (encoding of their signals e.g. multiple phases) are important design parameters. If the auditory nerve is damaged, an auditory brainstem implant (ABI) can be used to directly send signals to the brain.

Visual Prostheses: to allow sight in visually-impaired or blind people

Depending on which stage of the visual pathway is damaged, different levels of intervention are required. Stimulation can occur at the retina or the visual cortex, with varying degrees of information pre-processing and encoding of the input required. Bio-inspired photovoltaic devices are currently under research, which use semiconductive polymers to excite neurons in the retina.

CNS and PNS Implants: to stimulate particular areas of the nervous system.

There is a trade-off between invasiveness and signal resolution. The dura of the brain acts as a low-pass filter, removing important information, so subdural electrodes are required for clear signals.

- Electrocorticography (ECog): long electrodes for deep brain stimulation (DBS). The incoming electrical signals interrupt signals that cause tremors/rigidity/stiffness, although the neuromodulatory mechanism is not understood.
- Brain-computer interface: activate motor neurons directly from signals in the brain.
- Spinal cord stimulation: can relieve chronic pain in the back, neck, legs or arms.
- Single nerve stimulation: e.g. phrenic nerve for assisted breathing, sacral nerve for incontinence, PNS for drop foot, oesophagus for reflux.
- Electroceuticals: stimulation of the vagus nerve using a specific neural biomarker (code) to induce specific changes e.g. reducing inflammation. Finding such markers is an active area of research for a variety of disorders.

Implants can induce the foreign body response (broken capillaries on entry → protein release and adhesion → summoning of macrophages → macrophage fusion into giant cell → ECM deposition), which creates a deadzone around the electrode. It is difficult to prevent entirely, but can be reduced using e.g. hydrogels to match mechanical properties with surface nanostructures and immunomodulatory coatings.

20.6.2. Cutaneous Devices

Cutaneous (on the skin) electrophysiology uses electrodes to perform:

- Recording: brain (electroencephalography, EEG), heart (electrocardiography, ECG), muscles (electromyography, EMG)
- Stimulation: transcranial direct current stimulation (tDCS), transcutaneous electrical nerve stimulation, electroconvulsive therapy (ECT), defibrillation

Simple metal electrodes include Ag/AgCl (Ohmic, non-polarisable). Modern developments include inks or textiles with conductive polymers.

EEGs measure 'brain waves', coordinated synchronised nerve impulses, by an array of cutaneous electrodes. The frequency of the EEG signal can indicate the state of the brain: delta (0.5-4 Hz) → deep sleep, theta (4-7 Hz) → light sleep, alpha (8-13 Hz) → relaxed, beta (13-30 Hz) → alert/focussed, gamma (>30 Hz) → high-level cognition/memorising/problem-solving.

Transcranial direct current stimulation (tDCS) uses low currents between two electrodes; ECT uses much higher currents to induce seizure. These treatments can often be effective despite uncertainty on their mechanism of action: it is thought to act as a 'soft reset', inducing changes in neural chemistry connectivity, breaking or deactivating neural circuits associated with various mental disorders. Temporally-interfering fields can localise excitation to specific parts of the brain, especially targeting deep brain stimulation rather than neocortical regions.

Electrical impedance tomography (EIT) can be used as an imaging technique in which the impedance is reconstructed from fast-switching AC pulses through a set of electrodes around the perimeter of the target. It has also been applied to touch-sensitive biomimetic skins (tactile sensors).

Glucose meters are biosensors that use a small filament-like needle as an electrode to measure glucose concentration in the interstitial fluid. In an electrochemical biosensor (Section 13.5.12), an immobilised enzyme (e.g. glucose oxidase with FAD) reacts with glucose and produces FADH_2 , which undergoes a redox reaction to generate a current signal indicative of glucose concentration. There is a short time lag between blood glucose and measured glucose. Glucose meters are useful for patients with diabetes, and can be coupled with insulin autoinjectors as part of a control system.

EMGs can be used as data sources for machine-learning training of personalised prosthetic limbs, in which muscle signals of the stump are mapped to target robot pose movements, although surface electrodes (sEMG) produce noisier and less area-precise data than subcutaneous (needle) EMG.

Iontophoresis involves inducing the release of small molecules using a small current between two electrodes, as a form of drug delivery. Can be used in combination with biosensors for signalled release.

20.6.3. *In-vitro* Medical Devices

In-vitro Electrophysiology: recording electrical activity on cell tissues only

Useful for drug discovery and toxicology, and helps to minimise the use of animals. In 2022, the FDA (USA regulatory body) approved the sale of new drugs without requiring any animal testing data.

Extracellular IVE involves growing cell culture on a sensor, which can detect signals of order $\sim 100 \mu\text{V}$. Intracellular IVE involves use of thin electrodes being pushed into individual cells (patch clamp technique with a micromanipulator), which is high-effort, low-throughput and the cells die within ~ 24 hours. Using a gentle pick-up, a piece of the cell membrane can be extracted, which will contain ion channels, which can then be recorded individually. The signals are much clearer ($\sim 50 \text{ mV}$).

Organoids: physical models of organs to test e.g. drug pharmacokinetics.

Organ on a chip: simulates tissue activity in vitro. Use of microfluidics allows for fluid flow through micro-scale channels (e.g. blood through vessels, air through bronchioles).

L21. CHINESE (中文)

21.1. Basics of Chinese

21.1.1. Hanyu Pinyin Romanisation of Chinese Characters

Pinyin (拼音) is the official and most common romanisation system for Chinese.

Initials:

b, p, m, f, d, t, n, l, g, h, j, q, x, zh, ch, sh, r, z, c, s, y, w

Finals:

a, o, e, i, u, ü, ai, ei, ui, ao, ou, iu, ie, üe, er, an, en, in, un, ün, ang, eng, ing, ong, uang, iang, uai

Tones:

1: ā (prolonged), 2: á (rising), 3: ǎ (fall-rise), 4: à (falling), 5: a (neutral)

Alternative systems: Wade-Giles (older, unofficial), Yale (Cantonese: Hong Kong / Macau), bopomofo (Taiwan, uses phonetic Chinese syllable characters).

21.1.2. Stroke Order of Written Chinese Characters

Chinese characters must be drawn in the following order(s):

- top to bottom;
- left to right;
- horizontals before verticals;
- right-to-left diagonals before left-to-right diagonals;
- centre first in vertically symmetric characters;
- move from outside to inside, close frames last.

When writing with a brush, such as in calligraphy, this order helps to avoid smudging.

Some illustrative examples:

长 (cháng) 丿 一 长 长
 出 (chū) 丨 丨 丨 出 出
 女 (nǚ) ㇇ 女 女
 非 (fēi) 丨 丨 丨 丨 非 非 非 非
 巨 (jù) 一 冂 巨
 门 (mén) 丨 丨 门
 母 (mǔ) 丨 冂 母 母 母
 旅 (lǚ) 丨 丨 丨 方 方 方 方 旅 旅 旅

21.1.3. Common Radicals

	Association	Pīnyīn	Example usage		Association	Pīnyīn	Example usage
亻	person	rén	你 you (nǐ)	竹	bamboo	zhú	笔 pen (bǐ), 简 simple (jiǎn)
彳	road, walking	chì	街 street (jiē), 往 toward (wǎng)	足	foot	zú	踢 kick (tī), 跑 run (pǎo)
氵	water	shuǐ	河 river (hé), 洗 wash (xǐ)	辶	walk, action, time period	chuò / zouzhi	进 enter (jìn), 远 far (yuǎn)
冫	ice	bīng	冰 ice (bīng), 冻 freeze (dòng)	纟 (糸)	silk, thread, string	mì	线 thread (xiàn), 丝 silk (sī)
火	fire / burning	huǒ	灯 lamp (dēng), 烧 burn (shāo)	宀	roof	mián	家 home/family (jiā), 室 room (shì)
灬	fire / fire from below	huǒ	蒸 steam (zhēng), 热 hot (rè)	口	mouth, opening	kǒu	唱 sing (chàng), 和 and (hé)
日	day, sun, time	rì	时 time (shí), 晴 sunny (qíng)	囗	boundary, enclosure	wéi	国 country (guó), 园 garden (yuán)
月	moon, month	yuè	明 tomorrow (míng), 服 clothes (fú)	衤	clothes	yī	裙 skirt (qún), 衫 shirt (shān)
门 (門)	door	mén	间 room (jiān), 闭 shut (bì)	疒	sickness	nè	病 disease (bìng), 痛 pain (tòng)
女	female, woman	nǚ	好 good (hǎo), 妈 mother (mā)	阝	terrain, hill, city, town	yì	部 section (bù), 都 both (dōu)
子	child	zǐ	孩 child (hái), 孙 grandchild (sūn)	厂	factory, yard	hàn	厅 hall (tīng), 厂 factory (chǎng)
扌	hand	shǒu	推 push (tuī), 拉 pull (lā)	宀	wide, shelter	yǎn	店 shop (diàn), 府 mansion (fǔ)
讠 (言)	word, language, speech	yán	说 say (shuō), 语 language (yǔ)	心	heart	xīn	想 want (xiǎng), 忘 forget (wàng)
艹	grass	cǎo	花 flower (huā), 菜 vegetable (cài)	忄	feeling, mentality	xīn	情 emotion (qíng), 忙 busy (máng)
土	earth, soil	tǔ	地 ground (dì), 场 field (chǎng)	力	strength, power, force	lì	助 help (zhù), 加 add (jiā)
钅 (金)	metal	jīn	银 silver (yín), 铁 iron (tiě)	车 (車)	car, vehicle, cart	chē	车 car (chē), 轨 rail/track (guǐ)
饣 (食)	food, eat	shí	饭 rice/meal (fàn), 饮 drink (yǐn)	鱼 (魚)	fish	yú	鲜 fresh (xiān), 鲍 abalone (bào)
木	tree, wood	mù	林 forest (lín), 树 tree (shù)				

Note: radicals in brackets e.g. (門) denote the traditional character, often used in Hong Kong and Taiwan. Traditional characters are sometimes used alone for artistic purposes.

21.2. Basic Vocabulary

21.2.1. Basic Verbs

	Pinyin	English		Pinyin	English
是	shì	to be	发	fā	to send (emails)
有	yǒu	to have	送	sòng	to give / send
问	wèn	to ask	寄	jì	to send (letters)
吃	chī	to eat	忘	wàng	to forget
喝	hē	to drink	记得	jìdé	to remember
知道	zhīdào	to know (sth)	洗	xǐ	to wash
认识	rènshí	to know (sbd)	找	zhǎo	to look for / search
叫	jiào	to call / name	参观	cānguān	to visit
学	xué	to learn / study	参加	cānjiā	to take part in
懂 / 明白	dǒng / míngbái	to understand	穿	chuān	to wear (clothes)
说	shuō	to say / speak	戴	dài	to wear (accessories)
要	yào	to want to do	代表	dàibiǎo	to represent
想	xiǎng	to think / want	看见	kànjiàn	to look / see / watch
觉得	juéde	to feel	听	tīng	to listen / hear
写	xiě	to write	会	huì	to be able to / can
画	huà	to draw / paint	告诉	gàosù	to tell
住	zhù	to live	唱歌	chànggē	to sing
坐	zuò	to sit	跳舞	tiàowǔ	to dance
玩	wán	to play	游泳	yóuyǒng	to swim
睡觉	shuìjiào	to sleep	踢	tī	to kick
用	yòng	to use	打	dǎ	to hit
希望	xīwàng	to hope	打扫	dǎsǎo	to clean
来	lái	to come	做饭	zuòfàn	to cook
去	qù	to go	开车	kāichē	to drive

Verbs (continued):

	Pinyin	English		Pinyin	English
哭	kū	to cry	读	dú	to read
笑	xiào	to laugh	上班	shàngbān	to go to work
微笑	wéixiào	to smile	害怕	hàipà	to be scared
帮助	bāngzhù	to help	取	qǔ	to take
起床	qǐchuáng	to get up	讲	jiǎng	to state, explain
刷牙	shuāyá	to brush teeth	讲价	jiǎngjià	to bargain, haggle
跑步	pǎobù	to run	欢迎	huānyíng	to welcome
服务	fúwù	to serve	回答	huídá	to answer
锻炼	duànliàn	to exercise, work out	介绍	jièshào	to introduce
回	huí	to return	走	zǒu	to walk
买	mǎi	to buy	准备	zhǔnbèi	to prepare
卖	mài	to sell	等	děng	to wait
换	huàn	to exchange	排队	páiduì	to queue
试	shì	to try	约会	yuēhuì	to date / make appointment

21.2.2. Basic Adjectives

	Pinyin	English		Pinyin	English
好	hǎo	good	强	qiáng	strong
坏	huài	bad	弱	ruò	weak
快	kuài	fast	便宜	piányí	cheap
慢	màn	slow	旧 / 老	jiù / lǎo	old
漂亮	piàoliang	pretty	新	xīn	new
难看 / 丑	nánkàn / chǒu	ugly	贵	guì	expensive
有意思	yǒuyìsi	interesting	重要	zhòngyào	important
没意思	méiyìsi	boring	近	jìn	near
干净	gānjìng	clean	远	yuǎn	far
脏	zàng	dirty	不可缺少	bùkě quēshǎo	indispensable
忙	máng	busy	基本	jīběn	basic
累	lèi	tired	生气	shēngqì	angry
饿	è	hungry	高兴	gāoxìng	happy
渴	kě	thirsty	好吃	hào chī	tasty
伤心	shāngxīn	sad			

21.2.3. Adverbs

Adjectives can be turned into adverbs by adding 地. e.g. 生气 → 生气地 (angry → angrily).

Adverbs of degree (quantifiers):

	Pinyin	English		Pinyin	English
很	hěn	is [very]	实在	shízài	truly, honestly
非常	fēicháng	very	还	hái	still, yet
真的	zhēn de	really	最	zuì	most
特别	tèbié	especially	差不多	chàbùduō	almost, nearly

21.2.4. Pronouns

Possessive pronouns can be formed using 'pronoun + 的'.

	Pinyin	English		Pinyin	English
我	wǒ	I	它	tā	it
你	nǐ	you	你们	nǐmen	you (plural)
您	nín	you (formal)	他们	tāmen	they
他	tā	he			
她	tā	she			

21.2.5. Connectives

Connectives (conjunctions) join simple phrases to make compound sentences.

	Pinyin	English		Pinyin	English
和	hé	and (between nouns)	因为...所以		
因为	yīnwèi	because, since	但是只有...才行	dànshì zhǐyǒu...cái xíng	but only if...
所以	suǒyǐ	so	虽然...但是	suīrán...dànshì	although...but
也	yě	also	如果...那么	rúguǒ... nàme	if...then
而且	erqiě	moreover	除了...以外	chúle.. yǐwài	besides...
此外	cǐwài	in addition			
即使	jíshǐ	even though			
虽然	suīrán	although			
因此	yīncǐ	therefore			

Transportation

	Pinyin	English		Pinyin	English
走路	zǒulù	walk / on foot	飞机	fēijī	plane
自行车	zìxíngchē	bicycle	直升机	zhíshēngjī	helicopter
汽车	qìchē	car	船	chuán	boat
出租车	chūzū chē	taxi	渡轮	dùlún	ferry
面包车	miànbāo chē	van	邮轮	yóulún	cruise
公交车	gōngjiāo chē	bus	缆车	lǎnchē	cable car / gondola
火车	huǒchē	train	磁悬浮列车	cíxuánfú lièchē	maglev train
电车	diànchē	tram			

Media, Politics and Current Affairs

	Pinyin	English		Pinyin	English
新闻	xīnwén	news	资本主义	zìběn zhǔyì	capitalism
报纸	bàozhǐ	newspaper	共产主义	gòngchǎn zhǔyì	communism
记者	jìzhě	journalist / reporter	国际	guójì	international
媒体	méitǐ	media	经济	jīngjì	economy
总统	zǒngtǒng	president	政治	zhèngzhì	politics
国家	guójiā	country	新华	Xīnhuá	Xinhua News
世界	shìjiè	world	中国共产党	zhōngguó gòngchǎndǎng	Communist Party of China (CPC / CCP)
政府	zhèngfǔ	government	习近平	Xí Jìnpíng	Xi Jinping
西方	xīfāng	the West	中华文化圈	zhōnghuá wénhuà quān	sinosphere
部长	bùzhǎng	minister			

21.3. Themed Vocabulary

21.3.1. Food and Drink

Food (nouns):

苹果 (píngguǒ)	— apple	柠檬 (níngméng)	— lemon
牛肉 (niúròu)	— beef	面条 (miàntiáo)	— noodles
面包 (miànbāo)	— bread	橙子 (chéngzi)	— orange
蛋糕 (dàngāo)	— cake	凤梨酥 (fènglí sū)	— pineapple cake
鸡肉 (jīròu)	— chicken	比萨 (bǐsà)	— pizza
点心 (diǎnxīn)	— dim sum / snack	猪肉 (zhūròu)	— pork
鸭肉 (yāròu)	— duck	粥 (zhōu)*	— porridge / congee*
饺子 (jiǎozi)	— dumplings	土豆 (tǔdòu)	— potato
榴莲 (liúlián)	— durian	米饭 (mǐfàn)	— rice
鸡蛋 (jīdàn)	— egg	海鲜 (hǎixiān)	— seafood
鱼肉 (yúròu)	— fish	小吃 (xiǎochī)	— snack
薯条 (shǔ tiáo)	— fries / chips	汤 (tāng)*	— soup*
葡萄 (pútáo)	— grape	包子 (bāozi)	— steam stuffed bun
汉堡包 (hànbǎobāo)	— hamburger	茶叶蛋 (cháyè dàn)	— tea egg
火锅 (huǒguō)	— hotpot	蔬菜 (shūcài)	— vegetables
冰淇淋 (bīngqílín)	— ice cream	西瓜 (xīguā)	— watermelon

Drinks (nouns):

苹果汁 (píngguǒ zhī)	— apple juice	冰水 (bīng shuǐ)	— iced water
啤酒 (píjiǔ)	— beer	柠檬水 (níngméng shuǐ)	— lemonade
红茶 (hóngchá)	— black tea	牛奶 (niúniǎi)	— (cow's) milk
珍珠奶茶 (zhēnzhū nǎichá)	— pearl / bubble tea	矿泉水 (kuàngquán shuǐ)	— mineral water
白酒 (báijiǔ)	— Chinese spirit liquor	红葡萄酒 (hóng pútáojiǔ)	— red wine
可乐 (kělè)	— Coca Cola / Coke	汽水 (qìshuǐ)	— soft drink
咖啡 (kāfēi)	— coffee	烧酒 (shāojiǔ)	— soju
水果汁 (shuǐ guǒzhī)	— fruit juice	豆浆 (dòujiāng)	— soy milk
绿茶 (lǜchá)	— green tea	雪碧 (xuěbì)	— Sprite
热巧克力 (rè qiǎokèlì)	— hot chocolate	白葡萄酒 (bái pútáojiǔ)	— white wine

Condiments (nouns):

香醋 (xiāngcù)	— balsamic vinegar	蚝油 (háoyóu)	— oyster sauce
豆瓣酱 (dòubànjiàng)	— bean sauce	花生酱 (huāshēngjiàng)	— peanut butter
黄油 (huángyóu)	— butter	胡椒 (hújiāo)	— pepper
辣椒酱 (làjiāojiàng)	— chilli sauce	盐 (yán)	— salt
蒜蓉 (suànróng)	— minced garlic	芝麻油 (zhīmayóu)	— sesame oil
味精 (wèijīng)	— MSG	酱油 (jiàngyóu)	— soy sauce
		醋 (cù)	— vinegar

* use the verb 喝 despite being listed as a 'food'.

Culinary equipment and places (nouns):

早餐 (zǎocān)	— breakfast
咖啡厅 (kāfēi tīng)	— cafe
厨师 (chúshī)	— chef
筷子 (kuàizi)	— chopsticks
甜点 / 点心 (tiándiǎn / diǎnxīn)	— dessert
餐厅 (cāntīng)	— dining area
晚餐 (wǎncān)	— dinner
叉子 (chāzi)	— fork
清真食品 (qīngzhēn shípǐn)	— halal food
小贩中心 (xiǎofàn zhōngxīn)	— hawker centre
厨房 (chúfáng)	— kitchen
刀 (dāo)	— knife
乳糖不耐症 (rǔtáng bù nài zhèng)	— lactose intolerance
午餐 (wǔcān)	— lunch

菜单 (càidān)	— menu
微波炉 (wéibōlú)	— microwave
烤箱 (kǎoxiāng)	— oven
盘子 (pánzi)	— plate
酒吧 (jiǔbā)	— pub / bar
饭店 (fàndiàn)	— restaurant
盐 (yán)	— salt
水槽 (shuǐcáo)	— sink
勺子 (sháozi)	— spoon
炉子 (lúzi)	— stove
水龙头 (shuǐlóngtóu)	— tap / faucet
纯素食 (chún sùshí)	— vegan (adj.)
素食 (sùshí)	— vegetarian (adj.)
服务员 (fúwùyuán)	— waiter / waitress
炒锅 (chǎo guō)	— wok / frying pan

Preparing and eating food (verbs):

烘焙 (hōngbèi)	— to bake
红烧 (hóngshāo)	— to braise
叫外卖 (jiào wàimài)	— to call a takeaway
煮 / 做饭 (zhǔ / zuǒfàn)	— to cook
喝 (hē)	— to drink
吃 (chī)	— to eat
吃这里 (chī zhèlǐ)	— to eat in

点菜 (diǎn cài)	— to order dishes
烤 (kǎo)	— to roast / grill
上菜 (shàng cài)	— to serve
蒸 (zhēng)	— to steam
炖 (dùn)	— to stew
炒 (chǎo)	— to stir-fry / sauté
带走 (dài zǒu)	— to take out

Describing food (adjectives):

苦 (kǔ)	— bitter
淡 (dàn)	— bland
冷 (lěng)	— cold
美味 / 好吃 (měiwèi / hàochī)	— delicious
令人恶心 (lìngrén ǎixīn)	— disgusting
脂肪 (zhīfáng)	— fatty
有气泡 (yǒu qìpào)	— fizzy / bubbly
新鲜 (xīnxiān)	— fresh
冷冻 (lěngdòng)	— frozen
健康 (jiànkāng)	— healthy

热 (rè)	— hot
中毒 (zhòngdú)	— poisoned
生 (shēng)	— raw
咸 (xián)	— salty
酸 (suān)	— sour / acidic
变质 (biànzhì)	— stale / gone bad
含糖 (hán táng)	— sugary
甜 (tián)	— sweet
鲜味 (xiānwèi)	— umami / savoury
不健康 (bùjiànkāng)	— unhealthy

21.3.2. Hobbies and Pastimes

Activities (verbs and verb phrases):

足球 (zúqiú)	— football / soccer
橄榄球 (gǎnlǎnqiú)	— rugby / American football
跑步 (pǎobù)	— running

Thinking and emotions (adjectives):

无聊 (wúliáo)	— boring / bored
-------------	------------------

21.3.3. Describing People

Parts of the body and face:

手臂 (shǒubi)	— arm
胡须 (húxū)	— beard / moustache
身体 (shēntǐ)	— body
眼睛 (yǎnjīng)	— eyes
眉 (méi)	— eyebrows
睫毛 (jiémáo)	— eyelashes
脚 (jiǎo)	— feet
手指 (shǒuzhǐ)	— finger
头发 (tóufǎ)	— hair

手 (shǒu)	— hand
腿 (tuǐ)	— leg
嘴唇 (zuǐchún)	— lips
口 (kǒu)	— mouth
脖子 (bózi)	— neck
鼻子 (bízi)	— nose
脚趾 (jiǎozhǐ)	— toe
舌头 (shétou)	— tongue

Describing people's attributes:

美丽 (měilì)	— beautiful
可爱 (kě'ài)	— cute
胖 (pàng)	— fat
火辣 (huǒ là)	— hot / sexy
肌肉发达 (jīròu fādá)	— muscular

短 (duǎn)	— short
高 (gāo)	— tall
瘦 (shòu)	— thin
丑 (chǒu)	— ugly

Clothing and accessories:

领结 (lǐngjié)	— bowtie
胸罩 (xiōngzhào)	— bra
手镯 (shǒuzhuó)	— bracelet
旗袍 (qípáo)	— Chinese dress (Cheongsam)
衣服 (yīfú)	— clothes
外套 (wàitào)	— coat / jacket / hoodie
连衣裙 (liányīqún)	— dress
着装要求 (zhuózhāng yāoqiú)	— dress code
耳环 (ěrhuán)	— ear ring
口罩 (kǒuzhào)	— face mask (sanitary)
眼镜 (yǎnjìng)	— glasses
手套 (shǒutào)	— gloves
发夹 (fǎ jiā)	— hair bow / hair tie
手提包 (shǒutí bāo)	— handbag
帽子 (màozi)	— hat / cap
发带 (fǎ dài)	— headband
耳机 (ěrjī)	— headphones
证件卡 (zhèngjiàn kǎ)	— ID badge

挂绳 (guà shéng)	— lanyard
名称标签 (míngchēng biāoqiān)	— name tag
项链 (xiàngliàn)	— necklace
大衣 (dàyī)	— overcoat (longline coat)
戒指 (jièzhǐ)	— ring (for finger)
围巾 (wéijīn)	— scarf
衬衫 (chènshān)	— shirt
鞋子 (xiézi)	— shoes
裙子 (qúnzi)	— skirt
袜子 (wàzi)	— socks
丝袜 (sīwà)	— stockings / tights
西装 (xīzhuāng)	— suit
领带 (lǐngdài)	— tie
裤子 (kùzi)	— trousers / pants
T恤 (T xù)	— T-shirt
内裤 (nèikù)	— underpants
制服 (zhìfú)	— uniform
手表 (shǒubiǎo)	— watch

21.3.4. In the House

Rooms:

阁楼 (gélóu)	— attic
阳台 (yángtái)	— balcony
地下室 (dìxiàshi)	— basement
浴室 (yùshì)	— bathroom
卧室 (wòshì)	— bedroom

餐厅 (cāntīng)	— dining room
门厅 (méntīng)	— entrance hall
厨房 (chúfáng)	— kitchen
客厅 (kètīng)	— living room
书房 (shūfáng)	— study (room) / studio
窗户 (chuānghù)	— window

Things found in the home:

床 (chuáng)	— bed
椅子 (yǐzi)	— chair
餐桌 (cānzhuō)	— dining table
壁炉 (bìlú)	— fireplace
台灯 (táidēng)	— lamp (on a desk)

洗衣 (xǐyī)	— laundry
淋浴 (línǚ)	— shower (noun or verb)
沙发 (shāfā)	— sofa
桌子 (zhuōzi)	— table
电视 (diànshì)	— television
衣柜 (yīguì)	— wardrobe

Routines:

起床 (qǐchuáng)	— to get up (out of bed)
洗澡 (xǐzǎo)	— to take a shower / bathe

21.3.5. Travelling and Tourism

Modes of transportation:

自行车 (zìxíngchē)	— bicycle	高铁 (gāotiē)	— high-speed rail
船 (chuán)	— boat	磁悬浮列车 (cíxúánfú lièchē)	— maglev train
公交车 (gōngjiāo chē)	— bus	飞机 (fēijī)	— plane
缆车 (lǎnchē)	— cable car / gondola	软座 (ruǎn zuò)	— soft seat
汽车 (qìchē)	— car	软卧 (ruǎn wò)	— soft sleeper
邮轮 (yóulún)	— cruise	出租车 (chūzū chē)	— taxi
渡轮 (dùlún)	— ferry	火车 (huǒchē)	— train
硬座 (yìng zuò)	— hard seat	电车 (diànchē)	— tram
硬卧 (yìng wò)	— hard sleeper	面包车 (miànbāo chē)	— van
直升机 (zhíshēngjī)	— helicopter	走路 (zǒulù)	— walk / on foot

Navigation:

遥远 (yáoyuǎn)	— far away	街 (jiē)	— street
左边 (zuǒbiān)	— left side	迷路 (mílù)	— to be lost
地图 (dìtú)	— map	找 (zhǎo)	— to look for
附近 (fùjìn)	— nearby	左转 (zuǒ zhuǎn)	— to turn left
右边 (yòubiān)	— right side	右转 (yòu zhuǎn)	— to turn right
路 (lù)	— road	旅游指南 (lǚyóu zhǐnán)	— travel guide

In the city:

银行 (yínháng)	— bank	学校 (xuéxiào)	— school
酒吧 (jiǔbā)	— bar	商店 (shāngdiàn)	— shop
大楼 (dàlóu)	— building	人行道 (rénxíngdào)	— sidewalk / pavement
公交车站 (gōngjiāochē zhàn)	— bus stop	街道 (jiēdào)	— street
咖啡馆 (kāfēiguǎn)	— cafe	路灯 (lùdēng)	— street light
教堂 (jiàotáng)	— church	路牌 (lùpái)	— street sign
医院 (yīyuàn)	— hospital	地铁站 (dìtiě zhàn)	— subway station
酒店 (jiǔdiàn)	— hotel	超市 (chāoshì)	— supermarket
图书馆 (túshūguǎn)	— library	出租车 (chūzūchē)	— taxi
市场 (shìchǎng)	— market	剧院 (jùyuàn)	— theatre
博物馆 (bówùguǎn)	— museum	红绿灯 (hónglǜdēng)	— traffic light
公园 (gōngyuán)	— park	斑马线 (bānmǎxiàn)	— zebra crossing
餐厅 (cāntīng)	— restaurant		
饭馆 (fànguǎn)	— restaurant		

Famous landmarks:

紫禁城 (zǐjìnchéng)	— Forbidden City
长城 (chángchéng)	— Great Wall
天安门广场 (tiān'ānmén guǎngchǎng)	— Tiananmen Square

外滩 (wàitān)	— The Bund
长江 (chángjiāng)	— Yangtze River
长江大桥 (chángjiāng dàqiáo)	— Yangtze River bridge

Countries:

澳大利亚 (Àodàliyǎ)	— Australia
巴西 (Bāxī)	— Brazil
英国 (Yīngguó)	— Britain / UK
加拿大 (Jiānádà)	— Canada
中国 (Zhōngguó)	— China
法国 (Fàguó)	— France
德国 (Déguó)	— Germany
希腊 (Xīlà)	— Greece
印度 (Yīndù)	— India
印度尼西亚 (Yīndùnìxīyà)	— Indonesia
意大利 (Yìdàlì)	— Italy
日本 (Rìběn)	— Japan
哈萨克斯坦 (hāsàkèsītǎn)	— Kazakhstan
马来西亚 (Mǎláixīyà)	— Malaysia

蒙古 (Ménggǔ)	— Mongolia
尼日利亚 (Nírìliyǎ)	— Nigeria
巴基斯坦 (Bājīstǎn)	— Pakistan
菲律宾 (Fēilǚbīn)	— Philippines
俄罗斯 (Èluósī)	— Russia
新加坡 (Xīnjiāpō)	— Singapore
韩国 (Hánguó)	— South Korea
西班牙 (Xībānyá)	— Spain
台湾 (Táiwān)	— Taiwan
泰国 (Tàiguó)	— Thailand
乌克兰 (Wūkèlán)	— Ukraine
美国 (Měiguó)	— United States / USA
越南 (Yuènnán)	— Vietnam

Popular cities and islands for tourists:

雅典 (Yǎdiǎn)	— Athens
巴厘 (Bālì)	— Bali
曼谷 (Màngǔ)	— Bangkok
北京 (Běijīng)	— Beijing
迪拜 (Dībài)	— Dubai
爱丁堡 (Àidīngbǎo)	— Edinburgh
河内 (Hénnèi)	— Hanoi
胡志明市 (Húzhì míng shì)	— Ho Chi Minh City
香港 (Xiānggǎng)	— Hong Kong
高雄 (Gāoxióng)	— Kaohsiung
吉隆坡 (Jílóngpō)	— Kuala Lumpur
拉斯维加斯 (Lāsī wéijīāsī)	— Las Vegas
伦敦 (Lúndūn)	— London

洛杉矶 (Luòshānjī)	— Los Angeles
马德里 (Mǎdé lǐ)	— Madrid
马略卡 (Mǎlǚèkǎ)	— Majorca
迈阿密 (Mài'āmi)	— Miami
纽约市 (Niǚyuē shì)	— New York City
巴黎 (Bālì)	— Paris
罗马 (Luómǎ)	— Rome
旧金山 (Jiùjīnshān)	— San Francisco
首尔 (Shǒu'ěr)	— Seoul
上海 (Shànghǎi)	— Shanghai
深圳 (Shēnzhèn)	— Shenzhen
台北 (Táiběi)	— Taipei
东京 (Dōngjīng)	— Tokyo

21.3.5. Media and Technology

Digital media:

据说 (jùshuō)	— allegedly / reportedly	审查 (shěn chá)	— to censor
百度 (bǎi dù)	— Baidu	聊天 (liáo tiān)	— to chat
抖音 (dǒu yīn)	— Douyin / TikTok	下载 (xià zài)	— to download
电子邮件 (diàn zǐ yóu jiàn)	— email	发 (fā)	— to send (an email)
防火墙 (fáng huǒ qiáng)	— firewall	上网 (shàng wǎng)	— to surf the web
环球时报 (huánqiú shíbào)	— Global Times	打字 (dǎ zì)	— to type
互联网 (hù lián wǎng)	— internet	上传 (shàng chuán)	— to upload
记者 (jìzhě)	— journalist / reporter	网站 (wǎng zhàn)	— website
媒体 (méitǐ)	— media	微信 (wēi xìn)	— WeChat
网民 (wǎng mín)	— netizen	微博 (wēi bó)	— Weibo
新闻 (xīnwén)	— news	新华 (xīnhuá)	— Xinhua News
报纸 (bàozhǐ)	— newspaper	知乎 (zhī hū)	— Zhihu
社交媒体 (shè jiāo méi tǐ)	— social media		
消息来源 (xiāoxī lái yuán)	— source (of info)		

Famous people (cultural, historical and contemporary public figures):

李小龙 (Lǐxiǎolóng)	— Bruce Lee	周杰伦 (Zhōujiélún)	— Jay Chou
林鄭月娥 (Lín zhèngyuè'é)	— Carrie Lam	江泽民 (Jiāng Zémín)	— Jiang Zemin
孔子 (Kǒngzǐ)	— Confucius	老子 (Lǎozǐ)	— Lao Tzu
邓小平 (Dèng Xiǎopíng)	— Deng Xiaoping	毛泽东 (Máo Zédōng)	— Mao Zedong
范冰冰 (Fàn Bīngbīng)	— Fan Bingbing	孙子 (Sūnzi)	— Sun Tzu
马云 (Mǎyún)	— Jack Ma	蔡英文 (Cài Yīngwén)	— Tsai Ingwen
成龙 (Chénglóng)	— Jackie Chan	习近平 (Xí Jìnpíng)	— Xi Jinping
王嘉尔 (Wáng Jiā ěr)	— Jackson Wang	姚明 (Yáomíng)	— Yao Ming

21.3.6. Politics and Current Affairs

Government:

中国共产党 (zhōngguó gòngchǎndǎng) — CPC / CCP	部长 (bùzhǎng)	— minister
民主 (mínzhǔ)	政治 (zhèngzhì)	— politics
独裁 (dúcái)	总统 (zǒngtǒng)	— president
政府 (zhèngfǔ)		

Business and Economics:

资本主义 (zīběn zhǔyì)	— capitalism	率 (lǜ)	— rate
共产主义 (gòngchǎn zhǔyì)	— communism	产业 (chǎnyè)	— sector
公司 (gōngsī)	— company / corporation	股东 (gǔdōng)	— shareholder
经济 (jīngjì)	— economy	发展 (fāzhǎn)	— to develop
行业 (hángyè)	— industry	增加 (zēngjiā)	— to increase
通货膨胀 (tōnghuò péngzhàng)	— inflation	增长迅速 (zēngzhǎng xùnsù)	— to grow rapidly
		台积电 (táijīdiàn)	— TSMC (abbr.)

Law and crime:

被控 (bèi kòng)	— accused / charged	罚款 (fákuǎn)	— fine / penalty
案件 (ànjàn)	— case	法律 (fǎlǜ)	— law
罪行 (zuìxíng)	— crime	警察暴行 (jīngchá bàoxíng)	— police brutality
罪犯 (zuìfàn)	— criminal	监狱 (jiānyù)	— prison
拘留所 (jūliú suǒ)	— detention centre	小偷 (xiǎotōu)	— thief
被告 (bèigào)	— defendant	被逮捕 (bèi dàiǔ)	— to be arrested
毒品 (dúpǐn)	— drugs	谋杀 (móushā)	— to murder / to kill

Geopolitics and international relations:

国家 (guójiā)	— country	中华文化圈 (zhōnghuá wénhuà quān)	— Sinosphere
外交官 (wàijiāo guān)	— diplomat	西方 (xīfāng)	— the West
亚洲四小龙 (yàzhōu sì xiǎolóng)	— Four Asian Tigers	联盟 (liánméng)	— union / alliance
国际 (guójì)	— international	战争 (zhànzhēng)	— war
和平 (héping)	— peace	世界 (shìjiè)	— world
		世界大战 (shìjiè dàzhàn)	— world war

Environment:

气候变化 (qìhòu biànhuà)	— climate change
环境 (huánjìng)	— environment
洪水 (hóngshuǐ)	— flooding
全球变暖 (quánqiú biàn nuǎn)	— global warming

污染 (wūrǎn)	— pollution
垃圾 (lèsè)	— rubbish
浪费 (làngfèi)	— wastage

Society:

乞丐 (qǐgài)	— beggar
侨民 (qiáomín)	— expat / diaspora
住房 (zhùfáng)	— housing
饥饿 (jī'è)	— hunger
移民 (yímín)	— immigrant

网友 (wǎngyǒu)	— netizen
人口 (rénkǒu)	— population
社会 (shèhuì)	— society
交通 (jiāotōng)	— traffic
失业 (shīyè)	— unemployed

Personal and interpersonal affairs:

无神论 (wúshénlùn)	— atheism
双性恋 (shuāngxìngliàn)	— bisexual
佛教 (fó jiào)	— Buddhism
基督教 (jī dū jiào)	— Christianity
公民权利 (gōngmín quánlì)	— civil rights
道教 (dào jiào)	— Daoism / Taoism
外遇 (wàiyù)	— extramarital affair
同性恋 (tóngxìngliàn)	— gay / homosexuality
同性恐惧症 (tóngxìng kǒngjùzhèng)	— homophobia
人权 (rénquán)	— human rights
伊斯兰教 (yī sī lán jiào)	— Islam
女同性恋 (nǚ tóngxìngliàn)	— lesbian

生活 (shēnghuó)	— life
穷 (qióng)	— poor / poverty
宗教 (zōng jiào)	— religion
富 (fù)	— rich
风险 (fēngxiǎn)	— risk / hazard
上瘾 (shàngyǐn)	— to be addicted to
出柜 (chū guì)	— to come out (as LGBTQ)
谈恋爱 (tán liàn'ài)	— to date / fall in love
跨性别恐惧症 (kuà xìngbié kǒngjùzhèng)	— transphobia
异性恋 (yìxìngliàn)	— straight / heterosexuality

Medicine and wellbeing:

针灸 (zhēnjiǔ)	— acupuncture
细菌 (xìjūn)	— bacteria
中药 (zhōngyào)	— Chinese medicine
新冠疫情 (xīn guān yìqíng)	— coronavirus pandemic
冠状病毒病 (guānzhhuàng bìngdú bìng)	— COVID-19
饮食习惯 (yǐnshí xíguàn)	— eating habits
有害的 (yǒuhài)	— harmful
超重 (chāozhòng)	— overweight
大流行 (dà liúxíng)	— pandemic

症状 (zhèngzhuàng)	— symptoms
检测 (jiǎncè)	— test (for an illness)
对...过敏 (duì ... guòmǐn)	— to be allergic to...
减肥 (jiǎnféi)	— to lose weight
戒烟 (jièyān)	— to stop smoking
疫苗 (yìmiáo)	— vaccine
病毒 (bìngdú)	— virus
西药 (xīyào)	— Western medicine

21.3.7. Science

Biology and medicine:

氨基酸 (ānjīsuān)	— amino acid
碳水化合物 (tàنشuǐ huàhéwù)	— carbohydrate
细胞 (xìbāo)	— cell
脱氧核糖核酸 (tuōyǎng hétáng hésuān)	— DNA
酶 (méi)	— enzyme
进化 (jìnhuà)	— evolution
化石 (huàshí)	— fossil
基因编辑技术 (jīyīn biānjí jìshù)	— gene editing

葡萄糖 (pútáotáng)	— glucose
线粒体 (xiànlìtǐ)	— mitochondrion
信使核糖核酸 (xìnshǐ hétáng hésuān)	— mRNA
突变 (túbiàn)	— mutation
细胞核 (xìbāohé)	— nucleus (of cell)
光合作用 (guānghé zuòyòng)	— photosynthesis
蛋白质 (dànbáizhī)	— protein
呼吸作用 (hūxī zuòyòng)	— respiration

Chemical elements and compounds:

氨 (ān)	— ammonia / ammonium
钙 (gài)	— calcium
碳化 (tànhuà)	— carbide
碳 (tàn)	— carbon
二氧化碳 (èryǎng huàtàn)	— carbon dioxide
碳酸 (tànsuān)	— carbonate / carbonic acid
氯化 (lǜ huà)	— chloride
氯 (lǜ)	— chlorine
乙烷 (yǐwán)	— ethane
乙酸 (yǐsuān)	— ethanoic acid / acetic acid
乙醇 (yǐchún)	— ethanol
乙烯 (yǐxī)	— ethene / ethylene
氦 (hài)	— helium

氢气 (qīngqì)	— hydrogen
氢氧化 (qīng yǎnghuà)	— hydroxide
锂 (lǐ)	— lithium
镁 (měi)	— magnesium
甲烷 (jiǎwán)	— methane
硝酸 (xiāosuān)	— nitrate / nitric acid
氮 (dàn)	— nitrogen
氧化 (yǎnghuà)	— oxide
氧 (yǎng)	— oxygen
磷 (lín)	— phosphorus
钾 (jiǎ)	— potassium
钠 (nà)	— sodium
氯化钠 (lǜhuà nà)	— sodium chloride
硫酸 (liúsuan)	— sulfate / sulfuric acid

Chemistry:

溶液 (róngyè)	— aqueous solution
原子 (yuánzǐ)	— atom
原子轨道 (yuánzǐ guǐdào)	— atomic orbital
化学 (huàxué)	— chemistry
共价键 (gòng jià jiàn)	— covalent bond
电子 (diànzǐ)	— electron
火焰 (huǒyàn)	— flame
空穴 (kōng xué)	— hole (in semiconductors)
离子键 (lízǐ jiàn)	— ionic bond
分子 (fēnzǐ)	— molecule
分子轨道 (fēnzǐ guǐdào)	— molecular orbital
中子 (zhōngzǐ)	— neutron

氧化 (yǎnghuà)	— oxidation
沉淀 (chéndiàn)	— precipitate
质子 (zhízǐ)	— proton
反应 (fǎnyìng)	— reaction
还原 (huányuán)	— reduction
试管 (shìguǎn)	— test tube
加入 (jiārù)	— to add in
溶解 (róngjiě)	— to dissolve
过滤 (guòlǜ)	— to filter
得到 (dé dào)	— to get / to obtain
观察 (guānchá)	— to observe

Materials and their properties:

铝 (lǚ)	— aluminium
陶瓷 (táocí)	— ceramic
钴 (gǔ)	— cobalt
复合材料 (fùhé cáiliào)	— composite material
混凝土 (hùnníngtǔ)	— concrete
铜 (tóng)	— copper
水晶 (shuǐjīng)	— crystal
贫铀 (pínyóu)	— depleted uranium
钻石 (zuànshí)	— diamond
镝 (dī)	— dysprosium
玻璃 (bōli)	— glass
金 (jīn)	— gold
磁性 (cíxìng)	— magnet
材料 (cáiliào)	— material
金属 (jīnshǔ)	— metal

钕 (nǐ)	— neodymium
镍 (niè)	— nickel
塑料 (sùliào)	— plastic
铂 (bó)	— platinum
聚乙烯 (jùnyǐxī)	— polyethylene
聚合物 (jùhéwù)	— polymer
钢筋混凝土 (gāngjīn hùnníngtǔ)	— reinforced concrete
硅 (guī)	— silicon
银 (yín)	— silver
钢 (gāng)	— steel
石头 (shítou)	— stone
钛 (tài)	— titanium
制造 (zhìzào)	— to manufacture
钨 (wū)	— tungsten
木 (mù)	— wood

Physics:

加速度 (jiāsùdù)	— acceleration
能隙 (néng xì)	— band gap / energy gap
电池 (diànchí)	— battery
电容 (diànróng)	— capacitance / capacitor
导体 (dǎotǐ)	— conductor
电流 (diànliú)	— current
密度 (mìdù)	— density
位移 (wèiyí)	— displacement / position
掺杂 (chānzá)	— doping (of semiconductors)
电场 (diànchǎng)	— electric field
焓 (hán)	— enthalpy
熵 (shāng)	— entropy
力 (lì)	— force
重力 (zhònglì)	— gravity
电感 (diàngǎn)	— inductance / inductor
动能 (dòngnéng)	— kinetic energy

磁场 (cíchǎng)	— magnetic field
磁通量 (cítōngliàng)	— magnetic flux
质量 (zhìliàng)	— mass
动量 (dòngliàng)	— momentum
光子 (guāngzǐ)	— photon
pn结 (pn jié)	— p-n junction
势能 (shìnéng)	— potential energy
放射性 (fàngshèxìng)	— radioactive
电阻 (diànzǔ)	— resistance / resistor
半导体 (bàndǎotǐ)	— semiconductor
超导体 (chāodǎotǐ)	— superconductor
温度 (wēndù)	— temperature
变压器 (biànyāqì)	— transformer
晶体管 (jīngtǐguǎn)	— transistor
速度 (sùdù)	— velocity / speed
电压 (diànyǎ)	— voltage

21.4. Basic Grammar Points

21.4.1. Simple Sentences

SVO Word Order: Subject + Verb + Object.

他们吃素。 你喝茶吗？ 我去学校。 弟弟喜欢冰淇淋。

Adjectives: Noun + 很 + Adjective.

数学很难。 她很累。 老板很懒。 王嘉尔很火辣！

Nouns: Noun + 是 + Noun.

我是学生。 他们是有钱人。 这是我男朋友。 那是什么菜？

Possession: Noun 1 + 的 + Noun 2; Subject + 有 + Object.

你的手机 上海的天气 你女朋友很高。 你有房子吗？

21.4.2. Simple Questions

Yes/No Question: a statement followed by 吗？

你喜欢咖啡吗？ 你是大学生吗？ 妈妈会做饭吗？ 你没有工作吗？

These questions may be answered with 对 / 嗯 (casual 'yes') or by repeating the verb (affirmative) or by negating the verb (negative, e.g. 没有 / 不来).

Affirmative-Negative Question: use a verb or adjective and its negative.

他们来不来？ 这里的咖啡贵不贵？ 他吃不吃鱼？ 你女朋友漂不漂亮？

Two-character verbs/adjectives may be shortened to the first character for the positive.

Reciprocal Questions: giving a statement then asking for follow-up using 呢.

我很好。你呢？ 你爸爸是上海人，你妈妈呢？ 北京下雨了。上海呢？

Question Words: the interrogatives 什么，哪里 / 哪儿，那个，谁，什么时候，为什么，怎么，多少 are positioned in a sentence to replace the subject of the question.

我是谁。？ 你喜欢吃什么菜？ 我的自行车在哪儿？ 你在哪个房间？

21.4.3. Noun Suffixes

Character	Pinyin	Examples
子	zi	桌子，椅子，筷子，橙子，儿子
家	jiā	画家，科学家，作家
员	yuán	球员，演员，团员
儿	er	花儿，事儿，画儿
者	zhě	读者，患者

21.3.4. Measure Words

Typical pattern: [quantity] + measure word + noun

Character	Pinyin	Associated nouns
个	gè	generic; people, 这个 / 那个
岁	suì	age (years old: no noun required)
年	nián	periods of time, years
天	tiān	periods of time, days
口	kǒu	people in a family
只	zhī	animals, birds, pairs of body parts (hands, arms, legs, feet)
条	tiáo	long and thin things (rivers, roads, ribbons, strings)
支	zhī	long, round, cylindrical things (pencils, pens)
双	shuāng	pairs of things (shoes, socks)
张	zhāng	flat things (papers, tables, cards)
本	běn	book-like things (books, newspapers, magazines, textbooks)
瓶	píng	bottles
被	bēi	cups, glasses
份	fèn	portions of food, gifts, jobs, reports

A quantity of 'two things' uses the number 两, not 二.

每 can be used before a measure word to mean 'every'.

21.4.5. Adverbs

Negation: 不 + Verb / Adjective; if the verb is 有 then negate with 没有:

我今天不想工作 孩子不喝酒 我没有时间 这个不贵

All and Both: Subject + 都 + Verb / Adjective :

我们都住在上海 你们都认识约翰马? 我们都要冰水 我和我太太都不吃肉

Also: Subject + 也 + Verb / Adjective:

你也很高 他们也是法国人吗? 我也是学生 你的房子也很漂亮

Descriptive State Complement: Verb / Adjective + 得 + Description:

你说得很好 他来得有点晚 哪个城市发展得最快?

Degree Complement: 太 + Adjective + 了 / Adjective + 极了 / 死了 / 坏了!

21.4.6. Conjunctions**And:** Noun + 和 + Noun:

老板喜欢咖啡和茶

手机和电脑都很贵

他和他奴朋友都喜欢中国菜

Or, for questions: Option 1 + 还是 + Option 2:

辣的还是不辣的？

上海还是北京？

你喜欢我还是我的钱？

Or, for statements: Possibility 1 + 或者 + Possibility 2:

星期六或者星期天，都可以。 今天晚上我想吃披萨或者寿司。

Either / Or: 或者 + Possibility 1, 或者 + Possibility 2:

只有一块蛋糕，或者你吃或者我吃。 咱们或者今天去或者明天去，一定要去。

21.4.7. Numbers, Ages, Dates and Times**Digits:** 零，一，二，三，四，五，六，七，八，九**Magnitudes:** 十 (10) ，百 (100) ，千 (1,000) ，万 (10,000) ，亿 (100,000,000)**Ordinals:** 第一 (1st) ，第二 (2nd) ，第十三 (13th)**Ages:** A: 你多大了？B: 我是二十一岁。**Dates:** 今天是2023年3月28日/号。**Times:** 上午九点 (9 am) ，下午四点 (4 pm) ，五点半 (5:30) ，两点零九分 (2:09) ，一点四十分 (1:40) ，九点一刻 (9:15) ，六点三刻 (6:45) ，差五分三点 (2:55)

21.4.8. Verbs and Auxiliary Verbs

Being somewhere: Subject + 在 + Place

Somewhere having something: Place + 有 + Object

Being named: Subject + 叫 + Name; Subject + 姓 + Surname

Going somewhere: Subject + 去 + Place

Ability / Possibility: Subject + 能 + Verb

Learned skills: Subject + 会 + Verb

Will do / want to do something: Subject + 要 + Verb (+了)

Permissions: 可以 + Verb

How to do something: 怎么 + Verb ?

Negation in past tense: Subject + 没有 + Verb

Negative commands: 不要 + Verb

SOV Structure: Subject + 把 + Object + Verb phrase or Subj. + 把 + Obj. 1 + Verb + 给 + Obj. 2

Often used with 放 (to put) to avoid ungrammatical constructions.

In the second case, 给 is a preposition e.g. 我们把礼物送给客人了。

21.4.9. Perfect Tense (Completed Actions with Complements)

Common form for past tense: Subject + Verb + 了

他们到了。 我的小狗吃了。 今天我吃了早饭。 老师问了五个问题。

Past perfect progressive: 你来北京多长时间了？

21.4.10. Prepositions

From: 从, and **From...To...:** 从 ... 到 ...

从今天开始，我要每天学习中文。

21.4.11. Grammatical Complements

Complements are constructed verbs or verb phrases.

Result Complement: indicates the result of a verb.

Verb + RC

Examples: 看见 (to see), 听到 (to listen), 做完 (to finish doing) , 买到 (to buy successfully), 写对 (to write correctly), 学会 (to master), 洗干净 (to wash and clean), 计划好 (to plan well)

Directional complement: indicates direction of a verb.

Verb + 来 / 去 or Verb + Object + 来 / 去

来 indicates 'towards the speaker'. 去 indicates 'away from the speaker'.

Common verbs used are 上 (up), 下 (down), 出 (out), 进 (in), 回 (back), 过 (go over), 起 (get up).

Examples: 下来 (come down), 出来 (come out), 回去 (go back), 站起来 (stand up),

拿几个碗来 (bring a few bowls), 回中国来 (come back to China)

21.5. Sentences for Reference by Theme

21.5.1. Myself, Friends and Family

Vocabulary in red, orange and green. Structures in blue. Other useful words in purple.

我爸爸比我叔叔高。

Wǒ bàba bǐ wǒ shūshu gāo.

My dad is taller than my uncle.

21.5.2. Leisure and Tourism

Vocabulary in red, orange and green. Structures in blue. Other useful words in purple.

我喜欢游泳、但是只有水很热才行。

Wǒ xǐhuān yóuyǒng, dànshì zhǐyǒu shuǐ hěn rè cái xíng.
I like swimming, but only if the water is hot.

因为我的牛肉面很冷、所以我感觉一点儿伤心。

Yīnwèi wǒ de niúròu miàn hěn lěng, suǒyǐ wǒ gǎnjué yīdiǎnr shāngxīn.
I feel a little sad because my beef noodles are cold.

我通常星期六和朋友一起去看电影，特别是有新片的时候。

Wǒ tōngcháng xīngqīliù hé péngyǒu yīqǐ qù kàn diànyǐng, tèbié shì yǒu xīnpian de shíhòu.
On Saturdays, I generally go to see a movie with my friends, especially when there are new ones.

五月我去了西班牙度假。

Wǔ yuè wǒ qùle xībānyá dùjià.
In May, I went on vacation to Spain.

这个博物馆有很多历史遗迹，其中一些来自商朝。

Zhège bówùguǎn yǒu hěn duō lìshǐ yíjī, qízhōng yīxiē láizì Shāng cháo.
This museum has many historical relics, among which some come from the Shang dynasty.

我跟我朋友一起坐出租车去四川菜馆。

Wǒ gēn wǒ péngyǒu yīqǐ zuò chūzū chē qù Sìchuān cài guǎn.
My friends and I took a taxi to the Sichuan cuisine restaurant.

21.5.3. School and Careers

Vocabulary in red, orange and green. Structures in blue. Other useful words in purple.

我在清华大学学习化学，所以我可以成为一名科学家。

Wǒ zài qīnghuá dàxué xuéxí huàxué, suǒyǐ wǒ kěyǐ chéngwéi yī míng kēxuéjiā.

I am studying chemistry at Tsinghua University so I can become a scientist.

21.5.4. Science, Technology and Current Affairs

Vocabulary in red, orange and green. Structures in blue. Other useful words in purple.

在亚洲四小龙中（台湾、香港、新加坡和韩国）、台湾的半导体行业发展得最快。

Zài yà zhōu sì xiǎo lóng zhōng (Táiwān, Xiānggǎng, Xīnjiāpō hé Hánguó), Táiwān de bàndǎotǐ hángyè fāzhǎn dé zuì kuài.

Among the Four Asian Tigers (Taiwan, Hong Kong, Singapore and South Korea),

Taiwan's semiconductor industry has developed the most rapidly.

我乘坐磁悬浮列车从上海浦东机场到龙阳路站、最高速度达到了300公里每小时。

Wǒ chéngzuò cíxuánfú lièchē cóng shànghǎi pǔdōng jīchǎng dào lóng yáng lù zhàn, zuìgāo sùdù dá dào le 300 gōnglǐ měi xiǎoshí.

I took the maglev train from Shanghai Pudong airport to Longyang Road station, and it reached a maximum speed of 300 km/hr.

L22. KOREAN (한국어)

22.1. Basics of Korean

22.1.1. Hangeul (한글)

Vowels:

ㅏ	ㅑ	ㅓ	ㅕ	ㅗ	ㅛ	ㅜ	ㅠ	ㅡ	ㅣ
a	ya	eo	yeo	o	yo	u	yu	eu	i
ㅐ	ㅒ	ㅔ	ㅖ	ㅚ		ㅜ		ㅟ	
ae	yae	e	ye	oe		wi		ui	
				ㅘ		ㅙ			
				wa		wo			
				ㅙ		ㅞ			
				wae		we			

Consonants:

ㄱ	ㄴ	ㄷ	ㄹ	ㅂ	ㅅ	ㅇ	ㅇ	ㅈ	ㅊ	ㅋ	ㅌ	ㅍ	ㅎ
g	n	d	m	b	s	l/r	-/ng	j	ch	k	t	p	h
ㄲ		ㄸ		ㅃ	ㅆ			ㅉ					
kk		tt		pp	ss			jj					

The double consonants (ㄲ, ㄸ, ㅃ, ㅆ, ㅉ) have a short, sharp, tense pronunciation.

When occurring as ending consonants:

- ㄱ, ㅋ, ㄲ are all pronounced as 'k'
- ㄷ, ㅌ, ㅅ, ㅆ, ㅈ, ㅊ, ㅎ are all pronounced as a soft 't'
- ㅇ is pronounced 'l/r' (in between these sounds: it is always the same)
- ㅂ, ㅍ are pronounced 'p'
- ㅇ is pronounced 'ng'
- If the next character has an initial ㅇ then the pronunciation reverts back to being an initial.
- If the final is a double consonant and the next character does **not** have an initial ㅇ then only the second consonant is pronounced.

Examples: 하 (hya), 렌 (len), 여 (yeo), 꾀 (gokk), 식 (sik), 극어 (geug-eo), 닭도 (dak-do)

Note: these pronunciations are romanisations (**not** IPA) and are very approximate.

22.1.2. Korean Keyboard Layout (Korean IME)

~ ,	! 1	@ 2	# 3	\$ 4	% 5	^ 6	& 7	* 8	(9) 0	- _	+ =	 ₩	←
Tab ↔	Q ㅅ	W ㅅ	E ㅅ	R ㄹ	T ㄷ	Y ㅅ	U ㅅ	I ㅅ	O ㅅ	P ㅅ	{ [}]	
Caps Lock ⬆	A ㅏ	S ㄴ	D ㅇ	F ㄹ	G ㅎ	H ㅏ	J ㅏ	K ㅏ	L ㅣ	:	"	'	↵ Enter	
Shift ⬆	Z ㅏ	X ㅅ	C ㅅ	V ㅅ	B ㅏ	N ㅏ	M ㅏ	< ,	> .	?	/	Shift ⬆		
Ctrl	Win Key	Alt	한 자				한 영	Alt	Win Key	Menu	Ctrl			

서울대 왜 안 가고 싶어요?

Why don't you want to go to **Seoul National University (SNU)**?

나중에 외국에서 일하고 싶으세요?

Do you want to **work abroad in the future**?

서울대 가는 게 나쁘지 않을 듯요.

I don't think going to **Seoul National University** would be a **bad** idea.

재벌이나 외국 기업에서 일하고 싶으세요?

Would you rather **work** at a **chaebol** or a **foreign company**?

